SPIE

2013 BiOS

SPIE Photonics West

2–7 February 2013

Technical Summaries

www.spie.org/pw

Conferences & Courses
2–7 February 2013

Exhibition
BiOS Expo: 2–3 February 2013
Photonics West: 5–7 February 2013

Location
The Moscone Center
San Francisco, California, USA

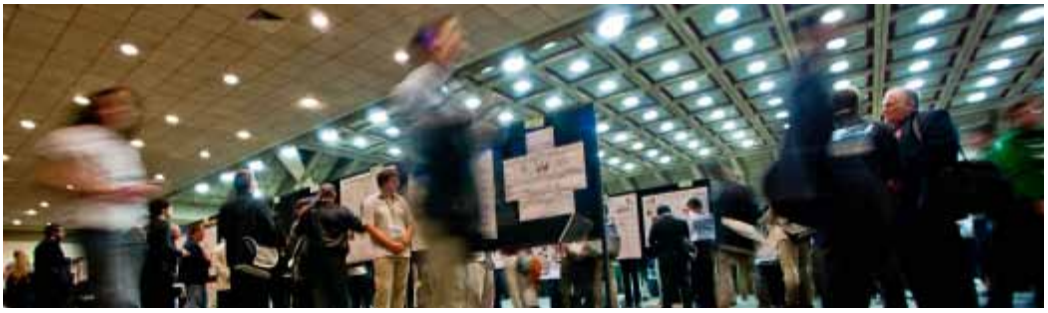

BiOS

SPIE Photonics West

Symposium Chairs

James Fujimoto
Massachusetts Institute of Technology (USA)

R. Rox Anderson M.D.
Wellman Ctr. for Photomedicine, Massachusetts General Hospital (USA) and Harvard School of Medicine (USA)

Contents

Click on the Conference Title to be sent to that page

Return to Contents

8565-1, Session 1

Confocal microscopy to guide laser ablation of non-melanoma skin cancers: a preliminary feasibility study

Bjorg A. Larson, Jason C. Chen, Milind Rajadhyaksha, Memorial Sloan-Kettering Cancer Ctr. (United States)

Laser ablation may be a promising method for removal of skin lesions, with the potential for better cosmetic outcomes and reduced pain, scarring and infection and may be a good choice for patients who are susceptible to cancerous lesions, such as those with nevoid basal cell carcinoma (BCC) syndrome, widespread actinic damage, or immunosuppression. However, an obstacle to implementing laser ablation is that the treatment leaves no tissue for histopathological analysis, which is routinely performed to examine for residual tumor. Confocal microscopy offers noninvasive optical sectioning of intact tissue, and has been shown to detect BCCs with high sensitivity and specificity, both in vivo as well as in excised tissue. Thus, pre-operative mapping of the depth and extent of BCCs may guide the initial ablation of the tumor, and subsequent intra-operative imaging may guide further ablation until all tumor is removed. We demonstrate preliminary feasibility of confocal microscopy to guide laser ablation of BCCs in freshly excised tissue from Mohs surgery. A pulsed Er: YAG laser, operating at 2940 nm wavelength, provides efficient ablation of tumor with reduced thermal damage to the surrounding tissue. Varying fluence up to 25 J/cm2 determines the ablation depth, up to 100 um. Tissue was examined for tumor before and after ablation using a confocal microscope with the imaging results confirmed by histopathology. A key challenge for this technique will be the development of contrast agents for vital staining of nuclear morphology to enable imaging of residual BCC tumors, ultimately on patients.

8565-2, Session 1

Automated localization of wrinkles and the dermo-epidermal junction in obliquely-oriented reflectance confocal microscopic images of human skin

Jamshid Sourati, Northeastern Univ. (United States); Milind Rajadhyaksha, Memorial Sloan-Kettering Cancer Ctr. (United States); Jennifer G. Dy, Deniz Erdogmus, Dana H. Brooks, Northeastern Univ. (United States)

Reflectance confocal microscopic (RCM) imaging of obliquely-oriented optical sections, rather than with traditional z-stacks, shows depth information that more closely mimics the appearance of skin in orthogonal sections of histology. This approach may considerably reduce the amount of data that must be acquired and processed. However, as with z-stacks, purely visual detection of certain structures, such as the dermal-epidermal junction (DEJ), in oblique images remains challenging due to low contrast in reflectance and textural variability in epidermal and dermal layers. We previously developed a machine learning approach to locating the DEJ in z-stacks. We have now extended that approach for obliquely-oriented sections. In addition we have developed a new algorithm to locate wrinkles in oblique sections. Since wrinkles are known to effectively change the local shape of DEJ, this algorithm, in addition to its intrinsic merit, gives useful information for localization of the DEJ. Automatically finding such morphological structures is not straightforward due to factors which include imaging artifacts, reflectance from the floor of wrinkles and the so-called “horny-plug” feature. As with our original algorithm, the approach combines feature sets based on image processing techniques and machine learning methods devised to cope with these difficulties.

8565-3, Session 1

Investigating the metastatic potential and pigment chemistry of melanomas using pump-probe imaging *(Invited Paper)*

Mary Jane Simpson, Jesse W. Wilson, Francisco E. Robles, Maria A. Selim, Marshall Phipps, Duke Univ. (United States); Warren S. Warren, Duke Univ. (United States) and Duke Univ. Medical Ctr. (United States)

Pump-probe microscopy non-destructively differentiates eumelanin and pheomelanin and can be used to quantify melanin distributions in thin biopsy slices. The nature of the technique makes it compatible with stained slides and suitable for in vivo imaging of moles. Monitoring the intensity and phase of the modulation transferred as a function of interpulse delay gives unique spectroscopic signatures to eumelanin and pheomelanin. Here we have extended that work for imaging melanin heterogeneity on a sub-cellular scale, investigating melanin degradation, and identifying features of metastatic melanomas.

We have found that melanin heterogeneity, characteristic of melanomas, persists on the sub-cellular scale, particularly in nested melanocytes. Other cells such as benign keratinocytes, do not have as much variation in pigment type in individual cells. High resolution melanin imaging has also allowed a comparison of the size of melanin granules in different types of cells.

We have also found spectral changes associated with melanin undergoing oxidative degradation, which breaks the biopolymer into monomers. This may be useful for differentiating melanophages from melanocytes and identifying pigmented cells experiencing oxidative stress due to malignancy or other damage.

We have analyzed a collection of archived melanomas with known sentinel lymph node biopsy results to avoid the uncertainty associated with a melanoma diagnosis by a pathologist. This study has revealed differences between the melanomas that had positive sentinel lymph node biopsies and the melanomas that showed no evidence of metastases following the excision of the primary tumor.

8565-4, Session 1

State-of-the-art clinical in vivo multiphoton tomography

Karsten Koenig, Univ. des Saarlandes (Germany) and JenLab GmbH (Germany)

Clinical multiphoton tomography based on femtosecond near infrared laser pulses for in vivo high-resolution skin imaging has been employed to thousands of volunteers and patients. The novel multimodal multiphoton tomograph MPTflex with its mechano-optical arm, active beam control, dual detector and wide-field imaging (up to 5x5 mm2) is in use in clinics in Japan, California, and Europe. Two-photon cellular autofluorescence and second harmonic generation of collagen can be detected with single-photon sensitivity and submicron spatial resolution. Using TCSPC, clinical two-photon FLIM has been used to distinguish fluorophores and to control therapeutical effects on patients suffering from dermatitis. Also in vivo clinical CARS has been realized to image intratissue lipids and water. Novel developments focus on multimodal hybrid imaging to generate optical tissue biopsies with subcellular resolution, deep-tissue information, and chemical fingerprints. Wide-field imaging tools such as dermoscopes, optical coherence tomographs as well as ultrasound and photoacoustics devices can be integrated. The hybrid tomographs have the potential to detect cosmetics and pharmaceutical components such as sunscreen nanoparticles and anti-aginging products in humans. Skin cancer such as malignant melanoma as well as dermatitis can be detected at an early stage and the efficiency

of the treatment can be monitored. Multiphoton tomographs will become biopsy-free and label-free imaging tools in personalized medicine, pharmacy, biotechnology as well as cosmetic research.

8565-5, Session 2

Comparison of single-photon and two-photon fluorescence properties of human skin and skin fluorophores

Jianhua Zhao, The BC Cancer Agency Research Ctr. (Canada); Mengzhe Shen, The Univ. of British Columbia (Canada); Edward Yu, The BC Cancer Agency Research Ctr. (Canada); Shuo Tang, Harvey Lui, The Univ. of British Columbia (Canada); Haishan Zeng, The BC Cancer Agency Research Ctr. (Canada)

Fluorescence spectroscopy is one of the most sensitive optical techniques for in vivo measurement of tissue biochemical and morphological properties. There is considerable interest in developing fluorescence-based spectroscopic and imaging techniques in biomedicine, particularly for early diagnosis of cancers and other diseases. Recently, two-photon fluorescence (TPF) imaging has gained popularity in biological and biomedical studies because of its advantages over single-photon fluorescence (SPF). Significant endogenous fluorophores in biological tissues include collagen, keratin, elastin, nicotinamide adenine dinucleotide (NADH), and flavin adenine dinucleotide (FAD). Understanding the fluorescence properties, concentrations and distributions of these fluorophores within tissue is important in optimizing the spectroscopic and imaging techniques and algorithms. It is believed that the TPF properties of these endogenous fluorophores are close to their SPF counterparts. However, there is no systematic compared study on the TPF and SPF properties of these endogenous fluorophores as of to date, due partially to the limitation of instrumentation. Very recently, we developed a video-rate TPF imaging system with the capability of measuring the two-photon excitation-emission matrix (EEM) spectroscopy. In this paper, we will present the SPF and TPF properties of the above mentioned biological fluorophores and human skin using single-photon EEM and two-photon EEM systems. We find that there are similarities and differences between SPF and TPF for these fluorophores and these differences demonstrate that caution must be exercised when interpreting tissue TPF properties based on the source of SPF reference spectra or vice versa.

8565-6, Session 2

Differential diagnosis of pigmented skin lesions based on harmonic generation microscopy

Ming-Rung Tsai, National Taiwan Univ. (Taiwan); Yi-Hua Liao M.D., National Taiwan Univ. Hospital (Taiwan); Chi-Kuang Sun, National Taiwan Univ. (Taiwan)

In clinical diagnosis, pigmented lesions are usually diagnosed using the naked eye and are with similar appearance. This may result in misdiagnosis and differential diagnosis of benign versus malignant lesions is thus important to ensure proper prognosis and treatment. Biopsy is currently the gold standard to make the definitive diagnosis, but this medical procedure is invasive and painful for patients. Recently in vivo harmonic generation microscopy (HGM) has been reported to have a superior performance on healthy human skin and oral mucosa. With the noninvasive nature, high penetration capability, and a high resolution, HGM could serve as an ideal virtual biopsy tool for in vivo, in situ, and immediate differential diagnosis of pigmented skin lesions. It is thus critical to investigate if the endogenous contrast provided by the HGM enough to diagnose the differences between the pigmented skin lesions. In this paper, we summarize our current clinical trial to perform in vivo and ex vivo HGM on pigmented skin lesions, including melanoma, pigmented basal cell carcinoma (BCC), nevocellular nevus, and seborrheic keratosis. Based on ex vivo study, histopathological correlated HGM imaging criteria for differential diagnosis were established. Three features of melanoma and four features of BCC were specified and statistically evaluated. Sensitivity values up to 100% (87-100%) and specificity values up to 99% (95-99%) were achieved for diagnostic classification. HGM presents a great potential to become a noninvasive diagnostic tool for the disease prescreening and clinical management of malignant diseases.

8565-7, Session 2

Video-rate in vivo human skin imaging using co-registered multiphoton and reflectance confocal microscopy

Hequn Wang, Anthony M. Lee, Zack Frehlick, The BC Cancer Agency Research Ctr. (Canada); Harvey Lui M.D., David I. McLean M.D., The BC Cancer Agency Research Ctr. (Canada) and The Univ. of British Columbia (Canada) and Vancouver Coastal Health Research Institute (Canada); Shuo Tang, The Univ. of British Columbia (Canada); Haishan Zeng, The BC Cancer Agency Research Ctr. (Canada) and The Univ. of British Columbia (Canada) and Vancouver Coastal Health Research Institute (Canada)

Combining reflectance confocal microscopy (RCM) and multiphoton microscopy (MPM) imaging potentially allows greater clinical diagnostic utility as complementary information can be revealed using these two techniques. Here we present a multimodal in vivo skin imaging instrument that is capable of simultaneously acquiring multiphoton and reflectance confocal images at up to 27 fps with 256?256 pixel resolution. A tunable (720-950nm) 80MHz femtosecond Ti:Sa laser was scanned into the back aperture of a 60X (NA=1.0) long working distance water immersion objective using a paired resonance/galvanometer scanner. A combination of beamsplitters, dichroic mirrors, and filters separated and directed the reflectance confocal (RCM), two-photon fluorescence (TPF) and second harmonic generation (SHG) signals onto their respective detectors. Images from all channels were simultaneously captured by a multichannel frame grabber. Imaging all channels with only one excitation laser source ensures perfect image registration between the RCM, TPF, and SHG images. Images and videos acquired with our system show that the three imaging channels provide complementary information in in vivo human skin measurements. In the epidermis, cell boundaries are clearly seen in the RCM channel, while cytoplasm is better seen in the TPF imaging channel; in the dermis, SHG and TPF channels show collagen bundles and elastin fibers, respectively. The demonstrated fast imaging speed and multimodal imaging capabilities of this MPM/RCM instrument are essential features for future clinical noninvasive applications of this technique.

8565-8, Session 2

Modeling semiconductor lasers for In vivo confocal-laser-scanning-microscopy in dermatology

Meng-Mu Shih, Univ. of Florida (United States)

Different lasers have clinical and research applications in dermatology and plastic surgery. Semiconductor lasers have attractive features such as small-size, low-power, and various wavelengths. Grating-embedded semiconductor lasers make not only the size more compact but the emitting wavelength more stable and precise.

This talk promotes applications of such lasers in this biomedical field. A skin-imaging technique using in vivo confocal-laser-scanning-microscopy (CLSM) serves as an example. The modeling results related to structures and materials of lasers are presented numerically by the optical and the photonic approaches. Interpretations based on numerical results provide insights into the modeling and design of laser-based applications.

8565-9, Session 3

Investigation of fractional laser photothermolysis and visualization of microthermal zone with optical coherence tomography

Feng-Yu Chang, Cheng-Hsing Fan, Cheng-Kuang Lee, Meng-Tsan Tsai, Chang Gung Univ. (Taiwan); Chih-Hsung Yang M.D., Chang-Gung Memorial Hospital (Taiwan)

Laser photothermal therapy is an effective method for skin resurfacing, including using ablative CO2 pulsed laser or non-ablative Er: Glass laser. However, it is difficult to evaluate the effect of laser treatment in real-time since the parameters including the density of incident beams, the penetration depth and the beam diameter cannot be obtained immediately. Therefore, in this study, we propose to use a noninvasive optical imaging technique, optical coherence tomography (OCT), to investigate the effect of laser treatment with three-dimensional imaging. In our experiments, the phantom and human skin including facial and belly skin were scanned with our SS-OCT system after laser treatments. From the scanning results, several parameters can be obtained such as the penetration depth, the zone of thermal damage, and the recovery time. Also, the treatment effects are compared by using CO2 pulsed laser and Er: Glass laser. With OCT scanning, it can provide the real-time information to evaluate the parameters of microthermal zones and penetration depth of optical beams, enabling to help the physicians determine the treatment parameters.

8565-10, Session 3

Microvasculature imaging for clinical scar assessment *(Invited Paper)*

Yih Miin Liew, Robert A. McLaughlin, Peijun Gong, The Univ. of Western Australia (Australia); Fiona M. Wood M.D., The Univ. of Western Australia (Australia) and Burns Service of Western Australia, Royal Perth Hospital (Australia); David D. Sampson, The Univ. of Western Australia (Australia)

Pathological scarring, such as hypertrophic scars and keloids, can result in major functional, cosmetic and psychosocial impairment of patients. Examination of scar progression is important in assessing response to treatment, and in early identification of pathological scarring. Redness of scarring is a commonly graded clinical indicator, indicating the level of scar vascularity. Angiogenesis occurs at an early stage of wound healing and may progress under pathological conditions long after wound closure, therefore causing pathological scars (keloid and hypertrophic) to appear very red. Scar vascularity is expected to reduce towards maturation as indicated by the reduction in their redness comparable to the surrounding normal skin. However, manual assessment of scar appearance can be subjective and suffer significant inter-observer variability. We demonstrate the first clinical application of optical coherence tomography (OCT) for in vivo, non-invasive and contrast agent-free quantification of the microvasculature network in human skin scars. In OCT imaging, vascular areas have been shown to undergo rapid speckle decorrelation, and this was used to delineate the microvasculature. Automatic techniques were then developed to quantify the degree of vasculature, including estimates of average vessel diameter and total amount of vasculature. Measurements were performed on eight human burns scar patients, comparing scar tissue with contralateral healthy tissue. Results showed a substantial difference between the scar and the normal tissue, with a significant increase in the measured density of vasculature present in scarred tissue.

8565-11, Session 3

Optical coherence tomography demonstrates epidermal thinning of human forearm volar skin after 2 weeks application of a topical corticosteroid.

Stephen J. Matcher, Zenghai Lu, Michael Cork, The Univ. of Sheffield (United Kingdom)

The use of topical corticosteroids (TCS) to treat inflammatory skin disorders such as atopic dermatitis is clinically established. However there is a strong interest in developing non-steroidal alternatives to TCS because the latter compounds are known to have strong effects on, for example, skin barrier function. In this report we present a human volunteer study in which optical coherence tomography (OCT) was used to non-invasively quantify the effects of a potent TCS on the structure of volar forearm skin and compare this with a non-steroidal alternative eczema treatment.

Methods: two matching sites were chosen on the left and right forearm of a human volunteer. The sites were recorded using nearby skin features and baseline OCT images recorded. OCT imaging was performed using a 1300 nm swept-source OCT system. 4x2 mm B-scans were recorded, revealing the epidermis and dermis as dark and bright band respectively. One arm was then treated using a potent TCS (betamethasone valerate 0.1%) whilst the other was treated using a non-steroidal immunosuppressant eczema treatment (Tacrolimus). After 14 days OCT images were collected at the same sites.

Results: The OCT images of the Tacrolimus-treated skin showed no discernible difference between pre- and post-treatment. In contrast the skin treated with bethamethasone valerate showed a substantial (~50%) decrease in the epidermal thickness as measured from the OCT image.

Conclusion: OCT is capable of detecting changes in skin structure induced by clinically approved eczema treatments. It is thus a viable tool for assessing the physical effects of alternative treatments.

8565-12, Session 3

Quantitative monitoring of tissue rejuvenation using 3D OCT

Areun Kim, Jeonghyeon Lee, Taeho Kim, Ulsan National Institute of Science and Technology (Korea, Republic of); Haekwang Lee, Sunghoon Lee, AmorePacific Corp. (Korea, Republic of); Woonggyu Jung, Ulsan National Institute of Science and Technology (Korea, Republic of)

Nowadays, laser therapy is a common method for treating various dermatological troubles, because it provides effective care of acne, pigmentation and wrinkle etc. in the skin. Although laser treatment becomes a routine procedure in medical and cosmetic fields, there are few studies investigating laser-tissue interaction and the prevention of side effect such as hyperpigmentation, redness and burning. This results from the lack of optimal imaging modality enabling fast feedback and quantitative information of tissue during therapeutic procedure.

In this study, we introduce a quantitative tissue monitoring tool using 3D optical coherence tomography (OCT) to observe tissue rejuvenation after laser irradiation. OCT has been used to image skin in dermatology, but previous approach was mostly focused on the diagnosis of disease with 2D image which has restriction to explore large area of tissue dynamically. In order to overcome these limit, we fabricated video integrated high speed 3D OCT which is capable of large field of cross-sectional imaging as well as surface imaging. Automatic segmentation software enabling the calculation of 3D volume was also developed accordingly. Engineered skins were irradiated by fractional laser, and analyzed by developed system and software. The experiment was repeated every two hours to observe the tissue rejuvenation for five days. Through this experiment, we found that laser irradiated engineered skin was mostly recovered within two days which has similar tendency with

histological evaluation. Our result shows that 3D OCT could be promising tool to be used in laser therapeutic procedure to monitor and quantify skin.

8565-13, Session 4

Effective dermal heating with temporal squared millisecond Nd:YAG pulses visualized using subsurface thermo imaging

Rudolf M. Verdaasdonk, Vrije Univ. Medical Ctr. (Netherlands) and Free Univ. Amsterdam (Netherlands); Albert Van der Veen, Divya Chandrabose, Vrije Univ. Medical Ctr. (Netherlands); Vladimir Lemberg, BonCheol L. Goo M.D., Lutronic Corp. (Korea, Republic of)

Various non-ablative treatment strategies have been introduced for effective skin rejuvenation. A wide beam millisecond long pulse Nd:YAG laser (CLARIA, Lutronic) was used to deliver thermal energy inside the dermis preserving the epidermis. The temporal pulse shape could contribute significantly to the heat accumulation inside the tissue.

The heat accumulation of ‘square’ and ‘non-squared’ pulses were compared in relation to beam diameter (5-20 mm), pulse length (1-100 ms, at 5 Hz) and energy (5-20 J) using thermal imaging in a model tissue simulating the treatment technique. A layer of chicken skin was position on an IR absorbing polyacrylamide gel and imaged from the side (‘underneath the surface’) with a thermo camera showing the absolute temperature dynamics in a ‘2 ? D geometry’.

The squared pulse showed to be more effective in heat accumulation (~25 %) compared to the non-squared pulse. A maximum temperature increase of 50 degree C occurred around 1 mm underneath the surface after 5 s exposure. Thermal relaxation was in the order of 30 seconds (however, in a model without perfusion). Larger spot sizes provide a more homogeneous temperature distribution inside the tissue.

Thermo imaging in a ‘subsurface’ geometry provided an insight in the temperature dynamics of non-ablative skin rejuvenation therapy showing that temporal square shaped pulses are more effective in heating tissue.

8565-14, Session 4

Comparative analysis of the thermal distribution of a radio frequency fractional system using high speed thermo imaging techniques

Rudolf M. Verdaasdonk, Vrije Univ. Medical Ctr. (Netherlands) and Free Univ. Amsterdam (Netherlands); Albert Van der Veen, Divya Chandrabose, Vrije Univ. Medical Ctr. (Netherlands); Vladimir Lemberg, BonCheol L. Goo M.D., Lutronic Corp. (Korea, Republic of)

Fractional RF treatment has become the effective skin rejuvenation procedure. The RF energy build up in the skin dermis creates the fractionated thermal damage and collagen denature. To control the clinical effect and adverse effects, it is important to know the thermal distribution in the dermis created by RF pulses. High speed (Schlieren) imaging techniques were applied to study the thermo dynamic effects in transparent tissue models (polyacrylamide gel or pig cornea) imaging from the side (‘underneath the surface’) of a RF Fractional System (INFINI, Lutronic) complimented with a standard thermo imaging. The RF system consisted either of a array of 7x7 surface electrodes or an array of 7 x 7 RF needles that are spring loaded injected 1-4 mm into the tissue to expose the tissue for 100 - 500 ms.

The dynamic images of the localized heating around the tip of the electrode at several mm depth in the tissue and consequent thermal relaxation gave good insight in heating mechanism (10 ms resolution). Additionally, the ‘subsurface’ thermal images showed local temperature rise of 50 degree C and relaxation times in the order of 1-2 seconds.

High speed thermo imaging in a ‘subsurface’ geometry provided an insight in the temperature dynamics during the application of RF electrodes to control and improve of non-ablative skin rejuvenation therapy .

8565-15, Session 4

Preclinical in vivo evaluation of combination photodynamic therapy and pulsed dye laser treatment on normal vasculature

Wesley Moy, Justin Moy, Kristen M. Kelly M.D., Bernard Choi, Beckman Laser Institute and Medical Clinic (United States)

Port wine stain (PWS) is a congenital birth mark commonly found on the face and neck regions. It consists of abnormally-enlarged vasculature in the dermis. Current treatments typically involve the use of a pulsed dye laser (PDL) combined with cryogenic cooling of the skin. Yellow light, from 585-595 nm wavelengths, is strongly absorbed by hemoglobin. The clinical goal is to achieve photocoagulation of the targeted vasculature in a selective manner.

Based on past studies, we postulate that PDL therapy is ineffective to acute consistent photocoagulation of smaller vasculature. Over the past decade, we studied the use of photodynamic therapy (PDT) as an alternate treatment option, either as a standalone procedure or in combination with PDL therapy. We hypothesize that combined use of PDT and PDL therapy can achieve photocoagulation of targeted vessels while reducing the radiant energies required for each therapy, resulting in a safer, more effective treatment option.

We devised a protocol that involves use of an intravascular photosensitizer followed by PDL treatments. To assess therapeutic efficacy, we used the mouse dorsal window chamber model and laser speckle imaging to monitor blood-flow dynamics. We defined a successful treatment outcome as achieving persistent vascular shutdown within the window, seven days following the combined PDT and PDL treatment.

With our preclinical data, we applied dose response curve analysis to identify a characteristic radiant exposure to achieve a successful treatment. We studied PDT threshold radiant exposures with the PDL treatments to achieve successful outcomes. Our preliminary data suggest that the combination PDT and PDL therapy is a viable treatment option for PWS vasculature.

8565-16, Session 4

Blue LED treatment of superficial abrasions

Domenico Alfieri, Light4Tech Firenze S.r.l. (Italy); Stefano Bacci, Univ. degli Studi di Firenze (Italy); Riccardo Cicchi, Istituto Nazionale di Ottica (Italy) and European Lab. for Non-linear Spectroscopy (Italy); Gaetano De Siena, Univ. degli Studi di Firenze (Italy); Francesco S. Pavone, European Lab. for Non-linear Spectroscopy (Italy); Roberto Pini, Francesca Rossi, Francesca Tatini, Istituto di Fisica Applicata Nello Carrara (Italy)

A compact and easy-to-handle photocoagulation device was used for inducing an immediate coagulation effect in skin large superficial abrasions, reducing the recovering time and improving the wound healing process. The handheld illumination device consists of a high power LED, emitting in the blue region of the spectrum, mounted in a suitable and ergonomic case, together with power supply, electronics, and batteries. The working principle of the LED-based photocoagulator is a photothermal effect: the blue light (420 nm) is selectively absorbed by the haemoglobin content of the blood and then converted into heat. Here we present an in vivo study performed on animal models. 10 Sprague Dawley rats (Harlan, Italy, weighing 200-250 g) were used to study the wound healing process. On the back of each rat, four large

abrasions were mechanically produced: two of them were used as a control, while the other two were treated with the photocoagulator, keeping it at a constant distance (2 mm) from the target, in continuous slow motion (treatment time: tens of seconds). The induced photothermal effect was monitored by an infrared thermocamera in order to avoid accidental thermal damage and to control the temperature dynamics during treatment. Objective observations, histopathological analysis and non-linear microscopy performed in a 8 days follow-up study showed no adverse reactions and no thermal damage in the treated areas and surrounding tissues. Moreover, a faster healing process and a better recovered morphology was evidenced in the treated tissue.

8565-18, Session 5

Elimination of single-beam substitution error in diffuse reflectance measurements using an integrating sphere

Luka Vidovic, Jo?ef Stefan Institute (Slovenia); Boris Majaron, Jo?ef Stefan Institute (Slovenia) and Univ. of Ljubljana (Slovenia)

Diffuse reflectance spectroscopy (DRS) is a popular approach to objective characterization of various skin test sites. A common DRS setup involves an integrating sphere (IS), in which spectrally broad illumination light is multiply scattered and homogenized. To account for illumination spectrum, each measurement begins by placing a highly reflective “white standard” against the IS sample opening and collecting the reflected light at the signal output port. After replacing the white standard with skin site of interest, DRS of the latter is determined by dividing the two signals at each involved wavelength.

However, because skin samples are invariably less reflective than the white standard, such a substitution modifies the illumination field inside the IS. This is known as a “single-beam substitution error” (SBSE) and leads to underestimation of skin’s reflectivity and distortion of measured DRS, with adverse consequences for subsequent quantitative analysis. Barring the use of much more complex dual-beam experimental setups, involving dedicated IS, literature states that only approximate corrections of SBSE are possible, e.g., by using look-up tables generated with lower-reflectivity standards.

We have established a way to eliminate SBSE by using IS equipped with an additional “reference” output port (e.g., ISP-REF by Ocean Optics). In a theoretical derivation, we show that two additional measurements performed at this port (of the white standard and skin sample, respectively) enable accurate compensation of the IS throughput alteration, thereby eliminating SBSE. We also demonstrate that the difference between DRS measured with and without such correction (reaching 7%) behaves according to theoretical predictions.

8565-19, Session 5

Characterization of a multi-modal probe for early skin cancer detection using Raman, reflectance and fluorescence spectroscopies

Manu Sharma, Liang Lim, The Univ. of Texas at Austin (United States); Eric Marple, EmVision, LLC (United States); William Riggs, DermDx (United States); James W. Tunnell, The Univ. of Texas at Austin (United States)

The development of technologies which focus on noninvasive pathology detection and diagnosis are imperative as their noninvasive nature improves patient care and their early detection capabilities reduce patient morbidity and mortality. The combination of different spectroscopic techniques, with each modality providing complementary information, has proven to be a very successful and relatively cheap option. Here we describe the design and testing of a novel optical fiber probe, which combines three optical spectroscopy modalities, and forms a key component in the development of a system to be used for the early detection of skin cancer.

Our probe collects light for fluorescence, Raman and reflectance spectroscopies. An effective multi-modal probe design must cater to the specifics of each technique such as a high Raman collection efficiency and the source-detector geometry for physiological measurements from reflectance spectra. Our solution involves an innovative gradient-index (GRIN) lens configuration to focus and collect light from the same area.

We have tested our prototype in both tissue-simulating phantoms and on human skin. Diagnostically important spectral features (Amide I/III, Q/Soret bands) can be identified and physiologically important parameters have been extracted, demonstrating adequate Raman collection efficiency and appropriate source-detector separation. Results from our clinical trial demonstrate that a multi-modal approach is a superior skin cancer diagnostic tool compared to any one single modality.

These initial results suggest that our multi-modal probe offers considerable promise for early skin cancer detection purposes. Our probe performance indicates that it could be well-applied to any biomedical multi-modal application.

8565-20, Session 5

Quantitative assessment of response of generalized Argyria to Nd:YAG treatment using diffuse optical spectroscopy

Rolf B. Saager, Beckman Laser Institute and Medical Clinic (United States); Khaled M. Hassan, Univ. of California, Irvine (United States); Clement Kondru, Anthony J. Durkin, Beckman Laser Institute and Medical Clinic (United States); Kristen M. Kelly, Univ. of California, Irvine School of Medicine (United States)

Generalized argyria is a blue-gray hyperpigmentation of the skin resulting from repeated ingestion of products as silver colloid. While some case reports have noted improvement after Q-Switched 1064nm Nd:YAG laser treatment to small surface areas, no reports have objectively monitored laser treatment of generalized argyria over large areas of skin, nor have long-term outcomes been evaluated.

We have developed a novel fiber probe which can be used in combination with diffuse optical spectroscopic (DOS) methods, to noninvasively determine full spectrum optical properties of superficial in-vivo skin in the wavelength range from 650-1000nm. This probe uses a highly scattering layer to diffuse photons emitted from a collimated light source, and relies on a two-layer diffusion model to determine tissue absorption coefficient ?a and reduced scattering coefficient ?s’. This technique was used to quantify the concentration of silver particles in the skin prior to laser treatment, as well as multiple time intervals up to 1 year thereafter.

We were able to estimate from the quantitative absorption data that there was, on average, a 0.042 mg/mL concentration of silver in the tissue prior to treatment through direct comparison of reference measurements of silver colloid in solution (H2O) taken in a spectrophotometer. There was no detectable presence of silver after a single treatment of the tissue area and no indication of recurrence up to one year. Additionally, the tissue optical properties indicated that there was no collateral tissue damage that resulted from these treatments, in agreement with clinical observation.

8565-21, Session 5

Non-invasive, in vivo fluorescence monitoring as an objective tool to examine wound healing progression following low level laser therapy

Vijendra Prabhu, Edward M. Fernandes, Satish B. S. Rao, Krishna K. Mahato, Manipal Univ. (India)

Collagen represents major protein component of the extracellular

matrix (ECM) and hence it could be used as an ideal tool for assessing wound healing following any therapy. Presently, there is a great need to develop quick, objective, non-destructive method to monitor collagen levels during progression of wound healing. The applicability of the laser induced fluorescence (LIF) towards wound healing monitoring by measuring collagen levels at different stages of the healing progression is the main idea behind the current work. Six to eight weeks old Swiss albino mice with ccircular wounds of 15 mm diameter were illuminated with single exposure of 2 J/cm2 from He-Ne laser (632.8 nm; 7 mW power; 4.02 mW/cm2 power density) along with un-illuminated and un-wounded controls. Spectroscopic changes were monitored by recording in vivo fluorescence spectra from each animal under anesthesia at different post-wounding days (5th, 10th, 30thday) by exciting wound granulation tissue/skin with 325 nm He-Cd laser. The autofluorescence from the tissue/skin was recorded from four different sites and four spectra were recorded from each. A total of 2160 spectra were recorded from 45 animals and analysed. The present study have shown significant increase ($P<0.05$) in collagen synthesis upon treatment with optimum laser dose of 2 J/cm2 immediately following wounding as compared to un-illuminated control group. In conclusion, in vivo fluorescence measurement is effective in monitoring wound healing and hence could be used over ex vivo method as an objective and non-intrusive method to monitor collagen levels

8565-22, Session 5

Theoretical study on Raman properties of normal human skin using Monte Carlo method with a multi-layered tissue model

Shuang Wang, Northwest Univ. (China); Jianhua Zhao, The BC Cancer Agency Research Ctr. (Canada) and The Univ. of British Columbia (Canada) and Vancouver Coastal Health Research Institute (Canada); Harvey Lui M.D., British Columbia Cancer Agency Research Ctr. (Canada) and The Univ. of British Columbia (Canada) and Vancouver Coastal Health Research Institute (Canada); Qingli He, Zhaoyu Ren, Jintao Bai, Northwest Univ. (China); Haishan Zeng, The BC Cancer Agency Research Ctr. (Canada) and The Univ. of British Columbia (Canada) and Vancouver Coastal Health Research Institute (Canada)

The Raman properties of normal human skin were studied theoretically using Monte Carlo simulation. Skin tissue was represented as a turbid eight-layered medium. The scattering, absorption and anisotropy propagation of the excitation light and regenerated Raman photon was modeled in this medium. Ex vivo Raman spectra from different skin layers were measured from skin sections to define the intrinsic Raman properties. The reconstructed Raman spectra reached reasonable agreement with the measured in vivo skin spectra, demonstrating the validity and usefulness of our modeling method. This theoretical work outlines a new way to investigate Raman properties of human tissue.

8565-23, Session 6

Hyperspectral imaging as a diagnostic tool for chronic skin ulcers

Martin Denstedt, Norwegian Univ. of Science and Technology (Norway); Brita S. Pukstad M.D., Norwegian Univ. of Science and Technology (Norway) and St.Olavs Hospital, Univ. Hospital of Trondheim (Norway); Lukasz A. Paluchowski, Norwegian Univ. of Science and Technology (Norway); Julio E. Hernandez-Palacios, Norwegian Univ. of Science and Technology (Norway) and Norsk Elektro Optikk AS (Norway); Lise L. Randeberg, Norwegian Univ. of Science and Technology (Norway)

Chronic wounds like venous leg ulcers, pressure sores and diabetic ulcers represent a major health problem in western countries. The healing process of a wound is complex, and the complete pathogenesis is not fully known. Diagnosis and follow-up of such wounds are currently based on visual inspection, biopsies and collection of samples from the wound surface. Hyperspectral imaging is a technique that combines spectroscopy and high resolution imaging into one modality, providing non-contact, high resolution measurements. The main aim of this study was to investigate the feasibility of this modality as a diagnostic tool in wound care.

Hyperspectral images (400-1000 nm) were collected from patients with venous leg ulcers using a pushbroom-scanning hyperspectral camera (VNIR 1600, Norsk Elektro Optikk AS). The scan duration was about 30 seconds, imaging skin regions approximately 10 by 20 cm in size, with a spatial resolution of approximately 60 µm and a spectral resolution of 3.7 nm. The patients were recruited from the outpatient clinic at Trondheim University Hospital. Wounds were examined regularly over 12 weeks. The patients were evaluated by a dermatologist at every appointment, and samples of wound fluid and bacterial samples were collected for further examination.

The results were analyzed using band ratio metrics as well as more complex statistical image analysis methods. Information about e.g. tissue oxygenation, area and structure of the wound was extracted and used to distinguish between different phases of healing. Preliminary results indicate that the system has a potential for fast in vivo diagnosis of wounds.

8565-24, Session 6

Non-invasive imaging of dermal lymphatic reconstitution using near-infrared laser angiography

Ah-Reum Jeong, Johns Hopkins Univ. School of Medicine (United States) and Keck School of Medicine, of Univ. of Southern California (United States); Gabriel A. Brat M.D., Kate J. Buretta, Joani M. Christensen, Gerald Brandacher M.D., Justin M. Sacks M.D., Johns Hopkins Univ. School of Medicine (United States)

Lymphatic channels and drainage play a major role in the rejection of vascularized composite allotransplants (VCA), such as hand and face transplants. In particular, the skin, as the most immunogenic organ, has a dominant role. The aim of this study was to characterize lymphatic regeneration using a translational model. We present the first part of this project using near-infrared (NIR) laser imaging with intradermal Indocyanine green (ICG) injection as a promising minimally invasive technology for lymphatic imaging.

Syngeneic, full-thickness skin grafts measuring 2?2cm were transplanted to the dorsolateral thigh of 15 Lewis rats. Each rat was imaged using commercially available NIR laser imaging over 1 hour at either post-operative day 6, 7, 8, 9, or 14 by intradermal injection of 4?L of 2.5mg/mL ICG. After imaging, sentinel lymph nodes were harvested to confirm presence of ICG. Intradermal acrylic blue dye injection was used to validate the pathway of lymphatic images, and its travel to the sentinel lymph node.

Lymphatics were readily seen in a full-thickness skin graft model as early as post-operative day 8. Acrylic blue dye injection and lymph node dissection confirmed lymphatic reconstitution. These results provide insights into the characteristics of lymphatic reconstitution in skin grafts and will serve as the foundation for examining acute rejection of the skin in VCA.

8565-25, Session 6

Diffuse reflectance imaging system for spectral analysis of skin cancer in vivo

Sheldon F. Bish, Youmin Wang, Manu Sharma, Nicholas Triesault, The Univ. of Texas at Austin (United States); Jason Reichenberg M.D., Univ. Medical Ctr. Brackenridge (United States); Xiaojing Zhang, James W. Tunnell, The Univ. of Texas at Austin (United States)

Diffuse reflectance spectroscopy provides a noninvasive means to determine tissue optical properties and has been used as a diagnostic tool for early cancer detection in several organ sites including the skin, cervix, and oral cavity. Until recently, these measurements were made on a single point of tissue, missing the spatial context to investigate critical features such as margins and shape. To expand on these point measurements, we have developed a diffuse reflectance spectroscopy imaging (DRSI) system capable of acquiring wide field optical property maps of tissue. This system uses a white light source and a portable spectrometer to acquire high resolution UV-VIS spectra. Currently, image acquisition time is approximately 10 seconds for a 50x50 pixel image. A nonlinear optimization fitting routine was used to fit a look-up table (LUT) model to the DRSI spectral images resulting in spatially resolved fits for reduced scattering, hemoglobin and melanin concentration. The system was validated across biologically relevant levels of reduced scattering (7% Error) and absorption (10% Error) using tissue simulating phantoms. DRSI optical property maps of suspected basal cell carcinoma and melanoma were acquired in vivo. These quantitative maps showed consistency with the known optical properties found in literature such as decreased reduced scattering within lesion margins. Here we have presented the latest edition of our DRSI system, demonstrating the potential as an effective tumor margin delineation tool for clinicians.

8565-26, Session 6

An initial development of laser speckle imaging for application in the inflammatory arthritis disease

Taeyoon Son, Won Hyuk Jang, Jihoon Park, Byungjo Jung, Yonsei Univ. (Korea, Republic of)

Rheumatoid arthritis (RA) is one of most common inflammatory joint disease. RA leads to damage to the articular cartilage, bony erosion and, finally, articular destruction. As the treatment in RA moves toward early and aggressive therapy more sensitive imaging techniques are needed to evaluate the effectiveness of early therapy. Common joint imaging modalities to diagnosis arthritis are conventional and digital radiography, CT, US, MRI and nuclear imaging. But, there exist some drawbacks. That is low soft tissue contrast and patient exposure to ionizing radiation expensive and not as widely available as US or CR for CT, difficulty to assess the structural changes within the bone, performance is highly dependent on the skills of operator for US, high cost, need for contrast agent long data acquisition time, in some cases impossible to use for MRI and poor spatial resolution and limitation of anatomical information for nuclear imaging. Optical imaging such as Laser speckle imaging (LSI) offers unique advantages - nonionizing noninvasive method - over existing imaging methods for medical imaging and diagnosis of arthritis. In this study, adjuvant-induced arthritis model was used and mouse feet were imaged. The mouse was divided into two groups – control (with no arthritis) and test (with inflammatory arthritis). The acquired images were analyzed into speckle contrast index and erythema index and compared conventional diagnosis method. The results show that the test group represent higher index for both LSI and erythema imaging compared to control group. From the results, LSI shows the potential of early diagnosis for inflammatory arthritis

8565-27, Session 7

Assessment of reconstructive flap occlusion in a preclinical model: A comparison of spatial frequency domain imaging to conventional digital color imaging

Eren Taydas, Beckman Laser Institute and Medical Clinic (United States); Adrien Ponticorvo, Beckman Laser Institute and Medical Clinic, University of California Irvine (United States); Amaan Mahzar, Modulated Imaging, Inc. (United States) and Beckman Laser Institute Photonics Incubator (United States); Thomas Scholz M.D., Jonathan Rimler M.D., Hak-Su Kim, Univ. of California, Irvine Medical Ctr. (United States); June Tong, Beckman Laser Institute and Medical Clinic (United States) and Univ. of California, Irvine (United States); Gregory R. D. Evans M.D., Univ. of California, Irvine Medical Ctr. (United States); David J. Cuccia, Modulated Imaging, Inc. (United States) and Beckman Laser Institute Photonics Incubator (United States); Anthony J. Durkin, Beckman Laser Institute and Medical Clinic (United States) and Univ. of California, Irvine (United States)

Tissue transfer techniques are commonly used in reconstructive surgery to replace damaged tissue. While typically successful, there is a 40-60% failure rate for tissue flaps that require additional surgery. The current technique for diagnosing tissue flap failure is to monitor the flap on an hourly basis and look for signs of discoloration. Because the chances of salvaging a tissue flap improve the earlier a problem becomes apparent, a technique that is capable of detecting changes before they are clinically noticeable has the potential to improve post-operative flap management. The research presented here aims to compare clinical appearance as recorded via digital camera with spatial frequency domain imaging (SFDI), a non-invasive imaging technique utilizing wide field patterned illumination at multiple wavelengths to generate images of tissue oxygen saturation. To mimic different levels of tissue failure, flaps were created in a swine model where blood flow was monitored with ultrasound probes and controlled with vascular occlusion cuffs. Blood flow was reduced by 25%, 50%, 75%, and 100% of baseline values in each of the flaps. The color changes recorded in the digital camera images were quantified in order to predict which occlusion conditions were visible to the human eye. The results of the color change analysis are compared to the oxygen saturation images generated by the SFDI system. Results indicate that while the human eye can reliably perceive changes at 100% occulsion, SFDI is able to detect changes as small as 50%, thereby improving the potential response time and reducing the potential for flap failure.

8565-28, Session 7

Quantitative longitudinal measurement in a rat model of controlled burn severity using spatial frequency domain imaging *(Invited Paper)*

John Quan M. Nguyen, Tuan Mai, Christian Crouzet, Beckman Laser Institute and Medical Clinic (United States); Nicole Bernal, Univ. of California, Irvine (United States); Bernard Choi, Anthony J. Durkin, Beckman Laser Institute and Medical Clinic (United States)

Despite an estimated 500,000 burn injuries reported each year in the United States, clinical diagnosis of burn wound severity still remains a challenge. Whether an injury will be able to heal by itself or require surgical excision and grafting is highly dependent on the wound's burn depth. In particular, partial thickness burn wounds are very difficult for clinicians to identify, and as such, result in delays in grafting and extended hospital stays. Here, we present a multi-day pre-clinical study in which we utilized a non-invasive wide-field functional imaging

modality known as Spatial Frequency Domain Imaging (SFDI) in order to quantitatively evaluate burn wound severities in a rat model. Imaging was conducted at 17 evenly spaced wavelengths from 650 to 970 nm using a broadband tungsten light source and liquid crystal tunable filter. Three groups of rats were given three categories of burn injuries (superficial, partial-thickness, and full thickness) according to a controlled burn protocol. Imaging and biopsy were conducted before and after burn injury, then on days 2, 3, and 7. Over the course of the one week healing period, we were able to map quantitative changes in spatially resolved tissue oxygen saturation, oxy/deoxy hemoglobin concentration, and reduced scattering coefficient. Overall, the results of this study suggest that SFDI can provide a quantitative means for tracking burn related tissue changes in a pre-clinical animal model.

8565-29, Session 7

Development of a wide-field fluorescence imaging system for evaluation of wound re-epithelialization

Walfre Franco, Enoch Gutierrez-Herrera, Martin Purschke, Ying Wang, Joshua Tam, R. Rox Anderson M.D., Apostolos G. Doukas, Massachusetts General Hospital (United States)

Normal skin barrier function depends on having a viable epidermis, an epithelial layer formed by keratinocytes. The transparent epidermis, which is less than a 100 mum thick, is nearly impossible to see. Thus, the clinical evaluation of re-epithelialization is difficult, which hinders selecting appropriate therapy for promoting wound healing. An imaging system was developed to evaluate epithelialization by detecting endogenous fluorescence emissions of cellular proliferation over a 10 mm x 10 mm field of view. A custom-made 295 nm ultraviolet (UV) light source was used for excitation. Detection was done by integrating a near-UV camera with sensitivity down to 300 nm, a 12 mm quartz lens with iris and focus lock for the UV regime, and a fluorescence bandpass filter with 340 nm center wavelength. To demonstrate that changes in fluorescence are related to cellular processes, the epithelialization of skin substitute constructs was monitored in vitro. Skin substitute constructs were made by embedding microscopic live porcine skin tissue columns, 700 mum in diameter and spaced 1 mm apart, in acellular porcine dermis. Surface images after embedding show circular profiles of the microscopic skin columns clearly defined by the UV signals. Images on a weekly basis show the extent of radial surface proliferation of keratinocytes and, eventually, full surface coverage. Functional validation of UV images was done by comparison to histology at the same time points. A simple, user-friendly way of imaging the presence of skin epithelium would improve wound care in civilian burns, ulcers and surgeries.

8565-30, Session 7

A novel spectral imaging system for quantitative analysis of hypertrophic scar

Pejhman Ghassemi, The Catholic Univ. of America (United States); Jeffrey W. Shupp M.D., Lauren T. Moffatt, Washington Hospital Ctr. (United States) and MedStar Health Research Institute (United States); Jessica C. Ramella-Roman, The Catholic Univ. of America (United States)

Scarring can lead to significant cosmetic, psychosocial, and functional consequences in patients with hypertrophic scars from burn injuries. Therefore, quantitative assessment of scar is needed in clinical diagnosis and treatment. The Vancouver Scar Scale (VSS), the accepted clinical scar assessment tool, was introduced in the nineties and relies only on the physician subjective evaluation of skin pliability, height, vascularity, and pigmentation. To date, no entirely objective method has been available for scar assessment yet there is a continued need for better techniques to monitor patients with scars. We introduce a new spectral imaging system combining out-of-plane Stokes polarimetry, Spatial Frequency Domain Imaging (SFDI), and three-dimensional (3D) reconstruction. The main idea behind this system is to estimate hemoglobin and melanin contents of scar using SFDI technique, roughness features with Stokes polarimetry, and height and general shape with 3D reconstruction. Our proposed tool has several advantages compared to current methodologies. First and foremost, it is non-contact and non-invasive and thus can be used at any stage in a wound healing without causing harm to the patient. Secondarily, the height, pigmentation, and hemoglobin assessments are co-registered and are based on imaging and not point measurement, allowing for more meaningful interpretation of the data. Finally, the algorithms used in the data analysis are physics based which will be very beneficial in the standardization of the technique. A swine model has also been developed for hypertrophic scarring and an ongoing pre-clinical evaluation of the technique is being conducted.

8565-17, Session PSun

Fiber 1.56-1.9 µm lasers in treatment of vascular malformations in children and adults

Ivan A. Abushkin, Valeriy A. Privalov, Chelyabinsk State Medical Academy (Russian Federation); Alexander V. Lappa, Chelyabinsk State Univ. (Russian Federation); Vladimir P. Minaev, IRE-Polus Co. (Russian Federation)

Our many years' experience (Proc. SPIE 7883, 78830H, 2011) of successful treatment of hemangiomas with NIR diode lasers (920-1060 nm) allowed us to take attempts to apply the experience to treatment other vascular pathologies: malformations. But the used lasers failed in these applications. Analysis of the failure reasons led us to fiber lasers of 1.5-2 µm wavelength.

Four new low invasive technologies with using these lasers were developed for treatment of:

- capillary malformations (port-wine stains),
- venous and venous-arterial malformations,
- micro and small cystic lymphangiomas,
- large cystic lymphangiomas.

1st technology is based on distant blood photocoagulation with the help of 1.56 µm fiber laser (for anatomically complicated parts of strains) and high intensive light (IPL) (for simple large areas). About 150 patients (children - 87%) were treated, good cosmetic effect have been achieved in 95% cases.

2nd technology uses endovascular blood photocoagulation with 1.56 µm laser or that in combination with 1.9 µm laser excision. More than 100 patients (children - 50%) with venous malformations and 5 children with venous-arterial ones were treated; excelent and good results have been achieved in all cases.

3rd technology uses laser actions of 2 types: distant ablation and interstitial thermotherapy with 1.9 µm laser. 6 children were treated, all with good result.

4th technology uses endocystic ablation and excision with 1.9 µm laser. 3 newborns with very extensive large cystic lymphangiomas were treated. Results are good.

8565-31, Session PSun

Treatment of toe nail fungus infection using an AO Q-switched eye-safe erbium glass laser at 1534 nm

Michael J. Myers, Jeffrey A. Myers, Baoping Guo, Christopher R. Hardy, Sean Myers, Angelo Carrabba, Kigre, Inc. (United States); Carmen Trywick, May River Dermatology, LLC (United States); Stewart Bryant, Clemson Univ. (United States); John Robert Griswold, Ave Maria Univ. (United States); Aggie Mazzochi,

Beauty & the Beach (United States); Franziska Roth, Kigre, Inc. (United States)

We report on “eye-safe” erbium glass laser operating at Short-Wave Infra-Red (SWIR) region at 1534nm, to treat Onychomycosis or toenail fungus. Infected toenails of 12 patients were treated over a 3 month period using both long pulse and Q-switched laser output pulses. Our results compared favorably to Neodymium Yittrium Aluminum Garnet (Nd:YAG) laser fungus treatment studies as reported in literature. Nd:YAG laser devices, operating in the Near Infra-Red, (NIR) region at 1064nm, have recently become an effective alternative treatment to traditional oral medications used to treat nail fungal infections. Conventional nail infection treatments employ medications such as allylamines, azoles and other classes of antifungal drugs that are unpopular due to numerous side-affects and drug interactions. Side-effects of these drugs include headache, itching, loss of sense of taste, nausea, diarrhea, heart failure and even potential death from liver failure. The effectiveness of conventional oral antifungal medications varies. In addition, antifungal prescription drugs are administered for long periods ranging from 6 weeks to 18 months. Nd:YAG antifungal laser treatment reports claim high success rates (65-95%) in eradicating toenail fungus and without adverse side-affects. Multiple laser treatments are administered over a 3 to 6 month period. Our initial treatments performed with the Er:glass laser on toenail fungus patients required only 1 to 2 treatments for cure. This same SWIR laser was used in experiments to treat Athlete’s Foot fungal infections. The 1534nm Er:glass laser emission has been found to be well optimized for dermatological treatments due high transmission properties of human skin in the SWIR region. Increased depth of tissue penetration is well-tolerated and provides for effective treatment of various skin conditions. “Eye-safe” Class I lasers provide for practical skin and nail tissue treatment without the need for eye-protection goggles. Laser safety filters may inhibit a practitioner’s vision and ability to distinguish skin and nail regions exhibiting different colors and textures. The laser is “eye-safe” due to the fact that Megawatt peak power Q-switched lasers operating at 1.54um in the narrow spectral window between 1.4um and 1.6um are approximately 8000 times more eye-safe than other laser devices operating in the visible and near infrared. Long-pulse or free running lasers operating in this wavelength range are ~ 2000 times more eye-safe.

8565-32, Session PSun

Phenylalanine gas phase and solvated models applied to skin NMF simulation by DFT calculations

Bruna G. Carvalho, Leandro Raniero, Airton A. Martin, Priscila P. Favero, Univ. do Vale do Paraíba (Brazil)

The L-phenylalanine is an essential amino acid to the organism. It is the precursor of tyrosine molecule participating in the synthesis of melanin. In the skin, it is one of the amino acids which compose the Natural Moisturizing Factor (NMF) that is responsible for the hydration of the skin. Thus, in medicine, the phenylalanine plays a relevant role when applied in topical and systemic therapy against diseases such as vitiligo. Based on this motivation, we present electronic proprieties analysis. We calculate the electronic density of state spectra, charge density plot for HOMO and LUMO states and energies of the systems. The data were obtained using the Vienna Ab-initio Simulation Package (VASP) program that is based on the density of functional theory (DFT). The molecule was modeled in vacuum and water, in nonionic and zwitterionic forms, this evaluation shows characteristics as hydrophilicity and hydrophobicity. In order to understand the environment dependence, the models were made with ammonia and urea which are molecules found in the NMF of the stratum corneum of the skin. Our data were validated with the calculation of the vibrational modes and the errors calculation between theoretical and experimental data obtained by FT-IR and Raman spectroscopy. The results show that the vibrational modes can be calculated with a difference between experiment and theory lower than 3% for any model. However electronic properties, like charge density, depend on the adopted model and environment. In the case of optical or electronic evaluation the most complete model (solvated) is the recommended.

8565-33, Session PSun

Discriminating model for skin cancer diagnosis in vivo through Raman spectroscopy

Fabrício L. Silveira, Univ. Camilo Castelo Branco (Brazil); Landulfo Silveira Jr., Camilo Castelo Branco Univ. (Brazil); Benito Bodanese M.D., Univ. Comunitária da Região de Chapecó (Brazil); Renato A. Zângaro M.D., Marcos T. T. Pacheco, Univ. Camilo Castelo Branco (Brazil)

The incidence and mortality rates of skin cancer have increased dramatically over the last decade in Brazil, mainly due to prolonged exposure of workers/farmers in the countryside to solar radiation, and general population in leisure time (especially beaches). The early diagnosis of precancerous and cancerous lesions through non-invasive diagnostic techniques such as Raman spectroscopy can help to reduce this incidence. The objective of this work is to develop a discriminating model, using near-infrared Raman spectroscopy, based on the estimated concentration of selected biochemical components presented in skin tissues, in order to discriminate normal and benign skin lesions from malignant tissues in vivo. Raman spectra were collected in patients who underwent excision surgery of suspicious lesions at the lesion site and at a normal circumjacent site, right before tissue withdrawn. A spectral model was developed in order to estimate the relative amount of selected biochemical compounds presented in skin, such as actin, collagen, elastin, nucleic acids, triolein, phenylalanine, ceramide and melanin, using least squares fitting. This amount was used to discriminate tissues according to the pathological condition. The results showed that the Raman spectra of normal skin, benign and malignant lesions have differences in the spectral regions of proteins and lipids (800-1000, 1200-1350 and 1450-1670 cm-1), indicating different biochemical constitution. The spectral model showed changes in the relative amount of the basal constituents, such as reduction in collagen and increase in actin and triolein for normal, benign and malignant tissues, which could be used to discriminate these tissues in vivo.

8565-34, Session 1

Optical diagnosis of painful bladder syndrome/interstitial cystitis

Babak Shadgan M.D., Andrew J. Macnab M.D., Lynn Stothers M.D., The Univ. of British Columbia (Canada)

Painful bladder syndrome/interstitial cystitis (PBS/IC) is defined as a syndrome of urgency, frequency, and suprapubic pain in the absence of positive urine culture or obvious bladder pathology. As no specific etiology has been identified yet, no specific methodology exists for diagnosis of this condition. One potential etiology of PBS/IC is bladder mucosa inflammation associated with abnormal angiogenesis and ulcerative lesions in bladder mucosa. A method capable of evaluating bladder wall metabolism may therefore be relevant for diagnosis of PBS/IC. Near infrared spectroscopy (NIRS) is a noninvasive optical technique using light to monitor tissue oxygenation and hemodynamics. The purpose of this study was to examine ability of NIRS to differentiate subjects identified as PBS/IC from other marked bladder conditions.

Twenty four adult patients with lower urinary tract dysfunction were divided into two groups, PBS/IC (4 male) and non-PBS/IC (8 male and 12) after standard diagnostic investigations. Detrusor oxygen saturation percentage (TSI%), were studied in all subjects using a spatially-resolved (SR) NIRS instrument, simultaneous to UDS study. After one minute baseline measurement in rest position, the detrusor TSI% was recorded by the NIRS instrument that was placed over the bladder. Statistical difference of the detrusor TSI% values between two groups were studied.

Mean resting values of detrusor TSI% were significantly different ($P<0.0005$) between two groups (74.2%±4.9 in PBS/IC vs. 63.6%±5.5 in non-PBS/IC).

Noninvasive NIRS interrogation of the bladder demonstrated significant increase in detrusor oxygen saturation in patients diagnosed as PBS/IC. This study presents potential application of SR-NIRS for noninvasive diagnosis of PBS/IC.

8565-35, Session 1

Using OCT to predict post-transplant renal function

Peter M. Andrews, Georgetown Univ. Medical Ctr. (United States); Yu Chen, Jeremiah Wierwille, Univ. of Maryland, College Park (United States); Danial Joh, Peter Alexandrov, Derek Rogalsky, Patrick Moody, Georgetown Univ. Medical Ctr. (United States); Wei Gong, Univ. of Maryland, Baltimore (United States) and Fujian Normal Univ. (China); Hsing-Wen Wang, Univ. of Maryland, Baltimore (United States)

The treatment of choice for patients with end-stage renal disease is kidney transplantation. However, there are not enough healthy kidneys available to meet this growing need. Acute tubular necrosis (ATN) induced by an ischemic insult (from prolonged ex vivo storage times or non-heart beating cadavers) is a major factor limiting the availability of donor kidneys. In addition, ischemic induced ATN is a significant risk factor for eventual graft survival and can be difficult to discern from rejection. Currently, there are no rapid and reliable tests to determine ATN suffered by donor kidneys and whether or not donor kidneys might exhibit delayed graft function. OCT (optical coherence tomography) is a rapidly emerging imaging modality that can function as a type of “optical biopsy”, providing cross-sectional images of tissue morphology in situ and in real-time. In recent pilot clinical trials, we found that OCT imaging of human donor kidneys both prior to and following their transplantation will provide data that allows the clinician to better predict the extent of ATN. In donor kidneys studied thus far, when the proximal convoluted tubules exhibit fully open lumens (i.e., tubule lining cells are not swollen), the kidneys functioned immediately and post-transplant serum creatinine levels rapidly returned to normal. However, when the proximal tubules lumens remain obscure or closed (i.e., due to swollen/damaged lining cells), the patients exhibited delayed renal function as indicated by a prolonged elevation of post-transplant serum creatinine levels. These findings suggest that OCT may be a valuable methodology to help access the status of the donor kidneys and predict post-transplant renal function.

8565-36, Session 1

ex vivo OCT study on encrustation of urologic double pigtail catheters

Ronald Sroka, Michaela Puels, Laser-Forschungslabor (Germany); Herbert Stepp, Katja Zilinberg, Markus Bader, Patrick Weidlich, Ludwig-Maximilians-Univ. München (Germany)

Introduction: Ureteric stenting is a commonly used endourologic procedure for temporary and long-term drainage of an obstructed upper urinary tract. The indication for ureteric stenting is obstruction due to intrinsic (intraureteral stones, strictures, or tumors) or extrinsic (for example compressing pelvic or retroperitoneal mass) causes. Despite the fact that stents do certainly have proven benefits in all fields of urology, there are potential morbidities. The most common problem of indwelling ureteral stents is infection. As foreign body in the urinary system, stents act as a nidus for bacteria colonization, crystallization and encrustation. Bacteria induced biofilm formation predisposes for the crystallization of lithogenic salts, such as calcium-phosphate, calcium-oxalate, magnesium-phosphate on the surface initiating stent encrustation. It was the objective of this study to evaluate whether optical coherence tomography (OCT) using both the surface and the endoluminal technique is feasible to investigate the locations and degree of encrustation process in clinically used ureteral stents.

Patients and methods: After removal from patients, fourteen polyurethane JJ stents were investigated. A fresh JJ served as a control. The external surfaces were examined using an endoscopic surface OCT whereas the intraluminal surfaces were investigated by an endoluminal radial OCT device. The focus was on detection of encrustation or crystalline sedimentation.

Results: In 12 female and 2 male patients, the median indwelling time of the ureteral catheter was 100 days (range 19-217). Using the endoluminal OCT, the size and grade of intraluminal encrustation could be expressed as a percentage relating to the open lumen of the reference stent. The maximum encrustation observed resulted in a remaining unrestricted lumen of 15-35% compared to the reference. The luminal reduction caused by encrustation was significantly higher at the proximal end of the ureteral stent as compared to its distal part. The extraluminal OCT-investigations facilitated the characterization of extraluminal encrustation.

Conclusion: OCT techniques were feasible and facilitated the detection of encrustation of double pigtail catheters on both the extra and intra luminal surface. Quantitative expression of the degree of intraluminal encrustation could be achieved, with the most dense and thickened occurrence of intraluminal incrustation in the upper curl of the JJ stent.

8565-37, Session 1

Full-field OCT can distinguish tumor from benign in human kidney and bladder tissue and assess kidney fibrosis in a rat model

Jonathan Caron, INSERM (France) and Univ. Paris VI (France); Sushmita Mukherjee, Manu Jain, Bekheit Salomoon, Maria M. Shevchuk, Douglas S. Scherr, Weill Cornell Medical College (United States); Isabelle Brocheriou, Hôpital Tenon (France); Jean-Jacques Boffa, INSERM (France) and Univ. Paris VI (France) and Hôpital Tenon (France); Katharine Grieve, Institut Langevin (France); Fabrice Harms, Bertrand Le Conte de Poly, LLTECH SAS (France); Albert C. Boccara, Institut Langevin (France) and LLTECH SAS (France)

Full-Field Optical Coherence Tomography (FF-OCT) is an alternative approach to Fourier-domain OCT, allowing parallel acquisition of en-face optical sections. Using medium numerical aperture objectives, isotropic resolution of approximately 1x1x1 µm is achieved.

In this study, FF-OCT was used to image human kidney and bladder, consisting of both benign and malignant specimens. Additionally, in rat kidney, a quantitative assessment of the state of fibrosis of the tissue was possible.

In benign bladder specimens, all normal tissue components such as urothelial cells, connective tissue and muscle bundles were readily identified. In tumor-free kidney, renal tubules, glomeruli, vasculature and interstitial tissue were clearly recognized. Features of the injured kidney such as sclerotic glomeruli and interstitial fibrosis defined as increased collagen fiber density were clearly visible. In bladder tumors, we could differentiate flat from papillary lesions. Furthermore, increased nuclear-cytoplasmic (N:C) ratio was seen in high-grade tumors. In kidney tumors, we saw a complete loss of normal architecture, associated with increased cellularity. At this time, we cannot confidently distinguish cellular clusters as inflammatory versus malignant.

In the rat model of hypertensive nephropathy, we present images in control, early fibrosis and advanced fibrosis states, and report on a quantitative method to assess renal fibrosis. Our preliminary results show that FF-OCT is a valuable method to rapidly assess sclerotic glomeruli in depth of fresh kidney tissue. The sum of serial images allows highlighting of peritubular capillaries which are not visible on histological analysis. We believe that FF-OCT could have clinical applications in fibrosis assessment in various tissues.

8565-38, Session 2

in vivo photoacoustic imaging of urinary bladders with dye-enhanced carbon nanotubes

Jasung Koo, Hyun Wook Kang, Pukyong National Univ. (Korea, Republic of); Jeehyun Kim, Kyungpook National Univ. (Korea, Republic of); Chulhong Kim, Univ. at Buffalo (United States); Junghwan Oh, Pukyong National Univ. (Korea, Republic of)

Photoacoustic tomography (PAT) is a nonionizing and noninvasive imaging technique with high ultrasonic resolution and functional information. Visualizing bladders (cystography) is a key procedure for diagnosing bladder-related diseases such as bladder cancer. However, the organ is clinically imaged by harmful ionizing imaging tools that induce significant damage on connective tissues. The purpose of the study was to demonstrate the feasibility of mapping a urinary bladder in small animals by using modified single-walled carbon nanotubes (SWNTs) as a nonionizing photoacoustic (PA) contrast agent. To improve the PA sensitivity of the SWNTs, indocyanine green (ICG) was conjugated to SWNTs and the optical absorption of SWNTs-ICG was enhanced by ~4 times compared to that of plain SWNTs at the concentration of 0.3 ?M. In vivo PA imaging results showed that the bladder was clearly visualized due to accumulation of SWNTs-ICG. A clinical PAT system with higher sensitivity may be able to use relatively low concentration of SWNTs-ICT with sub-nM sensitivity and sub-mm spatial resolution. The current results demonstrated that SWNTs-ICG could be potentially utilized to track vesicoureteral reflux (VUR) in combination with PA imaging due to its high optical contrast and good ultrasonic resolution without any ionizing radiation and invasiveness.

8565-39, Session 2

Subsurface optical stimulation of the rat prostate cavernous nerves using a 1490-nm diode laser

Serhat Tozburun, Charlotte D. Stahl, Thomas C. Hutchens, The Univ. of North Carolina at Charlotte (United States); Gwen A. Lagoda, Arthur L. Burnett M.D., Johns Hopkins Medical Institutions (United States); Nathaniel M. Fried, The Univ. of North Carolina at Charlotte (United States)

Introduction: Successful identification and preservation of the cavernous nerves (CN's), which are responsible for sexual function, during prostate cancer surgery, requires detecting CN's through a thin layer of overlying fascia. Subsurface optical nerve stimulation (ONS) of CN's has been previously reported in a rat model in which fascia is placed over CN's, using 1455 and 1550 nm infrared lasers. This study explores an alternative intermediate wavelength laser at 1490 nm, which combines advantages of both 1455 and 1550 nm lasers.

Methods: A 150-mW, single-mode, narrow linewidth, 1490-nm diode laser was used to stimulate the CN in continuous-wave mode in 8 rats through a fiber optic probe with 1-mm-diameter spot. This wavelength provides an optical penetration depth of ~520 micrometers, sufficient to penetrate typical thicknesses of both fascia and nerve for successful stimulation. ONS was measured by an intracavernous pressure response (ICP) in the rat penis.

Results: ONS was observed at 1490 nm through fascia layers up to 380 micrometers using a minimum incident laser power of ~53 mW. ICP response times averaged 10.4 + 1.8 s near the stimulation threshold and 4.6 + 0.2 s using higher laser powers (~75 mW) just below the thermal damage threshold. ICP signal-to-noise ratios of 3:2 were recorded.

Conclusions: The 1490-nm laser is capable of stimulating the CN at 2-3 times depth of 1455-nm laser, and it is also a lower cost, higher power, and higher quality laser alternative to the 1550-nm laser, for easy integration into a compact and inexpensive all-single-mode-fiber ONS system.

8565-40, Session 2

Temperature-controlled optical stimulation of the rat prostate cavernous nerves

Serhat Tozburun, The Univ. of North Carolina at Charlotte (United States); Gwen A. Lagoda, Johns Hopkins Medical Institutions (United States); Michael A. McLain, The Univ. of North Carolina at Charlotte (United States); Arthur L. Burnett M.D., Johns Hopkins Medical Institutions (United States); Nathaniel M. Fried, The Univ. of North Carolina at Charlotte (United States)

Introduction: Optical nerve stimulation (ONS) may be useful for intra-operative identification and preservation of the prostate cavernous nerves (CN's), responsible for erectile function, during prostate cancer surgery. ONS relies on a photothermal mechanism of laser-tissue interaction in which elevating nerve temperature to within a narrow range (~ 42-45 C) is critical to successful nerve activation without thermal damage. Closed-feedback loops utilizing an infrared (IR) sensor for real-time control of tissue surface temperatures during laser therapy have previously been reported (e.g. for laser tissue welding/soldering). This preliminary study explores a prototype temperature-controlled laser system for maintaining

a constant nerve temperature during short-term ONS of the rat prostate CN's.

Methods: A 150-mW, 1455-nm diode laser was operated in continuous-wave mode during stimulation of the rat CN's for 30 s through a fiber optic probe with 1-mm-diameter spot. The all-single-mode ONS system was controlled by a computer which opened and closed an in-line mechanical shutter in response to an IR sensor, with a temperature set-point of 45 C. Thermal camera temperature measurements and ONS without temperature control were performed for comparison.

Results: Strong correlation was observed between IR sensor and camera temperatures. With temperature control, CN temperature was maintained at 45.0 +/- 1.5 C. Without IR sensor feedback, CN temperatures continued to rise during ONS, reaching unsafe levels of ~50 C.

Conclusions: With further development, temperature-controlled ONS may provide a rapid, stable, and safe method for stimulation of the prostate cavernous nerves.

8565-41, Session 2

A new optical method enables fluorescence guided diagnosis of bladder tumours in the outpatient department and reveals significant photo bleaching problems in established inpatients photo dynamic diagnostics (PDD) techniques.

Lars R. Lindvold, Risø National Lab. (Denmark); Gregers G. Hermann, Frederiksberg Hospital (Denmark)

Photo dynamic diagnosis (PDD) is a convenient and well-documented procedure for diagnosis of bladder cancer and tumours using endoscopic techniques. At present, this procedure is available only for use in an operating room (OR) and often with substantial photobleaching effects of the photosensitizer.

We present a novel optical design of the endoscopic PDD procedure that allows the procedure to be performed in the outpatient department (OPD) and not only in the OR. Thereby, inpatient procedures lasting 1-2 days may be replaced by a few hours lasting procedure in the OPD.

Urine blurs the fluorescence during PDD used in the OPD. Urine contains fluorescent metabolites that are excited by blue light giving an opaque green fluorescence confounding the desired red fluorescence (PDD) from the tumour tissue.

Measurements from the clinical situation has shown that some systems for PPD based on blue light illumination (PDD mode) and white light illumination used for bladder tumour diagnosis and surgery suffers some inherent disadvantages, i.e., photo bleaching in white light that impairs the possibility for PDD as white light usually is used before the blue light for PDD.

Based on spectroscopic observations of urine and the photoactive dye Protoporphyrin IX used in PDD, a novel optical system for use with the cystoscope has been devised that solves the problem of green fluorescence from urine. This and the knowledge of photo-bleaching pitfalls in established systems make it possible to perform PDD of bladder tumours in the OPD and to improve PDD in the OR.

8565-42, Session 3

Fiber optic suctioning of urinary stone phantoms during laser lithotripsy

Richard L. Blackmon, The Univ. of North Carolina at Charlotte (United States); Jason Case, Susan Trammell, Univ of North Carolina at Charlotte (United States); Pierce B. Irby M.D., Carolinas Medical Ctr. (United States); Nathaniel M. Fried, The Univ. of North Carolina at Charlotte (United States)

Introduction: Fiber optic attraction of urinary stones during laser lithotripsy may be exploited to pull stone fragments inside the urinary tract without insertion of mechanical grasping tools, thus saving the urologist time and space in the working channel of the ureteroscope. In this study, we compare the experimental Thulium fiber laser (TFL) high pulse rate/low pulse energy operation to conventional Holmium:YAG low pulse rate/high pulse energy operation for fiber optic suctioning and manipulation of stone phantoms.

Methods: A TFL with wavelength of 1908 nm, pulse energy of 35 mJ, pulse duration of 500 microseconds, and pulse rate of 10-350 Hz, and Holmium laser with wavelength of 2120 nm, pulse energy of 35-350 mJ, pulse duration of 300 microseconds, and pulse rate of 20 Hz were tested, using 270-micrometer-core fibers. Plaster-of-Paris, 4-mm-diameter, stone phantoms were used. Stone drag speed was calculated by video recording distance moved per unit time. Five samples were averaged for each laser parameter set.

Results: A peak drag speed of ~2.5 mm/s was measured for both TFL at 35 mJ and 150-250 Hz and Holmium laser at 210 mJ and 20 Hz. However, TFL provided more stable manipulation over larger range of laser parameters.

Conclusions: Fiber optic "suctioning" of urinary stone phantoms is feasible. TFL operation at high pulse rates/low pulse energies is superior to Holmium operation at low pulse rates/high pulse energies for rapid and stable stone pulling. With further development, this technique may be useful for manipulation of stone fragments inside the urinary tract.

8565-43, Session 3

Dependence of laser-induced bubble collapse shockwave and fluence during Q-switched Tm:YAG laser lithotripsy

Danop Rajabhandharaks, Jian J. Zhang, Hui Wang, Jason R. Xuan, Ray Chia, Thomas Hasenberg, American Medical Systems (United States); Hyun Wook Kang, Pukyong National Univ. (Korea, Republic of)

Q-switched Tm:YAG laser ablation mechanisms on urinary calculi are still unclear to researchers. In this study, two parameters that may affect calculus ablation performance were investigated: laser-induced bubble collapse shockwave and laser fluence. For the effect of laser-induced bubble collapse shockwave study, calculus phantoms (Plaster of Paris) were ablated at single pulse and contact mode in air and in water. Ablation volume was obtained 0.006 mm3 and 0.008 mm3 in air and water group, respectively. High-speed photography showed formation of half-spherical bubble in contact mode with associated minimal collapse shockwave pressure, captured by a hydrophone. When a phantom was placed 1 mm away from the fiber tip to allow construction of full-spherical bubble, calculus ablation was very minimal and negligible compared with that obtained from the contact mode. Bubble collapse shockwave may not be the primary mechanism for calculus ablation during Q-switched Tm:YAG laser lithotripsy. Water surrounding calculus and fiber can help cool down the fiber tip to avoid catastrophic melting of the fiber and can help soften the calculus phantom to reduce the damage threshold. However, it may not significantly enhance calculus ablation volume. For dependence of fluence on calculus ablation study, calculus phantoms were ablated at single pulse and in contact mode with various pulse energies and fiber core sizes. Ablation was initiated at 12 J/cm2 (threshold) and became saturated after 28 J/cm2. The efficacy of using Q-switched Tm:YAG laser for urinary calculus lithotripsy is still under investigation and more feasibility experiments will be conducted in the future.

8565-44, Session 3

Comparison of detachable and tapered fiber optic tips for use in thulium fiber laser lithotripsy

Thomas C. Hutchens, Richard L. Blackmon, The Univ. of North Carolina at Charlotte (United States); Pierce B. Irby M.D., Carolinas Medical Ctr. (United States); Nathaniel M. Fried, Univ. of North Carolina at Charlotte (United States)

Introduction: The single-mode Thulium fiber laser (TFL) beam profile has previously been shown to allow coupling of higher power laser radiation into smaller fibers than the conventional multimode Holmium laser beam profile without proximal fiber tip degradation. This is significant because larger, more rigid optical fibers inserted into the working channel of a flexible ureteroscope may hinder ureteroscope deflection and prevent easy access to the upper urinary tract during lithotripsy. Furthermore, Holmium laser lithotripsy is typically performed with expensive, single-use optical fibers due to fiber tip degradation and sterilization issues. In this study, we propose use of inexpensive, detachable, and disposable large-core-diameter fiber tips in combination with a flexible, small-core "trunk" fiber.

Methods: A TFL with wavelength of 1908 nm, pulse energy of 40 mJ, pulse duration of 500 microseconds, and pulse rate of 100 Hz was used. A disposable, spring-loaded, twist-lock, 300-micrometer-core silica fiber optic tip was manually inserted and self-aligned with a 150-micrometer-core, 1-m-long trunk silica fiber. Fiber optic transmission tests and ex vivo stone ablation studies were performed using human urinary stone samples.

Results: The fiber optic system provided a transmission rate of ~77%. Human calcium oxalate monohydrate stones were ablated without damage to the trunk/tip interface, and the fiber probe delivered greater than 30,000 pulses without distal fiber tip degradation.

Conclusion: A novel fiber optic design incorporating an inexpensive, detachable, and disposable fiber optic tip was successfully tested. Future work will involve further miniaturization of the fiber optic design for potential integration into a flexible ureteroscope.

8565-45, Session 3

Laser lithotripsy retropulsion varies with stone mass

Joel M. Teichman M.D., St. Paul's Hospital (Canada); Michael E. Robinson, The Univ. of British Columbia (Canada)

INTRODUCTION AND OBJECTIVES: The Ho:YAG laser fragments stones by a photothermal mechanism. As fragment debris is ejected off the stone surface, it exerts a force in the opposite direction producing retropulsion. As pulse energy is increased, ablation crater volumes and retropulsion both increase. A recent study using 6 mm stone phantoms showed an overall benefit using low pulse energy at high pulse frequency. However, retropulsion has not been characterized for larger stones. We hypothesize that retropulsion would be minimal if treating a large bladder or renal calculus even at high pulse energy.

MATERIALS AND METHODS: Stone phantoms were constructed to uniform cube sizes of 0.5 cm to 2.0 cm. Stones were positioned in a cylindrical tube in a water bath, and irradiated with a 365 um fiber using Ho:YAG pulse energies 0.5 to 3.5 J to a constant total energy applied. Displacement was measured. Analysis of variance was used for statistics.

RESULTS: At any given pulse energy, retropulsion decreased as stone size increased, $p<0.05$. At high pulse energy (3.5 J), median retropulsion was 18 mm, 11 mm, 3 mm, 1 mm, and 0 mm for stones 0.5 cm, 1.0 cm, 1.5 cm, 2.0 cm, and 2.5 cm, respectively, $p<0.01$.

CONCLUSIONS: For most ureteral stones, low pulse energy at high frequency delivers efficient fragmentation, low retropulsion, and small fragments. For large bladder and renal stones, high pulse energy may be more efficient as retropulsion is minimal. The results are consistent with Newtonian mechanics. More study is warranted.

8565-46, Session 3

in vitro assessment of fragmentation and repulsion of handheld lithotripsy devices

Ronald Sroka, Thomas Pongratz, Giovanni Crameri, Laser-Forschungslabor (Germany); Nicolas Haseke, Univ. Hospital Munich (Germany); Markus Bader, Ludwig-Maximilians-Univ. München (Germany)

Introduction: Different laser-systems are currently used for stone fragmentation in the upper urinary tract. The aim of our study was to evaluate probe velocity and displacement, retropulsion and fragmentation characteristics two novel devices the electromechanically driven EMS LithoBreaker® (EMS Medical), and of the CO2 cartridge driven LMA StoneBreaker® (Cook Urological) in vitro test models.Testing of the LithoBreaker® included additionally two different probe guides (harder, softer) to assess the effect of the damper properties on the impulse characteristics.

Patients and methods: Maximum probe velocities and displacements were measured using high-speed photography at a resolution of 100.000 frames per second. Repulsion testing was conducted through a 7.5 Fr ureteroscope in an underwater set-up. The probes were projected against a non-frangible led mass placed in a 15 Fr horizontally mounted silicone tube as an in-vitro model of the ureter. Repulsion was determined by measuring the distance the lead mass (0.98g) was displaced. Fragmentation efficiency was assessed by measuring the number of single shots required to break Bego Stone phantoms hard (15:3) and soft (15:6) with an average size of 7.5 mm x 5.5 mm placed on a metal mesh (edge length 3.15mm) into < 3 mm fragments. Mean and standard deviation were computed for all groups and statistical analysis was performed (student's t-test).

Results: The StoneBreaker® yielded the highest velocity of 22.0 ± 1.9 m/sec. followed by the LithoBreaker® assembled with the hard probe guide of 14.2 ± 0.5 m/sec and the soft probe guide of 11.5 ±0.5 m/sec. accordingly. The maximum probe displacement for the StoneBreaker® was 1.04 mm and for the LithoBreaker® 0.9 mm and 1.1 mm (hard versus soft probe guide). Retropulsion produced using the 1mm probes showed no statistical differences between the devices. Using the 2mm probes, the hardness of the damper used significantly changed the repulsion behaviour of the LithoBreaker®. Using the 1mm probe, the amount of single shots for fragmentation of soft Bego Stones was significantly higher for the LithoBreaker® with soft probe guide: mean 31.5 ± 11.31 and hard probe guide: mean 21.5 ± 5.29 compared to the StoneBreaker®: mean 11.2 ± 2.65. Fragmentation efficiency for the hard Bego Stones showed similar statistically significant results.

Conclusion: The electromechanic LithoBreaker® and the pneumatic Stonebreaker® were shown to be effective in cracking stone phantoms with relatively low number of pulses. Fragmentation characteristics improved substantially with the higher hardness of the probe support higher velocity equals higher fragmentation performance of the LithoBreaker®. Retropulsion produced were at comparable levels. More testing is required to more detailed information on impulse frequency and capacity for stone clearance time to be used in clinical practice.

8565-50, Session P1

Near infrared spectral polarized imaging using Cybesin: a receptor-targeted contrast agent of prostate cancer

Yang Pu, Wubao Wang, Guichen Tang, The City College of New York (United States); Samuel Achilefu, Washington Univ. School of Medicine in St. Louis (United States); Robert R. Alfano, The City College of New York (United States)

Near-infrared (NIR) optical imaging is a powerful tool in cancer research that relies on activating endogenous chromophores and applying smart contrast agents that can target cancer cells. In order to observe

fluorescence from a substantial distance within the body, the emission wavelength must be in the NIR wavelength window in which light passing through tissue is less likely to be absorbed or scattered. Over the past decade, cyanine dyes have been investigated as contrast agents for optical detection of tumors because their emission range is in the tissue "optical window". Indocyanine Green (ICG), the only clinically approved NIR dye by FDA, is one of the most investigated. As a small ICG-derivative dye-peptide, Cybesin, was synthesized and used as a contrast agent to detect the over-express bombesin receptor in pancreas tumors in an animal model a few years ago. It was observed that the bombesin receptors are over-expressed on the membranes of human prostate cancer cells.

In this study, Cybesin was used to target over-expressed bombesin receptors in human prostate cancer tissue. We report on the NIR spectral polarization imaging study using Cybesin as an optical smart contrast agent marker to differentiate human prostate cancerous and normal tissues. The absorption and fluorescence spectra of Cybesin were studied in the wavelength region from 650 nm to 900 nm. The model prostate samples consisting of a small piece of normal prostate tissue and a small piece of prostate cancer tissues stained with Cybesin were imaged. The results indicate that this receptor-targeted Cybesin was preferentially taken up by prostate cancerous tissue compared to prostate normal tissues.

8565-51, Session P1

Magnetic nanoparticles-assisted cellular imaging for cervical cancer: preliminary study

Jasung Koo, Hyun Wook Kang, Pukyong National Univ. (Korea, Republic of); Jeehyun Kim, Kyungpook National Univ. (Korea, Republic of); Junghwan Oh, Pukyong National Univ. (Korea, Republic of)

Optical coherence tomography (OCT) has been applied to detect the movement of magnetic nanoparticles uptaken by cells and tissues under externally high-strength continuous magnetic fields, referred to as magneto-motive OCT (MM-OCT). The current study investigated the feasibility of PMM-OCT to track the mechanical movement of the remote magnetically-labeled cells eventually for early detection of cervical cancer. For non-contact cellular imaging, pulsed magneto-motive optical coherence tomography (PMM-OCT) was developed to reduce environmental temperature in the measurement volume and to expand the effective magnetic field distance from a pulse source. The PMM-OCT system consisted of a spectral-domain OCT system and a customarily-designed electrical pulse generator. Pulsed and sinusoidal modes were compared along with presence and non-presence of an iron core in the generator. Temperature as well as magnetization was quantitatively characterized for each condition in terms of distance and time. Due to the characteristics of pulsed mode and an iron core in the magnetic generator, the magnetic field was enhanced by up to 4 folds (6.5 kG with the core vs. 1.5 kG without the core) without significant temperature increase. M-mode images demonstrated that the system with higher magnetic field was able to image the presence of the magnetically-labeled HeLa cells in a distance as far as 30 mm away from the pulse generator. As an easy, sensitive, and non-contact approach, the proposed PMM-OCT may be beneficially applied to a molecular-level imaging systems for diagnosing cervical cancer.

8565-52, Session P1

Could the differences in the biochemistry of prostate carcinoma compared to benign prostate tissue biopsy fragments be evaluated through Raman spectroscopy?

Landulfo Silveira Jr., Camilo Castelo Branco Univ. (Brazil); Kátia R. M. Leite M.D., Miguel Srougi M.D., Univ. de São Paulo (Brazil); Fabrício L. Silveira, Marcos T. T. Pacheco, Univ. Camilo Castelo Branco (Brazil); Carlos A. Pasqualucci M.D., Univ. de São Paulo (Brazil)

It has been proposed a spectral model to evaluate the biochemical differences between prostate carcinoma and normal biopsy fragments using dispersive Raman spectroscopy, aiming the discrimination of lesions from normal tissues. We have examined 51 prostate fragments from surgically removed PrCa; each fragment of about 3 mm2 was snap-frozen and stored (-80ºC) prior spectral analysis. Raman spectrum was measured using a Raman spectrometer (830 nm excitation) coupled to a fiber-optic probe. Integration time and laser power were set to 50 s and 300 mW, respectively. It has been collected triplicate spectra from each fragment (total 153 spectra). Samples exhibited a strong fluorescence, which was removed by a 7th order polynomial fitting. It has been developed a spectral model based on the least-squares fitting of the spectra of pure biochemicals (actin, collagen, elastin, carotene, glycogen, phosphatidylcholine, hemoglobin, and water) with the spectra of tissues, where the fitting parameters are the relative contribution of the compounds to the tissue spectrum. The spectra (600 - 1800 cm-1 range) are dominated by bands of proteins; it has been found a small difference in the mean spectra of PrCa compared to the normal tissue, mainly in the 1000-1400 cm-1 region, indicating similar biochemical constitution. The spectral model revealed that elastin and phosphatidylcholine were increased in PrCa, whereas blood and water were reduced in malignant lesions ($p < 0.05$). A discrimination of PrCa from normal tissue using Mahalanobis distance applied to the contribution of phosphatidylcholine and hemoglobin resulted in sensitivity of 79% and specificity of 60%.

8565-53, Session P1

in vivo laser ablation study with 150 W diode laser: preclinical study

Malte Rieken, Basel Univ. Hospital (Switzerland); Hyun Wook Kang, Pukyong National Univ. (Korea, Republic of); Ed Koullick, Bayer Healthcare (United States); Alexander Bachmann, Basel Univ. Hospital (Switzerland)

Anatomic, tissue ablation and coagulation, and histopathologic outcomes of the 150-W 980-nm diode laser selective light vaporization (SLV) of the prostate in living canines were analyzed. Ten dogs underwent anterograde SLV with the 150-W 980-nm laser delivered by a side-firing fiber. Postoperatively, two dogs were euthanized at 3 hours as planned, six at 2–7 days due to complications, and two, without complications, at 8 weeks as planned. Laser energy and time were recorded. Prostates were sectioned, measured, and histologically analyzed after hematoxylin and eosin (H&E), triphenyltetrazolium chloride (TTC), or Gomori trichrome (GT) staining. SLV acutely and hemostatically created a 0.6±0.3 cm3 cavity in the 3-hour group accompanied by H&E- and TTC-identified coagulation necrosis of up to 9.5mm (6.1±1.2mm) that led to prostatic slough-induced obstruction and perforation in six of eight (75%) surviving animals, necessitating unplanned euthanasia within 2–7 days. H&E- and GT-stained prostates at 8 weeks postoperatively showed large (9.6±1.4 cm3) re-epithelialized prostatic cavities with persistent diffuse interstitial prostatitis and collagenous fibrosis. SLV with the 150-W 980-nm diode laser in living canines produced small cavities acutely, and was accompanied by deeply necrotic prostatic slough-induced obstruction and perforation in a majority of animals. A minority survived SLV and had favorable anatomic outcomes whereas histology revealed persisting inflammation. Further in vivo studies and a cautious clinical approach are recommended to finally evaluate the potential of SLVTM with the 150-W 980-nm diode laser.

8565-47, Session 4

Shining light on prostate cancer: image guided optical biopsy of the prostate

Daniel M. de Bruin, Berrend G. Muller, Academisch Medisch Ctr. (Netherlands); Arjen Amelink, Erasmus MC (Netherlands); Ton G. van Leeuwen, Jean J. de la Rosette, Dirk J. Faber, Academisch Medisch Ctr. (Netherlands)

Background

Current treatment in prostate cancer aims at systemic or radical procedures, with considerable side effects such as erectile dysfunction and/or incontinence. Small tumors occupying less than 5–10 % of the prostate volume are detected earlier. These tumors tend to have a unifocal or unilateral location. Accurate identification, grading and demarcation of a lesion is paramount for treatment. This is not provided by currently used imaging methodology and biopsy protocols.

Methods

We developed image guided optical biopsy (IGOB), a synergistic application of ultrasound (US) guided optical coherence tomography (OCT) and diffuse reflectance spectroscopy (DRS). IGOB provides tissue related optical properties associated with the location of a lesion. Moreover, tissue alterations occurring during cancer development are detectable in vivo using IGOB and could potentially enable tumor grading. IGOB could reduce the amount of biopsies due to a large measurement volume per biopsy. Each IGOB probe is delivered through a small needle, minimizing damage to the prostate. For this paper, the newly combined methods are first tested on silicon based optical phantoms.

Results

A phantom resembling the optical and US properties of normal prostate tissue and tumorous prostate tissue is fabricated. Co-localized grid based optical absorption and scattering information from a human prostate phantom is extracted from this phantom and correlated to prior knowledge of the phantom geometry. Transversal probe location in the prostate phantom is confirmed with US.

Conclusion

We have shown the potential application of IGOB for the detection of a leasion in the prostate, based on the optical properties.

8565-48, Session 4

Noninvasive imaging of prostate cancer progression in nude mice using iRFP gene reporter

Banghe Zhu, The Univ. of Texas Health Science Ctr. at Houston (United States); Grace Wu, The Univ. of Texas School of Health Information Sciences at Houston (United States); Holly Robinson, Nathaniel Wilganowski, Eva M. Sevick-Muraca, The Univ. of Texas Health Science Ctr. at Houston (United States)

Prostate cancer (PCa) is the second most common cancer in US men. Metastasis is the final step of tumor progression and remains the primary cause of PCa death. Hence preclinical, orthotopic models of PCa metastasis are necessary to develop new therapeutics against metastatic disease. Yet unlike irrelevant subcutaneous tumor models, the deployment of orthotopic models of cancer metastasis in drug research and development is limited by the inability to longitudinally monitor cancer progression/regression in response to administration of experimental pharmaceuticals. Recently, a near-infrared fluorescent protein (iRFP) was created for deeper imaging [1]. Imaging prostate tumor growth and lymph node metastasis in nude mice therefore becomes possible using this new fluorescent gene reporter. In this study, we first developed an intensified CCD (ICCD)-based iRFP fluorescence imaging device. Then human PCa PC3 cell lines expressing iRFP gene reporter were orthotopically implanted in male Nu/Nu mice at 8-10 weeks old. After 8-10 weeks, in vivo, in situ and ex vivo fluorescence imaging was performed. In vivo iRFP fluorescence imaging showed that the detected fluorescence concentrated at the prostate and became stronger over time, indicating the growth of implanted PCa. Fluorescence was non-invasively detected at locations of prostate-draining lymph nodes as early as 5 weeks post implantation, indicating the metastasis to lymph nodes. In situ and ex vivo fluorescence imaging demonstrated that the detected signals from PCa and lymph nodes were correlated with cancer positive status of tissues as assessed through standard pathology. Supported in part by NIH U54 CA136404 and the Wilson Foundation.

[1] Grigory S. Filonov, Kiryl D. Piatkevich, Li-Min Ting, Jinghang Zhang, Kami Kim, and Vladislav V. Verkhusha, “Bright and stable near-infrared fluorescent protein for in vivo imaging”, Nature Biotechnology, 29, 757-761, 2011.

8565-49, Session 4

Influence of tissue treatment onto the Raman spectra obtained from prostate histopathological slides for diagnostics purposes

Sinisa Vukelic, Bucknell Univ. (United States)

In recent years Raman spectroscopy has emerged as a potentially viable tool for automated cancer diagnostics. However, due to the complexity of the signal obtained from a tissue most of the studies have been confined to statistical analysis of the spectra with principal component analysis being most often reported as analysis of choice. These types of analyses are sensitive to modification of the Raman spectra due tissue processing. The study presented here addresses the modifications of the Raman spectra obtained from prostate tissue histopathological slides due to the tissue treatment and its influence on the automated cancer diagnostics via Raman spectroscopy.

8565-54, Session 1

Large field of view OCT-otoscope for diagnosing middle-ear infection

Kibeom Park, Kyungpook National Univ. (Korea, Republic of); Areun Kim, Ulsan National Institute of Science and Technology (Korea, Republic of); Nam Hyun Cho, Jeong Hun Jang, Sang Heun Lee, Kyungpook National Univ. (Korea, Republic of); Stephen A. Boppart, Univ. of Illinois at Urbana-Champaign (United States); Jeehyun Kim, Kyungpook National Univ. (Korea, Republic of); Woonggyu Jung, Ulsan National Institute of Science and Technology (Korea, Republic of)

We have developed a large field of view handheld Optical coherence tomography (OCT)-Otoscope which is able to image surface and cross-sectional structure of tympanic membrane. The handheld OCT-Otoscope utilized 2-axis MEMS scanner, micro optics, miniature CCD-based color video camera for compactness. The distal end of OCT-Otoscope was constructed by modifying the same metal ear tip used in existing commercial otoscopes. This allowed for the use of disposable ear specula for each patient. Since the exit of ear specular restricts the scanning aperture of OCT beam, we employed scanning optics similar to one for retinal OCT imaging in order to enhance the lateral scanning range. Current scanning optics was designed to cover the half of diameter of tympanic membrane (> 4 mm). The OCT-Otoscope was integrated to high speed spectral domain OCT system. Our probe has two different OCT beam scanning modes, single lateral scanning and rotational scanning. In the rotational scanning mode, single lateral scanning beam is rotated as clockwise within assigned the value of angle. Each 2D OCT images acquired by beam rotation were visualized as the cylindrical 3D volume image after post image processing. Data were acquired and processed at 70422 axial scans per second, or an image rate of ?70 frames/s with each image having 1000 axial scans (columns) of data. In order to demonstrate the use and performance of developed handheld OCT-Otoscope, tympanic membrane on human was imaged, which clearly identified the normal tissue morphology.

8565-55, Session 1

Noninvasive in vivo detection of human middle-ear biofilms in otitis media using an OCT-based primary care imaging system

Stephen A. Boppart M.D., Univ. of Illinois at Urbana-Champaign (United States)

Primary Care Medicine, including Family Practice and Pediatrics, has traditionally relied on physical exam skills and simplistic instruments for critical disease screening, diagnostic decision making, monitoring, and referral to medical specialists. The otoscope and ophthalmoscope are two historical and ubiquitous instruments that largely only illuminate and magnify tissue surfaces in the ear and eye, respectively. We have developed a new Primary Care Imaging system integrating optical coherence tomography (OCT) and video imaging with a MEMS-based handheld scanner and portable system to advance the screening, diagnostic, and monitoring capabilities in primary care, and to more effectively manage and refer patients based on quantitative data. One of our initial focus areas is on detecting otitis media and associated bacterial biofilms in the human middle ear. We have completed a 20-patient study involving 13 clinically-infected adult patients and 7 healthy human volunteers. Over 18,537 axial scans and 742 images were collected and analyzed. All middle ears with chronic otitis media showed evidence of biofilms, and all normal ears did not. Ongoing studies are examining differences between chronic and acute otitis media, and between adult and pediatric patients. Information on the presence of a biofilm, along with its structure and response to antibiotic treatment, will not only provide a better fundamental understanding of biofilm formation, growth, and eradication in the middle ear, but also may provide much-needed quantifiable data to enable early detection and quantitative longitudinal treatment monitoring of middle ear biofilms responsible for chronic and recurrent otitis media.

8565-56, Session 1

Monitoring structural vibrations of mouse middle and inner ear by swept-source optical coherence tomography

Jesung Park, Esteban F. Carbajal, Texas A&M Univ. (United States); Simon S. Gao, Patrick Raphael, Anping Xia, John S. Oghalai M.D., Stanford Univ. School of Medicine (United States); Brian E. Applegate, Texas A&M Univ. (United States)

Hearing loss is critical impairment to the quality of life. Clinical diagnosis of hearing loss by visualizing the cellular and tissue damage of ear is currently limited due to the difficulty of access and imaging resolution in the inner and middle ear. An optical device with high resolution using miniature endoscopic technology can be a potential diagnostic tool. We have developed a fiber-based swept source optical coherence tomography (SS-OCT) to characterize vibrational motion of the middle and inner ear in a mouse model with sound stimulus. SS-OCT mainly consists of a commercialized swept source, a pair of galvanometers, balanced detector and fiber-based optical components including circulator, attenuator and optical delay line. The swept source operates with a wavelength of 1310nm, tuning bandwidth of 110nm and sweep rate of 50KHz. For high-speed real-time performance, OCT data was acquired with PXI (PCI Extensions for Instrumentation) and proceeded by Labview based field programmable gate array (FPGA). The SS-OCT system has signal-to-noise ratio of 105dB and fall-off of ~6mm. Vibrational motion was first tested by OCT Alines phase noise from a piezoelectric element, and then analyzed structural vibration inside the mouse cochlea by applying sine-wave signals with precision signal generator. Monitoring real-time morphological and vibrational images of cochlea by high-performance OCT is a promising method to diagnose hearing loss.

8565-57, Session 1

A miniaturized laser-Doppler-system in the ear canal

Tobias Schmidt, Technische Univ. Ilmenau (Germany)

Gathering vibrational data from the human middle ear is quite difficult. To this date the well-known acoustic probe is used to estimate audiometric parameters, e.g. otoacoustic emissions, wideband reflectance and stapedius reflex data. An acoustic probe contains at least one microphone and one loudspeaker. For distortion product otoacoustic emissions (DPOAE) measurements, two loudspeakers are necessary. The acoustic parameter determination of the ear canal is essential for the comparability of test-retest measurement situations. Compared to acoustic tubes, the ear canal wall cannot be described as a sound hard boundary. Sound energy partly is absorbed by the ear canal wall. In addition the ear canal features a complex geometric shape. Those conditions are one reason for the high variability in input impedance measurement data of the tympanic membrane. During the measurement, the human ear is stimulated by a miniature loudspeaker. Sound waves

propagating along the ear canal are partly reflected at the ear drum. The sound field along the ear canal can be described using the evanescent wave model. The microphone is used for the determination of sound pressure in the ear canal. Measured variables depend on the acoustic parameters of the ear canal. Gathering spatial vibrational data from the tympanic membrane could provide help indicating beginning hearing disorders (e.g. otosclerosis, tympanosclerosis).

The method of Laser-Doppler-Vibrometry is well described in literature. Using this method the surface velocity of vibrating bodies can be determined contact-free. Conventional Laser-Doppler –Systems (LDS) for auditory research are mounted on a surgical microscope. Using a LDS the vibration of the ear drum can be measured directly, and not only by the sound field in the ear canal. Assuming a free line of view to the ear drum, handling of those laser-systems is complicated. We introduce a miniaturized vibrometer which is applied directly in the ear canal for contact-free measurement of the tympanic membrane vibration.

8565-58, Session 1

OCT otoscope for assessment of conductive hearing loss

Tracy C. Petrie, Sripriya Ramamoorthy, Hrebesh M. Subhash, Oregon Health & Science Univ. (United States); Ruikang K. Wang, Univ. of Washington (United States); Alfred L. Nuttall, Steven L. Jacques, Oregon Health & Science Univ. (United States)

An otoscope was built and tested that utilizes 1310-nm Fourier-domain optical coherence tomography (OCT), which allows imaging of the ossicles through an intact tympanic membrane and measurement of ossicle vibration in response to an applied auditory signal. The key advantage is the ability to non-invasively assess conductive hearing loss rather than surgically cutting the tympanic membrane to enable examination. The system measures vibration on the 1-300 nm scale. This report presents pilot testing in cadaveric ears.

8565-59, Session 1

Moments of inertia and alternative lever arms for mobile and fused ossicular chains in several land mammals

Ryan P. Jackson, Stanford Univ. (United States)

No Abstract Available

8565-60, Session 2

Laser assisted implantation of nitibond prothesis

Ronald Sroka, Thomas Pongratz, Laser-Forschungslabor (Germany); Florian Schroetzelmair, Univ. Hospital Munich (Germany); Fabian Suchan, Laser-Forschungslabor (Germany); Joachim D. Mueller, Univ. Hospital Munich (Germany); David Saal, Detlef Russ, Univ. Ulm (Germany)

Introduction: One problem during stapes prothesis implantation is the fixation to the ambos. Dislocalisation, bone necrosis and non-contact to the vestibulum are common side effects. Stapes implants consisting of shape memory alloys are promising candidates to reduce these side effects. Such NitiBOND-implants could be activated by laser. This study was carried out to investigate thermal properties and the absorption capacity of the implant material at commonly available laser wavelengths for proper laser induced activation.

Patients and methods: First investigation on bulk material of shape memory alloy was carried out by using ellipsometry. Thereafter the sample was irradiated under defined conditions and spatial and temporal temperature profile was recorded with a high speed thermal camera. To determine the thermal and optical properties heat diffusion was calculated with finite difference method and compared with the experimental data. In this way the specific thermal and optical material parameters could be determined to fit the experimental data. In a next step heat diffusion at a NitiBOND implant within an power range sufficient to exceed the transition temperature of the shape memory alloy were recorded. Additionally, the degree of shaping was investigated using a variety of laser parameters (wavelengths, pulse duration, energy per pulse). Finally, first clinical applications were performed.

Results: Comparison the experimental data with the numerical simulations of heat diffusion in the finite difference model the optical and thermal parameters of the shape memory alloy could be determined. Based on this data heat application during the transition process can be optimized. The thermal images of the real implants show the rapid spread of heat crossing the joints between the segments designed for deformation. The degree of shaping depends highly on the intensity and pulse duration. Clinically, a safe procedure could be established by using fibre assisted energy application in a contact free mode. A stepwise shaping of the NiTiBOND-implant to the ambos was achieved without laser interaction to surrounding tissue.

Conclusion: NitiBOND-prothesis are suitable for laser assisted fixation to the ambos. Thus a reproducible material dependent fixation could be performed, thus promising reduced side effect. In clinical trials the optimised parameters and application systems should be proven. An improved hearing and a reduced sound wave conduction component during clinical diagnosis could be observed. Clinical results seemed independent to the experience of the physician when using non-contact laser assisted implantation of NitiBOND implants.

8565-61, Session 2

Functional outcome after Er:YAG versus CO2 laser assisted stapedotomy

Justus F. Ilgner M.D., Univ. Hospital Aachen (Germany)

No Abstract Available.

8565-62, Session 2

Effect of LLLT on vestibular system

Chung-Ku Rhee M.D., Dankook Univ. Hospital (Korea, Republic of)

No Abstract Available.

8565-63, Session 3

In vivo visualization of endolymphatic hydrops using optical coherence tomography (OCT)

Tatsunori Sakamoto, Yosuke Tona, Takayuki Nakagawa, Juichi Ito, Kyoto Univ. Graduate School of Medicine (Japan)

Meniere's disease is one of common inner ear disorders, representing with repeated symptoms of hearing impairment and vertigo. Endolymphatic hydrops, dilatation of membranous compartment of inner ear, is commonly found in the postmortem histological examination in Meniere's disease patients and its model mice, and believed as the cause of this disease. However, its diagnosis was not easy, because live imaging method to visualize intracochlear structures has not been established. In this study, optical coherence tomography (OCT) was used to visualize endolymphatic hydrops in mice with targeted disruption of Slc26a4 (formerly known as Pendrin). Littermates of Pds-knockout mice at the age of 11 weeks were used in this study. By physiological tests, homo mice were deaf, and hetero and wild type littermates had normal

hearing functions. Under general anesthesia, bulla was removed to expose the bony wall of cochlea, and OCT images were acquired using SS-OCT with 1300 nm central wavelength (Thorlabs). After series of image acquisitions, animals were fixed, temporal bones were removed and postfixed with 4% PFA. Hematoxylin and eosion staining of 10-μm-thick frozen sections were used for the morphological study.

Homo mice showed profound inner ear dysfunction, and hetero and wild-type (wt) mice were normal. In heteros and wts, Reissner's membranes were visible at normal position in the cochlea. While, in homo mice, OCT images showed extreme enlagement of scala media with thinned basal membrane, which is consistent with the histology. In conclusion, OCT have the potential to visualize structural abnormality in vivo.

8565-64, Session 3

Sensing and three-dimensional OCT imaging of the cochlea and temporal bone: image-guided cochlear implantation

Mingtao Zhao, Jin U. Kang, John Niparko, Russell H. Taylor, Johns Hopkins Univ. (United States)

Optical coherence tomography (OCT) offers a highly useful non-destructive, cross-sectional imaging modality. Prior work suggests that OCT is highly effective in informing the surgeon of the position of neural and sensorineural structures during freehand or robotically-assisted cochlear implantation. In this abstract, we describe a novel dual-functional OCT system that provides real-time sensing and imaging of temporal bone structures, including the cochlear labyrinth. The system images intra-cochlear partitions with 3-D OCT real-time imaging and senses surgical planes with a fiber probe integrated with a sapphire ball lens. A lensed probe design with sensing distances up to 5 mm and lateral resolution 11 ?m was implemented for forward sensing. To prevent facial nerve injury, 3-D visualization can assist in navigation of anatomical landmarks in the facial recess; subsurface features of cochlea critical to preserving neuronal integrity are also mapped in 3-D. A graphics processing unit (GPU) boosts the speed of swept source optical coherence tomography, which realizes a real time 3-D rendering of intra-cochlear structures. Both the basal turn and facial nerve bundles inside the cadaveric human cochlea temporal bone can be clearly identified in our 3-D OCT volumetric rendering.

This project was supported by Cochlear Corporation and NIH R01 EY021540.

8565-65, Session 3

Measurement of in vivo basal-turn vibrations of the organ of Corti using phase-sensitive Fourier domain optical coherence tomography

Sripriya Ramamoorthy, Fangyi Chen, Tracy C. Petrie, Yuan Zhang, Oregon Health & Science Univ. (United States); Hrebesh M. Subhash, National Univ. of Ireland, Galway (Ireland); Niloy Choudhury, Michigan Technological Univ. (United States); Ruikang K. Wang, Univ. of Washington (United States); Steven L. Jacques, Alfred L. Nuttall, Oregon Health & Science Univ. (United States)

A major reason we can perceive faint sounds and communicate in noisy environments is that the outer hair cells of the organ of Corti enhance the sound-evoked motions inside the cochlea. To understand how the organ of Corti works, we have built and tested the phase sensitive Fourier domain optical coherence tomography (PSFDOCT) system. This system has key advantages over our previous time domain OCT system (Chen et al, 2011). The PSFDOCT system has better signal to noise ratio and simultaneously acquires vibration data from all points along the z-axis (Wang and Nuttall, 2010). Feasibility of this system to measure in vitro cochlear vibrations in the apex were demonstrated earlier (Subhash et al, 2012). In this study, we measure the in vivo basal-turn vibrations of the organ of Corti using PSFDOCT. In order to visualize the orientation of the tissue inside the cochlea for setting up the PSFDOCT measurement, we have supplemented the system with a sample-view camera using minimal parts. The set-up and preliminary data from the basal turn organ of Corti will be presented in this report.

8565-66, Session 3

Comparison of high-resolution microendoscope images and histopathological sections in ex vivo middle ear cholesteatomas and surrounding tissue

James A. Bradley, Lauren Levy, Andrew Sikora M.D., Mount Sinai School of Medicine (United States); Rebecca Richards-Kortum, Rice Univ. (United States); Eric Smouha, Mount Sinai School of Medicine (United States)

Objective: To investigate the concordance between optical images obtained with high-resolution microendoscopy (HRME) and conventional histopathology for ex vivo cholesteatoma specimens and surrounding middle ear epithelium.

Methods: After resection of cholesteatoma and surrounding middle ear epithelium from surgical patients, tissues were stained with a contrast agent, proflavine, and the HRME fiberoptic scope was placed directly on each tissue specimen. 4-10 short movie clips were recorded for both the cholesteatoma and surrounding middle ear epithelium specimens. The imaged areas were sent for standard histopathology, and the stained specimens were correlated with the HRME images. IRB approval was obtained, and each patient was consented for the study.

Results: Ten cholesteatoma specimens and 9 middle ear specimens were collected from 10 patients. In each case, cholesteatoma was easily discriminated from normal middle ear epithelium by its hyperfluorescence and loss of cellular detail. Qualitative analysis for concordance between HRME images and histological images from the same surgical specimen yielded a strong correlation between imaging modalities.

Conclusions: Keratinizing cholesteatoma and surrounding middle ear epithelium have distinct imaging characteristics. Loss of cellular detail and hyperfluorescence with proflavine are the hallmark characteristics of cholesteatoma which allow for differentiation from normal middle ear epithelium. Real-time optical imaging can potentially improve the results of otologic surgery by allowing for extirpation of cholesteatomas while eliminating residual disease. We anticipate performing an in vivo study to test this hypothesis.

8565-67, Session 3

Nonlinear optical imaging of the mammalian cochlea

Shelly Batts, Stanford Univ. (United States)

No Abstract Available

8565-68, Session 4

Infrared neural stimulation in the cochlea

Ken Zhao, Suhrud M. Rajguru, Claus-Peter Richter, Northwestern Univ. (United States)

No Abstract Available

8565-69, Session 4

Pulse shaping effects on optical induced auditory brainstem responses

Marc Kannengießer, Dietmar J. Hecker, Univ. des Saarlandes (Germany); Martin Sänger, Technische Univ. Kaiserslautern (Germany); Cathleen Schreiter, Univ. des Saarlandes (Germany); Hans-Jochen Foth, Technische Univ. Kaiserslautern (Germany); Achim Langenbucher, Bernhard Schick, Gentiana I. Wenzel, Univ. des Saarlandes (Germany)

Green light can activate the peripheral hearing organ (Wenzel et al 2009). However, this is not enough to improve the quality of life for hearing impaired patients. A controlled frequency specific activation of the complete audible frequency spectrum is mandatory to make speech and complex sounds of daily life perceptible and intelligible. As a first step, on the way to the development of a frequency modulation method, we thought to assess the effects of laser-pulse shaping on the optical induced auditory brainstem responses (ABR), in an animal model.

Click - ABRs were recorded preoperatively in anesthetized guinea pigs to confirm normal hearing. A 100 µm diameter optic fiber was inserted into the outer ear canal and directed to the ear drum. Optically induced ABRs were recorded in response to laser stimulation with Q-switched 10 ns, 532nm laser pulses from a diode-pumped solid state Nd:YAG laser (Xiton Photonics GmbH, Kaiserslautern, Germany).

Optical stimulation of the ear was possible with pulse energies from 0-17 µJ/pulse and repetition rate up to 20 kHz. Increasing the laser-repetition rate, lead to the superposition of the optical induced ABR´s.

These findings suggest that laser-pulse shaping based on variable temporal pulse distributions, a process that is well known in physics, applies for biological systems as well. Further studies are on the way to determine the optimal pulse shaping strategy for the activation of the complete auditory spectrum.

8565-70, Session 5

Software for automatic analysis of image and sound data simultaneously acquired from high-speed videoendocopy

Tao Jiang, Santa Clara Univ. (United States); Shouhua Luo, Southeast Univ. (China); Yuling Yan, Santa Clara Univ. (United States)

No Abstract Available.

8565-71, Session 5

Analysis of long-range OCT of subglottic stenosis in a rabbit model

Ashley Hamamoto, Univ. of California Irvine (United States)

No Abstract Available.

8565-72, Session 5

In vivo imaging of subglottic stenosis using long-range OCT: preliminary results in adults and children

No Abstract Available.

8565-73, Session 5

Compact divided-pupil line-scanning confocal microscope for investigation of human tissues

Christopher Glazowski, Gary Peterson, Milind Rajadhyaksha, Memorial Sloan-Kettering Cancer Ctr. (United States)

Divided-pupil line-scanning confocal microscopy (DPLSCM) can provide a simple and low-cost approach for imaging of human tissues with pathology-like nuclear and cellular detail. Using results from a multidimensional numerical model of DPLSCM, we found optimal pupil configurations for improved axial sectioning, as well as control of speckle noise in the case of reflectance imaging. The modeling results guided the design and construction of a simple (<10 component) microscope, packaged within the footprint of an iPhone, and capable of cellular resolution. We present the optical design with experimental video-images of in-vivo human tissues.

8565-74, Session 5

Remote image guided laser for endoscopic surgery

Ricardo Toledo-Crow, Stefan Kirov, Yongbiao Li, Snehal Patel, Milind Rajadhyaksha, Memorial Sloan-Kettering Cancer Ctr. (United States)

Surgical lasers have many benefits as surgical instruments but their widespread implementation has been limited by difficulties in manipulating and delivering the beams. As a consequence, significant progress in their development and adoption has been stagnant for a decade. For head and neck surgery their use requires special training and is restricted to procedures with direct access to the tissue. We are developing a Remote Controlled Image Guided Laser for Endoscopic Surgery, with the goals of: (a) expanding the use of lasers in H&N and other minimally invasive surgical procedures (MIS) to sites without direct access, (b) improve their control and accuracy, (c) reduce the training needed for their use. The device is small enough to be inserted into confined anatomical spaces (e.g. head and neck, gastrointestinal, etc.) and gives the surgeon the ability to control the path, speed and intensity of the laser remotely from a video console. It contains a laser steering mechanism, video camera, and instrument channels, in a package that can be adapted to existing endoscopic and robotic surgical technology. We made a prototype of the device that demonstrated good performance with the necessary opto-mechanical characteristics and size for endoscopic procedures within reasonable costs. We present our latest results in our effort overcome technical challenges to translate the device to the clinic and to commercialization.

8565-75, Session 6

Optical coherence tomography for monitoring late oral radiation toxicity

Bahar Davoudi, Univ. of Toronto (Canada); Melanie Morrison, Univ. of Toronto (Canada); Beau A. Standish, Ryerson Univ. (Canada); Kostadinka Bizheva, Univ. of Waterloo (Canada); Victor Yang, Ryerson Univ. (Canada); Wilfred Levin, Univ. of Toronto (Canada); Alex I. Vitkin, Ontario Cancer Institute (Canada)

Late oral radiation complication occurs in 47% of the patients who undergo radiation therapy for head and neck cancer [1]. These complications include conditions such as mucosal atrophy and xerostomia (dry mouth), decreasing the quality of life of the patients [2]. Currently, treatments for these complications are prescribed based on the sub-optimal information that the oncologist gathers through superficial visual inspection of the oral cavity. However, it has been shown that

damage to the subsurface components of the oral tissue (such as epithelium or the microvasculature in the lamina propria) occurs prior to the superficial surface-visible alterations [2]. Therefore, a need exists for a non-invasive method that can monitor the subsurface microstructural and microvascular changes due to radiation toxicity. In this study, we have used optical coherence tomography (OCT) as a high resolution, non-invasive subsurface imaging tool to address this clinical need.

A spectral-domain OCT system and an oral imaging probe were built to acquire microstructural and microvascular (Doppler and speckle variance OCT) images of the human oral tissue in vivo [3]. Firstly, the oral cavity of healthy human volunteers was imaged to generate an 'OCT atlas' of common microstructural and microvascular features in the oral subsurface layers [3]. After acquiring approval from Princess Margaret Hospital Ethics Board (Toronto, Canada), the OCT system was transported to the Radiation Late Effect Clinic for OCT imaging of late oral radiation toxicity patients.

Preliminary OCT images of these patients reveal changes in oral subsurface layers compared to that of healthy volunteers. While the epithelium (characterized as a low reflective layer in OCT images) and lamina propria (the highly reflective fibrous layer) are easily distinguishable in 3D structural OCT images of healthy volunteers, they cannot be discerned in the regions of patients' oral cavity which had received high radiation dose (>65Gy). Moreover, Doppler images of the vessels in these regions show larger and more turbulent flow compared to the vessels of same diameter in healthy volunteers. Currently, more quantitative measurements are being performed on the images to assess the changes in these patients.

[1] F. Denis et al., Int. J. Radiat. Oncol. Biol. Phys. 55, 93-8, 2003

[2] J. J. Sciubba and D. Goldenberg, Lancet Oncol. 7, 175-83, 2006

[3] B. Davoudi et al., Biomed. Opt. Express 3, 826-39, 2012

8565-76, Session 6

Miniaturization does not impair the ability of ESS to assess malignancy in human thyroid nodules

Jennifer E. Rosen, Irving J. Bigio, Boston Univ. (United States); Ousama M. A'Amar, Boston Univ. (United States); Stephanie L. Lee, Boston Univ. (United States); Faris Azar, Boston Univ. (United States)

Miniaturization of optical probe to fit through a 23 gauge needle does not alter the ESS signature in thyroid nodules.

8565-77, Session 6

Characterization of oral precancerous lesions based on higher-harmonic generation microscopy

Chen-Yu Lin, National Taiwan Univ. (Taiwan); Chih-Feng Lin, National Taiwan Univ. (Taiwan) and National Taiwan Univ. Hospital and College of Medicine (Taiwan); Chi-Kuang Sun, National Taiwan Univ. (Taiwan) and Molecular Imaging Ctr. National Taiwan Univ. (Taiwan) and Academia Sinica (Taiwan)

It is generally accepted that oral cancer arises in the presence of oral precancerous lesions. However, the clinical course of these lesions are quite unpredictable, and a fundamental enigma remains that when and how these lesions turn to malignant growth. Characterization of these potentially malignant lesions is thus important and could serve as early indicators of this neoplastic transformation process, potentially facilitates the treatment outcome and improves the survival rate. Higher generation microscope (HGM), providing images with a <500nm lateral resolution at a 300?m penetration depth, without leaving photodamages in the tissues, was used for this purpose. Oral cavity biopsies were obtained from 10 patients with clinical suspected oral precancerous lesions scheduled for surgical biopsy. HGM images were compared with histological images to determine the results. By visualization of subtle cellular and morphological changes, the preliminary result of this HGM image discloses excellent consistency with traditional histolopathology studies, without the need for fixation, sectioning and staining. More specifically speaking, the keratin thickness was found to be increased comparing with normal adjacent controls. In some cases, variations in cell size, nuclear size and increased nuclear/cytoplasmic ratio, and increased size of nucleoli were identified, indicating different stages of malignant transformation. These results together indicated that HGM provides the capability to characterize features of oral precancerous lesions as well as oral cancer progression, and holds the greatest potential as an ideal tool for clinical screening and surveillance of suspicious oral lesions.

8565-78, Session 7

Simultaneous two-photon fluorescence (2PEF), second harmonic generation (SHG) and confocal large field imaging of vocal folds

Romain Deterre, Ecole Polytechnique de Montréal (Canada); Mathias Strupler, Sainte-Justine Mother and Child Univ. Hospital Ctr. (Canada) and Ecole Polytechnique de Montreal (Canada); Nadir Goulamhoussen, Etienne De Montigny, Ecole Polytechnique de Montréal (Canada); Shilpa Ojha M.D., Harvard Medical School (United States); Christopher J. Hartnick M.D., Massachusetts Eye and Ear Infirmary (United States); Caroline Boudoux, Ecole Polytechnique de Montréal (Canada) and Sainte-Justine Mother and Child Univ. Hospital Ctr. (Canada)

The Hirano model depicts the vocal fold lamina propria as a three-layer system distinguishable by their respective concentration in collagen and elastin. Imaging modalities based on nonlinear interactions such as second harmonic generation (SHG) and two photon excitation fluorescence (2PEF) may be used to respectively image collagen and elastin. Therefore, we believe that nonlinear microscopy, with its cellular resolution and long penetration depth, is a perfect candidate to study vocal folds structures and eventually diagnose vocal fold pathologies.

In order to validate images obtained by nonlinear imaging, we built a multimodal benchtop microscope for simultaneous confocal, SHG and 2PEF imaging. The system is based on a 35 fs Ti:Saph laser beam sent to two galvanometer mounted mirrors for a rapid raster scan of the sample. A 0.8 NA water immersion microscope objective is used to obtain a 200 µm by 200 µm field of view. However, a larger field of view is necessary to compare nonlinear microscopy images with histopathology slides. By placing the sample on a 3-axis motorized translation stage and using an automated acquisition software, 10 mm by 3 mm stitched images can be obtained with the three modalities in a few minutes. Images obtained with the nonlinear modalities match the results of histopathology stained slides, showing efficiently the epithelium, lamina propria and underlying muscle of the vocal folds, but also glandular structure formation associated with intubation of the human subjects from which samples were extracted. This preliminary study highlights the potential of this technique for vocal fold imaging.

8565-79, Session 7

Comparison of porcine vocal fold ultrafast laser ablation parameters using 780-nm vs. 1550-nm excitation wavelengths

Murat Yildirim, Onur Ferhanoglu, The Univ. of Texas at Austin (United States); James B. Kobler, Steven M. Zeitels, Massachusetts General Hospital (United States); Adela Ben-Yakar, The Univ. of Texas at Austin (United States) and

Massachusetts General Hospital (United States)

Vocal fold scarring is one of the major cause of voice disorders and may arise from overuse or post surgical wound healing. One promising treatment aimed at restoring viscoelasticity of the outermost vibratory layer of the vocal fold, superficial lamina propria (SLP) utilizes the injection of soft biomaterials. To enhance treatment effectiveness, we are investigating a technique to ablate sub-epithelial planar voids in vocal fold using ultrafast laser pulses to better localize the injected biomaterial.

We present an in-depth analysis of surgery parameters at 780 and 1550 nm respectively. Specifically, we study the spatial extent of the void ablation by comparing initial bubble area to the targeted ablation area and collapse time of these bubbles at these two wavelengths. We create voids at a depth of 90 μm depth, which is the interface of the epithelium and SLP.. We deliver the pulses of a high repetition rate (300 kHz- 2 MHz) ultrafast fiber laser (Raydiance Inc.) using a home-built nonlinear laser scanning microscope.We acquire second harmonic generation, two-photon autofluorescence and third-harmonic generation signals from porcine vocal folds. Each imaging modality highlights different tissue signatures and types, and together they provide a complementary view of tissue. We demonstrate that initial bubble area with 2.1 uJ pulse energy at 1550 nm shows similar characteristics to the initial bubble area obtained using 750 nJ at 780 nm. We observed that all voids created using 780 nm pulses collapsed after an hour whereas permanent voids are created at 1550nm.

8565-80, Session 7

Study of vocal fold development using optical coherence tomography

Fouzi Benboujja, Ecole Polytechnique de Montréal (Canada); Shilpa Ojha M.D., Harvard Medical School (United States); Mathias Strupler, Ecole Polytechnique de Montréal (Canada); Stephen Maturo M.D., Scott Infusino, Christopher J. Hartnick, Harvard Medical School (United States); Caroline Boudoux, Ecole Polytechnique de Montréal (Canada)

The outcome of pediatric vocal fold surgery is highly dependent on the vocal maturation stage of the patient, since the identification of the appropriate time for surgery depends on the developmental stage of the vocal folds. However, our knowledge of pediatric vocal fold development is incomplete. Therefore, a deeper understanding of the development of the lamina propria is critical, as it could lead to specialized and adapted treatments for patients.

This highlights the need for developing quantitative features describing the vocal fold layers using a non-invasive imaging modality. In this study, we explore the use of Optical Coherence Tomography (OCT) to distinguish and model the vocal fold layers. Three groups were studied, each representing a different model and stage of maturation of the lamina propria: human fetus (1 layer), swine (2 layers), human adult (3 layers). Samples were imaged on a bench-top swept source OCT system (?0=1310nm, ??=100nm) and compared with histology. From the RAW OCT images, characteristics and repetitive patterns in the pixel intensity distribution were analyzed statistically using an automated algorithm. The results were compiled in a database of OCT features describing each specimen group. As excised vocal fold specimen are hard to come by, we designed a high-resolution OCT in vivo endoscope to increase the number of specimens in the database and acquire more information about the evolution of vocal folds. This imaging system will be suitable for longitudinal studies starting from neonates up to adulthood to yield a better understanding of the evolution of the vocal fold and ultimately provide surgeons with a more accurate pre- and per-operative visualization tool.

8565-81, Session 7

A concise algorithm for detection of vibration from Fourier domain OCT

Steven L. Jacques, Sripriya Ramamoorthy, Tracy C. Petrie, Alfred L. Nuttall, Oregon Health & Science Univ. (United States)

A concise and succinct algorithm for detection of vibration from an M-scan measurement of OCT versus time is presented. The algorithm draws on previously published work by others, but has distilled the process to the simplest code for vibration analysis.

8565-82, Session 7

Viability of porcine trachea post electromechanical reshaping

Syed F. Hussain, Beckman Laser Institute and Medical Clinic (United States)

The trachea or the airway leading to the lungs is a cartilaginous anatomical structure particularly prone to stenosis as a result of trauma and or intubation. In previous experiments, the application of voltage over time or electromechanical reshaping (EMR) has been known to significantly reshape cartilaginous tissue (Wong et. al). Porcine Trachea, largely cartilaginous in its composition, was used in this study to evaluate the viability of cartilaginous cells or chondrocytes after treatment using EMR. The cartilage samples were stained in a Hanks balanced salt solution with Calcein AM and Homodimer, DNA dyes that fluoresce under excitation of laser scanning microscope Zeiss Meta LSM 510. The rendered images depicted regions of green and red fluorescence representing live and dead chondrocytes, respectively. The rendered images were serially montaged and the resulting live-dead assay showed entire tissue samples consisting of largely viable chondrocytes post-EMR. Live-dead assays of the samples were quantified for cell death around regions of cathodes and anodes. While such numbers help quantify the degree of damage sustained by the cartilage tissue, a majority of the same was alive after treatment of EMR.

8565-83, Session 7

Near-infrared imaging for diagnosis of maxillary sinusitis

Joon S. You, Cyrus Manuel, Andrew E. Heidari, Praxis BioSciences, LLC (United States); Naveen Bhandarkar M.D., Univ. of California, Irvine School of Medicine (United States); Brian Wong M.D., Albert E. Cerussi, Beckman Laser Institute and Medical Clinic (United States)

Efficient management of chronic sinusitis remains a great challenge for primary care physicians. There is no simple, inexpensive, and safe method to accurately confirm the presence/extent of sinus disease. There is a great need for a simple office-based diagnostic technique that can reduce the time and cost related to under-treatments and unnecessary over-treatments (i.e. antibiotics) of chronic sinusitis. Previously, we reported that near-infrared imaging of maxillary sinus may provide means for assessing the presence of sinus disease. Here, we report development of a new generation of optical imaging setup for quick and simple assessment of sinusitis in primary care settings. It exploits the relative lack of attenuation in near-infrared region and its potential sensitivity to the sinus structures and fluid characteristics. Significant improvement in the performance has been achieved in the new imaging system in comparison to the previous version while keeping the cost of materials suitable for primary care uses. NIR imaging of patients with confirmed sinusitis was performed and compared with computed tomography scans. Comparison between CT scans and NIR image patterns demonstrates correlation between the NIR image intensity and the frontal bone structures of the maxillary sinuses. Results from the

patient study showed that air-filled and fluid/tissue-filled spaces can be reasonably distinguished by their differing NIR signal penetration patterns as well as reduced transmittance of NIR light by fluid build-up. We are currently conducting a small clinical trial to validate the efficacy of this NIR imaging technique as a tool in primary care doctors.

8565-84, Session 7

High speed in vivo upper airway imaging using long range optical coherence tomography

Joseph Jing, Univ. of California, Irvine (United States); Jun Zhang, Univ. of California, Irvine (United States) and Beckman Laser Institute (United States); Anthony Chin Loy, Univ. of California Irvine (United States); Brian Wong M.D., Univ. of California, Irvine (United States) and Beckman Laser Institute (United States); Zhongping Chen, Univ. of California, Irvine (United States) and Beckman Laser Institute (United States)

The human upper airway is a structurally complex anatomic region that plays an important role in respiration, deglutition, and production of speech. Obstruction in the upper airway can often cause reductions in breathing or gas exchange efficiency and lead to rest disorders such as sleep apnea. Long range optical coherence tomography (OCT) has the potential to provide high speed three dimensional tomographic images with high resolution and without the use of ionizing radiation. In this manuscript, we present work on the development of a long range OCT endoscopic probe (1.2 mm OD, 20 mm working distance) used in conjunction with a modified Fourier domain OCT system to acquire both structural and anatomical datasets of the human airway. Comprehensive in vivo imaging thru the upper airway from nasal fossa to the larynx is completed within 40 seconds. Separate 3D tracking is utilized to reconstruct an accurate 3D representation of the airway on which future computational fluid modeling can be performed to determine the sites of greatest obstruction.

8565-85, Session 8

Development of real-time automated image analysis algorithms for multi-modal optical imaging of oral neoplasia

Timothy Quang, Noah Bedard, Mark C. Pierce, Richard A. Schwarz, Rice Univ. (United States); Vijayashree S. Bhattar, The Univ. of Texas M.D. Anderson Cancer Ctr. (United States); Sharon Mondrik, Rice Univ. (United States); Jana Howe, Michelle D. Williams, Ann M. Gillenwater, The Univ. of Texas M.D. Anderson Cancer Ctr. (United States); Rebecca Richards-Kortum, Rice Univ. (United States)

Multispectral optical imaging techniques have emerged in recent years as a potentially useful adjunct to standard oral cancer screening. Recent studies suggest that acquiring optical images at multiple spatial scales in a multi-modal imaging system can aid in identifying neoplastic lesions by first rapidly screening an area with a large field of view using wide-field autofluorescence imaging, and then using high resolution imaging to interrogate suspicious regions on the cellular level. While initial studies have supported the use of multi-modal imaging as a clinical adjunct, one limitation is that images obtained still require post-hoc image analysis to classify imaging sites. In addition, the image analysis requires user input in terms of specifying regions of interest in the image to analyze. To provide real-time, automated feedback for the clinician, two image processing algorithms were developed for the multi-modal imaging system. One algorithm quantitatively analyzes wide-field images to identify at-risk regions for neoplasia while the other increases the field of view of the high resolution modality by stitching together consecutive frames into a mosaic and quantifies nuclear morphology in real-time.

The algorithms were evaluated by performing automated analysis of multi-modal data from 30 patients that had previously been analyzed using conventional methods with user input. Algorithm performance was then compared to previously published results. Image results suggest that these image analysis algorithms have the potential to improve the utility of multi-modal imaging in oral cancer screening.

8565-86, Session 8

Validation of an ESS signature to predict benign from malignant human thyroid nodules

Jennifer E. Rosen, Irving J. Bigio, Boston Univ. (United States); Ousama M. A'Amar, Boston Univ. (United States); Stephanie L. Lee, Boston Univ. (United States); Faris Azar, Boston Univ. (United States); Eladio Rodriguez-Diaz, Boston Univ. (United States)

Validation of an ESS signature to predict benign from malignant human thyroid nodules.

8565-87, Session 8

In vivo detection of circulating tumor cells during tumor manipulation

Mazen A. Juratli M.D., Ekaterina I. Galanzha, Mustafa Sarimollaoglu, Dmitry A. Nedosekin, James Y. Suen M.D., Vladimir P. Zharov, Univ. of Arkansas for Medical Sciences (United States)

Many cancer deaths are related to metastasis to distant organs due to dissemination of circulating tumor cells (CTCs) shed from the primary tumor. For many years, oncologists hypothesized some medical procedures may provoke metastasis; however, no direct evidence has been reported. A new, noninvasive technology, in vivo integrated photoacoustic flow cytometry (PAFC), provides ultrasensitive detection of CTCs. When CTCs with light-absorbing intrinsic melanin or green fluorescent protein pass through a laser beam aimed at a peripheral blood vessel, laser-induced acoustic waves or fluorescence from CTCs were detected using an ultrasound transducer and photodetector. We focused on melanoma of the head and neck due to the current lack of an effective treatment. Head and neck melanoma is aggressive, and has a poorer prognosis than other skin sites. The goal of this research was to determine if melanoma manipulation, (compression, incisional biopsy, or tumor excision) could enhance penetration of cancer cells from the primary tumor into the circulatory system. The ears of nude mice were inoculated with human melanoma cells. Blood vessels were monitored for the presence of CTCs using in vivo PAFC. We discovered compression of the tumor, or incisional biopsy, either initiated CTC release in the blood which previously contained no CTCs, or dramatically increased (10-30–fold) CTC counts above the initial level. Our results warn oncologists to use caution during physical examination, and surgery. A preventive anti-CTC therapy during or immediately after surgery, by intravenous drug administration could serve as an option to treat the resulting release of CTCs.

8565-88, Session 8

Reflectance confocal microscopy to distinguish thyroid, parathyroid and lymph node: a feasibility study

Frank Palmer, Bjorg A. Larson, Andre Moreira, Safina Ali, Milind Rajadhyaksha, Snehal Patel, Memorial Sloan-Kettering Cancer Ctr. (United States)

During thyroid surgery, preservation of the parathyroid glands (PG) is standard practice to minimize the risk of postoperative hypocalcemia. However, visual distinction of PG from adjacent thyroid tissue, fat or lymph node can be challenging. Surgeons currently rely on immediate histopathological frozen section analysis of suspected PG. If histopathological analysis confirms PG, the tissue is re-implanted into a suitable muscular bed. This paradigm of intraoperative examination is important in cancer surgery, to avoid confusing normal PG with malignant thyroid nodules or lymph nodes. A real-time intraoperative microscopic technique to identify PG from other adjacent tissue will be useful. We have used reflectance confocal microscopy (RCM) to analyze the nuclear and cellular details of freshly excised thyroid tissue, lymph node, and parathyroid glands, using a confocal microscope VivaScope 2500 (Lucid, Rochester, NY) with illumination wavelength of 658 nm. Image mosaics over approximately 5 ? 5 mm2 of tissue from 29 patients were acquired and analyzed. RCM images were correlated with traditional H&E-stained histopathology, which was performed en face on all specimens. The thyroid specimens included well and poorly differentiated thyroid carcinomas, follicular and hurthle cell adenomas, nodular hyperplasia, and goiter. The lymph node specimens included well and poorly differentiated thyroid carcinoma, squamous cell carcinoma, and benign lymph tissue. The parathyroid specimen was adenoma. RCM images correlated well with histopathology, allowing for differentiation between thyroid, parathyroid and lymph node. We hypothesize that intraoperative RCM may enable real-time in vivo identification of PGs during thyroid surgery.

8565-89, Session 9

Phase I clinical trial of TPCS2a induced photochemical internalization of bleomycin

Waseem K. Jerjes, Univ. College London (United Kingdom)

No Abstract Available

8565-90, Session 9

Photothermal treatment of head and neck squamous cell carcinoma using macrophage as vector for gold nanoshells

Seung-Kuk Baek M.D., Korea Univ. College of Medicine (Korea, Republic of); Taeseok D. Yang, Korea Univ. (Korea, Republic of); Wonshik Choi, Korea Univ. College of Medicine (Korea, Republic of); Tai Hyun Yoon, Korea Univ. (Korea, Republic of); Kyoung Jin Lee, Jae-Seung Lee, Korea Univ. (Korea, Republic of); Min-Goo Lee M.D., Min Woo Park M.D., Kwang-Yoon Jung M.D., Korea Univ. College of Medicine (Korea, Republic of); Sangyong Park, Beckman Laser Institute and Medical Clinic (United States)

Photothermal treatment(PTT) using nanoparticle has gained attention as the promising alternative therapies for malignant tumor. One of the strategies to increase the selectivity of PTT is the use of macrophage as cellular vector for nanoparticles. The aim of the present study is to examine the ability of macrophage as a cellular vector for efficient PTT and to determine the adequate power and time of NIR laser. The thermally-induced cell injury and death of cancer cells was started at 44 - 45℃ of temperature, which was made by PTT effect using gold nanoshell(NS) and NIR laser light at irradiance of 2W for 5 minutes. The peritoneal macrophage had an efficient ability as a cellular vector for NS and the cancer cells around NS loaded macrophages selectively lost the cellular viability by irradiation of NIR laser. Even if the toxicity of nanoparticles is an important limitation for clinical application, the cellular vector such as macrophage may reduce uncontrollable spread and toxicity of nanoparticles and should enable more selective PTT on cancer cell.

8565-91, Session 9

Treatment planning and control for laser therapy of head and neck cancer

Gal Shafirstein, Roswell Park Cancer Institute (United States)

No Abstract Available

8565-92, Session 9

Electromechanical reshaping device

Joon S. You, Cyrus Manuel, Crystal Bong, Richard Staebler, Chao Shen, Praxis BioSciences, LLC (United States); Brian Wong, Praxis BioSciences, LLC (United States) and Beckman Laser Institute (United States)

Every year, more than 600,000 operations are performed to alter the shape of the structural cartilage frameworks of the ear (otoplasty) and nose (rhinoplasty and septoplasty) for both functional and aesthetic purposes, accounting for more than $1 billion in expenditure. Current methods of reshaping cartilage in the head, face and upper airway require carving, cutting, suturing, or crushing this viscoelastic biologic charged polymer into a new desired shape in order to balance the innate forces that resist deformation. The results are highly variable and dependent on the skills and techniques of the surgeon. Recently, a new minimally-invasive technique has been developed based on the fact that cartilage mechanical properties can change in response to low-level, low-current DC electric fields. This technique called Electromechanical Reshaping (EMR) has recently been demonstrated using animal ears both ex vivo and in vivo. The procedures use expensive bench-top power supply with individual needles being applied by hand. Here we report development of the next generation(s) of benchtop and portable EMR devices along with needle applicators that can be used specifically for otoplasty. Each device allows real-time monitoring of electrical charge delivered to the tissues so that users can control the dosimetry. The needle applicators have been built to accommodate the mechanical bending of ears and simple application of needles. To minimize collateral damage in the skin tissue caused by electrochemical reactions, inactive areas of needles have been coated with dielectric materials. The new devices have been tested using ex vivo animal ears.

8565-93, Session 9

Skin photosensitivity in a phase I clinical trial of Amphinex® induced photochemical internalization of Bleomycin

Waseem K. Jerjes, Univ. College London (United Kingdom)

No Abstract Available

8565-94, Session 9

Comparison of 1470-nm diode laser vs c02-laserlaser for tonsillotomy and a clinical feasability trial on the use of 1940 nm

Ronald Sroka, Thomas Pongratz, Laser-Forschungslabor (Germany); Miriam Havel, Elsa Englert, Univ. Hospital Munich (Germany); Thomas Kremser, StarMedTec GmbH (Germany); Christain S. Betz, Univ. Hospital Munich (Germany); Andreas Leunig, HNO-Praxis (Germany)

Introduction: The need for reduction of post-tonsillectomy hemorrhage has led to promotion of tonsillotomy techniques for tonsil tissue reduction in obstructive tonsillar hypertrophy. A first study compares ablative tissue

effects using 1470nm diode laser and CO2-laser for tonsillotomy in an intraindividual design. A number of different laser systems have been used for volume reduction of hyperplastic nasal turbinates. The aim of a 2nd clinical feasibility study was to show the coagulative and tissue reducing effects using a novel Tm: fiber laser system emitting at ? = 1940 nm

Patients and methods: First 21 children aged 3 -13 years (mean age 6.3 years) underwent laser tonsillotomy for obstructive tonsillar hypertrophy in this double blind, prospective, randomized, clinical feasibility trial. In each case, tonsillotomy was performed using fibre guided 1470nm diode laser (contact mode, 15 W power) on the one side and CO2-laser (12 W power) on the other side. An independent physician documented clinical presentation and patients' symptoms preoperatively and on day 1, 3, 7, 14 and 21 postoperatively using standardized questionnaire including VAS (was ist das) for each side separately. The 2nd clinical feasibility trial included 11 patients suffering from hyperplastic inferior nasal turbinates, who were therapy-refractory to conservative medical treatment. The obstructive nasal cavity was treated using the 1940 nm Tm: fiber laser at < 5 W output power. The treatment was performed in non-contact mode under endoscopic control. Patients ' symptoms were documented both preoperatively and on days 1 – 3 and 28 postoperatively using a non-validated questionnaire. Additionally, an endoscopic examination was performed.

Results: Mean duration of single tonsillotomy operative treatment was 2.7 min using 1470nm laser and 4.9 min using CO2 laser respectively. Intraoperative bleeding and the frequency of bipolar forceps use for intraoperative bleeding control was significantly less pronounced using the 1470nm diode laser system. There was no difference in postoperative pain scores between the CO2-laser treated and the 1470nm fibre guided diode laser treated side. No infections, hemorrhages or other complications occurred in the course of the three weeks postoperative period.

In the turbinate study, none of the patients showed infections, and no hemorrhages or other complications occurred intra- or postoperatively. The mean laser activation time was extremely short being 28.0 ??8.5 s. In conjunction with a low power setting (median, 3 W; mean ??standard deviation, 3.3 ??1.1 W), a low energy of 90.2 ??37.8 J was applied. A significant reduction in nasal obstruction could be documented in all patients on day 28 postoperatively. Evaluation, as assessed preoperatively and 4 weeks postoperatively, showed significant subjective improvements.

Conclusion: A fiber-guided 1470nm diode laser system offers an efficient and safe method for tonsillotomy as treatment of obstructive tonsillar hypertrophy. Compared to our standard practice with CO2-laser, 1470nm laser application provides comparable tissue ablation effects with less intraoperative bleeding and shorter operation time. The treatment of

hyperplastic inferior turbinates using a 1940 nm Tm: fiber laser provides sufficient tissue reduction in a short operation time using low total energy. Patients described a significant improvement in nasal breathing postoperatively.

8565-95, Session 9

3-um CW lasers for myringotomy and microsurgery

Kurt J. Linden, Spire Corp. (United States); Christian P. Pfeffer, Children's Hospital Boston (United States); John G. Sousa, Nicholas D'Alleva, Sheaumann Laser, Inc. (United States); Arash Aslani, Spire Corp. (United States); Grzegorz Gorski, Margaret Kenna, Dennis S. Poe, Children's Hospital Boston (United States)

This paper describes the development and implementation of 3 µm lasers for myringotomy and microsurgery. Two different lasers were investigated. The first, an Er-doped, CW zirconate glass fiber laser optically pumped by a 970 nm diode laser, emitted > 1 W of CW power at 2712 nm with concomitant green incoherent emission that served as a convenient visible illumination beam. The second, a 1 W CW Er:YAG solid-state laser also optically pumped by a 970 nm diode laser, emitted > 1 W of CW power at 2940 nm, coincident with the strongest water optical absorption peak. Running CW, both lasers avoid the loud acoustical shocks associated with pulsed lasers. Myringotomies were carried out with the Er:YAG laser on anaesthetized guinea pigs and the effects of the laser were documented. Laser ablated samples of tympanic membrane, soft tissue and bone were histologically examined. Histology results indicated that the CW Er:YAG laser is a potential candidate for a new myringotomy tool and possibly for otologic microsurgery, but deliverable power levels need to be increased to the 2 W (or higher) level. This work was funded under NIH SBIR Grant No. 5R44DC004899.

8565-239, Session 9

iPDT and chemotherapy for recurrent HNSCC

Nestor Rigual, Roswell Park Cancer Institute (United States)

No Abstract Available

8565-96, Session 1

Optical imaging in the clinic *(Invited Paper)*

Septimiu D. Murgu M.D., Univ. of California, Irvine (United States)

No Abstract Available

8565-97, Session 1

Co-registered optical coherence tomography and autofluorescence imaging methods

Hamid Pahlevaninezhad, Anthony M. Lee, Daryl Chulho Hyun, Calum E. MacAulay, Stephen Lam, Pierre M. Lane, The BC Cancer Agency Research Ctr. (Canada)

Autofluorescence (AF) imaging using blue light illumination to excite natural tissue fluorescence has proven to be extremely effective for the early detection and staging of airway lesions. Optical coherence tomography (OCT), the optical equivalent of ultrasound, enables in vivo imaging of airway morphology with a resolution approaching that of histology. When used in combination, in a simultaneous and co-registered fashion, AF-OCT imaging can provide rich biochemical information co-localized with tissue morphology that cannot be achieved by either imaging modality alone.

Effective AF excitation wavelengths lie in the short wavelength range (400-460 nm), while OCT systems operate in the near IR range (1000-1600 nm). This large wavelength gap introduces challenges in the design of co-registered dual-modality systems. Many research groups have combined the two modalities in free space that precludes the applications involving tissue imaging inside human body. Especially for lung cancer, the most common cause of cancer death, fiber-based systems are more practical. In this paper, we present our results of dual-modality systems based on double-clad fibers, pump-signal combiners and tapered-end fibers for pulmonary airways imaging. Owing to the large effective area, these components can efficiently collect fluorescence light at the endoscope tip. We present and compare results from in vivo and ex vivo dual-modality AF-OCT systems.

8565-98, Session 1

OCT imaging in chronic obstructive pulmonary disease

Keishi Ohtani M.D., Rosa Lopez-Lisbona M.D., Anthony M. Lee, Daryl Chulho Hyun, Tawimas Shaipanich M.D., Annette M. McWilliams M.D., Pierre M. Lane, The BC Cancer Agency Research Ctr. (Canada); Harvey O. Coxson, Vancouver General Hospital (Canada); Calum E. MacAulay, Stephen Lam M.D., The BC Cancer Agency Research Ctr. (Canada)

Introduction: A recent ex-vivo study using micro-CT in patients with chronic obstructive pulmonary disease (COPD) showed that narrowing and disappearance of small conducting airways precedes the onset of emphysematous destruction in COPD. Until recently, the airway remodeling process could not be studied in detail in-vivo. In this study, we investigated the repeatability of navigating an Optical Coherence Tomography (OCT) catheter to image the same airways in smokers with and without COPD.

Method: OCT imaging was performed by inserting the catheter through a sub-segmental airway to a small bronchiole. Three-dimensional OCT imaging of 5 cm of airway segments was obtained. The catheter was removed and reinsertion into the same airway was attempted. The number of airway generations and quantitative measurements of the airway wall area were investigated.

Results: Sixty-three airways in 30 subjects were analyzed. Repeated insertion into the same airway was observed at 53.8 %, 92.3% and 70.8% of the time in the upper, middle and lower lobes respectively. The percentage differences of paired measurements of airway wall area between matched and unmatched airways in bronchioles were 5.8 ± 4.6 % and 7.3 ± 5.4 % respectively.

Conclusions: Repeated OCT imaging of airways is possible in the majority of cases except in the upper lobes. For airways that are not completely matched, some of the airway segments can still be used for comparison by careful alignment of the airway. OCT may be a useful method to study the remodeling process in small airways and the effect of therapeutic intervention.

8565-99, Session 1

Characterization of pre-neoplastic and neoplastic bronchial lesions using laser Raman spectroscopy

Hanna C. Pawluk, Michael A. Short, Stephen Lam M.D., Annette M. McWilliams M.D., Tawimas Shaipanich M.D., The BC Cancer Agency Research Ctr. (Canada); Diana N. Ionescu, The Univ. of British Columbia (Canada); Haishan Zeng, The BC Cancer Agency Research Ctr. (Canada)

Autofluorescence bronchoscopy has a high sensitivity but low specificity for localization of pre-neoplastic lesions and early bronchial cancers. Previously we have shown that addition of a point laser Raman spectroscopy (LRS) measurement increased the specificity to over 90% for differentiating high grade dysplasia and carcinoma in situ from benign lesions with little loss is sensitivity. We have also described improvements to this laser Raman spectroscopy system, including the incorporation of the latest charge coupled device to result in decreased noise and greater collection sensitivity for the inherently weak Raman signal emissions. Here, we build on the initial success of the pilot study, by expanding our sample size to 267 additional measurement sites using the improved Raman system. It was found that the sensitivity and specificity of the new generation system remain similarly high with the larger sample cohort.

8565-100, Session 1

Monitoring the response to segmental allergen challenge in allergic asthmatics

Melissa J. Suter, Matthew B. Applegate, Alyssa J. Miller, Daniel Hamilos M.D., Josalyn L. Cho, R. Scott Harris, Alex C. Chee, Khay M. Tan, Andrew D. Luster, Benjamin D. Medoff, Massachusetts General Hospital (United States) and Harvard Medical School (United States)

Asthma is a chronic inflammatory condition that is characterized by airway inflammation, remodelling and hyperresponsiveness. However, the exact mechanisms behind the pathophysiology of asthma remain uncertain. Eleven allergic asthmatic and fourteen allergic non-asthmatic volunteers were enrolled in this study. OFDI imaging was conducted in entire airway segments immediation prior to, and 24 hours post, titrated allergen delivery. Our results indicate that the asthmatic subjects have a greater baseline mucosal thickness than the non-asthmatic subject. Post allergen results reveal that both the allergic asthmatics and allergic non-asthmatics experience significant bronchoconstriction when compared to baseline values. There was no statistical difference in post allergen mucosal thickness values between groups.

8565-101, Session 2

Flexible transbronchial optical frequency domain imaging smart needle for biopsy guidance

Khay M. Tan, Alex C. Chee M.D., Milen Shishkov, Lida P. Hariri, Matthew B. Applegate, Brett E. Bouma, Melissa J. Suter, Massachusetts General Hospital (United States)

Lung cancer is the leading cause of cancer related death. Macroscopic imaging techniques such as computed tomography are highly sensitivity at detecting small, ≤ 2cm, peripheral pulmonary lesions (PPLs) in the lung but lack the specificity necessary for diagnosis. Transbronchial needle aspiration (TBNA) is a procedure routinely performed to diagnose PPLs but is hindered with a low diagnostic yield due to inappropriate needle placement. We have developed a flexible transbronchial optical frequency domain imaging (TB-OFDI) catheter that functions as a 'smart needle' to confirm the needle placement within the target lesion prior to biopsy. The TB-OFDI smart needle consists of a flexible and OFDI catheter that operates within a standard 21-gauge TBNA needle. The OFDI catheter can be easily removed from the needle to facilitate subsequent aspiration or biopsy acquisition. The OFDI imaging core consists of an angled-polished ball lens with a spot size of 25 μm at a working distance of 160 μm from the catheter sheath. The ball-lens was designed to have an ellipsoid shape in order to compensate for the astigmatism caused by encasing the optics within a protective sheath. Transbronchial imaging of inflated excised swine lung parenchyma with the TB-OFDI smart needle yielded clear images of alveoli. In-vivo transbronchial imaging was also performed on three swine with artificial lesions injected transthoracially. Our results suggest that the TB-OFDI smart needle may be a useful tool for guiding biopsy acquisition to increase the diagnostic yield of PPLs.

8565-102, Session 2

Endoscopic fluorescence-guidance system for lung cancer surgery: monitoring ICG with or without human serum albumin premixing

Yujin Oh, Korea Univ. (Korea, Republic of); Yuhua Quan, Hyun Koo Kim, Korea Univ. College of Medicine (Korea, Republic of); Beop-Min Kim, Korea Univ. (Korea, Republic of)

Near infrared (NIR) fluorescence endoscopic imaging system has been developed for detection of sentinel lymph node (SLN) during lung cancer surgery. The system provides both color and IR fluorescence images simultaneously, which are overlaid for clear visualization of the dye activities. It was found that the SLN was clearly visible in the rat thigh and the pig lung using our system. We monitored perfusion of the Indocyanine green (ICG) only and ICG molecules pre-mixed with human serum albumin (ICG-HSA). Fluorescence signal intensity to background ratio at SLN for both dyes were estimated and compared. Our results indicate that both dyes provide similar retention at SLN and premixing of ICG with HAS makes little difference in in vivo studies. Our system is currently under optimization process and will be used for clinical studies in the near future.

8565-103, Session 2

Diffuse optical spectroscopy monitoring of pulmonary physiological and metabolic effects of combined smoke-cyanide exposure

Jangwoen Lee, Beckman Laser Institute and Medical Clinic (United States); Sasan Sain, Univ. of California, Irvine School of Medicine (United States); David Mukai, David Yoon, Sari Mahon, Beckman Laser Institute and Medical Clinic (United States); Gerry R. Boss, Univ. of California, San Diego (United States); Matthew Brenner, Univ. of California, Irvine (United States) and Pulmonary and Critical Care Medicine Div., Univ.of California, Irvine Medical Ctr. (United States)

Smoke inhalation is the major cause of death in fire victims. Combined cyanide and carbon monoxide poisoning is frequent in smoke inhalation victims, and mortality correlates more closely with cyanide levels than carbon monoxide exposure levels. There is currently no available treatment for mass casualty cyanide exposure, since treatment of individual victims requires administration of intravenous antidotes, and some antidote agents are contraindicated in smoke inhalation. Additionally, there is no adequate monitoring modality since the onset of cyanide poisoning is rapid and the presence of cyanide in blood is not easily measured by current in-vivo rapid assay technology. We have previously demonstrated that non-invasive diffuse optical spectroscopy (DOS) can be used to detect the physiologic events occurring during development of CN toxicity in an animal model and we are developing a novel cyanide antidote, cobinamide, which could be administered intravenously or intramuscularly in mass casualty cyanide poisoning scenarios. Six ventilator-supported New Zealand white rabbits were exposed to cold smoke breaths until toxic carbon monoxide levels were achieved (~30%), concurrent with intravenous cyanide infusion (0.167mg NaCN in 0.9% NaCl/min for 60 minutes). Animals were monitored with continuous gas exchange, hemodynamics, blood gases, cyanide levels, and DOS, providing tissue oxy-and deoxyhemoglobin and cytochrome c oxidase redocx state measures in vivo. Cobinamide was then injected intramuscularly for the reversal of cyanide. DOS was capable of monitoring the relevant physiological changes during smoke-cyanide exposure and cobinamide treatment. Intramuscular cobinamide injection shows promise as a potential antidote for cyanide poisoning in smoke inhalation exposure.

8565-104, Session 2

High speed three dimensional endoscopic optical frequency domain imaging for lung cancer diagnosis

Jianan Li, Jianhua Mo, Frank Helderman, Mattijs de Groot, Johannes F. de Boer, Vrije Univ. Amsterdam (Netherlands)

We present here a high speed three dimensional endoscopic optical frequency domain imaging (OFDI) system with a miniature motorized probe. With a 1.65 mm outer diameter and a rotation speed of 3,000 – 12,500 rpm, this is the smallest motorized high speed OCT probe to our knowledge.

The motorized distal end provides a significant advantage over proximally driven probes since it does not require a drive shaft to transfer the rotational torque to the distal end and functions without a fiber rotary junction, therefore might reduce non-uniform rotation distortion (NURD) and enable higher scanning speeds.

The probe has a focal Full Width at Half Maximum of 9.6 μm and a working distance of 0.47 mm. Integrated in a high-speed OFDI setup at 1310 nm, it is capable to acquire 3D high resolution images in real time. We demonstrated its performance with preliminary ex vivo and in vivo images of porcine bronchial through the working channel of a human bronchoscope. Its small dimension allows getting deeper into smaller bronchiole branches. Future work includes developing polarization sensitive and Doppler imaging functions as well as development of multimodality systems for early diagnosis of lung cancer.

8565-105, Session 3

Four-dimensional visualization of healthy and diseased subpleural alveolar dynamics in vivo

William C. Warger II, Eman Namati, Massachusetts General Hospital (United States); Carolin I. Unglert, Massachusetts General Hospital (United States) and Air Liquide (France); Alex C.

Chee M.D., Univ. of Calgary (Canada); Brett E. Bouma, Guillermo J. Tearney M.D., Massachusetts General Hospital (United States)

Pulmonary alveoli are sacs that terminate the distal airways within the lung and are responsible for the exchange of oxygen and carbon dioxide during the respiratory cycle. While this process is crucial to sustaining life, no unifying hypothesis exists for mechanical alveolar changes during respiration, thereby limiting the ability to provide prognostic indicators and treatment of alveolar-based injuries and diseases. The uncertainty of alveolar mechanics is based on the miniature size of alveoli (100-300 ?m in diameter for humans) and the constant motion during respiration that has prevented three-dimensional imaging techniques, such as CT and MRI, from visualizing continuous alveolar dynamics in vivo. Optical techniques have provided much of the knowledge of alveolar dynamics, but these analyses have been limited to a single en-face plane. Recently, however, optical coherence tomography (OCT) techniques have shown promise for imaging and measuring three-dimensional volumes of alveoli in vivo. Here we present a comparison of healthy and emphysematous subpleural alveolar dynamics within living swine ventilated at 4-20 cmH2O. Preliminary results indicate a significant difference (p=0.0003) between the maximum volume of the healthy (0.27 nl (0.13,0.80)) and emphysematous (1.3 nl (0.64,1.98)) alveolar air spaces, reported as median (25th, 75th percentiles). A significant difference (p=0.0007) was also observed between the maximum percentage change in volume of healthy (82% (54,144)) and emphysematous (44% (36,66)) alveolar air spaces. These results demonstrate the ability of OCT to visualize and quantify four-dimensional alveolar dynamics to provide insight and knowledge into the mechanics for both healthy and diseased alveoli.

8565-106, Session 3

Three-dimensional ultrahigh-resolution optical coherence tomography imaging of lung tissues

Shutaro Ishida, Norihiko Nishizawa, Nagoya Univ. (Japan); Masashi Kitatsuji, Hiroyoshi Ohshima, HOYA Corp. (Japan); Miyoko Matsushima, Tsutomu Kawabe, Nagoya Univ. (Japan)

We have been investigating ultrahigh resolution optical coherence tomography (UHR-OCT) imaging of lung tissues using fiber based super continuum (SC) sources. The high power, low-noise, Gaussian shaped SC generated with ultrashort pulses and optical fibers at several wavelength regions were used as the broadband light sources for UHR-OCT. Since the lung connsists of tiny alveoli which are separeted by thin wall, the UHR-OCT is supposed to be effective for lung imaing. The normal and disease lung tissues were observed without invasive procedures to the lung itself. The clear images of alveoli were observed with index matching effect by saline.

In this work, we investigated the three-dimensional UHR-OCT imaging of lung structure. The lung of mouse and rat inflated with 5 cmH2O, 15 cmH2O, and 20 cmH2O air pressure were prepared as the sample for investigation of size and shape of the lung structure. These sampels were fixed with paraformaldehyde. A thin wall, the interveolar septum separating the alveoli was clearly observed. The difference of size and shape of alveoli and thier three-dimensional network was clearly observed from the UHR-OCT images. The clear images of alveoli were observed with index matching effect of paraformaldehyde. We investigated the wavelength dependence of 3D UHR-OCT image of lung structure at 800 nm, 1060 nm, and 1300 nm wavelength regions. The 3D UHR-OCT images of lung structure of rat were clearly observed in all wavelength regions and wavelength dependence of imaging contrast was observed.

8565-107, Session 3

Absolute measurements of subpleural alveolar compliance in vivo using OCT and model-based refraction correction

Carolin I. Unglert, Wellman Ctr. for Photomedicine (United States) and Air Liquide (France); William C. Warger II, Massachusetts General Hospital (United States); Eman Namati, Wellman Ctr. for Photomedicine (United States) and Massachusetts General Hospital (United States) and Harvard Medical School (United States); Jeroen Hostens, Bruker microCT (Belgium); Reginald Birngruber, Univ. zu Lübeck (Germany); Brett E. Bouma, Guillermo J. Tearney, Wellman Ctr. for Photomedicine (United States)

Accurate visualization and quantification of alveolar volume changes is crucial to advance our understanding of normal and diseased alveolar physiology. Optical coherence tomography (OCT) has been used increasingly to visualize mammalian pulmonary alveoli, but refraction artifacts hinder the measurement of absolute volumes and important physiologic parameters such as alveolar compliance.

We have compared measurements of fixed, air-filled subpleural alveoli obtained from OCT and micro-CT images and found that the alveoli were best generalized by a superellipse cross section within the micro-CT images, and OCT volumes underrepresent the absolute alveolar volume depending on the height/width ratio (form factor f) of the alveolar airspace. A two-dimensional ray-tracing model, which calculates the refraction of light through superellipse cross sections, confirmed the form factor dependence of the error (E_pred) by: E_pred= -8.655*f^2 + 39.06*f + 6.154*f*n +27.09*n-40.94, where n is the refractive index of the tissue. The rescaling of the fixed, air-filled swine alveoli based on f and OCT measurements of n reduced the error in overall volume measurements from 40 % to 9%. We further adopted the same approach for the analysis of 60 alveoli measured from four-dimensional OCT images acquired in-vivo to calculate a measure of alveolar compliance. Over the evaluated intratracheal pressure range of 3 to 20 cmH2O, the absolute change in alveolar volume was 8.0 pl/cmH2O on average.

In this study, we have shown that absolute measurements of alveolar volumes can be approximated from OCT images when corrected for refraction effects. This enabled quantification of alveolar volumes and compliance in-vivo.

8565-108, Session 3

Improved in situ imaging of alveoli with a side-facing OCT needle probe

Bryden C. Quirk, Robert A. McLaughlin, Alex M. Pagnozzi, Brendan F. Kennedy, Peter B. Noble, David D. Sampson, The Univ. of Western Australia (Australia)

Many lung diseases affect the structure of alveoli and the smaller airways. We are developing new techniques utilizing OCT needle probes for in situ lung imaging. We have developed a side-facing, OCT needle probe capable of imaging lung parenchyma located several centimeters below the lung surface. The all-fiber focusing optics consists of no-core and GRIN fiber, and a small mirror to redirect the light. The probe is attached to a common-path swept-source OCT system and mounted on a stepper motor for rotation and retraction. Multiple data sets were acquired on isolated sheep lungs, demonstrating the ability to image individual alveoli and bronchioles.

8565-109, Session 4

Measuring cystic fibrosis mucus viscosity using micro-optical coherence tomography

Bradford J. Diephuis, Massachusetts General Hospital (United States) and Harvard Medical School (United States); Eric Wilsterman, Linbo Liu, Kengyeh K. Chu, Kevin Boehm, Massachusetts General Hospital (United States); Alex Smith, Yao Li, Grace Houser, The Univ. of Alabama at Birmingham (United States); Gregory Dierksen, Massachusetts General Hospital (United States); Steven M. Rowe, The Univ. of Alabama at Birmingham (United States); Guillermo J. Tearney M.D., Massachusetts General Hospital (United States)

It is well established that the ion transport abnormalities affect mucus viscosity in cystic fibrosis (CF) afflicted airways. Investigation of mucus viscosity is therefore an active component of the research on the pathogenesis and treatment of CF. Past research has measured mucus viscosity using either bulk rheometers or microscopic fluorescent particle tracking. Here we introduce a method for measuring viscosity using Micro-Optical Coherence Tomography (μOCT), our recently developed form of OCT that has sufficient resolution to track either exogenous beads or endogenous inclusions in the mucus.

Our μOCT technology is capable of visualizing particles as small as 500nm at high frame rates (40 fps). As in fluorescent particle tracking micro-rheology, dynamic viscosity is computed by measuring the mean squared displacement of particles in the mucus and applying the generalized Stokes-Einstein relationship. Particles are tracked using a standard centroid-locating algorithm.

We validated our methodology on dextran solutions of varying concentrations with exogenous 500nm beads, which yielded strong concordance with published data. Furthermore, we were able to locate and track native micron-scale particles in human mucus with sufficient accuracy to distinguish CF from wild type mucus based solely on viscosity. ($p<.05$, $n=5$) Preliminary results suggest that this method can be performed in the presence of transverse motion, such as that seen in mucus flow in vivo, by subtracting the bulk motion vector from all particle tracks.

Because endogenous particles can be used, μOCT rheology provides two key benefits over current fluorescent particle tracking methods. Our methodology both eliminates the potential for interactions between mucus and exogenous particles as a source of error and enables the measurement of viscosity in situations where addition of fluorescent beads is not feasible, including in vivo applications.

8565-110, Session 4

Imaging of the mouse lung with scanning laser optical tomography

Marko Heidrich, Laser Zentrum Hannover e.V. (Germany); Manuela Kellner, Rebecca Beigel, Hannover Medical School (Germany); Raoul-Amadeus Lorbeer, Laser Zentrum Hannover e.V. (Germany); Lars Knudsen, Medizinische Hochschule Hannover (Germany); Tammo Ripken, Laser Zentrum Hannover e.V. (Germany); Alexander Heisterkamp, Friedrich-Schiller-Univ. Jena (Germany); Heiko Meyer, Laser Zentrum Hannover e.V. (Germany); Mark P. Kühnel, Matthias Ochs, Hannover Medical School (Germany)

New optical techniques have the potential to fill the gap between radiological and microscopic approaches to assess the lung's internal structure. If an imaging method should allow for quantitative assessment of lung structure, it needs to fulfill the requirements of unbiased sampling and measurement principles in the whole lung. Therefore, access to the whole lung for imaging purposes while providing sufficient resolution for visualizing details is important. To address this request, we applied Scanning Laser Optical Tomography (SLOT) for the three dimensional imaging of mouse lung ex vivo. SLOT is a highly efficient fluorescence microscopy technique allowing for 3D imaging of specimen of sizes up to several millimeters. In this study, previously fixed lung lobes were optically cleared and subsequently imaged with SLOT while making use of intrinsic contrast mechanisms like absorption and autofluorescence. Here, we demonstrate imaging of airways, blood vessels and parenchyma from whole mouse lung lobes with an optical resolution down to the level of single alveoli. The internal structure of the lung can be analyzed non-destructively and quantitatively in 3D datasets in any preferred planar orientation. Moreover, the procedure preserves microscopic structure of the lung and allows for subsequent correlative histologic studies. In summary, the study has shown that SLOT is a useful technique to visualize and survey the internal structure of mouse lung. Potential applications of SLOT in lung research are e.g. quantitative phenotype analysis of mouse models of human lung disease in combination with stereological methods.

8565-111, Session 4

Visualizing neutrophil trans-epithelial migration using μOCT

Linbo Liu, Massachusetts General Hospital (United States) and Harvard Medical School (United States); Wayne G. Shreffler, Gregory Dierksen, Mark E. Kusek, Eric Wilsterman, Kengyeh K. Chu, Bryan P. Hurley, Guillermo J. Tearney M.D., Massachusetts General Hospital (United States)

Integral to the effective functioning of neutrophils in host defense in the lung and other organs is their ability to egress from the vasculature and migrate through tissues including across mucosal epithelial barriers to sites of infection. While neutrophil trans-epithelial migration in the context of an inflammatory response is inherently beneficial for pathogen clearance, there is compelling evidence from observations in humans and in experimental models that in pathologic circumstances, neutrophils can serve as primary perpetrators of inflammatory injury to the mucosal surface. An imaging tool that can visualize this process at the cellular level without the aid of contrast agent will facilitate the understanding of this process in vivo and will likely provide new insights into developing organ-specific treatment strategies to reduce the deleterious consequences of mucosal inflammation.

μOCT is a reflectance micro-endoscopic tool developed in our lab that provide cross-sectional images of untreated tissue with a spatial resolution of 1-2 micron and a penetration depth of 300 um. The μOCT desktop system was used to image neutrophil migration across cultured respiratory, intestinal, and esophageal epithelial cells induced by chemoattactant or bacterial infection without any special preparation or use of exogenous contrast agent. The transmigration process was monitored at video rate (40 Hz) in the cross-sectional plane, or using 3D scan at 40images/hour. Epithelium and individual neutrophils can be clearly visualized and distinguished, and individual neutrophils can be tracked throughout the entire transmigration process.

Our results indicate that μOCT is capable of imaging neutrophil trans-epithelial migration at the cellular level in 3D (video rate cross-sectional) and 4D (3D + time). Further development of an in vivo imaging probe will facilitate evaluation of new treatment strategies to combat mucosal inflammatory diseases in humans.

8565-112, Session 4

Multi-scale fluorescence imaging of bacterial infection of the lung

Joel N. Bixler, Ying Kong, Jeffrey D. Cirillo, Kristen C. Maitland, Texas A&M Univ. (United States)

Tuberculosis, caused by Mycobacterium tuberculosis (Mtb), currently affects roughly one third of the world's population. Drug resistant strains

of Mtb decrease the effectiveness of current therapeutics and demand the development of new antimicrobial therapies. In addition, the current vaccine, Bacille Calmette Guérin (BCG), has been shown to be at best 80% effective in disease prevention. Current animal studies are often limited by sacrifice at discrete time points and tissue homogenization, which greatly reduce spatial and temporal resolution. Optical imaging offers the potential for a minimally-invasive solution to imaging on a macroscopic and microscopic scale, allowing for high resolution study of infection.

We have integrated a fluorescence microendoscope into a Caliper IVIS Lumina II whole-animal optical imaging system, allowing for simultaneous microscopic and macroscopic imaging of tdTomato expressing BCG in vivo. A 535 nm LED was collimated and launched into a 10,000 element fiber bundle with outer diameter of 0.66 mm. Fluorescent emission is then collected by the bundle and imaged onto the surface of a CCD camera. The fiber bundle can be inserted through an intra-tracheal catheter into the lung of a mouse, allowing for imaging of bacteria fluorescence with a 450 um field of view and 3 um resolution. Whole-body images can be collected simultaneously, allowing for multi-scale imaging. Results from microendoscopic imaging indicate the potential to detect and image bacterial infections down to 100 colony forming units. This novel imaging technique has the potential to allow for functional studies, enhancing the ability to assess new therapeutic agents.

8565-113, Session 4

3D functional imaging of lung vasculature using Doppler optical coherence tomography

Anthony M. Lee, Hamid Pahlevaninezhad, Daryl Chulho Hyun, Keishi Ohtani, Rosa Lopez Lisbona, Tawimas Shaipanich, Annette M. McWilliams, Stephen Lam, Calum E. MacAulay, The BC Cancer Agency Research Ctr. (Canada); Victor X. D. Yang, Ryerson Univ. (Canada); Pierre M. Lane, The BC Cancer Agency Research Ctr. (Canada)

Remodeling of the bronchial and pulmonary vasculature architecture is important in the pathogenesis of diseases such as asthma, chronic obstructive pulmonary disease (COPD), and lung cancer. Additionally, the detection and avoidance of larger blood vessels are necessary in procedures such as biopsy and airway bypass. However, there is a dearth of methods that can detect and map bronchial and pulmonary vasculature in vivo. Here we present a new instrument that uses Doppler optical coherence tomography (DOCT) for functional imaging of lung vasculature. DOCT not only allows for location of vasculature within the surrounding tissue, but also allows for time-course monitoring of natural blood flow or blood flow changes in response to intervention.

Our Doppler OCT instrument consists of a 50.4kHz, 1310nm-centered swept source laser, and a side-looking, rotating 0.9mm diameter fiber optic probe. Frame rates up to 100Hz, and pullbacks, and hence imaging volumes up to 50mm in length are possible with our probes. In vivo imaging is performed by passing the probe down the instrument channel of a standard bronchoscope. DOCT image acquisition and processing parameters are explored to optimize vascular imaging.

8565-114, Session 5

Pulmonary pathology *(Invited Paper)*

Lida P. Hariri, Massachusetts General Hospital (United States)

No Abstract Available

8565-115, Session 5

Quantitative label-free multimodality nonlinear optical imaging for in situ differentiation of cancerous lesions

Xiaoyun Xu, Xiaoyan Li, Jie Cheng, The Methodist Hospital Research Institute (United States); Zhengfan Liu, The Methodist Hospital Research Institute, System Medicine and Bioengineering Department (United States); Michael J. Thrall, Xi Wang, Xu Chen, Zhiyong Wang, Stephen T. C. Wong, The Methodist Hospital Research Institute (United States)

The development of real-time, label-free imaging techniques has recently attracted research interest for in situ differentiation of cancerous lesions from normal tissues. Different molecule-specific intrinsic contrast can arise from label-free imaging techniques such as Coherent Anti-Stokes Raman Scattering (CARS), Two-Photon Excited AutoFluorescence (TPEAF), and Second Harmonic Generation (SHG), which, in combination, would hold the promise of a powerful label-free tool for cancer diagnosis. Among cancer-related deaths, lung carcinoma is the leading cause among both sexes. Although early treatment can increase the survival rate dramatically, lesion detection and precise diagnosis at early stage is unusual due to its asymptomatic nature and limitations of current diagnostic techniques that make screening difficult. We investigated the potential of using multimodality nonlinear optical microscopy that incorporates CARS, TPEAF, and SHG techniques for differentiation of lung cancer from normal tissue. Fresh cancerous and non-cancerous lung tissue samples from patients were imaged using CARS, TPEAF, and SHG for comparison. These images showed good pathology correlation with hematoxylin and eosin (H&E) stained sections from the same tissue samples. Further, images at various penetration depths were recorded showing the three-dimensional morphologies of tumor cell nuclei using CARS, elastin using TPEAF, and collagen using SHG. Next, a classification algorithm was developed to quantitatively extract the above features and utilize them to separate normal from cancerous lesions. Our results indicate that via real-time morphology and classification analyses, a multimodality nonlinear optical imaging platform potentially offers a powerful minimally-invasive way to differentiate cancer lesions from surrounding non-tumor tissues in-vivo for clinical applications.

8565-116, Session 5

Pre-clinical study: use of full-field OCT to distinguish between malignant human lung tissue and adjacent tumor-free areas

Sushmita Mukherjee, Manu Jain, Bekheit Salomoon, Navneet Narula, Nasser Altorki, Weill Cornell Medical College (United States); Fabrice Harms, LLTECH SAS (France); Katharine Grieve, Institut Langevin (France); Bertrand Le Conte De Poly, LLTECH SAS (France); A. Claude Boccara, Institut Langevin (France) and LLTech SAS (France)

Full-field OCT (FFOCT) differs from traditional OCT in that en face tissue slices are captured using a CMOS camera and a pair of immersion microscope objectives of relatively high numerical aperture, which provide high lateral and axial resolution (1?m in three dimensions). Native field size is 1mm2, and stitching allows the capture of large fields, up to 25mm in diameter. 3D image stacks are obtained by stepping through the depth of the sample. FFOCT does not require exogenous contrast; it uses the back-scattered light due to refractive index variations in the tissue as a source of endogenous contrast.

Here we present FFOCT imaging results from 13 fresh (unprocessed and unstained) human lobectomy specimens. From each specimen, two sections were procured: tumor and adjacent tumor-free lung tissue. After FFOCT imaging, all specimens were processed for routine H&E histopathology, and the images were compared.

In tumor-free lung tissue, all normal components of lung such as alveoli, blood vessels and pleura were readily identified with FFOCT. In contrast, areas with tumor showed either clusters of cells with recognizable lung architecture or complete loss of normal lung architecture (replaced by sheets of cells). Presence of tumor was correctly identified in 94% of the stacks. In one case, bronchioalveolar carcinoma (adenocarcinoma with lepidic-predominant pattern) was diagnosed as “equivocal”. In tumor-free lung, absence of tumor was reported with confidence in 50% of the stacks, while the rest was considered “equivocal”. This false positive diagnosis was mainly encountered in areas with a collapse of the lung architecture.

8565-117, Session 5

Optical frequency domain imaging of peripheral lung nodules

Lida P. Hariri, Matthew B. Applegate, Mari Mino-Kenudson, Eugene J. Mark, Michael Lanuti, Colleen L. Channick, Guillermo J. Tearney M.D., Melissa J. Suter, Massachusetts General Hospital (United States)

Peripheral lung nodules frequently require transbronchial needle aspiration (TBNA) for diagnosis, which have variable diagnostic yields. Confirmation of needle placement within the nodule during TBNA could significantly enhance diagnostic yield. Needle-based optical frequency domain imaging (OFDI) provides non-destructive, high-resolution microstructural images of tissue with potential to distinguish nodules from adjacent parenchyma. Needle-based OFDI catheters compatible with standard bronchoscopic TBNA have been developed, but diagnostic criteria are required for peripheral nodules. We developed and validated OFDI criteria for peripheral nodules and lung parenchyma in ex vivo lung resection specimens. OFDI criteria for lung parenchyma and peripheral nodules were developed and validated in 111 ex vivo resection specimens in a blinded assessment with 6 independent readers (two pathologists, pulmonologists, and OFDI experts). All readers received a 15 minute training session with a single example each of lung parenchyma and peripheral nodule. Lung parenchyma images show signal-void alveolar spaces with signal-intense backreflections at tissue-air interfaces. Peripheral nodules were characterized by more homogeneous appearances, which lacked both signal-void alveolar spaces and signal-intense intense backreflections. Independent validation of OFDI criteria by pulmonologists, pathologists, and OFDI experts yielded a sensitivity and specificity of 93.5 and 97.3%, 93.5 and 98.2%, and 99.1 and 99.1%, respectively. The overall sensitivity and specificity were 95.4 and 98.2%, respectively. We have developed and validated OFDI criteria for peripheral nodules and lung parenchyma, achieving sensitivity and specificity > 95%. Needle-based OFDI has strong potential as a complementary imaging modality to confirm needle placement during TBNA and potentially increase diagnostic yield.

8565-118, Session 5

Polarization-sensitive optical frequency domain imaging: identifying fibrosis in peripheral lung nodules

Lida P. Hariri, Martin L. Villiger, Matthew B. Applegate, Khay M. Tan, Mari Mino-Kenudson, Eugene J. Mark, Brett E. Bouma, Melissa J. Suter, Massachusetts General Hospital (United States)

Bronchial biopsy and transbronchial needle aspiration (TBNA) can be limited by insufficient diagnostic tissue, which is in part due to the presence and inadvertent biopsy of tumor-associated fibrosis. The ability to target high-yield tumor-rich tissue during bronchoscopy is likely to improve diagnostic yield. Polarization sensitive OFDI (PS-OFDI) generates high resolution microstructural images while simultaneously measuring tissue birefringence. PS-OFDI could dramatically increase diagnostic tissue yield by identifying regions of tumor and differentiating from tumor-associated fibrosis. PS-OFDI was obtained in ex vivo lung resection specimens with either a custom-built bronchoscopic 2.4 Fr (0.8mm diameter) helical scanning catheter or a dual-axis bench top scanner. On structural OFDI, carcinomas exhibited architectural disarray, loss of normal airway/alveolar structures, and rapid light attenuation. In cases of solid, poorly-differentiated carcinomas with adjacent fibrosis, the distinction between tumor and fibrosis was not clear with structural OFDI alone. However, PS-OFDI demonstrated strong birefringence in fibrotic regions and little to no birefringence in the areas of carcinoma. Tumors with admixed early, loosely-organized desmoplastic fibrosis showed mild to moderate birefringence, and tumors with little connective tissues showed little to no birefringent signal. This study is the first demonstration of PS-OFDI in pulmonary pathology. Although this work is preliminary, it highlights the potential of PS-OFDI to provide additional insights into the tissue composition than is currently appreciable in standard structural OFDI images. The ability to identify tumor and differentiate from tumor-associated fibrosis during bronchoscopic biopsy and TBNA could be used to guide biopsy site selection and increase diagnostic tumor yield.

8565-119, Session 6

Quantitative optical imaging of impaired ciliary flow performance using a microfluidic chip-based mixing assay

Stephan Jonas, Yale Univ. (United States) and RWTH Aachen (Germany); Elaine Zhou, Engin Deniz M.D., Yale Univ. (United States); Brendan Huang, Yale School of Medicine (United States); Yu Wu, Rong Fang, Yale Univ. (United States); Mustafa K. Khokha M.D., Michael A. Choma M.D., Yale School of Medicine (United States)

Motile cilia continuously transport mucus out of the lungs. We hypothesize that intermediate levels of ciliary dysfunction, dysfunction that is undetectable by current diagnostics, is a major modifier of common respiratory diseases. Here, we analyze cilia-driven flow performance by quantifying cilia-driven microfluidic mixing as an integrated readout for cilia function. We fabricated a PDMS microfluidic chip with the following design specifications: (i) controlled delivery of flow contrast agent into a mixing well containing a ciliated sample, (ii) multiple inflow channels for the delivery of flow contrast agents and drugs, (iii) securing of ciliated samples using suction, and (iv) reusability. We used ciliated Xenopus embryos as a genetically manipulable ciliated surface. Flow was seeded with dye and mixing was imaged using videomicroscopy. We used a novel angiography-like preprocessing resulting in background-free images without the need for a key reference frame or fluorescence microscopy. Since mixing can be seen as a disordering process, Shannon information entropy was used to quantify mixing efficiency. Our preliminary results show that mixing efficiency is inversely proportional to fluid viscosity, that is, higher fluid viscosities lead to less efficient mixing. Reduced mixing efficiency was ascertained by: (i) subjective evaluation of mixing movies, (ii) comparison of entropy vs. time curves at different viscosities, and (iii) quantification of mixing efficiency using the rate of change of entropy as a readout measure. Ongoing work includes using the mixing assay as a complementary method to quantitative OCT flow imaging in understanding the different genetic determinants of ciliary flow performance.

8565-120, Session 6

Automated micro-optical coherence tomography image processing for cystic fibrosis

Bradford J. Diephuis, Massachusetts General Hospital (United States) and Harvard Medical School (United States); Christine P. Fleming, Linbo Liu, Massachusetts General Hospital (United States); Steven M. Rowe, The Univ. of Alabama at Birmingham (United States); Guillermo J. Tearney M.D., Massachusetts General Hospital (United States)

Airway surface liquid (ASL) depth, periciliary layer (PCL) depth, ciliary beat frequency (CBF) and mucociliary transport rate (MCT) have been identified as important functional parameters in cystic fibrosis (CF). Using our laboratory's high-resolution (1 ?m) Micro-Optical Coherence Tomography (?OCT) technology, we have previously described manual measurements of ASL depth, PCL depth, CBF and MCT in CF cell cultures and swine tissue. We now present methods for automated algorithmic measurement of these parameters.

Automated ASL depth measurement is performed using a Laplacian of Gaussian edge-detection algorithm that detects the apical border of epithelial cells and the top of the mucosal secretion. Images are pre-processed by time-averaging over 40 frames to reduce false edge detection due to flowing microparticles or transient noise. Work is ongoing to similarly automate the measurement of PCL depth.

CBF measurement utilizes the same edge detection algorithm to identify the ciliary region of interest on the apical border. A Fourier transform of pixel intensities on each 3?mx3?m segment within this region of interest is performed. Regions of active ciliary motion show frequency peaks, which are identified using standard peak detection algorithms to yield CBF. MCT is computed using 2D-cross correlation to track the movement of microparticles undergoing transverse motion, using the circular Hough transform to identify trackable particles.

We compared our automated results to manual measurement on 6 data sets of CF and wild-type cell cultures. We found agreement within 95% for ASL and MCT and 90% for CBF on all datasets and a paired t-test showed no significant difference between the methods. Compared to manual measurement, automated calculation both provides more reproducible values and enables the usage of these parameters in a high-throughput drug screen.

8565-121, Session 6

High throughput screening of primary airway epithelial cells in culture using µOCT

Kengyeh K. Chu, Linbo Liu, Massachusetts General Hospital (United States); Grace Houser, The Univ. of Alabama at Birmingham (United States); Gregory Dierksen, Eric Wilsterman, Christine P. Fleming, Bradford J. Diephuis, Massachusetts General Hospital (United States); Steven M. Rowe, The Univ. of Alabama at Birmingham (United States); Guillermo J. Tearney M.D., Massachusetts General Hospital (United States)

It is well established that the primary defect in cystic fibrosis (CF) results in abnormal mucociliary clearance (MCC) associated with dysregulation of the airway surface liquid (ASL) depth. However, the study of CF has been limited by the absence of an imaging technology for visualizing the respiratory mucosa at the cellular level. Direct imaging of motile cilia, which effect the primary mechanism of mucociliary clearance in normal airways, would be particularly impactful. Such technology could facilitate the discovery of new treatments by providing a means to prioritize agents active against the ion transport defect. Recently, we established a new high-resolution cross-sectional optical reflectance imaging technique termed Micro-Optical Coherence Tomography (µOCT) for imaging respiratory mucosa in situ and primary human airway cells in vitro. Preliminary data using novel systems developed in our laboratory provided a spatial resolution of < 2 µm and a rate of 32 frames per second, capable of visualizing prominent and reproducible anatomic differences between CF and normal respiratory epithelia, including simultaneous measurements of collapsed ASL height, reduced cilia beat frequency (CBF), and delayed mucus transport in CF cells and tissues. In the present study, we have developed and tested a dedicated µOCT system suitable for moderately high throughput evaluation of primary human bronchial epithelial cells treated with various ion transport modulators.

Compared with its previous iteration, the new system incorporates further improvements in imaging sensitivity and frame rates, making high-speed image acquisition possible. We have incorporated an automated plate scanning system and implemented automated analytic methods. Our system acquires a 4-sec video at each of 3 different locations within a primary culture well and completes a full-plate scan of a 24-wells in 6 minutes. The new device has been tested and validated by simultaneously measuring ASL depth, CBF, mucus transport, and periciliary layer morphology during the application of known ion transport modulators. Results demonstrate that µOCT high-throughput screening is feasible and could define target compound profiles required to restore normal epithelial function.

8565-44, Session 1

Plaque Biomechanics

Seemantini K. Nadkarni, Harvard Medical School (United States)

No Abstract Available

8565-45, Session 1

Artery Tissue Characterization

Gijs van Soest, Erasmus MC (Netherlands)

No Abstract Available

8565-46, Session 1

Myocardial Optical Imaging

Christine P. Fleming, Columbia Univ. (United States)

No Abstract Available

8565-13, Session 2

Magnetomotive optical coherence tomography for the assessment of atherosclerotic lesions using ?v?3-targeted microspheres

Adeel Ahmad, Jongsik Kim, Marina Marjanovic, Eric J. Chaney, Jonathan Rasio, Zita Hubler, Joanne Li, Kenneth S. Suslick, Stephen A. Boppart M.D., Univ. of Illinois at Urbana-Champaign (United States)

Magnetomotive optical coherence tomography (MM-OCT) has been shown to generate dynamic contrast in OCT images by utilizing the nanoscale displacements of magnetic nano/micro particles induced by an external magnetic field. By modifying these magnetic agents to target specific molecules and cellular receptors, molecular-specific contrast can be generated in OCT. In this study, we engineered oil-filled microspheres with Nile red and magnetic nanoparticles encapsulated inside the core. These microspheres were functionalized with an RGD-peptide sequence to target the ?v?3 integrin receptor for the localization of atherosclerotic lesions. Using an atherogenic rabbit model, diseased aortas were extracted and individually placed in a custom-designed flow chamber. The microspheres were circulated through the aortas in the custom-built flow chamber at physiologically-relevant pulsatile flow rates, pressures, and temperature to mimic the conditions in the living rabbit. Catheter-based OCT imaging was performed during perfusion while MM-OCT, fluorescence confocal microscopy, and histology were performed on the ex vivo aorta specimens after perfusion. Results showed successful targeting of the functionalized microspheres to the atherosclerotic lesions, good co-registration across the imaging modalities, and the ability of these microspheres to significantly enhance image contrast using MM-OCT. Further studies are being conducted to find the optimum solenoid coil configuration required for in vivo applications and for detecting magnetic particles in a flowing medium, which can potentially enable in vivo catheter-based MM-OCT imaging.

8565-14, Session 2

Towards intracoronary polarimetry

Martin L. Villiger, Ellen Z. Zhang, Wellman Ctr. for Photomedicine (United States); WangYuhl Oh, KAIST (Korea, Republic of); Gijs van Soest, Heleen M. M. van Beusekom, Erasmus MC (Netherlands); Benjamin J. Vakoc, Wellman Ctr. for Photomedicine (United States); Seemantini K. Nadkarni, Harvard Medical School (United States); Brett E. Bouma, Wellman Ctr. for Photomedicine (United States)

Intracoronary Optical Frequency Domain Imaging (OFDI) provides detailed information on the microstructure of coronary vessels. Polarization sensitive (PS) measurements could provide additional contrast related to the organization and density of fibrillar collagen in the vessel. Quantitative assessment of these parameters in the fibrous cap of atherosclerotic plaques could serve as a measure of plaque stability, which was suggested in ex vivo studies of aortic plaques. However, the implementation of PS to intracoronary OFDI has so far been hindered by the presence of polarization mode dispersion (PMD) that occurs as the light travels through the rotary junction and the fiber optic probe. We have developed a signal processing strategy that reconstructs sample birefringence in a robust fashion, rejects PMD, and is insensitive to fiber motion. Using the new algorithm, we measured intracoronary birefringence maps of catheterized human cadaveric hearts, which corresponded well with quantitative analysis of collagen content measured from picrosirius red stained sections. We have also demonstrated the feasibility of performing PS-OFDI in vivo in a diabetic, hypercholesterolemic swine model of atherosclerosis.

8565-22, Session 2

Association between macrophage phagocytosis and inflammatory activity assessed by ?OCT

Manabu Kashiwagi, Massachusetts General Hospital (United States); Chen-Hsin Sun, Wellman Ctr. for Photomedicine (United States); Linbo Liu, Joseph A. Gardecki, Massachusetts General Hospital (United States); Atsushi Tanaka M.D., Guillermo J. Tearney, Wellman Ctr. for Photomedicine (United States)

Macrophages play important functions in all phases of atherosclerosis, from atherogenesis to plaque rupture and acute coronary syndromes. Initially, circulating peripheral monocytes adhere to the vessel walls and transmigrate, at which time they differentiate into macrophages. In the coronary artery, macrophages phagocytize oxidized LDL, apoptose and form necrotic cores. We have recently developed a 1-μm resolution optical coherence tomography technology termed “?OCT”. μOCT enables cross-sectional imaging of human tissue with axial and lateral resolutions that are approximately an order of magnitude better than those of conventional OCT systems. This resolution improvement of ?OCT enables coronary artery microstructure to be imaged at a scale that is comparable to histopathology. In this study, we scanned human cadaver coronary artery samples with μOCT and found that some macrophages contained highly scattering constituents within their cytoplasm. We hypothesize that these intracellular inclusions are phagocytosed cholesterol crystals. Upon further analysis of μOCT images of 35 cadaver plaques, we found that there was a correlation between plaques containing macrophages with these inclusions and inflammatory cell adhesion ($R = 0.55$; $p < 0.0005$). These results suggest that μOCT may be useful for establishing a link between macrophage phagocytic activity and inflammatory cell recruitment in human coronary artery disease.

8565-23, Session 2

Ultrahigh frame-rate intravascular 2G-OCT

Han Saem Cho, Tae Hwan Kim, Sun-Joo Jang, KAIST (Korea, Republic of); Alexey V. Dan-Chin-Yu, Hyunjoo In-Tech Co., Ltd. (Korea, Republic of); Taegee Min, S&H Co., Ltd. (Korea, Republic of); O-ki Kwon, Seoul National Univ. Bundang Hospital (Korea, Republic of); WangYuhl Oh, KAIST (Korea, Republic of)

Acute myocardial infarction (AMI), most frequently caused by the disruption of a vulnerable atherosclerotic plaque, is the leading cause of death in the western world. Among all the clinical imaging modalities currently being used for studying and detecting vulnerable plaques, only optical coherence tomography (OCT) can provide sufficient resolution to visualize the pathologic features associated with the vulnerable plaque.

With the advent of second-generation OCT (2G-OCT), which enables orders of magnitude faster imaging than its first-generation version, three-dimensional visualization of microscopic structure of long coronary vessel wall recently became possible during a brief clear liquid flush (typically ~ 5s).

However, the clinical routine requires even faster imaging speed for couple of reasons. First of all, reducing amount of clear liquid flush is highly desirable to avoid potential flush-induced complications including contrast-induced nephropathy and ventricular arrhythmia. We also need to reduce the longitudinal imaging pitch, which is currently several times longer than the resolution of the OCT, for real 3D high-resolution imaging.

We demonstrate ultrahigh frame-rate intravascular 2G-OCT addressing these issues. Thanks to the high-speed 2G-OCT system and the ultrahigh-speed rotational driving unit that spins the intravascular imaging catheter, endoscopic imaging of the vessel is performed at a rate of 400 frames per second (604 lines per frame). The high-speed 2G-OCT system provides an A-line rate of 240 kHz with the axial resolution of 10 ?m and the imaging scan diameter of 13 mm. 6.4 cm long aorta of a New Zealand white rabbit was imaged ex vivo in 0.8 second with a conventional 200 ?m longitudinal imaging pitch. For three-dimensional high-resolution visualization, we also performed imaging of 3.6 cm long rabbit aorta with 25 ?m longitudinal pitch in 3.6 seconds.

8565-7, Session 3

Automated tissue characterization using intra-vascular optical coherence tomography

Giovanni J. Ughi, Katholieke Univ. Leuven (Belgium); Tom Adriaenssens, Univ. Hospitals Leuven (Belgium); Peter R. Sinnaeve, Walter Desmet, Katholieke Univ. Leuven (Belgium) and Univ. Hospitals Leuven (Belgium); Jan D'Hooge, Katholieke Univ. Leuven (Belgium)

Background– Intra-vascular optical coherence tomography (IV-OCT) is rapidly becoming the method of choice for in-vivo investigation of coronary artery disease. While IV-OCT visualizes atherosclerotic plaques with a resolution <20µm, image analysis in terms of tissue composition is currently performed visually by a time-consuming manual procedure based on the qualitative interpretation of image features.

Methods– We propose an algorithm for the automated and systematic characterization of IV-OCT atherosclerotic tissue. The method consists of a supervised classification of image pixels according to textural and geometrical features combined with the estimated value of the local attenuation coefficient µt. Textural features are computed through gray-levels co-occurrence matrices while µt is estimated by automatic iterative fitting of IV-OCT A-lines to a signal model.

IV-OCT images of 64 atherosclerotic plaques, from 49 in-vivo IV-OCT datasets, constituted the algorithm training and testing datasets. Validation was obtained by comparing automated analysis results to the manual assessment of the test-set images.

Results– An overall pixel-wise accuracy of 81.5% with a classification feasibility of 76.5% and per-class accuracy of 89.5%, 72.1% and 79.5% for fibrotic, calcific and lipid-rich tissue respectively, was found.

Conclusions– An algorithm for automated tissue characterization was developed and validated using in-vivo human data, proving that it can be applied to clinical IV-OCT data. This might be an important step towards the integration of IV-OCT in cardiovascular research and routine clinical practice.

8565-12, Session 3

Quantification of bright spots in IVOCT images of human coronary arteries

Jennifer E. Phipps, The Univ. of Texas Health Science Ctr. at San Antonio (United States); Deborah Vela, The Texas Heart Institute (United States); J. Jacob Mancuso, David L. Halaney, The Univ. of Texas Health Science Ctr. at San Antonio (United States); Thomas E. Milner, The Univ. of Texas at Austin (United States); Marc D. Feldman, The Univ. of Texas Health Science Ctr. at San Antonio (United States)

Background and introduction: Intravascular optical coherence tomography (IVOCT) is used to identify features of plaque vulnerability in vivo. Often, punctate bright regions (bright spots) in IVOCT images of human coronary arteries are thought to represent macrophages. We propose a method to identify bright spots with a brightness reference based on the IVOCT system and a normalization technique to account for light attenuation in tissue.

Methods: IVOCT pullbacks were acquired from coronary arteries of human hearts. A reference pixel brightness value was calculated based on the optoelectronics of the IVOCT system. A threshold to identify bright pixels was developed based on the reference brightness value and pixel depth to account for light attenuation with tissue depth. Tissue regions that demonstrated bright spots were then compared to histology (H&E, Movat's pentachrome, CD68, and Von Kossa).

Results: N=3 human hearts were analyzed (4 coronaries). Brightness was quantitatively observed in 122 images and correlated with fibrous tissue, macrophage-rich areas, cholesterol crystals, and calcium.

Discussion and Conclusion: A novel quantification method for unbiased identification of bright spots in IVOCT images is demonstrated and shows for the first time that bright spots can be caused by fibrous tissue.

These results indicate a new source of bright spots and a quantitative method of identification that corrects for variability in the light source and tissue depth.

8565-17, Session 3

Validation of an ex-vivo model for atherosclerotic tissue characterization using optical coherence tomography

Muthukaruppan Gnanadesigan, Erasmus MC (Netherlands); Steve White, Thomas Johnson, Univ. of Bristol (United Kingdom); Antonius F. W. van der Steen, Erasmus MC (Netherlands) and Netherlands Heart Institute (Netherlands); Gijs van Soest, Erasmus MC (Netherlands)

Coronary Heart Disease was the cause of 13 percent of deaths in the world in 2011 and the rupture of the vulnerable atherosclerotic plaque is the biggest contributor. Knowledge of plaque components associated with the plaque, necrotic core and the macrophage content can help a large extent in the assessment of the vulnerability of the plaque.

Optical coherence tomography (OCT) is an imaging technique which is widely used for the characterization of the plaque components. OCT uses a low coherence light to form images based on the backscattered light. Different tissue types attenuate light to a different extent and therefore we aim to use the attenuation coefficient obtained from OCT data to

distinguish between tissue types. To do so, we studied the effect of fixation and temperature changes on the light attenuation of the tissues.

The ex-vivo model we used to validate consists of a whole heart cadaveric specimen and facilitates catheter imaging modalities. OCT imaging of the coronary arteries were performed at different temperature conditions and pre and post fixation. The OCT data was analyzed using a mathematical model for OCT signals to retrieve the attenuation coefficient. Different tissue types were identified by comparing accurately with the histology and the attenuation coefficient of the same homogenous tissue type under different conditions were compared. The results indicate an increase in the value of the attenuation coefficient in fibrous tissue with fixation. The necrotic core and macrophages exhibit higher attenuation at room temperature than at cold and hot conditions.

8565-41, Session 3

Computer-aided image analysis for intravascular OCT

David L. Wilson, Zhao Wang, Hong Lu, David Prabhu, Hiram G. Bezerra M.D., Marco A. Costa M.D., Andrew M. Rollins, Case Western Reserve Univ. (United States)

Intravascular OCT (iOCT) is rapidly becoming an important tool for diagnosis, treatment planning, and therapy assessment in atherosclerotic disease. Major applications include characterization of atherosclerotic plaques and assessment of coronary stents. Data sizes overwhelm manual analysis with >200 images in a pullback. For example, our Cardiovascular Imaging Core Lab has manually analyzed (@6-16hrs/stent) iOCT image data from >20 international clinical stent trials including >2000 stents. To meet this need, we have developed highly automated methods for both off-line and point-of-care image analysis. Applications include automated assessment of artery stenosis, stent tissue coverage analysis, plaque calcifications, and 3D fibrous cap thickness to assess vulnerability. Advanced image processing techniques such as machine learning and graph search give robust, accurate results with few manually tuned parameters. Meaningful validations are done against clinical data. For example, using a dynamic programming method, we segmented thin-cap fibroatheroma (TCFA) to aid determination of plaque vulnerability. Over a total 323 images from 14 lipid rich lesions, automatic segmentation of cap thickness gave minimum thicknesses, a measure of vulnerability, within the range of values recorded by 3 observers. Unlike conventional visual determination of the thinnest part of a TCFA, the automated method is reproducible and gives entire 3D TCFA morphology and vulnerability heat maps. Stent strut detection and area measurements also compare favorably to manual assessments and can be optionally edited. Throughout, we will discuss how intravascular OCT image analysis meets clinical needs.

8565-5, Session 4

Intravascular near-infrared fluorescence imaging with intravascular ultrasound guidance

Adam J. Dixon, William H. Guilford, John A. Hossack, Univ. of Virginia (United States)

Intravascular imaging techniques are of increasing importance to the diagnosis and management of cardiovascular diseases. Near-infrared fluorescence (NIRF) catheters have demonstrated potential to characterize the molecular signatures of inflamed atherosclerotic plaques by detecting exogenous molecularly targeted fluorescent probes. However, NIRF catheters provide no structural information, which prevents quantification and spatial localization of the NIRF signal. We present a combined intravascular ultrasound (IVUS) and NIRF catheter capable of acquiring co-registered intravascular ultrasound and fluorescence images. The combined catheter has an outer diameter of 1.6 mm (4.8 F) and is comprised of a 400 µm diameter side-fired optical fiber and a 600 µm diameter IVUS transducer. A micro-lens focuses the excitation light into the tissue, which has improved the minimum detection sensitivity from approximately 1 nanomolar to 10 picomolar concentrations of DiR and has improved the angular resolution by 24% compared to unfocused side-fired fibers. The IVUS transducer operates at 40 MHz with an axial resolution of approximately 40 µm and a penetration depth of up to 8 mm. The IVUS and side-fired optical fiber are rotated independently, which enables fast IVUS acquisition speeds (>10 fps) while also allowing for the acquisition of co-registered long-exposure fluorescence measurements. Estimates of catheter-to-vessel wall distance are measured automatically from IVUS images using an active contours segmentation algorithm and are used to normalize the fluorescence signals for varying acquisition distances. We demonstrate the feasibility of this combined IVUS/NIRF catheter in an in vitro vessel phantom and ex vivo porcine carotid arteries.

8565-8, Session 4

Fully integrated intracoronary optical coherence tomography-ultrasound catheter for in vivo real-time assessment of vulnerable plaques

Jiawen Li, Univ. of California, Irvine (United States); Xiang Li, The Univ. of Southern California (United States); Aidan Raney, Dilbahar Mohar, Univ. of California, Irvine School of Medicine (United States); Joseph Jing, Univ. of California, Irvine (United States); Abbey Johnston, Univ. of California, Irvine School of Medicine (United States); Jun Zhang, Shanshan Liang, Sari Mahon, Matthew Brenner, Univ. of California, Irvine (United States); K. Kirk Shung, Qifa Zhou, The Univ. of Southern California (United States); Pranav M. Patel, Univ. of California, Irvine School of Medicine (United States); Zhongping Chen, Univ. of California, Irvine (United States)

The majority of coronary events are caused by the rupture of a thin-cap fibroatheroma (TCFA), a plaque with large lipid or necrotic core covered by relatively thin fibrous caps. Accurate assessment of TCFA is crucial to prevent death in patients with CAD. Current diagnostic techniques are often limited by either spatial resolution or penetration depth or soft tissue contrast. In this manuscript we show the successful development and use of an integrated OCT-IVUS system to image and classify atherosclerotic plaques in vivo using a single fully-integrated catheter. This novel technique provides high resolution (OCT) and deep penetration (IVUS) to visualize the two major characteristics of TCFA simultaneously.

The OCT-IVUS catheter, with a outer diameter of 1.2mm, is made by a OCT-IVUS probe covered by a commercial IVUS catheter sheath (with a guidewire rail and X-ray detective bands). 3D helix scan is performed during experiments. The rotational speed of this integrated catheter can reach to 20 rotations/s.

By this catheter-based IVUS-OCT system, we demonstrate the first OCT-IVUS imaging in the coronary artery of a live swine, a model commonly used prior to human research. The imaging procedures are done by the conventional femoral access, X-ray guidance and Omnipaque flushing. We also present OCT-IVUS images of a “thick” cap fibroatheroma from a live rabbit atherosclerotic plaque model and evaluations of plaques in cadaveric coronary specimens.

8565-26, Session 4

Continuous monitoring of mixed venous oxygen saturation by transesophageal near-infrared echo-oximetry: a feasibility study

Li Li, Massachusetts General Hospital (United States); Balachundhar Subramaniam, Brett A. Simon, Harvard Medical School (United States); Guillermo J. Tearney, Wellman Ctr. for

Photomedicine (United States)

Mixed venous oxygen saturation (SvO2), measured from pulmonary arteries, is vital for medical decision making during and after cardiac surgery. This measurement reflects the dynamic balance between the global oxygen supply and consumption. An abnormal low SvO2 is an effective prognostic marker of post-operative mortality and morbidity, and goal-oriented hemodynamic therapy that maintains SvO2 above a normal threshold could improve surgical outcomes. Historically, SvO2 was measured by transcutaneous pulmonary artery catheters. However, these invasive devices are associated with potential severe complications, and significant measurement error results from the incorrect placement. Thus, noninvasive, reliable and continuous monitoring of SvO2 remains an unmet clinical need.

We have developed an echo-oximeter by coupling an optical source to an echocardiographic probe. It noninvasively assesses pulmonary arteries through the esophageal wall. By detecting acoustic signals generated from blood by optical pulses with multiple near-infrared wavelengths, we can calculate the localized blood oxygenation from the recovered spatial-spectral map of optical attenuation. Using the echo-oximeter, we measured the oxygen saturation of blood vessels at various depths in tissue-mimicking phantom and en-bloc model of porcine heart and esophagus. Our predictions were compared with the gold-standard measurements by a CO-oximeter following invasive blood sampling. Results showed the echo-oximeter could continuously monitor blood oxygenation between 0~100% at a depth of up to 2 cm with an excellent accuracy (mean bias: 1.6%, standard deviation: 1.9%). Our study indicates that echo-oximeter enables safe and accurate longitudinal monitoring of SvO2, thus could become a useful tool in managing patients undergoing high-risk cardiac surgeries.

8565-29, Session 4

Design and validation of a small-profile rotational catheter for combined fluorescence lifetime imaging (FLIm) and intravascular ultrasound (IVUS) imaging of coronary arteries

Julien Bec, Dinglong M. Ma, Diego R. Yankelevich, Laura Marcu, Univ. of California, Davis (United States)

This paper presents the development and validation of a new, small-profile design of intravascular catheter which enables high speed bi-modal imaging of coronary arteries using fluorescence lifetime imaging (FLIm) and intravascular ultrasound (IVUS). The catheter is based on a bifurcated design that presents a 3 Fr diameter single lumen imaging section and a 5 Fr dual lumen shaft, housing independently rotating ultrasonic and optical channels. The two channels consist of the imaging elements of a commercial; 40 MHz IVUS 3 Fr catheter and a side viewing UV-grade silica fiber optic (300 ?m core). Data for each modality are acquired sequentially via helical scanning within the imaging section: only the channel actively acquiring data is present in the imaging section while the other channel is pulled back in the shaft, enabling bi-modal scanning without increase of the tip bulk compared to a standard IVUS catheter. Co-registration accuracy is achieved by anchoring the catheter in the vessel using a compliant balloon integrated proximally to the imaging section. The proximal occlusion created by the balloon, combined with flushing, provides blood removal from the optical pathway. Due to its compatibility with standard 0.014" guide-wires and 6 Fr catheter guides, this catheter integrates seamlessly with standard catheterization procedures and allows straightforward imaging of larger coronary arteries. Current tests conducted in vessel phantoms and swine showed the ability of the system to robustly acquire co-registered IVUS and FLIm data during a clinically realistic vessel occlusion time (15 – 30 seconds), enabling future study of atherosclerotic cardiovascular diseases.

8565-36, Session 4

Integrated multispectral fluorescence lifetime imaging (FLIm) and intravascular ultrasound (IVUS) system for real-time bimodal imaging of arterial wall pathologies

Dinglong M. Ma, Univ. of California, Davis (United States); Diego R. Yankelevich, Univ. of California, Davis (United States); Julien Bec, Jing Liu, Laura Marcu, Univ. of California, Davis (United States)

This communication demonstrates the development of a bimodal imaging system combining fluorescence lifetime imaging (FLIm) and intravascular ultrasound (IVUS) for simultaneous assessment of biochemical and morphological features of arterial vessels. Tissue autofluorescence is induced with a pulsed fiber laser (Fianium, 355 nm, 20 ps, 60 nJ pulse, 1 MHz repetition rate) and spectrally resolved using a tandem array of dichroic beam-splitters and filters that collects the autofluorescence into four wavelength sub-bands (390, 452, 542, and 629 nm center frequencies) with different optical delay. A fast MCP-PMT detects the emission pulses spanning 250 ns sequentially using a pulse sampling method to retrieve the fluorescence dynamics. The FLIm data is acquired by an 8 GS/s (3 GHz bandwidth) digitizer. IVUS imaging is provided by a commercial system (Boston Scientific, iLab system). Helical scanning of 400 RPM rotational speed and 0.75 mm/s pullback speed is achieved with FLIm image pixel size of 100 x 100 micrometers. Bimodal images are co-registered based on the shadow of IVUS transducer in FLIm images and the shadow of the fiber-optic in ultrasound images. The system is applied intravascularly through a bimodal catheter that combines a 300 ?m side-viewing multi-mode fiber for FLIm and a commercial 40 MHz IVUS transducer. The ability of this system to continuously scan arterial segments and analyze the bimodal data was validated in ex-vivo pig heart coronary arteries and in-vivo in swine femoral arteries. Current results demonstrate successful co-registration of relevant biochemical and morphological features in tissue detected with the bimodal system.

8565-38, Session 4

Optoacoustic processing algorithms for intravascular imaging using interferometric line ultrasonic sensors

Pablo González, Daniel C. Gallego, Horacio L. Lamela, Univ. Carlos III de Madrid (Spain)

OptoAcoustic Imaging (OAI) is a new biomedical imaging technology based on the use of laser-generated ultrasound. It combines optical contrast with low ultrasound scattering resulting in high spatial resolution in the range of several millimetres to centimetres. Therefore, it has great specificity on detecting haemoglobin, lipids, water and other light-absorbing chromophores. (Dima & Ntziachristos, Expert Opinion on Medical Diagnostics May 2011)

In the context of intravascular imaging, OAI provides interesting advantages compared to ultrasound imaging and other classical techniques in fields such as atherosclerosis diagnosis and treatment (van Soest et al., SPIE Photons Plus Ultrasound: Imaging and Sensing 2011 Vol. 7899) or coronary stents assessment and check, which luck endogenous ultrasound contrast (Karpiouk AB, Wang B, Emelianov SY., Rev Sci Instruments 2010). For this purposes, in addition to previous characteristics of both contrast and resolution, OAI allows discrimination of different tissue types by using multiwavelength photoacoustic responses.

In this work, we present the results of an optoacoustic intravascular endoscope based on a laser beam rotated within the vessel and moved lengthwise through it, and an interferometric ultrasonic sensor (H. Lamela, D. Gallego, A. Oraevsky, Optics Letters 2009), modeling an integrating interferometric line sensor (D. Gallego, H. Lamela, M. Wang, J. Hiltunen, M. Kinnunen, R. Myllylä, SPIE PW 2012 Vol. 8370).

The system is tested over different absorbent geometries, showing the capabilities and limitations of the algorithms. We compare the results obtained by the exact time-domain reconstruction formula and some approximate time-domain filtered back-projections reconstruction algorithms. A wavelet transform implementation using a wavelet family resembling the theoretical N-shaped OA signal can be used to sharpen object boundaries while simultaneously preserving high contrast of the reconstructed objects, reducing noise effects.

8565-6, Session 5

Fully-automatic 3-dimensional imaging of intravascular optical coherence tomography for stent assessment

Giovanni J. Ughi, Katholieke Univ. Leuven (Belgium); Tom Adriaenssens, Univ. Hospitals Leuven (Belgium); Walter Desmet, Katholieke Univ. Leuven (Belgium) and Univ. Hospitals Leuven (Belgium); Jan D'Hooge, Katholieke Univ. Leuven (Belgium)

Background– Intravascular Optical Coherence Tomography (IV-OCT) is an appropriate imaging modality for the assessment of intracoronary stents. Recent publications pointed to the fact that 3D visualizations have potential advantages compared to conventional 2D images. The major pitfall is that image analysis required for 3D visualizations is currently performed manually resulting in a very time-consuming procedure. The aim of the current study was the development of a rapid and fully-automatic algorithm for the 3D visualization of IV-OCT pullbacks.

Methods– IV-OCT pullbacks are first processed segmenting the imaging catheter through a rapid algorithm based on Hough transform, allowing for automatic pullback calibration and catheter removal. Then guide-wire boundaries are located implying 3D spatial continuity. Vessel lumen and stent struts are subsequently segmented by a previously developed algorithm and stent apposition quantified. 3D visualization is then generated through dedicated software for volume rendering.

Imaging catheter and guide-wire segmentation were validated by comparison to manual analysis while 3D images were visually compared to angiography and stent patterns known a priori.

Results– The segmentation algorithms showed a correlation with manual analysis of 0.99 while Bland-Altman statistics did not show significant bias. Visual inspection of automatic 3D IV-OCT results showed consistency with angiography and stent manufacturer's data. Computational time required for an entire IV-OCT pullback 3D rendering resulted to be <2min.

Conclusion– An algorithm for the rapid and fully-automatic 3D detection and visualization of stent was developed and validated. This potentially allows for the use of 3D IV-OCT in clinical routine and percutaneous coronary intervention optimization.

8565-21, Session 5

High-speed automatic segmentation of intravascular stent struts in optical coherence tomography images

Myounghee Han, Dongkwan Kim, WangYuhl Oh, Sukyoung Ryu, KAIST (Korea, Republic of)

Recently, Optical Coherence Tomography (OCT) has become one of the preferred clinical techniques for intracoronary diagnostic imaging. Thanks to its high resolution imaging capability, the OCT technique allows to identify microscopic features associated with various types of coronary plaque and it also allows to track stent position, malaposition and neo-intimal tissue growth after stent implantation. Accurate high resolution visualization of stent struts can help to examine the status of implanted stents potentially leading to proper treatment of the coronary artery disease. However, unfortunately, current stent identification involves time-consuming segmentation algorithms sometimes requiring labor-intensive manual analysis processes.

To resolve the problem, we propose a high-speed automatic segmentation algorithm of intravascular stent struts in OCT images. Unlike the other "automatic" stent segmentation algorithms, mainly based on time-consuming machine learning algorithms with manual addition and removal of stent struts for correction during the analysis processes, our algorithm does not require any manual adjustments of stent struts. We first analyze 10 consecutive cross-sectional OCT images to take boundary information into account to enhance the accuracy of guide-wire segmentation and lumen segmentation. Then, using the previously segmented guide-wire information, we perform stent segmentation to automatically eliminate the guide-wire signals. Our implementation uses the Intel(R) IPP library on CPU and the CUDA technology on GPU, which achieves the average analysis time of 0.24s/frame and the detection rate ranging from 84% to 88.6% for about 120 continuous images per patient. As such, the proposed algorithm is robust and fast enough to be integrated in clinical routine.

8565-34, Session 5

Effect of neointimal coverage on strut size measurements in IV-OCT imaging of coronary artery stents

Sahar Elahi, The Univ. of Texas at Austin (United States); Marc D. Feldman, The Univ. of Texas Health Science Ctr. at San Antonio (United States); Jouke Dijkstra, Leids Univ. Medisch Ctr. (Netherlands); Thomas E. Milner, The Univ. of Texas at Austin (United States)

Inasmuch as degree of neointimal formation over stent struts is an important indicator of vascular healing response and treatment effectiveness, accurate post-deployment assessment is of clinical interest. IV-OCT can provide ultrahigh resolution images of stents and is a superior candidate to assess neointimal thickness. A 3mm lumen diameter phantom blood vessel was constructed from a mix of polydimethylsiloxane (PDMS) and titanium dioxide to simulate the elastic and optical properties of the arterial wall. A TAXUS® Liberté™ stent was deployed within the phantom vessel and a layer of PDMS was formed over the stent to simulate neointimal coverage. High resolution Micro-CT images of the stent strut were recorded as a gold standard and to create a three-dimensional representation of a strut that was imported into a computer model. An IV-OCT catheter was specified and rotation of the light beam over the stent strut was simulated. Varying neointimal thicknesses were considered in the computer model to study scattering and reflection of light from the stent strut. Measured length of selected struts from Micro-CT images was 199, 318, 143 and 383um corresponding to neointima with thicknesses of 390, 366, 420, and 383um. Strut lengths measured from the corresponding IV-OCT images were 275, 435, 314, and 445um, respectively. Computer model results for neointimal thicknesses of 0, 10, 50, 100, 250um give predicted IV-OCT strut lengths of 75, 94, 132, 151, and 188um while actual strut length is 90um. Experimental and computer model results suggest thicker neointimas give elongated stent struts in IV-OCT images.

8565-25, Session 6

Micrometer resolution optical coherence tomography (?OCT) imaging of human calcific aortic valve disease

Chen-Hsin Sun, Duke-NUS Graduate Medical School (Singapore) and Wellman Ctr. For Photomedicine (United States); Linbo Liu, Manabu Kashiwagi, Joseph A. Gardecki, Massachusetts General Hospital (United States); Guillermo J. Tearney, Wellman Ctr. for Photomedicine (United States)

Calcific aortic valve disease (CAVD) is a progressive disorder characterized by a buildup of calcium deposits within the aortic valve leaflets. When CAVD progresses to symptomatic aortic stenosis and is left untreated, it has very high morbidity and mortality, with an average survival rate of 2 years and a 5-year survival rate of less than 20%. To date, there is no effective therapy for CAVD except surgical and transcatheter aortic valve replacement, which are expensive and have relatively high morbidity/mortality. A pharmacologic therapy, applied much earlier in the disease progression, would greatly improve patient outcomes and the management cost of this disease. One key barrier for developing drugs that halt the progression of CAVD is that its pathogenesis is poorly understood, which is in part due to the absence of a high resolution imaging tool that is capable of studying early stage CAVD in animal models and human patients in vivo. We have developed a new imaging technique termed micro-optical coherence tomography (?OCT) with a resolution of 1 ?m. Using ?OCT, we have imaged 30 ex-vivo human aortic valve leaflets from autopsies and post aortic valve replacement procedures and have compared the ?OCT images to corresponding H&E, Masson Trichrome, Movat's Pentachrome and Von Kossa stained slides. Our results show a good correspondence between ?OCT and histology, demonstrating inflammatory cell infiltration, ECM disorganization, cholesterol crystals deposition, micro-calcification, and calcium nodule formation. We believe that this technology has the potential become a valuable tool for the future study and diagnosis of CAVD.

8565-39, Session 6

Association of neointimal morphology by optical coherence tomography with rupture of neoatherosclerotic plaque very late after coronary stent implantation

Antonios Karanasos, Jurgen Ligthart, Karen Witberg, Erasmus MC (Netherlands); Konstantinos Toutouzas, Univ. of Athens (Greece); Joost Daemen, Gijs van Soest, Muthukaruppan Gnanadesigan, Robert-Jan van Geuns M.D., Peter de Jaegere, Evelyn Regar M.D., Erasmus MC (Netherlands)

Purpose: Neoatherosclerosis within a stent has been recently described as a culprit of late stent failure. We investigated by optical coherence tomography (OCT) the association of neoatherosclerotic plaque morphology with neointimal rupture (NR) and clinical presentation in patients late after coronary stent implantation.

Methods: From 1/1/2007 to 31/1/2012, 74 patients from two institutions underwent OCT assessment of a coronary stent implanted at least 18 months prior to OCT study. Native atherosclerosis criteria were used for neointimal characterization.

Results: Neoatherosclerosis was observed in 59.5% of the stents (n=44). Stents with neoatherosclerosis were more often associated with symptoms compared to stents without neoatherosclerosis (59.1% acute coronary syndrome (ACS), 25% stable angina (SA), and 15.9% asymptomatic versus 43.3% ACS, 6.7% SA, 50% asymptomatic, p<0.01). Among neoatherosclerotic lesions (n=44), NR was detected in 19 (43.2%) and had higher incidence in ACS (61.5%) than in SA (18.2%) and asymptomatic (14.3%) (p<0.05). Thrombus was detected in all NR cases. Fibrous cap thickness was lower in NR lesions compared to lesions without NR (48±21?m versus 104±58?m, p<0.01). Lipid content tended to be higher in lesions with NR (260±103o versus 203±85o, p=0.051). Lesions with NR had more often dense macrophage infiltration (84.2% versus 44.0%, p<0.05). There were no differences in neovascularization or calcifications between lesions with or without NR.

Conclusions: Neoatherosclerosis is frequent and more common among symptomatic patients. Importantly, neointimal rupture is associated with ACS late after stent implantation. Specific morphological characteristics, such as cap thickness and macrophage infiltration are associated with rupture of neoatherosclerotic plaques.

8565-40, Session 6

In-stent neoatherosclerosis: are first generation drug eluting stents different than bare metal stents? an optical coherence tomography study

Antonios Karanasos, Karen Witberg, Jurgen Ligthart, Konstantinos Toutouzas, Gijs van Soest, Muthukarrupan Gnanadesigan, Joost Daemen, Nicholas van Mieghem, Felix Zijlstra, Evelyn Regar M.D., Erasmus MC (Netherlands)

Purpose: In-stent neoatherosclerosis has been recognised in pathologic specimens of bare metal stents (BMS), and recently in first generation drug eluting stents (1st-DES) as well. However, in vivo data are scarce. By optical coherence tomography, we investigated the incidence and morphological characteristics of neoatherosclerosis (NA) very late after BMS or 1st-DES implantation.

Methods: From 1/1/2007 to 31/1/2012, 52 patients from two institutions underwent >24 months follow-up OCT assessment of a BMS or a 1st-DES (13 BMS – 39 1st-DES). NA was characterized using criteria for native atherosclerosis.

Results: Differences between BMS and 1st-DES are presented in the table. BMS had longer follow-up interval but no differences in clinical presentation at follow-up. No significant differences were evident in the incidence of NA, neointimal rupture, lipid content, neovascularization or macrophage infiltration between BMS and 1st-DES. There was however a trend for lower fibrous cap thickness (FCT) and for higher calcification in BMS (FCT: 51±31?m vs. 92±59?m, p=0.057; calcifications: 46.2% vs. 15.4%, p=0.051). 1st-DES with neoatherosclerosis had longer interval from implantation compared to 1st-DES with homogeneous coverage [Median 71 months (range 25-130) vs. 57 months (24-68), p<0.05], but there was no difference for BMS with or without neoatherosclerosis [Median 125 months (range 90-201) vs. 168 months (132-168), p=0.54].

Conclusions: The incidence and morphological characteristics of NA are similar between 1st-DES and BMS of more prolonged follow-up. Our findings suggest a time-dependent pattern in the incidence of NA in 1st-DES with 2-11 years follow-up.

8565-42, Session 6

Microscopic aortic valve imaging within the beating heart with OFDI

William C. Warger II, Joseph A. Gardecki, Kevin A. Gallagher, Luis Guerrero, Farouc A. Jaffer M.D., Guillermo J. Tearney M.D., Massachusetts General Hospital (United States)

Calcific aortic valve disease (CAVD) is present within approximately 25% of people 65-74 years of age and within 48% of people ≥84 years of age. CAVD is a progressive disorder characterized by focal areas of valve thickening and a build-up of calcium deposits within the aortic valve leaflet. Current noninvasive imaging techniques for detecting CAVD, such as echocardiography, CT, and MR, do not provide adequate resolution to detect microscopic calcification during the early stages of development,

when CAVD might be more responsive to medical therapies that could obviate the need for aortic valve surgery. Here we describe the development and testing of several intravascular optical frequency domain imaging (OFDI) catheter designs to image the aortic valve in vivo. The OFDI catheters were inserted through a 7F guide catheter within the femoral artery and positioned within the aortic sinus under x-ray fluoroscopy. Three-dimensional images were then acquired of the beating valves over 2-20 second intervals with the corresponding EKG. Preliminary results with these catheters have visualized the ventricularis, fibrosa, and spongiosa layer architecture of the valve within living swine during natural cardiac cycles. These results suggest that OFDI could provide a new imaging modality for visualizing the progression of CAVD to help develop therapeutic methodologies for non-surgical treatment of the disease.

8565-11, Session 7

Application of dual-modality optical frequency domain imaging and near-infrared fluorescence imaging in intravascular optical imaging of preclinical animal studies

Ehsan Hamidi, Wellman Ctr. for Photomedicine (United States); Tetsuya Hara, Eric A. Osborn, Adam Mauskapf, Massachusetts General Hospital (United States); Hongki Yoo, Hanyang Univ. (Korea, Republic of); Farouc A. Jaffer M.D., MGH Cardiovascular Research Ctr. (United States); Guillermo J. Tearney, Wellman Ctr. for Photomedicine (United States)

Co-registered Optical Frequency Domain Imaging (OFDI) and Near Infra-Red Fluorescence (NIRF) imaging can be an invaluable diagnostic and investigational tool in cardiology. In this dual-modality imaging technique based on a single catheter with a double cladding fiber, OFDI provides microstructural information through the core while NIRF imaging provides molecular information through the inner cladding simultaneously. We investigate and report our findings on the application of this novel imaging technology in preclinical animal studies. Stent thrombosis is an adverse complication of implanted coronary stents. In two separate studies we investigate stent healing in rabbit models.

In the first study, the disposition of stents to thrombosis that is characterized by fibrin deposition is investigated. A newly developed NIRF imaging molecular agent (FTP11-CyAm7) for molecular imaging of fibrin is utilized with intravascular NIRF-OFDI system to image in vivo the bare-metal stents implanted in the iliac artery of normal rabbits.

Patients with diabetes are at higher risk for restenosis and stent thrombosis due to impaired stent healing and more aggressive restenosis as a result of enhanced endovascular inflammation. In the second study, we investigate the healing of drug-eluding and bare-metal stents implanted in the infrarenal aorta of diabetes-induced rabbits. Prosense 750, a NIRF imaging molecular agent that identifies caspase enzyme activity, is utilized to image inflammation in vivo with intravascular NIRF-OFDI system post-stenting.

In vivo imaging results were compared to histology outcomes. Our findings verify that dual-modality OFDI NIRF Imaging is a promising tool for intravascular imaging and studying stent thrombosis.

8565-18, Session 7

Ex vivo imaging of human coronary atherosclerotic plaques by multimodality near-infrared autofluorescence and optical frequency domain imaging

Hao Wang, Wellman Ctr. for Photomedicine (United States) and Boston Univ. (United States); Paulino Vacas Jacques, Ehsan Hamidi, Wellman Ctr. for Photomedicine (United States); Joseph A. Gardecki, Massachusetts General Hospital (United States); Hongki Yoo, Hanyang Univ. (Korea, Republic of); Guillermo J. Tearney M.D., Wellman Ctr. for Photomedicine (United States)

Plaque progression is a complex process involving both chemical and structural changes within the atherosclerotic lesion and determines the plaque stability. Optical frequency domain imaging (OFDI) provides high-resolution microscopic images of coronary walls, and reveals structural features of calcification, lipid pool and fibrous plaques. However, additional compositional information of the plaque will aid in the assessment, diagnosis and patient treatment.

Previously, we have demonstrated that near infrared autofluorescence (NIRAF) spectroscopy has been used to differentiate broad classes of atherosclerotic disease in ex vivo spectroscopy studies (Based on NIRAF intensity, the 95% confidence interval is lipid rich plaque: (14.34±2.90)?107 counts; calcified plaque: (8.93±0.96)?107 counts; normal tissue: (1.52±0.13)?107 counts. One way ANOVA shows they are significantly different, $p<0.001$). Because these two techniques provide synergistic relevant information from the artery wall, we have developed a multimodality OFDI-NIRAF system and coronary catheter. Here we describe a histopathologic correlative study that compares the OFDI-NIRAF images with corresponding histology from arteries prosected from 5 cadaver hearts. Examples of different classes of coronary plaques will be discussed. These results indicate that multimodality OFDI-NIRAF technology may be useful for improved characterization of coronary artery disease when implemented in human patients.

8565-20, Session 7

Multimodal clinical system for fluorescence and optical frequency domain imaging to study the natural history of plaque progression

Paulino Vacas-Jacques, Hao Wang, Ehsan Hamidi, Wellman Ctr. for Photomedicine (United States); Ali M. Fard, Harvard Medical School (United States); Hongki Yoo, Hanyang Univ. (Korea, Republic of); Joseph A. Gardecki, Massachusetts General Hospital (United States); Brett E. Bouma, Guillermo J. Tearney, Wellman Ctr. for Photomedicine (United States)

Background

Ischemic heart disease, including atherosclerosis, is a recurrent type of malady, accounting for a yearly mortality of 16%. In atherosclerosis, vulnerable plaques that form and rupture can cause thrombosis leading to blockage of the coronary artery. Vulnerable plaques exhibit features that are structural, chemical, and molecular in nature. We present a multimodal clinical system to detect such features.

Our system performs structural imaging with micron-scale resolution by means of optical frequency domain imaging (OFDI). Chemical and molecular information is obtained by employing fluorescence imaging. Both modalities are acquired simultaneously with a new generation of double-clad fiber-based (DCF) catheters.

Methods

The OFDI system incorporates a swept-source laser implemented in a fiber sigma ring cavity. The FSR of the laser is 110nm, with an instantaneous linewidth of ~0.15nm. The laser operates at 100kHz with a duty cycle greater than 90% and an emitted power of 70mW. The laser illuminates a dual-balanced polarization diverse interferometer that is incorporated into a clinical grade cart.

The detection of molecular information is based on a fluorescence subsystem that is integrated within the OFDI console. For fluorescence the excitation wavelength was 633nm, the emission wavelengths ranged

from 680–750nm. Fluorescence was detected at 100kHz, synchronized with each OFDI A-line, using a high-speed photomultiplier.

The clinical DCF catheter enables coregistration of OFDI and fluorescence information. OFDI light is transmitted through the core, while fluorescence excitation/emission is guided through the cladding. The luminescent background of our clinical multimodality catheter is comparable to that of bare fiber.

Results

We describe signal-to-noise ratio, point-spread-function, and roll-off characteristics for the OFDI system. We report the salient parameters of the PMT-based fluorescence system, including SNR. Finally, we present coregistered structural and molecular data of tissue mimicking phantoms and ex-vivo human coronary tissue that demonstrate the functionality and accuracy of the multimodality clinical system.

8565-28, Session 7

Simultaneous high-resolution morphological and biochemical optical imaging of atherosclerosis

Paritosh Pande, Sebina Shrestha, Jesung Park, Fred Clubb, Texas A&M Univ. (United States); Brial Walton, The Texas Heart Institute (United States); Brian E. Applegate, Javier A. Jo, Texas A&M Univ. (United States)

Background: A detailed in vivo mapping of the morphological and biochemical development of atherosclerotic plaques has the potential to vastly improve our understanding of plaque pathogenesis. Objective: To develop and validate a novel imaging technology for high-resolution morphological and biochemical imaging of coronary atherosclerotic plaques. Methods: Optical Coherence Tomography (OCT) generates high-resolution 3D images of plaque morphology. Endogenous Fluorescence Lifetime Imaging Microscopy (FLIM) characterizes plaque biochemical composition. Both methods rely on intrinsic optical characteristics of the plaque, thus contrast agents are not required. A multimodal OCT/FLIM system has been developed to generate morphological and biochemical maps of the plaque, composed of a high-resolution (7/13 ?m axial/lateral) structural volumetric image superimposed with a luminal biochemical map (100 ?m lateral resolution). Fresh postmortem human coronary segments were imaged and included: intimal thickening (IT, n=11), pathological intimal thickening (PIT, n=2), PIT having >50% of collagen content (FIB-PIT, n=7), PIT with superficial infiltration of foam cells (FC-PIT, n=11), fibroatheroma (FA) having >50% of collagen content in the cap (FIB-FA, n=3), FA with superficial infiltration of foam cells (FC-FA, n=2), thin-cap fibroatheroma (TCFA, n=2), and/or calcified FA (CA-FA, n=8) as determined by histopathology. Results: Overall, 93.5% of the plaques (43 out of 46) were correctly identified based on the combined OCT-FLIM evaluation having the histopathology evaluation as the gold standard. Conclusion: The developed technology enables the characterization of plaque morphology and biochemistry with micron resolution and the identification of all histopathological types of coronary atherosclerotic plaque. Based on the success of this study an intravascular OCT/FLIM imaging system is being developed for the in vivo study of mechanisms of atherosclerosis development.

8565-35, Session 7

Multimodality intravascular endoscope for diagnosis of vulnerable plaques

Shanshan Liang, Beckman Laser Institute and Medical Clinic (United States) and Dalian Univ. of Technology (China); Joseph Jing, Univ. of California, Irvine (United States); Xiang Li, The Univ. of Southern California (United States); Jiawen Li, Univ. of California, Irvine (United States); Jun Zhang, Beckman Laser Institute and Medical Clinic (United States); K. Kirk Shung, Qifa Zhou, The Univ. of Southern California (United States); Zhongping Chen, Beckman Laser Institute and Medical Clinic (United States)

In order to increase the chance of survival for patients who suffer from atherosclerosis, researchers keep trying to find out more effective ways to diagnose atherosclerosis at earlier stage. The most commonly used method is intravascular ultrasound (IVUS) endoscope, and it has been used clinically to diagnose atherosclerosis for over 20 years. In recent years, optical coherence tomography (OCT) has also become a very useful tool for intravascular imaging, due to its high axial resolution and ability to detect the different layer structures of plaques. However, biomolecular information is still needed for more accurate diagnoses. By using fluorescence molecular imaging technique, the biochemical properties of biological samples can be examined. It would be very useful to get deep penetration depth, high axial resolution images and biomolecular information at the same time. Therefore, we built up an integrated system and fabricated an endoscope based on a double-clad fiber (DCF) combiner and a side view ultrasound transducer. Single-mode core of the DCF was used to transmit both OCT and fluorescence excitation light, and the multimode inner cladding was used to detect fluorescence emission signal. Ultrasound transducer was placed side by side with the optical part of the probe, allowing the three modalities to be co-registered. In vitro experiments have been done to demonstrate the capability of this integrated system.

8565-3, Session 8

Electrophysiological and histological effects on canine right atrium by photosensitization reaction under catheterization in vivo

Mei Takahashi, Emiyu Ogawa, Sayaka Motohashi, Tetsuya Nakamura, Hiroshige Kawakami, Naoki Machida, Arisa Ito, Keio Univ. (Japan); Takehiro Kimura, Seiji Takatsuki, Kotaro Fukumoto, Shunichiro Miyoshi, Keiichi Fukuda, Keio Univ. School of Medicine (Japan); Tsunenori Arai, Keio Univ. (Japan)

We investigated electrophysiological and histological effect on canine right atrium by photosensitization reaction (PR) via a manipulatable 7 Fr. laser catheter during PR and one week after PR with the aim of establishing a non-thermal tachyarrhythmia treatment. Talaporfin sodium and a 663 nm diode laser were used. The PR was performed to anatomical isthmus, which is located between inferior vena cava and tricuspid annulus in canine right atrium. Posterior right atrial wall was also ablated by PR. Since talaporfin sodium metabolization in canine is 8.2 times faster than human, we continuously administrated the photosensitizer via a left femoral vein to maintain photosensitizer concentration of 25-35 ?g/ml in blood plasma. Fifteen-minute after the kickoff of the photosensitizer administration, the laser irradiation via the laser catheter was operated with irradiance of 10 W/cm2. The laser irradiation was operated by point-to-point technique with contact to myocardium for 30 s. After 20 times irradiations, a 20-30 ms delay of the electrical signal propagation along tricuspid annulus was observed. This result might demonstrate the acute electrical conduction block induced by PR. The canine heart was extracted 1 week after PR and Azan staining specimen was histologically evaluated to investigate the myocardial damage by PR. The transmural fibrosis in isthmus with 2.2 mm in depth was found. This result might demonstrate the permanent electrical conduction block. We think that we might demonstrate the possibility of the PR-induced acute and permanent electrical conduction block in vivo.

8565-4, Session 8

Infrared laser sealing of blood vessels: preliminary ex vivo tissue studies

Christopher M. Cilip, Sarah B. Rosenbury, Thomas C. Hutchens, Gino R. Schweinsberger, Nicholas Giglio, The Univ. of North Carolina at Charlotte (United States); Duane E. Kerr, Cassandra Latimer, William H. Nau Jr., Covidien (United States); Nathaniel M. Fried, The Univ. of North Carolina at Charlotte (United States)

Introduction: Suture ligation of blood vessels during surgery can be time-consuming and skill-intensive. Energy-based, electrosurgical and ultrasonic devices have recently replaced sutures for many surgical procedures, providing rapid hemostasis during surgery. However, these devices have the potential to create an unnecessarily large collateral zone of thermal damage and tissue necrosis. This study explores infrared laser energy for rapid and precise thermal coagulation and sealing of vessels.

Methods: Multiple infrared lasers with wavelengths ranging from 808 - 2120 nm were tested during these preliminary studies. All tests were performed using fresh porcine renal vessels, ex vivo, with diameters of 1-7 mm, compressed to a fixed thickness. Cylindrical beam shaping optics were used to transform the circular beam to a linear beam profile, which was then applied normal to the vessel for narrow, full-width thermal coagulation. The laser irradiation time was fixed at 5 s. Vessel burst pressure measurements were performed and values greater than 3 times systolic pressure (360 mmHg) were judged successful.

Results: The 1470 nm wavelength was capable of sealing a wide range of small-to-large blood vessels from 1-7 mm diameter. A 1908 nm laser was also capable of sealing intermediate vessels up to 4 mm diameter, but failed to provide sufficient thermal coagulation and sealing of large vessels. The 1850-1880 nm wavelengths also performed well, but low laser power output limited further evaluation.

Conclusions: Near-infrared laser radiation providing intermediate penetration depths of 0.3-0.7 mm were capable of rapid and precise sealing of a wide range of vessel diameters.

8565-16, Session 8

Thermal ablation of WHHLMI rabbit atherosclerotic plaque by quantum cascade laser in the 5.7 ?m wavelength range

Keisuke Hashimura, Katsunori Ishii, Osaka Univ. (Japan); Naota Akikusa, Tadataka Edamura, Harumasa Yoshida, Hamamatsu Photonics K.K. (Japan); Kunio Awazu, Osaka Univ. (Japan)

We evaluated the utility of a compact and high-power quantum cascade laser (QCL) in the 5.7 ?m wavelength range for less-invasive laser angioplasty. Atherosclerotic plaques mainly consist of cholesteryl esters. The wavelength of 5.75 ?m is well absorbed in C=O stretching vibration mode of cholesteryl esters. Our previous study achieved to make cutting differences between a normal tunica intima of an artery and an atherosclerotic lesions using a nanosecond pulsed laser by differ-ence-frequency generation (DFG laser) at the wavelength of 5.75 ?m. For realizing a clinical appli-cation of this technique, a compact laser device is required. In this study, QCL irradiation effects to an atherosclerotic artery of myocardial infarction-prone Watanabe heritable hyperlipidemic rabbit (WHHLMI rabbit, provided from Institute for Experimental Animals, Kobe University Graduate School of Medicine) and an normal artery were observed and compared with the results of the DFG laser. As a result, the QCL could make cutting difference between the atherosclerotic artery and the normal artery. On the other hand, the QCL induced more thermal damage than the DFG laser at the irradiation condition of comparable ablation depth. It is considered that the pulse interval of the QCL was not sufficient for thermal diffusion of artery. In conclusion, the possivility of less-invasive and selective treatment of atherosclerotic plaques using the QCL in the 5.7 ?m wavelength range was revealed, although improvement of QCL was required to prevent the thermal damage of a normal artery.

8565-31, Session 8

Optical pacing of the adult rabbit heart

Yves T. Wang, Yongqiu Q. Doughman, Michiko Watanabe, Case Western Reserve Univ. (United States); Yuanna Cheng M.D., Cleveland Clinic Lerner Research Institute (United States); Andrew M. Rollins, Michael W. Jenkins, Case Western Reserve Univ. (United States)

Previously, we demonstrated that a pulsed laser can noninvasively pace embryonic quail hearts without exogenous agents or genetic modifications. Here, the feasibility of optically pacing an adult rabbit heart was explored. Whole, intact hearts from adult New Zealand White rabbits (n = 10) were excised, cannulated and perfused on a modified Langendorff apparatus. Pulsed laser light (? = 1851 nm) was directed to either the left or right atrium through a 400-μm multimode fiber. Simultaneous recordings of an ECG signal from the left ventricle and a transistor-transistor logic (TTL) pulse from the laser were used to determine when capture was achieved. Successful optical pacing was demonstrated by obtaining pacing capture, stopping, then recapturing as well as by maintaining capture while varying the laser pulse frequency. In addition, 1:1 capture with optical pacing was achieved for several minutes without skipping beats. Stimulation thresholds taken at various pulse durations suggested that longer pulses (8 ms) had a lower energy capture threshold. Further, to determine if optical pacing caused tissue damage, hearts were perfused with 30 μM of propidium iodide and analyzed histologically. Minor damage was sometimes observed at radiant exposures near the stimulation threshold and probably limited the ability to maintiain pacing for extended periods. In this study, we demonstrated that short-term optical pacing (~minutes) is feasible in the adult rabbit heart. Future optimization of optical pacing will be directed at lowering the stimulation threshold and allow for longer-term pacing.

8565-33, Session 8

Laser-driven short-duration heating angioplasty: dilatation performance in cadaver atherosclerotic femoral arteries

Natsumi Shimazaki, Sho Naruse, Tsunenori Arai, Nobuaki Imanishi, Sadakazu Aiso, Keio Univ. (Japan)

The purpose of this study was to investigate the artery dilatation performance of the short-duration heating balloon catheter in cadaver stenotic arteries. Thermal angioplasty, which was proposed in 1980s, provided successful revascularization with thermal denaturation (softening) of the collagen fibers in artery media. On the other hand, several literatures suggested that the thermal angioplasty resulted in severe restenosis and abnormal artery remodeling in chronic phase caused by thermal injury in artery adventitia and outer artery surroundings. To reduce the thermal injury in artery adventitia and outer artery surroundings, we proposed a short-duration heating balloon angioplasty. We designed a prototype short-duration heating balloon catheter that can heat artery media to around 60ºC in 15?25s by a combination of laser-driven heat generation and continuous fluid irrigation in the balloon. We performed ex vivo short-duration heating dilatation in the cadaver atherosclerotic femoral arteries (initial percent diameter stenosis 40-100%), with the maximum balloon temperature of 65±5ºC, laser irradiation duration of 25s, and balloon dilatation pressure of 3.5atm. The artery lumen configurations before and after the dilatations were assessed with a commercial IVUS system. After the short-duration heating dilatations, the percent diameter stenosis was reduced below 30% without any artery tears or dissections (N=6). We estimated that the artery media temperature was raised to around 60? in which plaque thickness was <0.8mm by a thermal conduction calculation. The estimated maximum temperature in artery adventitia and surrounding tissue was up to 45?. We found that the short-duration heating balloon could sufficiently dilate the cadaver stenotic arteries, without thermal injury in artery adventitia and surroundings.

8565-10, Session 9

Simultaneous microstructural and compositional imaging using co-registered optical frequency domain imaging and near-infrared spectroscopy for cardiovascular disease diagnostics

Ali M. Fard, Harvard Medical School (United States); Ehsan Hamidi, Paulino Vacas-Jacques, Hao Wang, Guillermo J. Tearney M.D., Wellman Ctr. for Photomedicine (United States)

Coronary artery disease (CAD) is the most common cause of death worldwide. This type of disease is the result of the buildup and rupture of atherosclerotic plaque within the coronary artery walls. Understanding and diagnosis of these plaques requires the knowledge of their microscopic structure as well as their composition. While optical frequency-domain imaging (OFDI) has been successfully used to acquire microstructural images of the coronary walls in vivo, it fails to identify and quantify the lipid contents (e.g., necrotic cores) that are associated with biomechanical instability and hence plaque rupture.

Here we report a dual-modality imaging system for simultaneous microstructural and compositional imaging of coronary artery walls using co-registered OFDI and diffuse near-infrared spectroscopy (NIRS) via a rotationally scanning catheter. The combination of OFDI and NIRS techniques in a single imaging modality would significantly enhance the ability to visualize, identify, and quantify the chemical composition of the tissue such as water, collagen, and cholesterol. Our dual-modality imaging system employs a high-speed (100 kHz) wavelength swept source (1240nm-1360nm) for both OFDI and NIRS, delivers the light to the tissue through the core of a rotating double-clad optical fiber and collects the scattered light via the core and inner cladding of the same fiber. In order to extract microstructural and compositional images, the two collected signals are split and processed separately. In this talk we will present the design of our catheter-based OFDI-NIRS system and will show results obtained from phantoms and human coronaries ex vivo.

8565-15, Session 9

Lipid distribution imaging in in-vitro artery model by 1.7-?m spectroscopic spectral-domain optical coherence tomography

Masato Tanaka, Mitsuharu Hirano, Takemi Hasegawa, Ichiro Sogawa, Sumitomo Electric Industries, Ltd. (Japan)

We demonstrate visualization of lipid distribution in in-vitro artery model by 1.7-?m spectroscopic spectral-domain optical coherence tomography (SD-OCT). In the demonstration, we measure spectral fringes by a spectrometer with an extended InGaAs line sensor and a super-continuum (SC) light source whose spectrum is arranged to have its maximum intensity in 1.7-mm band. The OCT system has an axial resolution of 18 ?m, a measurement range of 5 mm and a sensitivity of 103 dB with an A-scan rate of 0.96 kHz, which is limited by the noise of the available SC light source. The in-vitro model is made by injecting lipid into swine carotid artery, which is compared to intact artery. We perform B-scan of the model in water by connecting an OCT probe to the OCT system and pulling the probe back at 0.027 mm/sec with a rotation rate of 112 rpm. For visualizing lipid distribution, we adopt a spectroscopic OCT algorism where the detected spectral fringe is divided into six sub-bands, the set of the sub-band A-scans are fitted to a model accounting absorption characteristics of lipid with its peak at 1726 nm, and the content of lipid is estimated as lipid score. As a result, the p-value of the lipid score between the normal model and the plaque one is less than 1E-10 in 1-mm depth from the surface, which is significant of visualization of lipid distribution.

8565-19, Session 9

Intravascular spectroscopic optical coherence tomography for automated detection of lipid

Christine P. Fleming, Joseph A. Gardecki, Massachusetts General Hospital (United States); Jocelyn Eckert, Atsushi Tanaka M.D., Wellman Ctr. for Photomedicine (United States); Melissa W. Haskell, Massachusetts General Hospital (United States); Giora Wiesz, Columbia Univ. Medical Ctr. (United States); Brett E. Bouma, Guillermo J. Tearney, Wellman Ctr. for Photomedicine (United States)

Optical frequency domain imaging (OFDI) can identify key components related to plaque vulnerability but may suffer from artifacts that could prevent accurate identification of lipid rich regions. We present a model of depth resolved spectral analysis algorithm for intracoronary plaque classification based on spectroscopic optical coherence tomography (SOCT).

To accurately classify depth-resolved spectra, a quadratic discriminant analysis model was developed to classify depth resolved spectra. Model parameters to classify lipid were developed using OFDI images of phantoms with known chemical compositions of water, cholesterol, collagen, and calcium (n=355 images). To confirm spatial localization of lipid detection, the model was applied to OFDI images of artificial plaques of lipid deposits injected in swine aorta ex vivo with corresponding histological analysis (n=18 artificial plaques). These artificial plaques were designed to give the appearance of a lipid rich plaque within OFDI images, by injecting of fat emulsions into the tunica media layer of fresh normal swine aorta. Thereafter, the algorithm was applied to intravascular pull-back datasets from patients undergoing interventional procedures (n=20 patients).

Our results show that the addition of spectral information can improve the accuracy of detecting chemical compositions ($p<0.05$). The addition of spectral shape provided complementary information compared with standard attenuation coefficient analysis, increasing the classification accuracy ($p<0.05$). Importantly, depth-resolved spectral analysis was able to spatially localize lipid within artificial plaques and intracoronary pullback datasets of patients. This method can facilitate comprehensive visualization of lipid within of OFDI images, which can potentially improve diagnosis and/or assist in guiding therapeutic procedures.

8565-24, Session 9

Near-infrared hyperspectral imaging of atherosclerotic plaque in WHHLMI rabbit artery

Katsunori Ishii, Akiko Kitayabu, Kota Omiya, Norihiro Honda, Kunio Awazu, Osaka Univ. (Japan)

Hyperspectral imaging (HSI) of rabbit atherosclerotic plaque in near-infrared (NIR) wavelength range from 1150 to 2400 nm was demonstrated. A method to identify vulnerable plaques that are likely to cause acute coronary events has been required. The object of this study is identifying vulnerable plaques by NIR-HSI for an angioscopic application. In this study, we observed hyperspectral images of an atherosclerotic plaque in WHHLMI rabbit (atherosclerotic rabbit) artery under simulated angioscopic conditions by NIR-HSI. NIR-HSI system was constructed by a NIR super continuum light and a Mercury-cadmium-telluride camera. Spectral absorbance values (log (1/R) data) were obtained in the wavelength range from 1150 to 2400 nm at 10 nm intervals. The hyperspectral images were constructed with spectral angle mapper algorithm. As a result, the detections of atherosclerotic plaque under angioscopic observation conditions were achieved especially in the wavelength around 1200 nm, which corresponds to the second overtone of CH stretching vibration mode. The NIR-HSI was considered to serve as an angioscopic diagnosis technique to identify vulnerable plaques without clamping and saline injection.

8565-27, Session 9

Heat as a contrast agent to enhance thermal imaging of blood vessels

Jason R. Case, Susan R. Trammell, Madison A. Young, Michael X. Crown, Uriah Israel, The Univ. of North Carolina at Charlotte (United States)

We are using heat as a contrast agent to provide enhanced thermal imaging (8-10 μm) of vascular structures. This imaging technique has applications in mapping blood vessels just beneath the skin and during open surgeries. This study used high-power LED sources at 405nm and 530nm to selectively heat hemoglobin in blood relative to the water-rich tissue. The LED sources offer a low-cost alternative to lasers as heating sources. We present preliminary experimental results and Monte Carlo simulations that indicate high-contrast thermal imaging of vascular structures can be obtained. We measured the heating as a function of time in water-rich tissues versus blood (from a porcine donor) after exposure to 405nm or 530nm LED sources. We also conducted preliminary blood flow tests using vessels within a sample of heart tissue. We used a FLIR SC600 thermal camera to obtain images. Monte Carlo simulations were used to model the photon propagation for our LED sources in blood and soft tissue. Our Monte Carlo simulations indicate that the majority of the energy from both the 405nm and 530nm light sources was deposited in blood rather than surrounding soft tissues. Our experimental results demonstrate that the temperature of blood increases more rapidly than soft tissue after illumination with both the 405nm and 530nm LED sources (13 times faster at 405nm). Our preliminary blood flow tests indicate that this imaging technique can be used as a method to obtain high contrast thermal images of blood vessels without damaging surrounding tissue.

8565-162, Session 1

Hyperspectral functional imaging of the human brain

Vladislav Toronov, Ryerson Univ. (Canada)

Near-infrared light has been used in hundreds of functional studies and even a number of commercial systems have become available. However, a problem of significant distortions of cerebral signals or loss of information in optical data due to a low penetration of light into the adult human brain requires further development of both instrumentation and algorithms. Recent technological advances have brought to the market a number of models of low cost spectrometers with high signal to noise ratio. This allows for building multichannel broadband spectroscopy and imaging systems for brain imaging. We show that broadband imaging not only resolves a debate on which wavelengths of light are optimal for brain imaging, but also allows for a very effective signal filtering and extraction of cerebral signals based on specific spectral patterns.

8565-164, Session 1

Spontaneous FAD dynamics reveal functional connectivity patterns in mice

Patrick W. Wright, Adam Q. Bauer, Brian R. White M.D., Joseph P. Culver, Washington Univ. School of Medicine in St. Louis (United States)

Functional connectivity (FC), defined as correlated inter-regional brain activity, has the potential to act as a biomarker sensitive to progression of a neuropathology. Currently, hemodynamic changes in response to cognitive demand are the most commonly imaged and measured markers of functional cortical activity, often imaged in mice as the optical intrinsic signal (OIS). However, FC maps constructed using OIS are sensitive to altered neurovascular coupling that can occur in disease states. These bilateral FC maps can be difficult to interpret and not representative of underlying physiology. Whereas the hemodynamic response to neural activity is indirect via a multi-step neurovascular coupling process, optical signals via metabolites (e.g. flavin adenine dinucleotide, FAD) allow for imaging of cellular mechanisms known to be part of individual synaptic potential events. Wild-type Swiss Webster mice were imaged transcranially with sequential illumination provided by three collimated, collinear LEDs. A blue LED was used for FAD excitation, while red and green LEDs were used in combination to construct the OIS signal. Electrical forepaw stimulation was used to quantitatively evaluate the spatial and temporal resolution of the FAD signal as compared to OIS. Evaluation of spontaneous FAD signals demonstrated the feasibility of mapping FC patterns directly from metabolite dynamics. Evoked responses by forepaw stimulation also revealed that the OIS time-to-peak response lagged the time course of FAD emission. Mouse-specific FC mapping could provide a link between molecular level mouse models of disease and a clinical human disease, with FAD and OIS imaging providing alternative views of underlying neuronal mechanisms.

8565-166, Session 1

A time-gated near-infrared spectroscopic imaging device for human brain activation

Patrick Poulet, Wilfried Uhring, Univ. de Strasbourg (France); Walter Hanselmann, montena emc (Switzerland); Rene Glazerborg, Photonis (Netherlands); Farouk Nouizi, Chantal-Virginie Zint, Univ. de Strasbourg (France); Werner Hirschi, montena emc (Switzerland)

A time-resolved, spectroscopic, diffuse optical tomography device was assembled for clinical applications like brain functional imaging. The entire instrument lies in a unique setup that includes a light source, an ultrafast time-gated intensified camera and all the electronic control units. The light source is composed of four near infrared laser diodes driven by a nanosecond electrical pulse generator working in a sequential mode at a repetition rate of 100 MHz. The light pulses are less than 80 ps FWHM. They are injected in a four-furcated optical fiber ended with a frontal light distributor to obtain a uniform illumination spot directed towards the head of the patient. Photons back-scattered by the subject are detected by the intensified CCD camera. There are resolved according to their time of flight inside the head. The photocathode is powered by an ultrafast generator producing 50 V pulses, at 100 MHz and a width corresponding to a 200 ps gate. The intensifier has been specially designed for this application. The whole instrument is controlled by an FPGA based module. All the acquisition parameters are configurable via software through an USB plug and the image data are transferred to a PC via an Ethernet link. The compactness of the device makes it a perfect device for bedside clinical applications. The instrument will be described and characterized. Preliminary data recorded on test samples will be presented and compared to simulation results.

8565-168, Session 1

Orthogonal diffuse near-infrared reflectance spectroscopy allows to assess cerebral dysfunction and temperature variations following heatstroke on a mouse model

David Abookasis, Elad Zafrir, Elimelech Nesher, Albert Pinchasov, Shmuel Sternklar, Ariel Univ. Ctr. of Samaria (Israel); Marlon S. Mathews, Beckman Laser Institute and Medical Clinic (United States)

In this study, we used orthogonal diffuse reflectance spectroscopy (DRS) to assess brain dysfunction and to monitor internal temperature variations during heatstroke in intact mice brains (n=6). Heatstroke is a medical emergency defined by abnormally elevated body temperature greater than 40°C that causes biochemical, physiological and hematological changes (multiorgan damage). Therefore, quick diagnosis and management of heatstroke victims is essential for positive prognosis. Current clinical methods for monitoring temperature (invasive and noninvasive) suffers from several drawbacks such as complexity, cost, portability, safety, etc. To overcomes these deficiencies, a DRS working at the spectral range of 600-1000nm in orthogonal mode together with numerical processing have been applied to First, monitor cerebral optical changes, Second, evaluate rise in temperature and Third, to predict internal temperature noninvasively. Heatstroke was induced by exposing of the anesthetized mouse body, placed above controlled heating pad, to a high ambient temperature with increasing intervals of 1°C until death. Experimental results show variations in both absorption and scattering during heatstroke which emphasizes the changes in brain chromophores and morphology that occur during temperature elevation. In addition, a reflectance-temperature index was developed and found to correlate well with the measured temperature. Our preliminary results suggest orthogonal DRS have the potential to monitor and assess internal temperature variations and thus may serve as a useful tool in clinical and laboratory settings.

8565-170, Session 1

Generation of spreading depolarization and prolonged hypoxia in rat brain exposed to a laser-induced shock wave

Satoko Kawauchi, Shunichi Sato, National Defense Medical College (Japan); Izumi Nishidate, Tokyo Univ. of Agriculture and Technology (Japan); Hiroshi Nawashiro, Hiroshi Ashida, National Defense Medical College (Japan)

Blast-induced traumatic brain injury (bTBI) is a recent major concern in neurotraumatology. However, the mechanism and symptoms of bTBI are poorly understood and thus, reliable and easy-to-handle animal models are needed. We have been proposing the use of a laser-induced shock wave (LISW) to simulate bTBI in small animals. The method is characterized by safety and high spatiotemporal controllability in the shock wave energy. In our previous experiments, we locally applied an LISW to the rat brain and observed the generation of spreading depolarization and prolonged hypoxia. These two events might be correlated, but their causality is not clear. In this study, we investigated spatiotemporal characteristics of the spreading depolarization and prolonged hypoxia that occurred in the rat brain after LISW application to reveal their correlation. We also quantified the level of hypoxia, which might cause neuronal cell death. CCD-based reflectance imaging showed that immediately after the application of an LISW (peak pressure, ~95 MPa), depolarization wave was generated focally and propagated over the cortex in the hemisphere at a rate of 2.4-3.0 mm/min. During and after the propagation of the depolarization wave, long-lasting brain hypoxia was observed for up to ~3 h both by the diffuse reflectance and polarographic measurements. The oxygen partial pressure decreased up to about 55% of its initial level. Since spreading depolarization is known to be accompanied by a rapid consumption of the cerebral ATP, it would be a key event to cause hypoxia in the rat brain.

8565-172, Session 2

in vivo and in situ detection of atherosclerotic plaques using full-range complex-conjugate-free spectral domain optical coherence tomography in the murine carotid

Yong Huang, Robert Wicks, Johns Hopkins Univ. (United States); Kang Zhang, GE Global Research (United States); Mingtao Zhao, Lee Hwang, Johns Hopkins Univ. (United States); Betty Tyler, Gustavo Pradilla, The Johns Hopkins Hospital (United States); Jin U. Kang, Johns Hopkins Univ. (United States)

Stroke is the fourth leading cause of death in the United States. Carotid endarterectomy (CEA) has been shown to be superior to medical therapy for prevention of stroke. Approximately 140,000 CEA procedures are performed in the US each year. There is a need for a high-resolution, real-time, intraoperative imaging technique for detection of atherosclerotic plaque position and morphology. Optical coherence tomography (OCT) provides non-invasive cross-sectional imaging with a micrometer resolution. Eight wild-type mice (Nml) and 16 apolipoprotein E-deficient (ApoE-/-) mice, age 16 weeks, were randomized to three treatment groups: 1) Nml mice on a diet of regular rodent chow (n=8); 2) ApoE-/- on a high-fat, atherosclerotic diet (HFD) (n=8); and 3) ApoE-/- mice on a HFD given daily pravastatin (n=8). Mice were anesthetized and the left common carotid was exposed via left lateral neck dissection. Full-range, complex-conjugate-free spectral domain optical coherence tomography was utilized in 2D and 3D imaging of the area of interest in real-time through graphics processing unit accelerated algorithm. Mice were then perfused with saline and formalin. In-situ imaging after perfusion was performed for comparison with the in-vivo detection result. Carotid arteries were then resected, paraffin embedded and stained with hematoxylin and eosin for histologic comparison. Intraoperative OCT imaging showed clear plaque development in the ApoE-/- mice with less plaque in the ApoE-/- given pravastatin. The findings were confirmed with OCT imaging after perfusion and histology. Intraoperative OCT imaging during CEA offers the potential for real-time, detailed plaque imaging, potentially improving surgical accuracy and outcomes.

8565-173, Session 2

Optical coherence tomography detection of shear wave propagation in inhomogeneous tissue equivalent phantoms

Marjan Razani, Adrian Mariampillai, Beau A. Standish, Victor X. D. Yang, Michael C. Kolios, Ryerson Univ. (Canada)

In this work, we explored the potential of measuring shear wave propagation using Optical Coherence Elastography (OCE) based on a swept-source optical coherence tomography (OCT) system. Shear waves were generated using a piezoelectric transmitting sine-wave bursts of 400 ?s, synchronized with the OCT swept source wavelength sweep. The acoustic radiation force was applied to inhomogeneous phantoms. Differential OCT phase maps, measured with and without the acoustic radiation force, demonstrate microscopic displacement generated by shear wave propagation in these phantoms of different stiffness. The OCT phase maps are acquired with a swept-source OCT (SS-OCT) system. We present a technique for calculating tissue mechanical properties by propagating shear waves in inhomogeneous tissue equivalent phantoms with Acoustic Radiation Force (ARF), and measuring the shear wave speed and its associated properties with OCT phase maps. This method lays the foundation for future studies of mechanical property measurements of heterogeneous tissue structures, as well as potential research applications in pathology, aneurysm and intravascular studies.

8565-175, Session 2

Windows to the brain: novel concept for providing non-invasive, chronic access to brain for optical diagnostics and therapeutics

Yasaman Damestani, B. Hyle Park, Devin K. Binder, Javier E. Garay, Masaru P. Rao, Guillermo Aguilar, Univ. of California, Riverside (United States)

Every year only in the U.S., two million Traumatic Brain Injury (TBI) cases lead to 56,000 death and 18,000 survivors suffering from neurological impairment; and, 66,000 new cases of brain tumors are diagnosed. Patients with TBI, brain tumors, congenital deformities, or decompressive craniectomies require adequate reconstruction which provides chronic optical access to brain. Optical access is essential for precise postoperative imaging and therapy without future highly-invasive procedures. Our goal is to develop a transparent polycrystalline Yttria-Stabilized-Zirconia (YSZ) cranial implant (“window”) that enables chronic, non-invasive delivery and/or collection of laser light into/from affected areas within the brain.

The YSZ cranial implant is fabricated using current-activated pressure-assisted densification technique. The biocompatibility of YSZ implant is confirmed in vitro by cell growth and cytotoxicity assays of mouse embryonic fibroblast cells grown on the implant surface. In vivo, a part of mouse skull is replaced with the implant during craniectomy. Comparison of optical coherence tomography (OCT) images of murine brain with native cranium and YSZ implant confirms that the implant improves OCT axial and lateral resolution and laser penetration depth.

Also, the biological reaction of YSZ implant on murine calvarial bone after one week is assessed using histological analysis. In the prolong study, optical clearing agents are delivered with minimally-invasive microneedling technique to make the scalp that permanently covers the window temporarily transparent.

The results of this study suggest that transparent YSZ implant provides

biomechanical stability, cerebral protection, optimal cosmetic results, and chronic optical access to brain.

8565-236, Session 2

Blood flow velocity measurement by endovascular Doppler optical coherence tomography

Cuiru Sun, Univ. of Toronto (Canada); Barry Vuong, Felix Nolte, Ryerson Univ. (Canada); Kyle Cheng, Kenneth K. C. Lee, Univ. of Toronto (Canada); Beau A. Standish, Ryerson Univ. (Canada); Brian K. Courtney M.D., Sunnybrook Health Sciences Ctr. (Canada); Tom R. Marotta, St. Michael's Hospital (Canada); Adrian Mariampillai, Victor X. D. Yang, Ryerson Univ. (Canada)

Blood flow velocity and volumetric flow measurements are important parameters for assessment of the severity of stenosis and the outcome of interventional therapy. However, feasibility of intravascular flow measurement using a rotational catheter based phase resolved Doppler OCT is difficult. Motion artefacts induced by the rotating optical imaging catheter, and the radially dependent noise background of measured Doppler signals are the main challenges encountered. In this study, custom-made data acquisition system and algorithms are developed to remove non-uniform rotational distortion (NURD) induced phase shift artefact by tracking the phase shift observed on catheter sheath. The flow velocity is calculated from Doppler shift obtained by Kasai autocorrelation after motion artefact removal. A quality-guided phase unwrapping algorithm was used to unwrap the phase map.

Blood flow velocity profiles in porcine carotid arteries in vivo were obtained at 100 frames/s with 500 A-lines/frame and Doppler OCT images were taken at 20 frames/s with 2500 A-lines/frame. Three dimensional reconstruction of the vessel wall with the catheter from pull-back OCT imaging were employed and estimated the Doppler angle. Time-varying velocity profiles were obtained at a circular cross-section of a carotid artery and at an artery branch. Furthermore, the identification of vein adjacent to the catheterized vessel based on the color Doppler signal was also observed. Imaging results demonstrated that the system can measure the flow velocity as high as ~ 51 cm/s and a minimum detectable flow velocity ~ 2 mm/s. As a result, the absolute measurement of intravascular flow using a rotating fiber catheter is demonstrated, which can provide insights to different stages of interventional treatment of stenosis in coronary or carotid arteries.

8565-176, Session 3

Video-rate resonant scanning multiphoton microscopy: an emerging technique for intravital imaging

Euiheon Chung, Gwangju Institute of Science and Technology (Korea, Republic of); Nathaniel D. Kirkpatrick, Daniel C. Cook, Xiaoxing Han, Gabriel Gruionu, Shan Liao, Lance L. Munn, Timophy P. Padera, Dai Fukumura M.D., Rakesh K. Jain, Massachusetts General Hospital (United States)

The abnormal tumor microenvironment fuels tumor progression, metastasis, immune suppression, and treatment resistance. Over last several decades, developments in and applications of intravital microscopy have provided unprecedented insights into the dynamics of the tumor microenvironment. In particular, intravital multiphoton microscopy has revealed the abnormal structure and function of tumor-associated blood and lymphatic vessels, the role of aberrant tumor matrix in drug delivery, invasion and metastasis of tumor cells, the dynamics of immune cell trafficking to and within tumors, and gene expression in tumors. However, traditional multiphoton microscopy suffers from inherently slow imaging rates—only a few frames per second, thus unable to capture more rapid events such as blood flow, lymphatic flow, and cell invasion. Here, we report the development and implementation of a video-rate multiphoton microscope (VR-MPLSM) based on resonant galvanometer mirror scanning that is capable of recording at 30 frames per second and acquiring intravital multispectral images. We show that the design of the system can be readily implemented and is adaptable to various experimental models including brain metastasis. As examples, we demonstrate the utility of the system to directly measure flow within tumors, capture metastatic cancer cells moving within the brain vasculature and cells in lymphatic vessels, and image acute responses to changes in a vascular network. VR-MPLSM thus has the potential to further advance in vivo imaging and provide new insight into the biology of the tissue microenvironment.

8565-177, Session 3

Multimodal microscopy imaging of oxygen delivery in mouse cerebral microvasculature

Sava Sakad?ic, Emiri T. Mandeville, Massachusetts General Hospital (United States); Anna Devor, Massachusetts General Hospital (United States) and Univ. of California, San Diego (United States); Mohammad A. Yaseen, Joe J. Musacchia, Massachusetts General Hospital (United States); Louis Gagnon, Harvard-MIT (United States); Katharina Eikermann-Haerter, Massachusetts General Hospital (United States); Emmanuel Roussakis, Univ. of Pennsylvania (United States); Vivek J. Srinivasan, Cenk Ayata, Eng H. Lo, Massachusetts General Hospital (United States); Anders M. Dale, Univ. of California, San Diego (United States); Sergei A. Vinogradov, Univ. of Pennsylvania (United States); David A. Boas, Massachusetts General Hospital (United States)

Detailed microscopic measurements of oxygen delivery from cerebral microvasculature are needed to better understand cerebrovascular pathologies and to guide interpretation of macroscopic measures such as fMRI blood-oxygen-level dependence (BOLD). However, majority of intravascular PO2 measurements in the past were performed using invasive point measurement methods with limited spatial resolution below cortical surface, such as oxygen sensitive electrodes. In this work we present a multi-modal microscopy platform for imaging oxygen delivery in cerebral microvasculature in small rodents.

We combined two-photon microscopy imaging of oxygen partial pressure (PO2) based on measuring oxygen-dependent phosphorescence lifetime with Doppler Optical Coherence Tomography (Doppler OCT) – based imaging of cortical blood flow. Two independent scanning arms allowed independent optimization of scanning protocols for each imaging modality. Micro-angiograms were acquired by both modalities and used for corregistration.

Imaging was performed through a sealed cranial window in anesthetized C57BL/6 mice. We have obtained the high-resolution and high-density PO2 maps and detailed PO2 distributions in microvascular segments down to 450 um depth from the mouse cortical surface. The maps of PO2 values were analyzed using the graph representation of the actual microvascular trees. The methodology was used to infer cortical microvascular oxygenation distribution as a function of various vascular morphological parameters and to assess the influence of elevated blood flow during hypercapnia on microvascular oxygen delivery. While significant portion of SO2 (up to 20%) is reduced before the blood reaches the capillaries, the biggest SO2 increase during hypercapnia was measured in the capillaries distal to precapillary arterioles.

8565-178, Session 3

Investigation of human multiple sclerosis lesions using high resolution spectrally unmixed CARS microscopy

Kelvin W. Poon, Craig Brideau, Wulin Teo, Univ. of Calgary (Canada); Geert J. Schenk, Roel Klaver, Vrije Univ. Medical Ctr. (Netherlands); Jean H. Kawasoe, Univ. of Calgary (Canada); Jeroen Geurts, Vrije Univ. Medical Ctr. (Netherlands); Peter K. Stys, Univ. of Calgary (Canada)

The pathology of multiple sclerosis (MS) involves both the gray and white matter regions of the brain and spinal cord. It is characterized by various combinations of demyelination, inflammatory infiltration, axonal degeneration, and later gliosis in chronic lesions. While acute and chronic white matter plaques are well characterized and easily identified, evidence indicates that the CNS of MS patients may be globally altered, with subtle abnormalities found in grossly normal appearing white matter (NAWM) and in diffusely abnormal white matter (DAWM) where histochemical stains and advanced magnetic resonance imaging indicate altered tissue composition. Thus, the prototypical acute inflammatory lesion may merely represent the most obvious manifestation of a chronic widespread involvement of the CNS, which is difficult to examine reliably.

The current study deals with the microstructure and biochemistry of demyelination, remyelination and axonal loss in various regions of post-mortem human MS brain, including NAWM, DAWM and more typical acute and chronic lesions. The myelin sheath, neuroglia and perivascular spaces were investigated using a novel Coherent Anti-Stokes Raman Scattering (CARS) microscope with simultaneous Two-Photon Excited Fluorescence (TPEF) imaging. The active CH stretching region between ~ 2800 and 3015 cm-1 was probed to provide chemically specific, high resolution, label-free imaging pertaining to the progression of the disease. CARS data were correlated with TPEF and conventional histochemical stains.

Our novel CARS microscopy system provides detailed morphological and biochemical information regarding CNS pathology in MS and possibly other neurodegenerative disorders.

8565-179, Session 3

Comparative evaluation of methylene blue and demeclocycline for enhancing optical contrast of brain neoplasms

Dennis J. Wirth, Univ. of Massachusetts Lowell (United States); Matija Snuderl, Harvard Medical School (United States); Sameer A. Sheth, Churl-Su Kwon, William Curry, Massachusetts General Hospital (United States); Anna N. Yaroslavsky, Univ. of Massachusetts Lowell (United States) and Massachusetts General Hospital (United States) and Harvard Medical School (United States)

Contrast agents have shown to be useful in the detection of cancers. The goal of this study was to compare enhancement of brain cancer contrast using reflectance and fluorescence confocal imaging of two fluorophores, methylene blue (MB) and demeclocycline (DMN). Both contrast agents are nuclear stains and mimic the staining pattern of H&E histopathology. MB absorbs light in the red spectral range and fluoresces in the near infrared. It is FDA-approved for in vivo staining of human skin and breast tissue. However, its safety for staining human brain is questionable. Thus, DMN, which absorbs light in the violet spectral range and has a broad emission band covering green and yellow wavelengths, could provide a safer alternative to MB. Fresh excessive human brain tissues, obtained from surgeries, were cut in two pieces and stained with aqueous solutions of MB and DMN, respectively. Stained tissues were imaged using in-house built multimodal confocal imagers. The resulting reflectance and fluorescence optical images were compared and correlated with H&E histopathology, processed from each imaged tissue. The results indicate that the images of tissues stained with both stains exhibit comparable contrast and resolution of morphological detail. Further studies are required to establish the safety and efficacy of these contrast agents for use in human brain.

8565-180, Session 3

Three-dimensional imaging of whole rat sciatic nerve treatment response by tissue clearing

Yookyung Jung, Wellman Ctr. for Photomedicine (United States) and Harvard Medical School (United States) and Massachusetts General Hospital (United States); Cameron P. Keating, Prabhu Senthil-Kumar, Harvard Medical School (United States) and Massachusetts General Hospital (United States); Jonathan N. Soriano, Joanna Ng, Mark A. Randolph, Massachusetts General Hospital (United States); Jonathan M. Winograd, Harvard Medical School (United States) and Massachusetts General Hospital (United States); Conor L. Evans, Wellman Ctr. for Photomedicine (United States) and Harvard Medical School (United States) and Massachusetts General Hospital (United States)

Recently, studies have reported enhanced behavioral recovery from completely severed nerves after treatment with microsuturing in combination with administration of methylene blue (MB) and polyethylene glycol (PEG). The improved recovery observed in rat sciatic nerves has been proposed to arise from accelerated reconnection of cut axons. For accurate evaluation of this mechanism of nerve repair, direct observation and visualization of regenerated or reconnected axons at the lesion site is needed. Fluorescence microscopy has the ability to play an important role in such studies, as it provides both high resolution and specificity to image individual axons. However, the penetration depth of confocal and even standard multiphoton fluorescence microscopy is at most 100~300 ?m in rat sciatic nerves, preventing complete visualization of repair processes.

The problem of limited imaging depth can be solved using tissue clearing methods. In tissue clearing, water in nerve tissue is replaced by chemicals that have the same refractive index as the tissue itself, leading to substantially decreased light scattering and enhanced imaging penetration depth. We have found that tissue clearing preserves the structure of axons and the fluorescence from the green fluorescent protein (GFP) or fluorescent labeling of axonal neurofilaments, enabling three dimensional, whole sciatic nerve imaging. Using tissue clearing, we have performed time-course studies visualizing both microsuture and MB/PEG chemical repair of severed rat sciatic nerves. Imaging experiments have also been focused on correlated axonal changes observed in repaired nerves with functional changes observed in innervated muscle through measurements of motor endplate connectivity.

8565-181, Session 4

Concurrent multi-scale imaging combining optical coherence tomography with MRI for neurosurgery guidance

Chia-Pin Liang, Il Kyoon Kim, Bo Yang, Univ. of Maryland, College Park (United States); George Makris, Univ. of Maryland School of Medicine (United States); Jaydev Desai, Univ. of Maryland, College Park (United States); Rao L. Gullapalli, Univ. of Maryland School of Medicine (United States); Yu Chen, Univ. of Maryland, College Park (United States)

We developed a novel platform based on a teleoperated robot to perform high-resolution optical coherence tomography (OCT) imaging under

continuous MRI guidance. The superior soft tissue contrast and versatile imaging protocols of intra-operative MRI make it a promising guidance tool for high-precision functional neurosurgical interventions. Although useful for guidance, MRI alone may not have the resolution to detect micro-anatomical landmarks surrounding the targets. Microscopic OCT imaging on the other hand can visualize these landmarks and has been used to guide deep brain surgeries in small rodents in vivo and target human brain nuclei ex vivo. The limited field of view of OCT however necessitates that the OCT be selectively transported to the specific site of interest under MRI guidance. The combination of large-scale MRI tissue morphology and high-resolution OCT micro-anatomy in a concurrent and co-registered manner has great potential to improve the accuracy of various neurosurgical procedures. In this first ever development of MRI-compatible OCT imaging system, we integrated the OCT probe into a titanium cannula and navigated toward the target using a MRI-compatible robot. The OCT probe was scanned linearly using a piezoelectric transducer. The concurrent MRI/OCT dynamic images (imaging speed 0.25 frames/s for MRI and 15 frames/s for OCT) on sheep brain ex vivo demonstrated that OCT can reveal many MRI occult structures. The large-scale MRI image can be used to plan the trajectory and monitor the coarse instrument position relative to the target and real-time, high resolution OCT image can detect the important micro-landmarks for high-precision targeting.

8565-182, Session 4

Developing intraoperative confocal microscopes for guiding brain tumor resection

Steven Y. Leigh, Danni Wang, Ye Chen, Arnavi Varshney, Jonathan T. C. Liu, Stony Brook Univ. (United States)

Mounting evidence suggests that more extensive neurosurgical resection of gliomas is associated with increased overall survival. In a recent phase III trial led by Stummer et al., fluorescence image-guided surgery (FIGS) using contrast provided by 5-aminolevulinic acid (5-ALA)-induced PpIX fluorescence was associated with doubling the extent of resection and a 40% increase in overall survival. However, there are limitations to these wide-field imaging methods that have been discussed in the literature. For example, glioma margins are diffuse and lack a distinct transition between tumor and normal tissue. Wide-field (low-resolution) approaches, such as FIGS and MRI, provide pixel intensities that represent an average value from many cells, resulting in a diminished ability to detect the sparse fluorescent cell populations in low-grade gliomas and at the margins of all diffuse tumors. Therefore, a potential valuable complement to wide-field imaging would be an intraoperative optical-sectioning microscope capable of detecting and quantifying the presence of sparse populations of labeled cells. We have developed a surgical microscope utilizing a novel dual-axis confocal architecture for deep optical sectioning within tissues. The dual-axis configuration has been shown – through diffraction-theory modeling, Monte-Carlo scattering simulations, tissue phantom studies, and tissue-imaging experiments – to efficiently reject out-of-focus and multiply scattered light for high-contrast optical sectioning within tissues. Our surgical prototype incorporates a custom-designed biaxial-scanning MEMS mirror for high-speed imaging over a large field of view. Ex vivo and in vivo imaging studies have been performed on preclinical animal models stained with targeted and nontargeted fluorescent contrast agents, such as fluorescent antibodies and 5-ALA, respectively.

8565-183, Session 4

High sensitive time-resolved thermography and multivariate image analysis of the cerebral cortex for intrasurgical diagnostic

Julia Hollmach, Nico Hoffmann, Christian Schnabel, Technische Univ. Dresden (Germany); Saskia Kuchler, Stephan B. Sobottka, Matthias Kirsch, Gabriele Schackert, Edmund Koch, Universitätsklinikum Carl Gustav Carus Dresden (Germany); Gerald Steiner, Technische Univ. Dresden (Germany)

Time-resolved thermography is a novel method to assess thermal variations and heterogeneities in tissue and blood. The recent generation of thermal cameras provides a sensitivity of less than mK. This high sensitivity in conjunction with non-invasive, label-free and radiation-free monitoring makes thermography to a promising tool for intrasurgical diagnostic. In brain surgery, time-resolved thermography can be employed to distinguish between normal and anomalous tissue. In this study, we investigated and discussed the potential of time-resolved thermography in neurosurgery for the intraoperative detection of functional areas and demarcation of tumor borders. Algorithms for segmentation, reduction of movement artifacts and image fusion were developed. The preprocessed image stacks were subjected to multivariate data analysis methods to examine the response of induced stimuli. Principle Component Analysis was used for image evaluation to reveal small variances within the image sequence. The image evaluation shows significant differences for both types of tissue. Tumor and normal tissues have different time characteristics in heat production and transfer. Furthermore, active brain areas and perfusion profiles could be highlighted. These results demonstrated that time-resolved thermography is able to support the detection of tumors, circulatory disorders and functional areas in a contactless manner without any side effects for the tissue. The intraoperative usage of time-resolved thermography improves the accuracy of stenosis and tumor resections to prevent irreversible brain damage during surgery.

8565-184, Session 4

Non-invasive imaging of tumorous and healthy tissue in the human brain

Fabrice Harms, LLTECH SAS (France); Bertrand Devaux, Pascale Varlet, Hôpital Sainte Anne (France); Katharine Grieve, Anne Latrive, Institut Langevin (France); Bertrand Le Conte De Poly, LLTECH SAS (France); A. Claude Boccara, Institut Langevin (France) and LLTECH SAS (France)

Full-field OCT captures en face slices in tissue at 1 um resolution in 3D. In contrast with time or Fourier domain OCT, full-field OCT directly captures “en face” images using megapixel cameras and gel or water immersion microscope objectives of medium numerical aperture that provide high lateral and axial resolution (typically~1?m ?1?m?1?m).

Mosaicing of 1mm2 native field images produces large field views of macroscopic tissue architecture, on which a digital zoom reveals the microscopic structures. Depth stacks can subsequently be captured in areas of interest. The imaging process is non-invasive and requires no staining, which makes the technique particularly suitable for applications in pathology.

Here we use full-field OCT to image the human brain. Myelin fibers are clearly defined, grey matter can be discriminated from white matter, and axon bundles, glial cells and neurons are visible. We report on progress of a pre-clinical study to evaluate the use of full-field OCT in diagnosis and margin assessment of brain tumors, and we present cases of imaging meningioma, glioma, epileptic cortex and hippocampus in excised human brain specimens. This study constitutes a first step toward use of full-field OCT in the operating room for real-time diagnosis on excised samples during brain surgery.

Furthermore we are developing a similar system with a rigid probe to allow in vivo and in situ high-resolution imaging. Our probe could thus guide the surgeon before and during excision and ensure a more precise gesture.

8565-185, Session 4

Progress in translating multimodal nonlinear microscopy from basic research into neurosurgical praxis

Jürgen Popp, Tobias Meyer, Anna Medyukhina, Institut für Photonische Technologien e.V. (Germany); Martin Baumgartl, Thomas Gottschall, Jens Limpert, Andreas Tünnermann, Friedrich-Schiller-Univ. Jena (Germany); Benjamin Dietzek, Institut für Photonische Technologien e.V. (Germany); Michael Schmitt, Friedrich-Schiller-Univ. Jena (Germany)

Multimodal nonlinear microscopy utilizing NIR lasers is one of the most promising techniques for molecular imaging with respect to future application in clinics. This technique uniquely combines label-free chemical contrast and diffraction limited spatial resolution with low phototoxicity and moderate depth penetration in the range of few 100 µm. However, a complex and maintenance-intense instrumentation needs to be overcome in order for the technique to mature into a routine imaging tool for the clinics. Additionally, multimodal microscopy provides generally lower image contrast compared to the golden standard, staining histopathology, an issue of equal importance to be tackled.

In this contribution a portable and robust multimodal nonlinear microscope for simultaneous CARS, SHG and TPEF imaging is presented, utilizing an ultra compact fiber laser light source, which is ideally suited for implementation into an endoscope. In addition to the novel instrument, automated image processing routines have been developed and tested for automated image contrast enhancement and segmentation. The image analysis presented allows for extraction of histopathologically relevant parameters of the tissue, e.g. nucleus to cytoplasm ratio, cell density, nuclear size and shape, which are routinely used in pathology for grading of neoplasms of the human brain.

Financial support from European Union via the ‘Europäischer Fonds für Regionale Entwicklung (EFRE)’ and the ‘Thüringer Ministerium für Bildung Wissenschaft und Kultur (TMBWK)’ (projects: B578-06001, 14.90 HWP and B714-07037) and the German Federal Ministry for Science and Education (BMBF) MediCARS (FKZ: 13N10773 and 13N10774) is gratefully acknowledged.

8565-186, Session 4

Raman and infrared spectroscopic imaging for biochemical and morphological assessment of brain tumors

Christoph Krafft, Norbert Bergner, Institut für Photonische Technologien e.V. (Germany); Bernd F. M. Romeike, Rupert Reichart, Rolf Kalff, Friedrich-Schiller-Univ. Jena (Germany); Kathrin D. Geiger, Gabriele Schackert, Technische Univ. Dresden (Germany); Jürgen Popp, Institut für Photonische Technologien e.V. (Germany) and Friedrich-Schiller-Univ. Jena (Germany)

Raman and infrared spectroscopy enables label-free assessment of brain tissues and tumors at molecular and microscopic level. This contribution presents Raman and infrared images collected from low grade brain tumors (astrocytoma grade II), high grade brain tumors (astrocytoma grade III, glioblastoma multiforme) and brain metastases. A two level discrimination model for Raman and infrared data distinguished normal brain, necrosis and tumor tissue, and subsequently determined the primary tumor. Unsupervised unmixing of Raman images was applied for morphochemical analysis of non-dried brain tumor specimens. The spectral signatures and abundances of cholesterol, cholesterol ester, nucleic acids, proteins, lipids, carotene and buffer were identified. Lipid-to-protein ratios and nucleic acid-to-protein ratios were determined from the data that correlated well with the tumor grade. Furthermore, a nucleus-to-cytoplasm parameter was derived that also correlated with the tumor grade. An outlook will be given how to decrease collection time using coherent anti-Stokes Raman scattering (CARS) and to couple Raman systems with fiber optic probes for intraoperative applications.

Acknowledgements: Financial support of the European Union via the “Europäischer Fonds für Regionale Entwicklung” (EFRE) and the ”Thüringer Ministerium für Bildung, Wissenschaft und Kultur” (project: B714-07037) and the Federal Ministry of Education and Research (BMBF) (project: MediCARS) is highly acknowledged.

8565-187, Session 4

Analysis of specific factors of the heme biosynthesis in correlation to 5-?ALA induced fluorescence in gliomas

Georg Widhalm, Barbara Kiesel, Daniela Lötsch, Mauricio Moreno-?? M.D., Engelbert Knosp, Walter Berger, Stefan Wolfsberger, Medizinische Univ. Wien (Austria)

Fluorescence-guided resection of malignant gliomas using 5-aminolevulinic acid (5-ALA) established as a promising technique in many neurosurgical centers. In contrast, 5-ALA is not capable to visualize low grade glioma tissue in the majority of patients. Recently, specific factors of the heme biosynthesis were described that might play a key role for the presence of visible 5-?ALA fluorescence in different tumor tissues. Therefore, we analyzed specific factors of the heme biosynthesis in multiple tumor samples with strong and negative 5-ALA fluorescence of gliomas.

8565-161, Session 5

Monitoring of human brain function in risk decision-making task by near-infrared spectroscopy using a pixel-wised general linear model

Lin Li, Zi-Jing Lin, Mary Cazzell, Hanli Liu, The Univ. of Texas at Arlington (United States)

Risk decision making is an important cognitive process and thus is an essential topic in the field of neuroscience. The balloon analogue risk task (BART) is a valid experimental model and has been commonly used in behavioral measures to assess human risk taking action and tendency while facing risks. In this study, we have utilized a modified BART model including the win/lose and voluntary/involuntary parameters with a blocked design to investigate hemodynamic responses in the prefrontal and frontal cortical areas during decision-making. We have also defined and utilized a risk-taking level score with two measurable quantities that can be acquired by the modified BART model and diffuse optical tomographic (DOT) technique. Those methods were performed on 40 human participants (23 males and 17 females) to obtain hemodynamic changes and risk-taking scores during risk-task performance. In this work, we plan to demonstrate the ability of recording and analyzing DOT images of brain activity using a 36-channel DOT system. The measured hemodynamic response changes induced by BART were analyzed by a pixel-wised general linear model. A clear and significant change can be quantitatively obtained from the intuitive cerebral activation maps in the dorsal-lateral prefrontal cortex during the active choice mode, which is consistent with the results given by fMRI studies. Moreover, the results also indicated a significant gender difference during the active choice mode.

8565-163, Session 5

Validation of fNIRS in the visual cortex of neonates via simultaneous fNIRS/fMRI imaging

Jeffrey W. Barker, Ardalan Aarabi, Ashok Panigrahy M.D., Theodore J. Huppert, Univ. of Pittsburgh (United States)

INTRODUCTION: Functional near infrared spectroscopic (fNIRS) imaging has great potential as a bedside diagnostic tool for the neonate population because of its low cost and portability. In this study, we developed a magnetic resonance imaging (MRI) compatible NIRS probe for simultaneous MRI/NIRS in neonates. We compared simultaneous fNIRS/fMRI measurements for the resting state and for a visual stimulus paradigm. METHODS: We developed an MR compatible tomographic fNIRS probe for imaging the occipital cortex in neonates. We acquired simultaneous frequency modulated NIRS (FM-NIRS; ISS Imagent) and fMRI data in neonates during resting state and for a functional stimulus consisting of a 60° arc of LED lamps, which could be flashed at 4Hz in unison for full-field illumination or sequentially illuminated to give the impression of motion. Concurrent fMRI-BOLD and NIRS signals were recorded. The infant structural MR image was segmented into a 3-layer model (skin/scalp, CSF, brain) and used to model the diffusion approximation using the NIRFAST software. Both baseline scattering and absorption maps, as well as functionally-evoked changes in hemoglobin were reconstructed from the tomographic data and compared to fMRI results. RESULTS: Our preliminary results show strong correlation (R between 0.39-0.86) between the fMRI and fNIRS time-courses extracted from regions-of-interest from within the visual cortex of the infant during resting state scans. CONCLUSION: Simultaneous fMRI and fNIRS measurements are highly correlated in the visual cortex of neonates. This supports the validity of fNIRS as a potential independent modality for functional imaging of neonates.

8565-165, Session 5

Test-retest assessment of functional near-infrared spectroscopy to measure risk decision making in young adults

Lin Li, Zi-Jing Lin, Mary Cazzell, Hanli Liu, The Univ. of Texas at Arlington (United States)

Determining the reliability and reproducibility of hemodynamic responses measured by functional near-infrared spectroscopy (fNIRS) is important in order to interpret and understand the results of fNIRS experiments. We performed an fNIRS study, which was designed to associate hemodynamic responses in several cortical regions with risk decision making behavior in 9 young adults among a 3-week test-retest period. The Balloon Analog Risk Task (BART) is a protocol to evoke a risk-taking environment by introducing a gambling-like balloon game procedure. BART has been widely used to study the level of risk taking ability in the field of psychology, but it is the 1st time to be investigated by fNIRS. Repeated fNIRS measurements of young adult subjects were taken to identify brain activity changes in response to BART. In this study, we recorded the behavior performances simultaneously with the cerebral changes in oxygenated-hemoglobin (HbO) and deoxygenated-hemoglobin (HHb) concentrations. Both behavioral data and the observed hemodynamic patterns of brain activation support the hypothesis that the hemodynamic responses to BART are highly reproducible over the 3-week test-retest period.

8565-167, Session 5

Noninvasive optical evaluation of low frequency oscillations in prefrontal cortex hemodynamics during visual verbal working memory

Ting Li, Univ. of Science and Technology of China (China)

The low frequency oscillation (LFO) around 0.1 Hz has been observed recently in cerebral hemodynamic signals during rest/sleep, enhanced breathing, and head- up-tilting. Previous studies have shown that cerebral autoregulation can be accessed by LFOs. However, many brain function researches require direct measurement of LFOs during its specified brain function activities. This pilot study explored using near-infrared spectroscopy (NIRS) to noninvasively and simultaneously detect LFOs of prefrontal cerebral hemodynamics (i.e., oxygenated/deoxygenated/total hemoglobin concentration: [HbO2]/[Hb]/THC) during N-back visual verbal working memory task. The LFOs were extracted from the measured variables using power spectral analysis. We found the brain activation sites struck clear LFOs while other sites did not. The LFO of [Hb] acted as a negative pike and ranged in (0.05, 0.1)Hz, while LFOs of [HbO2] and THC acted as a positive pike and ranged in (0.1, 0.15) Hz. The amplitude difference and frequency lag between [Hb] and [HbO2]/THC produced a more focused and sensitive activation map compare to hemodynamic amplitude-quantified activation maps. This study observed LFOs in brain activities and showed strong potential of LFOs in accessing brain functions.

8565-169, Session 5

Study of resting state functional connectivity on the prefrontal cortex by using functional optical topography

Ching-Cheng Chuang, National Yang-Ming Univ. (Taiwan); Yao-Sheng Hsieh, National Taiwan Univ. (Taiwan); Kuen Feng Lin, National Yang-Ming Univ. (Taiwan); Tsan-Chi Liu, Chung Yuan Christian Univ. (Taiwan); Chia-Wei Sun, National Chiao Tung Univ. (Taiwan)

Resting state functional connectivity aims to identify spontaneous cerebral hemodynamic fluctuations that reflect neuronal activity at rest. As a promising non-invasive imaging technique, resting state studies of spontaneous fluctuations in the functional optical topography (fOT) has recently earned increasing attention and shown great promise in mapping the intrinsic functional organization of human brains. The purpose of this study was to assess hemodynamic changes over the prefrontal cortex (PFC) during the resting state by using a 52-channel fOT system (ETG-4000). This study consisted of a total of 20 healthy adult subjects. The mean age was 27 (± 3) years old. Regional mean time series were estimated by averaging the time series of all channels in this region. The Pearson's correlation coefficients were computed between each pair of source-detector combinations for each subject. The fOT signal is based on the intrinsic absorption of hemoglobin, therefore providing distinct maps for HbO2 and Hb. The result of correlations in the prefrontal cortex showed different patterns for HbO2 and Hb and showed the strong correlations between two hemispheres of PFC. Our findings suggest that fOT measurement could be applied to resting state functional connectivity studies. Besides, fOT may provide a high potential to determine whether functional connectivity between the regions identified as parts of the intrinsic functional organization were altered in patients with schizophrenia and dementia.

8565-171, Session 5

Simultaneous NIRS and kinematics study of planning and execution of motor skill task in subjects with and without cerebral palsy

Ujwal Chaudhary, Jean Gonzalez, Young-Jin Jung, Jennifer Davis, Patricia Gonzalez, Kyle Rice, Martha Bloyer, Leonard Elbaum, Anuradha Godavarty, Florida International Univ. (United States)

Cerebral palsy (CP) describes a group of motor impairment syndromes that occur in response to genetic and/or acquired disorders brain development. In the current study, NIRS and motion capture were simultaneously to be used in conjunction with kinematic studies in order to correlate the brain's planning and execution activity during and with arm movement in typically developing and subjects with cerebral palsy. The prefrontal region of the brain is non-invasively imaged using a custom built continuous-wave based near infrared spectroscopy (NIRS) system. The kinematics of the arm movement during imaging studies is recorded using an infrared based motion capture system, Qualisys. During the study, the subjects (over 18 years) performed 30-sec of arm movement followed by 30-sec of rest for 5 times, both with their dominant and non-dominant arm. The optical signal acquired from NIRS system was processed to elucidate the activation and lateralization in the prefrontal region of the participants. The preliminary NIRS results indicate differences in activation and lateralization in the prefrontal cortex across the stimuli and subject group. Currently simultaneous NIRS imaging and kinematics data are acquired in both the subject groups in order to correlate brain activity to arm movement in real-time. The study has significant implication in understanding the correlation between the planning and execution of arm movement (from NIRS imaging) to the actual arm movement (from kinematics). On a long run, the study has potential in augmenting the customizing the training or rehabilitation regime for individuals with CP via kinematic monitoring and brain imaging.

8565-188, Session PSun

Changes in cerebral hemodynamics in response to medical therapy for patent ductus arteriosus: prediction of treatment outcome in preterm infants

Mustafa Ridha, Lawson Health Research Institute (Canada); Rohit Arora, David Lee, Royal Victoria Hospital (Canada); Keith St. Lawrence, Lawson Health Research Institute (Canada); Ting-Yim Lee, Robarts Research Institute (Canada)

Echocardiography and BP measurements are traditionally used to diagnose hemodynamically significant patent ductus arteriosus (hsPDA) and to assess response to medical interventions. Changes in cerebral blood flow (CBF) may also estimate the hemodynamic significance of PDA and correlate with outcome.

CBF was measured before and after 3-day course of ibuprofen (IBU) or indomethacin (INDO) treatment to close hsPDA in preterm neonates. Quantitative CBF and cerebral metabolic rate of oxygen (CMRO2) were acquired by near infrared spectroscopy (NIRS) technique in conjunction with indocyanine green (ICG) tracer concentration curves. Treatment was deemed successful if no further intervention was necessary for the PDA.

16 preterm neonates (GA, 27±1.8wks; BW, 1007±200g; 10M:6F) with echo-confirmed hsPDAs were treated at a mean age of 6.3 days (11 with IBU and 5 with INDO). Treatment was successful in 9 (group A, 7 IBU, 2 INDO); the remaining 7 (group B) required further therapy and 4 needed surgical ligation. In group A, there was a significant increase in diastolic BP (+5.8 mmHg, p=0.03) and mean BP (+3.6 mmHg, p=0.04). The changes in diastolic BP correlated with changes in CBF in group A only (correlation coefficient=0.45). In this preliminary sample, 8 of 9 infants in group A had an increase in CBF; whereas only 2 of 7 in group B showed an increase in CBF, giving a positive predictive value (PPV) of 80% for PDA closure. The corresponding PPV for BP to predict outcome is 62%. CMRO2 values showed no change, suggesting that cerebral metabolism has not changed with PDA closure

Change in CBF may be used as a predictor of PDA outcomes post treatment independent of blood pressure and echo findings. The NIRS technique combined with ICG bolus-tracking is a rapid and simple bedside procedure that can provide valuable quantitative information on cerebral hemodynamics.

8565-189, Session PSun

Spatial frequency domain imaging for quantitative fluorescence image-guided brain tumor surgery: a comparative study

Mira Sibai, Princess Margaret Hospital (Canada); Michael J. Daly, MaRS Ctr. (Canada); Israel Veilleux, Princess Margaret Hospital (Canada); Anthony Kim, Sunnybrook Health Sciences Ctr. (Canada); Rolf B. Saagar, Beckman Laser Institute and Medical Clinic (United States); David J. Cuccia, Modulated Imaging, Inc. (United States); Brian C. Wilson, Princess Margaret Hospital (Canada)

Aminolevulinic acid-induced protoprophyrin IX (PpIX) provides fluorescence image contrast to assist in tumor margin resection, as in glioma. Although this enhances tumor delineation, visual assessment remains subjective and qualitative, which is problematic since the apparent fluorescence is distorted due to tissue's strong attenuation at the excitation and fluorescence emission wavelengths.

We have previously shown that quantitative measurement of the PpIX tissue concentration, [PpIX], derived from fluorescence and diffuse reflectance spectra and realized by an intraoperative fiber optic probe, increases sensitivity, resulting in more complete resection. However, this approach is limited to point measurements and thus time consuming. Hence, we propose extending to quantitative, wide-field fluorescence imaging by solving for the tissue optical properties across the field of view using spatial frequency domain imaging .

Here, both simulations and experimental measurements in tissue-simulating phantoms are presented. The instrumentation consists of multiple solid state light sources combined with a MEMS spatial light modulator to project intensity-patterned light onto the tissue surface. The spatially-modulated diffuse reflectance and the planar fluorescence images are captured by a CCD camera coupled with a liquid tunable crystal, providing spatial and spectral information to convert the fluorescence images to [PpIX] maps. Both uniform and non-uniform tissue fluorescent phantoms, comprising of haemoglobin and Intralipid as the absorber and scatterer, PpIX as the fluorophore, and agar as tissue matrix, are used to test the performance of the quantitative algorithm and optimize the modulation parameters yielding the most accurate [PpIX] measurements, both on the tissue surface and at depth.

8565-190, Session PSun

Hemodynamic responses to odor stimulation in the main olfactory bulb of rats using NIRS

Seungduk Lee, Korea Univ. (Korea, Republic of); Jaewoo Shin, Hwan Gon Lee, Chin Su Koh, Jae-Hong Park, Changkyun Im, Hallym Univ. (Korea, Republic of); Choong-Ki Kim, Korea Univ. (Korea, Republic of); In Seok Seo, Hyung-Cheul Shin, Hallym Univ. (Korea, Republic of); Beop-Min Kim, Korea Univ. (Korea, Republic of)

Odorant receptors in olfactory bulb are specialized to recognize physicochemical features such as chemical structures of odorant molecules, which are then translated into neural signals. In this study, we

tested whether the hemodynamic responses in the olfactory bulb can be used to distinguish different odorants including plain air as a reference (Blank), 2-Heptanone (HEP), Isopropylbenzene (IB), Isoamyl acetate (IAA) and 1-Pentanol (PEN). Our results show that odor-specific changes have regional dependency inside the olfactory bulb. Also, it was found that the temporal fluctuations of oxy-hemoglobin for various odorants could be additional marker for odor discrimination. Considering the good temporal resolution, we believe that NIRS may be useful for real-time interpretation of various odorants.

8565-191, Session PSun

Monitoring brain radiation therapy effects using speckle analysis in optical coherence tomography images

Andras Lindenmaier, Ontario Cancer Institute (Canada) and Univ. of Toronto (Canada); Kelly Burrell, Hospital for Sick Children (SickKids) (Canada); Leigh Conroy, Ralph DaCosta, Ontario Cancer Institute (Canada); Costel Flueraru, National Research Council Canada (Canada); Gelareh Zadeh, Univ. of Toronto (Canada) and Toronto Western Hospital (Canada); Alex I. Vitkin, Ontario Cancer Institute (Canada)

A significant proportion of the world population is affected by cancer at some point in their lifetime. ~50% of these are treated with X-ray radiation therapy,1 however the efficacy of the treatment is generally unknown for several weeks/months after treatment completion. This makes the adjustment of the treatment based on early response, and identification of non-responding patients, nearly impossible.

Some evidence suggests that optical coherence tomography (OCT) allows for the detection of early (1-3 weeks) structural and functional changes in tissue, by exploiting the information in the speckle features of the OCT images. This sub-resolution tissue information is not readily visible from the OCT structural images, but could potentially provide new biological metrics using advanced image analysis methods.2 For example, it has been shown that the temporal characteristics of OCT speckle are related to underlying tissue viscosity (microvasculature, interstitial fluid), and its spatial features are related to the cellular organizational microstructure of tissue.3

Here we show the results of an in-vivo mouse window chamber study, using non-obese diabetic immunodeficient NODSCID cranial window chamber mice with U87 glioblastoma xenografts. Both normal and human xenograft tumour tissues were treated with X-rays to monitor the changes due to ionizing radiation using speckle OCT. Different single doses in the 2-15 Gy range were delivered to tumour-bearing mice; these, as well as the un-irradiated controls, were imaged longitudinally for ~3 weeks after irradiation. The images were analyzed using quantifiable metrics based on OCT speckle statistics developed to differentiate between the different tissue types and irradiated and non-irradiated tumours. One set of metrics, intensity histogram based ones, allow for the differentiation of tumour and normal tissue as well as assessment of irradiation effects.

These newly developed OCT analysis methods report on functional and structural tissue changes due to ionizing radiation in-vivo, with potential for improving the optimization/delivery of radiation therapy as well as having fundamental scientific value in “shedding light on radiotherapy”.

References:

1. Halperin EC et al, Perez and Brady’s Principles and Practice of Radiation Oncology, Lippincott Williams and Wilkins (2008)

2. Dhawan AP, Huang HK and Kim DS, Principles and Advanced Methods in Medical Imaging and Image Analysis, World Scientific (2008)

3. Mariampillai A et al, Opt Lett 35, 1257-9 (2010)

8565-192, Session PSun

Effects of combined photochemical internalization and hyperthermia are sensitively dependent on radiant exposure

Steen J. Madsen, Christina Schlazer, Aaron Andersen, Stephanie Molina, Univ. of Nevada, Las Vegas (United States); Henry Hirschberg, Univ. of California, Irvine (United States)

Photochemical internalization (PCI) is designed to improve the delivery of therapeutic molecules in a site specific manner. It is a special version of photodynamic therapy (PDT) in which a plasma membrane localizing photosensitizer and a macromolecule (e.g. bleomycin) are localized in endocytic vesicles of target cells. PCI-mediated delivery of bleomycin has been shown to be effective in vitro against human glioma spheroids. In contrast to PCI, hyperthermia (HT) is a well-established therapeutic modality that has been used alone, or as an adjuvant for the treatment of a variety of cancers. The purpose of the present study was to determine whether the combination of PCI and HT results in enhanced toxicity compared to either treatment alone.

Human glioma spheroids (400-500 µm dia.) were irradiated with 670 nm laser light in a small incubator at temperatures ranging from 37 to 50 oC. For each temperature investigated (45 min. heating time), spheroids were divided into 5 groups: control, dark control, bleomycin-only, photodynamic therapy (PDT), and PCI. PDT and PCI spheroids were exposed to radiant exposures ranging from 0.5-3.0 J cm-2 using an irradiance of 5 mW cm-2. Toxicity was evaluated from spheroid growth kinetics.

The results show that PCI and HT interact in a synergistic manner over a very narrow range of radiant exposure (1.5-2.5 J cm-2) and temperature (40-42oC). This is the first observation of a synergistic interaction between PCI and HT.

8565-235, Session PSun

Unidirectional x-ray microbeam radiosurgery of infantile neuraxial malignancies: estimations of tolerable valley doses

Albert L. Hanson, Brookhaven National Lab. (United States); Jean A. Laissue, Univ. Bern (Switzerland); Daniel N. Slatkin, Nanoprobes, Inc. (United States)

Hindbrains of 11-13 days postpartum rats were irradiated horizontally from the right with a 1 cm-square array of 48 minimally divergent, upright, 19-39 µm-wide wiggler-generated X-ray microbeams. The spacing between the microbeams was either 105 or 210 µm, the peak entrance dose in each microbeam was either 50 or 150 Gy, and the median energy of each microbeam was ≈120 KeV. Doses and dose distributions were simulated applying the MCNPX radiation transport code with thirty billion incident photons per distribution per microbeam spacing. The hindbrains were modeled using a virtual water phantom, then doses were computed in ≈33 µg voxels throughout it, exemplified by displaying peak and nadir valley doses in twenty-seven selected regions distributed evenly throughout the phantom. Estimates of uncertainties attributable to various microbeam widths were also computed. The highest neurologically inconsequential minimum doses between contiguous microbeams fifteen months after irradiation were ≈5 Gy. Putatively, unidirectional microbeam radiosurgery using such doses should palliate infantile neuraxial malignancies with neurologically tolerable sequelae.

8565-194, Session 1

Thresholds of sensation and selective activation of nociceptors in the healthy human hand and foot

Ernest L. Scott, Thomas Johnson, Colorado State Univ. (United States)

The current technique for diagnosing and determining the degree of diabetic neuropathy is antiquated. The use of 2.01 Thulium-YAG laser light to determine more accurate sensation thresholds and selectively activate A-delta and C nociceptors may prove to be a much better technique. The first step in proving this is to determine the thresholds for sensation and the energy-pulse combinations to selectively activate A-delta and C nociceptors in the healthy human hand and foot. The data obtained can then be compared to the same type of data from the hands and feet of people with Type II Diabetes to determine the threshold at which diabetic neuropathy begins and the effect of neuropathy on A-delta and C nociceptors. The primary purpose of this study is to determine if the thresholds of sensation and energy-pulse combinations to selectively activate A-delta and C nociceptors. The secondary purpose is to prove whether or not these thresholds and energy-pulse combinations change in an individual over a six month to one year testing period. If they do not change over time in an individual then this data may be compared to the data from people with Type II Diabetes in a later study.

8565-195, Session 1

Optical activation of hippocampal neurons using short pulse laser

Jaemyung Jang, Seoul National Univ. (Korea, Republic of); Chanyoung Lee, Ulsan National Institute of Science and Technology (Korea, Republic of); Sungchul Bae, Accendo Systems (United States); Nooli Jeon, Seoul National Univ. (Korea, Republic of); Woonggyu Jung, Ulsan National Institute of Science and Technology (Korea, Republic of)

One of the many questions in neural engineering is whether light activates neural tissue without any interruption of foreign materials. This method should avoid to damaging neural tissue including in heating, putting pressure on it, and any other factors. Here, we show that hippocampal neurons in vitro were activated using optical stimulation at 780nm wavelength without any damage. In order to stimulate hippocampal neurons in safe area, we attempted optical stimulation using Ti-Sapphire femtosecond laser. Microelectrode arrays (MEAs) system was used to investigate neuronal response to optical stimulation, monitoring on the electrodes near the target neurons.

And neurons on the experiment were kept alive in a live cell chamber on the microscope. In our experiment, femtosecond pulse at 800 nm focused through new optic fibers on the cell body, allowed repeatable population burst with precise spike timing seen as electrically evoked stimulation. Neuronal activity was also seen for more than 24 hours in the live cell chamber showing that wave shape and spike rate were increased due to optical stimulation.

Results indicated that femtosecond pulse at 780 nm has an effect on hippocampal neuron, which may offer an alternative tool in neural engineering.

8565-199, Session 1

Optogenetic stimulation of cholinergic projection neurons as a potential therapy for Alzheimer's Disease

James J. Mancuso, Yuanxin Chen, Zhong Xue, The Methodist Hospital Research Institute (United States); Zhen Zhao, The Methodist Hospital Research Institute (United States) and Southest Univ. Medical School (China); Stephen T. C. Wong, The Methodist Hospital Research Institute (United States)

Activation of the cholinergic nuclei has emerged as a powerful potential treatment for a number of neurological disorders and is currently in clinical trial for Alzheimer's therapy. While effective in treatment for conditions ranging from depression to epilepsy, the currently accepted approach deep brain stimulation (DBS) remains somewhat unpredictable due to the heterogeneity of the projection neurons that are activated, including glutamatergic, GABAergic, and cholinergic neurons, leading to side effects ranging from apathy to depression or even suicidal behavior. It would be highly advantageous to confine stimulation to specific populations of neurons, particularly in diseases involving complex network interactions such as Alzheimer's. Optogenetics, now firmly established as an effective approach to render genetically-defined populations of cells sensitive to light activation, provides this capability and has already been proposed as a potential therapy for Parkinson's disease. Cholinergic dysfunction and degeneration are a hallmark of Alzheimer's disease such that restoration of cholinergic function is a logical goal in its treatment. Transgenic mice currently available from the Jackson laboratory [Zhao et al., 2011] express the optogenetic activator channelrhodopsin-2 specifically in cholinergic neurons. Here we deliver light or electrical stimulation directly to the basal cholinergic nuclei and evaluate relative effects on cortical blood flow, neuronal network activity, and astrocyte activation in anesthetized mice by intravital two-photon microscopy. Our results are intended as a proof of principle that optogenetic activation of cholinergic neurons could serve as a more specific alternative to DBS for treatment of neurodegenerative disorders.

8565-201, Session 1

Characteristics of cellular-scale neural responses to holographically-patterned photo-thermal and optogenetic stimulation

Shy Shoham, Nairouz Farah, Alaa Zoubi, Technion-Israel Institute of Technology (Israel); Inna Reutsky, Ruppin Academic Ctr. (Israel); Suhail Matar, Lior golan, Inbar Brosh, Technion-Israel Institute of Technology (Israel)

Artificially generating meaningful percepts using neuro-photonic interfaces will require display methods that can selectively excite across large neuronal populations. Recently, we introduced holographic optogenetic and photo-thermal photo-stimulation as a suitable projection/excitation strategy that can be used to selectively control large retinal neuronal populations, with high temporal precision (msec) and efficient use of light. Here, we explore the qualitative and quantitative aspects of cellular response characteristics to holographic stimulation patterns using optogenetic and photo-absorber induced neural-thermal stimulation (PAINTS) in cortical and retinal in vitro preparations.

Responses were measured using a multi-electrode array (MEA) and calcium imaging with organic dyes or the genetically encoded calcium indicator GCamP3. The neurons exhibit spatially-selective responses with single-cell resolution, and are optimally-driven with high fidelity using stimulation patches that are matched to the soma's outline. Interestingly, the response characteristics are nicely captured by simple and general mathematical relations: the thresholds for photo-thermal excitation were accurately captured using predictions from a physical-biophysical temperature-rate model, while the response probability and latency for

optogenetic stimulation are well fit by sigmoidal and power relations, respectively.

These results can help improve our understanding of the engineering requirements from cellular-resolution neuro-photonic interfaces, and provide further evidence that high-rate holographic projection could be an enabling photo-stimulation tool in the development of neuro-prosthetics with high spatial-temporal precision.

8565-202, Session 1

in vivo optical activation of astrocytes as a therapeutic strategy for neurodegenerative diseases

Yuanxin Chen, James J. Mancuso, Zhong Xue, Zhen Zhao, Stephen T. C. Wong, The Methodist Hospital Research Institute (United States)

Neurovascular dysfunction in many neurodegenerative diseases, such as Alzheimer's disease (AD), reduces blood flow to affected brain areas such that the local vasculature loses responsiveness to a number of the factors that normally precisely control blood flow in response to neuronal activity. We developed a new optical approach of activating astrocytes in vivo in animal models to increase local cerebral blood flow as a potential therapy for AD. Our technique uses fluorescent labeling of vasculature and astrocytes coupled with the tissue clearing technique known as Scale and two-photon microscopy to reconstruct and model the astrocyte-vascular relationship in thick cortical samples from normal and afflicted mice. Computational modeling of these reconstructions allow us to plot changes in local blood flow in specific at risk regions of the cerebral cortex and the number of astrocytes available locally to modulate blood flow. Calcium uncaging and optogenetics using channelrhodopsin-2 are applied to activate specific cell types, e.g., astrocytes, in vivo with high spatial and temporal resolutions. Using intravital two-photon microscopy imaging, we measured that single endfoot optical activation around an arteriole induced a 25% increase in arteriole diameter, which in turn increases local blood flow in down-stream capillaries. Reconstruction and modeling of the diseased astrocyte-vascular region determined the quantity of astrocyte activation required to restore normal neurovascular function in a particular brain volume. Thus, optogenetic activation of populations of astrocytes in vivo in afflicted brain areas of neurodegeneration models provides a therapeutic strategy to restore normal blood flow in those regions.

8565-206, Session 1

Closing a Venus Flytrap with electrical and mid-IR photon stimulations

David M. Eisen, Univ. of Maryland, Baltimore County (United States); Douglas Janssen, Greater Grace Christian Academy (United States); Xing Chen, Fow-Sen Choa, Dan Kostov, Univ. of Maryland, Baltimore County (United States); Jenyu Fan, AdTech Optics, Inc. (United States)

Plants have mechanisms to perceive and transmit information between its organs and tissues. These signals had long been considered as hormonal or hydraulic in nature, but recent studies have shown that electrical signals are also produced causing physiological responses. In this work we show that Venus Flytrap, Dionaea muscipula, can respond to both electrical and optical signals beside mechanical stimulations. While the Venus Flytrap does not have any neurons, it does contain transport cells with very similar characteristics to neurotransmitters and uses ionic mechanisms, as human neurons do, to generate action potentials.

In our electrical stimulation study, electrodes made out of soft cloth were soaked in salt water before placing to the midrib (+) and lobe (-). The flytrap's surface resistance was determined by subtracting out the average electrode resistance from the measured electrode to plant surface resistance, yielding an average contact resistance of around 0.98M?. A logarithmic amplifier was used to monitor mechanical stimulation generated electrical signals. Two electrical pulses were generated by mechanical touching the trigger hairs in the lobe twice within 20 seconds. By discharging around 600μC charge stored in a capacitor we demonstrated electrically closing of the flytrap. For optical excitation we found in our FTIR study it's tissue contains very similar protein absorption peaks to that of insects. A 7.35μm laser with ~50mw power was then used for the stimulation study. Electrical action potential was generated twice by Mid-IR photons before the closure of the flytrap.

8565-193, Session 2

Comparison of three pulsed infrared lasers for optical stimulation of the rat prostate cavernous nerves

Charlotte D. Stahl, Serhat Tozburun, Thomas C. Hutchens, The Univ. of North Carolina at Charlotte (United States); Gwen A. Lagoda, Arthur L. Burnett M.D., Johns Hopkins Medical Institutions (United States); Matthew D. Keller, Lockheed Martin Aculight (United States); Nathaniel M. Fried, The Univ. of North Carolina at Charlotte (United States)

Introduction: Optical nerve stimulation (ONS) is being explored for identification and preservation of the cavernous nerves (CN's), responsible for erectile function, during prostate cancer surgery. This study compares three pulsed infrared lasers to determine whether differences in spectral linewidth and/or temporal pulse profile influence successful ONS of the CN's.

Methods: Infrared laser radiation from the Capella diode laser (1873 nm, 5 ms, 10 Hz), Thulium fiber laser (TFL) (1873 nm, 5 ms, 10 Hz), and solid-state Holmium:YAG laser (2120 nm, 300 microseconds, 5 Hz) were transmitted through 400-micrometer-core-diameter fibers, producing a 1-mm-diameter-spot on nerve surface. These three wavelengths have ~400 micrometer optical penetration depth in tissue, closely matching the CN diameter for uniform irradiation. Successful ONS was judged by an intracavernous pressure (ICP) response in the penis in a total of 7 rats.

Results: The narrow linewidth TFL (~0.5 nm) and broad linewidth Capella laser (~12 nm) performed similarly, producing ICP responses with a threshold radiant exposure of ~0.6 J/cm2, and ICP response times of 10-14 s. The Holmium laser, with its unique spiking, long-pulse, temporal profile was capable of ONS at ~0.9 J/cm2 and response times of 45-60 s, due to its lower duty cycle (shorter pulse duration and lower pulse rate).

Conclusions: Capella, TFL, and Holmium lasers all demonstrated successful ONS of CN's. ICP response times and stimulation thresholds were dependent on rate of energy deposition into CN's, consistent with previous variable pulse rate TFL studies (10-100 Hz, CW), rather than linewidth or temporal pulse profile.

8565-205, Session 2

Reduced artifact from optical point stimulation enables optical mapping of embryonic quail hearts

Yves T. Wang, Shi Gu, Case Western Reserve Univ. (United States); Andreas A. Werdich, MetroHealth Medical Ctr. (United States); Andrew M. Rollins, Michael W. Jenkins, Case Western Reserve Univ. (United States)

Cardiac pacing is an important tool for studying cardiac electrophysiology. However, millimeter-long electrical space constants in cardiac tissue result in spatially large artifacts from electrical stimulation that impede recordings in small tissues. Here, for the first time, we demonstrate the ability to record surface electrical activity using optical mapping in embryonic hearts while pacing with optical point stimulation.

Excised embryonic quail hearts were stained with voltage-sensitive di-4-anepps and contractions stopped with cytochalasin D. A 1440-nm diode laser coupled through a single mode fiber and focused to a 10-?m spot was used to pace the hearts. High resolution optical mapping was acquired using a microscope with a 10x objective and a 128x128-element CCD camera.

Optical mapping detected an optical pacing artifact with a length constant of 56?m, over an order of magnitude smaller than the electrical artifact produced by traditional pacing. Artifact-free recordings were obtained away from the pacing site. The artifact appeared as a darkening around the pacing site. The main cause of the artifact was not electrical, but rather was thermal lensing, as distortion of the water-based medium alone can be observed. Some of the electrical activity in the affected region can be recovered with additional processing.

Optical pacing overcomes limitations of traditional electrical pacing, enabling both easily positioned point stimulation and electrical mapping of small embryonic hearts. A pacing artifact was observed with optical mapping, but was much smaller than that created by electrical pacing. Optical point stimulation will enable new studies of cell-to-cell coupling in embryonic hearts.

8565-214, Session 2

Radiant energy during infrared neural stimulation at the target structure

Claus-Peter Richter, Northwestern Univ. (United States); Suhrud M. Rajguru, Univ. of Miami (United States); Ryan Stafford, Alison M. Yates, Bryan J. Norton, Lockheed Martin Aculight (United States); Agnella I. Matic, Northwestern Univ. (United States); Stuart R. Stock, Northwestern Univ. Feinberg School of Medicine (United States)

No Abstract Available

8565-217, Session 2

Inhibiting neurons with infrared light

Austin R. Duke, Vanderbilt Univ. (United States); Hillel Chiel, Case Western Reserve Univ. (United States); E. Duco Jansen, Vanderbilt Univ. (United States)

No Abstract Available

8565-208, Session 3

Optical control the visual perception of awake non-human primate with infrared neural stimulation

Gang Chen, Jonathan M. Cayce, Xiang Ye, E. Duco Jansen, Anita Mahadevan-Jansen, Anna W. Roe, Vanderbilt Univ. (United States)

We previously reported that cortical responses can be modulated by pulsed infrared light in cortex of anesthetized non-human primates (Roe et al SPIE 2012). Infrared neural stimulation is a safe and relatively non-invasive way to modulate neuronal activity; it is achieved without viral or chemical substance injection and lacks disadvantages of current spread accompanied by electrical stimulation. We have now examined whether such optical stimulation applied to the brain can affect behavior. To examine this, a macaque monkey was trained to maintain visual fixation on a spot presented on a monitor; eye position was monitored with an infrared eye tracker. After an optical window was implanted over visual cortex, pulsed infrared light was applied via a fiber optic to visual cortical locations in the window. We found that application of laser light induced the monkey to repeatedly shift its gaze to a visual location on the monitor corresponding to the retinotopic location stimulated on the cortex. Such eye movements were not observed in the absence of laser light application. Thus, these results suggest that infrared neural stimulation can induce visual percepts and affect behavior in awake subjects. Optical stimulation may therefore have potential application in human brain-machine interfaces such as restoring vision in blind patients and treatment of other neurological disorders.

8565-212, Session 3

Responses to amplitude modulated infrared stimuli in the guinea pig inferior colliculus

Claus-Peter Richter, Northwestern Univ. (United States)

No Abstract Available

8565-213, Session 3

Masking of infrared neural stimulation (INS) in hearing and deaf guinea pigs

Hunter Young, Sama Smit Kadalia, Claus-Peter Richter, Northwestern Univ. (United States)

No Abstract Available

8565-215, Session 3

Longterm infrared neural stimulation in the chronic implanted cat

Agnella I. Matic, Northwestern Univ. (United States); Alan M. Robinson, Northwestern Univ. Feinberg School of Medicine (United States); Hunter Young, Suhrud M. Rajguru, Stuart R. Stock, Northwestern Univ. (United States); Claus-Peter Richter, Northwestern Univ. (United States) and Northwestern Univ. Feinberg School of Medicine (United States)

No Abstract Available

8565-216, Session 3

Evaluating the cellular mechanisms of Infrared neural stimulation in the rat somato-sensory cortex

Jonathan M. Cayce, Vanderbilt Univ. (United States); Matthew B. Bouchard, Columbia Univ. (United States); Mykyta Chernov, Vanderbilt Univ. (United States); Brenda Chen, Lauren Grosberg, Columbia Univ. (United States); E. Duco Jansen, Vanderbilt Univ. (United States); Elizabeth M. Hillman, Columbia Univ. (United States); Anita Mahadevan-Jansen, Vanderbilt Univ. (United States)

No Abstract Available

8565-207, Session 4

Flexible optitrode for localized light delivery and electrical recording

Wei-Chuan Shih, Univ. of Houston (United States)

The twisted-wire tetrode (TWT) for neuronal unit recording in the deeper regions of the brain, such as the hippocampus, has been indispensible to our understanding of how the neural mechanisms underlying normal learning and memory are usurped by drug addiction or disrupted by neuronal diseases. This simple device is fabricated by twisting four ~13 ?m insulated nickel-chrome wires together, thermally fusing the insulation, and clipping the end to create a probe with four closely spaced electrodes in a plane perpendicular to the cut wires. This talk describes the integration of a high-efficiency optical channel to deliver light to the sensing electrodes of a TWT while maintaining the fundamental flexibility of the TWT. Such a device could be used for molecularly specific control of in vivo neural activities by optogenetic stimulation and silencing with simultaneous electrical recording, which are essential for potential closed-loop feedback control.

We present optitrode, a miniaturized flexible probe for integrated, localized light delivery and electrical recording. Two platform technologies are currently under development. One is based on micro-assembly of an annular light guide with a conventional tetrode, while the other features thin-film electrodes patterned on a thin optical fiber. We will show preliminary characterization of light delivery efficiency and impedance measurements. We will also show results from in vivo experiments planned within the next few months.

8565-209, Session 4

Modeling ultra-violet metal-semiconductor lasers for neurophotonics

Meng-Mu Shih, Univ. of Florida (United States)

In 2012, optogenetics researchers utilized ultra-violet lasers in eyesight restoration and pain control. More activities of different neurons may be optically manipulated. Semiconductor lasers have features such as small size, low power and various wavelengths so that they can be widely used in biomedicine. Such lasers, with built-in metal gratings, can make wavelength stable and precise. This work applies theoretical models to calculate the coupling coefficients by using the photonic and the optical methods. Numerical results show how materials and structures can affect the coefficients. Physical interpretations of results provide insights for the modeling and design of such lasers.

8565-210, Session 4

Optrode arrays for infrared neural stimulation

Tanya Vanessa F. Abaya, Univ. of Utah (United States); Mohit Diwekar, Steve Blair, Prashant Tathireddy, The Univ. of Utah (United States); Loren Rieth, The Univ. of Utah (United States); Gregory A. Clark, Florian Solzbacher, The Univ. of Utah (United States)

Penetrating waveguide arrays made of glass (SiO2) and silicon were fabricated for infrared (IR) neural stimulation to provide 3D access to the brain or peripheral nerves for selective deep-tissue stimulation with different spatiotemporal patterns. Comprehensive bench characterization was performed to determine light delivery and loss mechanisms. Fused silica/quartz arrays have optrodes of constant geometry with a pyramidal tip at the end of a straight-edge shank; length, width, and tip angle of each optrode can be varied independently from array to array. Undoped silicon arrays are similar in form to the Utah Slant Electrode Array, which has tapered microneedles of varying length in one direction.

Light transmission efficiency was investigated with input from different optical fibers. With a 70-um wide and 1.5-mm long glass optrode having a tip taper angle of 30 degrees with respect to the optical axis, 70% of IR light from a butt-coupled 50-um fiber is transmitted out of the tips; shank length and tip taper does not affect the output power. However, transmission is only 39% for a 1.5-mm long Si optrode, and less for shorter more tapered optrodes. Similar beam profiles were obtained for both arrays when glass optrodes have a 45-degree tip taper; decreasing the glass optrode tip angle to 30 degrees increases the full-angle divergence from 15 to 55 degrees, which leads to a wider yet shallower illumination volume.

Results reveal that the dominant source of loss in both devices is from total internal reflection within the tips. Additional losses in the Si array include tapered shank radiation and reflection from its high refractive index. Insertion tests in tissue were also performed and were successful.

8565-211, Session 4

Infrared neural stimulation hardware development and challenges

Matthew D. Keller, David M. Braun, Lockheed Martin Aculight (United States); Matthew M. Dummer, Mary Hibbs-Brenner, Vixar Inc. (United States)

Infrared neural stimulation (INS) has emerged as a complementary technology to electrical stimulation of nervous system activity. In several applications, including the cochlea, vestibular system, and cardiac tissue, INS imparts the ability to stimulate with greater precision and no stimulation artifact. Historically, studies have been performed with the Ho:YAG laser and Lockheed Martin Aculight's (LMA) Capella laser. To explore the full range of optical parameters that may be useful for INS, LMA has recently produced several alternate versions of the Capella at different wavelengths. LMA has also developed wearable laser packs to facilitate chronic animal experiments, and has partnered with Vixar, Inc. to develop vertical cavity surface emitting lasers (VCSELs) to enable the development of fully implantable optical neuroprostheses. To work toward acute nerve monitoring applications, hand-held probes providing uniform light delivery have been investigated as well. Performance characteristics of these devices will be presented, as will the technical challenges that need to be overcome to implement this technology for human use.

8565-196, Session 5

Use of functional near-infrared spectroscopy to monitor cortical plasticity induced by transcranial direct current stimulation

Bilal Khan, Nathan Hervey, The Univ. of Texas at Arlington (United States); Ann Stowe, Timea Hodics, The Univ. of Texas Southwestern Medical Ctr. at Dallas (United States); George Alexandrakis, The Univ. of Texas at Arlington (United States)

Electrical stimulation of the human cortex in conjunction with physical rehabilitation has been a valuable approach in facilitating the plasticity of the injured brain. One such method is transcranial direct current stimulation (tDCS) which is a non-invasive method to elicit neural stimulation by delivering current through electrodes placed on the scalp. In order to better understand the effects tDCS has on cortical plasticity, neuroimaging techniques have been used pre and post tDCS stimulation. Recently, neuroimaging methods have discovered changes in resting state cortical hemodynamics after the application of tDCS on human subjects. However, analysis of the cortical activity for a physical task during and post tDCS stimulation has not been studied to our knowledge. A viable and sensitive neuroimaging method to map cortical activation patterns during and post tDCS is functional near-infrared (fNIR) imaging. In this study, the cortical activity during an event-related, left wrist curl task will be measured using fNIR imaging before, during, and after tDCS stimulation on healthy adults. Along with the fNIR imaging optodes, two electrodes will be placed over the primary motor hand areas of both brain hemispheres to apply tDCS. We will present changes in both resting state cortical connectivity and cortical activation patterns that occur during and post tDCS application. Additionally, changes to surface electromyography (sEMG) measurements of the wrist flexor and extensor of both arms during the wrist curl movement will be analyzed and related to the changes in cortical plasticity.

8565-197, Session 5

Induction of chronic epileptic seizure and corresponding hemodynamic monitoring in mouse model

Seungduk Lee, Korea Univ. (Korea, Republic of); Areum Jo, Jeong-Eun Sim, Sungkyunkwan Univ. (Korea, Republic of); Choong-Ki Kim, Hyuna Song, Korea Univ. (Korea, Republic of); Minah Suh, Sungkyunkwan Univ. (Korea, Republic of); Beop-Min Kim, Korea Univ. (Korea, Republic of)

Injection of FeCl2 or FeCl3 into the cortex was performed to induce chronic epileptic seizure, which is known to cause epileptiform discharges in animals. In this study, we investigated horizontal and vertical hemodynamic reactions to epileptic seizure simultaneously using two different optical techniques including optical recording of intrinsic signal (ORIS) and near-infrared spectroscopy (NIRS), respectively. We observed that cerebral hemodynamic responses were significantly disrupted in iron-injected hemisphere compared to the contralateral hemisphere. On the other hand, in contralateral hemisphere, hemodynamics was tightly coupled to epileptifom activities both for superficial and deep regions. In addition, we found that both parvalbumin expressing neurons and astrocytes were reduced in iron-injected site. Our result suggests that cortico-cortical and cortico-thalamic coupling can be effectively investigated for small animals using the dual optical techniques.

8565-198, Session 5

Concurrent functional near-infrared imaging and motion tracking to assess functional improvement of children with cerebral palsy after constrained induced motion therapy

Bilal Khan, Nathan Hervey, The Univ. of Texas at Arlington (United States); Laura Shagman, The Univ. of Texas at Dallas (United States); Fenghua Tian, Hanli Liu, The Univ. of Texas at Arlington (United States); Duncan MacFarlane, The Univ. of Texas at Dallas (United States); George Alexandrakis, The Univ. of Texas at Arlington (United States)

A special interest in functional neuroimaging is to quantify brain plasticity as identified by changes in cortical activation patterns after therapy. In this work we will image cortical plasticity in children with cerebral palsy (CP) after they have undergone occupational therapy. In recent studies we have demonstrated that functional near-infrared (fNIR) imaging is a viable and sensitive method for mapping motor cortex activities in children with CP. FNIR imaging metrics such as Time-to-Peak (TtP), Duration, Laterality Index (LI), and Area of Activation (AoA) were found to be significantly different between CP and age-matched healthy children. In addition to fNIR imaging, quantitative information about the action performed during imaging can be used to correlate the child's physical improvement to the changes seen in cortical activity. Thus in this study, fNIR imaging and measurements of the movement will be performed concurrently. Additionally, the fNIR imaging field of view will be expanded to include the secondary motor areas (premotor cortex and supplementary motor area), and both tapping and sequential tapping will be performed by the children during the imaging. Both types of tapping will be tracked by a 6-camera motion tracking system which will determine the three dimensional positions of retro-reflective targets placed on the fingers, wrists, and arms of the children. These measurements will be done on four children with CP before and immediately after two weeks of constrained induced motion therapy (CIMT), and on 5 age-matched healthy controls. Improvements in motor performance will then be determined by the changes in motion tracking metrics before and after therapy and these will be correlated to the spatio-temporal changes in cortical activity patterns.

8565-200, Session 5

Chronic multiphoton microscopy of simultaneous neuronal activity from all cortical layers in awake mice using microprisms

Michael J. Levene, Yale Univ. (United States); Mark Andermann, Harvard Univ. (United States); Markus Wolfel, Nathan Gilfoy, Yale Univ. (United States); Glenn Goldey, Northeastern Univ. (United States); Robert N. S. Sachdev, David A. McCormick, Yale Univ. (United States); Clay Reid, Harvard Univ. (United States)

Multiphoton microscopy of cortical brain activity has largely been restricted to superficial layers. Thus, conventional in vivo imaging techniques are not capable of monitoring activity of neurons across all cortical layers. We achieved simultaneous in vivo multiphoton microscopy of neuronal activity throughout all cortical layers using glass microprisms inserted directly into cortex. We successfully imaged neuronal activity with the calcium indicator GCaMP3 in acute preparations and in chronic preparations for several weeks after surgery. Simultaneous spontaneous and stimulus-evoked activity in hundreds of active neurons in layers 2/3, 5 and 6 could be recorded across days in primary visual cortex of awake, head-restrained mice.

Electrical recordings of neuronal spiking and local field potentials were obtained in order to evaluate the impact of the prism implant on electrophysiological measures of neural activity. Whisker-evoked responses could be recorded in barrel field somatosensory cortex in anesthetized, head-restrained mice within minutes after prism insertion, and for weeks thereafter.

By combining Cre-dependent fluorescence expression with transgenic mice that express Cre in a cell type- or layer-specific manner, we can examine the response properties and correlated activity of identified neural populations across all layers of neocortex. We conclude that the simultaneous imaging of neuronal activity throughout the depth of the cortex is readily available through the use of microprisms.

8565-203, Session 5

A common path optical coherence tomography based electrode for structural imaging of nerves and recording of action potentials

M. Shahidul Islam, Md. Rezuanul Haque, Christian M. Oh, Yan Wang, B. Hyle Park, Univ. of California, Riverside (United States)

This study is aimed to develop an optical system for both structural and functional imaging of nerves. The first part of this study is about polarization-sensitive optical coherence tomography (PS-OCT) imaging of rat sciatic nerves where PS-OCT combined with regular intensity based OCT has been demonstrated to be a very useful tool to extract important features of peripheral nerve microstructure. Our recently published results include measurement of epineurium thickness, estimation of tissue extinction coefficient and birefringence, quantification of bands of Fontana and determination of boundaries between different tissues. The second part is aimed to develop an optical tool to image the changes in nerve structures that correspond with neural activity. A major portion of current technologies for neural recording use either different varieties of electrodes or exogenous contrast agents and both of these are invasive to some extent. Nerves undergo small rapid transient thickness change during action potential propagation and this sub-nanometer thickness change (~1-50nm) has good temporal correlation with action potential. Our developed common path pr-OCT system is currently capable of detecting thickness changes as small as 0.5nm with a temporal resolution of 10?s. Recently, electrical recording of "single action potentials" from the optic nerve of lateral eye of horseshoe crab (Limulus polyphemus) has been demonstrated. Preliminary optical measurements from Limulus optic nerve have shown evidences of neural activity which

matched very well with concurrent electrical recording. KCl has been added to the nerve solution to block the action potentials and thus the accuracy of optical measurements is verified.

8565-204, Session 5

Altered functional connectivity and hemodynamics following ischemic stroke in mice

Adam Q. Bauer, Andrew Kraft, Patrick Wright, Washington Univ. School of Medicine in St. Louis (United States); Jin-Moo Lee, Washington Univ. in St. Louis (United States); Joseph P. Culver, Washington Univ. School of Medicine in St. Louis (United States)

Ischemic injury alters brain function and behavioral performance. Recent functional magnetic resonance imaging (fMRI) in humans and rats suggests that a brain-wide assessment of functional connections provides an indicator of prospective behavioral improvement. While interhemispheric connectivity between homotopic regions has been linked to recovery potential, interpretation of regional functional connectivity (fc) can be confounded by biology (e.g. neurovascular coupling) and data processing. In particular, a standard fcMRI procedure is removal of a common mode signal across the whole brain. Whole brain signals become less well-defined following stroke, as injured tissue lacks the same physiology and neural activity as healthy tissue. We examined this issue within a mouse model of stroke using fc optical intrinsic signal imaging (fcOIS). Functional connectivity patterns and evoked responses were mapped before and 72 hrs after transient middle cerebral artery occlusion. Mice were separated into three groups depending on infarct size, and analyzed using whole-field and hemi-field regression signals. We found decrements in interhemispheric connectivity and evoked response commensurate with infarct size. Importantly, the reduction in connectivity monotonically decreased with hemi-sphere regression signals, whereas traditional full brain regression produced artifact negative correlations that do not fit the expected physiology. Additionally, relative to the healthy hemisphere, the infarct hemisphere voxels had attenuated high frequency content, and were temporally delayed. The sensitivity afforded by fcOIS to detect small connectivity changes from multiple contrasts positions itself as a useful tool to for understanding how fc may influence functional and behavioral recovery.

8565-218, Session 1

A novel approach to Paget's disease diagnosis and monitoring using near-infrared spectroscopy *(Invited Paper)*

Diana C. Sordillo, The City Univ. of New York (United States); Yury Budansky, Peter P. Sordillo, Laura A. Sordillo, Robert R. Alfano, The City College of New York (United States)

Paget's disease of bone affects about 1 to 3 percent of people over 40 years of age in the United States. Characterized by an increase in the rate of bone remodeling due to excessive osteoclast activity, patients with Paget's disease can develop severe bone deformities. Pagetoid bones are large, fragile and prone to fractures. A hallmark of Paget's disease of bone is a marked increase in vascularization in bones. The determinants of vascularization are deoxyhemoglobin (Hb) and oxyhemoglobin (HbO2), which are the key chromophores in the NIR "tissue optical window" from 700nm to 1200nm. A Bone Optical Analyzer utilizing optical spectroscopy imaging to non-invasively measure the changes of Hb and HbO2 would enable early diagnosis and monitoring of disease progression in Paget's disease. Using inverse imaging algorithms, based on the diffusion equation, 2D and 3D maps of the bone's internal structure can be reconstructed. The use of NIR light may allow for repeated studies on patients with Paget's disease quickly, safely, inexpensively and without the risks associated with standard procedures. The model will be tested on bone tissue phantoms which mimic the scattering properties of human bone. This will be the foundation for the future use of this device in vivo.

8565-219, Session 1

Transcutaneous monitoring of murine bone composition with Raman spectroscopy *(Invited Paper)*

Jason R. Maher, Univ. of Rochester (United States); Jason Inzana, Univ. of Rochester Medical Ctr. (United States); Hani A. Awad, Andrew J. Berger, Univ. of Rochester (United States)

Recently, vibrational spectroscopy has been used to explore the biochemical differences between normal and osteoporotic bone. In fact, the results of an ex vivo study on exposed bone suggest that Raman spectroscopy could potentially provide predictions of fracture risk that are more accurate than those based upon the clinically-used parameter of bone mineral density [1]. While these results are promising, further work is necessary to make accurate transcutaneous measurements in vivo.

Transcutaneous Raman spectroscopy of bone is complicated by scattering, absorption, and fluorescence in the overlying soft tissue. Furthermore, type I collagen is present in both bone and soft tissue and separating the overlapping spectral contributions is difficult. In this presentation, we introduce a novel method to transcutaneously acquire bone spectra that are of sufficient quality to generate accurate predictions of fracture risk. This method, which is based upon fitting with a separately-acquired library of spectra, is utilized to detect biochemical differences in the tibiae of two genotypes of mice: wild-type and oim/oim (a mouse model of osteogenesis imperfecta). Recent results of in vivo and longitudinal studies will also be discussed.

[1] J. R. Maher, M. Takahata, H. A. Awad, and A. J. Berger, "Raman spectroscopy detects deterioration in biomechanical properties of bone in a glucocorticoid-treated mouse model of rheumatoid arthritis," Journal of Biomedical Optics 16(8), p. 087012, 2011.

8565-220, Session 1

Optical spectroscopy methods to probe key spectral fingerprints of bone

Diana C. Sordillo, The City Univ. of New York (United States); Laura A. Sordillo, Peter P. Sordillo, Robert R. Alfano, The City College of New York (United States)

We investigated the molecular fingerprints of bone using Raman spectroscopy, resonance Raman spectroscopy, visible and near-infrared absorption spectroscopy and fluorescence spectroscopy. The absorption spectra of animal bones from chicken, pig, lamb, cow and duck were analyzed and compared in the spectral range of 200 nm to 1600 nm. From 400 nm to 550 nm the absorption spectrum of HbO2 was observed. From 900 nm to 1600 nm absorption spectrum of H2O was observed. The fluorescence spectra from an excitation of 300 nm, 340 nm, 400 nm and 500 nm were investigated showing these key components: tryptophan, collagen, which is the main organic material in bone, flavins and porphyrins (due to blood within the bone). Resonance Raman with 514.5 nm laser excitation and Raman spectroscopy using a 785 nm laser were also performed. With these spectroscopic methods the important molecular features and components of bone can be studied and will be presented.

8565-221, Session 1

High temperature heat source generation with a very low power level

quasi-CW(continuous wave) semiconductor laser for medical use

Takahiro Fujimoto M.D., Clinic F (Japan) and Tokai Univ. (Japan); Yusuke Imai, Kazuyoku Tei, Tomoo Fujioka, Shigeru Yamaguchi, Tokai Univ. (Japan)

In most of medical and dental laser treatments, high power pulsed laser have been used as desirable light sources employing with an optical fiber delivery system. The treatment process involves high temperature thermal effect associated with direct laser absorption of the materials such as hard and?soft tissues, tooth, bones and so on. Such treatments sometimes face technical difficulties suffering from their optical absorption properties. We investigate a new technology to create high temperature heat source on the tip surface of the glass fiber proposed for the medical surgery applications. Using a low power level (4~6W) semiconductor laser at a wavelength of 980 nm, a laser coupled fiber tip was pre-processed to contain certain amount of TiO2 powder with a depth of 400?m from the tip surface so that the irradiated low laser energy could be perfectly absorbed to be transferred to thermal energy. Thus the laser treatment can be performed without suffering from any optical characteristic of the material. Semiconductor laser was operated quasi-CW mode pulse time duration of 180ms and more than 95% of the laser energy was converted to thermal energy in the fiber tip. by Based on two-color thermometry by using a gated optical multichannel analyzer with 0.25m spectrometer in visible wavelength region, the temperature of the fiber tip was analyzed. The temperature of the heat source was measured to be in excess 3500K. Demonstration of laser processing employing this system was successfully carried out drilling through holes in ceramic materials simulating bone surgery.

8565-222, Session 1

Optical methods for knee osteoarthritis detection

Yanping Chen, Xiamen Univ. (China)

Osteoarthritis is one of the most common diseases nowadays. One with serious damage of osteoarthritis would get disabled of joint, and life quality decreased. Optical methods for knee osteoarthritis detection were reviewed in this paper. Firstly, the advantages and disadvantages of some common imaging diagnostic techniques, for example X-ray/CT and MRI, were briefly summarized. Then three kinds of typical optics methods for the detection were introduced emphatically, such as coherence tomography (OCT), diffuse optical tomography (DOT) and photoacoustic tomography (PAT). After the introductions of some features of these three optical imaging methods on OA detection, this paper briefly forecasts their application prospect in early OA detection.

8565-223, Session 2

Future of bone pathology, bone grafting, and osseointegration in oral and maxillofacial surgery: how applying optical advancements can help both fields *(Invited Paper)*

Rahul Tandon D.D.S., Alan S. Herford D.D.S., Loma Linda Univ. (United States)

Introduction: In recent years, advances in technology are propelling the field of osteology into new realms. Diagnosis of bone pathology, bone graft substitution, and osseointegration of implants are three of the most researched and scrutinized topics in the field of osteology. In the field of Oral and Maxillofacial surgery, the alveolar mucosa that overlies the underlying bone is rather thin, allowing for significant diagnostic and therapeutic advantages over other areas of the body. However, there remains an enormous gap between advancements in physics, in particular optics, and oral and maxillofacial surgery; the aim of this presentation is to bridge that gap.

Bone Pathology: Bone pathology, in particular, provides a significant avenue in which modern technology may be able to advance the field. Pathologies and their severities vary significantly amongst their different types and amongst the individuals themselves. Nevertheless, improvements in diagnosis, classification, and treatment are still being sought after as advancements in technology continue to progress. By combining the clinical, histological, and pathological characteristics with these advancements, patients with such debilitating pathologies may have more promising options regarding lifestyle and prognosis.

Bone Grafting: Tissue grafting has become the treatment of choice for both clinicians and patients when correcting defects of any type. While soft tissue grafting such as skin grafting continues to be a popular choice, it still possesses significant disadvantages. Hard tissue grafting, in particular bone grafting, provides unique characteristics that bypass such disadvantages. Defects of the facial bones, in particular the jaws, may be due to a number of reasons: pathology, trauma, infections, congenital deformities, or simply due to atrophy. These defects can vary in size from small alveolar defects to segments of an entire jaw (mandible or maxilla). Bone grafting possesses a unique advantage in that new bone formation arises from tissue regeneration, and the combination of osteoblasts with collagen synthesis help to propel the success of the graft. At our institution we helped to usher in the use of such materials as Bio-Oss, a xenograft that can be used as a bone substitute for a variety of defects, and BMP-2, an osteoinductive protein which can induce the present osteoblasts to secrete bone matrix.

Osseointegration: The field of Dentistry has experienced a significant growth in the field of dental implants in the last 25 years. Dental implants have become the treatment of choice for most patients, replacing traditional methods of root canals and dentures. The actual process of the direct contact between the viable and bone without an intervening soft tissue layer is termed osseointegration. Nevertheless, the precise biological mechanism for the stable anchoring of titanium (the most commonly used metal for dental implants) in bone is still not fully understood. True chemical bonding at the interface between bone and commercial grade pure titanium has not been demonstrated and presents a potentially groundbreaking topic that should be investigated. While there are varying theories, the methods for investigation have not provided conclusive proof

supporting one theory over another.

Conclusion: The primary goal of this lecture is to introduce pioneers in the field of optics to the field of oral and maxillofacial surgery. With a brief introduction into the procedures and techniques, we are hopeful to bridge the ever widening gap between the clinical science and the basic sciences. At our institution we have begun evaluating the quality of bone using Raman Spectroscopy, and applying other areas of oral and maxillofacial surgery into such studies: bone grafting and dental implants. While our initial studies are promising, we believe that with a broader base of collaborations, we can make a quicker transition into clinical application.

8565-224, Session 2

Ultrafast laser ablation and machining of bone *(Invited Paper)*

Qiyin Fang, Ran An, Ghadeer K. Khader, Emilia Wilk, Harold K. Haugen, Gregory R. Wohl, Brett Dunlop, Mehran Anvari, McMaster Univ. (Canada)

Accurate and precise cutting/drilling of hard tissue is required in many clinical applications. For example, in pedicle screw spinal fixation, the screw insertion requires a very high degree of precision to avoid potential damage to the spinal cord. Compared to conventional mechanical burr drills, laser ablation has several potential advantages including: (i) no mechanical vibration, (ii) non-contact intervention that is compatible with real-time feedback mechanisms, and (iii) sub-millimeter precision with minimal collateral damage. We will summarize clinical applications with good potential for laser ablation and review recently relevant technological advances (e.g. compact fiber lasers, scanning technology, real-time monitoring, etc.). We will also present an experimental study in which we produced deep, high aspect ratio pilot holes in the pedicle of vertebral bone using ultrafast lasers. A number of laser ablation parameters (pulse duration, incubation effect, fluence, etc.) were investigated on unpolished fresh porcine cortical bone. The machining of millimeter-size structures was also explored under different ablation strategies. X-ray computed micro-tomography was employed to analyze the morphology of these structures.

8565-225, Session 2

Primary investigations on the potential of a novel diode pumped Er:YAG laser system for bone surgery

Karl Stock, Florian Hausladen, Holger Wurm, Raimund Hibst, Univ. Ulm (Germany)

Flashlamp pumped Er:YAG-lasers are successfully clinically used for both precise soft and hard tissue ablation is well known. As an alternative, actually a novel diode pumped Er:YAG laser system (Pantec Engineering AG) becomes available, with mean laser power up to 15W and pulse repetition rate up to 1kHz.

The aim of the presented study is to investigate the effect of this laser system on bone tissue at various irradiation parameters, particular at repetition rates exceeding 100 Hz.

For reproducible experiments, firstly an appropriate experimental set-up was realized with a beam delivery and focusing unit, a computer controlled stepper unit with sample holder, and a shutter unit. It allowed to move the sample (1mm-3mm sawed slices of pig bone) with a defined velocity while irradiation by various laser parameters. A water spray

served to moisten the sample surfaces. After irradiation the grooves were analyzed by light microscopy and laser scanning microscopy regarding to the ablation quality, the groove geometry, the ablation efficacy, and the thermal effects.

The resulting grooves are slightly cone shaped (groove depth up to 3mm, width about 200µm) with sharp edges at the surface. At 1W, 200Hz, 5mm/s sample movement and with water irrigation the measured ablation speed ?z/?t is 10.8 mm/s. The ablation depth per pulse is 54µm.

In conclusion, these first experiments demonstrate that the diode pumped Er:YAG laser system is an efficient tool for use in bone surgery.

8565-226, Session 2

Highly efficient nonthermal ablation of bone under bulk water with a frequency-doubled Nd:YVO4 picosecond laser

Cristian Tulea, Hud Wahab, Nils Gehlich, Jan Caron, Marco Höefer, Dominik Esser, Bernd Jungbluth, Achim Lenenbach, Reinhard Noll, Fraunhofer-Institut für Lasertechnik (Germany)

Several laser systems in the infrared wavelength range, such as Nd:YAG, Er:YAG or CO2 lasers are used for efficient ablation of bone tissue, while the application of short pulses in coaction with a thin water film results in reduced thermal side effects. Nonetheless up to now there is no laser-process for bone cutting in a clinical environment due to lack of ablation efficiency. Investigations of laser ablation rates of bone tissue using a rinsing system and handling bleedings have not been reported yet. In our study we investigated the ablation rates of bovine cortical bone tissue, placed 1.5 cm deep in water under laminar flow conditions, using a short pulsed (25 ps), frequency doubled (532 nm) Nd:YVO4 laser with pulse energies of 1 mJ at 20 kHz repetition rate. The enhancement of the ablation rate due to debris removal by an additional water flow from a well-directed blast pipe as well as the negative effect of the admixture of bovine serum albumin to the water were examined. Optical Coherence Tomography (OCT) was used to measure the crater volume. An experimental study of the depth dependence of the ablation rate confirms the theoretical prediction containing Beer-Lambert law, Fresnel reflection and a Gaussian beam profile. Conducting precise incisions with widths less than 1.5 mm the maximum ablation rate was found to be 0.2 mm3/s at depths lower than 100 µm, while the maximum depth was 3.5 mm.

8565-227, Session 2

Laser ablation in temporomandibular joint disorders and a case report involving an ossifying fibroma: how optics could potentially advance treatments in oral and maxillofacial surgery

Timothy W. Stevens D.D.S., Loma Linda Univ. (United States)

Introduction: The field of oral and maxillofacial surgery provides many applications for the use of lasers and optical analysis. The temporomandibular joint and gross bone grafting after surgical resection are just two of the areas that could benefit significantly from advancements in optics. It is the goal of this lecture to utilize the new advancements in optics so that patient care can be improved.

Laser Ablation: Low level laser ablation has been used in a variety of joint adhesion cases, including arthritis of the hand and foot. In the field of oral and maxillofacial surgery, this method has been used to treat pain and mobility dysfunction in patients with temporomandibular joint disease. Oftentimes the causes of such discomfort arises from adhesion between the cartilage and the surrounding bone. While the outcomes have been promising, lack of familiarity with the device or doubt about its effects have reduced its use, which has left the actual process of laser ablation relatively unchanged.

Case presentation: The patient in question was a 25 year old female who presented for a mandibular resection due to an ossifying fibroma. The area resected was reconstructed using a reconstruction bar overlying a bone graft taken from her iliac crest. Over the course of several months, her reconstructed area displayed significant signs of infection, as well as graft failure. X-rays, which were used as the primary indicator for graft status, did not display the actual metabolic activity and as a result her treatment was altered and went through several modifications. Although the patient was reconstructed successfully thereafter, it is our belief that with more advanced technology to assess her progression the patient could have endured far less suffering.

Conclusion: While there are many more areas of oral and maxillofacial surgery that could potentially benefit from advances in optical technology, we have chosen to highlight these two areas due to their prevalence within our community. It is our goal that by providing specific examples, we can bridge the gap that lies between the clinical sciences and basic sciences.

8565-228, Session 3

Multispectral photoacoustic method for the early detection and diagnosis of osteoporosis disease *(Invited Paper)*

Idan Steinberg, Avishay Eyal, Israel Gannot, Tel Aviv Univ. (Israel)

Osteoporosis a major health problem worldwide, with healthcare costs of billions of dollars annually. Optical methods are of great interest for probing bone pathologies due to their inherent noninvasiveness and the spectroscopic information they provide on tissue constituents. The risk of bone fracture depends on the Bone Mineral Density as well as its microstructure which is not measured in common clinical practice.

We propose the use of a multispectral photoacoustic technique to simultaneously measure the bone absorption spectrum and the generation efficiencies and propagation speeds of acoustic modes in the bone. Scanning is performed along both the optical wavelength as well as the acoustic frequency to obtain spectra and dispersion curves. A Monte-Carlo computer simulation of both light and sound propagation through the cylindrical bone was developed. Initial ex-vivo experiments were performed on of fowl tibia bone. A tunable Ti:Sapph laser @ 700-900 nm, followed by an Acousto-optic modulator, was used to generate photoacoustic signals at 0.5 - 2.5 MHz. The laser intensity was set to meet safety standards for skin exposure. Phase measurements along the cortical part of the bone were performed using spectrum analyzer to achieve high sensitivity to the detected photoacoustic signals.

Preliminary results are encouraging and show both theoretically and experimentally the potential of such method to successfully measure photoacoustic signals from bones with great flexibility. The interpretation of the measured speed and dispersion curves as a predictor of risk of fracture will be presented and discussed.

8565-229, Session 3

Non-invasive imaging of zebrafish with spinal deformities using optical coherence tomography: a preliminary study

Liane Bernstein, Ecole Polytechnique de Montréal (Canada); Kathy Beaudette, Ecole Polytechnique de Montréal (Canada) and CHU Sainte-Justine (Canada); Kessen Patten, Sainte-Justine Mother and Child Univ. Hospital Ctr. (Canada); Emilie Beaulieu-Ouellet, Ecole Polytechnique de Montréal (Canada); Mathias Strupler, Sainte-Justine Mother and Child Univ. Hospital Ctr. (Canada) and Ecole Polytechnique de Montréal (Canada); Florina Moldovan, Sainte-Justine Mother and Child Univ. Hospital Ctr. (Canada); Caroline Boudoux, Ecole Polytechnique de Montréal (Canada) and CHU Sainte-Justine (Canada)

The zebrafish model is increasingly being used to evaluate gene function in bone development and study various genetic mutations that might lead to spinal deformities such as scoliosis. However, current imaging techniques make it difficult to perform longitudinal studies of this condition. The goal of this project is to determine whether optical coherence tomography (OCT) is a viable non-invasive method to image zebrafish exhibiting spinal deformities.

Images of both live and fixed malformed zebrafish 5 to 21 days postfertilization as well as wild-type fish 5 to 29 days postfertilization were acquired non-invasively using a commercial SD-OCT system, with a laser source centered at 930nm (??=100nm), permitting axial and lateral resolutions of 7 and 8μm respectively. Using two-dimensional images and three-dimensional reconstructions, it was possible to identify the malformed notochord as well as deformities in other major organs at different stages of formation. A segmentation algorithm was developed to facilitate the visualization of the notochord and the angle of curvature of the deformed fish was calculated from the isolated spine. OCT images were compared to H&E histological staining and the “gold standards” of zebrafish bone imaging: calcein and alizarin red staining.

Because of the possibility of performing longitudinal studies on a same fish and reducing image processing time as compared with staining techniques and histology, the use of OCT would facilitate phenotypic characterization in studying genetic factors leading to spinal deformities in zebrafish and could eventually contribute to the identification of the genetic causes of spinal deformities such as scoliosis.

8565-230, Session 3

Photoacoustic and ultrasonic signature of early bone density variations

Bahman Lashkari, Andreas Mandelis, Univ. of Toronto (Canada)

This study examines the application of backscattered ultrasound (US) and photoacoustics (PA) for assessment of bone structure and density variation. Both methods are applied in the frequency-domain, employing linear frequency modulation chirps. An 800-nm CW laser and a 3.5-MHz ultrasonic transducer are used for transmitting the signal. The backscattered pressure waves are detected by a 2.2-MHz US transducer. Experiments are focused on detection and evaluation of PA and US signals from in-vitro animal and human bones with cortical and trabecular sublayers. Osteoporotic changes in the bone are simulated by using a very mild demineralization solution (EDTA 0.5M). The changes in the time-domain signal as well as integrated backscattering spectra are compared for each sample before and after demineralization. Results show the ability of US to generate detectable signal from deeper bone sublayers, whereas the PA signals show higher sensitivity to the variation in bone density. While US signal variation with changes in the cortical layer is insignificant, PA has shown to be able to detect minor variation of the cortical bone density.

8565-231, Session 3

Raman spectroscopy analysis of breast cancer metastasis induced bone quality alterations

Xiaohong Bi, Julie A. Sterling, Jeffry S. Nyman, Daniel S. Perrien, Anita Mahadevan-Jansen, Vanderbilt Univ. (United States)

Bone is one of the most common metastatic sites for breast cancer. Bone metastases result in pathologically active bone remodeling process and cause bone degradation or osteolytic lesions in breast cancer [1]. Thus breast cancer patients suffer high risk of pathologic fracture due to the elevated bone deterioration. Detailed characterization of cancer-induced changes in metastatic bone is important for disease diagnosis and treatment evaluation. In this study, Raman spectroscopy was applied to detect the molecular structure and composition of bones with or without osteolytic lesions in a breast cancer mouse model. Female athymic nude Balb/C mice aged 4 weeks, was injected with PBS or luciferase labeled human MDA-231 breast cancer cells by intra-cardiac injection as control and tumor-bearing groups, respectively. Tibiae and femora were collected and clear of soft tissues after the mice sacrificed at 4 weeks post tumor inoculation. Raman spectra were collected from the surface of the intact tibiae and femora at multiple locations using a confocal Raman microscope with a 785nm laser diode source. Each acquired spectrum consisted of three accumulations with an exposure time of 10 seconds and a binning of 3.

The tumor-bearing bones with osteolytic lesions have shown lower degree of collagen mineralization and decreased mineral crystallinity, suggesting enhanced bone degeneration in the presence of breast cancer cells. The elevated carbonation level and hydroxyproline content in cancerous bones also suggested active bone remodeling. These results demonstrated the potential of Raman spectroscopy in studying cancer bone metastasis.

8565-232, Session 4

Validating transcutaneous Raman spectroscopy in humans *(Invited Paper)*

Francis W. Esmonde-White, Michael D. Morris, Univ. of Michigan (United States)

Analysis of excised bone has shown that Raman spectroscopy can measure properties of bone related to composition, mechanical properties, and disease state. Futhermore, transcutaneous Raman spectroscopy of bone has been demonstrated in animals (ex vivo and in vivo) and human cadavers. This has suggested the potential for in vivo Raman assessment of human bone. To date no study has demonstrated human in vivo transcutaneous measurements of bone and validation against measurements of exposed bone in vivo and ex vivo.

In this study, we compare measurements in human subjects taken transcutaneously, on surgically exposed bone, and on recovered bone fragments according to an IRB-approved protocol. The Raman spectrum of bone is first measured transcutaneously (in vivo) in a pre-operative visit. Next, the exposed bone is measured in vivo during anterior cruciate ligament (ACL) repair surgery. Finally, a specimen of bone recovered during the normal surgical procedure is examined by microspectroscopy (ex vivo). A commercially available Raman spectrograph and optical probe operating at 785 nm excitation are used for the in vivo measurements.

Results for the transcutaneous and exposed bone measurements will be presented and discussed. We will discuss how we have dealt with ambient light in the surgical suite, as well as the other important requirements for performing Raman spectroscopy during a surgery.

8565-233, Session 4

Polarization Raman spectroscopy implicates orientation-composition in

a novel mouse model of bone brittleness

Alexander J. Makowski, Tennessee Valley Healthcare System (United States) and Vanderbilt Univ. (United States); Anita Mahadevan-Jansen, Vanderbilt Univ. (United States); Jeffry S. Nyman, U.S. Dept. of Veterans Affairs - Tennessee Valley Health Care System (United States) and Vanderbilt Univ. Medical Ctr. (United States) and Vanderbilt Univ. (United States)

Activation Transcription Factor 4 (ATF-4) is essential for osteoblast maturation and proper collagen synthesis. Loss of ATF-4 results in Coffin-Lowery Syndrome in humans. Genetic knockout in mice leads to similar dwarfism phenotypes. We recently found that these bones demonstrate a rare brittleness phenotype, independent of bone strength, that worsens with age. We utilized a confocal Renishaw Raman microscope (50x objective; NA=.75) to evaluate embedded, polished cross-sections of

mouse tibia from both wild-type and knockout mice at 8weeks and 20weeks of age (48 mice, n>=8 per group). Analysis of peak ratios indicated statistically significant changes in both mineral and collagen; however, compositional changes did not fully encompass biomechanical differences. To investigate the impact of material organization, we acquired colocalized spectra aligning the polarization angle parallel and perpendicular to the long bone axis from wet intact femurs of the same mice. Polarization angle difference spectra show marked significant changes in orientation of these compositional differences in both 8wk and 20wk mice. Relative to wild-type, 8wk knockout bones show significant differences (t-test; $p<0.05$) in Hydroxyproline, v4Phosphate, Carbonate, and CH2 peaks; however, older samples indicate a recovery of differences in Hydroxyproline and carbonate but persistent CH2 and v4Phosphate differences. Development of significant differences in AmideIII and v2Phosphate with age further explains biomechanical observations. Use of polarization specific Raman measurements has implicated a structural profile that furthers our understanding of this model of bone brittleness. Polarization content of Raman spectra may prove significant in future studies of brittle fracture and human fracture risk.

8565-234, Session 4

A survey of practical polarization bias optimization options for confocal Raman spectroscopy of bone

Alexander J. Makowski, Tennessee Valley Healthcare System (United States) and Vanderbilt Univ. (United States); Jeffry S. Nyman, U.S. Dept. of Veterans Affairs - Tennessee Valley Health Care System (United States) and Vanderbilt Univ. Medical Ctr. (United States) and Vanderbilt Univ. (United States); Anita Mahadevan-Jansen, Vanderbilt Univ. (United States)

Polarization of laser sources has been used previously to determine collagen fiber orientation and discriminate osteonal lamellae in both human and mouse bone. This proves a useful tool to establish the interaction between bone tissue composition and organization; however, to obtain a true measure of composition, this polarization bias must be eliminated. Polarized Raman literature implies the potential of three methods (sometimes used as controls or proof of principle): decreasing numerical aperture, selection of less sensitive peaks, and depolarization. To further knowledge of inherent polarization bias, we measured transverse cuts of polished human cadaveric femur to determine the phase angle and consistency of each peak under highly polarized Raman conditions (linear polarizers added to Renishaw confocal Raman microscope). Modeling according to Malus' Law, magnitude of intensity oscillation was used to quantify polarization sensitivity. Phase information was used to generate more and less sensitive peak ratio metrics for mineral to matrix ratio, carbonate substitution, and crystallinity. Replication of data and bone rotation in lower polarization regimes (removal of added optics and use of lower numerical aperture objectives) confirms that sensitive peaks retain polarization bias. Raman Mapping shows how the use of phase matched ratios further minimizes bias when quantifying compositional differences. Finally replicate Raman maps of the same bone using standard instrumentation, lowering numerical aperture, and employing circular polarization allow for comparison of the strengths and weakness of these methods, including throughput, efficacy of bias reduction, and practicality in modification of commercially available instrumentation.

8565-237, Session 5

Comparison of control and quality of bone cutting by using optical topographical imaging guided mechanical drill and 1070 nm laser with in-line coherent imaging

Marjan Razani, Yasaman Soudagar, Karen Yu, Ryerson Univ. (Canada); Christopher M. Galbraith, Paul J. Webster, Cole P. Van Vlack, Queen's Univ. (Canada); Cuiru Sun, Univ. of Toronto (Canada); Adrian Mariampillai, Beau A. Standish, Ryerson Univ. (Canada); James M. Fraser, Queen's Univ. (Canada); Victor X. D. Yang, Ryerson Univ. (Canada)

Precision depth control of bone resection is necessary for safe surgical procedures in the spine. In this paper, we compare the control and quality of cutting bovine tail bone, as an ex vivo model of laminectomy and bony resection simulating spinal surgery, planned with micro-CT data and executed using two approaches: (a) mechanical milling guided by optical topographical imaging and (b) optical milling using closed-loop inline coherent imaging (ICI) to monitor and control the incision depth of a high-power 1070 nm fiber laser in situ.

OTI provides the in situ topology of the 2-dimensional surface of the bone orientation in the mechanical mill which is registered with the treatment plan derived from the micro- CT data. The co-registration allows the plan to be programmed into to the mill which is then used as a benchmark of current surgical techniques.

For laser cutting, 3D optical landmarking with coaxial camera vision and the ICI system is used to co-register the treatment plan. The unstable, carbonization-mediated ablation behaviour of 1070 nm light and the unknown initial geometry of bone leads to unpredictable ablation which substantially limits the depth accuracy of open-loop cutting.

However, even with such a non-ideal cutting laser, we demonstrate that ICI provides in situ high-speed feedback that accurately limits the laser's cut depth to effectively create an all-optical analogue to the mechanical mill.

8565-238, Session 5

Photodynamic therapy as a local therapeutic adjunct for the treatment of vertebral metastases

Albert Yee, Shane Burch, Univ. of Toronto (Canada); Margarete K. Akens, Sunnybrook Health Sciences Ctr. (Canada); Emily Won, Victor Lo, Stuart Bisland, Univ. of Toronto (Canada); Brian C. Wilson, Ontario Cancer Institute (Canada); Cari M. Whyne, Sunnybrook Health Sciences Ctr. (Canada)

Background: Metastatic cancer causes the majority of tumors in bone, most frequently found in the spinal column. Skeletal complications cause pain and neurologic impairment. Photodynamic therapy (PDT) has been used to treat a variety of cancers. Minimally invasive surgical (MIS) strategies may allow targeted light application essential for PDT within bone structures.

Purpose: To quantify the effects of PDT on both tumor and bone tissues within the metastatic spine and translation of PDT for spinal metastases toward clinical practice.

Methods: Pre-clinical (rnu/rnu rat) vertebral metastasis models of osteolytic (MT-1 breast cancer) and mixed osteolytic/osteoblastic (ACE-1 prostate cancer) disease were used to evaluate the effect of PDT. PDT alone and in combination with other standard local (radiation therapy, RT) and systemic (bisphosphonates, BP) therapies was evaluated via bioluminescence imaging, micro-CT based stereology, histology, and biomechanical testing. The safety and feasibility of MIS+PDT were evaluated in scale-up animal studies.

Results: Single PDT treatment (photosensitizer BPD-MA, 690nm light) ablated tumor tissue in targeted vertebrae. PDT led to significant increases in bone structural properties, with greatest benefits from combined BP+PDT therapy:76% and 19% increases in bone volume fraction in treated tumor-bearing and healthy untreated controls, respectively. Similar synergistic improvements (but of lesser magnitude) were found in combined PDT+RT treatments. Scale-up porcine and canine models validated the feasibility, safety and potential efficacy of PDT in treating tumors in bone through targeted MIS approaches.

Discussion/Conclusion: The positive effects of PDT on tumor and bone have led to a MIS Phase I safety clinical trial of PDT for vertebral metastases that is now in progress.

8566-2, Session 1

Monitoring of enamel lesion remineralization by optical coherence tomography: an alternative approach towards signal analysis

Alireza Sadr, Mona Mandurah, Syozi Nakashima, Yasushi Shimada, Yuichi Kitasako, Junji Tagami, Tokyo Medical and Dental Univ. (Japan); Yasunori Sumi, National Ctr. for Geriatrics and Gerontology (Japan)

Early detection, monitoring and remineralization repair of enamel lesions are top research priorities in the modern dentistry focusing on minimal intervention concept. We investigate the use of swept-source optical coherence tomography system (SS-OCT) without polarization-sensing at 1319nm wavelength developed for clinical dentistry (Dental OCT System Prototype 2, Panasonic Healthcare Co., Ltd., Japan) in quantitative assessment of artificial enamel lesions and their remineralization. Bovine enamel blocks were subjected to demineralization to create subsurface lesions approximately 130 µm in depth, and subjected to remineralization in solutions with different compositions for up to two weeks. Cross-sectional images of sound, demineralized and remineralized specimens were captured under hydrated conditions by the OCT. At 14d, the specimens were cut into sections for cross-sectional nanoindentation to measure hardness from surface through the lesion under 2mN load. OCT images of lesions showed a boundary closely suggesting the lesion depth. Reflectivity had increased with demineralization. After remineralization, the boundary depth gradually decreased and nanoindentation showed 50%-60% overall hardness recovery. A significant negative correlation was found between the slope power-law regression as a measure of attenuation and overall nano-hardness for a range of data covering sound, demineralized and remineralized specimens (r=0.89 95% CI for r = 0.95 to 0.74). In conclusion, OCT could provide clear images of early enamel lesion extent and signal attenuation could indicate its severity and recovery. Clinical data of natural lesions obtained using Dental OCT and analyzed by this approach will also be presented. Study supported by GCOE IRCMSTBD and NCGG.

8566-3, Session 1

Multimodal optical detection of early childhood caries: a clinical prototype

Liang Zhang, Jeremy S. Ridge, Leonard Y. Nelson, Joel H. Berg D.D.S., Eric J. Seibel, Univ. of Washington (United States)

There is an increasing need for a safe and effective device for detection, diagnosis, and monitoring the therapy of early caries without the need for surgical intervention. We have developed a multimodal clinical dental device that will be clinically evaluated for the management early childhood caries. This laser based optical device combines a high contrast and high resolution surface imaging modality with a dual wavelength fluorescence modality to screen and identify caries lesions and erosions. Using a modified ultrathin laser-based scanning fiber endoscope (SFE) with 405 nm laser illumination, the highly sensitive surface imaging modality directs the attention of a clinician to suspicious regions on a tooth. Severity of the suspected lesion is then quantified by laser induced autofluorescence (AF) using dual 405 nm and 532 nm laser excitation during video-rate imaging. An AF ratio is computed from the acquired 405 nm and 532 nm spectra and displayed to the clinician, thus providing a quantifiable measure of lesion severity. Additionally, presence of spectral peaks due to light emission from porphyrin compounds in oral bacteria are also detected and analyzed. Here, we describe the implementation of this new multimodal optical prototype device and review the scientific principles behind the technology. Additionally, future plans including a low-cost version of the device is proposed for communities having less developed dental services.

8566-4, Session 1

Clinical monitoring of early caries lesions using cross polarization optical coherence tomography

Daniel Fried, Michal Staninec, Cynthia L. Darling, Kenneth H. Chan, Univ. of California, San Francisco (United States)

No Abstract Available

8566-5, Session 1

Polarization sensitive camera for the in vitro diagnostic and monitoring of dental erosion

Anke Bossen, Berner Fachhochschule Technik und Informatik , Optolab (Switzerland); Christoph Meier, Berner Fachhochschule Technik und Informatik , Otpolab (Switzerland); Ekaterina Rakhmatullina, Adrian Lussi, Bern Univ. Hospital (Switzerland)

Due to a frequent consumption of acidic food and beverages, a prevalence of dental erosion increases worldwide. In an initial erosion stage, the hard dental tissue is softened due to acidic demineralization. As erosion progresses, a gradual tissue wear occurs resulting in thinning of the enamel. Complete loss of the enamel layer can be observed in severe clinical cases. Therefore, it is essential to provide a diagnosis tool for an accurate detection and monitoring of dental erosion already at early stages.

We present the development of the polarization sensitive imaging camera for the visualization and quantification of dental erosion. The system consists of two CMOS cameras mounted on two sides of a polarizing beamsplitter. A horizontal linearly polarized light source is positioned orthogonal to the camera to ensure an incidence illumination and detection angles of 45°. The specular reflected light from the enamel surface is collected with an objective lens mounted on the beam splitter and divided into a horizontal (H) and vertical (V) components on each associate camera. Images of non-eroded and eroded enamel surfaces at different erosion degrees were recorded and assessed with a diagnosic software. The software was designed to generate and display two types of images: distribution of the reflection intensity (H) and polarization ratio (H-V)/(H+V) throughout the analyzed tissue area. The measurements and visualization of these two optical parameters, i.e. specular reflection intensity and the polarization ratio, allowed detection and quantification of enamel erosion at early stages in vitro.

8566-6, Session 1

Methods for monitoring erosion using optical coherence tomography

Kenneth H. Chan, Cynthia L. Darling, Daniel Fried, Univ. of California, San Francisco (United States)

No Abstract Available

8566-7, Session 2

Imaging biofilm growth on resins containing silver nanoparticles using CP-OCT

Bethany Kjellgren, Ruoqiong Chen, Corola Carrera, Conrado Aparicio, Alex Fok, Joel Rudney, Robert S. Jones, Univ. of Minnesota, Twin Cities (United States)

Antibacterial components such as silver nanoparticles have shown

promise in reducing bacterial biofilm growth on dental materials. There is great need to improve the longevity of dental resin composites with antimicrobial additives to existing formulations. This preliminary in vitro study used a 1310-nm based cross polarization swept source OCT (CP-OCT) system to image silver nanoparticle (10 nm) embedded resins. The initial aim of this project was to examine silver nanoparticle disbursement within dental primer and adhesive systems using CP-OCT imaging. After examining the disbursement of nanoparticles at different volume concentrations, the disks containing silver nanoparticles were placed in a CDC Biofilm reactor where complex multi-species dental biofilms grew within the reactor system. The multispecies biofilms were derived from plaque samples along the interface of composite or amalgam restorations in children with a history of early childhood caries. CP-OCT imaged the disbursement of silver nanoparticles in the resin by measuring an increase in scattering and depolarization changes of the resin. The overlaying biofilm on the resin with silver nanoparticles could be visualized using CP-OCT imaging.

8566-8, Session 2

Tooth structure characterization and dentin-enamel zone identification based on Stokes-Mueller calculation

Kuen Feng Lin, National Yang-Ming Univ. (Taiwan); Yao-Sheng Hsieh, National Taiwan Univ. (Taiwan); Ching-Cheng Chuang, National Yang-Ming Univ. (Taiwan); Tsan-Chi Liu, Chung Yuan Christian Univ. (Taiwan); Chia-Wei Sun, National Yang-Ming Univ. (Taiwan)

This study is a first using optical Stokes-Mueller measurement to characterize tooth structure and identify dentin-enamel zone (DEZ). By measuring the Stokes elements and Mueller matrices based on polarimetry technique. The Stokes vectors of a cross-sectional tooth slice were measured with various polarization input. The polarization state of incident light was controlled by half- and quarter-waveplates. Because of the direction of DEZ is different to enamel and dentin structures, the Stokes profiles show the specific characterization for DEZ identifying. For one-dimensional optical scanning, the tooth sample and light source were put on moving stages for optical scanning and calibration. After Stokes-Mueller calculation, the retardance of each tooth tissue can be obtained. Moreover, previous studies indicate that the dentin-enamel zone (DEZ) description is more accurate then DEJ since a progressive changing was observed. Therefore, this study demonstrates an in-vitro method based on Stokes calculation that can be applied to tooth DEZ identification. A cross-section tooth slice was measured for polarization property analysis. The one dimensional Stokes vector distribution indicates the DEZ characteristics anisotropically and the structural direction of tooth layers can be obtained. This optical method could carry out to dentin hypersensitivity diagnosis without any invasive operation because of the structure changing of DEZ could be observed. By tracking the changing of Stokes parameter distributions, an advisable therapy will be applied to avoid the occurrence of dentin hypersensitivity. The optical assessment with non-invasive, non-destructive, non-radiative scanning/imaging method may offer a great potential for other clinical disease diagnosis applications and postoperative monitoring of tooth.

8566-9, Session 2

Microleakage detection based on dental optical coherence tomography

Yao-Sheng Hsieh, National Taiwan Univ. (Taiwan); Chih-Wei Lu, Industrial Technology Research Institute (Taiwan); Yi-Ching Ho, Shyh-Yuan Lee D.D.S., National Yang-Ming Univ. (Taiwan); Ching-Cheng Chuang, National Chiao Tung Univ. (Taiwan); Wei-Cheng Huang, Industrial Technology Research Institute (Taiwan); Chia-Wei Sun, National Chiao Tung Univ. (Taiwan)

Caries may be the greatest problem because of the high prevalence. Dentists usually remove the lesion part and fill restoration materials or realize the root canal treatmen. However, the patients who were treated will under the risk of microleakage and secondary caries. The main reasons to secondary caries are the microleakage between dental resin and healthy teeth. Food debris stuck in these microleakages and produced acid to destroy enamel. This challenges the survival of the tooth and artificial crown of elders and children. Moreover, because of the senseless of hard tissues and canal treated tooth, the secondary caries are usually diagnosed when they almost lose the tooth. A good method with high accuracy for microleakage detection is necessary. The traditional tools to detect microleakage is based on clinical examination using dental probing and radiographs. The poor reliability and reproducibility of dental probing causes a fail diagnosis with tiny leakage width. Same problem occurs when radiography is applied. In addition, the radiation exposure is accompanied by radiography measurement. The optical coherence tomography (OCT) may provide another way to resolve this dilemma. In dental science, OCT can be an effective tool for assessing oral diseases. It may be an effective tool because of the non-invasive, non-destructive, non-radiated, and real-time monitoring properties. It also can provide sufficient information for dental clinical applications. This study demonstrated a preliminary study of microleakage detection for advanced secondary caries prevention based on SS-OCT in vivo with fiber handheld scanning probe. The microleakage between resin and enamel was observed in our OCT images obviously.

8566-10, Session 2

Utilizing optical coherence tomography for CAD/CAM of indirect dental restorations

Ravishankar N. Chityala, Univ. of Minnesota, Twin Cities (United States); Robert S. Jones, Univ. of Minnesota, Twin Cities (United States)

After dental decay is surgically removed, the lost tooth structure can be restored with the computer-aided design and computer-aided manufacturing (CAD/CAM) of a highly precise replacement material. This indirect method to restore the cavity preparation can offer improved long term durability and resistance to marginal leakage and wear over direct placement of photocured resin materials. This in vitro study investigated the ability of an intraoral 1310-nm based cross polarization swept source OCT (CP-OCT) system with a two axis tilt MEMS scanning mirror to construct 3D cavity prep molds. This study used hydroxyapatite disks (n=18) with and without surface morphology as a dental cavity model. The effect of hydration was also explored. Using acquired CP-OCT 3D data sets and a series of custom image segmentation and registration algorithms, 3D cavity replacement molds were created. In this study, water hydration had a negative effect on precisely replicating the lost tooth structure dimensions due to the optical delay in the OCT signal path length. This significance of this study is that the caries detection ability of CP-OCT can be combined with the clinical usefulness of utilizing CP-OCT for CAD/CAM fabrication of indirect dental restorations.

8566-11, Session 3

Selective excavation of human carious dentin using the nanosecond pulsed laser in 5.8 ?m wavelength range

Tetsuya Kita, Katsunori Ishii, Osaka Univ. (Japan); Kazushi Yoshikawa, Kenzo Yasuo, Kazuyo Yamamoto, Osaka Dental Univ. Hospital (Japan); Kunio Awazu, Osaka Univ. (Japan)

Less-invasive treatment of caries has been needed in laser dentistry. Er:YAG laser, which utilizes the wavelength of 2.94 ?m corresponding to the absorption peak of water, has become an alternative technique to a conventional dental drill, but cannot selectively remove carious dentin. Based on the absorption property of dentin, 6 ?m wavelength range shows specific absorptions and promising characteristics for the

excavation. In the previous study, 5.8 ?m wavelength range was found to be effective for selective carious dentin excavation and restoration using composite resin by the irradiation experiment with bovine sound and demineralized dentin. In this study, availability of 5.8 ?m wavelength range for selective excavation of human carious dentin was investigated. Human carious dentin was used for revealing the ablation property with a mid-infrared tunable nanosecond pulsed laser by difference-frequency generation. After irradiation experiment, surface morphologies were observed by scanning electron microscope and ablation depths were measured by confocal laser microscope. Ablation depths at normal and carious lesions were compared to evaluate selective excavation. Irradiation experiments indicated that 5.8 ?m wavelength range showed the selective excavation of carious dentin, but efficiency of ablation was less than the results of bovine dentin. Ablation property was different with respect to each carious dentin because of the different caries progression. Evaluation of caries progression and ablation property should be conducted simultaneously. In conclusion, 5.8 ?m wavelength range was found to be effective for selective excavation of human carious dentin.

8566-12, Session 3

Contact versus non-contact ablation of the artificial enamel caries by Er:YAG and CTH:YAG laser radiation

Tatjána Dostálová M.D., Charles Univ. in Prague (Czech Republic); Helena Jelínková, Jan ?ulc, Michal N?mec, Czech Technical Univ. in Prague (Czech Republic); Mitsunobu Miyagi, Tohoku Institute of Technology (Japan); Michaela Bucková, M. Ka?parová, Charles Univ., 2nd Medical Faculty (Czech Republic)

The physical basis of ablation of hard tissue by the Erbium family of lasers is related to the transfer of laser energy to the tissue that cause rapidly occurring of thermal and thermo- mechanical phenomena. The aim of study is to compare the ablation effect of contact and non-contact interaction of Er:YAG and CTH:YAG laser radiation with artificial enamel caries lesion. Demineralization process of enamel is usual e.g. after an orthodontic bracket debonding. Laser radiation can help in the process of micro-preparation or remineralization. The artificial caries was prepared in intact teeth to simulate demineralized surface and the laser radiation was applied. Contact and non-contact ablation was compared. Two laser systems Er:YAG 2.94um (non-contact 600 mJ, 6 Hz, and contact (sapphire tip - 250 mJ, 15 Hz) and CTH:YAG 2.1 um (non-contact 300 mJ, 1 Hz, and contact (waveguide with cap - 300 mJ, 1Hz) were used. The enamel artificial caries were gently removed by laser radiation and flow resin GC G-ænial and Sonic fill composite were inserted. Scanning electron microscope was use to evaluate the enamel surface structure, cross section of teeth (the enamel – resin bond) was analyzed.

8566-13, Session 3

A USPL functional system with articulated mirror arm for in-vivo applications in dentistry

Florian Schelle, Jörg Meister, Claudia Dehn, Christoph Bourauel, Mathias Frentzen D.D.S., Rheinische Friedrich-Wilhelms-Univ. Bonn (Germany)

Ultra-short pulsed laser (USPL) systems for dental application have overcome many of their initial disadvantages. However, a problem that has not yet been addressed and solved is the beam delivery into the oral cavity. The functional system that is introduced in this study includes an articulated mirror arm, a scanning system as well as a handpiece, allowing for freehand preparations with ultra-short laser pulses.

As laser source an Nd:YVO4 laser is employed, emitting pulses with a duration of <10 ps at a repetition rate of up to 500 kHz. The centre wavelength is at 1064 nm and the average output power can be tuned up to 9 W. The delivery system consists of an articulated mirror arm, to which a scanning system and a custom made handpiece are connected, including a 75 mm focussing lens. The whole functional system is compact in size and moveable. General characteristics like optical losses and ablation rate are determined and compared to results obtained in prior studies employing a fixed setup on an optical table. Furthermore classical treatment procedures like cavity preparation are being demonstrated on mammoth ivory and extracted human teeth. Clinically relevant treatment times are measured and temperature is monitored employing an infrared camera system.

This study indicates that freehand preparation employing an USPL system is possible but challenging, and accompanied by a variety of side-effects. The ablation rate with fixed handpiece is about 10 mm3/min in dentin. Factors like defocussing and blinding affect treatment efficiency.

8566-14, Session 4

The efficacy of selective calculus ablation at 400 nm: comparison to conventional calculus removal methods

Joshua E. Schoenly, Univ. of Toronto (Canada); Wolf D. Seka, Univ. of Rochester (United States); Georgios Romanos, Stony Brook Univ. (United States); Peter Rechmann, Univ. of California, San Francisco (United States)

No Abstract Available

8566-15, Session 4

Influence of USP laser radiation on cell morphology: HaCat and MG-63 cell lines for bone and soft tissue modelling in dentistry

Jörg Meister, Florian Schelle, Imke Beier, Christoph Bourauel, Matthias Frentzen D.D.S., Dominik Kraus, Rheinische Friedrich-Wilhelms-Univ. Bonn (Germany)

Due to the high intensities of USP laser radiation, the interaction with matter is always attended with a plasma formation. Therefore the surrounding tissue can be influenced by heat generation and additional light emission from the UV up to the near and mid infrared. In dentistry it is of importance that the treatment of bone and soft tissue, i.e. oral mucosa, with a USP laser should not cause any kind of morphological changes on the cell level leading to a delayed wound healing or cell mutation.

HaCat keratinocyte cells were used for epidermal (soft tissue) and MG-63 osteoblast-like cells for hard tissue (bone) modelling. Cell growing was realized on glas cover slips. Irradiation was carried out with a USP Nd:YVO4 laser having a center wavelength at 1064 nm. Based on the pulse duration of 8 ps and a pulse repetition rate of 500 kHz the laser emits an average power of 9 W. For efficiency testing of cell removal on glas cover slips, 1, 5, 25, 50 and 75 repetitions of the scanning pattern (scan loops) were used. Heat distribution during laser irradiation was measured with an infrared camera system. Subsequently haematoxylin staining and SEM investigations were used to analyse the morphological changes.

Differences of cell removal efficiency were observed with repetitions less than 25. Irradiated areas with repetitions greater than 50 were cell-free. Additionally, repetitions grater than 25 showed side effects for both cell lines. Cell destruction in both cell lines could be verified using the haematoxylin staining and the SEM pictures.

8566-16, Session 4

Photodynamic therapy for inactivation of endodontic bacterial biofilms and effect of tissue inhibitors on its antibacterial efficacy

Annie Shrestha, Anil Kishen II, Univ. of Toronto (Canada)

Complex nature of bacterial cell membrane and structure of biofilm has challenged the efficacy of antimicrobial photodynamic therapy (APDT) to achieve effective disinfection of infected root canals. In addition, tissue-inhibitors present inside the root canals are known to affect APDT activity. The current study aims to assess the effect of APDT on bacterial biofilms and evaluate the tissue-inhibitors effect on the antibacterial activity of PDT. Rose-bengal (RB) and methylene-blue (MB) were tested on Enterococcus faecalis (gram-positive) and Pseudomonas aeruginosa (gram-negative) biofilms. In vitro 7-day old biofilms were sensitized with RB and MB, and photodynamically activated with 20-60 J/cm2. Photosensitizers were pre-treated with different tissue-inhibitors (dentin, dentin-matrix, pulp tissue, bacterial lipopolysaccharides (LPS), and bovine serum albumin (BSA)) and tested for antibacterial effect of PDT. Microbiological culture based analysis was used to analyze the cell viability, while Laser Scanning Confocal Microscopy (LSCM) was used to examine the structure of biofilm. Photoactivation resulted in significant reduction of bacterial biofilms with RB and MB. The structure of biofilm under LSCM was found to be disrupted with reduced biofilm thickness. Complete biofilm elimination could not be achieved with both the photosensitizers used. APDT effect using MB and RB was inhibited in a decreasing order by dentin-matrix, BSA, pulp, dentin and LPS ($P < 0.05$). Both strains of bacterial biofilms resisted complete elimination after APDT and the tissue inhibitors existing within the root canal reduced the antibacterial activity at varying degrees. Further research is required to enhance the antibacterial efficacy of PDT in an endodontic environment.

8566-17, Session 4

Microhardness and acid resistance of hard tooth tissues after single mode YLF: Er laser treatment

Andrei V. Belikov, Ksenia V. Shatilova, Alexei V. Skrypnik, National Research Univ. of Information Technologies, Mechanics and Optics (Russian Federation)

At the moment attempts to use the radiation of different lasers have been made to increase in microhardness and acid resistance of human hard tooth tissues. CO2, Er-lasers, Nd:YAG, Ho-lasers, eximer, and argon lasers radiation was used for these purposes. In this work enamel, dentine and cementum treatment was carried out by diode-pumped YLF: Er laser radiation with wavelength of 2.84 ?m, at single- or multi- pulse impact. We treated tissues surface with laser radiation energy below the ablation threshold of hard tooth tissues. Thus treatment of tissue was carried out in order to achieve changes in the structure of tissue, but not its destruction. We did a series of experiments and investigated the combination of various parameters such as pulse duration (300-1000 ?s), pulse repetition rate (3-250 Hz), pulse energy (0.11-0.90 mJ) and number of pulses (1-600 pulses). It was shown that acid resistance of tissues increases and microhardness of enamel increases by 15% at pulse duration of 300 ?s, pulse repetition rate of 3 Hz, pulse energy of 0.90 mJ and number of pulses of 100. Microhardness of dentine increases by 30% at pulse duration of 300 ?s, pulse repetition rate of 250 Hz, pulse energy of 0.25 mJ and number of pulses of 55. Microhardness of tooth cementum increases by 20-40% at pulse duration of 300 ?s, pulse repetition rate of 250 Hz, pulse energy of 0.14-0.22 mJ and number of pulses of 55.

8566-18, Session PSun

High definition near-IR imaging of occlusal caries lesions

William A. Fried, Daniel Fried, Kenneth H. Chan, Cynthia L. Darling, Univ. of California, San Francisco (United States)

No Abstract Available

8566-19, Session PSun

Remineralization studies of early simulated lesions generated by pH cycling

Hobin Kang, Cynthia L. Darling, Kenneth H. Chan, Daniel Fried, Univ. of California, San Francisco (United States)

No Abstract Available

8566-20, Session PSun

Acoustic comparison of Er,Cr:YSSG laser and dental high speed handpiece for primary anterior tooth preparation

Monserrat Jorden, U.S. Naval Hospital (Japan); Jung-Wei Chen, Loma Linda Univ. (United States); Elisabeth Easley, Arizona School of Dentistry & Oral Health (United States); Yiming Li, R. Steven Kurti Jr., Loma Linda Univ. (United States)

The acoustics of a dental hard tissue laser (Er,Cr:YSSG laser, Waterlase MD, Biolase, USA) and a traditional dental high speed hand piece (Midwest®, Dentsply International, USA) were compared in vitro using a simple approach that can be easily adapted for in vivo studies. Thirty one extracted caries and restoration free primary anterior teeth were selected. These teeth were sectioned along a symmetry axis to give two identical sets for use in a split study. These halves were randomly assigned to either the laser (experimental) or the high speed (control) group. A miniature electret microphone was coupled to the sample using a polymer and used to collect the acoustic signal at the interface of the pulp chamber. This signal was captured periodically by a digitizing oscilloscope and multiple traces were stored for subsequent analysis. 2x1x1mm^3 preparations were made according to manufacturers recommendations for the given method. Each cavity was prepared by the same experienced clinician and calibration tests were performed to ensure consistency. The measurements indicated that the peak acoustic pressures as well as cumulative acoustic effects (due to duty cycle) were significantly higher ($P<.001$, T -test) with the dental hand piece than with the dental laser. Our study suggests the need for more detailed investigations into the neurological implications of acoustic effects in dental applications such as pain studies.

8566-21, Session PSun

Laser investigation of the non-uniformity of fluorescent species in dental enamel

Stephanie U. Tran, Human Photonics Lab. (United States) and Univ. of Washington (United States); Jeremy S. Ridge, Leonard Y. Nelson, Eric J. Seibel, Human Photonics Lab. (United States)

Many different fluorophores have been explored as the possible source of autofluorescence in dental enamel, with no definitive identification of the primary causative fluorescent species. One possible fluorescent species is a collagen residue in the enamel matrix; specifically non-reducible HP and LP crosslinkers. Collagen has long been known to be present in dentin and the dental enamel junction due to the secretion of a

collagenous predentin matrix during odontogenesis, but many textbooks claim the adult enamel to be free of collagen. In this study, we propose that the local environment of the fluorescent species in the enamel matrix is likely non-uniform in distribution within the enamel of extracted human teeth. Interprismatic and prismatic regions of enamel were isolated using acetic acid and EDTA respectively. Acetic acid preferentially dissolves the enamel prisms leaving behind the interprismatic region (type I etch), while EDTA preferentially dissolves the interprismatic area leaving the prismatic region behind (type II etch). Scanning electron micrograph images were also obtained post laser measurements to confirm specimens were properly etched. By examining the 405nm to 532nm fluorescence ratio change from sound enamel to eroded enamel we find significant differences in this ratio between type I and type II erosions. Type I erosion fluorescence ratios remained relatively the same with increased etch times while type II erosion fluorescence ratios decreased upon increased etch times. The fluorescence ratio differences and SEM images indicate a non-uniform distribution of fluorescent species in the interprismatic region as compared to the prismatic region.

8566-22, Session PSun

Determination of the suitable laser parameters in periodontal surgery

Ayse S. Sarp, Murat Gülsoy, Bogaziçi Üniv. (Turkey)

The use of modern laser technology in periodontal surgery has many advantages that are not accessible to conventional surgical techniques. Besides lots of advantages, thermal effect during the laser radiation on dental tissues can cause undesirable results. Erikkson et al. found that the threshold level for bone survival as 470C for 1 minute . Each wavelength has its own limitations and disadvantages like different penetration depths or thermal damages to tissue. Some do not have sufficient penetration into the adjoining tissue because of their high water absorptions. The aim of this study is to develop a better technique than existing methods, comparing a new wavelength with generally used two different wavelengths and also minimize the side effects of other laser applications. The surgical capability of a new fiber laser 1940- nm Thulium fiber Laser (IPG Laser; GMBH) will be explored in our study, and determined the suitable Laser parameters for periodontal surgery and keeping that intrapulpal temperature changes below the threshold value. This wavelength's effect is compared with a 809 nm diode laser a 1070 nm fiber laser. The temperature changes are recorded by a K-type Thermocouple for limiting the injury or pain. Three different power values, 0.5 Watt, 1.0 Watt and 1.5 Watt were examined for each wavelengths. Temperature rise were below the threshold value for each group. Significantly more coagulation time required for 0.5 and 1 Watt groups that were irradiated with 1940 nm fiber laser. Also, there were no difference in the histological examinations, all groups have the same depth of the incisions. Significantly less coagulation diameter observed in group 0.5 Watt group irradiated via 1940 nm fiber laser. As a result, this new wavelength laser can be effective in surgical procedures and can significantly enhance the long- term success of the treatment with optimum parameters.

8567-1, Session 1

Improved visualization of human retinal and choroidal vascular networks with phase-variance optical coherence tomography

Dae Yu Kim, Jeff Fingler, California Institute of Technology (United States); Robert J. Zawadzki, UC Davis Medical Ctr. (United States); Malvika Verma, California Institute of Technology (United States); Daniel Schwartz, Univ. of California, San Francisco (United States); John S. Werner, UC Davis Medical Ctr. (United States); Scott Fraser, California Institute of Technology (United States)

We acquired a phase-variance optical coherence tomography (pvOCT) volume data set of a normal subject and visualized blood circulation in the retina and the choroid. A semi-automatic segmentation program separated two retinal layers from an acquired volumetric data set and generated en face projection views from these layers. In addition, the processed pvOCT images will be compared to current standard imaging modalities used for retinal and choroidal vasculature visualization in clinical settings, including fluorescein angiography and indocyanine green angiography.

8567-2, Session 1

Investigation of exudative macular disease by multi-functional optical coherence angiography

Young-Joo Hong, Univ. of Tsukuba (Japan); Masahiro Miura, Tokyo Medical Univ. Kasumigaura Hospital (Japan); Myeong Jin Ju, Univ. of Tsukuba (Japan) and Univ. of British Columbia (Canada); Shuichi Makita, Yoshiaki Yasuno, Univ. of Tsukuba (Japan)

In this paper, we investigate exudative macular disease by high-penetration Doppler optical coherence angiography (HP-D-OCA). In addition, we also introduce a newly developed multi-functional OCA (MF-OCA) enabling simultaneous Doppler and Jones matrix investigation of the eye for the vasculature imaging and the discrimination of RPE and exudate at pathologic regions.

Ten eyes of 9 subjects, including 2 myopic choroidal neovascularization (mCNV), 3 age-related macular degeneration, and 4 polypoidal choroidal vasculopathy cases, were investigated by HP-D-OCA. Vasculature of en face projection image of slow Doppler mode is well correlated with the appearance of intermediate phase of indocyanine green angiography image. Hyper-scattering in en face projection image of OCT is well correlated with hyper-fluorescence in the late phase of fluorescence angiography image regardless of activity of CNV.

Two CNV eyes of non-proliferative diabetic retinopathy and angioid streaks were investigated by MF-OCA. the MF-OCA was performed by calculating OCT intensity, power of Doppler shift, and degree of polarization uniformity (DOPU) images from single measurement data. Vasculature and hard-exudate located in retina are not easily discriminable with OCT image, however vasculature shows non-zero Doppler shift and DOPU value close to 1, while hard-exudate shows zero Doppler shift and DOPU value around 0.5. When the RPE elevation and exudation occurred together in the lower part of retinal detachment, discrimination between RPE and exudation is not easy with OCT and Doppler images, however, these are discriminable by DOPU, due to the different polarization scramble property.

Structure, vasculature, exudate and RPE discriminable imaging was demonstrated by MF-OCA.

8567-3, Session 1

in vivo human optic nerve and laminar cribrosa microstructural and vasculature evaluation using ultrahigh sensitive optical microangiography

Lin An, Lee Peng, Gongpu Lan, Ruikang K. Wang, Univ. of Washington (United States)

Glaucoma is a group of eye diseases that can be characterized by the degeneration of optic nerve and death of retinal ganglion cell axons in optical nerve head (ONH), resulting in irreversible vision loss and ultimately blindness of patient. Though the detailed mechanism of Glaucoma has not been established yet, substantial evidences suggested that the compression and distortion of the lamina cribrosa (LC) is the initial step before the injury of retinal ganglion cell (RGC) axons [1]. The lamina cribrosa is a three-dimensional porous structure in ONH, which could provide protective support and nutrients to RGC axons. The elevated intraocular pressure (IOP) will have two effects on RGC axons. The first one is it will directly damage the axons [2] and the second one is it will disturb the LC capillary flows and hamper the nutrients transportation to the lamina axons [3]. Better assessments of lamina cribrosa from both structural and vasculature aspects would greatly enrich the knowledge about mechanism of Glaucoma and its early phases before the optical nerve loss, which could prevent the irreversible vision loss. A approach which can simultaneously reveal micro structure and vasculature information of LC is needed. Ultrahigh sensitive Optical micro angiography (UHS-OMAG) is a functional extension of Fourier Domain Optical Coherence Tomography (FDOCT), which could noninvasively provide high resolution high sensitivity depth resolved micro-structural and micro-vasculature information of biological tissue simultaneously. Combining with complex full range FDOCT system setup, the UHS-OMAG could achieve double imaging depth range and utilize the high sensitivity region for vasculature imaging. In this paper, we demonstrate the micro- structure and micro-vasculature results of the LC captured from a healthy volunteer in our lab using an ultrahigh speed UHS-OMAG system. Two experiments were performed. In the first experiment, a larger field of view traditional FDOCT scan was performed to achieve overall information of ONH. In the second experiment, a high resolution optical probe and a smaller field of view were employed to focus onto the bottom of the optic disc cup to achieve better visualization of the LC. The structural and vasculature maps of LC were then been qualitatively and quantitatively evaluated.

8567-4, Session 1

Classification of choroid based on blood vessel structure using high penetration optical coherence tomography

Lian Duan, Young-Joo Hong, Univ. of Tsukuba (Japan); Myeong Jin Ju, Univ. of Tsukuba (Japan) and Univ. of British Columbia (Canada); Yoshiaki Yasuno, Univ. of Tsukuba (Japan)

The choroid is a densely vascularized layer of the eye, accounting for most of the blood supply to the retina. It is known to be roughly classified to three layers including choriocapillaris, Sattler's, and Haller's layers. Visualization and evaluation of the individual layers of blood vessels in the choroid may promote the understanding to the blood circulation in the choroid and provide potential to improve diagnostic abilities for diseases such as age-related macular degeneration and diabetes. High penetration optical coherence tomography (HP-OCT) has demonstrated the ability to image the choroid and sclera.

Since the blood is less scattering than its surrounding tissue, the choroidal blood vessels can be segmented by intensity thresholding method. Firstly, the choroidal vessel was segmented by an adaptive thresholding in the en-face cross-sections at each depth of the choroid.

Successively, the choroidal vessel diameter was evaluated using a series of morphological operations in the segmentation results obtained in the first step. Finally, the local averaging of the diameter was further employed as a parameter to characterize the choroid.

In summary, a choroidal blood vessel classification and evaluation method is presented and applied to evaluate the internal property of the choroid using HP-OCT. This method characterizes the choroid based on the diameter of blood vessels. This characterization might be useful to diagnose posterior disorders associated with vasculature abnormality.

8567-5, Session 1

Quantitative analysis of retinal blood vessels based on 3D vasculature maps generated by optical microangiography

Ruikang K. Wang, Lee Peng, Lin An, Gongpu Lan, Univ. of Washington (United States)

In this paper, we utilized a newly developed ultrahigh speed UHS-OMAG system that is capable of achieving detailed microvasculature network of human retina. Two faster line scan CMOS are sequentially controlled to achieve ~500 kHz A-lines capturing rate, based on which the imaging time and motion artifacts during the experiments could be significantly reduced. For in vivo experiments, 800 A-lines were captured to form one B-scan to cover ~4 mm on X-direction, with which the system could achieve ~500 Hz frame rate. One Y-direction, 1500 B-frames were captured to cover ~3mm. Overall, it cost ~ 3 seconds to finish one 3D scan. After poste processed using the UHS-OMAG algorithms, the blood vessel images were first segmented into three different layers and then projected to a vasculature map through maximum projection method. For each layer, three quantitative parameters (vasculature networks could be quantified through Fractal Dimension, length fraction and area density) was used to evaluate the characteristic of the obtained vasculature networks. For all three parameters, the inner plexiform layer is high than ganglion cell layer and outer plexiform layer. The ganglion cell layer is similar to the outer plexiform layer. Initial statistical test indicates that there is no significant difference in blood vessel density among parafeveal and perifoveal regions; perifoveal region are significantly higher than that of the parafoveal region.

8567-6, Session 1

Vision changes in astronauts and the study of choroidal circulation

Rafat R. Ansari, NASA Glenn Research Ctr. (United States); Keith Manuel, NASA Johnson Space Ctr. (United States); Kwang I. Suh, NASA Glenn Research Ctr. (United States); Su-Long Nyeo, National Cheng Kung Univ. (Taiwan); Jerry Sebag M.D., The Univ. of Southern California (United States)

A recent report (Mader et al., Ophthalmology 2011) presented a case study of astronauts regarding in-flight vision changes. To date, there have been no studies characterizing the exact nature of this visual dysfunction and thus no focused studies of ocular physiology have been undertaken to identify the cause(s). We present an experimental study of choroidal microcirculation on 25 volunteer subjects ranging in age from 23-50 years onboard “zero” gravity aircraft while flying parabolic trajectories to begin advanced research on the effects of zero and hyper gravity on choroidal circulation. A compact head-mounted laser Doppler Flowmetry apparatus was used to test the hypothesis that ocular blood flow is altered at zero gravity.

8567-7, Session 2

Retinal safety of near-infrared femtosecond lasers in cataract surgery

Jenny Wang, Christopher Sramek, Stanford Univ. (United States); Yannis M. Paulus, Stanford Univ. School of Medicine (United States); Daniel Lavinsky, Stanford Univ. (United States); Georg Schuele, Dan E. Anderson, OptiMedica Corp. (United States); Daniel V. Palanker, Stanford Univ. (United States)

Application of femtosecond lasers to cataract surgery has added unprecedented precision and reproducibility. However, retinal safety limits, which constrain the laser repetition rate, for near-infrared lasers employed in cataract surgery are not well-quantified. Use of higher repetition rates can help reduce the effect of eye movements and improve patient comfort by reducing total procedure time. Establishing retinal safety limits for laser cataract surgery is therefore crucial for optimizing the technology. We determined retinal damage thresholds for scanning patterns while considering the effects of reduced blood perfusion from rising intraocular pressure and retinal protection from light scattering on bubbles and tissue fragments produced by laser cutting.

We measured retinal damage thresholds of a stationary 1030 nm continuous-wave laser with 2.6 mm retinal spot size for 10 and 100 second exposures in rabbits to be 1.35 W (68% CI: 1.26 – 1.42) and 0.78 W (0.73 – 0.83) respectively, and 1.08 W (0.96 – 1.11) and 0.36 W (0.33 – 0.41) when retinal perfusion is blocked. These results were used to calibrate the computational model of ocular heating.

We calculated damage thresholds for cataract surgery patterns by requiring that the tissue temperature does not exceed the damage threshold temperature course for the stationary beam. Light scattering on microbubbles and tissue fragments produced by 150 fs laser pulses decreased the transmitted power by 88%, adding a significant margin for retinal safety. These results can be used for assessment of the maximum permissible exposure during laser cataract surgery under various assumptions of treatment duration and scanning patterns.

8567-8, Session 2

In vivo performance of photovoltaic subretinal prosthesis

Yossi Mandel M.D., Georges Goetz, Daniel Lavinsky M.D., Phil Huie, Stanford Univ. (United States); Keith Mathieson, Univ. of Strathclyde (United Kingdom); Lele Wang, Theodore I. Kamins, Stanford Univ. (United States); Richard Manivanh, Stanford Univ. School of Medicine (United States); James Harris, Daniel V. Palanker, Stanford Univ. (United States)

We have developed a photovoltaic retinal prosthesis, in which camera-captured images are projected onto the retina using pulsed near-IR light. Each pixel in the subretinal implant directly converts pulsed light into local electric current to stimulate the nearby inner retinal neurons. 30 micron-thick implants with pixel sizes of 280, 140 and 70 μm were successfully implanted in the subretinal space of wild type (WT, Long-Evans) and degenerate (Royal College of Surgeons, RCS) rats. Optical Coherence Tomography and fluorescein angiography demonstrated normal retinal thickness and healthy vasculature above the implants upon 6 months follow-up. Stimulation with NIR pulses over the implant elicited robust visual evoked potentials (VEP) at safe irradiance levels. Thresholds increased with decreasing pulse duration and pixel size: with 10 ms pulses it went from 0.5 mW/mm^2 on 280 micron pixels to 1.1 mW/mm2 ^on 140 μm pixels, to 2.1 mW/mm^2 on 70 μm pixels. Latency of the implant-evoked VEP was at least 30 ms shorter than response evoked by the visible light, due to lack of phototransduction. Amplitude of the implant-induced VEP increased logarithmically with peak irradiance and pulse duration. It decreased with increasing frequency similar to the visible light response in the range of 2 - 10 Hz, but decreased slower than the visible light response at 20 - 40 Hz. Modular design of the photovoltaic arrays allows scalability to a large number of pixels, and

combined with the ease of implantation, offers a promising approach to restoration of sight in patients blinded by retinal degenerative diseases.

8567-9, Session 2

Optical modulation of transgene expression in retinal pigment epithelium

Daniel V. Palanker, Daniel Lavinsky M.D., Stanford Univ. (United States); Thomas W. Chalberg Jr., Avalanche Biotechnologies, Inc. (United States); Yossi Mandel, Stanford Univ. (United States); Phil Huie, Stanford Univ. School of Medicine (United States); Roopa Dalal, Stanford Univ. (United States); Michael Marmor, Stanford Univ. School of Medicine (United States)

Over a million of people in US alone are visually impaired due to the neovascular form of age-related macular degeneration (AMD). The current treatment is monthly intravitreal injections of a protein which inhibits Vascular Endothelial Growth Factor, thereby slowing progression of the disease. The immense financial and logistical burden of millions of intravitreal injections signifies an urgent need to develop more long-lasting and cost-effective treatments for this and other retinal diseases.

Viral transfection of ocular cells allows the creation of a “biofactory” that secretes therapeutic proteins. This technique has been proven successful in non-human primates, and is now being evaluated in clinical trials for wet AMD. However, there is a critical need to down-regulate gene expression in the case of total resolution of retinal condition, or if patient has adverse reaction to the trans-gene products.

The site for genetic therapy of AMD and many other retinal diseases is the retinal pigment epithelium (RPE). We developed and tested in pigmented rabbits, an optical method to down-regulate transgene expression in RPE following vector delivery, without retinal damage. Microsecond exposures produced by a rapidly scanning laser vaporize melanosomes and destroy a predetermined fraction of the RPE cells selectively. RPE continuity is restored within days by migration and proliferation of adjacent RPE, but since the transgene is not integrated into the nucleus it is not replicated. Thus, the decrease in transgene expression can be precisely determined by the laser pattern density and further reduced by repeated treatment without affecting retinal structure and function.

8567-10, Session 2

Cell-targeted holographic retinal photo-stimulation in vivo

Adi Schejter, Limor Tsur, Nairouz Farah, Technion-Israel Institute of Technology (Israel); Inna Reutsky-Gefen, Ruppin Academic Ctr. (Israel); Shy Shoham, Technion-Israel Institute of Technology (Israel)

Degenerative diseases of the outer retina lead to photoreceptor loss and eventually cause blindness. However, the retinal ganglion cells (RGCs) are relatively preserved. Artificial photo-stimulation of these functional cells could be the key to developing retinal neuroprosthetic devices, which will restore patients’ vision. A successful retinal prosthesis should induce activity patterns which will enable downstream circuits to correctly interpret the artificially generated stimulus as the intended image. In previous work, we demonstrated patterned photo-stimulation of RGCs in-vitro, using optogenetic and photo-thermal mechanisms.

The research presented here constitutes a first step in advancing towards in-vivo retinal stimulation. We present and characterize a system which integrates precise spatiotemporal holographic photo-stimulation with high resolution fundus imaging. This system allows targeting of a holographically projected pattern at specific locations with single-cell resolution, in order to excite specific RGCs in rodent retinas in-vivo.

Finally, we will describe the system’s application to functional calcium imaging of neuronal population activity as part of the development of a novel optical retinal prosthesis.

8567-11, Session 2

To be announced *(Keynote Presentation)*

No Abstract Available

8567-12, Session 3

Large-field high-speed polarization sensitive optical coherence tomography of the diseased eye

Stefan Zotter, Michael Pircher, Bernhard Baumann, Teresa Torzicky, Medizinische Univ. Wien (Austria); Hirofumi Yoshida, Futoshi Hirose, Canon Inc. (Japan); Mitsuro Sugita, Philipp Roberts, Markus Ritter, Christopher Schütze, Erich Götzinger, Wolfgang Trasischker, Clemens Vass, Ursula Schmidt-Erfurth, Christoph K. Hitzenberger, Medizinische Univ. Wien (Austria)

In this study we present novel measurement results on an improved polarization sensitive optical coherence tomography system (PS-OCT). PS-OCT in general is a functional extension of intensity based OCT, which allows the differentiation of several retinal layers due to the different light tissue interactions. This technique is able to distinguish between polarization preserving layers (e.g. photoreceptor layer), birefringent layers (e.g. retinal nerve fiber layer (RNFL) or Henle’s fiber layer) and depolarizing (polarization scrambling) layers (e.g. retinal pigment epithelium (RPE)), which is important for segmentation and to retrieve quantitative information about these layers. The new PS-OCT system supports scan angles of up to 40°x40° with a line scan rate of 70kHz. The high-speed imaging together with the large field of view considerably increases the informative value of the measurement results. In order to demonstrate the good performance of the new PS-OCT system we measured several healthy subjects and patients with various diseases such as AMD, glaucoma, Stargardt’s disease, Morbus Best and albinism. A comparison with clinically established methods such as autofluorescence, scanning laser polarimetry and intensity based OCT shows that the new PS-OCT system is capable to combine several abilities of these imaging techniques.

8567-13, Session 3

High-sensitive detection of keratoconus and keratoconus suspect by corneal birefringence measured by Jones matrix tomography

Yoshiaki Yasuno, Univ. of Tsukuba (Japan); Masahiro Yamanari, Tomey Corp. (Japan); Shinichi Fukuda, Sujin Hoshi, Simone Behergaray, Yiheng Lim, Testuro Oshika, Univ. of Tsukuba (Japan) and Computational Optics and Ophthalmology Group (Japan)

Systematic study of utility of polarization sensitive optical coherence tomography (PS-OCT) for keratoconus diagnosis is presented. Keratoconus is non-inflammatory disorder of cornea characterized by ecstatic abnormal thinning. The current standard methods of keratoconus, such as corneal topography based on ring projection, Scheimpflug camera, or OCT, provides reasonable sensitivity and specificity for moderate cases, its diagnosis ability for subclinical cases are low.

Since the keratoconus is expected to be associated with corneal tissue abnormality and cornea is a highly birefringent collagenous tissue, its abnormality could be detected by measuring its birefringence. In this paper, we discuss the utility PS-OCT for the detection of early and subclinical keratoconus.

63 eyes of 49 subjects including 31 keratoconic eyes, 7 keratoconus suspect eyes and 25 normal control eyes were involved. The eyes were examined by PS-OCT. Radially sectored en-face phase retardation map of the cornea were created. The phase retardations at each sector

are evaluated for its ability of detection of keratoconus by area-under-receiver-operating-characteristic curve (AROC) analysis.

The PS-OCT showed higher ability to discriminate preclinical keratoconus to normal control than standard topometry. On the other hand PS-OCT has low ability to discriminate preclinical to advanced keratoconus. This fact indicates that PS-OCT is sensitive for subclinical alteration of corneal tissue, and hence has high sensitivity for subclinical keratoconus detection.

8567-14, Session 3

Non-invasive assessment of corneal crosslinking changes using polarization sensitive optical coherence tomography

David Alonso-Caneiro, Queensland Univ. of Technology (Australia); Masahiro Yamanari, Tomey Corp. (Japan); Shinichi Fukuda, Sujin Hoshi, Univ. of Tsukuba (Japan); Satoko Nagase M.D., Tokyo Medical Univ. (Japan); Tetsuro Oshika, Yoshiaki Yasuno, Univ. of Tsukuba (Japan); Michael J. Collins, Queensland Univ. of Technology (Australia)

In recent years, a new minimally invasive procedure, called collagen crosslinking (CXL) has shown promising results in the prevention of the progression of keratoconus and corneal ectasia. The procedure alters the corneal biomechanical properties by increasing its stiffness and slowing down the progression of the condition. While some techniques have shown promise for in-situ imaging of CXL corneal changes, to the best of our knowledge there is no technique that allows identification of the treatment zone after CXL. Therefore, new methods are required to assess the regional effects on the corneal stroma of CXL treatment.

Polarization sensitive optical coherence tomography (PS-OCT) is a functional extension of the well developed OCT. The lamellar structure of the cornea (collagen fibres) has birefringence properties, which are altered by microscopic change of the collagen lamellar structure during CXL. Hence, CXL in the cornea can be monitored by PS-OCT.

In this study, a set of ex-vivo porcine eyes were treated with a chemical CXL agent (glutaraldehyde), while PS-OCT recordings were taken simultaneously to assess the sensitivity of the technique to distinguish changes in the corneal tissue. The results obtained in this study show a significant correlation between histological corneal changes and the phase retardation changes measured by PS-OCT after CXL. Thus, PS-OCT may be a suitable technique to measure CXL changes in-situ and assess the local changes in the treated region of the cornea.

8567-15, Session 3

Mapping scleral fiber orientation and birefringence in the rat eye in vivo using polarization sensitive optical coherence tomography

Bernhard Baumann, Marco Bonesi, Sabine Rauscher, Erich Götzinger, Michael Pircher, Harald Sattmann, Stefan Zotter, Teresa Torzicky, Wolfgang Trasischker, Medizinische Univ. Wien (Austria); Christoph M. Eigenwillig, Benjamin R. Biedermann, Wolfgang Wieser, Robert A. Huber, Ludwig-Maximilians-Univ. München (Germany); Christoph K. Hitzenberger, Medizinische Univ. Wien (Austria)

We present polarization sensitive optical coherence tomography (PS-OCT) for non-invasive imaging and quantification of the birefringence characteristics of the sclera in the rat eye in vivo. The biomechanical properties of the sclera are based on the collagen fiber organization and have been linked to the pathogenesis of glaucoma. PS-OCT gives access to the intrinsic birefringence properties of the sclera with micrometer scale resolution. In this study, high speed PS-OCT based on swept source technology and polarization maintaining (PM) fiber optics was used for imaging the retina and sclera around the optic nerve head (ONH). Three dimensional (3D) PS-OCT data sets were recorded in rat eyes in vivo and maps of the birefringent properties of the sclera were computed. Strong birefringence was observed in the sclera as a dramatic increase of phase retardation values with depth. The birefringent optic axis varied considerably dependent on the location around the optic nerve and exhibited a radial dependence in the posterior sclera. Unlike previously reported methods for investigating the scleral structure around the ONH, PS-OCT is a non-invasive technique which can be performed in vivo and therefore permits to enable longitudinal studies of pathologic changes in animal models of glaucoma.

8567-16, Session 3

Retardation of Henle's fiber layer: a comparison of polarization-sensitive methods

Donald T. Miller, Indiana Univ. (United States); Stefan Zotter, Medizinische Univ. Wien (Austria); Qiang Wang, Indiana Univ. (United States); Christoph K. Hitzenberger, Medizinische Univ. Wien (Austria)

Introduction: The structured organization of Henle's fiber layer (HFL) in the retina is well known to exhibit birefringence. While changes in HFL birefringence has been suggested as a sensitive indicator of disease onset, uncertainty remains as to the distribution and magnitude of its retardance in the normal eye. A key confounding issue is that the few studies to date have been based on different measurement methods and imaged different eyes. To address this uncertainty, we compared HFL retardance measurements on the same eyes using three methods: a GDx confocal scanning laser polarimeter (Carl Zeiss Meditec) and two laboratory polarization-sensitive optical coherence tomography (PSOCT) methods, one based on normal optical fiber and the other on polarization-maintaining fiber. Methods: Measurements were collected on three healthy subjects free of ocular disease (six eyes). All polarization images were acquired over at least 14degx14deg area centered on the fovea. The double pass phase retardation (DPPR) induced by HFL was extracted by comparing the Stokes vectors or phase retardance at the inner limiting membrane to that at the interface between the inner-and-outer segments (IS/OS) of the photoreceptor layer. Results and Conclusion: The projected DPPR map showed the characteristic "donut" pattern of elevated retardance centered on the fovea. Repeatability of the two PSOCT methods were comparable with standard deviations of ~0.45deg that is significantly smaller than the variation in DPPR across the six eyes measured of 1.75deg. The two PS-OCT methods yielded consistent radially-averaged DPPR traces on the same eyes. In contrast, GDx was elevated and more variable.

8567-17, Session 3

PS-OCT-based methodology for measuring age and population differences in phase retardation of Henle's fiber layer

Qiang Wang, Indiana Univ. (United States); Barry Cense, Utsunomiya Univ. (Japan); Omer P. Kocaoglu, Zhoulin Liu, Donald T. Miller, Indiana Univ. (United States)

We investigated a new methodology based on the technology of polarization-sensitive optical coherence tomography (PS-OCT) in conjunction with extensive post processing for measuring age and population differences in phase retardance of Henle's fiber layer (HFL).

To assess the efficacy of the methodology, double pass phase retardation (DPPR) of HFL was measured in a population of healthy subjects free of ocular disease (n=20; range=23-63 yrs; 8 females and 12 males) by comparing Stokes vectors at the inner limiting membrane (ILM) to that at the interface between the inner-and-outer segments (IS/OS) of

photoreceptors. ILM and IS/OS were segmented using a computer-aided manual procedure. To increase signal-to-noise, radial averages of DPPR about the foveal center were computed. To improve sensitivity, a six order polynomial fit was used to locate the maximum DPPR value and corresponding retinal eccentricity. Linear regression was then performed on the maximum DPPR value and retinal eccentricity as a function of age.

The projected DPPR map revealed the characteristic “donut” pattern of elevated retardance centered on the fovea. Averaged across all eyes, maximum DPPR was 24.9 deg and occurred at 2.0 deg retinal eccentricity. Subject variation about this average was +/- 4.65 deg, significantly larger than method repeatability (~0.45 deg). Linear regression found a correlation of maximum DPPR retinal eccentricity with age that decreased at 0.006 deg/yr (R^2=0.26, p=0.05), which was significant. Linear regression showed an overall thinning of the retina (OPL to IS/OS), decreasing at 0.20µm/yr (R^2=0.30, p=0.04), again significant. Results from the study indicate the PS-OCT-based methodology can detect significant age and population differences.

8567-18, Session 4

Clinically validated quantitative multi-surface corneal topography utilizing OCT

Ryan P. McNabb, Francesco LaRocca, Duke Univ. (United States); Sina Farsiu, Duke Univ. (United States) and Duke Univ. (United States); Anthony N. Kuo, Joseph A. Izatt, Duke Univ. (United States)

Surgical treatment of astigmatism requires accurate characterization of the magnitude and direction of the refractive astigmatic power of the cornea. Inaccurate measurements result in insufficient correction or even increased astigmatism for the patient. Keratometry and topography are currently used to measure corneal astigmatism but consider only the anterior surface contribution of the cornea. OCT images provide both the anterior and posterior surfaces to better characterize the optical properties of the cornea as a whole and have been used to provide high resolution information about corneal surface elevation and the derived spherical refractive power from these surfaces. These OCT measurements, however, are sensitive to patient motion which can corrupt the accuracy and hence clinical utility of the reported measurements. We have previously shown that distributed scanning OCT (DSOCT) can selectively filter patient motion from corneal OCT volumes and improve clinical measurements of spherical power. In this current study, we extended this work for astigmatic power measurement. In a clinical pilot study, we found the mean paired difference between DSOCT steep axis refractive power and topography was -0.05 D and 1.6 degrees; the flat axis difference was 0.15 D. Between DSOCT and Scheimpflug photography, the mean paired difference for the steep axis was -0.03 D and 2.2 degrees with a flat axis difference of 0.14 D. Surface curvature power maps were found to be qualitatively comparable across all three platforms. DSOCT shows promise for the accurate clinical characterization of astigmatic corneal refractive power comparable to current standards.

8567-19, Session 4

Assessing the change in axial eye length during accommodation with optical coherence tomography

Carolina De Freitas, Marco Ruggeri, Bascom Palmer Eye Institute (United States); Fabrice Manns, Bascom Palmer Eye Institute (United States) and Univ. of Miami (United States); Arthur Ho, Brien Holden Vision Institute (Australia) and Bascom Palmer Eye Institute (United States) and Univ. of New South Wales (Australia); Jean-Marie Parel, Bascom Palmer Eye Institute (United States) and Univ. of Miami (United States) and Brien Holden Vision Institute (Australia)

The goal of the present study is to verify if there is any change in axial eye length (AEL) during accommodation with an optical coherence tomography (OCT). A spectral domain OCT system capable of measuring intraocular distances with 8 µm axial resolution along the entire depth of the eye was used. The accommodative response to a step stimulus alternating between 0 D and 8 D was imaged five times in the right eye of two subjects, aged 24 and 35. The intra-ocular optical distances were measured along the central axis on the OCT frame, then divided by their group refractive indices and then and summed to determine the geometrical axial eye length. Dimensions from the relaxed state were compared to the fully-accommodated state and in all measurements, the change in axial eye length was well within the measurement variability with a range of -0.010 mm to +0.007 mm in the 24 year old subject and a range of -0.029 mm to +0.015 mm in the 35 year old subject. We found that within the precision of our method, no quantifiable axial eye length change can be measured while the eye is responding to accommodation.

8567-20, Session 4

3D ocular morphometry and biometry of accommodating eyes using full eye length imaging with SS-OCT

Ireneusz Grulkowski, Jonathan J. Liu, Massachusetts Institute of Technology (United States); Benjamin M. Potsaid, Massachusetts Institute of Technology (United States) and Thorlabs Inc. (United States); Vijaysekhar Jayaraman, Praevium Research, Inc. (United States); Alex E. Cable, Thorlabs Inc. (United States); David Huang, Casey Eye Institute OHSU (United States); Jay S. Duker, Tufts Univ. (United States); James G. Fujimoto, Massachusetts Institute of Technology (United States)

Accommodation is an ability of the eye to change optical power in order to maintain a focused image on the retina as image distance varies. It is largely due to alterations in parameters of the crystalline lens. We demonstrate novel ultra-long range volumetric imaging of the eye using swept source SS-OCT with vertical cavity surface-emitting laser (VCSEL) technology. Extremely long coherence length of VCSEL and high speed detection enable acquisition of images of the anterior segment and posterior pole of the eye (full eye length imaging). A prototype swept source OCT system utilizing VCSEL light source technology with integrated Badal optometer to induce accommodative demand is used in this study. Volumetric data sets of the eye at different ocular vergence levels (accommodative demands) are acquired. The application of 3-D refraction correction algorithms allows comprehensive quantitative characterization of the eye morphology during accommodation. The extracted parameters of the eye include topography of the cornea and the crystalline lens (phakometry), pupil diameter (pupillometry) as well as intraocular distances, including axial eye length (ocular biometry). The results demonstrate the ability of the full eye length imaging to characterize ocular dimensions and topographic parameters of the ocular structures.

8567-21, Session 4

Natural motion of the optic nerve head revealed by high speed phase-sensitive OCT

Keith OHara, Tilman Schmoll, Clemens Vass, Rainer A. Leitgeb, Medizinische Univ. Wien (Austria)

Glaucoma is a disease involving death of ocular nerve cells, and is associated with chronic deformation of the optic nerve head. If transient deformations of the nerve head due to the natural pulse can be measured clinically, they might reveal which optic nerve heads are susceptible to chronic damage. We developed a high speed phase-sensitive OCT system to measure the deformation of the optic nerve head during the pulse cycle. The spectral-domain OCT system acquired 100k A-scans per second, with measurements from a commercial pulse oximeter

recorded simultaneously, correlating OCT data to the subject's pulse. Data acquisition lasted for 2 seconds, to cover at least two pulse cycles. Acquiring 250 A-scans while scanning 2.4-mm across the optic nerve results in a frame rate of 400 B-scans per second, which is fast enough that speckle in successive B-scans is largely correlated, and meaningful phase differences can be taken between B-scans.

Bulk motion of the entire eye dominates the phase difference. We subtracted the best-fit linear trend from the phase difference images, to give a sequence of phase images encoding the relative motions only. About 5 to 10 µm/s motion of the cup, and retinal-pigment-epithelium edge, synchronous with the measured pulse, is seen relative to the retinal nerve fiber layer.

8567-22, Session 4

Determination of eye shape by ultrawide-field MHz-OCT

Thomas Klein, Wolfgang Wieser, Tom Pfeiffer, Robert A. Huber, Ludwig-Maximilians-Univ. München (Germany)

Determination and subsequent monitoring of the true three-dimensional shape of the human eyeball may be a helpful tool in the clinical management of certain risk groups. For instance, patients with highly myopic eyes are prone to pathologic myopia. Shape measurements are typically performed with stereoscopic ophthalmoscopy, ultrasound imaging or magnetic resonance imaging. These methods are either subjective, offer poor resolution or are prohibitively expensive. Ultrawide-field MHz OCT of the posterior pole may provide a valuable means for high-resolution, cost-effective and non contact shape analysis of the retina. In addition to shape, OCT B-scans are available for further analysis, perfectly co-registered to the overall shape. MHz-OCT provides sufficient speed for acquisition of large datasets suitable for shape analysis in short time. With a Fourier-domain mode locked (FDML) swept laser, large OCT datasets spanning ~60 degrees field of view can be acquired in-vivo. For shape analysis, OCT images need to be corrected for several distortions that affect the position of each voxel. These distortions can be divided into static and dynamic distortions. While static distortions need to be determined only once, dynamic corrections depend on the optical properties of each eye, and moreover on the exact position of the eye in relation to the scanning system. We will discuss all relevant distortions, their relative impact on the accuracy of shape analysis, and methods for distortion correction. Particular emphasis will be placed on the importance of suitable image preview functionality to allow precise alignment for increased reproducibility.

8567-23, Session 5

Simultaneous denoising and interpolation of SDOCT image via sparse representation

Leyuan Fang, Hunan Univ. (China) and Duke Univ. Medical Ctr. (United States); Shutao Li, Hunan Univ. (China); Ryan P. McNabb, Anthony N. Kuo, Cynthia A. Toth, Duke Univ. (United States); Joseph A. Izatt, Duke Univ. (United States) and Duke Univ. Medical Ctr. (United States); Sina Farsiu, Duke Univ. (United States) and Duke Univ. (United States)

We introduce an image restoration method to recover high-quality SDOCT images from clinical data. Our algorithm is an extension of the sparsity based denoising (MSBTD) algorithm that we recently introduced for reducing speckle noise [Fang et al. BOE 2012]. Our new algorithm is capable of both interpolating missing data and removing noise. To achieve this, we have modified the MSBTD algorithm in two ways. First, from the training dataset, we construct two structural sparse representation dictionaries offline: one that corresponds to high-quality images and another that corresponds to their degraded versions. Second, unlike our previous work, we do not need to acquire even a single high-quality image from the target patient in clinic. That is, we have constructed a comprehensive sparse representation dictionary from a previously collected dataset. This allows us to rapidly capture low-density noisy images and recover high-density low-noise images in the post-processing step using the constructed dictionary. Compared to previous attempts in utilizing compressive sampling for SDOCT interpolation, our algorithm has significant performance advantages, is mathematically better justified, and does not require complex sampling schemes. Our algorithm was tested on simulated and real retinal SDOCT images captured in the clinic. Experiments showed that our algorithm qualitatively and quantitatively outperforms a previous compressive sampling method as well as the state-of-the-art BM3D image interpolation method. In conclusion, for retinal SDOCT images, our algorithm is the most effective interpolation and denoising method to date. At the time of publication, we will make the code and dataset freely available online.

8567-24, Session 5

Automated multilayer segmentation and characterization in 3D spectral-domain optical coherence tomography images

Zhihong Hu, Doheny Eye Institute (United States); Xiaodong Wu, The Univ. of Iowa (United States); Amirhossein Hariri, SriniVas R. Sadda, Doheny Eye Institute (United States)

Spectral-domain optical coherence tomography (SD-OCT) is a 3-D imaging technique, allowing direct visualization of retinal morphology and architecture. The various layers of the retina may be affected differentially by various diseases. In this preliminary study, an automated graph-based multilayer approach was developed to sequentially segment eleven retinal surfaces including the outer retinal bands in normal SD-OCT volume scans at three different stages. For stage 1, the four most easily detectable surfaces were identified in four times downsampled images and were used as a priori positional information to limit the graph search for other surfaces at stage 2. Eleven surfaces were then detected in two times downsampled images at stage 2, and refined in the original image space at stage 3 using the graph search integrating the estimated morphological shape model. Twenty macular SD-OCT (Heidelberg Spectralis) volume scans from 20 normal subjects (one eye per subject) were used in this study. The overall mean and absolute mean differences in border position between the automated and manual segmentation for all 11 segmented surfaces were -0.20 ± 0.53 voxels (-0.76 ± 2.06 µm) and 0.82 ± 0.64 voxels (3.19 ± 2.46 µm). Intensity and thickness properties in various retinal layers were also investigated. This investigation in normal subjects may provide a comparative reference for subsequent investigations in eyes with disease.

8567-25, Session 5

Polarization based segmentation of the choroid-sclera interface and choroidal thickness measurement in 3D data sets of the human eye

Teresa Torzicky, Michael Pircher, Bernhard Baumann, Stefan Zotter, Wolfgang Trasischker, Erich Götzinger, Christoph K. Hitzenberger, Medizinische Univ. Wien (Austria)

In our current work we are using a polarization sensitive optical coherence tomography (PS-OCT) system with a central wavelength of 1040 nm, which allows increased penetration depth, for acquiring 3D data sets of the polarization characteristics of retina, choroid and sclera in vivo. Based on the acquired images a segmentation algorithm for identifying the retinal pigment epithelium (RPE) and the choroid-sclera interface (CSI), for investigation of the choroidal thickness in 3D data sets, was developed. The challenge of this work was that in 3D data sets averaging over a high number of frames, which is usually done for the segmentation in 2D data sets, is not possible. Therefore less signal

from deep layers like the sclera is detected, which hinders the acquisition of the scleral birefringence. To overcome this issue we developed an approach, where a polynomial is fitted through the CSI segmentation data points found by the algorithm, in order to compensate for the A-scans where the signal was too low for defining the CSI directly. With this approach a segmentation of the whole data set is possible, but in areas where changes in retardation values are not smooth, the segmentation result is not following the measured retardation characteristics accurately. Different approaches to overcome this issue are tested and discussed.

8567-26, Session 5

Validated automatic segmentation of photoreceptors in adaptive optics scanning ophthalmoscope images

Stephanie J. Chiu, Adam M. Dubis, Duke Univ. (United States); Robert F. Cooper, Marquette Univ. (United States) and Medical College of Wisconsin (United States); Alfredo Dubra, Joseph Carroll, Medical College of Wisconsin (United States); Joseph A. Izatt, Sina Farsiu, Duke Univ. (United States)

With the advent of adaptive optics imaging devices, visualizing photoreceptors in vivo is now possible. In recent years, algorithms have been developed to extract cone density, spacing, and reflectance from these images in order to characterize retinal degenerative diseases with varying rates of success. In this work, we developed a customized implementation of our generalized graph theory and dynamic programming GTDP framework for closed contour structures, to segment photoreceptors in adaptive optics scanning ophthalmoscope images. We first attained pilot estimates of cone locations by performing local maxima operations. To more precisely locate the cones, we then transformed each cone into the quasi-polar domain to segment the cone's closed contour shape as a layer. The centroid was then computed to locate the cone center. Finally, after detecting the most prominent cones, this entire process was repeated with higher sensitivity to detect cones in lower contrast regions. We then validated our GTDP algorithm for accuracy against the state-of-the-art technique and compared both fully automatic methods to the semi-automatic gold standard. Results show that our technique improved the cone detection rate by nearly a factor of three in comparison to the other automated method, on average correctly identifying 98% of the cones. Furthermore, our technique even located cones missed by the gold standard. Finally, we show that our algorithm extracted cone density and spacing metrics closer to the gold standard than the existing technique. Overall, these results are highly encouraging for reducing the time and manpower required to identify photoreceptors in ophthalmic studies.

8567-27, Session 5

Robust 3D-OCT motion correction with applications in pathology imaging, Doppler OCT, and OCT angiography

Martin F. Kraus, Friedrich-Alexander-Univ. Erlangen-Nürnberg (Germany); WooJhon Choi, Jonathan J. Liu, Massachusetts Institute of Technology (United States); Yali Jia, Casey Eye Institute OHSU (United States); Jason Zhang, New England Eye Ctr. (United States); Mehreen Adhi M.D., Tufts Univ. School of Medicine (United States); Benjamin M. Potsaid, Ireneusz Grulkowski, Massachusetts Institute of Technology (United States); David Huang M.D., Casey Eye Institute OHSU (United States); Jay S. Duker, New England Eye Ctr. (United States); Joachim Hornegger, Friedrich-Alexander Univ. Erlangen-Nuernberg (Germany); James G. Fujimoto, Massachusetts Institute of Technology (United States)

We present advances in the robustness of 3D OCT motion correction using orthogonal scan patterns and image registration. A new two stage optimization approach is employed to allow for the correction of low quality input data sets, such as commonly found in pathologic eyes. The first stage registers the two or more input volumes using a reduced numbers of degrees of freedom for optimization. The roughly corrected output of the first stage is then used as input for a full per A-Scan optimization in the second stage. Both stages employ multi-resolution optimization. Applications of motion correction and merging techniques to functional OCT such as Doppler OCT, and correlation based angiography are presented. For Doppler OCT processing we take special care of the fact that Doppler shift is a phase. Experiments show the ability to motion correct and merge low quality clinical input volumes and to motion correct functional OCT datasets and merge functional information. Experiments on angiography data show better connectivity of the vessels as well as higher SNR. In conclusion we think that these techniques can play a valuable role in structural and functional OCT imaging.

8567-28, Session 6

Development of a retinal phantom for OCT performance evaluation

Jigesh Baxi, Anant Agrawal, William R. Calhoun III, William R. Calhoun III, U.S. Food and Drug Administration (United States); Scott A. Mathews, The Catholic Univ. of America (United States); Daniel X. Hammer, Ilko Ilev, Ilko Ilev, Josh Pfefer, U.S. Food and Drug Administration (United States)

The purpose of this project is to develop a phantom to assess the performance of clinical optical coherence tomography (OCT) devices used to image the retina. Phantoms form the basis of many performance test methods for medical imaging systems, but few currently exist for OCT. We developed a retina-mimicking phantom to assess image quality and system accuracy. The retinal phantom is a layered structure, where each layer is designed to mimic the corresponding optical properties and thickness while also representing global anatomical features such as the foveal pit and optic disk. The phantom is embedded in an eye model capsule to simulate the focal length of the human eye and for ease of use with clinical OCT systems. Critical parameters such as system contrast and image distortion may be quantitatively measured. Furthermore, phantom thickness measurements can assess device and segmentation algorithm accuracy. Such an analysis may provide better insight into the clinical limitations of different OCT systems and serve as a standardization tool in performance evaluation and quality assurance of OCT devices.

8567-29, Session 6

Real-time Hartmann-Shack autorefractor: slit-lamp mounted prototype

Victor M. Hernandez, Stephanie Delgado, Bascom Palmer Eye Institute (United States) and Univ. of Miami (United States); David Borja, Univ. of Miami (United States) and Bascom Palmer Eye Institute (United States); Arthur Ho, Ophthalmic Biophysics Ctr., Bascom Palmer Eye Institute (United States) and Univ. of Miami (United States) and Univ. of New South Wales (Australia); Fabrice Manns, Bascom Palmer Eye Institute (United States) and Univ. of Miami (United States); Jean-Marie Parel, Bascom Palmer Eye Institute (United States) and Univ. of Miami (United States) and Brien Holden Vision Institute (Australia)

There are several surgical procedures, such as intraocular lens implantation and corneal transplant surgery that can benefit from real-time intraoperative measurement of refraction as a means to verify or optimize or the postoperative visual outcome. Current manual or

microscope-mounted intraoperative refractors do not allow continuous real-time measurements of refraction. As a first step towards the development of a microscope-mounted real-time intraoperative autorefractor, we present preliminary real-time refraction results obtained on an eye model using a prototype device mounted on a slit-lamp. The basic design is a modification of a slit-lamp mounted Hartmann-Shack autorefractor which measures the ocular wavefront but without using the traditional 4f relay system. Two different implementations were tested. An “outside-coupled” design where the autorefractor is coupled to the biomicroscope externally through a mirror mounted between the two observation channels, and an “inside-coupled” where the biomicroscope objective is one of the relay lenses of the system. Experiments were performed on the inside-coupled system using an eye model and a set of trial spectacle lenses that produced refractive errors ranging from -20D to +20D. Measurements were acquired in real-time at a rate of 10Hz. The experimental wavefront sphere-versus-refraction results were compared with predictions from a paraxial model of the system. This study demonstrates the feasibility of a compact biomicroscope-mounted real-time autorefractor with large dynamic range using a modified Hartmann-Shack aberrometer design without moving parts.

8567-30, Session 6

Real-time SLO eye tracking for improved phase-resolved OCT angiography

Boy Braaf, Kari V. Vienola, Rotterdam Ophthalmic Institute (Netherlands); Christy K. Sheehy, Univ. of California, Berkeley (United States); Qiang Yang, Montana State Univ. (United States); Koenraad A. Vermeer, Rotterdam Ophthalmic Institute (Netherlands); Pavan Tiruveedhula, Univ. of California, Berkeley (United States); David W. Arathorn, Montana State Univ. (United States); Austin Roorda, Univ. of California, Berkeley (United States); Johannes F. de Boer, Rotterdam Ophthalmic Institute (Netherlands) and Vrije Univ. Amsterdam (Netherlands)

Phase-resolved Optical Coherence Tomography (OCT) detects blood flow in tissue by the analysis of phase changes that are caused by the Doppler effect from moving particles. This technique relies on repeated A-scan measurements at (nearly) the same lateral location with micrometer accuracy. Eye motion can therefore easily create artifacts and increased noise levels. In this paper we present phase-resolved OCT in combination with active eye tracking to improve the imaging of the retinal micro-vasculature. Phase-resolved OCT was performed using inter-B-scan comparison with a 10 ms inter-frame time-delay using a 1050 nm wavelength phase-stabilized optical frequency domain imaging (OFDI) instrument. Simultaneous high-speed eye tracking was performed with an 850 nm Scanning Laser Ophthalmoscope (SLO) that measured retinal motion through the analysis of distortions within successive SLO images. The measured motion was used to correct the OFDI XY-scanners in order to lock the OCT scanning grid onto the same retinal area with a correction bandwidth of just over 30 Hz. At this bandwidth, distortions due to eye drift and gaps/jumps due to microsaccades were prevented in the OCT data. For events in which the tracking lock was lost (e.g. blinks, large saccades, fixation loss) the eye tracker signalled the OFDI instrument to rescan those lost area sections in real-time. This further decreased the amount of artifacts in micro-vasculature images. Additionally, eye tracking enabled the measurement of multiple datasets at the same location from which a compounded dataset with improved image quality was created.

8567-31, Session 6

Low cost active retinal tracker for optical coherence tomography

Yiheng Lim, Utsunomiya Univ. (Japan); Roy de Kinkelder, Univ. van Amsterdam (Netherlands); Barry Cense, Utsunomiya Univ. (Japan)

A retinal tracker for optical coherence tomography was implemented by integrating a line scanning laser ophthalmoscope (SLO) that runs simultaneously with the relatively slow scanning galvanometer mirror of an OCT system. The addition of the line scanning SLO requires integration of a few extra optical components, keeping the system small and low cost. A 785 nm laser diode and a cylindrical lens were used to form a line illumination for tracking. A line scan camera was used to acquire the fundus image of retina. The illumination of the tracker was descanned by the galvanometer raster scanner of the OCT system, so that a fundus image could be obtained simultaneously with each OCT B-scan. Eye motion was then detected after cross-correlating fundus images, and an XY correction signal was sent to the OCT galvanometer scanner. One subject was imaged. Voluntary eye motion of the subject was successfully compensated as OCT scans at the same retinal position were obtained independent from eye motion. The active tracker improves the success rate of acquiring multiple scans to average OCT images for speckle reduction, so that smaller structures are better visible.

8567-32, Session 6

4D dynamic imaging of the eye using ultrahigh speed SS-OCT

Jonathan J. Liu, Ireneusz Grulkowski, Massachusetts Institute of Technology (United States); Benjamin M. Potsaid, Massachusetts Institute of Technology (United States) and Thorlabs Inc. (United States); Vijaysekhar Jayaraman, Praevium Research, Inc. (United States); Alex E. Cable, Thorlabs Inc. (United States); Martin F. Kraus, Massachusetts Institute of Technology (United States) and Univ. Erlangen-Nuremberg (Germany); Joachim Hornegger, Friedrich-Alexander Univ. Erlangen-Nuernberg (Germany); Jay S. Duker M.D., Tufts Univ. (United States); James G. Fujimoto, Massachusetts Institute of Technology (United States)

Recent advances in swept-source / Fourier domain optical coherence tomography (SS-OCT) technology enable in vivo ultrahigh speed imaging, offering a promising technique for four-dimensional (4-D) imaging of the eye. Using an ultrahigh speed tunable vertical cavity surface emitting laser (VCSEL) light source based SS-OCT prototype system, we performed imaging of human eye dynamics in three different imaging modes: 1) Pupillary reaction to light at 200,000 axial scans per second, 9?m resolution, and 5.6mm imaging range in tissue. 2) Anterior eye focusing dynamics at 100,000 axial scans per second, 9?m resolution, and 13.7mm imaging range in tissue. 3) Retinal blood flow at 800,000 axial scans per second, 12?m resolution, and 2.5mm imaging range in tissue. Image processing methods such as image registration can correct motion artifacts and register sequential volumes. The combination of tunable ultrahigh speeds and long coherence length of the VCSEL along with the outstanding roll-off performance of SS-OCT makes this technology an ideal tool for time-resolved volumetric imaging of the eye. Visualization and quantitative analysis of 4-D OCT data can potentially provide insight to functional and structural changes in the eye during disease progression. In sum, ultrahigh speed imaging using SS-OCT promises to enable novel 4-D visualization of real-time dynamics of the human eye. Furthermore, this non-invasive imaging technology is a promising tool for research studies to characterize and understand a variety of visual functions.

8567-33, Session 6

Non-mydriatic confocal retinal imaging using a digital light projector

Matthew S. Muller, Aeon Imaging LLC (United States); Ann E. Elsner, Indiana Univ. (United States)

A 2nd generation confocal non-mydriatic retinal camera, the DLP-Cam, is presented, which uses digital light projector (DLP) technology to achieve advantages in size, cost, robustness, and flexibility over standard retinal

cameras.

The DLP-Cam substitutes a DLP for the traditional illumination and scanning elements in a confocal imaging system. To simulate continuous line scanning, the DLP rapidly projects adjacent lines across the field of view. The backscattered light from each illumination line is not descanned, but rather synchronized to a CMOS sensor's rolling shutter to achieve spatial filtering.

The DLP-Cam uses Texas Instruments' DLP LightCrafter to perform real-time imaging at 27.3 Hz with a retinal field of view of 33 x 25 deg. The retina is illuminated using the DLP's built-in red (640 nm) or green (530 nm) LED channels with a line width of 0.26 deg. An entrance/exit pupil of only 1.6 mm permits non-mydriatic imaging. Red and green image frames are registered, averaged, and overlaid to produce a color fundus photo with a resolution of 1024 x 768 pixels. The DLP-Cam occupies a footprint of 6.5 x 7.6 x 3.1 inches and weighs just 2.3 lbs.

Color retinal images of 8 undilated subjects taken using the DLP-Cam demonstrated good vessel contrast. For an undilated 27 year old male Caucasian subject, the DLP-Cam showed equal or better fine vessel visibility and contrast as compared to the Carl Zeiss GDx Polarimeter, Heidelberg Spectralis SLO, and Topcon TRC NW6S non-mydriatic fundus camera.

8567-34, Session 6

Handheld combined SLO/OCT system design

Francesco LaRocca, Derek Nankivil, Al-Hafeez Dhalla, Ryan P. McNabb, Duke Univ. (United States); Sina Farsiu, Duke Univ. (United States) and Duke Univ. (United States); Joseph A. Izatt, Duke Univ. (United States)

Scanning laser ophthalmoscopy (SLO) and optical coherence tomography (OCT) are widely used retinal imaging modalities that can assist in the diagnosis of retinal pathologies. SLO provides real-time, high contrast en face views of the retina, while OCT provides depth slices at similar rates. Alone, OCT can provide retinal volumes, which can be summed to produce en face views, however patient motion often distorts the volumetric data. The combination of SLO and OCT provides a more comprehensive imaging system and a method to register OCT images to produce motion corrected retinal volumes. While high quality, bench-top SLO/OCT systems have been discussed in the literature and are available commercially, there are currently no handheld designs. We describe the first design and validation of a handheld SLO/OCT system. The optical design was optimized in Zemax to achieve 7.0 µm and 7.5 µm lateral resolutions for the SLO and OCT, respectively, for a common field of view (FOV) of 20°. The mechanical system was created in SolidWorks with a form factor of 10.6" x 4.6" x 7.1". A table-top mock-up of the hand-held deisgn was assembled as a proof of concept. High SNR SLO and OCT images were acquired separately from a normal subject spanning a 13.5° FOV at 16 frames per second (fps). Incident powers on the eye for the SLO and OCT comprised 48% and 51% of the ANSI Z136.1 thermal hazard MPE limit, supporting the potential for simultaneous imaging.

8567-35, Session 7

Compact adaptive optics line scanning retinal imager: recent improvements and pilot clinical study

Mircea Mujat, R. Daniel Ferguson, Nicusor Iftimia, Ankit H. Patel, Physical Sciences Inc. (United States); Neeru Sarin, Laura Clark, Sina Farsiu, Cynthia A. Toth M.D., Duke Univ. (United States); Daniel X Hammer, U.S. Food and Drug Administration (United States)

The performance of clinical confocal SLO and OCT imagers is limited by ocular aberrations. Adaptive optics (AO) addresses this problem, but most research systems are large, complex, and less well suited to the clinical environment. Recent technological advances in this field made it possible to reduce the size of AO systems and integrate them into portable platforms without significantly reducing their performance. PSI's recently developed compact AO-LSO system is designed for rapid, automated generation of cone photoreceptor density maps. The system combines the power of AO correction with PSI's patented line-scanning (LSO) technology. The device has a compact foot-print suitable for clinical deployment. This allows clinicians and researchers to resolve and rapidly map photoreceptors for screening or exploring retinal structures with high resolution dynamically corrected to each subject's eyes. Potential retinal targets include cone photoreceptors, vessels and blood flow, nerve fibers bundles, lamina cribrosa and optic nerve head, drusen, edema, lesions, geographic atrophy, and other features of interest in the normal and diseased eye. The system previously presented at Photonics West has been upgraded to include a spectral-domain OCT channel. The wavelength of the LSO raster has been reduced to 750 nm to enhance system resolution. These upgrades significantly enhance the capabilities of the AO-LSO imager, providing the clinician with simultaneously-acquired (registered) en face photoreceptor images and AO-OCT retinal cross-sections. We present a detailed discussion of these new features and preliminary results from a pilot clinical study performed with this system at Duke University.

8567-36, Session 7

In-the-plane design of an off-axis ophthalmic adaptive optics system using toroidal mirrors

Zhuolin Liu, Omer P. Kocaoglu, Qiang Wang, Ravi S. Jonnal, Donald T. Miller, Indiana Univ. (United States)

Adaptive optics (AO) ophthalmoscopes have garnered increased clinical and scientific use for imaging the microscopic retina. Unlike conventional ophthalmoscopes, however, AO systems are commonly designed with reflective optics (spherical mirrors) that must be used off-axis. This arrangement causes astigmatism to accumulate, degrading image quality at the retina and generating unwanted beam displacement and distortion at pupil conjugate planes. To mitigate these and to tap the full potential of AO, we investigated a novel solution based on toroidal mirrors. We theoretically calculated the necessary tangential and sagittal radii of curvature of each toroidal mirror using Coddington equations in conjunction with ray trace modeling in Zemax optical design software. A minimum of three toroidal mirrors (out of the ten possible in the Indiana AO-OCT system) was predicted necessary to achieve diffraction-limited image quality and negligible beam displacement for 3.6°x3.6° field of view (FOV) of the retina. For the three toroidal mirrors combination, the wavefront RMS range was reduced to just 0.02? to 0.07? across the FOV. Likewise, beam displacement was reduced to below the lenslet pitch of the system's Shack-Hartman wavefront sensor (SHWS), thus enabling the full sensitivity of the SHWS to high spatial frequencies. Based on this theoretical result, custom toroidal mirrors were fabricated and implemented in the Indiana AO-OCT system. Wavefont aberrations measured at the eye pupil plane confirmed diffraction-limited system performance over the 3.6°x3.6° FOV. Maximum beam displacement at the pupil conjugate planes was measured to be less than the SHWS lenslet pitch, consistent with predicted design performance.

8567-37, Session 7

Small animal adaptive optics imaging system

R. Daniel Ferguson, Ankit H. Patel, Mircea Mujat, Nicusor Iftimia, Physical Sciences Inc. (United States); Daniel X. Hammer, Physical Sciences Inc. (United States) and U.S. Food and Drug Administration (United States); James D. Akula, Children's Hospital Boston (United States) and Harvard Medical School (United States)

Rodent models of human eye disease have increased the demand for in vivo animal fundus imaging modalities with cellular resolution. The

small eyes of rodents have the largest NA among mammals. Our present application is multimodal imaging (AOSLO/SDOCT) in albino rodent models of neurovascular disease (such as ROP) in which both inner and outer retinal structure and choroidal structure are potentially significant in disease and development. Special care is required for wavefront sensing to exploit the large NA while isolating selected layers for precision AO correction. Larger primary aberrations and defocused layers in very thick retinas, especially in unpigmented animals, significantly complicate wavefront sensing and correction. A number of novel features have been incorporated into our imaging system.

A high dynamic range hybrid wavefront sensor combining Shack-Hartman and discrete pupil-scanning method was tested. Serially displacing the pupil in discrete steps allows the WS maps to be interpolated at arbitrary density without spot overlap, even for large corrections. The optical design is very compact with four pupil conjugates for scanning/DMs. An SDOCT platform was integrated with the reference arm on a Badal optometer slide which locks the OCT reference and sample arms for up to 60D of sphere correction with no shift of OCT images.

Sprague-Dawley albino rats were imaged. All procedures were approved by the Animal Care and Use Committee at Children's Hospital, Boston, and the PSI IACUC. In conclusion, portable, flexible user-friendly AO platforms with adaptable wavefront sensing will increase their range of application to existing and emerging rodent models of eye disease.

8567-38, Session 7

Adaptive optics optical coherence tomography with dynamic retinal tracking

Omer P. Kocaoglu, Indiana Univ. (United States); R. Daniel Ferguson, Physical Sciences Inc. (United States); Ravi S. Jonnal, Indiana Univ. (United States); Zhuolin Liu, Indiana Univ (United States); Qiang Wang, Indiana Univ. (United States); Daniel X. Hammer, Physical Sciences Inc. (United States); Donald T. Miller, Indiana Univ. (United States)

Adaptive optics optical coherence tomography (AO-OCT) is a highly sensitive and noninvasive method for three dimensional imaging of the microscopic retina. Like all in vivo retinal imaging techniques, however, it suffers the effects of involuntary eye movements that occur even under normal fixation. The resulting image blur and distortion diminish the visibility of retinal structures, especially those at the cellular level. Further improvement can be gained using registration/dewarping algorithms and dynamic retinal tracking with additional hardware. The latter is particularly attractive for AO-OCT as it can compensate for eye motion larger than the imaging field of view and permit repeated imaging of the same retinal patch, both not correctable by post-processing. Considering these advantages, a customized retina tracker module from Physical Sciences Inc. was integrated into the sample arm of 2nd-generation Indiana AO-OCT system and its performance evaluated. Closed-loop tracking performance was assessed by comparing volume videos acquired with and without dynamic retinal tracking. En face projections of the AO-OCT volumes along the A-scan direction allowed assessment of lateral retinal motion. Tracking was found effective at stabilizing the retinal image. The average maximum displacement of the retina was no larger than 18±5um (with tracking) compared to 150±107um (without tracking) for the five video sessions. An additional benefit of tracking was that it repeatedly found the same retinal patch across imaging sessions. These results demonstrate, to the best of our knowledge, the first demonstration of AO-OCT image stabilization with a dynamic retinal tracker.

8567-39, Session 7

Dry age related macula degeneration investigated with a novel lens based adaptive optics ophthalmoscope

Franz Felberer, Julia-Sophie Kroisamer, Ursula Schmidt-Erfurth, Christoph K. Hitzenberger, Michael Pircher, Medizinische Univ. Wien (Austria)

In this study we investigate the applicability of a novel lens based adaptive optics scanning laser ophthalmoscope (AO-SLO) for imaging patients with dry age related macula degeneration (AMD). The high resolution images of the diseased retina are compared with images obtained with state of the art ophthalmological instruments (e.g. SD-OCT, IR fundus imaging).

8567-40, Session 7

The focusing of polychromatic stimuli by the human eye investigated with adaptive optics

Enrique-Josua Fernández, Alejandro Mira-Agudelo, Pablo Artal, Lab de Óptica Univ. de Murcia (Spain)

An open question in Physiological Optics is which wavelength is at focus on the observer retina for a white light object. The human eye presents a significant chromatic aberration, preventing the simultaneous focusing of different wavelengths. Monochromatic aberrations are also present, affecting the quality retinal images. In addition, the distinct efficiency of the three types of photoreceptors defines a particular spectral sensitivity curve. All of these factors were investigated in the current work using adaptive optics and invisible light wavefront sensing, merged in a single instrument. The aberrations of nine human eyes were measured with infrared light at 1050-nm while subjects focused some stimuli emitting at monochromatic wavelengths of 450-nm, 550-nm, 633nm, white light, and using a magenta filter. The accommodation response of the subjects viewing the stimuli was measured in real time for the normal and corrected aberrations. A weighting function was applied for determining which wavelength is focused on the retina. Observers focused the retinal images optimizing those wavelengths closer to the maximum of emission of the stimuli weighted by the eye's spectral sensitivity. Chromatic aberration may help the eye for efficiently selecting the brightest image in white light. The results showed the absence of effect when focusing the stimuli, irrespectively of the illumination, with monochromatic aberration correction. This result differs somehow from previous studies on the relative impact of monochromatic and chromatic aberrations [McLellan et al., 417 Nature (2002)]. Understanding how polychromatic light is distributed on the retina is relevant for both vision and retinal imaging.

8567-41, Session 8

Understanding the early morphological changes in the photoreceptor layer induced by sodium iodate in the rat retina as observed with UHR-OCT

Man Chun Alan Tam, Denise Hileeto, Donghyun Lee, Kostadinka Bizheva, Univ. of Waterloo (Canada)

A high speed, high resolution SD-OCT system was used to observe in-vivo early morphological changes in the rat retina, induced by administration of sodium iodate (NaIO3). Images acquired from the same location in the retina prior and post NaIO3 injection showed changes in the optical reflectivity and layer thickness of the photoreceptor IS and OS. Those changes were assessed with a custom retinal layer segmentation code that allowed for precise quantification of the retinal layer thickness and reflectivity. The formation of a new low reflective layer between the photoreceptor OS and the RPE was observed in all tested animals (20 rats). This new layer appeared as early as 1hour, increased in thickness by hour 6, and disappeared by hour 12 post NaIO3 injection. The low optical reflectivity and the dynamics of this new layer suggest that it is most likely fluid accumulation. Comparison with H&E stained histological sections and IgG immunohistochemistry revealed minimal photoreceptor OS cell swelling at hour 1, detachment of the OS from the RPE by hour 3, and breaking of the blood-retina barrier with significant fluid accumulation by hour 6 post NaIO3 injection. This study has

demonstrated that optical reflectivity and layer thickness changes, as observed non-invasively and in real time with UHR-OCT corresponded to the histologically observed and confirmed cell swelling, rearrangement and detachment of the protoreceptor OS and RPE layers. Therefore, the optical reflectivity and the thickness measurements can serve as markers in future non-invasive, in-vivo studies of disease- or drug- induced outer retinal degeneration.

8567-42, Session 8

In utero monitoring of embryonic eye development with OCT

Narendran Sudheendran, Maleeha Mashiatulla, Saba H. Syed, Univ. of Houston (United States); Irina V. Larina, Mary E. Dickinson, Baylor College of Medicine (United States); Kirill V. Larin, Univ. of Houston (United States)

Mice are an attractive model to study human ocular diseases due to the wide availability of different mutant strains. Previously we have demonstrated that Optical Coherence Tomography (OCT) technique is capable of live imaging of mice embryos in vitro and in utero. In this study, we have used a swept-source OCT (SSOCT) system to obtain 3D images of embryo eyes at different stages of development ranging from E13.5 to E18.5 in utero. The volume of the eye lens and the globe were obtained from 3D OCT images. The results indicate that the volume of the eye lens and the eye globe increases exponentially from 0.05 mm3 to 0.5 mm3 and from 0.1 mm3 to 1.2 mm3 as the embryo ages from E13.5 to E18.5, respectively. Therefore, we have demonstrated that OCT can be useful tool for longitudinal studies of embryonic development in utero.

8567-43, Session 8

Imaging pigment chemistry in melanocytic conjunctival lesions with nonlinear pump-probe microscopy

Jesse W. Wilson, Duke Univ. (United States); Lejla Vajzovic M.D., Duke Univ. School of Medicine (United States); Francisco E. Robles, Duke Univ. (United States); Thomas J. Cummings M.D., Prithvi Mruthyunjaya M.D., Duke Univ. School of Medicine (United States); Warren S. Warren, Duke Univ. (United States)

Conjunctival melanocytic lesions are challenging to diagnose clinically. Conjunctival melanoma is a primary concern, and shares similarities with cutaneous melanoma. The distinction between conjunctival benign nevi, pre-malignant primary acquired melanosis (PAM), and malignant melanoma may be difficult to draw, and becomes more difficult with earlier detection. However, unlike cutaneous melanoma, ocular tissue is limited and pathology specimens are small in size with significant crush and fixation artifact. All these factors lead to tendency to overdiagnose and unnecessary invasive procedures.

Here we extend a femtosecond laser microscopy technique, recently demonstrated to image the microscopic distribution of eumelanin and pheomelanin in unstained cutaneous biopsy sections, to the case of conjunctival melanocytic lesions. The technique operates by directing two optical pulse trains, one at 720 nm, the other at 810 nm, into a laser scanning microscope, and looking for instantaneous and time-delayed nonlinear interactions between the two. We have examined the microscopic distribution of pigmentation chemistry as a functional indicator of cutaneous melanocyte activity, and also as a means to give the pathologist more information in cutaneous pathology.

The conjunctiva provides a bridge into ocular biology, sharing morphologic similarity to skin. In these specimens, we have observed eumelanin, pheomelanin, hemoglobin, and surgical ink. We will discuss prospects for an in vivo ‘optical biopsy’ in anticipation of the ability to provide additional information before having to perform invasive procedures.

8567-44, Session 8

In vivo confocal intrinsic optical signal mapping of localized physiological lesion in laser-injured frog eye

Xincheng Yao, Qiu-Xiang Zhang, Rongwen Lu, The Univ. of Alabama at Birmingham (United States)

The purpose of this study is twofold: 1) to investigate physiological mechanism of stimulus-evoked fast intrinsic optical signal (IOS) recorded in dynamic confocal imaging of the retina, and 2) to demonstrate the feasibility of in vivo confocal-IOS mapping of localized retinal photoreceptor dysfunction. A rapid line-scan confocal ophthalmoscope was constructed to achieve in vivo confocal-IOS imaging of frog (Rana Pipiens) retinas at cellular resolution. In order to investigate physiological mechanism of the confocal-IOS, comparative IOS and electroretinography (ERG) measurements were conducted using normal frog eyes activated by variable intensity stimuli. Dynamic spatiotemporal filtering algorithm was developed to reject the contamination of hemodynamic changes on fast IOS recording. Laser-injured frog eyes were employed to test the potential of confocal-IOS mapping of localized retinal dysfunction. Comparative IOS and ERG experiments revealed a close correlation between the confocal-IOS and retinal ERG, particularly the ERG a-wave which has been widely used to evaluate photoreceptor function. IOS imaging of laser-injured frog eyes indicated that the confocal-IOS can unambiguously detect localized (<30 μm) functional lesion in the retina before detectable morphological abnormality. We anticipate that the confocal-IOS imaging can provide applications in early detection of age-related macular degeneration (AMD), retinitis pigmentosa (RP) and other eye diseases that can cause pathological changes in retinal photoreceptors.

8567-45, Session 8

In vivo three-dimensional characterization of aqueous outflow pathway using optical coherence tomography in human

Peng Li, Gongpu Lan, Tueng Shen, Murray Johnstone, Ruikang K. Wang, Univ. of Washington (United States)

The abnormalities of aqueous outflow system cause the elevation of intraocular pressure (IOP), followed by optic nerve damage and visual field loss. The detection of the aqueous outflow abnormalities may provide information for diagnosing initial and progressive glaucoma. This pilot study aims to explore the feasibility of using anterior segment optical coherence tomography (AS-OCT) to visualize, in parallel, the in vivo aqueous outflow pathway and its surrounding microcirculations in humans. An AS-OCT system was optimized for the 3D imaging of the anterior segment of the human eyes. An optical microangiography (OMAG) method, which is able to effectively separate the optical signals originated by blood flow from those by the static tissue elements, was applied to the OCT dataset to extract the microstructural and microvascular images, in parallel. These images together were used to identify the entire aqueous outflow pathway and to characterize the activity of aqueous outflow. The elemental tissue components of aqueous outflow system, including trabecular meshwork (TM), Schlemm’s canal (SC), collector channels (CCs), the aqueous (AV) and the episcleral (EV) veins, were identified. The associated depth-resolved microcirculation, including the conjunctival (CP), episcleral (EP) and intrascleral (IP) plexus, was mapped without the use of exogenous contrast agents. Particularly, there exists a regional difference (temporal, nasal and inferior quarter) in EP and IP distribution, which may suggests a regional variation of aqueous outflow. The proposed AS-OCT was capable of simultaneously visualizing the normal in vivo aqueous outflow system and its surrounding microcirculation. Further studies would be needed in order to explore the sensitivity of the proposed method to the abnormal aqueous outflow. The future applications can be found in the diagnosis, monitoring and treatment of glaucoma.

8567-46, Session 8

Flicker-induced near-infrared reflectance changes of the human ocular fundus

Nithiyanantham Palanisamy, Univ. degli Studi di Modena e Reggio Emilia (Italy) and Erode Sengunthar Engineering College (India); Luigi Rovati, Univ. degli Studi di Modena e Reggio Emilia (Italy); Charles E. Riva, Univ. de Lausanne (Switzerland); Mauro Cellini, Corrado Gizzi, Ernesto Strobbe, Emilio C. Campos, Univ. degli Studi di Bologna (Italy)

Purpose: An ocular fundus reflectometer was built to measure non-invasively the NIR reflectance changes in response to diffuse flicker stimulation at three visible wavelengths (430, 523 and 572 nm).

Methods:6 normal human subjects were studied. A modified fundus camera was used to image changes in retinal reflectance at 770 nm in response to visual stimulus at 523 nm. Multiscale framework algorithm evaluates the amount of x, y shift and rotation ? for all images with respect to the first image of the sequence and same was applied to each image during registration process to compensate unavoidable eye motions.The characteristics of the flicker-induced hemodynamical response in different regions of the eye was studied

Results: Preliminary results show a significant (average of 6 ± 2.1%) decrease in near-infrared reflectance from the human retina corresponding to astimulus at the wavelength of 523 nm.

Conclusion: This study demonstrates the feasibility of imaging changes in intrinsic optical properties of the human optic disc and peripapillary region in response to increased neural activity by flicker.

Keywords: Ocular fundus reflectometry, Functional imaging, Diffuse luminance flicker, Multiscaleframework, Fundus reflectance

References

1. C.E.Riva, E.Logean, and B.Falsini. Temporal dynamics and magnitude of the blood flow response at the optic disk in normal subjects during functional retinal flicker-stimulation. Neurosci. Lett., 75-78,Vol. 356, 2004.

2.M.Crittin and C.E.Riva. Optic nerve and retinal reflectance changes in response to physiological stimuli. Optics and Laser in Engineering, Vol. 43, 583-589, 2005.

3.M.Crittin and C.E.Riva. Functional imaging of the human papilla and peripapillary region based on flicker-induced reflectance changes. Neurosci. Lett., Vol. 360, 2004.

4.C.E.Riva, E.Logean, and B.Falsini., Visually evoked hemodynamical response and assessment of neurovascular coupling in the optic nerve and retina. Prog. Retin. Eye Res., Vol. 24, 2005

8567-47, Session 8

Functional imaging of hemodynamic stimulus response in the rat retina with ultrahigh-speed spectral / Fourier domain OCT

WooJhon Choi, Massachusetts Institute of Technology (United States); Bernhard Baumann, Medizinische Univ. Wien (United States) and Tufts Univ. (United States); Allen C. Clermont, Edward P. Feener, Joslin Diabetes Ctr. (United States); David A. Boas, Massachusetts General Hospital (United States); James G. Fujimoto, Massachusetts Institute of Technology (United States)

While the role of basal retinal blood flow as a possible early marker for retinal diseases is still under investigation, it is thought that the reduction in functional hyperemia, a rapid transient increase in retinal blood flow in response to flicker stimulus due to neurovascular coupling, may be one of the earliest markers for diabetic retinopathy. In this study, we investigated functional imaging of retinal hemodynamics in response to flicker stimulus in the rat retina using an ultrahigh speed spectral / Fourier domain OCT system at 840nm with an axial scan rate of 244kHz. At 244kHz the nominal axial velocity range that could be measured without phase wrapping was +/-37.7mm/s. Pulsatile total retinal arterial blood flow as a function of time was measured using an en face Doppler approach where a 200µm x 200µm area centered at the central retinal artery was repeatedly raster scanned at a volume acquisition rate of 55Hz. Three-dimensional capillary imaging was performed using speckle decorrelation which has minimal angle dependency compared to other angiography techniques based on OCT phase information. A flicker stimulus could be applied to the retina simultaneously during OCT imaging by inserting a dichroic mirror in the imaging interface. An acute transient increase in total retinal blood flow could be detected. An increase in visible capillary density in speckle decorrelation images could also be observed in some cases, which indicates an increase in the velocity of blood at the capillary level. This method promises to be useful for the investigation of small animal models of ocular diseases.

8567-48, Session 9

Clinical usefulness of Neural Rim Area, recorded with the Heidelberg RetinalTomograph, for glaucoma follow up

Per G. Söderberg, Uppsala Univ. (Sweden)

No Abstract Available

8567-49, Session 9

Comparison of RNFL thickness and RPE-normalized RNFL attenuation coefficient for glaucoma diagnosis

Koenraad A. Vermeer, Josine van der Schoot, Rotterdam Ophthalmic Institute (Netherlands); Hans G. Lemij M.D., Rotterdam Eye Hospital (Netherlands); Johannes F. de Boer, Rotterdam Ophthalmic Institute (Netherlands) and Vrije Univ. Amsterdam (Netherlands)

Recently, a method to determine the retinal nerve fiber layer (RNFL) attenuation coefficient, based on normalization on the retinal pigment epithelium, was introduced. In contrast to conventional RNFL thickness measures, this novel measure represents a scattering property of the RNFL tissue. In this paper, we compare the RNFL thickness and the RNFL attenuation coefficient on 10 normal and 8 glaucomatous eyes by analyzing the correlation coefficient and the receiver operator curves (ROCs). The thickness and attenuation coefficient showed moderate correlation (r=0.82). The full separation between normal and glaucomatous eyes based on the RNFL attenuation coefficient yielded an area under the ROC (AROC) of 1.0. The AROC for the RNFL thickness was 0.9875. No statistically significant difference between the two measures was found. RNFL attenuation coefficients may thus replace or be combined with current RNFL thickness measurements to improve glaucoma diagnosis.

8567-50, Session 9

Direct trabecular meshwork imaging in porcine eyes through multiphoton gonioscopy

Tim C. Lei, Univ. of Colorado Denver (United States); Omid Masihzadeh, Malik Y. Kahook M.D., Univ. of Colorado Denver School of Medicine (United States); Emily Gibson, Univ. of Colorado Denver (United States); David A. Ammar, Univ. of Colorado Denver School of Medicine (United States)

Observing the ocular aqueous outflow system (AOS) is important in understanding the pathophysiology of glaucoma. Our previous attempt

of using multiphoton microscopy (MPM) to image the murine irido-corneal region directly through the sclera was successful but due to optical scattering the image resolution was suboptimal and limited some observations of fine structures in the AOS. In this work, the porcine irido-corneal angle was successfully imaged through the transparent cornea using a gonioscopic lens to avoid the laser beam scattering qualities of scleral tissue. MPM for simultaneous multi-modal imaging by two-photon autofluorescence (2PAF) and second harmonic generation (SHG) was performed. Trans-corneal multiphoton microscopy of the porcine irido-corneal angle resulted in high-resolution images of the trabecular meshwork (TM). Mesh-like structures were observed through mostly SHG signals, indicating collagen based tissue within the TM region. Areas lacking SHG and 2PAF signal were assumed to be fluid-filled pores which range in size from ~10 to 50 μm closer to the juxtacanalicular TM to as large 150 μm near the corneosclaral TM. In general the diameters of these pores have been shown to be narrow at deeper depths within the TM, similar to those seen in electron microscopy of the porcine eye. The use of a gonioscopic lens to obtain SHG and 2PAF signals allowed for label free imaging without disruption of the TM or surrounding tissues. Gonioscopic MPM is a promising non-invasive imaging tool for high-resolution studies of the AOS and research continues to explore the potential for future clinical applications in humans.

8567-51, Session 9

In vivo meibomian gland imaging using Fourier-domain OCT

Tae Joong Eom, Gwangju Institute of Science and Technology (Korea, Republic of); Ho Sik Hwang, Seoul St. Mary's Hospital (Korea, Republic of); Jun Geun Shin, Byeong Ha Lee, Gwangju Institute of Science and Technology (Korea, Republic of); Choun Ki Joo, Seoul St. Mary's Hospital (Korea, Republic of)

We imaged human meibomian glands under the eyelid using real time display Fourier-domain OCT (FD-OCT). The FD-OCT system has a 52-kHz A-scan rate and a headset to image the everted eyelid. The wavelength swept source for the FD-OCT system uses the Fourier-domain mode locking method with 1310nmcenter wavelength. The use of the near infrared wavelength is helpful to image the meibomian glands under the conjunctiva layer. The real time display of the OCT system minimize unwanted motion artifact to reduce imaging time. The data acquisition time is 21 msec, and the processing time of the OCT data (4096 FFT-size ? 500 A-scans with 2 times average) is 16 msec, respectively. We cropped the volume data to remove the image of the palpebral conjunctiva and to highlight the region of the meibomian glands. The 3D volume image of the meibomian glands is reconstructed using 200 OCT tomograms following a developed image processing protocols, and the OCT image is compared with a near infrared (NIR) camera image. The 3D image shows the grape-like patterns of the meibomian glands and is consistent with the pre-measured NIR camera images. The meibomian glands are parallel to each other and the saccular acini are clearly visible. We estimated that the glands lay ~265 μm under the conjunctiva surface, and the glands structure to be about 570 μm thick. The refractive index of the conjunctiva and the gland are considered as 1.36 and 1.45, respectively.

8567-52, Session 9

Dynamic OCT measurements of corneal biomechanical properties after UV cross-linking in the rabbit

Michael D. Twa, Jiasong Li, Ravi K. Manapuram, Floredes M. Menodiado, Manmohan Singh, Univ. of Houston (United States); Salavat Aglyamov, Stanislav Emelianov, The Univ. of Texas at Austin (United States); Kirill V. Larin, Univ. of Houston (United States)

Structural properties of the cornea determine the shape and optical quality of the eye. Keratoconus, a structural degeneration of the cornea, is often treated with UV-induced collagen cross-linking to increase tissue resistance to further deformation and degeneration. Optimal treatments would be customized to the individual and consider pre-existing structural properties as well as the effects induced by treatment and this requires the capability to noninvasively measure tissue properties. The purpose of this study is to use novel methods of optical elastography to study the effects of UV-induced corneal collagen cross-linking in the rabbit eye. Low-amplitude (<1μm) surface waves were generated using focused air-pulse stimulation. Surface wave propagation was measured over a 6x6mm area using Phase Stabilized Swept Source Optical Coherence Elastography (PhS-SSOCE) with a sensitivity of (~ 10 nm). Surface wave amplitude and velocity were computed and compared in tissues before and after UV cross-linking. Wave amplitude was highest near the excitation position and was decreased after cross-linking. Wave velocity was greater in cross-linked tissue than it was in the untreated cornea. Decreased wave amplitude and increased wave velocity after cross-linking is consistent with increased tissue stiffness. This was confirmed by conventional mechanical tension testing (Instron). These results demonstrate that the combination of the PhS-SSOCE and focused air pulse stimulation is capable of measuring low amplitude tissue excitation and quantifying corneal stiffness.

8567-53, Session 10

The legacy of Pascal Rol

Jean-Marie Parel, Bascom Palmer Eye Institute (United States)

No Abstract Available

8567-54, Session PSun

Quantitative comparison of different-shaped wavefront sensors and preliminary results on a mechanical eye

Luis A. V. Carvalho, Univ. de São Paulo (Brazil) and Escola Paulista de Medicina - UNIFESP (Brazil) and Wavetek Technologies, LLC (United States)

Cartesian symmetry wavefront sensors (such as the Hartmann-Shack (HS) sensor) have become a standard in the fields of astronomy and vision science. Nevertheless, for the cylindrical symmetry of the eye we believe there are other sensor symmetries that should be tested. In this work, we have developed and compared three types of wave-aberration sensors, each with a very distinct symmetry/configuration: a dodecagonal (DOD), a cylindrical (CIL) and a conventional HS sensor. Each sensor was mounted on a laboratory optical bench and a commercial mechanical eye and trial lenses were used for tests. 10 different defocus aberrations were generated and compared. Measurement for each aberration was taken using each of the three sensors and a commercial auto-refractor as control. Results for the DOD, HS and CIL sensors were, respectively, as follows: mean of root mean square (RMSE) for all defocus aberrations, when theoretical Zernike coefficients were used as control, was 0.22, 0.66 and 0.26 microns; RMSE of sphere-cylinder values when compared to auto-refractor measurements was 0.18D, 0.22D and 0.35D for sphere, 0.14D, 0.24D and 0.17D for cylinder, 30, 40 and 20 for axis; RMSE of sphere-cylinder values when theoretical values were used as control was 0.11D, 0.29D and 0.46D for sphere, 0.15D, 0.28D and 0.17D for cylinder, 10, 20 and 10 for axis. Our conclusion is that, although all sensors furnished similar results when compared to the auto-refractor, the alignment of the DOD and CIL symmetry sensors to the eye pupil center is much more intuitive.

8567-55, Session PSun

Ocular UV protection: revisiting safe limits for sunglasses standards

Liliane Ventura, Univ. de São Paulo (Brazil); Mauro Masili, UNICEP São Carlos (Brazil); Homero Schiabel, Univ. de São Paulo (Brazil)

The International Commission on Non-Ionizing Radiation Protection – ICNIRP - establishes that safe limits regarding ultraviolet radiation exposure in the spectral region 180nm–400nm, incident upon the unprotected eyes, should not exceed 30 Jm-2 effective spectrally weighted; and the total (unweighted) ultraviolet radiant exposure in the spectral region 315nm–400nm should not exceed 104 Jm-2. However, it should be considered that the spectral range from 180nm–280nm does not reach the surface of the Earth, since it is absorbed by the ozone layer of the atmosphere. The Brazilian Standard for sunglasses protection, NBR15111(2004), as well as the British Standard BSEN1836(2005) and American Standard ANZI Z80.3(2009), requires the UV protection in the spectral range 280nm–380nm, but does not take into account the total (unweighted) UVA radiant exposure. These limits are discussed in this work and calculations have been made for 27 state capitals of Brazil determine parameters for ocular protection of the Brazilian population. These calculations and considerations may be extended to other countries as well. As a conclusion, we show that the upper limit for the UVA protection of 400nm should be considered to be included in the Brazilian standard, as well as the irradiance limits. Furthermore, the parameters for the resistance to irradiance test required on the Brazilian and British standards are also discussed herein as well the significance of this test. We show that the test should be performed by the sun simulator for a longer period than currently required.

8567-56, Session PSun

Prototype for measuring polarization angles of sunglasses according to Brazilian standard NBR15111

Luís E. Lopes, Liliane Ventura, Univ. de São Paulo (Brazil)

The use of polarizing filters in sunglasses has become popular worldwide. The Brazilian standard NBR15111 has specific requirements for its use (position and efficiency) and yet there is not on the market an adequate system for its determination. This paper describes the development of a prototype that measures the angle of polarization of the pair of sunglasses lenses, as well as the angle between them, according to the Brazilian Standard. The prototype consists of a 2000lx CIE D65 standard daylight simulator (metamerism index MIvis B or better for visible light), and two polarizing filters orthogonally assembled , placed in front of a perfect eye match light sensor, which is connected to a 10 bit analog to digital converter. The prototype is able to determine the polarizing efficiency up to 10:1, for the critical situation (less than 8% of light transmittance), and has 0.6° of resolution for positioning measurements, which was verified using a mounted graduated polarizer. The results are in accordance with the standard accuracy requirements of ±5° for filters position and 8:1 filters efficiency.

8567-57, Session PSun

Method for transmittance measurements in sunglasses for a kiosk

Marcio Makiyama Mello, Matheus Figueiredo, Ricardo A. Konda, Liliane Ventura, Univ. de São Paulo (Brazil)

Light transmittance measurements through sunglasses lenses is one of the required tests of the Brazilian Standard NBR15111(2004). Its measurement establishes the category of the sample and determines the required ultraviolet, visible and infrared protection, as well as the attenuation coefficient for signal light recognition. However, these measurements are usually performed by spectrophotometers and educated users, who are acknowledged to manage the equipment, use the weighting functions (WF) and interpret the data. We propose an alternative method, which consists in having matching optics and electronics to obtain a close WF to be used in transmittance measurements, and create an accessible device, for public self-use, providing a simple way for measuring and educating the public about sunglasses protection. The UV test is performed for the 280 – 400nm range, where UVA and UVB light sources and two photodiode sensors with Erythema action response are assembled. As for the visible test, a polynomial regression is obtained using a programmable color sensor, while the infrared test is performed by several LEDs that provide the 780 – 2000nm range, and an infrared sensor. Transmittances were simulated by applying mathematical filters (low, high and band-pass, simulating sunglasses filters) through the proposed WF and compared by using the original WF. The transmittances were within the deviation limit required by NBR15111. The results have led us to build a self service kiosk for public use providing the category, UV protection and IR protection of the sunglasses as well as the information regarding its use for driving.

8567-58, Session PSun

Semi-automatic evaluation of intraocular lenses (IOL) using a mechanical eye model

Andreas Drauschke, Elisabeth Rank, Lukas Traxler, Mathias Forjan, Fachhochschule Technikum Wien (Austria)

As cataracts are the most common reason for loss of vision with an age over 55, the implantation of intraocular lenses (IOL) is one of the most common surgical interventions. The quality measurement and test instructions for IOL are defined in the ISO 11979-2. However, the optical imaging quality of the implanted IOL is not always satisfactory for the patients. Therefore more efforts are put into the individualisation of IOL in order to achieve better imaging properties.

Two examples of typical quality standards for IOL are the modulated transfer function (MTF) and the Strehl ratio which can be measured in vivo or also in mechanical eye models. A mechanical eye model, based on optical properties published by Liou & Brennan, in the scale 1:1 is presented. It has been designed to allow the measurement of the MTF and Strehl ratio and simultaneous evaluation of physiological imaging quality. The eye model allows the automatic analysis of an IOL especially focused on the tolerance for tilting and decentralization. Cornea, iris aperture and IOL type are interchangeable, because all these parts are implemented by the use of separated holders. The IOL is mounted on a shift plate. Both are mounted on a tilt plate. This set-up guarantees an independent decentralization and tilt of the IOL, both moved by electrical drives. This set-up allows a two-dimensional tolerance analysis of decentralization and tilt effects. Different 100´100 point (decentralization´tilt) analyses for various iris apertures, needing only approximately 15 minutes per measurement, are presented.

8567-59, Session PSun

Choroidal imaging with dual-beam Doppler OCT using piezo steering mirror for fast adjustable velocity range

Franck Jaillon, Tomey Corp. (Japan); Shuichi Makita, Yoshiaki Yasuno, Univ. of Tsukuba (Japan)

Dual beam Doppler OCT with one-micrometer probe wavelength, using polarization multiplexing for generating two probing spots on the retina, is a technique that can image retinal and choroidal vasculatures. Its measureable velocity range is altered by the spatial separation between the probing spots. We here present an improvement of this method to dynamically change the measurement velocity range by using a piezo steering mirror in the sample arm. By dynamically changing the velocity range, ocular vessels with a wide range of flow velocities are visualized,

and a more complete representation of vasculature is obtained. Main advantages of this new implementation are shorter experimental time and consequently reduction of spatial displacements occurring between volumes acquired with different beam separations. This finally makes the method more suitable to be applied in clinical conditions. An emmetropic eye was scanned by this system. Three successive volumes are acquired with 3 different beam separations and a total acquisition time of 7 seconds.

8567-60, Session PSun

Longitudinal imaging of the human choroid using 1-micron swept-source optical coherence tomography

Yukari Jo M.D., Osaka Univ. Graduate School of Medicine FOM (Japan); Yasushi Ikuno M.D., Osaka Univ. (Japan); Yoshiaki Yasuno, Univ. of Tsukuba (Japan); Satoshi Sugiyama, Nobuyori Aoki, Naoko Hara, Tsutomu Ohmori, Tomey Corp. (Japan); Kohji Nishida, Osaka Univ. Graduate School of Medicine, FOM (Japan)

Purpose: Various macular diseases, including age-related macular degeneration, originate in the choroid, and the choroidal thickness changes in some pathological conditions. Because the choroid is highly vascularized, the thickness might be affected by the general circulation (i.e., pulsation). We measured the sequential longitudinal choroidal thicknesses over time using optical coherence tomography.

Methods: The choroids of three healthy volunteers (1 man, 2 women; mean age, 27.0 years) were observed using the prototype swept-source optical coherence tomography (center wavelength, 1,050 nm; 100,000 A-scans/second). The B-scans were comprised of 256 A-scans taken sequentially over time at a speed of 10 frames per second; the longitudinal choroidal thicknesses were assessed manually for 10 seconds in the volunteers. The images were divided into 10 sectors and the coefficient of variation was calculated. One hundred identical control images were traced to rule out observer bias.

Results: The mean coefficient of variation in each sector was 2.14% (range, 1.10%-3.32%), 2.17% (range, 1.53%-3.22%), and 1.73% (range, 1.23%-3.61%) in each subject. The values in the control experiment were 1.20% (range, 0.70%-2.14%), 1.53%, (range, 1.17%-1.85%), and 0.84% (range, 0.66%-0.98%), respectively. The control experiment had significantly smaller variations in all subjects ($P<0.01$ for all comparisons).

Conclusions: The choroidal thickness changes at times. Systemic pulsation may be one of the contributing factors.

8567-61, Session PSun

Semi-automatic detection in optical coherence tomography images of hard exudates in diabetic patients

Joel A. Papay, Indiana Univ. (United States); Ann E. Elsner, Indiana Univ. (United States) and Aeon Imaging, LLC (United States); Victor E. Malinovsky, Christopher A. Clark, Bryan P. Haggerty, Andrea V. Walker, Stuart B. Young, Shane G. Brahm, Colleen M. McIntyre, Indiana Univ. (United States); Taras V. Litvin, Glen Y. Ozawa, Jorge A. Cuadros, Tracy Wang, Univ. of California, Berkeley (United States); Matthew S. Muller, Indiana Univ. (United States) and Aeon Imaging, LLC (United States)

Optical Coherence Tomography (OCT) is widely used for management of the most common cause of vision loss of working adults in the US, diabetic macular edema (DME). One commonly used OCT measurement, central macular thickness, takes advantage of the axial resolution of OCT, but pools information laterally over a large retinal region. Developments in OCT technology such as spectral domain OCT (SDOCT) have improved axial quantification, but conventional DME measurements are still insensitive due to variable normative values, gender differences, unrelated increases in retinal tissue thickness, and retinal thinning due to cell death. In this report, we investigate image processing techniques that also include the use of reflectivity and feature information in SDOCT data from patients with DME. Hard exudates, which are the focal build-up of lipids and proteins resulting from vascular leakage, are a key feature in DME and should appear bright. Focal pockets of edema are another key feature, which lead to multiply scattered light and should appear dark. SDOCT b-scans of 74 adult diabetic patients were analyzed for gray scale information, and then used to develop quantification methods for hard exudates and edema in DME. Segmentation of the b-scans removed unwanted bright layers, i.e. the nerve fiber layer and photoreceptor/RPE complex. The hard exudates and focal edema each had consistent and significantly different distributions, $176 + 31.6$ and $16.8 + 9.79$ gray scale units, ($p < 0.0001$). Some eyes with extensive hard exudates had low values of central macular thickness, indicating the need for metrics beyond thickness.

8567-62, Session PSun

Laser welding in penetrating keratoplasty and cataract surgery of pediatric patients: early results

Francesca Rossi, Roberto Pini, Istituto di Fisica Applicata Nello Carrara (Italy); Luca Menabuoni, Alex Malandrini, Annalisa Canovetti, Ivo Lenzetti, Azienda USL 4 (Italy); Paolo Capozzi, Paola Valente, Luca Buzzonetti, Bambino Gesù Children's Hospital (Italy)

Diode laser welding of ocular tissues is a procedure that enables minimally invasive closure of a corneal wound. This procedure is based on a photothermal effect: a water solution of Indocyanine Green (ICG) is inserted in the surgical wound, in order to stain the corneal tissue walls. The stained tissue is then irradiated with a low power infrared diode laser, delivering laser light through a 300-μm core diameter optical fiber. This procedure enables an immediate closure of the wounds: it is thus possible to reduce or to substitute the use of surgical threads. This is of particular interest in children, because the immediate healing closure improves refractive outcome and anti-amblyopic effect; moreover this procedure avoids several general anesthesia for suture management. In this work, we present the first use of diode laser welding procedure in pediatric patients. 5 selected patients underwent cataract surgery (Group 1), while 4 underwent fs-laser-assisted penetrating keratoplasty (Group 2). In Group 1 the conventional surgery procedure was performed, while no stitches were used for the closure of the surgical wounds: these were laser welded and immediately closed. In Group 2 the donor button was sutured upon the recipient by 8 single stitches, instead of 16 single stitches or a running suture. The laser welding procedure was performed in order to join the donor tissue to the recipient bed. Objective observations in the follow up study evidenced a perfect adhesion of the laser welded tissues, no collateral effects and an optimal restoration of the treated tissues.

8567-63, Session PSun

All-femtosecond laser-assisted in situ keratomileusis

Egle Gabryte, Light Conversion Ltd. (Lithuania) and Vilnius Univ. (Lithuania); Danieliene Egle, Private Ophthalmological Practice (Lithuania); Agne Vaiceliunaite, Osvaldas Ruksenas, Mikas Vengris, Vilnius Univ. (Lithuania); Romualdas Danielius, Light Conversion Ltd. (Lithuania)

We present a femtosecond solid-state Yb:KGW laser system capable of performing complete LASIK (laser-assisted in situ keratomileusis) ophthalmic procedure. The fundamental infrared 1030 nm radiation is used to create the corneal flap, and subsequently the corneal stroma

ablation is performed using the ultraviolet pulses of the fifth harmonic (206 nm). During the first stage of the surgery the cornea is immobilized using curved applanation interface and ~100 ?m thickness corneal flap is created by scanning focused laser beam in spiral pattern. The duration of 10 mm diameter corneal flap formation is less than 20 s. Myopic correction of 1 D with femtosecond UV pulses within an optical zone of 5 mm in diameter is performed in 3.7 s at 20 kHz repetition rate and peak fluence of 130 mJ/cm^2. Although these durations meet the typical standards of the LASIK procedures, the speed of both surgery stages in our setup have potential to be increased significantly. In vivo experiments demonstrate that heating of cornea, ablated surface quality, and healing outcomes of the surgeries performed using femtosecond UV laser pulses are better or statistically indistinguishable from the results obtained in experiments using a conventional clinical ArF excimer laser as the UV source. The results of this research indicate the feasibility of clinical application of femtosecond UV lasers for stromal ablation. Ability of switching between laser harmonics allows for fast changeover from infrared to the UV mode implying that a wide range of ophthalmic procedures can be performed using this solid-state laser device.

8567-64, Session PSun

A low coherence interferometry-based eye length optometer

Alexander Meadway, The Univ. of Albama at Birmingham School of Medicine (United States); Christine F. Wildsoet, Yue M. Liu, Univ. of California, Berkeley (United States); Yuhua Zhang, The Univ. of Alabama at Birmingham (United States)

Interest in eye growth regulation has burgeoned with the rise in myopia prevalence world-wide. Eye length and eye shape are fundamental metrics for related research, although current in vivo measurement techniques are generally uni-dimensional, limited to the optical axis of the eye. We describe a high resolution, low coherence, time domain-based interferometry (LCI) system designed to measure eye length over a 200 field of view. The system uses a superluminescent laser diode (SLD) as a source, and includes a custom long-stroke, fast scanning linear motor with built-in precision displacement encoder, which allows a full length eye scan in the reference arm, and thus the entire eye length to be measured in one step, contrasting with the more typical systems that require multiple path lengths in the reference arm. Balanced detection is used to achieve an optimal signal-to-noise ratio. The measurement precision of this instrument is 10 micron, based on tests using a model eye. 3-D reconstructions of the ocular surfaces, including lens and retina, can be created from the collected data. Eye length data collected from a tree shrew, one of the mammalian models for myopia, are presented along with 3-D reconstruction of the ocular surfaces from cornea to retina.

This new system provides more detailed information about eye shape changes, through the measurement of eye length not only along the optical axis but also off-axis.

8567-65, Session PSun

Study of the possibility of diagnostic cataract in the THz range

Anna Ezerskaya, Olga Smolyanskaya, National Research Univ. of Information Technologies, Mechanics and Optics (Russian Federation); Aleksandra Goncharenko, FSBI Academy S.N. Fyodorov (Russian Federation)

It was revealed correlation between the optical density of the lens's nucleus in terahertz range with its density, determined according to the L. Buratti classification. Consolidation of the lens fibers caused by senile cataract, increases the reflectivity of the lens in the THz range. The temporal structure of reflected THz signals allows to determine the spatial distribution of density in the lens.

8567-66, Session PSun

Symbolic algebra approach to the calculation of intraocular lens powers following cataract surgery

David P. Hjelmstad, Arizona State Univ. (United States) and The Eye Ctr. (United States); Samir I. Sayegh M.D., The Eye Center (United States)

We present a symbolic approach based on matrix methods, to allow for the analysis and computation of intraocular lens power (IOL) following cataract surgery. We extend the basic matrix approach corresponding to paraxial optics to include astigmatism and other aberrations. The symbolic approach allows for a refined analysis of the potential sources of errors ("refractive surprises"). We demonstrate the computation of lens powers including toric lenses that correct for both defocus (myopia, hyperopia) and astigmatism. A specific implementation in Mathematica allows an elegant and powerful method for the design and analysis of these intraocular lenses.

We demonstrate the case of IOL design/selection easily establishing the fundamental theoretical formula used in most modern IOL calculations. We show how it can be analyzed to identify the more significant sources of errors and refractive surprises that arise for example following Laser in Situ Keratomileusis (LASIK). We extend the method to astigmatic systems represented by 4x4 matrices treated symbolically and analyze both orthogonal and non-orthogonal systems. We also exploit the methodology to outline the design of alternative intraocular lens systems.

8567-67, Session PSun

Adaptive optics-assisted optical coherence tomography for imaging of patients with age related macular degeneration

Kenta Sudo, Barry Cense, Utsunomiya Univ. (Japan)

Age related macular degeneration (AMD) is one of the leading blinding diseases that affect the maculas of our aging population. Recently, we introduced an imaging method that fills a gap between standard OCT and adaptive optics OCT, which we have called adaptive optics-assisted OCT. Because of the combination of a 10 degrees by 10 degrees isoplanatic patch and high lateral resolution (2.75 times the resolution of a standard OCT system), we think that adaptive optics-assisted OCT is particularly suitable for imaging of AMD pathology, as pathology occurs over a large field of view, but can have features that are small in size. In this paper, we seek to demonstrate the performance of the AOa-OCT system for imaging of AMD. Measurements were obtained in the retina of patients with drusen and AMD. Data was acquired after the wavefront sensor indicated diffraction-limited performance. The measurement time needed for the acquisition of one volume was less than 5s. Data was post-processed in Matlab, ImageJ and 3DSlicer.

8567-68, Session PSun

Volumetric imaging of the intraocular propagation medium using differential OTF wavefront sensing

Johanan L. Codona, The Univ. of Arizona (United States); Nathan Doble, New England College of Optometry (United States)

We first presented Differential OTF (dOTF) at the SPIE Astronomical Telescopes and Instrumentation meeting in Amsterdam, July 2012. (http://leitzel.as.arizona.edu/SPIE/) We validated the revolutionary new method using a diverse set of demonstration experiments, showing that simple optical setups and processing can measure wavefronts to better than 10 nm accuracy---potentially at fast video frame rates. The basic method uses two point source images differing by a small localized

change introduced into the periphery of the pupil. The two images are Fourier-transformed and differenced, giving a complex map of the field back-propagated to the pupil from the point-of-view of the camera. When used with a constellation of point sources, two images including all of the sources can be used to find the pupil field back-propagated along each of the various lines-of-sight, allowing tomographic reconstruction of the transmission and index of refraction within the overlapping propagation volumes. We will report on our efforts to add a dOTF imaging mode to the New England College of Optometry's (NECO) AO Fundus Camera using a diffraction pattern of laser spots on the retina as the constellation. Due to the dynamic nature of the eye in vivo, both the baseline and modified images will be taken simultaneously, although initial static tests will be serial. We will cover the concepts, basic instrument design, constellation and laser flux requirements, simulations and initial experimental results. We will also discuss the potential of this new method for opthalmic study and diagnosis.

8567-69, Session PSun

Cataract screening by minimally trained remote observer with non-mydriatic digital fundus camera

Ann Choi, Univ. of Illinois at Urbana-Champaign (United States) and The Eye Ctr. (United States); David P. Hjelmstad, Arizona State Univ. (United States) and The Eye Ctr. (United States); Jessica N. Taibl, The Eye Center (United States) and Univ. of Illinois at Urbana-Champaign (United States); Samir I. Sayegh, The Eye Center (United States)

Cataracts are the number one cause of blindness and visual disability worldwide. They are typically age related but can be accelerated due to a variety of reasons including trauma, inflammation, diabetes and myopia. Detecting the presence of cataracts can help restore a patient's vision but also hint at a patient's diabetic state or other underlying pathologies. Given the huge backlog of cataracts worldwide, rapid determination of the patients in most need for surgery is an important public health task.

We present a quick and simple method to determine the presence of a cataract that is usable by an observer with minimal training and no previous knowledge of cataract pathology or grading systems. The method is based on the comparison of a photo of the fundus obtained using a standardized setting of a digital non-mydriatic fundus camera, to that of a similar photo of a non cataractous eye. The novel aspect in our methodology is the minimal need for training and the provision of a computerized learning environment where rapid recognition of cataractous states can be learned by an untrained remote observer in less than half day. Right to left, preoperative and postoperative eye and eyes from different patients comparisons are included in the training database as these discrimination tasks are all relevant to the goal of referral and allocating resources.

The method specificity is significantly enhanced by the inclusion of a minimum of historical data.

8567-70, Session PSun

Real-time eye motion compensation in OCT imaging with tracking SLO

Kari V. Vienola, Boy Braaf, Rotterdam Ophthalmic Institute (Netherlands); Christy K. Sheehy, Univ. of California, Berkeley (United States); Qiang Yang, Montana State Univ. (United States); Pavan Tiruveedhula, Univ. of California, Berkeley (United States); David W. Arathorn, Montana State Univ. (United States); Johannes F. de Boer, Rotterdam Ophthalmic Institute (Netherlands) and Vrije Univ. Amsterdam (Netherlands); Austin Roorda, Univ. of California, Berkeley (United States)

Optical coherence tomography (OCT) is an interferometric imaging modality that allows cross-sectional imaging of internal biological structures. Involuntary fixational eye movements (e.g. microsaccades and drift) are a major source of artifacts in OCT images. In this paper, we present a combined system with optical frequency domain imaging (OFDI) instrument (also known as swept-source OCT) with a scanning laser ophthalmoscope based eye tracker to show OCT images with reduced eye motion artifacts. A phase-stabilized OFDI system operating at center wavelength of 1050 nm was used simultaneously with an 850 nm SLO to image the retina. Retinal texture tracking was performed using real-time analysis of the distortions within SLO frames and used to keep the OCT scanning grid locked on the same retinal location throughout the measurement, with an accuracy of 4 μm and correction bandwidth of 32 Hz. In the case of a tracking lock failure (e.g. blink or large saccade), the eye tracker signalled the OFDI system to rescan corrupted B-scans in real-time. With the use of TSLO, we were able to reduce the motion to 0.8 minutes of arc in OCT images and prevent distortions from saccades and jumps in the data. With these features, high quality optic nerve head images with reduced artifacts were obtained along with enface images from the blood vessels that showed negligible artifacts from eye motion.

8567-71, Session PSun

Comparing different imaging modalities for optimal visualization of lamina cribrosa features

Zach Nadler, UPMC Presbyterian (United States); Daniel X. Hammer, U.S. Food and Drug Administration (United States); R. Daniel Ferguson, Physical Sciences Inc. (United States); Larry Kagemann, Hiroshi Ishikawa M.D., Jessica E. Nevins, Gadi Wollstein M.D., Joel S. Schuman M.D., UPMC Presbyterian (United States)

The lamina cribrosa (LC) is a meshwork structure deep within the optic nerve head (ONH) thought to be a primary locale of axonal insult in glaucomatous optic neuropathy, and is the subject of several recent imaging studies, incorporating various technologies. Using a multimodal adaptive optics (AO) retinal imaging system which simultaneously acquires high resolution confocal scanning laser ophthalmoscopy (CSLO) and optical coherence tomography (OCT), images of the ONH of 15 healthy and 30 glaucoma subjects were taken at the University of Pittsburgh Medical Center (UPMC) Eye Center. A subset of eyes was also imaged with a commercially available CSLO system (HRT-III, Heidelberg Engineering, Heidelberg, Germany), and SD-OCT system (Spectralis, Heidelberg Engineering, Heidelberg, Germany). The LC was visualized using the different modalities and examined for microstructure such as laminar pores and beams. The relative advantage of each modality was considered.

8567-72, Session PSun

Device for imaging fundus autofluorescence with lock-in detection technique

Katarzyna Komar, Patrycjusz Stremplewski, Maciej Szkulmowski, Marta Motoczy?ska, Maciej Wojtkowski, Nicolaus Copernicus Univ. (Poland)

Fundus autofluorescence (FAF) plays a significant role among different retinal imaging modalities. However, there is still challenge in improving quality of obtained images, because of number of limitations causing that the FAF signal measured in vivo is weak.

In this contribution we show a new detection metod in retinal autofluorescence imaging, which may help to improve the metod sensitivity. Additionally, the proposed instrument combines functionality of autofluorescence with Fourier domain OCT. Autofluorescence of fundus was excited by fast modulated (up to 500 MHz) diode laser of wavelength 473 nm and detected in spectral range 500-680 nm by

photomultiplier and lock-in amplifier. Average power on the cornea surface during FAF measurements was ~50 ?W.

8567-73, Session PSun

Reflective afocal adaptive optics-optical coherence tomography retinal imaging system

Sang Hyuck Lee, John S. Werner, Robert J. Zawadzki, UC Davis Medical Ctr. (United States)

Over the last decade, development of adaptive optics (AO) retinal imaging instruments have made possible routine imaging of in vivo human retina at the cellular scale. However, the first reports of in-vivo imaging of the small-diameter foveal cones and rod photoreceptors have only recently been published. One of the reasons for achieving improved performance and resolution of AO systems can be attributed to aberration-free design of AO imaging instruments. Here we present progress on developing the next generation adaptive optics system that implements an aberration-free and pupil wander-free design using refractive optics. Similar to our original design, we used a cascade of focal telescopes (created by pairs of spherical mirrors) to produce conjugate planes of the eye pupil with all key optical components, including X and Y scanning mirrors, wavefront correctors and a Hartmann-Shack (H-S) wavefront sensor (which uses the OCT imaging light for wavefront reconstruction). The main difference is that the current design places optical elements out of the single plane in order to minimize system residual aberration. The optical performance of this instrument is compared to our previous multimodal AO-OCT/AO-SLO retinal imaging system using Optical Design Software Code V. The feasibility of new instrumentation for improved visualization of microscopic retinal structures will be discussed and tested. Examples of images acquired with old and new AO-OCT designs will be presented.

8567-74, Session PSun

Human retinal imaging using a conjugate-resolved 1050-nm swept source OCT with enhanced signal-to-noise ratio

Zhijia Yuan, Zhenguo Wang, Charles Reisman, Kinpui Chan, Topcon Medical Systems, Inc. (United States)

We have developed a complex spectral interferogram detection method for resolving the conjugate ambiguity in Fourier domain OCT to achieve full range imaging. Our method employs a phase alternation technique, through which a complex-valued spectral interferogram is encoded by a compact phase modulator placed in the reference arm. Comparing to other full range OCT techniques where the conjugate part is usually removed as artifact, the present method utilizes the entirety of the acquired signal to form the complex spectral interferogram, and thus offers an additional advantage of ~3dB signal intensity enhancement. The present method was implemented in a 100-kHz 1050-nm swept source OCT prototype system. The conjugate suppression ratio was measured to be at least 58dB in the point spread function test and ~40dB (limited by background noise) in human retinal imaging. Along with the low signal roll-off offered by the swept source, the present method enabled an extended imaging range of 5.2 mm in tissue with less than 7dB signal roll-off. Deep range OCT measurements of human eyes were performed, and their results are presented.

8567-75, Session PSun

Three-dimensional high spatial resolution retinal imaging: full field OCT with adaptive optics

Guillaume Chenegros, Observatoire de Paris à Meudon (France) and Observatoire de Meudon (France); Marie Glanc, Marie Blavier, Observatoire de Paris à Meudon (France); Gérard Rousset, Roderick Dembet, LESIA - Observatoire de Paris (France)

Retinal pathologies, like ARMD or glaucoma, need to be early detected, requiring imaging instruments with spatial resolution at a cellular scale. However, in- vivo retinal cells studies and early diagnoses are severely limited by the lack of resolution on eye-fundus images from classical ophthalmologic instruments because of the eye aberrations. Today, 2D high resolution retinal imager with adaptive optics are currently used by physicians. If the 2D resolution in the image field is good (about 2µm), the resolution along the optical axis is given by the eye depth of field (about 75µm) in fundus eye cameras. Each recorded image is the superposition between the retina plane in the focal plane and the other retina planes defocused with respect to this plane. To increase the resolution in the third dimension, we propose a new instrument. It is coupling both adaptive optics technic (to obtain a good resolution in the image plane) and the time domain full-field optical coherence tomography (to increase the resolution along optical axis). The four interferometric images, required to reconstruct the image in the retina depth, are simultaneously acquired, to limit the deleterious effect of eye movements. We will present the setup and features of this instrument, test results obtained with a prototype and the first 3D high resolution images of ex-vivo pig retinas recorded in laboratory.

8567-76, Session PSun

Multimodal imaging in clinical diagnosis and treatment of macular disease

Jessica N. Taibl, Univ. of Illinois at Urbana-Champaign (United States) and The Eye Ctr. (United States); Nancy Ayad, Samir I. Sayegh, The Eye Center (United States)

Accurate diagnosis and treatment of disease is a function of how well the pathology can be imaged. Different imaging modalities are sometimes necessary with each offering a different set of data. Co -registering images from different modalities can offer significant advantages. Combined PET/CT scanning has become an important tool, and PET/MRI, MRI/FT, MRI/SPECT are emerging as viable/useful options. Multi-modal imaging is finding its place in Ophthalmology and we illustrate and analyze its use in macular disease. Macular edema for example can result in accumulation of fluid in and around the macula. Fluorescein Angiography (FA) remains the gold standard to evaluate fluid and leakage while optical coherence tomography (OCT) is establishing a prominent role in its semi-quantitative analysis and layer-by-layer visualization of the retina. While the dynamic aspect of blood flow in the retina is better described by FA, OCT allows for cross-sectioning of the macula and the ability to characterize the presence of fluid and determine its location, distribution and volume. The synergistic use of FA and OCT provides more relevant information than using either modality alone and new technologies have provided the ability to simultaneously capture FA and OCT images, allowing dynamic analysis at the exact point of interest. Through an analysis of clinical data obtained in a busy retina clinic over a period of 6-months, we establish that the combined imaging protocol is easier and faster for both patient and technician, and ultimately and most importantly more capable of guiding the physician to a diagnosis and treatment.

8567-77, Session PSun

Picosecond laser ablation of porcine sclera

Wojciech S. Góra, Heriot-Watt Univ. (United Kingdom); Eleanor M. Harvey, The Univ. of Edinburgh (United Kingdom); Baljean Dhillon, NHS Lothian (United Kingdom); Simon H. Parson, The Univ. of Edinburgh (United Kingdom); Robert R. J. Maier, Duncan P. Hand, Jonathan D. Shephard, Heriot-Watt Univ. (United

Kingdom)

Lasers have been shown to be successful in certain medical procedures and they have been identified as potentially making a major contribution to the development of minimally invasive procedures. However, the uptake is not widespread and there is scope for many other applications where laser devices may offer a significant advantage in comparison to the traditional surgical tools. The purpose of this research is to assess the potential of using a picosecond laser for minimally invasive laser sclerostomy.

Experiments were carried out on porcine scleral samples due to the comparable properties to human tissue. Porcine sclera has similar histology, collagen fibres structure and water content (~70%) consequently porcine scleral samples can be used as a substitute for human samples in early stage research. Samples were prepared with a 5mm diameter trephine and were stored in lactated Ringer's solution. After laser machining samples were fixed in 3% glutaraldehyde, then dried and investigated under SEM.

The laser used in experiments is an industrial picosecond TRUMPF TruMicro laser operating at wavelength of 1030nm, pulse length of 6ps, repetition rate of 1 kHz and a focused spot diameter of 30?m.

The laser beam was scanned across the samples with a use of galvanometer scan head and various ablation patterns were investigated. Processing parameters (pulse energy, spot and line separation) which allow for the most efficient laser ablation of scleral tissue without introducing any collateral damage were investigated. The potential to create various shapes, such as linear incisions, square cavities and circular cavities was demonstrated.

8567-78, Session PSun

Sapphire ball lensed fiber probe for common-path optical coherence tomography in ocular imaging and sensing

Mingtao Zhao, Yong Huang, Jin U. Kang, Johns Hopkins Univ. (United States)

We describe a novel common-path optical coherence tomography (CP-OCT) fiber probe design using a sapphire ball lens for cross-sectional imaging and sensing in ophthalmology. The probe is specifically designed for use in both freehand and robotically assisted microsurgery. A theoretical sensitivity model for CP-OCT was proposed to assess its optimal performance based on an unbalanced photodetector configuration. Two probe designs with working distances (WD) 415?m & 1221?m and lateral resolution 11?m & 18?m, respectively, were implemented with sensitivity up to 88dB. The reference plane of the probe at the distal beam exit interface of the single-mode fiber (SMF) was encased within a 25-gauge hypodermic needle by the sapphire ball lens, facilitating its applications in bloody and harsh environments. The performances of the fiber probe with 11?m of lateral resolution and 19?m of axial resolution were demonstrated by cross-sectional imaging of a cow cornea and retina in vitro with a 1310nm swept source CP-OCT system. To show that the new probe can be highly effectively in our developed smart surgical tool setting, we used a phantom to mimic the inner limiting membrane, which has a high reflectivity to assess its performance. Experimental result shows that the lensed probe could sense the phantom surface over a wide viewing angle and can be used to maintain a stable distance of tool top to target surface up to 3.5mm using a PZT motor and active proportional-integral-derivative (PID) control algorithm. The amplitude of the tremor was reduced from 71.7?m to 12.7?m.

8567-79, Session PSun

High quality optical microangiography of ocular microcirculation and measurement of total retinal blood flow in mouse eye

Zhongwei Zhi, Xin Yin, Suzan Dziennis, Charles Alpers, Ruikang K. Wang, Univ. of Washington (United States)

Visualization and quantification of ocular blood flow especially absolute measurement of retinal blood flow (RBF) is important to the diagnosis and management of different eye diseases, including diabetic retinopathy. As a variation of Spectral-domain OCT, Optical microangiography (OMAG) is developed for generating 3D dynamic microcirculation image and later refined into ultra-high sensitive OMAG (UHS-OMAG) with the capability of imaging true capillary vessels. Here, we present the application of OMAG imaging technique for visualization of depth-resolved vascular network within retina and choroid as well as measurement of total retinal blood flow in mice. A fast speed spectral domain OCT imaging system at 820nm with a line scan rate of 140 kHz was developed to image mouse posterior eye. By applying UHS-OMAG scanning protocol and processing algorithm to extract the blood flow out of the background tissue, we achieved true capillary level imaging of retina and choroid vasculature in mouse eye. The microvascular pattern within different retinal layers and choroid after segmentation was presented. An en face Doppler OCT approach without knowing Doppler angle was adopted for the measurement of total retinal blood flow. The axial blood flow velocity is measured in an en face plane by raster scanning and the flow is calculated by integrating over the vessel area. Total RBF could be measured from both retinal arteries and veins with a high correlation. We applied OMAG to evaluate the microvasculature pattern change and quantify the total retinal blood flow change in early diabetic mice models compared with wild type mice.

8567-80, Session PSun

Contact focusing multimodal probes for potential use in ophthalmic surgery with the Erbium:YAG laser

Arash Darafsheh, Thomas C. Hutchens, S. Adam Burand, Kenneth W. Allen, The Univ. of North Carolina at Charlotte (United States); Amir Fardad, PhotonTech, LLC. (United States); Andrew N. Antoszyk, Uniformed Services Univ. of the Health Sciences (United States); Howard S. Ying, Johns Hopkins Univ. (United States); Nathaniel M. Fried, Vasily N. Astratov, The Univ. of North Carolina at Charlotte (United States)

Recently, we developed a novel contact focusing multimodal probe for ophthalmic surgery based on the mode filtering capability of chains of dielectric microspheres. We showed that for spheres with an index n~1.73, these chains filter lossless radially polarized periodically focused modes which are ultimately suitable for focusing multimodal incident beams. The last focused beam produced at the tip of the end sphere has a diameter on the order of a few wavelengths and can be used for ultra-precise contact surgery. Using a multimode flashlamp pumped Er:YAG laser with 0.1 mJ pulse energies and 75 μs pulse duration the probe was tested with porcine corneal tissue, ex vivo, where it produced ablation craters with average diameters in the 17-44 μm range with 8-26 μm depths.

In this work we study the possibility of the device integration with modern compact diode pumped lasers which can be electronically modulated at high frequencies up to 1000 Hz. The studies are performed with a single-mode, 1.5 W, Er:YAG laser (Sheaumann Laser, Marlborough, MA) with 0.1-1.0 ms pulse duration. By using a virtual imaging technique we show that these beams can be focused to wavelength-scale dimensions. Additional tests with burn paper confirm extremely compact holes sizes of ~15 μm produced in carbon paper. The energy density was found to be slightly below the tissue ablation threshold ~1.6 J?cm2, however

similar studies with 10 times more powerful, 15W, Er:YAG lasers (Pantec Engineering AG, Liechtenstein) are likely to produce a fast cutting portable system for ultra-compact intraocular surgery.

8567-81, Session PSun

Automatic algorithm for measuring visually evoked pupil size changes from OCT images

Chenyi Liu, Beijing Univ. of Posts and Telecommunications (China) and Univ. of Waterloo (Canada); Alireza Akhlagh Moayed, Alexander Wong, Paul Fieguth, Univ. of Waterloo (Canada); Hongxia Bie, Beijing Univ. of Posts and Telecommunications (China); Vivian Choh, Kostadinka Bizheva, Univ. of Waterloo (Canada)

The pupil is an aperture, located in the center of the iris of the eye that regulates the amount of light incident on the retina. Because of the corneal curvature, the pupil appears larger than it is during direct observation. We have designed a new approach to determining the pupil's physical size based on a fast scanning, functional ultrahigh resolution optical coherence tomography system and a novel automated computer algorithm. This approach allows for imaging of the iris and pupil with high spatial (15μm lateral and 3μm axial) and temporal (11μs) resolution, precise measurement of the pupil's physical size and automatic tracking of visually-evoked pupil dynamics. The computerized algorithm tracks the highly reflective edges of the iris in the OCT tomograms by applying a three-step strategy: a) a noise compensation reconstruction for reducing the effect of speckle on the edge tracking accuracy; b) a region-based maximum likelihood tracking; and c) an outlier compensation for calculation of the pupil size. The performance of the algorithm was tested in an animal model, where 2 week old chicken were dark adapted and then visually stimulated with 7ms long red, blue and green light flashes. OCT images of the pupil were acquired before, during, and after the onset of the visual stimulus. Data analyzed with the novel algorithm suggests that the pupil magnitude and rate of constriction and dilation are dependent on the color and intensity of the light flash, as well as the type and duration of the anesthesia.

8567-82, Session PSun

Quantification of phase retardation in corneal tissues using a femtosecond laser

William R. Calhoun III, Alexander Beylin, Richard P. Weiblinger, Ilko Ilev, U.S. Food and Drug Administration (United States)

The use of femtosecond lasers in ophthalmic procedures, such as LASIK, lens replacement (cataract surgery) as well as several other treatments, is growing rapidly. The treatment effect is based on photoablation of ocular tissue by a series of ultra short laser pulses. However, the laser beam characteristics change dynamically due to interactions with the birefringent corneal tissue, which may affect the outcome of the treatment. To better understand the effect the cornea has on the laser characteristics we developed a system for measuring phase retardation and validated it with precise, standard phase retarders. Then we measured the phase retardation of femtosecond lasers through bovine corneas and found that there is a considerable, location dependent, variation in retardation values. This information can potentially help optimize femtosecond laser parameters to make their application in ophthalmic procedures safer and more effective.

8567-83, Session PSun

Combination of optical coherence tomography and reflectometry for ophthalmologic measurements

Hui Lu, Michael R. Wang, Univ. of Miami (United States)

Tear film is very important to support normal eye functions in that it lubricates and protects the eye. Clinical evaluation of tear film provides valuable references for eye disease research and diagnosis of dry eyes. Reflectometry technique and optical coherent tomography are two important tools among the currently available techniques for tear film measurement. The existing reflectometry evaluation of tear film introduced by us can offer high resolution (0.3 μm) measurement of the tear thickness. While optical coherent tomography measurement can cover the whole cornea of the eye and the anterior segment, it suffers from less measurement precision (~ 3 μm). We report herein the combination of the two systems (OCT and optical reflectometry) to achieve simultaneously high resolution tear film thickness evaluation and anterior segment OCT imaging. Position dependent tear film thickness distribution on the cornea as labeled by OCT image can be revealed. The combined device is used to evaluate the artificial tear film on a model eye and analyze the anterior structure and tear film distribution.

8567-84, Session PSun

Study of zonule arrangement in human and non-human primates using fluorescent confocal microscopy

Heather A. Durkee, Ophthalmic Biophysics Ctr., Bascom Palmer Eye Institute (United States) and Univ. of Miami (United States); Steven Bassnett, Yanrong Shi, Washington Univ. School of Medicine in St. Louis (United States); Esdras Arrieta, Sonia Yoo, Bascom Palmer Eye Institute (United States); Jean-Marie Parel, Bascom Palmer Eye Institute (United States) and Univ. of Miami (United States) and Vision Cooperative Research Ctr. (Australia)

We present the experiments to quantify the zonular architecture in vitro using confocal microscopy and indirect immunostaining. Experiments were conducted on baboon, cynomolgus, rhesus, and human eyes. The eyes were dissected to expose the zonular fibers and the specimen was placed in 10% formalin for 48 hours. The zonules were stained by indirect immunostaining using goat-anti-MAGP-1 and donkey-anti-goat AlexaFluor488 and Draq5 nuclear stain. Images were acquired with a Leica TCS SP5 confocal microscope. The protocol produced exquisite images of the detailed three-dimensional anatomy of the zonules.

Preliminary findings show on the posterior side of the lens, at the lens capsule the zonules begin as individual fibers and bundle together as you move towards the ciliary processes. Some of these bundles form a sheet that covers the ciliary processes, but it currently unclear where and how this sheet attaches at the pars plana. Some zonules seem to attach at one point on a ciliary process by extending finger-like projections, but afterwards the zonules cable themselves again and continue toward the pars plana in parallel.

The long term goal of this study is to characterize the arrangement of the zonular fibers and its changes with age in human and non-human primates. The information will be used to enhance mechanical models of accommodation and to investigate the role of the zonular architecture in presbyopia.

8567-85, Session PSun

Ultrahigh precision diamond machining of contact lenses from advanced polymers

Khaled Abou-El-Hossein, Oluwole Olufayo, Nelson Mandela Metropolitan Univ. (South Africa); Vanessa Moodley, Univ. of KwaZulu-Natal (South Africa); Tony Bunn, South African Medical Research Council (South Africa); Johannes H. Neethling, Nelson Mandela Metropolitan Univ. (South Africa)

Advanced contact and intraocular lenses (CLs and IOLs) are made from hi-tech polymers that possess special properties. High quality ophthalmic lenses are shaped by cutting using the process of ultra-high precision machining (UHPM) based on turning operation using a diamond tool. This paper reports on the performance of UHPM in the production of CLs and IOLs from advanced materials such as hydrophilic polymers. UHPM process performance is measured in terms of form accuracy and machined surface integrity of the machined ophthalmic lenses and in terms of diamond tool wear. The study investigates the effect of varying the machining parameters of diamond turning such as depth of cut, feed rate and cutting speed on the mechanisms of tool wear. Few different grades of hydrophilic polymers are machined using single-point mono-crystalline diamond inserts having positive rake angle and relatively large clearance. The initial results show that for certain combinations of diamond machining parameters tool wear can be intensive and this can lead to noticeable deterioration of the machined polymers surfaces.

8567-86, Session PSun

Adaptive optics for reduced threshold energy in femtosecond laser induced optical vreakdown in water based eye model

Anja Hansen, Tammo Ripken, Alexander Krueger, Laser Zentrum Hannover e.V. (Germany)

In ophthalmic microsurgery tissue dissection is achieved using femtosecond laser pulses to create an optical breakdown. For vitreo-retinal applications the irradiance distribution in the focal volume is distorted by the anterior components of the eye causing a raised threshold energy for breakdown. In this work, an adaptive optics system enables spatial beam shaping for compensation of aberrations and investigation of wave front influence on optical breakdown. An eye model was designed to allow for aberration correction as well as detection of optical breakdown. The eye model consists of a plano-convex lens for modeling the eye's refractive power, a water chamber for modeling the tissue properties, and a PTFE sample for modeling the retina's scattering properties. Aberration correction was performed using a deformable mirror in combination with a Hartmann-Shack-sensor. The influence of an adaptive optics aberration correction on the pulse energy required for photodisruption was investigated using transmission measurements for determination of the breakdown threshold and video imaging of the focal region for study of the gas bubble dynamics. The threshold energy is considerably reduced when correcting for the aberrations of the system and the model eye. Also, a raise in irradiance at constant pulse energy was shown for the aberration corrected case. The reduced pulse energy lowers the potential risk of collateral damage which is especially important for retinal safety. This offers new possibilities for vitreo-retinal surgery using femtosecond laser pulses.

Conference 8568: Optical Methods for Tumor Treatment and Detection: Mechanisms and Techniques in Photodynamic Therapy XXII

Saturday - Monday 2 –4 February 2013 • Part of Proceedings of SPIE Vol. 8568 Optical Methods for Tumor Treatment and Detection: Mechanisms and Techniques in Photodynamic Therapy XXII

8568-1, Session 1

Determinants of reactive oxygen species formation during PDT *(Invited Paper)*

David H. Kessel, Michael Price, Wayne State Univ. (United States)

Two photosensitizing agents are known to localize in lysosomes, but form different ROS upon irradiation. The chlorin NPe6 produces a high yield of singlet oxygen while the Pd-bacteriopheophorbide produces only oxygen radicals in an aqueous environment. Clonogenic studies in 1% vs. 20% oxygen revealed that photokilling by NPe6 was relatively independent of the level of oxygenation. In contrast, photokilling by WST11 was reduced in an atmosphere containing 1% oxygen. Photobleaching studies and information obtained with fluorescent probes, in a cell-free system, revealed that formation of oxygen radicals by NPe6 or WST11 was correlated with the level of oxygenation. In contrast, both rate of photobleaching and singlet oxygen formation using NPe6 were unaffected by reducing the oxygen concentration. This information provides a rationale for the clonogenic data. Possible implications for PDT protocol design will be discussed.

8568-2, Session 1

Determinants of treatment resistance in 3D cellular models of cancer

Tayyaba Hasan, Massachusetts General Hospital (United States)

Photodynamic Therapy (PDT) appears to be synergistic or additive with several conventional therapeutic modalities for cancer. Disease models that have reasonable fidelity to the pathology being studied and are also amenable to efficient evaluation of combination treatments would therefore be very valuable in defining a role for PDT in the treatment of cancer. We propose that 3D in vitro models where both the cellular and extracellular matrix components may be tuned to match the disease of interest may present such an option. In early studies a comparison of 2D and 3D models of ovarian and pancreatic cancer cells demonstrates that the 3D models are more resistant to treatments including PDT and a variety of chemotherapy agents. This presentation will attempt to gain some understanding of what factors might be influencing this lack of response in 3D model and perhaps provide insights into the lack of concordance between conventional 2D cell culture and in vivo treatment response.

8568-3, Session 1

High-content image-based screening platforms for the optimization of PDT against select tumor populations

Oliver J. Klein, Yookyung Jung, Brijesh Bhayana, Conor L. Evans, Wellman Ctr. for Photomedicine (United States)

A major barrier to the effective treatment of cancer is heterogeneity, both between individual lesions, and within tumors itself. In ovarian cancer, for example, the selective pressures caused by different tumor implantation sites can lead to the formation of distinct genotypes and phenotypes within an individual patient. Tumors themselves are also often heterogeneous, containing a range of cellular populations and microenvironmental conditions. For example, even within metastatic tumor nodules, oxygen concentrations can range from normoxic to below 1%, with the extracellular pH ranging from neutral to as low as 5.5. This tumor heterogeneity can cause significant subpopulations of cells to go untreated, opening the door for recurrence and the rise of treatment resistance.

We are working to develop combination photodynamic therapy regimens to address heterogenous conditions through the use of high-content, high-throughput multimodal 3D in vitro tumor screening systems. In recent studies, we screened a small library of cationic EtNBS derivatives across tens of thousands of heterogenous ovarian cancer tumor nodules. Using a combination of wide-field and confocal microscopy, we identified an optimized treatment regimen for hypoxic tumor cells. Recent work has focused on developing new screening capabilities based on time-lapse optical coherence tomography, with morphometric analysis routines allowing for comprehensive volumetric identification of apoptosis and tumor nodule viabilities. Current therapeutic studies are focused on developing photodynamic therapy regimens capable of selectively targeting and eliminating normally resistant populations, including cells in poorly perfused and acidic environments.

8568-4, Session 2

A theoretical comparison of macroscopic and microscopic modeling of singlet oxygen during HPPH mediated-PDT

Baochang Liu, Univ. of Pennsylvania (United States); Michele M. Kim, Univ. of Pennsylvania School of Medicine (United States); Xing Liang, Timothy C. Zhu, The Univ. of Pennsylvania Health System (United States)

Mathematic models were developed to simulate the complex dynamic process of photodynamic therapy (PDT). Macroscopic or microscopic modeling of singlet oxygen (1O2) is particularly of interest because it is the major cytotoxic agent causing biological effects during PDT. Our previously introduced macroscopic PDT model incorporates the diffusion equation for the light propagation in tissue and the macroscopic kinetic equations for the production of the 1O2. The distance-dependent distribution of reacted 1O2 can be numerically calculated using finite-element method (FEM). We recently improved the model to include microscopic kinetic equations of oxygen diffusion from uniformly distributed blood vessels and within tissue. In the model, the cylindrical blood capillary has radius in the range of 4-10 μm and a mean length of 0.22mm, which supplies oxygen into tissue. Blood vessel network is assumed to form a 2-D square grid perpendicular to a linear light source. The spacing of the grid is 0.05 mm. Oxygen can also diffuse along the radius and the axial of the cylinder within tissue. The generation of 1O2 during HPPH-PDT can be simulated using both macroscopic and microscopic approaches. The comparison of the simulation results will be shown in this study. The simulation results will also be compared with experimental results from mouse studies.

8568-5, Session 2

Photonic cancer therapy: modulating cellular metabolism with light

Isabel Coutinho, Thiagarajan Viruthachalam, Gnana P. Gajula, International Iberian Nanotechnology Lab. (Portugal); Steffen B. Petersen, Maria Teresa Neves-Petersen, International Iberian Nanotechnology Lab. (Portugal) and Aalborg Univ. (Denmark)

The epidermal growth factor receptor (EGFR) belongs to the ErbB family of receptor tyrosine kinases. EGFR activation by binding of ligands (such as EGF and TGF) results in cell signaling cascades that promote cell proliferation, survival and inhibits apoptosis. As reported for many solid tumors, EGFR overexpression or overactivation is associated with tumor development and progression, resistance to various cancer treatment

approaches and poor prognosis. Therefore, inhibition of EGFR function is a rational cancer treatment approach. Our earlier studies demonstrated that UV illumination on aromatic residues nearby the disulphide bridges leads to the disulphide disruption. Since the human EGFR is rich in disulphide bridges and aromatic residues, structural changes can be induced upon UV excitation that may allow to regulate the ligand binding nature of EGFR and consequently over the tumor growth process. Here, we report the structural changes induced by UV light on the extracellular domain of EGFR. Steady state and time resolved fluorescence spectroscopy, circular dichroism, infrared spectroscopy and binding assays are being done. Our goal is to gain insight at the protein structure level that explains the way the new photonic cancer therapy works. This technology can be applicable to the treatment of various forms of cancer, and can be used in combination to the classical photodynamic therapy and other cancer therapies to improve treatment outcome.

8568-6, Session 2

Mechanism of enhanced responses after combination photodynamic therapy (cPDT) in carcinoma cells involves C/EBP-mediated transcriptional upregulation of the coproporphyrinogen oxidase (CPO) gene

Sanjay Anand, Cleveland Clinic Lerner Research Institute (United States); Tayyaba Hasan, Wellman Ctr. for Photomedicine (United States); Edward V. Maytin M.D., The Cleveland Clinic (United States)

Photodynamic therapy (PDT) with aminolevulinate (ALA) is widely accepted as an effective treatment for superficial carcinomas and pre-cancers. However, PDT is still suboptimal for deeper tumors, mainly due to inadequate ALA penetration and subsequent conversion to PpIX. We are interested in improving the effectiveness of photodynamic therapy (PDT) for deep tumors, using a combination approach (cPDT) in which target protoporphyrin (PpIX) levels are significantly enhanced by differentiation caused by giving Vitamin D or methotrexate (MTX) for 3 days prior to ALA-PDT. In LNCaP and MEL cells, a strong correlation between inducible differentiation and expression of C/EBP transcription factors, as well as between differentiation and mRNA levels of CPO (a key heme-synthetic enzyme), indicates the possibility of CPO transcriptional regulation by the C/EBPs. Sequence analysis of the first 1300 base pairs of the murine CPO upstream region revealed 15 consensus C/EBP binding sites. Electrophoretic Mobility Shift Assays (EMSA) proved that these sites form specific complexes that have strong, moderate or weak affinities for C/EBPs. However, in the context of the full-length CPO promoter, inactivation of any type of site (strong or weak) reduced CPO promoter activity (luciferase assay) to nearly the same extent, suggesting cooperative interactions. A comparative analysis of murine and human CPO promoters revealed possible protein-protein interactions between C/EBPs and several neighboring transcription factors such as NFkB, Sp1, AP-1, CBP/p300 and CREB (an enhanceosome complex). Overall, these results confirm that C/EBP's are important for CPO expression via complex mechanisms which upregulate PpIX and enhance the outcome of cPDT.

8568-7, Session 2

Addition of erlotinib to photodynamic therapy improves therapeutic benefit through multiple mechanisms

Shannon Gallagher-Colombo, Cory T. Rice, Joann Miller, Shirron L. Carter, Theresa M. Busch, Univ. of Pennsylvania (United States)

Overexpression of the epidermal growth factor receptor (EGFR) is a common characteristic of many aggressive cancers. While EGFR is currently a favorite molecular target for treatment of these cancers, inhibition of the receptor with small molecule inhibitors (e.g., erlotinib) or monoclonal antibodies (e.g., cetuximab) does not provide long-term therapeutic benefit as stand-alone treatment. In a combined modality setting, we have found that the addition of erlotinib to photodynamic therapy (PDT) with the photosensitizer verteporfin can improve long-term tumor responses in xenografts of non-small cell lung carcinoma (H460) and head and neck squamous cell carcinoma (SQ20B). This enhanced therapeutic benefit was mediated through multiple mechanisms that included increases in vascular damage, as well as direct effects on tumor cells. Furthermore, the balance between these mechanisms of erlotinib effect differed between H460 tumors, in which PDT led to activation of EGFR, and SQ20B tumors, in which PDT itself did not change EGFR activation although the addition of erlotinib did decrease its expression. Taken together, these data suggest that PDT-induced increases in EGFR activation are not required for the enhanced therapeutic benefit achieved with combination therapy. Continuing studies in other histologies treatable with PDT, yet with reported resistance to erlotinib, are being used to evaluate how the molecular interaction between PDT and erlotinib plays a role in the success of combination therapy.

8568-8, Session 2

Spatial measurement of subsurface PpIX fluorescence in vivo with ultrasound-guided tomographic spectroscopy

Brendan P. Flynn, Alisha V. D'Souza, Stephen C. Kanick, Brian W. Pogue, Thayer School of Engineering at Dartmouth (United States)

Aminolevulinic acid (ALA)-induced Protoporphyrin IX (PpIX)-based photodynamic therapy (PDT) is an effective treatment for skin cancers including basal cell carcinoma (BCC). Topically applied ALA promotes PpIX production preferentially in tumors, and many strategies have been developed to increase PpIX contrast in tumors, especially in deeper tumors. Deep tumors respond poorly to PDT treatment, and the relationship between PpIX distribution and PDT treatment efficacy at depths > 1-2mm is not fully understood. While surface imaging techniques provide useful diagnosis, dosimetry, and efficacy information for superficial tumors, these methods cannot interrogate deeper tumors. We have developed an ultrasound-guided, white-light-informed, fluorescence tomography system for the regional quantification of PpIX at depths up to 5mm. System details, including specifications, methodology, and concentration and depth sensitivities will be presented separately.

To better understand the decline in PDT treatment efficacy at increasing tumor depth, we will investigate the ALA-induced spatial production of PpIX within subcutaneous A431 (human skin carcinoma) tumors in athymic nude mice. We will also measure relative tumor stiffness using ultrasound elastography and the vascular density and collagen content using histology. In addition, the white light imaging system will provide bulk measurements of water content and oxygen saturation in the tumors and surrounding tissue. Preliminary studies show an informative but complex relationship between the measured parameter set and the dynamics of drug delivery, and we expect analysis of the full dataset to be instructional for future directions of PDT treatment.

8568-9, Session 3

Development a point measurement dosimeter to quantitatively monitor protoporphryin IX fluorescence in skin during photodynamic therapy

Stephen C. Kanick, Scott C. Davis, Martin E. Isabelle, Dartmouth College (United States); Edward V. Maytin M.D., The Cleveland Clinic (United States); Tayyaba Hasan, Massachusetts General

Hospital (United States); Brian W. Pogue, Dartmouth College (United States)

Quantitative interpretation of fluorescence emission spectra measured in tissue is complicated by the distortive influence of background tissue optical properties. Classically, studies have used information about the optical properties of the tissue gained from white light reflectance spectra to inform the correction of raw fluorescence. This approach is complicated in skin, as the absorption coefficient of melanin located in the epidermal layer shows a wavelength-dependent profile that is similar to the inverse of the background scattering spectrum, making these influences difficult to decouple. Additionally, the layered structure of skin tissue leads to wavelength-dependent depth sampling in the UV-VIS wavelength range, which complicates estimation of vascular physiological parameters sampled from the underlying dermal layer. Moreover, localized point-sampling is achieved by using a probe with small source and collection fibers (e.g. 0.2 mm in diameter) placed adjacent to one another; this sampling geometry will sample reflectance and fluorescence that may have different sensitivities to not only the reduced scattering coefficient, but also the scattering phase function spectrum. This study will utilize both simulations and experiments to develop a correction algorithm that returns estimates of quantitative fluorescence independent of theses listed effects for a fiber optic point-measurement probe. This algorithm will be utilized to interpret preliminary clinical data obtained from photodynamic therapy treatments of actinic keratosis using aminolevulinic acid induced protoporphryin IX excited at either 405 nm or 635 nm.

8568-10, Session 3

Photodynamic therapy light dose modeling using arterial and venous contrast CT information

Michael Jermyn, Scott C. Davis, Brian W. Pogue, Thayer School of Engineering at Dartmouth (United States); Matthew T. Huggett, Stephen P. Pereira, Univ. College London (United Kingdom); Tayyaba Hasan, Wellman Ctr. for Photomedicine (United States)

Using light modeling techniques, the light dose in the zone of necrosis produced by photodynamic therapy can be estimated. As a part of the VERTPAC-1 trials, CT scans are obtained of the pancreas and surrounding tissue of the patient before and after treatment, as well as during needle placement. The arterial and venous information from these scans is used to estimate blood content, and provide structural information of the pancreas and nearby blood vessels. After segmenting the blood vessels, light simulations are run to create maps of light fluence within the pancreas. These maps are then used to visualize light dose overlaid on the original CT scans. Using post-treatment scans, the light dose can be estimated at the boundary of the necrotic zone. Trials are being performed on multiple patients, and the aim of these light simulation studies is to assist pre-treatment planning by providing information about light dose threshold and structural information for needle placement. Currently, both the arterial and venous information from contrast CT are incorporated into the blood content estimation procedure, allowing for more accurate values of absorption. This is done by calculating the difference images for both phases (in implementation an ROI operation due to the high deformation between scans). The grayscale values in the blood vessels of these difference images are considered to be full blood content for the corresponding phase. The grayscale values in the pancreas tissue are then scaled based on the blood vessel values to produce a map of blood content. Using assumed values of oxygen saturation for arterial and venous, the blood content map is transformed into a map of absorption values. This absorption map is then used in labeling the optical properties for light modeling.

8568-11, Session 3

Theoretical and experimental examination of fluorescence generated during PDT treatment of enclosed cavities

Kara Lambson, Xing Liang, Timothy C. Zhu, Jarod C. Finlay, The Univ. of Pennsylvania Health System (United States)

Photosensitizer fluorescence emitted during photodynamic therapy (PDT) is of interest for monitoring the local concentration of the photosensitizer and its photobleaching. In this study, we use Monte Carlo (MC) simulations to evaluate the relationship between treatment light and fluorescence, both collected by an isotropic detector placed on the surface of the tissue. In treatment of the thoracic and peritoneal cavities, the light source position changes continually. The MC program is designed to simulate an infinitely broad photon beam incident on the tissue at various angles to determine the effect of angle. For each of the absorbed photons, a fixed number of fluorescence photons are generated and traced. The theoretical results from the MC simulation show that the angle theta has little effect on both the measured fluorescence and the ratio of fluorescence to diffuse reflectance. However, changes in the absorption and scattering coefficients, ?a and ?s', do cause the fluorescence and ratio to change, indicating that a correction for optical properties will be needed for absolute fluorescence quantification. Experiments in tissue-simulating phantoms confirm that an empirical correction can accurately recover the sensitizer concentration over a physiologically relevant range of optical properties.

8568-12, Session 3

Imaging of absolute PpIX concentration during PDT

Ulas Sunar, Andrew Kowalczewski, Daniel J. Rohrbach, Janet Morgan, Natalie Zeitouni, Barbara W. Henderson, Roswell Park Cancer Institute (United States)

Photodynamic Therapy has proven to be an effective treatment option for nonmelanoma skin cancers. The ability to quantify the concentration of drug in the treated area is crucial for effective treatment planning as well as predicting outcomes. We utilized spatial frequency domain imaging for quantifying the accurate concentration of protoporphyrin IX (PpIX) in phantoms and in vivo. First we quantified the absorption and scattering of the tissue non-invasively. Then, we corrected raw fluorescence signal by compensating for optical properties to get the absolute drug concentration. After phantom experiments, we used basal cell carcinoma model in Gli mice to determine optical properties and drug concentration in vivo before and after PDT.

8568-13, Session 3

Binding of new cationic porphyrins to plasma proteins: study by spectral and molecular docking analysis methods

Aram G. Gyulkhandanyan, Lusine Z. Gyulkhandanyan, Institute of Biochemistry (Armenia); Robert K. Ghazaryan, Yerevan State Medical Univ. (Armenia); Vehary A. Sakanyan, Univ. de Nantes (France) and ProtNeteomix Co. Ltd. (France); Grigor V. Gyulkhandanyan, Institute of Biochemistry (Armenia)

Porphyrins have a unique aromatic structure determining particular photochemical properties that make them promising photosensitizers for anticancer therapy. Previously, we synthesized a set of artificial porphyrins by modifying side-chain functional groups and introducing different metals into the core structure. Here, we have performed a comparative study of the binding properties of 29 cationic porphyrins

with plasma proteins by using microarray, spectroscopic approaches as well as molecular docking analysis method. The porphyrins were non-covalently immobilized onto hydrogel-covered glass slides and probed to bio-conjugated human and bovine serum albumins, as well as to human hemoglobin. The signal detection was carried out at the near-infrared fluorescence wavelength (800 nm) that enabled the effect of intrinsic visible wavelength fluorescence emitted by the porphyrins tested to be discarded. Competition assays on porphyrin microarrays indicated that long-chain fatty acids (palmitic and stearic acids) decrease porphyrin binding to both serum albumin and hemoglobin. The binding affinity of different types of cationic porphyrins for plasma proteins was quantitatively assessed in the absence and presence of fatty acids by fluorescent and absorption spectroscopy. Molecular docking analysis confirmed results that new porphyrins and long-chain fatty acids compete for the common binding site FA1 in human serum albumin and meso-substituted functional groups in porphyrins play major role in the modulation of conformational rearrangements of the protein.

8568-14, Session 3

Modelling hypersensitivity of cancer cells to infra-red laser irradiation: breaking ROS defence machinery

Sergei G. Sokolovski, Univ. of Dundee (United Kingdom); Alexey Goltsov, Univ. of Abertay Dundee (United Kingdom); Edik U. Rafailov, Univ. of Dundee (United Kingdom)

Quantum-dot (QD) laser diodes (LDs) emitting in infra-red spectrum range (around 1265 nm) was reported (Sokolovski SG et al., SPIE Proceedings, 2012) to induce the oxidative stress predominantly in cancer cells through direct triplet ? single oxygen transition designating a novel direction in cancer phototherapy equally with photodynamic therapy. For further development of this approach towards increasing the efficacy of killing cancer cells by 1265nm irradiation we used in vitro and in silico approaches to study in detail the response of normal and cancer cells to QD LD irradiation beneath thermal threshold.

Experimental and modelling results revealed that main impact to cellular oxidative state makes the delayed cascade of secondary reactive oxygen species (ROS) production from laser-pulse-induced primary singlet oxygen pool and secondly laser pulse irradiation (3 min, <90 J/cm2) effecting both normal and cancer cells causes most dramatic ROS generation and depletion of thioredoxin/glutathione antioxidant defence system in cancer cells as compared with normal cells. Based on this features of cell response to QD LD impulse irradiation we proposed the following strategy of laser impulse action to kill cancer cells where the first impulse destroys cellular antioxidant systems and makes the cancer cells more vulnerable to the next cascade of ROS generation by following impulses. Optimization of the intensity and periodicity of laser pulses targets to reach maximal selectivity managing of oxidative stress in normal and cancer cells and trigger ROS mediated cancer cell death through apoptotic way at non-thermal irradiation doses.

8568-15, Session 4

Photodynamic therapy for the treatment of retinoblastoma: revisiting an old concept with new ideas *(Invited Paper)*

Charles J. Gomer, Children's Hospital Los Angeles (United States) and Univ. of Southern California (United States)

Retinoblastoma (Rb) is the most common intraocular malignancy in childhood, affects 1 in 15,000 children, and accounts for 12% of infant cancers. Tumors occur as sporadic (unilateral) lesions or hereditary (bilateral) lesions. Therapy decisions depend on the size and location of the lesion(s) at the time of diagnosis and treatment options include enucleation for unsalvageable lesions and various localized procedures including external beam radiation therapy, scleral plaque radiation brachytherapy, combination chemotherapy including carboplatin, topotecan, focal laser therapy, and cryotherapy. Current procedures focus on maintaining useful vision, increasing cytotoxic tumor responses, and reducing side effects. Unfortunately tumor recurrences are still observed following treatment and the potential late effects of chemotherapy remain an issue. Anatomical and optical properties of Rb lesions suggest that Photodynamic Therapy (PDT) would be an ideal procedure to treat this localized malignancy. However, a previous clinical study using Photofrin mediated PDT to treat Rb resulted in a high rate of tumor recurrence. We hypothesize that Rb responsiveness to PDT is correlated with expression of prosurvival molecules within the treated lesions. We further hypothesize that targeted inhibition of prosurvival molecules will enhance PDT effectiveness by selectively increasing apoptosis in malignant Rb cells. We will present results on PDT activation of prosurvival molecules in Rb cells and on Rb tumoricidal responses when PDT is combined with agents targeting the expression and function of prosurvival molecules.

8568-16, Session 4

KillerRed as a potential genetically encoded photosensitizer for PDT of cancer

Elena V. Zagaynova M.D., Marina V. Shirmanova, Nizhny Novgorod State Medical Academy (Russian Federation); Ekaterina O. Serebrovskay, Konstantin A. Lukyanov, Shemyakin-Ovchinnikov Institute of Bioorganic Chemistry of the Russian Academy of Sciences (Russian Federation); Ludmila B. Snopova M.D., Ekatarina A. Minakova, Nizhny Novgorod State Medical Academy (Russian Federation); Ilya V. Turchin, Vladislav A. Kamensky, Institute of Applied Physics (Russian Federation); Sergey A. Lukyanov, Shemyakin-Ovchinnikov Institute of Bioorganic Chemistry of the Russian Academy of Sciences (Russian Federation)

Promising application of the protein KillerRed is a precise light-induced killing of the target cell populations. The phototoxicity of KillerRed has been found to depend greatly on its intracellular localization.

HeLa Kyoto cell line stably expressing KillerRed in mitochondria and in fusion with histone H2B were obtained by lentiviral transduction.The tumors were induced by injecting 5x106 HeLa cells into the mouse flank of female athymic nude mice. A total of 16 mice were randomly divided into four groups of four animals (two treated and two untreated control with and without KillerRed correspondingly). A diode pumped solid state yellow laser with 593 nm wavelength was used throughout this study. Whole-body in vivo fluorescence imaging was performed. 24 hours after the light treatment, tumors were excised, sectioned, and stained for light and electron microscopy.

It was found that after the irradiation fluorescence of KillerRed in tumors was less than that before the procedure by 31.6±9.4 %. Histological examination showed that control groups with HeLa tumors consisted of large polymorphic cells tightly packed together. The cancer cells without any morphological changes amounted to 80% of the total number of cancer cells in the field of view. In contrast, extensive morphological changes were observable in the treated tumors expressing KillerRed in nuclei and mitochondria. The portion of the dystrophically changed cells increased from 9.9 % to 63.7 %, and the cells with apoptosis hallmarks from 6.3% to 14%. The results of this study suggest KillerRed as a potential genetically encoded photosensitizer for photodynamic therapy of cancer.

8568-17, Session 4

Modeling physical and stromal determinants of 3D tumor growth to inform PDT-mediated combination treatments

Imran Rizvi, Massachusetts General Hospital (United States) and Harvard Medical School (United States) and Wellman Ctr. for Photomedicine (United States); Umut A. Gurkan, Brigham and Women's Hospital (United States) and Harvard Medical School (United States); Nermina Alagic, Wellman Ctr. for Photomedicine (United States) and Massachusetts General Hospital (United States); Sriram R. Anbil, Massachusetts General Hospital (United States) and Wellman Ctr. for Photomedicine (United States); Jonathan P. Celli, Univ. of Massachusetts (United States) and Wellman Ctr. for Photomedicine (United States) and Massachusetts General Hospital (United States); Savas Tasoglu, Brigham and Women's Hospital (United States) and Harvard Medical School (United States); Lawrence Mensah, Zhiming Mai, Iqbal Massodi, Massachusetts General Hospital (United States) and Wellman Ctr. for Photomedicine (United States); Utkan Demirci, Brigham and Women's Hospital (United States) and Harvard Medical School (United States); Tayyaba Hasan, Massachusetts General Hospital (United States) and Harvard Medical School (United States) and Wellman Ctr. for Photomedicine (United States)

The fate and phenotype of metastatic tumors is determined by a complex array of physical and biological factors that include flow-induced stress and signaling with stromal partners. Shed tumor cells develop into metastatic nodules under the influence of fluidic currents with support from multiple cell populations. The resultant advanced stage disease prognosticates the poorest outcomes. Among the critical stromal partners being investigated by our group and others, tumor endothelial cells are emerging as dynamic regulators of metastatic progression and mediators of treatment susceptibility. Bioengineered models that integrate these critical microenvironmental cues could serve as important complements to existing research systems, and could aid in identifying and optimizing mechanism-based combination therapies. We describe the development of three-dimensional (3D) platforms to evaluate the impact of hydrodynamic forces and stromal partners on the biological characteristics of tumor micronodules. The influence of fluidic streams on the aggressiveness of micrometastatic tumors will be presented. The incorporation of endothelial cells into 3D ovarian micronodules based on a characterization of multiple co-culturing techniques will be described. This approach supports a framework for developing therapeutic strategies that target the effects of stromal and dynamic physical forces.

8568-18, Session 4

Photodynamic characterization and optimization using multifunctional nanoparticles for brain cancer treatment

Kristen Herrmann, Yong-Eun Lee Koo, Daniel A. Orringer, Oren Sagher, Raoul Kopelman, Univ. of Michigan (United States)

To provide a better approach for treating cancer patients, a minimally invasive localized treatment Photodynamic Therapy (PDT) has been utilized to specifically treat cancer cells. PDT uses exogenously administered photosensitizers activated by light to induce cell death via formation of singlet oxygen and other free radicals. A variety of nanoparticle (NP) matrixes, photosensitizers, and targeting components have been utilized to make NP-based PDT improvements to current PDT efficiency. Our NPs have excellent tumor targeting qualities which are not achievable with molecular PDT drugs. These nanoparticles consist of a polyacrylamide (PAA) matrix with covalently linked photosensitive dyes obtaining surface conjugation with F3-peptide for active tumor targeting.

In vivo irradiation was performed using a 671nm solid-state red laser to test the efficacy of various fluency rates and illumination times. The photosensitizer in the form of free dye and embedded within PAA NPs at a dose of 0.86 mg dye/kg, was administered via the femoral vein of the rat models and incubated for an assortment of durations before irradiation to test the optimal incubation time for maximal NP accumulation within the tumor. Tumorigenic response to various photodynamic treatment conditions were examined by observing tumor tissue deviations within Sprague Dawley Rat models adorning a cranial window, allowing for a visual surveillance of tumor growth patterns.

PDT treatments with photosensitive-PAA NPs, F3-targeted or PEGylated, produced significant arrest of tumor growth over control groups, which clearly demonstrates the advantages of NP-based PDT agents for the eradication of local tumors, leading to the potential palliation of the advancing disease.

8568-19, Session 5

Photodynamic therapy in the treatment of pancreatic lesions *(Invited Paper)*

Kenneth K. Wang M.D., Mayo Clinic (United States)

We will review research to date using PDT for pancreatic cancer. The human trials will be discussed as well as new experimental evidence of the efficacy of HPPH for pancreatic cancer along with data looking at synergistic application of additional agents. New data will include work done in 3-D cultures and mouse models looking at the efficacy of PDT. We have found that PDT dramatically and significantly reduces tumor growth in mice.

8568-20, Session 5

Effects of surgical resection on outcomes following intraoperative photodynamic therapy *(Invited Paper)*

Keith A. Cengel, Charles B. Simone M.D., Theresa M. Busch, Joseph S. Friedberg, Univ. of Pennsylvania School of Medicine (United States)

We have previously demonstrated that multi-modality therapy including surgical resection with intraoperative photodynamic therapy (PDT) can be highly effective in the treatment of patients with malignant pleural mesothelioma (MPM). However, a subset of patients treated with this approach experience aggressive local or systemic relapse of MPM within the first 12 months. In this study, we combine analysis of clinical data and pre-clinical models to examine the hypothesis that cytokine signaling stimulated by the surgical resection can impair the efficacy of PDT. Patients who have undergone surgery followed by HPPH-mediated PDT experience distinct patterns of inflammatory cytokine release. Patients experiencing a significant increase in pro-inflammatory cytokines plasma levels from surgery prior to PDT appear to exhibit a greater degree of systemic toxicity and earlier recurrences than patients who did not experience a pro-inflammatory reaction to surgery. We have modeled this phenomenon in mice with syngeneic MPM tumors in which the tumor is incompletely resected and PDT is then performed. These experiments reveal that surgery appears to impair the efficacy of PDT. In vitro experiments suggest that a least one mechanism behind this phenomenon is the ability of surgically induced cytokines to promote cancer cell survival following PDT. Taken together, these results suggest that pro-inflammatory cytokines produced during surgical resection can have a negative impact on the efficacy of intraoperative PDT.

8568-21, Session 5

Photodynamic therapy and the treatment of head and neck malignancies *(Invited Paper)*

Merrill A. Biel M.D., Univ. of Minnesota, Twin Cities (United States) and Virginia Piper Cancer Institute (United States)

Photodynamic therapy has been successfully used to treat various cancers of the head and neck. Four hundred ninety one patients with neoplastic diseases of the larynx, oral cavity and pharynx have been treated with PDT with follow-up to 60 months. Those patients with primary or recurrent carcinoma in situ and T1 carcinomas obtained a complete response after one PDT treatment and 88% remain free of disease. Patients with T2 and T3 carcinomas treated with PDT obtained a complete response but in most cases they recurred locally, many with normal overlying mucosa. This is due to the inability to adequately deliver laser light to the depths of the tumor despite aggressive use of interstitial implantation. Intraoperative adjuvant PDT was used in 19 patients with recurrent head and neck cancers and only two developed local recurrences.

PDT is effective for the curative treatment of early carcinomas of the head and neck. It may also be of benefit as an adjuvant intraoperative treatment of large recurrent tumors.

8568-49, Session 5

Photodynamic therapy of locally advanced pancreatic cancer (VERTPAC study): final clinical results *(Invited Paper)*

Matthew T. Huggett, Univ. College London (United Kingdom); Michael Jermyn, Thayer School of Engineering at Dartmouth (United States); Alice Gillams, Univ. College Hospital (United Kingdom); Sandy Mosse, Univ. College London (United Kingdom); E. Kent, Univ. College Hospital (United Kingdom); Stephen G. Bown M.D., Univ. College London (United Kingdom); Tayyaba Hasan, Massachusetts General Hospital (United States); Brian W. Pogue, Thayer School of Engineering at Dartmouth (United States); Stephen P. Pereira, Univ. College London (United Kingdom)

Background: We undertook a phase I study of verteporfin photodynamic therapy (PDT) in 15 patients with locally advanced pancreatic cancer. The study consisted of two parts: i) dose-escalation profile to obtain the optimum laser energy to achieve safe and effective pancreatic tumour necrosis, ii) feasibility study of multiple fibre treatment.

Methods and Results: Needle placement and laser delivery were technically successful in all patients. Thirteen patients were treated with a single laser fibre. Three treatments were carried out each at 5, 10 and 20 J/cm2; and 5 treatments (4 patients) at 40 J/cm2. A further 2 patients were treated with 2 or 3 laser fibres at 40 J/cm2. Tumour necrosis was measured on CT by two radiologists 5 days after treatment. Axial and sagittal CT with segmentation of the necrotic zone was used for volume rendering. Plasma and lip fluorescence were measured for pharmacokinetics. There was a clear dose dependent increase in necrosis, with a median area of 20 x 16 mm (range 18 x 16 to 35 x 30 mm) at 40 J/cm2. In the 2 patients treated with multiple fibres, necrosis was 40 x 36 mm and 30 x 28 mm, respectively. There were no early complications in patients treated with a single fibre. Both patients treated with multiple fibres had CT evidence of inflammatory change anterior to the pancreas, but there were no clinically significant sequelae.

Conclusion: Single fibre verteporfin PDT is safe in a clinical setting up to 40J/cm2 and produces a dose-dependent area of pancreatic necrosis.

8568-22, Session 6

Clinical studies of combined photodynamic therapy using 5-fluorouracil and methylaminolevulinate in patients at high risk for squamous cell carcinoma

Edward V. Maytin M.D., Sara Lohser M.D., Alejandra Tellez M.D., Lauren C. Wene, The Cleveland Clinic (United States)

Photodynamic therapy (PDT) using aminolevulinic acid or its methyl ester, methyl-aminolevulinate (MAL), is an increasingly recognized approach for treating squamous neoplasia of the skin. Advantages of MAL-PDT include its ability to cover broad diseased areas (field treatment), and to do multiple sessions with little-to-no risk of scarring or mutagenesis. MAL-PDT is especially valuable in certain populations at high risk for skin cancer, including Caucasian patients with extensive solar damage, and organ transplant recipients (OTR) who take immunosuppressive drugs to prevent graft rejection. The latter group has a 65-200 fold increased risk of developing squamous cell carcinoma (SCC), a major cause of mortality. Therapeutic options for those patients, other than frequent surgeries, are very limited. Topical 5-Fluorouracil (5-FU), frequently prescribed in normal patients for pre-SCC of the skin, is only minimally effective in the OTR group. MAL-PDT, however, has ~40% efficacy for pre-SCC in OTR patients. Based upon our preclinical studies in mouse tumor models, which showed that preconditioning with 5-FU can drive higher accumulation of target protoporphyins (PpIX), we proposed a rational combination regimen of 5-FU and MAL-PDT in humans. A clinical trial was designed to test the hypothesis that a combination of 5-FU followed by MAL-PDT will elevate PpIX levels and achieve better clinical outcomes in high-risk OTR patients. Primary endpoints include PpIX levels and biochemical markers (p53) measured noninvasively and in skin biopsies. Lesion clearance and recurrence (via photographs and clinical exam) are secondary endpoints. Ongoing results of this clinical trial will be presented.

8568-23, Session 6

Real-time treatment feedback guidance of pleural PDT

Timothy C. Zhu, The Univ. of Pennsylvania Health System (United States); Michele M. Kim, Univ. of Pennsylvania (United States); Xing Liang, Baochang Liu, The Univ. of Pennsylvania Health System (United States); Julia Sandell, Univ. of Pennsylvania (United States); Jarod C. Finlay, Andreea Dimofte, Carmen E. Rodriguez, Charles B. Simone M.D., Keith A. Cengel, Joseph S. Friedberg, The Univ. of Pennsylvania Health System (United States)

Pleural photodynamic therapy (PDT) has been used as an adjuvant treatment with lung-sparing surgical treatment for mesothelioma with remarkable results. In the current intrapleural PDT protocol, a moving fiber-based point source is used to deliver the light and the light dose are monitored by 7 detectors placed in the pleural cavity. To improve the delivery of light dose uniformity, an infrared (IR) camera system is used to track the motion of the light sources. A treatment planning system uses feedback from the detectors as well as the IR camera to update light fluence distribution in real-time, which is used to guide the light source motion for uniform light dose distribution. We have improved the GUI of the light dose calculation engine to provide real-time light fluence distribution suitable for guiding the surgeons to delivery light more uniformly. A dual-correction method is used in the feedback system, so that fluence calculation can match detector readings using both direct and scatter light models. An improved measurement device is developed to automatically acquire laser position for the point source. Comparison of the effects of the guidance is presented in both phantom and patient studies.

8568-24, Session 6

Effects of modelled optical properties on recovered fluorophore concentration during image-guided fluorescence tomography

Alisha V. D'Souza, Brendan P. Flynn, Stephen C. Kanick, Brian W. Pogue, Thayer School of Engineering at Dartmouth (United States)

In fluorescence molecular tomography, optical boundary data and diffusion theory are used to reconstruct fluorophore distribution in the tissue being imaged via an iterative error minimization algorithm. Normalizing the fluorescence signal with the excitation signal, also called Born normalization, has been shown to correct for source and detector inconsistencies. It can also correct for tissue heterogeneities and inaccuracies in the model to some extent, but in the absence of known values, tissue optical properties must be guessed based on data in the literature. Using computer simulations and an ultrasound-guided fluorescence tomography system designed for spatial quantification of Protoporphyrin IX, we will first characterize the errors introduced in fluorophore concentration recovery by choice of incorrect optical properties. In both simulations and experimentation, we will measure tissue optical properties using white light spectroscopy to obtain a more accurate model. Accuracy of recovered fluorophore concentration with and without the use of the white light source will be compared, and the potential benefits of the use of white light-informed optical properties in tomographic fluorophore reconstruction will be discussed.

8568-25, Session 6

A robotic multi-channel platform for interstitial photodynamic therapy

Anna V. Sharikova, Jarod C. Finlay, Timothy C. Zhu, The Univ. of Pennsylvania Health System (United States)

A custom-made robotic multichannel platform for interstitial photodynamic therapy (PDT) and diffuse optical tomography (DOT) was developed and tested in a phantom experiment. The system, which is compatible with the operating room (OR) environment, has 16 channels for independent positioning of light sources and/or isotropic detectors in separate catheters. Each channel's motor has an optical encoder for position feedback, allowing resolution of 0.05 mm, and a maximum speed of 5 cm/s. Automatic calibration of detector positions was implemented using a red light beam that defines the starting position of each motor and by means of feedback algorithms controlling individual channels. As a result, the accuracy of zero position of 0.05 mm for all channels was achieved. We have also employed scanning procedures where detectors automatically cover the appropriate range around source positions. Thus, total scan time for a typical DOT was about 30 seconds using linear sources, and 1.5 minutes using point sources. The DOT was used to reconstruct 3D distributions of optical properties in the phantom based on the measured light fluence rates. The optical properties play a significant role in the light-photosensitizer interaction, and therefore the efficiency of PDT treatment. Additional features of our platform include automatic realignment of linear sources for PDT treatment, and optimized simultaneous stepping control of multiple sources during light delivery. These enhancements allow a tremendous improvement of treatment quality for a bulk tumor compared to the systems employed in previous clinical trials.

8568-26, Session 7

Monitoring photosensitizer uptake using two photon fluorescence lifetime imaging microscopy

Shu-Chi Allison Yeh, Kevin R. Diamond, Michael S. Patterson, David W. Andrews, Zhaojun Nie, Joseph E. Hayward, Qiyin Fang, McMaster Univ. (Canada)

Photodynamic Therapy (PDT) provides an opportunity for treatment of various invasive tumors by the use of a cancer targeting photosensitizing agent and light of specific wavelengths. However, real-time monitoring of drug uptake is desirable because the induction of the phototoxic effect relies on interplay between the dosage of localized drug and light. Fluorescence emission in PDT may be used to monitor the uptake process but fluorescence intensity is subject to variability due to scattering and absorption. In contrast, fluorescence lifetime is the time it takes for a fluorophore to drop to its ground state from the excited energy state, which is intensity independent while sensitive to the changes of its adjacent microenvironment. Therefore, using fluorescence lifetime as an additional imaging contrast may be beneficial to probe site-specific drug-molecular interactions and cell damage, and can potentially be a robust measurement at different cellular models. We have investigated the fluorescence lifetime changes of photosensitizers at various intracellular components in different cell lines. The fluorescence decays were analyzed using a bi-exponential model, followed by segmentation analysis of lifetime parameters. With establish of these characteristics, this study provides future references towards the co-culture and tissue platforms for real time visualization of the treatment efficacy.

8568-27, Session 7

Monte Carlo simulation of light fluence calculation during pleural PDT

Julia Sandell, The Univ. of Pennsylvania Health System (United States); Michelle M. Kim, Univ. of Pennsylvania School of Medicine (United States); Timothy C. Zhu, The Univ. of Pennsylvania Health System (United States)

The amount of light target tissues receive in Photodynamic therapy (PDT) helps determine how effective the resulting cell kill will be. Subsequently, a thorough understanding of light distribution in the desired tissue is necessary for accurate light dosimetry in PDT. Solving the problem of light dose depends, in part, on the geometry of the tissue to be treated. In particular, when considering PDT in the thoracic cavity for treatment of malignant, localized tumors such as those observed in malignant pleural mesothelioma (MPM), changes in light dose caused by the cavity geometry should be accounted for in order to improve treatment efficacy. Cavity-like geometries demonstrate what is known as the "integrating sphere effect" where multiple light scattering off the cavity walls induces an overall increase in light dose in the cavity. Current pleural cancer protocol assigns a standard light dose for the clinician to treat the patient to and is not based on the effects on fluence of the cavity geometry. We present a Monte Carlo simulation of light fluence based on a spherical and an elliptical cavity geometry with various dimensions. The tissue optical properties as well as the non-scattering medium (air and water) varies. We have also introduced small absorption inside the cavity to simulate the effect of blood absorption. We expand the MC simulation to track photons both within the cavity and in the surrounding cavity walls. Simulations are run for a variety of cavity optical properties determined using spectroscopic methods. We concluded from the MC simulation that the light fluence inside the cavity is inversely proportional to the surface area.

8568-28, Session 7

Light dosimetry and dose verification for pleural PDT

Andreea Dimofte, Anna V. Sharikova, The Univ. of Pennsylvania Health System (United States); Michele M. Kim, Univ. of Pennsylvania School of Medicine (United States); Timothy C. Zhu, The Univ. of Pennsylvania Health System (United States)

In-vivo light dosimetry for patients undergoing photodynamic therapy

(PDT) is critical for predicting PDT outcome. Patients in this study are enrolled in a Phase I clinical trial of HPPH-mediated PDT for the treatment of non-small cell lung cancer with pleural effusion. They are administered 4mg per kg body weight HPPH 48 hours before the surgery and receive light therapy with a fluence of 15-60 J/cm2 at 661 and 665nm. Fluence rate (mW/cm2) and cumulative fluence (J/cm2) are monitored at 7 sites during the light treatment delivery using isotropic detectors. Light fluence (rate) delivered to patients is examined as a function of treatment time, volume and surface area. In a previous study, a correlation between the treatment time and treatment volume and surface area was established. However, we did not include the direct light and the effect of the shape of the pleural surface on the scattered light. A real-time infrared (IR) navigation system was used to separate the contribution from the direct light. An improved expression that accurately calculates the total fluence at the cavity wall as a function of light source location, cavity geometry and optical properties is determined based on theoretical and phantom studies. The theoretical study includes an expression for light fluence rate in an elliptical geometry instead of the spheroid geometry used previously. The calculated light fluence is compared to the measured fluence in patients of different cavity geometries and optical properties. The result can be used as a clinical guideline for future pleural PDT treatment.

8568-29, Session 7

LEDs as excitation source for time resolved singlet oxygen luminescence detection in cell suspensions

Steffen Hackbarth, Annegret Preuss, Tobias Perna, Jan C. Schlothauer, Beate Röder, Humboldt-Univ. zu Berlin (Germany)

While the number of medical applications of Photodynamic Therapy is rising worldwide and some of them have been approved by health agencies in several countries, the direct observation of the main mediator – singlet oxygen – becomes more and more important. NIR-Photomultipliers for singlet oxygen luminescence detection are available already several years now. However, the number of groups that are able to detect such signals in cell suspensions or tissue is still limited, mainly due to the high costs for pulsed laser systems, their limited wavelength versatility as well as the difficult handling and maintenance.

We want to present a new versatile LED based singlet oxygen luminescence detection method that requires the space of two shoe boxes. The optical pathway is designed maintenance and adjustment free so non-specialists are able to perform measurements at highest quality. LEDs available for excitation cover the whole visible range so far and are superior to any other light source in terms of day to day reproducibility. Time correlated multi photon counting with a channel width of 20 ns enables an accuracy of 0.1 µs for the involved decay times even in cell suspensions with only minor effect on the cell viability.

We will demonstrate the high performance of this method with measurements of singlet oxygen luminescence from incubated cell suspensions that were recorded for a number of excitation wavelengths covering the UV-Vis range.

8568-30, Session 7

2D-scanning of singlet oxygen luminescence in skin using fiber optics

Jan C. Schlothauer, Steffen Hackbarth, Beate Röder, Humboldt-Univ. zu Berlin (Germany)

While the number of medical applications of photodynamic therapy is rising worldwide and some of them are also approved by health agencies in several countries, the direct observation of the main mediator – singlet oxygen – still is a challenging task which cannot be done as part of a clinical procedure. To be able to observe the generation and interaction of singlet oxygen in tissue during photodynamic therapy will allow for an optimization of drug and light dosage to reduce treatment stress for patients.

Ex vivo skin from pig ear is used for investigations. A Photosensitizer in a crème is topically applied to the skin and removed from the surface before measurement so only PS that penetrated into the skin is measured. The singlet oxygen luminescence is detected time resolved. The excitation and detection is done through fiber optics, which would allow implementing this method in a clinical application. Using parallel detection of the Photosensitizer fluorescence a correlation to the singlet oxygen luminescence can be shown.

8568-31, Session 7

In vivo luminescence model for the study of tumor regression and regrowth following combination regimens with differentiation-promoting agents and photodynamic therapy

Kishore Reddy Rollakanti, The Cleveland Clinic (United States); Sanjay Anand, Cleveland Clinic Lerner Research Institute (United States); Edward V. Maytin M.D., The Cleveland Clinic (United States)

Photodynamic therapy with aminolevulinic acid can be modified by pretreatment regimens with drugs such as 5-Fluorouracil (5-FU) or Vitamin D (calcitriol) that enhance accumulation of protoporphyrin IX (PpIX) within tumor tissue which presumably will enhance the therapeutic response to light. However, histological approaches for monitoring therapeutic responses are poorly suited for studying long term survival because large numbers of mice need to be sacrificed. To address this limitation, a non-invasive model to monitor tumor regression and regrowth has been established. Breast cancer cells, stably transfected with firefly luciferase (MDA-Luc cell line), are implanted subcutaneously in nude mice (0.25 - 1 x 106 cells/site), and monitored 0-36 min after i.p. injection of luciferin, with Xenogen in vivo imaging system. Luminescence is detectable at day 1 post-implantation. Tumors are suitable for experimentation on day 6, when daily injections of pretreatment agents (5-FU, 300 mg/kg; calcitriol, 1 ug/kg) begin. On day 9, ALA (75 mg/kg i.p.) is given for 4 hr, followed by illumination (633 nm, 100 J/cm2). Tumor luminescence post-PDT is monitored daily and compared with caliper measurements. Pretreatments (5-FU, calcitriol) by themselves do not inhibit luciferase expression, and all tumors grow at a similar rate during the pretreatment period. Results from in vivo survival experiments can be correlated to survival responses of MDA-Luc cells grown in monolayer cultures ± PDT and ± pretreatments, and additional mechanistic information (e.g. Ki67 and E-cadherin expression) obtained. In summary, this noninvasive model will permit testing of the therapeutic survival advantages of various pretreatments during cPDT.

8568-46, Session 7

Overcoming therapeutic resistance in pancreatic cancer with photodynamic therapy (PDT): development of pre-clinical models to evaluate the role of tumor-stroma interactions

Jonathan P. Celli, Univ. of Massachusetts (United States); Imran Rizvi, Iqbal Massodi, Massachusetts General Hospital (United States) and Wellman Ctr. for Photomedicine (United States); Michael Glidden, Univ. of Massachusetts (United States); Tayyaba Hasan, Massachusetts General Hospital (United States) and Wellman Ctr. for Photomedicine (United States)

Cancer of the pancreas remains one of the most dismal prognoses in medicine, due in large part to late diagnoses that preclude surgical resection, combined with resistance to virtually all available chemotherapy agents. This problematic drug resistance is traditionally

explained by the exceptionally rigid, hypovascular, fibrous stroma these tumors are noted for, which is thought to serve as a physical barrier to drug penetration, although a growing body of evidence suggests that even in scenarios where there is no barrier to penetration, the stroma gives rise to treatment resistance through complex biochemical and mechano-sensitive signaling. Further evidence however, suggests that photodynamic therapy (PDT) may have the potential to bypass and/or interrupt these very interactions which render these tumors non-responsive to other modalities. Taken together with positive early preclinical and clinical results with PDT for treatment of pancreatic cancer, these findings suggest promise for this modality to achieve meaningful improvements for this otherwise treatment-resistant disease, provided that suitable platforms conducive to more focused and deliberate development of the concept of targeting tumor-stroma interactions with PDT can be developed. Here, we introduce new in vitro pancreatic tumor models, which restore critical tumor stroma interactions. Combined with high-content quantitative imaging, these model systems reveal the roles of interactions with extracellular matrix components and stromal fibroblasts that contribute to stromal-mediated drug resistance, and provide a means for comprehensive mechanistic studies to develop PDT-based regimens for overcoming these complex pancreatic tumor survival strategies.

8568-47, Session 7

The impact of tumor endothelial cells on the biological characteristics of three-dimensional ovarian micronodules

Sriram R. Anbil, Imran Rizvi, Nermina Alagic, Iqbal Massodi, Massachusetts General Hospital (United States); Jonathan P. Celli, Univ. of Massachusetts (United States); Tayyaba Hasan, Massachusetts General Hospital (United States)

Ovarian carcinoma is the fifth-leading cause of cancer deaths among women and has a 5-year survival rate of less than 30%. In particular, metastatic disease is associated with the worst prognosis. The poor treatment response of multifocal disseminated nodules is due in part to their interactions with the local microenvironment. Tumor endothelial cells (TEC's) are among the important microenvironmental supporting cell populations and have been observed clinically in small peritoneal nodules. The conventional role ascribed to TECs has been largely focused on angiogenesis. However, the role of TECs as key signaling partners is emerging as an important area of discovery. TECs have recently been shown to directly influence tumor aggressiveness and proliferation. There is a need to develop more physiologically relevant models that will allow for an improved understanding how tumor-stroma interactions impact the progression of disease. We have adapted and characterized several approaches to culture multiple cell populations in three-dimensional (3D) models, and incorporated TEC's into 3D ovarian micronodules on a stromal bed. The biological characteristics of endothelialized 3D ovarian tumors will be presented. This model will facilitate improved development of therapeutic strategies that target tumor–stroma interactions in the treatment of multifocal disease.

8568-32, Session PMon

Parameter determination for singlet oxygen modeling of BPD-mediated PDT

Dayton D. McMillan, Daniel Chen, Michele M. Kim, Xing Liang, Timothy C. Zhu, Hospital of the Univ. of Pennsylvania (United States)

Photodynamic therapy (PDT) offers a cancer treatment modality capable of providing minimally invasive localized tumor necrosis. To accurately predict PDT treatment outcome based on pre-treatment patient specific parameters, an explicit dosimetry model is used to calculate apparent reacted 1O2 concentration ([1O2]rx) at varied radial distances from the activating light source inserted into tumor tissue and apparent singlet oxygen threshold concentration for necrosis ([1O2]rx, sd) for type-II PDT photosensitizers. Inputs into the model include a number of photosensitizer independent parameters as well as photosensitizer specific photochemical parameters ?, ?, and ?. To determine the specific photochemical parameters of benzoporphyrin derivative monoacid A (BPD), mice were treated with BPD-PDT with varied light source strengths and treatment times. All photosensitizer independent inputs were assessed pre-treatment and average necrotic radius in treated tissue was determined post-treatment. Using the explicit dosimetry model, BPD specific ?, ?, and ? photochemical parameters were determined which estimated necrotic radii similar to those observed in initial BPD-PDT treated mice using an optimization algorithm that minimizes the difference between the model and that of the measurements. Photochemical parameters for BPD are compared with those of other known photosensitizers, such as Photofrin. The determination of these BPD specific photochemical parameters provides necessary data for predictive treatment outcome in clinical BPD-PDT using the explicit dosimetry model.

8568-33, Session PMon

A novel LED-based light source for PDT applications in 96 well plate

Hasim O. Tabakoglu, Mehmet N. Burgucu, Tugba Sagır, Mehmet Senel, Sevim Isik, Fatih Univ. (Turkey)

Photodynamic therapy (PDT) can be applied wide range of medical conditions in clinics, recognized as both minimally invasive and minimally toxic treatment method. Light source is one of the important key components which involved in activation of photosentizers in PDT applications.

Aim of this study is to develop a novel light source for photodynamic therapy (PDT) applications. Light emitting diode (LED) based system has been developed. This structure was designed in accordance with cell culture studies. Power and energy distribution of light on 96 well plate was measured and set. According to results overall maximum light power was around 20 mW. Minimum light power was measured as 12 mW.

LED system was controlled by an open source electronics prototyping platform (Arduino). Modulation can also be established by using the system. Duration intervals were set from user interface program on computer screen.

LEDs emitted in different wavelength in red light spectrum (630 nm-660 nm) and blue light spectrum (430nm-460nm) was settled in different perforated boards. Effect of white light will also be examined. Perforated board is designed such that become compatible with the size of 96 well plate.

As a photosensitizer, PAMAM modified porphyrin molecule will be used. Effect of red and blue wavelengths as well as effect of white light on this molecule will be examined.

Effect of the system mentioned above will be tried on different cancer cell lines such as MCF-7 and HeLa. Viability essay WST-1 results will be presented in conference.

8568-34, Session PMon

A novel near real-time laser scanning device for geometrical determination of pleural cavity surface

Michele M. Kim, Timothy C. Zhu, Univ. of Pennsylvania School of Medicine (United States)

During HPPH-mediated pleural photodynamic therapy (PDT), it is critical to determine the anatomic geometry of the pleural surface quickly as there may be movement during treatment resulting in changes with the cavity. We have developed a laser scanning device for this purpose,

which has the potential to obtain the surface geometry in real-time. A red diode laser with a holographic template to create a pattern and a camera with auto-focusing abilities are used to scan the cavity. In conjunction with a calibration with a known surface, we can use methods of triangulation to reconstruct the surface. Using a chest phantom, we are able to obtain a 360 degree scan of the interior in under 1 minute. The chest phantom scan was compared to an existing CT scan to determine its accuracy. The laser-camera separation can be determined through the calibration with 5mm accuracy. The device is best suited for environments that are on the scale of a chest cavity (around 40cm range). This technique has the potential to produce cavity geometry in real-time during treatment. This would enable PDT treatment dosage to be determined with greater accuracy. Works are ongoing to build a miniaturized device that moves the light source and camera via a fiber-optics bundle commonly used for endoscopy with increased accuracy.

8568-35, Session PMon

Photodynamic therapy mediated by Cerenkov radiation from beta-emitting radionuclides

David Boucher, Brad Hartl, Laura Marcu, Simon R. Cherry, Univ. of California, Davis (United States)

The utilization of photodynamic therapy (PDT) in the treatment of deep tumors is significantly limited by the penetration depth of light. Furthermore, current implementation of PDT is limited to identifiable tumors, and cannot readily be applied to metastatic disease. To overcome these limitations, we demonstrate here the use of Cerenkov radiation generated by 90Y as a localized, internal light source for the activation of protoporphyrin IX, the active metabolite of 5-aminolevulinic acid (ALA). As proof of principle, in vitro assays were conducted in which U87 glioma cells were cultured in the presence of ALA and continually exposed to varying levels of 90Y. WST-1 assays confirmed a significant decrease in metabolic activity of cells treated with both ALA and 90Y. Control groups left untreated or treated with either ALA or 90Y further confirm that this observation is not simply an additive effect. In addition, preliminary in vivo studies have been completed in which animals bearing orthotopic U87-derived tumors were injected at a single time point with 150 µCi of the radiotherapeutic 90Y-DOTATOC and given a daily dose of ALA. Confirmation of probe delivery and conversion of ALA to protoporphyrin IX at the tumor site is provided by Cerenkov luminescent and fluorescent optical imaging, respectively, and effect of treatment was assessed by histology and tumor volume measurements from MRI images. Preliminary results suggest there is significant potential for synergies between radionuclide therapies and PDT mediated by Cerenkov radiation in the treatment of metastatic cancer.

8568-36, Session PMon

Assessing patient response during PDT in head and neck lesions with diffuse optical spectroscopies

Daniel J. Rohrbach, Nestor Rigual, Erin Tracy, Andrew Kowalczewski, Kenneth Keymel, Michele T. Cooper, Heinz Baumann, Barbara W. Henderson, Ulas Sunar, Roswell Park Cancer Institute (United States)

There is strong evidence that imprecise dosimetry results in variations in clinical responses to photodynamic therapy (PDT). Quantitative tools are likely to play an essential role in bringing PDT to a full realization of its clinical benefits. These tools can provide real-time feedback to surgeons in the operating room which will allow for the standardization of site-specific individualized protocols that are used to monitor both light and drug (photosensitizer) dose. Additionally the tissue response for individual patients can be assessed immediately after treatment.

Here, we present results from a Phase I clinical trial of HPPH-mediated PDT of head and neck cancer. We used a custom instrument that combined three spectroscopic techniques of diffuse correlation spectroscopy (DCS), diffuse reflectance spectroscopy (DRS), diffuse fluorescence spectroscopy (DFS) to quantify blood flow, blood volume fraction, blood oxygen saturation and photosensitizer concentration. Non-invasive measurements were acquired before and after PDT in the oral cavity. Our results indicate significant contrast in these parameters between the lesion and peripheral tissue before treatment. We also observed significant PDT-induced changes in these parameters, which correlated with the crosslinking of signal transducer and activator of transcription 3 (STAT3), a molecular marker of accumulated PDT dose. Our results suggest non-invasive diffuse optical spectroscopies can provide clinicians with functional parameters in real-time for treatment optimization and assessment of patient response

8568-37, Session PMon

A probe specific empirical light transport model for improved quantification of optical parameters during PDT

Daniel J. Rohrbach, Andrew Kowalczewski, Bouri Chen, Ulas Sunar, Roswell Park Cancer Institute (United States)

Diffuse reflectance spectroscopy (DRS) is a common technique for assessing the components of tissue both quickly and non-invasively. However, choosing the correct model for light-tissue interaction is very important for accurate quantification. Frequently used models like the diffusion approximation are only valid for certain ranges of tissue optical properties and specific probe geometries. In cases such as head and neck cancer in the oral cavity, where the topography of the oral cavity does not allow for probes with large separations, a different model needs to be used. For improved quantification with DRS over a wide range of optical properties and for a shorter source detector separation, a probe-specific light transport model can be more effective. To develop the light transport model, optical phantoms with precise optical properties were created to cover a range of absorption and scattering. Measurements were acquired from each phantom to determine the diffuse reflectance signal. By generating a grid of reflectance values at known optical properties, an empirical look-up-table was created. We will present our model in tissue simulating phantoms. In the future, we will apply it to the analysis of 40 patients from a clinical trial for head and neck cancer in the oral cavity.

8568-38, Session PMon

Imaging nonmelanoma skin cancers at pre- and post-PDT with combined ultrasound-photoacoustic microscopy

Ulas Sunar, Roswell Park Cancer Institute (United States)

Nonmelanoma skin cancers (NMSCs) have increased dramatically, with more than a million new cases worldwide each year. Treatment is usually either by excision or Mohs micrographic surgery and alternatively may include photodynamic therapy (PDT). PDT has become a treatment of choice especially for the cases with multiple sites and large areas. However, the efficacy of PDT is limited for thicker and deeper tumors. Depth and size information as well as vascularity can provide useful information to clinicians for planning and evaluating PDT. We utilized combined ultrasound-photoacoustic microscopy for imaging a basal cell carcinoma (BCC) tumor at pre- and post-PDT. Transgenic mice over expressing sonic hedgehog in the skin activate hedgehog signaling. These mice overexpress the downstream Gli2 transcription factor and develop spontaneous BCCs in skin. Reconstructed ultrasound and photoacoustic images showed that the ultrasound image provided structure of the tumor such as thickness and photoacoustic image provided vascular response of the tumor. Our results indicate that combined ultrasound-photoacoustic imaging can be useful tool for imaging NMSCs during PDT.

8568-39, Session PMon

PDT dose dosimetry for pleural photodynamic therapy

Anna V. Sharikova, Jarod C. Finlay, The Univ. of Pennsylvania Health System (United States); Xing Liang, Univ. of Pennsylvania (United States); Timothy C. Zhu, The Univ. of Pennsylvania Health System (United States)

PDT dose is defined as a product of the concentration of photosensitizer and the light fluence in target tissue. Existing systems are capable of measuring the light fluence but so far in vivo measurement of photosensitizer in the treated tissue has been lacking. We have developed and tested a new method to simultaneously acquire light dosimetry and photosensitizer fluorescence data via the same isotropic detector, and employing treatment light as the excitation source. A dichroic beamsplitter is used to split light from the isotropic detector into two fibers, one for light dosimetry, the other, after the 665 nm treatment light is removed by a band-stop filter, to a spectrometer for fluorescence detection. The light fluence varies significantly during treatment because of the source movement. The fluorescence signal is normalized by the light fluence measured at treatment wavelength. Tests performed in mouse experiments with HPPH photosensitizer have demonstrated the feasibility of this method. A BALB/c mouse with an AB12 tumor was injected with 0.25 mg/kg HPPH 24 hours before PDT treatment. We have shown that the absolute photosensitizer concentration can be obtained by an optical properties correction factor and linear spectral fitting. Tissue optical properties are determined using an absorption spectroscopy probe immediately before PDT at the same sites. This novel method allows accurate real-time determination of delivered PDT dose using existing isotropic detectors, and may lead to a considerable improvement of PDT treatment quality compared to the currently employed systems. Preliminary data in patient studies will be presented.

8568-40, Session PMon

Cytokine-reported inflammation after pre-PDT tumor excision is correlated with PDT-induced hypoxia measured by diffuse optical spectroscopy in mesothelioma patients

So Hyun Chung, Univ. of Pennsylvania (United States); Keith A. Cengel, Charles B. Simone M.D., Joseph S. Friedberg, Hospital of the Univ. of Pennsylvania (United States); Steven M. Albelda, Madeline E. Winters, Julien Menko, Univ. of Pennsylvania (United States); Jarod C. Finlay, Timothy C. Zhu, Eli Glatstein, Hospital of the Univ. of Pennsylvania (United States); Arjun G. Yodh, Univ. of Pennsylvania (United States); Theresa M. Busch, Hospital of the Univ. of Pennsylvania (United States)

The presence of pre-existing or treatment-initiated hypoxia can limit therapeutic response to photodynamic therapy (PDT). In a clinical trial of intra-operative HPPH-mediated PDT for malignant pleural mesothelioma, we have used Diffuse Correlation Spectroscopy (DCS) and Diffuse Optical Spectroscopy (DOS) to measure the effect of PDT on blood flow and hemoglobin concentration, respectively. Patients initially underwent debulking surgery for mesothelioma, including a radical pleurectomy. PDT immediately followed by delivering 661 nm illumination through a dilute intralipid solution filling the thoracic cavity. DCS and DOS measurements were made using a probe sutured to tissue within the illumination field. Resulting data showed the extent of treatment-created hypoxia, measured as reductions in the concentration of oxy-hemoglobin, to vary substantially among the first 8 patients that we have analyzed. Furthermore, among these patients, those with less PDT-created hypoxia trended toward a better prognosis than those with more severe treatment-associated hypoxia. In an effort to assess potential causes for inter-patient variability in PDT-created hypoxia, blood samples were collected at multiple timepoints and analyzed for cytokine induction. Unsurprisingly, these revealed that surgery could lead to increases in the pro-inflammatory cytokine IL-6. In fact, a correlation was found between the relative increase in IL-6 as a result of surgery and the subsequent development of PDT-created hypoxia (R=0.72, p-value: 0.044). This suggests to us that IL-6 induction by surgery may have led to vasoconstriction during PDT, and DOS measurement of oxy-hemoglobin during PDT may be able to communicate the effect of surgery and related prognosis of the patients.

8568-41, Session PMon

Targeted imaging of ovarian cnacer cells using viral nanoparticles doped with indocyanine green

Yadir A. Guerrero, Baharak Bahmani, Bonsu Jung, Valentine I. Vullev, Univ. of California, Riverside (United States); Vikas Kundra, The Univ. of Texas M.D. Anderson Cancer Ctr. (United States); Bahman Anvari, Univ. of California, Riverside (United States)

Our group has constructed a new type of viral nanoparticles (VNP) from genome-depleted plant infecting brome mosaic virus (BMV) that encapsulates FDA-approved near infrared (NIR) indocyanine green (ICG)1. We refer to these VNPs as optical viral ghosts (OVGs) since the constructs lack the genomic content of wild-type BMV. One of our areas of interest is the application of OVGs for real-time intraoperative NIR fluorescence imaging of small peritoneal ovarian tumor nodules. We target human epidermal growth factor receptor-2 (HER-2) expression in ovarian cancer as a biomarker associated with ovarian cancer, since its over-expression is linked to the disease's progression to death. We functionalize the OVGs with anti-HER2 monoclonal antibodies using reductive amination methods. We used flow cytometry and fuorescence imaging to quantify the relative uptake of functionalized OVGs by ovarian cancer cells, and compare the results with cases when the cells were incubated with free ICG and non-functionalized OVGs. We make use of the SKOV-3 cell line (high HER-2 expression) and the OVCAR3 cell line (low HER-2 expression) to compare uptake levels based on HER-2 overexpression. While developing our VNPs we have addressed some of the innate issues of ICG fluorescence quenching to develop OVGs with relative fluorescence emission levels greater than those observed for ICG free in solution. Our results suggest the possibility of using anti-HER2 conjugated OVGs in conjunction with cytoreductive surgery to detect small tumor nodules (<5cm) which currently are not excised during surgery

8568-42, Session PMon

An ultrasound-guided fluorescence tomography system: design and specification

Alisha V. D'Souza, Brendan P. Flynn, Sason Torosean, Stephen C. Kanick, Brian W. Pogue, Thayer School of Engineering at Dartmouth (United States)

An ultrasound-guided fluorescence molecular tomography system is under development for in vivo quantification of Protoporphyrin IX (PPIX) during Aminolevulinic Acid - Photodynamic Therapy (ALA-PDT) of Basal Cell Carcinoma. The system is designed to combine fiber-based spectral sampling of PPIX fluorescence emission with co-registered ultrasound images to quantify local fluorophore concentration. A single white light source is used to provide an initial estimate of the optical properties of tissue layers. Optical data is obtained by sequential illumination of a 633nm laser source at 4 linear locations with parallel detection at 5 locations interspersed between the sources. Acquired fluorescence spectra are processed to eliminate tissue auto-fluorescence. Tissue regions from segmented ultrasound images, optical boundary data, white light-informed initial optical properties and diffusion theory are used to estimate the fluorophore concentration in these regions. Our system and methods allow interrogation of both superficial and deep tissue locations;

this along with simulation results and phantom studies that establish depth and concentration sensitivity limits for recovered PPIX will be presented.

8568-43, Session PMon

Photodynamic therapy: diagnostic and therapeutic applications

Ivy M. Ndhundhuma, Council for Scientific and Industrial Research (South Africa)

Although pathologic examination remains the gold standard for diagnosis, cancer has the potential to be diagnosed through minimally invasive approaches because of its cutaneous location. A pathologist's ability to detect cutaneous cancers in their earliest form has been amplified. However, the problem with skin biopsy is that a pathology report is highly dependent on the quality of the biopsy that is submitted and when it is performed incorrectly, and without appropriate clinical information, a pathologist's interpretation of a skin biopsy can be severely limited. As current approaches are refined and new techniques are developed, the improved ability to diagnose cancer will hopefully enhance reaching the goal of reducing cancer mortality rates.

Photodynamic therapy has been established as a selective treatment modality for some medical indications during the last three decades. Photodynamic diagnosis (PDD), a fluorescence based technique defined from the photodynamic therapy principle, involves a combination of a fluorescent tumor-localizing photosensitizer with light and is currently under investigation as an early cancer detection tool. Much evidence has shown that a suitable photosensitizer for PDT or PDD should selectively localize in tumor cells than in normal cells. In this study, a laser scanning confocal microscope (LSCM) was used to compare fluorescence localization of aluminum (III) phthalocyanine chloride tetrasulphonate, in normal (fibroblasts) and cancerous skin cells (malanoma). A higher uptake and fluorescence localization of aluminum (III) phthalocyanine chloride tetrasulphonate in cancer cells was observed.

References

1. Peng Q, Juzeniene A, Chen J, Svaasand L O, Warloe T, Giercksky K E and Moan J 2008 Lasers in medicine Rep. Prog. Phys. 71 056701

2. Moghissi K, Stringer M R, Dixon K 2008 Fluorescence photodiagnosis in clinical practice Photodiagnosis Photodyn Ther 5 235

3. Huang Z, Xu H, Meyers A D, Musani A I, Wang L, Tagg R, Barqawi A B, Chen Y K 2008 Photodynamic therapy for treatment of solid tumors – potential and technical challenges, Technol Cancer Res Treat 7(4) 309

8568-45, Session PMon

Towards image guided drug delivery and therapy of glioblastoma

Srivalleesha Mallidi, Harvard Medical School (United States); Lawrence Mensah, Massachusetts General Hospital (United States); Kimberley S. Samkoe, Dartmouth College (United States); Brian W. Pogue, Thayer School of Engineering at Dartmouth (United States); Tayyaba Hasan, Massachusetts General Hospital (United States)

Glioblastoma (GBM) is an aggressive cancer with dismal survival rates and few new treatment options. Fluorescence guided resection of GBM followed by photodynamic therapy (PDT) has shown promise in several chemo- or radiotherapy non-responsive GBM treatments clinically. PDT is an emerging light and photosensitizer (PS) mediated cytotoxic method. However, as with other therapeutic modalities, the outcomes are variable largely due to the non-personalization of dose parameters and the highly localized nature of conventional PDT that ignores distant disease. The variability can primarily be attributed to the inter-patient differences in two key parameters - PS concentration and tumor oxygenation. These need to be incorporated in the design of patient-specific PDT. Also, because PDT has built in dual selectivity (confinement of light and localization of PS), using targeted PS would impact distant disease, an approach not yet exploited in GBM PDT. Building upon our previous findings, we are exploring several approaches to achieve this goal including nanotechnology and combination-based treatments. This presentation will discuss our efforts in creating multifunctional drug delivery constructs and their efficacy in in-vitro and in-vivo models of GBM.

8568-48, Session PMon

Calculation of singlet oxygen formation from one and two photon absorbing photosensitizers used in PDT

Mary J. Potasek, Mary J. Potasek, Gene Parilov, Karl Beeson, Simphotek Inc. (United States)

Advances in biophotonic medicine require new information on photodynamic mechanisms. In photodynamic therapy (PDT), a photosensitizer (PS) is injected into the body and accumulates at higher concentrations in diseased tissue compared to normal tissue. The PS absorbs light from a light source and generates excited-state triplet states of the PS. The excited triplet states of the PS can then react with ground state molecular oxygen to form excited singlet-state oxygen or form other highly reactive species. The reactive species react with living cells, resulting in cell death. This treatment is used in many forms of cancer including those in the prostrate, head and neck, lungs, bladder, esophagus and certain skin cancers. We developed a novel numerical method to model the photophysical and photochemical processes in the PS and the subsequent energy transfer to O2, improving the understanding of these processes at a molecular level. Our numerical method simulates light propagation and photo-physics in PS using methods that build on techniques previously developed for optical communications and nonlinear optics applications. We investigate both single photon and two-photon absorbing PS used in PDT and provide results of commonly used PS.

8568-50, Session PMon

CT imaging of orthotopic pancreas tumors in Rabbit correlating to verteporfin uptake

Jason Gunn, Kenneth M. Tichauer, Thayer School of Engineering at Dartmouth (United States); Karen L. Moodie, Dartmouth Hitchcock Medical Ctr. (United States); Susan Kane, Thayer School of Engineering at Dartmouth (United States); P. Jack Hoopes, Geisel School of Medicine (United States); Brian W. Pogue, Thayer School of Engineering at Dartmouth (United States)

No Abstract Available

8568-51, Session PMon

Photodynamic therapy for cancer with tyrosine kinase inhibitors: the power of combination therapy

Andrea Weiss, Ecole Polytechnique Fédérale de Lausanne (Switzerland); Judy van Beijnum, VU Univ. Medical Center, Amsterdam (Netherlands); Debora Bonvin, Hubert E. van den Bergh, Ecole Polytechnique Fédérale de Lausanne (Switzerland); Arjan . W Griffioen, VU Univ. Medical Center (Netherlands); Patrycja M. Nowak-Sliwinska, Ecole Polytechnique Fédérale de Lausanne (Switzerland)

Photodynamic therapy (PDT) when used for cancer induces secondary tissue responses that ameliorate the outgrowth of cancer cells, limiting its application. The combination with recently developed anti-angiogenic drugs may therefore improve treatment outcome. Here we demonstrate in two xenograft tumor models, for ovarian- and colorectal carcinoma, that angiogenesis inhibition can significantly improve the anti-tumor effect of PDT using the photosensitizer Visudyne®. We show that treatment with axitinib and sorafenib immediately after PDT results in a synergistic anti-tumor activity. Interestingly, treatment with sunitinib was not found to result in synergistic activities, while bevacizumab, although effective as a monotherapy, did not improve PDT at all. The synergistic activity of axitinib and sorafenib was measurable at the level of microvessel density, confirming the anti-angiogenic activity of both treatment strategies. Molecular analysis by real-time PCR revealed that the combination therapy results in suppression of VEGFR-2 expression in the vasculature. Scheduling studies were performed in order to understand the mechanism of the synergy. Since PDT is dependent on the presence of tissue oxygen, it was hypothesized that treatment with an angiogenesis inhibitor prior to application of PDT would improve the anti-tumor effect further. Surprisingly, improvement was not observed. Instead, giving axitinib prior to PDT resulted in worse outcome. Bevacizumab pretreatment even resulted in loss of PDT effects. The current data suggest that Visudyne®-PDT in combination with clinically approved anti-angiogenic agents can be applied for selective and efficient anti-cancer therapy. In addition, angiostatic treatment is best given after the PDT treatment.

8569-1, Session 1

The DOSE in LLLT: still no consensus *(Invited Paper)*

Tomas Hode, Immunophotonics, Inc. (United States); Lars Hode, Swedish Laser-Medical Society (Sweden); Peter A. Jenkins, SpectraMedics (United States)

It is well known that the light parameters in LLLT are of paramount importance to the results. Said parameters are typically wavelength, intensity, total energy, energy density, bandwidth, polarization, illumination time, etc. The most important light parameter is the dose (amount of light energy), but despite the fact that lasers have been used for almost 50 years for medical applications (McGuff, 1963), there is still no consensus on how to define “dose”. Dose in general means “amount” and in the case of LLLT, amount of light (photons), or light energy. The most common way to present dose is in number of joules per surface unit (for example J/cm2). Unfortunately, it is more complicated than that, which can be illustrated with the following fictional example:

A researcher performs an animal study and uses a 1 mW laser that illuminates a 1 mm2 surface area during 10 seconds, which gives a dose of 1 J/cm2. Another researcher decides to repeat the study, and uses a 100 mW laser that illuminates a 1 cm2 area, thus also providing a dose of 1 J/cm2. But in the latter case, the total energy provided is 100 times higher, which means that the outcome of the study is likely to be quite different!

As illustrated above, the fact that there is no consensus in the scientific community on how to define the dose is problematic. We will suggest a schedule of parameters that we will offer all scientific journals publishing articles on LLLT.

8569-2, Session 1

Low-level laser/light therapy (LLLT) direct and indirect targets *(Invited Paper)*

James D. Carroll, THOR Photomedicine Ltd. (United Kingdom)

The common method for applying LLLT is to aim light at an injury or lesion to promote healing, reduce inflammation or induce analgesia. However there is more to LLLT then just treating stressed cells around a pathology. Nerves, lymph, trigger points and blood are also influenced by light and not just by treating at the site of injury. Many laboratory and clinical research studies have shown that treatments remote from the site of injury produce statistical and clinically meaningful improvements to a range of pathologies. Analgesia can be induced anywhere proximal or distal to an injury as long as it is on the same nerve pathway. Myofascial trigger points distant from a pathology cause muscle tightness and shortening; they contribute to pain and dysfunction in arthritic joints and tendinopathies (as well as being a pathology in their own right), these can be deactivated with light. Lymph flow can be improved by treating nodes and lymph vessels proximal to an injury. There is sufficient evidence that blood irradiation improves flow, reduces oxidative stress and influences a variety of blood related products (platelets, red blood cells and lymphocytes). All of these will have power density, time, energy and fluence dependent effects. This presentation will be a brief overview of evidence; the wavelengths, power density, treatment time, treatment intervals and where to treat will be presented.

8569-3, Session 1

The wavelength, beam size, and type dependences of cerebral low-level light therapy: a Monte Carlo study on visible Chinese human

Ting Li, Univ. of Electronic Science and Technology of China (China)

Low level light therapy (LLLT) has been clinically utilized for many indications in medicine requiring protection from cell/tissue death, stimulation of healing and repair of injuries, pain reduction, swelling and inflammation. Presently, use of LLLT to treat stroke, traumatic brain injury, and cognitive dysfunction is attracting growing interest. Near-infrared light can penetrate into the brain tissue, allowing noninvasive treatment to be carried out with few treatment-related adverse events. Optimization of LLLT treatment effect is one key issue of the field; however, only a few experimental tests on mice for wavelength selection have been reported. We addressed this issue by low-cost, straightforward and quantitative comparisons on light dosage distribution in Visible Chinese human head with Monte Carlo modeling of light propagation. Optimized selection in wavelength, beam type and size were given based on comparisons among frequently-used setups (i.e., wavelengths: 660 nm, 810 nm, 980 nm; beam type: Gaussian and flat beam; beam diameter: 2 cm, 4 cm, 6cm).This study provided an efficient way to guide optimization of LLLT setup and selection on wavelength, beam type and size for clinical brain LLLT.

8569-4, Session 1

Mapping optical properties of rat brain for LLLT dosimetry

Marcelo V. P. Pires de Sousa, Univ. de São Paulo (Brazil); Renato Prates, Ilka Kato, Caetano Sabino, Tania Yoshimura, Luis Suzuki, Martha Ribeiro, Instituto de Pesquisas Energéticas e Nucleares (Brazil); Elisabeth M. Yoshimura, Univ. de São Paulo (Brazil)

Over the last few years, low-level light therapy (LLLT) has shown an incredible suitability for a wide range of applications for central nervous system (CNS) related diseases. In this therapeutic modality light dosimetry is extremely critical so the study of light propagation through the CNS organs has extreme importance. To better understand how light dosage can be delivered to the most relevant neural sites we evaluated optical properties, such as scattering and absorption coefficients, point by point in the rat brain. We obtained these optical properties for red (? = 660 nm) and near infrared (? = 808 nm) diode laser light analyzing the penetration and distribution in the whole brain. A fresh wistar rat (Rattus novergicus) brain was illuminated with both wavelengths on spots above the cortical surface. Horizontal, sagittal and coronal slices were made to compare the light transmission through substructures in all three directions. A high-resolution digital camera was employed to acquire data from transmitted light. Profiles of transmitted intensities were obtained from the images. Peaks and valleys in the profiles spatially showed sites where light was less or more attenuated. The signal peak intensities provide information about total attenuation and their width are correlated to the scattering coefficient at that individual portion of the sample. The outcomes of this study provide remarkable information for LLLT dose-dependent studies involving CNS and highlight the importance of LLLT dosimetry in CNS organs for large range of applications in animals and humans diseases.

8569-5, Session 1

Red and infrared light distribution in blood

Ana Carolina de Magalhaes, Elisabeth M. Yoshimura, Univ. de São Paulo (Brazil)

Low level laser therapy (LLLT) is used in several applications, including the reduction of inflammatory processes. It might be used to prevent the systemic inflammatory response syndrome (SIRS), which some patients develop after cardiopulmonary bypass (CPB) surgery applied to solve some heart diseases. The objectives of this study were to investigate light distribution inside blood, in order to implement the LLLT during CPB, and, through this study, to determine the best wavelength and the best way to perform the treatment. The blood, diluted to the same conditions of CPB procedure was contained inside a cuvette and an optical fiber was used to collect the scattered light. Two wavelengths were used: 632.8 nm and 820 nm, the results were compared to a Monte Carlo simulation. Light transmission through CPB tube walls and light distribution in blood inside CPB tubes were also evaluated. Compared to the 820 nm light, the 632.8 nm light is scattered further away from the laser beam, turning it possible that a bigger volume of blood be treated. Simulated and experimental data have a good agreement. The blood should be illuminated through the smallest diameter CPB tube, using at least four distinct points around it, in only one cross section, because the blood is kept passing through the tube all the time and the whole volume will be illuminated.

8569-7, Session 2

Exposing human retinal pigmented epithelial cells to red light in vitro elicits an adaptive response to a subsequent 2 ?m laser challenge

Kurt J. Schuster, TASC, Inc. (United States); Larry E. Estlack, Conceptual MindWorks, Inc. (United States); Jeffrey C. Wigle, Air Force Research Lab. (United States)

The objective of this study was to elucidate cellular mechanisms of protection against laser-induced thermal killing utilizing an in vitro retina model. When exposed to a 1 sec pulse of 2-µm laser radiation 24 hr after illuminating hTERT-RPE cells with red light (preconditioning), the preconditioned cells are more resistant to thermal challenge than unilluminated controls (adaptive response). Results of efforts to understand the physiology of this effect led us to two genes: Vascular Endothelial Growth Factor C (VEGF-C) and Micro RNA 146a (miR-146a). Transfecting “wild type” (WT) cells with siRNA for VEGF-C and miR-146a mRNA resulted in “knockdown” strains (VEGF-C(KD) and miR-146a(-)) with ~10% and ~30% (respectively) of the constitutive levels expressed in the WT cells. To induce gene expression, WT or KD cells were preconditioned with 1.44 to 5.40 J/cm2, using irradiances between 0.40 and 1.60 mW/cm2, of either 671-nm (diode) or 637-nm (laser) radiation. Probit analysis was used to calculate threshold damage irradiance, expressed as ED50, between 10 and 100 W/cm2 for the 2-µm laser pulse. In the WT cells there is a significant increase in ED50 ($p \leq 0.05$) with the maximum response occurring at 2.88 J/cm2 in the preconditioned cells. Neither KD cell strain showed a significant increase in the ED50, although some data suggest the response may just be decreased in the knockdown cells instead of absent. So far the response does not appear to be dependent upon either wavelength (637 vs. 671 nm) or coherence (laser vs. LED), but there is an irradiance dependence.

8569-8, Session 2

How low-level laser therapy can change mechanical properties of cells

Ana Carolina de Magalhaes, Diana Martinez, Ellisabeth M. Yoshimura, Adriano M. Alencar, Univ. de São Paulo (Brazil); Marcia Z. Z. J. Ferreira, Univ. Estadual de Campinas (Brazil); Cristina M. Chavantes M.D., Instituto do Coração (Brazil)

Low level laser therapy (LLLT) is used as a treatment of several conditions, including of inflammatory processes. Possible changes in mechanical properties of cells, caused by illumination, are investigated with optical magnetic twisting cytometry (OMTC), which is a technique used to evaluate mechanical properties in cell culture. Ferromagnetic microbeads are bound to cell cytoskeleton, the bead is magnetized horizontally and a vertical twisting magnetic field is applied causing a torque that deforms the cell, the bead rotates and translates. Based on the lateral displacement of the bead, elastic shear (G’) and loss (G”) moduli are obtained. Samples of human bronchial epithelial cell culture were divided in two groups: one was a control group and the other was illuminated with a 30 mW power 660 nm laser for 10 s, 1.9 J/cm2. Both elastic shear and loss moduli increased for illuminated samples. Elastic shear modulus increased by a factor of 1.5 and loss modulus increased by a factor of 2.0, which means that the cells became tenser. Standard deviations have also increased. Those results indicate that illumination causes structural changes in cell surface. Hence, OMTC is an important technique which can be used to aggregate knowledge for light effect in cell cytoskeleton and even LLLT mechanisms in inflammatory processes.

8569-9, Session 2

Study on the Curcumin dynamics and distribution through living biofilms

Mariana T. Carvalho, Univ. de São Paulo (Brazil); Livia N. Dovigo, Alessandra N. S. Rastelli, Univ. Estadual Paulista (Brazil); Vanderlei S. Bagnato, Univ. de São Paulo (Brazil)

The understanding of how the association of a photosensitizer and light acts against oral biofilms is still an important goal in antimicrobial PDT field. This study aimed to use confocal microscopy to evaluate different microorganisms and how different photosensitizers (PS) acts and binds to it. For this purpose we characterize each microorganism, evaluating its relation with the PS. Understanding how the PS binds to the microorganism cell can be an indicative on its effectiveness. The aim of our study was initially to determine how the PS would be distributed through the living biofilm. Our biofilms were grown on plastic, polystyrene, coupons, which are placed in uncontaminated custom designed glass wells for microscopy. These ensure that the environment and the sample were not cross contaminated. In this paper, we describe the work developed with Curcumin as the Photosensitizer agent in two different biofilms. We worked with a fungus (Candica albicans) and a bacterium (Streptococcus mutans). For the fungus, the biofilms were 2 days old, and for the bacterium, we worked with biofilms up to two weeks old. Each of the worked microorganisms has a different response for this PS during the photodynamic therapy. Therefore, we tried to correlate the know response from the PDT of this microorganisms for different incubation time. We realize there was a dynamics throughout the microorganism that could be correlated with the time of its first contact with the PS. Therefore, we present a fluorescence lifetime study of the Curcumin distribution in the biofilm.

8569-28, Session 2

Tissue regeneration with photobiomodulation

Praveen R. Arany, National Institute of Dental and Craniofacial Research (United States)

Low level light therapy (LLLT) has been widely reported to reduce pain and inflammation and enhance wound healing and tissue regeneration in various settings. LLLT has been noted to have both stimulatory and inhibitory biological effects and this process has been termed Photobiomodulation (PBM). Several elegant studies have shown the key role of Cytochrome C oxidase and ROS in initiating this process.

The downstream biological responses remain to be clearly elucidated. Our work demonstrates activation of an endogenous latent growth factor complex, TGF-?1, as one of the major biological events. TGF-?1 has critical roles in various biological processes such as inflammation and immune responses, wound healing and stem cell biology. This presentation will outline the distinct molecular mechanisms involved in activation of the latent growth factor complex. A broad panel of biochemical, biophysical and biological assays was used in vitro to explore each step of this process. Further, experiments in small animal models were used to establish the in vivo efficacy of this mechanism. While there are clearly demonstrated LLLT effects on both intracellular and extracellular biological molecules, which are dependent on the wavelength and energy density, this presentation will address one of these mechanisms involving LLLT-generated ROS activation of latent TGF-?1. This data highlights the use of PBM to activate an endogenous factor to direct differentiation of native, resident stem cells providing evidence for the use of LLLT as an innovative clinical tool in regenerative medicine.

8569-10, Session 3

Low-intensity laser for treatment of Herbes Simplex on Escherichia coli cultures and DNA repair

Adenilson S. Fonseca, Univ. do Estado do Rio de Janeiro (Brazil); Roberta S. Marciano, Luiz Phelippe S. Sergio, Giovanni Augusto C. Polignano, Oscar R. Guimaraes, Mauro Geller, Ctr. Univ. Serra dos Órgãos (Brazil); Flavia Paoli, UFJF (Brazil)

Low intensity red lasers are proposed for treatment of herpes simplex based on biostimulative effects. However, effects of low intensity lasers at fluences used in clinical protocols on DNA are controversial. The aim of this work was to evaluate the effects of low intensity red laser on survival and induction of filamentation of Escherichia coli cells, and induction of DNA lesions in bacterial plasmids. Escherichia coli cultures were exposed to laser (660 nm, 100 mW, 45 and 60 J/cm2) to study bacterial survival and filamentation. Also, bacterial plasmids were exposed to laser to study DNA lesions by electrophoretic profile and action of DNA repair enzymes. Data indicate low intensity red laser: (i) had no effect on survival of E. coli wild type, endonuclease III and formamidopyrimidine DNA glycosylase/MutM protein but decreased the survival of exonuclease III and endonuclease IV deficient cultures; (ii) induced bacterial filamentation, (iii) there was no alteration in the electrophoretic profile of plasmids in agarose gels, (iv) there was no alteration in the electrophoretic profile of plasmids incubated with formamidopyrimidine DNA glycosylase/MutM protein, endonuclease III, endonuclease IV and exonuclease III. Low intensity red laser at therapeutic fluences used for treatment of herpes simplex has effect on survival of E. coli exonuclease III and endonuclease IV deficient cells and induces bacterial filamentation in E. coli cultures proficient and deficient in DNA repair depending of growth phase.

8569-11, Session 3

Effects of speckle-like laser irradiation on growth of bacteria in vitro

Andreiy Yu. Popov, Nataliya A. Popova, Aleksandr V. Tyurin, Odessa National Univ. named after I. I. Mechnikov (Ukraine); Valentin M. Grimblatov, Photonics Life Technologies (United States)

There is ongoing debate about the importance of coherence of the light going through biological tissue for phototherapy. It has been argued that speckle phenomenon related to the coherence can play the major role in photobiostimulation. Several mechanisms have been proposed to explain biological effects of the speckles but no experimental work has been performed.

In this work we, for the first time, have experimentally demonstrated stimulation of bacterial growth inhibition by laser with interference pattern of intensity distribution and propose a mechanism for photobiomodulation by small-scale inhomogeneous laser irradiation.

In our experiments we measured the growth of Staphylococcus aureus and Peudomonas aeruginosa bacteria in vitro with and without antibiotic illuminated by laser light with homogeneous or interference spatial distribution of intensity. The spatial frequency of the interference field was controlled and study included control.

The effect of stimulation of bacterial growth compared to control was demonstrated. The effect varied significantly with changes of the spatial frequency of the interference field. Maximum inhibition of the bacteria growth was achieved at the spatial frequency 1000 1/mm. There was no stimulation of the growth inhibition with homogeneous distribution of the illumination

A potential explanation of photobiomodulation by laser speckles can rely on the photostimulated diffusion of ions (Dember effect) similar it is in inorganic media under inhomogeneous illumination. The Dember photo-induced local electric fields can alter the charge state of the membranes and stimulate penetration of biologically active substances through them, i.e. lead to changes in the life cycle of cells or microorganisms

8569-12, Session 3

Biostimulative effect of 809-nm diode laser and indocyanine green on p. aeruginosa instead of photodynamic effect

(Invited Paper)

Nuray Aysan, Nermin Topaloglu, Sahru Yueksel, Murat Gulsoy, Bogaziçi Üniv. (Turkey)

Photodynamic therapy (PDT) is a safe and alternative antimicrobial treatment that consists of a chemical agent, called photosensitizer, which can be activated by light of an appropriate wavelength to produce reactive oxygen species (ROS). PDT can be used for photoinactivation of bacteria in an attempt to overcome the problem of bacterial multidrug resistance. In particular, it is an effective antimicrobial treatment against infected wounds that have antibiotic resistance and wound infections would otherwise lead to mortality and morbidity.

The main purpose of this study was to demonstrate the importance of PDT dosimetry (light dose and concentration of photosensitizer). If the dosimetry of PDT was not optimized properly, photoinactivation of bacteria cannot be achieved and even worse biostimulation on pathogens could be observed. This study investigated whether there is a biostimulative effect due to free oxygen radicals of PDT when light dose and photosensitizer concentration are too low.

In this study, the biostimulative effect on P. aeruginosa strain was observed instead of the PDT effect, when 84 J/cm2 of energy dose (809-nm diode laser) was applied with 20, 50, 100 and 150 ?g/ml of ICG concentrations. The killing effect of PDT was observed with higher ICG concentrations, such as 200, 250 ?g/ml of ICG. However the killing effect was not enough to destroy pathogen efficiently with these high concentrations of ICG.

8569-13, Session 3

Transcranial low-level light therapy induces neurogenesis and synaptogenesis in mice *(Invited Paper)*

Michael R. Hamblin, Weijun Xuan, Shih-Fong Huang, Qiuhe Wu, Ying-Ying Huang, Wellman Ctr. for Photomedicine (United States)

We have previously shown that transcranial low level light therapy (LLLT) can ameliorate brain damage in mice subjected to traumatic brain injury and improve neurological function. We used a 810-nm laser and delivered

18 J/cm2 at an irradiance 25 mW/cm2. LLLT was either delivered once at 4 hours after controlled cortical impact TBI, once a day for 3 days, or once a day for 14 days. One and 3 applications of LLLT had beneficial effects on the mice, with 3 being better than 1, but 14 applications had no beneficial effect. We now report immunofluorescence studies in mouse brain sections that offer some explanation for this intriguing finding. Mice were injected with BrdU for 1 week before sacrifice (a marker for proliferating cells) and antibodies to double cortin (DCX-1,a marker of migrating neurons), Tuj-1 (a marker of neuroprogenitor cells), BDNF (brain derived neurotrophic factor) and synapsin-1 (a marker for newly formed synaptic connections between existing neurons). We found increased BrdU incorporation indicating proliferating cells in the dentate gyrus of the hippocampus, the subventricular layer of the lateral ventricle, as well as the brain tissue surrounding the cortical lesion. Interestingly these cells were more abundant at 7 days than at 28 days post TBI. Co-labeling of BrdU with Neu-N was performed indicating that the proliferating cells were in fact neuronal in nature. Mice with 3 laser treatments had much more BrdU incorporation than mice with 14. Upregulation of BDNF was seen at 7 days, and increased expression of DCX-1 and Tuj-1 was seen at 28 days in the lesion region, indication that neuroprogenitor cells may have migrated there from sites of neurogenesis. Increased syapsin-1 was seen in the cortex at 28 days indicating that neural plasticity may be stimulated by LLLT. Taken together these data suggest that transcranial LLLT may have applications beyond TBI in areas such as neurodegenerative disease and psychiatric disorders.

8569-20, Session PSat

Raman study of the effect of LED light on grafted bone defects

Luiz Guilherme P. Soares, Antônio Luiz B. Pinheiro D.D.S., Gilbeth Tadeu S. Aciole D.D.S., Jouber Mateus S. Aciole, Artur F. Barbosa, Univ. Federal da Bahia (Brazil); Landulfo Silveira Jr., Camilo Castelo Branco Univ. (Brazil)

Benefits of the isolated or combined use light and biomaterials on bone healing have been suggested. Our group has used several models to assess the effects of laser on bone. A Raman spectral analysis on surgical bone defects grafted or not with Hydroxyapatite (HA), treated or not with LED was carried out. 40 rats were divided into 4 groups. On Group I the defect was filled with the clot. On Group II, the defect was filled with the HA. On groups III the defect was filled with Clot and further irradiated with LED and on group IV the defects was filled with the HA and further irradiated with LED. LED (?850 ± 10nm, 150mW, A= 0.5cm2, 68s, 20 J/cm2 per session, 140 J/cm? per treatment) was applied at 48 h intervals during 15 days. Specimens were taken after 15 and 30 days after surgery and kept on liquid nitrogen, and underwent Raman analysis. For this, the peak of hydroxyapatite (~960 cm-1) was used as marker of bone mineralization. Significant difference was observed at both times ($p<0.05$). When the biomaterial was used higher peaks were observed. Association with LED further improved the intensity. Conclusion: It is concluded that LED light improved the effect of the HA.

8569-21, Session PSat

Green LED associated to hydrogen peroxide 20% for dental bleaching: nanomorfology study of enamel by scanning electron microscopy

Priscila C. Oliveira D.D.S., Susana P. S. Olivera D.D.S., Juliana S. Monteiro D.D.S., Gustavo M. P. Santos, Fernando J. P. Sampaio D.D.S., Maria Gesteira D.D.S., Maria Antonia de Fatima Zanin D.D.S., Antônio Luiz B. Pinheiro, Univ. Federal da Bahia (Brazil)

Dental bleaching is a very requested procedure in clinical dental practice and widely related to dental esthetics. The literature is contradictory regarding the effects of bleaching agents on the morphology and desmineralization of enamel after bleaching. The aim of this study was to analyze in vitro by scanning electron microscopy (SEM) the effect of hydrogen peroxide at 20% at neutral pH, cured by the green LED, to evaluate the action of these substances on dental enamel. We selected 15 pre-molars, lingual surfaces were sectioned and previously marked with a central groove to take the experimental and control groups on the same specimen. The groups were divided as follows.The mesial hemi-faces were the experimental group and distal ones as controls. For morphological analysis were performed 75 electron micrographs SEM with an increase of 43X and 220X and its images were evaluated by tree observers. Was also performed quantitative analysis of the determination of the surface atomic composition of the samples through microanalysis with the aid of scanning electron microscope. The use of hydrogen peroxide at a concentration of 20% at photoactivated green LED showed no significant changes in mineral composition of the samples or the dental morphological structure of the same when compared to their controls, according to the study protocol.

8569-22, Session PSat

Traditional phenothiazine derivatives as promising photosensitizers for a photodynamic antimicrobial chemotherapy (PACT) against parasites of Leishmania braziliensis: in vitro study

Artur F. Barbosa, Univ. Federal da Bahia (Brazil); Bruno B. Sangiorgi, Fundacao Oswaldo Cruz (Brazil) and Centro de Pesquisas Gonçalo Moniz (Brazil); Suely L. Galdino, Univ. Federal de Pernambuco (Brazil); Manoel B. Netto, Fundacao Oswaldo Cruz (Brazil); Ivan R. Pitta, Univ. Federal de Pernambuco (Brazil); Antônio Luiz B. Pinheiro, Univ. Federal da Bahia (Brazil)

According to WHO leishmaniasis representing a worldwide public health problem. The disease is estimated to cause 1.6 million new cases each year, of which an estimated 500 000 are visceral and 1.1 million cutaneous or mucocutaneous. Pentavalent antimonials, including sodium stibogluconate (Pentostam) and meglumine antimoniate (Glucantime), have been used in the treatment of leishmaniasis for over 50 years and they exhibit several limitations like severe side effects. Photodynamic Antimicrobial Chemotherapy (PACT) presents itself as a new proposal for a therapy against parasites. We aimed to verify the effectiveness of PACT in vitro, as a new technique for the treatment of Leishmaniasis. We used a semiconductor laser (? = 660nm, 40mW, 8,4 J/cm2, CW) associated to phenothiazine's derivatives (5 and 10 µg/ml, TBO, Methylene Blue or Phenothiazine) on the promastigotes form of Leishmania braziliensis in a single session. The parasites were incubated for 60 min in the presence of photosensitizers for subsequent irradiation. Viability of the parasites was assessed in quadruplicates of each group. The samples were removed and analyzed in a hemocytometer 72h after PACT. We found an important decrease in the number of viable parasites on all treated groups in comparison to their controls. Our results demonstrated significant percentage of lethality (above 95%), even using concentrations below those reported in the literature.

8569-23, Session PSat

Use of laser phototherapy on oral mucositis associated with CMF in FAC chemotherapy protocols in patients with breast cancer

Fabiola B. Carvalho D.D.S., Maria F. Ferreira, Susana Carla P. Oliveira D.D.S., Juliana S. Monteiro D.D.S., Gustavo M. P. Santos, Maria Gesteira, Tereza C. Maia, Antônio Luiz B. Pinheiro, Univ. Federal da Bahia (Brazil)

The aim of this study was to evaluate the efficacy of laser phototherapy in the prevention and treatment of oral mucositis induced by chemotherapy CMF (cyclophosphamide, methotrexate, 5-Fluouracil) and FAC (5 Fluouracil + Adriamycin + Cyclophosphamide) protocols in breast cancer patients. 28 patients undergoing one of the protocols were divided into three groups: A - 8 patients (Protocol FAC + Routine dental protocol + Laser), B - 6 patients (Protocol CMF + + Routine dental protocol + Laser), C - was divided into two sub-groups: Group C1 - 8 patients (Control Group 1: Protocol FAC + Routine dental protocol) and C2 - 6 patients (Control Group 2: Protocol CMF + + Routine dental protocol). Patients in Groups A and B received Laser 24 hours before chemotherapy cycle and repeated at every 48 hours up to one week after conclusion of the cycle. The results showed that Groups A and B presented oral mucositis grade 0 (64.29%), grade I (7.14%), grade II (14.29%), grade III (7.14 %), grade IV (7.14%). Group C1 and C2 presented mucositis grade 0 (35.71%) in the initial evaluation, grade I (21.43%), grade II (28.57%), grade III (14.29%), grade IV (0.00%). The results showed pain relief in 42.86% patients who used the laser as a preventive or therapeutic. It is concluded that the Laser caused immediate pain relief and accelerated healing.

8569-24, Session PSat

Photodynamic antimicrobial chemotherapy (PACT) using Phenothiazines derivatives associated with the red LED against staphylococcus aureus (ATCC 23529): in vitro

Anderson F. S. Miranda, Fundacao Oswaldo Cruz (Brazil); Gustavo M. Pires-Santos, Fundacao Oswaldo Cruz (Brazil) and a+ Medicina Diagnóstica (Brazil); Susana Carla P. Oliveira, Juliana S. Monteiro, Fernando J. P. Sampaio, Maria Gesteira, Fátima A. Zanin, Univ. Federal da Bahia (Brazil); Marcos A. V. Santos, Fundacao Oswaldo Cruz (Brazil); Antônio Luiz B Pinheiro, Univ. Federal da Bahia (Brazil)

The objective of this study was evaluating the bactericidal effect of PACT using phenothiazine derivatives at a concentration of 1.0µg/ mL and red LED at doses of 12J/cm? against S.aureus. The PACT is a treatment based on cytotoxic photochemical reaction in which a source of intense light activates a photosensitizer. This activation induces series of reactions which lead to the increase in free radicals (ROS) and subsequent cell death. For this research, tests were performed in quadruplicate, with four groups: Control (L-P-); LED (L+P-); LED and phenothiazine (L+P+); only phenothiazine (L-P+). Therefore, we analyzed the PACT bactericidal potential of phenothiazine associated with the red LED by means of turbidimetry and production of ROS, via fluorescence microscopy (FM), employing dihydroethidium (DHE) probe. This treatment protocol did not show statistically significant mortality between the groups when we analyzed the numbers of bacteria. Furthermore in the qualitative evaluation by FM was not observed labeled bacteria were visualized with probe in the control, in the group with only the phenothiazine or in the group treated only with LED. Though, in the L+P+ group most bacteria present was marked by DHE showing the production of ROS after LED application. Due to the production of ROS already provided it is believed that enhancing the production of it in these protocol will become more lethal against S. aureus. Therefore, it was concluded that the phenothiazine compounds when combined with red LED increase the production of ROS in bacteria and therefore can be regarded as promising treatment protocol.

8569-25, Session PSat

The response of human retinal pigment epithelium cells in vitro to changes in [NO] stimulated by low-levels of red light

Brent J. Lavey, U.S. Air Force (United States); Larry E. Estlack, Conceptual MindWorks, Inc. (United States); Kurt J. Schuster, TASC, Inc. (United States); Benjamin A. Rockwell, Air Force Research Lab. (United States); Jeffrey C. Wigle, U.S. Air Force (United States)

This research is to elucidate the role of nitric oxide (NO) in regulating the physiological response of hTERT-RPE cells in vitro following exposure to low levels of red light (photobiomodulation). In hTERT-RPE cell cultures exposed to 2.88 J/cm2 of red light (671 nm LED or 637 nm fiber laser) intracellular NO levels begin to increase within 1 hr of exposure and adenosine triphosphate (ATP) levels have about doubled at 4 hr post exposure. The increase in NO is followed by peaks in the levels of NF-?B and Bcl-2 mRNAs at 6 hr post exposure, and their respective proteins at 24 hr post-exposure; NF-?B is a protein that controls the transcription of DNA and Bcl-2 is an anti-apoptosis protein. In contrast, 24 hr post-exposure to red light, the level of Bax, a pro-apoptosis protein, is less than 50% of unexposed controls. The initiating event is thought to be photo-excitation of cytochrome c oxidase (Cco), which results in ejection of NO from the active site of Cco. This allows O2 to replace NO, which facilitates electron transfer and ATP synthesis. However, despite the increase in intracellular NO, exposure to red light did not affect the levels of inducible NO synthase (iNOS) mRNA, and NO and ATP levels in iNOS inhibited cells were not different from controls. This suggests that light-induced NO production is dependent on Cco, supporting the notion that Cco is the primary chromophore in low-level red light stimulation and that NO plays a role in the downstream effects of photobiomodulation.

8569-26, Session PSat

Photodynamic antimicrobial chemotherapy (PACT) using phenothiazines derivatives associated with the red LASER against staphylococcus aureus (ATCC 23529) in vitro

Gustavo M. P. Santos, Fundacao Oswaldo Cruz (Brazil) and a+ Medicina Diagnóstica (Brazil); Juliana S. Monteiro, Univ. Federal da Bahia (Brazil); Susana C. de Oliveira, Anderson F. S. Miranda, Fundacao Oswaldo Cruz (Brazil); Fernando J. P. Sampaio, Maria Gesteira, Univ. Federal da Bahia (Brazil); Marcos A. V. dos Santos, Fundacao Oswaldo Cruz (Brazil); Fatima A. Zanin, Antônio Luiz B. Pinheiro, Univ. Federal da Bahia (Brazil)

The objective of this study was to evaluating the bactericidal effect of PACT using phenothiazine at a concentration of 1.0µg/mL and red LASER at doses of 2.4J/cm? against S.aureus. The PACT is a treatment based on cytotoxic photochemical reaction in which a source of intense light activates a photosensitizer. This activation induces a series of reactions which lead to the increase in free radicals (ROS) and subsequent cell death. For this research, tests were performed in quadruplicate, with four groups: Control (L-P-); LASER (L+P-); LASER and phenothiazine (L+P+); only phenothiazine (L-P+). Therefore, we analyzed the PACT bactericidal potential of phenothiazine associated with red LASER by means of turbidimetry and production of ROS, via fluorescence microscopy (FM), employing dihydroethidium (DHE) probe. This treatment protocol did not show statistically significant mortality between the groups when we analyzed the bacteria numbers. Furthermore, the qualitative evaluation by FM was not observed labeled bacteria were visualized by probe in the control, in L-P+. However, immediately after the treatment L+P- was possible observed ROS presence, but few prokaryotes were marked. Though, in the L+P+ group most bacteria present was marked by DHE showing the production of ROS after LASER application. Due to the production of ROS already provided it is believed that enhancing the production of ROS this protocol will become more lethal against S.aureus. Therefore, it was concluded that the phenothiazine when combined with red LASER increase the production of ROS in prokaryotes and therefore can be regarded as promising treatment protocol.

8569-27, Session PSat

Low-level laser therapy (LLLT) using 635-nm light emitting diode (LED) inhibits bone resorptive osteoclast formation by regulating the actin cytoskeleton

Hyun-Ju Lim, Jang-In Shin, Man-Seok Bang, Chung-Hun Oh, Dankook Univ. (Korea, Republic of)

Bone diseases such as osteoporosis are mainly caused by up-regulated activity of osteoclasts. The present study was designed to examine the effects of Low Level Laser Therapy (LLLT) on the formation and activity of multinucleated osteoclasts, specifically 'round-shaped' osteoclast cells (ROC) in mouse derived macrophage lineage cell line, RAW264.7. The cells were irradiated by 400~900nm LED arrays during cultures (30mW/cm2 or 2mW/cm2). The cell viability was evaluated by MTT assay. The amount of total TRAP+ osteoclast and the number of ROC cells were estimated by TRAP solution assay and TRAP staining, respectively. Actin rings were stained with rhodamine-conjugated phalloidin, and resorption assay was performed by dentin slices. In addition, gene expression levels between the control and irradiation groups were evaluated by RT-PCR. In a morphological analysis, the formation of ROC was significantly inhibited by 635nm at 2mW/cm2 for 72hrs. Actin rings were seen at cell peripheries in most ROC cells of the control group but patches containing disorganized actin were found in the irradiation group. The number of ROC and bone resorption activity was much lower in the irradiation group than in the control group. Also, the gene expression levels involved in actin ring formation such as integrin ?3 and c-Src decreased in RT-PCR analysis. Overall, LLLT using 635nm LED may play a pivotal role in regulating bone remodeling, and it may prove to be a valuable tool for the treatment of bone diseases such as osteoporosis.

8569-14, Session 4

Photobiomodulation protects against retinal degeneration in a rodent model of retinitis pigmentosa

Janis T. Eells, Sandeep Gopalakrishnan, Heather Schmitt, Univ. of Wisconsin-Milwaukee (United States); Adam M. Dubis, Joseph Carroll, Medical College of Wisconsin (United States)

PURPOSE: Irradiation by light in the far-red to near-infrared (NIR) region of the spectrum (photobiomodulation, PBM) has been demonstrated to attenuate the severity of neurodegenerative disease in experimental and clinical studies. The purpose of this study was to test the hypothesis that 830 nm PBM would protect against the loss of retinal function and improve photoreceptor survival in a rodent model of retinitis pigmentosa, the P23H transgenic rat. METHODS: P23H rat pups were treated once per day for 180 seconds with an 830 nm LED array (25 mW/cm2; fluence 4 joules/cm2) (QBMI Photomedicine, Barneveld WI) from postnatal day (p) 10 to p25. Sham-treated rats were restrained for 180 seconds, but not exposed to NIR light. The status of the retina was determined at p30 by measuring photoreceptor function by ERG and retinal morphology by Spectral Domain Optical Coherence Tomography (SD-OCT). RESULTS: 830 nm PBM profoundly attenuated retinal degeneration in the P23H transgenic rat. NIR treatment preserved retinal function and retinal morphology in treated animals in comparison to the sham-treated group. Using the ISCEV protocol the rod photoreceptor response was 8.8 ± 0.7 µV in sham treated animals and 14.8 ± 2.2µV in PBM treated animals ($P<0.05$, n=4). CONCLUSIONS: Results from this study demonstrate the retinoprotective effects of 830nm PBM in a transgenic animal model of retinal degeneration and support the use of PBM as an innovative, non-invasive therapeutic approach for the treatment of retinal degenerative disease.

8569-15, Session 4

Study of T lymphocytes activation in cutaneous repair of diabetic rats treated with low-level laser therapy

Cristiane M. França D.D.S., Cristiano L. Santana, Brunna P. A. Sampaio, Fabiana Santos, Kristianne P. S. Fernandes D.D.S., Alessandro M. Deana, Raquel A. Mesquita-Ferrari, Daniela F. Silva, UNINOVE (Brazil)

The healing process of diabetic patients is often inefficient leading to chronic ulcers. Laser therapy is a promising tool to assist the closure of these wounds. This study evaluated T lymphocyte activation in wound repair of diabetic animals which underwent laser therapy, comparing two systems of delivery of laser light. 54 male Wistar rats (Rattus norvegicus albinus) with diabetes induced by intraperitoneal injection of streptozotocin (50mg/kg) were used. The ulcer was made using a 8 mm-punch in the back of the animal after trichotomy. Experimental groups: (1) control group (CG) - the sore back was not treated, (2) single dose (SDG) - dorsal ulcer received laser therapy two hours after the wound, (3) fractionated dose (FDG) - the ulcer received laser therapy on days 0, 3, 8, 10. Laser parameters for application in SGD: ? = (660 ± 2) nm, I = 6mW/cm2, D= 4 J/cm2, t = 668 s; and for FDG group were four doses of ? = (660 ± 2) nm, I = 6mW/cm2, D= 1 J/cm2, t = 167 s totalizing 4 J/cm2. At days 0, 3, 8, 10 and 14 the animals were euthanized and the ulcers were removed, routinely processed for hematoxylin & eosin stain and for immunohistochemistry to CD3 and CD45RO antigens. The presence and type of the inflammatory infiltrate, presence of granulation tissue, number of T lymphocytes, and activated T lymphocytes will be presented.

8569-16, Session 4

Influence of two laser light delivery protocols in the cutaneous healing of diabetic rat: morphological and myofibroblast evaluation

Brunna P. A. Sampaio, Cristiano L. Santana, Fabiana Santos, Kristianne P. S. Fernandes D.D.S., Raquel A. Mesquita-Ferrari, Alessandro M. Deana, Daniela F. Silva, Cristiane M. França, UNINOVE (Brazil)

Chronic ulcers in diabetic individuals are one of the main causes of amputation. Laser therapy is a promising tool to assist the closure of these wounds. This study compared tissue repair of diabetic ulcers under two systems of delivery of laser light. 54 male Wistar rats (Rattus norvegicus albinus) with diabetes induced by an intraperitoneal injection of streptozotocin (50mg/kg) were used. The ulcer was made using a 8 mm-punch in the back of the animal after trichotomy. Experimental groups: (1) control group (CG) - the sore back was not treated, (2) single dose (SDG) - dorsal ulcer received laser therapy two hours after the wound, (3) fractionated dose (FDG) - the ulcer received laser therapy on days 0, 3, 8, 10. Laser parameters for application in SGD: ? = (660 ± 2) nm, I = 6mW/cm2, D= 4 J/cm2, t = 668 s; and for FDG group were four doses of ? = (660 ± 2) nm, I = 6mW/cm2, D= 1 J/cm2, t = 167 s totalizing 4 J/cm2. At days 0, 3, 8, 10 and 14 the animals were euthanized and the ulcers were removed, routinely processed for hematoxylin & eosin stain and for immunohistochemistry to alpha smooth muscle actin, a myofibroblast marker. The presence and type of the inflammatory infiltrate, granulation tissue, number of myofibroblasts will be presented.

8569-17, Session 4

Laser immunotherapy for advanced breast cancer: a case report

Tomas Hode, Immunophotonics, Inc. (United States); Orn Adalsteinsson, International Strategic Cancer Alliance (United States); Gabriela L. Ferrel, Hospital Nacional Edgardo Rebagliati Martins (Peru); John A. Lunn, Commonwealth Medical Research Institute (Bahamas); Xiaosong Li, Chinese PLA General Hospital (China); Robert E. Nordquist, Immunophotonics, Inc. (United States); Wei R. Chen, Univ. of Central Oklahoma (United States)

Laser Immunotherapy is a drug/device combination therapy that utilizes a local intervention to induce a systemic anti-tumor immunity. The two principles underlying LIT are (1) local destruction of tumor cells resulting from direct delivery of laser energy into the tumor, which liberates tumor antigens and in itself induces a local immune response, and (2) local administration of an immunoadjuvant to elicit a much stronger systemic immune response. The fundamental mechanism behind LIT is the activation of antigen-presenting cells, such as dendritic cells, and subsequent exposure of the activated APCs to tumor antigens in vivo so that a tumor-specific T cell response is induced. Several late stage cancer patients have been treated with LIT with engouraging results. Here we present a case report of a metastatic breast cancer patient, and we also discuss the importance of using advanced imaging modalities for assessing the response to the treatment.

8569-18, Session 4

Influence of wavelength on the outcome of treatment of TMJ disorders: TMDS

Antônio Luiz B. Pinheiro D.D.S., Aparecida Maria C. Marques D.D.S., Carolina M. Carvalho D.D.S., Maria Cristina T. Cangussu D.D.S., Luiz Guilherme P. Soares, Univ. Federal da Bahia (Brazil)

It is known that wavelength influences the outcome of many clinical protocols. Laser-phototherapy (LPT) and LEDs have been used on the treatment of pain of several origins including Temporomandibular disorders - TMDs. TMDs are common painful multifactorial conditions affecting the temporomandibular joint whose treatment depends on the type and symptoms. Initially it requires pain control and for this, drugs, biting plates, oclusal adjustment, physiotherapy or their association are used. This work reports a series of patients of the Center of Biophotonics of the Federal University of Bahia over 10 years. Following standard anamneses, clinical and imaginologic examination and with the diagnosis of any type of TMD, the patients were set for light treatment. Treatment consisted of three sessions a week during six week. Prior irradiation, the patients were asked to score their pain using a VAS. ?780, ? 790, ? 830nm and/or ?660 and ?680nm lasers or LED were used on each session. Most patients were female (~46years old). At the end of the 12 sessions the patients were again examined and score their pain using VAS. No other intervention was carried out during the treatment. The results were statistically analyzed and showed that most patients were asymptomatic or improved after treatment and that the association of wavelengths was very efficient on the symptomatic group. It is concluded that the association of both wavelengths was effective on pain reduction on TMJ disorders of several origins.

8569-19, Session 4

Laser-acupuncture for autism/autism spectrum disorder: a randomized sham controlled trial

Shahzad Anwar, Anwar Shah's First C.P. and Paralysis Clinic and Research Ctr. (Pakistan)

OBJECTIVES: To evaluate the efficacy, safety, and compliance of laser-acupuncture in children with autism spectrum disorder (ASD). DESIGN: Randomized, sham controlled, double blind trial, with blinded evaluation, statistical analysis of results and standardized parent report. SUBJECTS AND INTERVENTIONS: Children with ASD were randomly separated into two groups one receiving laser-acupuncture (LA) group (n=60) and the other sham laser-acupuncture (SLA) group (n=56) matched by age and severity of autism. The LA group received laser-acupuncture for selected acupoints while the SLA group received sham laser-acupuncture to sham acupoints. A total of 24 LA and SLA sessions over 12 weeks were given. Primary outcome measures included Functional Independence Measure for Children (WeeFIM), Pediatric Evaluation of Disability Inventory (PEDI), Leiter International Performance Scale- Revised (Leiter-R), and Clinical Global Impression- Improvement (CGI-I) scale. Secondary outcome measures consisted of Aberrant Behavior Checklist (ABC), Ritvo-Freeman Real Life Scale (RFRLS), Reynell Developmental Language Scale (RDLS), and a Standardized Parental Report. Data were analyzed by the Mann-Whitney test. RESULTS: There were significant improvements in the language comprehension domain of WeeFIM (p=0.02), self-care caregiver assistant domain of PEDI (p=0.028), and CGI-I (p=0.003) in the LA group compared to the SLA group. As for the parental report, the LA group also showed significantly better social initiation (p=0.01), receptive language (p=0.006), motor skills (p=0.034), coordination (p=0.07), and attention span (p=0.003). All children with ASD adapted to laser-acupuncture easily. Mild side effects of irritability during laser-acupuncture were observed. CONCLUSION: A twelve-week (24 sessions) course of laser-acupuncture is useful to improve specific functions in children with ASD, especially for language comprehension, social initiation, motor skills and self-care ability.

8570-1, Session 1

A computational approach to optimize microring resonators for biosensing applications

Brett R. Wenner, Air Force Research Lab. (United States); Justin C. Wirth, Purdue Univ. (United States) and Birck Nanotechnology Ctr. (United States); Monica S. Allen, Jeffery W. Allen, Air Force Research Lab. (United States); Minghao Qi, Purdue Univ. (United States) and Birck Nanotechnology Ctr. (United States)

Microcavity structures have recently found utility in chemical/biological sensing applications. The appeal of these structures over other refractive index-based sensing schemes, such as those based on surface plasmon resonance, lies in their potential for producing a highly sensitive response to binding events. High-Q devices, characterized by sharp line widths, are extremely attractive for sensing applications because the bound analyte provides an increased optical pathlength, thus shifting the resonant frequency of the device. In this work, we design and simulate resonant microrings using full-wave finite element models. In addition to structure design, integration of the biological recognition element on the resonator is also considered. This is equally important in dictating the sensitivity of the sensing device. To this end, we take a four-step theoretical approach to optimizing the sensor. We begin by using FEM analysis to obtain the characteristic resonant wavelength, line width, and quality factor for bare ring resonators absent of surface functionalization. Next, we simulate the structure with a biorecognition element attached to the surface. The third step is to model the functionalized microring to mimic the interaction with the target analyte. At each step, we derive the transmission spectra, electric field distributions and coupling efficiencies, as well as wavelength dependence using empirical data for the refractive indices of biorecognition element and analyte. Finally, the geometry of the microrings is optimized in conjunction with the constituent material properties and the recognition chemistry using FEM combined with an optimization algorithm to maximize the sensitivity of the integrated biosensor.

8570-2, Session 1

Cascaded microring resonators for biomedical applications: improved sensitivity at large tuning range

Alethea V. Zamora Gomez, Daniel Pergande, Peter Lützow, Helmut Heidrich, Fraunhofer-Institut für Nachrichtentechnik Heinrich-Hertz-Institut (Germany)

The progress in the biomedical analysis has placed a growing demand on the innovation of reliable, miniaturized and low cost optical sensor systems based on integrated optical devices. We present a detailed analysis of sensor elements for applications in aqueous solutions based on two cascaded microring resonators by using the Vernier effect (VE). This approach is beneficial for ultra-high sensitivity at large free spectral range (FSR) and fabrication tolerances, aspects of crucial important for the practical detection of biomolecules such as peptides. The architecture consists of two silicon nitride microrings connected via a bus waveguide. The FSR of individual rings is slightly different in order to achieve VE. Meanwhile the external refractive index of the reference ring is fixed; the second one varies due to the presence of the analyte. The precise operating is controlled by using spectral tuning via integrated micro-heaters. Theoretical analysis has been performed for different structural parameters. A sensitivity of 10^4 nm/RIU can be predicted for the TE polarization and 10^5 nm/RIU for the TM polarization. The realization and experimental characterization of first devices will be presented. The devices include tapered grating couplers in order to couple light between fibers and the chip at moderate alignment tolerances in a reliable manner. Therefore, by combining the VE and the spectral tuning, cascaded microring resonators will be an optical configuration very promising for sensing applications.

8570-3, Session 1

FDTD simulation of microring resonator-based sensing

Dan T. Nguyen, Robert A. Norwood, College of Optical Sciences, The Univ. of Arizona (United States)

Recently, there has been great progress in the field of biosensors with extreme sensitivity down to single molecules or single particles of micron- or even nanometer scales. The enhancement mechanism responsible for this high sensitivity is the use of whispering gallery modes (WGM) in optical micro-cavities such as microrings, microspheres and microdisks, in which the WGM resonance enables multiple interactions between the guided light and the sensing object (SO). As a result, the WGM resonance enhances the sensitivity to a level at which a single molecule or particle can be detected. Usually, simplified analytic models based on coupled-mode theory are used to calculate the shift of the WGM wavelength in the presence of the SO, assuming the change of the optical path in the cavity when it couples with a SO depends on the refractive index and size of the sensing object. However, these analytical approaches fail to encompass many significant and complex factos, such as using the real shape and eigenmodes of the SO, determining the radiation losses of the light field in the tapered fiber and in the micro-cavity, as well as the scattering loss in the system. All of these factors can be addressed through FDTD simulation as presented in this paper. More importantly, the FDTD can yield the resonant modes of the sensing object, which are easier to observe than the small resonance wavelength shift predicted by coupled-mode theory.

8570-5, Session 1

Detection of small and large molecules using a porous silicon grating-coupled Bloch surface wave label-free biosensor

Gilberto A. Rodriguez, Judson D. Ryckman, Yang Jiao, Vanderbilt Univ. (United States); Robert L. Fuller, Villanova Univ. (United States) and Vanderbilt Univ. (United States); Sharon M. Weiss, Vanderbilt Univ. (United States)

A grating coupled porous silicon (pSi) Bloch Surface Wave (BSW) biosensor capable of supporting a surface mode is demonstrated for the real-time detection of both small and large molecules. Porous silicon is a powerful label-free biosensing platform for small molecules due to its tunable optical properties, enhanced surface area, as well as its rapid and cost-effective fabrication. Most pSi sensor platforms, however, are unable to perform high sensitivity detection of large molecules that do not infiltrate into the porous matrix. In this work, we show that the grating-coupled pSi-BSW sensor with a flow cell attached has more than 15% of the energy density confined to the surface of the structure, which allows for the high sensitivity detection of surface-bound large molecules.

Angle-resolved reflectance measurements are performed to quantify the detection sensitivity of the pSi BSW sensor towards one large molecule and two small molecules: 40-base thiol-modified probe DNA, 3 aminopropyltriethoxysilane, and Sulfosuccinimidyl-4-(N-maleimidomethyl) cyclohexane-1-carboxylate, respectively. The performance of the sensor is experimentally and theoretically compared to pSi waveguide and microcavity sensors. The sensors show comparable sensitivity towards the detection of the small molecules while the BSW sensor is superior for detection of the large molecule. The experimental results are in good

agreement with simulations based on rigorous coupled wave analysis and the transfer matrix method. We conclude that the grating-coupled pSi BSW sensor is a versatile sensor for the detection of a variety of molecules bound inside as well as on the surface of the structure.

8570-6, Session 2

Silicon photonic crystal microarrays for high throughput label-free proteomics for detection of cancers with sensitivity and specificity *(Invited Paper)*

Swapnajit Chakravarty, Omega Optics, Inc. (United States); Ray T. Chen, Wei-Cheng Lai, Yi Zou, The Univ. of Texas at Austin (United States); Robert M. Gemmill, Medical Univ. of South Carolina (United States)

Detection of biomolecules on microarrays based on label-free on-chip optical biosensors is very attractive since this format avoids complex chemistries caused by steric hindrance of labels. Application areas include the detection of cancers and allergens, and food-borne pathogens to name a few. We have recently demonstrated photonic crystal microcavity biosensors with high sensitivity down to 1pM concentrations. High sensitivities were achieved by slow light engineering which reduced the radiation loss and increased the stored energy in the photonic crystal microcavity resonance mode. Resonances with high quality factor Q~26,760 coupled with larger optical mode volumes allowed enhanced interaction with the analyte biomolecules which resulted in sensitivities down to 10 cells per micro-liter to lung cancer cell lysates. The specificity of detection was ensured by multiplexed detections from multiple photonic crystal microcavities arrayed on the arms of a multimode interference power splitter. Specific binding interactions and control experiments were performed simultaneously at the same instant of time with the same 60 micro-liter sample volume. Specificity is further ensured by sandwich assay methods in the multiplexed experiment. Sandwich assay based amplification increased the sensitivity further resulting in the detection of lung cancer cell lysates down to concentrations of 2 cells per micro-liter. The miniaturization enabled by photonic crystal biosensors coupled with waveguide interconnected layout thus offers the potential of high throughput proteomics with high sensitivity and specificity. We will review our recent work.

8570-7, Session 2

Evanescent field trapping of bacteria using photonic crystal cavities

Thijs van Leest, Jaap Caro, Technische Univ. Delft (Netherlands)

For societal needs such as monitoring the quality of drinking water, lab-on-a-chip techniques combining photonics with microfluidics are promising for on-site and early detection of hazardous bacteria. In this context, our research focuses on single cell optical trapping and Raman-sensing using the enhanced evanescent field of resonators at the scale of a bacterium. Photonic crystals (PhCs) can provide the versatile platform where cavities are engineered as sites with strong field enhancements, exploited for evanescent field trapping and Raman excitation.

In the work to be presented we focus on the optical trapping aspect. Three types of cavities, of different size compared to a bacterium, are investigated for their suitability to trap with the evanescent field. The cavities are situated in a hole type planar silicon PhC with triangular lattice. The simulation study involves optimization of the designs with 3D FDTD simulations to maximize the energy in the cavity, under the limiting condition of the perturbing effect of the bacterium on the cavity itself. We calculate the optical trapping force acting on a bacterium in the trap using the Maxwell stress tensor. The optimized cavities are fabricated in silicon-on-insulator using e-beam lithography and dry-etching, followed by integration into a microfluidic channel fabricated in a dry-film resist. The devices are characterized from the transmission spectra. Optical trapping events are recorded with a microscope from top. We experimentally demonstrate optical trapping with PhC cavities, using polystyrene beads as force probes as well as bacteria. Further, we compare experimentally derived trapping forces with simulated values.

8570-8, Session 2

Two-dimensional photonic crystal biosensor as a platform for label-free sensing of virus simulants

Rashmi Sriram, James E. Baker, Univ. of Rochester Medical Ctr. (United States); Philippe M. Fauchet, Vanderbilt Univ. (United States); Benjamin L. Miller, Univ. of Rochester Medical Ctr. (United States)

Resonant optical microcavites of two-dimensional photonic crystals (2D PhC) are responsive to refractive index changes in the immediate vicinity and thus constitute a label-free platform for sensing biological molecules. Because their active sensing volume is ~ 1 μm3, exceptionally sensitive detection of biomolecules is in principle achievable from complex biological samples. Previously, we have demonstrated detection of human-IgG proteins and virus-like particles by measuring the optical transmission spectrum from the chip after it has been treated and dried. However, this drying step precludes practical utility of the platform especially in the case of clinical diagnostics wherein multiple samples need to be tested in shorter times. To address this challenge, we present a proof-of-concept demonstration of virus simulant detection in a fluidic environment by integrating microfluidic channels with the 2D PhC biosensor. Results from computational modeling will be presented in addition to the experimental data.

8570-9, Session 2

High yield silicon photonic crystal microcavity biosensors with 100fM detection limit

Yi Zou, The Univ. of Texas at Austin (United States); Swapnajit Chakravarty, Omega Optics, Inc. (United States); Wei-Cheng Lai, Ray T. Chen, The Univ. of Texas at Austin (United States)

We will experimentally demonstrate a silicon photonic crystal (PC) microcavity biosensor with 100 femto-molar detection limit. The device consists of a linear L-type PC microcavity coupled to a W1 PC waveguide (PCW). We have recently demonstrated PC microcavity biosensors with high quality factors Q ~26,760 and high sensitivity down to 1pM concentrations. Our devices have demonstrated sensitivities higher than than competing optical platforms at concentration of 0.1microgram/ml across a range of dissociation constants KD 1 micro-molar to 1 femto-molar. High sensitivities were achieved by slow light engineering which reduced the radiation loss and increased the stored energy in the PC microcavity resonance mode which contributed to high Q as well as enhanced optical mode overlap with the analyte. Slow light engineering also enhanced coupling efficiencies from the input ridge waveguide into the PCW at the resonance frequencies of the PC microcavity. The detection principle is based on the shift in the resonance wavelength when a probe biomolecule in analyte medium binds specifically to its conjugate target biomolecule that is immobilized on the surface functionalized silicon photonic crystal microcavity. The specific binding of avidin to biotin is investigated and the specificity further confirmed by control experiments with bovine serum albumin. High device fabrication yields of PC microcavity biosensors reaching almost 90% have been achieved by coupling light into our devices with chip-integrated sub-wavelength grating couplers instead of end-fire coupling used previously. Sub-wavelength grating couplers are fabricated in the same step as the photonic crystal.

8570-10, Session 3

Microscale tools for measuring spatiotemporal chemical gradients in biological systems *(Invited Paper)*

Charles Henry, David S. Dandy, Stuart Tobet, Colorado State Univ. (United States)

Chemical gradients drive many processes in biology, ranging from nerve signal transduction to ovulation. At present, microscopy is the primary tool used to understand these gradients. Microscopy has provided many important breakthroughs in our understanding of the fundamental biology, but is limited due to the need to incorporate fluorescent molecules into a biological system. As a result, there is a need to develop tools that can measure chemical gradient formation in biological systems that do not require fluorescent modification of the molecules in question, can be multiplexed to measure more than one molecule and is compatible with a variety of biological sample types, including in vitro cell cultures and ex vivo tissue slices. Work from our group centered on the development of microscale tools to measure chemical gradients will be presented. In this project, we have developed a microfluidic interface that allows for sampling from underneath a tissue slice or in vitro cell culture system. The sampling system can resolve up to 19 different ports and can be interface with either electrochemical or fluorescence-based detection methods. Using these two detection methods, we are capable of analyzing the release of either small molecule metabolites or proteins and peptides using immunoassays.

8570-11, Session 3

Detection, isolation, and capture of circulating breast cancer cells with photoacoustic flow cytometry

Kiran D. Bhattacharyya, Martin Njoroge, Brian Gaffigan, Benjamin S. Goldschmidt, Kyle Rood, John A. Viator, Univ. of Missouri-Columbia (United States)

According to the CDC, breast cancer is the most common cancer among women and also the second leading cause of cancer related deaths among women. Metastasis, or the presence of secondary tumors caused by the spread of cancer cells via the circulatory or lymphatic systems, significantly worsens the prognosis of any breast cancer patient. In this study, a technique is developed to detect circulating breast cancer cells in human blood using in vitro photoacoustic flow cytometry. A Q-swtiched laser at 532nm is used to interrogate cells as they flow through the beam path. Cells with pigment emit ultrasound after irradiation as a result of the photoacoustic effect. Rare concentrations of circulating tumor cells in the presence of thousands of non-pigmented leukocytes can be detected with this method. Chromophores are selectively attached to breast cancer cells using immunochemistry. First, the device is calibrated to demonstrate a single-cell detection limit. Then cultured breast cancer cells are added to whole blood to reach a concentration of about 25 - 45 breast cancer cells/mL of blood, a biologically relevant number. An in vitro photoacoustic flow cytometer is used to detect and isolate these cells into a small volume followed by capture with the use of a micromanipulator. This method can not only be used to determine the disease state of the patient and the response to therapy, it can also be used for genetic testing and in vitro drug trials since the circulating cell can be captured and studied.

8570-12, Session 3

A compact spatially encoded flow cytometry apparatus for the detection of fluorescent particles

Félix-Antoine Lavoie, David Béliveau-Viel, Olivier Ratelle, Danny Brouard, Denis Boudreau, Univ. Laval (Canada)

The ability to detect and count single fluorescent particles with sensitivity and accuracy is a significant advantage for cell research and biosensing applications. Fluorescence microscopy is often used for this purpose, but the low throughput of this approach may be problematic. In recent years, flow cytometry has become a popular and powerful tool for the characterization and counting of fluorescent particles because of its flexibility and high throughput. Inspired by the work of Kiesel et al. [1], we have developed a capillary-based spatially encoded flow cytometer specifically for the detection of fluorescent nanoparticles. We use a barcoded capillary to spatially block excitation light and fluorescence emission from the particle in order to temporally encode the fluorescence signal. With suitable data treatment, this provides an enhancement of signal to noise ratio and the possibility to accurately count multiple beads located simultaneouly in the probed volume. This poster will describe the methodology developed to create a gold barcode pattern inside the capillary and present results for the detection of fluorescent particles.

[1] P Kiesel, M Bassler, M Beck and N Johnson (2009), Appl. Phys. Lett. 94(4), 041107. doi:10.1063/1.3070536.

8570-13, Session 3

Biophotonics: a European perspective

Thierry Robin, Jacques Cochard, TEMATYS (France); Frédéric Breussin, Yole Développement (France)

The final objective of the present work is to determine the opportunities and challenges for Biophotonics business development for the next five years with a focus on sensors and systems:

- For health diagnostics and monitoring especially for personalized medicine,

- For air, water and food safety and quality control.The development of this roadmap was initiated and supported by EPIC (The European Photonics Industry Consortium).

European research in Biophotonics is diverse, well represented and of world class. But, there is a large gap between scientists and engineers developing new technologies and the potential end users.

Our study aims to analyse key barriers to overcome before deployment of technology innovations and to chart pathways to their commercial exploitation:

At the technological level:

- Trade-off between spatial resolution, sampling volume or area, and effective interrogation depth,

- Specificity / sensitivity limitations,

- Acquisition speed/throughput,

- Genetically-encoded / biomarker-targeted optical probes,

- Label-free functional monitoring.

At the user level:

- User interface and ergonomics,

- Invasive nature & Miniaturization,

- Reliability,

- Use by non specialist (point-of-care, field-based, on line …)

- Minimal sample preparation.

At the system/integration level:

- Quantitative and rugged information,

- Key components and subsystems,

- Integration of multi-modal approaches providing complementary information,

- Biomedical certification,

- Manufacturing/Cost of the solutions.

We summarize the final roadmap recommendations and data:

- Market application segments and trends,

- Comparison of the situations in Europe, North America and Asia,
- Analysis of the industrial value chains in Europe,
- Analysis of the technology trends and major bottlenecks and challenges per application,
- Aspects related to regulation and standards.

8570-14, Session 4

Taking single virus detection and sizing to the limit with molecular sensitivity within a syringe needle: the birth of nanoplasmonic-microcavity hybrid sensors *(Invited Paper)*

Stephen Arnold, Polytechnic Institute of New York Univ. (United States)

The BioPhotonics community is buzzing at the prospect that ulta-small bio-nanoparticles such as Polio virus and protein can be detected and sized one at a time. As the awareness that the claim of label-free single protein sensing through the frequency shift of a bare microcavity by Armani et al in 2007 fades from lack of independent confirmation, a new approach has captured the community's interest. It is a product of a marriage between nano-optics and micro-photonics, and is poised to take label-free sensing to the limit. Simply stated a nanoplasmonic receptor attached to a microcavity can enhance the frequency shift of the cavity by orders of magnitude upon analyte binding. I will discuss the "Reactive Sensing Principle" that originally led us to this NanoPlasmonic-Microcavity hybrid sensor, and show recent results that confirm its validity. Following this, I will present the design of a Photonic-plasmonic-molecule that can speed up detection rates, maintain sensitivity at the molecular level, and remove thermal noise fluctuations from single bio-nanoparticle measurements. With time permitting I will describe how the most ubiquitious of biomedical gear, a syringe needle, can use these ideas to become smart.

8570-15, Session 4

Sub-wavelength fluorescent polymer coatings to convert standard glass capillaries into robust microfluidic refractometric sensors

Kristopher J. Rowland, Alexandre Francois, Tanya M. Monro, The Univ. of Adelaide (Australia)

A capillary microresonator platform for refractometric bio-sensing is demonstrated by coating the interior of standard thick-walled silica capillaries with a sub-wavelength layer of high-index, dye-doped polymer via a solvent evaporation method. Since no intermediate processing, such as etching or tapering, of the capillary is required, it is anticipated that the sensor can be readily interfaced to existing biological sensing and sorting platforms such as capillary electrophoresis. This architecture produces a resonator that is largely protected from its outer environment, interacting only with samples flowed through its interior via interfacing with standard microfluidic tubing and apparatus. Side illumination and detection of the polymer layer reveals a fluorescence spectrum that is periodically modulated by the presence of whispering gallery modes (WGMs) azimuthally trapped within it. Spectral shifts of the WGMs' resonances are experimentally evaluated by flowing aqueous glycerol dilutions through the capillary and calculating the mode shifts via a Fourier analysis technique. A semi-analytical eigenvalue model is used to calculate the sensitivity, quality factor limit and mode content of the polymer layer and is compared with the experimental results, showing how the thin layer, and low interior (aqueous) index, quenches the higher order radial modes, effectively enabling the excitation and detection of only the fundamental radial layer resonance. This interior polymer coating method could enable the exploitation of a wide range of material and optical properties for microfluidic bio-sensor design, while combining the benefits of a capillary flow cell format with remote fluorescence excitation and detection of the supported WGMs.

8570-16, Session 4

A fiber tip label free biological sensing platform for in vivo applications

Alexandre Francois, Kristopher J. Rowland, Tanya M. Monro, The Univ. of Adelaide (Australia)

Fluorescence labelling based techniques have been extensively used for in-vivo sensing application, however these techniques do not allow real time, label free in-vivo sensing. The novel platform presented in this paper is design to answer these challenges by bringing together a refractive index transducing mechanism based on Whispering Gallery Modes (WGM) in micron scale dye doped polystyrene microspheres combined with an Microstructured optical Fiber (MOF). Positioning the resonator onto the tip of a MOF allows to easily manipulate the microresonator and insert it into the target using a catheter, while the MOF provides the remote excitation and collection of the fluorescence modulated WGM spectra. Here, we demonstrate for the first time the ability of this fibre tip sensing platform to be operated above its lasing threshold, enabling higher performance, for the detection of specific proteins in a dip sensing architecture alleviating the need of complex microfluidic interface and paving the way toward in-vivo biological sensing.

8570-17, Session 4

Tapered optical fibers for aqueous and gaseous phase biosensing applications

Branden J. King, Peter E. Powers, Andrew M. Sarangan, Joseph W. Haus, Ighodalo Idehenre, Karolyn M. Hansen, Univ. of Dayton (United States)

This study focuses on the design, fabrication, and characterization of tapered optical fibers for label-free, biomolecular sensing in both aqueous and gaseous environments. Single mode fibers were tapered to a diameter of approximately 10 microns allowing for the propagation of multiple modes that create an interference pattern in the output signal. The physical dimensions of the tapered fibers were measured for use in multimodal output simulations, which were then compared to the empirically determined output signal. Tapered regions serve as the sensing interface, such that the light propagating through/around the fiber interacts with molecules tethered to the tapered surface. Tapered regions are functionalized with biomolecules for capture/detection of analytes in both aqueous (antibody) and vapor phases (DNA, peptides). Molecular binding of analytes with recognition molecules changes the refractive index and the thickness of the biolayer, which can be measured as a phase shift in the output. The sensing platform (fiber and PDMS flowcell) was designed such that the device could be fabricated and constructed quickly and economically. This study will include a discussion on refinement of surface chemistry (molecular layer thickness) to maximize molecular interactions for detection of low concentrations of analytes. We envision the use of tapered optical fibers in array format for detection of multiple analytes in complex samples for biomedical (blood, saliva, breath), environmental, and homeland security applications.

8570-18, Session 5

Controlled release of theophylline from poly(vinyl alcohol) hydrogels/porous silicon (SiP) nanostructured systems

Gabriela Palestino, Nancy Ayerim Cervantes-Rincon, Francisco Javier Medellín-Rodríguez, Univ. Autónoma de San Luis Potosí (Mexico); Vladimir Escobar-Barrios, Instituto Potosino de Investigación Científica y Tecnológia (Mexico)

Over the past few decades, advances in hydrogel technologies have

spurred development in many biomedical applications including controlled drug release. The advantage of using hydrogel is that the drug release rates can be controlled and triggered intelligently by interactions with biomolecular stimuli; however one difficulty that should be overcome in this system is the amount of the medicament absorbed for the hydrogel matrix is quite low, which produces that the drug doesn´t be administered in the required therapeutic dose. During this project, we synthesized by the freezing/thawing method, poly(vinyl alcohol) (PVA) an inert, no toxic; hydrophilic hydrogel characterized by its excellent biocompatibility. We assessed the impact of PVA concentration, the number of freezing/thawing cycles, the freezing time and the freezing temperature on gel formation as well as on the water absorption (grade of swelling) and quantity of drug released. Then, to increase the drug charge, the PVA matrix with the best properties was modified with porous silicon nanostructured particles (PSiNsP) previously charged with theophylline, a bronchodilator used in asthma treatment. Hence, by controlling the degree of swelling, crosslinking density, and PSiNsP concentration, delivery kinetics were engineered according to the desired drug release schedule. Additionally thermal, physicochemical and mechanical properties were evaluated for PVA/PSiNsP system as function of PSiNsP concentration. We observed that the addition of PSiNsP change the glass transition temperature and the mechanical properties of the PVA hydrogel.

8570-19, Session 5

Whispering gallery mode biosensing of translocation events through a single solid-state nanopore

Kyujung Kim, Max Planck Institute for the Science of Light (Germany); Gaurav Goyal, Min Jun Kim, Drexel Univ. (United States); Frank Vollmer, Max Planck Institute for the Science of Light (Germany)

Whispering gallery modes (WGM) biosensing is an emerging sensing technique for label free detection of biomolecules, their conformation and interactions. The biomolecules are detected as they interfere with a WGM optical resonance excited in a miniature ~50-300 ?m microsphere. Although the WGM biosensor has been developed for ultra-sensitive detection tasks with detection limits theoretically down to the single molecule level, this technique requires analyte molecules, which are initially randomly distributed throughout a sample, to localize on the most sensitive area of a WGM. In the past, optical trapping has been suggested as one possibility to achieve such high spatial localization of analyte.

Here we show that electrical translocation through a single nanopore in free standing silicon nitride membrane can localize particles and molecular analytes for most sensitive detection using WGMs. We first show the feasibility of this approach by detecting bacteria Escherichia coli using a 5 ?m diameter micropore. Next we show potential for detecting down to 50 nm sized gold nanoparticles with a 300 nm diameter nanopore in real time. The results demonstrate that the nanopore merged WGM biosensor provides opportunities for localizing nanoparticles and molecules for sensitive label-free optical detection, and provides a platform for exploring new optical detection and manipulation modalities in nanopore sensing.

8570-20, Session 5

Quantum bio-nanosensors based on quantum dot-metallic nanoparticle systems

Seyed M. Sadeghi, The Univ. of Alabama in Huntsville (United States)

In conventional plasmonic nanosensors adsorption of biological molecules to metallic nanoparticles shift the wavelengths of their localized surface plasmon resonances (LSPRs). When metallic nanoparticles are put in the vicinity of semiconductor quantum dots and driven with a coherent light source, however, the intrinsic plasmonic near fields of the metallic nanoparticles can be replaced with completely new types of fields (coherent-plasmonic fields). These fields are the result of coherent coupling between intrinsic resonances of the quantum dots (excitons) and metallic nanoparticles (LSPRs). In this contribution we discuss how the coherent-plasmonic field of a metallic nanoparticle can lead to a significantly larger field enhancement than that caused by its LSPR. Utilizing this, we investigate how such a coherent field enhancement can improve the sensitivities plasmonic nanosensors used to detect single biological molecules. We discuss how, instead of LSPR shifts, as in conventional nanosensors, the signal transduction methods in the proposed quantum nanosensors can include detection of the emission of the semiconductor quantum dots and even the heat generated by the metallic nanoparticles. We also discuss different configurations of such sensors based on applications of different shapes of metallic nanoparticles (spherical and nanorods) and materials (gold and silver).

8570-21, Session 5

Properties of resonant modal-plasmonic multiparametric biosensors *(Invited Paper)*

Robert Magnusson, Jaewoong Yoon, The Univ. of Texas at Arlington (United States); Debra D. Wawro, Resonant Sensors Inc. (United States)

We introduce a new class of label-free optical biosensors made with resonant periodic thin films. The sensors contain metals and dielectrics to admit cooperative resonance effects based on simultaneous guided leaky modes and surface-plasmon polaritons. Whereas ordinary surface-plasmon resonance (SPR) sensors admit only a single polarization state, namely transverse-magnetic (TM) polarization, the incorporation of guided-mode resonance (GMR) capability enables dual-polarization sensing. In fact, as the proposed dielectric-metal system can support multiple modes for each polarization state, multiple individual and mixed SPR/GMR resonance locations can be monitored. For example, monitoring two resonance events, one in each polarization, permits two parameters (e.g., sample background refractive index and biolayer thickness) to be determined simultaneously in each sensor-system channel. This attribute is unique to GMR-sensor technology and is not possessed by any competing methods; its application protects against false readings and erroneous conclusions and represents a major strength of this technology relative to other sensor methods. SPR biosensors are extremely sensitive with a long history of commercial use. The well-known prism-coupled SPR systems are typically bulky in system architecture and are not readily implemented into high-density arrays. In contrast, grating-based sensor systems provide compact sensor-chip arrays with potentially thousands of channels and freedom in addressing. Dielectric gratings can provide the coupling means for SPR sensors; these are fabricated easily and economically. Applying the hybrid plasmonic-modal sensor concept as proposed here potentially leads to new, compact, high-sensitivity biosensors for multiparametric detection. We provide initial computed and experimental results pertinent to this sensor class.

8570-22, Session 6

Single nanoparticle and virus imaging using computational on-chip microscopy

Onur Mudanyali, Euan R. McLeod, Wei Luo, Alon Greenbaum, Ahmet Faruk Coskun, Univ. of California, Los Angeles (United States); Jean-Marc Dinten, Yves Hennequin, Cédric P. Allier, CEA-LETI (France); Aydogan Ozcan, Univ. of California, Los Angeles (United States)

Visualization of nano-particles (e.g., viruses, small pathogens, etc.) using optical imaging and sensing techniques is a challenging task due to the

weakly scattering nature of nano-scale objects. Therefore, advanced imaging platforms (e.g., electron microscopy) are typically needed to observe the nano-world despite their high-cost, low-throughput and complex operation. Here we present a low-cost and high-throughput nano-imaging method based on a wide-field on-chip imaging platform that uses self-assembled aspheric liquid nano-lenses around individual nano-particles to directly image sub-100 nm particles across a large field-of-view of >20 mm2, i.e., more than two orders-of-magnitude larger than existing nano-imaging techniques. We use gravitational or evaporative-driven flow of a biocompatible aqueous buffer solution to form these nano-lenses around sedimented nanoparticles. Observation of individual nano-particles surrounded by the nano-lenses is performed with lensfree holographic pixel super-resolution microscopy that converts the enhanced phase contrast provided by the nano-lenses into intensity oscillations at the detector. Analytical and numerical modeling of the lens formation process and its influence on the optical signatures of the nanoparticles agrees well with our experimental results and explains why the lenses provide such a significant image enhancement. In order to demonstrate the performance of this novel nano-imaging approach, we imaged, for the first time in on-chip microscopy, various polystyrene nano-bead samples and single influenza A (H1N1) viral particles. Validated by 100X oil-immersion objective-lens and SEM (Scanning Electron Microscopy) comparisons, these imaging results provide the basis for a high-throughput, highly-sensitive, and field-deployable alternative to conventional nano-imaging platforms.

8570-23, Session 6

Rapid detection of malignant bio-species using digital holographic pattern recognition and nanophotonics

Sergey S. Sarkisov Sr., SSS Optical Technologies, LLC (United States); Tatjana Kukhtareva, Nickolai Kukhtarev, Michael J. Curley, Vernessa Edwards, John Corda, Marylyn Creer, Alabama A&M Univ. (United States)

There is a great need for rapid detection of bio-hazardous species particularly in applications to food safety and bio-defense. It has been recently demonstrated that the colonies of various bio-species could be rapidly detected using culture-specific and reproducible patterns generated by scattered non-coherent light. However, the method heavily relies of a digital pattern recognition algorithm, which is rather complex, requires substantial computational power and is prone to ambiguities due to shift, scale, or orientation mismatch between the analyzed pattern and the reference from the library. The improvement could be made, if, in addition to the intensity of the scattered optical wave, its phase would be also simultaneously recorded and used for the digital holographic pattern recognition. In this feasibility study the research team recorded digital Gabor-type (in-line) holograms of colonies of mold fungi Altenaria, namorphic Gaphium, and Aspergillus with a laser diode as a low-coherence light source and a lensless high-resolution (2.0x2.0 micron pixel size) digital image sensor. The colonies were grown in conventional Petri dishes using standard methods. The digitally recorded holograms showed low sensitivity to the lateral shift of the light beam. Besides pattern recognition with popular holographic methods, such as the Joint Transform and the VanderLugt correlator, reconstructive scanning across a colony depth of several millimeters was implemented. The fungi colonies have been also generating nanocolloidal silver during their growth in specially prepared matrices. The silver-specific plasmonic optical extinction peak at 410-nm was also used for rapid detection and growth monitoring of the colonies.

8570-24, Session 6

Towards a simple tuberculosis diagnosis through the exhaled breath: A liquid fluorimeter with an excitation at 265 nm

Jean B. Hue, Mathieu G. Dupoy, Severine Vignoud, Jean-Luc Ricaud, CEA-LETI (France); Thu-hoa Tran-Thi, Commissariat à l'Énergie Atomique (France); Sandrine Karpe, Ctr. National de la Recherche Scientifique (France); Armelle Novelli-Rousseau, Frédéric Mallard, BioMérieux (France)

The struggle against the tuberculosis is one of the World Health Organization priorities. Recovering from this infectious and deadly disease (2 millions of death per year) is possible with a correct diagnosis to give an appropriate treatment.

The most common tuberculosis tests are:

- skin tests : not reliable at 100% and need 2 days,

- blood tests : costly and sophisticated technology,

- chest X-ray : the first step before the sputum tests used for a bacterial culture with a final diagnosis given within 2 weeks.

A tuberculosis test based on exhaled breath is a prospective non invasive solution, cheap and easy to transport. In this paper, it is assumed, that niacine is a specific tuberculosis biomarker, that selected probe is specific to niacine and finally that the exhaled breath does not contain any interfering species.

To address this problem, a fluorimeter is developed with a cheap cooled CCD (~2k$) as a sensor to easily determine the suitable "fluorescent zone". In comparing aqueous solutions with and without niacine, 250 pM of niacine have been detected. With a commercial fluorimeter (Fluorolog from Horiba), only 200 nM of niacine are detected. The present detection remains 10 times above the estimated targeted value for a tuberculosis test.

The excitation source is a LED, which emits 20 micro Watts at 265 nm through a fiber. The emission signal is detected around 545 nm. A typical exposure lasts 700 seconds.

Analysis of biomarkers with a liquid fluorimeter are generic and promising as health diagnostics.

8570-25, Session 6

Optical characterization of microporous ceramics and applications for gas detection

Liang Mei, Lund Univ. (Sweden) and Zhejiang Univ. (China) and Joint Research Ctr. of Photonics (China); Sune Svanberg, Lund Univ. (Sweden) and Joint Research Ctr. of Photonics (China) and South China Normal Univ. (China); Gabriel Somesfalean, Lund Univ. (Sweden) and Zhejiang Univ. (China) and Joint Research Ctr. of Photonics (China)

Microporous ceramics can be utilized as components in many advanced technological applications, e.g., filters, sensors, catalyst supports and bio reactors. Information about their pore structure – e.g., porosity and pore size – is fundamentally important both for basic research and in industrial applications. In the present work, a tunable diode laser is utilized to evaluate the relative optical porosity of ceramics with different pore sizes and physical porosities. The relative optical porosity – which corresponds to the physical porosity of the ceramic – is defined as the ratio between the optical path length through the pores and the mean optical path length (MOPL) through the whole material. According to the Beer-Lambert law, the gas absorption signal is linearly proportional to the product of gas concentration and path length when absorption is very weak. When the gas concentration is known, the optical path length through the gas-filled pores of the ceramics can be retrieved by the so-called gas in scattering media absorption spectroscopy (GASMAS) technique complemented with wavelength modulation spectroscopy. At

the same time, the MOPL through the whole ceramic can be obtained by utilizing frequency domain photon migration (FDPM), which is a method widely used to assess optical properties in turbid media. Applications towards optical sensing of gas are demonstrated using the GASMAS-based technique in combination with Microporous ceramics.

8570-26, Session PSun

Enhance the detection limit of SiNW-FET biosensor by cholic acid treatment

Wen-Ti Hsu, Chia-Chang Tsai, Shi-Ya Hsu, An-Cheng Li, Jr Hau He, Shuchen Hsieh, Kuang-Hung Cheng, Hay-Yan Jack Wang, Kung-Kai Kuo, Li-Wei Tu, National Sun Yat-Sen Univ. (Taiwan)

3-aminopropyltriethoxysilane (APTES) is used as interfacing molecules, and assembly of these molecules is essential in surface modification technologies. In this study, we try to enhance the biosensor detection limit by increasing the APTES modification ratio. APTES modification ratio is related to the quantity of Si surface hydroxyl radical (-OH), so we can increase the APTES modification ratio by increase the quantity of -OH. In this study, biosensor chips are first soaked in 2% cholic acid in alcohol for 12 hrs to generate -OH on the SiO2 surface. The fluorescence test shows that after the cholic acid treatment the brightness increased. We use microelectronic techniques to fabricate silicon nanowires field effect transistors (SiNWs-FET). Then we modified APTES and biotin on SiNWs-FET sequentially to detect streptavidin. For SiNWs-FET, variation in molecular charge is reflected in a change in the wire current. The response of the drain-source current of biotin-modified SiNWs-FET to changes in streptavidin concentration was measured by using a lock-in technique. Control experiment was carried out before biotin modified, and the SiNWs-FET did not exhibit a current change when 10-7 M streptavidin passed through the microfluidic channel. APTES modified conditions can be determined by the source-drain current versus the voltage curve (Isd-Vsd curve). The resistance change ratio of cholic acid-treated SiNW-FET is higher than that without cholic acid treatment. And the sensitivity of streptavidin detection was lowered to 10-9 M from 10-8 M.

8570-27, Session PSun

Combined sensing platform for advanced diagnostics in exhaled mouse breath

Paula R. Fortes, Univ. Estadual de Campinas (Brazil); Andreas Wilk, Felicia Seichter, Univ. Ulm (Germany); Merima Cajlakovic, Stefan Köstler, Volker Ribitsch, JOANNEUM RESEARCH Forschungsgesellschaft mbH (Austria); Ulrich Wachter, Josef Vogt, Peter Radermacher, Univ. Ulm (Germany); Ivo M. Raimundo Jr., Univ. Estadual de Campinas (Brazil); Boris Mizaikoff, Univ. Ulm (Germany)

Efforts toward the development of integrated sensors platforms capable of performing exhaled breath (EB) analysis with required sensitivity and molecular discrimination have been carried out with particular focus on evaluating the potential for online and noninvasive monitoring and continuous analysis. Assessment of biomarkers present in EB provides a useful tool in medical diagnosis, as breath metabolites, e.g., after drug administration or breath compounds endogenously produced due to a particular physiological status may be accomplished online. Regarding mouse breath analysis, quantification of selected constituents at ppm-ppb concentration levels in minute sample volumes (few mL) is required.

Mid-infrared sensing schemes based on hollow waveguides [1-3] combined with luminescent sensors (LS) are used herein for non-invasively and simultaneously analyzing total CO2, the 12CO2/13CO2 ratio, and O2 in exhaled mouse breath. The LS sensor is integrated into the MIR-HWG such that a single diagnostic platform is established, as both sensors simultaneously interact with the same breath sample volume. Furthermore, coupling IR-HWG sensors with luminescent-based sensors extends the range of application of such combined breath diagnostic sensing platforms and provides an attractive concept for advanced research in the field of breath analysis.

Acknowledgements: The authors thank FAPESP (Proc. 12/05573-6) for financial support.

[1] C. Charlton, et al., Appl. Phys. Lett., 86, 194102/1-3 (2005).

[2] S.-S. Kim, et al., IEEE Sensors, 10, 145-158 (2010).

[3] A. Wilk, et al., Anal. Bioanal. Chem., 402, 397-404 (2012).

8570-28, Session PSun

Charge injection through nanocomposite electrode in microfluidic channel for electrical lysis of biological cells

Madhusmita Mishra, Anil Krishna, Manish K. Priydarshi, B. M. Shenoy, Gopalkrishna M. Hegde, D. Roy Mahapatra, Indian Institute of Science (India)

Several concepts have been developed in the recent years for nanomaterial based integrated MEMS platform in order to accelerate the process of biological sample preparation followed by selective screening and identification of target molecules. In this context, there exist several challenges which need to be addressed in the process of electrical lysis of biological cells. These are due to (i) low resource settings while achieving maximal lysis (ii) high throughput yield of target molecules to be detected (iii) automated extraction and purification of relevant molecules such as DNA and protein from extremely small volume of sample (iv) requirement of fast, accurate and yet scalable methods (v) multifunctionality toward process monitoring and (vi) downward compatibility with already existing diagnostic protocols. This paper reports on the optimization of electrical lysis process based on various different nanocomposite coated electrodes placed in a microfluidic channel. The nanocomposites are synthesized using Carbon Nanotube and ZnO nanorod dispersion in polymer. The efficiency of electrical lysis with various different electrode coatings has been experimentally verified in terms of DNA concentration, amplification and protein yield. The influence of the coating thickness on the injection current densities has been analyzed. We further correlate experimentally the current density vs. voltage relationship with the extent of bacterial cell lysis. A coupled multiphysics based simulation model is used to predict the cell trajectories and lysis efficiencies under various electrode boundary conditions as estimated from experimental results. Detailed in-situ fluorescence imaging and spectroscopy studies are performed to validate various hypotheses.

8571-1, Session 1

Joint aperture detection for angle-resolved ophthalmic MHz OCT

Thomas Klein, Raphael André, Wolfgang Wieser, Tom Pfeiffer, Robert Huber, Ludwig-Maximilians-Univ. München (Germany)

Joint-aperture optical coherence tomography (JA OCT) is a novel angle-resolved OCT method, in which illumination from an active channel is simultaneously probed by several passive channels. The passive channels point on the sample at the same position, but under an angle with respect to the illuminating active channel. JA OCT increases the collection efficiency of the OCT system and provides angular scattering information about the sample in a single acquisition. Thus, JA OCT is especially suitable for in-vivo imaging, since both image quality and acquisition speed of the active channel is equivalent to that of standard OCT. JA OCT will be compared to other angle-resolved techniques, and the relation between joint aperture imaging, adaptive optics, coherent and incoherent compounding will be discussed. We present angle-resolved imaging of the human retina at an axial scan rate of 1.68MHz, and demonstrate the benefits of JA OCT at this very high speed: Speckle reduction, signal increase and suppression of specular and parasitic reflections. Moreover, in future JA OCT may allow for the reconstruction of the full Doppler vector and tissue discrimination by analysis of the angular scattering dependence.

8571-2, Session 1

Dual-wavelength photothermal optical coherence tomography for blood oxygen saturation measurement

Biwei Yin, The Univ. of Texas at Austin (United States); Roman V. Kuranov, The Univ. of Texas Health Science Ct.r. at San Antonio (United States); Austin B. McElroy, Thomas E. Milner, The Univ. of Texas at Austin (United States)

We report design and demonstration of a dual wavelength photothermal (DWP) optical coherence tomography (OCT) system for imaging of a phantom vessel and measurement of microvasculature hemoglobin oxygen saturation (SO2) level. DWP-OCT contains a swept-source (SS) two-beam phase-sensitive (PhS) OCT system (1060 nm) and two intensity modulated photothermal excitation lasers (770 nm and 800 nm). The PhS-OCT probe beam (1060 nm) and photothermal excitation beams are combined into one single-mode optical fiber. A galvanometer based two-dimensional (2D) achromatic scanning system is designed to provide 14 ?m lateral resolution for the PhS-OCT probe beam (1060 nm) and 13 ?m lateral resolution for photothermal excitation beams. DWP-OCT system's sensitivity is 102 dB, axial resolution is 13 ?m in tissue and uses a real-time digital dispersion compensation process, and optical pathlength noise floor is 300 pm in the working range of photothermal modulation frequencies. Blood SO2 level is calculated from measured optical pathlength (op) variations in a 300 ?m diameter blood vessel phantom introduced by the two photothermal excitation beams. En-face and B-scan images of a phantom vessel are recorded, and six blood samples' SO2 levels are measured using DWP-OCT; results are compared with the values provided by a commercial blood oximeter.

8571-3, Session 1

Off-axis full-field swept-source optical coherence tomography using holographic refocusing

Dierck Hillmann, Medizinisches Laserzentrum Lübeck GmbH (Germany) and Thorlabs GmbH (Germany); Gesa L. Franke, Institut für Biomedizinische Optik Luebeck (Germany) and Medizinisches Laserzentrum Luebeck GmbH (Germany); Peter Koch, Thorlabs GmbH (Germany); Gereon Hüttmann, Univ. zu Lübeck (Germany) and Medizinisches Laserzentrum Luebeck GmbH (Germany)

We demonstrate a full-field swept-source optical coherence tomography (FF-SS-OCT) setup with an off-axis reference illumination as used in Hilbert phase microscopy or digital holographic microscopy. It obtains diffraction limited resolution over the entire measurement depth by using holographic refocusing techniques. This is achieved efficiently by Fourier domain resampling as in inverse scattering solutions and holoscopy. Compared to a standard on-axis setup, spatial filtering of the recorded interference pattern allows the suppression of artifacts and autocorrelation signals. It also doubles the measurement depth by resolving the complex conjugate ambiguity, effectively allowing full-range OCT. Images at moderate and high NA are shown, demonstrating the advantages of off-axis FF-SS-OCT.

8571-4, Session 1

Chromatic visualization of reflectivity variance within hybridized directional OCT images

Vikram S. Makhijani, Austin Roorda, Jan Kristine Bayabo, Kevin K. Tong, Carlos A. Revera-Carpio, Brandon J. Lujan M.D., Univ. of California, Berkeley (United States)

This study presents a new method of visualizing hybridized images of retinal spectral domain optical coherence tomography(SDOCT) data comprised of varied directional reflectivity. Due to the varying reflectivity of certain retinal structures relative to angle of incident light, SDOCT images obtained with differing entry positions result in non-equivalent images of corresponding cellular and extracellular structures, especially within layers containing photoreceptor components. Harnessing this property, cross-sectional pathologic and non-pathologic macular images were obtained from multiple pupil entry positions using commercially-available OCT systems, and custom segmentation, alignment, and hybridization algorithms were developed to chromatically visualize the composite variance of reflectivity effects. In these images, strong relative reflectivity from any given direction visualizes as relative intensity of its corresponding color channel. Evident in non-pathologic images was marked enhancement of Henle's fiber layer (HFL) visualization and varying reflectivity patterns of the inner limiting membrane (ILM) and photoreceptor inner/outer segment junctions (IS/OS). Pathologic images displayed similar and additional patterns. Such visualization may allow a more intuitive understanding of structural and physiologic processes in retinal pathologies.

8571-5, Session 1

Using guide stars with computational adaptive optics for correcting spatially-varying optical aberrations in coherence-based imaging

Nathan D. Shemonski, Steven G. Adie, Adeel Ahmad, Paul S. Carney, Stephen A. Boppart M.D., Univ. of Illinois at Urbana-Champaign (United States)

In adaptive optics (AO), typically a guide star is used for wavefront sensing which provides a closed-loop feedback metric for aberration

correction. Previously, we have shown that these techniques can be mimicked computationally to correct global aberrations using tissue phantoms and image metrics. Aberrations, though, are frequently a spatially-distributed local phenomenon which adaptive optics systems have difficulty correcting due to time averaging of wavefronts. In addition, aberrations caused by tissue or other heterogeneous structures can be of much higher-orders than a standard SLM or deformable mirror can correct. Here, we present the utilization of guide stars in computational AO for correcting spatially-varying aberrations in spectral-domain optical coherence tomography (SD-OCT). An iterative technique is used to move beyond the classical aberration characterization model of Zernike polynomials to correct for more general, higher-order aberrations.

8571-6, Session 1

Sensorless modal deformable mirror correction in adaptive optics: optical coherence tomography

Stefano Bonora, Univ. degli Studi di Padova (Italy); Steven S. Jones, Lawrence Livermore National Lab. (United States); Robert J. Zawadzki, UC Davis Medical Ctr. (United States)

We demonstrated that the modal sensorless correction can be used in Optical Coherence Tomography (OCT) with the use of a recently developed resistive deformable mirror. The Modal Deformable Mirror (MDM) is an electrostatic membrane DM where the actuators are composed by a resistive layer which continuously distributes the electrostatic pressure on the membrane. Wavefront sensorless control is a viable option for imaging biological structures for which AO-OCT cannot establish a reliable wavefront that could be corrected by wavefront corrector. Future refinements of this technique, beyond simple implementation presented in this manuscript, should allow its extension to in-vivo applications.

8571-7, Session 2

Efficient sweep buffering in swept source optical coherence tomography using a fast optical switch

Al-Hafeez Z. Dhalla, Kevin Shia, Joesph A. Izatt, Duke Univ. (United States)

We describe a novel buffering technique for increasing the A-scan rate of swept source optical coherence tomography (SSOCT) systems employing low duty cycle swept source lasers. This technique differs from previously reported buffering techniques in that it employs a fast optical switch, capable of switching in 60 ns, instead of a fused fiber coupler at the end of the buffering stage, and is therefore substantially more efficient. The use of the switch also eliminates patient exposure to light that is not used for imaging that occurs at the end of the sweep, thereby increasing the system sensitivity. We also demonstrate how numerical compensation techniques can be used to modify the signal from a Mach-Zehnder interferometer (MZI) clock obtained from the original sweep to recalibrate the buffered sweep, thereby reducing the complexity of systems employing lasers with integrated MZI clocks. Combining these methods, we constructed an SSOCT system employing an Axsun technologies laser with a sweep rate of 100kHz and 6dB imaging range of 5.5mm. The sweep rate was doubled with sweep buffering to 200kHz, and the imaging depth was extended to 9mm using coherence revival. We demonstrated the feasibility of this system by acquiring images of the anterior segments and retinas of healthy human volunteers.

8571-8, Session 2

MEMS tunable 1065nm and 1310nm VCSEL technology for flexible ultrahigh speed, ultralong imaging range, and Doppler OCT

Benjamin M. Potsaid, Massachusetts Institute of Technology (United States) and Thorlabs Inc. (United States); James Y. Jiang, Thorlabs Inc. (United States); Vijaysekhar Jayaraman, Praevium Research, Inc. (United States); Ireneusz Grulkowski, Woo Jhon Choi, Jonathan J. Liu, Massachusetts Institute of Technology (United States); Jens Peupelmann, Thorlabs GmbH (Germany) and IJP (Germany); Peter J. S. Heim, Thorlabs Quantum Electronics, Inc. (United States); James G. Fujimoto, Massachusetts Institute of Technology (United States); Alex E. Cable, Thorlabs Inc. (United States)

In this paper, we demonstrate 1065nm and 1310nm MEMS tunable Vertical Cavity Surface Emitting Laser (VCSEL) technology that achieves a flexible combination of ultrahigh sweep speeds, wide spectral tuning range, adjustability in sweep trajectory, and extremely long coherence length, which cannot be simultaneously achieved with any other previously demonstrated OCT light source technology. A low mass MEMS actuator in the VCSEL enables a single device to generate wavelength sweeps from 100kHz to 1.2MHz that are linearized, high duty cycle, and/or unidirectional or bidirectional for optimizing OCT imaging performance to an application. The sweep dynamics and intensity profile can be changed in real time, enabling versatile multi-speed, multi-resolution, and multi-imaging range instrumentation. The long coherence length of the VCSEL enables direct optical clocking of the A/D converter, eliminating the need for numerical fringe recalibration. When optical clocked, the VCSEL achieves excellent phase stability. We show ultrahigh speed 1.2MHz axial scan rate OCT imaging of the human retina (1065nm), long depth range imaging of the human anterior eye obtained at 100kHz axial scan rate (1310nm), and Doppler OCT imaging at 400 kHz axial scan rate (1065nm). High flow rates in the blood vessels can be observed at these high imaging speeds with negligible fringe washout and no phase wrapping artifacts. The ultrahigh speed and long imaging range results of this study combined with the flexibility in imaging modes and high phase stability suggest that the VCSEL will improve performance of existing applications and enable new applications in health care, research and industry.

8571-9, Session 2

4D OCT: full volumetric OCT at 25 Hz video rate

Wolfgang Wieser, Thomas Klein, Sebastian Karpf, Christoph M. Eigenwillig, Robert Huber, Ludwig-Maximilians-Univ. München (Germany)

We present video rate complete volumetric ultra high speed OCT imaging at 25 volumes per second. Each volume consists of 320 x 320 depth scans and each depth scan has 320 usable samples. The OCT system applies a 1310 nm Fourier domain mode locked (FDML) laser operated at 3.2 MHz sweep rate. Data acquisition is performed with two dedicated digitizer cards, each running at 2.4 GS/s, hosted in two separate computers. The acquired data is streamed directly into computer RAM allowing sustained volumetric imaging at 25.5 volumes/s for more than 30 seconds.

8571-10, Session 2

Ultrahigh resolution optical coherence tomography using high power fiber laser supercontinuum at 1.7 um wavelength region

Shutaro Ishida, Hiroyuki Kawagoe, Nagoya Univ. (Japan); Youichi Sakakibara, Emiko Omoda, Hiromichi Kataura, National Institute of Advanced Industrial Science and Technology (Japan); Norihiko Nishizawa, Nagoya Univ. (Japan)

The high power supercontinuum (SC) source at 1.7 um wavelength region based on high repetition rate single-wall carbon nanotube fiber laser was demonstrated for ultrahigh resolution optical coherence tomography (UHR-OCT). The optical spectrum of 242 nm and the output power of 43 mW were realized with 109 MHz repetition rate. The system sensitivity of 105 dB and axial resolution of 4.3 um in tissue were achieved. The UHR-OCT images of the pig thyroid gland were observed and the imaging depth and contrast were compared with those of the previous SC sources. The deeper penetration and higher contrast imaging were confirmed.

8571-11, Session 2

Enhancement of the depth range up to 13.8 mm with filtered external k-sampling-clock in an SS-OCT system using a reflective Fabry-Perot tunable laser

Hisashi Yamada, Yasuo Niimura, Fumiko Hiwatashi, Systems Engineering Inc. (Japan); Dong-Hac Choi, Kitasato Univ. (Japan); Koji Ohbayashi, Kitasato Univ. School of Medicine (Japan)

The purpose of this report is to develop a method to generate external k-clock sampling signals, which provides enhanced depth ranges up to 13.8 mm with commercial reflective Fabry-Perot tunable laser (RFPTL) type SS light sources. We investigated the signal generated when SS source light was passed through a Mach-Zehnder interferometer (MZI). The power spectra of MZI signals were obtained by FFT of the memorized data. In addition to the main interference peak, we found two side peaks which modulate the main peak. When the MZI signal was used for external sampling k-clock, the modulation by the parasitic side peaks caused jitter to make k-clocking sampling unstable. Appearance of these side peaks can be explained by presence of a reflecting surface in the laser cavity. The strategy to enhance the depth range of the SS-OCT system with externally generated k-sampling clock is to purify the MZI signal using electrical filters. Electrical low-pass and high-pass filters works gradually and have a certain roll-off frequency range. Therefore parasitic peaks must be separated from the main peak M at least more than the transient roll-off frequency range of filters. We found two ranges and one optical delay length, where enhanced depth ranges can be attained. We observed PSFs and OCT images at two selected depth ranges of 8.2 and 13.8 mm using developed external k-sampling-clock. OCT images of the anterior segment of the human eye are demonstrated.

8571-12, Session 2

High-speed Doppler OFDI using frequency multiplexed dual beam illumination

SunHee Kim, TaeJin Park, YomgKeun Park, Wang-Yuhl Oh, KAIST (Korea, Republic of)

Doppler optical coherence tomography (D-OCT) enables high resolution imaging of spatially-localized motion in the sample, especially in-vivo microvasculature imaging, utilizing the phase-resolved technique that is based on the detection of the phase shift between two temporally separated A-lines. To ensure correlation between the two phase measurements, conventional D-OCT over-samples in the transverse direction reducing the phase decorrelation due to the transverse displacement of the imaging beam at the expense of the imaging speed, i.e., frame rate. Recently several approaches such as optimization of beam scanning pattern in OFDI (optical frequency domain imaging) and dual-beam-scan using polarization multiplexing in SD-OCT (spectral-domain OCT) were demonstrated to address this issue. We present high-speed Doppler OFDI using frequency multiplexed dual beam illumination. The novel scheme provides a pair of spatially separated beams with an acousto-optic frequency shifter that illuminate the exactly same location on the sample with an adjustable time interval upon the imaging beam scan by the galvanometer. Since each beam is encoded with a distinct frequency shift, the two temporally separated beams are easily de-multiplexed in data processing. We demonstrate high-speed vasculature imaging of a mouse thigh in-vivo at 117.4 fps (1024 A-lines per frame) over 7 mm x 4 mm (transverse x depth). The 3D vasculature over 7 mm (X: 1024 lines) x 3.7 mm (Y: 518 lines) x 4mm (Z) volume is obtained in 4.41s.

8571-13, Session 3

Comprehensive structural and functional imaging of the human retina with ultrahigh speed swept source OCT using a VCSEL light source

WooJhon Choi, Massachusetts Institute of Technology (United States); Benjamin M. Potsaid, Massachusetts Institute of Technology (United States) and Advanced Imaging Group, Thorlabs Inc. (United States); Vijaysekhar Jayaraman, Praevium Research, Inc. (United States); Bernhard Baumann, Medizinische Univ. Wien (United States) and New England Eye Ctr. (United States) and Tufts Medical Ctr., Tufts Univ. (United States); Martin F. Kraus, Friedrich-Alexander-Univ. Erlangen-Nürnberg (Germany) and Pattern Recognition Lab., Friedrich-Alexander-Univ. Erlangen-Nürnberg (Germany) and School of Advanced Optical Technologies, Friedrich-Alexander-Univ. Erlangen-Nürnberg (Germany); Jonathan J. Liu, Ireneusz Grulkowski, Chen D. Lu, Massachusetts Institute of Technology (United States); Alex E. Cable, Thorlabs Inc. (United States); David Huang, Casey Eye Institute OHSU (United States); Jay S. Duker, New England Eye Ctr. (United States); Joachim Hornegger, Pattern Recognition Lab. (Germany) and Friedrich-Alexander-Univ. Erlangen-Nürnberg (Germany); James G. Fujimoto, Massachusetts Institute of Technology (United States)

Structural optical coherence tomography (OCT) imaging has become a clinical standard in many areas of ophthalmic clinical diagnosis and recent studies are investigating OCT for functional measurement of ocular blood circulation. Ultrahigh speed swept source OCT using VCSEL light sources is particularly attractive for dynamic imaging of the human retina because both time-resolved functional and structural information in three-dimensions can be measured using a single instrument, which facilitates large scale pre-clinical and clinical studies. In this study, we demonstrate the potential of ultrahigh speed OCT for comprehensive structural and functional imaging of the human retina using a VCSEL based swept source / Fourier domain OCT system at 1080nm with an imaging speed of 400kHz axial scans per second. A simple and efficient phase-stabilization approach using a fiber Bragg grating, necessary for phase-sensitive measurements, is presented. At 400kHz, the axial velocity range measurable with Doppler OCT without phase wrapping was ±80.0mm/s in tissue. With the ultrahigh speed OCT system, time-resolved pulsatile total retinal arterial blood flow can be measured with a volume acquisition rate of 7.6Hz. Large and small field of view angiography imaging over scan areas ranging from 12mm x 12mm to 3mm x 3mm is demonstrated with a total acquisition time of less than 4 seconds. Functional OCT information extracted from the data can

provide complementary information to co-registered three-dimensional structural OCT information on the retina and may be useful for assessing progression of retinal diseases like glaucoma and diabetic retinopathy.

8571-14, Session 3

Multi-functional optical coherence tomography for polarization and Doppler investigation of posterior eye

Myeong Jin Ju, Univ. of Tsukuba (Canada) and Univ. of Tsukuba (Japan); Young-Joo Hong, Yiheng Lim, Lian Duan, Shuichi Makita, Univ. of Tsukuba (Japan); Shuo Tang, The Univ. of British Columbia (Canada); Masahiro Miura, Tokyo Medical Univ. Kasumigaura Hospital (Japan); Yoshiaki Yasuno, Univ. of Tsukuba (Japan)

Functional optical coherence tomography (OCT), such as Doppler OCT and polarization sensitive OCT (PS-OCT), have been extensively applied into posterior eye imaging. Since each system provides unique information, the system was utilized for the specific purpose of the measurement. Doppler- and PS-OCT have been employed for assessing blood flow and classifying ocular tissues based on birefringence properties, respectively.

In this research, a multi-functional OCT (MF-OCT) capable to measure both Doppler phase shift and birefringence properties inside of retina, choroid, and sclera is presented. The MF-OCT based on passive polarization delay unit was previously introduced. The system depends on depth encoded polarization multiplexing, so its measurement depth range was quite limited. To overcome the limitation, the proposed MF-OCT system increase sampling frequency to 500 MHz with frequency rescaling technique. This advance improves the depth-resolution and measurement depth range. The MF-OCT has a depth resolution of 8.5 ?m in air, a sensitivity of 88 dB, and the depth range of 2.9 mm. Doppler OCT processing with a custom-made phase stabilization algorithm and Jones matrix analysis method are used for the Doppler phase shift and polarization change detection, respectively.

Two normal and two pathologic cases were measured in vivo. Detailed vasculature structure was visualized by power Doppler image. Birefringence characteristic of retina, choroid, and sclera were clearly recognized in the phase retardation image. The MF-OCT may have potentials to reveal retinal diseases accompanied by abnormalities of vasculature and birefringence.

8571-15, Session 3

Split-spectrum amplitude-decorrelation angiography and its quantification of optic nerve head blood flow

Yali Jia, Casey Eye Institute OHSU (United States); John C. Morrison M.D., Oregon Health & Science Univ. (United States); Jason Tokayer, The Univ. of Southern California (United States); Tan Ou, Lorinna Lombardi, Oregon Health & Science Univ. (United States); Bernhard Baumann, Chen D. Lu, WooJhon Choi, James G. Fujimoto, Massachusetts Institute of Technology (United States); David Huang M.D., Casey Eye Institute OHSU (United States)

To detect changes in optic nerve head (ONH) microcirculation in glaucoma patients using optical coherence tomography (OCT) angiography, one eye of each subject was scanned with a swept-source OCT system operating at the center wavelength of 1050 nm, speed of 100,000 axial scans per second, axial resolution of 6 µm and spot diameter of 18 µm (FWHM amplitude). The ONH region was scanned using a 3x3 mm volumetric angiography scan consisting of 200 MB-scans, each of which consisted of 8 consecutive B-scans at the same location, each in turn consisted of 200 A-scans. Four angiography scans were obtained in one session. Flow was detected by amplitude decorrelation values computed by cross-correlation between corresponding pixels on consecutive B-scans. The signal-to-noise ratio of flow detection was improved by the use of a recently developed split-spectrum amplitude-decorrelation angiography (SSADA) algorithm. En face maximum projection was used to obtain 2D disc angiograms, from which the percentage area occupied by vessels (vessel density) and average decorrelation values (flow index) were computed from the segmented disc areas. Unpaired t-test was used assuming unequal variance. Five pre-perimetric glaucoma (PPG) and Five normal human subjects were studied. Good signal strength and focus was obtained in all studied eyes. In normal subjects, a dense microvascular network was visible on the OCT angiography of the disc in addition to large retinal vessels. This network was visibly attenuated in all PPG subjects.The flow index was reduced by 28% and the vessel area was reduced by 28.3% in the PPG group. These reductions were statistically significant. The pooled coefficients of variation were 6.89% and 6.53% for flow index and vessel density, respectively. In summary, OCT angiography, generated by the new SSADA algorithm, was able to detect reduced ONH perfusion in a small group of early glaucoma patients. Further studies are needed to assess the potential of this new technology in glaucoma diagnostic and prognostic evaluation.

8571-16, Session 3

Wide field-of-view retinal capillary mosaic by ultrahigh-speed dual-beam Doppler optical coherence angiography

Shuichi Makita, Kazuhiro Kurokawa, Franck Jaillon, Yoshiaki Yasuno, Univ. of Tsukuba (Japan)

Non-invasive capillary imaging will be powerful tool for investigation and diagnosis of retinal pathologies. We have been developing high-sensitivity non-invasive blood flow imaging by using dual-beam-scan Doppler optical coherence angiography (DB-OCA). However, for high feasibility to clinical application, wide field-of-view imaging is preferred.

In this study, we demonstrate non-invasive wide field-of-view (FOV) retinal capillary imaging by ultrahigh speed DB-OCA. Light from a source which has 840 nm central wavelength and 50 nm bandwidth (FWHM) were divided into two polarization states to obtain two OCT signals. The acquisition rate of camera is 123,000 lines/s. DB-OCA with ultrahigh speed acquisition and large beam separation visualizes retinal capillary pattern within 4 x 4 mm^2. Moreover,

multiple imaging sessions are acquired by monitoring the en-face fundus image to cover wide FOV. A wide FOV en-face image was also obtained for the reference of monitoring and registration of multiple imaging patches.

The real-time fundus monitoring and wide FOV en-face imaging were achieved solely by OCT system with a fast en-face image processing of spectral interference fringes and a spiral beam scanning. An en-face fundus imaging with 12-mm diameter area is acquired within 0.6 s with increased line rate of 333,333 lines/s by decreasing the number of pixels. The 4-mm diameter area on the fundus is monitored at the frame rate of around 1.8. The wide FOV retinal capillary mosaic with multiple imaging sessions will be presented.

8571-17, Session 3

Angiography of the retina and choroid with phase-resolved OCT using interval-optimized backstitched B-scans

Boy Braaf, Koenraad A. Vermeer, Kari V. Vienola, Rotterdam Ophthalmic Institute (Netherlands); Johannes F. de Boer, Rotterdam Ophthalmic Institute (Netherlands) and LaserLAB, VU Univ. Amsterdam (Netherlands)

In conventional phase-resolved Optical Coherence Tomography (OCT) blood flow is detected from phase changes between successive A-scans. Especially in current high-speed OCT systems this results in a short evaluation time interval. This method is therefore often unable to visualize complete vascular networks since low flow velocities cause insufficient phase changes. In this paper this problem is solved by comparing B-scans (inter-B-scan comparison) instead of successive A-scans to create a larger evaluation time interval. Consequently a small evaluation time interval results in small B-scans with a limited lateral scan-width. A backstitched B-scan was therefore developed in which pairs of small repeated B-scans were stitched together in order to independently control the evaluation time interval and the total imaged lateral field size. High-resolution images of the vasculature of a healthy volunteer taken with conventional and inter-B-scan phase-resolved OCT are presented for a 20° x 26° field to show the advantage of longer time intervals. While conventional phase-resolved OCT only shows large blood vessels and suffers from signal loss due the cardiac cycle and Doppler angle orientation changes, inter-B-scan phase-resolved OCT shows complete vascular networks. A time interval of 2.5 ms was found effective to image the retinal vasculature down to the capillary level. The higher flow velocities of the choroid allowed a time interval of 0.64 ms to reveal its dense vasculature.

8571-18, Session 3

Enhanced vascular imaging by scattering and phase information of optical coherence angiography

Kazuhiro Kurokawa, Shuichi Makita, Young-Joo Hong, Yoshiaki Yasuno, Univ. of Tsukuba (Japan)

The retinal and choroidal vasculature plays significant role in maintaining visual function. Hence, vasculature imaging is the key to prevent significant visual impairment. To achieve three-dimensional enhanced vascular imaging, we used several vascular imaging techniques using scattering and phase information of optical coherence tomography (OCT): averaged intensity, intensity variance, averaged Doppler, maximum Doppler and intensity-Doppler variance. In addition, adaptive-optics is used to further enhance lateral resolution in capillary imaging. Then, we qualitatively compared the methods by generating several en face projections of the retinal and choroidal capillary network. The results showed that higher contrast capillary networks are more observed in the methods which use phase of OCT. The difference in the contrast mechanisms of the modalities might cause this variability of image contrast. Specifically, averaged intensity relies on scattering property of capillaries. Temporal variation of scattering provides the vascular contrast to the intensity variance. On the other hands, the contrasts of Doppler based methods, i.e., averaged Doppler and maximum Doppler, depend on the capillary blood flow velocity and its angle. Finally, intensity-Doppler variance is sensitive to the temporal variations of both scattering and phase. In conclusion, enhanced vascular imaging methods using scattering and phase information of OCT were demonstrated. These methods enabled the detailed investigation of the retinal and choroidal capillary network. At the capillary level, phase information of OCT is more sensitive to the dynamic tissue than scattering information of OCT.

8571-19, Session 3

Image acquisition and processing methods for artifact-reduced imaging and differentiation of retinal capillary beds using speckle variance optical coherence tomography

Hansford C. Hendargo, Theodore B. DuBose, Rolando Estrada, Stephanie J. Chiu, Sina Farsiu, Joseph A. Izatt, Duke Univ. (United States)

Recent developments in the ability to visualize blood flow and vasculature using ≥70kHz class spectral-domain and swept-source optical coherence tomography (SD/SSOCT) have enabled high resolution imaging of the retinal microvasculature. In particular, speckle and phase variance signal processing techniques allow for highly sensitive visualization and differentiation of retinal capillary beds, achieving non-invasive results comparable to fluorescein angiography and with the added advantage of depth-resolution. The ability to differentiate the superficial capillary plexus from the deep capillary plexus in the inner retina may allow for earlier detection, greater understanding, and improved treatment of pathologies, such as macular telangiectasia. Variance-based OCT techniques are well suited for depth-resolved imaging of these vessel layers, and development of variance OCT for clinical use is greatly desired.

Because acquiring a variance volume with a high-speed system still requires several seconds, patient motion may prevent proper visualization of the layered vasculature over an acquired retinal volume. Correction of motion in microvasculature images is difficult due to the complex structure of the capillaries. To enhance the clinical viability of variance OCT, we have developed image processing techniques using information from speckle variance OCT volumes to reduce motion artifacts by sub-dividing each image into motion free strips and creating a composite image with reduced motion artifacts using information from multiple volumes. We also show enhanced depth-resolved imaging of the distinct capillary beds using robust retinal segmentation algorithms we have developed previously to assist in vessel identification among the different retinal layers.

8571-20, Session 3

Retinal micro-capillaries blood flow estimation based on intensity information analysis of OCT data

Daniel Ruminski, Iwona M. Gorczy?ska, Maciej Szkulmowski, Danuta Bukowska, Nicolaus Copernicus Univ. (Poland); Robert Zawadzki, UC Davis Medical Ctr. (United States); Maciej Wojtkowski, Nicolaus Copernicus Univ. (Poland)

We propose an alternative OCT data processing method to visualize and quantitatively assess retinal blood flow in three dimensions using intensity information. We demonstrate that the proposed method is suitable for flow analysis in small retinal microvasculature.

8571-21, Session 4

First in human experience with tethered capsule OFDI endomicroscopy

Michalina J. Gora, Wellman Ctr. for Photomedicine (United States); Jenny S. Sauk, Robert W. Carruth, Kevin A. Gallagher, Melissa J. Suter, Norman S. Nishioka, Lauren E. Kava, Mireille Rosenberg, Massachusetts General Hospital (United States); Guillermo J. Tearney, Wellman Ctr. for Photomedicine (United States)

Videoendoscopy with subsequent biopsy, the gold standard for Barrett's esophagus (BE) diagnosis, requires sedation, making it costly and time-consuming. Additionally, it is not capable of accurately diagnosing dysplasia in BE. We have previously shown that optical frequency domain imaging (OFDI), when employed with a balloon-centering catheter, is capable of obtaining microscopic images of the entire distal esophagus (6cm length). However, OFDI balloon catheter must be implemented using the same sedated videoendoscopy.

Here, we introduce a new method for obtaining upper GI OFDI images that uses a tethered, swallowable capsule. The 12.8mm (diameter) by 24.8mm (length) transparent capsule is attached to a thin, 0.8mm dia. tether that contains an optical probe. The swallowed capsule traverses

the esophagus while circumferential OFDI images are acquired. In this paper, we report the first clinical study conducted with the tethered capsule OFDI endomicroscope. A total of 7 healthy volunteers and 6 subjects with a diagnosis of BE have been imaged without sedation. Four imaging passes through the esophagus were performed (two up and two down) in each patient. Contact between the esophagus and the pill was excellent, enabling high quality cross-sections over a mean esophageal length of 15cm. The procedure time lasted an average of 6 minutes. 12/13 subjects reported that they would prefer the capsule procedure to conventional upper endoscopy. These results demonstrate that unsedated, tethered capsule OFDI is a viable method for comprehensive microscopy of the upper GI tract. The relative simplicity of this procedure may make it a useful technique for BE screening in the outpatient setting.

8571-22, Session 4

Ultrahigh speed endoscopic optical coherence tomography using micro-motor imaging catheter and VCSEL technology

Tsung-Han Tsai, Yuankai K. Tao, Massachusetts Institute of Technology (United States); Benjamin M. Potsaid, Massachusetts Institute of Technology (United States) and Thorlabs Inc. (United States); Vijaysekhar Jayaraman, Praevium Research, Inc. (United States); Martin Kraus, Massachusetts Institute of Technology (United States) and Friedrich-Alexander-Univ. Erlangen-Nürnberg (Germany); Peter J. S. Heim, Thorlabs Quantum Electronics, Inc. (United States); Joachim Hornegger, Friedrich-Alexander Univ. Erlangen-Nuernberg (Germany); Hiroshi Mashimo, VA Boston Healthcare System (United States) and Harvard Medical School (United States); Alex E. Cable, Thorlabs Inc. (United States); James G. Fujimoto, Massachusetts Institute of Technology (United States)

We developed a micro-motor based miniature catheter with an outer diameter of 3mm for ultrahigh speed endoscopic optical coherence tomography (OCT) using vertical cavity surface-emitting laser (VCSEL) at a 1MHz axial scan rate. The micro-motor can rotate a micro-prism at 1,200-72,000rpm (corresponding to 20-1,200fps) with less than 5V driving voltage to provide fast and stable scanning, which is not sensitive to the bending of the catheter. The side-viewing probe can be pulled back for a long distance to acquire three-dimensional (3D) dataset covering a large area on the specimen. VCSEL provides high a-line rate to support dense sampling under high frame rate operation. With the use of a C++ based high speed data acquisition (DAQ) system, in vivo three-dimensional OCT imaging in rabbit GI tract with 1.6mm depth range, 11um axial resolution, 8um lateral resolution, and frame rate of 400fps is demonstrated.

8571-23, Session 4

Optical frequency domain imaging: guiding biopsy site selection in pulmonary nodules

Lida P. Hariri, Matthew B. Applegate, Massachusetts General Hospital (United States); Martin Villiger, Wellman Ctr. for Photomedicine (United States); Mari Mino-Kenudson, Eugene J. Mark, Colleen Channick, Michael Lanuti, Massachusetts General Hospital (United States); Guillermo J. Tearney, Wellman Ctr. for Photomedicine (United States); Brett E. Bouma, Melissa J. Suter, Massachusetts General Hospital (United States)

Lung cancer is the leading cause of cancer-related deaths. Tumor yields in bronchoscopic biopsies must be adequate in order to provide tissue for both histologic and molecular assessments, but can be low due to inadvertent biopsy of adjacent lung tissue, tumor-associated fibrosis, and/or necrosis. Optical frequency domain imaging (OFDI) has shown great promise in prior ex vivo pulmonary imaging to distinguish lung parenchyma from tumor. OFDI criteria for lung parenchyma and peripheral nodules were developed and validated in ex vivo resection specimens in a blinded assessment with 6 independent readers, achieving sensitivity and specificity of 95.4 and 98.2%, respectively. This demonstrates the ability of OFDI to differentiate parenchyma from tumor. However, even when tumor nodules are accurately targeted, biopsy of tumor-associated scar and/or necrosis can decrease tumor yield. Necrosis is identifiable in structural OFDI, but fibrosis can be difficult to distinguish from tumor. Polarization sensitive OFDI (PS-OFDI) provides both structural images to distinguish normal lung from tumor nodule and detects high birefringence from organized connective tissues. In solid, poorly-differentiated carcinomas with adjacent or admixed fibrosis, the difference between tumor and fibrosis was not readily apparent with structural OFDI alone. PS-OFDI demonstrated strong birefringence from fibrotic regions with little to no birefringence in the areas of carcinoma. Tumors with little connective tissues showed little to no birefringent signal. We believe that this study is the first demonstration of PS-OFDI of pulmonary pathology. These techniques could be used for real-time guidance of biopsy site selection to increase tumor yield during bronchoscopic biopsy.

8571-24, Session 4

High speed miniature motorized endoscopic probe for optical frequency domain imaging

Jianan Li, Jianhua Mo, Frank Helderman, Mattijs de Groot, Johannes F. de Boer, Vrije Univ. Amsterdam (Netherlands)

We developed a fiber based motorized distal scanning miniature probe for endoscopic Optical Frequency Domain Imaging (OFDI). With an outer diameter of 1.65 mm and a rotation speed of 3,000 – 12,500 rpm, this is the smallest motorized high speed OCT probe to our knowledge.

The motorized distal end provides a significant advantage over proximally driven probes since it does not require a drive shaft to transfer the rotational torque to the distal end of the probe and functions without a fiber rotary junction. The probe has a focal Full Width at Half Maximum of 9.6 µm and a working distance of 0.47 mm. We analyzed the non uniform rotation distortion and found a location fluctuation of only 1.87° in repeated measurements of the same object.

The probe was integrated in a high-speed Optical Frequency Domain Imaging setup at 1310 nm to acquire 3D images from ex vivo and in vivo pig bronchial tissue through the working channel of a human bronchoscope. Future work includes developing polarization sensitive and Doppler imaging function as well as development of multimodality systems.

8571-25, Session 4

Multimodal endoscopic Full-Field OCT imaging and elasticity mapping with a needle-like probe

Anne Latrive, Amir Nahas, Claude A. Boccara, Institut Langevin (France) and LLTech SAS (France)

We are interested in endoscopic OCT systems with a rigid probe for imaging and biopsy guidance of internal organs, for example breast, kidney, liver, or prostate, by penetrating inside the organ as with a needle. We propose to use the forward-viewing Full-Field OCT (FFOCT) approach in order to improve the lateral resolution and sectioning ability. Furthermore we worked on adding the elastic contrast to the FFOCT image using a static method.

Our endoscopic FFOCT system uses two coupled interferometers, a processing interferometer external to the probe and a distal interferometer at the end of the probe in contact with the sample. This way the probe is not part of an interferometer arm and is entirely insensitive to its environment. Moreover we use a very simple common-

path distal interferometer, so that it does not require any advanced miniaturized mechanical systems at the tip of the passive probe. Our rigid probe is based on a GRIN lens assembly with a diameter of 2 mm and a length of 150 mm. The axial and transversal resolution are 1.8 µm and 3.9 µm. Sensitivity was experimentally evaluated at -80 dB when averaging 20 images during about 1 second, which is enough to get signal from biological tissues and to image in vivo.

We imaged ex vivo samples of organs such as breast and kidney by inserting the probe into the tissue and taking images as we entered the organ. The pressure required for piercing the tissue depends on the probe geometrics and the tissue stiffness.

Further, we used our setup to perform elastography with a static method. We recorded a 3D image of the sample before and after compression by the probe, then we calculated the cross-correlation between the two stacks of images. By resolving the inverse problem we have access to the displacement and elastic modulus maps that provides a relative value of the local elastic properties along the optical axis. We show a proof-of-principle on a phantom and first results on biological tissues, beginning with mouse ear.

8571-26, Session 4

Optimum stent detection in intravascular OCT: A 3-D approach

Zhao Wang, George C. Linderman, Case Western Reserve Univ. (United States); Hiram G. Bezerra, Univ. Hospitals of Cleveland (United States); Marco A. Costa, David L. Wilson, Andrew M. Rollins, Case Western Reserve Univ. (United States)

Coronary stenting is the most common technique for coronary revascularization worldwide. Intravascular optical coherence tomography (OCT) is an important emerging imaging technique for stent analysis. We report a novel 3-D method using graph search techniques for automated stent strut detection. The presence of struts is first determined using a Bayesian network based on OCT image formation. Then, the depths of all detected struts in an entire pullback are simultaneously determined using a max-flow/min-cut graph algorithm. By incorporating some general shape knowledge of stents into spatial constraints during graph construction, the method can guarantee a global optimum solution for all struts under the constraint. This method is very robust to noises and artifacts, as high-level knowledge such as the stent shape, global context, and 3-D information are taken into account. The method also has great potentials for more accurate quantifications of stent area and tissue coverage, and is ideal for fast, automatic 3-D visualization.

8571-27, Session 4

Three dimensional calcified plaque segmentation of intravascular optical coherence tomography using interactive graph cuts

George C. Linderman, Zhao Wang, Case Western Reserve Univ. (United States); Hiram G. Bezerra, Univ. Hospitals of Cleveland (United States); Marco A. Costa, David L. Wilson, Andrew M. Rollins, Case Western Reserve Univ. (United States)

Coronary artery disease, the leading cause of death in America, is caused by the development of atherosclerotic plaques in the coronary artery. The presence and volume of calcified plaque can serve as a measure of total plaque burden and is an important consideration during stent placement. Intravascular optical coherence tomography (OCT) can be used to quantify superficial calcified plaque with unprecedented resolution. However, manual segmentation can be time consuming, as the plaque often spans many frames within a pull-back volume. Previous methods have been published for semi-automated 2D segmentation of calcified plaque, which operate on a frame-by-frame basis, but do not make use of information from surrounding frames. Such methods are subject to settling at a local optimum, and also are time-consuming for large volumes. We present a 3D segmentation method based on interactive graph cuts that overcomes these limitations by constructing a graph that represents the helical path of the intravascular OCT probe, weighting it based on regional and boundary information, and then finding the globally optimum segmentation using a maximum flow algorithm. Additionally, this algorithm allows for fast editing, such that if the segmentation result is not perfect, the user can make additional marks on the image and recalculate the improved segmentation in dramatically less time than the initial segmentation.

8571-91, Session 4

Intravascular spectroscopic optical coherence tomography for automated detection of lipid

Christine P. Fleming, Joseph A. Gardecki, Massachusetts General Hospital (United States); Jocelyn Eckert, Atsushi Tanaka, Wellman Ctr. for Photomedicine (United States); Melissa Haskell, Massachusetts General Hospital (United States); Giora Weiz, Columbia Medical Ctr. (United States); Brett E. Bouma, Guillermo J. Tearney M.D., Wellman Ctr. for Photomedicine (United States)

Optical frequency domain imaging (OFDI) can identify key components related to plaque vulnerability but may suffer from artifacts that could prevent accurate identification of lipid rich regions. Here, we report results based on attenuation, spectroscopy via spectroscopic OCT (SOCT), and a combination of attenuation and spectroscopy, for automated depth-resolved classification of lipid in atherosclerotic plaque.

To accurately classify depth-resolved spectra, a quadratic discriminant analysis model was developed to classify depth resolved spectra. Model parameters to classify lipid were developed using OFDI images of phantoms with known chemical compositions of water, cholesterol, collagen, and calcium (n=355 images). To confirm spatial localization of lipid detection, the model was applied to OFDI images of artificial plaques of lipid deposits injected in swine aorta ex vivo with corresponding histological analysis (n=16 artificial plaques). Thereafter, the algorithm was applied to intravascular pull-back datasets from patients undergoing interventional procedures (n=20 patients).

We have demonstrated that the addition of spectral information via SOCT to an attenuation model can improve the accuracy of detecting lipid rich regions, $p<0.05$. Importantly, depth-resolved spectral analysis was able to spatially localize lipid within artificial plaques and intracoronary pullback datasets of patients. These results may have important implications in a variety of coherence gating applications, such as coronary imaging, where there is endogenous absorption contrast within the light source bandwidth. By facilitating comprehensive visualization of lipid within of OFDI images, this technique can potentially improve diagnosis, facilitate automatic segmentation procedures, and provide more accurate information for interventional guidance.

8571-31, Session PMon

Direct electronic linearization for camera based spectral domain optical coherence tomography

Adrian G. Podoleanu, Andrew Payne, Univ. of Kent (United Kingdom)

An electronic method of k-space linearization for an analogue camera for use in optical coherence tomography is demonstrated. The method applies a chirp to the data transfer clock signal of the camera in order to temporally compensate for diffraction that is non-linear in wavenumber. The optimum parameters are obtained experimentally and theoretically and are shown to be in good accordance. Close to maximum measurable

axial optical path range, by applying this method, we report a narrowing of the FWHM of the point spread function by a factor of 5.6 and improve its magnitude by 9.8 dB. This method successfully maintains PSF width over a large OPD range and gives up to 8.8 dB improvement at 2 mm and 9.8 dB at 2.4 mm. The method was presented here on an analogue camera. However, the method can be easily incorporated into any CCD or CMOS, 1D or 2D digital cameras. The transport and readout clocks for the LSC were provided by external signal generators but in practical use the camera's clocks would be on board and controlled by an EPROM. Such a method allows gains in performance without the use of extra optical components or processor time, enabling higher quality images and faster signal output.

8571-84, Session PMon

Variable-range Doppler OCT using stabilized step scanning and phase variance binarized mask

Lei Shi, Jia Qin, Suzan Dziennis, Ruikang Wang, Univ. of Washington (United States)

Skipping various numbers of A-lines during conventional linear scanning is effective to obtain multi-range velocimetry using Doppler OCT (DOCT). High correlation between A-lines is a fundamental prerequisite for DOCT processing. Therefore, high oversampling is normally necessary, especially when skipping A-lines. That requires quite a long time imaging, which might not be acceptable on some occasions. Step-scanning protocol, which captures repeated A-scans, has been employed for multi-range DOCT previously. We develop it by waiting for the scanner to stabilize, but not capturing continuously. In this way the cross-correlation of step scanning maintains almost constant for all the captured A-lines, and is higher than that of linear scanning with the same imaging time. Due to the limited numbers of A-lines at each lateral position, we choose a previously proposed delay line high-pass filter to enhance flow sensitivity. Doppler processing is implemented after the filter, both of which utilize A-line skipping to achieve multiple velocity ranges. The obtained Doppler signal in blood flow is surrounded by much noise in non-flow area. This is because the static components are removed by the filter, leaving random phase noise. The phase variance as a flow indicator is employed to generate a binary mask to extract the Doppler signal out of noise. The technique is demonstrated in bi-directional cross-section and maximum projection en face images of middle cerebral artery (MCA) occluded mouse model with cranium left intact. The vasculature responses from artery down to capillary during baseline, occlusion and reperfusion are illustrated. In some arteries that branch from MCA the flow is reversed but not vanished.

8571-85, Session PMon

Quantitative transverse flow assessment using OCT speckle decorrelation analysis

Xuan Liu, Yong Huang, Johns Hopkins Univ. (United States); Jessica C. Ramella-Roman, The Catholic Univ. of America (United States); Jin U. Kang, Johns Hopkins Univ. (United States)

Doppler frequency shift, as well as interframe speckle variance of optical coherence tomography (OCT) signal have been used in blood flow detection. Optical coherence Doppler tomography (ODT) allows quantitative blood flow measurement; however, it is not able to measure flow in a plane that is normal to the imaging beam. Speckle variance OCT (svOCT) has higher sensitivity for the visualization of microvasculature; however, it is insensitive to the change of flow speed. In this study, we propose to use inter-Ascan speckle decorrelation of OCT signal for flow measurement The technique is based on our previous study which theoretically derived and experimentally verified the dependency of cross-correlation coefficient (XCC, ?) between Ascans on lateral displacement (?x): ?x=w[ln(1/?)]1/2. Here w indicates the beam width of the probing beam. This method allows quantitative measurement of flow perpendicular to the scanning beam. To experimentally validate our method, we fabricated a 300 µm diameter micro flow channel with bovine milk flowing in it. A precision syringe pump was used to control the flow speed. Cross-sectional images of the micro flow channel were obtained using a spectral domain OCT system operating at 845nm with 70 kHz Ascan rate with a 0.6?m lateral sampling interval. Using OCT images obtained at different pump speeds, we calculated ? between Ascans, extracted ?x from ?, and calculated the flow speeds. Results showed a close linear correlation between flow speeds extracted from our method and the pump rates, suggesting that cross-correlation analysis between Ascans can be used in quantitative flow measurement.

8571-86, Session PMon

Two-reference swept-source optical Doppler tomography of high operation flexibility

Ting-Ta Chi, Chiung-Ting Wu, Chen-Chin Liao, Yi-Chou Tu, Yean-Woei Kiang, Chih-Chung Yang, National Taiwan Univ. (Taiwan)

In Fourier-domain optical coherence tomography (OCT), the operation usually leads to the coexistence of the real and mirror images in the acquired result. Recently, a computation time-saving image processing method has been demonstrated for effectively suppressing the mirror image in a spatially localized (SL) manner by generating a system phase shift between the two neighboring A-mode scans. However, when there is a moving object in the sample, the Doppler phase shift will disturb the system phase shift and degrade the mirror image suppression result. Also, the computation for suppressing the mirror image will disturb the Doppler phase information. On the other hand, the two-reference technique has been demonstrated to also effectively suppress the mirror image. In this technique, the two reference arms provide us with the quadratic components for suppressing the mirror image. Therefore, the orientation of the beam splitter, which is used for combining the reference signals and sample signal and for controlling the relative phase (must be 90 degrees) between the two reference signals, must be precisely adjusted. This stringent condition makes the operation of a two-reference OCT system quite difficult. Here, we demonstrate a novel method for effectively suppressing the mirror image and extracting the optical Doppler tomography (ODT) signals by combining the two-reference OCT technique with the aforementioned "SL" image processing method. Using this method, the two-reference OCT system can be easily operated with any beam-splitter orientation except the condition of zero relative phase. The results of mirror image suppression and ODT signal extraction are demonstrated.

8571-87, Session PMon

Doppler frequency estimators under additive and multiplicative noise

Aaron C. Chan, Edmund Y. Lam, The Univ. of Hong Kong (Hong Kong, China); Vivek J. Srinivasan, Massachusetts General Hospital (United States)

In optical coherence tomography (OCT), unbiased and low variance Doppler frequency estimators are desirable for blood velocity estimation. Sub-optimality in the widely used Kasai autocorrelation estimator means that, unexpectedly, increasing the acquisition rate worsens the estimation performance. Here we suggest that maximum likelihood estimators (MLEs) that utilize prior knowledge of noise statistics may have better performance. We show that the additive white Gaussian noise maximum likelihood estimator (AWGN MLE) has a superior performance to the Kasai autocorrelation estimate under additive shot noise conditions. It can achieve the Cramer-Rao Lower Bound (CRLB) for moderate data lengths and signal-to-noise ratios (SNRs). However, it does not possess the wide-applicability that the non-parametric Kasai estimator has. We show that the AWGN MLE performs sub-optimally under multiplicative decorrelation noise. As maximum likelihood estimators make assumptions on the noise statistics, they are very sensitive to outliers,

signal contamination and deviations from noise model assumptions. We show that under multiplicative decorrelation noise conditions, the AWGN MLE performance deteriorates, while the Kasai estimator still gives reasonable estimates. Hence, we further develop a multiplicative noise MLE for use under multiplicative noise dominant conditions. This estimator is superior to both the AWGN MLE and the Kasai estimator under these conditions, but requires knowledge of the decorrelation statistics. Hence we conclude that it is preferable to use a maximum likelihood approach in OCT Doppler frequency estimation when noise statistics are known or can be accurately estimated.

8571-88, Session PMon

High-speed, high-sensitivity spectral-domain correlation mapping optical coherence tomography based modified scanning protocol

Hrebesh M. Subhash, Joey Enfield , Martin Leahy, National Biophotonics and Imaging Platform (Ireland)

Correlation mapping optical coherence tomography (cmOCT) is an alternative robust method for obtaining volumetric images of dynamic perfusion within the microcirculatory tissue beds in vivo. The cmOCT method uses a 2D correlation mapping algorithm on the intensity OCT images to extract depth resolved flow map from static tissue background. The earlier reported cmOCT was based on a commercial swept-source OCT system, which uses a scanning protocol with dense sampling between adjacent B-frame, such that the inter frame separation was within the resolution limit of the OCT system to ensure strong correlation between adjacent frames. However, this scanning protocol requires a relatively long scan time and high density B-frame images to reconstruct the volumetric perfusion map, which degraded the system performance for wide-field in vivo imaging applications. In order to overcome this limitation we implemented a custom built high-speed spectral domain OCT and introduced a new scanning protocol for high-speed and high sensitive imaging of cmOCT. The new scan protocol measures repeated B-scans at the same location to generate a high sensitivity correlation map between successive B-frames. This scanning protocol can provide better background suppression and wide scanning with relatively short scanning time.

8571-90, Session PMon

Absolute fast axis determination using non-polarization maintaining fiber-based polarization-sensitive optical coherence tomography

Zenghai Lu, Stephen J. Matcher, The Univ. of Sheffield (United Kingdom)

We report on a new calibration technique that permits the accurate extraction of sample Jones matrix and hence fast-axis orientation by using fiber-based polarization-sensitive optical coherence tomography (PS-OCT) that is completely based on non polarization maintaining fiber such as SMF-28. In this technique, two quarter waveplates are used to completely specify the parameters of the system fibers in the sample arm so that the Jones matrix of the sample can be determined directly. The device was validated on measurements of a quarter waveplate and an equine tendon sample by a single-mode fiber-based swept-source PS-OCT system.

8571-92, Session PMon

Investigation of polarization-sensitive optical coherence tomography towards the study of microstructure of articular cartilage

Deepa K. Kasaragod, Zenghai Lu, The Univ. of Sheffield (United Kingdom); Christine Le Maitre, Sheffield Hallam Univ. (United Kingdom); Mark Wilkinson, Stephen J. Matcher, The Univ. of Sheffield (United Kingdom)

We report on extended Jones matrix calculus based multi-angle study carried out to understand the depth-dependent structural orientation of the collagen fibers in articular cartilage using polarization-sensitive optical coherence tomography (PS-OCT). This study highlights a 3D lamellar model for the collagen fiber orientation, with a quadratic profile for the arching of the collagen fibers in transitional zone pointing towards an ordered arrangement of fibers in that zone. The PS-OCT based multi-angle measurements yield insight into depth-dependent collagen architecture of the articular cartilage samples.

8571-93, Session PMon

Brownian motion based glucose measurement spectral domain optical coherence tomography

Michal Vymyslicky, Kostadinka Bizheva, Univ. of Waterloo (Canada)

A high speed (47 kHz), high resolution (3 μm axial resolution) Spectral Domain OCT system, operating in the 1060nm spectral range was used to measure glucose concentration from liquid phantoms. The phantoms were composed of uniformly sized polystirene microspheres suspended in water and glucose, undergoing Brownian motion. The range of glucose concentrations was chosen to match the values typical for blood glucose in normal and diabetic subjects. A series of B-scans were collected from each phantom. Fluctuations in the intensity of the measured back scattered light were recorded and processed with Fast Fourier Transform. Data was averaged within each frame and across B-scans to improve the SNR of the measurement. The resulting power spectra were fitted with a Lorentzian probability density function to determine the particle self-diffusion coefficient, from which the viscosity of the sugar solutions was calculated. The measured viscosities correlated very well with the theoretically expected values.

8571-94, Session PMon

Ultrahigh-resolution optical coherence tomography imaging of protein crystals using gel inclusion technique

Norihiko Nishizawa, Shutaro Ishida, Nagoya Univ. (Japan); Mika Hirose, Shigeru Sugiyama, Tsuyoshi Inoue, Yusuke Mori, Kazuyoshi Itoh, Hiroyoshi Matsumura, Osaka Univ. (Japan)

Protein crystals are required for X-ray crystallography to determine three-dimensional structures of proteins at atomic resolution. The conventional microscopy is currently used for observation and screening of protein crystals. However, the three-dimensional imaging, which is important for automated treatment of protein crystal, is generally difficult by light microscopy. In addition, the protein crystals in the media are frequently difficult to identify by conventional light microscopy owing to the appearance of salt crystals or amorphous materials.

In this work, we successfully demonstrated micro-scale, non-invasive, three-dimensional cross-sectional imaging of protein crystals using ultrahigh resolution optical coherence tomography (UHR-OCT). A low noise, Gaussian like, high power supercontinuum at wavelength of 800

nm was used as the light source. The axial resolution of 2 um in sample and the sensitivity of 95 dB were achieved. Since the protein crystal has homogeneous nano-structure, the optical scattering is negligibly small. So we used gel-inclusion technique to enhance the intensity of scattered signals, and clear, sharp 3D cross-sectional images of protein crystals were successfully observed. As the gel concentration was increased, the OCT signal intensity was increased. Using this method, the protein crystals surrounded by substantial amount of precipitates could be visualized, which is difficult by conventional light microscopy. The discrimination of protein and salt crystals was also demonstrated by the OCT signal intensity. The wavelength dependence of OCT imaging for protein crystal was examined at wavelength of 800-1700 nm regions. It was confirmed that the finest images were observed using 800 nm wavelength system.

8571-95, Session PMon

Simultaneous measurement of the sweating dynamics of a few tens of eccrine sweat glands by optical coherence tomography

Masato Ohmi, Yuki Wada, Osaka Univ. (Japan)

Since the proposal of optical coherence tomography (OCT), OCT has been developed intensively for the clinical application in ophthalmology. In addition to the clinical applications, we recently demonstrated the dynamic OCT for in vivo observation of physiological functions of small organs such as eccrine sweat glands and peripheral vessels under the human skin surface. In our previous work, the dynamic OCT analysis of mental sweating of a single eccrine sweat gland was made using the time-domain OCT (TD-OCT). A lot of eccrine sweat glands align along the hill of fingerprint on human fingertips with the density of several hundred glands in cm2.

In this paper, we demonstrate the dynamic OCT analysis of mental sweating of a few tens of eccrine sweat glands on a human fingertip using the swept-source OCT (SS-OCT). We propose a novel method for evaluation of the amount of excess sweat in response to mental stress, where the en-face OCT images of the spiral lumen of the eccrine sweat gland are constructed by data acquisition of the 128 B-mode OCT images. The dynamic analysis of mental sweating is performed by the time-sequential piled-up en-face OCT images with the frame spacing of 3.3 sec. Strong non-uniformity is observed in mental sweating where the amount of excess sweat in response to sound stress and physical stress is different for each sweat gland. demonstrate the dynamic OCT possible for a few tens of eccrine sweat glands using the swept-source OCT (SS-OCT).

8571-96, Session PMon

Behavior of the thermal diffusivity of native and oxidized human low-density lipoprotein solutions studied by the z-scan technique

Antonio Figueiredo Neto, Priscila Santos, Thiago Genaro-Mattos, Andrea Monteiro, Sayuri Miyamoto, Univ. de São Paulo (Brazil)

Low-density lipoprotein (LDL) in vivo oxidative modifications play an important role in the development of atherosclerotic plaques. It is possible to distinguish native from in vitro oxidized LDL (oxLDL) samples using Z-scan (ZS) technique in millisecond time scale [1]. Part of the beam is absorbed and converted into heat, generating a refractive index gradient. The normalized transmittance, measured as a function of the sample position around the beam focus, provides a typical peak-to-valley curve, which is related to the thermal diffusivity of the sample by using the Thermal Lens model [2]. We prepeared copper-mediated oxLDL samples, which were oxidized sequentially from 10 to 90 minutes, in steps of 10 minutes. Our results show that the thermal diffusivity increases as a function of the LDL oxidation degree. This behaviour can be explained by the increase of the hydroperoxides production due to the oxidation process. The oxidation products translocate from one LDL to another, disseminating the oxidation process and caring the heat across the sample. This phenomenon leads to a quick thermal homogenization of the sample, avoiding the formation of the thermal lens in highly oxidized LDL solutions.

References

[1] S.L. Gómez et al., Chem. and Phys. Lipids 163, 545-551 (2010).

[2] Carter et al., Appl. Opt. 23, 476-481 (1984).

8571-97, Session PMon

Temperature dependence of the fluorescence spectrum of ZnCdS nanoparticles

Elena K. Volkova, Vyacheslav Kochubey, Julia Konyukhova, Alexander Skaptsov, N.G. Chernyshevsky Saratov State Univ. (Russian Federation)

We have investigated luminescent semiconductor nanoparticles, the wavelength of the fluorescence of which depends on ambient temperature. In our research we used ZnCdS semiconductor nanoparticles of the mixed type with polymer coating.

ZnCdS nanoparticles were synthesized from a mixture of aqueous solutions of cadmium chloride (CdCl2) and zinc chloride (ZnCl2) by addition of sodium sulphide solution at room temperature. The nanoparticles were not stabilized. Acrylic acid aqueous solution contained 200 ppm p-methoxyphenol inhibitor that was not removed before use was added into the nanoparticle suspension. The polymerization was induced by unfiltered radiation of 250-W mercury lamp during 15 minutes with continuous mixing of the solution. Experimentally found that with increasing temperature of the sample fluorescence intensity decreases and the fluorescence maximum shifts to longer wavelengths.

Temperature dependence of the fluorescence function of phosphors underlies the creation of a “noncontact” nano thermometers that can measure the intracellular temperature increase.

8571-98, Session PMon

Imaging of electro-kintetic properties of tissue by optical coherence tomography

Vladislav Toronov, Valentin Demidov, Yuan Xu, Victor Yang, Ryerson Univ. (Canada)

There are free and fixed charges in tissues. Free charges – mobile ions - can move during application of external electric field. Interactions of the fixed and free charges during application of the electric field are responsible for electro-kinetic effects in tissue such as electrophoresis and electroosmosis. These effects cause electrically-induced changes in tissues. It was shown that fixed charge density on cell membranes changes during tumor genesis in comparison with normal tissue. Our approach is to apply a physiologically safe electric field to a tissue sample and to measure changes in optical coherence signals. We employed the swept-source OCT engine with the broadband light source of 63-nm spectral bandwidth centered at 1300 nm and output power of 18 mW. Switching the polarity of the electric field induced significant reversible changes in both amplitude and phase of the OCT signal. However, since the phase signal was corrupted by the phase noise, it required a formidable signal processing development to obtain an image of electrically induced phase changes. In order to understand the electro-kinetic nature of the observed OCT signals we are currently developing the theory of the effects and tissue phantoms allowing controlling the electro-kinetic properties similar to those of the tissue. The results of these ongoing studies will be reported at the Conference.

8571-99, Session PMon

Swept source optical coherence microscopy using VCSEL technology

Osman Ahsen, Yuankai K. Tao, Massachusetts Institute of Technology (United States); James Y. Jiang, Thorlabs Inc. (United States); Benjamin M. Potsaid, Massachusetts Institute of Technology (United States) and Thorlabs Inc. (United States); Hsiang-Chieh Lee, Massachusetts Institute of Technology (United States); Yury Sheykin, Beth Israel Deaconess Medical Ctr. (United States); Aguirre D. Aguirre, Massachusetts Institute of Technology (United States) and Brigham and Women's Hospital (United States); Vijaysekhar Jayaraman, Praevium Research, Inc. (United States); James L. Connolly, Beth Israel Deaconess Medical Ctr. (United States); Alex E. Cable, Thorlabs Inc. (United States); James G. Fujimoto, Massachusetts Institute of Technology (United States)

Optical coherence microscopy (OCM) uses coherence-gated detection to remove out-of-focus light and enables improved contrast and imaging depth over conventional reflectance confocal microscopy for imaging in scattering tissues. Fourier domain/swept source OCM is an appealing alternative to conventional time domain OCM methods, as images from multiple depths are acquired simultaneously as well as it enables the usage of post processing algorithms to correct for dispersion and field curvature mismatches. However, to date, Fourier domain detection has not been widely used in OCM because of demanding imaging speeds.

Vertical Cavity Surface-Emission Laser (VCSEL) sources can operate at high speeds with sweep rates in the MHz range and have the potential to overcome the aforementioned limitations of swept source lasers for OCM applications. In this study, we demonstrate OCM with swept source / Fourier domain detection using a high speed prototype VCSEL light source. System uses a compact design suitable for imaging in the pathology laboratory. Resulting curvatures in the scanning field is corrected using a calibration field, providing a uniformly focused en face image. Large field mosaics are generated by scanning the sample with a precision translation stage and combining individual small field of view images by post-processing.

Pathologically relevant ex vivo samples, such as human breast, rabbit kidney and colon has been imaged and cellular features can be identified in the resulting images. With the newer developments in the VCSEL technology in terms of sweep rate and axial resolution, Fourier domain/ swept source OCM has the potential to replace time domain methods for microscopy applications.

8571-101, Session PMon

Simultaneous optical coherence tomography and autofluorescence microscopy with a single light source

Cuixia Dai, Shanghai Institute of Technology (China); Shuliang Jiao, Xiaojing Liu, The Univ. of Southern California (United States)

Optical coherence tomography (OCT) and Autofluorescence (AF) microscopy are two optical imaging modalities that can image different yet complementary contrasts of biological tissues. OCT provides high-resolution, depth resolved imaging mainly based on scattering contrast. AF imaging is based on fluorescence contrasts, which can provide maps of the distribution of endogenous molecules (fluorophores). Given their complimentary contrast mechanisms, the combination of OCT and AF imaging could potentially provide more sensitive and specific detection of disease than either modality alone. Several groups have investigated the combination of OCT with AF imaging. In their studies, two different light sources at different wavelengths were used for OCT imaging and fluorescence excitation, respectively.

In this paper, we have accomplished simultaneous spectral domain optical coherence tomography (SD-OCT) and AF microscopy with only one broadband light source centered at 415 nm. Since the two imaging modalities are provided by the same group of photons their images are intrinsically registered. The imaging system was successfully tested on imaging biological samples ex vivo and in vivo, and scattering and molecular contrasts were simultaneously achieved. In our dual-modality imaging system, if a broadband light source centered at other wavelengths, e.g. 500 nm, is used the system will be potentially useful for imaging the structure and lipofuscin of the RPE layer. Since the OCT and AF signals come from the same group of photons it is also possible to achieve depth resolved AF imaging if a relationship can be established or adding another OCT, for example, in the near infrared.

8571-102, Session PMon

200kHz A-line rate SS-OCT imaging at 1060nm using a time-multiplexed system architecture

Brian D. Goldberg, Bart C. Johnson, Walid Atia, Mark Kuznetsov, Dale Flanders, AXSUN Technologies Inc. (United States)

We demonstrate a novel laser and system configuration for high-speed swept-source optical coherence tomography (SS-OCT) that achieves a doubling of the effective A-line rate without the need for fiber based buffering. A common set of drive electronics is used to drive two independent swept laser sources at close to 50 percent duty-cycle. The sources are then combined using an external 3dB coupler in the so called "ping-pong" configuration. This approach offers several advantages compared with fiber-based buffering including size, cost, and system complexity. A 200 kHz A-line rate swept source system with 18.1 mW output power and 103 nm tuning bandwidth centered at 1040 nm is demonstrated.

8571-103, Session PMon

Passively mode locked swept lasers

Bart C. Johnson, Walid Atia, Mark Kuznetsov, Dale Flanders, AXSUN Technologies Inc. (United States)

Axsun short-cavity swept lasers for optical coherence tomography are shown here to be passively mode locked. The emitted pulses modulate the gain medium in such a way as to promote short to long tuning. Instead of new wavelengths being built up from spontaneous emission, each pulse hops to a longer wavelength by nonlinear means, tracking the MEMS tunable Fabry-Perot filter. This allows very high speed tuning. The pulsation is stable, so these lasers have low relative intensity noise and have demonstrated shot-noise-limited system performance.

Experimentally, this is shown through an "interference spectrogram" where the output of an interferometer is detected on a fast detector and a gated RF spectrum is computed. The interferometer path difference is adjusted so the pulses can be interfered with their nearest and second nearest neighbors. The resulting spectrogram is consistent with a laser that pulses twice per round trip, hops in frequency, and has chirped pulses.

These lasers were simulated using the mode locking theories of Haus as a starting point. We added the effect of the imaginary part of the gain, added a swept filter, and find numeric solutions. The experimental observations of pulsation, frequency hopping, and pulse chirp were confirmed by simulation. Coherence functions computed through simulation showed realistic coherence lengths, coherence revival, and that the coherence revival peaks are shifted from the zero beat as observed by other groups as well as ourselves.

8571-104, Session PMon

Fast wavelength sweep in dispersion-tuned fiber laser using a chirped FBG and a reflective SOA for OCT applications

Yuya Takubo, Shinji Yamashita, The Univ. of Tokyo (Japan)

We have demonstrated a wavelength-swept fiber laser based on dispersion tuning method. In this method, the light in a dispersive laser cavity is intensity modulated and actively mode-locked, and the lasing wavelength can be changed by controlling the modulation frequency. As the dispersion-tuned laser does not include any tunable filters, the sweep rate and range are not limited by mechanical moving parts. We have reported the wavelength-swept laser which has the tuning range of over 100nm with the sweep rate of 200kHz, and we have applied the laser to the swept-source OCT system. Although we have successfully obtained the OCT image of the human finger at 1kHz sweep rate, we could not obtain OCT images at higher sweep rate because of the performance degradation of the laser. As this laser cavity included 100m long dispersion compensating fiber (DCF), the long laser cavity increased the photon lifetime and resulted in the output power decrease and the linewidth broadening at higher sweep rate. In order to solve these problems, we inserted a reflective semiconductor optical amplifier (RSOA) and a chirped fiber Bragg grating (CFBG) into the laser cavity. Use of these devices made it possible to shorten the cavity length drastically and the laser performance at high sweep rate is significantly improved. We could achieve that the sweep range of 60nm and the output power of 8.4mW at 100kHz sweep. We applied the laser to swept-source OCT system and we successfully obtained images of an adhesive tape at up to 250kHz sweep.

8571-105, Session PMon

Combined tunable filters based swept laser source for optical coherence tomography

Minghui Chen, Univ. of Shanghai for Science and Technology (China); Zhihua Ding, Zhejiang Univ. (China); Cheng Wang, Chengli Song, Univ. of Shanghai for Science and Technology (China)

We demonstrate a novel ultra-broad tunable bandwidth and narrow instantaneous line-width swept laser source using combined tunable filters working at 1290 nm center wavelength for application in optical coherence tomography. The combined filters consist of a fiber Fabry-Perot tunable filter (FFP-TF) and a polygon mirror with scanning grating based filter. The FFP-TF has the narrow FSR but ultra high spectral resolution (narrow instantaneous bandwidth) driven at high frequency far from resonant frequency. The polygon filter in the Littrow configuration is composed of fiber collimator, polygon mirror driven by function generator, and diffractive grating with low groove. Polygon filter coarsely tune with wide turning range and then FFP-TF finely tune with narrow band-pass filtering. In contrast to traditional method using single tunable filter, the trade-off between bandwidth and instantaneous line-width is alleviated. The combined filters can realize ultra wide scan range and fairly narrow instantaneous bandwidth simultaneously. Two semiconductor optical amplifiers (SOA) in the parallel manner are used as the gain medium. The wide bandwidth could be obtained by parallel these SOAs to be suitable for sufficient wide range of the polygon filter's FSR because each SOA generates its own spectrum independently. The proposed swept laser source provides an edge-to-edge scanning range of 180 nm covering 1220 to 1400 nm with instantaneous line-width of about 0.03 nm at sweeping rate of 23.3 kHz. The swept laser source with combined filters offers broadband tunable range with narrow instantaneous line-width, which is especially benefiting for high resolution and deep imaging depth optical frequency domain imaging.

8571-106, Session PMon

High-speed miniaturized swept sources based on resonant MEMS mirrors and diffraction gratings

Stefan Gloor, Adrian H. Bachmann, Marc Epitaux, Tim Niederhäusern, Philipp Vorreau, Nicolai Matuschek, Kevin Hsu, Marcus Duelk, Christian Velez, Exalos AG (Switzerland)

High-speed wavelength-swept laser technology offers versatile applications in optical coherence tomography (OCT), bio-chemical spectroscopy, and fiber-optic sensing. Particularly in recent years, swept laser technology has been critical in advancing OCT applications in the field of bio-medical imaging and industrial imaging, imparting the advantages of real-time in-vivo diagnostics and high sensitivity. To realize real-time clinical imaging and broad-base commercial deployment, compact, small, and stable swept sources are of utmost importance.

We have developed a miniature external-cavity swept laser based on the Littrow configuration, with semiconductor optical amplifier broadband gain chip, high-speed resonant 1D Micro-Electro-Mechanical-System (MEMS) mirror, and proprietary diffraction grating all packaged into a temperature-controlled optical bench inside a 26-PIN butterfly (BTF) package. This hybrid BTF platform has the ability to generate lasers of different spectral regions (from 400nm to 1700nm) at different axial scan (A-scan) frequencies (2kHz to 150kHz).

We report the demonstration of a 40-kHz 1300-nm swept source with 10 mm coherence length realized in a compact butterfly package. Fast wavelength sweeping is achieved through a 1D 20-kHz MEMS mirror in combination with an advanced diffraction grating. The MEMS mirror is a resonant electrostatic mirror and performs harmonic oscillation only within a narrow frequency range, resulting in low-jitter and long-term phase-stable sinusoidal bidirectional sweep operation with an A-scan rate of 40 kHz. The source achieves a coherence length of 10 mm for both the up- and down-sweep and an OCT sensitivity of 105 dB.

8571-108, Session PMon

FPGA-based non-uniform fast fourier transform (NUFFT) algorithm for real-time OCT signal processing

Anke Bossen, Stefan Remund, Dominic Ernst, Christoph Meier, Berner Fachhochschule Technik und Informatik (Switzerland); Tim von Niederhäusern, Marcus Duelk, Exalos AG (Switzerland); Kalyanramu Vemishetty, National Instruments Corp. (United States)

Commercial OCT systems typically use real-time signal processing to allow instantaneous measurements and adjustments. Increasing data acquisition rates and imaging speeds of FD-OCT Systems therefore require efficient signal processing implementations to cope with the amount of the recorded data.

In this work, we present, to our knowledge, the first real-time implementation of a NUFFT algorithm for FD-OCT in an FPGA. First, the basic NUFFT algorithm is discussed and compared with cubic-spline interpolation regarding efficient re-sampling in k-space with different phase nonlinearities of sinusoidal swept sources. The algorithm was then adapted for an implementation in an FPGA unit and implemented on a NI PXIe-7965R FlexRIO FPGA module with Virtex-5 SX95T FPGA (National Instruments, USA) using the graphical programming language LabVIEW. The accuracy of the real-time FPGA-NUFFT OCT engine is compared with offline processing by means of simulated numerical data. For a continuous phase extraction with a Gaussian kernel of size 3 and an oversampling factor allowing a maximum of two interpolation points between the actual phase sampling points, the implemented algorithm allows a processing performance at a sampling rate of 100 MS/s. Furthermore, the OCT processing engine has been successfully tested with bidirectional sinusoidal swept sources at A-scan rates of 50 kHz with

real-time k-space calibration and linearization for up-sweep and down-sweep of the swept source.

8571-109, Session PMon

FPGA-based real-time swept-source OCT system for B-scan live-streaming or volumetric imaging

Marcel Jacomet, Vinzenz Bandi, Josef Goette, Berner Fachhochschule Technik und Informatik (Switzerland); Tim von Niederhäusern, Adrian H. Bachmann, Marcus Duelk, Exalos AG (Switzerland)

We have developed a high-speed, real-time Swept-Source OCT (SS-OCT) system with the signal-processing implemented in a Virtex-6 SX315T FPGA fabric, housed in standard, commercially available DAQ board, featuring a dual-channel 12-bit 500-MS/s digitizer. The SS-OCT system acquires on one input channel a k-clock reference signal, and performs, in real time for each A-scan, phase extraction based on the Hilbert transform to generate a remapping vector. The second input channel acquires the OCT signal itself, which is next k-space linearized using this remapping vector. Subsequently, a 2048-point FFT transforms each remapped A-scan. These processed A-scans are next sent to a host PC via PCIe at full frame rate for real-time visualization. The complete SS-OCT system is steered by a global control unit, that generates the needed synchronization signals for the 2D galvanometric scanners and AD converters to capture volumetric OCT images or to live-stream B-scans. We have successfully tested the real-time SS-OCT system with 1060-nm swept sources featuring continuous A-scans with 100 kHz sweep rates.

With the parallelization of our hardware algorithms, we have achieved high-speed, real-time signal processing at an oversampling rate of 500MS/s. An analysis of the OCT image quality reveals competitive results, despite the fact that we have implemented only a linear, but parallel and oversampled, remapping algorithm.

Because OCT algorithms are signal processing oriented, Matlab is our tool of choice for basic analysis. Therefore, we have followed the natural way to also use Matlab within our tool chain for OCT hardware algorithm development, synthesis and test.

8571-110, Session PMon

GPU-based real-time processing of Fourier domain OCT with zero-filling interpolation and fixed-pattern noise removal by partial median subtraction

Yuuki Watanabe, Yamagata Univ. (Japan)

Graphics processing unit (GPU) programming for real-time Fourier domain optical coherence tomography (FD-OCT) with fixed-pattern noise removal by subtracting mean and median was presented. In general, the fixed-pattern noise can be removed by the averaged spectrum from many spectra of an actual measurement. However a mean-spectrum results in artifacts as residual lateral lines caused by a small number of high-reflective points at a sample surface. These artifacts can be eliminated from OCT images by using medians instead of means. However, median calculations that are based on a sorting algorithm are known to consume a large amount of computation power and time. On the developed GPU programming highly reflective surface regions were obtained by calculating the standard deviation of the Fourier transformed data in the lateral direction. The medians and means were then subtracted at the observed regions and other regions such as backgrounds, respectively. Further the GPU programming was also performed the zero-filling interpolation, which is performed with a forward Fourier transform, zero padded to increase the data array length fourfold , inverse Fourier transformed back to the spectral domain, and linear interpolated in k-space. When the number of the median calculation was less than 320 positions of total 512 depths in an OCT image with 1024 A-lines, the GPU processing rate was faster than that of the line scan camera (46.9 kHz). Therefore, processed OCT images can be displayed in real-time using partial medians.

8571-111, Session PMon

A GPU accelerated real-time multi-functional SD-OCT system

Yan Wang, Christian M. Oh, Michael C. Oliveira, M. Shahidul Islam, Arthur Ortega, B. Hyle Park, Univ. of California, Riverside (United States)

We present a GPU accelerated multi-functional spectral domain optical coherence tomography system at 1300nm. A graphic processing unit (GPU) was utilized in the real-time processing program to fulfill the heavy computation of intensity, flow, phase retardation and en face images. The GPU-CPU hybrid processing program is capable of real-time processing and display of every intensity image, comprised of 1024 pixels by 2048 A-lines acquired at 20 frames per second. The update rate for all four images with size of 1024 pixels by 2048 A-lines simultaneously (intensity, phase retardation, flow and en face view) is approximately 10 frames per second, which is five times faster than the purely CPU processing program. The speed of the each facet of the multi-functional OCT GPU-CPU hybrid acquisition system, intensity, phase retardation, and flow, were separately demonstrated by imaging a horseshoe crab lateral compound eye, a non-uniformly heated chicken muscle, and a microfluidic device. Finally, a mouse brain with a thin skull preparation was imaged with all image views (intensity, phase retardation, flow, en face flow) updating at a rate of 10 frames per second with the en face flow view displaying blood vasculature and demonstrated our ability to do rapid identification of structures in OCT images. Real-time recorded videos when imaging samples listed above will be presented to demonstrate the fast processing speed and volume visualization ability of the hybrid GPU-CPU processing program.

8571-112, Session PMon

Method of performing Fourier transform of data not sampled on Cartesian grid and its validation on spectral domain optical coherence tomography data

Alexander A. Moiseev, Grigory V. Gelikonov, Pavel A. Shilyagin, Valentine M. Gelikonov, Institute of Applied Physics (Russian Federation)

In this paper we introduced a method of performed Fourier transformation of nonequidistantly spaced data. We show, that data resampling can be performed as “nonuniform convolution”, i.e. on convolution with the kernel which shape depends on position. Total number of requiwed calulations for performing nonuniform Fourier transform with proposed algorithm is O(mN+NlogN), where N is the length of realization and m is “convolution” kernel size. Because the length of such kernel can be choose relatively small (from 5 to 9) and no upsampling of the data as well as additional processing required, this operation can be computed numerically efficiently. Coefficients for such “convolution” are derived analytically and can be computed during performing transformation, or precomputed and stored. Method had been validated on Spectral Domain Optical Coherence Tomography (SD OCT) data.

8571-113, Session PMon

Improving resolution in spectral domain low coherence interferometry through FFT harmonic artifacts

Marcus P. Raele, Instituto de Pesquisas Energéticas e Nucleares (Brazil); Luiz V. G. Tarelho, Iakyra B. Couceiro, Carlos L. S. Azeredo, National Institute of Metrology, Standardization and Industrial Quality (Brazil); Anderson Z. de Freitas, Instituto de Pesquisas Energéticas e Nucleares (Brazil)

Low coherence interferometric setups in the Fourier domain can experience false structures after the Fourier Transform procedure due to signal saturation, giving rise to imaging artifacts. These structures are located at multiple frequencies of the original, and real scattering signals, also referred to as harmonics, are present. In this study, a better understanding of this phenomenon is described, simulated and measured in a real setup. The aim of the present work is to show that these features can be used to improve resolution in highly reflective samples. Using an OCT system and calibrated step height standards, it was possible to achieve a resolution greater than the coherence length of the light source.

This increased resolution was possible because the difference between peak positions from step height surfaces are directly related with harmonic order, the pixels number separation is bigger for higher orders than for lower orders, resulting in lower uncertainty as well.

8571-114, Session PMon

Blue light spectral optical coherence tomography with spectrally encoded illumination

Sylwia M Maliszewska, Nicolaus Copernicus Univ. (Poland); Robert J. Zawadzki, UC Davis Medical Ctr. (United States); Maciej Wojtkowski, Nicolaus Copernicus Univ. (Poland)

In this paper we present Spectral Optical Coherence Tomography modality which employs blue light in the spectral range of 365-445 nm and enables theoretically imaging with the axial resolution down to 1.8 ?m in air.

Recently first attempts on use of blue light in Optical Coherence Tomography imaging have been reported. However, in the reported setup configurations light coming from second harmonic (SHG) occurring in nonlinear crystals was centered at 415 nm and the full width at half maximum equaled to about 8 nm resulting in 12 ?m of axial resolution in air

To obtain broadband blue light we used second harmonic generation as well. Since the second harmonic component resulting from single SHG even in thin crystals and for high power lasers is very narrowband, we introduced angular scanning of the Ti:Saphh laser beam in a nonlinear crystal and obtained blue light with a spectrum swept in time in wavelength range from 365 to 445 nm.

Generated in this way broadband second harmonic light creates on imaged sample spatially dispersed – spectrally encoded line rather than a single spot – different parts of blue spectrum illuminate different place in the object at certain time. Therefore acquired “B-scans” include spectral signal from different parts of the sample. This spectrally encoded line illumination on the imaged object requires additional beam scanning and numerical data processing before A-scan equivalent spectral data are generated and standard OCT Fourier transformation can be applied to retrieve the image.

8571-115, Session PMon

Interferometric synthetic aperture microscopy implementation on a floating point multi-core digital signal processor

Adeel Ahmad, Univ. of Illinois at Urbana-Champaign (United States); Murtaza Ali, Texas Instruments Inc. (United States); Fredrick South, Guillermo L. Monroy, Steven G. Adie, Nathan Shemonski, Paul S. Carney, Stephen A. Boppart, Univ. of Illinois at Urbana-Champaign (United States)

Current generation optical coherence tomography (OCT) systems have scanning speeds approaching several hundred thousand A-lines per second. Optimum use of these high-speed systems not only requires sophisticated data acquisition techniques but also computational platforms with high compute capabilities. Recent developments in digital signal processors (DSPs) capabilities which include multi-core and floating-point operations support, coupled with the ease of programming and higher computations per watt, has made DSPs a strong contender for high performance computing applications in several areas. In this work, we describe the implementation of optical coherence tomography (OCT) and interferometric synthetic aperture microscopy (ISAM) processing on a floating point multi-core DSP (C6678, Texas Instruments). ISAM is a computationally intensive data processing technique that solves the depth-of-focus problem in OCT, yielding a spatially-invariant transverse resolution throughout the imaging depth. Computationally, ISAM requires Fourier transforms and re-sampling of the Fourier space of the data based on Stolt mapping (utilized in synthetic aperture radar). Preliminary results indicate that 2D-ISAM processing at 70,000 A-lines/sec and OCT at 180,000 A-lines/sec can be achieved with the current implementation using available DSP hardware. In the future, a complete embedded system incorporating camera-link interfaces and appropriate data input/output channels can be designed around the DSP chip to make a fully functional, portable, low cost and low power OCT system that may be useful for clinical and point-of-care settings.

8571-116, Session PMon

Wavefront control on optical coherence tomography for high penetration depth

Jaeduck Jang, KAIST (Korea, Republic of); Jaeguyn Lim, Samsung Advanced Institute of Technology (Korea, Republic of); Hyeonseung Yu, KAIST (Korea, Republic of); Hyun Choi, Jinyong Ha, Samsung Advanced Institute of Technology (Korea, Republic of); Wang-Yuhl Oh, KAIST (Korea, Republic of); Wooyoung Jang, Samsung Advanced Institute of Technology (Korea, Republic of); YongKeun Park, KAIST (Korea, Republic of)

We present a wavefront shaping approach on spectral domain optical coherence tomography (SD-OCT) for improving penetration depth. Recent SD-OCT system provides a penetration depth of around 2~3 mm depending on the optical characteristics of samples. In ophthalmology, the tissue structures are transparent, where multiple scattering is low, such that SD-OCT can achieve high penetration depth. Meanwhile, because other tissues such as a skin are nontransparent (heavily turbid), penetration depth is primarily limited by the scattering property between light source and tissues. An approach reduces the scattering by matching the refractive index of scatterers based on an optical clearing agent (Glycerol). However, the approach requires about 10 minutes after the addition of Glycerol. In addition, some approach called as spatial and frequency compounding regards multiple scattered phenomenon as background noise. The method acquires multiple uncorrelated measurements using slightly translated beam paths and multiple sources and only suppresses the background noise in a depth. In this paper, we propose a wavefront shaping approach for controlling scattering property. Generally, an optical phase conjugation (OPC) method, by changing the spatial phase of wavefront, can image the target through

turbid media in transmission mode. We apply the OPC method for OCT as reflection imaging mode to control the multiple scattering paths inside a sample. As the multiple scattering is reduced and the single scattering is strengthened, the SNR in deeper depths would be significantly enhanced. To implement wavefront shaping in OCT, we exploit spatial modulator at illumination part and optimally control a shape of wavefront by iterative feedbacks. Therefore, applying the wavefront shaping method, we can enhance the signal from deeper positions and extend the penetration depth.

8571-117, Session PMon

Combining Gabor and Talbot bands techniques to enhance the sensitivity with depth in Fourier domain optical coherence tomography

Adrian Bradu, Manuel Marques, Petr Bouchal, Adrian G. Podoleanu, Univ. of Kent (United Kingdom)

The purpose of this study was to show how to favorably mix two effects to improve the sensitivity with depth in Fourier domain optical coherence tomography (OCT): Talbot bands (TB) and Gabor-based fusion (GF) technique. TB operation is achieved by directing the two beams, from the object arm and from the reference arm in the OCT interferometer, along parallel separate paths towards the spectrometer. By changing the lateral gap between the two beams in their path towards the spectrometer, the position for the maximum sensitivity versus the optical path difference in the interferometer is adjusted. For five values of the focus position, the gap between the two beams is readjusted to reach maximum sensitivity. Then, similar to the procedure employed in the GF technique, a composite image is formed by edging together the parts of the five images that exhibited maximum brightness. The combined procedure, TB/GF is examined for four different values of the beam diameters of the two beams.

8571-118, Session PMon

Forward scanning probe for 3D optical coherence tomography (OCT)

Hinnerk Schulz-Hildebrandt, Daniel Kirsten, Gereon Hüttmann, Univ. zu Lübeck (Germany)

Optical coherence tomography (OCT) is a rapidly developing non-invasive imaging modality, which has become indispensable in ophthalmology. Integration of OCT with endoscopy opens a number of possible OCT applications diagnosing various diseases of inner organs. Various studies demonstrated the application of endoscopic OCT in cardiology or oncology. OCT can help to implement an optical biopsy, which makes histological diagnosis more precise and even may avoid the removal of tissue samples. Instead of waiting for the histo-pathologial evaluation of the biopsies, the physician could get diagnostic information in real-time during the intervention. Though several technical solution for endoscopic OCT probes were demonstrated, there is still a need for a 0° scanning probe which combines 3D imaging with variable scanning speed with a simple design for a single-use product. Here a special magnetic actuator is proposed as an alternative to piezo actuators.

Irradiation of from a single mode fiber (SMF-28e) is focused by a GRIN lens into the tissue. For scanning, the tip the fiber is moved magnetically in x- and y-direction 300 micro meter behind the GRIN lens. An image of the fiber end is formed 3.5 mm in front of the GRIN lens at a magnification of 1:2 . A lateral resolution of 39,5 micro meter was achieved. The position of the moving fiber is sensed optically in order to provide an undistorted OCT image. Total transmission of the probe was 73% for a single pass, which resulted in roughly 3 dB reduction of the OCT sensitivity by the probe. Volumetric image were obtained over up to 1.5 mm x 1.5 mm field of view. Low voltage operation at variable frequencies below the resonance is possible. A Simple cost-effective design of the mechanical and optical components was achieved.

8571-119, Session PMon

Complex artifact suppression using vestigial sideband filter in Fourier-domain optical coherence tomography

Hyun-Woo Jeong, Korea Univ. (Korea, Republic of); Jae-Guyn Lim, SAMSUNG Electronics Co., Ltd. (Korea, Republic of); Hyung-Jin Kim, Wonzoo Chung, Beop-Min Kim, Korea Univ. (Korea, Republic of)

Various complex artifact removal techniques, what we called the full-range complex (FRC) approaches, have been suggested for the mirror artifact suppression. One of the widely accepted approaches uses the phase modulation induced by the off-pivot illumination on the galvanometer, which does not require additional devices. In this method, acquired two-dimensional spectral data are Hilbert transformed to yield the complex signals along the B-scan direction. Then, the desired depth-resolved images without the mirror term can be reconstructed via Fourier transformation for each A-scan.

In Hilbert transform, the truncation length is the only parameter that can be adjusted to enhance the mirror term suppression. However, the truncation length is directly related to the computational load, thus it is critical to use the minimum truncation length which does not yield image distortion.

In this study, we employed vestigial sideband (VSB) filter, instead of conventional Hilbert transform, for the effective mirror artifact removal during the off-pivot, full-range approach in SD-OCT. It enables almost complete removal of one sideband by choosing appropriate filter parameters minimizing the filter distortion. To evaluate the optimal parameters, we acquired images of the IR card and analyzed the mirror suppression ratio of the card surface. Comparing images with similar mirror suppression ratio at each minimum truncation length (N) of both filters, it was found that the computational load was significantly reduced when using the VSB filter since much shorter truncation length was required. Finally, we present the anterior segment images of a human volunteer's eye processed using the VSB filter.

8571-120, Session PMon

Tunable linear in-wavenumber optical spectrometer for spectral-domain optical coherence tomography

Pavel A. Shilyagin, Grigory V. Gelikonov, Valentin M. Gelikonov, Institute of Applied Physics (Russian Federation)

A focusing lens distortion influence on spectrometer nonequidistance is observed. A detail analysis of a single-prism corrector of nonequidistance of grating-based spectrometer is made. A novel setup for optimal correction of spectrometer nonequidistance is proposed. The setup allows tuning of spectrometer to optimal correction of nonequidistance in wide range of illumination source's central wavelengths and focusing lens distortions.

A novel prism compensator setup, which uses prisms with very small material dispersion, and which is able to be tuned to optimal state for wide range of illumination source's central wavelengths and focusing lens distortions is proposed.

Using two separated prisms one can construct an optical deice, which is similar to a single prism with another prism angle. By tuning the angle between prisms and tilting the construction relatively to diffractive grating surface it is possible to obtain an optimal correction of spectrometer nonequidistance in wide range of source central wavelengths and focusing lens distortions.

8571-121, Session PMon

Ultrahigh resolution endoscopic spectral domain optical coherence tomography with a tiny rotary probe driven by a hollow ultrasonic motor

Ning Zhang, Tianyuan Chen, Tiancheng Huo, Chengming Wang, Jing-gao Zheng, Tieying Zhou, Ping Xue, Tsinghua Univ. (China)

This paper proposes a novel rotary endoscopic probe for spectral-domain optical coherence tomography (SD-OCT). The probe with a novel large N.A. objective lens is driven by an ultra-small hollow rectangular ultrasonic motor for circular scanning. Compared to the conventional driven techniques, the hollow ultrasonic motor enables the fiber to pass through its inside. Therefore the fiber, the objective lens and the motor are all at the same side. This enables 360 degree unobstructed imaging without any shadow resulted from power wire as in the conventional motor-driven endoscopic OCT. Moreover, it shortens the length of the rigid tip and enhances the flexibility of the probe. Meanwhile, the ultrasonic motor is robust, simple, quiet and of high torque, very suitable for OCT endoscopic probe. The side length of the motor is 0.7 mm with 5mm in length. The outer diameter of the probe is 1.2mm. A significant improvement in the lateral resolution is demonstrated due to the novel design of the objective lens, which is to our knowledge the highest lateral resolution in circular scanning endoscopic OCT. A right-angle lens is utilized instead of the traditional right-angle prism as the last optics close to the sample, leading to a reduction of the working distance and an enlargement of the N.A. of the objective lens. To demonstrate the performance of the endoscopic OCT system, a phantom and a chicken trachea are imaged with an axial resolution of ~7?m, a lateral resolution of ~6?m and a SNR of 88dB.

8571-122, Session PMon

In vivo human optic nerve and laminar cribrosa microstructural and vasculature evaluation using ultrahigh sensitive optical microangiography

Lin An, Peng Lee, Gongpu Lan, Ruikang Wang, Univ. of Washington (United States)

Optical nerve head, is a round or oval shaped structure of posterior part of human eye, where ganglion cell axons exit the eye to form millions of optical nerve fibers to transmit the visual information to the brain. The structural and vasculature information of ONH is an important indicator of glaucoma which is the second leading cause of blindness all over the word. Better assessments of ONH from both structural and vasculature aspects would greatly enrich the knowledge about mechanism of Glaucoma and its early phases before the optical nerve loss, which will cause irreversible vision loss. UHS-Optical micro angiography is a functional extension of Fourier Domain Optical Coherence Tomography, which could noninvasively provide high resolution high sensitivity depth resolved micro-structural and micro-vasculature information of biological information simultaneously. During the imaging process, a full rang vasculature imaging method proposed in was first performed to extend the imaging range and utilize the high sensitivity imaging region of the developed ultrahigh speed UHS-OMAG system. Together with a large field of view scanning pattern, we could achieve overall visualization of ONH both in micro structural and vasculature modes. For better visualizing the LC, a high resolution optical probe and a smaller field of view were employed to focus onto the bottom of the optic disc cup.

8571-123, Session PMon

Application of full range swept source optical coherence tomography for imaging anterior eye segments of the patients with keratoprosthesis implants

Raju Poddar, Dennis Cortes, Robert J. Zawadzki, Mark J. Mannis, John S. Werner, UC Davis Medical Ctr. (United States)

We constructed a high-speed complex conjugate resolved swept source optical coherence tomography system using coherence revival of the light source for clinical imaging of the anterior segment of the human eye. The performance of the system will be described in detail. The feasibility of our instrument for visualization of the anterior segment of patients with the Boston Keratoprosthesis (KPro) will be discussed. Examples of images acquired before and after the KPro lens [Type I and II] surgery will be presented along with an overview of the optical characteristics of the KPro lens.

8571-124, Session PMon

OCT corneal topography within ? diopter in the presence of saccadic eye movements

Samir I. Sayegh M.D., The Eye Center (United States)

Refractive surgeons and cataract surgeons need accurate measurements of corneal curvature/power. Increased expectations of patients, the increasing number of patients having undergone prior surgeries and patients with corneal pathologies dictate the need for reliable curvature measurements to enhance the predictability and the quality of surgical outcomes. Eye movements can negatively influence these measurements.

Current commercial OCT systems provide pachymetry measurements. Full corneal topographic information of anterior and posterior corneal surfaces for use in cataract surgery and refractive procedures remain a desirable goal and would add to the usefulness of anterior segment and posterior segment evaluation. Substantial progress has been made towards obtaining “average” central corneal power (D Huang), but its usefulness is limited as refractive cataract surgery has moved beyond the era of averages and into the new realm of individualized refractive corrections with no residual astigmatism. Power in different meridians and full topography have become a must and obtaining them with OCT is a natural choice as OCT delineates both the anterior and posterior surfaces, and therefore powers, of the cornea.

We present a model of eye movements based on peak saccade velocities and formulate criteria for obtaining OCT topography with ? of a diopter in the presence of these movements. Using these criteria we illustrate how next generation MHz systems will allow full corneal OCT topography in both healthy and pathological corneas.

8571-125, Session PMon

In vivo detection of cortical optical changes associated with seizure activity with optical coherence tomography

Melissa M. Eberle, Carissa L. Reynolds, Jenny I. Szu, Yan Wang, Anne M. Hansen, Mike S. Hsu, Devin K. BInder, B. Hyle Park, Univ. of California, Riverside (United States)

Epilepsy, affecting at least 2% of the population, encompasses a group of disorders of the brain characterized by the periodic and unpredictable occurrence of seizures. The most common technology for seizure detection is with electroencephalography (EEG), which has low spatial resolution and minimal depth discrimination. Optical techniques using near-infrared (NIR) light have been used to improve

upon EEG technology. Previous research has suggested that optical changes, specifically changes in near-infrared optical scattering, may precede EEG seizure onset in in vivo models and that these optical changes are due to pre-seizure physiological changes, in particular reduction in the extracellular space. Optical coherence tomography (OCT) is a high resolution, minimally invasive imaging technique, which can produce depth resolved cross-sectional images. In this study, OCT was used to detect changes in optical properties of cortical tissue in vivo in mice before and during the induction of generalized seizure activity. Generalized tonic-clonic seizures were induced with 100mg/kg pentylenetetrazol (PTZ) and imaging was performed through a thinned skull cortical window. We demonstrated that a significant decrease ($P < 0.001$) in backscattered intensity during seizure progression compared to the control measurements can be detected before the onset of observable manifestations of generalized (stage-5) seizures. The decrease in intensity was calculated through a rate of change analysis directly after PTZ injection. These results indicate the feasibility of minimally-invasive optical detection of seizures with OCT.

8571-126, Session PMon

Identification of in vivo brain structures using optical coherence tomography

Carissa Reynolds, Melissa M. Eberle, Jenny I. Szu, Mike S. Hsu, Yan Wang, Devin K. Binder, B. Hyle Park, Univ. of California, Riverside (United States)

Neurosurgery could greatly benefit from a tool which provides real-time imaging. Procedures such as tumor biopsies or placement of electrodes for deep brain stimulation require the insertion of probes into the brain. Currently there is no method for real-time imaging during probe placement. Surgeons rely on stereotactic navigation which utilizes computed tomography or magnetic resonance imaging scans taken before the surgery begins to plan the appropriate route of entry. However, this method cannot account for brain shift during the procedure. Optical coherence tomography, a nondestructive optical imaging technique with micrometer resolution and imaging depth on the order of a millimeter, could serve this purpose by providing real-time visualization of landmarks deep within the brain. This study investigated the ability of OCT to identify brain structures in vivo.

Using a spectral-domain OCT setup with a center wavelength of 1300 nm, we acquired images of in vivo mouse brain. The mouse was prepared with a thin-skull cortical window to allow for adequate imaging depth while preserving normal physiological conditions of the brain. India ink was injected through two small burr holes to define the boundaries of the OCT imaging plane. These markers were used to register the histology with OCT images. Comparison of the OCT images with histology identified the corpus callosum and two separate layers of the cerebral cortex. Attenuation coefficients for each of these regions were identified from OCT depth profiles. These results demonstrate the first layer specific registration of two-dimensional OCT images with histology to identify in vivo brain structures.

8571-127, Session PMon

Reflective type objective based spectral-domain phase-sensitive optical coherence tomography for high-sensitive structural and functional imaging of cochlear microstructures through intact bone of an excised guinea pig cochlea

Hrebesh M. Subhash, Oregon Health & Science Univ. (United States); Ruikang K. Wang, Univ. of Washington (United States); Fangyi Chen, Alfred L. Nuttall, Oregon Health & Science Univ. (United States)

Most of the optical coherence tomographic (OCT) systems for high resolution imaging of biological specimens are based on refractive type microscope objectives, which are optimized for specific wave length of the optical source. In this study, we present the feasibility of using commercially available reflective type objective for high sensitive and high resolution structural and functional imaging of cochlear microstructures of an excised guinea pig through intact temporal bone. Unlike conventional refractive type microscopic objective, reflective objective are free from chromatic aberrations due to their all-reflecting nature and can support a broadband of spectrum with very high light collection efficiency.

8571-128, Session PMon

History compounding: a novel speckle reduction technique for OCT guided cochleostomy

Yaokun Zhang, Karlsruher Institut für Technologie (Germany); Tom Pfeiffer, Wolfgang Wieser, Ludwig-Maximilians-Univ. München (Germany); Marcel Weller, Univ. Hospital Duesseldorf (Germany); Robert Huber, Ludwig-Maximilians-Univ. München (Germany); Thomas Klenzner, Univ. Hospital Duesseldorf (Germany); Joerg Raczkowsky, Heinz Woern, Karlsruher Institut für Technologie (Germany)

Optical coherence tomography (OCT) is a promising candidate for monitoring the bottom of the drilled channel during cochleostomy to prevent injury to the critical structure under the bone tissue. While the thickness of the overlaying bone tissue is changed during the drilling process, the wave front of the backscattered light is also altered and results in changing speckle patterns of the observed structure in the sequential history scans. By averaging these history scans, the speckle can be reduced and make the critical structure detection much easier.

Before averaging, the refractive index of bone tissue n_B has to be compensated so that the pixels representing the same structure in different history scans can be aligned together. For an accurate measurement of n_B, a bovine bone specimen with a stair-shaped surface is prepared using a CO2-Laser. An OCT scan of it is performed with a mirror underneath and the flat backside appears to be stair-shaped due to the uncompensated refractive index. By manually adjusting the value of n_B until the backside appears to be a straight line again we determine n_B=1.59.

A trail drilling is then conducted on fresh bovine bone plate fixed to an aluminum slab. Each time when the channel is deepened about 30-50?m, an OCT scan is taken. After refractive index compensation and history scans averaging, speckles below the drilled channel are reduced significantly, while those outside remain unchanged.

History compounding is therefore an effective, flexible and low cost technique for speckle reduction for OCT monitored hard tissue removal.

8571-129, Session PMon

Visualization of heart chamber of Drosophila with dual-beam optical coherence tomography

Cheng-Kuang Lee, Feng-Yu Chang, Meng-Tsan Tsai, Chang Gung Univ. (Taiwan); June-Tai Wu M.D., National Taiwan Univ. Hospital (Taiwan); Chih-Chung Yang, National Taiwan Univ. (Taiwan)

Drosophila (fruit fly) has been recognized as a powerful model for the studies on the heart development and diseases. However, the curvature of heart chamber, the high heart rate (4~6 beats/s), and the limited diameter of heart tube make imaging the entire heart chamber difficult. To non-invasive investigate the beating rhythms between the different heart

portions of Drosophila, we propose a new approach to visualize the entire heart camber including the conical chamber and ostia portions, and observe the retrograde and anterograde beats. In this study, a buffered Fourier-domain mode locking (FDML) laser is implemented to provide a high imaging speed with an A-scan rate of ~240 kHz. To increase the scanning range for the visualization of the entire heart chamber without sacrificing the frame rate of OCT system, the two output ports of the buffered FDML laser are used simultaneously to scan the different heart portions of Drosophila and two scanning images are combined as a single B-scan. Based on the dual-beam setup, one can see that the entire heart chamber can be observed to overcome the limitation of heart curvature. Furthermore, the beating behaviors of the different heart sections from young and old flies are also compared.

8571-130, Session PMon

Monitoring of the degradation in the rat's articular cartilage inducing osteoarthritis using common-path Fourier-domain optical coherence tomography

Chul-Gyu Song, Chonbuk National Univ. (Korea, Republic of)

No Abstract Available

8571-131, Session PMon

Ex-vivo bladder cancer study with combined two-photon microscopy and optical coherence tomography

Yeoreum Yoon, Bumju Kim, Junho Lee, Peng Xiao, Pohang Univ. of Science and Technology (Korea, Republic of); Ingul Kim, Ji Yeol Lee, The Catholic Univ. of Korea (Korea, Republic of); Ki Hean Kim, Pohang Univ. of Science and Technology (Korea, Republic of)

We tested feasibility of a combined two-photon microscopy (TPM) and optical coherence tomography (OCT), to identify of the cancer and to measure its extension into the bladder tissue using separate light sources. In combined system, TPM used a Ti-Sapphire laser having 780nm excitation wavelength for inducing fluorescence, and OCT used a wavelength swept source laser having 1310nm center wavelength respectively. TPM and OCT combined system was designed to have 300μm and 800μm field of view (FOV) with same objective lens, which has 20x, magnification. This system provided information at both the cellular and micro-structural level, which have sub-cellular resolutions and the deeper and wider tissue regions. An ex-vivo mouse bladder cancer model was used and the inner side of bladder tissue was exposed for imaging. 3D TPM imaging based on intrinsic fluorescence showed cellular structure of the normal and cancer bladder having 250~300μm depth range from surface. Umbrella cell, intermediate cell, collagen and upper muscle were visualized in the normal tissue, and the cancer tissue was distinguished due to its disorganized cellular structures. 3D OCT imaging showed several layered structures of normal bladder and the extension of the cancer into the bladder layers. The extension of the cancer invasion into bladder layers was founded between normal and tumor, and measured discrimination in low- and mild-grade staging, due to the no layered structure in tumor. We confirmed that TPM and OCT combined system has the potential to diagnosis bladder cancer preliminary with providing information at both cellular and structure levels, and this method expected to apply in various clinical purpose.

8571-132, Session PMon

Design of a swept-source, anatomical OCT system for pediatric bronchoscopy

Kushal C. Wijesundara, The Univ. of North Carolina at Chapel Hill (United States); Nicusor V. Iftimia, Physical Sciences Inc. (United States); Amy L. Oldenburg, The Univ. of North Carolina at Chapel Hill (United States)

We describe a swept source, anatomical OCT (aOCT) system designed to increase the scanning range of traditional OCT for imaging the geometry of the respiratory surface during bronchoscopy. A fiber-optic catheter with ball lens tip and an internally reflective polished flat surface is designed for sideways-directed imaging while maintaining sufficiently small (1.03 mm) diameter for insertion into a small-bore pediatric bronchoscope. The catheter is scanned distally by rotating and translating its optical fiber for helical scans. A large imaging range is enabled by the use of a long coherence length swept-source and a relatively long focal length (3.5 mm) from the fiber catheter, providing a working distance (12.0 mm) comparable to the maximum size of the upper airway in children less than 10 years of age. Measurements of the signal-to-noise ratio (SNR) roll-off as a function of distance from the catheter reveal the relative contributions of beam focusing, coherence length, and k-space nonlinearity, to the maximum imaging range. 3-D visualization of known plastic tubes and lung phantoms are obtained through helical data scans and image processing to locate the air-tissue interface, and comparisons with the known surface geometry is used for optimization of the aOCT system performance. Overall, accurate reconstruction of the airway geometry will enable predictive modeling of patients suffering from airway obstructions.

8571-133, Session PMon

Fingerprint fake detection by optical coherence tomography

Sven Meissner, Edmund Koch, Universitätsklinikum Carl Gustav Carus Dresden (Germany); Ralph Breithaupt, Bundesamt für Sicherheit in der Informationstechnik (Germany)

While every human fingerprint is unique, fingerprints can be faked very easily by using thin layer fakes. Because commercial fingerprint scanners use only a two-dimensional image acquisition of the finger surface, they can only hardly differentiate between real fingerprints and fingerprint fakes applied on thin layer materials. A Swept Source OCT system with an A-line rate of 20 kHz and a lateral and axial resolution of approximately 13 ?m, a centre wavelength of 1320 nm and a band width of 120 nm (FWHM) was used to acquire fingerprints and finger tips with overlying fakes. Three-dimensional volume stacks with dimensions of 4.5 mm x 4 mm x 2 mm were acquired. The layering arrangement of the imaged finger tips and faked finger tips was analyzed and subsequently classified into real and faked fingerprints. The manual classification between real fingerprints and faked fingerprints results in almost 100 % correctness. The outer as well as the internal fingerprint can be recognized in all real human fingers, whereby this was not possible in the image stacks of the faked fingerprints. Furthermore, in all image stacks of real human fingers the sweat gland ducts were detected. In contrast, in images of faked fingerprints we observe abnormal layer arrangements and no sweat gland ducts connecting the papillae of the outer fingerprint and the internal fingerprint. We demonstrated that OCT is a very useful tool to enhance the performance of biometric control systems concerning attacks by thin layer fingerprint fakes.

8571-28, Session 5

Optical-domain subsampling for data efficient Fourier-domain optical coherence tomography

Meena Siddiqui, Massachusetts Institute of Technology (United States) and Harvard Univ. (United States); Benjamin Vakoc, Wellman Ctr. for Photomedicine (United States) and Harvard Medical School (United States)

We introduce optical-domain subsampling as a method for imaging at high-speeds and over extended depth ranges but with a lower acquisition bandwidth than that required using conventional approaches. Optically subsampled laser sources utilize a discrete set of wavelengths to alias fringe signals along an extended depth range into a bandwidth limited frequency window. By detecting the complex fringe signals, optical-domain subsampling enables recovery of the depth-resolved scattering signal without overlapping artifacts. We demonstrate the principle of subsampled imaging using a polygon-filter based swept-source laser that includes an intra-cavity Fabry-Perot (FP) etalon.

8571-29, Session 5

Single-shot interpixel shifting for optical coherence tomography by oblique incidence spectroscopy

Hee Yoon Lee, Audrey K. Ellerbee, Stanford Univ. (United States)

Optical coherence tomography (OCT) is an imaging technique capable of generating high-resolution images of scattering tissue. Fourier domain methods of OCT – often preferred over their time-domain counterpart because of their increased sensitivity – can suffer from limited imaging depth due to a number of system-dependent parameters. For spectrometer-based systems in particular, one must often trade off between high resolution and large imaging depth due to limitations in the spectrometer design. Most methods implemented to improve the imaging range of OCT focus on addressing the complex conjugate artifact that occurs when structures are located near the position of zero pathlength delay. Alternative methods such as inter-pixel shifting (IPS) have also been shown to provide useful extended ranging depth for OCT, including with the use of comb functions to further reshape the fall-off graph. Unfortunately, previous demonstrations of IPS rely on multiple acquisitions and require moving parts. We demonstrate a new method of inter-pixel shifting with single-shot acquisition; the design of our system further improves the fall-off in the extended range, and can accommodate extensions in the ranging depth beyond simple factors of two. This design represents a new attempt at exploiting the inherent high pixel density of 2D array detectors for OCT and is a first step towards a new design for achieving large ranging depths with SD-OCT that can rival those attainable with swept-source variations.

8571-30, Session 5

Improvement of lateral resolution of optical coherence tomography images based on capon estimation of weighted multi-scatterer contributions

Evgenia Bousi, Costas Pitris, Univ. of Cyprus (Cyprus)

Improving the resolution of Optical Coherence Tomography (OCT) images has the potential to lead to superior diagnostic capabilities. In this summary, a novel method for lateral resolution improvement, which is independent of the delivery optics and the depth of focus, is presented. This technique is based on lateral oversampling, i.e. taking measurements at closely spaced, overlapping, resolution volumes, and subsequently utilizing the additional information to estimate a higher-resolution signal. For this purpose, each lateral OCT point is assumed to be a sum of signals from several high-resolution sub-volumes weighted by the point spread function (PSF). One approach to estimate these high-resolution sub-volumes, from the standard resolution volumes, is to directly solve for the inverse of their weighted sum. However, this inverse matrix technique is prone to noise amplification. Another approach is to take advantage of the correlation between the signals from adjacent volumes. This correlation is a direct result of the significant overlap in the lateral direction. Using Capon's method a set of weighting functions can be found which can be used to estimate the sub-resolution volumes from the oversampled OCT signal. Using this method, a lateral resolution improvement of about a factor of 4 has been achieved experimentally without a degradation of the signal-to-noise ratio (SNR). This method can provide simple and cost-effective means for improving the resolution of systems, such as those used in ophthalmology, where the imaging optics are constrained by the eye.

8571-32, Session 5

Real time 3D structural and Doppler OCT imaging on graphics processing units

Marcin Sylwestrzak, Daniel Szlag, Maciej Szkulmowski, Iwona M. Gorczynska, Danuta Bukowska, Maciej Wojtkowski, Piotr Targowski, Nicolaus Copernicus Univ. (Poland)

In this report the application of graphics processing unit (GPU) programming for real-time 3D Fourier domain optical coherence tomography (FdOCT) imaging with Doppler algorithms implementation for visualization of the flows is presented. One of the limitations of FdOCT is time of the data processing, which is generally longer than data acquisition. Utilizing an additional algorithms, like Doppler analysis, makes it even more time consumed. The general purpose computing on GPU (GPGPU) has been used successfully for structural imaging in OCT but real-time 3D Doppler OCT imaging has so far not been presented. In developed software the total speed of structural and Doppler OCT processing with visualization of 2D data consisting of 2000 A-scans generated from 2048 pixels spectra is higher than 120 Hz (refresh rate of a LCD monitor). The 3D imaging in the same mode of the volume data build of 100 x 100 A-scans is performed at a rate of about 9 frames per second. In this talk a software architecture, organization of the threads and applied optimization will be shown. For illustration the movies recorded during real time imaging of the human eye and the phantom (homogeneous water solution of Intralipid in glass capillary) will be presented.

8571-33, Session 5

GPU accelerated OCT processing at megahertz axial scan rate and high resolution video rate volumetric rendering

Yifan Jian, Kevin Wong, Marinko V. Sarunic, Simon Fraser Univ. (Canada)

OCT has undergone tremendous development since it was first invented in 1990s, especially in its acquisition speed. As the ultrahigh speed OCT acquisition has continuously been developed, there followed an increasing demand for real time volume visualization of OCT data to explore the full potential of the technology. In this report, we describe how to highly optimize a CUDA based platform to perform real time optical coherence tomography data processing and 3D volumetric rendering using commercial available cost-effective graphic processing units (GPUs). We used concurrent programming strategies to hide the latency of memory transfer, and developed a custom CUDA program for OCT data processing and volume rendering that is optimized for performance. The OCT data processing pipeline was implemented for both swept source OCT and spectral domain OCT. Additional post processing (bilateral filtering and frame averaging) was also implemented

to enhance the image quality. The maximum complete attainable axial scan processing rate (including memory transfer and rendering frame) was 2.2 megahertz for 16 bits pixel depth and 2048 pixels/A-scan. The maximum 3D volumetric rendering speed is 22 volumes/second (volume size: 1024x256x200). To the best of our knowledge, this is the fastest processing rate reported to date with single-chip GPU and the first implementation of real time video rate volumetric OCT processing and rendering that is capable of matching the ultrahigh speed OCT acquisition.

8571-89, Session 5

Polarization sensitive en face optical coherence tomography using multichannel acousto-optic deflectors

Mantas Zurauskas, John Rogers, Adrian G. Podoleanu, Univ. of Kent (United Kingdom)

We present a novel time-domain polarization sensitive optical coherence tomography configuration operating at 830 nm, equipped with multichannel acousto-optic deflectors (AOD)s. A pair of AODs are used in each interferometer arm. The system can be used to simultaneously acquire interference information from multiple polarization-sensitive channels. The method presented allows simultaneous collection of polarization information using the same photodetector receiver. The polarization information is encoded using radiofrequency. Information on the vertical and horizontal polarization is collected simultaneously and is encoded at two different radiofrequencies. The photodected signal is band pass filtered using two different filters, tuned on the two radiofrequency values. Such a scheme allows expandability, as the AODs can be driven with more than two radio frequency signals. Multiple radiofrequency excitation together with application of multiple waveplate elements between the AODs in one of the arms can be used to encode more than two orthogonal polarization directions.

The system enables measurement and imaging of backscattered intensity, birefringence, and fast optic axis orientation. The system is employed to demonstrate polarization sensitive imaging of a thermally damaged muscle tissue.

8571-34, Session 6

Mitigating polarization mode dispersion for polarization sensitive intracoronary imaging

Martin L. Villiger, Ellen Z. Zhang, Wellman Ctr. for Photomedicine (United States); William W. Oh, KAIST (Korea, Republic of); Seemantini K. Nadkarni, Benjamin J. Vakoc, Brett E. Bouma, Wellman Ctr. for Photomedicine (United States)

Polarization Mode Dispersion (PMD) has limited the implementation of polarization sensitivity (PS) into catheter based Optical Frequency Domain Imaging (OFDI). PMD describes the wavelength dependent polarization change as light travels along a single mode fiber or other optical components. PMD both increases the polarization noise floor and introduces artifactual birefringence values, which depend on the exact fiber position and change if the fiber is moved. This work investigates the mechanism by which PMD degrades the local birefringence and proposes an algorithm that reconstructs the sample birefringence in a robust fashion, mitigates the detrimental effects of PMD and speckle, and is insensitive to fiber motion. This is achieved by splitting the recorded spectrum of width ?k into several overlapping windows of reduced width ?k/N. The local retardation is computed for each window, using a least square estimator in the Stokes formalism, and then averaged to result in a 1/N^2 reduction of PMD effects. Because the finite axial distance dz over which the local retardation is extracted ultimately limits the axial resolution of the local birefringence, it is possible to tolerate the spreading of the axial point spread function by a factor N, to the point where it matches dz. With N=5 and dz=30um, we obtain detailed birefringence maps in the presence of more than 50fs system PMD. Using this new algorithm, we measured intracoronary birefringence maps of catheterized human cadaveric hearts, which corresponded well with quantitative analysis of collagen content measured from picrosirius red stained sections.

8571-35, Session 6

OCT speckle statistics can quantify micro-scale organization of tissue

Dirk J. Faber, Daniel M. de Bruin, Jeroen Kalkman, Ton G. van Leeuwen, Academisch Medisch Ctr. (Netherlands)

The development of disease is accompanied by morphological changes in the tissue down to the (sub)cellular level. These changes lead to changes in optical properties which can thus be used to monitor or diagnose disease progression. Usually optical properties are interpreted in terms of equivalent particle size and number density. These numbers may be hard to correlate with the images obtained from histology or microscopy. We derive a straightforward 1D mathematical model linking speckle variance as measured by functional optical coherence tomography (OCT) to optical properties of tissue (e.g. attenuation coefficient) and statistical measures of the samples composition (e.g. variance and correlation length of the refractive index fluctuation). We verify our model with numerical simulations of OCT speckle patterns. This approach allows both for extraction of information from very small volumes (thin layers) as well as providing metrics descriptive of the samples organization.

8571-36, Session 6

Numerical compensation of system polarization mode dispersion in polarization sensitive optical coherence tomography

Ellen Z. Zhang, Wellman Ctr. for Photomedicine (United States); Wang-Yuhl Oh, KAIST (Korea, Republic of); Martin L. Villiger, Wellman Ctr. for Photomedicine (United States); Liang Chen, Univ. of Ottawa (Canada); Brett E. Bouma, Benjamin J. Vakoc, Wellman Ctr. for Photomedicine (United States)

High noise levels in polarization-sensitive optical coherence tomography (PS-OCT) have broadly limited its clinical utility. Polarization mode dispersion (PMD) was identified as a dominant source of instrumentation noise in fiber-based PS-OCT system. PMD can be induced by circulators or even moderate lengths of optical fiber. Therefore it is very challenging, if not impossible, to entirely avoid PMD in a fiber-based system. In this presentation we propose a novel compensation method to measure instrumentation PMD in real time by means of three calibration signals and then numerically compensate PMD effects during post-processing. This requires phase stable acquisition of both input polarization states, which we achieve using a frequency multiplexing PS-OFDI setup. We validate our method by presenting significantly enhanced local birefringence images of intralipid, tendon, and muscle samples.

8571-37, Session 6

Dependent and multiple scattering unraveled by transmission and backscattered optical coherence tomography

Duc V. Nguyen, Edwin van der Pol, Dirk J. Faber, Ton G. van Leeuwen, Jeroen Kalkman, Academisch Medisch Ctr. (Netherlands)

Quantitative measurement of the attenuation coefficient of biological

tissue is hypothesized to provide information on tissue composition or pathology. To determine the range of validity of the measured attenuation by OCT, highly scattering samples are used. These high volume % scattering samples may exhibit dependent scattering, which can be observed as a non-linear and lower scattering value compared to the expected scattering (e.g. based on Mie theory). In back-scattered OCT measurements, both multiple as dependent scattering will be observed as lower measured attenuation and cannot be unraveled. In this work we use transmission and backscattered optical coherence tomography to distinguish the dependent and multiple scattering effects on the attenuation as measured by OCT. In samples with 2-20 % volume % silica beads, with diameters of 376, 759, 906 and 1215 nm as measured by TEM, diluted in water, we found that dependent scattering cannot be ignored for volume concentrations larger than 2%. With knowledge of these (dependent) scattering coefficients, the multiple scattering effects on the attenuation coefficient as determined by OCT (in back-scatter configuration), can be determined. We found that for the small spheres (376 nm, g = 0.24) multiple scattering is minimal. For the larger spheres, with g= 0.74, 0.78 and 0.87, multiple scattering results in an underestimation of the measured attenuation for the higher scattering samples.

8571-38, Session 6

Accurate and generic method for characterizing the optical properties of OCT contrast agents by using self-referencing OCT imaging

Jiefeng Xi, Yongping Chen, Xingde Li, Johns Hopkins Univ. (United States)

The use of nanoparticles in optical coherence tomography (OCT) as exogenous contrast agent has recently drawn a lot of attention. However, the optical properties of those nanoparticles were sometimes characterized via another instrument. And the accuracy and the sensitivity of the optical properties often fluctuate. Here we report an accurate generic method to characterize the optical properties of nanoparticles by using OCT itself. This characterization method could be simply applied to any nanometer-size OCT contrast agents. It can be potentially be applied to in vivo tissue imaging to assess the distribution of OCT contrast agents.

8571-39, Session 6

Imaging the complete set of optical and physical properties of biological tissue using inverse spectroscopic optical coherence tomography

Ji Yi, Vadim Backman, Northwestern Univ. (United States)

As an important approach to provide quantitative guidance for disease diagnosis or screening, measurement of tissue optical properties plays a key role in biophotonics research. Early techniques such as diffuse reflectance spectroscopy (DRS) measured the reduced scattering coefficient ?s based on diffusive transport theory. Improving upon DRS, other methods have been developed to measure optical properties within the sub-diffusive regime. Imaging techniques such as confocal reflectance microscopy, optical coherence tomography (OCT) and quantitative phase imaging are able to quantify spatially-resolved optical properties. However, the above-mentioned methods are insufficient to measure the full set of optical properties due to the backscattering detection scheme for in vivo noninvasive measurement, which only allows sampling over a small angular extent of the scattering field.

Here, we propose a novel methodology to measure and image the full set of optical properties using ISOCT. The forward model of ISOCT regards tissue as a medium with a continuously varying refractive index (RI). Since RI fluctuation in tissue is weak, the wavelength-dependent optical scattering properties can be derived under the first-order Born approximation. By the optical measurement of OCT, the RI spatial auto-correlation (RI correlation) function can be reversely deduced, and the entire optical scattering properties can be quantified. More importantly, the 3D imaging capability of OCT provides localized analysis which helps to directly visualize the optical properties.

8571-40, Session 7

En-face adaptive optics optical coherence tomography with 3D-motion correction

Franz Felberer, Gerold Aschinger, Julia S. Kroisamer, Christoph K. Hitzenberger, Michael Pircher, Medizinische Univ. Wien (Austria)

We present an en-face adaptive optics optical coherence tomography (AO-OCT) instrument that combines the high axial resolution of OCT with the high lateral resolution of AO. The instrument records OCT and scanning laser ophthalmoscope (SLO) images simultaneously which enables the correction of transverse motion artifacts in post processing. Active axial eye tracking is implemented into the OCT system using a separate Fourier Domain low coherence interferometer that measures the position of the cornea. This information is exploited to adapt the reference arm length via a rapid scanning optical delay line. Therefore the instrument is capable to provide motion artifact free high resolution 3D-images of the retina.

8571-41, Session 7

Rotational dove prism scanning dual angle Doppler OCT

Cedric Blatter, Séverine Coquoz, Branislav Grajciar, Amardeep S. Singh, René M. Werkmeister, Leopold Schmetterer, Rainer A. Leitgeb, Medizinische Univ. Wien (Austria)

Traditional Doppler OCT is highly sensitive to motion artifacts due to the dependence on the Doppler angle. This limits its reproducibility in clinical practice. To overcome this limitation, we use a bidirectional technique with a novel rotating scanning scheme. The volume is probed simultaneously from two distinct illumination directions with variable controlled orientations, allowing reconstruction of the true flow velocity, independently of the vessel orientation. A Dove prism in the sample arm permits a rotation of the illumination directions that can be synchronized with the standard beam steering device. The principle is implemented with Swept Source OCT at 1060nm with 100,000 A-Scans/s. We apply the system to human retinal absolute blood velocity measurement by performing circumpapillary time series scans around the optic nerve head. We also demonstrate microvasculature imaging by calculation of squared intensity differences between successive tomograms.

8571-42, Session 7

Intraoperative SDOCT for vitreo-retinal surgery with an integrated fundus camera for closed-loop surgical instrument tracking

Justin V. Migacz, Tomas Moreno, Duke Univ. (United States); Francisco Folgar, Duke Eye Center (United States); Adam Dubis, Sina Frasiu, Cynthia A. Toth, Duke Univ. (United States); Joseph A. Izatt, Duke Univ. (United States) and Duke Eye Ctr. (United States); Paul Hahn, Duke Univ. (United States)

In an ongoing clinical trial, we demonstrate the utility of microscope-integrated OCT (MIOCT) during ophthalmic microsurgical procedures. The system incorporates a current-generation clinical OCT system within a state-of-the art ophthalmic surgical microscope. The system can be installed and removed from the operating suite in under 10 minutes.

Many patient cases have been conducted successfully in which the surgeon has performed OCT imaging of patients with both the MIOCT and a commercial hand-held system. We have previously developed a feedback control system to track the OCT imaging location to the position of the surgical tool in the eye. To close the feedback loop, we have upgraded the MIOCT system with an integrated beam-viewing fundus camera. The fundus camera has the ability to simultaneously view both the visible color field and the near-IR light (?C=860nm) of the OCT beam incident on the retinal tissue.

8571-43, Session 7

High sensitive fundus autofluorescence imaging combined with speckle-free optical coherence tomography

Patrycjusz Stremplewski, Katarzyna Komar, Maciej Szkulmowski, Marta Motoczynska, Maciej Wojtkowski, Nicolaus Copernicus Univ. (Poland)

Scattering and fluorescence images provide complementary information about the health condition of the human eye, so getting them in a single measurement, using a single device may significantly improve a quality of diagnosis as it has been already demonstrated in Spectralis (Heidelberg Eng.) OCT instrument. There is still challenge to improve quality of fundus autofluorescence (FAF) images. The biggest obstacle in obtaining in vivo images of sufficient quality is very low fluorescence signal. For eye safety reasons, and because of patient comfort, using high-power fluorescence excitation is not an adequate solution to the low signal problem.

In this contribution we show a new detection method in the retinal autofluorescence imaging, which may improve the sensitivity. We used the fast modulated (up to 500 MHz) diode laser of wavelength 473 nm and detected fluorescence in the spectral range 500-680 nm by photomultiplier and lock-in amplifier. Average power of the collimated blue beam on the cornea used for FAF measurements was set to 50 ?W, 10 ?W, and even 4.5 ?W. The instrument was designed and constructed in Optical Biomedical Imaging Group laboratory, Institute of Physics, NCU, Torun, Poland. It combines functionality of imaging fundus of human eye by registration autofluorescence signal by Scanning Laser Ophtalmoscope (FAF-SLO mode of work) with speckle-free Fourier domain OCT (OCT mode of work).

8571-44, Session 7

Retinal tracking polarization sensitive optical coherence tomography

Mitsuro Sugita, Medizinische Univ. Wien (Austria) and Canon Inc. (Japan); Stefan Zotter, Michael Pircher, Medizinische Univ. Wien (Austria); Tomoyuki Makihira, Nobuhiro Tomatsu, Canon Inc. (Japan); Christoph K. Hitzenberger, Medizinische Univ. Wien (Austria)

Polarization sensitive optical coherence tomography (PS-OCT) is a powerful tool for differentiating retinal layers with polarization preserving, birefringent, and depolarizing characteristics, in ophthalmologic study use. In practical situations in ophthalmologic studies, involuntary eye motions tend to cause significant motion artifacts in the OCT images. In order for more robust and practical clinical studies of PS-OCT, we have built a PS-OCT setup combined with a retinal tracker. The tracker operates at up to 60Hz, with retinal position detection accuracy of about 10 μm. In order to show the effectiveness of the combination, in-vivo measurements with a healthy eye were carried out. A fixation target was configured to move circularly with diameter of about 1mm on retina, which guides the subject eye. The tracker detects the motion of the eye in the direction parallel to the retinal surface, and compensates the in-plane motion two-dimensionally. The measurement was done with 40Hz and 60Hz frequency tracking, and without tracking. The PS-OCT images were obtained in both B-scans and 3D raster scans. The results show effectiveness of the retinal motion correction, which improves depending on the tracking frequency from 40Hz to 60Hz.

8571-45, Session 7

Degree of polarization uniformity measured with polarization sensitive OCT as a function of the input polarization state

Stefan Zotter, Bernhard Baumann, Michael Pircher, Teresa Torzicky, Mitsuro Sugita, Erich Götzinger, Wolfgang Trasischker, Christoph K. Hitzenberger, Medizinische Univ. Wien (Austria)

Polarization sensitive optical coherence tomography (PS-OCT) is a functional extension of conventional intensity based OCT. Based on the different light tissue interaction mechanisms, PS-OCT allows to distinguish polarization preserving, birefringent and depolarizing structures. This is achieved by illuminating the sample with a defined polarization state and by using a polarization sensitive detection. Especially the capability of PS-OCT to reliably segment the RPE (which is based on the intrinsic polarization scrambling properties of the RPE) in age related macular degeneration (AMD) has proven to improve the reproducibility of lesion size detection in drusen or geographic atrophy. In this study we want to show that the depolarization effect of the RPE, measured with PS-OCT, strongly depends on the polarization state of the measurement beam. For this, healthy human volunteers and also tissue phantoms were measured with our PS-OCT system. The results show that the depolarization of the RPE and also of the tissue phantoms has a maximum when the polarization state of the incident beam is circular polarized, whereas it reaches a minimum when the polarization is changed to a linear state.

8571-46, Session 7

Detection of retinal degeneration using angle-resolved low coherence interferometry

Michael G. Giacomelli, Rolf Herrmann, Sanghoon Kim, Vadim Arshavsky, Adam Wax, Duke Univ. (United States)

Angle-resolved low coherence interferometry (a/LCI) is a light scattering technique related to optical coherence tomography (OCT) that has shown promise as a method of detecting dysplasia in vivo by analyzing variation in the angular dependence of scattered light. Previously, the detection of cellular features with sub-diffraction-limited accuracy has been demonstrated in limited numerical aperture systems. Recently, we have developed 2D a/LCI, an extension of the technique to measurement of the entire backscattered field in two dimensions. Here, we present a method of optical scattering analysis based on 2D a/LCI measurements that can recover depth-resolved information about the cellular and nuclear organization of retinal tissue. Using high-speed, Fourier-domain 2D a/LCI, we demonstrate that both short (subcellular) scale and long scale (tissue) features can be assessed using only the scattered intensity recovered over a limited range of angles. This technique is applied to imaging of the mouse retina to resolve individual layers using contrast generated by the organization of their cellular components. Variations in the organization of individual layers are demonstrated to produce reproducible and quantifiable levels of contrast across different subjects, and to vary in response to changes in cellular organization using a progressive retinal degeneration model.

8571-47, Session 7

Comparative optical coherence tomography and histological investigation of the outer retina

Xincheng Yao, Rongwen Lu, The Univ. of Alabama at Birmingham

(United States)

Given the excellent capability to identify morphological changes at individual functional layers of the retina, optical coherence tomography (OCT) has increasing application in eye disease detection. Early studies have disclosed four hyper-reflective OCT bands at the outer retina, i.e. photoreceptor side. Anatomic sources of these four OCT bands have been typically attributed as follows: first (1st) band at the outer limiting membrane (OLM); second (2nd) band at the photoreceptor inner/outer-segment (IS/OS) junction; third (3rd) band at the posterior tip of the OS; and fourth (4th) band at the retinal pigment epithelium (RPE). Anatomic correlates of the 2nd and 3rd bands remains controversial. The 2nd OCT band is widely attributed to the IS/OS junction, which cell biologists consider the connecting cilium (CC) between these structures. However, comparative alignment of OCT bands with an anatomically correct model of the outer retina suggested an alternative correlate, i.e., the IS ellipsoid, to the 2nd OCT band. This study was to experimentally test the anatomic correlate to the 2nd OCT band. In order to achieve sub-cellular resolution in both lateral and axial directions, a rapid line-scan OCT (LS-OCT) was developed. The LS-OCT combined technical merits of our recently demonstrated electro-optic phase modulator (EOPM) based functional OCT and line-scan confocal microscopy. Quantitative comparison of histological images and LS-OCT images revealed that dominant source of the signal reported as the 'IS/OS' OCT band actually originates from the IS. We speculate that the IS ellipsoid, which consists of abundant mitochondria, or the CC extended into the IS may contribute to the observed 2nd OCT band signal.

8571-48, Session 8

Photothermal optical lock-in optical coherence microscopy

Christophe Pache, Noelia L. Bocchio, Arno Bouwens, Martin Villiger, Corinne Berclaz, Joan Goulley, Theo Lasser, Ecole Polytechnique Fédérale de Lausanne (Switzerland)

Image contrast in optical coherence microscopy (OCM) is based on the intrinsic light scattering properties of the sample and is therefore label-free. While this is one of OCM's main strengths for live cell imaging, it is at the same time a drawback since it lacks molecular specificity. Among molecular imaging techniques, photothermal microscopy is a promising method because it does not suffer from the photobleaching problem encountered in fluorescence microscopy. Photothermal microscopy uses a modulated heating beam to probe the specific optical absorption of an extrinsic label such as the plasmon resonance of a gold nanoparticle. We have developed photothermal optical lock-in OCM (poli-OCM) to image the photothermal effect in three dimensions with high resolution and fast acquisition rate. In contrast to previous implementations of photothermal OCM, poli-OCM demodulates the photothermal signal optically using a resonant phase modulation in the reference arm. In this way, molecular contrast is introduced to OCM without sacrificing its high acquisition speed. We show that poli-OCM allows specific imaging of 40 nm gold nanoparticles within a highly scattering medium at 0.5 ?m lateral and 2 ?m axial resolution over a 50 ?m depth of focus. In addition to photothermal contrast, the poli-OCM instrument also provides intrinsic light scattering contrast with enhanced sensitivity using dark-field OCM. We have applied both imaging modalities to image living HeLa cells loaded with nanoparticles. The dark-field OCM modality images the overall cell structure, while the photothermal modality selectively images internalized nanoparticles.

8571-49, Session 8

Three-dimensional intracellular optical coherence phase imaging

Frank Helderman, Vrije Univ. Amsterdam (Netherlands); Bryan Haslam, Massachusetts Institute of Technology (United States); Mattijs de Groot, Johannes F. de Boer, Vrije Univ. Amsterdam (Netherlands)

Optical coherence tomography has been applied to the microscope domain to develop a three dimensional microscopy technique with a resolution on a sub micrometer scale. A common-path setup that uses for example the reflection of a cover glass as a local phase reference can sense optical path displacements smaller than a nanometer. Herewith, the motion of objects within the focal volume can be studied.

The need for detecting the cover glass limits the possibilities to use high numerical aperture objectives and thus the resolution, because the depth of field would become too short. Therefore, we designed a setup with a dual beam sample arm.

A polarizing beam splitter divides the sample beam into s- and p-polarized states that travel the same path, but in opposite directions through a Sagnac interferometer. There, a 4:1 telescope (f = -25 mm and f = 100 mm, Thorlabs) magnifies the width of the p-polarized beam and narrows the width of the s-polarized beam. The two beams share a common path towards the microscope. The broad beam will be focused into the sample for spatially specific phase information. The narrow beam with a long depth of field can detect the phase at the cover glass as a local reference.

The lateral resolution was 0.42 µm and the axial point spread function was 0.84 µm. The phase stability of 0.02 radians enabled detection of optical path displacements of 0.9 nm. This setup allows for three-dimensional intracellular phase imaging.

8571-50, Session 8

Label-free imaging of the dynamics of cell-to-cell string-like structure bridging in the free-space by low-coherent quantitative phase microscopy

Toyohiko Yamauchi, Hidenao Iwai, Yutaka Yamashita, Hamamatsu Photonics K.K. (Japan)

We report label-free and three-dimensional imaging of string-like structures bridging in the free-space between live cells, by using our low-coherent quantitative phase microscopy (LC-QPM). In past studies, three dimensional morphology of the string-like structures between cells had been investigated by electron microscopies and fluorescent microscopies and they were called "intercellular bridges" or "tunneling nanotubes". However, the electron microscopy kills the cells inevitably and the fluorescent microscopy is potentially an invasive method. In order to realize noninvasive imaging of live cells, we applied our LC-QPM which is a reflection-type, phase-resolved and full-field interference microscope employing a low-coherent light source. By means of low-coherence interferometry, LC-QPM is able to visualize the three-dimensional morphology of live cells without labeling. The lateral (diffraction limit) and longitudinal (coherence-length) spatial resolutions of LC-QPM were 0.5 micrometer and 0.93 micrometer, respectively and the repeatability of the phase measurement was 0.04 radians. We have successfully obtained three-dimensional morphology of live cultured epithelial cells (cell type: HeLa, derived from cervix cancer) and the individual string-like structures interconnecting the cells were clearly observed. When we performed volumetric imaging, 80 micrometer by 60 micrometer by 4.8 micrometer volume was scanned every 4.0 seconds and 22 frames of three-dimensional movie were recorded for the duration of 88 seconds. Moreover, the optical phase images gave us detailed information about the three-dimensional morphology of the string-like structure in sub-wavelength resolution. We expect that our LC-QPM will be a useful tool for the study of three-dimensional morphology of live cells.

8571-51, Session 8

2D and 3D static elastography using full field OCT

Amir Nahas, Anne Latrive, Institut Langevin (France) and LLTech

SAS (France); Stéphane Roux, Ecole Normale Supérieure de Cachan (France); Claude A. Boccara, Institut Langevin (France) and LLTech SAS (France)

Organ structures, tissues and cells are characterized by their intrinsic mechanical properties. Moreover, the mechanical properties of cells are related to their structure and function: changes in those properties can reflect cellular healthy or pathological states. Adding this contrast to morphological images could be a powerful help for diagnosis. In this study we add the elastographic contrast to the Full-Field OCT (FF-OCT) modality. FF-OCT is able to image biological tissues in 3D with a micrometer resolution. By combining it with elastography, we recreate a "virtual palpation" map at a micrometer scale.

In this study we present two static methods to add the elastographic contrast to FF-OCT images. In the first method we register a volumetric image before and after mechanical solicitation of the sample. From those two sets of images we estimate the 2D and 3D strain maps inside the sample by using two different algorithms: one based on cross-correlations and one based on finite elements. We use this method not only with a custom FF-OCT setup but also with an endoscopic FF-OCT setup. In the second method the sample is submitted to a low-amplitude periodical compression, and using a phase shifting modulation method derived from to the one used in classical FF-OCT imaging we are able to retrieve the local phase map modulation directly related to the local displacement. Those methods provide a relative value of the local elastic properties along the compression axis.

8571-52, Session 8

Self-interference fluorescence microscopy: three dimensional fluorescence imaging without depth scanning

Mattijs de Groot, Vrije Univ. Amsterdam (Netherlands)

We present a new method for high-resolution, three-dimensional fluorescence imaging. In contrast to beam-scanning confocal microscopy, where the laser focus must be scanned both laterally and axially to collect a volume, we obtain depth information without the necessity of depth scanning. In this method, fluorescence is collected in the backward direction and is sent through a phase plate that encodes the depth information into the phase of a spectrally resolved interference pattern. We demonstrate that decoding this phase information allows for depth localization accuracy better than 4 μm over a 500 μm depth-of-field. In a high numerical aperture configuration with a much smaller depth of field, a localization accuracy of 60 nanometers was achieved. This approach is ideally suited for miniature endoscopes, where space limitations at the endoscope tip render depth scanning difficult. We illustrate the potential for 3D visualization of complex biological samples by constructing a three-dimensional volume of the microvasculature of ex vivo murine heart tissue from a single 2D scan.

Early cancer diagnosis can be greatly improved by employing fluorescent labels that selectively target tumors. However, effective endoscopic imaging tools are needed to optimally exploit the potential of these markers. Depth resolved imaging of fluorescence will aid in the determination of the extent of invasion of a tumor in the underlying tissue in real time during intervention. The potential integration with OCT will provide both depth resolved tumor location and information about the surrounding tissue architecture. This could improve the effectiveness of therapy and response monitoring.

8571-53, Session 8

Using smart gold nanoparticles in photothermal optical coherence tomography combined with two-photon microscopy

Peng Xiao, Qingyun Li, Taejun Wang, Yeoreum Yoon, Yongjoon Joo, Jutaek Nam, Sungjee Kim, Ki Hean Kim, Pohang Univ. of Science and Technology (Korea, Republic of)

We applied phase-sensitive optical coherence tomography (OCT) to photothermal therapy with so-called "smart" gold nanoparticles (AuNPs) as an agent. "Smart" AuNPs are spheres of 10 nm in diameter, and become photothermal active only with aggregation. They are designed to have aggregation at low pH condition and can be targeted to cancerous cells and tissues. Two-photon microscopy (TPM) and OCT were used to visualize cells and "smart" AuNPs, and to measure photothermal therapy along with structural tissue information respectively. A system for the photothermal therapy and OCT was developed.

The system was applied to solution samples, cell samples and the mouse ear samples ex vivo by comparing to gold nanorods (AuNRs). In these studies, all the "smart" AuNPs and AuNRs have peak absorption of 660nm laser.

1. For solution sample, "smart" AuNPs with concentration of 2.6 nM was used by sandwiching it between coverslip and glass slide with a gap of 20?m. Photothermal laser was applied with modulation frequency of 100 Hz, 500 Hz and 1000 Hz. Measured phase shows transient changes corresponding to the different modulation frequency.

2. Cell samples were made by feeding HeLa cells with "smart" AuNPs and AuNRs in certain conditions on coverslips and sandwiched the cells with certain space from the coverslip and filled it with DI water. Photothermal laser modulation frequency is 100 Hz. The photothermal image we have gotten indicated the distribution and concentration of "smart" AuNPs and AuNRs in the cells.

3. Tissue samples were mouse ears injected by B16F10 mouse melanoma cells, which were incubated with "smart" AuNPs and AuNRs. Photothermal laser modulation frequency is also 100 Hz. TPM was applied to visualize cells and "smart" AuNPs and AuNRs while OCT to measure photothermal therapy along with structural tissue information respectively. Significant photothermal effects have been detected and the photothermal image also indicated the location and distribution of B16F10 mouse melanoma cells.

All the results show that "smart" AuNPs are a potential agent for photothermal cancer therapy. With the advantages of pH-induced aggregation, better endocytosis into cancerous cells and cancer targeting, "smart" AuNPs are sure to be a promising agent in photothermal cancer therapy. The combination with TPM gives us the possibility to see molecular and cellular structure. The next step is applying the technique to tissue samples in vivo. This will be a big advance for photothermal cancer therapy.

8571-54, Session 8

Visible spectrum optical coherence microscopy for live subcellular imaging

Arno Bouwens, Paul Marchand, Christophe Pache, Daniel Szlag, Theo Lasser, Ecole Polytechnique Fédérale de Lausanne (Switzerland)

The realm of three-dimensional tomographic subcellular imaging is currently almost exclusively occupied by confocal and two photon fluorescence microscopy. While these techniques offer molecular contrast, they are often ill suited for live cell studies because of the need for fluorescent labeling and the slow three-dimensional scan involved. The influence of fluorescent labeling on cell functioning is ambiguous and can interfere with the process under study. We present visible spectrum optical coherence microscopy (visOCM) with isotropic sub-micrometer resolution for fast label-free imaging of subcellular structures in living cells. By employing a supercontinuum light source with a large spectrum centered in the visible wavelength range (?0=560 nm, Δ?=180 nm), we obtain an axial resolution of 0.6 ?m in water. The broad visible spectrum can also be exploited for spectroscopic contrast and color imaging of cell structures. To simultaneously achieve a sub-micrometer lateral resolution, a high numerical aperture (NA) objective is used (effective NA=0.86), resulting in a lateral resolution of 0.4 ?m in water. The combination of a Bessel-like illumination and a Gaussian detection mode offers the dual advantage of an extended depth of focus and dark-field illumination. The extended focus allows a fast A-scan rate (140 kHz) and

the dark-field effect creates high sensitivity to light backscattered by cell samples. To cope with the increased dispersion in the visible spectrum, we have developed a combination of optical and numerical dispersion compensation. We demonstrate three-dimensional tomographic imaging of live cells with subcellular resolution revealing the cell nucleus as well as smaller subcellular structures.

8571-55, Session 8

High speed dispersion contrast coherence microscopy for imaging of cell dynamics

Branislav Grajciar, Cedric Blatter, Katharina Ludwig, Daniel Fechtig, Rainer A. Leitgeb, Medizinische Univ. Wien (Austria)

We introduce a parallel FD-OCM that combines the advantage of OCM as a promising technology for high-resolution cellular-level imaging in human tissues with the high speed and high phase sensitivity (stability) of a parallel FD-OCT system. The phase stability of the present system allows resolving path length differences with sub-nanometer sensitivity similar to spectral domain phase microscopy. Such high sensitivity over a full scanning field offers exciting new perspectives for label-free spectroscopic imaging. The residual dispersion of the system can be precisely calculated. Access to the sample dispersion due to the in general complex refractive tissue index allows us to differentiate biochemical properties and constituents. In addition the high-speed capability of parallel FD-OCM offers in vivo visualization of rapid dynamic processes on the cellular scale.

8571-56, Session 9

Double-clad-fiber needle probe for combined optical coherence tomography and fluorescence imaging

Dirk Lorenser, Bryden C. Quirk, The Univ. of Western Australia (Australia); Mathieu Auger, Wendy-Julie Madore, Ecole Polytechnique de Montréal (Canada); Rodney W. Kirk, The Univ. of Western Australia (Australia); Nicolas Godbout, Ecole Polytechnique de Montréal (Canada); David D. Sampson, The Univ. of Western Australia (Australia); Caroline Boudoux, Ecole Polytechnique de Montréal (Canada); Robert A. McLaughlin, The Univ. of Western Australia (Australia)

We present the first needle probe for combined optical coherence tomography (OCT) and fluorescence imaging. OCT needle probes are an enabling technology for minimally invasive imaging of solid tissues and organs. Whilst OCT provides valuable micrometer-scale structural image information of biological tissues, its diagnostic usefulness for a variety of applications can be significantly enhanced by combining it with a co-registered functional modality such as fluorescence imaging, providing complementary information about the biochemical composition of the tissue. Our needle probe uses double-clad fiber (DCF) which guides the OCT signal in the single-mode core and which collects and guides the returning fluorescence in a large-diameter multimode inner cladding. The side-facing 23G (0.64-mm diameter) needle probe is counter-rotated over 360 degrees and pulled back in 10 micrometer steps, thereby enabling 3D scanning. It is interfaced with a 1310-nm swept-source OCT system which has been modified to enable 488-nm fluorescence excitation and >500-nm emission detection by using a DCF coupler to couple out the returning fluorescence signal with high efficiency. The OCT and fluorescence signals are co-registered, yielding a 3D structural OCT image and a 2D fluorescence map in which each pixel represents the integrated fluorescence signal collected from the radial direction of the corresponding OCT A-scan. We present imaging results from an excised sheep lung with fluorescein solution infused through the vasculature. We were able to identify alveoli, bronchioles and blood vessels. The results demonstrate that the combined OCT + fluorescence needle images provide improved tissue differentiation over OCT alone.

8571-57, Session 9

Motion compensated hand-held common-path Fourier-domain optical coherence tomography probe for image-guided intervention

Yong Huang, Cheol Song, Xuan Liu, Jin U. Kang, Johns Hopkins Univ. (United States)

A motion-compensated hand-held common-path Fourier-domain optical coherence tomography imaging probe has been developed for image guided intervention during microsurgery. A hand-held prototype instrument was designed and fabricated by integrating an imaging fiber probe inside a stainless steel needle which is attached to the ceramic shaft of a piezoelectric motor housed in an aluminum handle. The fiber probe obtains A-scan images. The distance information was extracted from the A-scans to track the sample surface distance and a fixed distance was maintained by a feedback motor control which effectively compensated hand tremor and target movements in the axial direction. Graphical user interface, real-time data processing, and visualization based on a CPU-GPU hybrid programming architecture were developed and used in the implantation of this system. To validate the system, free-hand OCT images using various samples were obtained. The system can be easily integrated into other microsurgical tools and robotics, which will have a wide range of clinical applications. Such a tool could offer physicians greater freedom to access imaging sites of interest with reduced risk and higher image quality.

8571-59, Session 9

Towards microscopic resolution in holoscopy

Gesa L. Franke, Univ. zu Lübeck (Germany) and Medizinisches Laserzentrum Lübeck GmbH (Germany); Dierck Hillmann, Thorlabs GmbH (Germany) and Medizinisches Laserzentrum Lübeck GmbH (Germany); Christian Lührs, Peter Koch, Thorlabs GmbH (Germany); Gereon Hüttmann, Univ. zu Lübeck (Germany)

Holoscopy is an imaging approach, which overcomes limitations of conventional imaging by combining Digital Holography and full-field Fourier-domain optical coherence tomography. The interference pattern of the light scattered by a sample with a reference wave is recorded digitally at multiple wavelengths. By numerical processing of the data a 3D image of the sample is reconstructed with diffraction limited lateral resolution over the whole measurement depth. We successfully demonstrated holoscopy at low and moderate numerical apertures. Comparison with full-field optical coherence tomography at corresponding numerical aperture clearly showed the benefit of virtual refocusing compared to conventional imaging. Here we present measurements with higher resolution where this benefit of holoscopy over optical coherence tomography becomes even more important since the imaging depth of conventional imaging methods degrades significantly with numerical aperture. At a numerical aperture of 0.8 the imaging depth could be increased to approximately a hundred Rayleigh lengths with almost constant lateral resolution.

8571-60, Session 9

Freehand OCT with real-time lateral motion tracking

Xuan Liu, Yong Huang, Peter Gehlbach, Jin U. Kang, Johns Hopkins Univ. (United States)

Hand-held optical coherence tomography (OCT) systems without mechanical scanners can offer great freedom to access sites of interest for imaging. It is also simple, cost-effective, and easy to use. However, the scanning velocity of manual scan is not constant; therefore pseudo

B-scan images obtained by stacking sequentially acquired A-scans have a non-uniform spatial sampling rate in lateral dimension and distortion artifacts exist due to over or under sampling. To remove such artifacts, we used the decorrelation property of OCT speckle, particularly, cross correlation coefficient (XCC) between A-scans, to estimate the lateral motion of a probe that is manually scanned above a static sample, assuming motion is limited in lateral dimension and speckle decorrelation is only due to lateral displacement. The theoretical dependency of XCC on displacement was derived and validated by experimental data.

The manual-scanned OCT with real-time lateral motion tracking was based on a spectral domain OCT (SD OCT) operating at 840nm. For high-speed signal processing, we implemented massive computation via a general purpose GPU (Nvidia GeForce GTX 480). To build a simple, lightweight, and small probe which can have arbitrary length, we adopted a common path (CP) configuration for our interferometer and built a hand-held single-mode fiber probe.

With our real-time scanning speed corrected OCT system, we manually scanned an infrared viewing card, the finger and palm skin of a healthy volunteer, and the retina of a dissected cow eye. Images obtained are free of distortion artifact, suggesting that our speckle decorrelation method effectively achieved uniform spatial sampling.

8571-61, Session 9

Measurement of angle-resolved scattering property of ovarian tissue by use of OCT

Yi Yang, Tianheng Wang, Univ. of Connecticut (United States); Molly Brewer, Univ. of Connecticut (United States) and Univ. of Connecticut Health Ctr. (United States); Quing Zhu, Univ. of Connecticut (United States)

Angle-resolved optical scattering properties of ovarian tissue on different optical coherence tomography (OCT) imaging planes were quantitatively measured by fitting the compounded OCT A-lines into a single scattering model. Higher cross correlation value of angle-resolved scattering coefficients between different OCT imaging planes was found in normal ovaries than was present in malignant ovaries. The mean cross correlation coefficient (MCC) was introduced in this pilot study to characterize and differentiate normal and malignant ovaries. A specificity of 100% and a sensitivity of 100% were achieved by setting MCC threshold at 0.6 in the limited sample population. Other collagen properties such as content, structure and directivity were found to be different within OCT imaging penetration depth between normal and malignant ovarian tissue. The homogeneous three-dimensional collagen fiber network observed in the normal ovary effectively explains the stronger cross correlation of angle-resolved scattering properties on different imaging planes while the heterogeneity observed in the malignant ovary suggests a weaker correlation.

8571-62, Session 10

Ultrahigh-speed ultrahigh-resolution adaptive optics: optical coherence tomography system for in-vivo small animal retinal imaging

Yifan Jian, Simon Fraser Univ. (Canada); Robert J. Zawadzki, UC Davis Medical Ctr. (United States); Marinko V. Sarunic, Simon Fraser Univ. (Canada)

Small animal models of human retinal diseases are a critical component of vision research. Non-invasive ophthalmic imaging such as optical coherence tomography has become an important tool for small animal vision research programs and has greatly accelerated numerous preclinical studies. In this report, we investigated the strategies to overcome the general difficulties in ultrahigh-resolution small animal retinal imaging. In order to increase the lateral resolution, we incorporated an adaptive optics imaging system into the sample arm of our custom small animal OCT system that allows correction of aberrations in the imaging path, including the optics of the eye. An ultrahigh-resolution ultrahigh-speed adaptive optics optical coherence tomography system for small animal retinal imaging (mouse, fish, etc.) was designed and built. We adapted our imaging system to different types of small animals in accordance with the optical properties of their eyes. In our AO-OCT system, we used the same light beam for both wavefront sensing and imaging which allows us to monitor the layers that are at the focus in real time. Results of AO-OCT images of small animal retinas acquired with AO correction are presented. Cellular structures including nerve fiber bundles, capillary networks and detailed double-cone photoreceptors are visualized.

8571-63, Session 10

Phase-sensitive optical coherence tomography characterization of pulse-induced trabecular meshwork displacement in ex vivo non-human primate eyes

Peng Li, Roberto Reif, Zhongwei Zhi, Lin An, Elizabeth Martin, Tueng Shen, Murray Johnstone, Ruikang Wang, Univ. of Washington (United States)

Glaucoma is a blinding disease for which intraocular pressure (IOP) is the only treatable risk factor. The mean IOP is regulated through the aqueous outflow system, which contains the trabecular meshwork (TM). Considerable evidence indicates that trabecular tissue movement regulates the aqueous outflow and becomes abnormal during glaucoma; however, such motion has thus far escaped detection. The purpose of this study is to describe a novel use of a phase-sensitive optical coherence tomography (PhS-OCT) method to assess pulse-dependent TM movement. For this study, we used enucleated monkey eyes, each mounted in an anterior segment holder. A perfusion system was used to control the mean IOP as well as to provide IOP sinusoidal transients (amplitude 3 mmHg, frequency 1 pulse/second) in all experiments. Measurements were carried out at seven graded mean IOPs (5, 8, 10, 20, 30, 40, 50 mm Hg). We demonstrate that PhS-OCT is sensitive enough to image/visualize TM movement synchronous with the pulse-induced IOP transients, providing quantitative measurements of dynamic parameters such as velocity, displacement and strain rate that are important for assessing the biomechanical compliance of the TM. We find that the largest TM displacement is in the area closest to SC endothelium. While maintaining constant ocular pulse amplitude, an increase of mean IOP results in a decrease of TM displacement and mean size of the Schlemm's canal. These results demonstrate that the PhS-OCT is a useful imaging technique capable of assessing functional properties necessary to maintain IOP in a healthy range, offering a new diagnostic alternative for glaucoma.

8571-64, Session 10

Dynamic OCT measurement of the biomechanical properties of gelatin phantom and mouse cornea in vivo

Jiasong Li, Ravi K. Manapuram, Floredes M. Menodiado, Manmohan Singh, Univ. of Houston (United States); Salavat Aglyamov, Stanislav Emelianov, The Univ. of Texas at Austin (United States); Michael Twa, Kirill V. Larin, Univ. of Houston (United States)

The cornea provides approximately 2/3 of the optical refracting power of the eye and its shape and structure are the critical components of normal function of the eye. However, several diseases can alter biomechanical properties of the cornea and, thus, significantly reduce vision. Therefore, the use of elasticity imaging to evaluate corneal biomechanics is required for proper selection of several therapeutic procedures of the cornea, e.g. for clinicians performing refractive surgery, a practice that has

motivated much of the existing research in this field. Optical Coherence Elastography (OCE) is an emerging tool that allows noninvasive assessment of tissue biomechanical properties with high lateral and axial resolutions. Here we demonstrate the capability of OCT to assess surface mechanical wave propagation in tissue phantoms using a Phase Stabilized Swept Source Optical Coherence Tomography (PhS-SSOCT) system. Low-amplitude mechanical waves were introduced on surfaces of different concentrations gelatin phantoms using highly focused air puffs. The mechanical stimulus propagated through the phantom producing vibrations on the anterior and posterior surfaces of the phantom. The wave amplitudes and velocities were measured at spatially distributed points across the phantom surfaces using a phase-resolved method. The results demonstrate that this method allows measuring ultra-small changes in the wave amplitude (as small as 10 nm) as well as the wave velocities as a function of gelatin concentrations. Pilot experiments were performed to assess possibility of quantifying wave propagation in mouse cornea in vivo.

8571-65, Session 10

Simultaneous multi chromophore and in vivo pump-probe OCT imaging in Xenopus laevis

Oscar Carrasco-Zevallos, Ryan L. Shelton, Wihan Kim, Jeremy Pearson, Brian E. Applegate, Texas A&M Univ. (United States)

While optical coherence tomography (OCT) has been very successful imaging the morphology of turbid media such as tissue, it has very poor inherent molecular contrast. This is due to the fact that scattering properties do not vary significantly between molecular species. We present pump-probe optical coherence tomography (PPOCT), a technique capable of simultaneously imaging Methylene Blue (MB), a common biological dye, and hemoglobin in erythrocytes. PPOCT is a functional extension of OCT that merges the molecular specificity of pump-probe spectroscopy with the morphological information of conventional OCT. The presented PPOCT system employs a Nd:YVO4 532 nm laser for the pump. A pulsed Ti:Sapphire and a super luminescent diode (SLD), both centered at 830 nm, were interchanged for the probe / OCT beam. Using the pulsed Ti:Sapphire as the probe enabled precise control of interpulse delay, which was used to differentiate PPOCT signal from hemoglobin and MB, since the two chromophores exhibit different electronic state configurations, which are exploited in PPOCT imaging. PPOCT images of MB and whole blood in a capillary tube phantom were obtained. By varying the interpulse delay, PPOCT signals from MB and hemoglobin within the same image were easily separated. Simultaneous imaging of MB and hemoglobin could be used for developmental studies of the lymphatic (by injecting MB to add contrast) and vasculature systems in an animal model. Moreover, in vivo PPOCT cross-sectional images and volumes of Zenopus tadpole vasculature were obtained. OCT B-scans overlayed with thresholded PPOCT B-scans clearly depict microvasculature down to single capillary sensitivity.

8571-66, Session 10

OCT detection of neural activity in American cockroach nervous system

Iwona M. Gorczynska, Joanna Wyszkowska, Danuta Bukowska, Daniel Ruminski, Karol Karnowski, Maria Stankiewicz, Maciej Wojtkowski, Nicolaus Copernicus Univ. (Poland)

In this study we investigate the methods of OCT detection of stimulated neural activity in the American cockroach neural cord. We have constructed an experimental OCT setup allowing for imaging of the abdominal nerve cord excised from the insect, with resolution sufficient for visualization of giant axons located in the connectives. This system was used to develop methods for visualization of the sample response to the electric stimulus. Our main focus was on analysis of intensity and phase changes in the OCT signal. We will show that functional activity of the American cockroach neural cord can be stimulated in a simple experimental setup and detected with a classic, high resolution OCT system. Basic, qualitative experiments can be successfully performed without any sophisticated sample preparation or handling and without environmentally controlled conditions.

8571-67, Session 10

OCT imaging of early effects of ethanol exposure on the embryonic heart

Lindsy M. Peterson, Ganga H. Karunamuni, Shi Gu, Zhao Liu, Michael W. Jenkins, Michiko Watanabe, Andrew M. Rollins, Case Western Reserve Univ. (United States)

Alcohol-induced congenital heart defects are frequently life threatening and require surgical correction in the newborn. These ethanol-induced birth defects have been attributed to the mis-regulation of various signaling pathways, however most developmental cardiology studies fail to address the influential role of altered cardiac function on cardiogenesis. Alterations in several key cardiac functions and biomechanical forces can significantly influence gene expression in surrounding cells and thereby affect heart development. It has been difficult to assess the structure and function of the early heart development due to the lack of appropriate imaging tools. Here we use optical coherence tomography (OCT) and optical coherence microscopy (OCM) to directly monitor the developing heart. Through Doppler OCT imaging, pulsed Doppler traces were measured from HH stage 19 ethanol-exposed embryos and control embryos. The traces showed increased regurgitant flow and changes in the shape of the waveform which indicated an alteration in the atrio-ventricular cushions of ethanol-exposed embryos. To investigate changes in cushion formation 3-D OCM images of the cardiac cushions of excised hearts from both HH stage 19 ethanol-exposed embryos and control embryos were obtained. Volume measurements of the atrio-ventricular cushions showed a 52±14% decrease in cushion volume of the ethanol-exposed embryos when compared with the control embryos. Future studies will include repeating these measurements on earlier-stage embryos to better understand the causal link between altered hemodynamics and cardiac cushion formation.

8571-68, Session 11

Improved imaging of breast cancer using optical coherence elastography

Brendan F. Kennedy, Robert A. McLaughlin, Kelsey M. Kennedy, The Univ. of Western Australia (Australia); Andrea Curatolo, Univ. of Western Australia (Australia); Alan Tien, The Univ. of Western Australia (Australia); Bruce Latham, Royal Perth Hospital (Australia); Christobel M. Saunders, David D. Sampson, The Univ. of Western Australia (Australia)

Optical coherence elastography (OCE) has the potential to provide high resolution imaging of tissue micro-architecture in breast cancer. However, image quality in OCE is confounded by environmental vibrations and thermal drifts, making it difficult to implement in a clinical environment. We present a system that utilizes a common-path optical coherence tomography (OCT) configuration to significantly improve strain sensitivity, and demonstrate results acquired with a portable system in a clinical environment. We estimate strain introduced to excised breast tissue using a weighted least squares method recently developed in our laboratory. We present the first co-registered sets of en-face OCE, OCT and matching histology images for human breast tissue, highlighting features such as ducts, vessels and smooth muscle. The results show that OCE provides additional tissue differentiation over OCT, allowing improved visualization of micro-architecture in malignant human breast tissue.

8571-69, Session 11

Application of optical coherence tomography in brain cancer: detecting glioma invasion from non-neoplastic white matter in human ex vivo samples

Carmen Kut, The Johns Hopkins Hospital (United States); Jiefeng Xi, Johns Hopkins Univ. (United States); Shaan Raza M.D., The Johns Hopkins Hospital (United States); Jessica Mavadia, Johns Hopkins Univ. (United States); Wenxuan Liang, Johns Hopkins Univ. (United States) and The Johns Hopkins Hospital (United States); Hugo Guerrero-Cazares, Elliot McVeigh, Alfredo Quinones-Hinjosa M.D., The Johns Hopkins Hospital (United States); Xingde Li, Johns Hopkins Univ. (United States)

Recent studies on high grade gliomas(HGG) suggest positive association between extent of resection(EOR) and survival. Even with 5-ALA guidance, however, percentage of complete resection(65%) is far from optimal; moreover, fluorescence intensity varies among patients, especially at infiltrative regions. This highlights the need to better delineate and resect glioma margins efficiently and expeditiously, especially at transitional, infiltrative zones between tumor and normal white matter. In this study, we systematically investigated the feasibility of using optical coherence tomography(OCT) for delineating infiltrative tissues and thus potentially maximizing EOR. Fresh, ex-vivo tissues from 12 glioma(grades I-IV) and 5 control patients(temporal lobectomy) were imaged with an OCT system with central wavelength of 1310nm at ~16.0x9.0μm lateral x axial resolution and 40 frames/second imaging speed. Samples were subsequently processed for histology. OCT images were quantitatively analyzed to characterize optical attenuation and microscopic features. We found that the optical attenuation coefficients in the infiltrative zones from various tumor grades were consistently lower than normal white matter(2.6±1.2 versus 6.2±0.8mm) and the difference was statistically significant(p=0.0004). Further analyses revealed that an optimal sensitivity at 94% and specificity at 99% could be achieved using a cut-off value of 4.5/mm. Standard errors of sensitivity/specificity are being evaluated for additional testing datasets. We also identified two tumor features clearly visible under OCT: 1) Microcysts in ? of the patients for grade I-III and 2) necrosis/palisading features in all 8 patients. The results suggest the possibility of having clearer margins of resection intraoperatively using OCT to significantly improve surgical outcomes of glioma patients.

8571-70, Session 11

Optical coherence tomography and hyperspectral imaging of vascular recovery in a model of peripheral arterial disease

Kristin M. Poole, Wesley W. Sit, Jason Tucker-Schwartz, Craig L. Duvall, Melissa C. Skala, Vanderbilt Univ. (United States)

Peripheral arterial disease (PAD) leads to an increased risk of myocardial infarction and stroke, increased mortality, and reduced quality of life. The mouse hind limb ischemia (HLI) model is the most commonly used system for studying the mechanisms of collateral vessel formation and for testing new PAD therapies, but there is a lack of techniques for acquiring physiologically-relevant, quantitative data intravitally in this model. In this work, non-invasive, quantitative optical imaging techniques were applied to the mouse HLI model over a 21-day time course. Optical coherence tomography (OCT) imaged changes in blood flow (Doppler OCT) and microvessel morphology (speckle variance OCT) through the skin of haired mice with high resolution. Hyperspectral imaging was also used to quantify blood oxygenation. In ischemic limbs, blood oxygenation in the footpad and femoral blood flow distal to the ligation site significantly increased ($p<0.01$) over the 21-day time course, consistent with standard measures (laser Doppler perfusion imaging). Three dimensional images of the adductor muscle acquired with speckle variance OCT revealed changes in collateral vessel morphology consistent with published post-mortem results. Taken together, OCT and hyperspectral imaging enable intravital acquisition of both functional and morphological data which fill critical gaps in understanding structure-function relationships that contribute to recovery in the mouse HLI model. Therefore, these optical imaging methods hold promise as tools for studying the mechanisms of vascular recovery and evaluating novel therapeutic treatments in preclinical studies.

8571-71, Session 11

Characterization of middle ear effusions using phase variance and decorrelation OCT imaging

Guillermo L. Monroy, Cac Nguyen, Ryan Nolan, Nathan Shemonski, Univ. of Illinois at Urbana-Champaign (United States); Michael Novak M.D., Carle Foundation Hospital (United States); Stephen A. Boppart M.D., Univ. of Illinois at Urbana-Champaign (United States) and Carle Foundation Hospital (United States)

In acute and chronic cases of otitis media, the accumulation of liquid, commonly known as an effusion, develops with or leads to biofilm formation in the middle ear. Biofilms serve as a reservoir for infectious bacteria, and are considered the cause for recurrent infections. Otitis media is an extremely widespread disease, affecting over 80% of children before their third birthday. Acute otitis media is not typically severe and is often left untreated, which leads to the prevalence of chronic otitis media. At this more advanced stage, damage to the mastoid bone as well as bones in the middle ear may occur, leading to hearing loss and developmental delays in speech and language.

While traditional OCT images only provide a structural view of the sample, it is possible to distinguish liquid and solid structures, or provide characteristics such as the viscosity of the liquid, through additional signal processing. We first calculate phase variations between two adjacent B-mode OCT images, which helps to distinguish moving and non-moving structures in the middle ear. To characterize the liquid, when present, we process the Fourier transform of the cross-correlation of two M-mode OCT scans. We can then relate this signal to the diffusion constant of the Brownian motion of scatterers in the effusion, which can then be related to the viscosity. This information will give primary care physicians better diagnostic information on the state of the infection in the middle ear, and improve our fundamental understanding of the role effusions play in biofilm formation.

8571-72, Session 11

Sensing and three-dimensional imaging of cochlea and surrounding temporal bone using swept source high-speed optical coherence tomography

Mingtao Zhao, The Johns Hopkins Univ. (United States); Jin Kang, Johns Hopkins Univ. (United States)

We describe a novel dual-functional optical coherence tomography (OCT) system with both a fiber probe using a sapphire ball lens for cross-sectional imaging and sensing, and a 3-D bulk scanner for 3-D Oct imaging. A theoretical sensitivity model for Common Path (CP)-OCT was proposed to assess its optimal performance based on an unbalanced photodetector configuration. A probe design with working distances (WD) 415?m and lateral resolution 11 ?m was implemented with sensitivity up to 88dB. To achieve high-speed data processing and real-time three-dimensional visualization, we use graphics processing unit (GPU) based real-time signal processing and visualization to boost the computing performance of swept source optical coherence tomography. Both the basal turn and facial nerve bundles inside the cadaveric human cochlea

temporal bone can be clearly identified and 3D images can be rendered with the OCT system,which was integrated with a flexible robotic arm for robotic assisted microsurgery.

8571-73, Session 11

Measuring elastic contrast in human tissues using OCT needle probes

Kelsey M. Kennedy, Brendan F. Kennedy, Robert A. McLaughlin, David D. Sampson, The Univ. of Western Australia (Australia)

Optical coherence tomography (OCT) needle probes enable minimally invasive imaging of tissue microstructure centimeters below the surface. However, contrast based on OCT signal alone is often insufficient for distinguishing tissue types. An extension of OCT called optical coherence elastography (OCE) uses tissue elastic properties, which are indicative of tissue structure and pathology, as an additional contrast mechanism. To generate additional contrast in OCT needle images, we have developed the capacity to perform OCE measurements via a needle probe. Conventional OCE builds images by measuring deformation of tissue under an applied load, and analyzing the deformation to map variations in elastic properties. Our technique, needle OCE, uses an OCT needle probe to perform axial measurements of tissue deformation during needle insertion, allowing differentiation of tissues and identification of interfaces ahead of the needle. Our previous results have demonstrated the potential of needle OCE for subsurface detection of the boundaries of diseased tissue. In this paper, we assess the capability of needle OCE to delineate healthy and malignant human breast tissues. We describe our method for generating contrast based on tissue elasticity, and detail experiments performed in freshly excised human breast mastectomy samples. We compare needle OCE results with histopathology obtained along the insertion path of the needle, demonstrating differentiation of adipose, stroma, and malignant human breast tissues.

8571-74, Session 11

Ultrahigh resolution OCT of muco-ciliary activity on in vitro human airway epithelium

Amy L. Oldenburg, Raghav Chhetri, David B. Hill, Brian Button, The Univ. of North Carolina at Chapel Hill (United States)

OCT is uniquely suited for monitoring functional dynamics of the airway epithelium, especially in pulmonary diseases where mucus is characteristically thick or turbid. In particular, muco-ciliary clearance (MCC) is a key biomarker of pulmonary health. Here we show how ultrahigh resolution OCT can provide critical data relevant to MCC including mucus speed, height, and ciliary activity. Dynamic imaging methods including velocimetry using cross-correlation, and speckle fluctuation dynamics, are demonstrated in an actively transporting model of the human airway epithelium.

8571-75, Session 11

Characterization of ovarian tissue using polarization-sensitive optical coherence tomography

Tianheng Wang, Yi Yang, Quing Zhu, Univ. of Connecticut (United States)

Ovarian cancer has the highest mortality rate among all the gynecologic cancers because it is predominantly diagnosed in Stage III or IV due to the unreliable early symptoms and the lack of diagnostic techniques. Therefore, there is an urgent need to develop effective tools to detect ovarian cancer in earlier stages so that the survival rate can be increased. We characterized ovarian tissue using polarization-sensitive optical coherence tomography (PS-OCT) by quantitatively extracting optical scattering coefficient, phase retardation and phase retardation changing rate from 33 ex vivo ovaries (26 normal and 7 malignant ovaries) from 18 patients. In our previous study, optical scattering coefficient and phase retardation were extracted. In this report, a new parameter of phase retardation changing rate was extracted from ovarian tissue phase images, and it showed larger difference between normal and malignant ovary groups (Normal/malignant ratio=1.77) than scattering coefficient (ratio=1.36) and phase retardation (ratio=1.11). A generalized linear model was used to classify normal and malignant ovaries. By using these three parameters together, 100% sensitivity and 100% specificity were achieved. In addition, linear regression analysis showed that the phase retardation changing rate was positively correlated with collagen content measured from Sirius Red stained histology slides, with correlation coefficient R=0.74, which was higher than those from scattering coefficient (R=0.57) and phase retardation (R=0.47). Collagen was associated with the development of early ovarian cancers. These initial results showed that the quantitative analysis of PS-OCT could be a potentially effective tool for differentiating normal from malignant ovarian tissue.

8571-76, Session 12

Label-free optical imaging of blood and lymphatic vessels within tissue beds in vivo

Zhongwei Zhi, Yeongri Jung, Ruikang Wang, Univ. of Washington (United States)

Clinical and pathological observations suggest that, transport of tumor cells via lymphatics system is the most common pathway of initial dissemination for many carcinomas. Visualization of the lymph vessel plays a significant role in assessing patients with various malignancies and lymphedema. We report the use of an ultrahigh resolution optical microangiography (OMAG) system for simultaneous 3D imaging of microstructure, blood and lymphatic vessels without the use of an exogenous contrast agent. An OMAG system is developed that utilizes a broadband supercontinuum light source, providing an axial resolution of 2.3 ?m and lateral resolution of 5.8 ?m, capable of resolving the capillary vasculature and lymphatic vessels innervating microcirculatory tissue beds. An automatic algorithm is developed to segment the lymphatic vessels from the microstructural images based on the fact that the lymph fluid is optically transparent. Experimental demonstration is performed by showing detailed 3D lymphatic and blood vessel maps, coupled with morphology, within mouse ears in vivo. We have also demonstrated that the high resolution afforded by OMAG enables the visualization of the lymphatic valve structure, promising future investigation of the lymph flow dynamics within deep microcirculatory tissue beds. Currently, we are working on applying our technique for potential clinical applications, including monitoring the response of blood and lymphatic vessel to skin wounds on animal models. In future, the quantitative measurement of lymphatic vessel density will also be useful for the evaluation of lymphangiogenesis, which may be associated with the occurrence of various diseases especially tumor metastasis.

8571-77, Session 12

3d velocity vector measurement by 3-beam spectral-domain doppler optical coherence tomography

Wolfgang Trasischker, Stefan Zotter, Bernhard Baumann, Teresa Torzicky, Erich Götzinger, Michael Pircher, Christoph K. Hitzenberger, Medizinische Univ. Wien (Austria)

We present a three-beam Doppler Optical Coherence Tomography system for 3D velocity measurements of moving scatterers. The combination of three non-coplanar measurement directions enables the quantification of all three Cartesian velocity vector components as well as the absolute velocity value.

For each of the channels an individual SLD source with a central

wavelength at 840 nm is used. An in-house designed and built fiber collimator mount aligns the beams on the edges of an equilateral triangle and directs them towards the sample and reference arm. While sample and reference arm show a mutual bulk optics setup, the detection unit is comprised of three identical spectrometers.

For the measurement the three beams are focused down onto a mutual spot on the sample. This yields the beam geometry of a triangular pyramid.

In order to test the performance of our setup, measurements on a rotating and tilt-able disc were performed. With the known beam geometry it was possible to determine the velocity components in three dimensions and to measure the absolute velocity value independent of the vectors orientation and position.

With further development the setup might be used in ophthalmology to assess 3D velocity measurement of retinal blood flow and the possible diagnosis of ocular perfusion abnormalities.

8571-78, Session 12

High quality optical microangiography of ocular microcirculation and measurement of total retinal blood flow in mouse eye

Zhongwei Zhi, Xin Yin, Suzan Dziennis, Charles Alpers, Ruikang Wang, Univ. of Washington (United States)

Visualization and quantification of ocular blood flow especially absolute measurement of retinal blood flow (RBF) is important to the diagnosis and management of different eye diseases, including diabetic retinopathy. As a variation of Spectral-domain OCT, Optical microangiography (OMAG) is developed for generating 3D dynamic microcirculation image and later refined into ultra-high sensitive OMAG (UHS-OMAG) with the capability of imaging true capillary vessels. Here, we present the application of OMAG imaging technique for visualization of depth-resolved vascular network within retina and choroid as well as measurement of total retinal blood flow in mice. A fast speed spectral domain OCT imaging system at 820nm with a line scan rate of 140 kHz was developed to image mouse posterior eye. By applying UHS-OMAG scanning protocol and processing algorithm to extract the blood flow out of the background tissue, we achieved true capillary level imaging of retina and choroid vasculature in mouse eye. The microvascular pattern within different retinal layers and choroid after segmentation was presented. An en face Doppler OCT approach without knowing Doppler angle was adopted for the measurement of total retinal blood flow. The axial blood flow velocity is measured in an en face plane by raster scanning and the flow is calculated by integrating over the vessel area. Total RBF could be measured from both retinal arteries and veins with a high correlation. We applied OMAG to evaluate the microvasculature pattern change and quantify the total retinal blood flow change in early diabetic mice models compared with wild type mice.

8571-79, Session 12

Diabetes imaging: pancreatic vasculature and blood flow analysis using joint spectral and time domain OCM

Daniel Szlag, Nicolaus Copernicus Univ. (Poland) and Ecole Polytechnique Fédérale de Lausanne (Switzerland); Corinne Berclaz, Ecole Polytechnique Fédérale de Lausanne (Switzerland); Joan Goulley, Swiss Institute for Experimental Cancer Research (Switzerland); Arno Bouwens, Ecole Polytechnique Fédérale de Lausanne (Switzerland); Maciej Szkulmowski, Maciej Wojtkowski, Nicolaus Copernicus Univ. (Poland); Theo Lasser, Ecole Polytechnique Fédérale de Lausanne (Switzerland)

Faced with the overwhelming rise in the incidence of diabetes worldwide, the need to understand the underlying mechanisms of this disease becomes vital. Furthermore the possibilities for therapy require methods to assess their action and efficacy.

We demonstrate Optical Coherence Microscopy providing the possibility of combining the high resolution, high speed and high penetration depth 3-D structural imaging capability of OCM with the high speed 3-D flow measurement capabilities of JSTdOCT. We image the vascular architecture surroundings Langerhans' islet as well as an estimate of the direction and speed of blood flow without extrinsic labels.

8571-80, Session 12

Dynamic phase-resolved acoustic radiation force optical coherence elastography

Wenjuan Qi, Beckman Laser Institute and Medical Clinic (United States); Ruimin Chen, The Univ. of Southern California (United States); Lidek Chou, Gangjun Liu, Jun Zhang, Beckman Laser Institute and Medical Clinic (United States); Qifa Zhou, The Univ. of Southern California (United States); Zhongping Chen, Beckman Laser Institute and Medical Clinic (United States)

Changes in the biomechanical properties of tissues indicate tissue pathology in many diseases. Utilizing the correlation between tissue elasticity and pathology provides an additional insight into diagnosis and treatment of such diseases. In this paper, we report on the development of a phase-resolved acoustic radiation force optical coherence elastography method (PR-ARF-OCE) to evaluate the elastic properties of tissue. This method utilizes chirped acoustic radiation force to produce excitation along the sample's axial direction and uses phase-resolved optical coherence tomography (OCT) to measure the vibration of the sample. Under 500 Hz square wave modulated ARF signal excitation, A-mode phase maps of tissue-mimicking phantoms were generated by the ARF-OCE method and the resultant elastic modulus ratio was correlated with a standard compression test. The results verified that this ARF-OCE technique can efficiently measure sample elastic properties in an accurate and quantitative manner. Furthermore, a 3D ARF-OCE image of human atherosclerotic coronary artery was obtained. The result indicates that our dynamic phase-resolved ARF-OCE method is capable of delineating tissues with different mechanical properties.

8571-81, Session 12

Elastic restoring-force-free magnetomotive optical coherence tomography

Jongsik Kim, Adeel Ahmad, Stephen A. Boppart, Univ. of Illinois at Urbana-Champaign (United States)

Magnetomotive optical coherence tomography (MM-OCT) is a functional extension of OCT which utilizes magnetic nanoparticles (MNPs), and microspheres (MSs) containing MNPs, that are modulated by an external magnetic field for contrast enhancement and for elastography to assess the structural and viscoelastic properties of the surrounding tissues. Traditionally, the magnetomotive contrast had to rely on the presence of a micro-environmental restoring force acting on the particles after MNP displacement induced by an external magnetic field. We have developed a novel solenoid configuration to enable MM-OCT imaging in samples that do not have an elastic restoring force, such as liquids. Moreover, this coil is air-cooled with no significant heating, potentially enabling real-time MM-OCT imaging for extended durations.

8571-82, Session 12

Revealing viscoelasticity of soft tissue tumors using phase-sensitive optical coherence tomography and a focused air puff system

Shang Wang, Jiasong Li, Ravi K. Manapuram, Floredes M. Menodiado, Univ. of Houston (United States); Davis R. Ingram, The Univ. of Texas at Austin (United States); Michael D. Twa, Univ. of Houston (United States); Alexander J. Lazar, Dina C. Lev, Raphael E. Pollock, The Univ. of Texas M.D. Anderson Cancer Ctr. (United States); Kirill V. Larin, Univ. of Houston (United States) and Baylor College of Medicine (United States)

Here we report results on the use of an optical noncontact method for the detection of soft tissue tumors based on the viscoelastic properties of these tissues. A focused air puff system was used to excite surface mechanical waves (SMWs), which propagate on the surface of tissue. A high-speed phase-sensitive swept source optical coherence tomography (PhS-SSOCT) system was used to measure the amplitude decay, group velocity and dominant frequency of the SMWs as they propagate from the point of excitation. Amplitude exponential decay coefficient can be calculated to assess soft tissue viscosity. The quantification of group velocity and dominant frequency can be used to evaluate Young's modulus and the stiffness of tissues. Pilot experiments were performed on ex vivo human myxoma and normal fat. The viscoelasticity information of normal and pathological tissue was compared through the characterization of the SMWs. Kolmogorov–Smirnov test (K-S test) was utilized to examine the statistical significance of the difference in both location and shape of the data distribution. Conventional histological analysis (H&E-stained and light microscopy) was performed to confirm the OCT findings. Results indicate that myxoma can be well differentiated from normal fat based on the biomechanical assessment by OCT. This method of tissue viscoelasticity assessment is potentially useful for soft tissue tumors detection during surgery and can complement structural imaging.

8571-83, Session 12

In vivo imaging of gold nanorod contrast agents using photothermal optical coherence tomography

Jason M. Tucker-Schwartz, Travis A. Meyer, Chetan A. Patil, Craig L. Duvall, Melissa C. Skala, Vanderbilt Univ. (United States)

Photothermal optical coherence tomography (PT-OCT) has the potential to increase the molecular specificity of OCT for in vivo pre-clinical studies. However, in vivo PT-OCT of contrast agents has yet to be demonstrated. Here, we characterize PT-OCT imaging of gold nanorod (GNR) contrast agents in phantoms, and we further apply these techniques for in vivo GNR imaging. The PT-OCT signal was characterized and compared to the bio-heat equation with respect to varying photothermal chop frequency, photothermal laser power, OCT sample arm reflectivity, and concentration of GNRs. PT-OCT images were taken of GNR+ and GNR- solid agarose phantoms in capillary tubes, and 400 pM GNR matrigel injections into a mouse ear. Experiments revealed that PT-OCT signals varied as predicted with closed form models of the bio-heat equation. Increasing the concentration of GNRs caused a linear increase in the PT-OCT signal, with GNR sensitivity as low as 7.5 pM compared to a scattering control ($p<0.01$). PT-OCT images in capillary tubes and the live mouse ear demonstrated an appreciable increase in signal in the presence of GNRs compared to controls. Additionally, in vivo PT-OCT signals due to GNRs are spatially distinct from blood vessels imaged with Doppler OCT. The demonstrated in vivo PT-OCT sensitivity to GNR contrast agents is sufficient to image molecular expression, based on published molecular imaging studies employing GNR contrast agents in vivo. Therefore, this work demonstrates the translation of PT-OCT to in vivo imaging, and marks the next step towards its use as an in vivo molecular imaging tool.

8572-1, Session 1

Optical measurement of autonomic dysfunction in diabetic patients

Yuri An, Jungsul Lee, Chulhee Choi, KAIST (Korea, Republic of)

We have previously discovered that near-infrared optical imaging of indocyanine green (ICG) signal and analyzing its dynamics can be useful for measurement of blood perfusion rate and detection of Raynaud's syndrome. Raynaud's syndrome is one of autonomic dysfunction which is caused by many other diseases, such as systemic lupus erythematosus. This syndrome is closely related with abnormal vasomotor responses of diabetic vasculopathy and can progress to tissue necrosis due to excessively sustained vasoconstriction. Therefore, early detecting of Raynaud's syndrome has an important implication to prevent tissue damage from peripheral vascular disorders. In the current study, we tested whether the segmental and paired analysis of blood perfusion rate and Tmax value of ICG dynamics can be used for sensitive diagnosis of peripheral neuropathy and microvascular abnormalities which cannot be detected by conventional methods. From the NIR images of DM patients with vascular complications and without it, asymmetry of perfusion rate and Tmax value was observed. We assumed that decreasing local blood perfusion by peripheral neuropathy causes the asymmetric blood perfusion rate and Tmax value of right and left hands and feet. Furthermore, the asymmetry can be measured automatically, and features from this asymmetry may reflect the severity of peripheral neuropathy. These results collectively indicate that the proposed method can be used as a useful diagnostic tool of peripheral neuropathy or other neurological disorders, and also measuring the severity of DM.

8572-2, Session 1

New bilirubin sensors for total jaundice management using laser diodes, LEDs, and OLEDs

Mostafa Hamza, Mansoura Univ. (Egypt); Mohammad H. Sayed El-Ahl, Military Medical Academy (Egypt); Ahmad M. Hamza, National Research Ctr. (Egypt); Aya M. Hamza, Yahya M. Hamza, Tabarak Children's Hospital (Egypt)

It is important to detect jaundice in its early stages to prevent Kernicterus in newborn infants. When jaundice is properly diagnosed ,severe elevation of serum bilirubin can be prevented and effectively treated , preventing brain injury . However the accuracy and precision of the results obtained from conventional bilirubin meters have undesirable variability. In this paper the authors introduce the theory , design and operating principles of new non-invasive transcutaneous bilirubin sensors. The sensors are implemented using blue-green laser diodes and LEDs. The new design incorporates four wavelengths to avoid any spurious measurements due to the presence of melanin or due to skin maturity. The operation principle of these novel compact and low-cost bilirubin sensors is primarily based on the absorption characteristics of bilirubin in the blue-green region of the spectrum. The choice of these prescribed four wavelengths follows the principles of optical bilirubinometry. Accurate measurement of bilirubin concentration is a major determinant in the clinical management of neonatal jaundice. The management includes using blue laser diodes, or LEDs and Organic LEDs (OLEDs) for efficient phototherapy of jaundice. Non- invasive transcutaneous bilirubinometry using these novel sensors was used in our clinics and hospitals for the efficient and timely identification of neonates at risk of hyperbilirubinemia. The new system was found to provide an easy, quick and reliable screening of the neonates in the early stages of jaundice.

8572-6, Session 2

Photometric sensor system for a non-invasive real-time hemoglobin monitoring

Ulrich Timm, Jens Kraitl, Hartmut Ewald, Univ. Rostock (Germany)

Hemoglobin is a molecule which can be found in the red blood cells of the human body. Red blood cells are non-nucleated, biconcave discs that are filled with hemoglobin. Human beings have about 280 million hemoglobin molecules in each red blood cell. The primary function of hemoglobin is to transport oxygen from the lungs to the tissues and then transport carbon dioxide (CO2) back from the tissues to the lungs.

The absorption of whole blood in the visible and near infrared range is dominated by the different hemoglobin derivatives and the blood plasma that consists mainly of water. It is well known that pulsatile changes of blood volume in tissue can be observed by measuring the transmission or reflection of light through it. This diagnostic method is called photoplethysmography (PPG). The newly developed optical sensor system uses a multiplicity of discrete wavelengths for the measurement of the Hb concentration, oxygenation and pulse. This non-invasive multi-spectral measurement method is based on radiation of near monochromatic light, emitted by light emitting diodes (LED) in the range of 600nm to 1400nm, through an area of skin on the finger. Experimental results were obtained on human subjects during a calibration study in local blood donation centers, during dialysis session and and several surgery's . These results will be presented in comparison to other references as the blood gas analysis (BGA) and other on the market available devices.

8572-7, Session 2

Laser reflectance oximetry and Doppler flowmetry in assessment of complex physiological parameters of cutaneous blood microcirculation

Andrey V. Dunaev, Sergei G. Sokolovski, Neil A. Steward, Univ. of Dundee (United Kingdom); Victor V. Sidorov, SPE LAZMA Ltd. (Russian Federation); Edik U. Rafailov, Univ. of Dundee (United Kingdom)

High individual variability of blood microdynamics and tissue oxygenation measurements stimulated development of instrumental and methodological unification of various optical diagnostic techniques in a single device with software based on algorithms generating complex physiological parameters. This approach has been fully revealed in design of novel multifunctional laser-based non-invasive diagnostic system "LAKK-M" consisted of four optical approaches: laser Doppler flowmetry (LDF), tissue reflectance oximetry (TRO), laser fluorescence diagnostics (LFD) and pulse oximetry.

The study we present here demonstrates advantages of simultaneous recording of cutaneous peripheral blood microcirculation parameters: index of blood microcirculation (Im), tissue oxygen saturation (StO2), and relative blood volume (Vb) by LDF and TRO channels and their integral analysis. The long-term (over 1 month) variability of the parameters was assessed on adult volunteers without cardiovascular disease history. High variability in the initial parameters (Im and StO2 up to 16%) has been observed. All three parameters were then examined with built-in software including wavelet analysis that revealed five rhythmic components: endothelial, neurogenic, myogenic, breath and heart pulses which again demonstrated high variability (about 30-50%) might be due to hypersensitivity of middle finger tip pulp used as a test object.

It is also important to emphasize that during long-term observation of subject(s) individual variability in blood microdynamics and tissue

oxygenation demonstrated that all rhythmic components were synchronous with some latency between Im and StO2 in myogenic component underpinning the idea of strong correlation between peripheral hemodynamics and oxygen utilization in tissues.

8572-8, Session 2

Doppler diffuse optical multipatch imaging for microcirculatory monitoring

Liu Tsan Chi, Chung Yuan Christian Univ. (Taiwan); Ching-Cheng Chuang, National Taiwan Univ. (Taiwan); Yao-Sheng Hsieh, National Chiao Tung Univ. (Taiwan); Kuen Feng Lin, National Yang-Ming Univ. (Taiwan); Chia-Wei Sun, National Taiwan Univ. (Taiwan)

Microcirculation is the most important mechanisms to maintain tissue Metabolism, which can provide useful physiological information. A noninvasive methodology, Nearinfrared spectroscopy (NIRS) has been recently develop to assess ICU patients suffering from sepsis and heart failure, cerebral oxygenation and neuronal activity in humans. This study we proposed fDOI a new approach to combining Laser Doppler blood flowmetry (LDF) and continuous-wave nearinfrared spectroscopy (CW-NIRS), which is developed to measuring microcirculatory velocity of blood flowing, deoxygenated hemoglobin (Hb), oxygenated hemoglobin (HbO2), total hemoglobin (HbT) and oxygen saturation (StO2).

NIRS is used to evaluation spatial change in absorption and scattering in biological tissue, by monitoring changes in the concentration of oxygenated hemoglobin and deoxygenated hemoglobin. Deoxygenated hemoglobin is dominant lower than 805 nm absorption, rather oxy-hemoglobin dominates above 805 nm. Therefore, We use two light sources (780nm and 850nm) for measuring local changes in tissue oxygenation and perfusion, wavelength at 780nm also can measuring blood flowing.

In experiments, take advantage of far infrared illumination test in normal subjects to observing the body, which surrounding tissue oxygen and blood flowing changes due to the thermal effect of far infrared light. In the irradiation process, surrounding tissue microcirculation will change in the irradiation due to the body surface temperature increased by during irradiation, which lead to tissue blood flow increase then HbO2 rising. Integrated the following: (1) to achieve the purpose of the instrument miniaturization and low-cost by combining NIRS and LDF (2) far infrared illumination test is non-contact physiological intervention in the test method to provide more convenient and safe measurement. This system will have the opportunity to developed into Nursing in House system.

8572-9, Session 2

Non-contact tissue perfusion and oxygenation imaging using a LED based multi-spectral and a thermal imaging system: first results of clinical intervention studies

John H. Klaessens, Martin Nelisse, Univ. Medical Ctr. Utrecht (Netherlands); Rudolf Verdaasdonk, Vrije Univ. Medical Ctr. (Netherlands); Herke Jan Noordmans, Univ. Medical Ctr. Utrecht (Netherlands)

During clinical interventions objective and quantitative information of the tissue perfusion, oxygenation or temperature can be very useful for the surgical strategy. Local (point) measurements give limited information and affected areas can easily be missed, therefore imaging large areas is required .

A LED based multispectral imaging system (MSI, 17 different wavelengths 370nm-880nm) and a thermo camera were applied during clinical interventions: tissue flap transplantations (ENT), local anesthetic block and during open brain surgery (epileptic seizure). The images covered an area of 20x20 cm.

Measurements in clinical practice turned out to be more complicated compared to the laboratory experiment due to light fluctuations in the environment, movement of patient and limited angle of view in operation room. Using software, light fluctuations and movement were corrected.

Oxygenation concentration images could be calculated and combined with temperature images.

During brain surgery, changing in oxygenation on the cortex revealed the center of an epileptic attack. The effectivity of local anesthesia of a hand could be predicted in an early stage using the thermal camera and the reperfusion of transplanted skin flap could be imaged.

A LED based multispectral imaging system combined with thermal imaging provide complementary information on perfusion and oxygenation changes and are promising techniques for real-time diagnostics during clinical interventions.

8572-10, Session 2

Coherence-gated Doppler (CGD) for blood vessel detection

Chia-Pin Liang, Yalun Wu, Univ. of Maryland, College Park (United States); Joe Schmitt, St. Jude Medical, Inc. (United States); Cha-Min Tang, Univ. of Maryland School of Medicine (United States); Yu Chen, Univ. of Maryland, College Park (United States)

We developed a portable and low-cost CGD probe that can provide real-time audio feedbacks to the motion of moving scatters within a well-defined sample volume. The thin (0.125 mm) and flexible optical probe can be integrated within surgical tools for blood vessel detection. The diffuse optics design (sample volume mm-cm) of laser Doppler flowmetry (LDF) often includes high noises from surrounding tissues and thus not ideal for applications required high specificity, such as avoiding hemorrhage in deep brain and teeth pulp vitality testing. On the other hand, Doppler optical coherence tomography (DOCT) has high spatial resolution (~ 10 um), but requires complicated and expensive system to image the region of interest (ROI). Instead of imaging ROI, we fixed the path length of reference arm and tailored the sample volume to acquire the ensemble information from ROI (0.1-1 mm) by using the light source with appropriate coherent length and selecting the optics with proper focusing power. The interference fringe (~ kHz) reflecting the flow speed of moving scatters was directly converted to audio signal after amplification and frequency filtering. By placing CGD fiber probe on top of exposed rat femoral vessels, the distinctive audio feedbacks from artery, vein and surrounding tissues can be clearly differentiated. In the phantom studies, CGD probe demonstrated that it can detect and resolve a minute vessel (0.3 mm I.D.) in highly scattering environment (2% intralipid solution). CGD probe without expensive imaging components is a promising tool for blood vessel detection with superior resolution and specificity.

8572-11, Session 3

A multidimensional design for TCSPC-based diffuse optical/fluorescent tomography system

Wei Zhang, Yiming Lu, Liming Zhang, Feng Gao, Linhui Wu, Tianjin Univ. (China)

Techniques of time-correlated single-photon counting (TCSPC) have been widely used in diffuse optical tomography (DOT) and diffuse fluorescence tomography (DFT). While a multi-channel TCSPC-based DOT/DFT system can be conveniently constructed using independent modules, the state-of-the-art TCSPC technique has extended its multidimensional function by facilitating a compact and cost-effective design of the multi-channel as well as multi-wavelength data-acquisition. We herein present a revised multi-channel TCSPC system that is based

the multi-dimensional function of the TCSPC device. We also design a series of DOT and DFT experiments to validate effectiveness of the system.

8572-12, Session 3

A super-resolution method for arbitrary retrospective sampling in fluorescence tomography with raster scanning photodetectors

Xiaofeng Zhang, Duke Univ. (United States)

Dense optical sampling is required in high-resolution fluorescence molecular tomography and other biomedical optical imaging methods, such as diffuse optical tomography. Arrayed optical sensors, in particular charge coupled device cameras are commonly used mainly due to their high pixel count. Nonetheless, discrete-element optical sensors, such as photomultiplier tubes and avalanche photodiodes, are often desirable in many performance-demanding imaging applications. However, utilization of discrete-element sensors typically requires raster scanning of the sensor to achieve arbitrary retrospective sampling with high density. Care must be taken in using the relatively large active area of the discrete sensor to densely sample the image plane. In addition, off-line data analysis and image reconstruction often require full-field sampling. Pixel-by-pixel scanning is not only slow but also unnecessary for diffusion-limited imaging. We propose a super-resolution method that can recover the finer features of an image sampled with a coarse-scale sensor. This general-purpose method established the transfer function based on the known spatial characteristics of the scanning sensor with respect to the high-resolution true image, and achieved super-resolution by inversion of the linear transfer function. Regularized optimization algorithms were used to achieve optimized deconvolution. Compared to the untreated degraded image, the proposed super-resolution method significantly improved image quality. Using this method, the acquisition speed using a scanning photodetector can be dramatically improved without significantly sacrificing sampling density or flexibility.

8572-13, Session 3

Portable wide-field hand-held NIR scanner

Young-Jin Jung, Manuela Roman, Jennifer Carrasquilla, Sarah J. Erickson, Anuradha Godavarty, Florida International Univ. (United States)

Near-infrared (NIR) optical imaging modality is one of the widely used medical imaging techniques for breast cancer imaging, functional brain mapping, and many other applications. However, conventional NIR imaging systems are bulky and expensive, thereby limiting their accelerated clinical translation. Herein a new compact (6?7?12 cc), cost-effective, and wide-field NIR scanner has been developed towards contact as well as no-contact based real-time imaging in both reflectance and transmission mode. The scanner mainly consists of an NIR source light (between 700-900 nm), an NIR sensitive CCD camera, and a custom-developed image acquisition and processing software to image an area of 12 sq.cm. Phantom experiments have been conducted to estimate the feasibility of absorption and fluorescence medical imaging by using Indian-Ink, methylene blue and Indocyanine green as contrast agents. As a result, the developed NIR system measured the light intensity change in absorption-contrasted target up to 4 cm depth under transillumination mode. Preliminary in-vivo studies demonstrated the feasibility of real-time monitoring of blood flow changes. Currently, extensive in-vivo studies are carried out using the ultra-portable NIR scanner in order to assess the potential of the imager towards breast imaging and muscle oxygenation (towards sports injury applications).

8572-14, Session 3

Imaging functional brain networks in patients with deep brain stimulators using diffuse optical tomography

Amy R. Viehoever, Washington Univ. School of Medicine in St. Louis (United States); Adam T. Eggebrecht, Silvina L. Ferradal, Tasha Doty, Washington Univ. in St. Louis (United States); Tamara Hershey, Joseph P. Culver, Washington Univ. School of Medicine in St. Louis (United States)

Deep Brain Stimulation (DBS) is a surgically implanted therapy that has been shown to improve motor symptoms and quality of life in a number of movement disorders including Parkinson Disease (PD) and Dystonia. However, the mechanisms by which DBS produces these effects are not fully understood. Recently, resting state functional connectivity MRI and positron emission tomography (PET) analyses have identified cortical networks that are disrupted in various movement disorders; however, it is not known how these networks are affected by DBS. Due to safety concerns, it is not feasible to study patients following DBS placement with MRI.

We are using High Density Diffuse Optical Tomography (HD-DOT) to begin to understand how DBS affects functional brain networks. We are conducting studies on subjects who have had DBS placed for treatment of Parkinson's disease. Resting state functional connectivity and task based motor activations are measured using a large field of view HD-DOT system covering the occipital, temporal, motor, and some parietal and frontal cortical regions. Measurements are collected with the stimulator ON at optimized settings and then repeated with the stimulator OFF. The DOT images collected with stimulator ON are compared against images of stimulator OFF as well those collected from age matched controls. Preliminary results suggest that HD-DOT measures of cortical resting state functional connectivity and task based functional activations are feasible in DBS patients, a population that is unable to undergo fMRI studies.

8572-15, Session 3

Bedside diffuse optical tomography of resting-state functional connectivity in hospitalized neonates

Silvina L. Ferradal, Washington Univ. in St. Louis (United States); Steve M. Liao, Washington Univ. School of Medicine in St. Louis (United States); Adam T. Eggebrecht, Washington Univ. in St. Louis (United States); Terrie E. Inder, Joseph P. Culver, Washington Univ. School of Medicine in St. Louis (United States)

The high incidence of adverse neurodevelopmental outcomes in preterm infants remains a major clinical problem. Defining both anatomical and functional brain lesions may lead to a better understanding of the neural mechanism of adverse outcomes. Recent advances with resting-state functional connectivity MRI (fcMRI) provide an approach to defining functional lesions and have been used to investigate the maturation of the functional network architecture in neonates. Although fcMRI is an attractive tool because it does not require the subject to perform tasks, it has significant limitations for use in preterm infants due to challenges involved in the transportation to the scanner. Advances in high-density diffuse optical tomography (HD-DOT) techniques provide a portable and wearable alternative for evaluating the same hemodynamic physiology as BOLD-fMRI. We have previously shown the feasibility of detecting ischemia in an infant with an occipital stroke. In order to move forward with clinical applications of the technique, we first need to establish normal patterns of fcDOT maps in healthy infants and validate these results with those obtained with fcMRI. In this work, we demonstrate the feasibility of an expanded field of view HD-DOT system. Multiple functional connectivity networks are mapped over the occipital, parietal and temporal lobes of neonates. These preliminary results represent a

promising first step towards establishing a normative data set and serve as a foundation upon which to build studies of infants at greater risk for adverse outcome.

8572-16, Session 4

Label-free cell-based assay with spectral-domain optical coherence phase microscopy

SuHo Ryu, Chulmin Joo, Yonsei Univ. (Korea, Republic of)

Label-free cell assay technologies provide a means to study cell behaviours in various environments and to assess the effect of drugs on cells without any exogenous agents. Therefore, there have been much attention in developing new methods with enhanced throughput and sensitivity.

Conventional label-free cell assay systems detect changes of refractive index (RI) or optical path length near the cell-plate, as it offers information relevant to cell viability, toxicity and dynamic mass redistribution. Those methods typically use nanostructured substrate to improve the throughput and sensitivity at the surface, but the sophisticated patterned sensor surface required for operation increases the cost and manufacturing complexity.

We have developed a new label-free cell assay technology using spectral domain optical coherence phase microscopy (SD-OCPM). SD-OCPM is based on common-path spectral domain optical coherence reflectometry and has demonstrated its capability in measuring sub-cellular dynamics and molecular bindings at subnanometre length sensitivity. It can measure RI changes near the surface by detecting the phase change on sample surface within the coherence length of light source (1~6 um), without any modification of sensor surfaces.

We utilised this OCPM technology to detect cellular responses to various chemicals and drugs. In our preliminary experiment, OCPM successfully measured cell detachment from the glass substrate from trypsin-treated human breast cancer cells (MCF-7) with ~0.4 nm path length sensitivity. In this talk, we will briefly describe principle of operation and high-resolution, high-throughput implementation of our method, along with experimental results with various cell lines and chemicals (e.g. Colchicine).

8572-17, Session 4

A method to visualize lipid distribution within arterial vessel walls by 1.7 μm spectroscopic spectral-domain optical coherence tomography

Mitsuharu Hirano, Ichiro Sogawa, Takemi Hasegawa, Masato Tanaka, Sumitomo Electric Industries, Ltd. (Japan)

We report a method to visualize lipid distribution in axial and lateral direction within arterial vessel walls by spectroscopic spectral-domain Optical Coherence Tomography (OCT) at 1.7 μm wavelength for identification of lipid-rich plaque that is suspected to cause coronary events. In our method, an extended InGaAs-based line camera detects an OCT interferometric spectrum from 1617 to 1763 nm, which is then divided into six subbands, and A-scan OCT profile is calculated for each subband. The multi-spectral A-scan profiles are fitted to a model accounting the contributions from absorption by lipid that has a peak at 1730 nm, scattering that depends linearly on wavelength and scattering that does not depend on wavelength. Based on the fitting, lipid distribution in the cross section of vessel is visualized. In the fitting we assume that lipid content changes slowly in space and minimize the sum of fitting error and the norm of second spatial derivative of lipid content multiplied by a smoothing coefficient. We investigate numerically the effects of analyzing parameters such as number of subbands, number of points for numerical derivative and the smoothing coefficient, on the performance of lipid detection using simulated OCT spectral data, and have found optimum sets of parameters. Using the optimum parameters, we have confirmed that visualization of lipid distribution would be possible by our 1.7um OCT system that is currently being developed. The method is also verified by experiments that are reported separately.

8572-19, Session 4

Assessment of skin lesions with combined Reflectance confocal microscopy-optical coherence tomography

Nicusor Iftimia, Mircea Mujat, R. Daniel Ferguson, Physical Sciences Inc. (United States); William Fox, Lucid, Inc. (United States); Milind Rajadhyaksha, Memorial Sloan-Kettering Cancer Ctr. (United States)

A novel approach for combining reflectance confocal microscopy (RCM) and optical coherence tomography (OCT) within the same instrument with the goal to more effectively diagnose skin lesions is proposed. RCM can supplement OCT findings by providing images of the subcellular detail in the superficial epithelium (epidermis) and upper dermis with high resolution and high contrast. The RCM optical sectioning in the order of 1 to 3 um and its lateral resolution of 0.5 to 1.0 um are comparable to pathology capabilities. Thus, RCM might be used to evaluate skin lesions on a histomorphological level. However, RCM alone cannot reliably delineate the dermo-epidermal junction (DE junction), which is the boundary between the superficial epidermis and the underlying deeper dermis, and thus lesion depth is not reliably assessed. It also has limited imaging depth due to increasing aberrations and scattering at higher depths. Therefore, it can be used to complement OCT findings by highlighting morphological details in the epidermis and upper dermis. Thus, this dual-modality imaging technology could help clinicians to more reliably diagnose skin lesions by determining tissue structural integrity and viability. The simultaneous use of two high-resolution imaging technologies in diagnosing skin lesions will be discussed.

8572-20, Session 4

Intraoperative hand-held probe-based imaging of in situ breast tumor margins and lymph nodes using OCT and ISAM

Fredrick South, Marina Marjanovic, Steven G. Adie, Eric J. Chaney, Partha Ray M.D., Kimberly Cradock M.D., Univ. of Illinois at Urbana-Champaign (United States); John Brockenbrough M.D., George Liu M.D., Carle Foundation Hospital (United States); Guillermo Monroy, Ryan Nolan, Nathan D. Shemonski, Univ. of Illinois at Urbana-Champaign (United States); Jeffrey Putney, Donald Darga, Andrew J. Cittadine, Diagnostic Photonics, Inc. (United States); Paul S. Carney, Univ. of Illinois at Urbana-Champaign (United States); Stephen A. Boppart M.D., Univ. of Illinois at Urbana-Champaign (United States) and Diagnostic Photonics, Inc. (United States)

We present the development and translational clinical use of optical coherence tomography (OCT) and interferometric synthetic aperture microscopy (ISAM) as intraoperative high-resolution imaging techniques for real-time assessment of in-situ breast tumor margins and sentinel lymph nodes. Our portable OCT/ISAM system allows high-resolution imaging of tissue morphology in the operating room, providing critical diagnostic information for immediate surgical interventions.

OCT and ISAM are capable of providing high-resolution label-free images of intact tissue microstructure based on intrinsic optical scattering properties. We have previously shown that areas of higher scattering tissue with a heterogeneous pattern are indicative of tumor cells and tumor tissue in contrast to the lower scattering adipocytes found in normal breast tissue. Because of this, OCT/ISAM is able to visualize tumor margins on the micron scale to depths consistent

with histopathological evaluations. OCT/ISAM also have the potential for differentiating normal and metastatic lymph nodes based on microstructural scattering changes.

Our portable imaging system operates at a wavelength of 1300 nm and implements real-time OCT as well as real-time ISAM, which achieves depth-independent transverse resolution. This improved image resolution provides higher quality images with increased diagnostic value. Real-time in-situ imaging is made possible by our custom-designed hand-held probe which allows tissue to be imaged inside the surgical cavity and after resection. Both in-situ and ex-vivo images from over 20 patients have been acquired for correlation and comparison with post-operative pathology results. This system offers the potential for significantly reducing the exceedingly high re-operation rates in breast conserving surgeries.

8572-21, Session 4

Non-invasive assessment of sentinel node biopsies with full-field OCT

Katharine Grieve, Institut Langevin (France); Fabrice Harms, LLTECH SAS (France); Martine Antoine, Hôpital de Paris (France); Brigitte Sigal-Zafrany, Institut Curie (France); Osnath Assayag, Ecole Supérieure de Physique et de Chimie Industrielles (France); Bertrand Le Conte De Poly, LLTECH SAS (France); Claude Boccara, Institut Langevin (France) and LLTech SAS (France)

Full-field OCT (FF-OCT) is used to capture en face slices in tissue at 1 um resolution in 3D. In contrast to time or Fourier domain OCT, full-field OCT directly captures en face images using megapixel cameras and immersion microscope objectives of medium numerical aperture that provide high lateral and axial resolution (typically~1?m ?1?m?1?m). 3D image stacks can be captured by stepping through the depth of the sample. Mosaicing of 1mm2 native field images produces large field views of macroscopic tissue architecture, on which a digital zoom reveals the microscopic structures. The imaging process is non-invasive and requires no staining, which makes the technique particularly suitable for applications in pathology.

We have previously presented the use of FF-OCT in pre-clinical assessment of breast tissue in which blind diagnosis conducted on the FF-OCT images by two pathologists led to an assessment with 94% sensitivity and 76% specificity.

Here we follow on from this work to investigate the use of FF-OCT in sentinel node tissue assessment. To date we have imaged 40 specimens of freshly excised sentinel node tissue coming from a number of patients, with both healthy and cancerous samples. For each specimen we have taken 10x10mm FF-OCT images at 4 different depths. A single 10x10mm FF-OCT image is obtained in 2.5 minutes. Histology has been possible on 100% of the specimens. Microscopic features were easily recognizable and correlated with histology. Two pathologists have carried out diagnosis based on the FF-OCT images alone.

8572-22, Session 4

High-resolution spectrometer: solution to the axial resolution and imaging depth trade-off of SD-OCT

Tahereh Marvdashti, Audrey Ellerbee, Hee Yoon Lee, Stanford Univ. (United States)

We demonstrate a cross-dispersed spectrometer for Spectral Domain Optical Coherence Tomography (SD-OCT). The resolution of a conventional SD-OCT spectrometer is limited by the available sizes of the linear array detectors. This finite resolution has two major drawbacks: depth-dependent sensitivity falloff and limited axial field of view (i.e., ranging depth). More importantly, achieving practical imaging depths forces a trade-off between the axial resolution and the maximum imaging depth, which precludes high-resolution imaging.

Inspired by spectrometer designs for astronomy, we take advantage of very high pixel-density 2D CCD arrays to map a single-shot 2D spectrum to an OCT A-scan. The basic system can be implemented using a high-resolution Echelle grating crossed with a prism in a direction orthogonal to the dispersion axis. In this geometry, the interferometric light returning from the OCT system is dispersed in two dimensions; the resulting spectrum has more pixels than a traditional OCT spectrometer (which increases the ranging depth) and maintains good sensitivity over the ranging depth because of the improved fall-off resulting from the high-resolution grating. To our best of knowledge, we present the first demonstration of OCT image data using a cross-dispersed spectrometer. Potential applications for such a system include high-resolution imaging of the retina or anterior segment of the eye over extended imaging depths and small animal imaging.

8572-3, Session PSun

A glucose concentration detection method in interstitial fluid based on microdialysis for calibration of minimally invasive blood glucose monitoring

Ridong Wang, Tianjin Univ. of Commerce (China); Dachao Li, Tianjin Univ. (China)

There are two ways to detect the glucose level in interstitial fluid for minimally invasive blood glucose monitoring, the first one is transdermal extraction of interstitial fluid for detection, and the other one is the subcutaneous implantation of a micro glucose sensor. The results obtained by these two methods are not the real value of the glucose concentration of interstitial fluid, which requires a calibration by using the real value of the glucose concentration in interstitial fluid. But how to get this real value is a worldwide problem. In this article, a method based on microdialysis was presented to monitor glucose level in interstitial fluid continuously, and to provide the true value of the glucose concentration in interstitial fluid for the calibration of the minimally invasive blood glucose monitoring. An experimental system simulating the continuous variation of in vivo glucose concentration was built, and the influences on the recovery of microdialysis caused by flow rate, concentration, and temperature etc. were studied. The results led to the conclusion that the recovery fell by 71.7% when perfusion rate increased from 0.3 ?L/min to 3.0 ?L/min, while the different concentrations of glucose solutions scarcely contributed to the recovery instead, and the temperatures from 25 to 58 degrees Celsius caused the recovery to increase by 34.6%. The experiment on rabbit was carried out, the influence on in vivo recovery caused by flow rate was studied. The changes of glucose concentration in vivo were simulated through OGTT and insulin injections. The feasibility of using microdialysis to obtain the true value of the glucose concentration in interstitial fluid and to calibrate the minimally invasive blood glucose monitoring was verified.

8572-23, Session PSun

Normalized fluorescence lifetime imaging for tumor identification and margin delineation

Adria J. Sherman, Asael Papour, Univ. of California, Los Angeles (United States)

Fluorescence lifetime imaging requires complex instrumentation and algorithms to produce time-resolved images based on lifetimes of tissue fluorophores. These techniques have shown the ability to differentiate between a wide range of tissue types with sufficient specificity and sensitivity to identify malignant from benign tissue at the time of biopsy. However, the time and effort required to generate this information has limited the adoption of these techniques. Our group has developed a time-resolved imaging method that does not require the extraction of lifetimes or complex curve fitting algorithms to display the needed

information. The technique, entitled Normalized Fluorescence Yield Imaging (NoFYI), converts decay times at a range of wavelengths directly into contrast. Initial studies using Fluorescein and Rhodamine-B demonstrated the feasibility of this approach. Subsequent studies demonstrated the ability to separate collagen and elastin powders. The technique uses nanosecond pulsed UV LEDs at 370 nm for average illumination intensities of ~4.5 ?W on the tissue surface with detection by an Andor gated iCCD camera. To date, we have imaged 10 surgical brain biopsy specimens including 5 normal and 5 malignant gliomas. Images at multiple wavelengths clearly demonstrate differentiation between benign and malignant tissue, which was later confirmed by histology. Contrast was obtained between fluorophores with 35 ?m resolution and a dynamic range of ~40 dB allowing us to clearly define glioma tumor margins in this highly invasive cancer. This method appears to provide both anatomical and chemical information for the pathologist and the surgeon. These results suggest that this technology has a possible role in identifying tumors in tissue specimens and detecting tumor margins during procedures.

8572-51, Session PSun

An optimized algorithm of image stitching in the case of a multi-modal probe for monitoring the evolution of scars

Rami Kassab, FEMTO-ST (France); Sylvie Treuillet, Univ. d'Orléans (France); Franck S. Marzani, Univ. de Bourgogne (France); Christian Pieralli, Jean-Christophe Lapayre, Univ. de Franche-Comté (France)

We propose a new system that makes possible to monitor the evolution of scars after the excision of a tumorous dermatosis. The hardware part of this system is composed of a new optical innovative probe with which two types of images can be acquired simultaneously: an anatomic image acquired under a white light and a functional one based on autofluorescence from the protoporphyrin within the cancer cells. For technical reasons related to the maximum size of zone covered by the probe, acquired images are too small to cover the whole area of some scars. That is why a sequence of overlapping images is taken in order to cover the required area.

The main goal of this paper is to describe the creation of two panoramic images (anatomic and functional). Fluorescence images do not have enough salient information for matching the images; stitching algorithms are applied over each couple of white light images to produce an anatomic panorama of the entire scar. The same transformations obtained from this step are used to register and stitch the functional images. Several experiments have been implemented using different stitching algorithms (SIFT, ASIFT and SURF), with various transformation parameters (angles of rotation, projection, scaling, etc…) and different types of skin images. We present the results of these experiments that propose the best solution.

Thus, clinician has two panoramic images superimposed and usable for diagnostic support. A collaborative layer will be added to the system to allow sharing panoramas among several practitioners over different places.

8572-52, Session PSun

Handheld optical coherence tomography for human cutaneous chronic graft-versus-host disease

Mansik Jeon, Chulhong Kim, Univ. at Buffalo (United States); George L. Chen, Roswell Park Cancer Institute (United States)

Allogeneic hematopoietic cell transplant (alloHCT) is curative therapy for hematologic malignancies. However, its full potential is limited by chronic graft-versus-host disease (cGvHD), the major complication of alloHCT and the leading cause of non-relapse mortality after alloHCT. Chronic GvHD is the reaction of the donor's immune system against the recipient's tissues and is characterized by immune dysfunction and multi-organ fibrosis. Cutaneous disease is the most common manifestation, resulting in skin thickening and loss of elasticity, thereby limiting a patient's range of motion and decreasing quality-of-life. Cutaneous cGvHD assessments have heretofore been based on physical examination using descriptors such as the surface area, "movability", "pinchability", and skin appearance. Serial assessments of cutaneous cGvHD using these descriptors are difficult to objectively compare due to inter-observer differences. A quantitative method could improve serial assessment of cGvHD and facilitate the development of interventional clinical trials of new therapies. This paper presents the first known in vivo OCT imagery of human cutaneous cGvHD lesions. We imaged one patient with extensive cutaneous cGvHD at multiple disease affected sites and compared the results to OCT images of corresponding sites from a healthy control using a dual-modal handheld time-domain OCT (TD-OCT) and video imaging probe completely packaged in a mobile medical cart. We observed thickening of the stratum corneum, narrowing of the epidermis, and decreased surface waviness in cGvHD when compared to normal skin. These attributes can be quantified, suggesting that OCT may be a useful clinical diagnostic and therapeutic monitoring tool for cGvHD patients.

8572-53, Session PSun

A novel imaging strategy in 5-ALA-induced photodymanic diagnosis based on photobleaching of PpIX

Noriaki Koizumi M.D., Yoshinori Harada M.D., Eigo Otsuji M.D., Tetsuro Takamatsu M.D., Kyoto Prefectural Univ. of Medicine (Japan)

Photodynamic diagnosis (PDD) using 5-aminolevulinic acid (5-ALA) has been widely applied in clinical use. Following 5-ALA administration, 5-ALA-induced protoporphyrin IX (PpIX) is accumulated in cancer cells, and emits red fluorescence at around 635 nm on blue-violet light excitation. We have recently reported on 5-ALA-PDD to detect metastatic lymph nodes of gastrointestinal cancer. Through our examination, we revealed that PpIX fluorescence is sometimes disturbed by autofluorescence arising from tissue fluorophores, resulting in false-negative diagnosis of metastatic lesions. To resolve this issue, we sought to establish a new method to specifically detect 5-ALA-induced PpIX fluorescence based on PpIX photobleaching.

By continuous light irradiation, PpIX changes into another substance called photoprotoporphyrin (PPp) due to a photo-oxidative process of PpIX. According to this process, the fluorescence peak converts from 635 nm to 675 nm, although other endogenous fluorophores, such as collagen and flavins, show no spectral change even after light irradiation.

Since this spectral change associated with light irradiation is specific to PpIX, we could visualize PpIX accumulated in cancer cells specifically based on the change of spectral ratio from 675 nm to 635 nm. In particular, spectral images at 635 nm (I635nm) and 675 nm (I675nm) are sequentially acquired, and the ratio image of I675nm/I635nm (Rpre) is created by image processing. After light irradiation, we re-acquired the two spectral images and subsequently created another ratio image (Rpost). Finally, we created a ratioed ratio image (Rpost/Rpre) and could visualize PpIX localization specifically. This new method provides better diagnostic power than conventional PDD.

8572-54, Session PSun

The effect of borate polymer layers on measurement of glucose concentration by surface plasmon resonance

Jia Yang, Peng Wu, Dachao Li, Tianjin Univ. (China)

A new borate polymer PAA-ran-PAAPBA that can specifically adsorb

glucose was introduced into the glucose concentration measurement based on surface plasmon resonance. The borate polymer was bound onto the gold surface of SPR sensor using layer-by-layer (LBL) self-assembly method which can handle binding layer of polymer easily. Six layers and twelve layers of borate polymer were bound onto the SPR sensors respectively, and the effect of different layers of borate polymer on the glucose concentration measurement was studied. The experiment was conducted by three concentration ranges including 1~10mg/dL (interval ?=1mg/dL), 10~100mg/dL (?=10mg/dL) and 100~1000mg/dL (?=100 mg/dL), using both 6-layer-polymer sensor and 12-layer-polymer sensor. Glucose solution was injected into the experimental system, and the refractive index difference ?RU measured was fitted with their corresponding glucose concentration using quadratic curve. The experimental results are that the fitting degree are 0.47917 and 0.80343 in the range 1~10mg/dL , 0.90834 and 0.97941 in the range 10~50mg/dL ,and 0.99162 and 0.99377 in the range 10~1000mg/dL by using 6-layer-polymer sensor and 12-layer-polymer sensor respectively. Results showed that the performance of 12-layer-polymer sensor was better than that of the 6-layer-polymer sensor in the first two smaller ranges, and the measuring result was not significantly affected by polymer layers in the third range. It indicates that the enhancement of polymer layers on the surface of SPR sensor can dramatically improve the glucose measurement in the low concentration range, through which high-precision detection of glucose concentration in minimal volume of interstitial fluid can be realized.

8572-55, Session PSun

Cell phone based fluorescence dipstick reader for rapid diagnosis of Salmonella pathogen in water and beverages

Padmavathy Bakthavathsalam, Vinoth Kumar Rajendiran, The AU-KBC Research Ctr. (India); Jaffar Ali Baquir Mohammed, Pondicherry Univ. (India)

We report the development of fluorescence dipstick reader in a cell phone platform for diagnosis of Salmonella contamination in fruit juice. The technique uses a compact optical design containing a simple LED light source, an fluorescence filter set and a plano convex lens attached to the in-built camera of the commercial cell phone to detect the immunofluorescence in the dipstick membrane. The dipstick was developed for detection of Salmonella using FITC and Rubpy doped silica nanoparticles conjugated the anti- Salmonella sera and the sensitivity of the assay was compared with conventional gold nanoparticles based dipstick assay. The results were captured using the cell phone associated fluorescence dipstick reader and processed using open source image analysis software to obtain the characteristic intensity profile of the dipstick. It was found that the fluorescence dipstick showed increased sensitive detection compared to gold nanoparticles based read out. We also assayed the specificity of the assay on closely related Enterobacteriaceae members. The novel combination of fluorescence nanoparticles increased the sensitivity of dipstick detection when coupled with portable cell hone platform that can enable screening of various contaminated samples like food and water samples. Thus we demonstrate the cell phone assisted prototype fluorescence dipstick reader that can be potentially used in field applications for rapid pathogen diagnosis.

8572-56, Session PSun

Non-labeling imaging of rat colorectal cancers in vivo

Yoshinori Harada, Kiichiro Miyawaki, Katsuichi Imaizumi, Noriaki Koizumi, Keimei Nakano, Yoshihisa Yamaoka, Ping Dai, Tetsuro Takamatsu, Kyoto Prefectural Univ. of Medicine (Japan)

Macroscopic morphological changes are not sufficient to endoscopically reveal gastrointestinal tumors. Colorectal mucosa contains metabolism-related fluorophores, such as nicotinamide adenine dinucleotide (NADH), which might have potential to serve as biomarkers for detecting diminutive tumors. Our aim was to develop a non-labeling imaging technique for detecting rat colorectal cancers in vivo. Rat colorectal adenocarcinomas were induced by azoxymethane treatment. After autofluorescence images at 470 nm illuminated with dual-wavelength excitation at 365 nm (F365ex: NADH autofluorescence) and 405 nm (F405ex) were obtained, ratio images were created by dividing F365ex by F405ex. F365ex/F405ex ratio images indicated significantly higher signal values in the cancers than in the normal regions in-vivo. Small adenocarcinomas could be well delineated on F365ex/F405ex ratio images. These results showed that non-labeling imaging by using the dual-wavelength excitation method is efficient for visualizing rat colonic cancers in vivo and is a potential candidate for a novel diagnostic method applicable to clinical practice.

Ref) Imaizumi K, Harada Y, et al. Dual-wavelength excitation of mucosal autofluorescence for precise detection of diminutive colonic adenomas. Gastrointest Endosc 2012;75:110-7

8572-57, Session PSun

Raman spectroscopy using time-correlated photon-counting detection

Zhaokai Meng, Shuna Cheng, Georgi I. Petrov, Javier A. Jo, Vladislav V. Yakovlev, Texas A&M Univ. (United States)

A highly sensitive, shot-noise-limited Raman signal acquisition is achieved using frequency-time transformation in a single-mode fiber and time-correlated photon counting system. To spectrally disperse Raman signal excited by a picosecond laser pulse, the light is directed into a sufficiently long single-mode fiber. The output end of the fiber is coupled into a time-gated photon multiplier tube (PMT). Due to a frequency-time conversion provided by the fiber core, photons in different frequencies experience a different flight time. In this way, by measuring the arrival time of the registered photons, Raman peaks can be recorded and separated. Moreover, in some cases the fluorescence background can be eliminated from Raman signals due to its much longer life-time. Consequently, a fluorescence free Raman spectrum can be provided by time-correlated photon-counting Raman spectroscopy. In this presentation, by using a 400m SM600 single-mode fiber and a Hamamatsu R3809U-50 PMT, we demonstrate the Raman spectrum of dimethyl sulfoxide excited by a 532-nm picosecond pulsed laser.

8572-24, Session 5

Advanced fluorescence imaging system for clinical translation

Soren D. Konecky, Victor Ninov, Dar Bahatt, Jay Whalen, David Nilson, Heng Xu, Brad Rice, Caliper Life Sciences, Inc. (United States)

Fluorescence imaging of targeted probes enables non-invasive visualization of molecular processes in vivo. Typically, small animal fluorescence imaging systems utilize a light tight enclosure to prevent ambient light from obscuring the small signals emitted from fluorescent dyes. However, there are many exciting opportunities for fluorescence imaging in which a light enclosure is not feasible. These include pre-clinical applications such as large animal imaging, plus clinical applications such as fluorescence guided surgery, skin cancer imaging, and biopsy imaging. We present initial results using a newly designed enclosure-less imaging system which is designed to maintain the sensitivity of enclosed systems, while operating at high speeds with ambient light. Tissue is illuminated by rapidly alternating laser light with white light from an array of LEDs. Fluorescence emission is detected by an sCMOS sensor which is synchronized with the laser pulses, but rejects light from the LEDs. A second camera simultaneously acquires white light images. Short camera exposures and laser pulses reduce the contribution of ambient room light relative to emission light. A

compact and customized lens system is used for both illumination and detection. Rapid scanning of emission wavelengths using a liquid crystal tunable filter combined with real-time spectral unmixing enable us to multiplex probes while decreasing non-specific signal from tissue autofluorescence. We characterize the sensitivity of the new system over a wide range of parameters, and compare performance when imaging mouse models with traditional enclosed systems that utilize standard CCD technology.

8572-26, Session 5

Sentinel lymph nodes fluorescence and hyperspectral imaging using Patent Blue V

Franklin Tellier, Jerome Steibel, Renee Chabrier, Univ. de Strasbourg (France); Jean-Francois Rodier, Les Centres de Lutte Contre le Cancer (France); Genevieve Pourroy, Patrick Poulet, Univ. de Strasbourg (France)

Sentinel lymph node (SLN) biopsy is a surgical procedure in which the SLNs are identified, removed, and analyzed to detect a metastatic invasion from the primary tumour. A radioactive substance, a dye like Patent Blue V (PBV), or both are injected. We demonstrated that PBV fluorescence is about 34 times amplified, when the dye is mixed with human serum albumin (HSA) prior to use [1].

Using a probe based on optical fibers, one for excitation and the other for detection of scattered or fluorescence photons, we measured PBV detection thresholds lower than 2.5 nmol.L-1, with both methods. To obtain this sensitivity, the absorption by PBV should be discriminated from absorption by hemoglobins. The method using back-scattered photons requires a multiple wavelengths excitation and a spectral analysis [2].

As an extension of this single point detection, PBV distribution mapping can be obtained by fluorescence and by colour, hyperspectral, imaging. An experimental setup based on 4 low power laser diodes for colour imaging and one high power laser diode for fluorescence imaging, a frontal diffuser and a CCD camera was assembled. Evaluation of these methods for PBV distribution imaging were performed on test objects and on a preclinical model of swollen nodes on Lewis rats. We will present pictures of free PBV, PBV/HSA complex, and PBV bound on superparamagnetic iron oxides nanoparticules, the latter being synthesized for multimodal imaging.

1) F. Tellier el al. Biomedical Optics Express, to be published.

2) F. Tellier et al., Biomedical Optics Express, 1, 902-910, 2010.

8572-27, Session 5

Laser line scanning illumination scheme for the enhancement of contrast and resolution for fluorescence reflectance imaging

Frederic Fantoni, Lionel Hervé, Vincent Poher, CEA-LETI-Minatec (France); Sylvain Gioux, Beth Israel Deaconess Medical Ctr. (United States); Jérôme Mars, Institut National Polytechnique de Grenoble (France); Jean-Marc Dinten, CEA-LETI-Minatec (France)

Intraoperative fluorescence imaging in reflectance geometry is an attractive imaging modality as it allows to noninvasively monitor the fluorescence targeted tumors located below the tissue surface. The drawbacks of this technique are the poor resolution in the axial and lateral directions due to the multiple light scattering and the background fluorescence decreasing the contrast due to the wide-field illumination.

We propose a novel fluorescence imaging method based on laser line illumination in reflectance geometry. By scanning the medium with the laser line and choosing which part of the imaging field to detect, mask or subtract, we are able to enhance the contrast of fluorescent objects embedded in the medium. The optimal detection scheme depends on the depth of the object of interest. This technique allows us to reduce the contribution of parasite signals such as background fluorescence or excitation leaks and also enhances the resolution.

All the operations on the images can be done either digitally in post-processing or directly hardware implemented, allowing this technique to be integrated in a handheld device for real-time use.

This technique has been validated with tissue-like liquid phantoms with different levels of background fluorescence. Fluorescent inclusions are observed in several configurations at depths ranging from 1 mm to 1 cm. Results obtained with this technique are compared to those obtained with a more classical wide-field detection scheme.

Finally, we propose a setup to optically implement the masking detection that will dramatically fasten the detection scheme and optimize the fluorescence light throughput of the system.

8572-28, Session 5

Combination of widefield fluorescence imaging and nonlinear optical microscopy/ spectroscopy of oral epithelial neoplasia

Gracie Vargas, Kert Edward, Liang Ma, Tyra Brown, Suimin Qiu, Susan McCammon, The Univ. of Texas Medical Branch (United States); Massoud Motamedi, The Univ. of Texas Medical Branch (United States) and Univ. of Texas Medical Branch (United States)

Multiphoton autofluorescence microscopy (MPAM) and second harmonic generation microscopy (SHGM) are promising for the noninvasive assessment of neoplasia due to the ability to assess morphometry akin to pathological examination and biochemical information from endogenous fluorophores, however offer a limited field of view. Widefield fluorescence imaging on the other hand provides large area assessment with high sensitivity to abnormalities, but lacks specificity. The feasibility of combining a widefield approach with nonlinear optical microscopy for assessment of neoplastic epithelium was investigated in this study.

A hamster model for oral carcinogenesis involving the tri-weekly topical application of 9,10-dimethyl-1,2-benzanthracene (DMBA) to the buccal pouch was used. The full buccal pouch was imaged with a widefield autofluorescence setup using 405 nm illumination and emission in the blue and red (LP435nm; BP630 nm). Areas of interest were then imaged in vivo by MPAM/SHG microscopy/spectroscopy and with excitation wavelengths in the 780-890 nm range and detection of broadband emission and appropriate SHG wavelength. Imaged sites were biopsied immediately after imaging/spectroscopy and processed for histology then graded by a pathologist.

This proof-of-concept study demonstrated how the two modalities can be combined for large area low and subsurface microscopic evaluation of neoplastic tissue. As expected, widefield fluorescence revealed areas of interest corresponding to sites with precancers or early tumors, generally resulting in a decrease in blue emission or increase in red emission. In some cases a fluorescent change did not correspond to pathologist-graded neoplasia. MPM/SHG with spectroscopic provided specific subsurface cytological and stromal evaluation of suspicious sites.

8572-29, Session 6

Infrared dermal thermography on diabetic feet soles to predict ulcerations: a case study

Chanjuan Liu, Ferdi van der Heijden, Univ. Twente (Netherlands); Marvin E. Klein, DEMCON (Netherlands); Jeff G. van Baal, Hospital Group Twente (Netherlands); Sicco A. Bus, Hospital Group Twente (Netherlands) and Univ. van Amsterdam (Netherlands); Jaap J. Van Netten, Hospital Group Twente (Netherlands)

Diabetic foot ulceration is a major complication for patients with diabetes mellitus. If not adequately treated, these ulcers may lead to foot infection, and ultimately to lower extremity amputation, which imposes a major burden to society and great loss in health-related quality of life for patients. Early identification and subsequent preventive treatment have been proven useful to limit the incidence of foot ulcers and the lower extremity amputation. Thus, the development of new diagnosis tools has become an attractive option. The objective of our project is to develop an intelligent telemedicine monitoring system for frequent examination on patients' feet, to timely detect pre-signs of ulceration.

Inflammation in diabetic feet can be an earliest and predictive warning sign for ulceration, while temperature has been proven to be a vicarious marker for inflammation. Researches have indicated that infrared dermal thermography of foot sole can be one of the important parameters for assessing the risk of diabetic foot ulceration. This paper covers the feasibility study of using an infrared camera, FLIR SC305, in our setup, to acquire the spatial thermal distribution on the foot sole. With the obtained thermal images, automated detection through image analysis was performed to identify the abnormal increased/decreased temperature and assess the risk for ulceration. The thermography for feet sole of patients with diagnosed diabetic foot complications were acquired before the ordinary foot examinations. The assessment from clinicians and thermography were compared and four-month follow-up measurements were performed to inspect the prediction. Our preliminary studies indicate that dermal thermography in our proposed setup can be a screening modalities to predict ulcerations in daily foot care.

8572-30, Session 6

Laser scanning cytometry as a tool for biomarker validation

Anja Mittag, Univ. Leipzig (Germany) and Translational Ctr. for Regenerative Medicine (Germany); Christiane Füldner, Jörg Lehmann, Fraunhofer-Institut für Zelltherapie und Immunologie (Germany); Attila Tarnok, Univ. Leipzig (Germany)

Biomarkers are essential for diagnosis, prognosis, and therapy. As diverse is the range of diseases the broad is the range of biomarkers and the material used for analysis. Whereas body fluids can be relatively easily taken and analyzed, the investigation of tissue is in most cases more complicated. The same applies for the search and the evaluation of new biomarkers and the estimation of the binding of biomarkers found in animal models which need to be transferred into applications in humans. The latter in particular is difficult if it recognizes proteins or cells in tissue. The better way to find suitable cellular biomarkers for immunoscintigraphy or PET analyses may be therefore the direct ex vivo analysis of the respective tissue. In this study we present a method for biomarker validation using Laser Scanning Cytometry which allows the emulation of future in vivo analysis. The biomarker validation is exemplarily shown for rheumatoid arthritis (RA) on synovial membrane. Cryosections were scanned and analyzed by phantom contouring. Adequate statistical methods allowed the identification of suitable markers and combinations. The fluorescence analysis of the phantoms allowed the discrimination between synovial membrane of RA patients and non-RA control sections by using median fluorescence intensity and the "affected area". As intensity and area are relevant parameters of in vivo imaging (e.g. PET scan) too, the presented method allows emulation of a probable outcome of in vivo imaging, i.e. the binding of the target protein and hence, the validation of the potential of the respective biomarker.

8572-31, Session 6

Microendoscopy of small ducts as a potential tool for guiding and monitoring intruductual biopsy and therapy

Alexandre Douplik, Ryerson Univ. (Canada); Martin Hohmann, Friedrich-Alexander-Univ. Erlangen-Nürnberg (Germany); Asaf Shahmoon, Bar-Ilan Univ. (Israel); Azhar Zam, Friedrich-Alexander-Univ. Erlangen-Nürnberg (Germany); Zeev Zalevsky, Bar-Ilan Univ. (Israel); Michael Schmidt, Florian Stelzle, Friedrich-Alexander-Univ. Erlangen-Nürnberg (Germany); Hansgeorg Schaaf, POLYDIAGNOST GmbH (Germany)

The distinct changes in the tissue autofluorescence and spectral images between malignant and benign tissues potentially can facilitate visualization of lesions that are not seen under conventional white light ductoscopy. Spectral imaging is a large field of view and short integration time imaging modality allowing high-quality surveillance of the patient at video rate (24-30 fps), which is critical for endoscopy and endoscopic treatment when the duration of the procedure is limited. Real-time imaging may provide control of the therapeutic procedure, its monitoring and result assessment. Detection of cancer or other pathological lesions in hardly approachable ducts such as breast milk, pancreatic and Biliary ducts is becoming a priority because these malignancies are either engage a high number of patients (breast cancer) or grow aggressively leaving a short time (months) for in-time diagnostics and successful surgical interventions. At the first phase of the study, the ductoscope was coupled via a standard eyepiece to a fluorescence endoscopic imaging system (OncoLIFE, Xillix Technologies Corp, Canada: now PINPOINT, Novadaq Technologies Corp, Canada) with a spatial resolution of 3000 pixels at 0.7 mm diameter of the ductoscope (Fibertech, Japan). The next step was increasing the spatial resolution up to 10000 and 30000 pixels with a new microendoscope (Polydiagnost GmbH, Germany) using 0.7 and 1.3 mm diameter scopes consequently. The latest stage of the study employed a multicore-fiber microendoscope as a potential tool for diagnostics and surgery guidance facilitating up to 80000 pixels at 0.8 mm diameter scope.

8572-32, Session 6

Wide-field flexible endoscope for simultaneous color and NIR fluorescence image acquisition during surveillance colonoscopy

Pilar Beatriz Garcia Allende, Helmholtz Zentrum München GmbH (Germany); Wouter B. Nagengast, Univ. Medical Ctr. Groningen (Netherlands); Juergen Glatz, Vasilis Ntziachristos, Helmholtz Zentrum München GmbH (Germany)

Colorectal cancer (CRC) is the third most common form of cancer and, despite recent declines in both incidence and mortality, it still remains the second leading cause of cancer-related deaths in the western world. Colonoscopy is the standard for detection and removal of premalignant lesions to prevent CRC. The major challenges that physicians face during surveillance colonoscopy are the high lesion miss-rates and the lack of functional information to facilitate decision-making concerning which lesions to remove. Targeted imaging with NIR fluorescence would address these limitations. Tissue penetration is increased in the NIR range while the combination with targeted NIR fluorescent agents provides molecularly specific detection of cancer cells, i.e. a red-flag detection strategy that allows tumor imaging with optimal sensitivity and specificity. The development of a flexible endoscopic fluorescence imaging method that can be integrated with standard medical endoscopes and facilitates the clinical use of this potential is described in this work. A semi-disposable coherent fiber optic imaging bundle that is traditionally employed in the exploration of biliary and pancreatic ducts is proposed, since it is long and thin enough to be guided through the working channel of a traditional video colonoscope allowing visualization of proximal lesions. A custom developed zoom system magnifies the image of the proximal end of the imaging bundle to fill the dimensions of two cameras operating in parallel providing the simultaneous color and fluorescence video acquisition.

8572-33, Session 6

Real-time endoscopic guidance using near-infrared fluorescent light for thoracic surgery

Vivek Venugopal, Alan Stockdale, Florin Neacsu, Frank Kettenring, John V. Frangioni, Sidharta P. Gangadharan, Sylvain Gioux, Beth Israel Deaconess Medical Ctr. (United States)

Lung cancer is the leading cause of cancer death in the United States, accounting for 28% of all cancer deaths. Standard of care for potentially curable lung cancer involves preoperative radiographic or invasive staging, followed by surgical resection. With recent adjuvant chemotherapy and radiation studies showing a survival advantage in node-positive patients, it is crucial to accurately stage these patients surgically in order to identify those who may benefit. However, lymphadenectomy in lung cancer is currently performed without guidance, mainly due to the lack of tools permitting real-time, intraoperative identification of lymph nodes.

In this study we report the design and validation of a novel, clinically compatible near-infrared (NIR) fluorescence thoracoscope for real-time intraoperative guidance during lymphadenectomy. A novel, NIR-compatible, clinical rigid endoscope has been designed and fabricated, and coupled to a custom source and a dual channel camera to provide simultaneous color and NIR fluorescence information to the surgeon. The device has been successfully used in conjunction with a safe, FDA-approved fluorescent tracer to detect and resect mediastinal lymph nodes during thoracic surgery on Yorkshire pigs. Taken together, this study lays the foundation for the clinical translation of endoscopic NIR fluorescence intraoperative guidance and has the potential to profoundly impact the management of lung cancer patients.

8572-34, Session 7

Exploiting multimode waveguides for pure fibre based imaging

Tomá? ?i?már, Kishan Dholakia, Univ. of St. Andrews (United Kingdom)

There has been an immense drive in modern microscopy towards miniaturisation and fibre based technology. This has been necessitated by the need to access hostile or difficult environments in-situ and in-vivo. Strategies to date have included the use of specialist fibres and miniaturised scanning systems accompanied by ingenious microfabricated lenses. In parallel recent studies of randomized light fields and their holographic control opened up new ways for imaging. We present a novel approach for this field by utilising disordered light within a standard multimode optical fibre for minimally invasive lensless microscopy and optical mode conversion. We demonstrate the modalities of bright-field and dark-field imaging and scanning fluorescence microscopy at acquisition rates allowing observation of dynamic processes such as Brownian motion of mesoscopic particles. As the sample plane can be defined at any distance from the fibre facet, we eliminate the need for complex or elaborate focusing optics (e.g. miniaturized objectives, GRIN lenses) and instead reconfigure the system dynamically to image different axial planes. Furthermore, we show how such control can realise a new form of mode converter and generate various types of advanced light fields such as propagation-invariant beams and optical vortices. These may be useful for future fibre based implementations of super-resolution or light sheet microscopy. To the best of our knowledge, this technology represents the narrowest possible image guiding system based on light propagation.

8572-35, Session 7

A new spectroscopic paradigm for discrimination of lesions associated with breast microcalcifications

Narahara Chari Dingari, Ishan Barman, Jaqueline S. Soares, Massachusetts Institute of Technology (United States); Anushree Saha, Case Western Reserve Univ. (United States); Sasha McGee, The Univ. of North Carolina, Chapel Hill (United States); Luis H. Galindo, Massachusetts Institute of Technology (United States); Wendy Liu, Donna Plecha, Nina Klein, Case Western Reserve Univ. (United States) and Univ. Hospitals Case Medical Ctr. (United States); Ramachandra R. Dasari, Peter T. C. So, Massachusetts Institute of Technology (United States); Maryann Fitzmaurice, Case Western Reserve Univ. (United States)

Detection of microcalcifications is an early mammographic sign of breast cancer and considered as target for stereotactic breast needle biopsy. In this study, we develop and compare different approaches for developing Raman classification algorithms to diagnose invasive and in situ breast cancer, fibrocystic change and fibroadenoma that can be associated with microcalcifications. Briefly, Raman spectra were acquired from tissue cores obtained from fresh breast biopsies and analyzed using a constituent-based breast model. We have developed diagnostic algorithms based on the breast model fit coefficients using logistic regression, C4.5 decision tree classification, k-nearest neighbor (k-NN) and support vector machine (SVM) analysis, and subjected to leave-one-out cross validation. The best performing algorithm was based on SVM analysis (with radial basis function), which demonstrated a positive predictive value of 100% and negative predictive value of 96% for cancer diagnosis. Significantly, these results demonstrate that Raman spectroscopy provides adequate diagnostic information for lesion discrimination even in the presence of microcalcifications, which is the novel point of our work and has not been previously reported.

8572-36, Session 7

Mobile large area confocal scanner for imaging tumor margins: Initial testing in the Pathology Department

Sanjeewa Abeytunge, Bjorg Larson, Yongbiao Li, Memorial Sloan-Kettering Cancer Ctr. (United States); Emily Seltzer, Livingston High School (United States); Ricardo Toledo-Crow, Milind Rajadhyaksha, Memorial Sloan-Kettering Cancer Ctr. (United States)

Surgical oncology is guided by examining pathology that is prepared during or after surgery. The preparation time for Mohs surgery in skin is 20-45 minutes, for head-and-neck and breast cancer surgery is hours to days. Often this results in incomplete tumor removal such that positive margins remain. However, high resolution images of excised tissue taken within few minutes can provide a way to assess the margins for residual tumor. Current high resolution imaging methods such as confocal microscopy are limited to small fields of view and require assembling a mosaic of images in two dimensions (2D) to cover a large area, which requires long acquisition times and produces artifacts. To overcome this limitation we developed a confocal microscope that scans strips of images with high aspect ratios and stitches the acquired strip-images in one dimension (1D). Our “Strip Scanner” can image a 10 x 10 mm2 area of excised tissue with sub-cellular detail in about one minute. The strip scanner was tested on 17 Mohs excisions and the mosaics were read by a Mohs surgeon blinded to the pathology. After this initial trial, we built a mobile strip scanner that can be moved into different surgical settings. A tissue fixture capable of scanning up to 6 x 6 cm2 of tissue was also built. Freshly excised breast and head-and-neck tissues were imaged in the pathology lab. The strip-images were registered and displayed simultaneously with image acquisition resulting in large, high-resolution confocal mosaics of fresh surgical tissue in a clinical setting.

8572-37, Session 7

In-depth performance analysis and high impact applications of the HyperFlux spectrometer

Jeffrey T. Meade, Bradford B. Behr, Arjae Spectral Enterprises, Inc. (Canada); Andrew T. Cenko, Thunder Bay Regional Research Institute (Canada); Arsen R. Hajian, Tornado Spectral Systems (Canada)

We have conducted in-depth studies into the performance of Tornado Spectral Systems' HyperFlux spectrometer, and we have identified target applications that receive the greatest advantage from the technology. The HyperFlux is the world's first spectrometer to incorporate High Throughput Virtual Slit (HTVS) technology to greatly increase the light throughput of a high-resolution instrument by not using a slit. Typically the percentage of the total light collected by a high-resolution spectrometer that makes it to the focal plane is a few percent due to the slit blocking most of it . The HyperFlux spectrometer is able to offer an order of magnitude improvement over this performance level. With such a disruptive change in spectroscopic performance, applications never before possible are now achievable and it is important to understand in detail where the technological limitations of the HyperFlux are. Rigorous temperature and vibration tests, long term noise and alignment stability analysis, signal-to-noise ratio versus various system parameters, detector noise characterization, and effects of spurious optical artefacts have all been conducted and will be presented. Various applications where HyperFlux has the greatest impact will be discussed, such as Raman, multi-channel/imaging, fluorescence, emission/absorption, astronomical, and high-speed spectroscopy.

8572-38, Session 7

Multispectral digital colposcopy For detection of clinical cervical intraepithelial neoplasia

Michele Follen, The Univ. of Texas M.D. Anderson Cancer Ctr. (United States); Sylvia F. Lam, Martial Guillaud, Deanna Ceron, The BC Cancer Agency Research Ctr. (Canada); Judit Banath, The BC Cancer Agency Research Ctr (Canada); Jagoda Korbelik, The BC Cancer Agency Research Ctr. (Canada); Dennis D. Cox, Rice Univ. (United States); Neely Atkinson, The Univ. of Texas M.D. Anderson Cancer Ctr. (United States); Roderick Price, Texas Tech Univ. (United States); Timon P. H. Buys, The BC Cancer Agency Research Ctr. (Canada); Salvador Saldivar, Texas Tech Univ. (United States); Sarah Finlayson, Mark Heywood, Janice Kwon, Marette Lee, Jessica McAlpine, Tom Ehlen, Dianne Miller, The Univ. of British Columbia (Canada); Dirk van Niekerk, British Columbia Cancer Agency (Canada); Pierre M. Lane, Calum MacAulay, The BC Cancer Agency Research Ctr. (Canada)

Effective and affordable approaches to cervical cancer screening/diagnosis are desperately needed. Current standard of care for developed nations (Pap smear followed by colposcopy and histopathological review where abnormalities are detected) can be time consuming and require multiple visits, resulting in increased expenses. Though HPV vaccines may one day alter approaches to cervical neoplasia screening, the reality is that high demand for screening programs/colposcopic review is still expected for the foreseeable future. Further, use of HPV testing as a screening approach will also lead to increased demand for colposcopy (given the test's relatively low specificity). We have developed a multispectral digital colposcopy (MDC) device that visualizes the entire cervix, aiming to more effectively locate and diagnose disease. Our goal was to evaluate MDC images from patients undergoing loop electrosurgical excision procedure (LEEP) treatment for cervical intraepithelial neoplasia (CIN) against gold standard histopathological findings/colposcopic review, assessing whether MDC improves disease detection in vivo. Complete data from 53 subjects were obtained. MDC examination detected pathology-defined high grade disease (CIN II or III) in most instances (sensitivity, 99-68% [observer dependent]). The observed sensitivity of MDC images was moderate (86-34%). Data suggest the MDC may more accurately delineate disease boundaries than colposcopic review under white light. We conclude that CIN is detectable in vivo via MDC, suggesting clinical utility for this device when used in parallel with existing approaches. Our findings provide a strong rationale for larger planned trials that will assess the MDC in concert with a very specific spectroscopic point probe

8572-39, Session 8

Raman microspectrometer combined with scattering microscopy and lensless imaging for bacteria identification

Samy Andrea Strola, Emmanuelle Schultz, Cédric Allier, J. Lemmonier, J. Lemmonier, CEA-LETI-Minatec (France); Brandon DesRoches, Tornado Medical System (Canada); Jean-Marc Dinten, CEA-LETI-Minatec (France)

In this paper, we report on a compact prototype capable both of lensfree imaging, Raman spectrometry and scattering microscopy from bacteria samples. This instrument allows high-throughput real-time characterization without the need of markers, making it potentially suitable to field label-free biomedical and environmental applications.

Samples are illuminated from above with a focused-collimated 532nm laser beam and can be x-y-z scanned. The bacteria detection is based on emerging lensfree imaging technology able to localize cells of interest over a large field-of-view of 24mm2.

Raman signal and scattered light are then collected by separate measurement arms simultaneously. In the first arm the emission light is fed by a fiber into a prototype spectrometer, developed by Tornado Medical System based on Tornado's High Throughput Virtual Slit (HTVS) novel technology. The enhanced light throughput in the spectral region of interest (500-1800 cm-1) reduces Raman acquisition time down to few seconds, thus facilitating experimental protocols and avoiding the bacteria deterioration induced by laser thermal heating. Scattered light impinging in the second arm is collected onto a charge-coupled-device. The reconstructed image allows studying the single bacteria diffraction pattern and their specific structural features.

The characterization and identification of different bacteria have been performed to validate and optimize the acquisition system and the component setup.

The results obtained demonstrate the benefits of these three techniques combination by providing the precise bacteria localization, their chemical composition and a morphology description. The procedure for a rapid identification of particular pathogen bacteria in a sample is illustrated.

8572-40, Session 8

Classification of Raman spectra of bacteria using rank order kernels

Alexandros Kyriakides, Univ. of Cyprus (Cyprus); Evdokia Kastanos, Univ. of Nicosia (Cyprus); Katerina Hadjigeorgiou, Costas Pitris, Univ. of Cyprus (Cyprus)

The classification of Raman spectra can be very useful in a wide range of diagnostic applications including bacterial identification. Prompt and accurate diagnosis results in better patient prognosis and less chance of antibiotic resistance. However, the classification task is particularly challenging especially when the training and test data are truly independent or even taken at a different time and/or with dissimilar equipment. In this paper, a novel method, for classification of such spectra, is presented based on the bio-inspired Rank Order Kernel approach. A Rank Order Kernel operates on a two dimensional image

and is similar to a nonlinear spatial filter. The output of the Rank Order Kernel operation is a rank order code, i.e. a character string which represents the order of the corresponding pixel values on which the kernel operates. Rank Order Kernels are robust to noise due to the ranking they perform. For this work, the spectra were each converted to a two-dimensional image representation by using segment ratios. Each spectrum was divided into overlapping windows. The mean of the intensity values in each window was divided by every other mean intensity resulting in a two-dimensional matrix of ratios which was processed as an image. The images in the training set were then used to classify the images in the test set using a simple nearest neighbor algorithm and the Rank Order Kernel distance metric. This method results in higher accuracy compared to Support Vector Machines or Linear Discriminant Analysis which are currently the methods of choice.

8572-41, Session 8

Integrated fingerprint and high wavenumber confocal Raman spectroscopy for in vivo diagnosis of cervical precancer

Shiyamala Duraipandian, Zhiwei Huang, Wei Zheng, National Univ. of Singapore (Singapore); Joseph Ng, Jeffrey J. Low, Arunachalam Ilancheran, National Univ. Hospital (Singapore)

Raman spectroscopy is a vibrational spectroscopic technique capable of optically probing the compositional, conformational, and structural changes in the tissue associated with disease progression. The main goal of this work is to develop an integrated fingerprint (FP) and high wavenumber (HW) in vivo confocal Raman spectroscopy for simultaneous FP/HW tissue Raman spectral measurements. This work further explores the potential of integrated FP/HW Raman spectroscopy developed as a diagnostic tool for in vivo detection of cervical precancer. A total of 473 in vivo integrated FP/HW Raman spectra (340 normal and 133 precancer) were acquired from 35 patients within 5 s during clinical colposcopy. The major tissue Raman peaks are noticed around 854, 937, 1001, 1095, 1253, 1313, 1445, 1654, 2946 and 3400 cm-1, related to the molecular changes (e.g., proteins, lipids, glycogen, nucleic acids, water, etc.) that accompany the dysplastic transformation of tissue. The FP (800 - 1800 cm-1), HW (2800 - 3800 cm-1) and the integrated FP/HW Raman spectra were analyzed using partial least squares-discriminant analysis (PLS-DA) together with the leave-one-patient-out, cross-validation. The developed PLS-DA classification models and receiver operating characteristics (ROC) curves for the FP, HW and integrated FP/HW spectroscopy further discloses that the performance of integrated FP/HW Raman spectroscopy is superior to that of all others in discriminating the dysplastic cervix. The results of this work indicate that the co-contributions of underlying rich biochemical information revealed by the complementary spectral modalities (FP and HW Raman) can improve the in vivo early diagnosis of cervical precancer at clinical colposcopy.

8572-42, Session 8

Comparison of high and low frequency Raman spectra for colonic neoplasia detection

Michael A. Short, The BC Cancer Agency Research Ctr. (Canada); Isabella T. Tai, The Univ. of British Columbia (Canada); David Owen, Vancouver General Hospital (Canada); Calum MacAulay, Haishan Zeng, The BC Cancer Agency Research Ctr. (Canada)

Raman spectroscopy systems have good potential as adjunct devices for endoscopes to improve the in vivo identification of early cancers. Most systems currently under development utilize the traditional low frequency Raman measurement range since this contains the most spectral bands and by extension the most biochemical information. However there are significant masking emissions in the low frequency range which make it challenging to develop a routine clinical tool. One possibility is to use the high frequency Raman emissions which contain fewer spectral bands, but significantly less noise. To test this idea Raman emissions from colon tissue in the low and high frequency ranges were compared. Ex vivo tissues were used which allow for a more accurate comparison. Pathology predictive models were applied to the data using a multivariate statistical analyses on the spectra with a leave-one-out cross validation.

Raman spectra were obtained in the low (700-1750 cm-1) and high (2050-3100 cm-1) frequency ranges with clear peaks associated with tissue biomolecules. The spectra in the low frequency range contained a large number of Raman peaks, but also significant contributions from tissue autofluorescence and fibre optic emission despite extensive optical filtering. The spectra in the high frequency range were dominated by Raman emissions in a narrow band from 2700-3100 cm-1, but the tissue autofluorescence was only half as intense as the low frequency range and fibre optic emission was almost absent. Multivariate statistical analyses predicted the pathology with 100% sensitivity and a specificity close to 88% for both frequency ranges.

8572-43, Session 8

Quantitative and qualitative analysis of fluorescent substances and binary mixtures by use of shifted excitation Raman difference spectroscopy

Boris L. Volodin, PD-LD, Inc. (United States); William Yang, BaySpec Inc. (United States); Sergei Dolgy, PD-LD, Inc. (United States); Huawen Wu, BaySpec Inc. (United States); Chad Lieber, BaySpec, Inc. (United States)

Shifted Excitation Raman Difference Spectroscopy (SERDS) implemented with two wavelength-stabilized laser diodes with fixed wavelength separation is discussed as an effective method for dealing with the effects of fluorescence in Raman spectroscopic analysis. In this presentation we discuss the results of both qualitative and quantitative SERDS analysis of a wide variety of strongly fluorescing samples, including binary liquid mixtures. This application is enabled by the Volume Bragg Grating® (VBG®) technology, which allows manufacturing of compact low-cost high-power laser sources, suitable for extending the SERDS methodology to portable Raman spectrometers. We compare the accuracy, efficiency and practicality of using VBG-enabled SERDS method with conventional dispersive Raman analysis performed at the same excitation wavelength, as well as with dispersive Raman analysis performed at a longer excitation wavelength (e.g. 1064 nm), where no fluorescence is observed. Finally, the spectrum reconstruction algorithm enabling the qualitative analysis of strongly fluorescing samples by a human eye is discussed.

8572-44, Session 8

Tissue measurement using 1064-nm dispersive Raman spectroscopy

Chad A. Lieber, BaySpec, Inc. (United States); Huawen Wu, William Yang, BaySpec Inc. (United States)

To avoid the autofluorescence inherent to biological tissues, many biomedical Raman users long ago switched to near-infrared wavelengths like 785 or 830nm. Unfortunately, even at this end of the silicon spectral detection range, many tissue types still exhibit prohibitive fluorescence. Recent advances in spectrograph and detector technologies now allow dispersive Raman measurements at 1064nm with instrument quantum efficiency comparable to that of shorter wavelength systems. Using 1064nm dispersive Raman systems (both probe-based and microscopic), we have studied a variety of human and animal tissues, along with other biological samples. These studies show that the 1064nm Raman measurements are largely devoid of fluorescence, even in highly pigmented and porphyrin-rich tissues like kidney and

liver, with significantly higher signal-to-noise ratios. Furthermore, the longer wavelength approach allows a relaxation in sampling conditions, as interfering fluorescence and luminescence from glasses are also significantly reduced. Despite the wavelength-dependent reduction in Raman scattering efficiency versus 785nm approaches (approximately 3.4 times), permissible exposure limits allow a total compensation via an increase in laser power, such that equal integration times are afforded using both systems. Cellular studies are also presented using the 1064nm system, showing true confocal operation in the dispersive approach that has not been achievable by the geometry of previous FT-Raman systems. These studies demonstrate the suitability of dispersive 1064nm Raman for biomedical measurement, and evidences a new approach for studying highly fluorescent samples.

8572-45, Session 9

Utilization of moire technique for evaluation of wound dimensions and of healing progress

Marcia T. Saito, Elisabeth M. Yoshimura, Univ. de São Paulo (Brazil); Antonio C. L. Lino, Instituto Agronômico (Brazil); Francisco P. Fernández, Univ. de Oriente (Cuba); Marcelo V. P. Sousa, Univ. de São Paulo (Brazil)

The methods used for evaluating wound dimensions, especially of the chronic ones, are invasive and inaccurate. The Fringe Projection Technique with Phase Shift is an alternative non-invasive, accurate and low-cost optical method. Objective: The aim is to validate the technique through the determination of dimensions of objects with different geometries and colors simulating the wounds and tones of skin color and then compare with the known values. Taking into account the influence of skin wound optical factors, the technique will be used to evaluate actual patients' wound dimensions and to study its limitations in this application. Methods: Four sinusoidal fringe patterns displaced ? of the period each were projected in objects with different known dimensions, geometries and colors. The object dimensions were obtained from the unwrapped phase map through the observation of the fringe deformations caused by the object topography and using phase shift analysis. An object with simple geometry was used for dimensional calibration and the topography dimensions of the others were determined from it. After observing the compatibility with the data and validating the method, it was used for measuring the dimensions of real patients' wounds. Results and Conclusions: The discrepancies between actual topography and dimensions determined with Fringe Projection Technique and for the known object were lower than 0.5 cm. The method was successful in obtaining the topography of real patient's wounds. Objects and wounds with sharp geometries or causing shadow or reflection are difficult to be evaluated with this technique.

8572-46, Session 9

Fluorescence lifetime for blood stain age dating

Mikhail Y. Berezin, Washington Univ. School of Medicine in St. Louis (United States); Kevin Guo, Washington Univ. in St. Louis (United States); Samuel Achilefu, Washington Univ. School of Medicine in St. Louis (United States)

Bloodstain dating has remained an unsolved problem for the past two hundred years. Despite significant advancements in blood splatter, composition, and DNA analysis, techniques for ascertaining the age of bloodstains at crime scenes are surprisingly underdeveloped. Here, we propose a novel method for bloodstain dating based on the fluorescence lifetime of blood. We show that the intrinsic fluorescence lifetime, the average time needed for an excited molecule to return to the ground state, quickly and reliably reports the blood age. Our approach is based on the fact that the fluorescence lifetime of tryptophan – the major endogenous fluorophore in blood proteins - is highly sensitive to the protein conformation. We hypothesize that in the process of blood aging, the tryptophan bearing proteins, such as serum albumin and ?-globulins which constitute more than 95% of the protein mass in blood, undergo structural changes. Consequently, we expect that the proteins in blood and hence their fluorescence lifetime values would change with time and correlate with blood age. Preliminary results with blood from different dogs indicate the feasibility of our approach.

8572-47, Session 9

Using color intensity projections to visualize air flow in operating theaters with the goal of reducing infections

Keith S. Cover, Joost de Jong, Rudolf Verdaasdonk, Vrije Univ. Medical Ctr. (Netherlands)

Infection following neurosurgery is all too common. One possible source of infection is the transportation of dust and other contaminates into the open wound by airflow within the operating theater. While many modern operating theaters have a filtered, uniform and gentle flow of air cascading down over the operating table from a large area fan in the ceiling, many obstacles might introduce turbulence into the laminar flow including lights, equipment and personal. Schlieren imaging - which is sensitive to small disturbances in the laminar flow such as breathing and turbulence caused by air warmed by a hand at body temperature – was used to image the air flow due to activities in an operating theater. Color intensity projections (CIPs) were employed to reduce the workload of analyzing the large amount of video data. CIPs – which has been applied to images in angiography, 4D CT, nuclear medicine and astronomy – summarizes the changes over many gray scale images in a single color image in a way which most interpreters find intuitive. CIPs uses the hue, saturation and brightness of the color image to encode the summary. Imaging in an operating theater showed substantial disruptions to the airflow due to equipment such as the lighting. When these disruptions are combined with such minor factors as heat from the hand, reversal of the preferred airflow patterns can occur. These reversals of preferred airflow patterns have the potential to transport contaminates into the open wound. Further study is required to understand both the frequency of the reversed airflow patterns and the impact they may have on infection rates.

8572-48, Session 9

Universal rapid diagnostic test (RDT) reader on a cell-phone for real-time spatio-temporal mapping of infectious diseases

Onur Mudanyali, Stoyan Dimitrov, Uzair Y. Sikora, Swati Padmanabhan, Isa Navruz, Aydogan Ozcan, Univ. of California, Los Angeles (United States)

Diagnosis and monitoring of infectious diseases in resource limited environments still have serious drawbacks due to the lack of appropriate healthcare infrastructure and well-trained personnel. Toward this need, rapid diagnostic tests (e.g., lateral-flow based immuno-chromatographic tests) have been emerging to improve healthcare delivery by minimally trained technicians. In order to provide accurate digital reading of rapid diagnostic tests (RDTs) and real-time global mapping of infectious diseases, we developed a cell-phone based universal RDT reader platform that can automatically digitize and evaluate different types of RDTs. Weighing ~60 grams, this RDT reader attachment is installed at the back of the cell-phone camera unit and utilizes an inexpensive plano-convex lens and three light-emitting-diode (LED) arrays that are powered by either the cell-phone battery or two external AAA batteries. This hardware attachment enables digital acquisition of transmission and reflection images of various RDTs that are then digitally processed in real-time using a custom-developed application running on the cellphone to generate a digital evaluation report with semi-quantitative analysis of test results. The same cell-phone application wirelessly transfers the RDT

evaluation report to a secure server that organizes and presents the test results on a world-map through geo-tagging. Operating on both iPhone and Android phones, this universal RDT reader platform provides a valuable and timely tool not only for accurate and quantitative evaluation of RDTs but also for real-time spatio-temporal mapping of infectious diseases globally.

8572-49, Session 9

Label-free biosensor based on long period grating

Francesco Baldini, Francesco Chiavaioli, Ambra Giannetti, Massimo Brenci, Cosimo Trono, Istituto di Fisica Applicata Nello Carrara (Italy)

Long period gratings have been recently proposed as label-free optical devices for biochemical sensing. A biochemical interaction along the grating portion induces a refractive index change and hence a change in the fiber transmission spectrum. This provides an alternative methodology with respect to other label-free optical approaches, such as surface plasmon resonance, interferometric configurations and optical resonators. The fibre biofunctionalization has been carried out by means of a novel chemistry using Eudragit L100 copolymer as opposed to the commonly used silanization procedure. Antigen/antibody interaction has been analysed by means of an IgG/anti-IgG bioassay. The biosensor was fully characterised, monitoring the kinetics during the antibody immobilization and the antigen interaction and achieving the calibration curve of the assay. A comparison of the biosensor performance was made by using two different long period gratings with distinct periods. Experimental results demonstrated an enhancement of the biosensor performance when the fundamental core mode of the single-mode fibre couples with a higher order cladding mode. Considering an LPG manufactured on a bare optical fibre, in which the coupling occurs with the 7-th cladding mode, a dynamic signal range of 322 pm, a working range of 1.7 – 1450 mg L-1 and a LOD of 500 ?g L-1 were achieved.

8572-50, Session 9

A portable microfluidic-based biophotonic sensor for extracellular H2O2 measurements

Volodymyr Koman, Guillaume Suárez, Christian Santschi, Victor Javier Cadarso, Ecole Polytechnique Fédérale de Lausanne (Switzerland); Nadia von Moos, Univ. of Geneva (Switzerland); Jürgen Brugger, Ecole Polytechnique Fédérale de Lausanne (Switzerland); Vera I. Slaveykova, Institute F.A. Forel, Univ. of Geneva (Switzerland); Olivier J. F. Martin, Ecole Polytechnique Fédérale de Lausanne (Switzerland)

Hydrogen peroxide (H2O2), one of the most important reactive oxygen species (ROS), acts as a signaling molecule in a broad variety of signaling transduction processes, as an oxidative stress marker in ageing and disease, and as a defence agent in response to pathogen invasion. Therefore, the development of analytical tools providing information on the dynamics of H2O2 generation is of utmost importance to obtain better insights in the complex physiological processes of living cells and their response to environmental stress.

We present a portable analytical sensor for extracellularly monitoring release of H2O2 in real time. The biosensor is based on the optical detection of the oxidation state of cytochrome c (cyt c). A picomolar limit of detection is achieved by enhancing the absorption of cyt c via the multiscattering produced by random aggregates of polystyrene beads. Using ink-jet printing technique the sensing elements, namely cyt c loaded polystyrene aggregates are fabricated with high reliability in terms of repeatability and sensitivity. The detection of H2O2 released from stressed aquatic microorganisms is performed using such an ink-jet printed biosensor. Hydrogen peroxide has to be brought into contact with the sensing cyt c spot. To go beyond the diffusion limit, a specifically designed microfluidic system delivers the released H2O2 into the sensing region. In conclusion, this sensor provides a non-invasive way to monitor cell metabolism and its portability is especially of interest for point-of-care diagnostics.

8573-1, Session 1

Fluorescence advantages with microscopic spatiotemporal control *(Invited Paper)*

Debabrata Goswami, Debjit Roy, Indian Institute of Technology Kanpur (India); Arijit K. De, Indian Institute of Technology Kanpur (India) and Lawrence Berkeley National Lab. (United States)

We present a clever design concept of using femtosecond laser pulses in microscopy by selective excitation or de-excitation of one fluorophore over the other overlapping one. Using either a simple pair of femtosecond pulses with variable delay or a train of laser pulses at 20-50 Giga-Hertz excitation, we show controlled fluorescence excitation or suppression of one of the fluorophore with respect to the other through wavepacket interference, an effect that prevails even after the fluorophore coherence timescale. Such an approach can be used both under the single-photon excitation as well as in the multiphoton excitation conditions resulting in effective higher spatial resolution. Such high spatial resolution advantage with broadband pulsed excitation is of immense benefit to multiphoton microscopy and can also be an effective detection scheme for trapped nanoparticles with near-infrared light. Such sub-diffraction limit trapping of nanoparticles is challenging and a two-photon fluorescence diagnostics allows a direct observation of a single nanoparticle in a femtosecond high-repetition rate laser trap, which promises new directions to spectroscopy at the single molecule level in solution. The gigantic peak power of femtosecond laser pulses, even at low average powers, at high repetition rate provide huge instantaneous gradient force that most effectively result in a stable optical trap for spatial control at sub-diffraction limit. Such studies have also enabled us to explore simultaneous control of internal and external degrees of freedom that require coupling of various control parameters to result in spatiotemporal control, which promises to be a versatile tool for the microscopic world.

8573-2, Session 1

Optimal design for high-quality functional brain imaging by diffuse optical tomography *(Invited Paper)*

Hanli Liu, The Univ. of Texas at Arlington (United States)

Near infrared spectroscopy (NIRS) is the foundation of diffuse optical tomography (DOT), which has been developed and investigated intensively in recent years as a potential clinical tool for functional brain imaging. As compared to other functional brain imaging modalities, NIRS or DOT technology has many advantages, such as radiation free or strong magnetic field free, portable, low-cost, with fast temporal data acquisition, without very strict body confinement, and possible for repeated measurements within a short period of time. However, several technical challenges exist as road blocks to prevent DOT from becoming a practical tool to be used in clinical environments. These challenges can be solved or partially solved by improving the design and implementation of optical fiber probes and fiber array layouts, as well as by developing appropriate mathematical algorithms to compensate severe decays in optical signals by deeper tissue layers. This presentation is going to present a few solutions toward this direction; it will report our recent studies in brush-fiber design and implementation, probe geometry optimization, depth-compensation algorithm to improve depth localization accuracy in DOT, as well as to compare and discuss DOT image qualities using several DOT image processing algorithms. Overall, this talk will give an overview on current DOT probe and system designs as well as qualities for functional brain imaging.

8573-3, Session 1

Component and system evaluation for the development of a handheld point-of-care spatial frequency domain imaging (SFDI) device

Kyle P. Nadeau, Beckman Laser Institute and Medical Clinic (United States); Pierre Khoury, Amaan Mazhar, David J. Cuccia, Modulated Imaging, Inc. (United States); Anthony J. Durkin, Beckman Laser Institute and Medical Clinic (United States)

Recent advances in digital photography have made it an efficient and economic means to assist dermatologists in monitoring skin lesions during treatment. Typical applications include skin cancer, therapeutic response, and wound healing. However, conventional digital cameras only provide qualitative color information. To address this issue, we are developing a quantitative, handheld skin imaging camera that employs Spatial Frequency Domain Imaging (SFDI), a non-contact approach for determining optical properties over a wide field-of-view. In addition to calibrated color information, SFDI gives the absolute concentration of relevant chromophores such as oxy/deoxy-hemoglobin, total hemoglobin, and oxygen saturation. We have carried out a performance analysis of light sources, spatial light modulators, and detectors in order to identify components that will be appropriate for a compact form factor SFDI system. Broadband and LED light sources are investigated, with key measurements including power, spectra, and stability. For spatial light modulation, we investigate DMD-based projection systems, as well as slide-based systems. Relevant data includes input-output linearity, spectral throughput, and projection time. We evaluate both color and grayscale camera detectors, with key data including stability and sensitivity. We also present results from phantom studies of device prototypes. Custom layered tissue phantoms are fabricated to closely resemble the optical characteristics of actual human skin. Using these phantoms, we evaluate the precision of optical property calculations and color data.

8573-4, Session 1

Real-time multispectral diffuse optical tomography system for imaging epileptic activity and connectivity *(Invited Paper)*

Huabei Jiang, Tao Zhang, Jianjun Yang, Hao Yang, Univ. of Florida (United States)

We describe the design and evaluation of a multispectral continuous-wave diffuse optical tomography (DOT) system that can be used for real-time three-dimensional imaging of epileptic activity and connectivity. In vivo experiments using a rat model of epilepsy are demonstrated.

8573-5, Session 2

The design and integration of a custom broadband 15x zoom lens for NIR fluorescence-guided surgery *(Invited Paper)*

Julie Bentley, Univ. of Rochester (United States); John V. Frangioni M.D., Harvard Univ. (United States); Sylvain Gioux, Beth Israel Deaconess Medical Ctr. (United States)

Over the last few years, fluorescence imaging for biomedical applications has experienced very rapid growth. An application triggering significant interest is the use of fluorescence for image guidance during surgical

interventions. A 15x broadband (400-1000 nm) macro-zoom objective has been designed, manufactured, and tested for use in image-guided surgery that employs near-infrared (NIR) fluorescence imaging. The lens has been incorporated into a novel FLARE™ imaging system with an imaging head that can be positioned in space using an articulated arm during surgery. Pre-clinical images from the as-built system will be presented

8573-6, Session 2

An algorithm for automated selection of application-specific fiber optic probes

Andrew J. Gomes, Vadim Backman, Northwestern Univ. (United States)

Several optical techniques and systems have been designed to measure the optical properties of shallow tissue layers such as the epithelium and mucosa. While a wide range of options is often beneficial, it poses a problem to an investigator selecting which method to use for their biomedical application of interest. In this paper we present a methodology to optimally select a probe that matches the application requirements. Our method is based both on matching a probe's average penetration depth with the optimal diagnostic depth of the clinical application and on choosing a probe whose interrogation depth and path length is the least sensitive to alterations in the target medium's optical properties. Satisfying these requirements ensures that the selected probe consistently assesses the relevant tissue volume with minimum variability. To aid in probe selection, we have developed a publicly available graphical user interface (GUI) that takes the desired penetration depth and optical properties of the medium as its inputs and automatically ranks different techniques in their ability to robustly target the desired depth. Techniques investigated include single fiber spectroscopy, differential path length spectroscopy, polarization-gating, elastic light scattering spectroscopy, and diffuse reflectance. Analysis of the GUI on several case studies reveals that the choice of the optimum probe depends on the desired depth as well as the optical properties of the medium.

8573-7, Session 2

Design of a miniature objective lens for in vivo confocal microendoscopy

Tzu-Yu Wu, College of Optical Sciences, The Univ. of Arizona (United States); Arthur F. Gmitro, Andrew R. Rouse, The Univ. of Arizona (United States)

Confocal microendoscopy allows in vivo histologic diagnosis of epithelial surfaces of internal organs in real time during optical biopsy. A fluorescence confocal microendoscope typically requires a miniature objective lens with high resolution for visualization at the cellular level. This paper presents a design of a miniature water-immersion microscope objective lens that delivers nearly diffraction-limited performance over a 486 µm to 820 µm wide spectral range. This broad spectral bandwidth allows the objective lens to be used with a wide variety of fluorescent contrast agents. The lens design is a 15 mm long and 4.2 mm diameter multi-element assembly with a maximum clear aperture of 2.3 mm. The lens has a numerical aperture of 0.6 and a magnification of 2.2, which yield a tissue space lateral resolution of 1.5 µm over a 466 µm field of view. It is designed for, but not limited to, use in a flexible fiber-bundle-based fluorescence confocal imaging system that can operate in both grayscale and multispectral imaging modes. The lens is integrated into an imaging catheter that incorporates a focus mechanism and a contrast agent delivery channel. The catheter employs a flexible 50,000-element fiber bundle with a 1,025 µm diameter active area and can be routed through the instrument channel of a standard endoscope, adding microscopic imaging capability to a conventional endoscope. Primary applications of a system employing this miniature objective lens are early detection of cancer or disease in the gastrointestinal tract and female reproductive system via an endoscopic procedure.

8573-8, Session 2

A multiresolution foveated laparoscope

Yi Qin, College of Optical Sciences, The Univ. of Arizona (United States); Zhenrong Zheng, Zhejiang Univ. (China); Hong Hua, College of Optical Sciences, The Univ. of Arizona (United States)

Laparoscope plays an important role in minimally invasive surgery (MIS), which provides revolutionized patient care. However, the state-of-art laparoscopic technologies suffer a number of limitations. One limitation is the trade-off between wide field of view and high spatial resolution. Inspired by the fovea of human retina and the function of eye movements, we proposed a multi-resolution foveated laparoscope (MRFL) that addresses the FOV-resolution tradeoff. The MRFL system is able to (1) simultaneously provide both wide-angle and high-magnification images of a surgical area in real-time within a fully integrated system; (2) automatically scan and engage the high-magnification probe to any sub-region of the surgical field by optical tracking capability; (3) maintain a low profile.

In this paper, a prototype of the MRFL system with a functional computer user interface was demonstrated. The wide-angle probe of the prototype system has an 80-degree field of view and the high-magnification probe has a 26.6-degree field of view. The objective lens was designed to be diffraction limited with about 15% distortion. Each rod lens relay group works at a magnification of -1 and has a distortion less than 0.1%. The integrated high-magnification probe was designed to have a capability of resolving 100um in the object space. A compact mechanical case with high tolerance was designed for the integrated system. The performance tests were carried out for the objective lens group, each rod lens relay group as well as the entire integrated system. The experimental results demonstrated high optical performance comparable to the original optical design.

8573-9, Session 2

A virtual size-variable pinhole device for single photon confocal microscopy

Guangjun Gao, Retina Health Ctr. (United States); Bahram Khoobehi, LSU Health Sciences Ctr. (United States)

Pinhole is a critical device in single photon confocal microscopy (SPCM) owning to its ability to block the background noise scattered from back and forth of the focal plane. Without pinhole, the sectioning ability of SPCM will be degraded and many background noise signals will occurred together with useful signals, and sometimes these bad noises can submerge the details that we are interested. However a pinhole with too small diameter will block both background noises and part of signals and decrease the intensity of the image. Therefore in many cases pinhole size should be selected carefully. Unfortunately because of constrains in mechanics, a pinhole that can change its size continuously, for example from 10 µm to 100 µm, is unavailable. For most commercial confocal microscopies, only several discrete pinhole sizes are provided, such as 10 µm, 30 µm, 60 µm etc. Things will be even harder for some imaging systems which use the input interface of a single mode fiber as the pinhole of SPCM, and then the pinhole size of these systems will be fixed, which far limit the optimization of systems' performance.

In this paper, we design a size-variable pinhole setup that can offer a virtual pinhole with its diameter adjustable. This setup includes a physical pinhole (or single mode fiber) and a fine designed zoom relay (ZR) optical system. The magnification ratio of this ZR can vary smoothly while keeping the conjugation distance unchanged. The aberrations of the ZR are well balanced and diffraction-limited image performance are obtained so that the virtual pinhole can block background scattering noise and pass the in-focus signal effectively and accurately. Simulation results are also provided and discussed.

8573-10, Session 2

Using a mini aspheric lens as the objective of a miniaturized video-rate nonlinear optical microscope

Hsiang-Yu Chung, National Taiwan Univ. (Taiwan); Chi-Kuang Sun, National Taiwan Univ. (Taiwan) and Molecular Imaging Ctr., National Taiwan Univ. (Taiwan) and Institute of Physics & Research Ctr. for Applied Sciences, Academia Sinica (Taiwan)

In order to apply nonlinear optical microscopy for clinical applications, an optical imaging head with a miniaturized size, a larger field of view (FOV), and a video frame-rate is highly desired. A hand-held miniaturized system can provide conveniences during the observation and allow intravital applications. Larger fields of view allow more information to be revealed simultaneously. High frame rates can not only reduce the imaging acquisition time but also allow one to deal with the image blurring problem resulted from vibrations.

Aspheric lenses, which are known as their complicated lens surface profile designed for aberration reduction or replacement for a multi-lens system, are commonly used in cell phone cameras, optical disk drives, or laser diode collimators. With its smaller size and cheaper price, it could be an alternative to traditional objectives in miniaturized nonlinear microscopy systems. In this talk, we present our recent investigation on the potential to use a mini aspheric lens as the objective of the miniaturized nonlinear microscopy system. In this system, the mini aspheric lens was integrated with a tube lens pair for beam size magnification, a MEMS mirror as a scanner, and a dichroic beam splitter. We investigated its performance for TPF (two-photon fluorescence), SHG (second harmonic generation), and THG (third harmonic generation) microscopies. Comparison studies using the Blu-ray disk (BD) lens or a GRIN rod are also reported.

8573-11, Session 3

Multi-system comparison of optical coherence tomography performance with point spread function phantoms *(Invited Paper)*

Joshua Pfefer, U.S. Food and Drug Administration (United States); Chao-Wei Chen, Anthony Fouad, Univ. of Maryland, College Park (United States); Wei Gong, Univ. of Maryland, Baltimore (United States) and Fujian Normal Univ. (China); Peter Tomlins, Queen Mary, Univ. of London (United Kingdom); Peter Woolliams, National Physical Lab. (United Kingdom); Rebekah Drezek, Rice Univ. (United States); Anant Agrawal, U.S. Food and Drug Administration (United States); Yu Chen, Univ. of Maryland, College Park (United States)

Point spread function (PSF) phantoms based on unstructured distributions of sub-resolution particles in a transparent matrix have proven effective for evaluating resolution and its spatial variation in optical coherence tomography (OCT) systems. Measurements based on PSF phantoms have the potential to become a standard test method for consistent, objective and quantitative inter-comparison of OCT system performance. Towards this end, we have evaluated PSF phantoms based on 300-nm-diameter gold nanoshells, 1-micron-diameter iron oxide particles and 1.5-micron-diameter silica particles. The phantoms were imaged by spectral-domain, swept source and time-domain systems. Results indicate that iron oxide particles and gold nanoshells were highly effective for measuring spatial variations in the magnitude and shape of PSFs across the image volume. Mean particle concentrations on the order of 1000 per cubic mm provided optimal balance between accurate determination of performance metrics and minimization of overlap between neighboring PSFs. Significant system-to-system differences in resolution and signal intensity and their spatial variation were readily quantified. The phantoms proved useful for identification and characterization of irregularities such as astigmatism and PSF sidelobes. In this paper we discuss the utility of 3D visualization for PSF engineering as well as the development of algorithms to calculate standard performance metrics. Our multi-system study provides evidence of the effectiveness of PSF-phantom-based test methods for comparison of OCT system resolution and signal uniformity.

8573-12, Session 3

A one step vs. a multi step geometric calibration of an optical coherence tomography

Jesús Díaz Díaz, Maik Rahlves, Leibniz Univ. Hannover (Germany); Omid Majdani, Medizinische Hochschule Hannover (Germany); Eduard Reithmeier, Tobias Ortmaier, Leibniz Univ. Hannover (Germany)

In recent years, optical coherence tomography (OCT) has gained increasing interest not only as an imaging system in medicine but also as a measuring device in technical and life science applications. A major requirement for the latter is a high confidence in the validity and realness of the measurements. This contribution compares two approaches for the 3D landmark-based geometric calibration based on the identification of a parameterized grey-box OCT model. For this purpose, a one step and a multi step calibration is performed with a designed and manufactured 3D reference structure and a high-accurate 6 DoF parallel kinematic, respectively. The 3D reference structure is silicon-made and consists of an array of inverse multilevel pyramids with circular landmarks. We introduce the complete identification process beginning with a grey-box OCT model for geometric distortion correction. The theoretical framework is based on a maximum-likelihood parameter estimation finding the best suitable parameters by minimizing the error between via image processing localized (actual) and real (target) landmark coordinates in the least square sense. For evaluation purposes, common measurement errors in the field of medical surgery such as the Fiducial Registration and Localization Error are compared before and after geometric calibration. Experimental results show that both proposed methodologies reduce systematic errors by more than one order of magnitude, being the error slightly smaller for the multi step approach. These results affirm the possibility of integrating an OCT in a medical navigation system, and, due to its simplicity, the advantages of the one step calibration.

8573-13, Session 3

A quantitative evaluation of digital tissue phantoms for oximetry

David W. Allen, National Institute of Standards and Technology (United States); Ronald Xu, The Ohio State Univ. (United States); Joseph P. Rice, Maritoni Litorja, Jeeseong Hwang, National Institute of Standards and Technology (United States)

Digital tissue phantoms allow the evaluation of spectral imagers using scenes of real subjects. This enables the instrument under test to view medically relevant scenes of tissue with variable disease status. NIST has demonstrated the ability to collect hyperspectral imagery of tissue and project the scene using a hyperspectral image projector. To transition from using digital tissue phantoms as a qualitative tool to a quantitative tool, an application specific evaluation must be performed. In this work hyperspectral scenes were digitally generated with variable oxygenation levels. The ability to produce a given tissue oxygenation level and the precision with which the level can be controlled was determined. Additionally, the ability to reproduce a specific oxygenation state was determined to be well within the inherent variability of the tissue.

8573-14, Session 4

FDA regulation of in vitro diagnostic devices *(Keynote Presentation)*

Yun-Fu Hu, U.S. Food and Drug Administration (United States)

The Food and Drug Administration (FDA) regulates the sale and distribution of medical devices under a statutory and regulatory framework. This presentation will provide an overview of federal regulations of medical devices, including risk-based classifications of medical devices, and basic regulatory requirements that manufacturers, repackagers, relabelers, and/or importers of medical devices distributed in the U.S. must comply with. The basic elements that device manufacturers must include in any marketing applications to FDA for clearance or approval of in vitro diagnostic devices and the criteria that FDA uses to assess the safety and effectiveness of in vitro diagnostic devices will be described. Some examples of the issues and challenges that are discovered in the FDA review processes will be provided to help device manufacturers to better understand quality system requirements, and to design and conduct appropriate validation studies for a quicker premarket review. The mechanisms that the FDA uses to ensure the safety and effectiveness of in vitro diagnostic devices in the marketplace will also be briefly discussed.

8573-15, Session 5

Challenges and opportunities in clinical translation of fluorescence lifetime diagnostic techniques *(Invited Paper)*

Laura Marcu, Univ. of California, Davis (United States)

Fluorescence measurements can provide information about changes in the biochemical, functional and structural characteristics of fluorescent bio-molecular complexes in tissues and cells (e.g. structural proteins, enzyme metabolic co-factors, lipid components, and porphyrins). Typically, these changes are a result of either pathological transformations or therapeutic interventions. We research the development of instrumentation that utilizes label-free fluorescence lifetime contrast to detect and evaluate these molecular changes in vivo in patients and methodologies conducive to near-real time diagnosis of tissue pathologies. This presentation overviews the clinically-compatible time-resolved fluorescence spectroscopy (TRFS) and fluorescence lifetime imaging microscopy (FLIM) techniques developed in our laboratory; and studies that demonstrate the translational potential of these techniques. This includes the characterization of high-risk atherosclerotic plaques, primary brain tumors and head and neck tumors. Current results demonstrate that intrinsic fluorescence signals can provide useful contrast for diagnosis of these diseases. Challenges and solutions in the clinical implementation of these techniques are also discussed.

8573-16, Session 5

Delineation of clinical needs and device determinant parameters for oral applications of optical techniques *(Invited Paper)*

Petra Wilder-Smith, Beckman Laser Institute and Medical Clinic (United States)

The diagnostic tools that are currently available to clinicians are limited. For oral soft tissues, clinical examination and excisional biopsy remain the primary diagnostic tool. Given the often very similar appearance of many oral mucosal conditions, ranging from inflammatory or acute infectious and traumatic lesions to potentially premalignant and malignant lesions, additional diagnostic tools capable of evaluating specific biomarkers of oral mucosal disease are urgently needed. Periodontal disease spans the health of oral hard and soft tissues. Clinicians still lack tools to detect, quantify and monitor the inflammatory, vascular and other pathological processes that lead to the soft tissue attachment and bone loss caused by this condition. Oral hard tissue diagnostic needs include the evaluation of de- and remineralization processes on the tooth surface, as well as early caries detection. With the availability of effective remineralizing interventions to reverse enamel and dentine demineralization, the potential for thus avoiding caries development is limited primarily by the inability to map the mineralization status of specific tooth sites. Regenerative techniques for the dental pulp are becoming increasingly successful. Again, it is the inability to diagnose, quantify and monitor pulpal vitality that limits the widespread use of this very promising technique to avoid tooth devitalization and root canal therapy.

In this presentation, the specific design parameters and diagnostic biomarkers needed for novel diagnostic tools in the oral cavity will be defined and discussed.

8573-17, Session 5

Using multiphoton excitation for in vivo human clinical imaging: feasibility and possible applications. *(Invited Paper)*

Warren R. Zipfel, Cornell Univ. (United States)

Direct imaging of microscopic tissue morphology, pathology and metabolic state can be achieved using nonlinear imaging of intrinsic tissue fluorophores and second harmonic signals in intact tissue. UV-excitable chemotherapy agents are also easily accessible using nonlinear imaging and often lead to increased contrast of tumors and tumor borders. Possible designs of nonlinear imaging instruments for clinical applications ranges from small flexible endoscopes, to larger rigid laparoscopes, to ex vivo imaging of biopsy specimens. However, tissue autofluors are weak two-photon fluorophores and very often high laser powers are required for imaging. To design instruments targeted for these types of applications, several critical engineering parameters need to be elucidated, such levels of nonlinear excitation that are safe and sub-mutagenic, and levels of collection efficiency required to collect useable images at safe intensities. In this talk, data on typical average powers required for acquiring usable signal-to-noise imaging intrinsic tissue fluorescence images in vivo is reported and the risk potential at these intensity levels is accessed using a standard gene mutation assay. With 760 nm, 200 fs raster-scanned laser irradiation delivered through a 0.75 NA objective we found negligible mutagenicity at powers less than ~25 mW, while higher laser powers initiated a significant increase in genetic lesions.

8573-18, Session 5

Imaging of epithelial neoplasia by multiphoton autofluorescence and second harmonic generation microscopy/spectroscopy *(Invited Paper)*

Gracie Vargas, The Univ. of Texas Medical Branch (United States); Kert Edward, Univ. of the West Indies (Jamaica); Liang Ma, Suimin Qiu, Vicente Resto, Susan McCammon, The Univ. of Texas Medical Branch (United States)

In recent years there has been increased interest in the investigation of nonlinear optical microscopy toward assessment of disease and potential clinical applications due to the ability to evaluate tissues to hundreds of microns in depth at subcellular resolution and based on intrinsic signals altered by disease. Multiphoton autofluorescence microscopy (MPAM) and second harmonic generation microscopy (SHGM), for example, allow for noninvasive assessment of microstructure that may be correlated to pathologic evaluation. Additionally, they offer the ability to gain biochemical information from endogenous fluorophores altered with disease. The application of MPAM/SHGM (imaging, spectroscopy) to the

noninvasive evaluation of oral neoplasia will be discussed with aspects of study and method design.

In these studies oral mucosa is evaluated toward the goal of identifying image/spectroscopic based indicators of neoplastic transformation by nonlinear optical microscopy. MPAM/SHGM are performed on an in vivo hamster model for oral carcinogenesis and on ex vivo human tissues. Excitation wavelengths are in the 780-890 nm range and broadband emission is detected with appropriate SHG wavelength. Multiphoton microspectroscopy is performed in each layer of the oral mucosa and lamina propria. Sites are biopsied after imaging/microspectroscopy, processed for histology, and graded by a pathologist masked to imaging. Image/spectroscopic parameters are correlated to pathological grade.

Parameters based on intensity present challenges in maintaining reproducibility. Spectroscopy provides an additional avenue for reproducibility when differences are based on spectral shifts. Results show differences in morphometric and spectral features between normal and dysplasia/neoplasia making the combination promising for delineating normal from neoplastic epithelium.

8573-19, Session 5

Large field air flow visualization in the operating room to study potential sources for contaminations during surgery

Rudolf M. Verdaasdonk, Joost de Jong, Albert Van der Veen, Keith Cover, Vrije Univ. Medical Ctr. (Netherlands)

In the design of operating rooms (OR), a laminar flow of clear air is created above the field of surgery to prevent contaminations during after surgery. In a previous study, it was shown that equipment and people interfere with the ideal air flow using a special visualization technique. In this study, various air flow visualization techniques have been developed and compared to optimize for high sensitivity, large field of view and practical to be applied in a live OR setting.

The visualization techniques are based on contrast enhancement using either ‘analoge’ optical methods (Schlieren) or digital image processing methods enabling quantification of the images e.g. applying color intensity projection.

Small density gradients in air induced by e.g. temperature differences, will deflect light beams. By discriminating the deflected rays from background light using spatial filters or digital subtraction techniques, air flow can be visualized.

An enormous contrast enhancement was obtained with a classical Schlieren (CS) setup using concave mirror, however, the field of view was limited to the size of the mirror (35 cm). To enlarge the field of view, a background oriented Schlieren setup (BOS) was developed by placing a high contrast pattern (e.g. lines ~10/cm) in the background and subtracting the image before and during air flow either with a ‘analoge’ spatial filter or digitally. It was less sensitive compared to CS.

Schlieren techniques can visualize air flow enabling improvement in air flow management in the OR to prevent infection and contaminations

8573-30, Session 5

Image-guided liver surgeries using fluorescence goggle system

Yang Liu, Washington Univ. in St. Louis (United States); Walter J. Akers, Washington Univ. School of Medicine in St. Louis (United States); Gail P. Sudlow, Washington Univ. in St. Louis (United States); Kexian Liang, Samuel Achilefu, Washington Univ. School of Medicine in St. Louis (United States)

No Abstract Available

8573-20, Session 6

Photoacoustic microscopy based multimodal imaging system *(Invited Paper)*

Hao F. Zhang, Northwestern Univ. (United States); Shuliang Jiao, The Univ. of Southern California (United States)

Photoacoustic microscopy (PAM), especially optical-resolution PAM (OR-PAM), has the potential to become a mainstream microscopic tool for biomedical research. The key advantage of PAM is that it can measure the physiologically specific optical absorption properties in biological tissue, which is not available in any other existing optical microscopic modality. Moreover, by tuning the exciting optical wavelengths, PAM can achieve molecular imaging of several chromophores, such as hemoglobin oxygen saturation, without extrinsic labeling. However, the current OR-PAM mainly relies on mechanical scanning of either the sample or the optical/ultrasonic assembly during data acquisition. As a result, it is not only slow but also not compatible with other optical microscopic technologies for multimodal imaging. We developed a laser-scanning OR-PAM, which can complete a volumetric acquisition within a very short period, and further integrated it with spectral-domain optical coherence tomography (SD-OCT), fluorescence confocal microscopy, and adaptive optics for multimodal imaging based on various optical contrasts.

In the laser-scanning OR-PAM, the ultrasonic detector was kept stationary and only the laser light was raster-scanned by a two-dimensional galvanometer scanner within the field-of-view (FOV) during data acquisition. By employing the galvanometer scanning, PAM became compatible with existing optical microscopies, which permits integrating PAM with established optical technologies. In our multimodal system, a tunable dye laser system was used as the PAM and fluorescence confocal microscopy irradiation source and a superluminescent diode (SLD) was used as the SD-OCT light source. All modalities shared the same scanning and delivery optics and, therefore, images from PAM, SD-OCT, and confocal microscopy were intrinsically registered laterally.

8573-21, Session 6

Spectral variations in narrow band imaging depth-selectivity: mucosal scattering vs. hemoglobin

Quanzeng Wang, U.S. Food and Drug Administration (United States); Du Le, U.S. Food and Drug Administration (United States) and The Catholic Univ. of America (United States); Jessica Ramella-Roman, The Catholic Univ. of America (United States); Joshua Pfefer, U.S. Food and Drug Administration (United States)

Spectral variations in contrast enhancement of mucosal vasculature are a key feature of narrow band imaging (NBI) devices. In prior NBI studies, the enhanced visualization of larger, deeper vessels with green light (e.g., 540 nm) relative to violet light (e.g., 415 nm) has often been attributed to the well-known monotonic decrease in scattering coefficient with wavelength in biological tissues. We have developed and implemented numerical and experimental approaches to elucidate and quantify this and other light-tissue interaction effects relevant to NBI. A Monte Carlo model incorporating vessel-like inclusions with a range of diameters (20 to 300 microns) and depths (50 to 400 microns) was used to predict reflectance and fluence distributions in the tissue and calculate vessel contrast values. These results were compared to experimental measurements based on a liquid phantom with a hemoglobin-filled capillary. By comparing results for cases representing mucosa regions with and without blood, we were able to evaluate the relative significance of absorption and scattering on spectral variations in depth-selectivity. Results indicate that at 415 nm, detection of superficial vasculature with NBI is almost entirely dependent on the absorption coefficient of the blood in the vessel of interest. The enhanced visualization of deep vessels at 540 nm bands relative to 415 nm was due primarily to absorption by the superficial vasculature rather than a decrease in

scattering coefficient. While computationally intensive, our numerical modeling approach provides unique insights into the light propagation mechanisms underlying this emerging clinical imaging technology.

8573-22, Session 6

Biofilm formation on different stainless steel morphologies studied by hyperspectral imaging

Do-Hyun Kim, U.S. Food and Drug Administration (United States); Hanh N. D. Le, U.S. Food and Drug Administration (United States); Moon S. Kim, U.S. Dept. of Agriculture (United States); Jeeseong Hwang, National Institute of Standards and Technology (United States)

By offering high corrosion resistance and durability, stainless steel is widely used in many public health applications and products. Stainless steel devices in contact with food and medical environment are subject to internal and external contamination as well as cross contamination to the neighbor environment. Therefore, the hygienic safety level of stainless steel devices is an important area of investigation. The contaminant mainly originates from bacterial attachment which leads to biofilm development on device surfaces. Biofilm formation behavior is a customary indicator for device hygienic validation and will be discussed in our study with its different bacterial adhesion on various stainless finish morphologies. Signatures of Escherichia Coli biofilm and stainless steel configuration are collected by our macroscopic hyperspectral imaging system. Hyperspectral imaging methodology is used to distinguish similar spectra within the study region by indicating different unique peaks of each subject, thus enhancing the differentiation between bacterial signatures and various stainless steel configurations. Biofilm formation on different stainless steel morphologies is established with the study of Escherichia Coli biofilm configuration on four different stainless steel finishes including unpolished, mirror-like, fine and coarse grain-line brushed. The observation and discussion of different bacterial attachment degrees on stainless steel surfaces enhance the finding of a proper material that possesses a high hygienic safety level for public health related devices.

8573-23, Session 6

Label-free mapping and modeling of the distribution of intracellular molecules using hyperspectral microscopy

Daniel Stark, Ji Youn Lee, National Institute of Standards and Technology (United States); Fuyuki Tokumasu, National Institutes of Health (United States); Robert Chang, David W. Allen, Maritoni Litorja, Matthew Clarke, National Institute of Standards and Technology (United States); Do-Hyun Kim, U.S. Food and Drug Administration (United States); Jeeseong Hwang, National Institute of Standards and Technology (United States)

For optical imaging of endogenous biomarkers such as hemoglobin (Hb) and cytochrome, various spectroscopic imaging techniques have been developed to achieve image contrast from absorption spectra of the biomarkers. We will present a hyperspectral microscope technique and results on label-free, absorption-based hyperspectral imaging of single erythrocytes to resolve intracellular molecules including oxyHb, metHb, and hemozoin produced by a Plasmodium falciparum that causes malaria in human. We will also discuss on a cell-simulating model system with absorption standard materials towards quantitative label-free molecular imaging of disease-related endogenous biomarkers using hyperspectral imaging techniques.

8573-24, Session 6

Evaluation of shape recognition abilities for micro-lens array based optical detectors by a dedicated simulation framework

Xiaoming Jiang, Liji Cao, Wolfhard Semmler, Jörg Peter, Deutsches Krebsforschungszentrum (Germany)

Micro-lens array (MLA) based optical detector have shown to be effective optical devices which are able to capture 3D information of imaged objects from single projections. To further study their 3D object shape recognition ability - a feature that is very important for in vivo optical imaging - we have created a simulation environment using a physically based rendering code. This framework is also designed to evaluate the performance of the following shape recognition algorithms: optical flow and multi-projection surface reconstruction methods.

Instead of simple pinholes model which are used in MLA detectors, this framework simulates real physical processes of optical rays that pass through lenses and interact with the imaged object model. The commonly used DigiMouse dataset was adopted to generate image data for different detector parameters of interest (focal length, sensor pixel size and micro lens diameter). Results of this framework conform well with the depth-of-field theory. Reconstructed planar images from the set of elemental images, for which we developed an inverse mapping algorithm, show the same computational refocusing effect at different depths as is seen in acquired data.

This novel simulation framework has demonstrated to be suitable for supporting the development, evaluation and optimization of MLA based imaging systems. Both shape recognition algorithms yield comparable results corresponding to the phantom. The optical flow method reveals the relative shape of the phantom, although the spatial and depth resolution is low. The multi-projection surface reconstruction provide higher resolution data. However, the issue of concave regions arises, which needs further improvement.

8573-25, Session PSun

A novel method for MTF measurement based on resampling techniques

Zhongxing Zhou, Qingzhen Zhu, Feng Gao, Huijuan Zhao, Lixin Zhang, Tianjin Univ. (China)

The modulation transfer function (MTF) of radiographic systems is frequently evaluated by measuring the system's edge spread function (ESF) using a slightly slanted, attenuating sharp edge device. The oversampled ESF is always constructed in a very simple manner by rearranging the pixel data of N consecutive lines corresponding to a lateral shift of the edge by one pixel. A regular sub-sampling pitch is assumed for the oversampled ESF, which is given by the original pixel sampling distance divided by the integer number N. However, a lateral shift of the edge of exactly one pixel is, in general, not obtained by an integer number of lines. Therefore, the sub-sampling pitches are not uniformly distributed in the oversampled ESF. In this work, the non-uniformly distributed sub-sampling pitches are resampled into regular sub-sampling pitch before constructing the oversampled ESF. Synthetic edge images with known MTF were used as gold standards for determining the accuracy of our method. Then the edge method based on resampling techniques was then applied to images from a commercial digital x-ray system (Pixarray 100). Our method obtained more smooth Line spread function than conventional edge method. Overall, our method consistently computed MTFs which were in good agreement with the true MTF, and it provides an accurate measurement of the pre-sampled MTF for digital radiographic systems.

8573-26, Session PSun

Improving the fluorescence spectrometer sensitivity limit towards femtomolar concentrations

Manoel Veiga, Peter Kapusta, Sebastian Tannert, Felix Koberling, Matthias Patting, Marcus Sackrow, Michael Wahl, Rainer Erdmann, PicoQuant GmbH (Germany)

Detection sensitivity is a key parameter to meet today´s demand for handling smallest analyte amounts and short measurement times in the optical evaluation of pharmaceuticals and biotechnology products.

The introduction of single photon counting based data acquisition has proven to yield a major sensitivity increase and very high dynamic range - it is the ideal method for measuring weak luminescence. The achievable signal-to-noise ratio of this method is significantly higher than of methods based on analog detection. This allows for accurate quantification of extremely low concentration levels down to the femto-molar range.

In this communication we present the hardware and handling optimization of a state of the art spectrometer for steady state and time-resolved fluorescence measurements. We discuss critical components affecting the spectrometer sensitivity and present a step by step rundown of the measures needed to find optimal measurement conditions in order to reach the ultimate performance limit. Data of popular fluorescent dyes as well as the Raman spectrum of water were recorded under well defined and reproducible conditions with the goal of enabling straightforward comparison of different systems. Analyte concentrations towards the femtomolar regime were independently verified using lifetime assisted, single particle based Fluorescence Correlation Spectroscopy (FLCS).

8573-27, Session PSun

The performance evaluation of the Mach-Zehnder type full-field optical coherence imaging

Eun-Seo Choi, Joo Ha Kim, Seung Suk Lee, Chosun Univ. (Korea, Republic of)

We demonstrate the performance of fiber-based full-field optical coherence tomography(FF-OCT), which is consist of fiber based Mach-Zehnder interferometer and bulk-optic probing head. Using the fiber-based interferometer, several advantages such as compact design, fiber-based flexibility in design, and vibration-insensitive enhancement can be achieved. The designed compact head also has the merit in isolated imaging apart from the setup with easily adaptable small sized imaging probe. Fiber based interferometer can be implemented due to multi-functional optical delay line by using single fiber coupler or single fiber circulator, where optical path length is adjusted with applying phase stepping. All functions for mechanical control are given in the newly designed optical delay line. So optical head can only perform image collection without any mechanical movement. Using this proposed full-field optical coherence imaging setup, we obtain images of biological samples and non-biological samples. By analyzing the image, various property of the system such as point spread function, axial resolution, image contrast, and imaging speed was evaluated. The proposed setup can make conventional bulk-optic based FF-OCT system into portable FF-OCT system. This research was supported by Basic Science Research Program through the National Research Foundation of Korea(NRF) funded by the Ministry of Education, Science and Technology (No. 2010-0024886).

8573-28, Session PSun

Modeling near-infrared semiconductor lasers for microsurgery in stem cell studies

Meng-Mu Shih, Univ. of Florida (United States)

The microscope integrated with a laser can be utilized in the stem cell research. This compact design with the eye-safe laser inside the objective can facilitate ablation tasks in microsurgery. Semiconductor lasers with integrated gratings do not increase the device size and can improve the wavelength stability and precision to ensure the quality of microsurgery. This work demonstrates the modeling process of such lasers by using the photonic and optical methods. Numerical results show how structures and materials affect the laser. Physical interpretations of numerical results can provide insights into the modeling and design of the laser in this system.

8573-29, Session PSun

Conversion of a low cost off-the-shelf spectrometer into a broadband continuous-wave near-infrared spectrometer for deep tissue spectroscopy

Mamadou Diop, Eric Wright, Keith St. Lawrence, Lawson Health Research Institute (Canada)

Efficient light collection is critical in deep tissue spectroscopy since only a very small fraction of the injected signal emerges from the probed medium due to absorption and strong scattering of light by biological tissues. Light collection can be improved by optimizing the contact area between the detection system and the medium by means of light guides with large detection areas. Since the size of these light guides is not compatible with commercial spectrometers, which are typically equipped with a slit to improve their spectral resolution, deep tissue spectrometers are usually custom-built. However, off-the-shelf spectrometers have attractive advantages, such as low cost, small foot-print and availability, compared to custom-made units. Here we show that simple modifications to an off-the-shelf spectrometer (QE65000 from Ocean Optics) can make it suitable for deep tissue spectroscopy. The noise, spectral resolution and stability of the modified instrument were characterized and compared to a custom-built unit specifically designed for deep tissue spectroscopy. The average readout noise was found to be 1.2 counts/pixel which is comparable to the specification of the manufacturer (1.5 counts/pixel). The gain of the spectrometer was approximately 22.702 per electron and the dark electron accumulation rate was ~16 electrons/pixel at -20ºC. The spectral resolution and stability of the modified spectrometer were comparable to the values obtained with the custom-built unit. We also present in vivo measurements acquired simultaneously with the two spectrometers in a piglet model of newborn.

8573-31, Session PSun

Surgical oncology aided by fluorescence goggle system

Yang Liu, Washington Univ., St. Louis (United States); Walter J. Akers, Adam Q. Bauer, Washington Univ. School of Medicine in St. Louis (United States); Gail P. Sudlow, Washington Univ. in St. Louis (United States); Kexian Liang, Joseph P. Culver, Samuel Achilefu, Washington Univ. School of Medicine in St. Louis (United States)

No Abstract Available

8574-1, Session 1

Time resolved optical tomography locates fluorescent targets in a turbid medium

Binlin Wu, Wei Cai, Swapan K. Gayen, The City College of New York (United States)

We introduce a fluorescence optical tomography approach to locate targets embedded in a turbid medium. The approach extends time reversal optical tomography (TROT) to fluorescent signals. TROT uses a multi-source illumination and multi-detector signal acquisition scheme, along with TR matrix formalism, and multiple signal classification (MUSIC) to construct pseudo-image of the targets. The samples consisting of a single or two Indocyanine Green filled tubes as targets embedded in a 250 mm X 250 mm X 60 mm rectangular cell of Intralipid-20% suspension as the scattering medium were step scanned across the 790-nm excitation beam to realize multi-source probing. The ICG concentration was 1μM, and the Intralipid-20% concentration was adjusted to provide ~ 1-mm transport length for both excitation and fluorescence wavelengths. The data matrix was constructed using the diffusely transmitted fluorescence signals for all scan positions, and the TR matrix was constructed by multiplying data matrix with its transpose. A pseudo spectrum was calculated using the signal subspace of the TR matrix. Tomographic images were generated using the pseudo spectrum. The peaks in the pseudo images provided locations of the target(s) with sub-millimeter accuracy. Concurrent transmission TROT measurements corroborated fluorescence-TROT findings. The results demonstrate that TROT is a fast approach that can be used to obtain accurate three-dimensional position information of fluorescence targets embedded deep inside a highly scattering medium, such as, contrast-enhanced tumor in a human breast.

The research is supported in part by US Army Medical Research and Materiel Command under Contract Number W81XWH-07-1-0454.

8574-2, Session 1

Synchromodal optical in vivo imaging employing micro-lens-array optics: a complete framework

Jörg Peter, Deutsches Krebsforschungszentrum (Germany)

A novel concept and complete mathematical framework for in vivo optical imaging comprising bioluminescence imaging (BLI) and fluorescence imaging and tomography (FI/FT) is presented in which optical data is acquired in synchromodal (i.e. fully simultaneous) operation with secondary imaging modalities (SIM) such as positron emission tomography (PET). Technical realization thereof is accomplished by means of a per-SIM-compatible micro-lens-array (MLA) based light detector resembling a plenoptic-type camera. A multitude of such detectors, various excitation and illumination light-sources for multispectral imaging, emission filters, etc., as well as a complete mechanical gantry including actuators for independent detector and light source positioning is housed in a cylindrical enclosure, sized to be insertable within the target's SIM field-of-view. A complete multimodal operation framework has been developed and is implemented in which reconstructed tomographic data of any modality can be used as a priori information for finding the imaged object's 3D surface (gradient vector flow algorithm). Surface-controlled inverse mapping is performed to calculate and fuse the emission light map (BLI, FI) with the boundary of the imaged object. Triangulation and optical reconstruction (FT) or constrained flow estimation (BLI), both including the use of SIM priors, is performed to estimate the internal 3D emission light distribution. Even though the instrumentation concept and the complete implementation of mathematical procedures follows a 'single button' operation strategy, the mathematical framework is susceptible to a number of variables controlling convergence and computational speed. Experimental data are presented for synchromodal BLI-PET imaging.

8574-3, Session 1

Toward ideal imaging geometry for recovery independence in fluorescence molecular tomography

Robert W. Holt, Dartmouth College (United States); Frederic Leblond, Brian W. Pogue, Thayer School of Engineering at Dartmouth (United States)

One of the established challenges with fluorescence molecular tomography is the inconsistent quantification accuracy of recovered fluorescent contrasts with changing target depth. This work examines the optimization of source and detector placement as a means of recovering consistent contrast regardless of imaging depth. Established methods have typically relied on pure noise processing, spatially varying regularization, or examining linear combinations of data to produce uniform sensitivity. Here, a simulation study is performed to examine purely in a geometrical sense which distributions of optical projection measurements result in a uniform sensitivity function, as well as what projection angles are the most important for accurate and consistent target recovery as a function of depth. The capability of the ideal geometries to accurately recover fluorescent distributions is compared with that of established imaging geometries with respect to consistent size and contrast accuracy metrics. It is shown that full tomographic data is unnecessary (and possibly harmful) for accurate recovery of contrasts. In addition, it is emphasized that densely sampled data sets contain a great deal of redundant information and needlessly make a larger inverse problem. It is shown that intelligently sampling the possible field of data is more important than simultaneously utilizing as much data as possible.

8574-4, Session 1

A novel high-resolution optical imaging modality: photo-magnetic Imaging

Alex Luk, David Thayer, Yuting Lin, Univ. of California, Irvine (United States); Hao Gao, Emory Univ. (United States); Gultekin Gulsen, Univ. of California, Irvine (United States)

Introduction: Here, we introduce an entirely new imaging technique termed Photo-Magnetic Imaging (PMI), which overcomes the limitation of pure optical imaging and provides optical absorption images at MRI spatial resolution. PMI uses laser light to heat the medium under investigation but employs MR thermometry for the determination of spatially resolved optical absorption in the probed medium.

Methods: During PMI measurements, four 800nm CW lasers (1W) are used to simultaneously illuminate the medium from multiple views and heat for approximately 30 seconds inside the MRI. The temperature variation due to the laser heating is directly proportional to the local optical photon density and the local absorption coefficient. Dynamic MR phase maps are obtained before, during and after heating to monitor spatially and temporally varying temperature increase. We have successfully performed PMI using agar phantom and chicken breast samples under the ANSI limit. Currently, we are undertaking studies to show the performance of PMI in vivo.

Results: We have developed a FEM-based PMI inverse solver that reconstructs quantitative absorption images from the measured MRI maps. Inclusions located 1.5cm deep with target to background absorption contrast ratio of four to eight have been successfully resolved and their absorption coefficients are recovered with less than 10% error.

Conclusion: PMI has shown the ability to recover optical absorption at MR resolution by modeling photon migration and heat diffusion in tissue. Utilizing multiple wavelengths, PMI imaging can potentially provide the same functional information as diffuse optical imaging or PAT, but at MRI resolution in thick tissue. A FEM-based PMI inverse solver has

been developed by modeling photon migration and heat diffusion in tissue to reconstruct quantitative absorption images from the measured MRI maps. We have successfully performed PMI using agar phantom and chicken breast samples under the ANSI limit. Currently, we are undertaking studies to show the performance of PMI in vivo.

8574-5, Session 1

Design of a rotational ultrasound guided diffuse optical tomography system for whole breast imaging

Zixin Deng, Yuting Lin, Kenji Ikemura, Po-jung M. Tseng, Yu-wen Chang, Gultekin Gulsen, Univ. of California, Irvine (United States)

This study focuses on a multimodal imaging technique that integrates both structural and functional information using a priori ultrasound (US) information to assist near-infrared (NIR) diffuse optical tomography (DOT). Up to date, hand-held systems that integrates DOT and US have been demonstrated. Our system is designed to be fully-automated and non-contact. Our aim is to built an interface, in which the optical source and detector fibers will rotate around the breast together with the US transducer. However, in this study we built a prototype system which rotated the phantom and kept the transducers stationary for simplicity. Simulation and experimental studies were performed using a variety of source-detector configurations. The reconstruction results were compared with and without US a priori information. To collect the a priori US information, the multi-modality agar phantom was rotated 360° using a computer controlled rotational stage. The multi-modality phantom had an inclusion that had both optical absorption and US contrast. 360 US images were collected in 1° increments covering the entire phantom volume. The DOT data was also collected while the phantom is rotated with particular source-detector configurations. These results have shown that when the detectors were π /8 apart, and the phantom is rotating at π /16 increments with a total of 32 views provides the optimum image reconstruction. As expected, US a priori information further improved the quantification accuracy.

8574-6, Session 1

Simultaneous multimodal microscopy for head and neck tissue identification

Etienne De Montigny, Nadir Goulamhoussen, Ecole Polytechnique de Montréal (Canada); Mathias Strupler, Sainte-Justine Mother and Child Univ. Hospital Ctr. (Canada) and Ecole Polytechnique de Montréal (Canada); Caroline Boudoux, Ecole Polytechnique de Montréal (Canada) and Sainte Justine Univ. Hospital Ctr. (Canada)

Thyroid pathologies are the most common malignancies of the endocrine system. Treatment usually involves careful resection of the diseased gland, but complications may occur when parathyroid glands are accidentally removed or damaged. To facilitate tissue identification during surgery, we propose the use of an optical instrument compatible with endoscopy combining confocal microcopy and optical coherence tomography (OCT). Confocal microscopy provides a large magnification with sub-cellular information similar to histology, while OCT can act as a guiding tool with its larger field of view and penetration depth.

We have previously shown the possibility of performing multimodal imaging based on a dual-band wavelength-swept laser (centered at 780nm and 1310nm) allowing co-registered spectrally encoded confocal microscopy (SECM) and swept-source optical coherence tomography. To improve contrast and selectivity in identifying the structures in the head and neck area, near-infrared fluorescence imaging was integrated into the system, as recent literature has shown that major head and neck tissues exhibit some autofluorescence at 785nm (Paras et al, JBO, 2011).

A C++ acquisition platform allows acquisition rates up to 125MS/s and real-time simultaneous display of all modalities. The spectral bandwidth of our laser (35 nm at 780 nm and 90 nm at 1310 nm) allows for 1200 resolvable points in SECM and an axial resolution of 15µm in OCT . Identification of head and neck structures is facilitated by the orthogonal field of views and different magnifications and by the added contrast provided by the autofluorescence of parathyroid.

8574-7, Session 2

TBD *(Invited Paper)*

No Abstract Available

8574-8, Session 2

Static and quasi-static elastography adding contrast to full-field optical coherence tomography

Amir Nahas, Institut Langevin (France) and LLTECH SAS (France); Stéphane Roux, Ecole Normale Supérieure de Cachan (France); A. Claude Boccara, Institut Langevin (France) and LLTECH SAS (France)

Organs structures, tissues and cells are characterized by their intrinsic mechanical properties. Moreover, the mechanical properties of cells are related to their structure and function: changes in those properties can reflect cellular healthy or pathological states. Adding this contrast to morphological images is a powerful help for diagnosis. In this study we add the elastographic contrast to the Full-Field OCT (FF-OCT) modality. FF-OCT is able to image biological tissues in-depth and in 3D with a micrometerresolution. By combining it with elastography, we recreate a “virtual palpation” map at the scale given by FF-OCT.Our custom FF-OCT setup includes an elastography system that creates various levels of compression on the sample. We present in this study two methods for retrieving the elasticity map, one static and one quasi-static. In the first static method we record a 3D image of the sample before and after compression, then we calculate 3D cross-correlation between the two stacks of images. By doing so, we have access to a 3D map of displacements and stiffness. The second quasi-static method is a novel method we have developed, in which we have direct access to the local displacement map without any cross-correlation calculation. The sample is submitted to low-amplitude periodical compression, and from a similar 4 phases modulation method we use in classical FF-OCT imaging, we are able to retrieve the local phase map modulation directly related to the local displacement. Those methods provide a relative value of the local elastic properties along the compression axis.

8574-9, Session 2

in vivo monitoring of laser wound healing in the mouse cornea with two-photon microscopy

Jun Ho Lee, Changho Seo, Dongsik Kim, Pohang Univ. of Science and Technology (Korea, Republic of); Ho Sik Hwang, Choun Ki Joo, Seoul St. Marys Hospital (Korea, Republic of); Ki Hean Kim, Pohang Univ. of Science and Technology (Korea, Republic of)

Transparent cornea allows to image immune reaction. Lymphatic vessels, which are related to immune mechanism of mouse eye, are located widely in conjunctiva which encloses cornea. Wound healing process is one of the immune reaction processes of the cornea. Corneal wound healing process mechanism is already researched in previous study and also immune cell dynamics in corneal lymphatic vessels did. We want to image this under in-vivo state imaging through wound healing process of cornea. We induced inflammation to cornea by using femtosecond laser rather than suture what previous study already used because laser

surgery is popular in the corneal refractive surgery in now days. We used a mouse for this experiment. We made our custom two-photon microscope (TPM) to image and ablate the mouse cornea. We set up TPM and femtosecond laser ablation system. Customized mouse holder was made to hold the mouse eye during TPM imaging. Mouse is anesthetized using isoflurane and labeled the lymphatic vessel which is located near the cornea using ALEXA 488 dye. We ablate the cornea of mouse eye by using Ti-Sapphire laser to induce inflammation. We will Image the inflamed corneal tissue in vivo by using TPM on regular period and immune procedure in the cornea after corneal laser induced ablation. Therefore, we will apply TPM to visualize for migration of immune cell in inflamed corneal tissues during corneal wound healing in order to understand the biological process and to optimize the laser surgical parameters.

8574-10, Session 2

Optical design of a compound lens satisfying both optical coherence tomography and confocal microscopy constrains

Mathias Strupler, Ecole Polytechnique de Montréal (Canada) and Sainte Justine Hospital Research Ctr. (Canada); Etienne De Montigny, Ecole Polytechnique de Montréal (Canada); Caroline Boudoux, Ecole Polytechnique de Montréal (Canada) and Sainte Justine Hospital Research Ctr. (Canada)

To achieve virtual biopsies using optical imaging, a possible solution involves combining a large scale imaging modality to localize structures and a subcellular resolution modality to perform diagnoses. We believe that optical coherence tomography (OCT) and confocal microscopy (CM) could be used in combination to achieve this goal. Indeed, OCT can acquire large volumes (mm x mm x mm) but with a resolution limited to about 10 ?m, whereas CM has a subcellular resolution but is limited to a smaller field of view (FOV). However, OCT is performed using small numerical aperture (NA) telecentric scan lenses and CM uses high NA microscope objectives. We propose the design of a compound lens capable of accommodating both modalities simultaneously in a handheld probe.

Our compound lens is designed for an OCT system working at 1250-1350 nm and a CM system at 770-870 nm. We minimized the number of lens to two cemented achromatic doublets to increase the design manufacturability and decrease potentially detrimental back reflections. The design was optimized to be image telecentric for OCT and achromatic for the CM wavelength band. A glass window was also inserted to create a contact probe with a CM focus depth that can be changed from 0 to 0.5 mm. For lenses diameter of 8 mm, we achieved an OCT FOV >3 mm and a CM FOV >300 ?m with a NA >0.3. Future work will consist in machining the lens and in its integration in a sub-cm diameter handheld probe.

8574-11, Session 2

Integrated laser scanning photoacoustic and confocal microscopy for real-time imaging

Sang-Won Lee, Joo Hyun Park, Jae Yong Lee, Eun Seong Lee, Korea Research Institute of Standards and Science (Korea, Republic of)

Optical resolution photoacoustic microscopy (OR-PAM) can obtain noninvasive and in-vivo images with sub-micrometer resolution using optical absorption in confocal region. Recently, OR-PAM has been integrated with other optical imaging modalities based on optical scattering such as optical coherence tomography (OCT) and fluorescence confocal microscopy (FCM). However, most of OR-PAM had to need long acquisition time (from dozens of seconds to several hours) because of using a nanosecond pulsed laser with a slow repetition rate (10 Hz ~ 20 kHz). In this study, we constructed a dual-modality imaging system, which was integrated with OR-PAM and confocal microscopy. To provide real-time OR-PAM, we used a nanosecond pulsed Ytterbium fiber laser with an adjustable repetition rate (50 kHz ~ 600 kHz) at 532 nm. In addition, a CW argon laser at 633 nm was used for confocal microscopy. Lights merged by a dichroic mirror were scanned by 2D galvanometer mirrors. Scanned lights were focused and incident into the specimen via an objective lens with 0.4 NA. A 50 MHz ultrasound transducer and a photomultiplier tube (PMT) were used to detect the PA waves and optical signal, respectively. We could obtain simultaneous OR-PAM and confocal images with the real-time display speed of 1.1 fps at the repetition rate of 300 kHz. At that time, the image size was 512 x 512 pixels.

8574-12, Session 3

Using multimodal imaging techniques to monitor limb ischemia: a rapid noninvasive method for assessing extremity wounds

Rajiv Luthra, Naval Medical Research Ctr. (United States); Nicole J. Crane, Naval Medical Research Ctr. (United States) and Uniformed Services Univ. of the Health Sciences (United States); Jonathan Forsberg, Naval Medical Research Ctr. (United States) and Uniformed Services Univ. of the Health Sciences (United States) and Department of Orthopedics and Rehabilitation, Walter Reed National Military Medical Center, Bethesda (United States); Eric A. Elster, Naval Medical Research Ctr. (United States)

Almost 70% of military casualties resulting from Operation Iraqi Freedom (OIF) and Operation Enduring Freedom (OEF) were recorded as involving major limb injury. Of these, 90% were caused by blast injuries from improvised explosive devices (IEDs). Soldiers face traumatic amputations, open fractures, crush injuries, and acute vascular disruption. Ischemia is a major concern, as lack of blood flow to tissues leads to tissue deoxygenation and necrosis. If left unaddressed, a potentially salvageable limb may require amputation. Often, due to complications, the wound healing process is protracted, involving a series of debridements. During a debridement, surgeons visually inspect tissue and subjectively determine whether it is necrotic and requires removal. To minimize the number of debridements necessary, the need for an accurate and objective method for determining wound healing is evident.

In this study, our goal is to integrate two non-invasive, rapid, and low-cost techniques to develop an objective and quantitative model of wound perfusion and tissue viability. Integrating thermal and 3-charge coupled device (3-CCD) imaging techniques allows us to visually and quantitatively identify and track regions of tissue oxygenation and perfusion as they change in real time. To simulate the different types of injuries sustained by soldiers, two methods are used in a swine limb ischemia model: direct occlusion of the iliac vessels and pneumatic tourniqueting of the hind limb. Data collected from this study gives both a surface indication of tissue oxygenation as well as overall limb perfusion. The combined data analysis provides a more complete indication of tissue health.

This study aims to not only increase fundamental understanding of the processes involved with limb ischemia and reperfusion, but also develop tools to monitor overall limb perfusion and tissue oxygenation in a clinical setting. A rapid, objective diagnostic for extent of ischemic damage and overall limb viability could provide surgeons with a more accurate indication of optimized timing for wound closure. Reducing the number of surgical interventions required has the obvious benefits of reducing patient distress and decreasing both the overall recovery time and cost of rehabilitation.

8574-13, Session 3

TBD *(Invited Paper)*

No Abstract Available

8574-14, Session 3

Elasticity image analysis of optical-based tactile system used for breast tumor characterization

Jong-Ha Lee, Samsung Advanced Institute of Technology (Korea, Republic of); Chang-Hee Won, Temple Univ. (United States)

Elasticity is an important indicator of tissue health, with increased stiffness pointing to an increased risk of cancer. We investigate a tissue elasticity estimation method for application in early breast cancer screening. The estimation is performed through the analysis of elasticity images obtained by an optical-based tactile system. The system operates based on the total internal reflection principle. Near-infrared light is injected into the sensing probe of the system to allow for total reflection. If a tumor is embedded in tissue, when the system is compressed against the tissue, the trapped light in the sensing probe is scattered. The scattered light is captured by a high resolution camera. To estimate tissue stiffness by analyzing the captured elasticity image, 3-D finite element modeling based forward algorithm and scaled conjugate gradient based inversion algorithm are employed. The forward algorithm is used to extract three kinds of features (texture, morphological, and Fourier description-based features) from the image over different tissue stiffness values. Then, the stepwise regression method is applied to select an optimal subset of features. In the inversion algorithm, the mapping model between selected image features and tumor stiffness values is designed using forward algorithm results. From the generated mapping model, we estimate the tissue stiffness value from the newly obtained elasticity image. The proposed method has been validated in laboratory experiments on breast tissue models and in an ongoing clinical study. The obtained results prove that the proposed method has potential to become a screening and diagnostic method for breast cancer.

8574-15, Session 3

Multimodal tissue perfusion imaging using multi-spectral and thermographic imaging systems applied on clinical data

John H. Klaessens, Martin Nelisse, Univ. Medical Ctr. Utrecht (Netherlands); Rudolf M. Verdaasdonk, Vrije Univ. Medical Ctr. (Netherlands); Herke Jan Noordmans, Univ. Medical Ctr. Utrecht (Netherlands)

Clinical interventions influence tissue perfusion resulting in local oxygenation or temperature changes. Real-time imaging of these effects provides useful information to determine the surgical strategy or the understanding of physiological regulation mechanisms. Two non-contact large field perfusion imaging methods were tested using a LED based multispectral imaging (MSI, 17 narrow band wavelengths 370 nm-880 nm) and thermal imaging for stationary and dynamic applications.

From the MSI images at particular wavelengths, the oxygenation concentration changes were calculated comparing different analyzing methods based on either wavelength or time ratios. .

The choice of wavelengths, for hemoglobin concentration calculations was predetermined in laboratory conditions before being applied in clinical studies. In addition corrections were necessary for interferences during the clinical registrations (OR light fluctuations, tissue movements).

The multispectral and thermal imaging systems were clinically applied to observe perfusion change for (a) the reperfusion after tissue flap transplantation (ENT), (b) the effectiveness of local anesthetic block and (c) the localization of an epileptic center on the cortex during brain surgery. The multispectral imaging system clearly showed the dynamical changes of perfusion/oxygenation during clinical interventions. Thermal imaging showed the local heat distributions over tissue areas due to perfusion changes. Multispectral imaging and thermal imaging provide complementary information and are promising techniques for real-time diagnostics of physiological processes in medicine.

8574-23, Session PSun

Towards diffuse optical tomography of arbitrarily heterogeneous turbid medium using GPU-accelerated Monte-Carlo forward calculation

Xi Yi, Weiting Chen, Linhui Wu, Wei Zhang, Jiao Li, Xin Wang, Liming Zhang, Feng Gao, Tianjin Univ. (China)

At present, the most widely accepted forward model in diffuse optical tomography (DOT) is the diffusion equation, which is derived from the radiative transfer equation by employing the P1 approximation. However, due to its validity restricted to highly scattering regions, this model has several limitations for the whole-body imaging of small-animals, where some cavity and low scattering areas exist. To overcome the difficulty, we presented a Graphic-Processing-Unit (GPU) implementation of Monte-Carlo (MC) modeling for photon migration in arbitrarily heterogeneous turbid medium, and, based on this GPU-accelerated MC forward calculation, developed a fast, universal DOT image reconstruction algorithm. We experimentally validated the proposed method using a continuous-wave DOT system in photon-counting mode and a cylindrical phantom with a cavity inclusion.

8574-24, Session PSun

Dynamic fluorescence diffuse tomography methodology for imaging pharmacokinetic-rates of indocyanine green in small animal

Xin Wang, Xi Yi, Linhui Wu, Jiao Li, Liming Zhang, Wei Zhang, Feng Gao, Tianjin Univ. (China)

Related to the morphological differences in the vascularization between healthy and diseased tissues, pharmacokinetic-rate images of indocyanine green (ICG) can provide diagnostic information for tumor differentiation, and especially have the potential for differentiation and staging of tumors. To acquire pharmacokinetic-rate images, we firstly develop a dynamic fluorescence diffuse tomography method to acquire a time-course of the ICG concentration image from the measured boundary flux of the excitation and fluorescence at different moments. Then, the pharmacokinetic-rate images are estimated using an extended Kalman filter framework based on a two-compartment model composed of plasma and extracelluar-extravascular space (EES). Finally, to optimally evaluate the performance of the proposed methodology, the metabolic processes of ICG in mouse is dynamically simulated with a digimouse model. The results suggest that the methodology can obtain the pharmacokinetic-rate images of indocyanine green in mouse with a good robustness.

8574-25, Session PSun

Color intensity projections with hue cycling for intuitive and compressed presentation of motion in medical imaging modalities

Keith S. Cover, Frank J. Lagerwaard, Rudolf M. Verdaasdonk, Vrije Univ. Medical Ctr. (Netherlands)

Color intensity projections (CIPs) has been employed to improve the accuracy and reduce the workload of interpreting a series of grayscale images by summarizing the grayscale images in a single color image. CIPs – which has been applied to grayscale images in angiography, 4D CT, nuclear medicine and astronomy – uses the hue, saturation and brightness of the color image to encode the summary information. In CIPs, when a pixel has the same value over the grayscale images, the corresponding pixel in the color image has the identical grayscale color. The arrival time of a signal at each pixel, such as the arrival time of

contrast in angiography, is often encoded in the hue (red-yellow-green-light blue-blue-purple) of the corresponding pixel in the color image. In addition, the saturation and brightness of each pixel in the color image encodes the amplitude range and amplitude maximum of the corresponding pixel in the grayscale images. In previous applications of CIPs the hue has been limited to less than one cycle over the color image to avoid the aliasing due to a hue corresponding to more than one arrival time. However, sometimes in applications such as angiography and astronomy, in some instances the aliasing due to increasing the number of cycles of hue over the color image is tolerable as it increases the resolution of arrival time. Key to applying hue cycling effectively is interpolating several grayscale images between each pair of grayscale images. Ideally, the interpreter is allowed to adjust the amount of hue cycling in realtime to find the best setting for each particular CIPs image. CIPs with hue cycling should be a valuable tool in many fields where interpreting a series of grayscale images is required.

8574-26, Session PSun

Comparison of brain-related, systemic physiological, and instrumentation noise during a test-retest study of brain responses with concurrent MRI and NIRS

Theodore J. Huppert, Jeffrey W. Barker, Ardalan Aarabi, Univ. of Pittsburgh Medical Ctr. (United States)

Introduction

Brain imaging data is sensitive to biases from instrument related measurement noise, systemic physiology and from other factors affecting the magnitude of the brain response, such as intake of caffeine. In this study, 60 subjects were scanned in two or three sessions separated by 3-4 or 6-9months using concurrent MRI and NIRS. The purpose of this study was to quantify the variations in brain responses using concurrent multimodal information to distinguish physiological and measurement (e.g. modality-specific) sources of error in the estimation of brain activity.

Methods

A bilateral NIRS head cap containing sensors for both a continuous wave (TechEn CW6) and a frequency-domain (ISS; Imagent) NIRS system was used to record brain activity during median nerve stimulation during a concurrent 3T MRI scan. MR images of baseline blood flow and oxygen saturation were recorded using a pulsed arterial spin labeling (ASL) and a quantitative-BOLD (QBOLD) imaging technique. A 5% CO2 hypercapnia challenge was used in a subset of the participants to provide calibration of the MRI signal.

Results

We found that approximately 65-78% of the temporal variance of the fMRI signal is shared with fluctuations observed in the NIRS. Only about 21-25% of the variance in the BOLD signal can be directly attributed to systemic physiology. The remaining approximately 45% of the variance is related to single-trial variability in the brain response and background oscillations.

Conclusion.

We believe that this is the first large-scale study to quantitatively compare the sensitivity and systematic errors between fMRI and NIRS imaging methods.

8574-27, Session PSun

Multimodal tissue diagnostic technique combining fluorescence lifetime imaging (FLIm), ultrasound backscatter microscopy (UBM) and photoacoustic imaging (PAI): design and in vivo validation in a hamster oral carcinoma model

Feifei Zhou, Yang Sun, Hussain Fatakdawala, Hussain Fatakdawala, Abhijit J. Chaudhari, Julien Bec, Jing Liu, Diego Yankelevich, Univ. of California, Davis (United States); Shannon Poti, Steve P. Tinling, Gregory D. Farwell, Regina F. Gandour-Edwards, UC Davis Medical Ctr. (United States); Laura Marcu, Univ. of California, Davis (United States)

We report a multimodal imaging technique for characterization and diagnosis of oral carcinoma. The experimental apparatus integrates in a compact (6.5 mm total diameter at the distal end) scanning probe three detection channels: 2D fluorescence lifetime imaging (FLIm) sensitive to superficial molecular changes using a single silica fiber (600 ?m core diameter; 100?200 ?m image pixel size), ultrasonic backscatter microscopy (UBM) for assessment of the 3D tumor microanatomy using a single element ultrasonic transducer (41 MHz center frequency, 65 ?m and 37 ?m lateral/axial resolution), and 3D photoacoustic imaging (PAI) for functional imaging associated with optical absorption contrast (ultrasonic detection pathway shared with UBM, excitation at 532 nm by 16 plastic optical fibers 500 ?m core diameter tilted to generate a dark field illumination excitation). Experiments were conducted in a hamster oral carcinoma model (9 animals). Current results demonstrate the ability of this technique to provide co-registered and complementary information related to 1) the tissue biochemical features (collagen and NADH composition) at the tissue surface detected by FLIm with 2) the underlying tissue microstructure to >4 mm depth detected by UBM and with 3) the tissue blood vessels (capillaries) distribution within tissue volume detected by PAI. Current findings suggest the potential of this multimodal implementation for enhanced analysis of diagnosis of oral carcinoma.

8574-28, Session PSun

Simulation of action-potential-sensitive second harmonic generation response of unmyelinated afferents to temperature effects

Xinguang Chen, Zhihui Luo, Hongqin Yang, An Zhang, Shusen Xie, Fujian Normal Univ. (China)

In this paper, we studied the effects of temperature on the propagation properties of action potential on unmyelinated afferents by action-potential-sensitive second harmonic generation (SHG). A mathematical model was presented which combining with SHG imaging to study the action potential properties in an unmylinated fiber affected by temperature. The results showed that the action potential propagation along an unmyelinated fiber was sensitively probed by optical SHG imaging in real time. Meanwhile, the action potential properties on an unmyelinated fiber is obviously changed at innocuous temperatures through analyzing the changes of action-potential-sensitive SHG signals, including the increase of conduction velocity and the decrease of duration at higher temperatures. Our study indicates that optical second harmonic generation imaging may be a potential tool to investigate the underlying mechanisms of complex physiological phenomena such as nerve excitation.

8574-29, Session PSun

An optical 3D model construction system for medical imaging

Arezoo Movaghar, Reza Safabakhsh, Khosro Madanipour, Amirkabir Univ. of Technology (Iran, Islamic Republic of)

No Abstract Available

8574-16, Session 4

Diagnosing breast cancer using independent diffuse optical tomography and x-ray mammography scans

Maxim Fradkin, Jean-Michel Rouet, Philips France (France); Richard H. Moore, Daniel B. Kopans, Massachusetts General Hospital (United States); Keith Tipton, Sankar Suryanarayanan, Philips Healthcare, N.A. (United States); David A. Boas, Qianqian Fang, Massachusetts General Hospital (United States)

We have previously demonstrated the utilization of spatially co-registered diffuse optical tomography (DOT) and digital breast tomosynthesis (DBT) for joint breast cancer diagnosis. However, clinical implementation of such multi-modality approach may require development of integrated DOT/DBT imaging scanners, which can be costly and time consuming. Exploring effective image registration methods that combine the diagnostic information from a standalone DOT measurement and a separate mammogram can be a cost-effective solution, which may eventually enable adding functional optical assessment to all previously installed digital mammography systems.

In this study, we investigate a contour-based image registration method to convert independent optical and x-ray scans into co-registered datasets that can benefit from a joint image analysis. For the optical-alone scan, we utilize a low-cost camera to recovery breast surface and spatial landmarks by running a multi-view photogrammetry analysis. The reconstructed breast surface is used to register the breast contour extracted from an x-ray mammogram acquired separately. Applying the transformation yielded from the registration, we map the 2D mammogram to the optical measurement space and build structural constraints for optical image reconstruction. A non-linear reconstruction utilizing the structure-priors is then performed to generate hemoglobin maps with improved resolution. To validate this approach, we used a set of patient measurements with simultaneous DOT/DBT and a separate 2D mammographic scan. The images recovered from the registration procedure derived from DOT and 2D mammogram present similar image quality compared to those recovered from co-registered DOT/DBT measurements.

8574-17, Session 4

A dual oxygenation and fluorescence imaging platform for reconstructive surgery

Yoshitomo Ashitate, John N. Nguyen, Vivek Venugopal, Alan Stockdale, Florin Neacsu, Frank Kettenring, Bernard T. Lee, John V. Frangioni, Sylvain Gioux, Beth Israel Deaconess Medical Ctr. (United States)

There is a pressing clinical need to provide image guidance during surgery. Currently, assessment of tissue that needs to be resected or avoided is performed subjectively leading to a large number of failures, patient morbidity and increased healthcare costs. Because near-infrared (NIR) optical imaging is safe, noncontact, inexpensive, and can provide relatively deep information (several mm), it offers unparalleled capabilities for providing image guidance during surgery. These capabilities are well illustrated through the clinical translation of fluorescence imaging during oncologic surgery.

In this work, we introduce a novel imaging platform that combines two complementary NIR optical modalities: oxygenation imaging and fluorescence imaging. We validated this platform during facial reconstructive surgery on large animals approaching the size of humans. We demonstrate that NIR fluorescence imaging provides identification of perforator arteries, assesses arterial perfusion, and can detect thrombosis, while oxygenation imaging permits the passive monitoring of tissue vital status, as well as the detection and origin of vascular compromise simultaneously. Together, the two methods provide a comprehensive approach to identifying problems and intervening in real time during surgery before irreparable damage occurs.

Taken together, this novel platform provides fully integrated and clinically friendly endogenous and exogenous NIR optical imaging for improved image-guided intervention during surgery.

8574-18, Session 4

Multimodal investigation of neural-vascular coupling during somatosensory stimulation and resting state using concurrent MEG-NIRS and MRI-NIRS

Theodore J. Huppert, Avniel Ghuman, Univ. of Pittsburgh Medical Ctr. (United States)

Introduction

In this study, multi-channel functional near-infrared spectroscopy (NIRS) signals were recorded from the primary and secondary somatosensory cortex during concurrent magnetoencephalography (MEG) and functional MRI. A pulsed-pair median nerve stimulus was used to probe the relationships of the neural and vascular responses. Concurrent neural and vascular data was recorded during resting state fluctuations.

Methods

A total of 15 subjects were scanned on two sessions with concurrent MEG-NIRS and fMRI-NIRS at 3T. A pulsed pair median nerve stimulus was used with inter-pulse intervals between 50ms-2000ms were used to probe the dynamics of the neural refractory period during unilateral stimulation. In a separate study, 10 subjects were scanned during resting state while fixating on a cross-hair using MEG-NIRS and during a concurrent 7T MRI-NIRS scan. These subjects were also scanned at 3T for anatomical and diffusion tensor MRI tractography.

Results

Concurrent NIRS-MEG and NIRS-MRI showed similar activation areas within S1. Both MEG and MRI showed additional activations within the secondary sensory area (S2), which was below the spatial resolution of NIRS. Regions-of-interest from the area of S1 were examined as a function of the inter-pulse interval. The NIRS and MRI data both showed a U-shaped response profile indicating a minima in the response at 75-150ms corresponding to the neural refractory period. The ratio of the amplitude of the second to first pulse measured via MEG showed a similar response profile.

Conclusion.

Concurrent MEG-NIRS and MRI-NIRS results show tight coupling of the neural and vascular signals.

8574-19, Session 4

A device for multimodal imaging of skin

Janis Spigulis, Univ. of Latvia (Latvia); Valerijs Garancis, Telemedica, SIA (Latvia); Uldis Rubins, Eriks Zaharans, Janis Zaharans, Liene Elste, Univ. of Latvia (Latvia)

A prototype device for multimodal imaging of skin for improved diagnostics has been developed. Using a single CMOS image sensor, the skin area of diameter 30mm is examined by four consecutive image/

video measurement cycles:

(1) RGB image at white LED illumination via crossed polarizers to reveal subcutaneous structures;

(2) 5 spectral images at narrowband LED illumination (450nm, 540nm, 580nm, 660nm, 940nm) via crossed polarizers with further calculated maps of skin chromophores - melanin, oxy-hemoglobin, deoxy-hemoglobin and bilirubin;

(3) photoplethysmography video under green LED illumination with further calculated map of skin blood microcirculation perfusion;

(4) autofluorescence video under UV (365nm) LED irradiation with further calculated map of skin fluorophore clusters accordingly to the photo-bleaching rates.

Design details of the device as well as preliminary results of clinical tests will be reported.

8574-20, Session 5

Validation of diffuse optical tomography using a bi-functional optical-MRI contrast agent and a hybrid DOT-MRI system

Alex Luk, Yuting Lin, David Thayer, Anjani Hagan, Kristin Murray, Univ. of California, Irvine (United States); Burcin Unlu, Bo?aziçi Univ. (Turkey); Brian Grimmond, GE Gobal Research (United States); Anup Sood, GE Global Research (United States); Egidijus Uzgiris, Rensselaer Polytechnic Institute (United States); Orhan Nalcioglu, Gultekin Gulsen, Univ. of California, Irvine (United States)

Since diffuse optical tomography (DOT) is a low spatial resolution modality, it is desirable to validate its quantitative accuracy with another well-established imaging modality, such as MRI. However, simply co-injection of both MRI and DOT agents cannot cross-validate two modalities unless two different contrast agents have exactly the same pharmacokinetics. This necessitates multi-modality contrast agents, which provide not only co-localization but also the same kinetics and hence, a powerful way to cross-validate two imaging modalities. In this work, we have used a polymer based bi-functional MRI-optical contrast agent (Gd-DTPA-polylysine-IR800) in collaboration with GE Global Research . The agent has IR800 as the optical dye, which has its peak absorption at 760 nm (NIR range) that is suitable for in vivo imaging due to the deeper light penetration in tissue. Besides, the size of the polymer can be varied to obtain a spectrum of pharmacokinetic rates. Moreover, the ratio of MR and optical agent loading can be adjusted for optimal sensitivity for both imaging modality. In this study, we demonstrate that utilization of MR a priori structural information is important to get more accurate agent kinetics using DOT. Bi-functional agents are injected to the rats bearing AC 3230 breast cancer model and pharmacokinetics at the tumor site as well as other organs such as bladder and kidney are recovered using MR structural priori. Finally the results are cross-validated using DCE-MRI.

8574-21, Session 5

Multimodality pH imaging in a mouse dorsal skin fold window chamber model

Hui Min Leung, The Univ. of Arizona, College of Optical Sciences (United States); Rachel Schafer, Mark D. Pagel, The Univ. of Arizona (United States); Ian F. Robey, The Univ of Arizona (United States); Arthur F. Gmitro, The Univ. of Arizona (United States)

There is considerable interest in the study of extracellular pH (pHe) as a cancer biomarker. Low pHe is indicative of glycolytic metabolism in tumors and plays a role in extracellular tissue remodeling and, hence, cancer metastasis. In this work, multiple methodologies for in-vivo measurement of tumor pHe in a mouse dorsal skin fold window chamber (DSFWC) model were developed. The DSFWC is a support structure that holds a thin layer of skin tissue. The top layer of skin is removed and an optically clear window (coverslip) is placed over the exposed tissue. Cancer cells can be implanted into the exposed tissue layer to provide an accessible tumor model. We have developed a plastic DSFWC that is compatible with MR imaging as well as with optical imaging. The new DSFWC technique enables continuous study of the same tissue microenvironment on multiple imaging platforms.

For optical imaging of pHe, measurement is done with a tail-vein injection of SNARF-1 carboxylic acid and ratiometric measurement of its fluorescence signal using a confocal microscope. Imaging is done under well regulated temperature control of the animal. This optical pHe measurement method was used to study the alkalization of tissue when sodium bicarbonate is given to the mice as a potential treatment to reverse acidosis.

A second method to measure pHe is based on MRI using ULTRAVIST® (a clinically approved CT contrast agent), which acts as a Chemical Exchange Saturation Transfer (CEST) agent. A ratiometric analysis of water saturation signal at 5.6 and 4.2 ppm chemical shift provides an estimate of the local pH. In this work we evaluated the ability to utilize this CEST methodology in the DSFWC model.

8574-22, Session 5

Ultra-high sensitivity detection of bimodal probes at ultra-low noise for combined fluorescence and positron emission tomography imaging

Nikta Zarifyussefian, Univ. de Sherbrooke (Canada); Olivier Daigle, Nüvü Caméras Inc. (Canada); Elena Ranyuk, Réjean Lebel, Johannes Van Lier, Brigitte Guérin, Roger Lecomte, Univ. de Sherbrooke (Canada); Marc Massonneau, Quidd (France); Marie-Eve Ducharme, Nüvü Caméras Inc. (Canada); Yves Bérubé-Lauzière, Univ. de Sherbrooke (Canada)

A critical limitation encountered in combined fluorescence and positron emission tomography (PET) imaging using a bimodal biomarker is the forced link between the radioactive and fluorescence emission rates. Both rates cannot be made independent, as each biomarker molecule holds both a radioactive component (atom) and a fluorescent component. Hence, the concentration of these two components is necessarily the same. In PET imaging, one typically resorts to minute biomarker concentrations to limit radioactivity, which is harmful, and in order not to saturate the count rate of the PET camera which is typically an extremely sensitive device capable to detect and quantitate concentrations down to picomolars. This limits the availability of fluorescence for optical detection, because at such concentrations fluorescence is extremely faint. We hereby present results on detecting at ultra-low noise such faint concentrations of fluorescence in vivo in small animals using a phtalocyanine-based bimodal compound synthesized by our group that holds a 64Cu radioactive atom. We quantify the concentration floor at which fluorescence cannot be detected anymore. This is achieved using the ultra-sensitive and ultra-low noise EM N2 EMCCD camera from NüVü Caméras Inc. (Montréal, Canada) installed in the QOS imager (Quidd, S.A.S. France) modified for the purpose. At the heart of the camera's unsurpassed performances in low light imaging is the CCD controller for counting photons (CCCP) which generates significantly less clock-induced charges (CICs - the main source of noise of an EMCCD in photon counting conditions) than any other CCD controller available on the market (< 0.001 ?/pixel/frame).

8575-2, Session 1

Multicolor probe-based confocal laser endomicroscopy: a new world for in vivo and real-time cellular imaging

Hédi Gharbi, Tom K. Vercauteren, François Doussoux, Matthieu Cazaux, Francois Lacombe, Mauna Kea Technologies (France)

Since its inception in the field of in vivo imaging, endomicroscopy through optical fiber bundles, or probe-based Confocal Laser Endomicroscopy (pCLE), has extensively proven the benefit of in situ and real-time examination of living tissues at the microscopic scale. By continuously increasing image quality, reducing invasiveness and improving system ergonomics, Mauna Kea Technologies has turned pCLE not only into an irreplaceable research instrument for small animal imaging, but also into an accurate clinical decision making tool with applications as diverse as gastrointestinal endoscopy, pulmonology and urology.

The current implementation of pCLE relies on a single fluorescence spectral band making different sources of in vivo information challenging to distinguish. Extending the pCLE approach to multi-color endomicroscopy therefore appears as a natural plan. Coupling simultaneous multi-laser excitation with minimally invasive, microscopic resolution, thin and flexible optics, allows the fusion of complementary and valuable biological information, thus paving the way to a combination of morphological and functional imaging.

This paper will detail the architecture of a new system, Cellvizio Dual Band, capable of video rate in vivo and in situ multi-spectral fluorescence imaging with a microscopic resolution. In its standard configuration, the system simultaneously operates at 488 and 660 nm, where it automatically performs the necessary spectral, photometric and geometric calibrations to provide unambiguously co-registered images in real-time. The main hardware and software features, including calibration procedures and sub-micron registration algorithms, will be presented as well as a panorama of its current applications, illustrated with recent results in the field of pre-clinical imaging.

8575-3, Session 1

Needle endomicroscope with a plastic achromatic objective to perform optical biopsies of breast tissue

Matthew R. Kyrish, Jessica Dobbs, Rebecca Richards-Kortum, Tomasz S. Tkaczyk, Rice Univ. (United States)

In order to diagnose cancer in breast tissue, a sample must be removed, prepared, and examined under a microscope. As an alternative, a needle-like fluorescence endomicroscope that can perform optical biopsies is demonstrated. The system provides high resolution, high contrast images in real-time which can allow a diagnosis to be made during surgery without the need for tissue removal. Optical sectioning is achieved via structured illumination to select a thin tissue section and reject out of focus light. An image is relayed between the sample plane and the imaging system by a coherent fiber bundle with an integrated objective lens. The custom, achromatic objective provides correction for both excitation and emission wavelengths (452 nm and 515 nm, respectively). It also magnifies the object onto the distal tip of the fiber bundle to increase lateral resolution. Specifically, the objective is designed to work within the visible spectrum from 452 nm to 623 nm. The lenses are composed of Zeonex E48R, PMMA, and polystyrene, which are optical plastics that can be fabricated by single-point diamond turning (for prototyping) or injection molding (for manufacturing). The selected materials provide a sufficient variety in Abbe number to perform chromatic correction. The lenses are assembled using zero alignment fabrication techniques so no adjustment is necessary during assembly. The system performance, including lateral and axial resolution, was characterized using resolution targets and the slanted edge technique, and followed with ex vivo imaging of breast resections. The biological imaging results are compared to those from the Lucid VivaScope, a commercial, benchtop confocal microscope. In both cases, proflavine was used as a fluorescent dye. As with the commercial system, the endomicroscope is able to achieve optical sectioning and to resolve subcellular features including nuclei and intercellular connective tissue.

8575-4, Session 1

A near infrared angioscope visualizing lipid within arterial vessel wall based on multi-spectral image in 1.7 μm wavelength band

Takemi Hasegawa, Ichiro Sogawa, Hiroshi Suganuma, Sumitomo Electric Industries, Ltd. (Japan)

We have developed a near infrared (NIR) angioscope that takes multi-wavelength images in 1.7μm band for visualizing lipid-rich coronary plaques. The angioscope comprises light source, camera, and fiberscope. The light source, containing a supercontinuum source and a switching optical filter, emits 1.60, 1.65, 1.72 and 1.76μm wavelengths sequentially in synchronization to the camera frame. The supercontinuum is seeded by 1.55μm wavelength pulses, whose spectrum is spread by a nonlinear fiber designed to generate 1.7μm wavelength most efficiently. The switching filter contains 1x4 fiber-optic path switches and interferometric band-pass filters. The camera detects NIR images by an InGaAs/GaAsSb type-II quantum well sensor at 100frames/s. The filter wavelength and the camera frame are synchronized by an FPGA. The fiberscope, based on a silica-based image-guide designed for 1.7μm wavelength, transmits 1300pixel NIR images and has 0.7mm outer diameter, which is compatible with the conventional angioscope and suited for continuous flushing to displace blood. We have also developed image processing software that calculates spectral contribution of lipid as lipid score at each pixel and create lipid-enhanced color images from the lipid score at 11 frames/s. The system also includes conventional visible light source and camera, and takes visible light images synchronously with the lipid-enhanced images. The performance of the angioscope for detecting lipid-rich plaque has been verified in bench tests using a plaque model made by injecting lard into excised swine carotid arterial vessel. The plaque models are imaged in water at working distances of 0 to 3mm, and significantly distinguished from normal vessels.

8575-34, Session 1

Barrett's pathology update *(Invited Paper)*

Guillermo J. Tearney M.D., Wellman Ctr. for Photomedicine (United States)

No Abstract Available

8575-35, Session 1

Molecular imaging for endoscopic detection of neoplasia in Barrett's esophagus *(Invited Paper)*

Thomas D. Wang, Univ. of Michigan (United States)

No Abstract Available

8575-5, Session 2

µOCT Imaging probe for imaging functional anatomy of respiratory epithelium in Vivo

Ken Chu, Tzahi Grunzweig, Linbo Liu, Gregory Dierksen, Robert W. Carruth, Massachusetts General Hospital (United States); Ramses V. Martinez, George Whitesides, Harvard Univ. (United States); Steven M. Rowe, The Univ. of Alabama at Birmingham (United States); Guillermo J Tearney, Wellman Ctr. for Photomedicine (United States)

µOCT allows for fast imaging of three-dimensional tissue with microscale resolution. Previously, we were able to visualize and evaluate mucociliary clearance in respiratory airway and oviduct tissues using a bench-top µOCT system. Here, we present a µOCT probe that is capable of imaging the respiratory epithelium in the nasal cavity with sufficient resolution and acquisition speed to directly evaluate mucociliary clearance in vivo.

Our µOCT probe is a rigid, side-viewing endoscope with an outer diameter of 3 mm. The probe is driven by a linear motor at the proximal end so that the focused beam is scanned longitudinally at 40 Hz with a typical travel of 0.5 mm. The imaging console is the same as in the desktop system we used previously which provides an axial resolution of 1 um and an acquisition rate of 16,000 A-lines per second with a detected wavelength range of 800 ±200 nm. The gradient index (GRIN)-based probe provides a spot size of 2-3 um over a depth of focus of 320 µm.

The µOCT probe is a powerful tool that can be used to study and diagnose diseases associated with mucociliary clearance such as cystic fibrosis and primary ciliary dyskinesia in humans. Further development of an endobronchial probe will enable microstructural imaging of human pulmonary airways.

8575-6, Session 2

OFDI guided biopsy of Barrett's esophagus

Melissa J. Suter, Massachusetts General Hospital (United States); Michalina J. Gora, Wellman Ctr. for Photomedicine (United States); Gregory Lauwers, Arni T. Arnason, Jenny S. Sauk, Khay M. Tan, Kevin A. Gallagher, Lauren Kava, Massachusetts General Hospital (United States); Brett E. Bouma, Wellman Ctr. for Photomedicine (United States); Norman S. Nishioka, Massachusetts General Hospital (United States); Guillermo J. Tearney, Wellman Ctr. for Photomedicine (United States)

Surveillance protocols for patients with Barrett's esophagus involve the acquisition of random 4-quadrant biopsy acquisition along the extent of the visible Barrett's segment to identify dysplasia and adenocarcinoma. Due to the random nature of this biopsy protocol it is highly susceptible to sampling errors with <1% of the involved tissue generally assessed. We have developed a balloon-based optical frequency domain imaging (OFDI) system with laser marking capabilities to guide biopsy site selection with the goal of reducing this sampling error. 10 subjects undergoing surveillance of Barrett's esophagus were enrolled in this study. 3 target sites were selected and marked in each patient based on the intra-procedural interpretation of the comprehensive OFDI datasets. Tissue specimens of the targeted sites were subsequently obtained using jumbo biopsy forceps. Diagnosis of the OFDI, endoscopy, and histopathology images of the target sites was performed by independent blinded readers and were statistically compared to one another. Our results suggest that OFDI guided biopsy of the esophagus is safe and feasible and may significantly improve the accuracy of diagnosis in patients with Barrett's esophagus, leading to better management and earlier detection of malignancy.

8575-7, Session 2

Mesoscopic spectrally encoded tomography

Paulino Vacas-Jacques, Wellman Ctr. for Photomedicine (United States); Joseph A. Gardecki, Massachusetts General Hospital (United States); Brett E. Bouma, Guillermo J. Tearney, Wellman Ctr. for Photomedicine (United States)

Background: Developing a new approach for optical tomography is relevant because few technologies are capable of providing information in the mesoscopic regime. Currently, mesoscopic imaging is accomplished using modulated imaging and laminar optical tomography. For endoscopic applications, it would be desirable to have a single fiber solution because of size and flexibility constraints while imaging luminal organs. We introduce Mesoscopic Spectrally Encoded Tomography (MSET) a technique that uses a single optical fiber and spectral encoding to simultaneously collect light from a plurality of source-detector separations.

Methods: Our MSET configuration comprises emission and collection fibers, diffractive elements for the generation of sources and detectors, and a spectrometer-based detection scheme. A 20 mW superluminescent diode (Superlum, Ireland) with 833 nm center wavelength and 54 nm bandwidth is used as radiation source. Two holographic gratings, 1200 lines/mm at 830 nm (Wasatch Photonics, US), are employed for spectral encoding of the light. A sprint spL2048-140km camera (Basler, Germany) is the main component of the spectrometer. MSET was used to image an agar-based phantom with a central absorbing inclusion, and reconstructions were performed using MSET data, which is equivalent to the data employed in diffuse optical tomography in reflectance geometry, in conjunction with Monte Carlo calculations. MSET reconstructions were compared with phantom geometry.

Results: An absorbing inclusion located 4 mm below the surface of the phantom was assessed with a maximum source-detector separation of 10 mm. MSET data was obtained from the phantom. When compared to the phantom structure, reconstructed data correlated to the known absorber distribution.

Conclusions: Our preliminary results suggest that MSET may be a useful method for mesoscopic tomography in luminal organ applications.

8575-8, Session 2

Development of a fluorescence-labeled peptide for cervical cancer screening with microendoscope

Numfon Khemthongcharoen, National Electronics and Computer Technology Ctr. (Thailand) and Chulalongkorn Univ. (Thailand); Santi Rattanavarin, National Electronics and Computer Technology Ctr. (Thailand); Pongsak Sarapukdee, Chulalongkorn Univ. (Thailand); Satjana Pattanasak, National Science and Technology Development Agency (Thailand); Somchai Niruthisard M.D., Chulalongkorn Univ. (Thailand); Wibool Piyawattanametha, National Electronics and Computer Technology Ctr. (Thailand) and Chulalongkorn Univ. (Thailand)

Cervical cancer is the third most common cancer in women worldwide. Current cervical screening methods frequently present both false negative and false positive results. Moreover, those techniques require technical expertise to diagnose results and women need to be screened regularly. In this work, we develop a novel fluorescence-labeled peptide tracer for cervical cancer detection. Phage display random peptide library was used to identify a specific binding peptide for cervical cancer imaging probe development. Phage-displayed specific peptides and synthetic peptides sequence were experimentally tested for their sensitivity and penetrability into the cervical cancer cells by utilizing flow cytometry method and confocal cells imaging analysis. Then, imaging demonstration of the peptides was performed with dual-axis confocal microendoscope on tissue biopsies. Phage-displayed specific binding

peptides can be used for cervical cancer cells detection after the cells are permeabilized for at least 30 minutes. Difference in fluorescence signal intensity between cervical cancer cells versus normal fibroblast cells stained by specific binding phages is over 2 times higher than that of the control phages. Phage-displayed binding peptide particles also provide multi-labeling sites on their coated protein surface for fluorescence signal enhancing purpose. As the results, whole phage particles can potentially be used as a low cost specific tracer for ex vivo cervical cancer screening. Due to cells penetrability and patient safety reasons, synthetic peptides derived from phages combining with endoscopic imaging method are more suitable for in vivo cervical cancer imaging in order to improve an alternative cervical screening method known as “single visit approach.”

8575-9, Session 2

Detecting fluorescence hot-spots using mosaic maps generated from multimodal endoscope imaging

Chenying Yang, Timothy D. Soper, Eric J. Seibel, Univ. of Washington (United States)

Background: Fluorescence peptides targeting the molecular signature of cells are under investigation for imaging of adenocarcinoma and high-grade dysplasia in Barrett’s esophagus. These fluorescent peptides can be combined with a multimodal wide-field endoscopic imaging system to highlight suspect regions (hot-spots) within the esophageal mucosa. These hot-spots can be small and sparse, and the detection of fluorescence signal is dependent on background noise and distance to the endoscope. To enhance intraoperative visualization of these hot-spots, an image mosaicking algorithm is applied to endoscopic video to improve recognition of fluorescent regions by co-registering multiple image frames. The resulting video mosaic can be extended to create anatomical maps of the esophagus and labeled hot-spots to assist biopsy and document findings.

Method: A laser-based ultrathin scanning fiber endoscope (SFE) was used for multimodal (reflective and fluorescence) imaging. The algorithm used reflective images to register successive image frames using optical flow. Fluorescence frames were then registered to provide a wider field of view and to enhance weak fluorescence signal by multi-frame averaging.

Results: The algorithm was successfully run on simulated endoscopic images of a texture-mapped test targets and experimental SFE images both with/without fluorescence hot-spots. The resultant mosaic map contained enhanced fluorescent hot-spot recognition.

Conclusions: A mosaicking algorithm was developed specially tailored to multimodal imaging in esophagus. Future experiment on synthetic esophagus phantom with fluorescent hot-spots is needed to allow it to robustly adapt to large camera motions and rapidly red flag hot-spots for biopsy.

8575-10, Session 3

High-speed high-resolution noninvasive microscopy of blood

Lior Golan, Daniella Yeheskely-Hayon, Limor Minai, Dvir Yelin, Technion-Israel Institute of Technology (Israel)

Microscopic imaging of individual blood cells flowing within the vessels of a patient is a challenging task, requiring high-speed image acquisition for overcoming the rapid blood flow in vivo. We have recently demonstrated non-invasive, label-free imaging of red and white blood cells flowing within small capillary vessels inside patients, using a spectrally encoded confocal microscopy technique that repeatedly images a single line across the vessel with no moving parts.

Here, we report a novel spectrally-encoded blood microscopy system capable of imaging blood cells flowing at speeds of a few tens of millimeters per second without motion artifacts. The new system is comprised of a 100 kHz swept-wavelength source operating at 1060 nm and an interferometric detection scheme in the Fourier domain that enhances the system’s sensitivity and speed. Using Hilbert transform demodulation of the acquired spectral interferograms to extract the reflectivity at each resolvable point, we demonstrate high-resolution imaging of blood cells flowing at 10 mm/s within 70 um diameter vessels deep below the surface of the lower lip of a volunteer, revealing red blood cell deformations under normal physiological flow conditions. Imaging of large vessels would allow fast acquisition of large data sets, allowing extraction of various blood parameters with improved accuracy. The system presented in this work would be useful for non-invasive blood testing for the diagnosis and online monitoring of various medical conditions.

8575-11, Session 3

Tethered capsule spectrally encoded confocal endomicroscopy for eosinophilic esophagitis

Nima Tabatabaei, Dongkyun Kang, Harvard Medical School (United States) and Massachusetts General Hospital (United States); Robert W. Carruth, Massachusetts General Hospital (United States); Minkyu Kim, Harvard Medical School (United States) and Massachusetts General Hospital (United States) and Univ. of Tokyo (Japan); Guillermo J. Tearney, Harvard Medical School (United States) and Massachusetts General Hospital (United States) and Massachusetts Institute of Technology (United States); Tao Wu, Harvard Medical School (United States) and Massachusetts General Hospital (United States)

Eosinophilic esophagitis (EoE) is a prevalent food allergy disorder that manifests by eosinophilic infiltration within the esophageal wall. Currently EoE patients are treated by either dietary changes or topical steroids that eliminate the inflammatory infiltrate. Both treatments require multiple follow up sedated endoscopies with biopsies to confirm elimination of eosinophils. These procedures are expensive, time consuming, and difficult for patients to tolerate. Spectrally-encoded confocal microscopy (SECM) is a reflectance microscopy technique which assigns the wavelength components of a wavelength swept laser light spatially across a focal line inside the sample. In a prior bench top study, we have shown that SECM is capable of identifying eosinophils in biopsy samples. Here we describe the implementation of SECM in a miniaturized, tethered capsule which is capable of performing sub-cellular imaging of the esophagus in unsedated patients after the capsule has been swallowed. The capsule is filled with water and made out of fluorinated ethylene propylene (refractive index = 1.338) to maintain an optically-continuous layer between the objective lens and the tissue. This minimizes both the spherical aberration and specular reflection. Furthermore, single mode lensed fiber with a NA of 0.18 at 1300nm is used to shorten the length of the 7 mm diameter capsule to 30 mm. Experiments carried out with the first prototype indicate transverse and axial resolutions of 5 µm and 12 µm, respectively. Preclinical animal testing followed by a human pilot study will be carried out to investigate the performance of the capsule as an accurate and inexpensive endomicroscopy diagnostic tool for EoE.

8575-12, Session 3

Comprehensive confocal endomicroscopy of the esophagus in vivo using SECM

DongKyun Kang, Massachusetts General Hospital (United States); Simon Schlachter, Nine Point Medical (United States) and Massachusetts General Hospital (United States); Robert W. Carruth, Massachusetts General Hospital (United States); Minkyu Kim, Massachusetts General Hospital (United States) and Univ. of Tokyo (Japan); Tao Wu, Wellman Ctr. for Photomedicine (United States); Nima Tabatabaei, Nima Tabatabaei, Milen Shishkov,

Paulino Vacas-Jacques, Wellman Ctr. for Photomedicine (United States); Kevin Woods, Wellman Ctr. for Photomedicine (United States) and Emory Univ. Hospital (United States); Jenny S. Sauk, Norman S. Nishioka, Massachusetts General Hospital (United States); Brett E. Bouma, Guillermo J. Tearney, Wellman Ctr. for Photomedicine (United States)

Accurate diagnosis of Barrett's esophagus (BE), dysplasia, and esophageal cancer can sometimes be hampered by the sampling errors in endoscopic biopsy: only very small fractions of the distal esophagus are biopsied and examined during histomorphologic analysis. Confocal endomicroscopy can visualize key microscopic features associated with BE and other important esophageal diseases without taking excisional biopsies. However, the typical field size of confocal endomicroscopy is limited to less than 0.5 mm, and the imaging speed needs to be increased significantly in order to examine the large mucosal regions that may contain malignant changes. Spectrally encoded confocal microscopy (SECM) is a high-speed reflectance confocal microscopy technology that diffracts different wavelengths of light to distinct locations on the sample. With SECM, images can be acquired 10-100 times faster than video rate by utilizing a rapid wavelength-swept source and a large-bandwidth photodetector. The high imaging speed of SECM, combined with the helical scanning of the SECM optics, makes it possible to contemplate imaging the entire distal esophagus. Here, we present an endoscopic SECM probe for comprehensive imaging of the esophagus. The SECM probe uses a custom water-immersion objective lens (aspheric singlet; NA = 0.5w) and an index-matched guide tube to achieve high imaging resolution without significant spherical aberrations. The spectrally-encoded focal line is tilted relative to the tissue surface by angling the objective lens and covers a lateral field size of 280 ?m a ranging depth of 57 ?m. The distal SECM optics is assembled with a torque coil and helically-scanned by a fiber-optic rotary junction and a pull-back stage. Using this device, we have conducted esophageal imaging in vivo in swine following acetic acid administration using a spray catheter. Our results show that it is possible to acquire circumferential confocal microscopy data over a 5-cm-long segment of the swine esophagus in 2 minutes. SECM images allowed clear visualization of the nuclei of squamous epithelium. These results indicate that SECM may become a viable modality for imaging the cellular structure of the entire distal esophagus for the screening and surveillance of BE.

8575-13, Session 3

Compound vari-focal objective lens for confocal endomicroscopy

Minkyu Kim, Massachusetts General Hospital (United States) and Univ. of Tokyo (Japan); Dongkyun Kang, Robert W. Carruth, Massachusetts General Hospital (United States); Guillermo J. Tearney, Wellman Ctr. for Photomedicine (United States) and Massachusetts Institute of Technology (United States) and Harvard Medical School (United States); Tao Wu, Massachusetts General Hospital (United States); Nima Tabatabaei, Harvard Medical School (United States)

The diagnosis of esophageal disease such as Barrett's esophagus, eosinophilic esophagitis, dysplasia and intramucosal carcinoma remain important clinical problems. Imaging large areas of esophagus with microscopy resolution in vivo could provide an improved diagnostic solution, compared with standard of care random excisional endoscopic biopsy. Spectrally Encoded Confocal Microscopy (SECM) is an endomicroscopy technology that can image large areas of distal esophagus by helically scanning the probe optics. One key challenge for comprehensive endoscopic confocal microscopy is keeping the focus within the tissue at all times during the scan. This task can be accomplished by incorporating an adaptive focusing mechanism within the SECM probe. In this paper, we present a vari-focal objective lens that can hydraulically change the focal length while maintaining a high NA. The vari-focal objective is composed of an aspheric singlet that has been assembled with a vari-focal liquid lens. Most of the optical power is provided by the aspheric singlet, and the vari-focal liquid lens changes the optical power slightly to change the focal length. We have used an aspheric singlet (ALPS; molded glass aspheric singlet; material = L-LAH84; focal length = 1.6mm; NA = 0.44) and an internally fabricated vari-focal liquid lens (liquid = water; liquid refractive index = 1.33; liquid chamber thickness = 0.5mm; Polydimethylsiloxane membrane thickness: 130?m). This combination of elements provided a NA of 0.40-0.46 while the focal length was changed over a 617?m range.

8575-14, Session 4

High resolution large field-of-view endomicroscope with optical zoom capability

Dimitre G. Ouzounov, David R. Rivera, Watt W. Webb, Chris Xu, Cornell Univ. (United States)

To operate as an optical biopsy tool, a clinical endoscope must provide a large field-of-view (FOV) to survey large tissue area and subcellular spatial resolution to achieve real time tissue diagnostics. Miniature objective lens cannot achieve simultaneously these two requirements, and optical zoom capability is an essential functionality for a practical endoscope. Here, we present a miniature endomicroscope that combines large FOV (1.15 mm) reflectance modality and high-spatial resolution (~ 0.5 um) multiphoton imaging. The essential element of the endoscope is a 3 mm outside diameter (OD), catadioptric zoom lens based on the idea of separating the optical paths of excitation light with different wavelengths. The two imaging modes are switched by changing the wavelength of the excitation light and, therefore, the optical zoom operation is achieved without any mechanical adjustment at the endoscope distal end. We packaged the zoom lens with a previously demonstrated miniaturized resonant/non-resonant fiber raster scanner into a miniature (5 mm OD, 5 cm length) endoscopic probe. We tested the performance and confirmed the high resolution and large FOV of this miniature device by imaging a US Air Force test target in transmission. We acquired in vivo and ex vivo images of unstained mouse and rat tissues by using the large FOV mode to navigate to the site of interest and then using the high resolution modality to image with cellular details. The demonstrated endomicroscope with optical zoom capability is a significant step for developing clinical optical tools for real time tissue diagnostics.

8575-15, Session 4

Label free multiphoton imaging of human pulmonary tissues through two-meter-long microstructured fiber and multicore image-guide

Guillaume Ducourthial, Claire Lefort, XLIM Institut de Recherche (France); Donald A. Peyrot, Univ. Pierre et Marie Curie (France); Tigran Mansuryan, XLIM Institut de Recherche (France); Sergei G. Kruglik, Christine Vever-Bizet, Univ. Pierre et Marie Curie (France); Luc Thiberville, Rouen Univ. Hospital (France); Francois Lacombe, Mauna Kea Technologies (France); Geneviève Bourg-Heckly, Univ. Pierre et Marie Curie (France); Frédéric Louradour, XLIM Institut de Recherche (France)

This work deals with label free multiphoton imaging of the human lung tissue extracellular matrix (ECM) through optical fibers. Two devices were developed, the fisrt one using distal scanning of a double clad large mode area (LMA) air-silica microstructured fiber, the second one using proximal scanning of a miniature multicore image guide (30000 cores inside a 0.8 mm diameter). In both cases, the main issue has been excitation pulse linear and nonlinear distortion efficient pre-compensation. By inserting a compact (10 cm x 10 cm footprint) GRISM-based stretcher, made of readily available commercial components, before the delivery fiber, we achieved as short as 25-femtosecond-

duration pulses that were temporally compressed at the direct exit of a 2-meter-long fiber. Interestingly this femtosecond pulse fiber delivery device is also wavelength tunable over more than 100 nm inside the Ti: Sapphire emission band. Those unique features allowed us to record elastin (through two-photon fluorescence) and collagen (though second harmonic generation) fibered network images. These images were obtained ex-vivo with only 10 mW @ 80 MHz of IR radiation delivered to the alveoli or bronchus tissues. 3D imaging with 400-micrometer-penetration depth inside the tissue was possible working with a 2-meter-long LMA fiber, while the miniature image guide allowed us to perform endoscopic real time microimaging of the ECM ex vivo.

8575-16, Session 4

Development of a side-looking endoscopic imaging probe for combined two-photon microscopy and optical coherence tomography

Taejun Wang, Peng Xiao, Qingyun Li, Jun Ho Lee, Pohang Univ. of Science and Technology (Korea, Republic of); Pilhan Kim, KAIST (Korea, Republic of); Euiheon Chung, Gwangju Institute of Science and Technology (Korea, Republic of); Seungjae Myung, Asan Medical Ctr. (Korea, Republic of); Ki Hean Kim, Pohang Univ. of Science and Technology (Korea, Republic of)

Endoscopy is a well-known imaging technology for preclinical study. We developed a side-looking endoscopic probe for the combined imaging of two-photon microscopy (TPM) and optical coherence tomography (OCT). The probe is made of grin lenses, which are 2.0 mm in diameter, and a prism was attached at the distal end for the side-looking. This probe can be rotated and translated along its axis to image tubular organs such as the colon. In previous study, endoscopy system has been developed in the form of confocal microscopy generally. But we set up our endoscopic imaging probe by using the Ti:Sapphire laser for two-photon excitation of point-scanning process to provide more deeper axial-information and combined OCT which used a wavelength-swept source centered at 1300 nm to provide morphology in larger tissue region. This setup, which we have developed, is designed to do simultaneous imaging by combining TPM and OCT using the same scanner and objective lens. And also, this setup is able to do video-rate imaging. We will characterize the endoscopic probe with tissue phantoms, and will apply to the mouse colon both in ex-vivo and in-vivo.

8575-17, Session 4

Fiber optic nonlinear endomicroscopy for imaging biological tissues based on intrinsic contrast

Wenxuan Liang, Yuying Zhang, Johns Hopkins Univ. (United States); Meredith Akins, The Univ. of Texas Southwestern Medical Ctr. at Dallas (United States); Yongping Chen, Qi Mao, Johns Hopkins Univ. (United States); Ming-Jun Li, Corning Incorporated (United States); Kristine Glunde, Zaver Bhujwalla, Johns Hopkins Univ. (United States); Katherine Luby-Phelps, Mala Mahendroo, The Univ. of Texas Southwestern Medical Ctr. at Dallas (United States); Xingde Li, Johns Hopkins Univ. (United States)

Two-photon fluorescence (TPF) and second harmonic generation (SHG) microscopy technologies are sensitive to intrinsic fluorophores and structural proteins with near infrared excitation. They are capable of providing native physiological and structural information without introducing contrast agents, exhibiting strong promise for many clinical applications. Typical bench-top microscopes, however, have limited applicability in most, especially in vivo, clinical settings. Therefore a miniature nonlinear endomicroscope is pressingly needed. Our group demonstrated the very first, all-fiber-optic, and fully integrated scanning endomicroscope prototype capable of TPF imaging on stained tissue. This presentation will focus on recent advances that significantly improved the sensitivity, signal-to-noise ratio, and image quality of the system. Our newly-developed endomicroscope, whose diameter is only 2 mm, features a single customized double-clad fiber (with a larger inner clad) and a compound micro-objective lens with high-degree chromatic correction. It achieves high resolution, high fluorescence collection efficiency, and enables intrinsic TPF and SHG imaging at a frame rate of 2.7 fps with an excitation power of 20-30 mW. TPF imaging using the endomicroscope can clearly visualize subcellular structure of small intestines and other organs on mouse and rat models. Furthermore, with two detection channels, the system can collect TPF signals from NADH and FAD simultaneously to assess cellular redox ratio. In addition, SHG imaging with the endomicroscope has shown its capability of assessing cervical collagen remodeling during pregnancy. These results demonstrate the strong potential of the endomicroscopy technology for translating the high-resolution nonlinear imaging modality to broad in vivo and clinical applications.

8575-18, Session 4

Development of a coherent Raman scattering fiber optic probe

Richa Mittal, Mihaela Balu, Gangjun Liu, Zhongping Chen, Bruce J. Tromberg, Petra Wilder-Smith, Beckman Laser Institute and Medical Clinic (United States); Eric O. Potma, Univ. of California, Irvine (United States)

Coherent Raman scattering (CRS) is a label-free imaging technique for real-time examination of live tissues. CRS techniques have been used extensively in fundamental and applied research, however, there is a growing need to optimize these techniques for clinical implementations. To enable clinical translation, the optical components utilized in nonlinear microscopy need substantial miniaturization. A central challenge is to design focusing optics that reliably focus the two excitation beams, which have substantially different center wavelengths, to the same focal spot. We designed and fabricated a CRS imaging device with custom built achromatically corrected lenses and a fiber-scanning mechanism for live tissue imaging. This CRS imaging device enables real-time inspection of superficial tissues in hollow tracts of the human body.

8575-29, Session PSun

Compact 2D MEMS mirror for dual-axes confocal endomicroscope

Haijun Li, Zhen Qiu, Xiyu Duan, Wajiha Shahid, Quan Zhou, Kenn R. Oldham, Katsuo Kurabayashi, Thomas D. Wang, Univ. of Michigan (United States)

We have designed and fabricated a compact MEMS chip that integrates 2-dimensional (2D) resonant in-plane mirror with high fill-factor on a single SOI substrate for use in a dual-axes confocal endomicroscope (5 mm outer diameter). This 2D resonant in-plane scanner has an open gimbal frame to increase the fill factor of the mirror. The effective reflective surface area of the mirror is increased by ~20%. Backside islands were included in the design to enhance the mechanical structure of the gimbal frame and the mirror plate, thereby reducing dynamic deformations. A robust “three-mask, three-step deep reactive-ion etching (DRIE)” SOI process was developed to fabricate these devices with high yield of >90%. A layer of sputtered aluminum (~120 nm) was deposited onto the front side of the mirror’s silicon surface in the last step of the process to achieve a high quality reflective surface (reflectivity >80% from 488 to 600nm) with ~2nm rms surface roughness and ~1.67meters surface curvature. Experimental tests show that the fabricated 2D MEMS scanner can achieve large oscillation angles (?12° optical deflection angle) for both the inner and outer axes at low drive voltages (<50V) with

a tunable frequency bandwidth close to resonance (0.9 kHz for the outer (slow) axis and 2.5 kHz for the inner (faster) axis). This mirror was used in the dual axes confocal endomicroscope to collect fluorescence images from mice colon tissue.

8575-32, Session PSun

Ultrafast laser scalpel

Onur Ferhanoglu, Murat Yildirim, Adela Ben-Yakar, The Univ. of Texas at Austin (United States)

We present optical design and characterization results of an ultrafast laser probe for high speed microsurgery. The probe consists of an air core photonic crystal fiber for the delivery of high energy ultrafast laser pulses, a quadrant electrode piezo tube for fiber scanning, and two aspherical lenses for collimating and focusing the light. All components within this probe will be smaller than 3.2mm in diameter, to enable access to a wide variety of surgical sites. The probe is designed to ablate an area of 300µm x 300µm within 100 milliseconds using a high repetition rate (300 kHz or 2MHz) fiber laser. Optical simulations reveal that diffraction limited resolution of 0.65µm is preserved throughout the entire field of view. Using this probe, we have demonstrated 2-D ablation on a porcine vocal fold sample. With further development such a probe may serve as a precise ultrafast laser scalpel in the clinic.

8575-33, Session PSun

Evaluation of a compound eye type tactile endoscope

Kayo Yoshimoto, Kenji Yamada, Nagisa Sasaki, Maki Takeda, Sachiko Shimizu, Osaka Univ. (Japan); Toshiaki Nagakura, Osaka Electro-Communication Univ. (Japan); Hideya Takahashi, Osaka City Univ. (Japan); Yuko Ohno, Osaka Univ. (Japan)

Minimally invasive surgical techniques for endoscope become widely used, for example, laparoscopic operation, NOTES (Natural Orifice Translumenal Endoscopic Surgery), robotic surgery and so on. There are so many demand and needs for endoscopic diagnosis. Especially, palpation is most important diagnosis on any surgery. However, convenience endoscopic system has no tactile sensibility. There are many studies about tactile sensor for medical application. These sensors can measure object at a point. It is necessary to sense at area for palpation. To overcome this problem, we propose compound eye type tactile endoscope. The proposed system consists of TOMBO (Thin Observation Module by Bound Optics) and clear silicon rubber. Our proposed system can estimate hardness of target object by measuring deformation of a projected pattern on the silicon rubber. The purpose of this study is to evaluate the proposed system. We approximate silicone rubber by finite element model and object by spring model, and simulate silicone rubber deformation by computer. In computer simulation, the thickness of silicone correlates with the Young's modulus of object. And the resolution of object's Young's modulus by measuring the proposed system varies according to the Young's modulus of object. Based on this result we experiment by a prototype system and the known hardness object. The experimental results show similar to simulation results. These results suggest that the proposed system is useful as a tactile sensor for palpation. In future, we optimize system and experiment with tissue.

8575-19, Session 5

Phase sensitive imaging of acoustic vibrations using spectrally encoded interferometry

Ovadia Ilgayev, Dvir Yelin, Technion-Israel Institute of Technology (Israel)

Noncontact techniques for measuring acoustic vibrations are potentially important tools for diagnosing hearing and vocal folds disorders. Laser Doppler vibrometry is a well-established research tool for high-sensitivity measurements of acoustic vibrations of an object that is illuminated by a single laser beam. However, measuring the full vibrational patterns of a two-dimensional surface requires knowledge of not only the frequency and amplitude of the wave, but also the relative phases between different locations of the (three dimensional) surface. The high-speed imaging rates and high axial resolutions of interferometric spectrally encoded endoscopy (SEE) make it suitable for imaging of acoustic vibrations at the audible frequency range with high phase sensitivity. In this work, we demonstrate a bench-top interferometric phase-sensitive spectrally encoded imaging system, which is capable of imaging, for the first time, the three-dimensional acoustic vibration patterns of a surface at nanometer resolution. The vibration patterns of various surfaces of different materials vibrating at a range of frequencies were imaged by analyzing relative spectral phases that correspond to small axial displacements of a few nanometers in magnitude. Potential applications for imaging surface vibrations with nanometric resolution using compact imaging probes include diagnosis of various middle ear pathologies, for example by imaging the tympanic membrane or within the middle ear.

8575-20, Session 5

Dual-channel spectrally encoded endoscopic probe

Dvir Yelin, Guy Engel, Technion-Israel Institute of Technology (Israel)

High quality imaging through sub-millimeter endoscopes provides clinicians with valuable diagnostics capabilities in hard to reach locations within the body. Thanks to its potentially flexible, small diameter probes, spectrally encoded endoscopy (SEE) has been shown promising for such task; however, challenging probe fabrication and high speckle noise had prevented its testing in extensive in vivo studies. Here we demonstrate a novel miniature SEE probe that incorporates some of the recent progress in spectrally encoded imaging technology into a compact and robust endoscopic system. A high-quality miniature diffraction grating was fabricated using automated femtosecond laser cutting from a large bulk grating, and attached to a miniature gradient index lens at the distal end of the spectrally encoded imaging channel. Using a separate channel for incoherent illumination through a multi-mode fiber, the new system is characterized by a large depth of field, negligible back reflections, and well-controlled speckle noise, which depend on the core diameter of the illumination fiber. Using 500-micron diameter imaging channel, high groove density grating, and broadband illumination spectrum within the visible range, the new endoscopic system now allow significant improvements in almost all imaging parameters compared to previous spectrally encoded systems. We demonstrated high quality, real time imaging of a volunteer's finger, as well as color imaging, through an ultra-miniature, two-fiber endoscopic probe.

8575-21, Session 5

Fabrication of miniature endoscope using soft lithography

DongKyun Kang, Massachusetts General Hospital (United States); Ramses V. Martinez, George Whitesides, Harvard Univ. (United States); Guillermo J. Tearney, Wellman Ctr. for Photomedicine (United States)

Spectrally encoded endoscopy (SEE) is a miniature endoscopy technology that can conduct high-definition imaging through a sub-mm diameter probe. With SEE, broadband light is diffracted by a grating at the tip of the fiber, producing a dispersed spectrum on the sample. Light returned from the sample is detected using a spectrometer; each resolvable wavelength corresponds to reflectance from a different point on the sample. Previously, SEE has been demonstrated using

a 350 µm diameter probe, producing high-quality images in two- and three- dimensions. The main technical challenge for fabricating SEE probes has been to make a sub-mm transmission grating with a high diffraction efficiency and to precisely assemble the miniature grating with other optical components in the probe. In this paper, we describe a new method of building SEE probes using soft lithography. In this new fabrication approach, we first fabricated a h-PDMS stamp replicating an etched fused silica grating (groove density = 1379 lines/mm; diffraction efficiency at 530 nm = 86%). A drop of UV-curable epoxy that has a similar refractive index to fused silica was then placed between the distal tip of a GRIN lens and the h-PDMS stamp. The epoxy was cured with UV exposure and patterned to replicate the surface topology of the original fused silica grating. We have built a 500 µm diameter SEE probe using the new fabrication method. The diffraction efficiency of the miniature grating was measured to be 75%. The new fabrication method will provide an economic and reproducible way of making SEE probes.

8575-22, Session 5

Novel double clad fiber couplers for spectrally encoded endoscopy

Wendy-Julie Madore, Etienne De Montigny, Simon Lemire-Renaud, Etienne Duchesne De Lamotte, Ecole Polytechnique de Montréal (Canada); Mathias Strupler, Sainte Justine Mother and Child Univ. Hospital Ctr. (Canada); Nicolas Godbout, Ecole Polytechnique de Montréal (Canada); Caroline Boudoux, Ecole Polytechnique de Montréal (Canada) and Sainte Justine Univ. Hospital Ctr. (Canada)

Single fiber endoscopy has recently been demonstrated using different techniques such as spectral encoding (SEE). This technology could allow access to a more significant number of organs through miniature instruments. However, due to the coherent nature of laser light, reflectance single fiber endoscopy suffers from speckle noise. The use of double clad fibers (DCF) allows us to overcome this problem by reducing speckle contrast by up to a factor 5, while increasing the depth of field as well as signal collection by up to a factor 9.

To improve mechanical stability and decrease the coupling losses of the current free-space beam-splitter approach, all-fiber DCF couplers (DCFCs) were developed. Current DCFCs allow for the quasi-lossless transmission of the coherent single-mode signal (illumination and collection) and >40% transmission of the multimodal signal (collection). Previously demonstrated DCFCs have a theoretical multimodal collection efficiency limited to 50%. We herein present a novel DCFC design capable of collecting >70% of light from the inner cladding area, while still transmitting all the single mode signal over a wide spectral region (1250 nm to 1350 nm). This custom design allows for an improvement of the signal to noise ratio, which can be used to detect weaker signals (such as fluorescence or Raman) or to image in vivo samples faster. We also implemented this novel DCFC in a SEE setup, which allowed us to acquire speckle-free images (1000x1000 pixels) at 30 frames per second. Lastly, we created three-dimensional reconstructions by coupling the core signal to an interferometer.

8575-23, Session 6

Flexible fiber-bundle probe for endoscopic full-field OCT

Anne Latrive, Ecole Supérieure de Physique et de Chimie Industrielles (France) and LLTECH SAS (France); Claude A. Boccara, Institut Langevin (France) and LLTECH SAS (France)

Optical Coherence Tomography (OCT) has proven its interest for many biomedical fields thanks to its virtual slicing and 3D imaging capability. Full-Field OCT (FFOCT) is an approach that directly takes “en face” 2-D images with an isotropic resolution around 1µm; it has proven a powerful tool for imaging of biological tissue samples. However the standard bulky system is not suited for hardly accessible areas of the body; in order to perform an in situ minimally invasive optical biopsy one requires a millimeter-size system such as an endoscopic probe.

We present an endoscopic imaging system adapted from the Full-Field OCT principle. Our approach is based on the coupling of two interferometers under incoherent illumination: one is external to the probe, and one is placed at the distal end. The distal interferometer is common-path: interferences occur between the reference beam reflected at the tip of the probe and light backscattered by the tissue. The advantage compared to scanning systems is that it does not require any advanced miniaturized mechanical systems at the tip of the probe, which are likely to increase its diameter as well as its cost, and it can be adapted to any type of probe.

Here the probe we present is a 1 meter-long fiber bundle of 30,000 pixels for an outer diameter of 0.9mm with a 1 mm-diameter focusing GRIN lens at the distal end. The use of a fiber bundle in such an interferometric setup induces cross-talk phenomena between adjacent fibers and between modes inside each core, but we find imaging still possible. The axial and lateral resolutions are 1.8 and 4.9 µm respectively. We show ex vivo images on excised human breast tissue.

8575-24, Session 6

OFDI tethered capsule localization for unsedated gastrointestinal 3D imaging

Melissa W. Haskell, Massachusetts General Hospital (United States); Michalina J. Gora, Wellman Ctr. for Photomedicine (United States); Robert W. Carruth, Massachusetts General Hospital (United States); Martin Villiger, Guillermo J. Tearney, Wellman Ctr. for Photomedicine (United States)

Barrett’s esophagus is a metaplastic disorder that can undergo dysplastic progression, leading to esophageal adenocarcinoma. Upper endoscopy, which is costly and relatively inaccurate, is the standard of care for screening for BE. Optical frequency domain imaging (OFDI) has potential to overcome these shortcomings by detecting 3D microscopic tissue architecture is a non-sedated procedure.

We have developed a swallowable OFDI tethered capsule that enables real-time imaging of the esophagus through an unsedated procedure. In the first-generation capsule catheter distance between the capsule and the incisors was recorded using 5-cm-spaced marks on the tether. To improve OFDI tethered capsule 3D reconstruction, we have developed second-generation device with a laser sensing system tracking the tether’s movements during the imaging procedure. This tracking system is placed at the close vicinity of patient’s mouth and obtains data simultaneously with OFDI image acquisition.

In a pilot human study, we have successfully imaged the entire esophagus in 13 patients with the first generation capsule. When attempting to reconstruct the OFDI tethered capsule endomicroscopy dataset in three dimensions, we have found that peristalsis, breathing and cardiac motion, and inconstant pullback velocity impede reliable reconstruction. We have successfully tested the second-generation capsule in the laboratory setting for tracking the tether’s velocity in a manner that is non-invasive and designed to be comfortable for patients. We will test the device in a human study to validate that the new tracking sensor improves 3D reconstructions of OFDI images of the esophagus that are obtained in vivo.

8575-25, Session 6

Spiral-scanning, side-viewing optical coherence tomography endoscope for three-dimensional fully sampled in vivo imaging of the mouse colon

Weston A. Welge, College of Optical Sciences, The Univ. of

Arizona (United States); Jennifer K. Barton, The Univ. of Arizona (United States)

We have previously developed side-viewing endoscopic OCT systems to detect colorectal cancer in the murine model, which longitudinally scans the mouse colon at 8-16 discrete angular positions. This small number of angles is chosen to keep imaging time and the amount of data to analyze reasonable, but this azimuthal undersampling of the tissue may result in missed or incorrectly characterized adenomas. A need exists for a spiral-scanning OCT endoscope capable of generating 3D, in vivo OCT data sets that satisfy the Nyquist criterion for adequate sampling of the tissue.

Our new endoscopic system replaces the sample arm optics of a commercial OCT system (OCS1050SS, Thorlabs, Newton, NJ) with a spiral-scanning, gradient-index lens-based endoscope. The endoscope provides unit magnification at a working distance capable of producing a focal depth of 280 µm in tissue. The working distance accounts for a 41° rod prism that reflects the beam through the endoscopic window into the tissue while minimizing back reflection. A swept-source laser with a central wavelength of 1040 nm and spectral bandwidth of 80 nm provides an axial resolution of 12 ?m in air and 9 ?m in water. The endoscope has a theoretical diffraction-limited lateral resolution of 5.85 µm. We present fully sampled, 3D, in vivo images of the mouse colon and compare measurements of adenoma diameter to the 2D OCT system, as well as gold standard histology. Errors in diameter measurements of up to 42% are present in the 2D system, and nearly eliminated in the 3D spiral-scanning system.

8575-26, Session 6

Fluorescence-based SMC and OCT endoscope to study aberrant crypt foci in mouse model of colon cancer

Molly Keenan, The Univ. of Arizona (United States); R. Andrew Wall, College of Optical Sciences, The Univ. of Arizona (United States); Jennifer K. Barton, The Univ. of Arizona (United States)

The accepted model of colorectal cancer assumes the paradigm that aberrant crypt foci (ACF) are the earliest events in tumorigenesis and develop into adenoma, which further develop into adenocarcinoma. Under this assumption, basic research and drug studies have been performed using ACF as substitute markers for fully developed carcinoma. While studies have shown a correlation between the number of ACF present and the presence of adenoma/adenocarcinoma, a causal relationship has yet to be determined. The mouse has shown to be an excellent model for colorectal cancer; however, the outcomes of such experiments require sacrifice and histologic examination of ex vivo tissue. To better utilize the mouse model to study ACF and adenoma development, an endoscope was constructed for non-destructive in vivo surface visualization, molecular imaging and cross-sectional imaging of the colon. Our system combines surface magnifying chromoendoscopy (SMC) and optical coherence

tomography (OCT) to image colon microstructure. Sixteen mice, treated with the carcinogen azoxymethane, were imaged at 2 week intervals, to visualize carcinogenesis events. With this dual-modality system we are able to visualize crypt structure alteration over time as well as adenoma development over time.

8575-27, Session 6

OFDI tethered capsule endomicroscopy for unsedated gastrointestinal imaging

Michalina J. Gora, Wellman Ctr. for Photomedicine (United States); Jenny S. Sauk, Robert W. Carruth, Kevin A. Gallagher, Melissa J. Suter, Norman S. Nishioka, Massachusetts General Hospital (United States); Guillermo J. Tearney, Wellman Ctr. for Photomedicine (United States)

Currently, the gold standard for screening for Barrett's esophagus is videoendoscopy with subsequent biopsy, which is costly due in part to the requirement that patients typically be sedated prior to the procedure. Optical frequency domain imaging (OFDI) is an imaging technology that obtains comprehensive microscopy images of the esophagus in living patients without excising tissue. To date, we have used a balloon-centering catheter used in conjunction with sedated endoscopy to obtain comprehensive 3D microscopic images of the esophagus in patients.

We have developed a new technology that implements in-vivo microscopy in a swallowable capsule. The small capsule (12.8 x 24.6 mm) is connected to the OFDI instrument console through a flexible tether (OD ~1 mm and length ~1.6 m). The tether contains a rotating driveshaft, which encloses an optical fiber, delivering light to the optical probe focusing the near-infrared light at the tissue (30µm spot size). The tethered capsule catheter can be sterilized and reused.

We have tested the tethered capsule device in a human pilot study, where unsedated patients swallowed the capsule, providing real-time OFDI cross-sections while the device traversed the esophagus under the natural force of peristalsis. The tether allowed the operator to control position of the capsule in the esophagus also allowed for its retrieval, disinfection, and reusing. The entire procedure, including three-dimensional OFDI imaging of the entire esophagus repeated 4 times, lasted on average 6 minutes from capsule insertion to extraction.

These results demonstrate that comprehensive, unsedated microscopic imaging of upper GI tract organs is safe and feasible.

8575-28, Session 7

Achromatic surgical MEMS-based dual-axis confocal microscope for delineation of brain tumor margins

Steven Y. Leigh, Danni Wang, Ye Chen, Jonathan T. C. Liu, Stony Brook Univ. (United States)

A miniature achromatic MEMS-based confocal microscope based on a dual-axis architecture is presented. The device is an enhanced version of a previously described microscope that is now able to perform spatially coregistered fluorescence imaging at multiple wavelengths. This device has a 10 mm diameter scan head with a 2 mm diameter tip for convenient use during surgery to guide tumor resection. The MEMS mirror, which is adjustable to a focal depth of 20–200 micrometers, has its two orthogonal axes driven at their respective mechanical resonance frequencies, which enables imaging with an axial resolution of 9 micrometers and in-plane resolution of 4 micrometers over a field of view of 450 ? 450 micrometers. Simultaneous two-color imaging of individual optical sections is achieved by using a pair of volume phase holographic gratings paired with prism assemblies to compensate for chromatic dispersion in the 2-mm diameter gradient index (GRIN) relay lens at the distal end of the microscope. Experimental measurements of the axial response of the microscope as well as two-color images of a reflective bar target and fresh mouse brain tissues demonstrate the performance of our device and its potential for multicolor in vivo optical-sectioning microscopy.

8575-30, Session 7

Handheld multispectral dual-axis confocal microscope for cervical cancer screening

Pongsak Sarapukdee, Santi Rattanavarin, Numfon Khemthongcharoen, Ungkarn Jarujareet, Romuald Jolivot, National Electronics and Computer Technology Ctr. (Thailand); Il Woong Jung, Daniel Lopez, Argonne National Lab. (United States); Michael J. Mandella, Stanford Univ. School of Medicine (United States); Wibool Piyawattanametha, National Electronics and Computer Technology Ctr. (Thailand)

Cervical cancer is a leading cause of death in women around the world. Detection of precancerous lesions is essential strategies to reduce total incident rates of cervical cancer patients. Current techniques for precancerous detection need to be confirmed by histopathological examinations, which are time consuming and require medical experts to accurately diagnose the disease. Therefore, the goal is to develop a handheld multispectral dual-axis confocal (DAC) microscope for real-time in vivo cervical cancer screening.

The overall diameter of the DAC microscope is designed to be around 1 cm with a suitable length (20 cm) to image cervix. We used a gold coated MEMS scanner as a raster scanning element. Its die size is 3.25 ? 3.25 mm2 designed by Argonne National Laboratory and fabricated at Silex Microsystems. The laser source is a fiber coupled CW multi-wavelength generator (QIOPTIQ, UK). We coupled 561, 662, and 781 nm laser sources into a custom-made achromatic collimator made from a S630 single mode fiber and an achromatic lens NT65-568. The maximum insertion loss of the handheld microscope system is 30.8 dB at 662 nm laser wavelength. The measured full width at half maximum (FWHM) of transverse (X-Y direction) resolutions are 4.78, 5.77, 7.45 μm for 561 nm, 662 nm, and 781 nm, respectively while FWHM of axial (Z direction) resolutions are 6.2, 6.2, 5.6 μm for 561, 662, 781 nm, respectively. Multi-spectral imaging demonstration of the microscope is demonstrated on tissues biopsies (cervix and colon tissues) to demonstrate the capability of the microscope.

8575-31, Session 7

Vertical cross-sectional imaging by multi-color handheld dual-axes confocal microscope

Zhen Qiu, Xiyu Duan, Haijun Li, Choong-ho C. Rhee, Supang Khondee, Bishinu Joshi, Xiaoming Zhou, Kenn R. Oldham, Katsuo Kurabayashi, Thomas D. Wang, Univ. of Michigan (United States)

We have demonstrated vertical cross-sectional imaging with a near-infrared (NIR) dual-axes confocal fluorescence endomicroscope. This multi-color (671 and 785 nm) 3-dimensional (3D) handheld imaging instrument uses a novel 3D scanning mechanism that includes a 2-dimensional (2D) micro-mirror consisting of a resonant in-plane combdrive configuration MEMS scanner (RIMS) and z-axis actuation with a translational piezoelectric micro-motor. The 2D RIMS device, fabricated with a 4-mask SOI MEMS process, utilizes a parametric resonance mechanism. With low drive voltage, this scanner can achieve a large scanning angle (±6 deg mechanical) with a 200 Hz tunable frequency bandwidth close to resonance at ~3kHz. The dumb-bell shaped mirror is 2.71 mm in length and 650 um in width, and the surface is coated with Au/Cr to achieve optical reflectivity >90% from 671-785 nm. This compact NIR fluorescence imaging instrument has an outer diameter of 5 mm and a length of 20 mm at the distal end, and is fully packaged and sealed. A large field-of-view (800 um by 500 um) can be achieved in the XZ-plane with 5um lateral resolution and 7um translational resolution and 500um deep tissue penetration at 5 Hz frame rate. To demonstrate vertical cross-sectional imaging, we collect images from a 3D cyst phantom (ex = 671 nm) and from a 3D bead phantom with Cy5.5 (ex = 671 nm) and Cy7.5 (ex = 785 nm) fluorophores simultaneously. The XZ view shows the relationship among tissue micro-structures as they vary with depth. This instrument can achieve real time histopathology in vivo in the preferred view of pathologists.

8576-1, Session 1

Fabrication of a rugged polymer-coated silver hollow fiber with a vitreous film for the infrared

Katsumasa Iwai, Sendai National College of Technology (Japan); Mitsunobu Miyagi, Tohoku Institute of Technology (Japan); Yi-Wei Shi, Fudan Univ. (China); Yuji Matsuura, Tohoku Univ. (Japan)

A rugged hollow fiber is fabricated by all-liquid phase technique.

A silica glass capillary is used as the substrate and vitreous film is firstly coated on the inside of the capillary to protect the glass tube from moisture.

This protective coating keeps the thin-wall glass tube away from damage due to the following silver plating process.

On the protective coating, a silver film is deposited by a conventional mirror plating technique.

Subsequently, a polymer film is coated on the silver film to reduce transmission loss by employing interference effect of the polymer film.

Fabrication process and transmission properties of the rugged polymer-coated silver hollow fiber were discussed.

The loss for the 700-?m-bore size, 1-m-length rugged polymer-coated silver hollow fiber was 2 dB under straight condition, and 3.5 dB under the condition of a 270 degree bend with a 15-mm bending radius at the wavelength of 2.94 ?m.

8576-2, Session 1

Focused light delivery and all optical scanning from a multimode optical fiber using digital phase conjugation

Ioannis N. Papadopoulos, Salma Farahi, Christophe Moser, Demetri Psaltis, Ecole Polytechnique Fédérale de Lausanne (Switzerland)

In contrast to single mode optical fibers, multimode fibers offer a large number of degrees of freedom corresponding to the number of propagation modes in the fiber and therefore allow a higher peak power to be transmitted through. This feature, however, does not come without a cost, as the propagated field is coupled to the different modes and finally gets scrambled. In this context, control of light transmission through a multimode optical fiber is essential for the development of high-resolution endoscopes as well as for high power therapeutic applications.

We demonstrate the generation of a sharp focus spot (beam waist 2*w0 = 1.4?m) at the output of a multimode fiber (200?m core, 0.37 NA) using digital phase conjugation and we exploit the digital nature of the data to perform scanning of the focus spot over an area of 175?m diameter. Initially, a 532nm laser beam is focused at the distal end of the fiber and the speckled output at the proximal end is holographically recorded with a reference beam. The phase of the output speckle pattern is extracted and assigned onto a spatial light modulator (SLM) that is used to generate the optical phase conjugate field. The phase conjugate field is directed towards the proximal end of the fiber and comes into focus at its distal end. By focusing the excitation laser beam at different positions on the distal end of the fiber facet and recording the corresponding holograms, a look-up table is generated that allows scanning the focus spot over a region of 175?m diameter.

We believe that the generation of a sharp focus spot digitally scanned over the output end of a multimode fiber's tip is enabling new high resolution lensless endoscopic imaging modalities.

8576-3, Session 1

Dual-modality fiber-optic imager (DFOI) for intracellular gene delivery in human cervical cancer cell

Jaepyeong Cha, Jing Zhang, Saumya Gurbani, Min Li, Jin U. Kang, Johns Hopkins Univ. (United States)

Gene therapy is a fast growing method to treat cervical cancer, which is one of the major cancers among females. The most common optical method to validate cellular uptake of the gene is to detect tagged fluorescence signals from the cells that express fluorescence proteins. However, fluorescence detection is usually performed in vitro due to the limitation of commercially available standard microscopes. Therefore, to image the tissue in unperturbed physiological conditions, it is necessary to have an optical tool that enables the in vivo imaging of cancer cells. Advances in fiber optics have led to the development of several novel sub-cellular imaging methods, in vivo. Herein, we propose a highly sensitive dual-modality fiber-optic imager (DFOI), which permits ~3.5?m lateral resolution and can measure gene transfection efficiency. The DFOI used a 500 micron-diameter coherent fiber bundle as an imaging probe and two Silicon avalanche photodetectors for the simultaneous imaging of laser scanning confocal reflectance and fluorescent microscopy. Images obtained from both detectors were displayed simultaneously in near real-time at 1Hz. We have implemented an automated image analysis to calculate the number of fluorescent cells among the total cells in the imaging field of view (diameter: 460?m). To test the system performance we examined a non-viral gene delivery vector KDEL-CFP, the fluorescence tagged and targeted human cervical cancer cell lines (HeLa), in four commercially available reagents and compared the transfection efficiencies. Preliminary experimental results demonstrated that the DFOI is promising system for in vivo evaluation of intracellular gene delivery.

8576-4, Session 1

Numerical analysis of the diffusive mass transport in brain tissues with applications to optical sensors

Adrian Neculae, Univ. of West Timisoara (Romania); Andreas Otte, Univ. of Applied Sciences Offenburg (Germany); Dan Curticapean, Hochschule Offenburg (Germany)

In the brain-cell microenvironment, diffusion plays a crucial role: besides delivering glucose and oxygen from the vascular system to brain cells, it also moves informational substances between cells. The brain is an extremely complex structure of interwoven, intercommunicating cells, but recent theoretical and experimental works showed that the classical laws of diffusion, cast in the framework of porous media theory, can deliver an accurate quantitative description of the way that molecules are transported through this tissue. The mathematical modeling and the numerical simulations are successfully applied in the investigation of diffusion processes in tissues, replacing the costly laboratory investigations. Nevertheless, the modeling must rely on highly accurate information regarding the main parameters (tortuosity, volume fraction) which characterize the tissue, obtained by structural and functional imaging. One of the most promising techniques for obtaining the values for characteristic parameters of the transport equation is the direct optical investigation using optical fibers. The analysis of these parameters also reveals how the local geometry of the brain changes with time or under pathological conditions.

This paper presents a set of computations concerning the mass transport inside the brain tissue, for different types of cells. By measuring the time evolution of the concentration profile of an injected substance and using suitable fitting procedures, the main parameters which characterize the

tissue can be determined. This type of analysis could be an important tool in understanding the functional mechanisms of effective drug delivery in complex structures as the brain tissue.

8576-5, Session 1

Effects of sterilization methods on key properties of specialty optical fibers used in medical devices

Andrei A. Stolov, Brian Slyman, David T. Burgess, Adam S. Hokansson, Jie Li, R. Steve Allen, OFS Specialty Photonics Div. (United States)

Optical fibers with different types of polymer coatings were exposed to three sterilization conditions: multiple autoclaving, treatment with ethylene oxide and treatment with gamma rays. Effects of different sterilization techniques on key optical and mechanical properties of the fibers are reported. The primary attention is given to behavior of the coatings in harsh sterilization environments. The following four coating/buffer types were investigated: (i) dual acrylate, (ii) polyimide, (iii) silicone/PEEK and (iv) fluoroacrylate hard cladding/ETFE.

8576-6, Session 1

Laser-induced damage to large core optical fiber by high peak power laser

Xiaoguang Sun, Jie Li, OFS Specialty Photonics Div. (United States)

In this paper we will describe our experiment with laser-induced damage to large core multimode step index optical fiber. The laser used has a peak power up to 400kW and average power of 160W. A different failure mode of fiber was observed from those discussed in our previous studies with lower laser power level. We have tested different types of fibers with high power laser in a two point bend tester. The results will enable us to gain more knowledge about the new failure mechanism and optimize fiber design for delivering high peak laser power.

8576-7, Session 2

Flexible delivery of Er:YAG radiation at 2.94 µm with novel hollow-core silica glass fibres: demonstration of tissue ablation

Artur Urich, Robert R. J. Maier, Heriot-Watt Univ. (United Kingdom); Jonathan C. Knight, Fei Yu, Univ. of Bath (United Kingdom); Duncan P. Hand, Jonathan D. Shephard, Heriot-Watt Univ. (United Kingdom)

In this work we present the delivery of a high energy Er:YAG laser pulses operating at 2.94 ?m through a hollow-core negative curvature fibre (HC-NCF) and its use for the ablation of biological tissue. In HC-NCF fibres, which have been developed recently, the laser radiation is confined in a hollow core and by an anti-resonant or reflection principle (also known as ARROW). The fibre is made of fused silica which has high mechanical and chemical durability, is bio-inert and results in a fibre with the flexibility that lends itself to easy handling and minimally invasive procedures. The fibre structure consists of only one ring of capillaries around a very large core, followed by a protecting outer layer, hence the preform is easy to build compared to traditional (hollow-core) photonic crystal fibres. The core is constructed by a negative curvature (the curvature of the capillaries is opposite to the one of the fibre itself) of this inner ring structure. The measured attenuation at 2.94µm is 0.18dB/m with a single mode output beam profile. This is a significant advantage for surgical applications as the beam profile is maintained during fibre movement. We demonstrate high power delivery through this fibre, well above the thresholds needed for the ablation of biological tissue in non-contact and contact mode. Delivered energy densities reached > 750J cm-2 after 10 m of fibre.

This flexible high energy delivery system offers an alternative to existing beam delivery systems such as articulated arms and large core multi-mode fibres with enhanced capabilities.

8576-8, Session 2

Research on the FBG's high temperature sustainability influenced by the drawing process

Shuqiang Zhang, Feng Tu, Weijun Huang, Fei Liu, Jing Ma, Yingsong Li, Yangtze Optical Fibre and Cable Co., Ltd. (China)

The numerous potential applications of UV-induced fiber Bragg gratings (FBGs) in fiber optic sensing and telecommunications have generated a significant interest in this field in recent years. However, two major factors—the photosensitivity of the fiber in which the grating is written and the thermal stability of the grating—are of prime importance in terms of choosing the most appropriate fiber to use and of the long-term functionality of the grating over a wide range of temperatures. B/Ge-codoped fiber has been reported to give a much higher level of photosensitivity when compared with other fibers, and the technique of hydrogen loading can further enhance this property of the fiber, but the gratings written in these fibers, with or without pre-treatment or post-treatment, are reported to have a much poorer high-temperature stability.

Based on the plasma chemical vapor deposition (PCVD) process, the high Ge (Germanium) and Ge/B (Germanium/Boron) co-doped photosensitive fiber were developed. The photosensitive fibers with different drwaing temperature and drawing tension have been studied. Based on the experimental results obtained from studies of several kinds of photosensitive fiber on both the photosensitivity and the temperature sustainability of the FBGs written into them, the so-called cation hopping model has been used to explain, in which the size of the cation responsible for the temperature sustainability.

8576-9, Session 2

Large-mode area fiber for optical coherence tomography

Sucbei Moon, Kookmin Univ. (Korea, Republic of); Zhongping Chen, Beckman Laser Institute and Medical Clinic (United States)

We have investigated the use of multimode fiber in optical coherence tomography (OCT) with a mode filter that selectively suppresses the power of high-order modes (HOMs). With a moderate number of modes, a large-core fiber (LCF) is an attractive alternative to the conventional single-mode fiber (SMF) for its large mode area and the consequentially wide Rayleigh range of the exiting beam if the fundamental mode of the LCF was efficiently filtered by a mode filter installed in the middle. For this, a very simple scheme of mode filtering was developed with a fiber-coil mode filter. The LCF was coiled by an optimal bend radius with a fiber winder which was designed for reduced micro-bends. We also developed the methods of finding the optimal bend radius through theoretical analyses and experimental quantifications of the bend losses.

By utilizing the mode-filtered LCF, of which the core diameter was 20 micrometers, an OCT imaging probe was made with a very simple structure without an objective lens. This could be realized by the attractive feature of the mode-filtered LCF with a large mode area which allows a low divergence for the exiting beam to exhibit a long imaging range along the fiber axis. The OCT imaging capability was tested with a spectral-domain OCT at the conventional wavelength band of 1.3 micrometers. It has been successfully demonstrated that our mode-filtered LCF can provide a useful imaging or sensing probe without an objective lens which can greatly simplify the structure of the probing optics.

8576-10, Session 2

Dual-channel fiber-probe for simultaneous imaging of swept source optical coherence tomography and fluorescence spectroscopy

Eun Jung Min, Jae Hwi Lee, Jun Geun Shin, Byeong Ha Lee, Gwangju Institute of Science and Technology (Korea, Republic of)

We propose a dual concentric channel fiber scanning probe for simultaneous measurements of swept source optical coherence tomography (SSOCT) and fluorescence spectroscopy (FS). For the purpose, SSOCT and FS systems are combined by adopting the specially fabricated double cladding fiber (DCF) and wavelength division multiplexing (WDM) coupler. The DCF fiber in one of the output ports of the DCF coupler is directly used for the fiber-based probe of the sample arm. Moreover, the fiber was driven by a piezo bender for obtaining two dimensional OCT-FS image profile. Since the DCF has a dual channel configuration of core and inner cladding, it can deliver both the OCT and the FS signals at the same time. Therefore, the suggested system enables multifunctional imaging that would make it possible to determine a more specific diagnosis. The most advantage of the DCF-based dual-channel system is that both signals are emitting from the same fiber. Since both channels are concentric, we can use a common focusing lens without the problem of beam alignment. Introducing the piezo bender as a scanner, we can expect implementation of a practical system. To demonstrate the feasibility of the probe, a photosensitizer infected in-vivo mice was imaged with a scanning speed of 16 Hz and a scanning range of 2 mm.

8576-11, Session 3

Simultaneous measurement of radiation dose and strain using a micro-tapered long-period fiber grating incorporating an erbium-doped fiber

Young Bo Shim, Hyun-Joo Kim, Hanyang Univ. (Korea, Republic of); Young-Hoon Ji, Korea Institute of Radiological & Medical Sciences (Korea, Republic of); Young-Geun Han, Hanyang Univ. (Korea, Republic of)

We propose a new type of a hybrid sensing probe based on a micro-tapered long-period fiber grating (MT-LPFG) incorporating an erbium-doped fiber (EDF) for simultaneous measurement of radiation dose and strain. The effects of gamma radiation and strain on the transmission characteristics of the hybrid sensing probe based on the MT-LPFG and the EDF are investigated. The EDF was pumped by a 980 nm laser diode and its amplified spontaneous emission (ASE) light transmitted through the MT-LPFG was measured by using an optical spectrum analyzer. As the hybrid sensing probe based on the pumped EDF and the MT-LPFG was irradiated with 1.25-MeV 60Co gamma rays, the transmission was reduced because of the formation of the color center which absorbs the pump and the amplified spontaneous emission light. When the strain was applied to the hybrid sensing probe, the resonant peak of the MT-LPFG was shifted to shorter wavelengths because of the negative contribution of the photoelastic effect. Since the variation of the strain-induced refractive index modifies the coupling strength, the transmission of the MT-LPFG is also changed. By measuring the transmitted intensity and the resonant wavelength of the MT-LPFG, the radiation dose and strain can be determined simultaneously.

8576-12, Session 3

Real-time depth-resolved Raman endoscopy for in vivo diagnosis of dysplasia in Barrett's esophagus

Mads Sylvest Bergholt, Wei Zheng, Khek Yu Ho, Ming Teh, Khay Guan Yeoh, Jimmy B. Y. So, Zhiwei Huang, National Univ. of Singapore (Singapore)

Raman spectroscopy is a vibrational analytic technique sensitive to the changes in biomolecular composition and conformations occurring in tissue. With our most recent development of on-line near-infrared (NIR) Raman endoscopy integrated with depth-resolved Raman probe for selective interrogation of the epithelium, in vivo Raman tissue diagnosis (optical biopsy) during clinical gastrointestinal endoscopy has been realized under multimodal wide-field imaging (i.e., white- light reflectance (WLR), narrow-band imaging (NBI), autofluorescence imaging (AFI)) guidance.

A selection of 43 patients who previously underwent Raman endoscopy (n=146 spectra) was used to render diagnostic models for identifying dysplasia in Barrett's esophagus based on partial least squares - discriminant analysis (PLS-DA). The on-line Raman endoscopy technique was tested prospectively on (n=2) new esophageal patients for in vivo tissue diagnosis.

High quality in vivo Raman spectra can be acquired and evaluated in real-time within 0.5 sec during clinical endoscopic examinations. Significant differences in Raman spectra between normal and dysplastic tissue are observed reflecting the pathological transformation associated with Barrett's carcinogenesis (e.g., upregulated protein synthesis and elevated DNA content etc.). The depth-resolved Raman endoscopic technique developed could prospectively identify Barrett's dysplasia with a accuracy of 85.9% (sensitivity: 91.3% (21/23): specificity 83.3% (40/48)).

This study realizes for the first time real-time image-guided Raman endoscopy for in vivo diagnosis of precancer in the esophagus at the molecular level.

8576-13, Session 3

Microstructured optical fiber Bragg grating sensor for DNA detection

Alessandro Candiani, Michele Sozzi, Enrico Coscelli, Federica Poli, Annamaria Cucinotta, Alessandro Bertucci, Roberto Corradini, Univ. degli Studi di Parma (Italy); Maria Konstantaki, Foundation for Research and Technology - Hellas (Greece); Walter Margulis, Acreo AB (Sweden); Stavros Pissadakis, Foundation for Research and Technology - Hellas (Greece); Stefano Selleri, Sara Giannetti, Univ. degli Studi di Parma (Italy)

Microstructured optical fibers (MOFs) represent versatile photonic elements for sensing applications; the capillaries running along their length constitute a powerful microfluidic platform that can be surface functionalized for performing selective sensing experiments. Bragg reflectors inscribed in MOFs can be efficiently used for interrogating the changes occurring in the functionalized capillaries.

In this work the inner surface of a grape-fruit geometry MOF, where a Bragg grating was previously inscribed, has been functionalized using Peptide Nucleic Acid (PNA) probe, an OligoNucleotide (ON) mimic that is well suited for specific DNA target sequences detection. A solution of DNA molecules, matched with the PNA probes, has been infiltrated inside the fiber capillaries and hybridization has been realized according to the Watson - Crick Model. In order to achieve signal amplification, oligonucleotide-functionalized gold nanoparticles (ON-AuNPs) were then infiltrated and used to form a sandwich-like system. Experimental measurements show a clear wavelength shift of the high order mode in the reflected spectra for a 100 nM DNA solution. Several experiments have been carried out on the same fiber using the identical concentration,

showing the same modulation and proving a good reproducibility of the results, suggesting the possibility of the reuse of the sensor. Measurements have been also made using a 100 nM mis-matched DNA solution, containing a single nucleotide polymorphism, demonstrating the high selectivity of the sensor.

8576-14, Session 3

Hollow core photonic crystal fiber as a robust Raman biosensor

Altaf Khetani, Ali Monenpour, Jason Riordon, Vidhu S. Tiwari, Michel Godin, Hanan Anis, Univ. of Ottawa (Canada)

The present work demonstrates the integration of hollow core photonic crystal fibers (HC-PCF), microfluidics, and statistical analysis for monitoring biomolecules using Raman spectroscopy. HC-PCF as a signal enhancer has been proven by many researchers. However, there have been challenges in using HC-PCF for practical applications due to limitations such as coupling, stability, evaporation, clogging, consistent filling, and reusing the same fiber. This limited the potential of HC-PCF to detect low concentrations of liquid samples, which is why HC-PCF still hasn't transcended the lab barriers. The current device is based on an H-design lay-out which uses the pressure difference between the two ends of the fiber for filling and flushing the liquid samples. This mitigated several issues related to device performance by allowing us to fill the fiber with liquid samples consistently, rapidly and reproducibly. The resulting Raman signals were significantly more stable as various concentrations of ethanol in water were sequentially introduced into the fiber. The scheme also allowed us to overcome the barrier of predicting low concentrations by applying Partial Least Square (PLS) technique which was done for the first time using HC-PCF. Thus, the present scheme paves path for the inclusion of HC-PCF in the main stream point-of-care technology.

8576-15, Session 3

Augmenting convection-enhanced delivery through simultaneous co-delivery of fluids and laser energy with a fiber optic microneedle device

R. Lyle Hood, Rudy T. Andriani Jr., John L. Robertson, John H. Rossmeisl Jr., Christopher G. Rylander, Virginia Polytechnic Institute and State Univ. (United States)

Convection-enhanced delivery (CED) is a minimally-invasive surgical procedure for treatment of malignant glioma wherein a cannula is inserted into the CNS to a tumor site for local chemotherapy infusion. This study evaluated in vivo experiments using a novel, fiberoptic microneedle device (FMD) as a cannula capable of augmenting CED volumetric dispersal through co-delivery of laser energy during infusion. FMD technology is enabled by light-guiding capillary tubing capable of co-delivery (LTSP150375, Polymicro Technologies). The hypothesis is that non-damaging levels of photothermal heating (~42°C) will increase infusion dispersal volume.

Two FMDs were stereotactically placed in the brain parenchyma of anesthetized, male rats symmetrically in either hemisphere at a depth of 1.5 mm. Co-delivery was conducted at laser powers of 100-200 mW (1064 nm laser) and a fluid flow rate of 0.1 µL/min (2.5% albumin-bound Evans Blue). One FMD co-delivered laser and fluid simultaneously while the other delivered fluid alone (control). Both infusions were begun simultaneously and continued for one hour. Following infusion, the brains were immediately removed and formalin-fixed for 48 hours, after which the infusion sites were sectioned, stained, and inspected by a veterinary neurosurgeon. Quantitative analysis of the dye dispersal area in photographed sections was conducted through thresholding with ImageJ.

Results indicated that co-delivery improved dye dispersal over the infusion period. Area analysis of the stained sections showed a 322±0.35% increase in the section plane (N=3). These results indicate that the dispersal of infusates delivered through CED may be substantially improved through the simultaneous co-delivery of laser energy.

8576-16, Session 3

Controlled surgery using cw 2-µm laser systems with modified fiber tips

Rudolf M. Verdaasdonk, Vrije Univ. Medical Ctr. (Netherlands) and Free Univ. Amsterdam (Netherlands); Albert Van der Veen, Vrije Univ. Medical Ctr. (Netherlands); Tjeerd de Boorder, Herke Jan Noordmans, Univ. Medical Ctr. Utrecht (Netherlands); Peter Vandertop, Hans Daniels, Vrije Univ. Medical Ctr. (Netherlands); Aijt Pothen, Univ. Medical Ctr. Utrecht (Netherlands); Andreas Eing, LISA laser products (Germany)

The continuous wave 2 µm laser has proven to be a versatile tool for controlled ablation or cutting of tissue with hemostasis and minimal carbonisation due to effective tissue water vaporisation. The 2 µm wavelength can be considered 'eye safe' and fiber delivery enables endoscopic application in both air and water.

To improve the practical application in various endoscopic and robotic surgical procedures, the fiber delivery system was adapted by shaping the fiber tip for better control of the beam direction and enhancement of the tissue effect.

The optical characteristics of tapered, ball shaped and angled fiber tips and the ablation effects in tissues were studied using high speed and thermal imaging techniques. Beam properties were also analysed by ray-tracing. The modified tips were applied during surgery in the lungs to ablate diseased mucosa on the trachea wall, resection of tumors in the tongue and, in neurosurgery for 3rd ventriculostomy to treat hydrocephalus.

Due to an instant cyclic phase change between water and vapour, the beam direction can change dramatically and has to be accounted for in tip design and potential damage during clinical application. The tapered shape enabled precise contact surgery. An angled ball shape provides controlled side irradiation of the wall during endoscopic procedures e.g. in the trachea.

Modified fiber tips improve the control and versatility of the cw 2 µm laser for various clinical applications.

8576-17, Session 4

Ball lens fiber optic sensor based smart handheld microsurgical instrument

Cheol Song, Johns Hopkins Univ. (United States); Peter Gehlbach, Wilmer Eye Institute (United States); Jin U. Kang, Johns Hopkins Univ. (United States)

Dexterity and precision are required to perform the delicate freehand maneuvers necessary for vitreoretinal microsurgery. Here, we present an ergonomic design as well as medications that improve performance of our smart handheld microsurgical tool. The tool is composed of common path swept source optical coherence tomography (CP SS-OCT) and now incorporates a ball lens fiber optic distance sensor as well as a piezoelectric motor for tremor compensation. This increasingly practical surgical tool effectively suppresses unintended tool tip drift and dampens hand tremor while reacting to surgical target movement. The active compensation abilities of the tool are demonstrated by comparison of smart tool-assisted task performance to freehand performance.

We demonstrate that the ball lens fiber optic probe combined with a single mode fiber could increases the working angle of the tool to over 45 degree as compared to the limited working angle of the bare fiber sensor. This approach also increases the magnitude of the distance sensing

signal in water, which is optically analogous to vitreous body. The tool achieves real-time depth tracking using a PZT motor based closed-loop control scheme to "sense" and suppress unintended hand tremor on the order of 0-15 Hz. The tool allows more exact and versatile function during microsurgery. This novel microsurgical tool may serve as the platform used to combine dynamic fiber optic distance sensing and the motion cancellation scheme into one handheld instrument. Its clinical relevance includes increased stability and more precise instrument actions; micro-manipulation based cutting skills, minimization of clinical risk, and improved surgeon capabilities.

8576-18, Session 4

Non-circular core all silica fibers for irradiation and sensing medical applications

Bolesh J. Skutnik, CeramOptec Industries, Inc. (United States)

Medical treatments benefit from increased sharpness of radiation emission or detection. Non-circular core silica/silica optical fibers have benefits of better control of irradiation of diseased tissue and more uniform irradiations. Description of tested fiber structures and others available are presented.

Data will be presented on mechanical reliability of such fibers, primarily, medium-to-long term static fatigue experiments as well as shorter term strength experiments. Mandrel wrapped fibers in water environment are used to determine static fatigue in a wet environment similar to that of the human body. Samples have been tested from times as short as minutes up to about 2 years plus. The majority of testing was made on fibers with dimensions of 200x200 µm core :: 200x200/420/620/1100 structure Si/Si/ double plastic jacketing.

Weibull plot analysis yield static fatigue (SFN) parameters of 16-18 (negative slope of the Weibull plot) and intercepts at zero time of 7.4 to 7.8 GPa (750-800 Kpsi). Dynamic strength testing with a modified universal strength tester yield results in agreement with strengths determioned from short term static fatigue testing.

Spectral properties have been measured under several conditions. Generally the losses in the Vis to near-IR region as similar circular core fibers and depend on the chemistry and draw history of the core/clad materials. Losses in the UV depend on fiber dimensions a bit more thanfor circular core fibers of similar chemical and draw history.

Besides a flatter edge compared to circular core fibers, the loss of radial symmetry provides for more uniform output across the core face. Non-circular core silica/silca fibers have been found to have useful properties for sensing as well, which reflected on their use in astronomical applications in specialty telescope systems. They have been found to display mechanical properties remarkably as good as standard circular core fibers, with very high dynamic strengths and very good Static Fatigue Parameters.

8576-19, Session 4

Delivery systems with higher stability for 266 and 355-nm pulsed Nd-YAG laser light

Karl-Friedrich Klein, Cornell P. Gonschior, Technische Hochschule Mittelhessen (Germany); Moritz B. Klein, TransMIT GmbH (Germany); Jan C. Heimann, Technische Hochschule Mittelhessen (Germany)

In the past, the spectral stability of multimode UV-fibers in the deep UV-region has been mainly characterized using deuterium lamp with a broadband spectrum. Based on these results and for comparison of different UV fibers, the test procedures have to be standardized. Especially, the spectral UV-damage is length-dependent due to the variation of the optical power and spectral shape along the fiber. Current results for the preparation of a German test standard will be discussed in detail.

However, for fluorescence applications in analytics or sensing, improved pulsed Nd-YAG lasers with higher harmonics are interesting candidates for new systems. Because of the better beam quality, multimode with a core smaller than 100 µm or few-mode fibers can be recommended. On the other hand, the higher intensities stimulate higher UV-damage which can overlap with the laser wavelengths of 266 and 355 nm. Because of these new requirements, a new fiber design will be introduced here and specific fiber properties will be presented. Finally, the results of laser-induced UV-damage will be compared with above results using deuterium lamp.

8576-20, Session 4

Fluorescence image-guided photodynamic therapy of cancer cells using a scanning fiber endoscope

Eric J. Seibel, Mikias H. Woldetensae, Mark R. Kirshenbaum, Univ. of Washington (United States); Greg M. Kramer, Nortis Corp. (United States); Liang Zhang, Univ. of Washington (United States)

A scanning fiber endoscope (SFE) and cancer biomarker 5-aminolevulinic acid (5-ALA) were used to fluorescently detect and destroy superficial cancerous lesions, while experimenting with different dosimetry levels for concurrent or sequential imaging and laser therapy. The 1.6-mm diameter SFE was used to fluorescently image a confluent monolayer of A549 human lung cancer cells from culture, previously administered with 5 mM solution of 5-ALA for 4 hours. The SFE produced 500-line images of 405nm-excited fluorescence at 15 Hz using the red detection channel centered at 635nm. Twenty hours after therapy, cell cultures were stained to distinguish between living and dead cells using a laser scanning confocal microscope. To determine relative dosimetry for photodynamic therapy (PDT), 405nm laser illumination was varied from 1 to 5 minutes with power varying from 5 to 20 mW, all combinations delivering equal total energy delivered to the cell culture. The results show that PDT of A549 cancer cell monolayers using 405nm light for imaging and 5-ALA-induced PpIX therapy was possible using the same SFE system. Increased duration and power of laser illumination produced an increased area of cell death upon live/dead staining. The ultrathin and flexible SFE is able to direct PDT using wide-field fluorescence imaging of a monolayer of cultured cancer cells after uptaking 5-ALA. The correlation between light intensity and duration of PDT was measured. Increased length of exposure and decreased light intensity yields larger areas of cell death than decreased length of exposure with increased light intensity.

8576-21, Session 4

Development of a custom optical fiber device with four-wave mixing mitigation for CARS endoscopy

Pascal Deladurantaye, INO (Canada); Eric J. Seibel, Univ. of Washington (United States); Alex Paquet, David Gay, Michel Poirier, Benoît Fortin, Carl Larouche, INO (Canada); Brian C. Wilson, Ontario Cancer Institute (Canada); Ozzy Mermut, Jean-François Cormier, INO (Canada)

Coherent Anti-Stokes Raman scattering (CARS) endoscopy would be of significant clinical value for improving the specificity of cancer detection. However, implementing such a nonlinear technology in a fiber-based endoscope is challenging for several reasons. Principally, it is known that the propagation of the Stokes and pump waves in the core of a single-mode fiber leads to generation of a contaminating signal at the CARS wavelength, due to four wave mixing (FWM) processes in silica. Several approaches can be considered for the rejection of this FWM background; however, constraints inherent to scanning-mode operation and device compactness constitute practical limitations.

Here, we report on progress in developing a custom optical fiber device

that includes three potential approaches to mitigate the FWM effect for CARS endoscopy using: an ultra-high attenuation custom fiber module; cross-polarization propagation; and patterned rejection coating at the distal end of a custom double-clad polarization-maintaining fiber. Subsequently, we discuss the practical implementation of the special fiber device in a new spiral scanning-fiber endoscopic imaging technology developed at the University of Washington. This technology has ideal attributes for clinical use, including small footprint, adjustable field-of-view and high spatial-resolution up to video rates. Wide clinical applicability is anticipated, particularly in the early detection of endoluminal cancers without biomarker labeling.

8576-22, Session 4

Monitoring the impact of pressure on the assessment of skin perfusion and oxygenation using a novel pressure device

Jessica C. Ramella-Roman, Thuan Ho, Du V. N. Le, Pejhman Ghassemi, Thu Nguyen, The Catholic Univ. of America (United States); Alison Lichy, Suzanne Groah, National Rehabilitation Hospital (United States)

Skin perfusion and oxygenation is easily disrupted by imposed pressure. Fiber optics probes, particularly those spectroscopy or Doppler based, may relay misleading information about tissue microcirculation dynamics depending on external forces on the sensor. Such forces could be caused by something as simple as tape used to secure the fiber probe to the test subject, or as in our studies by the full weight of a patient with spinal cord injury (SCI) sitting on the probe. We are conducting a study on patients with SCI conducting pressure relief maneuvers in their wheelchairs. This study aims to provide experimental evidence of the optimal timing between pressure relief maneuvers. We have devised a wireless pressure-controlling device; a pressure sensor positioned on a compression aluminum plate reads the imposed pressure in real time and sends the information to a feedback system controlling two position actuators. The actuators move accordingly to maintain a preset value of pressure onto the sample.

This apparatus was used to monitor the effect of increasing values of pressure on spectroscopic fiber probes built to monitor tissue oxygenation and Doppler probes used to assess tissue perfusion.

8576-23, Session 5

Mid-infrared fiber optic approach for detecting surface biochemical contamination using Fourier transform infrared (FTIR) spectroscopy

Moinuddin Hassan, Xin Tan, Ilko Ilev, U.S. Food and Drug Administration (United States)

Surface organisms of medical devices play a critical role as they control many clinical properties including immediate response from the biological host. Accurate and real-time identification of microorganisms is clearly of great importance in medical fields to protect patient from high risk infection. Currently, some of the conventionally applied clinical detection methods are based on swab/wipe sampling, subsequent extraction and ex-situ detection using techniques such as High Performances Liquid Chromatography or Enzyme Immunoassay. However, since these techniques suffer from inefficiency and complexity, some alternative real-time, non-contact and quantitative methods to identify the presence of microorganisms in clinical setting are needed. In the present study, we demonstrate a FTIR fiber-optic based sensing approach for remote and in-situ measurement of biochemical contaminations on medical device surfaces in the mid-infrared (MIR) spectral range of 2.5 micron to 11 micron. A two-fiber sensor probe was designed using hollow fibers with a core diameter of 750 micron and a numerical aperture of 0.05. One of the fibers (illuminating) is coupled to the FTIR light source (Halogen) and the other fiber (detecting) to the FTIR detector (liquid Nitrogen cooled MCT). The measurements were carried out in a diffuse reflections mode. Protein samples of different concentrations under dry condition were used to investigate the sensitivity of the system. The results were validated by comparing with similar measurements using a conventional FTIR microscope setup.

8576-24, Session 5

Calcium detection in muscle tissue with fiber-optic based biofluorometer and UV-LED excitation

Mathias Belz, World Precision Instruments, Inc. (Germany); Alexander Dickson, Xavier O. Acevedo, World Precision Instruments, Inc. (United States); Karl-Friedrich Klein, Technische Hochschule Mittelhessen (Germany)

The detection of calcium in muscle fibers is of great importance to physiological research. This paper describes the design of a new UV-LED and fiber-optic based fluorescence detection system using the ratiometric properties of the fluorescent dye Fura-2 to measure free calcium in muscle fibers. The biofluorometer excites the muscle tissue alternatively at 340 nm and 380 nm wavelength using UV-LEDs. The respective emission, filtered limited around 510 nm wavelength, is detected with a miniature photomultiplier tube. Light is guided to and from the muscle tissue strips of 0.5 mm diameter and 3mm length by a newly designed fiber optic probe optimized for high light efficiency. Free calcium is detected in the physiological range by calculating the ratio of light emission excited at 340 nm and 380 nm respectively. Up to 1000 ratios per second can be measured. In parallel, a muscle analog consisting of a capillary tube with an inner diameter of 550 micrometer was designed. Studies on power budget, ratiometric dynamic range, linearity and signal to noise ratio have been carried out. Preliminary results on life muscle tissue will be reported.

8576-25, Session 5

Optical fiber probe for all-optical photoacoustic measurement

Yusuke Miida, Yuji Matsuura, Tohoku Univ. (Japan)

Combination of an optical-fiber based photoacoustic probe and a hollow optical fiber for laser light transmission is developed for all-optical photoacoustic endoscopy imaging. The photoacoustic fiber probe detects ultrasound by a thin polymer film attached at the end surface of silica optical fiber.It is confirmed that the sensitivity and frequency characteristics are comparable to PVDF hydrophone. In this presentation, experimental results of photoacoustic imaging are also shown.

8576-26, Session 5

Hollow waveguide with multiple dielectric layer for infrared cavity-ring-down spectroscopy

Ryo Ichikawa, Takashi Katagiri, Yuji Matsuura, Tohoku Univ. (Japan)

Ultra-low loss hollow waveguides with multiple dielectric layers are designed and fabricated for use in cavity ring-down spectroscopy. The waveguides are composed of four glass strips with dielectric multilayer that are formed in advance. Experimental results show that waveguides with three dielectric layers have lower losses at a target wavelength in the infrared than those with a single dielectric layer.

8576-27, Session 5

Measurement of blood glucose by infrared spectroscopy using hollow-optical fiber probe

Yuki Tanaka, Saiko Kino, Yuji Matsuura, Tohoku Univ. (Japan)

An infrared spectroscopy system based on a hollow-optical fiber probe for measurement of blood glucose concentration is developed. The probe consists of a flexible hollow-optical fiber and an ATR prism attached at the distal end of the fiber. This flexible probe enables measurement of oral mucosa and ear lobes that have blood capillaries near the skin surface. Experimental results show that absorption peaks of blood glucose are detected by the system. To improve measurement accuracy and reproducibility, precise control of area of prism that contacts on the sample surface.

8576-30, Session 5

Whispering gallery mode aptasensors for detection of blood proteins

Silvia Soria, Gualtiero Nunzi Conti, Andrea Barucci, Istituto di Fisica Applicata Nello Carrara (Italy); Simone Berneschi, Istituto di Fisica Applicata Nello Carrara (Italy) and Centro Fermi (Italy); Lorenzo Lunelli, Fondazione Bruno Kessler (Italy) and IBF-CNR Univ. of Trento (Italy); Cecilia Pederzolli, Laura Pasquardini, Fondazione Bruno Kessler (Italy); Masimiliano Insinna, Simone Salvadori, Univ. degli Studi di Firenze (Italy)

Whispering gallery mode resonators (WGMR) have been recently proposed as an efficient tool for the realisation of optical biosensors. A crucial step for producing reliable biosensors is their surface functionalization. In this work we report a functionalization process based on the use of a DNA aptamer. After a piranha activation, the WGMR was immersed in a mercaptopropyltrimethoxysilane (MPTMS) toluene solution. Two different thrombin and one vascular endothelial growth factor (VEGF) specific aptamers were then immobilized on WGMR. The silanization efficacy was evaluated morphologically by means of AFM (Atomic Force Microscopy) measurements. Using a fluorescent derivative of both aptamers, their immobilization was evaluated in terms of homogeneity using confocal microscopy analysis. Also the optical characterization of the functional WGMR was performed, confirming that their resonance properties are little affected by the treatments. The characterization of the immobilized aptamer layers suggests that a suitable density of biorecognition molecules is obtained.

The sensor performance for thrombin and VEGF detection was first characterize in tris(hydroxymethyl)aminomethane (TRIS) buffer. Control experiments with non-sense aptamers for testing the specificity were also performed. Then the potential use of the WGMR as a clinical laboratory testing device for blood protein detection was modeled and tested by measuring thrombin in 10% diluted, non-filtered human serum samples[1].

[1] L. Pasquardini, S. Berneschi, A. Barucci, F. Cosi, R. Dallapiccola, L. Lunelli, G. Nunzi Conti, C. Pederzolli, and S. Soria, “Whispering Gallery Modes Aptasensors for detection of blood proteins”, J. Biophotonics 1–10 (2012) / DOI 10.1002/jbio.201200013

8576-33, Session 5

Design and fabrication of multilayer thin film coated hollow waveguides for enhanced infrared radiation delivery

Carlos M. Bledt III, Jeffrey E. Melzer, James A. Harrington, Rutgers, The State Univ. of New Jersey (United States)

Metal coated Hollow Glass Waveguides (HGWs) incorporating single dielectric thin films have been widely used for the low-loss transmission of infrared radiation in applications ranging from surgery to spectroscopy. While the incorporation of single dielectric film designs have traditionally been used in metal/dielectric coated HGWs, recent research has focused on the development of alternating low/high refractive index multilayer dielectric thin film stacks for further transmission loss reduction. Continuing advances in the deposition of optically functional cadmium sulfide and lead sulfide thin films in HGWs have allowed for the simultaneous increase in film quality and greater film thickness control necessary for the implication of such multilayer stack designs for enhanced reflectivity at infrared wavelengths. This study focuses on the theoretical and practical considerations in the development of such multilayer stack coated waveguides and presents novel results including film growth kinetics of multilayer stack thin film materials, IR spectroscopic analysis, and IR laser attenuation measurements. The effects of incorporating progressive alternating cadmium sulfide and lead sulfide dielectric thin films on the optical properties of next generation dielectric thin film stack coated HGWs in the near and mid infrared regions are thoroughly presented. The implications of incorporating such dielectric multilayer stack coatings based on metal sulfide thin films on the future of IR transmitting hollow waveguides for use in applications ranging from spectroscopy, to high laser power delivery are briefly discussed.

8576-34, Session 5

Mid-infrared (IR) – a hot topic: the potential for using mid-IR light for non-invasive, early-detection of skin cancers in vivo

Angela B. Seddon, The Univ. of Nottingham (United Kingdom)

The tremendous significance of mid-IR spectroscopic sensing is highlighted. The remarkable progress made towards mid-IR spectral in vitro mapping of tissue and cancer detection is reviewed, with emphasis on diagnosis of skin cancer. The status quo of chalcogenide glass mid-IR fibreoptics and photonics for meeting opportunities for remote mid-IR sensing in general, and in in vivo cancer detection in particular, is assessed. Raman spectroscopy is a sister technique to mid-IR spectroscopy. The current success of Raman spectroscopy in medical diagnosis is appraised, with particular emphasis on Raman spectral imaging of tissue towards skin cancer diagnosis in vivo, based on a silica-glass fibreoptic sensor-head. The challenges to be met in chalcogenide glass science and technology towards facilitating analogous fibreoptic diagnostics based on mid-IR spectroscopy are addressed.

8576-28, Session PSun

Real-time optical fiber dosimeter probe

Hyun-Joo Kim, Young Bo Shim, Young-Hoon Ji, Young-Geun Han, Hanyang Univ. (Korea, Republic of)

We have fabricated a PMMA (poly-methyl-methacrylate) film-coated D-shaped optical fiber dosimeter probe for real-time radiation sensing applications. The D-shaped fiber with was firstly fabricated using a side polishing technique and then, the PMMA solution (MICROCHEM Corp., OCG PMMA 950K resist, solids: 7% in chlorobenzene) was spin-coated on the polished region of the D-shaped fiber. The remaining length of cladding region and the thickness of the PMMA film were estimated to be 1 ?m and 10 ?m, respectively. As the PMMA film plays a role in the formation of multimode slab waveguide, the resonant mode coupling between the D-shaped fiber and the PMMA overlay produces the harmonic resonant peaks in the transmission spectrum. The effect of gamma radiation on the transmission characteristics of the PMMA film-based D-shaped fiber probe was investigated. If PMMA film coated on the D-shaped fiber is exposed to gamma radiation, their optical properties are changed due to the main-chain scission and crosslinking in the PMMA matrix. As the PMMA film-based D-shaped fiber was

irradiated with 1.25-MeV 60Co gamma rays, the resonant wavelength was linearly shifted to shorter wavelengths due to the refractive index change of the PMMA film. The resonant wavelength shift of ~40 nm was observed for total dose of 10 kGy at dose rate of 100 Gy/h. Consequently, the radiation-induced refractive index change resulted in the resonant wavelength shift of the proposed optical fiber dosimeter, and the radiation sensitivity and resolution of the proposed optical fiber dosimeter were estimated to be -4 pm/Gy and 35 Gy, respectively.

8576-29, Session PSun

A glucose concentration measurement method based on fiber optic surface plasmon resonance sensor

Dachao Li, Zhu Rui, Peng Wu, Tianjin Univ. (China)

A glucose concentration measurement method based on fiber-optic surface plasmon resonance (FO-SPR) is proposed to achieve online, real-time detection of human blood glucose concentration by miniaturized sensor. The end-reflection structure of FO-SPR sensor was simulated and the impact of different parameters on sensor performance was analyzed as follows: when the fiber diameter increases, the normalized light intensity increases but curvature radius and attenuation of the SPR curve change small; The normalized light intensity and curvature radius decrease as the length of sensor area increases; When the gold film thickness increases, the SPR curve has a red shift and a larger curvature radius, the attenuation becomes larger first and then smaller; The impact of chromium layer thickness is little. The optimized structural parameters of FO-SPR sensor were obtained as follows, fiber diameter: 600?m, the length of the sensing area: 15mm, gold film thickness: 50nm, the thickness of chromium layer: 3-5nm. The FO-SPR sensor was manufactured according to the optimized parameters. A glucose concentration measurement system was set up, including halogen light source (360nm-2000nm), transmission fiber, Y-type optical fiber coupler, FO-SPR sensor, spectrometer (200nm-1000nm). Different concentrations of glucose solution were measured and the relationship between the concentration of glucose solutions and SPR resonance wavelength was obtained. The experiment results show that the correlation coefficient of fitting curve of glucose concentration and SPR resonance wavelength reaches 0.97386 within the human blood glucose concentration range of 0?200mg/dL. The measurement repeatability is also proved to be able to meet the requirements of blood glucose concentration detection in clinics.

8576-31, Session PSun

Interventional operation OCT probe with the function of real time temperature monitoring

Yuan Guo, Johns Hopkins Univ. (United States); Lian suo Wei, Qiqihar Univ. (China); Xuan Liu, Johns Hopkins Univ. (United States)

OCT is playing an important role in interventional operations now. And in many interventional operations the temperature of the tissue is one of the main factors that will influent the operation effect. So monitoring the temperature the operational tissue real time is critical for the operation. In this paper an OCT probe for interventional operation with real time temperature monitoring function was presented.

The probe contains two main parts. One is a micro OCT probe; the other is a fluorescence optical fiber thermometer. These two parts were installed in a base with a transparent shell and shared one light source. The optical fiber introduced the light and radiated to the reflector prism, which was stuck to the rotor of the front-motor, through a Grin lens. Then the light could be focused and irradiated to the operational tissue. And the motor drove the prism to realize rotating scan. At the same time the thermometer, which is along with the OCT probe, can monitor the temperature of the operational tissue real time. There are four basic components in the fluorescence thermometer: excitation light source, fluorescence sensitive material, optical detector and the circuit. The excitation light walked along the optical fiber and reached the fluorescence material stuck to the front of the optical fiber. Then the fluorescence material was excited. The excited fluorescent light would then be passed back along the optical fiber. And it can be detected by the photo detector and was transformed to the electrical signal. By amplified and filtered in the circuit, it was sent to the computer. Then the temperature can be get by processing the signals in the computer.

With this kind of interventional OCT probe that has the function of monitoring temperature, the optical biopsy can be realized and meantime the temperature of the operational tissue can be get. It will has broad clinical and research foreground especially in some significant interventional operations that temperature demanded strictly.

8576-32, Session PSun

Monitoring of the degradation in the rat's articular cartilage inducing osteoarthritis using common-path Fourier-domain optical coherence tomography

Chul-Gyu Song, Yong Kyun Oh, Dong Ho Shin, Jeong Hwan Seo, Min Ho Kim, Chonbuk National Univ. (Korea, Republic of); Jin U. Kang, Johns Hopkins Univ. (United States)

The objective of this experiment is to evaluate the utility and limitations of optical coherence tomography (OCT) for real-time, high-resolution structural analysis. We monitored the degradation of the rat's articular cartilage inducing osteoarthritis (OA) and the change of the rat's articular cartilage recovery by treatment medication, using our developed common-path Fourier-domain (CP-FD) OCT. Also, we have done a comparative analysis the rat's articular cartilage and OA grade. To observe the progression of OA, we induced OA by injecting the monosodium iodoacetate (MIA) into the right knee joint. After the injection of MIA, we sacrificed the rats at intervals of 3 days and obtained OCT and histological images. OCT and histological images showed the OA progress of similar pattern. These results illustrated the potential for non-invasive diagnosis about the grade of OA using CP-FD OCT.

The objective of this experiment is to evaluate the utility and limitations of optical coherence tomography (OCT) for real-time, high-resolution structural analysis. In this study, we induced OA into rat's knee joints and observed the stages of OA at weekly intervals. The progression of OA was monitored using CP-FDOCT. The results using the CP-FDOCT system were compared to biopsy results. A super-luminescent diode (D-855, Superlum Diode Ltd., Ireland) with the central wavelength of 846.5 nm; the spectral full-width at half maximum (FWHM) of ~100 nm was used as the light source; and the axial resolution of our system was found to be 3.153 um. The beam splitter used a 50/50 coupler (FC850-40-50-APC, Thorlabs Inc., USA) and only one branch on the right side because the reference signal simply used the reflected signal from the distal end of the fiber optic probe. To control the actuators and to perform image processing in our motorized stage–based CP-FDOCT system, OCT acquisition software was developed using the LabVIEW platform. In the histology after 1 week of exposer to MIA, a rough surface of cartilage was shown. In the week-2 image, the right part of the cartilage was degenerated, and the cartilage cell generally was destroyed. In the week-3 image, the whole cartilage surface had degenerated. The thickness of cartilage also was thin, and calcification had progressed too far. The OCT images acquired with the CP-FDOCT system show patterns similar to those in the corresponding histology. In this paper, a technique for the micrometer-scale imaging of arthritis cartilage using a high-resolution CP-FDOCT system, which is simpler than the conventional OCT system with two arms, has been proposed. In the OCT image, abnormalities such as cartilage destruction were indicated and matched up with the pattern of the histology. The possibility of having an inexpensive, real-time, high-resolution, nondestructive diagnosis technique for articular cartilage could be realized by combining the use of the endoscope with other clinical imaging techniques. In future work, we plan to make a real-time 3D OCT system for imaging osteoarthritis.

8577-1, Session 1

The efficacy of Stokes Shift Spectroscopy to detect prostate and breast cancer in human tissues

Yang Pu, Wubao Wang, Yuanlong Yang, Robert R. Alfano, The City College of New York (United States)

Stokes Shift Spectroscopy (S3) offers a novel way to rapidly measure spectral fingerprints of complex molecular mixtures in tissue. The changes of key fluorophores from normal state to the malignant state can be reflected by alteration of S3 profiles. S3 measurements can be used to acquire enough information of different key fluorophores in one spectrum to speed up spectral acquisition time. It is desirable to achieve the efficiency by employing a single scan to obtain most critical information of the fingerprints of main fluorophores, which are valuable for cancer detection.

In this study, we demonstrate the usefulness of the S3 technique to distinguish the malignant samples from the normal specimen in breast tissues. The optimal wavelength shift constant (delta_lamda_c) of S3 measurements for the purpose of breast cancer detection will be determined and the reason will be discussed explicitly. The underlying physical and biological basis for S3 for the purpose of cancer detection will be discussed. We investigate the reason why S3 is superior over absorption, fluorescence and Excitation-Emission Matrix (EEM) measurements for cancer detection in tissue. For the first time, this presentation explicitly discloses how and why S3 is superior in comparison with other conventional spectroscopic techniques. We show the optimal delta_lamda_c for breast cancer detection. This study demonstrates that the S3 measurements can be used to acquire information of different key fluorophores in one spectrum and used to investigate the changes of the relative content of the key fluorophores in breast tissues during the development of cancer.

8577-2, Session 1

Diagnosis of colorectal cancer using autofluorescence combined with diffuse reflectance spectra

Lina Liu, Fujian Normal Univ. (China) and Fujian Normal Univ. (China); Zhihai Qiu, Yingbin Nie, Fujian Normal Univ. (China); Weihua Li, Fujian Provincial Hospital (China); Lisheng Lin, Shusen Xie, Buhong Li, Fujian Normal Univ. (China)

Autofluorescence (AF) and diffuse reflectance (DR) spectra of freshly excised colorectal tissues were obtained using a fiber optic probe-based portable optical system for diagnostics. A Y-type optic fluorescence probe with one fiber for detection and seven for excitation was used for light transmission. The light emanating from the tissue surface is delivered to a USB-based miniature fiber optic spectrometer. The AF under 337 nm excitation and DR spectra using a tungsten halogen light source with wavelength range of 360-2000 nm were sequentially measured. The fluorescence spectra of pure fluorophores known in colorectal tissues such as collagen, nicotinamide-adenine dinucleotide (NADH) were also measured with 337 nm excitation. AF spectra distorted by the effects of optical absorption and scattering in tissues were corrected by the corresponding DR spectra. The corrected spectra were analyzed using multivariate curve resolution (MCR) to reveal changes of relative contents of endogenous fluorophores in colorectal tissue. An algorithm combined principal component analysis (PCA) with Fisher's discriminant analysis (FDA) was developed for tissue classification with the corrected spectra. PCA was used to reduce the dimensionality of corrected AF spectra, while FDA was then performed to predict the tissue disease state with a leave-one-out cross validation. The results suggest that AF combined with DR spectra, in conjunction with MCR analysis and PCA-based FDA algorithm, have the potential to distinguish different colonic tissue types with higher sensitivity and specificity.

8577-3, Session 1

In vivo fluorescence lifetime imaging for detection of cancer biomarkers

Yasaman Ardeshirpour, Victor Chernomordik, Moinuddin Hassan, Rafal Zielinski, Jacek Capala, Amir Gandjbakhche, National Institutes of Health (United States)

Amplification of Human Epidermal Growth Factor 2 (HER2/neu) gene and overexpression of its receptor has been diagnosed in approximately 20-30% of invasive breast cancer cases. It is one of the important factors that is involved in poor porognosis and resistance to traditional chemotherapy treatments. Therefore, it is important to characterize the expression of the HER2 receptors in order to optimize the treatment procedure for these patients.

Current diagnostic gold standards for detection of HER2 expressions are semi-quantitative and are based on ex vivo methods, such as immunohistochemistry (IHC) and fluorescent in situ hybridization (FISH). These methods are all invasive and require biopsies from tissue specimens. However, inherently, biopsies have a risk of missing the malignant lesion and limitation of covering the details of whole heterogeneity of the tumor.

Fluorescence lifetime imaging is an imaging technique based on the differences in the exponential decay rate of fluorescent signal. In this study, we have designed a fluorescence probe specific to HER2 receptors and injected to nude mice with different level of HER2 expression. The lifetime of fluorescence at the tumor and contralateral sites was measured in-vivo and the correlation between the fluorescence lifetime and the level of HER2 overexpression has been studied.

8577-4, Session 2

Autofluorescence microscopy with sub-300 nm excitation for cellular diagnostics

Timothy E. Renkoski, College of Optical Sciences, The Univ. of Arizona (United States); Bhaskar Banerjee M.D., The Univ. of Arizona College of Medicine (United States); Logan R. Graves, College of Optical Sciences, The Univ. of Arizona (United States); Nathaniel S. Rial M.D., The Univ. of Arizona College of Medicine (United States); Brenda Baggett, Urs Utzinger, The Univ. of Arizona (United States)

Diagnosis of cancer in organs such as the breast and pancreas often involves a needle biopsy used to retrieve representative cells from a mass. The current cytologic procedure requires staining and careful evaluation by a skilled cytopathologist. Diagnostic results are delayed by this process and still lack the desired sensitivity and specificity. We have developed a novel fluorescence microscope including excitation below 300 nm to image the native fluorescence of living cell samples. Multiple excitation wavelengths allow us to rapidly measure distributions and levels of tryptophan, NADH, and FAD. These images are used to monitor cell functions which have been shown to change in cancerous cells. Tryptophan is tied to protein production, while NADH and FAD are involved in cell metabolism. We have taken images of living cells isolated from rat and human pancreas which show strong autofluorescence in response to UVC excitation and unique visualization of subcellular structure. We have also imaged cultured human cell lines of the breast and pancreas to identify differences in fluorescence intensity and cell structure between normal and cancerous cells. It is anticipated that a distinction in cell status will arise from the analysis. These results are in progress and will be presented at conference. This technique is of special interest because very few images of tryptophan fluorescence exist in the literature and high contrast is obtained without a stain. The work may lead to an accurate and more rapid diagnosis of cells obtained from needle biopsy.

8577-5, Session 2

Large area mapping of excised breast tissue by fluorescence confocal strip scanning: a preliminary feasibility study

Bjorg A. Larson, Sanjeewa Abeytunge, Melissa Murray, Milind Rajadhyaksha, Memorial Sloan-Kettering Cancer Ctr. (United States)

Lumpectomy, in conjunction with radiation and chemotherapy drugs, together comprise breast-conserving treatment as an alternative to total mastectomy for patients with breast tumors. The tumor is removed in surgery and sent for pathology processing to assess the margins, a process that takes at minimum several hours, and generally days. If the margins are not clear of tumor, the patient must undergo a second surgery to remove residual tumor. This re-excision rate varies by institution, but can be as high as 60%. Currently, no intraoperative microscopic technique is used routinely to examine tumor margins in breast tissue. A new technique for rapidly scanning large areas of tissue has been developed, called confocal strip scanning, which provides high resolution and seamless mosaics over large areas of intact tissue, with nuclear and cellular resolution and optical sectioning of about 2? microns. Up to 3.5 x 3.5 cm2 of tissue is imaged in 13 minutes at current stage speeds. This technique is demonstrated in freshly excised breast tissue, using a mobile confocal microscope stationed in our pathology laboratory. Twenty-five lumpectomy and mastectomy cases were used as a testing ground for reflectance and fluorescence contrast modes, resolution requirements and tissue fixturing configurations. It was concluded that fluorescent imaging provides the needed contrast to distinguish ducts and lobules from surrounding stromal tissue. Therefore the system was configured with 488 nm illumination, with acridine orange fluorescent dye for nuclear contrast, with the aim of building an image library of malignant and benign breast pathologies.

8577-6, Session 2

Steady state and time-resolved fluorescence spectroscopic characterisation of normal and cancerous urine

Rajasekaran Ramu, Prakasarao Aruna, Anna Univ. Chennai (India); Munusamy Balu David, Arignar Anna Memorial Cancer Hospital & Research Institute (India); Dornadula Koteeswaran, Meenakshi Ammal Dental College & Hospital (India); Kulandaivel Muthuvelu, Stanley Medical College and Hospital (India); Rai R., Dr. Rai Memorial Cancer Institute (India); Singaravelu Ganesan, Anna Univ. Chennai (India)

Urine is one of the diagnostically important bio fluids, as it has many metabolites and some of them are native fluorophores. There may be a variation in the distribution and the physiochemical properties of the fluorophores during any metabolic change and pathologic conditions. Fluorescence spectroscopy has been considered as a promising tool to characterize the fluorophores present in the urine. This is because, it is sensitive even at trace level, sensitive to the micro environmental changes and has many complementary techniques. In this study, we aimed at characterising the urine of both normal and patients with confirmed cancer using steady state and time-resolved fluorescence spectroscopy. Attempts were also made to statistically discriminate the cancer patients from normal subjects. The results of fluorescence emission spectral signatures and excited state kinetics of urine of normal subjects and cancer patients and its statistical significance will be discussed.

8577-7, Session 2

Time-resolved fluorescence polarization for breast cancer detection in vitro using an octreotide-indocyanine green conjugate

Laura A. Sordillo, Giovanni Milione, Peter P. Sordillo, Bidyut Das, Wubao Wang, Samuel Achilefu, Robert R. Alfano, The City College of New York (United States)

Time-resolved fluorescence was used to investigate malignant and normal adjacent breast tissues stained with a conjugate of indocyanine green, an FDA approved near-infrared dye, and octreotide, a somatostatin receptor ligand. Somatostatin is a naturally occurring human hormone with important effects on cell growth, blood sugar and many other regulatory functions. Somatostatin receptors can occur on human cancers, may be crucial to their development, and may be important determinants of their aggressiveness. Somatostatin receptors may also be important in determining patient prognosis and response to therapy. The cancer studied was a high-grade ductal carcinoma which was estrogen receptor, progesterone receptor and HER-2-neu positive (triple positive). The tumor was Ki-67, p53, E-cadherin and p120 catenin positive, but BCL 2 negative.

A marked increase in fluorescence lifetime intensity was seen in the breast cancer sample compared to the normal sample. A fast fluorescence lifetime decay of the parallel component and slow decay of the perpendicular component was observed due to the molecular rotation of the conjugate solution. These results confirm that somatostatin receptors occur on human breast carcinomas, suggest that the presence of somatostatin receptors should be investigated as a marker of breast cancer aggressiveness, and suggest that this conjugate might be used to detect the presence of residual breast cancer after surgery, allowing better assessment of tumor margins and reducing the need for second and repeat biopsies in selected patients.

8577-30, Session 3

Multimodal optical detection of breast cancers

Anna N. Yaroslavsky, Rakesh Patel, Univ. of Massachusetts Lowell (United States); Ashraf Khan, Robert Quinlan, Univ. of Massachusetts Medical School (United States)

Intra-operative delineation of breast cancer is a significant clinical problem in the surgical management of breast cancer. A reliable method for demarcation of benign and malignant breast tissue during surgery would aid in reducing the re-excision rate for patients due to positive margins. We present a novel method of identifying breast cancer margins using combined dye-enhanced wide-field polarization imaging for quick and accurate delineation of en face cancer margins and optical coherence tomography (OCT) for rapid cross-sectional evaluation. Ten ductal carcinoma specimens were acquired following surgeries, stained with methylene blue, and imaged. Wide-field reflectance images were acquired at 440 and 640 nm. Wide-field fluorescence images were excited at 640 nm and registered between 660 and 750 nm. OCT images were acquired using a commercial 1310 nm Thorlabs swept-source system. The imaging results were validated against corresponding histopathology processed from approximately the same planes that were imaged. Both wide-field polarization imaging and OCT provided useful diagnostic information with regards to cancer resection margins in breast tissue. Combined OCT and wide-field polarization imaging show promise for intra-operative detection of invasive ductal breast carcinoma.

8577-9, Session 4

Diagnosis of malignant and benign prostate tumor from spectra of blood plasma

Vadivel Masilamani, King Saud Univ. (Saudi Arabia)

Prostate cancer is a major problem in North America since human longevity is higher . In the clinical procedure and the conventional detection protocols there is sufficient confusion to discriminate the benign from the malignant growth . In this connection, the spectral biopsy of blood study presented here is capable of such discrimination with sensitivity and specificity over 80% . It is the simplicity of this approach that makes a possible future supplement for clinical diagnosis

The study has been done with a set of patients of Benign Prostate Hyperplasia , prostate cancer and age adjusted normal controls each of 25 in number We had employed fluorescence and stokes shift spectroscopy of blood plasma alone to obtain spectral features

Based on the relative intensities of bands of tryptophan , NADH and flavine we were able to make discrimination in three sets with an accuracy greater than 80%

8577-10, Session 5

Resonance Raman Spectroscopy for Human Cancer Detection of Key Molecules with Clinical Diagnosis

Yan Zhou, The General Hospital of the Air Force, PLA (China); Cheng-hui Liu, The City College of New York (United States); Jiyou Li M.D., Lixin Zhou M.D., Jingsheng He M.D., Beijing Cancer Hospital (China); Yi Sun, Yang Pu, The City College of New York (United States); Ke Zhu, Yulong Liu, Institute of Physics (China); Qingbo Li, BeiHang Univ. (China); Gangge Cheng, The General Hospital of the Air Force, PLA (China); Robert R. Alfano, The City College of New York (United States)

Raman spectroscopy can detect biological molecular vibrations and structure, composition, and interactions in the native state without any labels or contrast enhancing agents. Resonance Raman (RR) spectroscopy can also probe IR-active vibrations that are usually not evident in Raman spectra and therefore can additionally reveal so-called “silent modes,” vibrations that are seen neither in Raman nor in IR absorption spectra. RR spectroscopy can enhance particular vibrational bonds associated with key characterizing molecules excited with biological changes on molecular level.

In this report, RR spectra of human breast tissues and six kinds of brain tissues (meninges tissues in malignant, benign and normal; glioblastoma multiforme in grade IV; pituitary adenoma; acoustic neuroma benign) were measured using a micro confocal Raman system with excitation of 532 nm wavelength. RR spectral data from breast and brain tissues combined with clinical magnetic resonance imaging (MRI) and immunohistochemistry (IHC) image were analyzed. RR spectral differences between cancerous and normal tissues in meninges brain and breast tissues were evidenced, demonstrating high accuracy and reliability of RR spectroscopic technique as clinical optical pathology.

It was found in the RR experiment that extremely resonant enhancement at 532 nm excitation were obtained on amide II at 1548 cm-1 band both in breast and brain cancerous tissues. The energy contained in two photons with the wavelength of 532 nm lies exactly at the maximum of the DNA absorption band in the UV which is caused by the big enhancements of RR spectra on the nucleotide bases (T: 750 cm-1, A: 1306 and 1338 cm-1, and (A,G,T: 1378 cm-1) and mitochondria (1585 cm-1) bands. RR spectra of aromatic amino acids (phenylalanine: 1587 and 1605 cm-1, tyrosine: 1603 cm-1, tryptophan: 1578 cm-1) bands make strong contributions in cancerous tissues compared with non cancerous tissues due to the intense resonant effect. Amide I band characteristic of protein secondary structures shifted from center 1656 cm-1 to 1639 cm-1 with an RR gain was observed in cancerous tissues. Bayesian statistical theory, principal component analysis (PCA) and support vector machine (SVM) were performed on the RR spectral data acquired from eight types of breast and meninges tissues with a total of seventy one scanned spectra, yielding the diagnosis sensitivity of 80% and 90.9% and specificity of 100% and 100%, respectively.

8577-11, Session 5

Confocal resonance Raman probes the cell-cycle dependence of the spectra of proliferating normal and neoplastic single cells

Susie Boydston-White, Borough of Manhattan Community College (United States); Cheng-hui Liu, Robert R. Alfano, The City College of New York (United States)

Confocal resonance Raman (RR) spectra were collected from single proliferating cells and analyzed to detect spectral patterns that are cell-cycle dependent, as a consequence of cellular proliferation — normal or abnormal.

In eukaryotes, proliferation requires cells pass through the eukaryotic cell cycle — the interval between the completion of mitosis of the parent cell, and that of one or both daughter cells — which is divided into four main phases: gap 1 (G1), synthesis (S), gap 2 (G2) and mitosis (M), each representing a period with a particular set of events. Cells from two different cell lines: Human fibroblast — a normal proliferating cell line — and human fibrosarcoma — a cancerous proliferating fibroblast cell line — were cultured, then cells in the M phase were selected. The now-synchronized M-phase cells were cultured and harvested hourly for 24 hours. The cells’ biochemical age at each time point was confirmed by immunohistochemical staining to identify the presence or absence of cellular components that appear and/or disappear as the cells proceed through the cell-cycle. The RR spectra were collected and compared for each time point as the cells proceeded through the cell cycle to determine what spectral vibrational patterns are cell-cycle dependent.

In this study, the question is whether the cell-cycle dependent RR spectral patterns of the vibrational modes observed in proliferating normal and neoplastic single cells are due to a state of cancer or are simply the consequences of the cells’ changing internal biochemistry due to the process of cellular proliferation --- normal or abnormal.

8577-12, Session 6

An all-in-one demonstration of the diagnostic power of Raman spectroscopy in breast cancer: lesion discrimination and microcalcification identification

Ishan Barman, Narahara Chari Dingari, Jaqueline S. Soares, Massachusetts Institute of Technology (United States); Anushree Saha, Sasha McGee, Case Western Reserve Univ. (United States); Luis Galindo, Massachusetts Institute of Technology (United States); Wendy Liu, Donna Plecha, Nina Klein, Case Western Reserve Univ. (United States); Ramachandra R. Dasari, Peter T. C. So, Massachusetts Institute of Technology (United States); Maryann Fitzmaurice, Case Western Reserve Univ. (United States)

Breast cancer is the second leading cause of cancer death in women, with one in eight women likely to develop breast cancer in her lifetime. Microcalcifications are localized deposits of calcium species in breast tissue that are considered an early mammographic sign of breast cancer. Here we report, for the first time, the development of a Raman spectroscopy technique to simultaneously identify microcalcification status and diagnose the underlying breast lesion, in real time, during

stereotactic breast core needle biopsy procedures. In this study, Raman spectra were obtained ex vivo from 146 tissue sites from fresh stereotactic breast needle biopsy tissue cores from 33 patients, including 50 normal breast tissue sites, 77 breast lesions with microcalcifications, and 19 breast lesions without microcalcifications, using a compact clinical Raman system. The Raman spectra were modeled based on the breast tissue components and a support vector machine framework was used to develop a single-step, model-based diagnostic algorithm to distinguish normal breast tissue, fibrocystic change, fibroadenoma and breast cancer, in the absence and presence of microcalcifications. This algorithm was then subjected to leave-one-out cross validation, yielding a positive predictive value, negative predictive value and overall accuracy of 100%, 96% and 82%, respectively, for the diagnosis of breast cancer with or without microcalcifications. It should be noted that the majority of breast cancers diagnosed using this algorithm are ductal carcinoma in situ (DCIS), the most common lesion associated with microcalcifications, which could not be diagnosed using previous Raman diagnostic algorithm(s). Our study demonstrates the potential of Raman spectroscopy to not only detect microcalcifications but also diagnose the breast lesions associated with the microcalcifications, including DCIS, and thus provide real-time feedback to radiologists during stereotactic breast needle biopsy procedures, reducing non-diagnostic and false negative biopsies.

8577-13, Session 6

Analysis of healthy and regenerated bone tissue: use of the Fourier transform infrared spectroscopy (FT-IR) in the molecular identification in situ

Taciana D. Magrini, Herculano S. da Silva Martinho, Arnaldo R. dos Santos, UFABC (Brazil)

The analysis of bone repair is complex because for histological analysis it is used demineralization drastic process. That normally makes samples unviable for another form of analysis more refined as immunocitochemistry, or molecular assay. Otherwise, molecular analysis of bone samples does not preserve its morphology. So, generally one works with information (molecular and morphological) that cannot be directly integrated in the same sample.

The Fourier Transformed Infrared Spectroscopy (FTIR) is a vibrational spectroscopy technique that can be used for probing the molecular alterations associated with healthy, pathologic, wound or regenerated tissues. Spectral bands provide direct information about the biochemistry composition in situ without damage the sample.

In the present work it was studied healthy, regenerated and cartilage rat tibia histological material (not dyed and deparaffinized) by attenuated total reflection (micro ATR-FTIR) and histological imaging. Results were obtained after 14 days from the lesion.

The histological images were consistent with healthy, regenerated and cartilage bone tissue. The FTIR bands area revealed biggest differences between healthy and cartilage tissue (100% of the eight bands analyzed by T-student test with $p<0.005$). The more significant intensity differences ($p<0.005$) between regenerated and cartilage tissue are in the range 1486-1763 cm-1 (amide I and II of proteins) and 2841-3015 cm-1 (lipids) where regenerated absorbed more than cartilage. For regenerated and healthy tissue comparison, differences are in the range 3015-3514 cm-1 (water region) where there was more water intensity in the healthy tissue. It is expected a variation in the quantity of proteins for the regenerated tissue.

8577-14, Session 6

Could near-infrared Raman spectroscopy be correlated with the Metavir scores in liver lesions induced by hepatitis C virus?

Marcio C. R. Gaggini M.D., Ricardo S. Navarro, Aline R. Stefanini, Rubens S. Sano, Univ. Camilo Castelo Branco (Brazil); Landulfo Silveira Jr., Camilo Castelo Branco Univ. (Brazil)

The liver is responsible for several basic functions; most of the main proteins are synthesized by the liver. In present days, the viral hepatitis C is one of the highest causes of chronic hepatic illness worldwide, affecting around 3% of the world population. The liver biopsy is considered the gold standard for diagnosing hepatic fibrosis; however, the biopsies may be questioned because of potential sampling error, morbidity, possible mortality and relatively high costs. Spectroscopy techniques such as Raman spectroscopy have been used for bio-diagnosis of human tissues, with favorable results. Raman spectroscopy has been employed to distinguish normal from malignant hepatocytes through spectral features mainly of proteins, nucleic acids and lipids. In this study, eleven patients with diagnoses of chronic hepatitis C underwent hepatic biopsies having two hepatic fragments collected: one was scored through Metavir system and the other was submitted to near-infrared Raman spectroscopy using a dispersive spectrometer (830 nm wavelength, 300 mW laser power and 20 s exposure time). Five spectra were collected in each fragment and submitted to Principal Components Analysis (PCA). Results showed a good correlation between the Raman spectroscopy features and the stage of hepatic fibrosis. PCA showed that samples with higher degree of fibrosis presented higher amount of protein features (collagen), whereas samples of higher degree of inflammation presented higher features of hemoglobin, in accordance to the expected evolution of the chronic hepatitis.

8577-15, Session 7

Moving Raman spectroscopy into real-time, online diagnosis and detection of precancer and cancer in vivo in the upper GI during clinical endoscopic examination

Zhiwei Huang, Mads Sylvest Bergholt, Wei Zheng, National Univ. of Singapore (Singapore); Khek Yu Ho, Ming Teh, Khay G. Yeoh, Jimmy B. Y. So, Asim Shabbir, National Univ. Hospital (Singapore)

Raman spectroscopy is a vibrational spectroscopic technique sensitive to the changes of biomolecular structures and compositions occurring in tissue. With our very recent development of Raman endoscopy platform integrated with on-line diagnostic scheme, in vivo Raman tissue diagnosis (optical biopsy) in the upper GI during clinical gastrointestinal endoscopy has been realized under multimodal wide-field imaging (i.e., white-light reflectance (WLR), narrow-band imaging (NBI), autofluorescence imaging (AFI)) guidance.

A selection of over 340 patients who previously underwent Raman endoscopy (n=2469 spectra) was used to generate multivariate diagnostic models for diagnosis of gastric dysplasia and neoplasia based on partial least squares - discriminant analysis (PLS-DA). The on-line Raman endoscopy technique was used as a prospective screening technique on new gastric patients (n=4) for in vivo tissue diagnosis and characterization at endoscopy.

High quality in vivo Raman spectra can be acquired and processed in real-time within 0.5 sec during clinical endoscopic examinations. Significant differences in Raman spectra between normal and dysplastic tissue are observed reflecting the pathological transformation associated with gastric carcinogenesis (e.g., upregulated protein synthesis and elevated DNA content etc.). The on-line Raman endoscopic technique developed could prospectively identify gastric dysplasia with sensitivity of 81.5% (22/27) and specificity of 87.9% (29/33).

We realizes for the first time the novel image-guided Raman endoscopy

as a screening tool for on-line in vivo diagnosis of precancer and cancer in the upper GI at endoscopy.

8577-16, Session 7

Protein-like bulk model: a model for study the vibrational spectra of confined water in tissues

Herculano S. da Silva Martinho, Erika T. Sato, UFABC (Brazil)

Despite the extensive theoretical and experimental work devoted to understanding the properties of water, many of them still remain shrouded in mystery. The fact that water is often present in nanoscopic confined non-aqueous media brings up the need to understand these properties in confined spaces and near the interfaces. In this sense, since collagen is a protein essential role in the formation of extracellular matrix and is widely present in our body, we proposed the study of water confined in collagen in order to investigate their vibrational modes. Each cluster of water molecules was confined to an outline of collagen helixes, with 100 atoms. Collagen was obtained from a hydrated collagen peptide, derived from the Protein Data Bank. The results were interpreted with the aid of simulations for various structures of water (H2O)n, where n = 1-8 (H2O), (H2O)2, (H2O)3, (H2O)4, (H2O)5-cyclic, (H2O)6-cage, (H2O)7-low and (H2O)8-S4. We used the Density Functional Theory (DFT) and the CPMD program. The wave functions were optimized and vibrational analyses were performed using Raman responses. We were also calculated linear response of systems to obtain the values of polarization and polar tensors of each atom in the system. Thus, we could realize that water is of extreme importance in the interpretation of the characteristic peaks of each confinement and plays a key role in achieving these peaks. It was possible to see that the external hydration no exerts great influence on the characteristic peaks in the analyzed region, 2800-3600cm-1. It was also noted that there are characteristic bands for analyzed confinements. In this case, it was perceived that the vibrations are of protein only or protein more water. Among these, we highlight C4, which has a characteristic peak at 2888cm-1 and, as discussed. This peak probably is such that most favors the electron transfer processes, with the vibrations of protein atoms and water molecules. Protein–water interactions are known to play a critical role in the function of several biomacromolecular systems including protein tissues. Small changes in structure and dynamical behavior of water molecules at the peptide–water interface can effectively change both the structure and dynamics of the protein function. Thus, we could realize that the presence of different water clusters plays an important role in protein characteristic peaks and defines a greater affinity to the ROS. We concluded that the water is of extreme importance in protein functions and we confirmed that there are changes in vibrational modes of water-related structural organization of water, which is an important information for understanding biological processes in terms of bio-physical-chemical and physiological.

8577-17, Session 7

Identifying pathological bone mineralization in diabetic foot wounds by Raman spectroscopy

Karen A. Esmonde-White, Francis W. Esmonde-White, Univ. of Michigan (United States); Crystal Holmes, Univ. of Michigan Medical School (United States); Michael D. Morris, Univ. of Michigan (United States); Blake J. Roessler, Univ. of Michigan Health System (United States)

Raman spectroscopy is a valuable tool for measuring the chemical composition and molecular structure of bone and other musculoskeletal tissues. Diabetic osteomyelitis is a complication of diabetic foot ulcers and is a major risk factor for foot amputation. Current clinical imaging methods of detecting osteomyelitis, such as x-ray or MRI, are inadequate as these methods can only detect the late-stage changes. We hypothesized that Raman spectroscopy can be used to determine the chemical composition of bone infected by diabetic osteomyelitis to provide an early marker of bone infection. As part of a clinical study, bone fragments containing cortical and cancellous bone were removed from non-healing foot ulcers of study participants as part of their treatment for diabetic osteomyelitis. Bone fragments were examined by Raman microspectroscopy (785 nm) and fiber-optic Raman spectroscopy (830 nm). An additional study of human cadaveric feet was performed to test prototype fiber optic Raman probes for clinical measurements. Unexpectedly, Raman spectra of infected bone fragments contained bands from non-apatitic calcium phosphate minerals such as brushite. Non-apatitic minerals have not been observed in other bone pathologies, and the presence of these minerals may be a unique marker for diabetic osteomyelitis. Cadaveric studies demonstrated feasibility of clinical Raman measurements using custom-built fiber optic probes, even at poorly mineralized portions of the foot. We will discuss ongoing technology development studies, unexpected complications from the use of pathology marking dyes and logistical considerations for using a Raman probe in an infected wound bed.

8577-18, Session 7

Multicore fiber with integrated fiber Bragg grating for background-free Raman sensing

Sebastian Dochow, Ines Latka, Martin Becker, Ron Spittel, Jens Kobelke, Kay Schuster, Albrecht Graf, Sven Brückner, Sonja Unger, Manfred Rothardt, Institut für Photonische Technologien e.V. (Germany); Benjamin Dietzek, Institut für Photonische Technologien e.V. (Germany) and Univ. Jena (Germany); Christoph Krafft, Institut für Photonische Technologien e.V. (Germany); Jürgen Popp, Institut für Photonische Technologien e.V. (Germany) and Univ. Jena (Germany)

The combination of Raman spectroscopy with fiber optic probes enables analyzing the biochemical composition of tissues without markers in a non-destructive way. A small diameter (1 mm) fiber optic probe with one excitation fiber, 11 detection fibers and integrated filters (Emvision, USA) was recently coupled to a Raman spectrometer (Kaiser Optical Systems) to study excised arteries ex vivo and rabbit arteries in vivo. The current contribution introduces a novel fiber optic Raman probe with in-line fiber Bragg gratings (FBGs) as notch filter in the collection path. Multi-core single-mode fibers (MCSMF) were drawn integrating 19 and 61 single-mode cores to improve collection efficiency. Raman probes were assembled with one fiber for excitation and six MCSMF with inscribed FBGs for collection. Background suppression, collection efficiency and distance dependence of the probes were characterized and first Raman measurements are presented. The advantages of the novel probes are discussed.

Acknowledgements: Financial support of the European Union via the “Europäischer Fonds für Regionale Entwicklung” (EFRE) and the “ Thüringer Ministerium für Bildung, Wissenschaft und Kultur” (project: B714-07037) is highly acknowledged.

8577-19, Session 7

Spectral diagnosis of thalassemia: an innovative technique

Vadivel Masilamani, King Saud Univ. (Saudi Arabia)

World Health Organization (WHO)has reported, in 2008, about 7% are born with Sickle Cell Disease (SCD) and Thalasseamia Syndromes. Because of this, about 50,000-100,000 children with thalassaemia major die each year in developing countries The conventional method of detection of Thal is clinical examination followed with Complete Blood Counting (CBC), Electrophoreses, and High Performance Liquid Chromatography (HPLC). with Sensitivity of 92.9% Specificity of 83.9% The present spectroscopy study shown here has the potential for reliable and very fast screening of Thallasemia with a sensitivity and specificity

over 95% . It has the potential for prognostic evaluation of confirmed cases during and after treatment.

We had employed Fluorescence Emission Spectra (FES) with excitation at 325 nm and and Stokes's Shift Spectra(SSS) with 70nm offset on the blood samples obtained from patients of thallasemia (N=35)and normal age adjusted controls (N= 28) The spectral features of amino acids (eg ,tyrosene) and enzymes (eg ,NADH) are so distinct that an accuracy of 100 % could be achieved.

8577-20, Session 8

Overview of light transport in scattering biomedical-like media

Brian W. Pogue, Thayer School of Engineering at Dartmouth (United States)

No Abstract Available

8577-21, Session 8

Biomedical Raman spectroscopy in tissue diagnosis and characterization

Zhiwei Huang, National Univ. of Singapore (Singapore)

No Abstract Available

8577-22, Session 8

Complex light

Giovanni Milione, The City College of New York (United States)

No Abstract Available

8577-23, Session 8

The role of tissue optics in functional imaging

Bruce J. Tromberg, Beckman Laser Institute and Medical Clinic (United States)

No Abstract Available

8577-24, Session 9

In vivo three-dimensional optical coherence tomography and multiphoton microscopy in a mouse model of ovarian neoplasia

Jennifer M. Watson, Samuel Marion, Photini F. Rice, Dave Bentley, David G. Besselsen, Urs Utzinger, Patricia B. Hoyer, Jennifer K. Barton, The Univ. of Arizona (United States)

In order to determine early microscopic changes accompanying the development of ovarian tumors, 48 mouse ovaries were imaged in vivo, at multiple time points throughout their life, using optical coherence tomography (OCT) and multiphoton microscopy. Dosing mice with 4-vinylcyclohexene diepoxide and 7, 12-dimethylbenz[a]anthracene resulted in a variety of tumor types. For in vivo imaging, ovaries were accessed using a sterile surgical method. Three-dimensional OCT image stacks were obtained with a Thorlabs swept-source system using 1040 nm central wavelength and 80 nm bandwidth. Simultaneous second harmonic generation (SHG) and two-photon-excited fluorescence (TPEF) images were collected from the surface of the ovary to 100 µm depth in 10 µm increments with a TriM Scope using 780 nm excitation. Difficulty of accessing the ovary in live animals, due to adhesions from previous surgeries, prevented imaging of all ovaries at all three time points. We obtained images of 4 ovaries at one time point, 22 ovaries at two time points and 22 ovaries at all three time points. OCT visualizes gross structural changes in the ovary. SHG and TPEF images show changes in collagen structure and fluorophore concentration, respectively, with disease progression. Analysis to determine the source of intense punctate fluorescence is ongoing. With age and tumor development, collagen fibers reorganize and the quantity and size of fluorescent particles change. These results indicate that obtaining in vivo measurements in a human may be possible and such measurements may be useful in detecting early ovarian disease.

8577-25, Session 9

A novel intravital multi-harmonic generation microscope for early diagnosis of oral cancer

Yu-Hsiang Cheng, Chih-Feng Lin, National Taiwan Univ. (Taiwan); Chi-Kuang Sun, National Taiwan Univ. (Taiwan) and Institute of Physics & Research Ctr. for Applied Sciences (Taiwan) and Molecular Imaging Ctr. (Taiwan)

Oral cancer is one of the most frequently diagnosed human cancers and leading causes of cancer death all over the world, but the prognosis and overall survival rate are still poor because of delay in diagnosis and lack of early intervention. The failure of early diagnosis is due to insufficiency of proper diagnostic and screening tools and most patients are reluctant to undergo biopsy. Optical virtual biopsy techniques, for imaging cells and tissues at microscopic details capable of differentiating benign from malignant lesions non-invasively, are thus highly desirable. A novel multi-harmonic generation microscope, excited by a 1260 nm Cr:forsterite laser, with second and third harmonic signals demonstrating collagen fiber distribution and cell morphology in a sub-micron resolution, was developed for clinical use. To achieve in-vivo observation inside the human oral cavity, a small objective probe with a suction capability was carefully designed for patients' comfort and stability. By remotely changing its focus point, the same objective can image the mucosa surface with a low magnification, illuminated by side light-emitting diodes, with a charge-coupled device (CCD) for site location selection before the harmonic generation biopsy was applied. Furthermore, the slow galvano mirror and the fast resonant mirror provide a 30 fps frame rate for high-speed real-time observation and the z-motor of this system is triggered at the same rate to provide fast 3D scanning, again ensuring patients' comfort. Focusing on the special cytological and morphological changes of the oral epithelial cells, our preliminary result disclosed excellent consistency with traditional histolopathology studies.

8577-26, Session 9

Highly-sensitive detection of cancer cells using femtosecond dual-wavelength near-IR two-photon-excited fluorescence imaging

Aleksander K. Rebane, Montana State Univ. (United States) and National Institute of Chemical Physics and Biophysics (Estonia); Jean R. Starkey, Mikhail Drobijev, Montana State Univ. (United States); Nikolay S. Makarov, Los Alamos National Lab. (United States)

Various modalities of optical imaging of cancer are becoming increasingly useful instruments for refining early diagnosis, developing targeted therapies and monitoring of patient response to therapy. However, imaging in the visible region of the spectrum often suffers from poor light penetration of the tissues.

We develop a novel imaging protocol using commercial near-IR fluorophore Styryl-9M and show that it allows detection of small cancer

cell colonies deep inside tissue phantoms, as well as in a mouse mode, with high sensitivity and specificity. We image the two-photon-excited fluorescence in the Styryl-9M by tuning 1 kH, 100 micro joule energy, 100-fs duration pulses sequentially to two wavelengths, 1200 nm and 1100 nm, where the dye shows a large variation of the two-photon absorption on the local environment. Evaluating the normalized ratio of the dual-wavelength images yields the location of the cancer cells colony, even if it is surrounded by a large number of normal cells. The 2PEF showed a positive correlation with the levels of MDR1 proteins expressed by the cells, and, for high MDR1 expressors, as few as ten cancer cells could be detected. Similar high sensitivity is also demonstrated for tumor colonies induced in mouse external ears. By comparing normalized ratios of the signal intensity at different wavelengths we are able to distinguish between samples with cancer cells, without cells, and with normal cells. The proposed method is promising for non-invasive optical detection of cancer and may be applied in cancer diagnostics for differentiation of cancer vs. normal cells, as well as for precise localization of tumors.

8577-27, Session 9

High-spectral resolution nonlinear microspectroscopy and imaging of soft condensed and biological media

Feruz S. Ganikhanov, Shan Yang, Sanjay Adhikari, West Virginia Univ. (United States)

We elaborate and demonstrate a method that is capable of producing high spectral resolution dispersion data for the resonant third-order nonlinearity of a medium probed within microscopic volumes. Time-domain CARS transients traced with femtosecond pulses within orders of magnitude in the signal decay can lead to resolution of fine spectral features in dispersion that can not be reliably detected by frequency-domain Raman based spectroscopy techniques, including coherent methods. Dispersion data for the nonlinear susceptibility would be a major asset in microscopic characterization of complex biological media studied with chemical sensitivity. Using our approach, dispersion of ?(3) can be obtained from a medium probed within microscopic volumes with a spectral resolution of better than 0.1 cm-1.

The experimental method is based on three-color time-domain CARS with femtosecond pulses. We used two independently tunable synchronously pumped optical parametric oscillators (OPOs). The OPOs are simultaneously pumped by a high power femtosecond Ti:sapphire oscillator running at 76 MHz with details provided in our recent work. The OPOs can be tuned to a central wavelength within 950-1150 nm range in order to satisfy resonant condition for a particular Raman active mode with vibration energy up to 3000 cm-1. Typically, CARS-signal that was generated within approximately 0.2fL probe volume could be traced within five orders of magnitude as the delay time of the probe pulse is changed from the maximum signal position. We show that , in many cases, the macroscopic coherent amplitude generated by a pair of pulses is a real function and Fourier transform of the square root of the time-domain CARS signal provides dispersion of chi(3) with the equivalent spectral resolution determined by maximum delay time at which the signal is still detected. Since we are able to detect time-resolved CARS signal within more than 5 orders of magnitude, typically, spectral resolution of 0.05-0.1 cm-1 can be obtained for Raman lines in viscous media like oil, etc.

We will present results of the method's application in biological cells and tissue. Namely, we accessed a protein line at 1245 cm-1 in E-coli cell, major DNA and protein Raman active lines in red blood cells and in fat tissue.

8577-29, Session 10

Polarimetric Mueller microscopy as a tool for parametric studies of healthy and cancerous human colon tissue

Angelo Pierangelo, Sandeep Manhas, Bicher Haj-Ibrahim, Ecole Polytechnique (France); Abdelali Benali, Institut Mutualiste Montsouris (France); Tatiana Novikova, Ecole Polytechnique (France); Brice Gayet, Pierre Validire, Institut Mutualiste Montsouris (France); André Nazac, CHU Bicêtre (France); Antonello De Martino, Ecole Polytechnique (France)

Recently multi-spectral Mueller polarimetric imaging was demonstrated as a new promising optical technique for cancer diagnostics. This technique provides specific contrasts which can be used with exvivo samples for cancer staging (colon, A. Pierangelo et al, Opt. Express 19, 1582), detection of residual cancer after radiochemotherapy treatment (rectum) and of precancerous zones (uterine cervix). However, a proper understanding of the interaction of polarized light with such samples is needed both for its own sake and to optimize the implementation of the technique.

Healthy as well as cancerous tissues can be modeled as multilayer structures with various scatterers embedded in each layer [M.R. Antonelli et al, Biomed. Opt. Express, 2, 1836]. The observed polarimetric contrasts are related to the nature and size of the scatterers as well as the optical properties of the layers (absorption, optical index…). These contrasts thus depend on many parameters, which cannot be uniquely determined from backscattering polarimetric images of optically thick tissues which typically involve multiple photon scatterings.

In this study we used a multispectral Mueller microscope to analyze the images of unstained histological cuts of normal and cancerous colon samples in transmission and reflection modes in both real and Fourier spaces. These cuts are sufficiently thin (5 - 20µm) to make sure that single scattering is dominant. The data taken in these conditions are thus quite complementary to those obtained in backscattering imaging of thick samples for the determination of the optical model parameters. The first results of these studies will be presented and discussed.

8577-31, Session 10

Optical and terahertz biopsy of skin cancers

Cecil S. Joseph, Rakesh Patel, Univ. of Massachusetts Lowell (United States); Victor A. Neel, Massachusetts General Hospital (United States); Robert H. Giles, Univ. of Massachusetts Lowell (United States); Anna N. Yaroslavsky, Univ. of Massachusetts Lowell (United States) and Massachusetts General Hospital (United States)

Nonmelanoma skin cancers are the most common form of cancer. Reflection cross-polarized continuous wave terahertz imaging offers intrinsic contrast between normal and cancerous tissue, but lacks the resolution required to identify tissue morphology. Intrinsic polarized light imaging at optical frequencies, provides morphological detail at sufficient resolution but often lacks contrast between the lesion and normal skin. We combined these two modalities and determined terahertz cross-polarized reflectance threshold values for malignant and benign skin tissue structures. Thick fresh excisions of skin cancer specimens were obtained from Mohs surgeries. The samples were mounted and scanned using both a continuous-wave terahertz imaging system at 513 µm and an optical polarized light imager at 440 nm. The terahertz images were overlaid with the optical images and compared with H&E histology. Terahertz cross-polarized reflectance values were calculated for cancerous and normal structures of the samples. The average reflectivity values for basal cell carcinomas showed that cancer had lower reflectivity than normal tissue. Similarly, squamous cell carcinomas showed the same trend but the reflectivity values slightly higher than those for BCC samples. Overall the average cross polarized reflectivity of the tumor

and normal regions for all the samples investigated so far was found to be 0.69% ± 0.034% and 0.84% ± 0.010%, respectively. The difference between normal and cancer for representative sections averaged over all samples was significant ($p<0.001$). The combined optical and terahertz imaging shows promise for the detection of nonmelanoma skin cancers.

8577-32, Session 10

Formulaic ratio imaging for improved visualization of low contrast lesions in human colon specimens

Urs Utzinger, The Univ. of Arizona (United States); Timothy E. Renkoski, College of Optical Sciences, The Univ. of Arizona (United States); Bhaskar Banerjee, The Univ. of Arizona College of Medicine (United States); Logan R. Graves, College of Optical Sciences, The Univ. of Arizona (United States); Nathaniel S. Rial, The Univ. of Arizona College of Medicine (United States); Sirandon A. H. Reid, The Univ. of Arizona (United States); Vassiliki L. Tsikitis, Valentine N. Nfonsam, Piyush Tiwari, Hemanth Gavini, The Univ. of Arizona College of Medicine (United States)

The accepted screening technique for colon cancer is white light endoscopy, but it is known to miss polyps and flat neoplasms. Better visualization is needed to improve the endoscopists quality of examination. Results from existing commercial autofluorescence (AF) endoscopes have been mixed, with some showing increased detection of polyps, while others showed no difference to white light endoscopy and missed detection of flat lesions. We collected AF and narrow band reflectance (R) images of 30 fresh human colon resections at illumination wavelengths between 280 and 550 nm. AF at 440 nm exhibited the highest contrast between lesion and adjacent normal tissue with contrast of adenocarcinoma being larger than adenoma. Contrast was larger in distal lesions compared to proximal lesions, which could be attributed to differences in genetic mutations. Through the evaluation of color digital images we identified 10 samples as low contrast lesions (LCLs). We formed over 30 formulaic ratio images such as 1/A, A/B, 1/(A+B), A/(A+B), C/(A+B) etc. and evaluated them using multiple observers. We found that in LCLs, the ratio image AF 340 / AF 440 produced the largest number of exceptional images while it was effective in highlighting the lesion in 70% of LCLs. Contrast may be due to increased NADH levels, increased hemoglobin absorption, and reduced signal from submucosal collagen. A complementary ratio image (R 480/ R 555) combined two reflectance images and produced exceptional images especially in LCLs where AF 340 / AF 440 was ineffective. The newly discovered ratio images can potentially improve detection rate in screening with a novel AF colonoscope.

8577-33, Session 10

Study and discrimination of human cervical tissue Images through multi-fractal analysis

Jaidip M. Jagtap, Indian Institute of Technology Kanpur (India)

In our earlier study, we have shown that wavelet based multifractal analysis has potential to discriminate normal tissue sections from dysplastic ones. To further classify among the various grades of dysplasia, images with better resolution and fluctuation less light sources are needed. This study is done using the inverted confocal microscope with laser scanning fluorescence imaging. The periodic structure of collagen present in stromal region of cervical tissue gets disordered with progress in grade of dysplasia, leading to variation in birefringence. This has been studied through the ?-exponent of Fourier transform of confocal images enabling us to discriminate between normal and abnormal human cervical tissue sections. The holder exponent from 2D images further classifies various grades of dysplasia. In addition, since cellular density of epithelium increases with depth for various grades of dysplasia, images of the epithelium were analysed separately. The holder exponent which measures multifractality is higher for dysplastic tissue sections than normal ones because of their higher cellular density. Gd3 can be clearly distinguished from the normal through the holder exponent while Gd1 and Gd2 can be discriminated from FFT only. Extraction of subtle fluctuations from optical images through multifractal studies promise to be a powerful diagnostic technique.

8577-8, Session PWed

Investigation of native spectral difference among cancer cell lines with different risk levels

Yang Pu, City College of New York (United States); Jianpeng Xue, China Pharmaceutical Univ. (China); Baogang Xu, Washington Univ. in St. Louis (United States); Wubao Wang, The City College of New York (United States); Yueqing Gu, China Pharmaceutical Univ. (China); Rui Tang, Washington Univ. in St. Louis (United States); Samuel Achilefu, Washington Univ. School of Medicine in St. Louis (United States); Robert R. Alfano, The City College of New York (United States)

Previous study of optical screening of cancer has shown that difference of native fluorescence spectra can be used to distinguish cancer tissue from normal tissue. The native fluorophores, such as NADH and FAD, are involved in the oxidation of fuel molecules, and therefore, direct monitoring of NADH fluorescence dynamically can interpret the metabolic activity of cells. Usually the metabolic rate of advanced metastatic cancer cells is greater than that of less advanced cancer cells, causing the effect known as hypoxia, which was found by Warburg.

The aim of the present research is to determine if the native fluorescence spectroscopy approach is effective to detect changes of fluorophore compositions related to different types of cancer cell lines with different risk levels. Different types of cancer cell lines with different risk levels, such as primary tumor carcinoma (MCF-7), moderate metastatic (DU-145), and advanced metastatic (LNCap and PC-3) cell lines, were excited by the selective excitation wavelength of 300 nm. The contributions of principle biochemical components to fluorescence spectra from the cell samples were investigated using the different non-negative constraint blind source separation methods. The higher relative content of tryptophan was observed in the metastatic cancer cell lines in comparison with the moderate metastatic and non aggressive cell lines. This work shows the changes of relative contents of tryptophan and NADH obtained using native fluorescence spectroscopy may present potential criteria - for detecting different cancer cell lines with different risk levels.

8578-1, Session 1

Cerebral tissue oxygen saturation monitoring using frequency-domain near-infrared spectroscopy in anesthetized patients: a clinician's perspective of cerebral circulation physiology *(Invited Paper)*

Lingzhong Meng, Duke Univ. Medical Ctr. (United States); A. W. Gelb, Univ. of California, San Francisco (United States); W. W. Mantulin, Univ. of California, Irvine (United States); Albert E. Cerussi, Bruce J. Tromberg, Beckman Laser Institute and Medical Clinic (United States)

From 2010 to 2011, we applied frequency-domain near-infrared spectroscopy (FD-NIRS) (Oxiplex TS, ISS Inc., Champaign, IL, USA) in anesthetized surgical patients to investigate the effect of drug-induced change in systemic hemodynamics (blood pressure and cardiac output) and ventilation-induced change in blood carbon dioxide (CO2) on cerebral tissue oxygen saturation (SctO2). Our data show that FD-NIRS is a robust technology in SctO2 measurement and is sensitive and consistent in detecting SctO2 change caused by a change in systemic hemodynamics or blood CO2 level. However, when translating the change in SctO2 in the context of cerebral circulation physiology, difficulty occurs. First of all, FD-NIRS measures pooled blood; however, the clinically meaningful cerebral desaturation is venous, not arterial, desaturation because the systemic arterial blood which perfuses the brain is almost always well saturated if there is no major cardiopulmonary disease. Thus, the ability to differentiate arterial and venous saturation can better fulfill the clinical need. Second, a decrease in SctO2 can be due to an increased cerebral consumption of O2, a decreased O2 delivery to the brain, or a decreased arterial and/or increased venous blood contribution to NIRS measurement, alone or in any combination. The knowledge of the cause of cerebral desaturation can better facilitate clinical management. For example, our observation of the decrease in SctO2 secondary to a drug-induced increase in blood pressure may not be due to a decrease in cerebral blood flow. Instead, it may be caused by a decreased arterial blood contribution to NIRS measurement due to the blood pressure increase-induced arterial constriction per autoregulatory mechanism. If the later is true, cerebral desaturation in this scenario will have different physiological (intact cerebral autoregulation) and clinical (no intervention needed) implications. Unfortunately, the current NIRS technologies being applied in the clinical settings are not able to tell the cause of cerebral desaturation. Third, a clinician would wish NIRS can provide information regarding the integrity of neurovascular coupling which is often impaired in certain conditions and the status of cerebral vasomotor tone which relates to the integrity of cerebral autoregulation. The reasoning is that a better grasp of physiology helps with a better clinical management and neurovascular coupling and cerebral autoregulation are essential concepts in cerebral circulation physiology.

8578-2, Session 1

Validation of optically measured cerebral venous oxygen saturation in humans

Jennifer M. Lynch, Univ. of Pennsylvania (United States); Erin M. Buckley, Peter Schwab, Brian D. Hanna, Daniel J. Licht, The Children's Hospital of Philadelphia (United States); Arjun G. Yodh, Univ. of Pennsylvania (United States)

Diffuse Optical Spectroscopy (DOS) is a well-established and widely accepted modality for non-invasively measuring concentrations of oxy- and deoxy-hemoglobin ([HbO2] and [Hb]) in tissue. Specifically, it is well suited for measures of cerebral tissue oxygen saturation. While cerebral tissue oxygen saturation provides some insight into how oxygen is being utilized by the brain, an actual quantification of cerebral oxygen extraction requires separate measures of arterial and venous saturations. Measures of cerebral arterial oxygen saturation are easily attainable, but cerebral venous oxygen saturation is much more difficult to measure, especially non-invasively and without a perturbation such as venous occlusion.

We validate the use of diffuse optics as a non-invasive measure of cerebral venous oxygen saturation using a method described previously (Wolf 1997, Franceschini 2002). Instead of a perturbation that can be very dangerous in some critical care patients, this method relies only on a steady respiration rate that results in a steady, oscillatory venous blood volume. We validate this measurement of cerebral venous oxygen saturation against a "gold standard" measurement from a blood sample taken from the superior vena cava in a pediatric population for which this invasive measurement is part of clinical care. We also demonstrate the ability to apply this technique to other populations, including healthy adults and critically-ill neonates, a population for which this measurement would be invaluable.

8578-3, Session 1

Use of diffuse optical spectroscopy to monitor muscle and brain oxygenation dynamics during isometric and isokinetic exercise

Goutham Ganesan, Joshua Cotter, Univ. of California, Irvine (United States); Warren Reuland, Beckman Laser Institute and Medical Clinic (United States); Robert V. Warren, Soroush M. Mirzaei Zarandi, Univ. of California, Irvine (United States); Albert E. Cerussi, Bruce J. Tromberg, Beckman Laser Institute and Medical Clinic (United States); Pietro R. Galassetti, Univ. of California, Irvine (United States)

The goal of this research is to quantify tissue oxygenation responses to isometric exercise in healthy subjects. Because ischemia is a significant component of the physiological response to resistance exercise, it is important to accurately measure the degree to which ischemia is achieved during resistance exercise. We present measurements of muscle and prefrontal cortex (PFC) oxygenation using different Diffuse Optical (DOS) devices that provide near-infrared data acquired in continuous wave (CW), time-domain (TD, prototype by Hamamatsu) and frequency-domain (FD, prototype by Beckman Laser Institute) modes. The primary challenge employed in this study is a 30-s isometric contraction for elbow flexion at 90 degrees on a Biodex dynamometer. We aim to address several hypotheses, including: 1. DOS techniques improve detection of PFC oxygenation during exercise, and 2. Dynamic measurements of tissue scattering are necessary for accurate muscle oxygenation measurements, and will yield better correlations with other measures of muscle activation.

Results: TD data in five subjects suggests that a 30-s isometric contraction of the biceps muscle results in reduction of reduced scattering coefficients at three wavelengths from 17-20%. Additionally, the average difference in reported O2 saturation change between processing methods (with and without continuous scattering correction) was 16% (SEM = 7%). Additionally, we report preliminary correlations between scattering changes and torque production during a 30 second isometric contraction for elbow flexion. Finally, PFC Total Hemoglobin levels increased by 7.4 micromolar (SEM = 1.1) when measured without scattering correction, whereas including the correction resulted in no significant increase (-.69 ± .66 micromolar).

8578-4, Session 1

Investigation of human frontal cortex under noxious thermal stimulation of temporomandibular joint using functional near infrared spectroscopy

Amarnath S. Yennu, Rohit Rawat, Mayur Jadhav, Michael T. Manry, Hanli Liu, The Univ. of Texas at Arlington (United States)

According to American Academy of Orofacial Pain, 75% of the U.S. population experiences painful symptoms of temporomandibular joint and muscle disorder (TMJMD) during their lifetime. Thus, objective assessment of pain is crucial for efficient pain management. We used near infrared spectroscopy (NIRS) as a tool to reveal and understand hemodynamic responses in frontal cortex to noxious thermal stimulation of temporomadibular joint (TMJ). NIRS experiments were performed on 7 healthy male volunteers under both low pain stimulation (LPS) and high pain stimulation (HPS), using a temperature-controlled thermal stimulator. To induce thermal pain, a 16X16 mm¬¬2 thermode was strapped onto the right TMJ of the subject. Initially, subjects were asked to rate perceived pain on a scale of 0 to 10 for the temperatures from 41?C to 47?C. For the NIRS measurement, two magnitudes of temperatures, one rated as 3 and another rated as 7, were chosen as LPS and HPS, respectively. The experimental paradigm was a blocked design with 20-sec stimulation and a variable inter-stimulus-interval. By analyzing the temporal profiles of changes in oxy-hemoglobin concentration (HbO) using cluster-based statistical tests, we were able to identify several regions of interest (ROI), (e.g., secondary somatosensory cortex and prefrontal cortex), where significant differences ($p<0.05$) between HbO responses to LPS and HPS are shown. In order to classify these two levels of pain, a neural-network-based classification algorithm was used. Using leave-one-out cross validation from 7 subjects, the two levels of pain were identified with 88.5% sensitivity, 100% specificity, 94.2% accuracy, and 0.97 area under curve.

8578-5, Session 1

functional near-infrared spectroscopy (fNIRS) during vestibulo-ocular and postural challenges

Helmet T. Karim, Univ. of Pittsburgh Medical Ctr. (United States) and Univ. of Pittsburgh (United States); Joseph M. Furman M.D., Univ. of Pittsburgh (United States); Theodore J. Huppert, Univ. of Pittsburgh Medical Ctr. (United States)

Introduction

Functional near-infrared spectroscopy (fNIRS) is a non-invasive brain imaging method that uses light to record regional changes in cerebral blood oxygenation during functional tasks. In a set of experiments, we have applied fNIRS to study cortical brain activations during vestibular and posturography testing.

Methods

A 32-channel device was used to record brain activation during a series of vestibular experiments.

Caloric stimulation. A bilateral fNIRS probe was used to record brain activity from the frontal and temporal regions of 20 healthy persons: (N=10 young; N=10 older). Brain responses were recorded during warm (44oC) and cool (30oC) caloric irrigations. The older group showed increased bilateral activations of the superior temporal gyrus (STG) compared to the younger population.

Dynamic Posturography. FNIRS was recorded during sensory organization testing (SOT) on an EquitestTM platform in ten young healthy volunteers. Brain areas in STG and frontal cortex (FC) were activated during the SOT conditions.

Rotational testing. A 4-channel wireless fNIRS system was built to allow measurements in STG during earth-vertical axis rotational testing. Bilateral STG/SMG activation was recorded from twenty healthy volunteers (N=10 young; N=10 older) during sinusoidal rotation (0.1 Hz, 60 deg/sec) in the dark.

Results

In each of these experiments, significant changes in the superior temporal gyrus were recorded using fNIRS. This finding is consistent with the role of this part of the brain in cortical processing of secondary vestibular information.

Conclusions

These experiments demonstrate the feasibility of using fNIRS imaging for studying cortical activity during vestibulo-ocular and postural challenges.

8578-6, Session 1

Low frequency oscillations measured with near infrared spectroscopy shed light onto underlying cerebral hemodynamics

Jana M. Kainerstorfer, Michele L. Pierro, Angelo Sassaroli, Tufts Univ. (United States); Peter R. Bergethon, Boston Univ. (United States); Sergio Fantini, Tufts Univ. (United States)

Near-infrared spectroscopy (NIRS) is a non-invasive optical method that provides information about cerebral tissue oxygenation, as well as tissue concentrations of deoxy-hemoglobin ([Hb]) and oxy-hemoglobin ([HbO]). NIRS measurements on the human brain are sensitive to oscillatory hemodynamics associated with cardiac pulsation (~1 Hz), respiration (~0.3 Hz), and spontaneous low frequency oscillations (LFOs) at ~0.1 Hz. These hemodynamic oscillations reflect local changes in the cerebral blood volume (CBV), blood flow velocity (CBFV), and/or metabolic rate of oxygen (CMRO2) resulting from systemic and/or local physiological processes. We have developed an analytical method to decompose measured oscillations of [Hb] and [HbO] into individual components associated with CBV and CBFV/CMRO2 oscillations. The approach relies on a vector decomposition of the phasors of measured [HbO] and [Hb], which are fully characterized by the amplitude and phase of their oscillations, and offers the unique possibility of simultaneously monitoring CBV and CBFV oscillations. We present the application of this approach to measurements on the human brain under various conditions. One of those examples is phase and intensity changes of CBV and CBFV during sleep, where we demonstrate that different stages of sleep are characterized by different [Hb] and [HbO] phasors. In particular, we have found a reduction in the amplitude and an increase in the phase difference of [Hb] and [HbO] low-frequency oscillations during deep sleep compared to the wake state. By contrast, the phase difference between CBFV and CBV low frequency oscillations remained constant throughout all sleep states, suggesting that cerebral autoregulation is maintained during sleep.

8578-7, Session 2

Functional brain imaging with a supercontinuum time-domain NIRS system

Juliette J. Selb, Bernhard B. Zimmermann, Mark Martino, Tyler M. Ogden, David A. Boas, Massachusetts General Hospital (United States)

We have developed a time-domain near-infrared spectroscopy (TD-NIRS) system for baseline and functional brain imaging. The instrument uses a pulsed broadband supercontinuum laser emitting a large spectrum between 650 and 1700 nm, and a gated detection based on an intensified CCD camera. The source laser beam is split into two arms, below and above 780 nm. In each arm, a fast motorized filter wheel enables selection of bandpass filters at the required wavelength. The filtered laser beam is then launched into one of a 4?4 array of source fibers. The multiplexing through the array of fibers is implemented through a very compact home-made design consisting of two

galvanometer mirrors followed by an achromatic doublet. Source fibers are then recombined one-by-one from both arms into the 16 source optodes to be positioned on the head. Each optode therefore consists of two fibers for the two wavelength arms. For one of the two wavelengths, we use on the source side longer fibers and on the detection side shorter fibers, so that the overall introduced delay is the same at both wavelengths. In this manner, the pulses at both wavelengths arrive simultaneously on the ICCD camera, with half the detection fibers monitoring one wavelength and the other half the other wavelength. The combination of the fast source multiplexing and of the fiber-based spectral differentiation enables rapid multi-spectral detection adequate for functional imaging. We will present the instrumentation and show its preliminary functional imaging capabilities on the adult head.

8578-8, Session 2

Imaging high level functional networks with diffuse optical tomography

Adam T. Eggebrecht, Silvina L. Ferradal, Washington Univ. in St. Louis (United States); Amy Robichaux Viehoever, Washington Univ. School of Medicine in St. Louis (United States); Mahlega Hassanpour, Washington Univ. in St. Louis (United States); Abraham Z. Snyder, Joseph P. Culver, Washington Univ. School of Medicine in St. Louis (United States)

High-density diffuse optical tomography (HD-DOT) methods have improved localization and resolution compared to traditional near infrared spectroscopy (NIRS). However HD-DOT systems have generally suffered from a limited field of view (FOV) and studies have focused on sensory and motor areas. In order to consider a wider range of clinical applications, it is necessary to sample a large contiguous FOV that permits the study of high level functional brain networks. We have developed an HD-DOT cap that spans over 70% of the superficial cortical surface covering occipital, temporal, and much of the parietal and frontal lobes. In this study, subject-specific anatomical MRIs are used to generate accurate photon propagation models and the DOT image reconstructions are calculated within the subject-specific anatomical space. Data are affine transformed into a standard MNI atlas space to create group averages of the activations. Stimuli include somatosensory, visual, auditory and language tasks. Nodes within the language processing system are clearly separable into passive auditory and visual processing and active generation of verbal output of novel speech. Activation locations are validated with matched non-concurrent fMRI data on the same subjects. The locations of these task-based activations are used as seeds in functional connectivity analysis of resting state data measured via HD-DOT. The seeds chosen provide access to the visual, motor, language, attention, and default mode networks. Seed-based correlation maps of resting-state networks generated from HD-DOT data are then compared with fMRI. Cortical maps from both modalities show clear differentiation between the five networks investigated.

8578-9, Session 2

Improved depth specificity and spatial resolution in brain atlas-guided diffuse optical tomography

Fenghua Tian, Venkaiah C. Kavuri, Hanli Liu, The Univ. of Texas at Arlington (United States)

In diffuse optical tomography (DOT), researchers often face challenges to accurately recover the depth and size of the reconstructed objects. We recently developed a combined approach using depth compensation algorithm (DCA) to solve the depth localization problem and L1-norm regularization to solve the over-smoothing problem that degrades the spatial resolution. In order to conduct DOT in accordance with realistic human brain anatomy, in this report, we have generated a finite element mesh of a standard brain atlas (ICBM 152) using a publically available toolbox (iso2mesh). The combined DCA+L1 approach is implemented in brain atlas-guided DOT through the following procedures: (1) probabilistic registration is used to localize DOT measurements on the brain mesh by digitizing the coordinates of optodes along with several cranial landmarks; (2) mesh-based Monte Carlo (MMC) simulations or finite element modeling (NIRFAST) is utilized to solve the forward problem; (3) compensation of sensitivity matrix along depth, given in DCA, is applied in the process, followed by (4) inverse reconstruction based on L1-norm regularization. As an example, motor activation induced by a finger tapping task is utilized to validate the improved depth specificity and spatial resolution of reconstructed DOT images when combined DCA+L1 is used in brain atlas-guided DOT.

8578-10, Session 2

Dynamic contrast enhanced time-resolved near-infrared measurement of cerebral hemodynamics before and during ischemia

Jonathan T. Elliott, Lawson Health Research Institute (Canada) and Univ. of Western Ontario (Canada); Mamadou Diop, Laura B. Morrison, Lawson Health Research Institute (Canada); Ting-Yim Lee, Lawson Health Research Institute (Canada) and Univ. of Western Ontario (Canada); Keith St. Lawrence, Univ. of Western Ontario (Canada) and Lawson Health Research Institute (Canada)

We present a dynamic constrast enhanced near-infrared (DCE-NIR) technique that is capable of non-invasive quantification of cerebral hemodynamics in the adult subject. The challenge of removing extracerebral contamination is overcome through the use of multi-distance time-resolved DCE-NIR combined with the kinetic deconvolution optical reconstruction (KDOR) analytical method. As validation, cerebral blood flow, cerebral blood volume and mean transit time recovered with DCE-NIR are compared with CT perfusion values in adult pigs (n=8) during normocapnia, hypocapnia, and ischemia.

Measurements of blood flow acquired with DCE-NIR were compared against concomitant measurements using CT Perfusion. A strong correlation was observed between these groups of measurements ($p = 0.001$, $r = 0.854$, slope = 1.00, y-intercept = 1.357 mL/min/100g). In addition, measurements of cerebral blood volume were compared. The mean percent error in CBV between the two techniques was 11.72 ± 23.86%. In conclusion, we demonstrate that DCE-NIR can be used to measure cerebral hemodynamics directly at the bedside, providing measurments that are in good agreement with the current clinical standard of CT perfusion.

8578-11, Session 2

Optical characterization of two-layered diffusive media for absolute brain oximetry with frequency-domain near-infrared spectroscopy

Bertan Hallacoglu, Angelo Sassaroli, Irwin H. Rosenberg, Sergio Fantini, Tufts Univ. (United States)

Improving the accuracy, reliability, and reproducibility of absolute brain near-infrared measurements is crucial to establish their utility and validity for research and clinical use. In a recent study, we have used a diffusion-based homogenous model to perform absolute brain spectroscopy and oximetry using multi-distance frequency-domain data collected on the forehead of sixteen elderly subjects. We observed a strong intra-subject reproducibility of absolute measurements performed in separate sessions with cross-correlation coefficients of 0.9 for the absorption coefficient (?a) and 0.7 for the reduced scattering coefficient (??s). Despite the strong reproducibility, we observed a dependence of the measured optical coefficients on the range of source detector separations, indicating a depth-dependence of the tissue optical properties. Here, we make the

assumption that the forehead can be optically modeled by a two-layered diffusive medium, where first and second layers represent extracerebral (scalp, skull, dura, pia) and brain (cerebral cortex) tissues, respectively. We apply a diffusion-based, two-layer model to simultaneously measure the optical properties of the first (?a(1) and ??s(1)) and second (?a(2) and ??s(2)) layer and the thickness of the first layer (L). Monte Carlo simulations have shown that all five parameters can be measured with an accuracy of 5% for a range of optical properties and top-layer thickness that are representative of the human brain. We will also present results on two-layered tissue-like phantoms, and representative results on human subjects.

8578-12, Session 2

Phasor brain mapping of tissue hemoglobin concentration, blood volume, and flow velocity with near-infrared spectroscopy

Michele L. Pierro, Jana M. Kainerstorfer, Angelo Sassaroli, Tufts Univ. (United States); Peter R. Bergethon, Boston Univ. (United States); Sergio Fantini, Tufts Univ. (United States)

Near infrared spectroscopy (NIRS) has been extensively used to assess hemodynamic and oxygenation changes associated with brain activation. Moreover, the phase difference between oscillations of oxy- ([HbO]) and deoxy-hemoglobin ([Hb]) concentrations can be used as an additional indicator of underlying physiological and hemodynamic effects under resting and activation conditions. For example, spontaneous low frequency oscillations (~0.1 Hz) of [Hb] and [HbO] have been investigated to characterize baseline cerebral hemodynamics and autoregulation, resting networks, and functional connectivity in human subjects. We have developed a phasor-based approach to decompose measured oscillations of [Hb] and [HbO] into oscillations of local cerebral blood volume (CBV) and flow velocity (CBFV). This approach provides amplitude and phase data for the oscillatory components of [Hb], [HbO], and the underlying CBV and CBFV. As a result, one can generate spatial maps of the amplitude and phase of a variety of quantities that are directly related to oscillatory hemodynamics in the brain. We present phasor maps of hemoglobin concentration, blood volume and flow velocity measured on the human brain with NIRS. Measurements were performed with a Hitachi ETG 4000 CW system featuring 52 channels covering the frontal lobe. Phase maps under rest condition show that the spatial distribution of the relative phase of [Hb] and [HbO] has a much broader angle distribution than the relative phase of CBV and CBFV. These results suggest that low frequency oscillations of CBV and CBFV feature a spatially uniform phase relationship under rest conditions in healthy subjects.

8578-13, Session 3

Predicting breast cancer response to neoadjuvant chemotherapy using a generalized linear model *(Invited Paper)*

Quing Zhu, Univ. of Connecticut (United States); Liqun Wang, Univ. of Manitoba (Canada)

In this presentation, we report our recent progress of using ultrasound-guided near infrared tomography to assess and predict breast cancer response to neoadjuvant chemotherapy. 32 women were imaged prior to treatment, at the end of every treatment cycle, and before their definitive surgery. Pretreatment breast tumor hemoglobin content is a good predictor of patient response to neoadjuvant chemotherapy. The differences of mean maximum total hemoglobin (tHb) and the mean average tHb of responder and non-responder groups were statistically significant (P=0.005, P=0.009, respectively). The percentage of total hemoglobin changes normalized to the pretreatment level (%tHb) can be used to further predict pathological tumor response at early treatment cycles; and the differences between the two responder groups were statistically significant at the end of cycles 1-3. A Generalized Linear Model was developed to predict each individual patient response based on pretreatment hemoglobin parameters, %tHb changes during early treatment cycles, tumor characteristics and tumor receptor markers. If tumor grade and mitotic count, pretreatment tHb, deoxyHb and oxyHb, and %tHb measured at treatment cycles 1-3 were used as predictor variables, the prediction sensitivity and specificity achieved 100%, respectively. If tumor grade and mitotic count and tumor receptor markers of ER, PR and HER2, pretreatment tHb, deoxyHb and oxyHb, and %tHb measured at treatment cycle 1 were used as predictor variables, the prediction sensitivity and specificity achieved 100%, respectively. This model is indeed a powerful tool to assist oncologists in predicting and planning for neoadjuvant chemotherapy once validated by a larger patient pool.

8578-14, Session 3

Early prediction of neoadjuvant chemotherapeutic efficacy with multi-parametric diffuse optical methods

(Invited Paper)

Regine Choe, Univ. of Rochester Medical Ctr. (United States); David R. Busch, Univ. of Pennsylvania (United States); Turgut Durduran, ICFO - Institut de Ciències Fotòniques (Spain); Joseph M. Giammarco, Eastern Univ. (United States); Saurav Pathak, So Hyun Chung, Han Y. Ban, Ellen K. Foster, Tiffany Averna, Univ. of Pennsylvania (United States); Ki Won Jung, Peter Carlile, Univ. of Rochester (United States); Erin M. Buckley, Meeri N. Kim, Univ. of Pennsylvania (United States); Mary E. Putt, Carolyn Mies, Mitchell D. Schnall, The Univ. of Pennsylvania Health System (United States); Mark A. Rosen M.D., Hospital of the Univ. of Pennsylvania (United States); Angela DeMichele, The Univ. of Pennsylvania Health System (United States); Arjun G. Yodh, Univ. of Pennsylvania (United States)

Early prediction of cancer therapeutic efficacy is especially important for non-responders. With this information, non-responders can avoid unnecessary side effects and potentially increase chance for survival by switching to alternative therapies without losing time. Several studies have demonstrated that diffuse optical methods have potential to predict neoadjuvant chemotherapeutic efficacy in breast cancer. However, most studies did not have access to blood flow information, and focused on relatively late time points (e.g., one month). We have combined a diffuse correlation spectroscopy and a diffuse optical spectroscopy to simultaneously measure blood flow, total hemoglobin concentration, blood oxygen saturation, and tissue scattering to monitor neoadjuvant chemotherapy of breast cancer patients. Thirteen subjects with breast cancer undergoing neoadjuvant chemotherapy were measured at four time points with diffuse optics: before, 1-2 days after initial therapy, inter-regimen, and post-treatment time points. Subjects with breast cancer were grouped into a responding group (N=9) and a non-responding group (N=4). In addition, healthy subjects (N=4) were measured to quantify longitudinal physiological fluctuations. The optically derived parameters of tumor were normalized with pre-therapy values at each time point. Relative total hemoglobin concentration at the inter-regimen time in responding group was significantly lower than those in non-responding and healthy groups. For multivariate analysis, a probability of non-response was constructed through logistic regression by combining all four optical derived parameters. The probability of non-response for each subject was higher for most of non-responders and lower for responders at 1-2 days after initial therapy and middle of therapy.

8578-15, Session 3

Early optical predictors of neoadjuvant chemotherapy response in breast cancer measured using diffuse optical spectroscopic imaging (DOSI)

Darren M. Roblyer, Boston Univ. (United States) and Beckman Laser Institute (United States); Hideki Takeuchi, Shigeto Ueda, Albert E. Cerussi, Amanda F. Durkin, Anais Leproux, Beckman Laser Institute and Medical Clinic (United States); Ylenia Santoro, Univ. of California, Irvine (United States); Shanshan Xu, Beckman Laser Institute and Medical Clinic (United States); Rita S. Mehta, David J. Hsiang, John A. Butler, Univ. of California, Irvine (United States); Bruce J. Tromberg, Beckman Laser Institute and Medical Clinic (United States)

Currently, response to neoadjuvant chemotherapy in breast cancer patients is evaluated at the time of surgery after months of cytotoxic treatment. Those patients achieving a pathologic complete response (pCR) have been shown to have favorable outcomes. Predictors of response before the start of treatment and/or early feedback on tumor response would allow physicians to adaptively alter regimens to optimize individual outcomes. Our group has recently demonstrated early markers of response using Diffuse Optical Spectroscopic Imaging (DOSI) and we are currently exploring new measurement timepoints. We report the most recent results here. DOSI utilizes temporally modulated near-infrared light (50MHz – 600MHz) from multiple laser diodes in combination with broadband excitation to recover broadband absorption and scattering values from tissue. Concentrations of oxyhemoglobin, deoxyhemoglobin, water and lipids are fit to the recovered absorption spectra. Measurements are made using a simple handheld probe placed on the skin. Functional 2D image maps are created by interpolation between measurement points. In an investigation of 41 subjects, we observed that tumors achieving pCR had a higher baseline oxygen saturation compared with non-pCR tumors (77.8% versus 72.3%). In a retrospective study of 23 subjects, we observed a flare in tumoral oxyhemoglobin concentration (> 40%) on day 1 after the start of chemotherapy only in patients achieving a partial or pathologic complete response. Finally, in an ongoing study we have observed significant tumor hemodynamic fluctuations in 16 subjects during their first 4-6 hour chemotherapy infusion. These observations highlight the potential utility of DOSI technology for therapy response prediction.

8578-16, Session 3

Monitoring neoadjuvant chemotherapy responses with NIR spectral tomography

Shudong Jiang, Brian W. Pogue, Michael A. Mastanduno, Kelly E. Michaelsen, Fadi El-Ghussein, Keith D. Paulsen, Thayer School of Engineering at Dartmouth (United States); Wendy A. Wells, Peter A. Kaufman, Dartmouth Hitchcock Medical Ctr. (United States)

Near infrared spectral tomography (NIRST) has shown promise for reliably monitoring changes in breast cancer vascular and cellular composition through images of total hemoglobin concentration (HbT), tissue oxygen saturation (StO2), water fraction, as well as elastic scattering parameters. In this study, 43 patients under neoadjuvant chemotherapy (NAC) have been enrolled. For each patient, NIRST images of both breasts are acquired prior, during and after the treatment. After surgery, histopathological characteristics of the resected tissue are evaluated and a complete (pCR) or incomplete (pIR) pathological response to NAC is determined and compared with the NIRST results. Up to date, data of 14 patients who have a full complement of imaging data has been analyzed and the percentage change in HbT inside the tumor region between the images obtained during the last breast examination (performed within a 4-week period following the start of therapy) and the images obtained before treatment has been summarized. Comparing the results which appear in our previous paper (S.Jiang et al, Radiology, 252(2):551-60, 2009), the updated data show an even stronger statistically-significant separation of mean percentage change in HbT between subjects with pathological complete response (pCR) and pathological incomplete response (pIR) (p-value for difference in mean percentage change in HbT between the pCR and pIR groups is now 0.0017). The results are also compared to the data obtained from a hand-held Diffuse Optical Spectroscopic Imaging (DOSI) system, which is currently under evaluation in a national multi-center (ACRIN) trial.

8578-17, Session 3

Functional measurements of tumor response during neoadjuvant chemotherapy using diffuse optical spectroscopic imaging: preliminary results of the ACRIN #6691 trial

Anais Leproux, Amanda F. Durking, Montana Compton, Erin Sullivan, Darren M. Roblyer, Hideki Takeuchi, Albert E. Cerussi, Beckman Laser Institute and Medical Clinic (United States); Rita S. Mehta, Chao Family Comprehensive Cancer Ctr. (United States); Bruce J. Tromberg, Beckman Laser Institute and Medical Clinic (United States)

In April 2011 we activated the first multi-center clinical trial to evaluate breast cancer chemotherapy response using an optical technology in a study sponsored by the American College of Radiology Imaging Network (ACRIN). Sixty breast cancer patients receiving neoadjuvant chemotherapy will be measured using Diffuse Optical Spectroscopic Imaging (DOSI) in five academic clinical research centers: UC Irvine, Dartmouth, U Penn, UC San Francisco and Massachusetts General Hospital. This report is an update on the progress of this study (ACRIN #6691).

The study aims are: (#1) Advance DOSI technology by establishing procedures and methods for Quality Control and Instrumentation (QC/I), and (#2) Utilize the QC/I technology framework to conduct longitudinal DOSI and MRI measurements in limited multicenter clinical translational studies. Each ACRIN site features identical DOSI instruments and procedures. DOSI combines frequency-domain photon migration with steady-state tissue spectroscopy to measure broadband near-infrared absorption and reduced-scattering spectra (650-1000 nm) of breast tissue in vivo. Near-infrared spectra are acquired at discrete spatial locations and map the tissue concentration of oxy and deoxy -hemoglobin, water, and lipid. A tissue optical index (TOI), based on deoxy-hemoglobin, water, and lipid concentrations, is under investigation as a surrogate endpoint for pathological complete response.

Twenty-six patients have been enrolled between June 2011 and June 2012. Seven were excluded from the study because of various reasons and 9 patients have completed chemotherapy. We will outline the challenges we have faced and how standardized tests and analysis procedures have been developed to improve study data quality.

8578-18, Session 3

Dynamic optical breast imaging for neoadjuvant therapy monitoring

Stefan A. Carp, Christy M. Wanyo, Qianqian Fang, David A. Boas, Steven J. Isakoff, Massachusetts General Hospital (United States)

Near-infrared optical measurements have been shown to offer a promising non-invasive way for monitoring breast neoadjuvant chemotherapy (NAC) and predicting outcome. Here, we extend optical measurements to capture additional hemodynamic and metabolic

biomarkers revealed by dynamically imaging breast tissue during fractional mammographic compression. We are conducting a pilot feasibility study in female patients with unilateral locally advanced breast cancer undergoing standard-of-care NAC. Pre-treatment and day 7 post-treatment TOBI scans are obtained, with additional (optional) scans on day 1 of each subsequent chemotherapy cycle. Time-resolved oxy-(HbO), deoxy-(HbR), and total-(HbT) hemoglobin concentration and hemoglobin oxygen saturation (SO2) are calculated. The compression-induced rate of change of HbT correlates with changes in tissue blood volume indicative of biomechanical properties. The evolution of tissue SO2 is modeled to obtain an index of the ratio of oxygen metabolism to blood flow. Response is defined as >50% reduction in the largest tumor diameter. We focused our initial group analysis on 5 HER2+ patients, of which two were non-responders, and three were responders according to our criteria. In this subgroup, the non-responders had an average increase of 1% in total hemoglobin concentration from day 0 to day 7, while the responders had an average 12% decrease in HbT, respectively. We also noted different trends in the evolution of the tissue oxygen consumption to blood flow ratio, which increased 32% in non-responders from day 0 to day 7, while decreasing 11% in responders. These results suggest that dynamic diffuse optical tomography can detect changes due to treatment.

8578-19, Session 4

A diffuse optical tomography imaging system for monitoring tumor response to neoadjuvant chemotherapy in breast cancer patients

Jacqueline E. Gunther, Emerson Lim, Hyun-Keol Kim, Melinda Brown, Susan Refrice, Molly L. Flexman, Kevin Kalinsky, Columbia Univ. (United States); Dawn L. Hershman, Columbia Univ. Medical Ctr. (United States); Andreas H. Hielscher, Columbia Univ. (United States)

Breast cancer patients often undergo neoadjuvant chemotherapy to reduce the size of the tumor before surgery. Tumors which demonstrate a pathologic complete response associate with improved disease-free survival; however, as low as 9% of patients may achieve this status. The goal is to predict response to anti-cancer therapy early, so as to develop personalized treatments and optimize the patient's results. Previous studies have shown that tumor response can be predicted within a few days of treatment initiation. We have developed a diffuse optical tomography (DOT) imaging system for monitoring the response of breast cancer patients to neoadjuvant chemotherapy.

Our breast imaging system is a continuous wave system that uses four wavelengths in the near-infrared spectrum (765 nm, 808 nm, 827 nm, and 905 nm). Both breasts are imaged simultaneously with a total of 64 sources and 128 detectors. Three dimensional reconstructions for oxy- hemoglobin concentration ([HbO2]), deoxy-hemoglobin ([Hb]) concentrations, and water are performed using a PDE-constrained multispectral imaging method that uses the diffusion approximation as a model for light propagation.

Each patient receives twelve weekly treatments of Paclitaxel followed by four cycles of Doxorubicin and Cyclophosphamide (AC) given every other week. There are six DOT imaging time points: baseline, week 3 and 5 of Paclitaxel, before AC, cycle 1 and 2 of AC, and before surgery. Preliminary results show that there is statistical significance for the percent change of [HbO2] and [Hb] at week 2 from the baseline between patients with a pathologic response to chemotherapy.

8578-20, Session 4

Imaging the effects of neoadjuvant chemotherapy on the contralateral normal breast using MRI and diffuse optical spectroscopic imaging (DOSI)

Thomas D. O'Sullivan, Anais Leproux, Jeon-Hor Chen, Orhan Nalcioglu, Alex Matlock, Min-Ying Su, Bruce J. Tromberg, Univ. of California, Irvine (United States)

DOSI (Diffuse Optical Spectroscopic Imaging) provides a quantitative measure of tissue functional components allowing for quantitative imaging of breast tissue composition and metabolism. We hypothesize that DOSI can provide a quantitative metric to measure and track changes of breast density. In this study, DOSI was used to image the normal breast tissue of breast cancer subjects undergoing NAC and the results were compared to fibroglandular tissue volume measured by MRI (N=15 subjects, 9 pre- and 6 post-menopausal). Tissue concentrations of hemoglobin, water, and lipid were calculated at each DOSI measurement point on the contralateral normal breast and compared to breast density measured with MRI. Several DOSI parameters correlated strongly with MRI fibroglandular breast density at baseline, including tissue water concentration ($r=0.806$, $p=0.029$) and deoxyhemoglobin concentration ($r=0.963$, $p<0.001$). There was no correlation between density and scattering parameters or oxygen saturation. Examining the effect of NAC on chromophore concentrations yielded valuable information about the action of NAC on normal breast tissue. A steady reduction of oxyhemoglobin suggests that NAC agents act directly on the breast tissue by causing a reduction of perfusion. However, since a reduction in breast tissue water is more apparent in younger, premenopausal subjects, it is possible that NAC suppression of ovarian hormones have a role in reducing breast tissue density as well. Both mechanisms can explain and likely have a role in the NAC-induced reduction of breast density. These results suggest that DOSI is a low-cost, bed-side imaging modality capable of monitoring breast density as a prognostic marker.

8578-21, Session 4

Non-invasive in vivo characterization of cancer-cell proliferation and angiogenesis in breast cancer using dffuse optical tomography

So Hyun Chung, Univ. of Pennsylvania (United States); Michael D. Feldman, The Univ. of Pennsylvania Health System (United States); Daniel Martinez, The Children's Hospital of Philadelphia (United States); Helen Kim, David R. Busch, Univ. of Pennsylvania (United States); Regine Choe, Univ. of Rochester Medical Ctr. (United States); Arjun G. Yodh, Univ. of Pennsylvania (United States)

Cancer cell proliferation and angiogenesis changes indicate tumor growth. Characterization of these properties in in-vivo human breast cancer can magnify the importance of findings from in-vitro tissues. Diffuse Optical Tomography (DOT) was employed to measure 21 infiltrating ductal carcinoma patients. The breast was measured in a transmission geometry using multiple source locations and a CCD camera. The amplitude and phase properties of each source-detector pair were used to quantify oxy-, deoxy- and total-hemoglobin concentrations, tissue oxygenation and reduced-scattering-coefficients. Using Aperio® algorithms, cancer proliferation was quantified by calculating Ki67 positive nuclei percent and angiogenesis was estimated by measuring CD34 stained mean vessel area (um2). Out of 21 subjects, 8 had Ki67 positive staining in normal cells. The ratio of Ki67 expression in cancer cells to surrounding normal cells is correlated with DOT-measured tumor-to-normal ratio of volume-averaged tissue oxygen saturation (Correlation: 0.92, p-value: 0.001), oxy-hemoglobin concentration (Correlation: 0.93, p-value: 0.002), total-hemoglobin

concentration (Correlation: 0.81, p-value: 0.02) and reduced-scattering coefficients (Correlation:0.74, p-value: 0.046). Mean vessel area in cancer correlated with tumor-to-normal ratio of oxy-hemoglobin (Correlation: 0.65, p-value: 0.006, N=17) , total-hemoglobin (Correlation: 0.68, p-value: 0.003) and reduced-scattering coefficients (Correlation: 0.54, p-value: 0.028). The difference between the field of view needed to calculate a parameter value (i.e., macroscopic (cm3) for DOT and microscopic (um3) for histology) likely lowers the correlation between the two technologies. However, the results of this study clearly suggest that DOT measures tumor growth due to proliferation of cancer cells in oxygenated environment and angiogenesis in cancer-cell-surrounding stroma.

8578-22, Session 4

Broadband optical mammography: oxygenation mapping, edge-effect corrections, and depth discrimination

Pamela G. Anderson, Jana M. Kainerstorfer, Angelo Sassaroli, Elizabeth Rosenberg, Roni Cantor-Balan, Geethika Weliwitigoda, Fridrik Larusson, Eric L. Miller, Misha E. Kilmer, Tufts Univ. (United States); Marc J. Homer, Roger A. Graham, Tufts Medical Ctr. (United States); Sergio Fantini, Tufts Univ. (United States)

Optical mammography is an imaging modality which can provide functional information about breast tissue through absorption contrast of near infrared light. Functional information can aid in breast cancer diagnosis and monitoring response to therapy. We have previously reported broadband optical mammograms that allow for breast tumor detection on the basis of measured oxygen saturation of hemoglobin. We are in the process of confirming these initial results on a larger patient population. Using a broadband light source (650-900nm), we perform a collinear illumination-collection scan of the breast in transmission mode, and we apply a paired-wavelength spectral method for quantitative oximetry. The growing clinical data set allows us to re-evaluate and optimize two critical steps in the analysis of optical mammograms, namely edge effects correction, and spatial second-derivative processing. Since we do not collect frequency-domain data, rather than using phase information for tissue thickness assessment, we explore various spatial high-pass or band-pass filters to suppress edge effects. We also exploit the directional information of spatial second derivatives to aid the depth determination of detected tissue inhomogeneities. To this aim, we report data collected with off-axis illumination and collection optical fibers, which allow for depth discrimination in optical mammograms. On tissue-like phantoms, we have found depth assessment to be accurate to within 6 mm. We will report our latest results in the areas of oxygenation mapping on a screening patient population, optimal edge-effect correction based on continuous-wave data, and depth resolution as a supplement to 2D projection optical mammograms.

8578-23, Session 4

Improvisations on target specific optical reconstruction of breast cancer using NIR fluorescence-enhanced contrast agent

Francis K. J., Iven Jose, Christ Univ. (India)

Estrogen induced proliferation of mutant cells is a growth signal hallmark of breast cancer. Fluorescent molecule that can tag Estrogen Receptor[ER] can be effectively used for detecting cancerous tissue at an early stage. A novel target-specific NIRf dye conjugate aimed at measuring Estrogen Receptor[ER] status was synthesized by ester formation between 17-? estradiol and a hydrophilic derivative of ICG, cyanine dye, bis-1,1-(4-sulfobutyl) indotricarbocyanine-5-carboxylic acid, sodium salt. In-vitro studies provided specific binding on ER+ve [MCF-7] cells clearly indicating nuclear localization of the dye for ER+ve as compared to plasma level staining for MDA-MB-231. Furthermore, cancer prone cells showed ~4.5-fold increase in fluorescence signal intensity compared to control.

A model of breast phantom was simulated to study the in-vivo efficiency of dye with the parameters of dye obtained from photo-physical and in-vitro studies. The excitation (754nm) and emission (787nm) equation are solved independently using parallel processing strategies. The results were obtained by carrying out wavelet transformation on forward and the inverse data sets. An improvisation of the Information content of system matrix was suggested in wavelet domain. The inverse problem was addressed using Levenberg–Marquardt procedure with the minimization of objective function using Tikhonov approach. The multi resolution property of wavelet transform was explored in reducing error and increasing computational efficiency. Our results were compared with the single resolution approach on various parameters like computational time, error function and Normalized Root Mean Square (NRMS)error. A model with background absorption coefficient of 0.01mm-1with anomalies of 0.02mm-1 with constant reduced scattering of 2.0mm for different concentration of dye was compared in the result. The reconstructed optical properties were in concurrence with the tissue property at 787nm. We intend our future plans on in-vivo study on developing a complete instrumentation for imaging a target specific lipophilic dye.

8578-24, Session 4

Three-dimensional tomographic imaging using a Gen-2 hand-held optical imager: reflectance and transmission studies

Jean Gonzalez, Manuela Roman, Sarah J. Erickson, Jennifer Carrasquilla, Anuradha Godavarty, Florida International Univ. (United States)

The application and proliferation of optical imaging technology to breast cancer diagnosis and prognosis has produced a myriad of imaging devices. Recently, a novel Gen-2 hand-held optical imager was developed in our Optical Imaging Laboratory, which is capable of contouring to tissue curvatures, simultaneous multiple point illumination and detection, and imaging of large tissue surfaces both via reflectance and transmission approaches. The reflectance and transmission imaging capabilities of the hand-held imager was tested via extensive experimental using cubical tissue phantoms containing absorption based targets. The experimental studies determined that the hand-held optical imager could detect targets (from 2D surface images) up to 2.5 and 5 cm deep when employing reflectance and transmission imaging, respectively. Initial human subject studies conducted on healthy volunteers over the age of 21 also suggested successful 2D localization of absorption based targets placed in the infra-mammary fold. Currently extensive reflectance and transmission based phantom studies are performed in order to evaluate the 3D tomographic imaging capabilities of the imager. Additionally, in-vivo studies on normal breast tissues are also carried out to assess the effect of pressure on target detectability during reflectance and transmission imaging. The gen-2 hand-held optical imager has potential to be used as a reflectance based imager (similar to ultrasound) or as a transmission based imager (similar to x-ray mammography) in an actual clinical setting.

8578-91, Session PSun

Dual-source and dual-frequency endoscopic diffuse optical tomography reconstruction algorithm based on the effective detection area

Zhuanping Qin, Shanshan Cui, Yanshuang Yang, Ying Fan, Xiaoqing Zhou, Huijuan Zhao, Feng Gao, Tianjin Univ. (China)

In this paper, dual-source and dual-frequency endoscopic diffuse optical tomography reconstruction algorithm based on the effective detection

area is investigated for the reconstruction of the optical parameters including the absorption and reducing scattering coefficients. The forward problem is solved by the finite element method based on the dual-source and dual-frequency diffuse equation. A dual-frequency Newton-type algorithm is applied to obtain the solution. To further improve the image accuracy and quality, the above method based on the region of interest (ROI) is applied. The simulation and experiment are performed in the cervix canal model to verify the validity of the algorithm. Results show that the dual-source and dual-frequency reconstruction improves the image accuracy and quality compared to the results with single-source and single-frequency method. The contrast-to-noise ratio (CNR) is high as 9. The peak coefficients in ROI are equivalent to the true of the optical coefficients with RMS less than 10%. The percentage errors calculated for the mean optical coefficients in the ROI are less than 12%. Meanwhile, the source-detector distance can be further decreased with the dual-source diffuse equation. The results with the method based on ROI show that the CNR is improved by 13 and the maximum RMS of the peak coefficients in ROI are lower 1%, respectively.

8578-92, Session PSun

Resolution studies of a hand-held optical imager

Manuela Roman, Jean Gonzalez, Jennifer Carrasquilla, Sarah J. Erickson, Anuradha Godavarty, Florida International Univ. (United States)

Hand-held optical imaging devices are currently developed by several research groups as a non-invasive and non-ionizing method towards clinical imaging of breast cancer. In our Optical Imaging Laboratory, a Gen-2 hand-held optical imager has been developed capable of 2D surface imaging and 3D tomography. The optical imager is composed of an intensified charge-couple device (ICCD) based detector andsix 785nm laser diodes which are connected to the probe head of the hand-held probe via optical fibers. The hand held probe has a two-part forked design to enable both transmission and reflectance based imaging.

In the current work, the capability of the imager to resolve two closely placed targets is assessed via 2D and 3D tomographic studies. Resolution studies have been carried out under various experimental conditions using slab phantoms (filled with 45% organic milk). Reflectance studies were performed in which targets were placed in 10?10?10 cm3 phantoms at different depths (0.5 to 2.5cm) and different distances between targets (0.5 to 4cm). Targets of different sizes (0.5cm to 1.0cm diameter) filled with Indocyanine green have been used to represent real tumors under both absorbance and fluorescence conditions. Preliminary 2D surface images of reflected measurements have demonstrated the ability of the system to resolve 0.95cm diameter targets placed 1.5cm apart at 1cm depth. Three dimensional tomography reconstructions are currently performed to assess the resolution of the imager under different experimental conditions.

8578-93, Session PSun

EasyTopo: tool for rapid diffuse optical topography based on standard brain atlas

Fenghua Tian, Hanli Liu, The Univ. of Texas at Arlington (United States)

Near infrared spectroscopy (NIRS) based, diffuse optical topography remains a valid tool in functional brain imaging since it avoids solving the forward and inverse computational problems, which are encountered in diffuse optical tomography. Topography is particularly useful when a sparse array of optodes is used and depth specificity is not the main interest. In this study, we have developed an easy graphic tool for rapid diffuse optical topography ("EasyTopo") based on a standard brain atlas (ICBM 152). Probabilistic registration is required to register NIRS measurements onto the brain atlas by digitizing the coordinates of optodes along with several cranial landmarks. EasyTopo approximates the cortical layer of the brain as a hemispherical surface. Therefore, the stereotaxic coordinates of the brain surface and the co-registered NIRS measurements are converted into the spherical coordinates, where 2D angular interpolation of the measured data is implemented to obtain topographic images. Then, the interpolated image is projected back onto the brain surface in the original 3D stereotaxic coordinates. Compared with the existing 3D topography methods, EasyTopo is more computationally efficient and does not require any data extrapolation. Another advantage of EasyTopo is that the data between two spatially adjacent measurements is interpolated along their included angles (i.e., along the angular direction) rather than along a straight line going under the brain surface; the former geometry in principle matches better with the real measurement setup. To support the study, EasyTopo has been used and validated with published data. Now it is publically available.

8578-94, Session PSun

Mechanical indentation improves cerebral blood oxygenation signal quality of functional near-infrared spectroscopy (fNIRS) during breath holding

William C. Vogt, Edwin Romero, Virginia Polytechnic Institute and State Univ. (United States); Stephen M. LaConte, Virginia Tech Carilion Research Institute (United States) and School of Biomedical Engineering and Sciences, Virginia Tech (United States); Christopher G. Rylander, School of Biomedical Engineering and Sciences, Virginia Tech (United States)

Functional near-infrared spectroscopy (fNIRS) is a well-known technique for non-invasively measuring cerebral blood oxygenation, and many studies have demonstrated that fNIRS signals can be related to cognitive function. However, the fNIRS signal is attenuated by the skin, while scalp blood content has been reported to influence cerebral oxygenation measurements. Mechanical indentation has been shown to increase light transmission through soft tissues by causing interstitial water and blood flow away from the compressed region. To study the effects of indentation on fNIRS, a commercial fNIRS system with 16 emitter/detector pairs was used to measure cerebral blood oxygenation at 2 Hz. This device used diffuse reflectance at 730 nm and 850 nm to calculate deoxy- and oxy-hemoglobin concentrations. A borosilicate glass hemisphere was epoxied over each sensor to function as both an indenter and a lens. After placing the indenter/sensor assembly on the forehead, a pair of plastic bands was placed on top of the fNIRS headband and strapped to the head to provide uniform pressure and tightened to approx. 4 lbf per strap. Cerebral blood oxygenation was recorded during a breath holding regime (15 second hold, 15 second rest, 6 cycles) in 4 human subjects both with and without the indenter array. Results showed that indentation increased raw signal intensity by 85 ± 35%, and that indentation increased amplitude of hemoglobin changes during breath cycles by 313% ± 105%. These results suggest that indentation improves sensing of cerebral blood oxygenation, and may potentially enable sensing of deeper brain tissues.

8578-95, Session PSun

in vivo evaluation of atlas-based HD-DOT reconstructions over the occipital cortex

Silvina L. Ferradal, Adam T. Eggebrecht, Mahlega S. Hassanpour, Washington Univ. in St. Louis (United States); Abraham Z. Snyder, Joseph P. Culver, Washington Univ. School of Medicine in St. Louis (United States)

High-density diffuse optical tomography (HD-DOT) is a non-invasive imaging technology that measures hemodynamic physiology, similar to the BOLD signal of functional MRI (fMRI), with superior temporal resolution and moderate image quality. Due to its portability, HD-DOT

facilitates longitudinal monitoring desirable for studying clinically relevant populations such as stroke patients and premature infants. Previous studies have shown that anatomically-based head models derived from the patient's structural images can improve the accuracy of the DOT reconstruction. However, this modeling approach contradicts the portability premise of the DOT technique and becomes impractical for bedside monitoring. In this work, we propose a methodology to build atlas-based head models derived from the MNI152 atlas, a head template that exhibits high spatial resolution without being subject to the idiosyncrasies of single subject atlases. We validate the reconstruction accuracy relative to subject-specific head models as well as subject-matched fMRI maps of cortical responses to visual stimulation in five healthy adult subjects. Group averaged t-maps obtained for atlas-based DOT and fMRI cortical responses exhibit strong spatial agreement. Quantitative comparisons demonstrate that atlas-based DOT has an average localization error of (2.9+/-1.1) mm relative to subject-specific DOT and (8.3+/-1.6) mm relative to the gold standard of fMRI. These promising results suggest that the proposed technique provides adequate spatial localization in the absence of subject-specific structural information and illustrates the potential of atlas-based DOT as a valuable imaging tool for reporting brain function at the bedside.

8578-96, Session PSun

Development of quality control and instrumentation performance metrics for diffuse optical spectroscopic imaging instruments in the multi-center clinical environment

Samuel T. Keene, Albert E. Cerussi, Robert V. Warren, Brian Hill, Darren M. Roblyer, Anais Leproux, Amanda F. Durkin, Thomas D. O'Sullivan, Hosain Haghany, Bruce J. Tromberg, Beckman Laser Institute and Medical Clinic (United States)

Instrument equivalence and quality control are extremely important in multi-center clinical trials. We currently have five identical Diffuse Optical Spectroscopic Imaging (DOSI) instruments enrolled in the American College of Radiology Imaging Network (ACRIN, #6691) trial of at five academic clinical research sites in the US. In order to reliably compare DOSI measurements across different instruments, operators and sites, we must be confident that the data quality is comparable and require objective and reliable methods for identifying, correcting, and rejecting low quality data. To achieve this goal, we took frequency domain photon migration (FDPM) measurements of tissue-simulating phantoms using DOSI instruments at two of the ACRIN sites, and recovered optical properties (absorption and reduced scattering) that were within 5% of one another. Further, we performed a similar set of measurements using an ACRIN DOSI instrument and our newest miniature DOSI instrument prototype, and found that the two instruments also recovered optical properties that agreed within 5%. We also identified crucial sources of error in the broadband portions of our DOSI measurements and developed new calibration procedures to help eliminate these errors. Finally, we developed and tested an automated quality control algorithm that rejects data points that are below the noise floor of our instruments. Using a new protocol for obtaining dark-noise data, we were able to apply the algorithm to ACRIN patient data and successfully improve the quality of recovered physiological data, as well as identify measurements that could not be improved by rejecting noisy data points.

8578-97, Session PSun

Noninvasive quantification of in vivo optical properties and chromophores concentrations of different layers of human tissue using portable multichannel frequency domain photon migration system

Soroush Mirzaei Zarandi, Oren Gross, Hosain Haghany, Goutham Ganesan, Albert E. Cerussi, Bruce J. Trombeg, Univ. of California, Irvine (United States)

Non-invasive access to muscle and brain tissue hemoglobin oxygenation requires extracting information content through a top layer (e.g., fat or bone) with thickness ranging from a few mm to over a centimeter. In order to quantify the unique metabolism of each layer, it is important to decouple top and bottom layer optical properties because diffuse signals generally represent a mixture of both layer's optical properties. In this study, we separated arm (triceps brachii) and leg (gastrocnemius) muscle oxygenated and deoxygenated hemoglobin dynamics from fat layer dynamics during arterial occlusions using a two layer algorithm. We took reflectance measurements at multiple source-detector (s-d) separations using a multi-channel Frequency Domain Photon Migration (FDPM) system.

The multi-channel FDPM instrument measures phase and amplitude of four discrete near-infrared laser diodes modulated by sweeping from 50-500 MHz at 15, 20, 28 and 35mm s-d separations. A vascular cuff with an automated inflater was used on the dominant arm, while the FDPM probe was placed on the same muscle distal to the occlusion cuff. We took sequential measurements pre, during (2 minutes) and post occlusion. Instrument responses from measurements (frequency-dependent phase and amplitude) were calibrated using phantoms simulating muscle. In next step, phase differences and amplitude ratios of multiple pairs of distances were fitted to a two layer model to recover absorption and reduced scattering coefficients of both layers. Oxy- and deoxyhemoglobin concentrations were then extracted from the wavelength-dependent absorption coefficients. We observed significant changes in muscle oxy- and deoxyhemoglobin concentrations and only slight changes in fat.

8578-99, Session PSun

Fluorescence imaging of vascular endothelial growth factor in mice tumors using targeted liposome ICG probe

Saeid Zanganeh, Yan Xu, Univ. of Connecticut (United States); Marina V. Backer, Joseph M. Backer, SibTech, Inc. (United States); Quing Zhu, Univ. of Connecticut (United States)

VEGF targeted liposome loaded ICG (Lip/ICG) probe for fluorescence tomography was synthesized and its in vivo targeting capability of deeply-seated mice tumors was demonstrated. In the in vivo study, two groups of experiments with mouse tumors located at imaging depths of 1.5 and 2.0 cm were conducted. In the first group, 50 Micro Molar targeted Lip/ICG (n=6) and non-targeted Lip/ICG (n=6) was injected to mice with tumors located at 1.5 cm depth. The second group was injected with 50 Micro Molar targeted Lip/ICG (n=2) and non-targeted Lip/ICG (n=2) with tumors located at 2 cm depth to compare the depth sensitivity of the dyes. The result has shown that non-targeted Lip/ICG was washed out after 60 minutes, however the targeted Lip/ICG remained in the tumor site until 270 minutes. At target depth of 1.5 cm, the fluorescence strength of VEGF targeted Lip/ICG was significantly higher than that of non-targeted Lip/ICG at 30 minutes ($P=0.002$ and Bonferroni-Holm corrected $Pc=0.0083$) and remains significant at 60 minutes ($P=0.001$, $Pc=0.0071$), 90 minutes ($P<0.001$, $Pc<0.001$), 150 minutes ($P<0.001$, $Pc<0.001$), 210 minutes ($P<0.001$, $Pc<0.001$) until 270 minutes ($P=0.011$, $Pc=0.055$). This difference in wash out time suggests that the optimal time window to image VEGF targeted Lip/ICG probe is

between 30 to 270 minutes. At target depth of 2 cm, the fluorescence signal strength of non-targeted and targeted dyes showed similar tread on wash out time and optimal imaging window. In summary, VEGF targeted Lip/ICG has enhanced detection of deeply-seated tumors

8578-100, Session PSun

Brain and muscle oxygenation monitoring using near-infrared spectroscopy (NIRS) during all-night sleep

Zhongxing Zhang, Ramin Khatami, Clinic Barmelweid (Switzerland) and Univ. of Zürich (Switzerland) and Univ. Hospital Zurich (Switzerland)

The hemodynamic changes during sleep are still not well understood. NIRS is ideally suited for monitoring the hemodynamic changes during sleep due to the properties of local measurement, sub-second time resolution, totally safe and good tolerance to motion. Several studies have conducted to monitor cerebral hemodynamics using NIRS in both normal subjects and patients during all-night sleep, but scarce data exist on muscular hemodynamic changes. In the present study, we assessed brain and muscle oxygenation changes in 7 young adults during all-night sleep with combined polysomnography measurement. We found that muscle oxygenation showed similar changes as brain oxygenation during sleep initiation and the transitions between different sleep stages. A decrease in HbO2 and tissue oxygenation index (TOI) while an increase in Hb were observed immediately after sleep onset, and an opposite trend was usually found after transition to deep sleep. Variances in HbO2 and Hb concentration changes were larger (F-test, $p<0.05$) in rapid eye movement (REM) sleep compared to non-rapid eye movement (NREM) sleep in both brain and muscle measures, while similar TOI changes were found only in the muscle, but not in the brain. These results indicate a possible common physiological mechanism to regulate the HbO2 and Hb changes in muscle and brain during sleep, but additional regulation mechanisms are responsible to maintain stable oxygen saturation in the brain.

8578-101, Session PSun

Digital lock-in detection system based on single photon counting for near-infrared functional brain imaging

Wei Meng, Ming Liu, Xi Yi, Linhui Wu, Zhuanping Qin, Huijuan Zhao, Feng Gao, Tianjin Univ. (China)

Near infrared imaging (NIRI) and diffuse optical imaging (DOI) are increasingly used to detect hemodynamic changes in the cerebral cortex induced by brain activity. For the sake of capturing the dynamic changes in real-time imaging applications, such as brain imaging, digital lock-in detection technique could be applied. Using particular modulation and sampling constraints and averaging filters, one can achieve optimal noise reduction and discrimination between sources of different modulation frequencies.

In this paper, we designed and developed a compact dual-wavelength continuous wave DOI system based on the single photon counting digital lock-in detection technique. According to the frequency division multiplexing light source coding technique, sine waves with different frequencies are generated so as to amplitude-modulate two laser sources with different wavelengths. The diffuse light is detected by photomultiplier tubes (PMT) and 13 detection channels collect the data simultaneously. A digital lock-in detection circuit for photon counting measurement module and a DDS (Direct Digital Synthesizer) signal generation module were separately implemented in two FPGA development platforms. We produced an in vitro flat phantom model of human forehead, which possesses absorption coefficients and reduced scattering coefficients that are similar to those of the prefrontal cortex. The probe geometry was designed to cover most of the phantom. To validate the feasibility and functionality of the developed system, a series of experimental tests were performed. Preliminary results were obtained which are in accord with the true parameter values of the phantom.

8578-102, Session PSun

The study of the ellipsoid parametric description of the shape-based diffusion optical tomography

Yuan Wang, Linhui Wu, Zhuanping Qin, Ming Liu, Xiaoqing Zhou, Huijuan Zhao, Feng Gao, Tianjin Univ. (China)

As a new non-invasive medical imaging technology, diffuse optical tomography (DOT) has become one of the focused topics, which can provide vast quantities of functional information of tissues. The reconstruction problem of DOT is highly ill-posed, meaning that a small error in the measurement data can bring about drastic changes of optical parameters. In this paper, it is proposed that the shape-based DOT can effectively reduce the ill-poseness under the assumption that the optical parameters of organizations in various organs are distributed uniformly. By use of the B-spline basis functions, the description of the shape, location, optical coefficients of the inhomogeneity, and the value of the background could be realized with only a small number of parameters. Since the structure of most human organs and tumors is kind of ellipsoid, the shape of the inhomogeneity boundary is described as an ellipsoid. In the forward problem, boundary element method (BEM) is implemented to solve the diffuse equation (DE). In the inverse calculation, a Levenberg-Marquardt algorithm with line search is implemented to solve the underlying nonlinear least-squares problem. Simulation results show that the algorithm is effective in reducing the ill-poseness and robust to the noise. The image quality is reliably improved. By use of continuous-wave measurement system, it is validated that the proposed shape-based DOT reconstruction algorithm has a reasonable accuracy.

8578-104, Session PSun

Near-infrared optical imaging of human brain based on the semi-3D reconstruction algorithm

Ming Liu, Wei Meng, Zhuanping Qin, Xiaoqing Zhou, Huijuan Zhao, Feng Gao, Tianjin Univ. (China)

In the non-invasive brain imaging with near-infrared light, precise head model is of great significance to the forward model and the imaging reconstruction. To deal with the individual difference of human head tissues and the problem of the irregular curvature, this paper extracted head model with Mimics software from the MRI image of a volunteer. This scheme makes it possible to assign the optical parameters to every layer of the head tissues reasonably and solve the diffusion equation with the finite-element analysis. During the solution of the inverse problem, a semi-3D reconstruction algorithm is adopted to trade off the computation cost and accuracy between the full 3-D and the 2-D reconstructions. In this scheme, the changes in the optical properties of the inclusions are assumed either axially invariable or confined to the imaging plane, while the 3-D nature of the photon migration is still retained. This therefore leads to a 2-D inverse issue with the matched 3-D forward model. Comparing to the conventional mode, the Semi-3D reconstruction algorithm reduced the time consumption, at the same time, provided effective depth information.

8578-105, Session PSun

Experimental investigation on region-based diffuse optical tomography

Linhui Wu, Wei Zhang, Limin Zhang, Yuan Wang, Yiming Lu, Huijuan Zhao, Feng Gao, Tianjin Univ. (China)

A region-based approach of image reconstruction using the finite element method is developed for diffuse optical tomography (DOT). The method is based on the framework of the pixel-based DOT methodology and on an assumption that different anatomical regions have their respective sets of the homogeneous optical parameter distributions. With this hypothesis, the region-based DOT solution greatly improves the ill-posedness of the inverse problem by reducing the number of unknowns to be reconstructed. The experimental validation of the methodology is performed on a solid phantom employing a multi-channel DOT system of lock-in photon-counting mode. The results demonstrate that the proposed DOT methodology presents a promising tool of in vivo reconstructing background optical structures with the aid of anatomical a priori.

8578-106, Session PSun

A novel fast image reconstruction of fluorescence diffuse optical tomography for non-contact 360° projection system

Xiaoqing Zhou, Ying Fan, Zhuanping Qin, Ming Liu, Qiang Hou, Huijuan Zhao, Feng Gao, Tianjin Univ. (China)

Fluorescence diffuse optical tomography (FDOT) is a promising technique to map molecular contrast for in vivo small animal. Dense sampling of the illumination and detection can offer an effective way of improving the image reconstruction performances of FDOT, at a cost of lengthy computation times. It is becoming more important to develop faster imaging reconstruction method as the measurement data sets increase in size as a result of the application of newer generation non-contact instruments. Here we provide a fast solution strategy that significantly reduces imaging effort for FDOT with large data sets. The fast imaging strategy firstly subsamples the measured data sets in detection space using a wavelet encoding to reduce the scale of the weight matrix dramatically. Then, L1-norm regularization instead of the L2-norm is utilized for the penalty term due to the sparsity characteristic of the fluorescent sources. As a result, the performance of this reconstruction method is greatly enhanced using the wavelet basis functions with the minimum numbers, which makes the reconstruction procedure more efficient. A non-contact, projection fluorescence tomography system using CCD-based detection and scanning source beam in free space has been established. And physical experiments on solid cylindrical phantoms are carried out to evaluate the fast inversion scheme. Results show that the proposed reconstruction method increases the speed of FDOT without sacrificing the reconstruction quality.

8578-107, Session PSun

Multi-wavelength diffuse optical tomography system using digital lock-in photon-counting technique

Weiting Chen, Hui Guo, Xi Yi, Feng Gao, Limin Zhang, Tianjin Univ. (China)

Diffuse optical tomography was recognized as one of the most potential methods to in-vivo breast imaging due to its advantages of non-invasiveness, high sensitivity and excellent specificity etc. This modality aims at portraying the concentration distribution of oxy-hemoglobin and deoxy-hemoglobin statically or dynamically by resolving the optical properties at multiple wavelengths. To further improve the instantaneity and sensitivity of the method, we have developed a continuous-wave diffuse optical tomography system based on lock-in photon-counting technique, which can perform multi-wavelength measurement simultaneously at ultra-high sensitivity. The system was configured by modulating the laser sources at different wavelengths with different frequencies and adopting a single photon-counting block based on the digital lock-in detection for the data demodulation. A series of phantom experiments were performed to evaluate the capability of the method.

8578-108, Session PSun

Near-infrared spectroscopy system with non-contact source and detector for in vivo multi-distance measurement of deep biological tissue

Tsukasa Funane, Hitachi, Ltd. (Japan) and Keio Univ. (Japan); Hirokazu Atsumori, Masashi Kiguchi, Hitachi, Ltd. (Japan); Yukari Tanikawa, National Institute of Advanced Industrial Science and Technology (Japan); Eiji Okada, Keio Univ. (Japan)

The near-infrared spectroscopy (NIRS) system for detecting the absorption change in deep biological tissues must currently use fiber-optics in contact with the skin to avoid artifacts induced by skin-reflected light or tissue movement. On the other hand, non-contact NIRS imaging has many promising applications such as monitoring the biological state of people that are driving or sleeping. The purpose of this study is the development and application of a non-contact NIRS scanning system with a phosphor cell placed on the skin for in vivo measurement of biological tissue. Because the phosphor is excited by the light that propagates in the tissue and the excitation light is cut by optical filters, the light that propagates in the tissue is selectively detected. The non-contact system was extended to a scanning system with flexible source positions using a galvano scanner. Non-contact measurement of the human forearm muscle was performed with the optical scanning system, and the dependence of optical density change (?OD) caused by the upper-arm occlusion and release on source-detector distance was investigated. The results demonstrate the effectiveness of the multi-distance measurement using this system for human forearm measurement. Furthermore, a human forehead was measured with the system, and the surface-layer subtraction method with short-channel regression was applied. Based on the correlation with a simultaneously measured laser-Doppler signal, a deep-layer signal was successfully extracted, which demonstrates that our optical scanning system can be used as a multi-distance NIRS system for measuring the human forehead.

8578-109, Session PSun

New nonlinear inversion technique for depth distribution of absorption by spatially resolved backscattering measurement

Kazuhiro Nishida, Takeshi Namita, Yuji Kato, Koichi Shimizu, Hokkaido Univ. (Japan)

To estimate the depth distribution of absorption coefficient in turbid medium, a new nonlinear inversion technique was developed. It can solve the difficulty of the nonlinear error of the conventional linear inversion techniques.

First, the turbid medium is divided into imaginary layers with arbitrary thickness. The spatial pathlength distribution (SPD) as a function of source-detector distance is obtained for each layer in the Monte Carlo simulation. In the integral operation using SPD's, we can obtain the absorption coefficient of each layer, or the depth distribution of absorption. This inversion process is based on the assumption that the light attenuation is linear with respect to the small pathlength of a photon. However, if we consider the variance of pathlength of many photons in each layer, this assumption results in nonlinear error. We developed a technique to solve this problem in the following three steps.

First, the initial values of absorption coefficient of each layer are obtained using conventional linear inverse matrix assuming that variance of pathlength of many photons does not exist. Then, improved absorption coefficients are obtained with these initial values and the pathlength variance of many photons using the same matrix. In this way, the nonlinear error is corrected. Repeating this process, the improved absorption coefficient approaches a true value.

The effectiveness of the proposed technique was confirmed in the Monte

Carlo simulation. The effect of measurement noise was analyzed in the simulation. Appropriate conditions of the measurement were obtained in the analysis.

8578-110, Session PSun

In vivo estimation of light scattering and absorption properties of rat brain using single reflectance fiber probe during cortical spreading depression

Izumi Nishidate, Chiharu Mizushima, Keiichiro Yoshida, Tokyo Univ. of Agriculture and Technology (Japan); Satoko Kawauchi, Shunichi Sato, National Defense Medical College (Japan); Manabu Sato, Yamagata Univ. (Japan)

Diffuse reflectance spectroscopy using fiber optic probe is one of most promising technique for evaluating optical properties of biological tissue. We present a new method determining the reduced scattering coefficients mus', the absorption coefficients mua, and tissue oxygen saturation StO2 of in vivo brain tissue using single reflectance fiber probe with two source-collector geometries. In this study, we performed in vivo recordings of diffuse reflectance spectra and the electrophysiological signals for exposed brain of rats during the cortical spreading depression (CSD) evoked by the topical application of KCl. The time courses of mua in the range from 500 to 584 nm and StO2 indicated the hemodynamic change in cerebral cortex. Time courses of mus' are well correlated with those of mua in the range from 530 to 570 nm, which also reflect the scattering by red blood cells. On the other hand, increases in mus' at 500 and at 584 nm were observed before the profound increase in mua and they synchronized with the negative shift of the extracellular DC potential. It is said that the DC shift coincident with a rise in extracellular potassium and can evoke cell deformation generated by water movement between intracellular and extracellular compartments, and hence the light scattering by tissue. Therefore, the increase in mus' at 500 and 584 nm before the profound increase in mua are indicative of changes in light scattering by tissue. The results in this study indicate potential of the method to evaluate the pathophysiological conditions of in vivo brain.

8578-111, Session PSun

Investigation of verbal and visual working memory by multi-channel time-resolved functional near-infrared spectroscopy

Davide Contini, Politecnico di Milano (Italy); Matteo Caffini, Univ. degli Studi dell'Aquila (Italy); Rebecca Re, Lucia M. G. Zucchelli, Politecnico di Milano (Italy); Lorenzo Spinelli, Consiglio Nazionale delle Ricerche–Istituto di Fotonica e Nanotecnologie (Italy); Sara Basso Moro, Silvia Bisconti, Marco Ferrari, Valentina Quaresima, Univ. degli Studi dell'Aquila (Italy); Simone Cutini, Univ. degli Studi di Padova (Italy); Alessandro Torricelli, Politecnico di Milano (Italy)

Working memory (WM) is fundamental for a number of cognitive processes, such as comprehension, reasoning and learning. WM allows the short-term maintenance and manipulation of the information selected by attentional processes. The goal of this study was to examine by time-resolved fNIRS neural correlates of the verbal and visual WM during forward and backward digit span (DF and DB, respectively) tasks, and symbol span (SS) task. A neural dissociation was hypothesised between the maintenance and manipulation processes. In particular, a dorsolateral/ventrolateral prefrontal cortex (DLPFC/VLPFC) recruitment was expected during the DB task, whilst a lateralised involvement of Brodmann Area (BA) 10 was expected during the execution of the DF task. Thirteen subjects were monitored by a multi-channel, dual-wavelength (690 and 829 nm) time-resolved fNIRS system during 3 minutes long DF and DB tasks and 4 minutes long SS tasks. The participants' mean memory span was calculated for each task: DF: 6±1.1 digits; DB: 6 ±1.3 digits; SS: 5±1.3 symbols. No correlation was found between the span level and the heart rate data (measured by pulse oximeter). As expected, DB elicited a broad activated area, in the bilateral VLPFC and the right DLPFC, whereas a more localised activation was observed over the right hemisphere during either DF (BA 10) or SS (BA 10 and 44). The robust involvement of the DLPFC during DB, compared to DF, is compatible with previous findings and with the key role of the central executive subserving in manipulating processes.

8578-112, Session PSun

Development of optical research platform to investigate hemodynamic and metabolic responses to breast cancer chemotherapy in animal models

Ki Won Jung, Natalie A. Mitchell, Hyun Jin Kim, Teresa Yung, Univ. of Rochester (United States); Timothy M. Baran, Univ. of Rochester Medical Ctr. (United States); Kelley S. Madden, Univ. of Rochester (United States); Edward B. Brown, Soumya Mitra, Univ. of Rochester Medical Ctr. (United States); Thomas H. Foster, Univ. of Rochester (United States) and Univ. of Rochester Medical Ctr., Imaging Sciences (United States); Regine Choe, Univ. of Rochester Medical Ctr. (United States)

In clinical research employing diffuse optics, several groups have demonstrated hemodynamic parameters have potential to predict outcome of breast cancer chemotherapy. However, the earliest and the optimal time to monitor hemodynamic parameters to distinguish good and poor responders are unclear, partly due to limited number of patients and practicality of frequent monitoring. Therefore, our lab is developing a research platform to investigate hemodynamic/metabolic responses to chemotherapy in animal models using athymic nude mice with MCF-7 or MDA-MB-231 (human breast cancer cells) injected in mammary fat-pads.

The hemodynamic/metabolic effects of chemotherapeutic drugs commonly used for patients (e.g., Adriamycin, Cyclophosphamide, Taxane) are investigated using the following methods. For hemodynamic response monitoring, the blood flow is measured using a diffuse correlation spectroscopy, and oxy-/deoxy-hemoglobin, water, and lipid concentrations along with tissue scattering are determined using a broadband diffuse optical spectroscopy. The hemodynamic/scattering parameters are measured daily, and their changes are quantified. While hemodynamic parameters have a potential to predict therapy, combining hemodynamic with metabolic parameters may enhance this predictability, based on clinical studies from nuclear medicine imaging. To investigate this, different near-infrared fluorescent contrast agents conjugated with deoxyglucose are being evaluated for their abilities to probe glucose metabolism. As the first step, pharmacokinetics and biodistribution of these agents in the whole body are quantified using a fluorescent stereomicroscope which can translate the stage and stitch individual fields to create a montage. For quantitative determination of dye concentration in deeper tissue, diffuse optical spectroscopy system with dye-specific filters will be used.

8578-113, Session PSun

Sparse signal recovery techniques in fluorescence diffuse optical tomography

An Jin, Birsen Yazici, Rensselaer Polytechnic Institute (United States)

Fluorescence diffuse optical tomography (FDOT) is an emerging molecular imaging modality that uses near infrared (NIR) light to excite the fluorophores injected into tissue; and to reconstruct the fluorophore concentration from boundary measurements. The FDOT

image reconstruction is a highly ill-posed inverse problem due to a large number of unknowns and limited number of measurements. However, the fluorophore distribution is often very sparse in the imaging domain since fluorophores are typically designed to accumulate in relatively small regions.

Recently, the emerging field of compressive sensing (CS) has shown that sparse signals can be recovered exactly from only a small number of measurements. In the last decade, a wide range of reconstruction techniques, which we refer to as sparse signals recovery techniques, have been developed to recover sparse signals from limited number of measurements. The sparse signal recovery techniques fall into two classes: greedy-type algorithms and relaxation techniques. In this paper, we give a brief review of a number of sparse signal recovery techniques in CS literature, and use these techniques to reconstruct the sparse fluorophore concentration map in the FDOT inverse problem. In 3D numerical simulation, we compare the image reconstruction performances of different sparse signal recovery techniques. We also apply the traditional Tikhonov regularization for comparative purpose. We show that most sparse signal recovery techniques have better reconstruction performances than that of traditional Tikhonov regularization, and the relaxation techniques generally outperform greedy-type algorithms in FDOT image reconstruction.

8578-114, Session PSun

Multi-channel time-resolved functional near infrared spectroscopy system

Davide Contini, Rebecca Re, Massimo Turola, Politecnico di Milano (Italy); Lorenzo Spinelli, IFN-CNR (Italy); Giuseppe Romano, Rinaldo Cubeddu, Alessandro Torricelli, Politecnico di Milano (Italy)

Functional near infrared spectroscopy (fNIRS) is a tool to non-invasively monitor task-related hemodynamic changes in the human brain. In this application, the problem of depth sensitivity is of great importance both for localization (e.g. discrimination between diffuse vs. focal changes during brain activation) and eventually for accurate quantification of response (e.g. tumor discrimination in optical mammography). Recent studies have shown either theoretically or experimentally, that in the time-domain depth sensitivity can be improved by exploiting the temporal information. The development of compact and portable time-resolved multi-wavelengths multi-distance systems for clinical application would therefore improve the effectiveness of functional studies. In this work we focus on the development and characterization of an advanced 16 sources and 8 detectors time-resolved system for functional studies with a high achievable SNR and fast images reconstruction/data analysis.

The system is based on a couple of pulsed diode laser heads at the two wavelengths of 690nm and 820nm (repetition frequency of 80MHz, average power of 1-2 mW), an optical system for multiplying the number of injection points on the sample (16 injection positions with minimum switching time of 10 ms), 8 independent single photon detection chains each of them composed by an hybrid single photon PMT and a time correlated single photon acquisition electronic board. The independent detection scheme and the multiplexing approach of the injection points/wavelengths permit to reach the limit in terms of counts and achievable SNR.

The system was tested both with phantoms and in vivo.

8578-115, Session PSun

Monitoring changes in the cerebral metabolic rate of oxygen consumption with diffuse optical and MRI susceptometry techniques in a pig model

Wesley B. Baker, Zachary Rodgers, Kejia Cai, Erin M. Buckley, Joel H. Greenberg, Univ. of Pennsylvania (United States); Turgut Durduran, ICFO - Institut de Ciències Fotòniques (Spain); Arjun G. Yodh, Ravinder Reddy, Univ. of Pennsylvania (United States)

The cerebral metabolic rate of oxygen consumption (CMRO2) is a promising biomarker for identifying diseased tissue in the brain. Combining the optical techniques of diffuse optical spectroscopy (DOS) and diffuse correlation spectroscopy (DCS) is a non-invasive approach to measure CMRO2 via a steady-state compartment model. A compartment model is also utilized to measure CMRO2 from combining the non-invasive MRI techniques of susceptometry based oximetry and velocity mapping. This is a cross validation study between diffuse optics measurements and MRI measurements of CMRO2 increases due to the injection (4.5 mg/kg) of the drug 2,4-dinitrophenol (DNP) in a pig model. DOS/DCS is dominantly sensitive to oxygen saturation and blood flow in the microvasculature while the MRI techniques are applied to measure oxygen saturation and blood flow in the sagittal sinus vein draining the cerebral tissue. The arterial saturation was measured from a blood gas sample taken from the femoral artery. To date, the diffuse optical and MRI techniques measured the same cerebral hemodynamic changes in one pig. Following DNP injection, oxygen saturation decreased by 15 percentage points, blood flow increased 40 percent, and CMRO2 increased 50 percent. More animals will be measured to confirm the agreement between these optical and MRI techniques. A third technique, proton detected 17O MRI, which is a direct measure of CMRO2 that does not rely on the compartment model, is currently being optimized and will ultimately be used to validate the optical and susceptometry measurements.

8578-116, Session PSun

Experimental results using a three-layer skin model for diffuse reflectance spectroscopy

Hanna Karlsson, Ingemar Fredriksson, Marcus Larsson, Tomas Strömberg, Linköping Univ. (Sweden)

We have previously presented a multiparameter three-layer semi-infinite skin model with epidermis of varying thickness, an upper dermis of 0.5 mm and an infinitely thick lower dermis layer for diffuse reflectance spectroscopy. The wavelength dependent scattering was equal in all layers. Monte Carlo simulations of photon transport for epidermal thickness and tissue scattering were used to calculate photon pathlength distributions in each layer. The effect of tissue chromophores was added in the post-processing. Recorded diffuse reflectance spectra at source-detector distances of 0.4 and 1.2 mm were white normalized and calibrated for the relative intensity between the two distances and matched to simulated spectra in a non-linear optimization algorithm. This study evaluates methodological considerations (system calibration and the optimization algorithm) and yields data on the internal model parameters and the main output parameters; RBC tissue fraction and oxygenation. Spectra were recorded on the volar forearm on 33 healthy subjects in a protocol involving a 5 min systolic occlusion. 8/33 recordings were excluded due to drift in the spectrometer (>10% intensity change using an intensity reference). An intensity relaxation factor of ±25% was applied to allow for temporal drift in the spectrometer. The remaining 25/33 recordings were modeled with an rms-error typically < 4%. The estimated RBC tissue fraction and oxygenation showed the expected response during occlusion and hyperemia. In conclusion, the model can predict spectra recorded at two distinctly different distances with good accuracy.

8578-117, Session PSun

Hybrid model for photon propagation in random media based on the radiative transfer and diffusion equations

Hiroyuki Fujii, The Tokyo Metropolitan Institute of Medical Science (Japan); Yoko Hoshi M.D., Tokyo Institute of Medical Science (Japan); Shinpei Okawa, National Defense Medical

College (Japan); Kosuge Tomoya, The Univ. of Electro-Communications (Japan); Satoru Kohno, The Tokyo Metropolitan Institute of Medical Science (Japan)

Recently, forward models based on the radiative transfer (RTE) and the diffusion equations (DE) have been discussed for improvement of the diffuse optical tomography (DOT). The DOT requires an accurate and efficient numerical model for photon propagation inside a random medium. Thus, in the paper, we have proposed a hybrid model based on the RTE and DE in the random medium with an anisotropic source at refractive-index-mismatched boundary to reduce the computational costs with a reasonable accuracy.

We have numerically solved the time-domain RTE and DE by using the finite-difference, discrete-ordinate method in a two-dimensional homogeneous medium for different values of the anisotropic factor. We have performed the time discretization in the forward Euler scheme. A spatial step size and temporal step size were determined for the numerical results to agree with analytical solutions of the RTE and DE within errors.

At first, we have examined a validity of the DE by comparing the fluence rates computed from the RTE and DE. Then, we have determined two length scales, where the DE holds, about 10 from the source and 3 from the boundaries in a normalized unit by the extinction coefficient. By using the two length scales, we have successfully constructed the hybrid model and confirmed a recovery of photon propagation computed from the RTE. We could reduce the computational costs by approximately half comparing with the costs of the RTE.

8578-25, Session 5

Use of a coherent fiber bundle for multi-diameter single fiber reflectance spectroscopy *(Invited Paper)*

Arjen Amelink, Chris Hoy, Henricus J. Sterenborg, Erasmus MC (Netherlands)

Multi-diameter single fiber reflectance (MDSFR) spectroscopy enables quantitative measurement of tissue optical properties, including the reduced scattering coefficient and the phase function parameter gamma. However, the accuracy and speed of the procedure are currently limited by the need for co-localized measurements using multiple fiber optic probes with different fiber diameters. We here present the use of a coherent fiber bundle acting as a single fiber with a variable diameter for the purposes of MDSFR spectroscopy. Using Intralipid optical phantoms with reduced scattering coefficients between 0.24 and 3 per mm, we find that the spectral reflectance and effective path lengths measured by the fiber bundle (NA = 0.40) are equivalent to those measured by single solid-core fibers (NA = 0.22) for fiber diameters between 0.4 and 1.0 mm (r = 0.997). This one-to-one correlation may hold for a 0.2 mm fiber diameter as well (r = 0.816); however, the experimental system used in this study suffers from a low signal-to-noise for small dimensionless reduced scattering coefficients due to spurious back reflections within the experimental system. Based on these results, the coherent fiber bundle is suitable for use as a variable-diameter fiber in clinical MDSFR quantification of tissue optical properties.

8578-26, Session 5

Masked diffuse scanning: towards real-time reconstruction-free diffuse optical depth sectioning

Joseph Angelo, Beth Israel Deaconess Medical Ctr. (United States) and Boston Univ. (United States); Vivek Venugopal, Beth Israel Deaconess Medical Ctr. (United States); Frederic Fantoni, CEA-LETI (France); Irving J. Bigio, Boston Univ. (United States); Lionel Hervé, Jean-Marc Dinten, Vincent Poher, CEA-LETI (France); Sylvain Gioux, Beth Israel Deaconess Medical Ctr. (United States)

Current methodologies for obtaining depth sensitive contrast information from an optically diffusive medium involve complex hardware and software implementations. In turn, such methods typically lead to long acquisition and long reconstruction times making them impractical for real-time use. In this work, we propose a hardware-only method capable of providing depth sensitive contrast information without any reconstruction and with rapid acquisition. This method, termed Masked Diffuse Scanning (MDS), relies on physically masking the point spread function from a collimated beam over a diffusive medium to isolate the contribution of the photon path lengths of interest. By continuously scanning and integrating the obtained images, MDS allows, for the first time, optical depth sectioning of a diffusive medium without any processing.

8578-27, Session 5

A handheld wireless device for diffuse optical spectroscopic assessment of infantile hemangiomas

Christopher J. Fong, Hyun Kim, Lauren Geller, Nicole Weitz, Molly L. Flexman, Maria Garzon M.D., Andreas H. Hielscher, Columbia Univ. (United States)

Infantile hemangiomas (IH) are common vascular growths, occurring in 5-10% of neonates. The clinical presentation is variable, and some hemangiomas have the potential to cause disfiguring and even life-threatening complications. Currently, there is no objective tool to monitor IH or to guide treatment.

A handheld wireless device (HWD) that uses diffuse optical spectroscopy (DOS) technology has been recently been developed by our group to measure absolute oxygenated and deoxygenated hemoglobin concentration as well as scattering in tissue. Chromophore reconstructions of these variables can be computed using a multispectral evolution algorithm. We adapted this general purpose device for specific measurements and use in assessment of IH. Advances and improvements include faster data acquisition, a lock-in detection scheme able to perform simultaneous illumination by multiple wavelengths, and an imaging head optimized for superficial tissue imaging.

We validated the new system by experimental studies in which two-layer liquid phantoms and homogeneous liquid phantoms where an object was placed at various depths were imaged. Results show the performance of the device against various layer thicknesses and sensitivity in measuring the optical objects placed at various depths. In addition, a clinical study is under way to assess the utility of DOI for characterizing and monitoring IH. We hypothesize that the HWD will be able to quantitatively characterize changes in perfusion in-vivo concurrently with or before a clinically apparent increase or decrease in lesion size. We also hypothesize that the HWD may provide an earlier indication for treatment assessment for problematic hemangiomas.

8578-28, Session 5

Imaging SERS nanoparticles with Raman tomography

Jennifer-Lynn H. Demers, Scott C. Davis, Brian W. Pogue, Dartmouth College (United States)

Gold core nanoparticles with an additional layer of Raman active material were designed in order to employ Surface Enhanced Raman Scattering (SERS) as an imaging agent for in-vivo measurements. By altering the Raman layer it is possible to create nanoparticles with different spectral features, which can then be imaged simultaneously. The number of particles that can be imaged in a multiplex approach is governed by the ability to generate independent spectra for each distinct Raman

active material. Work has been done showing up to 10 different Raman materials can be used in manufacturing SERS nanoparticles.

The Raman signal generated by the nanoparticles is measured in a tomographic arrangement. Imaging is completed using up to 16 parallel cooled-CCD coupled spectrometers that can be combined with MR images to obtain spatial prior information. Reconstructions of measured signal are completed using diffusion algorithms both with and without the inclusion of spatial priors. Phantom studies are useful to determine the limits of the system in spectrally resolving the various Raman materials. Future work will look at the imaging of targeted SERS nanoparticles to determine the distribution of particles to the target as well as compare the accumulation of targeted versus non-targeted nanoparticles.

8578-29, Session 5

A combined 3D and hyperspectral method for surface imaging of wounds

Lukasz A. Paluchowski, Thomas Røren, Martin Denstedt, Norwegian Univ. of Science and Technology (Norway); Brita S. Pukstad, Norwegian Univ. of Science and Technology (Norway) and St. Olavs Hospital, Univ. Hospital of Trondheim (Norway); Lise L. Randeberg, Norwegian Univ. of Science and Technology (Norway)

Information about the size and depth of a wound and how it is developing is an important prognostic tool in wound diagnosis. In this study a two-camera vision system has been developed to collect optical properties, shape and volume of chronic skin ulcers as tool for diagnostic assistance. This system combines the functionality of 2D imaging spectroscopy and 3D stereo-photogrammetry. A high resolution hyperspectral camera and a monochromatic video frame camera were mounted on the same scanning system. Stereo images were acquired using different baselines by controlling the position of the video camera in the scanning direction. This information was used for accurate estimation of the transformation matrices that bring the two images to epipolar orientation. A digital Surface Model (DSM) of the wound surface was computed after the rectification. The resulting DSM of undamaged surroundings of the wound was used to reconstruct the top surface above the wound and thus the wound volume. Additionally, the hyperspectral image was co-registered to the monochromatic frame image and an orthoimage was produced using the DSM. This allowed for metric measurements of parameters delivered from the spectral analysis (e.g. tissue oxygenation, pigmentation, classification). The analyses can, if desired, be limited to a certain depth of interest like the wound bed or wound border. Simultaneous analysis of the hyperspectral data and the surface model gives a promising, new, non-invasive tool for characterization of chronic wounds. Future work will concentrate on implementation of real time analysis and improvement of the accuracy of the system.

8578-30, Session 5

Diffuse optical tomography using wavelength-swept laser

Jae Du Cho, Pusan National Univ. (Korea, Republic of) and Univ. of California, Irvine (United States); Gukbin Lim, Myung-Yong Jeong, Pusan National Univ. (Korea, Republic of); Orhan Nalcioglu, Gultekin Gulsen, Univ. of California, Irvine (United States); Chang-Seok Kim, Pusan National Univ. (Korea, Republic of)

Diffuse optical tomography is powerful and cost-effective medical imaging technique that can provide functional information of thick tissue, such as saturation oxygen level of blood, lipid and water concentration deep inside tissue. Due to light-tissue interaction, wavelength dependent absorption and scattering occur and one can measure photon flux distribution with an optical instrumentation. Generally, individual laser diodes have been employed to measure light scattering and absorption. However, it is widely accepted that the more wavelength we use, the more accurate functional information we obtain.

In this paper, we introduce diffuse optical tomography system using wavelength-swept laser. We have focused on reducing spectral time and simplifying hardware complexity by replacing multiple light sources with a single wavelength-swept laser. The laser consists of two different semiconductor optical amplifiers, which are centered at 800 nm and 850 nm, a fiber optic band-pass filter, fiber directional couplers. Launched wavelength covers from 780 to 880 nm and averaged optical output power is 20 mW. Wavelength swept rate is 1000 times/second. We also introduce signal modulation techniques for wavelength-swept laser to obtain high signal-to-noise ratio and its novel signal processing methods as well.

8578-31, Session 5

Spectroscopic diffuse optical tomography with high yield

Martin B. van der Mark, Milan J. H. Marell, Philips Research Nederland B.V. (Netherlands)

Light from a super continuum source is dispersed into a number of wavelength bands, coded using a spatial light modulator and recombined into an optical fiber that delivers it to living tissue. Diffuse light emanating from the tissue is detected efficiently with an array of high numerical aperture, single-element photo detectors and spectrally resolved by demodulation. This method allows spectral changes in tissues to be imaged with high speed and sensitivity.

8578-32, Session 6

MRI-guided optical spectroscopy of breast cancer: optimized coupling to varying breast sizes and integration with clinical DCE-MRI

Michael A. Mastanduno, Shudong Jiang, Thayer School of Engineering at Dartmouth (United States); Roberta M. DiFlorio-Alexander, Dartmouth Hitchcock Medical Ctr. (United States); Brian W. Pogue, Keith D. Paulsen, Thayer School of Engineering at Dartmouth (United States)

In the current design of image-guided optical spectroscopy, the information can compliment that of contrast MR imaging of breast cancer with functional maps of tissue physiology. The optical systems used in the past have been limited by low sensitivity to lesions near the chest wall and its inability to image women with smaller breasts (A or B cup). We address these issues by implementing a breast interface that houses optical fibers directly within a clinical MRI breast coil and can accommodate a wide range of breast sizes and lesion locations. This interface especially improves sensitivity towards lesions located in the upper outer quadrant of the breast, and near the medial chest wall—two important regions where breast lesions are commonly found. In testing and optimizing the device, we present phantom data showing contrast recovery in this new imaging geometry within 5% of the expected value and successful imaging of healthy volunteers of all breast sizes, demonstrating improvement over previous designs.

Finally, we present results from an ongoing clinical study (target 60 patients) where this technology is used to try to separate malignant lesions from benign, prior to biopsy. Imaging results of suspicious regions are compared with histopathological analysis of biopsy samples from the same regions. In optimizing this multimodality imaging technique, we hope to be able to aid healthcare decisions while providing more information to clinical MRI exams. This combination provides complex anatomical and molecular information that may decrease the number of unnecessary biopsies thereby improving patient care.

8578-33, Session 6

Hybrid-PMT and photodiode-based multiwavelength diffuse optical tomography system for multiple chromophore recovery in the breast with MRI guidance

Fadi El-Ghussein, Shudong Jiang, Michael A. Mastanduno, Brian W. Pogue, Keith D. Paulsen, Thayer School of Engineering at Dartmouth (United States)

The design and evaluation of a breast diffuse optical tomography (DOT) spectral imaging system is described in detail. The system was created as a hybrid system, to combine frequency-domain (FD) detection of light below 850nm wavelengths, with continuous-wave (CW) detection of NIR light above 850nm. Both approaches utilize 240 data point measurements around the breast. A total of 9 lasers in the visible and near-infrared wavelenths (661 nm – 948nm) are used to quantify the four main chromophores found in the breast: hemoglobin, oxy-hemoglobin, water, and lipid. The frequency domain part of the system uses optimized circuitry for each of 15 photomultiplier tubes (PMTs) in order to record the intensity and phase of the 100MHz modulated signals. The CW part of the system uses 15 photodiodes to record the intensity of the low frequency modulated laser signal (below 100Hz). Evaluation of the system has shown an improvement over our previous systems, particularly in phase accuracy, stability, and reproducibility. The detection system has been incorporated into a MRI-coupled DOT system, allowing simultaneous MRI and NIR spectroscopy of breast tissues. Chromophore recovery and quantification shows an improvement due to the increased number of wavelengths used for imaging. Finally, the result of a first set of clinical trial on cancer patients is summarized.

8578-34, Session 6

Concurrent diffuse optical tomography and photoacoustic tomography with indocyanine green enhancement

Chen Xu, Patrick D. Kumavor, Yan Xu, Quing Zhu, Univ. of Connecticut (United States)

In order to overcome the intensive light scattering in the biological tissue, diffuse optical tomography (DOT) in the near infrared range for breast lesion detection is usually combined with other image modalities such as ultrasound, X-ray, and MRI, to provide guidance. However, these guided imaging modalities depend on different contrast mechanisms from the optical contrast used by DOT. As a result, they can't provide reliable guidance for diffuse optical tomography because some lesions may not be detectable by a non-optical modality but yet have high optical contrast. An image modality which can provide the guidance using optical contrast is desirable for DOT. In this paper, we present a system combined the diffuse optical tomography with the photoacoustic tomography (PAT) to detect and characterize the target embedded in a turbid medium. Photoacoustic tomography utilizes a short-pulsed laser beam to penetrate into tissue diffusively. Upon absorption of the light by the target, photoacoustic waves are generated and used to reconstruct, at ultrasound resolution, the optical absorption distribution that reveals optical contrast. The combined system comprises a 64-channel photoacoustic system integrated with a frequency-domain diffused optical system. To further improve the contrast, the exogenous contrast agent, indocyanine green (ICG) is used. Our experimental results showed that the combined system can detect the phantom up to 2.5 cm in depth and 10 μM in concentration in the intralipid solution with absorption coefficient about 0.068 cm-1. The animal experiments also confirmed that the combined system can detect the tumor region and monitor the ICG uptake and washout. A dose of 100μl of 100μM ICG was injected to the mouse. After twenty minutes, DOT absorption coefficient reached the peak which is about 20% more than the beginning state. This method can potentially improve the accuracy of detecting the small breast lesions or any lesions which are sensitive to the reference change, such as the lesions located on the chest wall.

8578-35, Session 6

Mitigating the effects of the chest wall boundary in diffuse optical tomography

Han Y. Ban, Univ. of Pennsylvania (United States); Manabu Machida, Univ. of Michigan (United States); David R. Busch, Univ. of Pennsylvania (United States); Frank A. Moscatelli, Swarthmore College (United States); Saurav Pathak, Univ. of Pennsylvania (United States); John C. Schotland, Univ. of Michigan (United States); Vadim A. Markel, Univ. of Pennsylvania School of Medicine (United States); Arjun G. Yodh, Univ. of Pennsylvania (United States)

Diffuse optical tomography has been used clinical settings to image physiologically important chromophores in turbid media such as breast tissue. However, these images often show degradations in image quality and artifacts due to boundary effects in the presence of a chest wall. Here we present a systematic bench-top study of the image quality of phantoms with sub-centimeter features in the presence of a large absorptive phantom with optical properties similar to that of a chest wall. We will show how artifacts introduced by the chest wall can be reduced by the exclusion of data near the non-diffuse regions using a linear algebraic reconstruction method.

8578-36, Session 6

Portable handheld broadband multi-channel diffuse optical spectroscopic imaging device for breast cancer applications

Hosain Haghany, Beckman Laser Institute and Medical Clinic (United States)

Diffuse optical spectroscopic imaging (DOSI) is a non-invasive technique based on multiply-scattered near-infrared (NIR) light for quantitative imaging and characterization of thick tissues. For the first time, we developed a portable multi-channel DOSI instrument that employs a handheld probe capable of acquiring broadband absorption and scattering spectra from four unique spatial views. Each view is defined by source-detector (SD) pairs separated by 15, 20, 28 and 35mm in reflectance geometry. Absorption and scattering spectra (650-1000 nm) are obtained by combining 50-500MHz multi-frequency, frequency domain photon migration (FDPM) at four NIR wavelengths (660, 690, 785 and 830) with time-independent broadband spectroscopy. Preliminary measurements of breast cancer patients revealed significant differences in tumor versus normal optical properties for each view in 2D maps. Tissue optical index (TOI=([ctH_2 O]?[ctHHb])/[Lipid]), a contrast function, distinguished between normal and diseased tissues at each probing depth. In a patient treated with neoadjuvant chemotherapy, TOI contrast of shorter channels (SD 15, 20 and 28mm) showed about 40% change during the course of neoadjuvant treatment; however for the longest channel (SD 35mm) it stayed almost constant. This suggest that our 4 channel design is capable of mapping spatially varying subsurface tissue metabolism such as tumors, as well as monitoring response to the neoadjuvant chemotherapy. Tomographic reconstructions of broadband optical properties are currently being explored.

8578-37, Session 6

Scattering estimation from digital breast tomosynthesis guiding near infrared spectral tomographic reconstruction

Kelly E. Michaelsen, Venkataramanan Krishnaswamy, Brian W. Pogue, Dartmouth College (United States); Stephen P. Poplack, Geisel School of Medicine at Dartmouth (United States); Keith D.

Paulsen, Dartmouth College (United States)

X-ray image pixel intensity and optical scattering are compared for several normal subjects to assess the feasibility of using X-ray imaging as a surrogate for optical scattering in near-infrared spectral tomography. If not adequately characterized, scattering mischaracterization can greatly affect quantification of hemoglobin and other tissue chromophores. Digital breast tomosynthesis (DBT) images and single point reflectance measurements of optical breast scattering are compared for a wide variety of breast sizes and densities to determine if scattering can be accurately predicted based on x-ray attenuation. DBT exams in both medio-lateral oblique and cranio-caudal views are obtained according to clinical protocol for normal subjects with x-ray intensities for fibroglandular and adipose tissue drawn from the central projection frame. These images are normalized for x-ray settings (kVp and mAs) and tissue thickness for comparison across patients. Completely co-registered near-infrared continuous wave data is collected nearly simultaneously. Scattering estimates are obtained from a stand-alone frequency domain photon migration unit with a two by two grid measurement in each quadrant and single measurements between each quadrant. Average scattering estimates are then used to reconstruct continuous wave data for tissue chromophores. Scatter values from the optical system will be compared with x-ray attenuation for all patients to evaluate any correlation between the two parameters. Lastly, hemoglobin recovery using the scattering estimated from the x-ray intensity will be compared to using the optical scattering from the hand held probe. If implemented, x-ray based scattering estimation will decrease exam time and cost as well as simplify the design of a newly developed integrated near infrared spectral tomography and digital breast tomosynthesis imaging system.

8578-38, Session 7

Light transport in biological media: analytical solutions, simulations, and experiments *(Invited Paper)*

Alwin Kienle, Andre Liemert, Florian Foschum, Univ. Ulm (Germany)

The light transport in biological media is studied theoretically and experimentally. We derived exact analytical solutions of the radiative transfer equation for different geometries in the steady-state, spatial frequency, frequency, and time domains both for two and three-dimensions. Arbitrary rotationally symmetric anisotropic scattering functions, e.g. the Henyey-Greenstein function or obtained from Mie theory, can be applied. The exact boundary conditions within the transport theory are implemented including Fresnel-reflection at mismatched interfaces. The analytical solutions of the fluence, the radiance, the reflectance, and transmittance are verified with the Monte Carlo method showing an agreement within the statistics of the simulations. In addition, analytical solutions derived from approximations of the radiative transfer equation, e.g. the diffusion equation and the simplified spherical harmonics equations, are found. For the important case of the semi-infinite geometry the analytical solutions are compared to experiments, e.g. to spatially resolved reflectance measurements. Experiments are performed with well-characterized tissue phantoms. As a liquid phantom fat emulsions including ink as absorber are employed, whereas as solid phantoms a resin matrix using titanium dioxide particles as scatterers and different pigments as absorbers is applied. Semi-infinite and layered geometries are considered. The use of the obtained analytical solutions and the Monte Carlo simulations is investigated for determining the optical properties of the considered geometries. Different algorithms for solving the inverse problem are investigated.

8578-39, Session 7

Efficient Green's function and Jacobian matrix calculations for optical tomography problems near boundaries using phase-function-corrected diffusion theory approximations

Roger J. Zemp, Univ. of Alberta (Canada)

Optical tomography and quantitative photoacoustic tomography problems typically have been limited in accuracy, conditioning, computational cost and image quality by the lack of analytical models of light transport that accurately describe light propagation in strongly absorbing turbid media or near the point of entry. Recently Vitkin et al. (Nat. Comm. 2011) described an elegant phase-function correction to the diffusion theory that describes steady-state time-independent radiative transport in these regimes with improved accuracy over diffusion models, P3, and other approximations. Their theory was developed for pencil-beams normally-incident on a semi-infinite turbid medium. We extend their theory to derive and compute Green's functions for the case of a buried directional point source in a semi-infinite turbid medium and provide analytical expressions for phase-function-corrected diffusion-theory estimation of Jacobian matrices for optical tomography problems near boundaries. Calculation of these Green's functions and Jacobian matrices would normally require solving the full radiative transport equation, a computationally burdensome task, however, the analytic approximations provide tremendous computational savings with at most 3D integration required. For now we restrict our efforts to perturbative optical tomography problems where optical heterogeneities are small variations about a homogeneous background. Application of the theory is discussed for DC diffuse optical tomographic estimation of absorption and scattering coefficients, for recovery of fluorophore distributions, and for multiple-illumination photoacoustic tomography. Model calculations for Green's functions are validated against Monte Carlo simulations with 2% accuracy and imaging simulations show improved reconstruction accuracy near boundaries over more traditional diffusion-theory methods in perturbative optical tomography phantom studies.

8578-40, Session 7

Normalized Born ratio of steady-state fluorescence in concave- and convex-shaped infinitely long cylindrical medium geometries

Anqi Zhang, Daqing Piao, Oklahoma State Univ. (United States)

The normalized Born ratio of steady-state fluorescence measurements in a concave or convex-shaped medium geometry is investigated by analytical and numerical methods. The "concave" geometry refers to a scattering-dominant medium enclosed by a long circular cylindrical applicator, and the "convex" geometry refers to a scattering-dominant medium enclosing a long circular cylindrical applicator. The numerical investigation uses finite-element-method, and the corresponding analytical evaluation is based upon a recently developed method of treating steady-state photon diffusion in both concave and convex geometries. The steady-state Born ratio associated with a source and a detector located on the medium-applicator interface is examined for the medium having a homogeneous distribution of fluorophore, and for the source and detector aligning either azimuthally or longitudinally in both concave and convex geometries. At a given set of optical properties and the same line-of-sight source-detector distance, the normalized Born ratio is always smaller in the concave and greater in the convex geometry, respectively, when comparing to that in the semi-infinite geometry. At a given set of optical properties, the increase rate of the normalized Born ratio versus the line-of-sight source-detector distance is the greatest along the azimuthal direction in the convex geometry among the studied cases. The change to the normalized Born ratio caused by containing a target with more or less fluorophore than the background

is also investigated numerically. The results indicate that the normalized Born ratio as well as its sensitivity to the same level of heterogeneity may be geometrically dependent.

8578-41, Session 7

Transport-theory-based transfer matrix for generalized optical system components in contact-free optical tomography

Jingfei Jia, Hyun-Keol Kim, Jong Hwan Lee, Andreas H. Hielscher, Columbia Univ. (United States)

Measurements for Optical Tomography (OT) are often limited to methods employing optical fibers, which are cumbersome to use when dealing with variable and complex geometries. To overcome the difficulties and inconvenience caused by adjusting the OT system to adapt to different objects, contact-free imaging technique are becoming more prominent in OT. These contact-free imaging modalities typically employ CCD cameras in combination with various optical components instead of fiber based systems. For these imaging systems a transfer matrix, which defines the linear mapping from the light intensity distribution on the object's surface to the pixel intensity on the CCD chip (image plane), is required to formulate the inverse problem. To date several groups have presented such transfer matrix using a diffusion model for light propagation in small animals. However, it is well known that the diffusion model does not account for angular dependents of light propagation and emission on the surface of objects. Angular-dependents is particular important for optically thin media, such as small animals, fingers, or media that contain void-like regions.

In this work we present the first transport-theory-based transfer matrix for contact free measurements. Unlike diffusion theory, transport theory provides information about the angular dependent of light propagation. The basic theory, formulations, and numerical results comparing the transport-theory approach to diffusion-theory-based transfer matrixes are presented. Furthermore, we show experimental validation for the case of a conical mirror imaging system. Our results demonstrate the need for accurate transport theory based transfer matrixes in small animal optical tomography.

8578-42, Session 7

Statistical inference for functional imaging data of HD-DOT using non-stationary cluster size analysis based on random field theory

Mahlega S. Hassanpour, Washington Univ. in St. Louis (United States); Brian R. White M.D., Washington Univ. School of Medicine in St. Louis (United States); Adam T. Eggebrecht, Washington Univ. in St. Louis (United States); Silvina L. Ferradal, Washington Univ. School of Medicine, Dept of Biomedical Engineering (United States) and Washington Univ. in St. Louis (United States); Abraham Z. Snyder, Joseph P. Culver, Washington Univ. School of Medicine in St. Louis (United States)

High density diffuse optical tomography (HD-DOT) is becoming a promising neuroimaging modality in neuro-scientific studies of brain in both bedside clinical and naturalistic settings, due to portability and wear-ability of its imaging system. Developing an accurate statistical analysis of data besides improving image quality plays a crucial role in understanding and interpreting neuroimaging results. Recently we have developed more realistic forward light modeling using MRI structural images. Due to differences in optical properties of different tissue types, HD-DOT sensitivity is inhomogeneous resulting in a spatially variant (non-stationary) imaging field. In this work we provide a robust statistical analysis stream for HD-DOT within the frame work of a general linear model (GLM). We estimate local temporal and spatial correlation structures of random fields from the residuals of the GLM. In order to solve the multiple comparison problem we implement a non-stationary cluster size analysis based on Gaussian random field theory. Gaussianized t-fields are generated by estimating temporal degrees of freedom and t-statistics at each voxel and local roughness is estimated by calculating the variance–covariance matrix of spatial partial derivatives of the standardized residuals. This analysis stream provides a general analytical tool to study more complex brain functions with accurate evaluation of statistical significance of the detected activation foci.

8578-43, Session 7

Systematic evaluation of the time-domain two-layer analytical model to estimate the adult brain optical properties

Juliette J. Selb, Tyler M. Ogden, Jay Dubb, Qianqian Fang, David A. Boas, Massachusetts General Hospital (United States)

Time-domain near-infrared spectroscopy (TD-NIRS) offers the ability to measure the absolute baseline optical properties of a tissue. Specifically, for brain imaging, the robust assessment of cerebral blood volume and oxygenation based on measurement of cerebral hemoglobin concentrations is essential for reliable cross-sectional and longitudinal studies. In adult heads, these measurements are complicated by the presence of thick extra-cerebral tissue (scalp, skull, CSF). For this reason, a simple semi-infinite homogeneous model of the head has proven to have limited use because of the large errors it introduces in the recovered brain absorption. An analytical two-layer model has shown improved results, as demonstrated by Monte-Carlo simulations on a semi-infinite two-layer geometry, and the method has been applied by multiple teams on experimental human data since then. However, no estimation of the method performance has been performed on actual head geometry.

Here we present a systematic assessment of the two-layer method to assess the brain optical properties based on realistic Monte Carlo simulations at different measurement locations over the whole head, and for different head structures obtained from MRI segmentations. Simulated optodes are positioned over the whole head with a 1 cm spacing grid configuration. Each optode serves successively as a source while all others serve as detectors. The simulated time-domain data at multiple source-detector separations are fitted to the two-layer model to recover the brain optical properties. We will present the performance and limitations of the method for different scalp locations, and discuss options to improve the results.

8578-44, Session 8

Convergence features of four Monte Carlo methods in the time domain *(Invited Paper)*

Angelo Sassaroli, Tufts Univ. (United States); Fabrizio Martelli, Univ. degli Studi di Firenze (Italy)

In photon migration, Monte Carlo (MC) methods are widely used because they provide a simple and practical tool to solve the radiative transfer equation under various conditions. For example, MC methods can be used to model arbitrary geometries and distribution of the optical properties. The flexibility and simplicity of MC methods are the reasons that they are often considered as a standard for transport calculations. In the literature, different MC methods have been proposed, each characterized by different ways to extract the pathlength between consecutive interaction events. These methods differ also for the assignment of the weight factor of each detected photon. We carry out a time-domain study of four different MC methods aimed at enhancing their different convergence characteristics. We have compared the performance of the MC methods for a wide variety of the optical properties, including both diffusive and non diffusive regimes, in the semi-infinite and slab geometries. This study can provide some guidelines to understand which MC method is more suitable for a given situation, according to the geometry and choice of the optical properties.

8578-45, Session 8

Image reconstruction techniques for ultrasound-modulated optical tomography

Samuel Powell, Terence S. Leung, Univ. College London (United Kingdom)

Ultrasound-modulated optical tomography (UMOT) is a hybrid technique which aims to exploit the optical contrast of biological tissues and the spatial resolution of focused ultrasound fields to produce images of the optical properties of biological tissues.

The insonfication of a coherently illuminated turbid medium gives rise to a 'virtual' optical source of distinct spectral qualities in the region of the acoustic field. This inherent localisation provides a degree of spatial resolution in boundary measurements which has been investigated by a number of authors. The underlying diffuse optical tomography problem within UMOT is, however, fundamentally non-linear: boundary measurements remain dependent upon the optical properties throughout the medium. Thus, the recovery of quantitative information requires that some form of inversion process is applied.

In this work we detail the solution of a forward model of the acousto-optic effect using a finite element formulation. This forward model is used to explore the sensitivity of the UMOT technique in scenarios common to standard diffuse optical tomography, and this information is used to optimise the optical and acoustical configuration employed in our UMOT reconstructions. With an optimised configuration, we assess the performance of various image reconstruction algorithms in recovering three-dimensional images of the optical properties of biological tissues with simulated measurements derived from our reference Monte-Carlo model.

8578-47, Session 8

Genetic algorithm-based approach for quantitative imaging of inhomogeneities in turbid medium using diffuse optical tomography

Atul Srivastava, Abhishek R. Sethi, Indian Institute of Technology Bombay (India)

The present work is concerned with the development and applications of genetic algorithm-based optimization scheme for the reconstruction of the optical inhomogeneities embedded in turbid medium using diffuse optical tomography (DOT). In the proposed inversion scheme, the task of image reconstruction is formulated as optimization problem which is solved using genetic algorithm to find the global minimum of the objective function. This approach preserves the full non-linear features of the problem and it can be applied for quantitative reconstruction over a wide range of contrast values where conventional linear and higher order reconstruction approaches show severe limitations. A genetic algorithm has, basically, five steps: creation of an initial population; evaluation of the fitness of each parent in a given environment; selection of parents based on their fitness; reproduction including recombination and mutation; and finally evaluation of the fitness of a reproduced population in a given environment to serve as parents for next generation. Successful implementation of the proposed scheme has been demonstrated for quantitative reconstruction of absorbing inhomogeneities (single as well as multiple) embedded in an otherwise homogeneous medium. In order to demonstrate its potential, reconstruction results have been presented for a wide range of parameters including size, location and contrast of the absorbing inhomogeneities embedded in the turbid medium. Relatively weak as well as high contrast levels of the embedded inhomogeneities have been considered. Results of the present study show that for small and relatively weakly absorbing inhomogeneities, the accuracy of reconstruction strongly depends on the number of parents considered in the initial generation. Errors associated with reconstruction were seen to decay with an increase in the number of parent population. Details of the proposed reconstruction methodology and primary findings of ther study would be presented in detail.

8578-48, Session 8

Numerical and experimental studies of x-ray luminescence optical tomography for small-animal imaging

Changqing Li, Univ. of California, Davis (United States); Arnulfo Martínez Dávalos, Univ. Nacional Autónoma de México (Mexico); Simon R. Cherry, Univ. of California, Davis (United States)

X-ray luminescence optical tomography (XLOT) is an emerging hybrid imaging modality in which x-ray excitable particles (phosphor particles) emit optical photons when stimulated with a collimated x-ray beam. XLOT combines the high sensitivity of optical imaging with the high spatial resolution of x-ray imaging. For XLOT reconstruction, we compared two reconstruction algorithms, conventional filtered backprojection (FBP) and a new algorithm, x-ray luminescence optical tomography with excitation priors (XLOT-EP), in which photon propagation was modeled with the diffusion equation and the x-ray beam positions were used as reconstruction priors. Numerical simulations based on dose calculations were used to validate the proposed XLOT imaging system and the reconstruction algorithms. Simulation results showed that XLOT can better detect inclusions of particles than CT alone. Nanoparticle concentrations reconstructed with XLOT-EP were much less dependent on target depths than those obtained with FBP. Measurements at just two orthogonal projections were sufficient for XLOT-EP to reconstruct an image for simple source distributions. The heterogeneity of the distribution of x-ray deposition was included in the XLOT-EP reconstruction and improves the reconstruction accuracy, suggesting that there is a need to calculate or measure the x-ray energy deposition for experimental XLOT imaging. We have built a prototype XLOT imaging system, in which a collimated x-ray beam is used to scan the samples and an electron multiplying charge couple device (EMCCD) is used to collect the optical photons emitted by the x-ray excitable particles. Phantom experiments have been performed to validate the XLOT system and the proposed reconstruction algorithms.

8578-49, Session 8

Continuous wave broadband analysis of tissues

Vladislav Toronov, Ryerson Univ. (Canada)

A fundamental problem in the biological tissue characterization and imaging is the high scattering of light which makes optical attenuation measurements ambiguous. This problem was conceptually resolved at some improving levels of practical accuracy by using time-domain and frequency-domain systems, which allow for the separation of absorption from scattering based on the time of flight or phase delay measurements. However, in spite of the progress in time- and frequency-domain hardware, continuous-wave systems offer higher signal-to-noise ratios, better portability, and, potentially, lower equipment and service costs. Although CW systems cannot separate absorption from scattering in unknown media at arbitrary isolated wavelengths of light, we have shown earlier that in biological tissues of known composition one can quantify the chromophore concentrations, such as oxy- and deoxyhemoglobin, water, and fat, and also quantify the reduced scattering coefficient by using broadband approach and by employing characteristic spectral features of chromophores. In this submission we report further developments of our hyperspectral technique, in particular for non-homogeneous tissues of complex structure.

8578-50, Session 8

Diffuse optical imaging system design with point-target Cramér-Rao bounds

Vivian E. Pera, Dana H. Brooks, Mark J. Niedre, Northeastern Univ. (United States)

A persistent topic in diffuse optical imaging has been how best to design source and detector configurations. A popular tool currently used for this purpose is singular value analysis (SVA), where one computes the singular value spectrum of the Jacobian (sensitivity matrix) associated with a particular system configuration and optimizes the configuration to maximize the number of singular values above a given threshold. SVA, however, does not make use of the information contained in the singular vectors of the Jacobian or the covariance of the measurements. In part to address these shortcomings, some have proposed using the Cramér-Rao lower bound (CRLB), which defines the best achievable precision of any estimator for a given data model or, equivalently, system configuration. Because the diffuse optical tomography problem is ill-posed, computing the CRLB is not straightforward; a common approach is to restrict the number of unknowns to be estimated.

In this work, we investigate the applicability of point-target (i.e., all image values are zero except for one) CRLBs to the general diffuse optical tomography problem, where all image values must be recovered. We use the NIRFAST software package to evaluate the performance of a two-dimensional circular imaging geometry for various detector apertures and system noise models. We find that although the point-target CRLBs are capable of predicting performance trends for a given system configuration as a function of depth, for example, in general, they are not useful predictors of system performance across different system configurations.

8578-51, Session 9

Measuring tumor cycling hypoxia and angiogenesis using a side-firing fiber optic probe *(Invited Paper)*

Bing Yu, The Univ. of Akron (United States) and Duke Univ. (United States); Amy Shah, Duke Univ. (United States) and Vanderbilt Univ. (United States); Bingqing Wang, Narasimhan Rajaram, Quanli Wang, Nirmala Ramanujam, Duke Univ. (United States); Gregory M. Palmer, Duke Univ. School of Medicine (United States); Mark W. Dewhirst, Duke Univ. (United States)

Hypoxia and angiogenesis can significantly influence the efficacy of cancer therapy and the behavior of surviving tumor cells. There is a growing demand for technologies to measure tumor hypoxia, particularly cycling hypoxia (CH), and angiogenesis temporally in vivo to enable advances in drug screening, development and optimization.

Frequency-domain photon migration (FDPM) or diffuse optical spectroscopy (DOS) is a noninvasive technology that can provide quantitative information about tissue hemoglobin content and oxygenation status. We have developed a six-wavelength FDPM instrument and a flat side-firing fiber optic probe for noninvasively measuring tumor hypoxia and angiogenesis. The side-firing probe can be easily and reliably attached to a flat skin surface, making it an ideal tool for continuous monitoring of tumor physiology and morphology change in preclinical tumor models. In this presentation, we report the use of the side-firing probe in a preclinical model for monitoring changes in the head & neck (FaDu) tumor physiology upon breathing carbogen gas, cycling hypoxic gas, or just room air. We demonstrated that significant increase in tumor oxygenation with carbogen gas breathing. Decrease in tumor oxygenation with reduced O2 supply during hypoxic gas breathing was captured and the general trend followed that of arterial blood oxygenation measured with a mouse pulse oximeter. Natural CH with patterns and frequency range similar to those reported in literature was also observed in some rats under room air. The studies demonstrated the potential of the technology for longitudinal monitoring of tumor CH during tumor growth or in response to therapy.

8578-52, Session 9

Ovarian tissue characterization using bulk optical properties

Behnoosh Tavakoli, Yan Xu, Quing Zhu, Univ. of Connecticut (United States)

The American Cancer Society reported the mortality rate of the patients diagnosed with ovarian cancer is more than 70% each year in the United States. Due to few symptoms and no reliable screening test, ovarian cancer is not often found in its early stages and therefore the survival rate has not improved remarkably in the past 40 years. Thus, there is an urgent need to improve the current diagnostic techniques or discover specific molecular markers of ovarian cancer. Optical imaging has a great potential to improve the ovarian cancer detection and diagnosis either through minimally invasive or noninvasive approaches. To the best of our knowledge, there is no published literature reporting ovarian tissue optical properties while these bulk parameters are critically important for researchers to understand the complex ovaries. In this study we have characterized the optical properties of 26 ovaries ex-vivo using a Diffuse Optical Tomography system assisted by Ultrasound localization. The feasibility of differentiating benign from malignant ovaries using bulk optical parameters is explored. The light absorption distribution in the ovary is directly related to the vasculature distribution and the scattering coefficient is largely related to the collagen content. Studies using other modalities have shown the relation between collagen content and ovarian cancer development. The quantitative discrimination has indicated that, in the postmenopausal group, malignant ovaries showed 1.3 times lower scattering coefficient than normal ones with the p-value of 0.0021. This encouraging result suggests optical imaging may have a potential role for improving diagnosis of ovarian cancers.

8578-53, Session 9

Monitoring changes in tissue optical properties during and after interstitial photothermal therapy of ex vivo human prostate tissue

Robert A. Weersink, Jie Hie, Israel Veilleux, John Trachtenberg M.D., Brian C. Wilson, Univ. Health Network (Canada)

Near-infrared laser interstitial thermal therapy (LITT) is currently undergoing clinical trials as an alternative to watchful waiting or radical surgery in patients with low-risk focal prostate cancer. Many focal tumors are located on the posterior zone of the prostate next to the rectum. Hence the greatest patient risk is overtreatment leading to localized damage to the rectal wall. To prevent this toxicity, we are developing a method of monitoring treatment progression using transrectal diffuse optical tomography (TRDOT) combined with transrectal 3D ultrasound (3D-TRUS), based primarily on increased tissue optical scattering associated with tissue coagulation. To properly develop the DOT system, absolute measurements of the prostate tissue optical scattering properties were made on ex vivo human prostate samples prior to and post coagulation. Prostate samples were fixed within gel to ensure stable positioning and prevent deformation arising from needle insertions. An interstitial photothermal treatment was delivered generating lesions ~10-15 mm in diameter. During treatment delivery, an optical probe positioned 5 mm from the treatment fiber was used to monitor local changes in tissue optical properties during the treatment. Measurements were also made during treatment using the TRDOT and 3D-TRUS system positioned next to the treatment zone. After treatment, the changes in the tissue optical properties were spatially mapped by repositioning the optical probe in other locations within the prostate, advancing it in 1 mm increments through the coagulation zone and collecting optical properties at each increment. The optical property estimates and spatial information obtained using each method was compared.

8578-54, Session 9

Dynamic contact-free continuous-wave diffuse optical tomography system for the detection of vascular dynamics within the foot

Michael A. Khalil, Hyun-Keol Kim, Andreas H. Hielscher, Columbia Univ. (United States)

We introduce a dynamic contact-free continuous-wave diffuse optical tomography system for the detection and monitoring of peripheral arterial disease (PAD) in the foot. Contact-Free imaging is highly desirable because of the presence of open ulcerations and gangrene wounds in many patients, which make fiber contact with the feet problematic. The system input unit is comprised of two laser diodes (? = 680 and 860nm) that deliver light to 20 collimated optical fibers via a MEMS optical switch. These fibers then shine collimated light onto various positions on the foot and the transmitted light is reflected off a silver coated mirror onto an electron multiplying charge coupled device (EMCCD) camera. The system is operated using a LabVIEW graphical user interface, which allows for ease of operation. The system can achieve a dynamic range of 86 dB with a frame rate of 4 Hz using 20 collimated source fibers and 2 wavelengths. Using this system we have performed first venous occlusion experiment on 3 patients and 2 healthy volunteers. Upon inflating a pressure cuff around the thigh we observe blood pooling and dynamic oxy-and deoxy hemoglobin concentration changes within the foot and subsequent return to resting state, when the thigh cuff is released, differences between healthy and PAD patients are pronounced.

8578-55, Session 9

Measurement of oxygen consumption during muscle flaccidity exercise by near-infrared spectroscopy

Keiko Fukuda, Tokyo Metropolitan Institute of Technology (Japan); Yuuta Fukawa, Tokyo Metropolitan College of Industrial Technology (Japan) and Tokyo Metropolitan Institute of Technology (Japan)

Near-infrared spectroscopy (NIRS) is a noninvasive method for measuring muscle oxygenation and is suitable for evaluating exercise. However, measurement results are influenced by blood volume change due to changes in the blood pressure. In order to evaluate changes in blood volume and to improve measurement accuracy, we applied three-wavelength light source (680nm, 808nm and 830nm) for the continued wave measurement. Two detectors (targeted detector and the reference detector) were placed near the target muscle and apart from it. With three-wavelength light source, the changes of the oxyhemoglobin and the deoxyhemoglobin concentrations are obtained and the scattering in tissue is also obtained.

We measured the blood volume change by controlling the blood pressure by a blood-pressure cuff. The total hemoglobin concentration measured with the target and the reference detectors are almost identical, thus the reference detector is effective for monitoring the blood volume change in the artery and the vain without the tissue oxygenation. We also measured the blood volume change during the handgrip exercise. This time, the total hemoglobin concentration measured by the targeted detector and that measured by the reference detector were different. A stepwise change of oxygen concentration at the timings of grasping and releasing was clearly measured with the reference detector, but was not clearly measured with the target detector. The difference is caused by the existence or non-existence of the tissue oxygenation.

These results show that our method is effective for evaluating blood volume change contained in oxygen concentration.

8578-56, Session 9

Development of transrectal diffuse optical tomography combined with 3D-transrectal ultrasound Imaging to monitor the photocoagulation front during interstitial photothermal therapy of primary focal prostate cancer

Jie He, Univ. of Toronto (Canada); Robert A. Weersink, Israel Veilleux, Ontario Cancer Institute (Canada); Daqing Piao, Oklahoma State Univ. (United States); John Trachtenberg M.D., Brian C. Wilson, Univ. of Toronto (Canada) and Ontario Cancer Institute (Canada)

Near-infrared laser interstitial thermal therapy (LITT) is currently undergoing clinical trials as an alternative to watchful waiting or radical surgery in patients with low-risk focal prostate cancer. Currently, we use magnetic resonance imaging-based thermography to monitor the growth of the photocoagulation zone and determine indirectly the completeness of the target tissue destruction while avoiding damage to adjacent normal tissues, particularly the rectal wall. However, incomplete tumor destruction has occurred in some patients due to premature termination of treatment since the photocoagulation zone is not directly observed. We propose transrectal diffuse optical tomography (TRDOT) in combination with transrectal 3D ultrasound (3D-TRUS) to address his limitation. Here, we present the results of forward simulations and image reconstruction of a growing coagulated lesion with optical scattering contrast, using an established finite element analysis software platform (NIRFAST). A range of source-detector configurations were simulated and compared, in terms of sensitivity to scattering changes in the region of interest. Different image reconstruction schemes were investigated and evaluated in terms of dynamic resolution, localization accuracy and computation efficiency, especially for the accurate delineation of the posterior boundary of the coagulation zone as the critical parameter for treatment guidance. The simulations were validated in tissue-simulating phantoms with measurements acquired in a state-of-the-art continuous wave (CW) TRDOT system, and the performance is compared to that of a frequency-domain (FD) DOT system.

8578-57, Session 9

Development of multispectral transrectal ultrasound compatible near infrared imaging system for early detection of prostate cancer

Venkaiah C. Kavuri, Hanli Liu, The Univ. of Texas at Arlington (United States)

We investigate the feasibility of trans-rectal near infrared (NIR) based diffuse optical tomography (DOT) for early detection of prostate cancer using a transrectal ultrasound (TRUS) compatible imaging probe. Image reconstruction of DOT in trans-rectal scenario faces the following challenges: (1) TRUS-based probe has the limited number of optode locations available (leading to an underdetermined problem), (2) TRUS-based probe has the limited diameter of the optical fibers (causing poor signal sensitivity for source-detector separations > 3cm), and (3) quantification of the absorption contrast depends upon the number wavelengths used. Motivated by these challenges, we designed a multi-wavelength, TRUS-compatible, NIR-based image system, in which the photo diodes were placed on the trans-rectal probe. The conventional TRUS probe can provide positioning information of the probe and guides DOT image reconstruction process by offering the hard prior information on anatomical regions of the target. The placement of photo diodes on the TRUS probe eliminates the issues related to the coupling of light into the optical fiber. A multi-spectral imaging system increases the quantification accuracy of light absorption. We used NIR light between 600-900 nm for the tissue interrogation. DC signals were recorded and used for estimating the absorption coefficient. For validation, we

prepared a laboratory phantom with gelatin-intralipid with an inclusion (having 2:1 contrast) placed at 2 cm depth. The proposed system will be utilized to generate absorption images. For further quantification, reconstructed images obtained from the proposed system will be compared with the reconstructed images using single or dual-wavelength systems.

8578-58, Session 10

Dynamics of tumor oxygen state after single irradiation

Anna V. Maslennikova M.D., Institute of Applied Physics (Russian Federation) and Nizhny Novgorod State Medical Academy (Russian Federation); Anna G. Orlova, Tatiana I. Pryanikova, German J. Golubjatnikov, Institute of Applied Physics (Russian Federation); Ludmila B. Snopova M.D., Nizhny Novgorod State Medical Academy (Russian Federation); Tatiana Smirnova, N.I. Lobachevsky State Univ. of Nizhni Novgorod (Russian Federation); Ilya V. Turchin, Institute of Applied Physics (Russian Federation)

The “oxygen effect” phenomenon and reoxygenation are known to be important factors influencing tumor’s radiosensitivity. This study objective was monitoring of oxygen state changes of rat’s tumor model after single irradiation. Experiments were carried out on white outbreed rats. Pliss’s lymph sarcoma was chosen as a model of rapidly growing poor oxygenated tumor. Irradiation (Co60, 1.25 MeV) was performed on the 5th day after tumor inoculation with single dose of 10 Gy. Distribution and dynamics of concentrations of total hemoglobin, oxygenated hemoglobin, deoxygenated hemoglobin, and blood oxygen saturation were estimated using diffuse optical spectroscopy (DOS). Experiments were performed by frequency-domain diffuse optical spectroscopy setup with single source-detector pair and parallel plane geometry (Institute of Applied Physics RAS, Russia). The results obtained by DOS were verified by direct measurements of pO2 of tumor tissue using needle oxygen sensor. In parallel, standard histology (hematoxylin and eosin) was done in 24 and 48 hours after irradiation.

Changes of tumor oxygenation after irradiation demonstrated a two-phase character. In 24 hours, a significant decrease of oxygen saturation of tumor tissue was observed, that appeared to be due to increase of deoxygenated hemoglobin concentration comparing to the initial level ($p=0.01$) while oxyhemoglobin decreased insignificantly. In 48 hours after irradiation tumor’s oxygen saturation increased because of the decrease of concentration of deoxyhemoglobin and increase the level of oxyhemoglobin. Oxygen saturation levels of tumor tissue measured by DOS and by pO2 sensor demonstrated a strong correlation ($r=0.88$, $p<0.0001$). Histological study in 24 hours after irradiation showed substantial damage of tumor perfusion: venous plethora, oedema, heamostasia and dystrophic changes of tumor cells. In 48 hours microcirculation changes appeared to be less expressed; dystrophic changes of tumor cells strengthened. So, the main reason of radiation-induced decrease of tumor oxygenation in 24 hours was blood flow damage. The reoxygenation in 48 hours aroused from decreased oxygen consumption by dystrophic tumor cells.

8578-59, Session 10

Detection of peripheral arterial disease within the foot using dynamic diffuse optical tomography

Michael A. Khalil, Hyun-Keol Kim, In-Kyong Kim, Martina Barbiero, Columbia Univ. (United States); Rajeev Dayal, New York Presbyterian Hospital (United States); Gautam Shrikande, New York-Presbyterian Hospital (United States); Andreas H. Hielscher, Columbia Univ. (United States)

Peripheral Arterial Disease (PAD) affects over 10 million Americans and is associated with significant morbidity and mortality. PAD is the narrowing of the functional area of the artery due to plaque build-up in the vascular walls. The traditional method for the diagnosis of PAD is the ankle-brachial index (ABI), which is the ratio of the patient’s systolic blood pressure in the dorsalis pedis artery in the foot to the systolic blood pressure in the brachial artery in the arm. An ABI reading less than 0.9 indicates that the subject has affected vasculature. PAD patients with co-morbidities such as diabetes are difficult to diagnose due to calcified arteries, which elevate blood pressure readings leading to false-negative diagnosis. Dynamic diffuse optical tomography (DDOT) promises to overcome the limitations of the current diagnostic techniques. We present results from a 30 patient pilot study, in which we employed DDOT to image the change in hemoglobin concentration in the foot in response to a thigh cuff occlusion. The patients were split into three cohorts 10 healthy, 10 PAD patients, and 10 diabetic PAD patients. Using the dynamic changes in the reconstructed DDOT images of hemoglobin-dependent parameters, such as oxy, deoxy , and total hemoglobin, we observe significant differences between healthy volunteers and PAD patients. Our results suggest that DDOT has the potential to become a reliable diagnostic tool for PAD, including diabetic patients.

8578-60, Session 10

Computer aided diagnosis of rheumatoid arthritis with frequency domain optical tomography

Ludguier D. Montejo, Andreas H. Hielscher, Hyun-Keol Kim, Columbia Univ. (United States)

We present a framework for identifying and using DOT image biomarkers to diagnose Rheumatoid Arthritis (RA). The framework was validated with DOT images of 219 proximal interphalangeal joints obtained from a recent clinical study (99 joints of patients with RA and 120 joints of healthy volunteers). First we extracted 594 features from DOT images and then utilized them to diagnose RA. These features were obtained from the reconstructed absorption and scattering maps, and include spatial-frequency coefficients, Gaussian mixture model parameters, and basic statistical values.

We used ROC curve analysis to identify the classification strength of each individual feature. The top 30 individual features were selected for multidimensional classification for which we employed five different machine learning algorithms; k-nearest neighbors (k-NN), linear discriminate analysis (LDA), quadratic discriminate analysis (QDA), self organizing maps (SOM), and support vector machines (SVM) were used to classify the DOT image of each joint as affected or not affected with RA. We report on the performance of each classification algorithm in terms of diagnostic sensitivity and specificity.

All five classification algorithms found feature combinations for which classification accuracies was better that 90% in terms of sensitivity and specificity. The highest sensitivity (99±1%) and specificity (98±1%) was achieved with the SVM algorithm (Youden index of 0.97). The features that are most predictive of RA are derived from the spatial variation of the optical properties and the absolute range in feature values.

8578-61, Session 10

Quantitative assessment of partial vascular occlusions in a swine pedicle flap model using spatial frequency domain imaging

Adrien Ponticorvo, Eren Taydas, Univ. of California, Irvine, Beckman Laser Institute (United States); Amaan Mazhar, Modulated Imaging Inc., Beckman Laser Institute Photonic Incubator (United States); Thomas Scholz M.D., Univ. of California, Irvine (United States); Jonathan Rimler, Hak-Su Kim, Univ. of California Irvine Medical Ctr. (United States); Gregory R.

D. Evans M.D., Univ. of California, Irvine (United States); David J. Cuccia, Modulated Imaging, Inc. (United States); Anthony J. Durkin, Beckman Laser Institute and Medical Clinic (United States)

The use of tissue transfer flaps has become a common and effective technique for reconstructing or replacing damaged tissue. While the overall failure rates associated with this procedure are relatively low (5-10%), the failure rates of tissue flaps that require additional surgery are significantly higher (40-60%). The reason for this is largely due to the absence of a technique for objectively assessing tissue health after surgery. A device that could definitively quantify various hemodynamic parameters associated with tissue health would be extremely useful for monitoring these tissue flaps. Here we have investigated spatial frequency domain imaging (SFDI) as a potential tool to do this. By projecting wide-field patterned illumination at multiple wavelengths onto a tissue surface, SFDI is able to quantify absolute concentrations of oxygenated and deoxygenated hemoglobin. We have used SFDI to study swine pedicle flaps that were controlled with a real-time vascular occlusion system and monitored by ultrasonic flow probes. We have performed a series of experiments where blood flow from either the arterial or venous vasculature was reduced for 30 minutes to 25%, 50%, 75%, or 100% of the baseline values. We will show that while blood flow changes in the pedicle flap do not become clinically apparent until they have been reduced by more than 75%, SFDI is capable of detecting changes as small as 50%. Additionally, the ability to monitor absolute values of oxygenated and deoxygenated hemoglobin can yield more valuable information about the tissue failure than looking at blood flow or oxygen saturation alone.

8578-62, Session 10

Near-infrared spectroscopy of renal tissue in vivo

Dirk Grosenick, Oliver Steinkellner, Heidrun Wabnitz, Rainer Macdonald, Physikalisch-Technische Bundesanstalt (Germany); Thoralf Niendorf, Max-Delbrück-Ctr. für Molekulare Medizin Berlin-Buch (Germany); Kathleen Cantow, Bert Flemming, Erdmann Seeliger, Charité Universitätsmedizin Berlin (Germany)

We have developed a method to quantify hemoglobin concentration and oxygen saturation of the renal cortex by near-infrared spectroscopy. A fiber optic probe was used to transmit the radiation of three semiconductor lasers at 690 nm, 800 nm and 830 nm to the tissue, and to collect diffusely remitted light at source-detector separations from 1 mm to 4 mm. To derive Hb concentration and blood oxygen saturation the spatial dependence of the measured cw intensities was fitted by a Monte Carlo model. In this model the tissue was assumed to be homogeneous. The scaling factors between measured intensities and simulated photon flux were obtained by applying the same setup to a homogeneous semi-infinite phantom with known optical properties and by performing Monte Carlo simulations for this phantom. To accelerate the fit of the tissue optical properties a look-up table of the simulated reflected intensities was generated for the needed range of absorption and scattering coefficients. The intensities at the three wavelengths were fitted simultaneously using Hb concentration, oxygen saturation, reduced scattering coefficient at 800 nm and scatter power coefficient as fit parameters. The capability of the method for absolute quantification of optical properties was checked by measurements on a set of phantoms with various optical properties known from time-resolved investigations. The method was employed to study the temporal changes of renal Hb concentration and oxygenation on an anesthetized rat during ischemia by arterial occlusion and subsequent reperfusion to simulate phenomena leading to acute kidney injury.

8578-63, Session 10

Importance of optical path length in determining brain hemodynamic properties in a pre-clinical mouse model of Alzheimer's disease

Alexander J. Lin, Adrien Ponticorvo, Bernard Choi, Anthony J. Durkin, Bruce J. Tromberg, Beckman Laser Institute and Medical Clinic (United States)

In this work, we present an economical spatial frequency domain imaging (SFDI) platform utilizing a commercially available LED projector (460nm, 530nm, and 632nm LEDs), cameras, and off-the-shelf optical components suitable for acquiring baseline optical properties. The ability to separate absorption and scattering in the visible wavelengths was shown in liquid blood and ink phantoms. We demonstrate in baseline SFDI of a mouse model of Alzheimer's disease (AD) that total hemoglobin (THb) is significantly decreased compared to controls (48.6 ± 3.5?M vs 66.5 ± 3.4?M, p=0.046) and the measured oxygen saturation is 89 ± 5% and 96 ± 2% (p=0.44) in control (n=8) and AD (n=5) mice, respectively.

In hindpaw stimulation experiments, we show significant differences between AD and control mice in area-under-the-curve (AUC) of the initial dip, the AUC of the subsequent overperfusion, and the relaxation time T50 of the overperfusion. SFDI correction of the differential pathlength factor (DPF) further showed significantly less change in the peak dip and slope of dip of the Hb concentration compared to controls. These results emphasize the importance of determining baseline optical properties for multispectral imaging, and their implications for relative change in cerebral metabolic rate of oxygen (rCMRO2) calculations will be discussed.

8578-64, Session 11

Fluorescence tomography applied to prostate cancer diagnosis using a white pulsed laser

Anthony Daures, Commissariat à l'Energie Atomique et aux Energies Alternatives (France); Jerome Boutet, Commissariat à l'Énergie Atomique (France); Lionel Hervé, CEA-LETI (France); Roland Sauze, Commissariat à l'Energie Atomique et aux Energies Alternatives (France); Emilie Heinrich, Commissariat à l'Énergie Atomique (France); Nicolas Grenier, Univ. Bordeaux 1 (France); Jean-Marc Dinten, CEA-LETI (France)

Prostate cancer diagnosis is based on PSA rate measurement and ultrasound guided biopsy. Recently criticised for its lack of specificity, new approaches are currently investigated: MRI, elastography, TEP, NIRS and Time Resolved (TR) fluorescence tomography. The advantage of TR fluorescence tomography relies on its good complementarity with the standard ultrasound protocol and on the possible localization of prostate tumors marked by specific probes.

After a first TR system based on a bulky titanium-sapphire laser, we designed a new one taking advantage of a more compact white pulsed laser (FIANIUM). The improved compactness is now fully compatible with clinical environment. This setup also allows localizing multiple fluorophore and performing oximetry measurements. The light, filtered by two linear variable filters to select a 770±20 nm window, is driven to the transrectal probe which also collects the fluorescence light emitted by the marker. The signal is detected by photomultipliers connected to TCSPC boards. A reconstruction algorithm based on intensities and time of flight allows a fast localization of the fluorophore.

We compared the performances of the new white laser system to the previous titanium-sapphire on prostate mimicking phantoms. The laser power delivered on the phantom by the new laser appeared to be suitable to fluorescence measurements, just below cutaneous maximum permitted exposure. The new system allowed us to localize fluorescent inclusions of an ICG nanoemulsion at fixed positions inside a prostate mimicking phantom. We investigate the possibility to reduce the influence

of background fluorescence by performing acquisition at multiple wavelengths.

8578-65, Session 11

Whole body fluorescence imaging in humans

Sophie K. Piper, Charité Universitätsmedizin Berlin (Germany); Jan Mehnert, Berlin NeuroImaging Ctr., Charité Universitätsmedizin Berlin (Germany) and Max-Planck-Institut für Kognitions- und Neurowissenschaften (Germany) and Machine Learning Department, Berlin Institute of Technology, Technical University Berlin (Germany); Christina Habermehl, Charité Universitätsmedizin Berlin (Germany); Andreas Wunder, Experimental Neurology, Charité Universitätsmedizin Berlin (Germany) and Ctr. for Stroke Research, Charité Universitätsmedizin Berlin (Germany); Christoph H. Schmitz, Berlin NeuroImaging Ctr., Charité Universitätsmedizin Berlin (Germany) and NIRx Medizintechnik GmbH (Germany); Hellmuth Obrig M.D., Berlin NeuroImaging Ctr., Charité Universitätsmedizin Berlin (Germany) and Max-Planck-Institut für Kognitions- und Neurowissenschaften (Germany) and Clinic for Cognitive Neurology, Univ. Hospital Leipzig (Germany); Jens M. Steinbrink, Ctr. for Stroke Research, Charité Universitätsmedizin Berlin (Germany) and Berlin NeuroImaging Ctr., Charité Universitätsmedizin Berlin (Germany)

Dynamic Near-Infrared Fluorescence (DNIF) imaging of fluorescent dyes has become an established tool in experimental biomedical research for studying the perfusion in small rodents, but also for local applications in humans, e.g. arthritis of finger joints or mammography. With our study we are the first who transferred the well known whole-body imaging approach for rodents directly to humans. Possible applications include a quick screening tool for peripheral vascular diseases of the whole body or its parts (e.g. diabetic feet). As tissue penetration depth of NIR light suffices to trans-illuminate small animals but not humans, it was expected to see mainly skin perfusion. However, analog to the results reported by E. Hillmann (Nat Photonics, 2007) in rodents, we took a focused look at the abdomen and the head of subjects to see if distinct perfusion properties of the organs or the brain may be discernible in humans.

Video sequences and static maps of perfusion depending parameters show, how the overall blood flow in the skin first appears in the head followed by the spreading throughout the trunk, abdomen, and periphery. Ghosting in the whole-body fluorescence data but clearly visible in the close-up measurements of the abdomen is a large internal structure possibly corresponding to the liver which starts fluorescing 4-6 sec earlier and stronger than the surrounding and caudal regions.

We regard this first experiment to be a convincing demonstration of the ability to track fluorescent dyes in the whole human body non-invasively with high spatial and temporal resolution.

8578-66, Session 11

Maximum likelihood reconstruction of extremely sparse solutions in diffuse fluorescence flow cytometry

Vivian E. Pera, Dana H. Brooks, Mark J. Niedre, Northeastern Univ. (United States)

The use of sparsity constraints to improve results obtained with traditional approaches to diffuse optical and diffuse fluorescence tomography has received increased attention in recent years. When the solution is known to be extremely sparse (i.e., all image values are zero except for one), we show that an effective way of imposing such a constraint is to re-parameterize the problem and solve it with the maximum likelihood (ML) method. We derive the ML estimate of the position of a cell in the field-of-view of an instrument designed to detect rare, fluorescently-labeled circulating cells in small animals. The instrument consists of two light sources and six detectors arranged in a ring around the limb to be imaged. The presence of a fluorescently-labeled cell gives rise to “spikes” at the detectors that vary in height depending on the position of the cell, thus permitting tomographic reconstruction. Only one cell is expected to be in the field-of-view at a time.

In the limit of high signal-to-noise ratio, ML estimators are known to achieve the Cramér-Rao lower bound for the precision of the estimate, which guarantees that no other unbiased algorithm will perform better. We compute the Cramér-Rao bound for our estimate, and this suggests that we can localize a cell to within 200 microns of its true position. Our algorithm does not depend on the selection of a regularization parameter, and each reconstruction takes about 0.02 s. We validate the algorithm on limb-mimicking phantoms imaged with the instrument.

8578-67, Session 11

Quantitative depth resolved imaging of protoporphyrin IX (PpIX) using spatial frequency domain imaging (SFDI)

Rolf B. Saager, Beckman Laser Institute and Medical Clinic (United States); Steve Saggese, David J. Cuccia, Modulated Imaging, Inc. (United States); Kristen M. Kelly, Univ. of California, Irvine School of Medicine (United States); Anthony J. Durkin, Beckman Laser Institute and Medical Clinic (United States)

The ability to quantitatively determine tissue fluorescence is critical for the development of dosimetric photodynamic therapy of skin cancer. We have previously reported a method to correct protoporphyrin IX (PpIX) fluorescence images for the affects of native tissue optical properties using spatial frequency domain imaging (SFDI). Whereas this method has been used to determine the concentration of PpIX to within 0.2?g/mL accuracy in phantoms, it assumes the drug is homogeneously distributed. We have extended our approach to account for the depth penetrance of topically-applied drug in addition to spatial resolution. Since SFDI can be used to determine the optical properties of tissue both at the excitation and emission wavelengths, the pathlengths of the interrogating photons can be calculated, which enables us to estimate the volume of tissue interrogated by our imaging system. By utilizing multiple wavelength excitation sources, each with distinct penetration depths, the determined PpIX concentration as a function of excitation source (i.e. as a function of volume interrogated). This can be used to determine the depth distribution.

Here we demonstrate the accuracy and depth resolution of this approach using layered phantoms ranging in discrete thicknesses from 1-5mm, where PpIX concentration and background optical properties have been varied. An in vivo example of depth resolved PpIX fluorescence from topical application of ALA (Levulan) in healthy skin will also be provided. We believe that this approach may be appropriate for providing quantitative insight into determination of photosensitizing drug concentration and distribution for improved photodynamic treatment of skin diseases.

8578-68, Session 11

A dual-reporter fluorescent imaging approach can be used to estimate sentinel lymph node tumor burden

Kenneth M. Tichauer, Kimberley S. Samkoe, Jason R. Gunn, Dartmouth College (United States); Tayyaba Hasan, Wellman Institute of Photomedicine (United States); Brian W. Pogue, Dartmouth College (United States)

Molecular imaging of targeted reporters is a powerful tool for investigating molecular processes in vivo. However, biological variability in factors such as blood flow or vascular permeability can have a significant affect on reporter uptake, making it difficult to acquire quantitative information about reporter binding (the parameter of interest) from images. In response, we have developed an approach for fluorescence imaging that includes measuring the uptake of a second, untargeted reporter to account for non-receptor mediated uptake of the targeted reporter. In this study, the utility of this dual-reporter approach to quantify tumor burden in sentinel lymph nodes was investigated. Sentinel lymph nodes are characterized by their proximity to a tumor, and the presence of metastatic tumor cells in these nodes is an important indicator in cancer therapy, the diagnosis of which requires invasive resection of the lymph node(s). The utility of the dual-reporter imaging approach to measure tumor burden in sentinel lymph nodes was investigated in a bioluminescent human breast cancer xenograph model in 6 female nude mice. Once the presence of tumor in the lymph node was confirmed by bioluminescent imaging, fluorescently labeled anti-EGFR antibody and an untargeted antibody (labeled with a different fluorophore) were injected intradermally, proximal to the lymph node, and the uptake of the two reporters was imaged simultaneously with a with a flat-panel fluorescent scanner. Preliminary results demonstrated a statistically significant correlation between the dual-reporter measured tumor burden and the bioluminescent measure of tumor burden.

8578-69, Session 11

Optimized methodology for low-contrast fluorescence recovery using a new approach for reference tracer normalization

Robert W. Holt, Kenneth M. Tichauer, Fadi El-Ghussein, Jason R. Gunn, Frederic Leblond, Brian W. Pogue, Dartmouth College (United States)

One of the main problems with in vivo fluorescence recovery with tomographic data is that it can only reliably recover images of high contrast to background ratio, an issue particularly when the fluorescent contrast in a region of interest is proximal to a significant source of background contrast, such as an organ of filtration. Contrast enhancement methods include background subtraction approaches using pre-injection optical scan data and the use of a continuously growing library of fluorescent dyes. This work shows a method of combining the resolution of structural image guidance with the benefits of using multiple fluorescent tracers in order to substantially improve the accuracy of recovered contrast values for targeted tracer concentration. The fluorescence image reconstruction is constrained with structural anatomical priors from microCT to define distinct regions in the imaging domain for the tumor and the organs of filtration. Anatomical priors decrease the conditioning of the inverse problem significantly, and make the calculation fast. Two fluorescent dyes, one targeted to the tumor of interest and one untargeted, with distinct excitation wavelengths, are concurrently administered in the subject and simultaneously imaged using a temporally staggered set of pulsed lasers at these distinct excitation wavelengths. The two data sets are intelligently differenced to enhance the recovered targeted contrast. The speed of the reconstruction calculation means that the process can be iteratively performed to update the intelligent differencing of the optical data sets to further enhance contrast. The method is supported by in vivo imaging of ASPC1 pancreas tumors in mice.

8578-70, Session 11

Fluorescence molecular tomography on animal model by means of multiple views structured light illumination

Nicolas Ducros, Andrea Bassi, Gianluca Valentini, Politecnico di Milano (Italy); Gianfranco L. Canti, Univ. degli Studi di Milano (Italy); Simon R. Arridge, Univ. College London (United Kingdom); Cosimo D'Andrea, Politecnico di Milano (Italy)

Fluorescence molecular tomography (FMT) is an optical imaging technique which aims at localyzing and quantifying 3D fluorochrome distribution in highly scattering animal model. FMT schematically consists in illuminating the sample at the excitation wavelength and acquiring (e.g. by means of a CCD) the fluorescence signal reaching the borders of the sample. By solving the inverse problem it is possible to reconstruct the 3D fluorochrome distribution within the sample. This procedure is quite demanding in terms of both acquisition and computational times. Different research groups have recently proposed compression approaches regarding both illumination (wide field structured light instead of raster point source) and detection (compression of the acquired images). In both cases, the aim is to reduce the acquisition and computational times while preserving the spatial resolution of the reconstructed fluorochrome distribution. Recently, the authors have proposed a fast FMT approach using compression of both illumination and detection spaces. This approach was demonstrated on a cylindrical phantom. Its generalization to real scenarios is quite challenging because real samples (e.g. mouse) have arbitrary shape with no symmetry axis. In this work, we propose a general approach that can address real scenarios. Results on both phantom (non cylindrical sample rotating off-axis) and animal model will be shown. The upgrades of the experimental and computational procedures that allow for extending the approach from cylindrical phantom to animal model will be thoroughly described in this work.

8578-71, Session 12

Imaging with ICG-loaded monocytes to distinguish infection and sterile inflammation

Joani M. Christensen, Yongping Chen, Gabriel A. Brat, Kate J. Buretta, Damon S. Cooney, Gerald Brandacher, Kristine E. Johnson, W. P. Andrew Lee M.D., Xingde Li, Justin M. Sacks M.D., Johns Hopkins Univ. (United States)

Distinguishing infection from sterile inflammation currently relies upon subjective interpretation of clinical parameters, microbiologic data, and nonspecific imaging. Assessing characteristic variations in leukocytic infiltration could provide more specific information. Homing of systemically administered monocytes tagged using the only FDA-approved near infrared dye, indocyanine green (ICG), may be assessed non-invasively using clinically-applicable laser angiography systems to investigate cutaneous inflammatory processes.

RAW 264.7 mouse monocytes were coincubated with ICG solution. Fluorescence was confirmed microscopically. Homing ability of loaded cells was assessed in vitro using a microplate chemotaxis assay. Labeled cells were injected systemically into mice with induced sterile inflammation (Complete Freund's Adjuvant inoculation) or infection (Group A Streptococcus inoculation) of the hind limb. Whole animal near infrared imaging was completed using a FDA-approved, commercially available laser angiography system. Fresh frozen tissue from the area of inoculation was examined microscopically for fluorescence.

Loaded cells displayed high near-infrared fluorescence intensities. Ability of loaded cells to chemotax in response to monocyte chemotactic protein-1 remained above baseline ($p < 0.01$). Following intravascular injection of loaded cells, whole animal imaging revealed local fluorescence at the inoculation site, with significantly different fluorescence ratios in the infection and inflammation model as early as 2 hours after injection ($p<0.01$). Microscopic examination of local tissue revealed punctate areas of fluorescence, consistent with the presence of ICG-loaded cells.

Development of a minimally invasive technique to rapidly image inflammation without radiation may lead to the development of new tools to distinguish infectious conditions from sterile inflammatory conditions at the bedside.

8578-72, Session 12

Target tumor hypoxia with 2-nitroimidazole-ICG dye conjugates

Yan Xu, Saeid Zanganeh, Younis Mohammad, Andres Aguirre, Tianheng Wang, Yi Yang, Michael B. Smith, Quing Zhu, Univ. of Connecticut (United States)

Tumor hypoxia is a major indicator of treatment resistance to chemotherapeutic drugs and fluorescence diffusive optical tomography has tremendous potential to provide clinically useful functional information by targeting tumor hypoxia. In this paper, a second generation 2-nitroimidazole-indocyanine green (ICG) conjugate using piperazine linker (2-nitro-ICG-p) was synthesized for robust tumor-targeted hypoxia fluorescence tomography. We have conducted three groups of in vivo experiments with mouse tumors located at imaging depths of 1.5 and 2.0 cm in a turbid medium. One group of mice was injected with ICG as control, the second group was injected with 2-nitro-ICG-p, and the last group was injected with 2-nitro-ICG-p and the first generation2-nitroimidazole-ICG using ethanol linker (2-nitro-ICG-e) to compare the two generation dyes. On average, the reconstructed maximum fluorescence concentration of mice injected with 2-nitro-ICG-p was 2.1-2.2 times higher than that injected with untargeted ICG, and was 1.2-1.3 times higher than that of 2-nitro-ICG-e beyond 3 hours post-injection. At the 15 uM lower injection concentration of 2-nitro-ICG-p, the reconstructed maximum fluorescence concentration was still 1.4 to 1.8 times higher than that of background and lasted for more than 7 hours, while ICG was completely washed out in less than 3 hours. These findings were supported with fluorescence images of histological sections of tumor samples using a Li-COR scanner and immunohistochemistry technique for targeting tumor hypoxia.

8578-73, Session 12

Monitoring of tumor growth in mice using fluorescence transillumination imaging setup with a single source-detector pair

Ilya V. Turchin, Mikhail S. Kleshnin, Ilya I. Fiks, Institute of Applied Physics (Russian Federation); Irina V. Balalaeva, N.I. Lobachevsky State Univ. of Nizhni Novgorod (Russian Federation)

We present a small animal fluorescence imaging system which combines epi-illumination and planar transillumination geometries. Epi-illumination for superficial measurements is providing by a CCD with a LEDs illumination board and a filter set. Synchronous scanning of an animal by a laser source and a photomultiplier tube or spectrometer as a detector allows implementing planar transillumination imaging for deep seated fluorophores. Such a technique provides better quality of 2D transillumination images in comparison with a wide-field CCD detection. The results of monitoring of tumor growth in nude mice with a tumor model labeled with far red fluorescent proteins using the developed setup will be presented. The developed system can also provide 3D reconstruction of the fluorophore distribution inside animal body which is based on the spectrally resolved measurements provided by a highly sensitive spectrometer in transillumination configuration. The reconstruction procedure utilizes the effect of fluorescence spectrum distortion while propagating through biological tissue due to the dispersion of absorption and scattering coefficients. The reconstruction technique reduces the autofluorescence effect using additional symmetric measurements of the investigated object, accomplished by exchanging source and detector positions. The results of experimental studies on tissue phantoms and small animals in vivo have shown high accuracy of the inverse problem solution for spatial distribution of the fluorophore concentration.

8578-74, Session 12

A fast full-body fluorescence/ bioluminescence imaging system for small animals

Jong Hwan Lee, Hyun-Keol Kim, Jingfei Jia, Christopher J. Fong, Andreas H. Hielscher, Columbia Univ. (United States)

Recently, whole body in vivo fluorescence and bioluminescence imaging of small animals has widened its applications and increased the capabilities for pre-clinical researches. However, most commercial and prototype optical imaging systems are a CCD camera based planar imaging systems using epi-illumination mode, which have a limited number of views from small animals. And for more accurate tomographic image reconstruction, additional data is necessary. To overcome this problem, researchers have suggested several approaches such as maximizing the detected sample area, including other high-resolution modalities such as CT, MRI or Ultrasound, and using multi-spectral signals. Here we present a new fluorescence/bioluminescence imaging system for small animals, which can image the entire surface of an animal simultaneously. The system consists of two conical mirrors, the source illumination part, the line laser scanner for the surface geometry extraction, and the camera system. Two conical mirrors are configured to capture and project the entire surface image onto the intensified CCD camera with one acquisition. A motorized translational and rotational gantry system positions the intensity modulated laser source on an animal surface. With our system, the detectable surface area can increase up to the entire surface of an animal and the unwanted consecutive back reflections of light between an animal and a conical mirror, which occur in a single conical mirror scheme, can be reduced. In addition, by providing unobstructed space around an animal, the other imaging modalities can be easily incorporated. We demonstrate the performance of our system with the simulation and small animal experiments.

8578-75, Session 12

Dynamic fluorescence mediated tomography

Metasebya Solomon, Washington Univ. in St. Louis (United States); Walter J. Akers, Kooresh I. Shoghi, Samuel Achilefu, Joseph P. Culver, Washington Univ. School of Medicine in St. Louis (United States)

Dynamic fluorescence imaging is an emerging technology that can provide enhanced non-invasive functional and molecular level detail. In this work, we demonstrate dynamic fluorescence mediated tomography (DyFMT) of diagnostic imaging agents in tumor bearing mice. Co-registered data was collected using a fiber based, video-rate (30 Hz) FMT system concurrent with preclinical microCT images as anatomical reference. A fluorescent probe was administered by a bolus tail vein injection. The dynamic fluorescence intensity was monitored continuously for 10 minutes after injection. To delineate the different internal organs based on differences in the kinetics of injected contrast agents, we used a seed-based correlation analysis. Time courses were extracted from the dynamic imaging series for target regions guided by organ locations in the corresponding anatomical X-ray CT images. For each region of interest (heart, lung, liver, kidney, tumor), a 1 mm3 volume seed region was chosen for correlation analysis. A correlation coefficient was calculated between each seed region and every other voxel's throughout the imaging volume. For each seed, the images show high correlation with the surrounding voxels and the expected shapes of the heart, lung, liver, kidney and tumor are retrieved. The anatomical co-registration in this dataset also served to validate the accuracy of the seed-based analysis in delineating the shapes of the internal organs. In summary, this technique provides a powerful dynamic analysis of optical agents which has potential for reporting the disease state of the internal organs and to monitor their response to therapeutic agents.

8578-76, Session 12

Assessment of tumour physiology by dynamic contrast-enhanced near-infrared spectroscopy

Kyle Verdecchia, Jonathan T. Elliot, Mamadou Diop, Lisa Hoffman, Lawson Health Research Institute (Canada) and Western Univ. (Canada); Ting-Yim Lee, Imaging Div., Lawson Health Research Institute (Canada) and Western Univ. (Canada) and Robarts Research Institute (Canada); Keith St. Lawrence, Lawson Health Research Institute (Canada) and Western Univ. (Canada)

The purpose of this study was to develop a dynamic contrast-enhanced (DCE) near-infrared spectroscopy (NIRS) technique to characterize tumour physiology. Dynamic data were acquired using two contrast agents of different molecular weights, indocyanine green (ICG) and IRDye 800CW carboxylate. The DCE curves were analyzed using a kinetic model capable of extracting estimates of tumour blood flow (F), mean capillary transit time (tc) and leakage of dye into the tumour interstitial space – characterized by the permeability surface-area (PS) product. Data were acquired from four nude rats with tumour xenografts (>10mm) implanted in the neck. Four DCE-NIR datasets (two from each contrast agent) were acquired for each rat. The dye concentration curve in arterial blood, which is required to quantify the model parameters, was measured non-invasively by dye densitometry. As expected, no differences in the hemodynamic parameters were found between the two contrast agents (F = 0.30±0.11 ml/g/min and tc = 10.8±3.1 s). However the PS product for the IRDye (0.051±0.033 ml/g/min) was significantly larger than the corresponding value for ICG (0.004±0.002 ml/g/min). This was expected since ICG binds to albumin and therefore has a molecular weight of 67 kDa compared to 1166 Da for IRD. This study demonstrates the ability of DCE-NIRS to quantify tumour physiology. The next step is to adapt this approach to diffuse optical tomography.

8578-77, Session 13

Time domain fluorescence lifetime tomography: theory and in vivo applications *(Invited Paper)*

Anand T. N. Kumar, Athinoula A. Martinos Ctr. for Biomedical Imaging (United States)

Molecular imaging is a rapidly evolving research discipline that seeks to provide a visual representation and characterization of cellular events at the macroscopic level, within intact living organisms under physiologically relevant conditions. We are developing tools for optical molecular imaging based on time domain excitation and detection technology, with specific emphasis on applications of fluorescence lifetime contrast. Fluorescence lifetime is a highly environment-sensitive molecular parameter that is also independent of concentration, excitation intensity or photo-bleaching. Microscopy techniques such as fluorescence lifetime imaging (FLIM) are widely used to detect lifetime changes that reveal bio-chemical processes and interactions at the cellular level. Much of the current applications involving lifetime sensitive fluorescent dyes are restricted to thin tissue samples, with high resolution (~10 microns) spatial lifetime maps revealing the local micro-environment of the dye. We have developed a model for in vivo tomographic lifetime imaging that is a direct extension of FLIM for several cm thick turbid tissue. This model is applicable for a wide range of optical properties and spatial scales relevant to biomedical imaging. Besides allowing a simple and clear interpretation of time resolved signals, we show that this model allows a direct and efficient calculation of fluorescence signals using the Monte-Carlo approach based on store photon path histories. We also explore the optimization of tomographic reconstructions with time domain fluorescence data. Finally, we will present applications of time domain fluorescence imaging for mouse models of cancer and cardiac disease.

8578-78, Session 13

A time-domain diffuse optical tomography scanner with multi-view non-contact dual wavelength detection for intrinsic and fluorescence small animal imaging

Yves Bérubé-Lauzière, Eric Lapointe, Julien Pichette, Univ. de Sherbrooke (Canada)

We present a high performance non-contact diffuse optical tomography (DOT) scanner with 360 degrees multi-view detection for localizing fluorescent biomarkers in small animals. It relies on time-domain (TD) detection after short pulse laser excitation. TD measurements are carried out using ultrafast time-correlated single photon counting and photomultiplier tubes. For light collection, 7 free-space optics non-contact dual wavelength detection channels comprising 14 detectors overall are placed around the subject, allowing parallel measurement of time point-spread functions at both excitation and fluorescence wavelengths. The scanner comprises a stereo camera pair for measuring the outer shape of the subject in 3D. Surface and DOT measurements are acquired simultaneously using the same laser beam. The scanner's hardware (optomechanics and electromechanics) and software architecture are discussed, along with characterization and calibration of channel time delays and instrument response functions (IRFs), with IRFs ranging from 115 to 285 ps. Results on the localization of fluorescent point-like inclusions immersed in a scattering and absorbing object mimicking biological tissues are presented. The localization algorithm relies on distance ranging based on the measurement of early photons arrival times (EPATs) at different positions around the subject. This requires exquisite timing accuracy. Further exploiting this capability, we show results on the effect of a scattering heterogeneity on EPATs. We also show absorption and scattering images reconstructed with an iterative full TD tomographic algorithm we developed and data acquired with our scanner. Through its free-space optics design and electro-optics used, our scanner shows unprecedented timing resolution compared to other multi-view TD scanners.

8578-79, Session 13

Design of an optimized time-resolved diffuse optical tomography probe to achieve deep absorption contrast reconstruction in a cylindrical geometry

Anne Planat-Chretien, Lionel Hervé, Michel Berger, Agathe Puszka, Jean-Marc Dinten, CEA-LETI (France)

We propose to use a Time-Resolved instrumentation coupled with a new method based on Mellin-Laplace Transform to reconstruct 3D optical characteristics deeply buried in diffusive tissues. The instrument is designed for new-born infant brain imaging, and 8cm-diameter cylindrical geometries are considered for this study. The MLT method we developed[1] enables to analyze TR measurements on time windows and focus on late photons to reconstruct deep optical parameters map. 2D simulations are performed on discs to optimize sources and detectors geometry given the background optical parameters. We show the limitations of reflexion geometries to achieve deep inclusions and emphasize the contribution of complementary reflexion and transmission geometries. Noise influence is discussed according to power density and acquisition time constraints. 3D TR simulation results are also provided on both cylindrical and spherical type objects. Explicit sensitivity matrix on such large datasets combined with the large size of the medium mesh would be intractable so reconstructions are performed without expressing it.

These simulation results allow us to size an experimental validation bench. A Femtosecond Laser coupled to 12 excitation fibres is used to sequentially excite the medium. The medium responses are simultaneously sampled with 12 detection fibres coupled with a High rate intensifier (HRI). By increasing the width of late time gates, we accurately

measure late photons which carry pieces of information of deep layers of the diffusing medium. The relevance of the different geometries are given for an 8cm cylindrical Delrin container filled with ink and intralipid mimicking the brain optical properties.

[1]Lionel Hervé, Agathe Puszka, Anne Planat-Chrétien, Jean-Marc Dinten, "Time-domain diffuse optical tomography processing by using the Mellin-Laplace transform", Applied Optics, In press

8578-80, Session 13

Robust imaging strategies in time-resolved wide-field optical tomography

Vivek Venugopal, Beth Israel Deaconess Medical Ctr. (United States); Jin Chen, Xavier Intes, Rensselaer Polytechnic Institute (United States)

Time-resolved imaging has been well-established as the most powerful imaging paradigm in optical tomography capable of providing rich information datasets for both functional and fluorescence tomography. The practical implementations of time-resolved imaging platforms however are limited by lengthy acquisition times and demand highly stable instrumentation for collection of robust datasets. In recent years, wide-field imaging strategies have been implemented for time-resolved imaging allowing a fast acquisition of information-rich datasets within relatively short acquisition times. In this work, we present wide-field illumination and processing strategies which significantly improve the signal-to-noise ratio of the measurements. We first demonstrate the use of an adaptive illumination scheme which allows a subject-independent optimization of illumination scheme providing more than 200% improvement in number of measurements at the excitation wavelength and more than 80% improvement in measurements at fluorescence wavelengths leading to improved localization and quantification in fluorescence molecular tomography. Secondly, we demonstrate the impact of temporal and photon noise on time-resolved measurements and compare the performance of various born-normalization schemes designed to improve the robustness of the tie-resolved data-types used for reconstruction. The adoption of these strategies alleviates some of the limitations associated with time-resolved imaging, thus allowing the wider acceptance of time-resolved methods in the scientific community.

8578-81, Session 13

An overview of time-domain diffuse fluorescence imaging: instrumentation and applications

Kenneth M. Tichauer, Robert W. Holt, Frederic Leblond, Brian W. Pogue, Dartmouth College (United States)

Rapidly pulsed laser excitation with high-rate signal detection allows the dispersion of emitted fluorescent signals through tissue to be measured. This "time-domain" approach to measuring diffuse fluorescence data offers a wide range of advantages over conventional "continuous-wave" fluorescence imaging. While continuous-wave imaging provides a measure of only fluorescence intensity at each source-detector pairing, time-domain approaches provide fluorescence intensity throughout the whole temporal response to the pulsed-laser excitation, adding a whole new dimension to the dataset. This presentation will cover the instrumentation required to collect time-domain data, dealing with complications and nuances of system and data calibration, and will introduce present applications of time-domain diffuse fluorescence imaging.

8578-82, Session 13

Time resolved functional near infrared spectroscopy by means of time gated system at small interfiber distance

Davide Contini, Alberto Dalla Mora, Laura Di Sieno, Alberto Tosi, Gianluca Boso, Alessandro Torricelli, Politecnico di Milano (Italy); Lorenzo Spinelli, Istituto di Fotonica e Nanotecnologie (Italy); Rinaldo Cubeddu, Antonio Pifferi, Politecnico di Milano (Italy)

Functional near infrared spectroscopy (fNIRS) is a tool to non-invasively monitor task-related hemodynamic changes in the human brain. In this work we focused on small (few millimeters) source-detector distance time-resolved measurements, which are predicted to have better contrast, better spatial resolution, and lower noise than the typical measurements performed at few centimeters.

The instrument is based on a fiber laser providing two independent output at 710nm and 820nm with a repetition frequency of 40MHz and a FWHM of few tens of picoseconds. In our instrumental set-up we exploited a fast-gating (<500ps) front-end electronics enabling a silicon Single-Photon Avalanche Diode (SPAD) for time-correlated single-photon counting. By means of this detector, we can acquire "late" (strongly attenuated) photons of the diffused light collected few millimeters apart from the injection point. Such photons traveled long paths through the head, then exploring the brain cortex. This is possible because the fast-gated SPAD rejects the huge amount of "early" photons which otherwise would saturate the detection electronic chain. Two fast time-gated detectors are used to acquire independently late photons at the two wavelengths in order to estimate concentrations of oxy- and deoxy-hemoglobin during brain activity. This prototype, differently from the previous ones, can follow the hemodynamic behavior of tissues for both oxy- and deoxy-hemoglobin at the same time with measurement at small distance between injection and detection points.

We validated the instrument on tissue phantoms attaining photon-timing resolutions of 100ps (FWHM) and photon-counting dynamic ranges of around 160dB. Preliminary results in-vivo show for the first time the possibility to detect the dynamic of oxygenated and deoxygenated hemoglobin concentration during a cerebral activation with an interfiber distance of few millimeters.

8578-83, Session 13

Three-dimensional diffuse optical tomography with full multi-view time-domain experimental data

Jorge Bouza Domìnguez, Yves Bérubé-Lauzière, Univ. de Sherbrooke (Canada)

In this work, time-domain data is collected with a state-of-the-art multi-view experimental scanner developed in our group for small animal imaging and used in a tomographic image reconstruction algorithm. The collected data comprises full time-dependent optical signals leaving the biological medium and acquired all around using time-correlated single photon counting and ultra-short laser pulse illumination. The diffuse optical tomography (DOT) algorithm relies on the time-dependent parabolic simplified spherical harmonics (TD-pSPN) equations as the forward model to recover the 3D absorption and diffusion coefficient maps of the medium. The inverse problem is cast and solved as an iterative constrained optimization problem where an objective function determines the accuracy of the forward model predictions at each iteration. Time-dependent adjoint variables are introduced to accelerate the calculation of the gradient of the objective function. Several experiments with homogeneous media and embedded absorbing and scattering heterogeneities are conducted. Cases involving small geometries and high absorption representative of common situations found in small animal imaging are presented. The results demonstrate that accurate quantitative 3D maps of optical properties of biological tissues can be retrieved using intrinsic measurements obtained with our experimental scanner along with our DOT algorithm.

8578-84, Session 14

Non-contact type time-domain fluorescence diffuse optical tomography for quantitative analysis of fluorophores *(Invited Paper)*

Goro Nishimura, Daisuke Furukawa, Kamlesh Awasthi, Hokkaido Univ. (Japan)

We will present a new design of non-contact type time-domain system for fluorescence diffuse optical tomography and the results with phantom and small animal measurements. In particular, we will discuss the detectability and quantification under the practical experimental environment.

For the image reconstruction, we employed an algorithm, fluorescence-assisted diffuse optical tomography (FA-DOT). This algorithm can quantify the absorption by the florophores in the heterogeneous system, using two images reconstructed by the excitation light and a sum of the excitation and emission data. In the calculation, a direct arithmetic between the excitation and emission temporal profiles is required and thus the stability of the measurement in both intensity and time is essential to improve the result.

The new system is designed to improve the stability employing non-contact type probes to eliminate the instability of the probe contact and a two-channel detection, which measures the excitation and emission simultaneously.

Since the temporal profile of the fluorescence is primarily determined by the geometry, position and lifetime of the fluorophores and modulated by the absorption of the fluorophores. Therefore, the temporal profile is less sensitive to the amount of the fluorophores. The time-domain FA-DOT is less sensitive to the smaller amount of the florophores but better than the normal DOT.

We conduct a measurement with a cylindrical phantom with an ICG-Intralipid target to show the performance of the system. Finally, we demonstrate with rats.

We will discuss the detectability of the target and the quantification and comparison between the conventional DOT and FA-DOT.

8578-85, Session 14

in vivo fluorescence lifetime imaging for monitoring the efficacy of the cancer treatment

Yasaman Ardeshirpour, Victor V. Chernomordik, Moinuddin Hassan, Rafal Zielinski, Jacek Capala, Amir H. Gandjbakhche, National Institutes of Health (United States)

Recent studies on Monoclonial Antibodies for cancer treatment show that their efficacy is strongly correlated with characterization of cancer biomarkers. On the other hand, currently, monitoring the effectiveness of therapy is limited to comparison of disease progression before and after therapeutic cycle. However, it is important to monitor the effectiveness of the drug on cancer biomarkers during the therapeutic cycles, especially at the early stages of the treatment.

In this paper, we studied the Human Epidermal Growth Factor 2 (HER2/neu) receptor. Amplification of Human Epidermal Growth Factor 2 (HER2/neu) gene and overexpression of its receptor has been diagnosed in approximately 20-30% of invasive breast cancer cases. It is one of the important factors that is involved in poor prognosis and resistance to traditional chemotherapy treatments.

Current diagnostic gold standards for detection of HER2 expressions are semi-quantitative and are based on ex vivo methods. These methods are all invasive and require biopsies from tissue specimens.

In this study, we used in-vivo fluorescence lifetime imaging which is an imaging technique based on the differences in the exponential decay rate of fluorescent signal. We made a fluorescence probe specific to HER2 receptor and injected to nude mice with HER2 positive tumors. The fluorescence lifetime was monitored continuously during the therapy and the correlation between the fluorescence lifetime and the efficacy of the treatment was studied.

8578-86, Session 14

ICG-bolus tracking based on time-resolved reflectometry for assessment of cerebral perfusion in post-traumatic brain injury patients

Daniel Milej, Anna Gerega, Institute of Biocybernetics and Biomedical Engineering (Poland); Wojciech Weigl, Warsaw Praski Hospital (Poland); Roman Maniewski, Adam Liebert, Institute of Biocybernetics and Biomedical Engineering (Poland)

We present results of time-resolved measurements of the diffuse reflectance and fluorescence carried out in healthy volunteers and post-traumatic brain injury patients. The distributions of times of flight (DTOF) of diffusely reflected photons were acquired together with distributions of times of arrival (DTA) of fluorescence photons during inflow and washout of the optical contrast agent (indocyanine green - ICG) injected intravenously. The methodology of data analysis is based on the observation of delays between the signals of statistical moments (number of photons, mean time of flight and variance) of DTOFs and DTAs related to the inflow of ICG to the extra- and intracerebral tissue compartments. The delays were determined by evaluation of the maximum of derivatives of the measured signals of the mentioned moments. The signal of number of diffusely reflected photons was considered in this analysis as a reference with assumption that this signal represents inflow and washout of the dye in the extracerebral tissues. It was observed in healthy volunteers that moments of higher order (especially variance of the DTOF) reflect inflow of the dye into the brain and the ICG inflow appears in these signals earlier than in the signals of number of photons. We will show results of data analysis carried out on time-resolved signals of diffuse reflectance and fluorescence in patients with critical brain perfusion disorders (intracranial haemorrhage, brain edema, brain death) resulting from post-traumatic brain injury. Statistical comparison of delays obtained in healthy volunteers and subgroups of patients will be presented.

8578-87, Session 14

Deconvolution improves the depth sensitivity of time-resolved techniques

Mamadou Diop, Keith St. Lawrence, Lawson Health Research Institute (Canada)

Time-resolved (TR) measurements from a single source-detector pair contain enough information to separate between superficial and deep absorption changes in tissues. In principle, photons in the late part of the temporal-point-spread-function (TPSF) have a higher probability of probing deep tissues than early-arriving photons. Consequently, time-windowing has been suggested as a method for improving the sensitivity of TR measurements to deep absorption changes. Since TR measurements also contain the effects of the instrument-response-function (IRF), we investigated the influence of the IRF on the depth-resolved absorption changes retrieved from TR measurements using time-windowing. Absorption changes were simulated in the lower-layer of a two-layer medium with 10 mm thick upper-layer and a semi-infinite lower-layer. IRFs of different widths (with and without after-pulse) were also generated and convolved with simulated TR data, to mimic experimental measurements, and the resulting TPSFs were analyzed using time-windowing. The analysis showed that after-pulse in the IRF - due to the use of PMT as detector – significantly reduces (up to a factor of 5) the sensitivity of late-arriving photons to absorption changes occurring in the lower-layer. Furthermore, we show that by applying our recently developed model-independent deconvolution technique,

the effects of the IRF could be efficiently eliminated. We subsequently demonstrate that deconvolved TR data have a higher sensitivity to deep absorption changes than raw measurements. Analysis of TR data acquired in a pig model of the adult head confirms the above theoretical predictions and shows that this method can substantially improve the sensitivity of TR measurements to brain signal in adult.

8578-88, Session 14

Development of an optical non-contact time-resolved diffuse reflectance scanning imaging system: first in vivo tests

Mikhail Mazurenka, Physikalisch-Technische Bundesanstalt (Germany); Laura Di Sieno, Gianluca Boso, Davide Contini, Antonio Pifferi, Alberto Dalla Mora, Alberto Tosi, Politecnico di Milano (Italy); Heidrun Wabnitz, Rainer Macdonald, Physikalisch-Technische Bundesanstalt (Germany)

We report on the development of a non-contact scanning imaging system for time-domain NIRS applications. The system is based on a null source-detector separation approach and utilizes polarization-sensitive detection and a state-of-the-art fast-gated single-photon avalanche diode. The system detects late photons only, bearing information about deeper layers of the biological tissue.

First in-vivo measurements have been performed to prove the feasibility and applicability of the non-contact system. To estimate depth sensitivity of the system experiments were done with both inhomogeneous tissue-like phantom and with various types of biological tissue in vivo. In particular, oxygenation-related changes in skin were measured (Valsalva – 3 volunteers), as well as muscles oxygenation (venous and arterial occlusions – 5 volunteers in both cases). Finally, tests on human brain activation were performed (motor cortex - 4 volunteers, the frontal lobe with cognitive task - 6 volunteers). Task-related changes in oxygenation were clearly detected for all volunteers for Valsalva, venous and arterial occlusions, while for brain activation tasks significant signals were detected only for one volunteer during a cognitive task and one volunteer for a motor task (different subjects). In other cases brain signals were overpowered by signals from superficial layers of the head.

The results of first in-vivo tests prove the feasibility of the non-contact scanning imaging system for further development into a prototype for biological tissue imaging with various medical applications. These tests also helped to find weak points in the current design. Work on improvements and preparation for new in-vivo measurements are currently under the way.

8578-89, Session 14

Analytical solutions of time-domain fluorescence molecular tomography based on simplified spherical harmonics equations

Limin Zhang, Tianjin Univ. (China); Wei Zhang, Tianjin Univ. (China) and Tianjin Univ. (China); Feng Gao, Jiao Li, Huijuan Zhao, Tianjin Univ. (China)

Fluorescence diffusion optical tomography (FDOT) is a technique to visualize specific biochemical events inside living subjects. The diffusion equation, which is derived from the radiative transfer equation (RTE) by employing the P1 approximation, is a widely accepted forward model in FDOT. But this methodology has several limitations for small-animal applications, especially for small-geometry and high-absorption. Lately, the simplified spherical harmonics equations (SPN equations) were introduced to overcome the defect of great computation of PN approximation and meanwhile maintain its validity.

The frequency domain (FD) and time-domain (TD) modes can reconstruct fluorescence yield and lifetime in FDOT. The lifetime-imaging in the FD mode generally requires an impractically high modulation frequency. However the TD technique offers a potential advantage of directly extracting the lifetime information. In this work, we propose an analytical fluorescent diffuse optical algorithm extended to the time domain based on SP3 equations, for semi-infinite geometry. To validate the proposed method, large absorption coefficients and small distances from the source are simulated. The solid phantom is made from Polyformaldehyde. To simulate fluorescent targets embedded in the tissue, a cylindrical hole is drilled in the phantom and filled with a mixed medium that consist of 1% Intralipid solution , Indian ink and Cy5.5 agent. By use of a time-correlation single photon counting (TCSPC) system, we experimentally validate that the proposed scheme can achieve simultaneous reconstruction of the fluorescent yield and lifetime distributions with a reasonable accuracy.

8579-1, Session 1

Ultrashort femtosecond laser pulses for imaging and nanomanipulation of living cells

Aisada Uchugonova, Karsten König, Univ. des Saarlandes (Germany)

Multiphoton microscopes have become important tools for sub-wavelength three-dimensional nanoprocessing as well as for non-destructive imaging of living biological specimens. A mode-locked 85 MHz Ti:Sapphire laser with an ultrabroad band spectrum and an in situ pulse duration at the target ranging from 12 fs up to 3 ps was employed for two-photon imaging and nanomanipulation of living cells. The results demonstrate the potential of extreme ultrashort femtosecond laser pulses at low mean μW powers for imaging and mean powers of 1-10 mW for nanosurgery of cells and cellular organelles without causing collateral damage.

We further aim to use this cutting-edge laser nanotechnology for highly efficient optical manipulation of stem cells for applications in the field of regenerative medicine.

8579-2, Session 1

Impact of a temporal pulse overlap on laser-tissue-interaction of modern ophthalmic laser systems

Nadine Tinne, Nicole Kallweit, Gesche Knoop, Eike Lübking, Laser Zentrum Hannover e.V. (Germany); Holger Lubatschowski, Rowiak GmbH (Germany); Alexander Krüger, Tammo Ripken, Laser Zentrum Hannover e.V. (Germany)

This study describes a time-resolved interaction analysis of the laser-induced optical breakdown (LIOB) by two and more temporally separated fs-laser pulses in water. Until recently, the fs-laser systems used in clinical application evolved a steady increase in the repetition rate, which resulted in a significant reduction of treatment duration. Thus, the immediate pulse-to-pulse interaction has become very important in the context of ophthalmic laser applications like the LASIK procedure. Whenever high-repetition rate ultra-short laser pulses are used to disrupt tissue in a liquid or biological environment, cavitation bubbles are produced, which interact with the surrounding tissue as well as with each other or even following laser pulses. While the interaction between single laser pulses and biological tissue has been studied extensively, the interaction of pulse-to-pulse interaction due to a spatial and temporal overlap has scarcely been studied yet. For that reason, we investigated the interaction of temporally separated laser pulses by time-resolved photography. Various regimes were created: Focusing a second laser pulse (i) into persisting gas bubbles, (ii) into an existing cavitation bubble and (iii) focusing several subsequent pulses. While in scenario (i), the probability of generating two successive LIOBs distinctly decreases, no second bubble oscillation can be observed within (ii). Though, the laser-tissue interaction might be accompanied by an increased laser energy transmission, which is strongly dependent on the temporal pulse overlap. In conclusion, the results of this study are of great interest for the prospective optimization of the surgical process with modern fs-lasers.

8579-3, Session 1

Investigation of the morphology of the features generated via femtosecond lasers in the interior of a bovine cornea sections

Sinisa Vukelic, Bucknell Univ. (United States); Panjawat Kongsuwan, Y. Lawrence Yao, Columbia Univ. (United States)

Nonlinear absorption of femtosecond laser pulses enables the induction of bubble cavities in the interior of eye cornea without affecting other parts of an eye, a phenomena utilized for flap formation in laser assisted corneal surgery. In the present study laser pulses were focused in the interior of the sections of bovine cornea. Tight focus of the laser pulses results in the plasma formation followed by its explosive expansion, which drives cavity formation. The morphology of the generated features as well as the nature of the physical mechanisms of the phenomenon as a function of process parameters is discussed. Numerical model is proposed to develop predictive capabilities for the feature size and shape and the results are compared against the experimental findings.

8579-4, Session 1

Comparison of laser-induced damage with forward-firing and diffusing optical fiber during laser-assisted lipoplasty

Changhwan Kim, Kyungpook National Univ. (Korea, Republic of); Ik-Bu Sohn, Gwangju Institute of Science and Technology (Korea, Republic of); Hoyong Park, Mingi Kang, Yong J. Lee, Ho Lee, Kyungpook National Univ. (Korea, Republic of)

Laser-assisted lipoplasty is made possible by using an optical fiber that delivers light endoscopically to subcutaneous fat tissue. Most optical fibers used for laser-assisted lipoplasty are designed to be irradiated in a forward direction. The emission pattern at the distal end of a forward-firing fiber resembles a “water jet” from a water pipe. In this study, we compared a forward-firing fiber configuration with a typical diffusing fiber for one use in laser-assisted lipoplasty. We hypothesized that the shape of the laser-induced coagulation zone in fat tissue is consistent with the beam emission pattern of the light delivery system. The light-emitting pattern of the diffusing fiber represents a uniform distribution from the distal end. Therefore, we hypothesized that a laser-induced coagulation pattern with a diffusing fiber would resemble the uniform distribution of laser light at the distal end, whereas the coagulation pattern of the forward-firing fiber would resemble a water jet shape. In contrast to our hypothesis, the overall shape of the laser-induced coagulation zone did not match the emission pattern of the forward firing-fiber. Based on our experiment results, we propose an interaction mechanism between laser and fat tissue with a forward-firing fiber. The coagulation zone is governed by both the beam emission pattern and a secondary energy transfer process in the fat tissue ablation.

8579-5, Session 1

Erbium laser induced water jet cleaning of root canals enhanced with gas bubbles

Rudolf M. Verdaasdonk, Vrije Univ. Medical Ctr. (Netherlands) and Free Univ. of Amsterdam (Netherlands); Vladimir Lemberg, BIOLASE Technology, Inc. (United States); Albert Van der Veen, Vrije Univ. Medical Ctr. (Netherlands); Dmitri Boutoussov, BIOLASE Technology, Inc. (United States)

Erbium lasers have shown to be effective for the root canal treatment in dentistry.

Previous studies have shown that explosive vapor bubble formation create high speed liquid motion associated with turbulence and cavitation effects. However, the effectiveness of various treatment strategies is not clear.

In this study, mechanism for effective cleaning and sterilization of the root canal was tested in relation to fiber tip shape (flat or tapered, 200 - 400

μm), tip position (above or inside canal) and presence of gas bubbles in canal.

The experiments were performed in a transparent tapered root canal model ending in small opening resembling the apex. The canal was filled with red colored water either plane or with small gas bubbles. In addition, the lower part of the canal was filled with sticky paste as model for debris. Simulating the clinical treatment, the mechanism and effectiveness of cleaning of the canal during laser exposure (20-50 mJ) was determined using high speed imaging (100 and 5 us resolution).

Faster canal clearing was obtained when gas bubbles were present inside the canal. Explosive vapor bubbles created by the Er laser pulses compress the gas bubbles along the canal down to the apex inducing high speed water displacement and jets dissolving debris. The mechanism of effective root canal cleaning is attributed to Erbium laser induced high speed water jets which is enhanced by gas bubbles and might potentially kill bacteria.

8579-7, Session 2

Determination of cell death mechanisms initiated during gold nanoparticle-mediated photothermal therapy

Varun Pattani, James Tunnell, The Univ. of Texas at Austin (United States)

Recent studies have shown that gold nanoparticle (GNP)-mediated photothermal therapy (PTT) is effective in treating cancer; however, the cell death mechanisms involved during PTT are not fully understood. PTT utilizes localized heat from the GNPs within the tumor to induce cellular damage. The purpose of this study was to determine whether PTT efficacy depends on GNP localization and elucidate the cell death mechanisms involved. We determined the threshold laser power to induce cell death during PTT for GNPs targeted extracellularly and intracellularly. GNP localizations were confirmed using two-photon microscopy. We measured the change in cellular temperature (?T) that correlates with the laser power threshold. Finally, we probed specific cell death pathways initiated for both GNP localizations during PTT, using fluorescent stains. We investigated necrosis, cell death due to external injury resulting in surrounding tissue inflammation, and apoptosis, programmed cell death without external inflammation, as the primary pathways. Cell death required a 50% higher fluence rate for membrane-bound GNPs (30 W/cm2) than for internalized GNPs (19 W/cm2). Similarly, we measured a significantly higher ?T ($p < 0.01$) for membrane-bound GNPs (8.3°C) than internalized GNPs (6.6°C) to induce cell death. These results suggest that GNP cellular concentrations alone did not solely account for the threshold fluence rate differences observed. Therefore, the GNP localization does seem to have a significant impact on the cell death pathways during PTT. A better understanding of the cell death mechanisms involved in GNP-mediated PTT may allow for increased efficiency and selectivity of such treatments and nanovector design.

8579-8, Session 2

Green's function representation of laser induced thermal dynamics and determination of thermal criteria for optically induced neural activation

Bryan J. Norton, Meghan A. Bowler, Lockheed Martin Aculight (United States)

Optical nerve stimulation (ONS) is rapidly becoming an important tool for basic research and a promising new clinical technology: selectively activating nerves to restore function, map the nervous system, and perform diagnostic procedures. The stimulation mechanism is photothermal, so understanding the heat distribution is fundamental to understanding ONS. This work develops both a framework describing the time evolution of the heat distribution induced by optical fluence and a novel method to extract thermal criteria for neural activation. We are first concerned with the general problem of describing the temperature distribution in a homogenous medium. To this end, we determine a Green's function solution to the heat diffusion equation and convolve it with the optical fluence. This provides a general closed form solution to the thermal problem of interest. This pursuit also yields an expression for the thermal relaxation time, providing a strong definition for thermal confinement in ONS applications. The insight we gain from this framework allows us to extract thermal criteria for neural activation from experimental data. Our work provides both insight into the mechanism for stimulation and understanding sufficient to aid in the development of ONS devices. Thermal criteria values will prove useful for choosing parameters such as spot size, pulse width, stimulation spacing, and stimulation depth in future ONS applications.

8579-9, Session 2

Infrared nerve stimulation: modelling of photon transport and heat conduction

Alexander C. Thompson, Scott A. Wade, Peter J. Cadusch, Will G. A. Brown, Paul R. Stoddart, Swinburne Univ. of Technology (Australia)

Infrared neural stimulation (INS) is a novel technique for stimulating neurons with infrared light, rather than the traditional electrical means. There has been significant discussion in the literature on the mechanisms behind INS, while recent work has shown that infrared light stimulates neurons by causing a reversible change in their membrane capacitance. Nevertheless, the effect of different laser parameters on neuronal responses is still not well understood. To better understand this and to assist in designing light delivery systems, modelling of spatial and temporal characteristics of light delivery during INS has been performed. Monte Carlo modelling of photon transport in tissue allows the spatial characteristics of light to be determined during INS and allows comparisons of varying geometries and fibre designs. Finite element analysis of heat conduction can then be used to reveal the behaviour of different pulse durations and the resulting temperature decay. The combination of the two methods allows for further insights into the mechanisms of INS and assists in understanding different mechanisms which promote INS. The model shows there are two regimes of INS, namely temperature limited for pulses under 100 ?s and temperature gradient limited for longer pulses. This is in accordance with previously published data. It also provides a tool for optimising the design of emitters and implants.

8579-10, Session 3

Nonlinear optical frequency conversions of femtosecond laser in corneal tissue

William R. Calhoun III, U.S. Food and Drug Administration (United States); Divya Kernik, U.S. Food and Drug Administration (United States) and Johns Hopkins Univ. (United States); Alexander Beylin, Richard P. Weiblinger, Ilko Ilev, U.S. Food and Drug Administration (United States)

Development of novel femtosecond laser (FSL) based technologies and medical devices is an emerging field with significant public health impact and applications in a variety of biomedical areas including ophthalmology, dentistry, neurosurgery, multiphoton imaging, nanotechnology etc. In the field of ophthalmology, since the first approval of FSL-assisted in-situ keratomileusis (LASIK), the FSL applications have been broadly expanded to new areas such as cataract surgery. The FSL treatment effect is based on photoablation of ocular tissue by a series of ultrashort pulses which create very intense optical fields at the treatment site. The intensity of these fields can reach levels that are above the thresholds required for certain nonlinear optical frequency conversion effects such as harmonics generation, sum-frequency

mixing and self-phase modulation. In the case of nonlinear multiphoton microscopy, the FSL intensity is very low and requires highly sensitive detection systems. However, clinical femtosecond therapeutic lasers are considerably more powerful and can generate significantly more intense spectral conversion effects which could potentially be of safety concerns to local or even distant ocular cells and structures. In the present study, using a clinically relevant therapeutic FSL and advanced optical sensing techniques, we develop test methods for studying and evaluating the efficacy and potential safety concerns of nonlinear conversion effects that are generated in bovine corneal tissue. This study provides new data and information on the FS laser-tissue interactions related to nonlinear effects and on understanding how these interactions affect the safety and efficacy of new FSL technologies and devices.

8579-11, Session 3

Plasmonic properties of gold nanoparticles can promote neuronal activity

Chiara Paviolo, Swinburne Univ. of Technology (Australia); John W. Haycock, The Univ. of Sheffield (United Kingdom); Jiawey Yong, Aimin Yu, Sally L. McArthur, Paul R. Stoddart, Swinburne Univ. of Technology (Australia)

Over the past decade, gold nanoparticles have attracted considerable interest for biological applications such as labeling, drug/gene delivery, heating, sensing and imaging [1]. They are attractive because they can be synthesised easily, support surface functionalization and have useful optical properties [1,2]. Gold nanorods (Au NRs) possess distinct surface plasmon resonances (SPRs) in transverse and longitudinal directions tunable across the visible to near infrared (NIR) region [2]. Herein we demonstrate that Au NRs SPR excitation can trigger neuronal cell differentiation and induce intracellular Ca2+ transients using NG108-15 neuronal cells, which extends to poly(sodium styrene sulfonate) PSS and SiO2 coated Au NRs.

Importantly, Au NRs assessed by live/dead staining and MTS cell viability showed no effect of significant toxicity. The effect of a 780 nm laser diode (LD) was then examined. A significant decrease in viability was observed initially (from 250 mW/cm2 upwards), with complete recovery measured after one day in culture. This suggested that the cells initially shocked by the laser, but not permanently damaged. We conclude from this that the laser powers selected were not harmful for neuronal cells.

Indeed the laser powers thereafter were observed to have a stimulatory effect on differentiation – according to the maximum neurite length, the number of neurites per neuron and the percentage of neurons with neurites. Significant increases were observed in the neurite length and of the percentage of neurons with neurites. In particular, NG108-15 cultured with NPs and irradiated with the 780 nm LD showed a neurite length increase versus control of almost 20 μm (at 7.5 W/cm2). To the best of our knowledge, this effect has never been reported before and it appears to be linked to the excitation of the localized surface plasmon resonance in the NRs.

The effect of the laser energy on intracellular Ca2+ signaling was then studied. NG108-15 neuronal cells are not regarded as excitable and no spontaneous activity was detected. Evidence of photo-generated transient calcium release was recorded, with a recovery time constant over a period of approximately 0.55 s. These findings are consistent with the observations of [3], where Ca2+ transients were triggered in rat ventricular cardiomyocytes by pulsed infrared radiation at 1862 nm. Our hypothesis is that the temperature increase caused by excitation of the plasmonic resonance of the nanoparticles is responsible for the calcium response in the present work. To the best of our knowledge, this effect has never been reported before and opens new opportunities for improving the efficiency of optical stimulation of nerves.

1. Sperling RA, Gil PR, Zhang F, Zanella M, Parak WJ. Biological applications of gold nanoparticles. Chemical Society Reviews 2008 Sep;37(9):1896-1908.

2. Harris N, Ford MJ, Mulvaney P, Cortie MB. Tunable infrared absorption by metal nanoparticles: the case for gold rods and shells. Gold Bulletin 2008;41(1):5-14.

3. Dittami GM, Rajguru SM, Lasher RA, Hitchcock RW, Rabbitt RD. Intracellular calcium transients evoked by pulsed infrared radiation in neonatal cardiomyocytes. Journal of Physiology-London 2011; 589(6):1295-1306.

8579-12, Session 3

Study of photosensitization reaction progress in a 96 well plate with photosensitizer rich condition using Talaporfin sodium.

Emiyu Ogawa, Mei Takahashi, Tsunenori Arai, Keio Univ. (Japan)

To quantitatively investigate photosensitization reaction against cells with photosensitizer rich condition using Talaporfin sodium in a 96 well plate, we studied photosensitization reaction characteristics in this well. We have proposed non-thermal conduction block of myocardium tissue using photosensitization reaction with laser irradiation shortly after Talaporfin sodium injection. In above situation, photosensitizer is located outside the myocardial cells in high concentration. To understand interaction of the photosensitization reaction in which the photosensitizer distributed outside cells, photosensitization reaction in the 96 well plate should be studied.

Talaporfin sodium solution of 2.8 mm in depth and a 663 nm diode laser were used. The photosensitizer solution concentrations of 12.5-37.5 ?M were employed. The photosensitizer fluorescence of 40 J/cm2 with 0.29 W/cm2 in irradiance was measured during the laser irradiation. The photosensitizer solution absorption and dissolved oxygen pressure after the laser irradiation were also measured.

We found that the photosensitization reaction had 2 distinctive phases of different reaction rate: rapid photosensitization reaction consuming dissolved oxygen and gentle photosensitization reaction with oxygen diffusion from the solution-air boundary. The dissolved oxygen pressure and photosensitizer solution absorbance were 30% and 80% of the initial values after the laser irradiation, respectively. Therefore, oxygen was rate-controlling factor of the photosensitization reaction in the 96 well plate with photosensitizer rich condition. In the second phase, the oxygen pressure was kept around 40 mmHg and it is similar than that of myocardium tissue in vivo. We think that our 96 well plate in vitro system may simulate PDT in myocardial tissue using photosensitization reaction parameters mentioned above.

8579-13, Session 3

Ursolic Acid Mediates Photosensitization by Initiating Mitochondrial-Dependent Apoptosis

Yuan-Hao Lee, The Univ. of Texas Health Science Ctr. at San Antonio (United States); Exing Wang, Indiana Univ. (United States) and Univ. of Texas Health Science Center (United States); Neeru C. Kumar, Randolph D. Glickman, The Univ. of Texas Health Science Ctr. at San Antonio (United States)

The signaling pathways, PI3K/Akt and MAPK, are associated with carcinogenesis, and may also be activated by light exposure. These pathways, however, may also be modulated or inhibited by naturally-occurring compounds, such as the triterpenoid, ursolic acid (UA). Previously, the transcription factors p53 and NF-kB, which transactivate mitochondrial apoptosis-related genes, were shown to be differentially modulated by UA. Our current work indicates that UA exerts these effects via the PI3K/Akt pathway. UA-modulated apoptosis, following exposure to UV radiation, is observed to correspond to differential levels of oxidative stress in retinal pigment epithelial (RPE) and skin melanoma (SM) cells. Flow cytometry and DNA fragmentation analyses showed that UA pretreatment potentiated radiation-induced apoptosis, even though the resultant DNA photo-oxidative damage (i.e. strand breakage) was reduced, presumably by some antioxidant activity of UA. The inhibitory effect of UA on NF-?B activation in SM cells was enhanced by wortmannin or rapamycin pretreatment, which indicates that all three

agents have similar antagonistic effects on the PI3K/Akt/mTOR pathway. In addition, the antagonistic effect of UA on the PI3K/Akt pathway was reversed by insulin leading to greater p53 activation. MitoTracker, a mitochondrial functional assay, indicated that mitochondria in RPE cells experienced reduced oxidative stress while those in SM cells exhibited increased oxidative stress upon UA pretreatment. When rapamycin was administered with UA, the mitochondrial oxidative stress was increased in RPE cells while decreased in SM cells. These results indicate that UA modulates p53 and NF-?B, initiating a mitogenic response to radiation that triggers mitochondria-dependent apoptosis.

8579-14, Session 3

Comparison of photoinduced conformational changes of human serum albumin bound to protoporphyrin IX and hemin

Sarah C. Rozinek, Lorenzo Brancaleon, The Univ. of Texas at San Antonio (United States)

The conformational effects of binding Protoporphyrin IX (PPIX) and hemin, respectively, to human serum albumin (HSA) as well as the bound systems' response to low-dose irradiation with a laser at 405 nm (Soret band) are examined at physiological and acidic pH conditions. The study uses a combination of optical methods, including steady-state fluorescence, fluorescence lifetime and circular dichroism (CD) measurements, along with computational simulations. Heme-albumin has been shown to possess enzymatic and allosteric properties that could be linked to biological functions. The possibility to trigger conformational changes at a known location in HSA, using laser irradiation, could enable us to artificially enhance or modify the properties of the heme binding site as well as allosteric sites. This could have repercussions in the future development of heme-albumin as an artificial enzyme, as a substitute for hemoglobin or myoglobin or as a catalyst in fuel cells. Spectroscopic data suggests that irradiation of the bound system is capable of modifying the globular protein structure by direct charge transfer mechanisms at both physiological and acidic pH conformations. Computational docking simulations predict lower free energy of binding for PPIX than for hemin, and the predicted porphyrin conformations agree with CD signals where PPIX maintains a planar ring structure and the hemin rings hold a saddled confirmation.

8579-34, Session 3

Detection of oxidative stress biomarker-induced assembly of gold nanoparticles in retinal pigment epithelial cells

Zannatul Yasmin, The Univ. of Texas at San Antonio (United States); Yuan-Hao Lee, Saher Maswadi, Randolph D. Glickman, The Univ. of Texas Health Science Ctr. at San Antonio (United States); Kelly L. Nash, The Univ. of Texas at San Antonio (United States)

Oxidative stress (OS) is increasingly implicated as an underlying pathogenic mechanism in a wide range of diseases, resulting from an imbalance between the production of reactive oxygen species (ROS) and the system's ability to detoxify the reactive intermediates or repair the resulting damage. ROS can be difficult to detect directly; however, they can be detected indirectly from effects on oxidative stress biomarkers (OSB), such as glutathione (GSH), 3-nitrotyrosine, homocysteine, and cysteine. Moreover the reaction of transition metals with biologically relevant molecules (BRM) oxidized by ROS can yield reactive products that accumulate with time and contribute to aging and disease. The study of the interaction between BRM and OSB using functionalized nanoparticles (fNPs) has attracted interest because of potential applications in bio-sensors and biomedical diagnostics. A goal of the present work is to use fNPs to detect and ultimately quantitate OS in retinal pigment epithelial (RPE) cells subjected to external stressors, e.g. nonionizing (light) and ionizing (gamma) radiation. Specifically, we are investigating the assembly of gold fNPs mediated by the oxidation of GSH in irradiated RPE cells. The dynamic interparticle interactions had been characterized in previously reported work by monitoring the evolution of the surface plasmon resonance band using spectroscopic analysis (UV-VIS absorption). Here we are comparing the dynamic evolution of fNP assembly using photoacoustic spectroscopy (PAS). We expect that PAS will provide a more sensitive measure allowing these fNP sensors to measure OS in cell-based models without the artifacts limiting the use of current methods, such as fluorescent indicators.

8579-39, Session 3

Discovery of photochemical damage mechanisms using in vitro and in silico models *(Invited Paper)*

Pamela K. Fink, Saint Mary's Univ. (United States); Michael L. Denton, TASC, Inc. (United States); Cherry Castellanos, 711 HPW/RHDO (United States); Amanda J. Tijerina, Conceptual Mindworks, Inc. (United States); Kurt J. Schuster, TASC, Inc. (United States); Jeffrey W. Oliver, Air Force Research Lab. (United States)

A computer-based model has been built that simulates the response of the retinal pigmented epithelial (RPE) cell to laser exposure in the photochemical (non-thermal) damage exposure range (≥ 100 s exposures). The modeling approach used is knowledge-based, modular, and hierarchical, allowing the explicit modeling of the cascades of intracellular events in response to laser application. Thus, the model can be used to both analyze existing in vitro data sets, as well as efficiently direct sampling strategies for future in vitro and in vivo studies. This model has been validated using laboratory data from several studies reported in the literature using blue light (413nm and 458nm) lasers with 100 s, 200 s, and 3600 s exposure durations. The model was able to predict the in vitro ED50 response curve from these studies, as well as the results for which we have no in vitro data (extrapolated based on irradiance reciprocity), within 1-6% for the shorter duration exposures. Based on exploration of this computer model using lethal vs. non-lethal laser exposure scenarios, the RPE cell's oxidative stress response differs quantitatively very little with respect to typical oxidative stress sources such as superoxide and hydrogen peroxide. However, in the lethal exposure scenarios the model points to a potential tipping point in the oxidative stress response of the mitochondrial-based cellular energetics. Further studies are underway to explore issues related to the levels of ATP/ADP and GSH/GSSG that are predicted by the model in these lethal vs. the non-lethal exposure scenarios.

8579-15, Session 4

Influence of different output powers on the efficacy of photodynamic therapy with 809-nm diode laser and indocyanine green

Nermin Topaloglu, Sahru Yuksel, Murat Gülsoy, Bogaziçi Üniv. (Turkey)

Photodynamic therapy (PDT) is an alternative antimicrobial treatment method. Different wavelengths of light sources mostly in the visible spectrum have been investigated for antimicrobial Photodynamic Therapy. Even though the wavelengths in near infrared spectrum have the advantage of higher penetration capability in biological tissue, they have not been preferred for PDT because of their possible photothermal effect in biological tissues. In our previous studies, the desired PDT effect was achieved with 809-nm diode laser and indocyanine green (ICG) on drug resistant pathogens. In this study, it was aimed to investigate the influence of different output powers during PDT applications with 809-nm diode laser to clarify whether there is a photothermal effect to kill the pathogens or only the photochemical effect of photodynamic therapy.

4 different output powers (500 mW, 745 mW, 1000 mW, 1500 mW) were examined in Laser-only and PDT groups of P. aeruginosa ATCC 27853 in vitro. In the PDT groups, a non-phototoxic ICG concentration (25 µl/ml) have been chosen to eliminate the effect of ICG and evaluate only the effect of output powers. Applied energy dose (252 J/cm2) was kept constant by increasing the exposure duration (300, 240, 180 and 120 seconds respectively). These output powers in Laser-only or PDT groups did not seem to cause photothermal effect. There was not any significant decrease or increase on bacterial load after the applications with different output powers. Higher output powers in PDT groups with the same ICG concentration did not cause higher killing efficiency.

8579-16, Session 4

Trigger effect of infrared femtosecond laser irradiation on neoplasm in experimental cervical cancer

Tatyana Gening, Olga Voronova, Igor Zolotovsky, Ulyanovsk State Univ. (Russian Federation); Alexey Sysoliatin, A. M. Prokhorov General Physics Institute (Russian Federation); Dinara Dolgova, Tatyana Abakumova, Ulyanovsk State Univ. (Russian Federation)

In the present study, we have analyzed the efficiency of a subpicosecond laser pulse system, providing pulse generation with low average and high peak power for cervical cancer treatment.

An effect of subpicosecond laser irradiation on proliferation and neoplasm metastasis, as well as tumor biological characteristics, has been studied to estimate the laser efficiency. To assess the influence of subpicosecond infrared laser radiation on neoplasm of CC-5 grafted white mice, (on the 20th and 30th day after transplantation) neoplasm was subjected to femtosecond laser irradiation (the operating wavelength ? = 1550 nm, the peak power of 6 kW, and the average power below 1.25 mW). The average energy density (energy dose) for one exposure was 0.24 J/cm2 and 0.36 J/cm2 for two groups of animals. There were 10 irradiation trails for both energy doses. After irradiation trials, the indicators of the “Lipid peroxidation - antioxidants” system: malondialdehyde (MDA), activity of catalase, superoxide dismutase (SOD), glutathione reductase (GR), and glutathione transferase (GT) have been determined in tumor tissue. Besides, a morphological analysis of tumor tissue has been performed. The mathematical analysis of obtained data based on the assumption of linear and nonlinear regression shows that irradiation effect (at low average power below 2 mW) is nearly independent of the energy density. The results suggest a trigger character of infrared femtosecond laser irradiation effect on redox-dependent processes in neoplasm of experimental CC. Such a mechanism, employed in biological tissues treatment, could provide an effective but sparing tool for cancer cure (including cervical cancer).

This work was supported by the Ministry of Education and Science of the Russian Federation within the framework of government order, Russian Foundation for Basic Research, and Grant of the President of the Russian Federation.

8579-17, Session 4

Thermodynamic finite-element-method (FEM) eye model for laser safety considerations

Nico Heussner, FZI Forschungszentrum Informatik (Germany); Lukas Holl, Karlsruher Institut für Technologie (Germany); Ariana Shults, Illinois Institute of Technology (United States); Thorsten Beuth, Harsha Umesh Babu, Leilei Shinohara, Siegwart Bogatscher, Karlsruher Institut für Technologie (Germany); Matthias Wippler, Karlsruhe Institut of Technology - Institute for Information Processing Technology (Germany); Wilhelm Stork, Karlsruher Institut für Technologie (Germany)

We present a complete thermodynamic eye model to aid simulations while determining laser safety requirements in the field of scanning laser devices. Considering the recent development of microdisplays, retinal displays and other emerging technologies, laser safety issues are becoming more and more important. It has recently been shown that existing standards and frameworks for laser safety do not cover the treatment of moving spots on the retina in sufficient detail. With the growing number of applications using scanning lasers, significant research is underway in order to generate appropriate extensions to the laser safety standards. We have developed a thermodynamic model of the whole human eye which would help in reducing animal experiments and provide a simulation tool to assist the manufacturers in their safety considerations. By using the software Hypermesh© and Ansys Fluent© we created a FEM-model capable of simulating the thermal behaviour of all parts of the eye, i.e. the temperature distribution at any point of the eye can be predicted. The model also includes the blood flow within the choroid coat, aiming for a precise description of the thermal behaviour in both, spatial and time domain.

8579-18, Session 4

Visualization of thermal lensing induced image distortion using Zemax ray tracing and BTEC thermal modeling.

Erica Towle, The Univ. of Texas at Austin (United States); Clifton D. Clark III, Fort Hays State Univ. (United States) and TASC, Inc. (United States); Michelle T. Aaron, Robert J. Thomas, Air Force Research Lab. (United States)

In recent years, several studies have been investigating the impact of thermal lensing in ocular media on the visual function of the human eye. These studies have shown that when near-infrared (NIR) laser light (1319 nm) is introduced to a human eye, the heating of the eye can be sufficient to alter the index of refraction of the media leading to changes in the visible wavefront through an effect known as thermal lensing, while remaining at a safe level. One of the main limitations of experimentation with human subjects, however, is the reliance on a subject’s description of the effect which can vary greatly between individual participants. Therefore, a computational model was needed which could accurately represent the changes to a visual field as a function of changes in the index of refraction. First, to model changes in the index of refraction throughout the eye, a computational thermal propagation model was used. These data were then used to generate a comprehensive ray tracing model of the human eye using Zemax (Radiant Zemax Inc, Redmond WA) via a gradient lens surface. Using this model, several different visual stimulus targets have been analyzed which represent real-world visual acuity so that the effect of different changes in the index of refraction could be related back to changes in a visual scene.

8579-35, Session PMon

Low level laser irradiation induces metabolic changes in bovine oocytes, improving the in vitro production of embryos

Carlos A. Soares, Kelly Annes, Thiago R. Dreyer, Taciana D. Magrini, Herculano S. da Silva Martinho, Marcella P. Milazzotto, UFABC (Brazil)

The in vitro maturation of oocytes (IVM) is a key process for in vitro embryo production (IVP) in which nuclear and cytoplasmic changes are necessary to support the early events of embryonic development. The present study aimed to test the use of low-level laser irradiation (LLLI) during IVM for improving the efficiency of bovine IVP. We used LLLI (? HeNe 633nm - 15mW - fluency 1J/cm2) at the beginning of IVM in cumulus oocyte complexes (COCs) retrieved from bovine ovaries. After that, oocytes were submitted to IVP. Non-irradiated COCs were used as negative controls. Granulosa cells, oocytes, and embryos were evaluated separately by means of mitochondrial activity, cell cycle progression, cell

viability, embryo production and quality. There was an increase in the mitochondrial membrane potential and the number of cells in S/G2/M phases of the cell cycle for irradiated granulosa cells when compared to the control. Moreover, there were changes in the expression pattern of genes related to the cell cycle and maintenance of cell viability. For irradiated oocytes, there were also changes in the expression pattern of genes related to cell cycle and changes in meiotic progression when compared to the control. Finally, embryos derived from irradiated COCs presented the same cleavage and blastocyst rates and there was no change in the number of viable cells. However, the total number of cells per blastocyst increased when compared to the control embryos. Based on these results, we can conclude that irradiation with LLL may be an alternative to improving bovine IVP.

8579-36, Session PMon

Effects of low level laser therapy on skeletal muscle repair following cryolesion

Raquel A. Mesquita-Ferrari, Agnelo N. Alves, Kristianne P. Fernandes D.D.S., Claudia A. V. Melo, Renato Y. Yamaguchi, Cristiane M. França, Sandra K. Bussadori, UNINOVE (Brazil); Fabio D. Nunes, Univ. de São Paulo (Brazil)

A growing body of evidence suggests that low-level laser therapy (LLLT) promotes skeletal muscle regeneration, but its effectiveness in the treatment of injury remains questionable and its therapeutic potential is not fully established. The aim of the study was to evaluate the effects of LLLT on skeletal muscle repair following cryoinjury in rat tibialis anterior (TA) muscle. Wistar rats were divided into four groups: 1) control; 2) sham; 3) cryoinjured without treatment; 4) cryoinjured and LLLT. The cryoinjured groups with and without treatment were analyzed after 1, 3 and 7 days following the injury procedure. The laser irradiation was performed daily on the injured region using the GaAlAs laser (780nm) with a beam spot of 0.4 cm2, an output power of 40mW, energy density of 10J/cm2 for 10 seconds. After sacrifice, the TA was removed for morphological analysis using the hematoxylin-eosin assay. Results: The morphological analysis revealed that the control group showed normal histological appearance with the presence of fibers with peripheral nuclei and absence of injury or inflammation. The sham group showed a discrete inflammatory infiltrate in the surface region of the muscle surgically exposed. After 1 and 3 days, the cryoinjured LLLT groups showed a decrease in inflammatory infiltrate, edema and myonecrosis in comparison to untreated groups in the same period. After 7 days, the treated and untreated cryoinjured groups exhibited similar reduction in inflammatory infiltrate, edema and myonecrosis. Conclusion: LLLT can modulate the muscle repair by reducing the inflammatory infiltrate, edema and myonecrosis in TA muscle

8579-37, Session PMon

A nondestructive diffuse reflectance calibration-free method for determine optical parameters of biological tissues

Alexander Lappa, Artem Kulikovskiy, Anton Kulikovskiy, Tamara Makarova, Chelyabinsk State Univ. (Russian Federation)

A method for nondestructive evaluation of absorption and reduced scattering coefficients μa, us' of turbid media (biological tissues, first of all) is presented in this work. The method refers to the spatially resolved diffuse reflectance techniques. There are four features in our method: new light propagation model and technique for inverse problem solving, minimally possible number of reading fibers, no preliminary calibration measurements on phantoms with known optical parameters, possibility of usage of monochromatic light sources.

Our light propagation model is kinetic one (bases on radiation transport equation), it allows correct consideration of processes dependent on photon directions (reflection and refraction on boundaries, angular aperture of optical fibers, and so on) in contrast to diffusion, P1, and some other non-kinetic approximations. Besides refractive index the model includes only 2 optical parameters.

The method uses a probe with 3 optical fibers: one illumination and two reading fibers. As the measured quantities to extract the parameters we suggest to use two ratios: Q1=D1/S and Q2=D2/D1, where D1, D2 - detector indications from the reading fibers, S – from the illumination one.

The technique of parameters determination includes preliminary calculations of Q1, Q2 at different ua, us' in sufficiently broad range (i.e. calculation of functions q1(ua,us')) with the original algorithm using the Green function approach, the similarity transformation, and a special non-analog correlated technique of the Monte Carlo method. Media parameters are found as numerical decision of equation system: q1(ua,us')=Q1, q2(ua,us')=Q2, where Q1,Q2 – measured values.

A series of phantom and in vivo experiments showed good performance of the proposed method.

8579-38, Session PMon

Resolution analysis of an angular domain imaging system with two-dimensional angular filters

Eldon Ng, The Univ. of Western Ontario (Canada) and Lawson Health Research Institute (Canada); Jeffrey J. L. Carson, Lawson Health Research Institute (Canada) and Univ. of Western Ontario (Canada)

Angular Domain Imaging (ADI) employs an angular filter to distinguish between quasi-ballistic and scattered photons based on trajectory. A 2D angular filter array was constructed using 3D printing technology to generate an array of microchannels 500 μm x 500 μm with a length of 12 cm. The main barrier to 2D imaging with the 2D angular filter array was the shadows cast on the image by the 500 μm walls of the angular filter. The objective of this work was to perform a resolution analysis of the 2D angular filter array. The approach was to position the AFA with a two dimensional positioning stage to obtain images of areas normally obstructed by the walls of the AFA. A digital light processor was also incorporated to generate various light patterns to improve the contrast of the images. A resolution analysis was completed by imaging a knife edge submerged in various uniform scattering media (Intralipid® dilutions with water). The edge response functions obtained were then used to compute the line spread function and the theoretical resolution of the imaging system. The theoretical system resolution was measured to be between 110 μm – 180 μm when the scattering level was at or below 0.7% Intralipid®. The theoretical resolution was in agreement with a previous resolution analysis of a silicon-based angular filter with a similar aspect ratio. The measured resolution was also found to be smaller than the size of an individual channel, suggesting that the resolution of an AFA based ADI system is not dependent on the size of the microchannel.

8579-19, Session 5

Raman Fiberoptic Probe for Monitoring Human Tissue Engineered Oral Mucosa Constructs

Alexander T. Khmaladze, Shiuhyang Kuo, Cynthia L. Marcelo, Stephen E. Feinberg, Michael D. Morris, Univ. of Michigan (United States)

In oral surgery, there is a need for tissue engineered constructs for dental implants, reconstructions due to trauma, oral cancer or congenital defects. A non-invasive quality monitoring of the development of tissue engineered constructs during their production and implantation is a required component of any successful tissue engineering technique. We demonstrate the design and application of a Raman spectroscopic probe for rapid and noninvasive monitoring of Ex Vivo Produced Oral

Mucosa Equivalent constructs (EVPOMEs). We conducted in-vitro studies to identify Raman spectroscopic failure indicators for EVPOMEs that are stressed by higher temperature or exposure to higher than normal concentration of calcium ions. Raman spectra of EVPOMEs exposed to thermal and calcium stress showed correlation of the band height ratio of CH2 deformation to phenylalanine ring breathing modes, providing a Raman metric to distinguish between viable and nonviable constructs. Further, we tested the Raman stress metrics (already developed in vitro). We have also verified that the technique is capable of observing the results of pretreatment of EVPOMEs with rapamycin - a drug that is expected to positively affect EVPOMEs' development, resulting in more viable constructs. We distinguished between EVPOMEs pre-treated with rapamycin and controls, using the ratio of the Amide III envelope to the phenylalanine band as an indicator. The goal of this project is to design of a stand-alone system, which will be usable in a clinical setting, as the data processing and analysis will be performed automatically, based on already established and tested Raman spectroscopic indicators for EVPOMEs.

8579-20, Session 5

A novel and real-time identification methodology for microcalcifications in breast needle biopsies

Jaqueline S. Soares, Ishan Barman, Narahara Chari Dingari, Massachusetts Institute of Technology (United States); Zoya Volynskaya, Massachusetts Institute of Technology (United States) and Aperio Technologies, Inc. (United States); Wendy Liu, Nina Klein, Donna Plecha, Case Western Reserve Univ. (United States) and Univ. Hospitals Case Medical Ctr. (United States); Ramachandra R. Dasari, Peter T. C. So, Massachusetts Institute of Technology (United States); Maryann Fitzmaurice, Case Western Reserve Univ. (United States) and Univ. Hospitals Case Medical Ctr. (United States)

Microcalcifications are a feature of particular diagnostic significance on a mammogram and often geographically target the location of the most important abnormality within the breast. There is an unmet clinical need for a tool that can provide real-time guidance during stereotactic biopsy procedures for microcalcification retrieval. Optical spectroscopy, especially Raman spectroscopy, has been previously employed due to its chemical specificity. In this work, we evaluate an alternate modality, diffuse reflectance spectroscopy, for detection of microcalcifications based on the variations in scattering and absorption signatures stemming from the size and nature of the lesions associated with the microcalcification clusters. Diffuse reflectance and Raman spectra were acquired ex vivo from 203 tissue sites in fresh breast biopsy tissue cores from 23 patients undergoing stereotactic breast needle biopsies, including 90 normal sites, 56 lesions without microcalcifications and 57 lesions with microcalcifications. The radiographic assessment was compared with the Raman and reflectance measurements and the sites were classified using principal component analysis and support vector machines. We report that a decision algorithm developed for detection of microcalcifications in breast tissue using only diffuse reflectance spectra shows high predictive power with positive (PPV) and negative predictive value (NPV) of 97% and 88%, respectively. While the Raman algorithm is expectedly more specific (PPV = 98%, NPV = 95%), the high diagnostic power obtained using diffuse reflectance spectra alone creates a new landscape for real time detection of microcalcifications due to the lower acquisition time and simpler instrument requirements of the latter.

8579-21, Session 5

Hyperspectral imaging of tissue mimicking phantoms: principle component analysis

Philip Wong, The Univ. of Western Ontario (Canada); Fartash Vasefi, SMI (United States); Muriel Brackstone, Lawson Health Research Institute (Canada); Bozena Kaminska, Simon Fraser Univ. (Canada); Jeffrey J. L. Carson, Lawson Health Research Institute (Canada)

Angular Domain Spectroscopic Imaging (ADSI) is a hyperspectral imaging technology that combines both optical spectroscopy and optical imaging into a single platform. The technique employs an array of micro-channels to perform angular filtration, whereby quasi-ballistic photons traversing a turbid sample are accepted and scattered photons (image-degrading) are rejected. The aim of the work reported here was to evaluate the effectiveness of the ADSI system at identifying targets buried within tissue-mimicking phantoms. Principal component analysis (PCA) was applied to spectral data-cubes to extract the main spectral features from the phantoms. Targets of various absorption levels (Indocyanine Green), depths beneath the phantom surface, and background scattering levels were evaluated. PCA components were analyzed with k-means clustering and the extracted features were grouped and classified and the sensitivity and specificity of the ADSI system were estimated. ADSI with PCA provided clear separation of targets at different Indocyanine Green concentrations and depths. The results led us to conclude that the technique holds potential for characterizing tissue specimens obtained during surgery.

8579-22, Session 5

Assessment of optical properties in turbid media using frequency-modulated continuous-wave diode lasers

Liang Mei, Lund. Univ. (Sweden) and Zhejiang Univ. (China) and Joint Research Ctr. of Photonics (China); Sune Svanberg, Lund Univ. (Sweden) and South China Normal Univ. (China) and Joint Research Ctr. of Photonics (China); Gabriel Somesfalean, Lund Univ. (Sweden) and Zhejiang Univ. (China) and Joint Research Ctr. of Photonics (China)

The optical properties – e.g., reduced scattering coefficient and absorption coefficient – are key components needed in many biophotonics applications. In the present work, a novel and technically undemanding method is proposed to evaluate these parameters, utilizing a frequency-modulated continuous-wave diode laser as a light source and examining the intensity fluctuation of the scattered light using a heterodyne detection scheme. Due to scattering in the turbid media, a time delay distribution between the scattered light and the reference light is introduced, leading to a frequency delay which generates a beat signal. The beat frequency is linearly proportional to the delay time between the scattered and reference light. Thus, the power spectrum of the detected light intensity is equivalent to the time-of-flight distribution for the light that passed through the solid turbid medium. However, in turbid liquid materials, apart from the frequency delay due to the light scattering, Doppler shifts due to the moving particles are also produced. Thus, the power spectrum of the detected light intensity corresponds to the combined effect of the Doppler shifts and the light scattering. Based on the diffusion approximation theory, a nonlinear fit to the power spectrum of the scattered light field from the solid or liquid turbid media is performed. In proof-of-principle measurements, the optical properties of liquid and solid turbid media could be retrieved.

8579-23, Session 5

A compensation algorithm for multiple scattering in laser speckle rheology of biological fluids

Zeinab Hajjarian Kashany, Seemantini K. Nadkarni, Harvard Medical School (United States)

Bio-fluids play key roles in different organs, owing to their distinct viscoelastic properties. Alteration of these properties is often an indicator of a pathological condition and tools that enable probing mechanics of bio-fluids are of invaluable diagnostic potential. Laser Speckle Rheology (LSR) is a novel optical approach that enables mechanical evaluation of biological specimens in a non-contact manner. In LSR, the specimen is illuminated by a laser beam and speckle intensity fluctuations are recorded via a high-speed camera. Speckle fluctuations are modulated by displacements of scattering particles. Since extent and scales of particle movements are related to viscoelasticity of the microenvironment, speckle fluctuations can be processed to evaluate mechanical properties. However, multiple scattering of light also modifies speckle fluctuations rate and complicates the extraction of particles' mean square displacement (MSD) from speckle movies. In this study, we propose a new algorithm to correct for variations in scattering concentrations. To this end, diffuse reflectance profile (DRP) of intensity is calculated from speckle frame series and optical properties are experimentally estimated. A Monte-Carlo ray tracing (MCRT) program is developed and used to extract MSD from speckle fluctuations, by taking into account the contribution of optical properties. Subsequently complex viscoelastic modulus, G*(?), is calculated from the MSD. Comparison of LSR measurements with conventional rheometery indicates a strong correlation between the two measurements for phantoms (R=0.996, P<10-5), bovine synovial fluid (R=0.927, P<10-5), and bovine vitreous humorous (P=0.997, P<10-5), demonstrating the promising prospect of LSR for evaluation biofluids' viscoelasticity.

8579-24, Session 5

Automated quantification of birefringence for assessment of muscle necrosis using polarization-sensitive optical coherence tomography

Lixin Chin, Univ. of Western Australia (Australia); Xiaojie Yang, Blake R. Klyen, Robert A. McLaughlin, Tea Shavlakadze, Miranda D. Grounds, David D. Sampson, The Univ. of Western Australia (Australia)

We present an automated technique for the optical assessment and quantification of tissue damage, through the calculation of birefringence from 3D volumetric polarization-sensitive optical coherence tomography (PS-OCT) scans. The technique is demonstrated using skeletal muscles from a mouse model of human muscular dystrophy, and validated against histology.

Birefringence is an optical property exhibited by many types of tissue, including those of the musculoskeletal system, due to the presence and arrangement of anisotropic tissue ultrastructures. Disease processes can disrupt these structures, leading to a corresponding reduction in birefringence, and quantification of birefringence can give an indication of the extent and severity of tissue damage. Birefringence manifests as an induced phase-retardation between orthogonal linearly polarized components of light, and this phase-retardation can be measured non-invasively using PS-OCT. We have developed a novel technique using quadrature demodulation and phase-unwrapping to calculate the value of birefringence in each depth scan in the PS-OCT volume. This produces a 2D en face map of birefringence quantification, which provides an indication of the extent of tissue damage.

This technique was applied to skeletal muscles from the mdx mouse model of Duchenne muscular dystrophy, which are prone to develop areas of necrosis. En face birefringence maps were generated for skeletal muscle samples from both mdx mice and healthy control C57 wild-type mice. Validation with co-located histology sections shows a strong correspondence between the resulting areas of low and high birefringence, and areas of necrotic and undamaged muscle respectively.

8579-25, Session 6

Skin microvascular and metabolic response to pressure relief maneuvers in people with spinal cord injury

Jessica C. Ramella-Roman, Du V. N. Le, Thu Nguyen, The Catholic Univ. of America (United States); Alison Lichy, Suzanne Groah, National Rehabilitation Hospital (United States)

Clinician's recommendations on wheelchair pressure reliefs in the context of the high prevalence of pressure ulcers that occur in people with spinal cord injury is not supported by strong experimental evidence. Some data indicates that altered tissue perfusion and oxygenation occurring under pressure loads, such as during sitting, induce various pathophysiologic changes that may lead to pressure ulcers.

Pressure causes a cascade of responses, including initial tissue hypoxia, which leads to ischemia, vascular leakage, tissue acidification, compensatory angiogenesis, thrombosis, and hyperemia, all of which may lead to tissue damage. We have developed an advanced skin sensor that allow measurement of oxygenation in addition to perfusion, and can be safely used during sitting. The sensor consists of a set of fiber optics probes, spectroscopic and Laser Doppler techniques are used to obtain parameters of interest.

The overriding goal of this project is to develop the evidence base for clinical recommendations on pressure reliefs.

In this paper we will illustrate the experimental apparatus as well as the results of a small clinical trial conducted at the National Rehabilitation Hospital.

8579-26, Session 6

Effect of xenon/hypothermia on cerebral blood flow and oxygen consumption in newborn piglets with a time-resolved near-infrared technique

Mohammad Fazel Bakhsheshi, Jennifer Hadway, The Univ. of Western Ontario (Canada); Mamadou Diop, Lawson Health Research Institute (Canada); Keith St. Lawrence, Ting-Yim Lee, The Univ. of Western Ontario (Canada)

OBJECTIVES: Clinical trials of hypothermia (HT) therapy in asphyxiated infants have demonstrated the therapeutic potential in cerebral ischemia. Xenon (Xe) is a rare noble gas with attractive anesthetic properties including minimal side effect and fast onset/emergence, also showing great promise as a neuroprotectant in both in vitro and in vivo experimental studies, particularly when combined with cooling1. We investigated the combination effect of Xenon/Hypothermia compared with Propofol/Hypothermia on the cerebral metabolic rate of oxygen (CMRO2) and cerebral blood flow (CBF) by a bolus-tracking method using indocyanine green (ICG) as a flow tracer with time-resolved near-infrared (TR-NIR) technique on new born piglets.

METHODS: Experiments were conducted on five new born piglets (<3 days) that were anesthetized by isoflurane (3% to 4% during preparatory surgery,1.5% post surgery). After surgery, piglets were maintained on 1-2% isoflurane at normothermia (NT37°C). After two measurements were collected, Isoflurane was discontinued and an intravenous infusion of propofol started (9-22.4 mg/kg h), coupled with ventilation on 70% nitrous oxide (N2O) and 30% oxygen (O2) with normo and hypothermic (HT33°C) condition. The propofol infusion pump displayed the estimated blood propofol concentration. After approximately 2-3 hours on this anesthetic combination, piglet was given to breath 40-50% Xe replaced with N2O using the closed-circuit Xe/O2 delivery system2. A femoral artery was catheterized to monitor heart rate and blood pressure and to intermittently collect arterial blood samples for gas (paCO2, paO2), pH and glucose analysis. A cannula was inserted into an ear vein for administrating of ICG. Animals were placed in a prone position, and

a custom-made probe holder was strapped to the head to hold the TR-NIRS emission and detection probes 2 cm apart, parasagittally, approximately 1.5 cm dorsal to the eyes. Temperature was altered by exposing piglet's body to room temperature until the rectal temperature decreased to 33°C. CBF/CMRO2 was then determined from brain ICG concentration curves as described previously3. For each temperature, two measurements were collected per anesthetic condition.

RESULTS: Both CBF and CMRO2 were affected by changing the anesthetic condition and also decreasing the brain temperature resulted in a decrease in CBF and CMRO2, as expected4. Both the Heart rate (HR) and mean arterial blood pressure (MAP) varied with the level of anesthesia and changing in temperature. There was a statistically significant increase in HR and when the anesthetic was switched from isoflurane to propofol/ N2O ($P < 0.003$). Similarly, Figure 2 shows that both CBF and CMRO2 were not significantly affected when the anesthetic was switched from propofol/ N2O to propofol/ Xe.

CONCLUSION: CBF and CMRO2 were measured by TR-NIR technique during hypothermia treatment with varying the plane of anesthesia in new born piglets. As the next step we will be validating our results in more newborn piglets.

REFERENCES

1-J Cereb Blood Flow Metab. Apr - 29(4):707-14 (2009)

2-Anesth Analg. Aug - 109(2) - 451-60 (2009)

3-Journal of Biomedical Engineering. 15(5) - 057004 – Sep-Oct (2010)

4-Proc. SPIE 8207, 82074R (2012)

8579-27, Session 6

Optical properties of tumor tissues grown on the chorioallantoic membrane of chicken eggs measured with a double integrating sphere and inverse Monte Carlo method in the wavelength range of 350-1000 nm

Norihiro Honda, Yoichiro Kariyama, Osaka Univ. (Japan); Takuya Ishii, Chiaki Abe, Katsushi Inoue, Masahiro Ishizuka, Tohru Tanaka, SBI Pharmaceuticals Co., Ltd. (Japan); Hisanao Hazama, Kunio Awazu, Osaka Univ. (Japan)

Photodynamic therapy (PDT) using 5-aminolaevulinic acid (ALA) is an attractive method because of the shorter decay time of photosensitivity compared with PDT using other drugs. However, the optimum conditions to perform ALA-PDT, e.g., drug dose, wavelength, and irradiation dose have never been clarified. To evaluate the effectiveness of PDT using ALA and its dependence on drug dose, wavelength, and irradiation dose in the treatment of tumors, the usefulness of a tumor model prepared with tumor cells grown on the chorioallantoic membrane of chicken eggs was studied by measuring the optical properties of the tumor model. The optical properties of tumor model were measured with a double integrating sphere optical setup and inverse Monte Carlo technique in the wavelength range from 350 to 1000 nm. The spectra of absorption and reduced scattering coefficients of the tumor model grown in the chicken eggs were compared with those of the other tumor model grown in mice. The measured optical properties of the tumor model using chicken eggs were similar to those of the tumor model using mice. These results indicate that the tumor model using chicken eggs are a suitable system to investigate the effectiveness of ALA-PDT. This in vivo assay system for tumors has advantages for evaluating antitumor effect of ALA-PDT because of its convenience, rapidity, and inexpensiveness.

8579-28, Session 6

High performance near-IR imaging for breast cancer detection

Yasser H. El-Sharkawy, Cairo Univ. (Egypt)

We present a method for the noninvasive determination of the size, position, and optical properties of tumors in the human breast. The tumor is first detected by photothermal imaging. It is then sized, located, and optically characterized using a deigned digital image processing and edge detection pattern recognition. Our method assumes that the tumor is a spherical in homogeneity embedded in an otherwise homogeneous tissue. We deposit a heat energy in the tissue by absorption of Nd:YAG laser and its subsequent conversion to heat via vibrational relaxation. This causes a rise in temperature of the tissue. Also heat will diffuse through the tissue causing a rise in temperature is the surrounding tissue. We can differentiate between normal and cancerous tissue using IR thermal camera. We report the results obtained on a 55-year-old patient with a papillary breast cancer. We found that the tumor absorbs and scatters near-infrared light more strongly than the surrounding healthy tissue. Our method has yielded a tumor diameter of 0.5 cm.

These results can provide the clinical examiner with more detailed information about breast lesions detected by photothermal imaging thereby enhancing its potential for specificity

8579-29, Session 7

Complex tissue phantoms using intralipid-infused solids for testing on fluorescence angular domain imaging

Rongen L. K. Cheng, Glenn H. Chapman, Mohammad Osama, Simon Fraser Univ. (Canada)

Optical imaging through biological tissue poses significant scattering problems which result in degradation of image resolution and quality. Utilizing organic materials as tissue test structures pose problems in biomedical imaging in vitro; tissues tend to have short lifetime which changes optical parameters and is difficult to manipulate for different imaging systems. We have been exploring to create long term stable phantoms with controllable scattering levels which have now measured to last for at least 10 months maintaining consistent optical characteristics to mimic skin characteristics by using solid organic scattering medium. A simple long term phantom is developed by encapsulating an intralipid-infused agar layer within clear polymer. For this work, we are targeted to create a complex testing structure which resembles collagen fluorescence under epidermis. The fabrication of multi-layered tissue phantoms consisted an intralipid-infused agar which replicates skin scattering characteristics ($\mu s = 20cm\text{-}1$, $g = 0.85$) and is positioned on top of multiple cylindrical tubing that are filled with either liquid/solid materials. These replicates blood vessels/injected fluorophores that lies beneath the epidermis. To verify the usage ability on imaging systems, we incorporated Angular Domain Imaging (ADI) to improve image quality by filtering out scattered light in the biological tissue based on the angular direction of photons. This technique is independent of wavelength, coherent, pulse, or duration compared to OCT or time domain imaging - hence more economic/convenient to apply on imaging systems. A type of ADI filter, SpatioFrequency filter with an acceptance angle of 0.286°, these embedded cylinders are detected.

8579-30, Session 7

Two-dimensional angular filter array for angular domain imaging with 3D printed angular filters

Eldon Ng, Jeffrey J. L. Carson, The Univ. of Western Ontario (Canada) and Lawson Health Research Institute (Canada)

Angular Domain Imaging (ADI) is an imaging technique that is capable of generating two dimensional shadowgrams of attenuating targets embedded in a scattering medium. In ADI, an angular filter is positioned between the sample and the detector to distinguish between quasi-ballistic photons and scattered photons. One implementation of ADI is with an Angular Filter Array (AFA). An AFA is a series of microchannels

with a high aspect ratio. Previous AFAs from our group were constructed by etching a silicon wafer, limiting the imaging area to a one dimensional line. Two dimensional images were acquired via scanning. The objective of this work was to extend the AFA design to two dimensions to allow for two dimensional imaging with minimal scanning. The second objective of this work was to perform initial characterization of the imaging capabilities of the two dimensional AFA. Our approach was to use rapid 3D prototyping techniques to generate an array of microchannels. The imaging capabilities were then evaluated by imaging a 0.9 mm graphite rod submerged in a scattering media. Contrast was observed to improve with longer angular filters. Contrast was also observed to improve two-fold when a second angular filter array was placed in front of the sample to mask the incoming light. A background scatter estimation method was also implemented by obtaining a second image with the mask intentionally misaligned to the AFA. Image contrast was improved when the scatter estimation image was subtracted from the original image obtained with the mask aligned to the AFA.

8579-31, Session 7

A discrete particle Monte-Carlo simulation of the effect of blood flow on the scattered light autocorrelation function

Noam Racheli, Ilan Breskin, Avihai Ron, Yaakov Metzger, Ornim Medical Ltd. (Israel); Giora Enden, Ben-Gurion Univ. of the Negev (Israel); Revital Shechter, Ornim Medical Ltd. (Israel)

Monte Carlo (MC) methods are widely used in biomedical applications. In particular, they are used to model light propagation in tissue. Here we present a Discrete Particle Monte Carlo (DPMC) simulation method to demonstrate how moving blood cells may affect the detected light autocorrelation function. Application of this effect can provide an important diagnostic tool for blood perfusion in tissue. Unlike common MC simulations, in which the light propagation within a medium is represented by a set of statistical rules and parameters, in the DPMC simulation the photon trajectories are calculated according to their interactions with pre-positioned matter particles. The advantage in applying the DPMC-based model is its ability to investigate directly and with relative ease the effect of particle displacements on photon trajectories, while in common MC simulations the particles' locations are not accounted for and particle displacements are introduced indirectly.

The DPMC model was described by a set of uniformly distributed particles. Particle displacements were introduced by repositioning them between consecutive time intervals according to their initial position and respective velocities. Photons reaching the detector face simultaneously created an interference according to their trajectories which was converted into light amplitude. The light intensity autocorrelation function was calculated for each set of particle displacements. Several simulation runs were performed over a range of different particle velocities.

We demonstrate that the detected light intensity autocorrelation function broadens as particles' velocity increases, as predicted.

8579-32, Session 7

Use of photoelastic modulator to linear dichroism measurement of bundles of collagen

Rosimere J. V. Moya, Victória Dias, Josiane A. F. Shibuya, Fernanda I. Correa, Cristiane M. França, Daniela F. Silva, UNINOVE (Brazil)

The phase of the light beam is modulated by either an electro-optic or photoelastic modulator. Differential absorption of linearly polarized light then produces a flux variation at the modulation frequency, which is detected by the phase-sensitive detection technique. The dichroism is a characteristic property of many transparent materials and depending sensitively upon the crystalline structure. Biomolecules also presents dichroism and findings have enabled the realization of the oriented arrangement of proteins and acid mucopolysaccharides in collagen sections. The measurement of this property is, therefore, a useful tool for studying biomolecules. The use of photoelastic modulator to linear dichroism measurement of bundles collagen before and after polarized and non polarized laser irradiation was realized and in this study and we shall describe our method for measuring and explain the laser influence on patterns dichroism of bundles collagen. In conclusion, the effect of the electric field on the collagen bundles is to align their molecules along the direction of the electric vector of the polarized light, increasing their molecular polarizability. Since this effect is of vectoral origin and thus, essentially no thermal, our findings stimulate researchers interested in this field to make further investigations to clarify mechanisms involved in the laser therapy. Despite the large number of studies about the action of the laser radiation, the mechanism of biostimulation has not been established and studies considering properties of polarized light are not usually performed.

8579-33, Session 7

Monte Carlo simulation of radiation transfer in human skin with geometrically correct treatment of boundaries between different tissues

Jan Premru, Univ. of Ljubljana (Slovenia); Matija Milanic, Jo?ef Stefan Institute (Slovenia); Boris Majaron, Jo?ef Stefan Institute (Slovenia) and Univ. of Ljubljana (Slovenia)

In customary implementation of three-dimensional (3D) Monte Carlo (MC) numerical model of light transport in highly scattering and heterogeneous biological tissues, the volume of interest is divided into voxels by a rectangular spatial grid. Because each voxel is assumed to have homogeneous optical properties, curved boundaries between neighboring tissues inevitably become serrated. This raises some concern with regard to realism of the model with regard to reflection and refraction of "photons" on such boundaries.

In order to investigate the above concern, we have implemented an augmented MC code, where tissue boundaries (e.g., blood vessel wall, epidermal-dermal junction) are defined by analytical functions and thus maintain their shape regardless of grid disretization.

Results of the customary and augmented model are compared for a few characteristic sample geometries, mimicking a port-wine stain vessel irradiatied with 532 nm laser beam of varying diameter.

We found that energy absorbed in boundary-containing voxels can vary by up to to 100% between the two models. At specific locations inside the vessel, absorbed energy values can still differ by up to 10%.

Even physically relevant integral quantities, such as linear density of the energy absorbed by the vessel, can differ between the two models as much as ±30%. Moreover, the values obtained with the customary model vary strongly with discretization step and don't dissappear with ever finer discretization. Meanwhile, our augmented model shows no such behavior, indicating that the customary approach suffers from inherent inaccuracy arising from physically flawed treatment of tissue boundaries.

8580-1, Session 1

In vivo microcirculation imaging of the sub-surface fingertip using correlation mapping optical coherence tomography (cmOCT)

Roshan I. Dsouza, Azhar Zam, Hrebesh M. Subhash, National Univ. of Ireland, Galway (Ireland); Kirill V. Larin, Univ. of Houston (United States); Martin J. Leahy, National Univ. of Ireland, Galway (Ireland)

We describe a novel application of correlation mapping optical coherence tomography (cmOCT) for sub-surface fingerprint biometric identification. Fingerprint biometrics including automated fingerprint identification systems, are commonly used to recognise the fingerprint, since they constitute simple, effective and valuable physical evidence. Spoofing of biometric fingerprint devices can be easily done because of the limited information obtained from the surface topography. In order to overcome this limitation a potentially more secure source of information is required for biometric identification applications. In this study, we retrieve the microcirculation map of the subsurface fingertip by use of the cmOCT technique. To increase probing depth of the sub surface microcirculation, an optical clearing agent composed of 75% glycerol in aqueous solution was applied topically and kept in contact for 15 min. OCT intensity images were acquired from commercial research grade swept source OCT system (model OCT1300SS, Thorlabs Inc. USA). A 3D OCT scan of the fingertip was acquired over an area of 5x5 mm using 1024x1024 A-scans in approximately 70 s. The resulting volume was then processed using the cmOCT technique with a 7x7 kernel to provide a microcirculation map. Studies have been conducted to monitor the microcirculation map of fingertip over period. We believe these results will demonstrate an enhanced security level over artificial fingertips. To the best of our knowledge, this is the first published demonstration of imaging microcirculation map of the subsurface fingertip.

8580-2, Session 1

Fractals and fluctuations: spatial and temporal correlations in optical coherence tomography of human breast cancer models

Zachary F. Phillips, Raghav K. Chhetri, Jason Cooper, Melissa A. Troester, Amy L. Oldenburg, The Univ. of North Carolina at Chapel Hill (United States)

The complex microenvironment surrounding human mammary epithelia is implicated in breast cancer development. Here we study both normal and pre-malignant mammary epithelial cells (MECs) in 3D tissue cultures as they form polarized, acinar structures similar to those found in vivo. Using Optical Coherence Tomography (OCT), we assessed the spatial and temporal characteristics of MECs co-cultured with stromal fibroblasts to characterize epithelial-fibroblast interactions. For spatial assessment, we used fractal analysis, which has recently emerged as a popular processing tool in many fields of computational biology and medical imaging. We employed a fractal box-counting method to calculate the fractal dimension of acini imaged in 3D using OCT as a function of increasing fibroblast concentration and culture time over 2 weeks. For temporal assessment, we performed speckle fluctuation spectroscopy, which has been previously used by others to identify cellular mechanisms such as apoptosis or motility. Here we use a compressive sampling method to acquire OCT images simultaneously across a large dynamic range of time timescales up to 40 frames per second. By rendering OCT contrast images of speckle fluctuations within specific frequency bands, we can observe the spatial pattern of cellular motility in and around the acini. We find that normal and pre-malignant acini and surrounding fibroblasts exhibit different rates of speckle fluctuation in different tissue culture conditions. These spatial and temporal metrics provide a new window into epithelial-stromal interactions in breast cancer.

8580-3, Session 1

Effect of scattering coefficient on laser speckle contrast imaging

Kosar Khaksari, Dennis Thomas, Sean J. Kirkpatrick, Michigan Technological Univ. (United States)

Laser speckle contrast imaging (LSCI) is a fast, efficient method to infer relative blood flow from the local contrast of a time integrated speckle pattern. Movement associated with scattering particles results in a reduction of the local contrast, where contrast is defined as the standard deviation of the intensity of the speckle pattern divided by the mean intensity and is usually calculated over a small window of pixels. Relative velocity can be inferred by quantifying the spatial (or temporal) speckle contrast.Contrast in LSCI can be affected by optical properties of the scattering medium. Scattering coefficient, μs, absorption coefficient, μa, and scattering anisotropy, g, are optical properties that may influence the calculated contrast. This work considers the effect of the reduced scattering coefficient in LSCI. The effect of changing the reduced scattering coefficient of various concentrations of a dilute milk solution on LSCI was investigated. LSCI measurements were made on a phantom structure consisting of an opaque polymeric block and a glass capillary. Dilute milk solutions with varying reduced scattering coefficients were flowed through the glass capillary at a constant velocity. All other imaging parameters were kept constant so that only g was varied between experiments. We determined the dependence of speckle contrast on the scattering coefficient for milk solutions with different lipid concentration. For a fixed optical setup, the speckle contrast decreased with increased scattering coefficient.

8580-4, Session 1

Optical vortex behavior in numerically and experimentally generated speckle fields with different phase correlations

Dennis Thomas, Kosar Khaksari, Michigan Technological Univ. (United States); Donald D. Duncan, Portland State Univ. (United States); Sean J. Kirkpatrick, Michigan Technological Univ. (United States)

The dynamic behavior of phase singularities (or optical vortices) in speckle fields generated both numerically and experimentally using a spatial light modulator (SLM), was investigated. Sequences of phase masks with known temporal decorrelation behavior were numerically generated. Fourier transforming these masks and multiplying by the complex conjugate yielded 2D speckle field sequences with pre-determined decorrelation characteristics. These same phase masks were uploaded to an SLM illuminated by a HeNe laser to produce dynamic speckle sequences with identical predetermined behavior experimentally. From the original phase fields, phase singularities were located based on local topological charge. Number density of the vortices, and vortex trail length were determined for the sequences. These spatio-temporal behaviors of the vortices were compared for the numerically generated true fields and the pseudo-fields calculated via a 2-D Hilbert transform of the numerically generated speckle patterns and the SLM generated speckle patterns. Decorrelation behavior of the numerically generated speckle patterns and the equivalent SLM generated speckle patterns was also investigated. The relationships between the spatio-temproal behavior of the numerically generated and SLM generated speckle patterns and the spatio-temproal behaviors of the optical vortices located in the true fields and the different realizations of the pseudo-fields will be the focus of this presentation.

8580-5, Session 1

On the relationship between speckle-field and vortex-field decorrelation behaviors

Sean J. Kirkpatrick, Michigan Technological Univ. (United States); Donald D. Duncan, Portland State Univ. (United States)

Phase information is not generally available in simple, non-interferometric optical imaging (intensity) configurations. Yet as initially shown by Siegert, the statistical relationship between the amplitude and the phase is retained and the relationship between the field autocorrelation function and the autocorrelation function of the corresponding intensity pattern is provided by the Siegert relation. However, speckle fields arising from scattering media contain singular locations of zero intensity and undefined phase. The phase in the vicinity of these singular points rotates through a full 2 pi radians along a circular path surrounding these points. These points are referred to as optical vortices. It has been suggested that because the vortices in a dynamic, stochastic optical field move in a manner correlated with the motion of the scattering particles, their spatio-temporal behavior can be used to help understand the dynamic behavior of the scattering media. In this study we numerically investigate the relationship between the decorrelation behavior of dynamic speckle fields and the decorrelation behavior of corresponding vortex 'fields'. Optical vortices in true and pseudo-fields calculated from dynamic speckle fields were identified based on values of the local topological charge. The 2-D matrix of the locations of the vortices was defined as the vortex field. The autocorrelation functions of intensity speckle patterns and corresponding vortex fields were determined for several different decorrelation behaviors and a relationship between the autocorrelation functions was determined. This study presents another approach to exploiting the spatio-temporal behavior of optical vortices to aid in our understanding of dynamic systems.

8580-6, Session 1

Measurement of dynamic scattering beneath stationary layers using multiple-exposure laser speckle contrast analysis

Evan R. Hirst, Oliver B. Thompson, Michael K. Andrews, Industrial Research Ltd. (New Zealand)

The retina/choroid structure is an example of a complex biological target featuring highly perfused tissues and vessel flows both near the surface and at some depth. Laser speckle imaging can be used to image blood flows but static scattering paths present a problem for extracting quantifiable data. The speckle contrast is artificially increased by any residual specular reflection and light paths where no moving scatterers are encountered.

Here we present results from phantom experiments demonstrating that the static and dynamic contributions to laser speckle contrast can be separated when camera exposures of varying duration are used. The stationary contrast parameter follows the thickness and strength of the overlying scatterer while the dynamic proportion of the scatter resulting from vessel flows and Brownian motion is unchanged. The importance of separating the two scatter components is illustrated by in vivo measurements from a scarred human retina, where the effect of the un-perfused scar tissue can be decoupled from the dynamic speckle from the intact tissue beneath it.

8580-7, Session 1

Effective frequency sensitivity of laser speckle contrast measurements

Oliver B. Thompson, Evan R. Hirst, Michael K. Andrews, Industrial Research Ltd. (New Zealand)

How does speckle contrast K, measured at camera exposures T around 10 ms, give us information about temporal autocorrelation of the speckle pattern with time constants ? < 1 ms, corresponding to Doppler shifts in the KHz range? We explore the implications of this question and show that for any particular assumed temporal speckle autocorrelation function, K measured at T >> ? accurately measures ?, but that K measurements at T < ? are required in order to determine the actual shape of the autocorrelation function. Determining the shape of the autocorrelation function is important if we wish to distinguish between different types of flow or movement in tissue, for example distinguishing Brownian motion or the randomly-oriented flows in capillary networks from more ordered flow in resolvable vessels.

8580-8, Session 1

Vortex lifetimes in dynamic speckle fields

Donald D. Duncan, James C. Gladish, Portland State Univ. (United States); Sean J. Kirkpatrick, Michigan Technological Univ. (United States)

Speckle fields contain optical vortices, or phase singularities, at points of zero intensity and thus undefined phase. For many years, the spatio-temporal variations in speckle fields have been exploited for inferring measures of the dynamics of scattering media (QLS, Laser Speckle Contrast Imaging, etc.). We are thus lead to hypothesize that the spatio-temporal behavior of optical vortices can be exploited as an indicator of biological activity as well. One such property of these phase singularities is their lifetime. Here we use Bayesian particle filters to estimate the first order statistics of vortex lifetimes. This is achieved by generating synthetic, dynamic speckle patterns with a given decorrelation time and tracking the vortices from birth to annihilation. The temporal extent of the resulting vortex trajectories is used to derive the probability density function describing vortex lifetimes. Measures of tortuosity are also of interest. We provide details of these probability density functions and the link between lifetime and tortuosity, and the more conventionally used speckle decorrelation time. Ultimately, these results will be useful in relating the persistence of phase singularities to the dynamic properties of the propagation medium.

8580-9, Session 1

Scatter characteristics of liquid crystal variable retarders

James C. Gladish, Donald D. Duncan, Portland State Univ. (United States)

Liquid crystal variable retarders (LCVRs) are computer-controlled birefringent devices that contain nanometer-sized birefringent liquid crystals (LCs). The LCs impart retardance effects through a global, uniform orientation change based on a user-defined drive voltage input. However, due to scattering by the LCs, these devices have a variable signal-to-noise ratio (SNR) that depends on the state of the LCVR. This scattering ultimately determines the SNR of a measurement system comprised of these LCVRs. For example, these LCVRS will ultimately be used in a spectral polarimeter for characterization of sub-wavelength structure of biological tissues. In this work, we investigate the SNR of these devices by measuring the voltage-dependent LC scattering signature with goniometric and spectral integrating sphere configurations. From these two types of measurements, we quantify SNR and show that the LCs produce scatter that is non-Rayleigh. This effect is described in terms of a voltage-dependent structure factor, which characterizes the sub-wavelength spatial organization of the LCs. This same type of analysis can also be applied to biological tissue. However, the main difference here is that the LC characterization includes a well-controlled experiment in which there is a significant amount of a priori knowledge of the scatterer organization.

8580-10, Session 2

Enhancing antibiofilm efficacy in photodynamic therapy: effect of microemulsion *(Invited Paper)*

Anil Kishen II, Univ. of Toronto (Canada)

In this study, we tested the hypothesis that a microemulsion containing oxygen carrier in photosensitizer formulation when activated would facilitate comprehensive disinfection of matured bacterial biofilm on infected dentin by photodynamic therapy (PDT). Experiments were conducted in different phases. In the phase 1 an imaging analysis was used to characterize the bubble dynamics generated in microemulsion, while in the phase 2, photosensitizing formulation containing microemulsion were tested for its photochemical properties. In phase 3, the efficacy of microemulsion containing photosensitizer formulation was tested on in vitro biofilm models of Enterococcus faecalis grown on dentin substrate. Microemulsion containing photosensitizer formulation was overall the most effective photosensitizer formulation for photooxidation, generation of singlet oxygen, and in disinfecting biofilm bacteria. This modified photosensitizer formulation will have potential advantages in dentin disinfection.

8580-11, Session 2

Bed-side monitoring of hemodynamics in ischemic stroke patients with diffuse correlation spectroscopy *(Invited Paper)*

Turgut Durduran, ICFO - Institut de Ciències Fotòniques (Spain)

Diffuse correlation spectroscopy (DCS) utilizes the temporal statistics of the laser speckles that persist even in diffuse light. The technology enables the researchers to measure microvascular cerebral blood non-invasively and when combined with near-infrared diffuse optical spectroscopy (NIRS-DOS) enables the derivation of a comprehensive view of the brain physiology. We describe the development and use of these methods for monitoring of patients who are at high risk or have suffered an ischemic stroke. We will describe our ongoing work in risk stratification of high-risk populations, monitoring the interventions at the emergency rooms and bed-side monitoring at the more acute stages. The ultimate goal is to introduce the diffuse optical monitors into clinical use for personalized medicine.

8580-12, Session 2

Investigating the response of mammalian cells to terahertz radiation

Jillian P. Giles, Cecil S. Joseph, Peter Gaines, Robert H. Giles, Univ. of Massachusetts Lowell (United States)

The advancement of medical and defense terahertz (THz) imaging applications, along with limited research on the response of biological systems to THz frequencies (0.1-10 THz), has driven further analysis of THz radiation-induced effects on cellular structures and viability. In this study, a CO2 optically-pumped FIR gas laser was used to irradiate human embryonic kidney (HEK) 293 cells at 584 GHz, 1.4 THz, and 2.4 THz. The HEK 293 cells were cultured in polystyrene, 96-well plates using DMEM (Dulbecco's Modified Eagle's Medium) supplemented with 10% fetal bovine serum. The cells were irradiated in the center wells of the 96-well plates for one hour at room temperature (~21°C), along with control plates incubated in the same conditions but in the absence of irradiation. The cells were then incubated at 37°C for 24 to 48 hours after irradiation. Following incubation, cell viability and cell proliferation were assessed using the cell metabolic MTS assay technique. The instrumentation employed and the analysis of biological responses will be presented.

8580-13, Session 2

Monitoring cells in engineered tissues with optical coherence phase microscopy: optical phase fluctuations as an endogenous source of contrast

Pierre O. Bagnaninchi, The Univ. of Edinburgh (United Kingdom); Christina Holmes, Maryam Tabrizian, McGill Univ. (Canada)

In tissue engineering there is a need for non-invasive, label-free monitoring of cell growth and health within 3D constructs. We have previously shown that optical coherence phase microscopy was sensitive enough to monitor intracellular motion. Here we demonstrate that intracellular motility can be used as an endogeneous contrast agent to image cells in various 3D engineered tissue architectures. Phase and intensity-based reconstruction algorithms are compared.

In this study, we used an optical coherence phase microscope set up in a common path configuration, developed around a Callisto OCT engine (Thorlabs) centred at 930nm, and an inverted microscope with a custom scanning head. Intensity data were used to perform in-depth microstructural imaging. In addition, phase fluctuations were measured by collecting several successive B scans at the same location, and the first time derivative of the phase, i.e. time fluctuations, was analysed over the acquisition time interval to map motility. Alternative intensity-based Doppler variance algorithms were also investigated. Two distinct scaffold systems seeded with adult stem cells, algimatrix (Invitrogen) and custom microfabricated poly(D,L-lactic-co-glycolic acid) fibrous scaffolds, as well as cell pellets were imaged.

We showed that optical phase fluctuations resulting from intracellular motility can be used as an endogenous source of contrast for optical coherence phase microscopy allowing the distinction of viable cells from the surrounding scaffold.

8580-14, Session 2

Characterization of the contributions of systemic physiology to functional NIRS data using single-channel ICA decomposition of fNIRS signals

Ardalan Aarabi, Theodore J. Huppert, UPMC Presbyterian (United States)

Introduction.

Functional near infrared spectroscopy (fNIRS) has been used to study hemodynamic changes associated with spontaneous neural activities in the brain. The fNIRS measurements reflecting changes in regional oxygenated and deoxygenated hemoglobin concentrations are often contaminated by physiological noise including changes related to blood pressure, respiration and cardiac activity. We developed an approach based on single-channel independent component analysis (scICA) to decompose resting-state fNIRS signal into its underlying source signals.

Methods.

The oxy-hemoglobin (oxy-Hb) and deoxy-hemoglobin (deoxy-Hb) recordings from 17 subjects were first preprocessed through band-pass filtering, noisy channel removal and motion artifact reduction. For each subject the frequency bands of the average normalized power spectral density of the fNIRS data were determined. Using the spectral bands, the number of independent sources required in the scICA-based approach was estimated. The fNIRS signals were then decomposed using scICA. Finally, the contributions of the components associated with frequency bands were estimated. A PCA-based clustering method was also used to group subjects based on their contribution of slow activity, respiration and cardiac activity.

Results.

Low frequency oscillations accounted for 40-55% of total power of the oxy-Hb and deoxy-Hb signals. Respiration and cardiac pulsations

accounted for 10-30% each. From the inter-subject clustering, we identified two types of physiological oscillations. Type-I contained a lower contribution of slow activity and a higher contribution for the respiration and cardiac activity within the deoxy-Hb, oxy-Hb signals in comparison with type-II.

Conclusion.

fNIRS signals can be decomposed using our approach to their underlying components with disjoint spectral support.

8580-15, Session 2

Delineation of the interaction of PAMAM dendrimer and skin by OCT

Amy Judd Judd, Keele Univ. (United Kingdom); Jon Heylings, Dermal Technology Lab., Ltd. (United Kingdom); Ka-Wai Wan, Univ. of Central Lancashire (United Kingdom); Gary Moss, Ying Yang, Keele Univ. (United Kingdom)

Polyamidoamine (PAMAM) dendrimers have been topically applied to the skin and utilised as a permeation enhancer for a range of therapeutic compounds. However, very little is known about the mechanism of enhancement. This study used optical coherence tomography (OCT) to investigate the influence of PAMAM dendrimers to alter surface refractive index (RI) in excised porcine skin. It is revealed that PAMAM dendrimers caused a sporadic disruption and disappearance of the white hyper-reflective band on the skin surface using OCT. Following the decontamination of the treated skin specimens, the entrance signal, resulting in the polarised light reflecting off the keratin of the upper skin strata, returned to normal. Further, PAMAM-induced changes in skin RI was benchmarked against glycerol, a known permeation enhancer and skin clearing agent. Changes in RI with PAMAM were only observed on the skin surface, suggesting that the dendrimer only modulates the outer layers of the stratum corneum. This is substantially different to the observed effect of glycerol, which permeated more deeply into the skin. The non-invasive and non-destructive OCT imaging technique may provide a convenient tool to investigate the mechanism of permeation enhancement and transdermal drug delivery.

8580-16, Session 3

Randomness in OCT and diffuse tomography *(Keynote Presentation)*

A. Claude Boccara, Sylvain Gigan, Institut Langevin (France)

The randomness of the refractive index and/or the position of the scatterers blur the images in biological tissues. OCT by selecting singly backscattered photons is a first approach that allows overcoming this problem. Even with incoherent sources the OCT signal exhibits a speckle distribution. We will examine the basic nature of the signal and what kind of supplementary information can be extracted from the OCT data such as local refractive index, density of scatterers and elasticity map.

Wavefront correction, introduced in astronomy, has found to be also useful in “ballistic” biomedical imaging by compensating tissue induced aberrations (typically over tens of modes) in direct or OCT retinal examination and 2-photon microscopy. More recently, mastering a larger number of modes (hundreds to thousands), it has been demonstrated that focusing through and in scattering media is possible with a wavelength or even a subwavelength resolution. This is achieved by using a spatial light modulator (SLM) or a phase conjugation (4-wave mixing) approach. We will discuss the basic principles of space and time focusing, present recent advances in this domain that occurs by using only optical waves or coupling optics and acoustics, underline difficulties linked to tissue imaging and try to forecast future developments.

8580-17, Session 4

Self-adaptation optical effects in photothermal treatment of tissue structures *(Invited Paper)*

Ilya V. Yaroslavsky, James J. Childs, Igor Perchuk, Mikhail Smirnov, Andrey V. Erofeev, Gregory B. Altshuler, Palomar Medical Technologies, Inc. (United States)

Photothermal effects form basis for many uses of optical energy to treat various medical conditions. Light-tissue interactions at high energy and/or power densities can become non-linear and, as such, no longer be accurately described by the simplistic linear models. These nonlinearities may profoundly affect resulting patterns of the light-tissue interaction; yet they are still poorly understood due to their complexity. In this work, we investigated the role of opto-thermal nonlinearities in light treatments of two important structures: skin and hair. In the first case, we used the Er:glass laser emitting at the wavelength of 1540 nm mostly absorbed by water; in the second, a diode laser emitting at 800 nm was used, with melanin as primary absorber. We have shown that both propagation of optical energy in the tissue and the resulting temperature field are significantly influenced by the non-linear effects. Moreover, the observed nonlinearities led to self-adaptation phenomena, such as canalization of the optical propagation pathways. These phenomena may be used to optimize photothermal procedures.

8580-18, Session 4

Non-invasive detection of antioxidants in human skin *(Invited Paper)*

Jürgen M. Lademann, Ruo-Xi Yu, Charité Universitätsmedizin Berlin (Germany); Wofgang Köcher, Opsolution GmbH (Germany); Martina C. Meinke, Alexa Patzelt M.D., Sabine Schanzer, Wolfram Sterry, Maxim E. Darvin M.D., Charité Universitätsmedizin Berlin (Germany)

In recent years optical investigation methods have been developed, which permit the non-invasive analysis of the dermal antioxidants, specifically the carotenoid concentrations which could serve as marker substances for the whole antioxidative status of the human skin. The use of resonance Raman spectroscopy and reflectance spectroscopy for non-invasive in vivo analysis of dermal carotenoids in humans is presented in this lecture. The investigations demonstrated that the antioxidant concentration measured in the skin of the investigated subject reflects his specific lifestyle and the stress he is exposed to. It could be shown in the investigations that subjects with high antioxidant concentrations in their skin were considerably less affected by skin ageing than comparable subjects with lower antioxidant concentrations. Consequently, a healthy diet rich in fruit and vegetables is the best prevention strategy against skin ageing. It is therefore particularly important to inform and educate adolescents about healthy lifestyles and avoidance of stressors. In this context, 50 senior high school students were measured for their antioxidant concentrations.

8580-19, Session 4

A preliminary investigation: the impact of microscopic condenser on depth of field in cytogenetic imaging

Liqiang Ren, Zheng Li, Yuhua Li, The Univ. of Oklahoma (United States); Bin Zheng, Univ. of Pittsburgh (United States); Shibo Li M.D., The Univ. of Oklahoma Health Sciences Ctr. (United States); Wei R. Chen, Univ. of Central Oklahoma (United States); Hong Liu, The Univ. of Oklahoma (United States)

As one of the important components of optical microscopes, the condenser has a considerable impact on system performance, especially on the depth of field (DOF). DOF is a critical technical feature in cytogenetic imaging that may affect the efficiency and accuracy of clinical diagnosis. The purpose of this study is to investigate the influence of microscopic condenser on DOF using a prototype of transmitted optical microscope, based on objective and subjective evaluations. Firstly, the relationship between condenser and objective lens is described, and the theoretical analysis of the condenser impact on system numerical aperture and DOF are discussed. Secondly, a standard resolution pattern and an evaluation function in spatial domain are used to objectively assess the condenser impact on DOF under 10?, 20? and 40? objective lenses, respectively. Finally, several cytogenetic samples are observed under a 40? objective lens to subjectively estimate the influence of the condenser. The experimental results of these objective and subjective evaluations are in agreement with the theoretical analysis. Although the above qualitative results are obtained under the experimental conditions with a specific prototype system, the methods presented in this preliminary investigation could offer useful guidelines for optimizing operational parameters in cytogenetic imaging.

8580-20, Session 4

Microcirculation imaging of the psoriatic plaques in vivo using correlation mapping optical coherence tomography

Haroon Zafar, National Univ. of Ireland, Galway (Ireland) and National Biophotonics and Imaging Platform (Ireland); Joey Enfield, Marie-Louise O'Connell, National Biophotonics and Imaging Platform (Ireland); Martin J. Leahy, National Univ. of Ireland, Galway (Ireland) and National Biophotonics and Imaging Platform (Ireland) and Royal College of Surgeons in Ireland (Ireland)

Vascular abnormalities play a critical role in skin diseases such as skin cancer, wine stain and psoriasis. Psoriasis is a chronic skin disease which affects 1% to 3% of the population. It results from abnormal immune function and is characterized by the presence of psoriatic plaques. The cause of psoriasis is not fully understood. To gain a better understanding of the vascular involvement in the psoriasis and its regular clinical assessment in vivo, non invasive imaging with high resolution and high sensitivity is needed. In this work correlation mapping optical coherence tomography (cmOCT) is used for microcirculation imaging of the psoriatic plaques in a completely non-contact and non-invasive manner. The cmOCT is a promising technique for microcirculation imaging that dense scanning OCT image acquisition and a novel software post processing protocol based on correlation statistics. This technique extracts the flow information from OCT data sets using purely the OCT signal intensity without the requirement of phase information. Promising results from microcirculation imaging of the psoriatic plaques in human forearm are presented. 3D microcirculation structure maps of the psoriatic plaques and healthy tissues are produced showing how these vessels relate to each other and within the plaque. Knowledge of the 3D microvascular architecture in psoriatic plaques will give fundamental insights into the disease and the possibility of identifying personalized treatments.

8580-21, Session 4

Mapping of spatial distribution of superficial blood vessels in human skin by double correlation analysis of optical coherence tomography images

Alexander Doronin, Sam Botting, Univ. of Otago (New Zealand); Marie Meglinski, Columba College (New Zealand); Karin M. Jentoft, Helmholtz Zentrum München GmbH (Germany); Igor V. Meglinski, Univ. of Otago (New Zealand)

2D/3D spatial distribution of superficial blood vessels in human skin in vivo was conducted by double correlation analysis of the swept source Optical Coherence Tomography (OCT) images. An adaptive Wiener filtering technique has been employed to remove background noise and increase the overall quality of the OCT images acquired experimentally. Correlation Mapping and Fourier domain correlation approaches have been subsequently applied to enhance spatial resolution of images of vascular network in human skin. The analysis of images performed on Graphics Processing Units (GPUs) utilizing the recently developed Compute Unified Device Architecture (CUDA) framework. This allows carrying out the Fast Fourier Transform (FFT) in parallel that significantly speed ups the correlation analysis of OCT images. It has been demonstrated that the double correlation approach permits obtaining 2D/3D images of superficial blood vessels and their distribution within the human skin with higher resolution compare to the similar techniques reported early.

8580-22, Session 4

PCA-based polarized fluorescence study for detecting human cervical dysplasia

Anita H. Gharekhan, C. U. Shah Science College (India); Seema Devi Khainchi, Jaidip M. Jagtap, Indian Institute of Technology Kanpur (India); Prasanta K. Panigrahi, Indian Institute of Science Education and Research Kolkata (India); Asima Pradhan, Indian Institute of Technology Kanpur (India)

A systematic investigation of the two highest principal components of the fluorescence spectra in visible region of dysplastic and normal human cervical tissues is analyzed using scatter plots and probability density functions. The fluorescence from dysplastic and normal parts of same patient were measured separately. The epithelial sides of samples were excited with a 450W Xenon lamp with 350 nm excitation wavelength and the components of fluorescence light which are parallel (co- or I?) and perpendicular (crossed- or I?) to the incident polarized light were recorded for the wavelength range of 380-650 nm. The dominant principal components i.e., the eigenvectors corresponding to the two largest eigenvalues of the covariance matrix, extracted using singular value decomposition. In this study, over 95% of the variance in the data was explained by the first two components of the PCA. Since the first and second principal components (PC1 & PC2) capture the highest proportion of variance present in the data, we have analyzed the two highest principal components using scatter plots and probability density functions. The scatter plots of PC1 versus PC2 show considerable differences between different tissue types. The difference of the parallel and perpendicular components shows remarkable difference as this is free from the diffusive component, so the intrinsic fluorescence is expected to manifest better here.

8580-23, Session 4

Delineating breast ductal carcinoma using combined dye-enhanced wide-field polarization imaging and optical coherence tomography

Anna N. Yaroslavsky, Rakesh Patel, Univ. of Massachusetts Lowell (United States); Ashraf Khan, Robert Quinlan, Univ. Massachusetts Memorial Medical Ctr. (United States)

Intra-operative delineation of breast cancer is a significant clinical problem in the surgical management of breast cancer. A reliable method for demarcation of benign and malignant breast tissue during surgery would aid in reducing the re-excision rate for patients due to positive margins. We present a novel method of identifying breast cancer margins using combined dye-enhanced wide-field polarization imaging for

quick and accurate delineation of en face cancer margins and optical coherence tomography (OCT) for rapid cross-sectional evaluation. Ten ductal carcinoma specimens were acquired following surgeries, stained with methylene blue, and imaged. Wide-field reflectance images were acquired at 440 and 640 nm. Wide-field fluorescence images were excited at 640 nm and registered between 660 and 750 nm. OCT images were acquired using a commercial 1310 nm Thorlabs swept-source system. The imaging results were validated against corresponding histopathology processed from approximately the same planes that were imaged. Both wide-field polarization imaging and OCT provided useful diagnostic information with regards to cancer resection margins in breast tissue. Combined OCT and wide-field polarization imaging show promise for intra-operative detection of invasive ductal breast carcinoma.

8580-24, Session 5

Optical clearing technology for in vivo tissue imgaing *(Invited Paper)*

Dan Zhu, Britton Chance Ctr. for Biomedical Photonics (China)

The high scattering in turbid biological tissues limits the penetration of visible and near-infrared light in tissue, which affects its applicability in preclinical and clinical medicine, and life science. The tissue Optical clearing technique based on immersion of tissues into optical clearing agents (OCAs) allows one to effectively control optical properties of tissues, leads to essential reduction of scattering, and therefore enhance the depth to which light penetrates in tissue. During the last several years, we have been focusing on optical clearing of tissue in vivo, such as skin and skull. In order to develop some safe, effective and reliable optical clearing methods to perform in vivo, non-invasive optical imaging, we firstly paid attention to mechanisms of tissue optical clearing and biocompatibility of OCAs. Secondly, we paid attention to the dynamical function and morphology of blood vessels caused by OCAs, the negative effect on blood vessel or skin depends on the dose of OCAs and type. Thirdly, some optical clearing were developed to make skin or skull transparent by topical application, and realize the visualization of subcutaneous and cortical microvessles. Combining optical clearing technique of tissue in vivo with laser speckle temporal contrast analysis, the blood flow at high resolution can be obtained. With transgenosis technique, it is possible for fluorecsence imaging to observe the neural activtiy in contex or the immune response.

8580-25, Session 5

Analysis of spontaneous fluctuations of optical signals in humans

Vladislav Toronov, Ryerson Univ. (Canada)

Near infrared light is sensitive to changes in blood volume and oxygenation. Modern near infrared spectroscopic devices allow for high speed data acquisition. These features make near infrared spectroscopy an ideal non-invasive tool to study dynamic processes associated with changes in blood volume and oxygenation. On the other hand, hemodynamic processes can be categorized into spontaneous vasodilation activity and functional activity. While it is known that various mechanisms of vasodilation include sympathetic nervous system and use of vasodilators such as nitric oxide, the structure and function of the overall vasodilation control system and even its purpose are poorly understood. In this study we acquired non-invasively hemodynamic optical signals on brain and muscles of healthy adult humans during rest and exercises. We also recorded simultaneously blood pressure changes and electro-encephalographic data. We used tools of non-linear dynamics and complex system techniques to understand main features of the underlying dynamic system.

8580-26, Session 5

Optical clearing for enhanced in utero mouse embryonic imaging

Narendran Sudheendran, Maleeha Mashitulla, Univ. of Houston (United States); Mohamad G. Ghosn, Baylor College of Medicine (United States); Valery V. Tuchin, N.G. Chernyshevsky Saratov State Univ. (Russian Federation); Mary E. Dickinson, Irina V. Larina, Baylor College of Medicine (United States); Kirill V. Larin, Univ. of Houston (United States)

Studying mammalian embryonic development in mouse models is crucial for understanding developmental defects in humans. Optical Coherence Tomography (OCT) has been previously used to image mice embryos at various stages of development. Recently, our group has demonstrated possibility of live in utero imaging of mice embryos allowing longitudinal monitoring and quantification of various morphological features. However, the uterine wall considerably attenuates the light and limits access to deep lying embryonic tissues. Tissue optical clearing has been demonstrated as valuable method to clear superficial regions of tissue. In these studies we investigated if application of clearing agents can reduce light attenuation by the uterine wall and enable deeper light penetration. We applied 20% and 40% glycerol solutions to clear the uterine wall and demonstrated improved embryonic imaging. We determined that optical signal in OCT images using 20% and 40% glycerol solution increased by 22% and 41%, respectively, over a period of 1 hour. These results suggest that optical clearing techniques can be used for in utero imaging.

8580-27, Session 5

Sample entropy of light transmission as a blood flow indicator

Jing Dong, Renzhe Bi, Kijoon Lee, Nanyang Technological Univ. (Singapore)

Sample Entropy (SampEn) is one of the non-linear complexity measures, gaining increasing popularity in biomedical time series data analysis such as heart rate variability, atrial fibrillation (AF) and the electroencephalographic. Originated from approximate entropy (ApEn) which determines the conditional probability of similarity between a chosen data segment and the rest with the same data length, sample entropy (SampEn) is a modified algorithm of ApEn. It is less biased statistic by avoiding counting self-matches of segments.

Recently, diffuse correlation spectroscopy (DCS) technology has been developed to extract tissue blood flow information out of diffuse reflectance signal. It requires high speed photon count detecting system to get autocorrelation function of the diffused photons, and the blood flow information can be extracted by fitting the autocorrelation function to the Brownian motion or random flow model.

In this paper, instead of calculating autocorrelation function and subsequently fitting the model to assess the flow, we attempted to utilize Sample Entropy (SampEn) on diffuse reflectance signal. It has several advantages such as the relative low requirement of sampling speed and can be calculated with relatively small number of data so that the high speed detector is not required. Moreover, the flow information is not based on fitting the model thus it is model-free. It suggests that SampEn is a good indicator for relative flow through flow phantom experimental data and cuff occlusion data. The dependence of SampEn analysis on template dimension (m), data size (N), and delay time (tau) will also be discussed in great detail.

8580-28, Session 5

Automatic soft tissue tumor margin detection with multiple analyses of optical coherence tomography images

Shang Wang, Narendran Sudheendran, Univ. of Houston (United States); Davis R. Ingram, Alexander J. Lazar M.D., Dina C. Lev, Raphael E. Pollock, The Univ. of Texas M.D. Anderson Cancer Ctr. (United States); Kirill V. Larin, Univ. of Houston (United States) and Baylor College of Medicine (United States)

We report on a multiple analyses model for optical coherence tomography (OCT) image processing in order to provide an improvement on the margin localization during the resection of soft tissue tumor. This model is based on the quantification of tissue scattering coefficient (TSC), speckles fractal dimension (SFD), and speckles intensity variance (SIV) through analyzing two-dimensional OCT images taken from the homogeneous human tissue parts ex vivo. The OCT images were first surface flattened. TSC was achieved by calculating the slope value of each intensity A-line. After removing the slopes from all the intensity A-lines, SFD was extracted by using one-dimensional fractal box-counting method from each intensity line in both transverse and vertical directions. SIV was also calculated from the same intensity lines for SFD. Reference values were quantified for the tissue types of liposarcoma, leiomyosarcoma, myxoma, fibrous tumor, muscle, collagen and fat. For assessing the feasibility of this model in margin detection, ex vivo muscle tissue with fibrous tumor was imaged and the quantified values of TSC, SFD and SIV were compared with the reference ranges. The tumor margin location was estimated along the imaging depth and confirmed by conventional histology analysis. Results demonstrate that the employed multiple analyses model for processing OCT images can be used for the automatic detection of soft tissue tumor margin. Future work will be focused on expanding the library reference data and including more tumor margin samples for statistical efficiency test of the model.

8580-29, Session 6

Evaluating image contrast in optical coherence elastography using finite element analysis *(Invited Paper)*

Kelsey M. Kennedy, The Univ. of Western Australia (Australia); Chris Ford, Curtin Univ. (Australia); Brendan F. Kennedy, Robert A. McLaughlin, Mark B. Bush, David D. Sampson, The Univ. of Western Australia (Australia)

Optical coherence elastography (OCE) is a dynamic optical imaging technique that differentiates tissues based on their mechanical response to stress, as measured with optical coherence tomography. In OCE images (elastograms), tissue strain is commonly used to indicate elasticity. However, proportionality of strain to elasticity assumes a uniform stress distribution, which is inaccurate for inhomogeneous tissue, due to stress concentrations that arise at interfaces and vary with geometry and boundary conditions. Thus, strain images are subject to mechanical artifacts, limiting their clinical utility. Previous OCE studies have proposed signal processing techniques for measuring deformation or novel excitation mechanisms for generating contrast, but none have investigated the limitations on contrast and image quality imposed by tissue mechanics. Understanding these limitations is necessary to reliably interpret elastograms and identify clinical applications for which OCE is suited. To elucidate sources of artifacts in elastograms and analyze their effects on image quality, we performed OCE measurements on tissue-mimicking phantoms with known properties and validated the resulting strain maps using finite element models (FEM). We will present elastograms for varying boundary conditions and geometries, including bi-layer and inclusion structures, and demonstrate their agreement with FEM simulations. We employ FEM to simulate the stress field in each case, identifying sources of non-uniformity. To quantify the accuracy of strain images in representing elasticity, we determine the ratio of strain contrast in elastograms to true elastic contrast for varying degrees of contrast. Results highlight the range of tissue mechanical parameters for which strain images provide accurate visualization of elasticity.

8580-30, Session 6

Structured illumination fluorescence correlation spectroscopy for velocimetry in Zebrafish embryos

Paolo Pozzi, Leone Rossetti, Laura Sironi, Stefano Freddi, Laura D'Alfonso, Maddalena Collini, Giuseppe Chirico, Univ. degli Studi di Milano-Bicocca (Italy)

We report on a study of the vascular system based on Fluorescence Correlation and Image Correlation Spectroscopy. The long term project addresses biologically relevant issues concerning vasculogenesis and cardiogenesis and in particular mechanical interaction between blood flow and endothelial cells. To this purpose we use Zebrafish as a model system since the transparency of its embryos facilitates morphological observation of internal organs in-vivo. Moreover the embryos are not completely dependent on a functional vascular system to continue to survive and develop (embryos receive enough oxygen by passive diffusion), thereby allowing a detailed analysis of animals with severe cardiovascular defects.The correlation analysis provides quantitative characterization of fluxes in blood vessels in vivo. We have pursued and compared two complementary routes in order to obtain complementary point of view. In a first one we developed a two-spots two-photon setup in which the spots are spaced at adjustable micron-size distances (1-40 microm.) along a vessel and the endogenous (autofluorescence) or exogenous (dsRed transgenic erythrocytes) signal is captured with an EM-CCD and cross-correlated. We exploit the two-photon infrared excitation (wavelength 800 nm) to induce autofluorescence in plasma proteins and its intrinsic 3D section capability. In this way we are able to follow the morphology of the Zebrafish embryo and simultaneously measure the heart pulsation and the velocity of red cells and of small plasma proteins. The analysis of the signal is made through the fitting of the cross-correlation function to models that account for the diffusion and drift of two populations of objects. Further refinements of these models account for the elasticity of the vessels and for the crowding of the erytrhocyte in the flux. The data acquired on a two-spot basis are compared to line scanning imaging along a vessel by means of a confocal setup. The two methods, coupled to numerical simulations and analytical models, allows to characterize the motion of plasma fluids and erythrocytes in healthy Zebrafish embryos to be compared in the future to pathogenic ones.

8580-31, Session 6

Fluorometry of ischemia reperfused rat lungs in vivo

Reyhaneh Sepehr, Kevin Staniszewski, Univ. of Wisconsin-Milwaukee (United States); Said Audi, Marquette Univ. (United States); Elizabeth R. Jacobs, VA Medical Ctr. (United States); Mahsa Ranji, Univ. of Wisconsin-Milwaukee (United States)

Objective: Previously we demonstrated the utility of optical fluorometry to evaluate lung tissue mitochondrial redox state in isolated perfused rats lungs under various chemically-induced respiratory states [1-3]. The objective of this study was to evaluate the effect of acute ischemia on lung tissue mitochondrial redox state in vivo using optical fluorometry. Under ischemic conditions, insufficient oxygen supply to the mitochondrial chain should reduce the mitochondrial redox state calculated from the ratio of the auto-fluorescent mitochondrial metabolic coenzymes NADH (Nicotinamide Adenine Dinucleotide) and FAD (Flavoprotein Adenine Dinucleotide).

Materials and methods: The chests of anesthetized, and mechanically ventilated Sprague-Dawley rat were opened to induce acute ischemia by

clamping the left hilum to block both blood flow and ventilation to the left lung for approximately 10 minutes. NADH and FAD fluorescent signals were recorded continuously in a dark room via a fluorometer probe placed on the pleural surface of the left lung.

Results: Acute ischemia caused a decrease in FAD and an increase in NADH, which resulted in an increase in the mitochondrial redox ratio (RR=NADH/FAD). Restoration of blood flow and ventilation by unclamping the left helium restored the RR back to its baseline. These results (increase in RR under ischemia) show promise for the fluorometer to be used in a clinical setting for evaluating the effect of pulmonary oxidative stress (e.g. chronic hyperoxia, ischemia-reperfusion) on lung tissue mitochondrial redox state in real time.

[1] R. Sepehr, K. Staniszewski, S Maleki, E. R. Jacobs, S. Audi, M. Ranji,, "Optical imaging of tissue mitochondrial redox state in intact rat lungs in two models of pulmonary oxidative stress," Journal of Biomedical Optics, vol. 17, p. 046010, Apr 2012.

[2] R. Sepehr, K. Staniszewski, E. R. Jacobs, S. Audi, M. Ranji, "Optical studies of tissue mitochondrial redox in isolated perfused rat lungs," in Proceedings of SPIE 8207D, San Fransisco, 2012; doi: 10.1117/12.909474

[3] K. Staniszewski, S. Audi, R. Sepehr, E. R. Jacobs, M. Ranji, " Surface Fluorescence Studies of Tissue Mitochondrial Redox State in Isolated Perfused Rat Lungs," Submitted to the Annals of biomedical engineering, July 2012.

8580-32, Session 7

Spectral encoding of spatial frequency approach for characterization of 3D structures

Sergey A. Alexandrov, National Univ. of Ireland, Galway (Ireland); Shikhar Uttam, Rajan K. Bista, Kevin D. Staton, Yang Liu, Univ. of Pittsburgh (United States)

Probing the sub-surface 3D internal structure of label-free objects, such as biological cells, tissues and nanofabricated materials, in their natural environments, with nano-scale accuracy and sensitivity is of great importance in many biomedical applications. We develop a new method to probe 3D structures which is based on spectral encoding of 3D spatial frequency (SESF) approach. Since an object's structure can be described using 3D scattering potential, or its Fourier transform (i.e., spatial frequency), SESF encodes different spatial frequencies of the scattering potential into corresponding wavelengths, which are translated into the image plane. Using a broadband light source in conjunction with a spectral device to record the spectrum at each image point, the information about the object's internal structure characterized by the axial spatial frequency can be reconstructed at each image point. Importantly, we demonstrate that this approach provides nanoscale accuracy and sensitivity in characterizing the axial structures with relatively simple optical instruments. We will present the theoretical basis of the SESF approach and validation of its nanoscale accuracy and sensitivity by numerical simulation. We will also demonstrate its feasibility to characterize nano-structures by experiments using complex 3D nanosphere aggregates and biological cells. Our results show that the SESF approach detects distinct differences in the spatial period in the label-free cells at different phases of the cell cycle, which is not detectable using conventional light microscopy. The potential applications of this technique can be broad, from probing macro-scale objects with nanoscale sensitivity, to detecting nano-structural changes of microscopic objects and quantifying nano-fabricated structures.

8580-33, Session 7

High-speed full-range spectral-domain correlation mapping optical coherence tomography

Hrebesh M. Subhash, Roshan I. Dsouza, Martin J. Leahy, National Biophotonics & Imaging Platform (Ireland)

In this paper, we introduce a full range spectral-domain correlation mapping optical coherence tomography (cmOCT) to utilize the whole depth imaging range of the spectrometer. The mirror image elimination is based on the linear phase modulation of the interferometer's reference arm mirror and with an algorithm that exploits Hilbert transform to obtain full range complex imaging in conjunction with the cm-OCT reconstruction technique. The proposed system is based on a high speed spectrometer at 91KHz with a modified scanning protocol to achieve higher acquisition speed with wide scan range. The estimated sensitivity of the system was around 102dB near the zero-delay line with ~14dB roll-off from 0.5mm to 2.5mm imaging-depth position. The estimated axial and lateral resolutions are 6.1 μm and 20 μm, respectively. A direct consequence of this complex conjugate artifact elimination is the enhanced flow imaging sensitivity for deep tissue imaging application by doubling the imaging depth. In turn, this also provides additional flexibility to explore the most sensible measurement range near the zero-delay line.

8580-34, Session 7

Depth selective flowmetry based on diffuse optical speckle analysis

Renzhe Bi, Jing Dong, Kijoon Lee, Nanyang Technological Univ. (Singapore)

Recently Diffuse Correlation Spectroscopy (DCS) is widely used for in vivo monitoring of blood perfusion at different depth, however the cost of the detection equipment, which includes single photon detector and hardware correlator, is relatively expensive, especially for multi-channel measurement. We propose a CCD based non-contact detection method, which takes advantage of the spatial correlation of diffuse laser speckle, to reduce the cost and achieve depth selective measurement with single exposure.

The light source is similar to traditional DCS equipment, which is a point laser source with long coherence length. Unlike DCS, where time autocorrelation of single laser speckle is applied, we use CCD as detector to catch the spatial distribution of diffuse laser speckles within a small surface area with short exposure time. By analysis of the speckle's spatial correlation, relative blood perfusion speed can be deduced. And by using larger imaging area, we can acquire measurements with different source-detector separations within one CCD image. Thus blood perfusion at different depth can be measured simultaneously. Both phantom experiment with controlled perfusion speed and in vivo experiments will be exhibited, and the results show good authenticity.

Comparing with traditional DCS machine, our setup is more cost effective and easier to implement. This setup can be used as non-contact and long-time monitor for blood perfusion inside deep layer tissue. Therefore it has high potential applications in biomedical functional study, such as brain function study and muscle dynamics study. And it will be a good supplement to the existing diffuse optical measuring methods.

8580-35, Session 7

Cross-polarized terahertz and optical imaging of nonmelanoma skin cancers

Cecil S. Joseph, Rakesh Patel, Univ. of Massachusetts Lowell (United States); Victor A. Neel, Massachusetts General Hospital (United States); Robert H. Giles, Univ. of Massachusetts Lowell

(United States); Anna N. Yaroslavsky, Univ. of Massachusetts Lowell (United States) and Massachusetts General Hospital (United States)

Nonmelanoma skin cancers are the most common form of cancer. Reflection cross-polarized continuous wave terahertz imaging offers intrinsic contrast between normal and cancerous tissue, but lacks the resolution required to identify tissue morphology. Intrinsic polarized light imaging at optical frequencies, provides morphological detail at sufficient resolution but often lacks contrast between the lesion and normal skin. We combined these two modalities and determined terahertz cross-polarized reflectance threshold values for malignant and benign skin tissue structures. Thick fresh excisions of skin cancer specimens were obtained from Mohs surgeries. The samples were mounted and scanned using both a continuous-wave terahertz imaging system at 513 μm and an optical polarized light imager at 440 nm. The terahertz images were overlaid with the optical images and compared with H&E histology. Terahertz cross-polarized reflectance values were calculated for cancerous and normal structures of the samples. The average reflectivity values for basal cell carcinomas showed that cancer had lower reflectivity than normal tissue. Similarly, squamous cell carcinomas showed the same trend but the reflectivity values slightly higher than those for BCC samples. Overall the average cross polarized reflectivity of the tumor and normal regions for all the samples investigated so far was found to be 0.69% ± 0.034% and 0.84% ± 0.010%, respectively. The difference between normal and cancer for representative sections averaged over all samples was significant ($p<0.001$). The combined optical and terahertz imaging shows promise for the detection of nonmelanoma skin cancers.

8580-36, Session 7

Functional connectivity patterns in spontaneous cerebral blood flow of mice

Karla M. Bergonzi, Adam Q. Bauer, Joseph P. Culver, Washington Univ. in St. Louis (United States)

We present the use of Laser Speckle Contrast Imaging (LSCI) to map resting-state functional connectivity (FC) based on cerebral blood flow (CBF) in mice. Patterns of regional, synchronized neural activity during rest provide maps of functional network connectivity at the systems level and show strong correspondence with those functionally active during task. A weakness with FC mapping using optical and MRI methods is that altered neurovascular coupling during disease can make disruptions in FC difficult to interpret. However, creating FC maps using spontaneous blood flow would provide a more comprehensive assay, potentially clarifying the mechanisms involved in FC disruption. Here, we present the use of LSCI to record spontaneous CBF in mice to map resting-state FC. LSCI uses the spatiotemporal statistics of laser interference at the cortex to measure the movement of red blood cells, thus providing a measurement of CBF. LSCI was performed through the mouse skull after reflection of the scalp, allowing for imaging of the brain over approximately 1cm2 of the dorsal cortex. A combination of spatial and temporal averaging was used to obtain sufficient signal to noise ratio for spontaneous correlation analysis. The spatial extent and correlation strengths of the CBF-based FC maps were found to be both robust and repeatable across mice and corroborate previously observed functional connectivity patterns in healthy mice using optical intrinsic signal imaging. Creating FC maps using spontaneous CBF will aid in providing a more complete assay of the mechanisms contributing to altered FC patterns in disease models.

8580-37, Session 7

Optimum polarimeter training sets for liquid crystal variable retarders

James C. Gladish, Donald D. Duncan, Portland State Univ. (United States)

Polarimeter training consists of presenting a set of known Stokes vectors (the training set) to the polarimeter, and then making polarimeter measurements on the training set to establish a measurement function. The measurement function describes how accurately the polarimeter can recover a given Stokes vector. The training set historically has been selected systematically due to limitations in the mechanical repositioning of the birefringent components making up the Stokes generator. However, the generation of a systematic training set can introduce systematic error, leading to inaccurate measurement functions. Here we propose a new technique to avoid the systematic generation of training sets. This technique is based on liquid crystal technology, and utilizes two liquid crystal variable retarders (LCVRs) to generate arbitrary Stokes vector training sets. LCVRs allow the user the freedom to choose an arbitrary set of Stokes vectors from anywhere on the Poincaré sphere. This provides an opportunity to optimize the training set, while also avoiding systematic error inherent with traditional techniques.

8580-38, Session 8

Effect of optical clearing agent at deeper tissue microcirculation using correlation mapping optical coherence tomography (cmOCT)

Azhar Zam, Martin J. Leahy, National Univ. of Ireland, Galway (Ireland)

Optical clearing is a method to enhance light penetration into biological tissue by using hyperosmotic and biocompatible agents. Hyperosmotic agents result in refractive index matching between cells which causes a reduction in optical scattering. In this paper, we investigate the effect of optical clearing at light penetration of deeper tissue microcirculation. We used two optical clearing agents, glycerin and fructose. We apply the optical clearing agents for 15 minutes to increase the resolution and penetration depth of the sub surface fingertip. We retrieve microcirculation map of the subsurface fingertip by use of cmOCT technique which was not easily retrieve without optical clearing.It is also possible to calculate the capillary loop density for the fingertip by counting the number of detected vessels. Studies have been conducted to compare the microcirculation map of fingertip from different optical clearing agent. We believe these results will show comparison between different optical clearing agent.

8580-39, Session 8

Doppler and photothermal optical coherence tomography for quantifying microvessel hemodynamics

Devin R. McCormack, Chetan A. Patil, Jason M. Tucker-Schwartz, Melissa C. Skala, Vanderbilt Univ. (United States)

Simultaneous imaging of blood oxygen saturation (sO2), vessel morphology, and blood flow dynamics at a microvascular level can give new insight into oxygen delivery and its role in multiple pathologies including cancer and ischemia. Currently, there are few technologies that can track all of these endpoints simultaneously and non-invasively in three dimensions; none of which can do so at microvascular resolution without exogenous contrast. The combination of Doppler optical coherence tomography (OCT) and photothermal OCT (PTOCT) may provide a single platform for imaging blood flow, microvessel morphology, and sO2 in three dimensions within an inherently co-registered system. PTOCT leverages the intrinsic NIR absorption differences between oxygenated and deoxygenated hemoglobin to ratiometrically determine sO2 at OCT imaging depths (1-3mm) and resolution (1-25μm). 715 and 732nm amplitude-modulated photothermal laser light is co-aligned with a spectral domain OCT system, and photothermal blood absorption at these wavelengths is extracted from the phase of the OCT interferogram. Phase information is additionally

used to determine Doppler flow profiles, while vessel morphology is constructed tomographically from the photothermal data. Photothermal derived sO2 values of canine blood phantoms flowing at physiological rates were found to be comparable to “gold standard” measures from a blood gas analyzer (<12% difference, n=4). In vivo feasibility has also been established with PTOCT images of mouse ear microvasculature. PTOCT-derived in vivo sO2 values of 86±6% (mean ± SEM, n=6) were calculated within microvessels, in agreement with published values. This work paves the way for multi-functional hemodynamic imaging of microvasculature in animal disease models.

8580-40, Session 8

Functional evaluation of the fast and slow response in neural activation using a multi-modality optical imaging system

Jia Qin, Lin An, Suzan Dziennis, Lei Shi, Roberto Reif, Siavash Yousefi, Ruikang Wang, Univ. of Washington (United States)

The coupling between neural activation and cerebral blood flow (CBF) is a fundamental aspect of brain physiology, and can aid in the understanding of physiopathology. However, directly imaging the intrinsic neuronal response and utilizing additional biomarkers, such as hemoglobin whose primary function is to transport oxygen to provide energy for regular organ function, could enable a comprehensive understanding of physiological and pathological conditions. Therefore, a multifunctional imaging modality that can synchronize and elicit the optical intrinsic signal and various biomarkers, such as the changes in CBF, oxygenated (HbO2), deoxygenated (Hb) and total hemoglobin (HbT) concentrations and cerebral metabolic rate of oxygen (CMRO2), can be advantageous as surrogate of neural activity involved in the physiological processes. A synchronized dual-wavelength laser speckle contrast imaging system, which contains two cameras that are synchronously triggered to acquire data, can acquire frames at a high spatiotemporal resolution (up to 500 Hz for ~1000?1000 pixels). Functional electrical stimulation is used to demonstrate the capability of the highly integrated system for imaging the fast response (neuronal response within tens of milliseconds) by quantifying the optical intrinsic signal, and slow response (blood flow and hemoglobin concentration response occurring in seconds) in the mouse brain, through an intact cranium. The capability to synchronize the fast and slow responses is not only valuable in pre-clinical applications for investigation of the mechanism of neurovascular and metabolic coupling, but also has potential in monitoring and diagnosing abnormalities in the human brain.

8580-41, Session 9

Full-scale blood flow response in functional electrical stimulation in mouse model evaluated by variable-range Doppler OCT

Lei Shi, Jia Qin, Siavash Yousefi, Suzan Dziennis, Ruikang K. Wang, Univ. of Washington (United States)

Depth-resolved microscopy is of great significance in evaluation of hemodynamic responses from neural activation, such as evoked by functional electrical stimulation. Doppler optical coherence tomography, which combines optical coherence tomography with Doppler algorithm, is an ideal tool to achieve this purpose with high spatiotemporal resolution. Previously due to the limits by phase wrapping and sensitivity, it is normally employed to detect fast blood flow, e.g. artery and vein. Here, we describe a comprehensive quantification of the vasculature from artery down to capillary using a variable-range Doppler OCT (VDOCT) technique. It captures repeated A-scans for multi-range velocimetry and uses a phase variance mask to extract the blood signal. The experiment was done by imaging the somatosensory cortex in a forepaw electrical stimulation mouse model with cranium left intact. The control and stimulated trials are given. The results revealed that fractional flow variances were mainly dependent on the vessel sizes: the larger the vessel, the smaller the change. The vasculature response sequence is also analyzed. By comparing the both sides of a stroke mouse, the healthy and infarction status are explicated. This can aid in the stroke study, which is critical on the blood flow supply. VDOCT lays a solid foundation for the detailed hemodynamic investigation in neural research. To further extend the imaging capability, we combined it with other imaging modalities, such as optical microaniography and laser speckle imaging, making the whole system a practical and promising tool for brain study.

8580-42, Session 9

Imaging the molecular diffusion in biological tissues with optical coherence tomography

Alexander Doronin, Anthony Karl, Adrián F. Peña Delgado, Ruth M. Empson, Igor V. Meglinski, Univ. of Otago (New Zealand)

Several investigations have been done to enhance the capacity of Optical Coherence Tomography (OCT) to achieve deep imaging in skin and other biological tissues. Optical clearing has emerged as the most suitable technique to accomplish this. In the current report we identify the front of molecular diffusion in mice skin in vivo and brain in vitro by using correlation analysis of the successive OCT images. The temporal changes of the diffusion front are associated with the morphology of the tissue, and thus provide additional information regarding tissue structure and abnormalities that are not observed by OCT under normal conditions.

8580-43, Session 9

Screening of molecular probes: optical and photophysical properties of new porphyrin

Grigor V. Gyulkhandanyan, Institute of Biochemistry (Armenia); Robert K. Ghazaryan, Yerevan State Medical Univ. (Armenia); Anna G. Gyulkhandanyan, Institute of Biochemistry (Armenia); Valery N. Knyukshto, Alexander S. Stasheuski, Boris M. Dzhagarov, Institute of Physics (Belarus)

The research and detailed analysis of the spectral and photophysical properties of new porphyrins and metalloporphyrins (21 compounds) have been conducted. This allowed conducting a preliminary selection of compounds suitable for photodynamic therapy of tumors (PDT) and photodynamic inactivation of microorganisms (FDI). For these compounds absorption and fluorescence spectra were measured. For all the complexes of metalloporphyrins containing atoms Co, Ag, Fe and Cu, are not detected own emission or the impurity luminescence of free porphyrin base. For other compounds, i.e. free porphyrins and their complexes with atoms Zn, characterized by the presence a significant fluorescence. The values of fluorescence quantum yields are a few percent and this are typical of the free bases and complexes with Zn. The essential influence of the nitrogen atom in the pyridyl ring on the spectral characteristics of luminescence is discovered. For free base porphyrins and their zinc complexes exhibit pronounced photosensitizing activity, which allows them to recommend for further study of their effectiveness in PDT and FDI. The nature of the aqueous solution does not affect the high efficiency of singlet oxygen generation of studied porphyrins (from 75% to 90%). The spectral characteristics, the values of fluorescence quantum yields, the kinetic parameters of the triplet states of porphyrins shows that all studied new water-soluble porphyrins and Zn-metalloporphyrins are promising for the creation of the basis of new fluorescent probes. The authors are grateful of BFFR (Project F11ARM-017) and SC of science of Ministry of Education and Science of Armenia (Project 11RB-016) for support.

8580-44, Session PMon

Validation and measurement of the positional floating reference point by near-Infrared (NIR) spectroscopy

Jingying Jiang, XuZheng Rong, Hao Zhang, Kexin Xu, Tianjin Univ. (China)

Previous studies have preliminarily validated the floating reference method and shown that it has the potential to improve the accuracy of non-invasive blood glucose sensing with Near-Infrared Spectroscopy. In order to make this method practical, it is necessary to precisely verify and measure the existence and variation features of the positional floating reference point. In this talk, a device which can precisely verify and measure the positional floating reference point is built. Therefore, as the light intensity of diffuse reflectance from the tested sample is very weak, we adopted a multipath probes system to improve the signal strength. And in this system, the probes are circularly arranged around the light source. Meanwhile, light source center is regarded as the probes's reference center while they are moving. In addition, these probes can be individually propel by hand or in motor-driven pattern with micrometers. Those micrometers reach an accuracy of 0.01mm and its marked surface makes it easy to read.Experimental results further demonstrate the existence characteristic of positional floating reference point as well as its variance characteristic for samples with different properties.

8580-45, Session PMon

Computer vision localization-based in vivo measurement by NIR spectroscopy

Jingying Jiang, Hao Zhang, Xuzheng Rong, Kexin Xu, Tianjin Univ. (China)

Near-Infrared spectroscopy analysis is a main method for non-invasive in vivo measurement of human body composition. However, the practical application of this technique is still unreachable because of the uncertainty of measurement conditions during in vivo measurement. The uncertainty would greatly influence the acquisition of spectral signal which reflects different concentrations of the constituent of human body. In this talk, Monte Carlo simulation has been used to investigate light transport within multi-layered nonuniform tissue. The location of optical sensor has been proved to be associated with the diffused reflection light. So we proposed a computer vision localization method which is based on image matching to localise optical sensor, and then the impact of optical sensor position and orientation variance can be decreased. The experimental results have shown that the uncertainty of measurement have been reduced significantly, signal-to-noise ratio have been enhanced greatly.

8580-46, Session PMon

Simulation on how to customize glucose adjustment method for noninvasive blood glucose sensing by NIRS

Jingying Jiang, Xiaolin Min, Da Zou, Kexin Xu, Tianjin Univ. (China)

Previous studies have shown the limitations of taking OGTT (Oral Glucose Tolerance Test) as the glucose adjustment recipe for non-invasive blood glucose sensing. Therefore, as the change of blood glucose under OGTT is excessively single, it is difficult to provide more comprehensive and reliable information for the establishment of predictive model. To solve this problem, a new try using other adjustment methods has been made based on a mathematical model of glucose metabolism system, IMM (the Integrated Minimal Model). In this talk, a further study would be focused on more detailed combination options of different glucose input types for glucose adjustment projects in non-invasive blood glucose sensing. Firstly, the changes of human blood glucose concentration under oral-taking, intravenous injection and intravenous drip were simulated under IMM. Meanwhile, the corresponding spectra were collected through Monte Carlo simulation of the three-layer skin model. And then calibration models by means of partial least squares (PLS) method have been established, which could be used to evaluate the quality of different glucose adjustment options. Finally, the use and combination guidelines for glucose adjustment were given. In conclusion, the calibration models under combined glucose input types, compared with OGTT, show a great enhancement in the stability, applicability and predictive power. This would finally improve the precision of non-invasive blood glucose sensing.

8580-47, Session PMon

Monte Carlo simulation on the effect of dermal thickness variances on noninvasive blood glucose sensing

Jingying Jiang, Da Zou, Xiaolin Min, Tianjin Univ. (China); Zhenhe Ma, Northeastern Univ. (China); Kexin Xu, Tianjin Univ. (China)

Near-infrared spectroscopy is an ideal measurement method for noninvasive blood glucose sensing. In that measuring process, the light transport path in skin tissue would affect the final near-infrared spectrum greatly. In this talk, the Monte Carlo simulation has been conducted to investigate the effect of dermal thickness variances on blood glucose sensing results. We adopt specific skin models for different measurement sites in the research. Results demonstrate that under certain circumstance, the dermal thickness change exerts a great impact on spectroscopy measurements. Further results prove that the dermal thickness has a key influence on the position of floating reference point and the prediction of blood glucose concentration by using partial least squares(PLS) modeling. It will lay a solid foundation for the further design of an advanced blood glucose detection probe to make the blood glucose sensing results more precise eventually.

8580-48, Session PMon

Wavelet-based recognition of oscillatory EEG-patterns

Alexey I. Nazimov, Alexey N. Pavlov, Alexander E. Hramov, Vadim V. Grubov, Alexey A. Koronovskii, N.G. Chernyshevsky Saratov State Univ. (Russian Federation); Evgenia Sitnikova, Institute of Higher Nervous Activity and Neurophysiology of RAS (Russian Federation)

Automatic recognition of specific oscillatory patterns on EEG represents an important problem in neurophysiology. Complex time-frequency organization of EEG-signals and the existence of many rhythmic components being close enough in the frequency domain lead to a hard procedure of experimental data analysis by human operators. At present, there are many techniques that are able to solve this problem with a required level of accuracy. Among them, wavelet-based methods are related to the most powerful tools.

In order to provide recognition procedure with wavelets, one needs: 1) to select an appropriate basis constructed from a single soliton-like function; 2) to select appropriate scale and translation parameters associated with the most informative wavelet-coefficients.

In this work we propose an optimization algorithm that allowed us to identify and recognize sleep spindles (SS) and spike wave discharges (SWD) using standard wavelet functions (MHAT, Morlet, etc.). The feature of this approach is that optimal parameters of the continuous wavelet-transform are estimated using two functionals and, therefore, this procedure does not depends on the experience of researcher who analyses experimental recordings.

We show that the proposed technique improves the quality of recognition of specific oscillatory patterns on EEG compared with standard recognition procedures used by many authors, e.g., in solving the problem of classification of neuronal activity from extracellular recordings of action potentials. The precision of recognition of specific EEG-patterns with the proposed approach exceeds 90% and can be improved when providing additional modifications of the optimization procedure.

8580-49, Session PMon

On-off intermittency of thalamo-cortical neuronal network oscillations in the electroencephalogram of rodents with genetic predisposition to absence epilepsy

Alexander E. Hramov, Vadim V. Grubov, Alexey N. Pavlov, N.G. Chernyshevsky Saratov State Univ. (Russian Federation); Evgenia Sitnikova, Institute of Higher Nervous Activity and Neurophysiology of RAS (Russian Federation); Alexey A. Koronovskii, N.G. Chernyshevsky Saratov State Univ. (Russian Federation); Anastasija E Runnova, REC ``Nonlinear Dynamics of Complex System", Saratov State Technical University (Russian Federation); Sveltlana A Shurugina, NG Chernyshevsky Saratov State University (Russian Federation); Alexey Ivanov, REC ``Nonlinear Dynamics of Complex System", Saratov State Technical University (Russian Federation)

Spike-wave discharges (SWD) are electroencephalographic hallmarks of absence epilepsy. SWD are known to originate from thalamo-cortical neuronal network that normally produces sleep spindle (SS) oscillations. Although both SS and SWD are considered as thalamo-cortical oscillations, functional relationship between them is still uncertain. The present study describes temporal dynamics of SWD and SS as determined in long-time electroencephalograms (EEG) recorded in WAG/Rij rat model of absence epilepsy.

We have proposed the novel mathematical method based on the continuous wavelet analysis and the empirical mode decomposition (EMD) for the automatic detection of SWD, SS (10-15 Hz) and 5-9 Hz oscillations in EEG. This method is based on the preliminary filtration of the EEG signals by means of the EMD-based method and subsequent wavelet transform and analysis of the wavelet energy in the typical frequency ranges for each oscillatory EEG patterns.

It was found that non-linear dynamics of SWD and SS fits well to the law of 'on-off intermittency'. Intermittency in sleep spindles and SWD implies that (1) temporal dynamics of these oscillations are deterministic in nature, and (2) it might be controlled by a system-level mechanism responsible for circadian modulation of neuronal network activity.

8580-50, Session PMon

An approach for identification of early pathological changes in cerebral blood flow

Alexey N. Pavlov, Oxana V. Semyachkina-Glushkovskaya, Vladislav V. Lychagov, N.G. Chernyshevsky Saratov State Univ. (Russian Federation)

Identification of the key reasons and studying of mechanisms responsible for the development of cerebral-vascular pathologies at newborns is related to the most actual medical problems. Scientific works devoted to vascular pathology of a brain at adults are numerous and extensive. However at children, especially in the neonatal period, works in this area are presented by individual researches.

Studying of vascular pathology of a brain at newborns is very important due to a high prevalence of the cerebral vascular diseases connected with hypoxemia and patrimonial traumas that are inevitably reflected in high growth of number of children with a delay of speech and psychomotor development.

In this work we perform researches aimed at the creation of a computer diagnostic complex for identification of early pathological changes in a brain blood flow. For this purpose we combine optical visualization methods with advanced data processing tools based on the wavelet-transform.

Our experimental study performed in 60 male newborn rats is based on optical coherent tomography (OCT). We consider this approach as one of the most powerful tool for early diagnostics of malfunctions of vegetative and molecular mechanisms of regulation of a brain blood flow. Further analysis of OCT-data is performed with wavelet-based approaches that provide: 1) the possibility to improve the quality of OCT images through advanced filtering technique; 2) the possibility to quantify time-frequency dynamics using a multi-resolution approach.

We study stress-induced distortions of brain vessels accompanied by increase in diameters of cerebral arteries and decrease of blood flow rate.

8580-51, Session PMon

4D display of outflow track of embryonic-chick-heart (HH 14-19) using a high-speed streak mode OCT

Siyu Ma, Rui Wang, Clemson Univ. (United States); Richard L. Goodwin, Univ. of South Carolina School of Medicine (United States); Roger R. Markwald, Thomas K. Borg, Medical Univ. of South Carolina (United States); Raymond B. Runyan, The Univ. of Arizona (United States); Bruce Z. Gao, Clemson Univ. (United States)

Congenital Heart Disease (CHDs) is the most common congenital malformation in newborns in the US. Although knowledge of CHDs is limited, their origin during early heart development has been confirmed, and altered blood flow is highly suspected to be the factor that changes the mechanical conditions and stimulates developmental responses that result in heart morphology remodeling, which ultimately cause CHDs. As a result, a high speed imaging tool is in critical need to capture the fast altering hemodynamic condition and morphology of embryonic heart in vivo to study CHDs. We present a high speed streak mode OCT that works at the center wavelength of 830nm and capable of giving 600?200 pixel size pictures of the outflow track of an embryonic chick heart at the rate of 1000 Hz. The modality gives a voxel resolution less than 10 ?m3 and a penetration depth of 0.97mm. The 2-second-long 4D images of outflow track were obtained every hour from HH 14 to HH17 for the quick morphology change during that period and every other hour from HH17 to HH19 for comparatively slow morphology change. Because of the fast scanning speed, there is no need for post acquisition interpolation such as gating techniques to give a fine 3D structure. In addition, the outflow track shows fluent curve and more details at the edge, which is an improvement from previous work in literature. With this information, further studies on the role of hemodynamic changes in CHDs will be accessible with the aid of particle image velocimetry.

8580-52, Session PMon

Reflectance spectroscopy of optical clearing of skin in vivo

Xiewei Zhong, Jing Wang, Xiang K. Wen, Dan Zhu, Britton Chance Ctr. for Biomedical Photonics (China)

Chemical agents with high refractive index, hyperosmotic, and biocompatibility are introduced into tissue, which will reduce the scattering of tissue, and enhance the penetration of light in tissue. Diffuse reflectance, as a common method, has been applied to assess optical clearing of skin in vivo, but the scattering characteristic during the optical clearing process has not been valuated quantitatively. In this work, a

diffuse reflectance spectroscopy, based on a lookup-table (LUT) based inverse model, is applied to calculate the scattering parameters of skin, such as reduced scattering coefficient at 500 nm, the Rayleigh scattering fraction. Optical clearing agents (OCAs) were topically treated rat skin in vivo, and the diffuse reflectance spectroscopy were measured. And then the reduced scattering coefficient at 500 nm, the Rayleigh scattering fraction can be extracted. The results show that the diffuse reflectance spectrum are decreased obviously, which reduces both the scattering parameters after the application of OCAs. This study provides evident directly for explore the mechanisms of optical clearing of skin in vivo.

8580-53, Session PMon

Scaling of photothermal effects accounting for localization of CW and pulse laser radiation within plasmonic nanoparticles

Alexander N. Yakunin, Yuri A. Avetisyan, Institute of Precision Mechanics and Control (Russian Federation); Valery V. Tuchin, N.G. Chernyshevsky Saratov State Univ. (Russian Federation) and Institute of Precision Mechanics and Control (Russian Federation)

We discuss the methodology of comparative analysis of laser irradiation impact on plasmonic nanoparticles used for inducing of photothermal effects in cells and tissues. To quantify the thermal effects of CW and pulse laser irradiation with various exposures, pulse duration and repetition rate it is proposed to use the newly introduced parameters. These parameters have a quantitative measure and provide the objectivity of heating control. They are: 1) integral time TAU_L of exceeding of a certain temperature level T_L, and 2) integral of specific energy E_L expended in excess of a temperature higher than T_L. It It is shown that the introduced parameters contribute to the generalization of the results of experiments by constructing the phenomenological models. Models, in their turn, provide a scaling of photothermal effects (e.g., cell optoporation) taking into account the localization of the field of laser radiation within plasmonic nanoparticles at arbitrary parameters of the laser pulses.

8580-54, Session PMon

Optical properties of the human finger nail

Alexey N. Bashkatov, Elina A. Genina, Valery V. Tuchin, N.G. Chernyshevsky Saratov State Univ. (Russian Federation)

The optical properties of human nail were measured in vivo in the wavelength range 400-2000 nm. In the wavelength range from 400 to 1000 nm the measurements were carried out using the commercially available fiber-optic spectrometer USB4000-Vis-NIR (Ocean Optics, USA) and the commercially available fiber-optic spectrometer NIRQUEST 256-2.1 (Ocean Optics, USA) have been used for the measurements in the wavelength range 950-2000 nm. All measurements were performed in reflectance mode with using fiber-optical probe QR400-7-Vis/NIR and integrating sphere ISP-80-8-REFL (Ocean Optics, USA). Two layers optical model of the tissue has been developed and the inverse Monte Carlo method was used to determine the absorption and reduced scattering coefficients of the tissue from the measurements.

8580-55, Session PMon

Structural change of adipose tissue at photodynamic treatment: in vivo study using OCT

Irina Y. Yanina, Valery V. Tuchin, N.G. Chernyshevsky Saratov State Univ. (Russian Federation)

Structural changes in the adipose tissue at photodynamic treatment were observed by time variation studied with OCT.

Group of 2-year old female rats of 10 animals kept 14 days in accordance with the European Convention for the Protection of animals used for experimental and other scientific purposes, besides the standard diet received 5 g sugar, 5 g dry milk, 5 g of sunflower oil and 5 g of egg powder in order to cause alimentary obesity. Animals were divided into 2 groups of 5 individuals. Hairs were removed. The action was carried out in area of the ribs on the side of the chest. The brilliant green (BG) and indocyanine green (ICG) in concentration of 0.5 mg / ml was injected on the side of left and right ribs. To the first group of rats injected BG was dissolved in saline (solution 1), while to the second group - injected ICG was dissolved in saline (solution 2). Within rat dye (solution 1 or 2 of the same concentration) was injected first, and then irradiated with a diode source. CW laser diode (ACCULASER, 810 nm; power density, 16-24 W/cm2; exposure time, 0.5 min) and dental diode irradiator Ultra Lume Led 5 (442 and 597 nm; power density, 75 mW/cm2; exposure time, 3 min) were used for irradiation.. Optical fiber tip was directed perpendicular to the tissue surface. Anesthesia of rats was carried out with a solution zoletil. Zoletil was administered intraperitoneally at a dose of 80 mg/kg.

The results indicate adipocytes' membrane destruction and thus a decrease adipose tissue volume induced by photodynamic treatment.

8580-56, Session PMon

Structural change of adipose tissue at photodynamic and photothermal treatment using encapsulated ICG

Irina Y. Yanina, Valery V. Tuchin, N.G. Chernyshevsky Saratov State Univ. (Russian Federation)

Structural changes in the adipose tissue of at photodynamic and photothermal treatment were observed by time variation of refractive index studied with OCT.

The 100-150 ?m fat tissues slices were used in in vitro experiments. A CW diode laser (ACCULASER, 810 nm) was used to irradiate tissue slices at power densities of 250, 375, 500, and 625 mW/cm2. The studies were conducted at physiological temperature (37ºC).

The 2 mg/ml ICG water solutions were encapsulated by a three-step procedure. First, CaCO3 particles filled with ICG were formed by co-precipitation of Na2CO3 and CaCl2 in ICG solution. Then polyelectrolyte shell was formed by layer-by-layer self-assembly method. Biocompatible cationic (chitozan) and anionic (dextran sulfate) polyelectrolytes were deposited from 1 mg/ml solutions in 0.15M NaCl. On the third step CaCO3 cores were dissolved by 2M EDTA water solution.

It was found that relative refractive index of the scatterers decreased with time elapsed after treatment that indicated the immersion optical clearing. These data support the hypothesis that photodynamic and photothermal treatment induces fat cell lipolysis for some period after treatment.

8581-1, Session 1

Photoacoustic intra-operative nodal staging using clinically approved superparamagnetic iron oxide nanoparticles

Diederik J. Grootendorst, Raluca M. Fratila, Martijn Visscher, Bennie Ten Haken, Univ. Twente (Netherlands); Richard J. A. Van Wezel, Radboud Univ. Nijmegen (Netherlands); Wiendelt Steenbergen, Srirang Manohar, Univ. Twente (Netherlands); Theo J. M. Ruers M.D., The Netherlands Cancer Institute (Netherlands)

Detection of tumor metastases in the lymphatic system is essential for accurate staging of various malignancies, however fast, accurate and cost-effective intra-operative evaluation of the nodal status remains difficult to perform with common available medical imaging techniques. In recent years, numerous studies have confirmed the additional value of superparamagnetic iron oxide dispersions (SPIOs) for nodal staging purposes, prompting the clearance of different SPIO dispersions for clinical practice. We evaluate whether a combination of photoacoustic (PA) imaging and a clinically approved SPIO dispersion, could be applied for intra-operative nodal staging. Metastatic adenocarcinoma was inoculated in Copenhagen rats for either 5 or 8 days. After SPIO injection, the lymph nodes were photoacoustically imaged both in vivo and ex vivo whereafter imaging results were correlated with MR and histology. Results were compared to a control group without tumor inoculation.

In the tumor groups clear irregularities, as small as 1 mm, were observed in the PA contrast pattern of the nodes together with an decrease of PA response. These irregularities could be correlated to the absence of contrast in the MR images and could be linked to metastatic deposits seen in the histological slides. The PA and MR images of the control animals did not show these features. We conclude that the combination of photoacoustic imaging with a clinically approved iron oxide nanoparticle dispersion is able to detect lymph node metastases in an animal model. This approach opens up new possibilities for fast intra-operative nodal staging in a clinical setting.

8581-2, Session 1

Real-time opto-acoustic imaging system for clinical assessment of breast lesions

Jason Zalev, Bryan Clingman, Remie Smith, Tom Miller, A. Thomas Stavros, Seno Medical Instruments, Inc. (United States); Sergey A. Ermilov, Dmitri Tsyboulski, Andre Conjusteau, Alexander A. Oraevsky, TomoWave Laboratories, Inc. (United States); Kenneth Kist, N. Carol Dornbluth, The Univ. of Texas Health Science Ctr. at San Antonio (United States); Pamela Otto, The Univ. of Texas Health Science Ctr. at Houston (United States)

We report on findings from the clinical feasibility study of the Imagio™ Breast Imaging System, which acquires two-dimensional opto-acoustic images co-registered with conventional ultrasound using a specialized handheld probe.

Dual-wavelength opto-acoustic technology is used to generate parametric maps based on total hemoglobin and its oxygen saturation in breast tissues. This provides functional diagnostic information pertaining to tumor metabolism and microvasculature, which is complementary to morphological information obtained with conventional grayscale ultrasound.

We examine performance of our technology on well characterized tissue phantoms constructed with specific optical and acoustic properties for breast tissue. We also present co-registered opto-acoustic and ultrasonic images of malignant and benign tumors from a recent clinical study. The clinical results illustrate that the technology has the capability to improve overall accuracy of breast tumor diagnosis. In doing so, it has the potential to reduce biopsies and to characterize cancers that were not seen well with conventional grayscale ultrasound alone.

8581-3, Session 1

Clinical prototype of portable photoacoustic flow cytometer for early diagnosis of multiple diseases

Vladimir P. Zharov, Ekaterina I. Galanzha, Mustafa Sarimollaoglu, Dmitry A. Nedosekin, Mazen A. Juratli M.D., Yulian A. Menyaev, Univ. of Arkansas for Medical Sciences (United States)

The safety of photoacoustic (PA) technologies allows using them in various clinical scenarios. We report the development of clinical prototype of label-free PA flow cytometer (PAFC) for early diagnosis of multiple diseases. Module principle allows us to use high pulse rate lasers (e.g., at 532 nm, 671 nm, 820 nm and 1064 nm) and fiber–based PA tips for the assessment of blood vessels in hands, legs, neck and other locations. Here we focus on a portable prototype using a 1064 nm laser, focused ultrasound transducers, and positive and negative PA contrast modes, and its preclinical testing for controlling of melanoma recurrence, and cardio-vascular disorders associated with clotting and red blood cell aggregation. In particular, approximately 90% of melanoma deaths are related to metastasis spreading by circulating tumor cells (CTCs). Due to small blood volume samples (a few mL), the sensitivity of existing CTC assays is limited, so incurable metastasis is already established at the time of initial diagnosis. This problem was overcome by using in vivo PAFC allowing the assessment of large blood volume in vivo, potentially the patient's entire blood volume (in adults ?5 L). If oncoming pilot clinical trials using the portable PAFC are successful, this technology can provide breakthroughs for the early detection of CTCs when metastasis has not yet developed and, hence well-timed therapy including phototherapy is more effective. We present also application of described prototype for in vivo dynamic monitoring of white, red and mixed clots and red blood cell aggregates.

8581-4, Session 1

Photoacoustic tomography through an intact adult human skull

Liming Nie, Xin Cai, Chao Huang, Alejandro Garcia-Uribe, Mark A. Anastasio, Lihong V. Wang, Washington Univ. in St. Louis (United States)

Photoacoustic tomography (PAT) of the human brain is very challenging since light is strongly scattered and decays and ultrasound signals are heavily attenuated by the skull (4-11 mm thickness). In this article, we first demonstrate the feasibility of PAT through the adult skull intact. A pulsed laser at 1064 nm irradiated the top or temporal area, and a transducer circularly scanned the skull to collect data at 200 positions. Initially, the target was moved inside the empty skull to subtract interference photoacoustic signals from the skull. Then phantoms and bovine blood enclosed by the human skull were imaged. Due to the skull thickness differences between the top and temporal area, higher imaging contrast could be gained by irradiating through the temporal area rather than through the top of skull. The cerebral cortex of a dog brain inside the human skull was clearly mapped. Our experimental results indicate that light can penetrate the thick human skull and that the produced ultrasound is sufficiently detectable. Thus, PAT can potentially be applied to human brain imaging.

8581-5, Session 1

Image reconstruction in photoacoustic tomography with heterogeneous media using an iterative method

Chao Huang, Kun Wang, Liming Nie, Lihong V. Wang, Mark A. Anastasio, Washington Univ. in St. Louis (United States)

There remains an urgent need to develop effective photoacoustic computed tomography (PACT) image reconstruction methods for use with acoustically inhomogeneous media. Transcranial PACT brain imaging is an important example of an emerging imaging application that would benefit greatly from this. Existing approaches to PACT image reconstruction in acoustically heterogeneous media are limited to weakly varying media, are computationally burdensome, and/or make impractical assumptions regarding the measurement geometry. In this work, we develop and investigate a full-wave approach to iterative image reconstruction in PACT for media possessing inhomogeneous speed-of-sound and mass density distributions and acoustic attenuation described by a frequency power law. A key contribution of the work is the formulation of a procedure to implement a matched discrete forward and backprojection operator pair, which facilitates the application of a wide range of modern iterative image reconstruction algorithms. This presents the opportunity to employ application-specific regularization methods to mitigate image artifacts due to measurement data incompleteness and noise, finite-sampling effects, and modeling errors. The forward and backprojection operators are based on the k-space pseudospectral method for computing numerical solutions to the PA wave equation in the time-domain. The developed operator pair was employed with a modern iterative image reconstruction algorithm that employed total variation regularization and was investigated in both computer-simulation and experimental studies. Our results establish that the proposed image reconstruction method can effectively compensate for acoustic aberration and attenuation, and reduces artifacts in the reconstructed image.

8581-6, Session 1

Noninvasive optoacoustic monitoring of cerebral venous blood oxygenation in rats with blast-induced traumatic brain injury

Karon E. Wynne, Douglas S. DeWitt, Yuriy Y. Petrov, Irene Y. H. Petrova, Andrey Petrov, Margaret A. Parsley, Rinat O. Esenaliev, Donald S. Prough, The Univ. of Texas Medical Branch (United States)

Blast-induced neurotrauma (BINT) is a major cause of combat-related death. Clinical data demonstrate that monitoring of cerebral venous blood oxygenation is useful to facilitate the management of patient with traumatic brain injury. The current method for monitoring cerebral venous blood oxygenation is invasive, while near-infrared spectroscopy (NIRS), the only noninvasive method for monitoring blood oxygenation, cannot measure cerebral venous blood oxygenation due to poor spatial resolution. In contrast, the higher resolution of the optoacoustic technique permits spatial localization of specific blood vessels, including the superior sagittal sinus (SSS), a large central cerebral vein, as we have demonstrated in large animals and humans. The present work demonstrates optoacoustic monitoring of SSS oxygenation in a rodent model of BINT. Mild, moderate or severe BINT was induced in anesthetized rats using a blast device driven by blank nail gun cartridges. SSS oxygenation was measured through an intact scalp and skull, using a multi-wavelength near-infrared optoacoustic system with a custom-made wide-band optoacoustic probe. Physiologic variables (arterial blood pressure, heart rate, temperature, etc.) were recorded simultaneously before and after the blasts. The system provided continuous, real-time SSS oxygenation measurements. The data demonstrated that optoacoustics can be used for monitoring cerebral venous blood oxygenation in a wide range (from 40% to 100%) in a rodent model of blast injury.

8581-7, Session 1

Noninvasive optoacoustic monitoring of cerebral venous blood oxygenation in patients with traumatic brain injury

Yuriy Y. Petrov, Donald S. Prough, The Univ. of Texas Medical Branch (United States); Claudia S. Robertson, Baylor College of Medicine (United States); Irene Y. H. Petrov, The Univ. of Texas Medical Branch (United States); Luciano L. Ponce Mejia, Santosh Sadasivan, Baylor College of Medicine (United States); Andrey Petrov, Rinat O. Esenaliev, The Univ. of Texas Medical Branch (United States)

Traumatic brain injury (TBI) is a major cause of combat-related death. Moreover, 150,000 civilian patients per year suffer moderate or severe TBI in the USA alone. Proper management of patients with severe TBI is facilitated by monitoring of cerebral venous oxygenation (CVO) because even one episode of CVO < 50% is associated with increased mortality. Invasive measurement of jugular bulb oxygenation is the “gold-standard” technique. However, this approach requires frequent recalibration and may result in complications. We proposed to use optoacoustic technique for noninvasive CVO monitoring by probing cerebral veins such as the superior sagittal sinus (SSS). Recently, we validated it in animal studies and built medical grade optoacoustic systems for CVO monitoring in patients with TBI. In this work, we performed the first tests of one of the systems in patients with TBI, in whom jugular venous bulb catheters had been inserted as a part of routine care. Optoacoustic signals were recorded continuously from the SSS and used for real-time processing and display of the SSS oxygenation. Simultaneously, invasive jugular bulb oxygenation was measured. Noninvasive optoacoustic measurements and jugular bulb oxygenation correlated highly. These data suggest that optoacoustics is a promising technology for noninvasive CVO monitoring. Ongoing studies will further validate the system performance in patients with severe TBI.

8581-8, Session 1

Real-time photoacoustic imaging system for clinical burn diagnosis

Taiichiro Ida, Yasushi Kawaguchi, Advantest Corp. (Japan); Satoko Kawauchi, Daizoh Saitoh, Shunichi Sato, National Defense Medical College (Japan); Toshiaki Iwai, Tokyo Univ. of Agriculture and Technology (Japan)

Burn depth assessment is crucial for the appropriate treatment plan to save severe burn patients, but the quantitative method of burn depth is not available. We previously showed the validity of photoaoustic (PA) diagnosis of burns in rats, where the PA signal originating from blood in the noninjured tissue layer located under the injured tissue layer with vascular occlusion was detected1. However, the measurement system was not practical because it was based on a single-element transducer. In this study, we have developed the real-time PA imaging system with the 10-mm-long linear-array transducer. The 532-nm Q-switched Nd:YAG laser is used as a light source, and it can be replaced with the custom fiber laser. The laser fluence used in the experiment is lower than the ANSI safety limit. PA tomograms can be obtained at 8~30 fps. The phantom study showed that a light absorber in the tissue-mimicking scattering medium can precisely be detected up to 5 mm in depth. The diagnostic experiments were conducted for three rat burn models: superficial dermal burn, deep dermal burn, and deep burn. The PA tomograms were compared with the results of histological analysis of the tissues biopsied after the imaging, showing good agreement between the zones of stasis indicated by PA imaging and histological injury. These results indicate the potential usefulness of the present system in clinical burn diagnosis. PA imaging of healthy volunteer human skin will also be presented.

1. S. Sato et al., J. Trauma 59, 1450 (2005).

8581-9, Session 2

Three-dimensional intravascular imaging of plaques by a vibrational photoacoustic endoscope in probe-scanning manner

Pu Wang, Purdue Univ. (United States); Wei Wei, Univ. of California, Irvine (United States); Michael Sturek, Indiana Univ.-Purdue Univ. Indianapolis (United States); Zhongping Chen, Univ. of California, Irvine (United States); Ji-Xin Cheng, Purdue Univ. (United States)

Photoacoustic imaging using the intrinsic contrast from harmonic vibration of C-H bonds allows selective mapping of lipids and connective tissues inside the artery wall. Towards the goal of diagnosing atherosclerosis in clinical setting, we herein demonstrate a miniaturized photoacoustic endoscope for intravascular lipid visualization. In our study, 1730 nm excitation was used to excite the first overtone vibration of C-H bonds. Iliac arteries from a high-fat-diet-fed Osabaw big served as sample with atherosclerotic lesion. A parallel aligned ultrasound transducer and optical fiber head was applied for side viewing excitation delivery and ultrasound detection. By scanning the probe with a combination of rotary and linear stages, three dimensional imaging of atherosclerotic plaques was performed. Our study pushes the development of photoacoustic endoscopy towards the clinical diagnosis of atherosclerosis.

8581-10, Session 2

Differentiating lipid types using intravascular photoacoustic spectroscopy

Krista Jansen, Antonius F. W. van der Steen, Erasmus MC (Netherlands) and Interuniversity Cardiology Institute (Netherlands); Geert Springeling, Min Wu, Adrie J. M. Verhoeven, Monique T. Mulder, Erasmus MC (Netherlands); Xiang Li, Qifa Zhou, K. Kirk Shung, The Univ. of Southern California (United States); Dominique P. V. de Kleijn, Univ. Medical Ctr. Utrecht (Netherlands); Gijs van Soest, Erasmus MC (Netherlands)

The rupture of a coronary atherosclerotic plaque and subsequent thrombogenesis is the main cause of acute coronary events. Plaque composition is an important determinant for its vulnerability – its susceptibility to rupture. Plaque progression is characterized by the accumulation of lipid varieties that are virtually absent in a healthy vessel wall. Of these, cholesterol, cholesterol oleate and cholesterol linoleate are most abundantly present (Stegemann, et al., 2011 Circ Cardiovasc Genet). It has been previously shown that intravascular photoacoustics (IVPA) can identify lipids in human atherosclerotic lesions, ex vivo (Jansen et al., 2011 OL). To show that IVPA can distinguish between lipid types, we performed spectroscopic IVPA imaging of lipids in human coronary atherosclerotic plaque ex vivo, peri-adventitial tissue and atherectomy material – atherosclerotic plaque removed from the carotid artery. In addition, we determined IVPA reference spectra of cholesterol, cholesterol oleate and cholesterol linoleate. We measured in the 1200 nm wavelength region, where the lipid absorption spectra show distinct peaks due to the second harmonic overtones of the C-H bond vibrations. The C-H configurations differ per lipid, which results in detectable variations in peak wavelengths and intensities between the spectra of the different lipids. After imaging, the peri-adventitial tissue and atherectomy material were analyzed chemically and by mass spectrometry to determine relative quantities of the different lipid constituents. Finally, we compared the IVPA spectra of the human material to those of the three separate lipids, as well as relevant lipid absorption spectra found in literature (Tsai et al., 2001 J Med Biol Eng).

8581-11, Session 2

Optical-resolution photoacoustic micro-endoscopy with ultrasound array system detection

Tyler Harrison, Parsin HajiReza, Roger J. Zemp, Univ. of Alberta (Canada)

Recently we demonstrated the feasibility of Optical-Resolution Photoacoustic Micro-Endoscopy (OR-PAME) using an image guide fiber. However, the use of an ultrasound transducer for signal collection limited useful applications. We demonstrate detection of OR-PAM signals using an external array transducer in order to make endoscopic imaging practical for clinical use for the first time. The array system is able to visualize the placement of the image-guide fiber using pulse-echo ultrasound then switch to an OR-PAME acquisition mode.

Photoacoustic signals are captured by a Verasonics ultrasound system using an L7-4 linear array transducer. A high-repetition-rate 532-nm fiber laser was used as the excitation source. This light was focused and raster-scanned into a 800?m-diameter image-guide fiber bundle consisting of 30,000 individual fiber elements. The operator finds the end of the endoscope using a flash ultrasound imaging mode, then captures endoscopic data by clicking a button. This activates the motion of scanning mirrors into the end of the image guide, and engages an endoscopic capture sequence. Endoscopic data are used to form a maximum amplitude image by simply taking the maximum of the absolute value of the signal across the 64 center channel lines used for capture. Using this technique, we have captured images of carbon fibers with a resolution of 6 microns at an SNR of greater than

30dB. Electronic focusing is expected to improve the SNR. The use of an ultrasound array transducer for both endoscope guidance and data collection allows for a much smaller endoscope footprint while opening up clinical possibilities.

8581-12, Session 2

Photoacoustic endoscopy of rat colorectal tumor in vivo

Chiye Li, Joon-Mo Yang, Washington Univ. in St. Louis (United States); Yu Zhang, Younan Xia, Georgia Institute of Technology (United States); Lihong V. Wang, Washington Univ. in St. Louis (United States)

Because of its strong spectroscopic and angiographic imaging ability, photoacoustic endoscopy could be a powerful tool for studying tumor development. Although many in vivo photoacoustic imaging studies based on tumors in rat models have been reported, to our knowledge, none of them were implemented in the endoscopic form and mostly made on the basis of xenografts. Here we report the first photoacoustic endoscopic imaging study of rat colorectal and melanoma tumor growth in vivo. By injecting the tumor cells (DHD/K12/TRb rat colonic carcinoma cell line and B16 melanoma cell line), we induced the formation of two different types of tumors (rat colorectal and melanoma tumors) in situ at the rectal walls of athymic nude mutant rats (Hsd:RH-Foxn1rnu/Foxn1+). Importantly, homograft implantations were performed for our rat tumor models. After the formation of the tumor, we monitored its development weekly over 3-5 weeks by recording dual-wavelength image data with a photoacoustic endoscopic probe. Each imaging session required a scanning time of ~3 minutes, and volumetric data were recorded for each wavelength, covering ~3 cm length and ~12 mm image diameter. Morphologic evolution of blood vessels was investigated near the tumor regions at each stage, and oxygen saturation of hemoglobin was also evaluated based on the dual-wavelength information. We observed obvious difference in vasculature development between the two tumor models. The presentation describes the detailed experimental method for tumor induction and the endoscopic imaging procedure, and shows the imaging results. Our study could lead to a useful methodology for studying tumor development in small animals.

8581-13, Session 2

Integrated intravascular catheter for high-resolution ultrasound and photoacoustic imaging

Andrei B. Karpiouk, Douglas E. Yeager, The Univ. of Texas at Austin (United States); James H. Amirian M.D., Richard W. Smalling M.D., The Univ. of Texas Health Science Ctr. at Houston (United States); Stanislav Y. Emelianov, The Univ. of Texas at Austin (United States)

Thin cap fibroatheroma (TCFA) – a type of atherosclerotic plaque prone to rupture and to induce acute coronary events. To identify TCFA, an imaging tool capable of resolving a thin fibrous cap (<65 ?m in thickness), large necrotic core, and increased macrophage infiltration is required. Previously, the intravascular photoacoustic (IVPA) imaging guided by intravascular ultrasound (IVUS) imaging was introduced as a means of visualizing both arterial morphology (IVUS) and composition (IVPA). The recently developed integrated IVUS/IVPA imaging catheter has been successfully demonstrated for the detection of lipid within arterial plaques in both ex vivo and in vivo studies. However, the thickness of the overlying fibrous cap could not be estimated reliably due to relatively low center frequency of ultrasound transducer. In the current work, we present and discuss a high-resolution integrated IVUS/IVPA imaging catheter based on 60-MHz single-element ultrasound transducer and custom-built light delivery system capable of high-resolution imaging of both morphology and composition of atherosclerotic plaques. The catheter was tested ex vivo using excised atherosclerotic and healthy arteries. Advantages and further optimization of the integrated IVUS/IVPA imaging catheter are discussed.

8581-14, Session 2

Photoacoustic imaging of the human carotid artery: simulations, phantom studies, and practical considerations

Pieter Kruizinga, Frits Mastik, Erasmus MC (Netherlands); Nico de Jong, Erasmus MC (Netherlands) and Interuniversity Cardiology Institute (Netherlands) and Delft Univ. of Technology (Netherlands); Antonius F. W. van der Steen, Erasmus MC (Netherlands) and Interuniversity Cardiology Institute (Netherlands); Gijs van Soest, Erasmus MC (Netherlands)

The human carotid artery is one of the main arteries of interest to cardiovascular research. The biological constituents that make up the artery wall are important parameters for the clinical evaluation of the carotid artery. Classification of an arterial plaque to be either safe or unsafe depends heavily on the tissue types involved. It was shown that photoacoustic imaging can be used to image the relevant biological chromophores that relate to tissue types involved in plaque formation [1,2]. However, the experiments reported in [1,2] were performed in an intravascular setting, where light delivery and ultrasound detection were in close proximity to the tissue of interest. This scenario does not apply to the case of non-invasive photoacoustic imaging of the carotid artery. The location of the organ (>1 cm underneath the skin) and the abundant presence of blood (a strong optical absorbing tissue type) will seriously affect the imaging capabilities. In this study we evaluate the possibility of imaging the human carotid artery wall by means of photoacoustic imaging. We discuss the optical illumination (wavelength, pulse duration and energies), associated ultrasound detection (desired frequency, bandwidth, size, position and number of elements) and properties of the relevant biological chromophores. These considerations are supported by simulations based on clinical CT, MRI and ultrasound datasets and associated phantom measurements. Based on our findings we define the optimal parameters and practical conditions for successful photoacoustic imaging of the human carotid artery.

References:

[1] Sethuraman S, Amirian JH, Litovsky SH, Smalling RW, and Emelianov SY. Spectroscopic intravascular photoacoustic imaging to differentiate atherosclerotic plaques. Optics Express,16:5, 3362-3367. 2008.

[2] Jansen K, Van der Steen AFW, Van Beusekom HMM, Oosterhuis JW, Van Soest G.Intravascular photoacoustic imaging of human coronary atherosclerosis. Optics Letters. 36:5, 597:599. 2011.

8581-15, Session 3

A brain tumor molecular imaging strategy using a new triple-modality MRI-photoacoustic-Raman nanoparticle

Adam de la Zerda, Stanford Univ. (United States); Moritz F. Kircher, Memorial Sloan-Kettering Cancer Ctr. (United States); Jesse V. Jokerst, Stanford Univ. (United States); Cristina L. Zavaleta, Stanford Univ. School of Medicine (United States); Paul J. Kempen, Erik Mittra, Stanford Univ. (United States); Ken Pitter, Ruimin Huang, Carl Campos, Memorial Sloan-Kettering Cancer Ctr. (United States); Frezghi Habte, Robert Sinclair, Stanford Univ. (United States); Cameron W. Brennan, Ingo K. Mellinghoff, Eric C. Holland, Memorial Sloan-Kettering Cancer Ctr. (United States); Sanjiv S. Gambhir, Stanford Univ. (United States)

The difficulty in delineating brain tumor margins is a major obstacle towards better outcomes for patients with brain tumors. Current imaging methods are limited by inadequate sensitivity, specificity and spatial resolution. Here we show that a unique triple-modality magnetic resonance imaging–photoacoustic imaging–Raman imaging nanoparticle (termed MPR) can accurately delineate the margins of brain tumors in living mice both preoperatively and intraoperatively. The MPR nanoparticle is a 60nm gold core surrounded by a Raman-active layer and a 30nm silica coating that is conjugated to DOTA-Gd. The MPRs exhibit a high relaxivity coefficient r1=3x10^6/mM/s, a strong absorbance peak at 540nm of 2.5x10^10/cm/M and a unique Raman signature. We measured the lowest detectable concentration in vitro to be 4.88pM for MRI, 1.22pM for photoacoustic and 610fM for Raman imaging. MPRs were then injected subcutaneously to living mice at concentrations of 50-1100pM. The sensitivity limit for both MRI and photoacoustic imaging was 50pM. Raman imaging clearly visualized the 50pM concentration with SNR=500, suggesting a sensitivity limit much lower than 50pM. Intravenous injection of MPRs into orthotopic glioblastoma-bearing mice led to MPR accumulation and retention by the tumor in less than 1h post-injection. No MPR accumulation was observed in the healthy tissue allowing for a noninvasive tumor delineation using all three modalities through the intact skull. We also used Raman imaging for intraoperative tumor resection, and confirmed its ability to accurately delineate the tumor margins through histological analysis. This new triple-modality–nanoparticle has promise for enabling more accurate brain tumor imaging and resection.

8581-16, Session 3

Photoacoustic tomography to identify angiogenesis for diagnosis and treatment monitoring of inflammatory arthritis

Xueding Wang, Univ. of Michigan Health System (United States); Justin R. Rajian, Univ. of Michigan Medical School (United States); Gandikota Girish, Univ. of Michigan Health System (United States); David L. Chamberland, Univ. of Michigan (United States)

Identifying neovascularity, i.e. angiogenesis, as a feature of inflammatory arthritis, can help in early accurate diagnosis and treatment monitoring of this disease. Photoacoustic tomography (PAT), as a hybrid imaging modality, relies on intrinsic differences in the optical absorption

among the tissues being imaged. Since blood has highly absorbing chromophores including both oxygenated and deoxygenated hemoglobin, PAT holds potential in identifying early angiogenesis associated with inflammatory joint diseases. In this study, we used PAT to identify the changes in the development of inflammatory arthritis, through the study on a well-established adjuvant-induced arthritis (AIA) rat model. Imaging at two different wavelengths, 1064 nm and 532 nm, revealed that there was a significant signal enhancement in the ankle joints of the arthritis affected rats when compared to the normal control group. Histological analysis of both the normal and the arthritic rats correlated well with the imaging findings. In another experiment, the images from AIA rats that had been treated with anti-rheumatic drug for 15 days were compared with those from non-treated AIA rats. Relative decreasing in photoacoustic signal intensity was observed as a result of the treatment, which was also confirmed by the measurements of the clinical score (measurement of joint size) and the imaging findings from positron emission tomography that was conducted on the same animals. The results from this study suggest that the emerging PAT technology could become a new tool for clinical management of inflammatory joint diseases.

8581-17, Session 3

Nanosensor aided photoacoustic measurement of pH in vivo

Aniruddha Ray, Hyung Ki Yoon, Univ. of Michigan (United States); Xueding Wang, Univ. of Michigan Health System (United States); Raoul Kopelman, Univ. of Michigan (United States)

pH plays a critical role in many aspects of cell and tissues physiology. A decrease in tissue pH in vivo reflects the body's stress conditions such as inflammation, interruption of normal blood supply, biochemical shock etc. Lower pH is also a typical characteristic of arthritic joints and tumor tissues. These pH anomalies are also exploited in different drug delivery mechanisms.

Here we demonstrate, for the first time, nanosensors aided pH sensing in vivo using spectroscopic photoacoustic measurements. The nanosensors consist of Seminaphtharhodafluor (SNARF-5), a pH sensitive dye, encapsulated in a specially designed polyacrylamide hydrogel matrix with a hydrophobic core. The photoacoustic intensity ratio between the excitation wavelengths of 585nm and 565nm increases in the pH range from 6.0 to 8.0 and is used to determine the pH of the local environment. These nanosensors are biodegradable, biocompatible, have a long plasma lifetime and can be targeted to any type of cells or tissues by surface modification using proper targeting moieties. The encapsulation of the dye prevents the interaction of the dye with proteins in plasma and also reduces the dye degradation. The SNARF-5 dye in its free form loses 90% of its absorbance in presence of albumin, a protein found in abundance in plasma, and this has severely limited its adaptation to in vivo environments. In comparison, the SNARF-5 nanosensors lose only 16% of their absorbance in the same environment. We employ these nanosensors to demonstrate the feasibility of pH sensing in vivo through photoacoustic measurements on a rat joint model.

8581-18, Session 3

High resolution photoacoustic imaging of microvasculature in normal and cancerous bladders

Zhixing Xie, William W. Roberts, Paul L. Carson, Univ. of Michigan Medical School (United States); Xiaojun Liu, Chao Tao, Nanjing Univ. (China); Xueding Wang, Univ. of Michigan Medical School (United States)

We explored the potential of an emerging laser-based technology, photoacoustic imaging (PAI), for bladder cancer diagnosis through high resolution imaging of microvasculature in the interior bladder tissues. Images of ex vivo canine bladders demonstrated the excellent ability of PAI to map three-dimensional microvasculature in optically scattering bladder tissues. By comparing the results from human bladder specimens affected by cancer to those from the normal control, the feasibility of PAI in differentiating malignant from benign bladder tissues was explored. The reported distinctive morphometric characteristics of tumor microvasculature can be seen in the images from cancer samples, suggesting that PAI may allow in vivo assessment of neoangiogenesis that is closely associated with bladder cancer generation and progression. By presenting subsurface morphological and physiological information in bladder tissues, PAI, when performed in a similar way to that in conventional endoscopy, provides an opportunity for improved diagnosis, staging and treatment guidance of bladder cancer.

8581-19, Session 3

Anatomical and molecular small-animal whole-body imaging using ring-shaped confocal photoacoustic computed tomography

Jun Xia, Muhammad R. Chatni, Konstantin I. Maslov, Lihong V. Wang, Washington Univ. in St. Louis (United States)

In preclinical and clinical cancer staging and treatment planning, simultaneous imaging of both anatomical structures and molecular contrasts, such as glucose metabolism, plays an important role. Currently, it can be done only by dual modalities such as PET-MRI and PET-CT, which not only cost dearly but also render low-resolution molecular images. Even with image co-registration, the spatial resolution of the metabolic imaging modality is not improved. Additionally, due to ionizing radiation, longitudinal monitoring of the same subject is usually not feasible. We introduce ring-shaped confocal photoacoustic computed tomography (RC-PACT), the first imaging method that provides simultaneous anatomical and metabolic contrast in a single modality. Utilizing the novel design of confocal full-ring light delivery and ultrasound transducer array detection, RC-PACT provides full-view cross-sectional imaging with high spatial resolution. Scanning along the orthogonal direction provides 3D imaging. While the anatomy was imaged with the endogenous hemoglobin contrast, the glucose metabolism was imaged with IRDye800-2DG, a near-infrared dye-labeled 2-deoxyglucose. Through mouse tumor models, we demonstrate that RC-PACT may be a paradigm shifting imaging method for preclinical research.

8581-20, Session 3

Three-dimensional single-shot optoacoustic visualization of excised mouse organs with model-based reconstruction

Xosé Luis Deán-Ben, Andreas Buehler, Vasilis Ntziachristos, Daniel Razansky, Helmholtz Zentrum München GmbH (Germany)

Optoacoustic imaging offers the unique capability of simultaneous excitation of a three-dimensional (volumetric) region with a single interrogating laser pulse. In this way, three-dimensional imaging with single-shot illumination is theoretically achievable, which in principle allows the visualization of dynamic events at a high frame rate mainly limited by the pulse repetition rate of the laser. Simultaneous acquisition of optoacoustic signals at a set of points surrounding the imaging sample is however required for this purpose, which is hampered by several technical limitations related to lack of appropriate ultrasound detection technology, digital sampling and processing capacities. Also, a convenient reconstruction algorithm must be selected to accurately image the distribution of the optical absorption from the acquired signals. Specifically, the resolution and quantitativeness of the images depend on the reconstruction procedure employed. Herein we describe an accurate three-dimensional model-based optoacoustic reconstruction

algorithm based on a convenient discretization of the analytical solution of the forward model. Subsequent algebraic inversion is done with the lsqr algorithm. The performance of the algorithm is showcased by reconstructing images of excised mouse organs with a custom made three-dimensional optoacoustic imaging system. In this system, 256 optoacoustic signals corresponding to single-shot excitation are simultaneously collected with an array of ultrasonic transducers disposed on a spherical surface, which allows three-dimensional imaging at a frame rate of 10 Hz.

8581-21, Session 4

A photoacoustic tomography and ultrasound combined system for proximal interphalangeal joint imaging

Guan Xu, Justin R. Rajian, Gandikota Girish, Xueding Wang, Univ. of Michigan Medical School (United States)

A dual modal system for proximal interphalangeal joint imaging combining photoacoustic tomography and ultrasound is introduced. The system integrates a tunable optical parametric oscillator laser pumped by the second harmonic output of an Nd:YAG pulsed laser as the illumination source. The 80mJ per pulse output of the laser system is tuned to 740nm and coupled to a fiber bundle consisting of 18 fiber optics for bilateral illumination of the examined finger joint. Due to the coupling efficiency and beam spreading, the power density delivered to the finger surface is approximately 4 mJ per pulse per square centimeter, which is significantly lower than the ANSI safety limit. A standard ultrasound system with an 8mm linear ultrasound transducer array including 128 10MHz-bandwidth elements captures the photoacoustic signals and ultrasound control images at the middle plane of the bilateral illumination. Preliminary in vivo evaluation of the system with a volunteer pool of 5 healthy finger joints revealed that the system can recover both the structural and functional information with decent resolution. Confirmed by the control ultrasound images, the system for the first time identified the functional contrast between the tendon and muscle tissue with photoacoustic tomography. The merits of utilizing the standardized ultrasound system thereby include the miniaturized transducer array and rapid data acquisition hardware, as well as a better understanding of the substructures in photoacoustic tomography when images from both modalities are co-registered. The system will be implemented to clinical scenarios for the diagnosis of inflammatory arthritis and the exploration of novel biomarkers to the disease.

8581-22, Session 4

3D laser optoacoustic ultrasonic imaging system

Sergey A. Ermilov, André Conjusteau, Travis Hernandez, TomoWave Laboratories, Inc. (United States); Richard Su, TomoWave Laboratories, Inc. (United States) and Univ. of Houston (United States); Vyacheslav V. Nadvoretskiy, Dmitri Tsyboulski, TomoWave Laboratories, Inc. (United States); Fatima Anis, Mark A. Anastasio, Washington Univ. in St. Louis (United States); Alexander A. Oraevsky, TomoWave Laboratories, Inc. (United States) and Univ. of Houston (United States)

In this presentation, we introduce a novel three-dimensional imaging system that combines optoacoustic tomography and laser ultrasound to obtain coregistered maps of tissue optical absorption and speed of sound (SoS). Volumetric SoS images provide valuable anatomical information on tissue structures. Simultaneously, the measured SoS data allows more accurate optoacoustic reconstruction of heterogeneous biological objects. The optoacoustic module includes an arc-shaped array of 128 ultrasonic transducers rotated 360 degrees with respect to the visualized volume allowing the full-view tomographic reconstruction. A Q-switched laser system is used to establish appropriate optoacoustic illumination pattern with two fixed (532 nm and 1064 nm) and one tunable (730-850 nm) output wavelengths, each operated at 10 Hz pulse repetition rate. A 532 nm wavelength, being mostly absorbed within a narrow superficial layer of skin, is used to outline the visualized biological object. The wavelengths of 757 nm, 800 nm, and 1064 nm are used to produce volumetric maps of total hemoglobin, blood oxygenation, and water content. Broadband wide-directivity laser ultrasound emitters are arranged in a spiral pattern and are positioned opposite to the array of transducers. This imaging geometry allows reconstruction of images that depict the 3D SoS distribution from the measured time of flight data. The reconstructed SoS map can subsequently be employed by an optoacoustic reconstruction algorithm to compensate for acoustic wavefield aberration and thereby improve the accuracy of the reconstructed optical absorption distribution. Two prototypes of the system are being developed for preclinical imaging research in small animal models and for clinical diagnostic imaging of breast cancer.

8581-23, Session 4

Accurate photoacoustic tomography using acoustic velocity maps in reconstruction

Srirang Manohar, Jithin Jose, Rene G. H. Willemink, Cornelis H. Slump, Univ. Twente (Netherlands); Ton G. Van Leeuwen, Univ. Twente (Netherlands) and Academisch Medisch Ctr. (Netherlands); Wiendelt Steenbergen, Univ. Twente (Netherlands)

Most photoacoustic (PA) studies and reconstruction algorithms are based on the assumption of tissue homogeneity which justifies the use of a single SOS value for the region of interest. Tissue has spatially heterogeneous SOS and cannot be accurately reconstructed under this assumption. We present experimental and image reconstruction methods that allow both PA and SOS distributions to be imaged.

For measurements we use the recently introduced PER-PACT approach, where speed-of-sound (SOS) inhomogeneities are simultaneously measured with photoacoustics. Further, we use an iterative reconstruction algorithm for retrieving SOS images, using the Eikonal equation to model refractive effects in the forward projection. We also introduce a novel iterative PA reconstruction algorithm utilizing SOS information, which accounts for ray-refraction also using the Eikonal equation. This approach is successful in obtaining artifact-free highly accurate PA tomograms. Both algorithms use a high accuracy fast marching method (HAFMM) for computation of TOF values at each pixel in the reconstruction grid.

The results show that our approach of using the hybrid measurement method and the new reconstruction algorithms, is successful in substantially improving the quality of PA images with a minimization of blurring and artefacts.

8581-24, Session 4

Dual-modality section imaging system with optical ultrasound detection for photoacoustic and ultrasound imaging

Robert Nuster, Gerhild Wurzinger, Sibylle Gratt, Günther Paltauf, Karl-Franzens-Univ. Graz (Austria)

Sectional imaging can be used as a less time consuming alternative compared to full 3D photoacoustic imaging. Recently, we have shown that an optical interferometer combined with a cylindrical acoustic reflector can be used for 2D photoacoustic slice imaging. Differently to “point-like” detectors the focused laser beam of the interferometer is regarded as an integrating line detector. Consequently, image reconstruction from the recorded signals requires the application of the inverse Radon transform.

In this work, we propose the further development of the optical detection setup towards dual-modality section imaging that combines photoacoustic (PA) and ultrasound (US) imaging. Both imaging modalities

use optical generation and detection of ultrasound waves. A one-sided chrome coated concave cylindrical optical lens is used as target to induce acoustic signals for US imaging and as acoustic mirror that forms acoustic images. By probing the temporal evolution of the acoustic images with an optical beam perpendicular to the acoustic axis and simultaneously rotating the object, data for reconstruction of a PA and a US slice image are acquired. All acoustic signals are excited optically via the thermoelastic effect using laser pulses coming from the same laser system. No image registration is required to overlay PA and US section images due to the simultaneous measurement of the signals with the same detector. The resolution and sensitivity of the detection system is investigated by simulations and experiments on phantom samples.

8581-25, Session 4

Simultaneous photoacoustic and optically mediated ultrasound microscopy: phantom study

Pavel V. Subochev, Alexey R. Katichev, Andrey N. Morozov, Anna G. Orlova, Vladislav A. Kamensky, Ilya V. Turchin, Institute of Applied Physics (Russian Federation)

In our paper, we implemented an original system combining US and PA microscopy techniques different from the known systems since the excitation of ultrasonic pulses is provided by the metalized surface of a spherically focused ultrasound transducer (outer electrode of a PVDF film) due to its absorption of pulsed laser radiation backscattered by the tissue investigated. Use of the same spherical surface for both generation and reception of US pulses provides the improved spatial resolution, since the original radiation pattern of the receiver becomes “squared.” Also, our system does not require additional bulky elements intended for the excitation of probing ultrasound pulses.

The PA part of the developed experimental setup is our fiber-optic counterpart of the acoustic-resolution PA microscope [H. F. Zhang, K. Maslov, G. Stoica, L. V. Wang, Nature Biotech. 24, 848 (2006)] based on conical lenses. The use of a fiber-optic illumination system makes it easy to optimize the spatial illumination field for transducers with different geometries and reception frequencies, which can be based on the results of numerical simulations.

The results of two-dimensional imaging of the agar phantom and post mortem rat head using PA and US methods will be presented.

8581-26, Session 4

Development of a hybrid fluorescence-photoacoustic imaging platform for in vivo diagnosis and interventional guidance in breast cancer

Jiachuan Bu, Ontario Cancer Institute (Canada); Azusa Maeda, Ontario Cancer Institute (Canada) and Univ. of Toronto (Canada); Bryce Nelson, Terrence Donnelly Ctr. for Cellular and Biomolecular Research (Canada); James Pan, Terrence Donnelly Ctr for Cellular and Biomolecular Research (Canada); Wey-Liang Leong, Ontario Cancer Institute (Canada) and Princess Margaret Hospital (Canada); Alexandra M. Easson, Ontario Cancer Institute (Canada); Susan J. Done, Univ. of Toronto (Canada) and Princess Margaret Hospital (Canada); Gang Zheng, Brian C. Wilson, Ontario Cancer Institute (Canada) and Univ. of Toronto (Canada); Sachdev Sidhu, Terrence Donnelly Ctr. for Cellular and Biomolecular Research (Canada); Ralph S. DaCosta, Ontario Cancer Institute (Canada) and Univ. of Toronto (Canada)

Background: Individualized breast tumor molecular characterization is crucial to determine the optimum therapies dependent on specific receptors (e.g. Trastuzumab for HER2+ tumors). Non-invasive imaging that identifies receptors could avoid the need for biopsy. Hence, we propose that a novel hybrid photoacoustic+fluorescence imaging instrument to be used with receptor-targeted contrast agents. The combined modalities could offer molecularly-specific imaging within deep tissue and additional guidance during surgical resection. In this preclinical study the aims were: 1) to evaluate the tumor-specificity of HER2-targeted agents in vitro, and 2) to test these agents in vivo for tumor binding affinity, pharmacokinetics and feasibility for fluorescence-guided tumor resection.

Methods: Human breast tumor cell line MDA-MB-231 (HER2-) and its H2N variant (HER2+) were used in vitro (in cell culture and phantoms) and in vivo (xenograft tumor in nude mice) to test the specificity of the fluorescently-labeled HER2-targeted probe comprising of antibody fragment (Fab). Fluorescence (MaestroTM, CRi) and photoacoustic (Vevo LAZR, VisualSonics Inc.) imaging were used for in vitro and in vivo experiments.

Results and Discussion: In vitro testing of anti-HER2 Fab demonstrated its specificity to HER2+ MDA-MB-231 H2N tumor cells using fluorescence imaging. Measurable photoacoustic signal could also be detected based on the optical absorption of the fluorescent dye at depth in tissue phantom (~5 mm). Preliminary in vivo testing of the probe demonstrated its accumulation in HER2+ tumor within 24 hours. Future work includes development of agents for other therapeutic targets, such as estrogen receptor, to perform multiplexed imaging.

8581-27, Session 4

Doppler photoacoustic and Doppler ultrasound in blood with optical contrast

Adi Sheinfeld, Avishay Eyal, Tel Aviv Univ. (Israel)

Photoacoustic Doppler (PAD) flowmetry may allow simultaneous measurement of blood flow and oxygen saturation. While in-vivo optical-resolution PAD was already implemented, acoustic-resolution PAD in blood, which can potentially facilitate larger imaging depths, is yet to be demonstrated.

Acoustic-resolution PAD as well as Doppler ultrasound (DUS) measurements were performed in tubes filled with flowing blood with indocyanin green (ICG) at different concentrations. The same ultrasonic transducer and similar modulation waveforms were used in both modalities. The setup comprised a directly-modulated fiber-coupled 830nm laser-diode and a 10MHz focused transducer. The modulation was either continuous wave at 10MHz or tone-bursts for depth-resolved measurements. The resulting signal was recorded and Fourier transformed to extract the Doppler signal.

In the PAD measurements, the amplitude of the Doppler peak was found to be proportional to the ICG concentration. While PAD velocity measurements could be performed on blood with ICG at human safe concentrations, it was difficult to obtain sufficient Doppler signal in whole blood. In contrast, DUS yielded the same Doppler signal for blood with and without ICG. Replacing the blood with carbon particles suspension yielded a significant increase in the Doppler signal in both modalities. These observations imply that the increase in PA Doppler signal with ICG concentration was due to the increased optical absorption and perhaps also due to increased inhomogeneity in the absorption, while in the carbon particles suspension there was also a change in the acoustical characteristics. A new setup whose excitation wavelength is with higher blood absorption is currently being implemented.

8581-28, Session 5

Calibration-free absolute quantification of oxygen saturation based on the dynamics of photoacoustic signals

Jun Xia, Amos Danielli, Lidai Wang, Lihong V. Wang, Washington Univ. in St. Louis (United States)

Photoacoustic (PA) tomography (PAT) is an emerging hybrid imaging technique that has broad preclinical and clinical applications. Based on the photoacoustic effect, PAT directly measures the optical absorption rather than the tissue-intrinsic optical absorption coefficient; the former is the product of the latter and the local optical fluence. Therefore, quantitative PAT requires knowledge of the optical fluence, which can only be estimated through invasive measurements or sophisticated modeling of optical absorption and scattering. In this report, we circumvent this requirement by quantifying absolute oxygen saturation (sO2), an important functional parameter of biology tissue, from the dynamics of PA signals. The new method works under two conditions: (a) the change in sO2 is localized (instead of systemic), and (b) the transition can be monitored with multiple wavelengths. Instead of using the absolute signal intensity, the ratio of signal change at each wavelength was utilized to compute the absolute sO2. The conversion to ratio automatically removes the contribution from optical fluence and allows calibration-free quantification of absolute sO2. The new method was validated in two PAT modalities: photoacoustic computed tomography (PACT) and photoacoustic microscopy (PAM). In PACT, near infrared excitation was utilized for deep tissue imaging, and in PAM, visible excitation was utilized for high spatial resolution imaging at a shallower depth.

8581-29, Session 5

Fluence mapping inside highly scattering media using reflection mode acousto-optics

Altaf Hussain, Khalid Daoudi, Erwin Hondebrink, Wiendelt Steenbergen, Univ. Twente (Netherlands)

Most of the optical imaging modalities which aim to image structures deep inside the scattering medium suffer from a quantification problem. The quantification problem is a result of an unknown fluence distribution of light and becomes more complicated to solve when the medium to be imaged is optically inhomogeneous. We propose a methodology to solve the problem of non-invasively mapping the fluence inside the optically inhomogeneous scattering medium without prior knowledge of its optical properties. We present an adapted theoretical model of our concept, which is based on two principles: the photon reversibility property of light propagation in scattering media and the possibility to label the light in a localized region inside the medium using acousto-optic modulation. The adaptation accounts for the effect of local optical absorption inside the ultrasound focus on the fluence rate of acoustically labeled photons. We provide the proof of our methodology with Monte-Carlo simulations and our results show that it is possible to measure the fluence inside highly scattering medium in absolute terms. We show experimental results of reflection mode acousto-optics to provide a relative map of the fluence distribution in highly scattering medium. Measurements could be obtained down to a depth of 15 mm, for a wavelength of 750 nm.

8581-30, Session 5

Quantitative photoacoustic tomography: acoustic and optical inversions

Teedah Saratoon, Univ. College London (United Kingdom); Tanja Tarvainen, Univ. of Eastern Finland (Finland) and Univ. College London (United Kingdom); Benjamin T. Cox, Simon R. Arridge, Univ. College London (United Kingdom)

Quantitative photoacoustic tomography (QPAT) offers the possibility of high-resolution molecular imaging by quantifying molecular concentrations in biological tissue. QPAT comprises two inverse problems: (1) the construction of a photoacoustic image from surface measurements of photoacoustic wave pulses over time, and (2) determining the optical properties of the imaged region. The first is a well-studied area for which a number of solution methods are available, while the second is, in general, a nonlinear, ill-posed inverse problem.

Model-based inversion techniques have been proposed to solve (2). These are usually based on the diffusion approximation of the radiative transfer equation (RTE) and typically assume the acoustic inversion step has been solved exactly. Here, neither simplification is made: the full RTE is used to model the light propagation, and the acoustic propagation and image reconstruction are included. In other words, the full quantitative inversion is tackled.

Newton-based minimisations are computationally cumbersome for large data sets, and hence impractical when dealing with three-dimensional images. Gradient-based minimisation schemes provide a practical alternative, since they avoid the storage of very large, dense Hessian or Jacobian matrices. Here, pressure time series were simulated using a k-space, pseudo-spectral time domain model, and a time-reversal reconstruction algorithm was used to form a photoacoustic image from which the optical coefficients are to be recovered. An adjoint-assisted gradient inversion using a finite element model of the RTE was used to determine the optical coefficients and Tikhonov and total variation regularisation schemes were used to dampen the effects of noise in the inversions.

8581-49, Session PSun

Handset pulsed laser probe for portable high frame photoacoustic imaging system

Khalid Daoudi, Univ. Twente (Netherlands); Olivier Rabot, Quantel Laser Diodes (France); Andreas Kohl, Quantel Group (France); Stéphane Tisserand, Silios Technologies (France); Peter J. Brands, Esaote Europe B.V. (Netherlands); Wiendelt Steenbergen, Univ. Twente (Netherlands)

Photoacoustics is a hybrid imaging modality that based on detection of acoustic wave generated by absorption of pulsed light by tissue chromophors. In current research, this technique uses large and costly photoacoustic systems with a low frame rate imaging. To open the door for widespread clinical use, a compact, cost effective and ultrafast system is required. In this work we report on the development of a small compact handset pulsed laser probe which can be used for portable and real time photoacoustic imaging system. The handset laser system is designed in the frame of European project. The probe integrates diode lasers connected to electrical driver developed for very short high power pulses. The driver can be triggered with an external system with high stability. The emitted beam is collimated and shaped with compact micro optics beam shaping system delivering a homogenized rectangular laser beam intensity distribution. It uses specifically developed highly efficient diode stacks with high frequency repetition rate up to 10 kHz, emitting at 800nm wavelength. This laser source is a building block to develop a low cost high frame rate photoacoustic imaging system and dramatically improve the temporal resolution.

8581-89, Session PSun

Efficient framework for optoacoustic image reconstruction using wavelet packets

Amir Rosenthal, Daniel Razansky, Vasilis Ntziachristos, Helmholtz Zentrum München GmbH (Germany)

The use of model-based algorithms in optoacoustic tomography offers many advantages over analytical inversion methods. However, the relatively high computational complexity of the model-based approaches often restricts their efficient implementation. In practice, a very large number of pixels/voxels is required for image reconstruction. Consequently, size of the forward-model matrix hinders the use of many inversion algorithms, often making model-based approaches impractical.

In this work, we present a new framework for model-based optoacoustic tomographic reconstructions, which is based on a wavelet-packet representation of the imaged object and the acquired projection data. The frequency localization property of the wavelet-packet base leads to an approximately separable model matrix, for which reconstruction

at each spatial frequency band is independent and requires only a fraction of the projection data. Thus, the large model matrix is effectively separated into a set of smaller matrices, facilitating the use of inversion schemes whose complexity is highly nonlinear with respect to matrix size. The performance of the new methodology is demonstrated for the case of two-dimensional optoacoustic tomography for both numerically generated and experimental data. In the case of partial-tomographic data, the wavelet-packet framework enabled employing regularization algorithms such as singular value decomposition, which were too resources consuming to be used on the total model matrix. Thus, the new framework enables extending the application of model-based techniques to image sizes which have in the past been prohibitive for this approach.

8581-91, Session PSun

Thermoacoustic imaging of fresh prostates up to 6-cm diameter

Sarah K. Patch, Univ. of Wisconsin-Milwaukee (United States); Eric Hanson, McGill Univ. (Canada); Majorca Thomas, Holly Kelly, Kenneth Jacobsohn, William A. See, Medical College of Wisconsin (United States)

Current imaging techniques typically reveal one (XR, CT, US) or very few (MRI) tissue parameters and they all fail to robustly visualize prostate cancer (PCa).

Thermoacoustic (TA) imaging provides a novel contrast mechanism that may enable visualization of cancerous lesions. Imaging entire prostate glands requires 6 cm depth penetration. Because VHF pulses are far less lossy in tissue than microwave and optical irradiation, they permit greater depth penetration – at the expense of SNR. We excite TA signal propagating high-power (40 kW peak), submicrosecond TE10 pulses with carrier frequency 100 MHz. This frequency can easily penetrate the abdomen of large adults, and we generate TA pulses with sufficient strength to survive 6 cm of outgoing travel to an ultrasound transducer.

A benchtop system designed for imaging large whole organs was optimized specifically for imaging smaller prostate glands. The system has smaller cross-section, increasing EM power deposition – and therefore TA signal strength. 15g/L glycine solution serves as acoustic couplant because it has low EM and acoustic loss, and is not absorbed by the tissue.

We will present TA images of fresh prostates. The urethra is routinely visualized as signal dropout; surgical staples formed from 100-micron wide wire bent to 3 mm length generate strong positive signal*. In conclusion, TA tomography robustly detects small high-contrast inclusions. Whether the microvasculature supporting aggressive tumor growth will provide sufficient contrast over a larger tumor volume remains TBD.

* surgical staples were inadvertently left on 2 of the first specimens imaged. We now remove them.

8581-92, Session PSun

Characterizing microscopic morphology in biological tissue with photoacoustic spectrum analysis: feasibility study with simulations and experiments

Guan Xu, Univ. of Michigan Medical School (United States); Irfaan Dar, Univ. of Michigan (United States); Chao Tao, Xiaojun Liu, Nanjing Univ. (China); Xueding Wang, Univ. of Michigan Health System (United States)

Photoacoustic imaging is a non-invasive imaging modality that physically combines the resolution of ultrasound and the functional contrast of optical imaging. Although photoacoustic images clearly reflect the macroscopic transitions of tissue optical properties, the less significant contrast fluctuations encoding the microscopic morphologies within the seemingly homogeneous regions in biological tissues are usually ignored. This study, following the major procedures of ultrasound spectrum analysis, which reveals the acoustic scattering properties of the microstructures within biological tissue, investigated the feasibility of characterizing the microstructures in biological tissue with photoacoustic spectrum analysis. The scope of this study was limited to analyzing the power spectra of one dimensional signals generated by spherical photoacoustic sources, with varied dimensions and concentrations, embedded in ultrasonically homogeneous and optically transparent background materials. Theoretical hypotheses were derived regarding the contribution of frequency or time domain components decomposed from photoacoustic signals to the total signal power spectra. The linear models fitted to the power spectra in both simulations and experiments, in agreement to the hypotheses, indicated that: a) the slope of the linear model decreases as the source dimension increases; b) the slope slightly decreases as the source concentration increases; c) intercept and midband fit of the linear model increase as the source dimension increases; d) intercept and midband fit increase as the source concentration increases. Differences and similarities between the photoacoustic and ultrasound spectrum analysis were extensively discussed. The conclusion of this study can potentially be extended to photoacoustic sources with shapes, dimensions and concentrations in larger ranges.

8581-93, Session PSun

Low-cost parallelization of optical fiber based detectors for photoacoustic imaging

Johannes Bauer-Marschallinger, Hubert Grün, Peter Burgholzer, Thomas Berer, RECENDT GmbH (Austria)

Optical fiber based detectors are an attractive alternative to point-like detectors for photoacoustic imaging because of their large aperture. Up to now, the realized setups consist only of a single optical fiber detector, caused by the high costs per channel. A one channel setup, however, results in relatively long measurement times. Thus, simultaneous measurements with multiple channels are essential for practical applications.

We present a multi-channel setup, made possible by replacing key components of the prior setups by low cost devices as used in telecommunication industries. The tunable low-bandwidth light source was replaced by a laser diode operating at 1550 nm. Due to the low coherence of the laser diode, the paths lengths of the interferometer have to be matched accurately. The two paths of the interferometer are brought to quadrature by an electro-optical phase shifter, instead of tuning the laser wavelength, and by using a low-cost microcontroller for working point stabilization. Additionally, commercial balanced photo-detectors were replaced by self-built high-bandwidth detectors.

Multichannel detection is demonstrated for a four channel ring detector array. The rings are made of graded index polymer optical fibers, which exhibit more sensitivity as standard glass optical fibers. Furthermore, we compare the performance (in terms of signal-to-noise-ratio and stability) of the presented setup with the one channel detector based on the tunable laser and a commercial photodetector.

8581-94, Session PSun

Phase modulated influences of curved trajectories in monte carlo simulations

Jacob W. Staley, Wiendelt Steenbergen, Univ. Twente (Netherlands)

In order to take into account the influence of refractive index gradients, and their resultant influence on photon trajectories and their phases, we employ the eikonal equation. By manipulating the eikonal equation into a form suitable for use with Monte Carlo simulations we show it is possible

to accurately propagate photons along curved paths. The curved paths arise from the continuously varying refractive index values encountered between consecutive scattering events. We demonstrate the applicability of the technique in 2-dimensional cases insonified with planar waves, as well as 3-dimensional cases under insonification of a simulated commercial ultrasound linear array.

8581-95, Session PSun

Millisecond-pulse Alexandrite laser for more sensitive acousto-optic imaging

Emilie Benoit, Francois Ramaz, Ecole Supérieure de Physique et de Chimie Industrielles (France)

Because of multiply scattering, imaging tissues with coherent light generates speckle that decorrelates within 1 ms. Acousto-optic imaging is able to measure the local optical properties of tissues (absorption, scattering) using an acoustic wave for localization and resolution. It is a coherent technique that is concerned by the time limitation of speckle correlation when imaging living tissues. In order to improve the efficiency of acousto-optic signal creation, we use a pulsed Alexandrite laser instead of classic CW lasers that concentrates the optical power within 1 ms at 10 Hz rate (200 mJ mean energy). The Alexandrite laser emits light in the therapeutic window (around 780 nm) which guaranties a several cm deep penetration in tissues.

The detection of the acousto-optic signal is performed with off-axis heterodyne digital holography and a resolution of 1 mm3 is achieved thanks to the implementation of a random phase jumps modulation on ultrasound and light. This technique called Acousto-Optical Coherence Tomography (AOCT) is relevant considering that we deal with long-duration signals. We have already successfully implemented it with a CW Ti:Sapphire laser [1]. Synchronization and timing is adapted to fit the use of our pulsed Alexandrite laser.

First experiments are carried out on tissue-mimicking phantoms composed of agar and Intralipid and containing small absorbing inclusions. Then biological tissues are imaged. An important work is done for speed improvement of camera detection and data processing in order to perform 3D imaging.

[1] E. Benoit a la Guillaume, S. Farahi, E. Bossy, M. Gross, and F. Ramaz, Opt. Lett. (2012), to be published.

8581-96, Session PSun

Joint acousto-optic and ultrasound images of small animals

Emilie Benoit, Jean-Luc Gennisson, Salma Farahi, Ecole Supérieure de Physique et de Chimie Industrielles (France); Alexander A. Grabar, Uzhgorod National Univ. (Ukraine); Mickael Tanter, Francois Ramaz, Ecole Supérieure de Physique et de Chimie Industrielles (France)

Acousto-optic imaging is an interferential technique that can image the volume of some cm thick scattering media, like biological tissues, in order to measure their local optical properties, i.e. the absorption or scattering coefficients. In contrast with photo-acoustic imaging, an optical signal is detected, whose localization and resolution are ruled by the ultrasound characteristics.

With the use of a Sn2P2S6 crystal in photorefractive holographic detection configuration, we are able to image in the therapeutic window. A fast detection is performed thanks to a single broadband photodiode and with the ultrasound burst technique [1], a one-dimensional profile is obtained in a few ms with a millimeter resolution. To perform 3D imaging without losing in speed, the acoustic mono-element transducer is replaced by a multi-element probe that can focus everywhere on a plane depending on the delay law ruling the piezo elements. A motorized scanning is required only in one direction so that well-resolved 3D images can be achieved rapidly.

As the multi-element ultrasound probe works both as an emitter and a receiver, a complementing standard echography examination can easily be performed without any change in the measurement configuration.

This bi-modal imaging device is first tested on agar and Intralipid scattering phantoms containing black-inked inclusions of different absorption coefficients. Then joint acousto-optic and ultrasound images are performed through the body of dead mice. The comparison of the two images enables to validate the potentiality of acousto-optic imaging of biological tissues.

[1] S. Farahi, G. Montemezzani, A. A. Grabar, J.-P. Huignard, and F. Ramaz, Opt. Lett. 35, 1798 (2010).

8581-97, Session PSun

Recognizing ovarian cancer from co-registered ultrasound and photoacoustic images

Umar S. Alqasemi, Patrick D. Kumavor, Andres Aguirre, Quing Zhu, Univ. of Connecticut (United States)

Co-registered ultrasound and photoacoustic images of ex vivo human ovaries with known diagnosis from biopsy were used. The images were processed in order to find exclusive classification between cancerous and non-cancerous cases. Initial image compression is done with wavelet transform, after that, mean Radon transform is computed for the photoacoustic part of the image then fitted with a Gaussian function to find the centroid of suspicious area for shift-invariant recognition process. After that, unique features are extracted from the images by several methods; including features from Fourier domain, image statistics, and the outputs of different composite filters made from the joint frequency response of different cancerous case images within the training set of images. These features are chosen based on careful observation of the training set of images, and extracted from more than 400 training images obtained from 33 human ovaries. The extracted feature values from the training set were used to train a support vector machine (SVM) structure for classification, and it was able to exclusively separate the cancerous cases from the non-cancerous ones for the training set of images. The trained SVM structure was then used to test 96 new images, obtained from 37 more human ovaries of different diagnoses, to evaluate and determine the test sensitivity and specificity for detection and diagnosis. The image recognition classifier was able to recognize the cancerous images from the non-cancerous images of the non-training data with 76.92% sensitivity and 95.18% specificity. If we assume that recognizing one image as cancerous case is sufficient to consider the ovary as cancerous, the classifier was able to recognize the cancerous ovaries from the non-cancerous ones with 100% sensitivity and 93.94% specificity. Note that, all the ovaries used in this study were obtained right after the oophorectomy from UCONN health center, and then returned to pathology department for final diagnosis.

8581-98, Session PSun

Two-photon photoacoustics ultrasound measurement by a loss modulation technique

Yu-Hung Lai, Chieh-Feng Chang, National Taiwan Univ. (Taiwan); Yu-Hsiang Cheng, Graduate Institute of Photonics and Optoelectronics, National Taiwan University (Taiwan); Chi-Kuang Sun, National Taiwan Univ. (Taiwan) and Academia Sinica (Taiwan)

In this work, we investigated the principle of the two-photon absorption (2PA) detection with loss modulation technique, and first demonstrated the existence of two-photon photoacoustics ultrasound excited by a femtosecond laser. By using the AO modulation with different modulation frequencies, we successfully create the beating of the light signal when the two arms of the beams are both spatial and temporal overlapping. The pulse train of the femtosecond laser causes the narrow

band excitation, providing the frequency selectivity and sensitivity. Moreover, the pulse energy is no more than 15nJ/pulse, which is at least 3 orders of magnitude smaller than that of the nanosecond laser, and therefore prevents the thermal damage of the sample. With the help of lock-in detection and low noise amplifier, we can separate the signal of two-photon absorption from one-photon absorption. We used ultrasonic transducer to detect the response of the sample, and verify the existence of the two-photon photoacoustics ultrasound generating by the femtosecond laser. Several contrast agents, such as the black carbon solution, the fluorescence dye and the nano-particles, are used in the experiment. This is a milestone to develop the two-photon photoacoustics microscopy, which, in principle, has the great potential to achieve the in vitro and in vivo high resolution deep imaging.

8581-100, Session PSun

A novel design for small animal PAT system

Zijian Deng, Changhui Li, Peking Univ. (China)

Small animal whole-body photoacoustic tomography (PAT) has drawn increasing attention recently. We report a PAT imaging system that relies on a novel design to optimize the light illumination and acoustic detection. Our method overcomes the conflict in the sharing of the transportation path for the illumination light and the acoustic wave. In addition to the theoretical simulation, we experimentally demonstrated that our design can help both the signal to noise ratio and the quantitative imaging of small animal deep tissues. Moreover, our design can be straightforwardly extended to various PAT imaging systems.

8581-101, Session PSun

Evaluation of tissue microstructure with a narrowband and low frequency photoacoustic tomography system

Yiqun Yang, Shaohua Wang, Chao Tao, Nanjing Univ. (China); Xueding Wang, Univ. of Michigan Health System (United States); Xiaojun Liu, Nanjing Univ. (China)

The characteristic microstructures in biological tissues could be used to differentiate tissue types, such as tumor vs. normal tissue. The spatial resolution of classical photoacoustic tomography (PAT) mainly depends on the wavelengths of the detected ultrasonic signals. In order to present the very detailed microstructures in a biological sample, the receiving bandwidth of the PAT system needs to be extremely wide. Another challenge in detecting the high frequency signals associated with microstructures is the strong acoustic attenuation which increases quadratically with ultrasound frequency.

In this study, we propose a novel photoacoustic spectral analysis (PSA) technique which evaluates the microstructures in tissues by analyzing the spectral parameters of detected photoacoustic signals. Experimental result verified that, using a limited 1-5 MHz working bandwidth, PSA could effectively differentiate two melanoma-mimicking phantoms containing different microstructures (49 ?m and 199 ?m absorber sizes respectively). In comparison, since the physical scales of the microstructures are too small and beyond the spatial resolution of the PAT system, classical tomographic imaging could not differentiate the two phantoms. The findings from this study suggest that the proposed PSA technique could help distinguish different tissue types, by evaluating the characteristic microstructures in tissues, without relying on the detection of high frequency signals which is extremely challenging when the target object is deep.

8581-102, Session PSun

Acoustic-resolution photoacoustic imaging system with simple fiber illumination

Yasuyuki Tsunoi, Keio Univ. (Japan); Shunichi Sato, Satoko Kawauchi, Hiroshi Ashida, National Defense Medical College (Japan); Mitsuhiro Terakawa, Keio Univ. (Japan)

Acoustic-resolution photoacoustic microscopy (AR-PAM) with dark-field confocal illumination enables unique high-resolution visualization of chromophores in tissue, such as microvasculatures, at depths of a few millimeters. However, most current systems are bulky and use complex optical components for illumination, thus requiring highly sensitive alignment. In this study, we developed a compact acoustic-resolution photoacoustic imaging system with simple fiber illumination. Around the high-frequency (30-MHz) ultrasound detector attached with the high-numerical-aperture acoustic lens, four quartz fibers were placed at the four directions. The setting angle of the fibers were determined to form a dark field on the tissue surface under the acoustic lens and for the four light beams from the fibers to be combined near the focal point of the acoustic lens, i.e., at a depth of around 1.2 mm in the tissue. The acoustic lens and the output ends of the fibers were capped with an acoustically and optically transparent engineering plastic sheet, whose surface can be directly placed and scanned on the tissue surface with ultrasound gel. The diameter and height of this imaging head were as small as 32 mm and 27 mm respectively. The phantom study showed that the lateral spread function of the present imaging system was 120 micrometers, which agreed well with the theoretical value of 112 micrometers. We then attempted to image the vasculatures in the rat skin ex vivo, demonstrating high-contrast visualization of the blood vessels of a few hundred micrometers in diameter in the tissue.

8581-103, Session PSun

Measuring non-radiative relaxation time of fluorophores by intensity-modulated laser induced photoacoustic effect

Behrouz Soroushian, Xinmai Yang, The Univ. of Kansas (United States)

Modulated tone-burst light was employed to measure nonradiative relaxation time of biological tissue samples through photoacoustic effect. To map nonradiative relaxation time relatively, modulated tone-burst light is used to generate photoacoustic signals. Then nonradiative relaxation time is indicated by the amplitude decay rate as modulation frequency increases. The results show that although blood is an optically weak absorber at 808 nm, by using this method a significant enhancement of contrast-to-noise ratio of a blood target compared to pulsed photoacoustic imaging at this wavelength is achieved. Furthermore, a theoretical model was developed to estimate nonradiative relaxation time through a fitting process for the quantitative study. Experiments were performed on solutions of new indocyanine green in two different solvents (water and dimethyl Sulfoxide (DMSO)). A 1.5 times slower non-radiative relaxation for the solution in DMSO was observed as compared with the aqueous solution. This result agrees well with general finding that non-radiative relaxation of molecules in triplet state depends on viscosity of solvents in which they are dissolved.

8581-104, Session PSun

Photoacoustic microscopy with 7.6-μm axial resolution

Chi Zhang, Konstantin I. Maslov, Junjie Yao, Lihong V. Wang, Washington Univ. in St. Louis (United States)

The axial resolution of photoacoustic microscopy (PAM) is much lower than its lateral resolution, which resolves down to the submicron level.

Here we achieved so far the highest axial resolution of 7.6 μm by using a commercial 125-MHz ultrasonic transducer for signal detection followed by the Wiener deconvolution for signal processing. The axial resolution was validated by imaging two layers of red ink in a wedge shape. Limited by the working distance, the high-frequency ultrasonic transducer can penetrate 1.2 mm into biological tissue from the ultrasound detection side. At this depth, the signal-to-noise ratio decreases by 11 dB, and the axial resolution degrades by 36%. Melanoma cells were imaged ex vivo, and the 3D PAM images were validated by bright field optical microscopy. Compared with a PAM system with a 50-MHz ultrasonic transducer, our high-axial-resolution PAM system resolved the blood vessels in mouse ears in vivo much more clearly in the depth direction.

8581-105, Session PSun

Exploring ultrasound-modulated optical tomography at clinically useful depth using the photorefractive effect

Puxiang Lai, Yuta Suzuki, Xiao Xu, Lihong V. Wang, Washington Univ. in St. Louis (United States)

For years, ultrasound-modulated optical tomography (UOT) has been proposed to image optical contrasts deep inside turbid media (such as biological tissue) at an ultrasonic spatial resolution. The reported imaging depth so far, however, has been limited, preventing this technique from finding broader applications. In this work, we present our latest experimental explorations that push UOT to clinically useful imaging depths, achieved through optimizing from different aspects. One improvement is the use of a large aperture fiber bundle, which more effectively collects the diffused light, including both ultrasound-modulated and unmodulated portions, from the turbid sample and then sends it to the photorefractive material. Another endeavor is employment of a large aperture photorefractive polymer film for demodulating the ultrasound-induced phase modulation. Compared with most UOT detection schemes, the polymer film based setup provides a much higher etendue as well as photorefractive two-beam-coupling gain. Experimentally, we have demonstrated enhanced sensitivity and have imaged through tissue-mimicking samples up to 9.4 cm thick at the ultrasonically-determined spatial resolution.

8581-106, Session PSun

Simultaneous multispectral coded excitation using periodic and unipolar M-sequences for photoacoustic imaging

Haichong Zhang, Kengo Kondo, Makoto Yamakawa, Tsuyoshi Shiina, Kyoto Univ. (Japan)

Photoacoustics (PA) enables optical-absorption imaging such as functional imaging with depth information by combining ultrasonics and optics. The task with PA is to increase the signal-to-noise ratio (SNR) because excitation light is attenuated with depth. Repeating irradiation worsens the frame rate, and it will be worse to acquire multispectral information. In previous research, we proposed the m-sequence family such as gold codes, which provide better SNR images than ensemble average. However, the sending procedure is so complex that it was essential to send sequences twice aperiodically since the negative codes of bipolar sequences must be sent separately, and the decoding artifacts of those bipolar sequences cannot be minimized in aperiodic sending, unlike periodic sending. This study proposes periodic and unipolar m-sequences (PUM): a unipolar sequence consisting of {1, 0}, selected from positive codes of bipolar m-sequences. Signals can be enhanced by decoding periodically sent PUM using bipolar sequences, and there are no coding artifacts at all for a single wavelength. Moreover, in multispectral simultaneous irradiation, the crosstalk in PUM remains low level on a stable, which is inherited from m-sequence. We demonstrated that PUM's improved SNR is superior to that of aperiodic m-sequence family codes or orthogonal Golay codes. Furthermore, the frame-rate, which is normally limited by acoustic time-of-flight, can be maximized up to the pulse repetition frequency since the decoding start point can be set in any code in periodic irradiation.

8581-107, Session PSun

Dual-modal photoacoustic and optical coherence tomography using one single near-infrared supercontinuum

Changho Lee, SeungHoon Han, Sehui Kim, Kyungpook National Univ. (Korea, Republic of); Mansik Jeon, Univ. at Buffalo (United States); Min Yong Jeon, Chungnam National Univ. (Korea, Republic of); Chulhong Kim, Univ. at Buffalo (United States); Jeehyun Kim, Kyungpook National Univ. (Korea, Republic of)

We report the development of a combined dual-modal photoacoustic and optical coherence tomography (PA-OCT) system using one single near-infrared (NIR) supercontinuum laser source which can provide both optical absorption and scattering contrasts simultaneously. By using a small sized pulsed Nd:YAG microchip laser and a photonic crystal fiber, we fabricated a pulsed broadband supercontinuum source from 600 to 1700 nm. Under the same optical hardware system, intrinsically registered PA and OCT images are acquired in a single scanning. In order to demonstrate feasibility of our system, we successfully acquired the PA and OCT images of black and white hairs images at the same time. The black hair was detected in both PA and OCT images, while the white hair appeared only in the OCT image. This result suggests the potential of compact, cost-effective, and simple dual-modal PA-OCT system. Moreover, we believe that this approach will be a key point for commercialization and clinical translation.

8581-108, Session PSun

Microring resonator aided vibrational photoacoustic tomography

Cheng Zhang, Sung-Liang Chen, Tao Ling, L. Jay Guo, Univ. of Michigan (United States)

Atherosclerosis is a chronic disease where the blood vessel walls gradually thicken as a result of accumulated fatty material such as lipids. Accurate characterization of lipid deposition on artery walls is critical for both diagnosing and treating of this disease. In order to obtain such information, many imaging modalities have been explored. Intravascular ultrasound imaging provides information on the morphology of the atherosclerotic plaques, but the acoustic contrast between lipid and surrounding tissues is quite low. In contrast, magnetic resonance imaging is capable of differentiating lipid deposition from the surrounding tissue, but the resolution needs to be improved. Therefore, an imaging modality that can reliably detect lipid distribution with both sufficient contrast and high resolution is desired. Recently, vibrational photoacoustic microscopy (VPAM) has been demonstrated. Compared with other imaging modalities, Photoacoustics enables label-free and bond-selective characterization of lipid deposition at clear contrast and good resolution. In this work, we exploit a microring resonator as a sensitive and wide bandwidth ultrasound detector for vibrational photoacoustic tomography (VPAT). Compared with VPAM, VPAT makes use of ultrasound signal generated from both quasi-ballistic and diffusive regime, and therefore, a further imaging depth is achieved. Besides, the microring resonator has ultrahigh sensitivity and is able to detect weak vibrational photoacoustic signals with good signal-to-noise ratio. In addition, its wide bandwidth (DC to over 90MHz) provides high resolution and enables imaging at multiple length scales. Such a tomography system provides accurate and good imaging quality at sufficient depth, which greatly benefits the study of atherosclerosis.

8581-109, Session PSun

A dynamic image reconstruction method with spatio-temporal constraints

Hyun-Keol Kim, Michael A. Khalil, Jacqueline E. Gunther, Ludguier D. Montejo, Andreas H. Hielscher, Columbia Univ. (United States)

Dynamic optical tomographic imaging (DOTI) has in recent years received increasing attention as a viable means to probe physiology in tissue over time. This technique can thus be used to detect tissue abnormalities as tumors. However, conventional dynamic imaging methods require a relatively very long computation time since thousands of images have to be reconstructed independently in a one-at-a-time manner to generate some meaningful dynamic information. To overcome this shortcoming, we propose here a novel fast dynamic imaging method that makes use of spatial-temporal constrains in the framework of PDE-constrained algorithm. This new approach enables using all data from different time points into the reconstruction. Therefore, this method reconstructs all time-dependent parameters from different time points at once, which leads to a great saving in the image reconstruction time. The performance of this method is tested with numerical and experimental data. As a result, this new approach showed that it can speed up dynamic imaging by a factor of 50 or greater provided that suitable basis functions are selected.

8581-110, Session PSun

iIn vivo optoacoustic tomography of the human anterior neck region

Alexander Dima, Vasilis Ntziachristos, Helmholtz Zentrum München GmbH (Germany)

The human anterior neck region is a common diagnostic site of diseases such as Carotid Artery Disease (CAD) or Thyroid Disease. CAD diagnosis often involves assessment of arterial lumen diameter and (in case of stenosis) of atherosclerotic plaque composition. Important parameters in the diagnosis of thyroid disorders include the shape and size or the level of vascularization of the thyroid gland or of nodules contained within. In both cases ultrasound imaging is routinely applied for diagnosis, because it offers high resolution anatomical information and high throughput point of care application. Similarly optoacoustic imaging could be applied as it provides the same resolution and is ideally suited for vascular imaging. Additionally, Multi-Spectral Optoacoustic Tomography (MSOT) significantly increases sensitivity to spectrally dependent molecular parameters such as blood oxygenation or externally administered contrast agents. We therefore show herein the feasibility of using a tomographic handheld optoacoustic imaging system for imaging the human neck region up to 20 mm below the skin surface. The system, based on in-plane epi-illumination and focused curved array detection, is capable of delivering high resolution images at 10 frames per second and was designed to achieve almost ideal optical and acoustic coupling while being fully handheld and ready for clinical adaption. We demonstrate live imaging performance on several human volunteers by imaging the common carotids, the jugular veins and both lobes of the thyroid gland. For validation we employ echo ultrasound and Doppler ultrasound imaging.

8581-111, Session PSun

Functional photoacoustic micro-imaging of cerebral hemodynamic changes in single blood vessels after photo-induced brain stroke

Lun-De Liao, National Univ. of Singapore (Singapore) and National Chiao Tung Univ. (Taiwan); You-Yin Chen, National Yang-Ming Univ. (Taiwan); Chin-Teng Lin, National Chiao Tung Univ. (Taiwan); Meng-Lin Li, National Tsing Hua Univ. (Taiwan)

Studying the functional hemodynamic roles of individual cerebral cortical arterioles in maintaining both the structure and function of cortical regions during and after brain stroke in small animals is an important issue. Recently, functional photoacoustic microscopy (fPAM) has been proved as a reliable imaging technique to probe the total hemoglobin concentration (HbT), cerebral blood volume (CBV) and hemoglobin oxygen saturation (SO2) in single cerebral blood vessels of rats. Here, we report the application of fPAM associated with electrophysiology recordings to investigating functional hemodynamic changes in single cortical arterioles of rats with electrical forepaw stimulation after photo-induced ischemic stroke. Because of the weak optical focusing nature of our fPAM system, photo-induced ischemic stroke targeting single cortical arterioles can be easily conducted with simple adaptation. Functional HbT, CBV and SO2 changes associated with the induced stroke in selected arterioles from the anterior cerebral artery system were imaged with 36 ? 65-um spatial resolution. Experimental results showed that after photo-occlusion of a single arteriole, the functional changes of nearby arterioles in cerebral cortex only can be observed immediately after the stroke. After a few minutes of stroke onset, there are no significant functional changes under the forepaw stimulation, suggesting that alternate blood flow routes are not actively recruited. The fPAM with electrophysiology recordings complements existing imaging techniques and has the potential to offer a favorable tool for explicitly studying cerebral hemodynamics in small animal models of photo-indcued ischemic stroke.

8581-112, Session PSun

Remote photoacoustic imaging on non-flat surfaces and appropriate reconstruction algorithms

Thomas Berer, Armin Hochreiner, Heinz Roitner, Hubert Grün, Peter Burgholzer, RECENDT GmbH (Austria)

The recently introduced remote photoacoustic imaging technique (rPAI) allows measurement of photoacoustic signals on non-planar surfaces without the need for a water bath or coupling agent. Hereby, photoacoustically generated ultrasonic displacements are detected without physical contact to the sample by utilizing laser interferometric techniques. Conventional reconstruction methods for PAI usually assume planar or spherically shaped detection surfaces. If the assumed surface does not match the actual sample surface, these algorithms produce strong image artifacts.

In this work we adapted different algorithms to allow reconstruction on non-planar surfaces and evaluate them on experimental and simulated data. Experimental data were obtained by utilizing our remote photoacoustic setup based on two-wave mixing (TWM) in a photorefractive crystal. Ultrasonic displacements were obtained on non-planar surfaces, the exact morphologies of which were determined by optical coherence tomography (OCT). Three-dimensional reconstructions of real measurement data is shown with synthetic aperture focusing technique (SAFT) and spectral-domain time reversal (SDTR) algorithms, whereupon the exact surface morphology, obtained from OCT scans, is taken into account. The results are compared to a standard Fourier domain SAFT (FSAFT) algorithm. Analysis of the performances of the different algorithms and the obtainable resolution on various surfaces is examined on simulated data. It is shown that SDTR gives the best result as the algorithm comprises the wave equation, whereas the SAFT algorithm leads to artifacts. We further improved the algorithms by taking into account that we measure the projection of the surface displacements in direction of the scanning beam and not the full displacements.

8581-113, Session PSun

Reconstruction of the optical properties of inhomogeneous medium from photoacoustic signal with lp sparsity regularization

Shinpei Okawa, Takeshi Hirasawa, Toshihiro Kushibiki, Miya Ishihara, National Defense Medical College (Japan)

A method to reconstruct the optical properties in optically inhomogeneous media from the photoacoustic (PA) signals is discussed. The forward models of the propagations of the excitation light and that of the PA wave are constructed with the finite element method. The inverse problem is formulated as a linear equation relating the optical properties to time-domain PA signals. By solving the inverse problem, the distribution of the optical properties in the optically inhomogeneous medium is reconstructed. The measurement noise and the mismatches between the actual measurement system and the forward model often cause artifacts in the reconstructed image. To reduce the artifacts and to obtain high resolved reconstructed image, we use the regularization method which minimizes the lp norm of the solution of the inverse problem.

It is demonstrated by some numerical simulations that the regularization method using lp norm reconstructs localized changes in the optical properties from the baseline. The images reconstructed with the lp sparsity regularization are compared to those with truncated singular value decomposition (TSVD). We also discuss the use of the images reconstructed with TSVD as an initial guess for the reconstruction with lp sparsity regularization. TSVD method can provide good initial guess and prevent the reconstructed image being too sparse and loosing deeply embedded PA sources for reconstruction in use of lp sparsity regularization.

8581-114, Session PSun

Analysis of laser parameters in the solution of photoacoustic wave equation

Hakan Erkol, Mustafa U. Arabul, Esra Aytac Kipergil, Burcin M. Unlu, Bogaziçi Üniv. (Turkey)

Imaging performance of photoacoustic microscopy depends primarily on laser parameters because short pulsed laser induces photoacoustic wave via thermal expansion. In the literature, photoacoustic wave equation is either solved for Dirac delta shaped spatiotemporal profiles containing no laser parameter dependency or solved with some approximations for Gaussian spatiotemporal profiles. For this reason, photoacoustics research has not usually focused on laser parameters (pulse duration and beamwidth of laser). Thus, studying laser parameter dependencies of photoacoustic signal will lead researchers to achieve optimal values for different imaging samples. In this work, for an optically absorbing spherical object, treating temporal profile of laser as Gaussian, we solve the photoacoustic wave equation analytically via the Fourier transform for rectangular and Gaussian radial profiles. Without any approximation, we obtain exact solutions and plot the photoacoustic signals as a function of time for different radial positions outside the spherical object. For realistic values of photoacoustic parameters, we present an expression for the photoacoustic signal that contains the laser parameters (pulse duration and beamwidth) and investigate the variation of the signal with respect to the corresponding parameters for Gaussian spatiotemporal profile. We also analyze effects of the other laser parameters (peak power, average power and the pulse energy) on the signal. The results presented here provide a theoretical basis for biomedical optics and guide photoacoustic imaging studies in terms of quantification of physical laser parameters.

8581-115, Session PSun

Deconvolution algorithms for photoacoustic tomography to reduce blurring caused by finite sized detectors

Peter Burgholzer, Heinz Roitner, Thomas Berer, Hubert Grün, RECENDT GmbH (Austria); Robert Nuster, Günther Paltauf, Karl-Franzens-Univ. Graz (Austria)

Most reconstruction algorithms for photoacoustic tomography, like back-projection or time-reversal, work ideally for point-like detectors. For real detectors, which integrate the pressure over their finite size, it was shown that the images reconstructed by back-projection or time-reversal show some blurring. Only iterative reconstruction algorithms or algorithms using an imaging matrix can take the finite size of real detectors into account, but the numerical effort is significantly higher. For spherical or cylindrical detection surfaces the blurring caused by a finite detector size is proportional to the distance from the rotation center and is equal to the detector size at the detection surface. We used several “deconvolution” algorithms to reduce the blurring on simulated and on experimental data: e.g. a “point-to-center” method, where the measurement data for each reconstructed point is time shifted in a way that each reconstructed point is in the rotation center; or a “Wiener deconvolution” where the deconvolution length is proportional to the radius. Experimental data were obtained on a plastisol cylinder with 6 thin holes filled with an absorbing liquid (OrangeG). The holes were loacated on a spiral emanating from the center of the cylinder. Data acquisition was done by utilization of piezoelectric detectors with diameters of 6 mm and 3mm which were rotated around the object at radii of 12 mm and 16 mm, respectively.

8581-116, Session PSun

Measurement of the Grueneisen coefficient of tissue by photoacoustic spectrometry

Da-Kang Yao, Lihong V. Wang, Washington Univ. in St. Louis (United States)

Photoacoustic tomography is a new medical imaging technique, capable of visualizing deep internal structures in biological tissue. In photoacoustic tomography, the Grueneisen coefficient of tissue is a constitutive parameter which relates optical absorption to acoustic pressure. Instead of direct measurement, the parameter is usually estimated in terms of the thermal expansion coefficient, heat capacity, and acoustic speed, which causes uncertainty in photoacoustic imaging. To minimize the uncertainty, we applied photoacoustic spectrometry (PAS) to directly measure the Grueneisen coefficient. In our PAS system, an OPO laser system emitted laser pulses at wavelengths between 460 and 1550 nm. After passing through a 1-mm-diameter hole and a beam sampler, the laser beam illuminated tissue samples. Pulse energy was measured by a photodiode detector. Acoustic pressure was detected by a 20 MHz water-immersion flat ultrasonic transducer. The relation between the amplitude (A) of a photoacoustic signal, the Grueneisen coefficient (?), the pulse energy (E), and the absorption coefficient (?a) of the tissue, is expressed as A/E=???a, where ? is a constant. We calibrated the PAS system by fitting the photoacoustic spectrum of water to its absorption spectrum at wavelengths between 1100 and 1550 nm. From this wavelength range, we found that the Grueneisen coefficient was 0.132 ± 0.001 (mean ± standard deviation) for bovine serum at room temperature (24oC). The Grueneisen coefficient was 0.144 ± 0.003 for bovine erythrocytes, 0.79 ± 0.01 for porcine lipid, and 0.74 ± 0.01 for porcine subcutaneous fat tissue at 24oC.

8581-117, Session PSun

Photoacoustic imaging of a genetically encoded photoswitchable fluorescent probe

Arie Krumholz, Washington Univ. in St. Louis (United States); Kiryl Piatkevich, Vladislav V. Verkhusha, Albert Einstein College of Medicine of Yeshiva Univ. (United States); Lihong V. Wang, Washington Univ. in St. Louis (United States)

Although many contrast agents, including nanoparticles and organic dyes, have been used with photoacoustic tomography (PAT), genetically encoded contrast agents are particularly powerful. Their contrast appears only under conditions that can be precisely controlled both spatially and temporally. Here we report on a novel near-infrared fluorescent protein characterized by low fluorescence quantum yield and absorption near a hemoglobin absorption minimum, making it ideal for PAT. Additionally, this protein can reversibly photoswitch between two states, denoted as “ON” and “OFF”, with absorbance maxima at 754 and 677 nm, respectively. The capability to photoswitch can be exploited to enhance contrast in PAT by probing the protein in both its “ON” and “OFF” states and producing a differential image. Here, we report the successful photoacoustic imaging of the genetically encoded reversibly photoswitchable iRFP variant ex vivo. The protein was selected based on PAT signal strength and photoswitchable contrast after comparison with other versions of the near-infrared photoswitchable fluorescent protein expressed in the Met-1 mouse mammary carcinoma cell line. To test the maximum imaging depth achievable with the proteins, a phantom was constructed by embedding sections of laboratory tubing in chicken breast tissue, with the cells expressing the proteins in one tube, and blood in the other for comparison. Subsequent depths were simulated by stacking sections of chicken on the sample. The photoswitchable performance was tested by imaging ten cycles between the “ON” and “OFF” states and measuring the difference in contrast per cycle.

8581-118, Session PSun

Quantitative imaging of bilirubin by photoacoustic microscopy

Yong Zhou, Chi Zhang, Da-Kang Yao, Lihong V. Wang, Washington Univ. in St. Louis (United States)

Noninvasive detection of both bilirubin concentration and its distribution is important for disease diagnosis. However, current noninvasive techniques, such as diffuse reflectance spectroscopy and hyperspectral imaging, cannot provide both bilirubin concentration and distribution information at the same time. In this study we implemented, for the first time, multi-wavelength photoacoustic microscopy (PAM) to detect bilirubin distribution. With high accuracy and spatial resolution, PAM has successfully quantified the oxygen saturation of hemoglobin (sO2) based on the different absorption spectra of oxyhemoglobin and deoxyhemoglobin. Similarly, here we show that PAM can also quantitatively map bilirubin distribution. We first demonstrate that our PAM system can measure absorption spectra of bilirubin and blood. Then, based on the absorption spectra, proper wavelengths are selected to measure pure bilirubin samples and bilirubin-blood mixtures. By detecting tissue-mimicking phantoms with various bilirubin concentrations, we show that the root-mean-square error of prediction (RMSEP) reaches 0.52 mg/dL and 0.83 mg/dL for pure bilirubin and for blood mixed bilirubin, respectively. We further image bilirbubin distributions in tissue-mimicking samples both with and without blood. Finally, we showed that bilirubin can be imaged without accuracy degradation down to >400 ?m in depth. Our results show that PAM has the potential to quantitatively image bilirubin in vivo for clinical applications.

8581-119, Session PSun

Novel micromachined silicon acoustic delay line systems for real-time photoacoustic tomography applications

Cheng-Chung Chang, Young Cho, Texas A&M Univ. (United States); Lihong V. Wang, Washington Univ. in St. Louis (United States); Jun Zou, Texas A&M Univ. (United States)

In current photoacoustic tomography (PAT) systems, ultrasound transducer arrays and multi-channel data acquisition (DAQ) electronics are used to receive the PA signals. To achieve real-time PA imaging, massive 1D or even 2D transducer arrays and large number of DAQ channels are necessary. As a result, the ultrasound receiver becomes very complex, bulky and also costly. In this paper, we report the development of novel micromachined silicon acoustic delay line systems, which are expected to provide a new approach to address the above issue. First, fundamental building block structures of the acoustic delay line systems were designed and fabricated. Their acoustic properties were characterized with ultrasound and photoacoustic measurements. Second, two different acoustic delay line systems (parallel and serial) were designed and fabricated using advanced micromachining processes to ensure compact size, high accuracy, and good repeatability. The transmission of multiple acoustic signals in the acoustic delay line systems were studied with both ultrasound and photoacoustic experiments. Experimental results show that the silicon acoustic delay line systems can guide multiple channels of PA signals with low loss and distortion. With the addition of a set of suitable time delays, the time-delay PA signals arrived at a single-element transducer at different times and were unambiguously received and processed by the following DAQ electronics. Therefore, the micromachined silicon acoustic delay line systems can be used to combine multiple signal channels into a single one (without the involvement of electronic multiplexing), thereby reducing the complexity and cost of the ultrasound receiver for real-time PAT application.

8581-120, Session PSun

in vitro and ex vivo evaluation of silica-coated super paramagnetic iron oxide nanoparticles (SPION) as biomedical photoacoustic contrast agent

Rudolf Alwi, Sergey A. Telenkov, Andreas Mandelis, Univ. of Toronto (Canada); Timothy Leshuk, Frank Gu, Univ. of Waterloo (Canada); Sulayman Oladepo, Kirk H. Michaelian, Natural Resources Canada (Canada)

The employment of contrast agents in photoacoustic imaging has gained significant attention within the past few years for their biomedical applications. In this study, the use of silica-coated superparamagnetic iron oxide (Fe3O4) nanoparticles (SPION) was investigated as a contrast agent in biomedical photoacoustic imaging. SPIONs have been widely used as Food-and-Drug-Administration (FDA)-approved contrast agents for magnetic resonance imaging (MRI) and are known to have an excellent safety profile. Using our frequency-domain photoacoustic correlation (the photoacoustic radar) with a modulated laser excitation, we examined the effects of nanoparticle size, concentration and biological media (e.g. serum, sheep blood) on its photoacoustic response in turbid media (intralipid solution). Maximum detection depth and minimum measurable SPION concentration were determined experimentally. The detection was performed using a single element transducer. The nanoparticle-induced optical contrast ex vivo in dense muscular tissues (avian pectus) was evaluated using a phased array photoacoustic probe and the strong potential of silica-coated SPION as a possible photoacoustic contrast agents was demonstrated. This study opens the way for future clinical applications of nanoparticle-enhanced photoacoustic imaging in cancer therapy.

8581-121, Session PSun

Combined photoacoustic and ultrasound imaging of human breast in vivo in the mammographic geometry

Zhixing Xie, Won-Mean Lee, Fong Ming Hooi, J. Brian Fowlkes, Renee W. Pinsky, Dean A. Mueller, Xueding Wang, Paul L. Carson, Univ. of Michigan Medical School (United States)

This photoacoustic volume imaging (PAVI) system is designed to study breast cancer detection and diagnosis in the mammographic geometry in combination with automated 3D ultrasound (AUS). The good penetration of near-infrared (NIR) light and high receiving sensitivity of a broad bandwidth, 572 element, 2D PVDF array at a low center-frequency of 1MHz were utilized with 20 channel simultaneous acquisition. The feasibility of this system in imaging optically absorbing objects in deep breast tissues was assessed first through experiments on ex vivo whole breasts. The blood filled pseudo lesions were imaged at depths up to 49 mm in the specimens. In vivo imaging of human breasts has been conducted. 3D PAVI image stacks of human breasts were coregistered and compared with 3D ultrasound image stacks of the same breasts. Using the designed system, PAVI shows satisfactory imaging depth and sensitivity for coverage of the entire breast when imaged from both sides with mild compression in the mammographic geometry. With its unique soft tissue contrast and excellent sensitivity to the tissue hemodynamic properties of fractional blood volume and blood oxygenation, PAVI, as a complement to 3D ultrasound and digital tomosynthesis mammography, might well contribute to detection, diagnosis and prognosis for breast cancer.

8581-122, Session PSun

Acousto-optic effect with audible sound and its application in classifying hidden colours

Terence S. Leung, Shihong Jiang, Univ. College London (United Kingdom)

Acousto-optic (AO) imaging is an imaging technique which provides spatial distributions of both optical and mechanical properties. It is based on the ultrasonic modulation of light phase with focused ultrasound, whose beam width also determines the spatial resolution. In this work, we investigate a closely related problem, i.e., the interaction between coherent light and audible sound for optical spectroscopy applications.

One major difference between ultrasound and audible sound is that the displacement of scatterers caused by audible sound is much larger (micrometres) than that by ultrasound (nm). The strong acoustic modulation of light phase due to audible sound gives rise to higher harmonics in the time-varying speckle intensity (the AO signal) which can be captured by a four-phase stroboscopic technique originally developed for AO imaging.

Because of the long wavelength, audible sound is not suitable for AO imaging. Here, we introduce a spectroscopy application which aims to classify the colour of an object (paper) hidden behind a 10 mm thick opaque slab with an air gap of 5 mm. Small displacements at 200 Hz were induced in the paper by attaching it to the diaphragm of a loudspeaker. Two coherent lasers (green and red) illuminated the front of the slab in turn, producing acoustically modulated speckle patterns which were captured by a CCD camera. The amplitude of the first harmonic of the AO signal, indicative of the hidden colour, was measured using the stroboscopic technique. The technique is able to classify hidden colours including green, yellow, orange and red.

8581-123, Session PSun

Photoacoustic imaging in the evaluation of laser controlled drug release using gold nanostructure agents

Yao Sun, King C. P. Li, Wake Forest Baptist Medical Ctr. (United States) and The Methodist Hospital Research Institute (United States); Brian E. O'Neill, The Methodist Hospital Research Institute (United States)

This paper presents an in vitro study in photoacoustic evaluation of laser controlled drug release by using gold nanostructure agents. Laser controlled drug release has been studied and reported by using high intensity nanosecond laser source and optical absorbing gold nanostructures. With the same nanosecond laser source in low intensity, photoacoustic imaging technique can be employed to evaluate the laser controlled drug release, which makes it promising to combine low energy photoacoustic imaging/evaluation with high energy laser controlled drug delivery in a non-radiation, low cost and minimum modified theranostic platform. As an effort to test the feasibility, gold nanoparticles and gold nanorods which have strong absorption of laser specifically in 532 nm and 808nm to trig the drug release in carriers were evaluated in high energy laser treatment and low energy photoacoustic imaging. More than 20% drop of the intensity in the photoacoustic images has been observed in both gold nanoparticles solutions and gold nanorods solutions, after being treated by high energy laser. This study suggests that it is possible to evaluate the high energy laser controlled drug release with low energy photoacoustic imaging method in a non-complex theranostic platform.

8581-124, Session PSun

Viewing individual cells and ambient microvaculature using two molecular contrasts

Zhixing Xie, Sung-Liang Chen, Univ. of Michigan Medical School (United States); Xunbin Wei, Shanghai Jiao Tong Univ. (China); Paul L. Carson, Univ. of Michigan Medical School (United States); Xueding Wang, Univ. of Michigan Health System (United States)

To view the individual cells and ambient microvasculature simultaneously will be helpful to study tumor angiogenesis and microenvironments. To achieve this, two molecular contrast mechanisms were exploited simultaneously by integrating two imaging modalities, confocal fluorescence microscopy (CFM) and photoacoustic microscopy (PAM). These share the same scanning optical path and laser source. The induced photoacoustic (PA) signal was detected by a highly sensitive needle hydrophone; while the back-traveling fluorescent photons emitted from the same sample were collected by an avalanche photodetector. Experiments on ex vivo rat bladders were conducted. The CFM image depicted the shape and size of the individual cells successfully. Besides large polygonal umbrella cells, some intracellular components can also be discerned. With the CFM image presenting morphologic cellular information in the bladder wall, the PAM image provides the complementary information, based on the endogenous optical absorption contrast, of the microvascular distribution inside the bladder wall, from large vessels to capillaries. Such multimodal imaging provides the opportunity to realize both histological assay and characterization of microvasculature using one imaging setup. This approach offers the possibility of comprehensive diagnosis of cancer in vivo.

8581-125, Session PSun

Multispectral photoacoustic imaging of tissue denaturation induced by high-intensity focused ultrasound treatment

Yao Sun, King C. P. Li, Wake Forest Baptist Medical Ctr. (United States) and The Methodist Hospital Research Institute (United States); Brian E. O'Neill, The Methodist Hospital Research Institute (United States)

This paper presents an ex vivo study in imaging high-intensity focused ultrasound induced tissue denaturation with multispectral photoacoustic approach. Beef tissues treated by both water bath and high-intensity focused ultrasound were imaged and evaluated by photoacoustic imaging method, where light in multiple optical wavelengths between 700nm and 900nm is applied. Tissue denaturation after being treated by water bath and high-intensity focused ultrasound has been observed in multispectral photoacoustic images. The denaturation is more striking in shorter optical wavelength photoacoustic images than in longer optical wavelength photoacoustic images. Multispectral photoacoustic images of the tissue denaturation were discussed and analyzed in this paper. This study suggests that multispectral photoacoustic imaging method is promising in the evaluation of tissue denaturation induced by high-intensity focused ultrasound treatment.

8581-126, Session PSun

Continuous high-speed volumetric photoacoustic microscopy via a field programmable gate array

Scott P. Mattison, Ryan L. Shelton, Brian E. Applegate, Texas A&M Univ. (United States)

The ability to collect data in real time is important in all biological imaging modalities that aim to image dynamic processes. Photoacoustic Microscopy (PAM) is a rapidly growing biomedical imaging technique that is often used to image microvasculature and melanoma, and is capable of fully rendering three-dimensional images. However, due to the bi-polar nature of the PAM signal, post processing through demodulation is required to accurately display morphological data. Typically, demodulation requires post processing of the data, limiting its use in real-time applications. This results in many PAM systems displaying data through maximum amplitude projection (MAP) images, completely ignoring the axial dimension of their scans and throwing away useful data. We overcome this processing limit by utilizing a configurable integrated circuit known as a Field Programmable Gate Array (FPGA). The FPGA allows us to perform quadrature demodulation of the photoacoustic signal as it is being collected. The result is a PAM system capable of producing continuous, morphologically accurate B-scans and volumes at a rate limited only by the repetition rate of the laser. This allows us to generate accurately rendered volumes at the same speed as MAP images. With a 100 KHz actively q-switched laser we are able to generate 200 by 200 pixel b-scans at a rate of 500 Hz. The imaging potential of the system has been demonstrated in volumes of human hair phantoms and chick embryo vasculature. This system is capable of 50 x 50 x 50 volume stacks processed and displayed at better than video rate.

8581-127, Session PSun

Nonionizing photoacoustic cystography with near-infrared absorbing gold nanostructures as optical opaque tracers

Mansik Jeon, Chulhong Kim, Univ. at Buffalo (United States); Jingyi Chen, Univ. of Arkansas (United States)

Cystography is a routine clinical diagnostic procedure that utilizes ionizing X-rays to visualize urinary bladders. The typical procedure involves voiding urine, injecting a radio-opaque dye (X-ray contrast) via a catheter, and then acquiring X-ray images with a fluoroscope or computed tomography scanner. The obtained X-ray images are used to assess bladder cancer, bladder polyps, vesicoureteral reflux, enlargement of prostate gland, tears in the bladder wall following trauma, obstruction of the ureters or urethra, neurogenic bladder, or hydronephrosis. Despite its relatively simple implementation and high resolution, the X-ray based imaging uses harmful ionizing radiation. Here we demonstrate the feasibility of nonionizing and noninvasive photoacoustic (PA) imaging of urinary bladders using near-infrared absorbing gold nanostructures, gold nanocages (GNCs), as an optical turbid tracer. We have successfully imaged a rat bladder filled with GNCs using a PA imaging system. After transurethral injection of 0.6-pmol GNCs, the PA amplitudes were enhanced by ~2240 % and the accumulation was confirmed by spectroscopic PA imaging. Both in vivo and ex vivo PA imaging results reveal that GNCs were naturally excreted via urination, thus no accumulation of GNCs in the bladder and kidney was observed. The PA cystography with transurethral injection of GNCs provides two crucial safety features over the exiting X-ray method: no radiation exposure and no long-term heavy metal accumulation, which will be keys for clinical translation.

8581-128, Session PSun

High resolution functional photoacoustic computed tomography of the mouse brain during electrical stimulation

MohammadReza NasiriAvanaki, Jun Xia, Lihong V. Wang, Washington Univ. in St. Louis (United States)

Photoacoustic computed tomography (PACT) is an emerging imaging technique which is based on the acoustic detection of optical absorption from tissue chromophores, such as oxy-hemoglobin and deoxy-hemoglobin. An important application of PACT is functional brain imaging of small animals. The conversion of light to acoustic waves allows PACT to provide high resolution images of cortical vasculatures through the intact scalp. Here, PACT was utilized to study the activated areas of the mouse brain during forepaw and hindpaw stimulations. Temporal PACT images were acquired at multiple wavelengths, enabling computation of hemodynamic changes during stimulation. The stimulations were performed by trains of pulses at different stimulation currents (between 1 to 10 mA) and pulse repetition rates (between 0.05 Hz to 0.01Hz). The response at four functional regions on the cortex, i.e., the primary motor cortex, secondary motor cortex, somatosensory cortex-forelimb, and somatosensory cortex-hindlimb, were investigated under various stimulation conditions. The Paxinos mouse brain atlas was used to confirm the activated regions. The study shows that PACT is a promising new technology that can be used to study brain functionality with high spatial resolution.

8581-129, Session PSun

Transvaginal photoacoustic imaging probe and system based on a multiport fiber-optic beamsplitter and a real time imager for ovarian cancer detection

Patrick D. Kumavor, Umar S. Alqasemi, Behnoosh Tavakoli, Hai Li, Yi Yang, Quing Zhu, Univ. of Connecticut (United States)

A real-time coregistered pulse-echo/photoacoustic imaging probe and system for ovarian cancer detection is presented. The probe consists of a transvaginal ultrasound transducer integrated with a high-power custom-made fiber-optic beamsplitting unit. This unit has an input fiber core diameter of 940 microns that is fused to 19 output fibers of 200 microns diameter each, with an overall insertion loss of 1.2 dB. 18 output fibers

are distributed around the transducer for the light delivery during imaging. The remaining fiber is used to monitor and compensate laser output. The energy density delivered by the probe on the tissue surface was measured at the 1/e-point intensity of the beam to be 15 mJ/cm2 for a 20 mJ/pulse input, which is below FDA limit. A light-weight protective frame, measuring 2.5cm in diameter and made of plastic, encloses the array of source fibers; this ensures that fibers do not cause injury to patient. The real-time imager is controlled by a Field Programmable Gate Array (FPGA). The FPGA controls the ultrasound transmission and reception, the photoacoustic data acquisition, the parallel processing and storage of the beam, and the real-time switching between the two modalities. These features make the probe and the system ideal for in vivo studies. The capabilities of the probe were characterized using phantoms made of blood tubing. Images of the phantom taken through a 1cm-thick chicken layer yielded a signal-to-noise ratio of 22dB. Ex vivo images of excised human ovaries showed blood vasculature that compared well with results obtained from H&E histological staining.

8581-130, Session PSun

Estimating oxygen saturation in vivo with photoacoustic imaging: a system developer's perspective

Andrew Needles, James Mehi, Minalini Lakshman, Andrew Heinmiller, Catherine Theodoropoulos, Desmond Hirson, VisualSonics Inc. (Canada)

Photoacoustic (PA) imaging can estimate the spatial distribution of oxygen saturation (sO2) in blood, due to its dependence on optical absorption. This talk will focus on the development of an sO2 imaging mode on a commercial system, emphasizing the practical challenges involved with implementing this parametric imaging technique.

A PA imaging system (Vevo LAZR, VisualSonics, Toronto) was operated using high-frequency linear array transducers with integrated optical fibers (LZ250, LZ550, 21 MHz and 40 MHz respectively, VisualSonics). Data was collected using a dual-wavelength approach (750 and 850 nm) and processed to form estimates of sO2. Blood was extracted from cannulated tail veins of healthy adult rats into polyethylene tubing, while the animal was inhaling either 100% oxygen or 5% oxygen. Oxygen partial pressure (pO2) readings were made in the tubing using the OxyLab pO2 E Series monitor (Oxford Optronix, Oxfordshire, UK), while simultaneously imaging with PA. sO2 estimates were compared to pO2 using the standard dissociation curve (Kelman, 1966).

Previous work (Needles, SPIE 2011) has shown that comparisons to known pO2 values for validating estimates of sO2 provides reasonable correlation (R2 = 0.8), however these estimates were performed offline, relied on averaging, and showed errors as high as 20%. The work presented in this current study was done in real-time on the imaging system. For real-time imaging the biggest issues faced are related to correct estimation of optical attenuation and fluctuations in optical fluence. Characterizations of attenuation and energy monitoring and compensation technology were developed to stabilize fluence estimates. The overall effect was the reduction in sO2 estimation error from the previously reported level of 20%. This improvement provides better reliability and confidence to researchers studying sO2 in preclinical animal models of human disease, while using PA imaging..

8581-131, Session PSun

Deep tissue fluorescence imaging using digitally time-reversed ultrasound-encoded light

Benjamin Judkewitz, Ying Min Wang, California Institute of Technology (United States); Charles A. DiMarzio, Northeastern Univ. (United States); Changhuei Yang, California Institute of Technology (United States)

Scattering of light by thick tissues severely limits our ability to study intact specimens at high resolution. Most current methods disregard scattered light, treating it as noise. The depth limits of these methods are thus related to the amount of ballistic light detected, which decreases exponentially with tissue thickness. However, scattered light contains valuable information. Xu et. al. (Nature Photonics 2011) recently suggested combining ultrasound encoding with time reversal to improve absorption contrast in scattering samples at millimeter resolution. However, to realize deep tissue fluorescence imaging, significant technical challenges need to be overcome – namely 1) the low optical gain of photorefractive crystal based phase conjugate mirrors and 2) the high diffuse background that accompanies the time reversed focus due to incomplete time reversal. Here, we overcome these technical challenges using digital time reversal of ultrasound-encoded light with high optical gain and adaptive background cancellation. We directly demonstrate focusing and fluorescence imaging deep inside biological tissues. We further illustrate the potential of our method for fluorescence bioimaging in the diffusive regime by imaging complex fluorescent objects and tumor microspheres 2.5 mm deep in biological tissues, at an anisotropic lateral resolution of 36 microns by 52 microns. Our results set the stage for a range of applications in biomedical research and medical diagnostics.

8581-132, Session PSun

Modification of a commercially available photoacoustic imaging system for the use of 1064-nm and 532-nm wavelengths to assess photoacoustic contrast agents

Andrew Heinmiller, VisualSonics Inc. (Canada); Kimberly A. Homan, Stanislav Y. Emelianov, The Univ. of Texas at Austin (United States); Adam J. Cole, Sanjiv S. Gambhir, Stanford Univ. (United States); Andrew Needles, Catherine Theodoropoulos, Desmond Hirson, VisualSonics Inc. (Canada)

The use of near-infrared wavelengths for photoacoustic (PA) imaging takes advantage of the relatively low inherent absorption of tissues and has encouraged the development of agents which show high contrast in this range. Here, we describe the modification of a commercially available PA imaging system (Vevo LAZR, VisualSonics, Toronto) to take advantage of the 532nm and 1064nm wavelengths inherent in the generation of the currently tuneable range of 680 to 970nm and in the use of these two wavelengths to assess contrast agents.

The photoacoustic imaging system generated light from a Nd/YAG laser modified to extract the 532 and 1064nm wavelengths in addition to its OPO-derived tuneable range (680 - 970 nm) and deliver this light through a fiber integrated into a linear array transducer (LZ250, VisualSonics).

Gold nanoplates (UT Austin), carbon nanotubes (Stanford U), DyLight 550 (Thermo Fisher) and blood were imaged in a phantom (PE20 tubing) and in a hindlimb subcutaneous tumor in vivo to determine their photoacoustic signal intensity at all wavelengths.

In the phantom and in vivo, all agents caused an enhancement of the photoacoustic signal at their respective peak absorbance wavelengths. These results show that the 532nm and 1064nm wavelengths could prove useful in biomedical imaging due to the contrast agents customized for them. The 1064nm wavelength in particular has the advantage of having very low generation of endogenous signal in vivo, making agents tuned to this wavelength ideal for targeted contrast imaging.

8581-133, Session PSun

Temperature-modulated fluorescence tomography: modulating tissue temperature using HIFU for high-resolution in vivo fluorescence tomography

Tiffany C. Kwong, Yuting Lin, Univ. of California, Irvine (United States); Uma Sampathkumaran, Shaaz Ahmed, InnoSense LLC (United States); Gultekin Gulsen, Univ. of California, Irvine (United States)

Low spatial resolution due to strong tissue scattering is one of the main barriers that prevent the wide-spread use of fluorescence tomography. To overcome this limitation, we previously demonstrated a new technique, temperature-modulated fluorescence tomography (TM-FT), which relies on key elements: temperature sensitive ICG loaded pluronic nanocapsules and high intensity focused ultrasound (HIFU), to combine the sensitivity of fluorescence imaging with focused ultrasound resolution. While conventional fluorescence tomography measurements are acquired, the tissue is scanned by a HIFU beam and irradiated to produce a local hot spot, in which the temperature increases nearly 5K. The fluorescence emission signal measured by the optical detectors varies drastically when the hot spot overlays onto the location of the temperature dependent nanocapsules. The small size of the focal spot (~1mm) up to a depth of 6 cm, allows imaging the distribution of these temperature sensitive agents with not only high spatial resolution but also high quantitative accuracy in deep tissue using a proper image reconstruction algorithm. Previously we have demonstrated this technique with a phantom study with nanocapsules sensitive to 20-25°C range [Lin et al, App. Phys. Letter 2012; Lin et al, JBO 2012]. In this work, we will demonstrate this method with nanocapsules optimized for in vivo animal imaging.

8581-134, Session PSun

Reconstruction in 2D nonhomogeneous photacoustic tomography

Cornelis H. Slump, Univ. Twente (Netherlands); Bernhard J. Hoenders, Univ. of Groningen (Netherlands)

This proposal for a poster contribution, reports in part on a larger study on the existence, uniqueness and stability of photo acoustic inverse source reconstructions for the biomedical application domain. We consider a cylindrical configuration for the experimental setup with a slowly rotating object and fixed positions for laser and ultrasound detectors. This is in essence a 2D problem. We present an analysis of the forward and inverse problem for the acoustical inhomogeneous object with validation by simulation and with reference to the pertinent experiments. The analysis of the imaging and reconstruction is completed with reconstructions from both simulated and experimental data.

The purpose of photo acoustic tomography is the reconstruction of the optical absorption distribution from the ultrasound shockwaves, which emerge by the local absorption of the optical energy from the irradiating laser pulses.

We start with some artificial and theoretically constructed optical absorption distribution examples and describe, combined with the acoustical velocity profile, the forward problem. First, we investigate the conditions for unique reconstruction analytically after some simplifying approximations. Also the full nonlinear problem is treated numerically with an iterative optimization algorithm. Special interest is in absorption distributions combined with velocity profiles that do not radiate when interrogated by the optical pulse. Sensitivity for noise, measuring (averaging) time, resolution of the reconstruction result as function of the number of required projections is indicated. The results are repeated for simulated breast tissue characteristics and the structures likely to be encountered are modeled. We compared results with a breast phantom from the literature.

8581-31, Session 6

Nanoparticle-augmented photoacoustics: signal generation and optimization

Stanislav Y. Emelianov, The Univ. of Texas at Austin (United States)

Photoacoustics (PA) has become a strong addition to the arsenal of biomedical imaging methodologies due to its non-invasiveness, deep tissue penetration, and high spatial and temporal resolution. Nanoparticle-augmented PA adds molecular imaging and even sensing to PA imaging by exploiting the high absorption cross sections of metal - particularly plasmonic - nanoparticles targeted to molecular markers. By using the nanoparticle as the optical absorber, a heterogeneous system is created with stress and thermal processes no longer confined. In nanosystems where thermal transport is dominant, the process of photoacoustic signal generation is not well understood. An analytical solution for the PA pressure generated from a spherically symmetric absorber, coated with a non-absorbing shell, and dispersed in a non-absorbing fluid environment is used to show the dominance of heat transfer from the nanoparticle to the fluid in the PA signal generation; in many cases the signal from the nanoparticle itself can be neglected. The model provides explanations for our recent experimental results that the modulation of the heat transfer from absorber to signal-generating fluid can lead to signal enhancement, and it allows for an estimate of the fluid volume that is most important for signal generation. We contrast the model with existing theoretical descriptions of PA signal generation, and point out the possibilities for signal amplification and contrast enhancement by designing the local environment of the nanoparticle. The results can be the basis for rational PA signal design using the unique features of nanoparticle-augments PA.

8581-32, Session 6

Evaluation of genetically expressed absorbing proteins using photoacoustic spectroscopy

Jan G. Laufer, Charité Universitätsmedizin Berlin (Germany); Amit Jathoul, Martin Pule, Paul C. Beard, Univ. College London (United Kingdom)

Genetically expressed contrast agents are of great interest in the life sciences as they allow the study of structure and function of living cells and organisms. Although fluorescent proteins originally developed for optical imaging have been used for photoacoustic imaging of small translucent organisms, they present disadvantages when used in mammalian organisms. For example, their absorption rarely extends into the near-infrared wavelength region where light penetration through tissue is greatest, and they often exhibit photoinstability, such as photobleaching or transient absorption changes. Novel, non-fluorescent absorbing proteins, called chromoproteins, may become an attractive alternative. In this study, a variety of red-shifted fluorescent proteins and chromoproteins were evaluated in vitro using photoacoustic spectroscopy to assess their photostability. A wavelength tuneable laser system provided nanosecond excitation pulses between 450nm and 680nm with which the samples were illuminated, and a Fabry-Pérot ultrasound sensor was used to detect the resulting photoacoustic waves. By plotting the signal amplitude as a function of wavelength, photoacoustic amplitude spectra were obtained. To test photobleaching, the excitation wavelength was tuned to the absorption peak of the protein and the signal amplitude was recorded as a function of time. The results showed that chromoproteins provide stronger photoacoustic signals, better spectral stability, and exhibit less photobleaching than fluorescent proteins. In addition, the successful expression of a chromoprotein in mammalian cells was demonstrated in a pilot study. This study has shown that chromoproteins are suitable for photoacoustic imaging.

8581-33, Session 6

Quantitative imaging of molecular targets using photoacoustic microscopy

Jason R. Cook, Wolfgang Frey, Stanislav Y. Emelianov, The Univ. of Texas at Austin (United States)

Molecular photoacoustic (PA) imaging uses targeted nanoconstructs and/or dyes to detect, identify, and monitor pathology in diseased tissues. Although the applicability of molecular PA imaging has been demonstrated, quantifying the amount of labeling remains a challenge. To address this problem, we developed a quantitative PA (qPA) imaging technique to locate and quantify molecular sensors. Our approach is based on the linear dependence between the amplitude of the PA pressure wave and the optical absorption by nanoparticle absorbers (NPAs). In the current study, we used a custom qPA nanoscope to demonstrate the ability to quantify iron-oxide NPAs. Initially, the linear dependence of the PA signal with local NPA concentration and fluence was determined in NPA phantoms. The linear dependences were then applied to qPA imaging of cell cultures with various NPA-loading concentrations, and the accuracy was validated using mass spectrometry with errors of less than 10%. Furthermore, qPA imaging of an unstained histology slide of a murine xenograft tumor was performed and compared with optical imaging of the slide stained with Prussian blue (a positive indicator of the presence of iron-oxide NPs). The results showed excellent correlation between pathological and anatomical information. Overall, PA is a powerful in-vivo molecular imaging technique, and the qPA approach can provide a new platform to accurately determine the distribution of molecular indicators of pathological tissue.

8581-34, Session 6

The influence of particle size on the photoacoustic conversion of gold nanorods embedded in biopolymeric scaffold

Lucia Cavigli, Marella de Angelis, Fulvio Ratto, Paolo Matteini, Francesca Rossi, Istituto di Fisica Applicata Nello Carrara (Italy); Sonia Centi, Univ. degli Studi di Firenze (Italy); Roberto Pini, Istituto di Fisica Applicata Nello Carrara (Italy)

Gold nanorods (GNRs) exhibit intense optical absorption bands in the near-infrared (NIR) region of principal interest for applications in biomedical optics, due to the excitation of surface plasmon resonances, which can be tuned according to the particle aspect ratio (AR). The high absorbance of GNRs at their resonance wavelength combined with the inertness of gold make these particles excellent candidates to improve the contrast in photoacoustic (PA) imaging and as phototransducers for the selective photothermolysis of cancer.

Main drawbacks for the application of GNRs as contrast agents in PA applications include their limited photostability. In particular, when GNRs are irradiated with nanosecond laser pulses in resonance with their plasmon oscillations, there may occur phenomena like reshaping into spherical particles, as well as fragmentation at higher laser fluences, which result into dramatic modifications of their optical absorption bands and substantial loss of PA conversion efficiency.

In this contribution we investigate the influence of size on GNRs stability, PA conversion efficiency and the ability to generate vapor bubbles from GNRs embedded in biomimetic scaffolds. GNRs with different average sizes and comparable AR are synthesized and then dispersed into 50-?m-thick chitosan films. The PA conversion efficiency and stability under NIR pulsed irradiation at different laser fluences are investigated, which reveals the occurrence of unique size effects, which are characterized by significant thresholds for the particle deformation and the ignition of vapor bubbles.

We expect these results to provide new inspiration for the design of plasmon resonant nanoparticles for specific PA applications in biomedical imaging and microsurgery.

8581-35, Session 6

A study on magnetic porous nano-silica beads with pore-filled gold nanorods as novel multi-functional contrast agents of photoacoustic imaging

Chih-Tai Fan, National Tsing Hua Univ. (Taiwan); Po-Jung Chen, National Chiao Tung Univ. (Taiwan); You-Yin Chen, National Yang-Ming Univ. (Taiwan); Tzu-Chen Yen, Chang-Gung Memorial Hospital (Taiwan); Dean-Mo Liu, San-Yuan Chen, National Chiao Tung Univ. (Taiwan); Meng-Lin Li, National Tsing Hua Univ. (Taiwan)

Photoacoustic (PA) imaging requires contrast agents which can enhance the contrast and efficiency of tumor targeting, own high photothermal stability and long circulation time, and are effective with low doses in vivo. In this study, we developed magnetic porous nano-silica beads with pore-filled gold nanorods (FeAuNSBs) as a multi-functional contrast agent of photoacoustic imaging. It owns the merits of gold nanorods (AuNRs) with silica coating – high biocompatibility, PA signal amplification and optical tunability for PA signal generation. The magnetic property of its embedded iron oxides is used to enable active tumor targeting, i.e., magnetic targeting. Phantom experiments were performed to confirm the tunability of FeAuNSB's optical absorbance in near-infrared light and demonsrate its magnetic targeting capability and high photothermal stability. Typically, it was found that the wavelength of peak optical absorption was sustained after pulsed laser exposure. In vivo experimental results showed that with the magnetic targeting to a tumor, contrast increase of about 10 dB over the tumor region in PA images was obtained and was higher than 2 dB achieved using conventional AuNRs. Overall, we proved the feasibility of FeAuNSBs as a good tumor targeting contrast agent of PA imaging. Future work will focus on verification of FeAuNSB's performance on photothermal therapy with PA image guidance.

8581-36, Session 6

Photoacoustic signal enhancement using optical vaporization of ICG-loaded nanodroplets

Alexander Hannah, Katheryne E. Wilson, Kimberly A. Homan, Stanislav Y. Emelianov, The Univ. of Texas at Austin (United States)

We have developed an imaging contrast agent – optically triggered nanodroplet, capable of improving ultrasound and photoacoustic imaging contrast as a result of vaporization. Consisting of FDA-approved materials – a perfluorocarbon core with encapsulated indocyanine green (ICG) dye, the nano-sized droplets, irradiated with 740 nm laser light, produce a transient photoacoustic signal of much greater magnitude than the signal from thermoelastic expansion of the droplet alone. The resulting bubbles provide ultrasound contrast. This imaging strategy employs nanoparticles and an external trigger for production of a vaporization photoacoustic signal, enhancing ultrasound and photoacoustic contrast under controlled conditions and safe energy levels.

8581-37, Session 6

Contrast enhancement by simultaneous ultrasound/laser pulse probing of gold nanosphere encapsulated emulsion beads

Kjersta Larson Smith, Chen-Wei Wei, Univ. of Washington (United States); Ivan Pelivanov, Univ. of Washington (United

States) and Moscow State Univ. (Russian Federation); Jinjun Xia, Danilo Pozzo, Thomas J. Matula, Matthew O'Donnell, Univ. of Washington (United States)

A new technique using pulsed laser heating of a nanocomposite contrast agent to stimulate harmonic generation in a scattered probe ultrasound (US) beam is proposed to increase specific contrast based on suppressing undesired background signals. The composite combines an emulsion bead core (250 nm in diameter) with amphiphilic gold nanospheres (GNSs- 12 nm in diameter) assembled at the interface. The absorption spectrum of the clustered GNSs red-shifts to the near infrared range (700 nm) from the typical 520 nm peak of distributed GNSs, enabling their use at depth in tissue. Illuminating the composite with a pulsed laser with appropriately chosen parameters can heat the composite through optical absorption by the GNSs and expand the emulsion droplet to form a bubble. By delivering an US pulse simultaneously or immediately after the laser pulse is delivered, harmonic signals are produced. The results show that a residual nonlinear image created by subtracting a laser-generated photoacoustic (PA) signal from simultaneous US/laser probing of these composites is more than 30 dB higher than that produced by US alone without the laser. Thus, the proposed composite contrast agent can be used not only for enhanced PA imaging, but also for simultaneous nonlinear US imaging, making it possible to dramatically increase the specificity with simultaneous US/laser probing.

8581-38, Session 7

Design considerations for ultrasound detectors in photoacoustic breast imaging

Wenfeng Xia, Daniele Piras, Univ. Twente (Netherlands); Spiridon van Veldhoven, Christian Prins, Oldelft Ultrasound B.V. (Netherlands); Ton G. van Leeuwen, Wiendelt Steenbergen, Srirang Manohar, Univ. Twente (Netherlands)

The ultrasound detector is the heart of a photoacoustic imaging system. In photoacoustic imaging of the breast there is a requirement to detect tumors located a few centimeter deep in tissue, where the light is heavily attenuated. Thus a sensitive ultrasound transducer is of crucial importance. As the frequency content of photoacoustic waves are inversely proportional to the dimensions of the absorbing structures, and in tissue can range from ranging from hundreds of kHz to tens of MHz, a broadband ultrasound transducer is required centered on an optimum frequency.

A single element piezoelectric transducer structurally consists of the active piezoelectric material, front- and back-matching layers and a backing layer. To have both high sensitivity and broad bandwidth, the materials, their acoustic characteristics and their dimensions should be carefully chosen.

In this paper, we present design considerations of an ultrasound transducer for imaging the breast such as the choice of detector output characteristics such as sensitivity and frequency response, and further the selection of active material and matching layers and their geometries. We iterate between simulation of detector performance and experimental characterization of functional models to arrive at an optimized implementation. For computer simulation, we use 1D KLM and 3D finite-element based models. The optimized detector has a large-aperture possessing a center frequency of 1 MHz with fractional bandwidth of more than 80%. The measured minimum detectable pressure is 0.5 Pa, which is two orders of magnitude lower than the detector used in the Twente photoacoustic mammoscope, and the lowest reported value for an ultrasound detector used in photoacoustic breast imaging.

8581-39, Session 7

Microstructured polymer optical fiber interferometric sensor for optoacoustic endoscopic applications

Daniel C. Gallego, Horacio L. Rivera, Univ. Carlos III de Madrid (Spain); Alessio Stefani, Ole Bang, Technical Univ. of Denmark (Denmark)

In the last two decades intravascular ultrasound (IVUS) arise as an important imaging method to visualize atheromatous plaque in the coronary arteries. Vulnerable atherosclerotic plaques (VP) are characterized by the presence a lipid-rich necrotic core, which is soft and mechanically unstable, covered by a thin fibrous cap, which is weakened by inflammation. The rupture of these VP releases the thrombogenic contents of the plaque into the bloodstream resulting in acute myocardial infarction or in a stroke with a high mortality rate. Such events cause the majority of acute cardiovascular events and sudden cardiac deaths, resulting in 17 million fatalities worldwide annually, representing 29% of all global deaths.

An IVUS catheter contains at its tip a transducer or an array of transducers which emits ultrasonic waves and receives the backscattered signal from the tissue. The tomographic views generated allows an accurate determination of location and morphology of atherosclerotic plaque but has a limited specifity for different soft tissue types and therefore to discriminate the plaque composition. Intravascular photoacoustics (IVPA), can complement IVUS information by mapping the optical absorption. In order to achieve a practical IVUS/IVPA catheter is mandatory to have a wideband ultrasonic detector with enough sensitivity despite the necessary miniaturization to be fitted in less than 1mm to pass through thin vasculature.

Detection ultrasound signals by optical techniques, like optical fiber sensors, have many advantages over traditional electrical methods such as immunity to electrical perturbations, large detection bandwidth and higher compactness with the same sensitivity. Our group demonstrated that ultrasonic sensitivity of an interferometric single mode polymer optical fiber sensor (SMPOF) is one order greater than a silica counterpart. However, these SMPOF are not easily commercially available and its performance in terms of loss and coupling light into is very poor what makes them impractical for real implementation. In contrast, microstructured polymer optical fiber (mPOF) can be made endlessly single-mode and presents a relative low loss at visible wavelength regime.

In this paper, we introduce and characterize in the MHz regime two interferometric mPOF sensors based on PMMA and humidity insensitive polymer TOPAS for to be used in an intravascular optoacoustic endoscope. This will be done based on the comparison of sensitivity, dynamic range, frequency bandwidth, spatial resolution and compactness.

8581-40, Session 7

Optical micromachined ultrasound transducer (OMUT) for high frequency imaging

Mohammad Amin Tadayon, Univ. of Minnesota (United States); Shai Ashkenazi, Univ. of Minnesota, Twin Cities (United States)

Piezoelectric ultrasound transducers are at the heart of almost any ultrasonic medical imaging probe. However, their sensitivity and reliability severely degrade in applications requiring high frequency (>20 MHz) and small element size (<0.1 mm). Alternative technologies such as capacitive micromachined ultrasound transducers and optical sensing and generation of ultrasound are being investigated. In this paper, we present our first steps in developing optical micromachined ultrasound transducers (OMUT) technology. OMUTs rely on microfabrication techniques to construct micron-size air cavities capped by an elastic membrane. The membrane functions as the active ultrasound transmitter and receiver. We will describe the design and testing of prototype OMUT

devices which implement a receive-only function.

The cavity detector is an optical cavity which its top mirror is deflected under the application of the pressure. The intensity of a reflected light beam is highly sensitive to displacement of the top membrane if the optical wavelength is at near-resonance condition. Therefore, US pulses can be detected by recording the reflected light intensity. The device sensitivity depends on the top membrane mechanical properties and optical characteristics of the optical cavity. The device was fabricated using SU-8 as a structural material and gold as a mirror. We have developed a new bonding method to fabricate a sealed, low roughness, high quality optical cavity.

The 60?m cavity with the 8.5?m top membrane is tested in water with 25MHz ultrasound transducer. The NEP of the device for bandwidth of 28MHz was 9.25kPa. The optical cavity has a finesse of around 23.

8581-41, Session 7

Optimized high-frequency ultrasonic transducer design for laser-scanning photoacoustic ophthalmoscopy

Teng Ma, The Univ. of Southern California (United States); Xiangyang Zhang, Univ.of Southern California (United States); Ruimin Chen, K. Kirk Shung, Shuliang Jiao, Qifa Zhou, The Univ. of Southern California (United States)

Photoacoustic ophthalmoscopy (PAOM) is an emerging high resolution three-dimensional imaging technology based on optical absorption contrast to accomplish high speed in vivo imaging of retinal micro-vasculature and retinal pigment epithelium. Moreover, it offers the unique optical-absorption information of retina without mechanically scanning of the ultrasonic transducers. With these attributes, PAOM could potentially contribute to the diagnosis of many retinal diseases, such as diabetic retinopathy and age-related macular degeneration. The image quality is directly related to the geometry and receiving sensitivity of the high-frequency ultrasonic transducer. To insure closer contact with the eyelid during the in vivo experiment, the ultrasonic transducer is optimized to have small aperture size, very high receiving sensitivity and large field of view without blocking the laser light. Results from 20MHz to 40MHz miniature transducers show that lower frequency (20MHz) transducer could provide the highest detection sensitivity with satisfactory axial resolution. Additionally, press-focusing technique could generate a more diverged beam in the far field, which enlarges the field of view of ultrasonic transducer with a trade-off of detection sensitivity. In this work, we will present our optimized design of the high frequency ultrasonic transducer for PAOM including material selection, frequency selection, and fabrication process. In vivo images of rat retina were acquired and quantitatively studied to demonstrate the optimized design. Lastly, we discuss the current limitations of single-element transducer, and consider the future development of 2D array for photoacoustic application.

8581-42, Session 7

Optical detection of ultrasound using AFC-based quantum memory technique in cryogenic rare earth ion doped crystals

Luke R. Taylor, Univ. of Otago (New Zealand); David L. McAuslan, Univ. of Queensland (Australia); Jevon J. Longdell, Univ. of Otago (New Zealand)

We present results of a novel and highly sensitive technique for the optical detection of ultrasound using frequency-selective storage in an atomic frequency comb (AFC) based quantum memory.

The ultrasound ‘tagged’ optical sidebands are absorbed within a pair of symmetric AFCs, generated via optical pumping in a Pr3+:Y2SiO5 sample (tooth separation ? = 150 kHz, comb finesse fc ~ 2 and optical depth ?L ~ 2), separated by twice the ultrasound modulation frequency (1.5 MHz) and centered on either side of a broad spectral pit (2 MHz width), allowing transmission of the carrier. The stored sidebands are recovered with 10-20% efficiency as a photon echo (as defined by the comb parameters), and we demonstrate a record 49 dB discrimination between the sidebands and the carrier pulse, high discrimination being important for imaging tissues at depth.

The technique is both considerably more sensitive than other techniques, and remains immune to speckle decorrelation. Indeed, we further demonstrate detector limited sensitivity of the same (~29 dB) using a highly scattered beam, and apply the technique to the imaging of a phantom immersed in a scattering medium, representative of a biological tissue sample.

Our results strongly suggest the suitability of this technique for high-resolution non-contact non-destructive in vivo deep tissue imaging.

8581-43, Session 7

Single-cell photoacoustic thermometry

Liang S. Gao, Lidai Wang, Chiye Li, Haixin Ke, Lihong V. Wang, Washington Univ. in St. Louis (United States)

Intracellular temperature sensing is an essential technique for understanding cellular thermodynamic behavior during events such as division, gene expression, and enzyme reaction. Although nano-scale thermocouple and temperature-sensitive fluorescence biosensors have been employed in single-cell thermometry, they present problems such as sensitivity to solution pH values and toxicity to cells. In addition, since most of these temperature-sensitive biosensors are custom-developed, currently single-cell thermometry is limited to a few labs.

Here, we present novel single-cell photoacoustic thermometry (SCPT) for studying the intracellular thermodynamics. With 3 seconds per frame imaging speed, a temperature resolution of 0.2 ? C was achieved in a photo-thermal cell heating experiment. Since the sensitivity to the local temperature in SCPT arises from the photoacoustic generation mechanism, SCPT features the unique advantage that any commercially available absorptive dyes or particles—even endogenous absorbers—can be used as the cellular temperature sensor. This advantage greatly simplified the experimental procedures and setup in the demonstrated cancer cell photo-thermal heating experiment, compared to the fluorescence-based approach (Nature Photonics, 6, 346, 2012). To the best of our knowledge, for the first time, SCPT enables simultaneous high-resolution imaging and temperature sensing of single cells without depending on custom-developed temperature-sensitive biosensors. This technique should facilitate the conversion of single-cell thermometry into a routine lab tool and make it accessible to a much broader biological research community.

8581-44, Session 7

Wideband robust optical detector of ultrasound for intravascular applications

Amir Rosenthal, Stephan Kellnberger, Miguel Angel Araque Caballero , Daniel Razansky, Vasilis Ntziachristos, Helmholtz Zentrum München GmbH (Germany)

Optical sensors of ultrasound are a promising alternative to piezoelectric techniques. Specifically, fiber-based sensors are attractive for intravascular optoacoustic imaging because of their miniature size and optical transparency. One of the major limitations of optical sensing technology is its susceptibility to environmental conditions, e.g. changes in pressure and temperature, which may saturate the detection. Additionally, the acoustic impendence mismatch between the fiber and water may lead to acoustic resonances, which limit imaging capabilities.

In this work a fiber-based optical sensor of ultrasound is demonstrated. The sensor is based on a pi-phase-shifted fiber Bragg grating with an effective sensing length of approximately 350 µm. A novel technique for optical readout of the sensor is developed which is based on pulse

interferometry. In contrast to standard coherent continuous-wave interrogation techniques, no locking of the laser's wavelength to the sensor's wavelength is required: The pulses possess a wide spectrum which covers the grating's notch under all practical conditions, enabling stable performance under strong external perturbations.

The new technique enables robust ultrasound detection under external perturbations and exhibits sensitivity equivalent to that of standard coherent continuous-wave techniques. A detection bandwidth of 30 MHz was demonstrated, comparable with intravascular piezoelectric transducers. Additionally, despite acoustic impendence mismatches, the sensor exhibited an orderly, resonance-free spatio-temporal response in the frequency band 6 MHz – 30 MHz, facilitating imaging applications.

8581-45, Session 8

Fundamental limitations on the sensitivity of photoacoustics

Amy M. Winkler, Konstantin I. Maslov, Lihong V. Wang, Washington Univ. in St. Louis (United States)

Recently, a number of optical imaging modalities have achieved single molecule sensitivity, including photothermal imaging, stimulated emission microscopy, ground state depletion microscopy, and transmission microscopy. These optical techniques are based on optical absorption contrast, extending single-molecule detection to non-fluorescent chromophores. Photoacoustics is a hybrid technique that utilizes optical excitation and ultrasonic detection, allowing it to scale both the optical and acoustic regimes with 100% sensitivity to optical absorption. However, the sensitivity of photoacoustics is limited by thermal noise. Due to background acoustic black body radiation in the medium itself at room temperature, even optical detection schemes are subject to this limitation. In this paper, we investigate the molecular sensitivity of photoacoustics, both theoretically and experimentally. We demonstrate a sensitivity of 100,000 methylene blue molecules for narrowband continuous wave photoacoustics (4,200 molecules estimated under optimum conditions) and 60 million methylene blue molecules for pulsed photoacoustics (30 million estimated under optimum conditions for a 50 MHz bandwidth). For oxygenated hemoglobin, we demonstrate a sensitivity of 86,000 molecules using narrowband continuous wave photoacoustics and extrapolate a sensitivity of 660 molecules under optimum conditions. The possibility of pushing the sensitivity of photoacoustics to the single molecule limit is discussed.

8581-46, Session 8

All-optical ultrasound detection using glancing angle deposited (GLAD) nano-structured films

Parsin Haji Reza, Kathleen M. Krause, Michael J. Brett, Roger J. Zemp, Univ. of Alberta (Canada)

We demonstrate, an all-optical Fabry-Perot-interferometer ultrasound detector using glancing angle deposition (GLAD) films. GLAD is a single-step physical vapor-deposition (PVD) technique used to fabricate nanostructured thin films. Using titanium dioxide (TiO2), a transparent conductor with a high refractive index (n = 2.4), the GLAD technique can be used to fabricate samples with tailored refractive index periodicities with a high level of control and hence provide customized high Q-factor reflectance spectra. Additionally, the average acoustic impedance of the films can be lower than bulk materials stacks which will improve acoustic coupling, – especially for high acoustic frequencies.

Two identical filters with high reflection (~ 95%) in the C-band range and transparent in the visible range (~80%) using GLAD films are fabricated. A 22µm Parylene C layer is sandwiched by these two GLAD films in order to form a Fabry Perot Interferometer (FPI). A high speed tunableing CW C-band laser is focused at the Fabry Perot Interferometer and the reflection is measured using a high speed photodiode. The ultrasound pressure will modulate the optical thickness of the FPI and hence its reflectivity. These reflections are proportional to ultrasound pressure.

The Fabricated sensor was tested by using a 10MHz unfocused transducer. The ultrasound transducer has been previously calibrated using a hydrophone. The minimum detectable acoustic pressure is measured as ~0.2 kPa and the frequency response is ~ 40MHz. Improved sensitivity and bandwidth are expected with further FPI optimization. We demonstrate the utility of the detector for optical-resolution photoacoustic microscopy (OR-PAM) using a 532-nm fiber-laser as excitation source.

8581-47, Session 8

Photoacoustic tomography using parallel acoustic delay lines

Murat Yapici, Khalifa Univ. of Science, Technology and Research (United Arab Emirates); Chulhong Kim, Univ. at Buffalo (United States); Cheng-Chung Chang, Texas A&M Univ. (United States); Mansik Jeon, Univ. at Buffalo (United States); Zijian Guo, Xin Cai, Washington Univ. in St. Louis (United States); Jun Zou, Texas A&M Univ. (United States); Lihong V. Wang, Washington Univ. in St. Louis (United States)

Achieving real-time photoacoustic (PA) tomography typically requires multi-element ultrasound transducer arrays and their associated multiple data acquisition (DAQ) electronics to receive PA waves simultaneously. In this paper, we report the first demonstration of a photoacoustic tomography (PAT) system using optical fiber-based parallel acoustic delay lines (PADLs). By employing PADLs to introduce specific time delays, the PA signals (on the order of a few micro seconds) can be forced to arrive at the ultrasonic transducers at different times. As a result, time?delayed PA signals in multiple channels can be ultimately received and processed in a serial manner with a single?element transducer, followed by single?channel DAQ electronics. Our results show that an optically absorbing target in an optically scattering medium can be photoacoustically imaged using the newly developed PADL-based PAT system. Potentially, this approach could be adopted to significantly reduce the complexity and cost of ultrasonic array receiver systems. Once fully developed and optimized, the PADL approach could be applied to enhance the clinical applications of real?time 2?D or even 3?D photoacoustic and ultrasound imaging with significantly reduced system cost.

8581-48, Session 8

Photoacoustic imaging with orthogonal reflecting detector arrays

Benjamin T. Cox, Univ. College London (United Kingdom); Leonid Kunyansky, The Univ. of Arizona (United States)

In recent years, high resolution photoacoustic images have been obtained using data recorded by Fabry-Perot sensor arrays, due to their wide bandwidth, high sensitivity and small sensor element size. These optically-addressed arrays are planar, and the high image quality has been obtained despite the fact that data from a planar array of finite extent can never give an exact PA image. This raises the exciting possibility that even higher quality images may be obtained by choosing an improved sensor array configuration. One way to achieve this without losing the advantages that the Fabry-Perot sensor offers is through a combination of two or more planar arrays arranged orthogonally. Such an arrangement poses a new challenge: in photoacoustic image reconstruction it has usually been assumed that the sensors do not affect the sound field and therefore reconstruction algorithms typically assume free space boundary conditions (ie. no boundaries). However, as the FP sensors are solid reflecting surfaces this is no longer the case and the reflections must be explicitly taken into consideration during the reconstruction. (This is also true of other types of planar array, eg.

piezoceramic, CMUT, and so this paper applies to those cases too.) A fast, Fourier-based exact reconstruction algorithm for cases such as this will be described and demonstrated.

8581-50, Session 8

Light emitting diodes as an excitation source for photoacoustic imaging

Thomas J. Allen, Paul C. Beard, Univ. College London (United Kingdom)

Semiconductor light sources, such as laser diodes or light emitting diodes (LEDs) could provide an inexpensive and compact alternative to traditional Q-switched lasers for photoacoustic imaging. So far, only laser diodes have been investigated for this purpose. It is here suggested that high power LEDs could provide a significantly cheaper alternative, as LEDs are typically an order of magnitude cheaper than laser diodes with some high power devices available for a few dollars. LEDs provide the advantage of being widely available in the visible wavelength range (400nm to 632nm) where blood is strongly absorbent (>10cm-1) and water absorption is weak (<0.01cm-1). Operating at these wavelengths could allow high contrast photoacoustic images of the superficial vasculature to be achieved. High power LEDs are generally operated in continuous wave mode and provide average powers of 1 or 2W. Two driving methods have been investigated in order to use these devices in pulsed mode for photoacoustic imaging. The first method investigated over driving by 10 to 100 times at a low duty cycle (<0.01%) and offers the prospect of achieving similar pulse energies (?10µJ) to that provided by high peak power pulsed laser diodes. The second method explored the possibility of using coded excitation schemes such as Barker codes and Golay codes to maximise the energy deposited in the tissue without compromising the bandwidth of the generated photoacoustic signals. In the first instant, experiments were undertaken to determine the maximum pulse energy which could be obtained from off-the-shelf LEDs when being over driven and the effect this had on their lifespan. Subsequently, these excitation sources were combined with a photoacoustic scanning system and both driving methods were used to image tissue mimicking phantoms as well as the micro-vasculature of the palm of a hand. This study demonstrated that LED could be used as an inexpensive and compact excitation source able to image superficial microvasculature.

8581-51, Session 8

High-efficiency time-reversed ultrasonically encoded optical focusing using a large area photorefractive polymer

Yuta Suzuki, Xiao Xu, Puxiang Lai, Lihong V. Wang, Washington Univ. in St. Louis (United States)

Time-reversed ultrasonically encoded (TRUE) optical focusing focuses light beyond one transport mean free path by phase-conjugating the ultrasonically tagged light. However, in previous works, only a small portion of the tagged light was phase-conjugated by using a photorefractive BSO crystal, due to its small active area (1?1 cm^2). In this work, we report high-efficiency TRUE focusing using a large area photorefractive polymer (5?5 cm^2), which demonstrated ~40 times increase in focused energy. Further, we imaged absorbers embedded in a turbid sample of thicknesses up to ~12 transport mean free paths.

8581-52, Session 8

Frequency domain photoacoustic tomography with a near-IR laser diode

Sergey A. Telenkov, Andreas Mandelis, Univ. of Toronto (Canada)

Tomographic implementation of the frequency domain photoacoustic method with a near-IR (808nm) laser diode as an optical source will be reported. The developed Photoacoustic Radar system features chirp-modulated laser excitation, 128-element concave transducer array rotating around the test specimen and a cross-correlation signal processing algorithm for spatially-resolved image formation. System characterization was carried out using tissue simulated phantoms with embedded optical contrast inclusions positioned at depths up to 3 cm. Feasibility of three-dimensional imaging of optical contrast using this frequency domain photoacoustic method was demostrated. Potential clinical applications of the proposed system may include breast cancer imaging and will be discussed in this presentation.

8581-53, Session 8

X-ray induced photoacoustic tomography

Liangzhong Xiang, Bin Han, Stanford Univ. (United States); Colin M. Carpenter, Stanford Univ. School of Medicine (United States); Lei Xing, Stanford Univ. (United States)

X-ray induced photoacoustic tomography (X-PAT) is proposed as a new biomedical imaging modality based on the selective x-ray excitation and ultrasound detection of X-ray-excitable photoacoustic signal. The photoacoustic effect results from the thermalization of the excited Auger electrons and photoelectrons. Both X-rays and ultrasound propagate long distances in tissue, it is particularly well suited for in vivo clinical relevant biomedical imaging.

In X-PAT, tomographic images are generated by irradiating the subject using a sequence of programmed X-ray pulsed beams, while sensitive ultrasound detectors measure the ultrasound emission out of the subject. Because X-rays do not scatter in tissue as much as optical photons, it has a very high penetration depth in biological tissue and provides a way to break through the 'hard depth limit' of optical imaging. The spatial resolution of the system can be made as high as needed by narrowing the beam aperture. In particular, 1 mm spatial resolution was achieved for a 1-mm-wide X-ray beam. In the theoretical part, we provide the formulas for both the forward and inverse problems of X-PAT and estimate the signal amplitude in biological tissues. In the experimental part, the experiment setup and methods are introduced and the signals and the image of a metal object by means of X-PAT are presented. The promising pilot experimental results suggest the feasibility of the proposed X-PAT approach.

8581-54, Session 8

in vivo universal flow cytometry integrating photoacoustic and fluorescence detection schematics

Dmitry A. Nedosekin, Mustafa Sarimollaoglu, Stephen B. Foster, Ekaterina I. Galanzha, Vladimir P. Zharov, Univ. of Arkansas for Medical Sciences (United States)

In vivo flow cytometry is a novel research tool which can provides noninvasive, real-time monitoring of circulating nanoparticles, normal and abnormal cells or drug delivery vehicles directly in the bloodstream, lymph flow or cerebrospinal fluid . This tool utilizes various detection platforms including photothermal (PT), fluorescence, photoacoustic (PA), or Raman techniques. However, the use of only one technique limits the range of objects to those with either non-radiative or radiative relaxation of the absorbed energy. This also restricts the number of tags available for multiplex targeting due to the overlapping of broad absorption or emission spectra. In particular, in vivo photoacoustic (PA) and fluorescence flow cytometry were previously used separately only using pulsed and continuous wave lasers, respectively, and preferentially positive contrast mode only. Herewith, we present an integrated platform combining PA and fluorescence detection techniques with positive and negative contrast modes for in vivo simultaneous detection of probes and cells with weak and strong absorption and fluorescent properties. The features, parameters and applications of this unique biological tool

are discussed. The applications include detection of liposomes loaded with florescent dye, B16F10 melanoma cells with intrinsic melanin and green fluorescent protein (GFP) as , C8161-GFP melanoma cells targeted by magnetic nanoparticles, MTLn3 adenocarcinoma cells expressing novel near-infrared iRFP protein, and quantum dot-carbon nanotube conjugates. The use of pulsed laser for time-resolved discrimination of objects with long fluorescence lifetime (e.g., quantum dots) from shorter autofluorescence background (e.g., blood plasma) is also highlighted. The supplementary nature of PA and fluorescence detection methods increased the versatility of the integrated tool for simultaneous detection of probes and cells having various absorbing and fluorescent properties, and provided verification of PA data, especially novel labeling of cells by conjugated nanoparticles directly in the bloodstream using a more established fluorescence-based technique.

8581-55, Session 8

Negative dynamic photoacoustic contrast: principle and application

Ekaterina I. Galanzha, Mustafa Sarimollaoglu, Dmitry A. Nedosekin, Vladimir P. Zharov, Univ. of Arkansas for Medical Sciences (United States)

Recently we introduced a negative, photocoustic (PA) contrast for label-free imaging and detection of low absorbing objects in a strong absorption background. Here we propose a novel, dynamic, negative contrast mode to increase PA sensitivity and resolution, and use new types of negative PA contrast agents. We also extended the principle of negative dynamic contrast on photothermal (PT) and fluorescent techniques and combined all methods in one universal tool to study cells with various absorption properties. The unique capability of these techniques has been demonstrated with focus on ultrasensitive and noninvasive detection of circulating single cancer cells, leukocytes and cell aggregates (clots) including clots as early diagnostic and prognostic biomarkers of cardiovascular disorders. Specifically, using preclinical mouse models of myocardial infarction and human blood samples, we observed that PA negative contrast can be used for detection of low-absorbing circulating clots by (i.e., signals from clots are below the background of blood) with the size down to 20 ?m. We demonstrated that the combination of this phenomenon with positive contrast can significantly extend the variety of detectable morpho-functional types of clots including white, red, and mixed (pink) clots. Taking into account the safe nature of the proposed biotechnology, we anticipate its quick translation for the use in humans.

8581-56, Session 8

Investigation into alternative sources of positive and negative contrast for thermoacoustic imaging

Olumide Ogunlade, Paul C. Beard, Univ. College London (United Kingdom)

In thermoacoustic imaging, the contrast results from the difference in dielectric properties of tissues. This dielectric contrast is due to the difference in water content and ionic content of various tissues. Traditionally, thermoacoustic imaging is based on positive contrast, that is, the high absorption of microwave energy of an inclusion of higher conductivity relative to a background. An example of this is a tumour in a fat dominated breast tissue, where the contrast in conductivity can be as much as a factor of three.

In this study, we investigate the of negative contrast where a weak microwave absorber is surrounded by a highly absorbing background. Such contrast could be endogenous, such as a lipid rich nerve sheath in surrounding high water content tissue. Negative contrast could also be due to the use of exogenous contrast agents which decrease the effective conductivity of tissue to which they aggregate. Previous investigations on contrast agents for thermoacoustic imaging have tended to focus on the use of contrast agents which provide positive contrast by increasing the effective conductivity of the tissue.

We characterise a number of positive and negative contrast agents by measuring their conductivity using a microwave resonator. The contrast agents include commercial MRI contrast agents, air filled microbubbles, as well as novel engineered lipid loaded agents. We then conduct thermoacoustic imaging experiments at 3GHz on realistic tissue mimicking phantoms using a cylindrical scanning system, before and after the introduction of these contrast agents. Thermoacoustic signals and reconstructed images will be presented to give an indication of the tissue discrimination obtainable, with these agents, in thermoacoustic imaging.

8581-57, Session 8

Vibrational photoacoustic imaging with a Ba(NO3)2 crystal based Raman laser

Rui Li, Mikhail N. Slipchenko, Purdue Univ. (United States)

With optical absorption as a contrast and ultrasonic resolution, photoacoustic (PA) tomography has been successfully applied to map animal or human organs such as breast, brain and skin. Over the past, the majority of the PA imaging studies has been using electronic absorption as the contrast. Recently, vibrational photoacoustic (VPA) imaging, which employs molecular overtone vibration as contrast mechanism, opens a new avenue for deep tissue bond-selective imaging. In particular, overtones of C-H bond vibration have been adopted to visualize lipid and collagen. In order to resonate with C-H bond vibration, laser wavelengths at 1210 nm or 1730 nm are used, where the absorption peaks of the second and first overtone reside. Currently, optical parametric oscillator (OPO) pumped by Nd:YAG laser is employed to generate the needed wavelengths. However, the OPO conversion efficiency at the above-mentioned specific wavelengths is quite low, making it difficult to generate high pulse energy needed for VPA tomography. In addition, the cost of OPO often exceeds that of the pump laser. Herein, We demonstrate for the first time the construction and use of a Ba(NO3)2 crystal based Raman laser for photoacoustic imaging of C-H overtone vibration. Using a Nd:YAG laser as the pumping source, up to 21.4 mJ pulse energy at 1197 nm was obtained, corresponding to a conversion efficiency of 34.8%. Three-dimensional photoacoustic imaging of intramuscular fat was performed to prove the concept of using a Raman laser to map lipid distribution in biological tissues. Our method holds great potential for vibrational photoacoustic tomography.

8581-58, Session 8

Optical phase conjugation applied to acousto-optic imaging of thick scattering media with a Nd:YVO4 gain medium

Baptiste Jayet, Institut Langevin (France); Jean-Pierre Huignard, Jphopto (France); Francois Ramaz, Institut Langevin (France)

Acousto-optic imaging is a technique using the modulation of light by ultrasound to probe the local optical properties of thick scattering media at visible or near IR wavelength with a millimetric resolution [1]. As the modulation frequency (a few MHz) is very small compared to the light frequency (several 100THz), a standard spectral filtering is hard to set up. A solution is to use detection techniques based on two or four wave mixing (phase conjugation) in nonlinear crystals to perform a wavefront adaption of the modulated light in order to detect it on a large area single detector.

Up to now, nonlinear photorefractive crystals (such as BSO or LiNbO3) were used for phase conjugation [2,3]; we demonstrate here the use of a new kind of crystal (Nd:YVO4), which exhibits a high gain @1064nm. As the local amplification gain depends on light intensity, if the crystal is illuminated with the interference pattern of a signal and a reference beam, the spatial modulation of the intensity will create a spatial modulation of gain in the crystal which can be seen as a gain hologram. Then, there

are two ways of detecting the acousto-optical signal. Either we use the diffraction of the reference beam (two-wave mixing) or the diffraction of a counter-propagating reference beam to generate the phase conjugate beam (four-wave mixing [4]).

The use of a Nd:YVO4 crystal enables to detect an acousto-optical signal through several millimetres of a living tissue with a response time around 90µs; much faster than the response time of a photorefractive crystal (around 10ms). This makes the gain media much more robust against speckle decorrelation in biological samples.

References

[1] S. Farahi, G. Montemezzani, A. A. Grabar, J.P. Huignard and F. Ramaz, “Photorefractive acousto-optic imaging in thick scattering media at 790nm with a SPS:Te crystal”, Opt. Lett., vol. 35, pp.1798-1800 (2010)

[2] P. Lai, X. Xu and L.V. Wang, “Time-reversed ultrasonically encoded optical focusing in biological tissue”, J. Biomed. Opt 17, 030506 (2012)

[3] Z. Yaqoob, D. Psaltis, M.S. Feld and C. Yang, “Optical phase conjugation for turbidity suppression in biological sample”, Nat photonics 2, 110-115 (2008)

[4] A. Brignon, L. Loiseau, C. Larat, J.-P. Huignard, J.-P. Pocholle, “Phase conjugation in a continuous-wave diode-pumped Nd :YVO4 laser”, Appl. Phys. B 69, 159-162 (1999)

8581-59, Session 8

Photoacoustic thermal diffusion flowmetry in tissue-mimicking phantoms

Adi Sheinfeld, Avishay Eyal, Tel Aviv Univ. (Israel)

We have recently introduced a new blood-flow measurement technique termed photoacoustic thermal diffusion flowmetry (PA-TDF). It utilizes photothermal heating and photoacoustic temperature monitoring to measure the tissue thermal conduction and convection time constants from which the blood velocity can be inferred.

Until now PA-TDF was only demonstrated in water immersed single tubes using CW modulation. In this work we extended our study to tissue-mimicking phantoms with multiple vessels at various diameters, structures and depths and experimentally verified the relations between the estimated time constants and the vessels and illuminating beam dimensions. We also demonstrated, for the first time, depth-resolved PA-TDF measurement using tone-burst PA excitation.

A pair of fiber-coupled, directly-modulated, 830nm laser diodes were used for excitation, one generated slow temperature oscillations (<10Hz) and the other induced the PA excitation. The phantoms were composed of agar and 1% intralipid solution, yielding scattering similar to soft tissue. 0.25mm and 1mm diameter tygon tubes, either single or bundles, were embedded at depths of 1-4mm and blood was driven into the tubes at velocities between 1-11 mm/sec. Frequency scan of the photothermal modulation yielded the system modulation frequency response. The results were fitted to Lorentzian curves to estimate the heat clearance time constants and the corresponding blood velocities. The measurement also yielded an effective heat clearance length which agreed well with the beam width in the phantom, as evaluated from Monte-Carlo simulation. The conduction time constants were found to be proportional to the ratio between the illuminated tube volume and its surface area.

8581-60, Session 8

Bayesian-based weighted optoacoustic tomographic reconstruction in acoustic scattering media

Xosé Luis Deán-Ben, Vasilis Ntziachristos, Daniel Razansky, Helmholtz Zentrum München GmbH (Germany)

The high optoacoustic resolution at depths beyond the diffusive limit of light stems from the low scattering of sound, as compared to photons, within biological tissues. However, some biological samples contain strongly mismatched tissues such as bones or lungs that generally produce acoustic reflections and scattering, and image distortion is consequently produced by assuming an acoustically homogeneous medium. We describe herein a statistical procedure to modify the reconstruction algorithms in order to avoid such distortion. The procedure is based on weighting the contribution of the collected optoacoustic signals to the reconstruction with the probability that they are not affected by reflections or scattering. A rough estimation of such probability by considering an area enclosing the sample allows significantly reducing the artefacts associated to acoustic distortion. Furthermore, the available structural information of the imaging sample can be incorporated in the estimation of the distortion probability, in a way that a further improvement in the quality of the reconstructed images is achieved. The benefit of the reconstruction procedure described herein is showcased by reconstructing tissue mimicking phantoms containing air-gaps and small animals containing several acoustically mismatched regions. In all cases, the image artefacts produced when no weighting is done are significantly reduced.

8581-99, Session 8

Functional photoacoustic ocular imaging

Shuoqi Ye, Peking Univ. (China) and Shanghai Jiaotong Univ. (China); Ning Wu, Peking Univ. (China); Qiushi Ren, Peking Univ. (China) and Shanghai Jiaotong Univ. (China); Changhui Li, Peking Univ. (China)

Ocular imaging plays a key role for the diagnosis of various ocular diseases. In this work, we have developed an ocular imaging system based on the photoacoustic tomography. This system has successfully imaged the entire eye of a mouse, from its iris to the retina region, and the imaging is label-free and non-invasively. In addition to the structural imaging, functional information, such as the oxygen saturation, can be also obtained with the spectroscopic imaging. The resolution of this system reaches several micron meters, allowing the study of microstructures in various ocular tissues. Our system has a potential to be a powerful non-invasive imaging method for ophthalmology.

8581-135, Session PMon

Modeling detector effects on optical phase conjugation of an ultrasonically encoded signal

Joseph L. Hollmann, Charles A. DiMarzio, Northeastern Univ. (United States)

Scattering in tissue limits the depth to which light may be focused, effectively limiting the use of optics in both diagnostic imaging and therapeutics. It has been shown the scattering effect may be reduced utilizing adaptive optics. A low-power optical signal is utilized to interrogate tissue. A focused ultrasound (US) beam modulates the optical signal that has traversed its waist, adding a frequency shift to it. The sidebands are then demodulated effectively isolating light that has traversed the US beam. Optical phase conjugation of these sidebands will then force light to retrace its trajectory and focus back at the US beam waist.

However, any real detection system will not be able to capture the entire emitted probe field due to numerical aperture and pixel and detector size limitations. This talk will analyze the portion of the phase signal necessary for successful focusing utilizing phase conjugation by simulating varying numerical apertures and detector placements against the performance of optical phase conjugation.

8581-136, Session PMon

A novel fiber laser development for photoacoustic microscopy

Seydi Yavas, Bilkent Univ. (Turkey); Esra Aytac Kipergil, Bogaziçi Üniv. (Turkey); Burcin M. Unlu, Bogaziçi Univ. (Turkey); Fatih Ö. Ilday, Bilkent Univ. (Turkey)

Photoacoustic microscopy (PAM), as an imaging modality, has shown promising results in imaging angiogenesis and cutaneous malignancies like melanoma, revealing systemic diseases including diabetes, hypertension, tracing drug efficiency and assessment of therapy, monitoring healing processes such as wound cicatrization, brain imaging and mapping. Clinically, PAM is emerging as a capable diagnostic tool. Parameters of the laser used in PAM, particularly, pulse duration, energy,pulse repetition frequency (PRF), and pulse-to-pulse stability affect signal amplitude and quality, data acquisition speed and indirectly, spatial resolution. Lasers used in PAM are typically Q-switched lasers, low-power laser diodes, and recently, fiber lasers. Significantly, the key parameters cannot be adjusted independently of each other, whereas microvasculature and cellular imaging, e.g., have different requirements. Here, we report an integrated fiber laser system producing nanosecond pulses, covering from 600 nm to 1300 nm, developed specifically for photoacoustic excitation. The system comprises of Yb-doped fiber oscillator and amplifier, an acousto-optic modulator (AOM) and photonic-crystal fiber to generate supercontinuum. Complete control over the pulse train, including generation of non-uniform pulse trains, is achieved via the AOM through custom-developed field-programmable gate-array (FPGA)electronics. The system is unique in that all the important parametersare adjustable: pulse duration(1-3ns), energy (up to 10 ?J),repetition rate(50 kHz-3 MHz). Different photocoustic imaging probes can be excited with the ultrabroad spectrum. The entire system is fiber-integrated;guided-beam-propagation rendersit misalignment free and largely immune to mechanical perturbations. The laser is robust,low-cost and built using readily available components.

8581-138, Session PMon

Photoacoustic assessment of oxygen saturation: effect of red blood cell aggregation

Eno Hysi, Ryerson Univ. (Canada) and Louisiana State Univ. (United States); Ratan K. Saha, Saha Institute of Nuclear Physics (India); Michael C. Kolios, Ryerson Univ. (Canada)

We report on using photoacoustic imaging/spectroscopy to study the effect of red blood cell (RBC) aggregation on the oxygen saturation. Aggregation is observed during atherosclerosis and cerebral ischemia due to flow-rate decreases or plasma fibrinogen increases. It leads to a plasma layer formation which reduces the frictional interaction with the vessel's endothelial cells. We hypothesize that RBC aggregates will affect the oxygen release into the surrounding environment.

Monte Carlo based methods were used to simulate, random non-aggregated RBC configurations. Aggregates were formed through hexagonal packing. Photoacoustic signals were generated using the frequency-domain solution to the wave equation for fluid spheres. Fully oxy/deoxygenated samples were simulated using the optical absorption coefficients at 750 and 1064nm. In-vitro experiments using porcine RBCs were conducted using the Imagio (Seno Medical Instruments Inc.) at 750 and 1064nm. Varying size aggregates were induced using Dextran-70 and the oxygen saturation level (SO2) was computed for each sample at various hematocrit levels.

Non-aggregated signal amplitude increased by ~1.5x when doubling the hematocrit level. Oxygenated samples were ~2.7x higher than deoxygenated samples for 750nm. The dominant frequency of the photoacoustic signals shifted by ~230MHz towards the clinical frequency-range as the size of the aggregate increased. Experimental signal amplitude for the largest aggregate was ~1.6x higher than the non-aggregated sample. The SO2 increased by 30%. For all aggregation levels, the 40% hematocrit SO2 was ~15% higher than the 10%. These results suggest that RBC aggregation significantly decreases the RBC oxygen release and this can be assessed with photoacoustic imaging/spectroscopy.

8581-139, Session PMon

Model-based tomographic optoacoustic reconstruction in media with small speed of sound variations

Xosé Luis Deán-Ben, Daniel Razansky, Vasilis Ntziachristos, Helmholtz Zentrum München GmbH (Germany)

The majority of optoacoustic reconstruction algorithms are based on the assumption that the speed of sound within the imaging sample is constant and equal to the speed of sound in the coupling medium, typically water. However, small speed of sound changes between different organs and structures are common in actual samples. The variations in the speed of sound within biological tissues are usually below 10% with respect to the speed of sound in water. Under these circumstances, the acoustic wave propagation can be modeled as acoustic rays and the main effect of the acoustic heterogeneities is the time-shifting of the optoacoustic signals. Herein, we describe a model-based reconstruction algorithm capable of accounting for such small speed of sound variations. It is based on modifying the integration curve in the forward optoacoustic model according to the time-shifting produced by differences in the speed of sound. The forward model is then discretized and inverted algebraically by means of the lsqr algorithm. The algorithm was tested experimentally with tissue-mimicking agar phantoms containing glycerine to simulate a higher speed of sound than water. The improvement in the image quality as compared to the results obtained by assuming a uniform speed of sound are discussed in this work.

8581-140, Session PMon

Photoacoustic endoscopic imaging of the rabbit mediastinum

Joon-Mo Yang, Christopher P. Favazza, Washington Univ. in St. Louis (United States); Ruimin Chen, The Univ. of Southern California (United States); Junjie Yao, Xin Cai, Chiye Li, Konstantin I. Maslov, Washington Univ. in St. Louis (United States); Qifa Zhou, K. Kirk Shung, The Univ. of Southern California (United States); Lihong V. Wang, Washington Univ. in St. Louis (United States)

Photoacoustic endoscopy is a promising tomographic endoscopy modality that provides a unique combination of functional optical contrast and high spatial resolution at clinically relevant depths, far exceeding the penetration depths of conventional high-resolution optical imaging modalities. Moreover, it can provide unprecedented physiological and functional information of the target tissue with the aid of endogenous or exogenous contrast agents. With these attributes, photoacoustic endoscopy's potential clinical contributions could rival or exceed those of current ultrasound endoscopy. Results from our recent transesophageal imaging study on rabbits demonstrate the technique's ability to image major organs in the mediastinal region, such as the lung, trachea, and cardiovascular systems (Nature Medicine, 2012). Also, the simultaneous, multi-wavelength spectral imaging capability of our system enables the provision of a wealth of functional information, such as the total hemoglobin concentration, the oxygen saturation of hemoglobin, and the dynamics of the lymphatic system. In this poster, we present features from photoacoustic images from the mediastinal region of several rabbits, acquired both in vivo and ex vivo. Additionally we compare possible clinical contributions of this technique with those of ultrasound endoscopy. Lastly, we discuss the current limitations of our

endoscopic imaging system, and consider directions of future technology development.

8581-141, Session PMon

Photoacoustic radiofrequency spectroscopy (PA-RFS): a technique for monitoring absorber size and concentration

Eno Hysi, Ryerson Univ. (Canada) and Louisiana State Univ. (United States); Dustin Dopsa, Michael C. Kolios, Ryerson Univ. (Canada)

Photoacoustic (PA) imaging displays the radiofrequency (RF) envelope-detected-amplitude as brightness pixels being prone to system-dependencies since signal acquisition is subjected to operator settings and the instrumentation used. Transducer-calibrated RF power-spectra can remove such dependencies. Linear-regression can be performed on the calibrated spectra yielding parameters such as spectral slope (SS) and midband fit (MBF). In ultrasound imaging these parameters are related to scatterer size and concentration. In PA imaging, the absorber size dictates the RF power-spectra content. We postulate that photoacoustic-radiofrequency-spectroscopy (PA-RFS) will provide information about the absorber size and concentration.

Gelatin-based-tissue-mimicking phantoms were constructed using black polystyrene beads (Polysciences Inc.). The bead diameter were 1±0.03 and 10±0.3μm. 3 phantoms were constructed for each bead with concentrations of 0.1, 0.2 and 0.3% (v/v). PA imaging was performed using the Imagio (Seno Medical Instruments Inc.) at 1064nm and the transducer frequency response was measured using a 200nm-thick gold film. The SS and MBF were computed for each phantom.

The 10μm-phantom signal amplitude was ~40% higher than the 1μm-phantom and increased linearly with increasing bead concentration. SS for the 1μm-phantom was 2.55dB/MHz and 1.92dB/MHz for the 10μm-phantom not changing with increasing bead concentration. This suggests that SS is sensitive to changes in absorber size, much like in ultrasound imaging. The MBF linearly increased with increasing bead concentration and was ~4dB higher for the 10μm-phantom for the 0.3% bead concentration. These results suggest that PA-RFS can potentially monitor changes in absorber size thus improving PA imaging in its ability to distinguish structural tissue variations.

8581-142, Session PMon

Optoacoustic monitoring of cutting and heating processes during laser ablation

Erwin Bay, Helmholtz Zentrum München GmbH (Germany); Alexandre Douplik, Ryerson Univ. (Canada); Daniel Razansky, Helmholtz Zentrum München GmbH (Germany)

Background: Laser-tissue interaction during laser surgery can be classified into two biophysical processes: tissue removal in the focal zone of the laser beam and heating in the surrounding tissue. In order to ensure a precise cut and minimal collateral thermal damage, the surgeon has to control several parameters, such as power, repetition rate and fiber movement velocity.

Method: In this study we propose utilizing optoacoustics for providing the necessary real-time feedback of cutting and heating processes. A single Q-switched Nd-YAG laser (532nm, 4 KHz, 18 W, pulse duration 7.6ns) was used for ablation and generation of optoacoustic signals in fresh bovine tissue samples. Both shockwaves, generated due to tissue removal, as well as normal optoacoustic responses from the surrounding tissue were detected using a single 10MHz piezoelectric transducer.

Results: It has been observed that rapid reduction in the shockwave amplitude occurs as more material is being removed from the focal zone, indicating decrease in cutting efficiency of the laser beam, whereas gradual decrease in the optoacoustic signal likely corresponds to coagulation around the ablation crater. Further heating of surrounding tissue leads to carbonization accompanied by a significant shift in the generated optoacoustic spectra.

Conclusion: Our results hold promise for real-time monitoring of cutting efficiency and collateral thermal damage during laser surgery.

8581-143, Session PMon

Improving the quality of photoacoustic images using short-lag spatial coherence imaging technique

Behnaz Pourebrahimi, Dustin Dopsa, Michael C. Kolios, Ryerson Univ. (Canada)

Clutter noise and phase aberrations are challenges in photoacoustic and ultrasound imaging as they degrade the image quality. In this paper, the Short-Lag Spatial Coherence (SLSC) imaging technique is proposed to reduce the clutter and phase aberrations in photoacoustic images.

SLSC imaging technique is based on the Van Cittert-Zernike theorem which states that the Fourier transform of the mutual coherence function of a distant, incoherent source is equal to its complex visibility. In this technique, images are obtained through the spatial coherence of photoacoustic signals at small spatial distances across the transducer aperture.

To demonstrate the performance of the SLSC technique for photoacoustic imaging, we used a fat tissue mimicking phantom with an embedded optical absorber lesion in the middle. The SLSC is applied on each frame of the photoacoustic data and the image is obtained by averaging the results. We compare the images obtained using SLSC with the images obtained through applying beamforming algorithm (sum and delay). A superior Contrast, CNR (contrast-to-noise ratio), and SNR (signal_to_noise ratio) is observed when SLSC method is used (an increase of 2.7, 11.5, and 1.25 times, respectively). We also show the impact of number of data frames on which SLSC is applied on the image quality. Our results show that with increasing number of frames, Contrast, CNR, and SNR are improved.

This technique is shown to improve the quality of photoacoustics images compared to beamforming technique and to detect the optical absorber structure surrounded by scattering tissues which is not detectable by ultrasound.

8581-144, Session PMon

Application of a new sensing principle for photoacoustic imaging of point absorbers

Zafer Do?an, Ivana Jovanovic, Ecole Polytechnique Fédérale de Lausanne (Switzerland); Thierry Blu, The Chinese Univ. of Hong Kong (China); Dimitri Van De Ville, Ecole Polytechnique Fédérale de Lausanne (Switzerland)

Photoacoustic tomography (PAT) is a hybrid imaging method that combines ultrasonic and optical imaging modalities, in order to overcome the individual deficiencies and to reinforce their strengths. It is based on the reconstruction of optical absorption properties of the tissue from the measurements of a photoacoustically generated pressure field. Current methods consider short-pulsed or continuous laser excitation of the tissue. Assuming thermal and stress confinement conditions, both excitation methods allow the generation of a propagating pressure field. Most of the previous approaches aim at recovering an initial pressure field based on the measurements of the generated field by iterative reconstruction algorithms in time- or Fourier-domain. Here, we propose an application of a new sensing principle that allows for efficient and non-iterative reconstruction algorithm for imaging point absorbers in PAT. We consider a closed volume surrounded by a measurement surface in an acoustically homogeneous medium and we aim at recovering the position and the amount of heat absorbed by point absorbers in

the domain. We propose a two step algorithm based on proper choice of the sensing functions. In the first step, we extract the projected positions on the complex plane and the weights by a sensing function that is well-localized on the same plane. In the second step, we recover the remaining z-location by choosing proper set of plane waves. We show that the proposed families of sensing functions are sufficient to recover the parameters of the unknown signal in continuous domain. The k-wave toolbox, developed by B. E. Treeby and B.T. Cox from UCL, is used to simulate the photoacoustic wave field. We also evaluate the performance of the proposed algorithm using the simulation sensor data of the same toolbox for different imaging mediums and measurement setups. We demonstrate that the proposed reconstruction algorithm can accommodate model mismatches in terms of sound speed, source support size, and sensor directionality.

8581-145, Session PMon

Carbon nanoparticles as a multimodal thermoacoustic and photoacoustic contrast agent

Xin Cai, Lina Wu, Wenxin Xing, Jun Xia, Liming Nie, Ruiying Zhang, Samuel A. Wickline M.D., Gregory M. Lanza, Dipanjan Pan, Lihong V. Wang, Washington Univ. in St. Louis (United States)

We demonstrated the potential of carbon nanoparticles (CNPs) as exogenous contrast agents for both thermoacoustic (TA) tomography (TAT) and photoacoustic (PA) tomography (PAT). In comparison to deionized water, the CNPs provided a four times stronger signal in TAT at 3 GHz. In comparison to blood, The CNPs provided a much stronger signal in PAT over a broad wavelength range of 450–850 nm. Specifically, the maximum signal enhancement in PAT was 33 times stronger in the near-infrared window of 635–670 nm. In vivo blood-vessel PA imaging was performed non-invasively on a mouse femoral area. The images, captured after the tail vein injection of CNPs, show a gradual enhancement of the optical absorption in the vessels by up to 230%. The results indicate that CNPs can be potentially used as contrast agents for TAT and PAT to monitor the intravascular or extravascular pathways in clinical applications.

8581-146, Session PMon

Classifying vascular tissues using photoacoustic signals

Behnaz Pourebrahimi, Ryerson Univ. (Canada); Jason Zalev, Seno Medical Instruments, Inc. (United States); Joris Nofiele, Azza Al-Mahrouki, Gregory J. Czarnota, Sunnybrook Health Sciences Ctr. (Canada); Michael C. Kolios, Ryerson Univ. (Canada)

Photoacoustic (PA) tomography is based on the detection of acoustic waves generated by the absorption of light. Blood has up to six orders of magnitude larger light absorption than the surrounding tissues and therefore the pressure wave from the blood vessels is much stronger. The vasculature of normal and abnormal tissues can be distinguished by their morphological structures: normal vasculature have a highly organized structure with a narrow range of branching angles while abnormal vasculature have an erratic structure with a wide distribution of branching angles.

This paper proposes a new method to classify vascular tissues in the range from normal to different degrees of abnormality based on the PA signals generated by vasculatures with different structures. The PA signals are generated by a mathematical model for pressure waves from fractal trees that simulate vascular tissues, and are detected by a 128 element transducer array. The classification of the vasculatures is achieved based on the statistical features such as energy, entropy, homogeneity, and correlation extracted from PA signals in wavelet domain. A feature vector for each vasculature is provided and the distance between feature vectors are computed as the measure of similarity between vasculatures. The approach proposed in this paper can help both detecting abnormal tissues and monitoring the treatment progress by measuring the similarity between tissues in different stages of treatment. The approach is applied to in vivo data from tumor bearing mice to detect cancer treatment effect. On the test data, the classification gives more than 90% accuracy.

8581-147, Session PMon

Combined optical- and acoustic-resolution photoacoustic microscopy based on an optical fiber bundle

Wenxin Xing, Washington Univ. in St. Louis (United States); Lidai Wang, Washingon Univ. in St. Louis (United States); Konstantin I. Maslov, Lihong V. Wang, Washington Univ. in St. Louis (United States)

Photoacoustic microscopy (PAM), whose spatial resolution and penetration depth are both scalable, has made great progress in recent years. According to their different lateral resolutions, PAM systems can be categorized into either optical-resolution (OR) PAM, with optical-diffraction-limited lateral resolution, or acoustic-resolution (AR) PAM, with acoustically limited resolution and a deeper maximum imaging depth. In this report, we present a combined OR and AR PAM system with resolutions of 2.2 μm and 40 μm, respectively, and imaging depth up to 3.0 mm. Sharing most components between the OR and AR implementations, the system achieves separated illumination for OR and AR imaging by an optical fiber bundle through different channels, and two discrete lasers are used to provide either high-power energy for AR imaging or high-repetition-rate pulses for OR imaging. The combined system can operate in two modes. The first is switchable-resolution mode, as in regular microscopy with switchable objectives. The system also can acquire OR and AR images simultaneously. By setting different step sizes and slightly separating the optical and acoustic focal points, the system enables automatically co-registered higher-resolution OR and deeper AR photoacoustic imaging. In summary, the design enables OR and AR photoacoustic imaging in one single system, which extends the usability of current photoacoustic systems and simplifies the imaging procedure.

8581-148, Session PMon

Combined 3D photoacoustic and 2D fluorescence imaging of indocyanine green (ICG) contrast agent flow

Ivan Kosik, Astrid Chamson-Reig, Jeffrey J. L. Carson, The Univ. of Western Ontario (Canada)

Photoacoustic imaging uses laser-induced ultrasound transients to generate optical absorption maps of the irradiated volume. Consequently, this technique is capable of gathering optical information at ultrasound resolution in deep tissue without suffering from the degrading effects of multiply scattered light associated with turbid media. In this work we used an Nd:YAG pumped OPO laser system to perform simultaneous photoacoustic and fluorescence imaging. A single 780 nm laser pulse generated both ultrasound and fluorescence, enabling reconstruction of images for both modalities with near perfect temporal co-registration. We used a custom built photoacoustic imaging system consisting of a 60-channel transducer array connected to a 50 MHz data acquisition system. The array featured a hemispherical geometry and the transducer elements had a center frequency of 2.6 MHz. Horizontal (xy) plane resolution was 0.5 mm while the vertical resolution was approximately 1 mm, due to the anisotropic transducer distribution. Fluorescence was captured using an 830 nm narrow band filter and a 12 bit CCD camera. The results indicated that the system could track the flow (10

?L/min) of 30-?M ICG within a 0.28 mm I.D. tube with high temporal and spatial resolution and accuracy, although artefacts were present in the photoacoustic images. Furthermore, 6 mm and 9 mm spherical agar phantoms impregnated with ICG were imaged with photoacoustic imaging at depths well beyond the capabilities of fluorescence imaging. The result highlights the ability of photoacoustic imaging to supplement fluorescence data when optical scatter reduces fluorescence resolution beyond its useful range.

8581-149, Session PMon

On the sensor influence in photoacoustic signal produced by point-like source

Carlos A. Bravo-Miranda, Arturo Gonzalez-Vega, Gerardo Gutierrez-Juarez, Univ. de Guanajuato (Mexico)

Photoacoustic signal is described by solutions to the photoacoustic wave equation for certain well known detection geometries, which include point-like sources. Important advances in photoacoustic imaging applications have been achieved considering models to describe the system in which the size of sensor is not taken into account. In order to explore the influence of a sensor on photoacoustic signal, we use the solution of the photoacoustic wave equation for a point-like source to study the behavior of a plane circular sensor of finite area. The circular sensor of known dimensions was simulated by a mesh of point-like sensors connected in parallel. Taking the origin of the system at the circular sensor center, we consider signal detection at different positions with respect to the sensor location. Also we simulated the behavior of the photoacoustic pressure when the source was fixed and the sensor was rotated and displaced respect to axes of coordinate system. We study the behavior of obtained signal by taking into account the amplitude, temporal width and signal shape. Moreover, this simulations allowed us monitoring the signal shape when sensor discretization changes and obtained results show variations in temporal width and amplitude when sensor rotations and displacements were carried out.

8581-150, Session PMon

Iterative algorithm for multiple illumination photoacoustic tomography (MIPAT) using transducer channel data

Peng Shao, Roger J. Zemp, Univ. of Alberta (Canada)

Photoacoustic imaging is a promising imaging modality offering high-resolution contrast with intrinsic optical contrast. However, quantification of photoacoustic imaging is challenging. One reason for this is that the local initial pressures generated when absorbed light pulses are converted to acoustic signals are proportional to not only the local optical absorption coefficient, but also the local laser fluence, which is in turn a complex nonlinear function of the distributed optical properties of the medium. The nonlinear inverse problem of estimating optical properties from photoacoustic data is further complicated by potential ill-posedness: a given photoacoustic absorbed energy distribution may be due to non-unique absorption-scattering distribution pairs. Recently we demonstrated a linearized non-iterative algorithm, namely multiple-illumination photoacoustic tomograpy (MIPAT), for recovering absorption-scattering distributions using multiple illuminations. This approach showed that multiple illuminations can significantly mitigate absorption-scattering non-uniqueness as demonstrated by simulations. The algorithm we reported used a diffusion-regime ratiometric approach and assumed that initial pressures could be reconstructed in an ideal way. Unfortunately, artefacts in the reconstructed initial pressure distribution can lead to undesirable errors when solving for optical properties. We present an algorithm for quantitative photoacoustic estimation of optical absorption and diffusion coefficients based on minimizing an error functional between measured photoacoustic data and a calculated forward model with a multiple-illumination pattern. The proposed method does not require ideal initial pressure estimation from photoacoustic tomographic data but rather uses un-reconstructed channel data. Simulations show promise for numerically robust optical property estimation as illustrated by well-conditioned Hessian singular values in 2D examples.

8581-151, Session PMon

Developement of a neonatal skull mimicking phantom for photoacoustic imaging of the infant brain

Pantea Tavakolian, Jeffrey J. L. Carson, Lawson Health Research Institute (Canada) and The Univ. of Western Ontario (Canada); Astrid Chamson-Reig, Lawson Health Research Institute (Canada); Fartash Vasefi, SMI (United States) and Lawson Health Research Institute (Canada); Rhiannon Todd, Lawson Health Research Institute (Canada); Keith St. Lawrence, Ivan Kosik, Lawson Health Research Institute (Canada) and The Univ. of Western Ontario (Canada)

Photoacoustic imaging (PAI) has been proposed as a non-invasive technique for the diagnosis and monitoring of disorders in the neonatal brain. However, PAI of the brain through the intact skull is challenging due to reflection and attenuation of photoacoustic pressure waves by the skull bone. The objective of this work was to develop a phantom for testing the potential limits the skull bone places on PAI of the neonatal brain. Our approach was to make acoustic measurements on materials designed to mimic the neonatal skull bone and construct a semi-realistic phantom. A water tank and two ultrasound transducers were utilized to measure the ultrasound attenuation properties (100 kHz to 5MHz) of several materials. Cured mixtures of epoxy and titanium dioxide powder provided the closest acoustic match to neonatal skull bone. Specifically, a sample 1.4 mm thick composed of 50% (by mass) titanium dioxide powder and 50% epoxy was closest to neonatal skull bone in terms of acoustic attenuation. A hemispherical skull phantom (1 mm skull thickness) was made by curing the epoxy/titanium dioxide powder mixture into a mold. The mold was constructed using 3D prototyping techniques using the hairless head of a realistic infant doll. The head was scanned to generate a 3D model, which in turn was used to build a 3D CAD version of the mold. The mold was CNC machined from two solid blocks of Teflon®. Utilizing the neonatal skull phantom, we plan to study the propagation of photoacoustic pressure waves experimentally under a variety of conditions.

8581-152, Session PMon

Potential for photoacoustic imaging of the neonatal brain

Pantea Tavakolian, Jeffrey J. L. Carson, Lawson Health Research Institute (Canada) and The Univ. of Western Ontario (Canada); Astrid Chamson-Reig, Lawson Health Research Institute (Canada); Keith St. Lawrence, Lawson Health Research Institute (Canada) and The Univ. of Western Ontario (Canada); Ivan Kosik, Lawson Health Research Institute (United States) and The Univ. of Western Ontario (Canada)

Photoacoustic imaging (PAI) has been proposed as a non-invasive technique for imaging neonatal brain injury. Since PAI combines many of the merits of both optical and ultrasound imaging, images with high contrast, high resolution, and a greater penetration depth can be obtained when compared to more traditional optical methods. However, due to the strong attenuation and reflection of photoacoustic pressure waves at the skull bone, PAI of the brain is much more challenging than traditional methods (i.e. near infrared spectroscopy) for optical interrogation of the neonatal brain. To evaluate the potential limits the skull places on 3D PAI of the neonatal brain, we constructed a neonatal skull phantom (1-mm thick) with a mixture of epoxy and titanium dioxide

powder that provided acoustic insertion loss (1-5MHz) similar to human infant skull bone. The phantom was molded into a realistic infant skull shape by means of a CNC-machined mold that was based upon a 3D CAD model. To survey the effect of the skull bone on PAI, a robotic photoacoustic point source was raster scanned within the phantom brain cavity to capture the imaging operator of a 3D PAI system (60 ultrasound transducers in a hemispherical arrangement) with and without the intervening skull phantom. The resultant imaging operators were compared to determine the effect of the skull layer on the PA signals in terms of amplitude loss and time delay. Utilizing this experimental approach we have a quantitative method to evaluate the limits the skull bone places on 3D PAI.

8581-153, Session PMon

A photoacoustic endoscope designed for human urogenital imaging

Chiye Li, Joon-Mo Yang, Washington Univ. in St. Louis (United States); Ruimin Chen, The Univ. of Southern California (United States); Konstantin I. Maslov, Washington Univ. in St. Louis (United States); Qifa Zhou, K. Kirk Shung, The Univ. of Southern California (United States); Lihong V. Wang, Washington Univ. in St. Louis (United States)

Photoacoustic endoscopy for human urogenital imaging has potential in diagnosing important diseases such as endometrial cancer and prostate cancer. We have developed a new photoacoustic endoscopic probe specifically designed for such applications. The endoscopic probe was constructed with a rigid form for operator's more convenient handling during diagnostic procedures, and the probe body has a streamlined structure with a dome shaped distal end for smooth cavity introduction. In the distal section, all optical and mechanical components are encapsulated in a stainless steel tubular housing with an outer diameter of 12.7 mm and ~50 cm in length. The endoscope employs a parabolic scanning mirror actuated by a stepper motor located at the proximal end and performs side scanning, providing an angular field of view of more than 250°. Via the scanning mirror, laser pulses and acoustic waves are delivered coaxially to achieve an efficient overlap of the illumination and acoustic detection over a large radial range. The parabolic mirror-based acoustic focusing has a lower acoustic geometric aberration than our previous acoustic lens-based focusing methods, while providing a high acoustic numerical aperture. We validated the new endoscope's imaging ability with phantom experiments. In future human subject imaging studies, the endoscope will co-operate with a portable pulsed laser system that provides dual-wavelength laser pulses with rapid switching to collect functional information. In the presentation, we provide more detailed information about the endoscope and discuss the advantages of the design, along with possible future application.

8581-154, Session PMon

Intravascular Imaging using a frequency domain photoacoustic method

Robin F. Castelino, Univ. of Toronto (Canada) and Sunnybrook Research Institute (Canada); Michael Hynes, Sunnybrook Research Institute (Canada); Chelsea E. Munding, Univ. of Toronto (Canada) and Sunnybrook Research Institute (Canada); Sergey A. Telenkov, Andreas Mandelis, Univ. of Toronto (Canada); F. Stuart Foster, Univ. of Toronto (Canada) and Sunnybrook Research Institute (Canada)

Intravascular ultrasound (IVUS) imaging is an established technology for diagnostic and guidance protocols in interventional procedures. Although routinely used, it is reported to have low sensitivity in the detection of thrombus and lipid-rich lesions due to the limited acoustic contrast of soft tissues. Intravascular photoacoustic (IVPA) imaging has potential to characterize lipid-rich structures based instead on the optical absorption contrast of these tissues. This method has been previously reported using pulsed laser systems. In this study, we demonstrate IVPA imaging with a continuous wave (CW) laser diode using the frequency domain photoacoustics approach, denoted FD-IVPA.

An agar vessel phantom with thin absorbing graphite rods was imaged using a planar IVUS transducer with an aperture of 2mm by 2mm, and a central frequency of 9.5 MHz. The CW source consisted of a diode-based, fibre-coupled laser delivering an average of 1.2W over an amplitude modulated linear chirp with a 4-12MHz bandwidth. The transducer and optical fibre were co-aligned and placed at the distal tip of a catheter. These were held in place within the lumen of a rotating vessel phantom, allowing for co-registration of the IVUS and FD-IVPA images.

This study demonstrates proof of principle of frequency domain methods for intravascular imaging. Although intravascular applications use much higher imaging frequencies, we were constrained by the inability of the laser driver to modulate at frequencies higher than 12MHz. This is not a limitation of the imaging method, but a limitation of our current system. Future studies will focus on ex vivo vessels specimens using higher imaging frequencies and faster modulating laser systems.

8581-155, Session PMon

Noninvasive photoacoustic computed tomography of mouse brain metabolism in vivo

Junjie Yao, Jun Xia, Konstantin I. Maslov, MohammadReza NasiriAvanaki, Washington Univ. in St. Louis (United States); Vassiliy Tsytsarev, Univ. of Maryland School of Medicine (United States); Alexei Demchenko, Univ. of Missouri-St. Louis (United States); Lihong V. Wang, Washington Univ. in St. Louis (United States)

To control the overall action of the body, brain consumes a large amount of energy in proportion to its volume. In humans and many other species, the brain gets most of its energy from oxygen-dependent metabolism of glucose. An abnormal metabolic rate of glucose and/or oxygen usually reflects a diseased status of brain, such as cancer or Alzheimer's disease. We have demonstrated the feasibility of imaging mouse brain metabolism using photoacoustic computed tomography (PACT), a fast, noninvasive and functional imaging modality with optical contrast and acoustic resolution. Brain responses to forepaw stimulations were imaged transdermally and transcranially. 2-NBDG, which diffuses well across the blood-brain-barrier, provided exogenous contrast for photoacoustic imaging of glucose response. Concurrently, hemoglobin provided endogenous contrast for photoacoustic imaging of hemodynamic response. Glucose and hemodynamic responses were quantitatively decoupled by using two-wavelength measurements. We found that glucose uptake and blood perfusion around the somatosensory region of the contralateral hemisphere were both increased by stimulations, indicating elevated neuron activity. The glucose response amplitude was about half that of the hemodynamic response. While the glucose response area was more homogenous and confined within the somatosensory region, the hemodynamic response area showed a clear vascular pattern and spread about twice as wide as that of the glucose response. The PACT of mouse brain metabolism was validated by high-resolution open-scalp OR-PAM and fluorescence imaging. Our results demonstrate that 2-NBDG-enhanced PACT is a promising tool for noninvasive studies of brain metabolism.

8581-156, Session PMon

Improving photoacoustic imaging contrast of brachytherapy seeds

Leo L. J. Pan, Ali Baghani, Robert N. Rohling, Purang Abolmaesumi, Septimiu E. Salcudean, Shuo Tang, The Univ. of

British Columbia (Canada)

Prostate brachytherapy is a form of radiotherapy for treating prostate cancer where the radiation source known as brachytherapy seeds are inserted non-surgically into the prostate region. Accurate seeds localization during prostate brachytherapy is essential to the success of intraoperative treatment planning. The current standard modality used in intraoperative seeds localization is transrectal ultrasound (TRUS). TRUS, however, suffers in image quality due to several factors such as acoustic shadowing due to microcalcifications, and off-axis seed orientation. Photoacoustic imaging (PAI), based on the photoacoustic phenomenon, is an emerging imaging modality. Contrast generating mechanism in PAI is optical absorption that is fundamentally different from conventional B-mode ultrasound which depends on acoustic impedance mismatch. A photoacoustic imaging system is developed using a commercial ultrasound system equipped with a data acquisition hardware SonixDAQ (Ultrasonix). Barchytherapy seeds embeded in tissue for up to ~2cm depth are deteceted. To further improve imaging contrast and depth, several methods are investigated. One modification is to apply a layer of absorption enhancing coating to the seeds. In comparison to bare seeds, approximately ten times increase in signal intensity as well as two times increase in imaging depth are achieved. We are also exploring surface plasmon resonance effect to improve seeds contrast. In addition, materials with high absorption and high thermal-elastic expansion coefficient such as dyed ethanol are being tested to act as contrast agent that can be inserted into a stranded seeds. Our results show that PAI has great promise in improving seeds localization and visualization compared to ultrasound.

8581-157, Session PMon

Acoustic and the photoacoustic scattering from transverse isotropic tissues

Yae-lin Sheu, I-Ching Ho, Pai-Chi Li, National Taiwan Univ. (Taiwan)

The angular dependence of integrated scatter (IS) of ultrasonic and photoacoustic waves from specimens consisting of transverse isotropic structures are investigated. Three dimensional simulations of ultrasonic and photoacoustic waves scattering in a cubic sample composed of aligned cylindrical scatterers, in which each has a diameter of 50 ?m and an aspect ratio of 60, were compared with experimental measurements. Simulations employed by the k-Wave: MATLAB toolbox [B. Treeby, et. al, J. Biomed. Opt. 15(2), 021314 (2010)] were justified by the time-domain Born approximation to elastic scattering model for ultrasonic backscattering. At 30 degrees, the ultrasonic and photoacoustic IS decreased by 15 dB and 1 dB, respectively, compared to 0 degree measurements. Experiments with a bundled hair sample also demonstrated that decrease in the ultrasonic IS was 20 dB, while in the photoacoustic IS was less than 3 dB. Note that 0 degree is the perpendicular direction to the cylindrical axes. A hypothesis to explain the reason why the photoacoustic wave propagation is less sensitive to the anisotropic structure was provided. Scattered ultrasonic waves were approximately in phase since the transmission could be considered planar. On the other hand, a point-like laser spot generated a spherical photoacoustic wave in the specimen and hence the incident angle at each scatterer varies, resulting in a collection of waves with incoherent phases at the detector. The finding implies that photoacoustic imaging has the potential to detect tissues with transverse isotropic structure that may be overlooked by conventional ultrasound imaging.

8581-158, Session PMon

A photoacoustic technique to measure the properties of single cells

Eric M. Strohm, Elizabeth Berndl, Michael C. Kolios, Ryerson Univ. (Canada)

Many methods to have been developed to measure the properties of single cells (such as sound speed, density and size). We demonstrate a new technique to non-invasively determine cellular properties using photoacoustic signals. Melanoma cells (containing melanin, an endogenous optical absorber) and MCF7 breast cancer cells (stained with trypan blue) were trypsinized and deposited onto a gelatin surface, then irradiated with a 532 nm laser (330 ps pulse width, up to 200 nJ/pulse). The photoacoustic signals were recorded using a 200 MHz transducer. The power spectrum was calculated using a Fast Fourier Transform and compared to established theory that use thermal expansion equations to calculate the emitted photoacoustic wave. The theoretical parameters (size, sound speed and density) were adjusted until a good fit between measured and theory was found.

The measured photoacoustic spectrum from MCF7 cells was in good agreement to well established theory, however the spectra from melanoma cells were not. In melanoma cells, the melanin particles are distributed throughout the cytoplasm but not the nucleus. A finite element model was developed to calculate the photoacoustic signal emitted from cells. The results were verified against theory and the MCF7 cell results using a homogenous spherical shape, and then applied to the melanoma cell configuration where the nucleus was omitted from the thermal expansion equations. The cell properties were in agreement with those found from other methods (sound speed = 1560 m/s, density = 1050 kg/m3). In summary, a photoacoustic method to determine the cellular properties is presented.

8581-159, Session PMon

Simulating the phenomenon of digitally time-reversed ultrasound-encoded light

Snow H. Tseng, Wei-Lun Ting, Yi-An Huang, National Taiwan Univ. (Taiwan)

Here we attempt to simulate the macroscopic light scattering phenomenon involving ultrasound-encoded light for deep-tissue imaging. The simulation is done by numerical solutions of Maxwell's equations, which can accurately account for phase and amplitude of light. The reported simulation enables qualitative and quantitative characterization that may provide important information for enhancement.

8581-160, Session PMon

Flow measurement by temporal-correlation laser scanning photoacoustic microscopy

Wenzhong Liu, Wei Song, Qing Wei, Hao F. Zhang, Northwestern Univ. (United States)

In this report, we demonstrate the feasibility of measuring optically-absorbing microsphere flow velocity and Doppler angle based on temporal-correlation method using a laser scanning photoacoustic microscopy. To measure the flow velocity, at each scanning position, we continuously acquired 40 photoacoustic waveforms (A-lines) with an interval of 50 ?s. Cross-correlation between consecutive A-lines was calculated to extract the time shift caused by moving absorbing microspheres. Multiplication of the time shift and ultrasound propagation speed in water gave the travel distance of the microspheres along the axis of acoustic detector within 50 ?s, which further gives the microsphere flow velocity component along the axis of the acoustic detector. To detect the Doppler angle, we collected the ultrasound travel time from multiple locations along the flow and calculated the Doppler angle from the three-dimensional data. In phantom experiment, we measured different flow velocities, from -60 mm/s to 60 mm/s, under the different Doppler angles, from 35 degree to 51 degree. The measured results agree with the preset values well.

8581-161, Session PMon

Feasibility study of two-photon absorption-dependent photoacoustic microscopy

Dongyuan Chen, Northwestern Univ. (United States); Shuliang Jiao, The Univ. of Southern California (United States); Hao F. Zhang, Northwestern Univ. (United States)

We explored the feasibility of employing the two-photon optical absorption in photoacoustic microscopy. Almost all the existing photoacoustic microscopy systems rely on the single-photon optical absorption to induce thermoelastic vibrations and, thus, photoacoustic waves for imaging. Taking advantage of nonlinear optical contrasts in photoacoustic microscopy may open up windows for new biomedical applications. In this study, we used an amplified fs laser system as the irradiation source. The pulse duration after the regenerative amplifier was 90 fs, the pulse repetition rate was 1 kHz, and the maximum pulse energy was 3.5 mJ. We first acquired the quadratic dependence of the photoacoustic signal amplitude on the input pulse energy in both cooper and hematoporphyrin/alcohol solution, which confirmed the nonlinear two-photon optical absorption in photoacoustic generation. Then we acquired three dimensional images of phantoms that made from cooper wire and hematoporphyrin/alcohol solution filled capillary tubes. In the future, we will optimize the imaging system to minimize the illumination pulse energy and to image biological tissue samples.

8581-162, Session PMon

Monitoring of the degradation in the rat's articular cartilage inducing osteoarthritis using 128 channel real time photoacoustic tomography

Chul-Gyu Song, Dong Ho Shin, Sang Hun Ryu, Yong Kyun Oh, Jeong Hwan Seo, Chonbuk National Univ. (Korea, Republic of)

Photoacoustic Tomography (PAT) is a promising medical imaging modality by reason of its particularity. It combines optical imaging contrast with the spatial resolution of ultrasound imaging, and can distinguish changes in biological features in an image. For these reasons, many studies are in progress to apply this technique for diagnosis. But, real-time PAT systems are necessary to confirm biological reactions induced by external stimulation immediately. Thus, we have developed a real-time PAT system using a linear array transducer and a custom-developed data acquisition board (DAQ). To evaluate the feasibility and performance of our proposed system, two types of phantom tests were also performed. As a result of those experiments, the proposed system shows satisfactory performance and its usefulness has been confirmed. We monitored the degradation of the rat's articular cartilage inducing osteoarthritis (OA) and the change of the rat's articular cartilage recovery by treatment medication, using our developed real-time PAT.

In this study, we developed a real-time PAT system for functional imaging in vivo and confirmed the feasibility of the proposed system through two types of phantom test. Also, we have done a comparative analysis the rat's articular cartilage and OA grade. To quantify the measured photoacoustic signals from the linear array transducer in real-time, a multi-channel DAQ device is necessary. The PCI extensions for an instrumentation(PXI)-platform-based DAQ are used, with 50 MHz sampling frequency, 12 bit resolution, 128 analog input channels and 192 Mb/sec transmission speed, using direct memory access (DMA) method and a control program developed in Labview software. A custom-developed trigger controller is dedicated to laser-emitting, and the trigger for acquisition timing generation and a linear array probe (L14-5/28, Ultrasonix) with 5 MHz center frequency and 128 element transducers were used to measure the photoacoustic signal. To amplify and filter the detected signal, a custom-developed pre-amplifier was placed ahead of the DAQ, and had 40 dB gain, 5 MHz passband and 128 channels. The results of phantom test show that our PAT system has enough performance to obtain a 570 * 300 pixel image at 15 frames/sec with approximately 0.3-mm resolution.

Also, we have done a comparative analysis the rat's articular cartilage and OA grade. To observe the progression of OA, we induced OA by injecting the monosodium iodoacetate (MIA) into the right knee joint. After the injection of MIA, we sacrificed the rats at intervals of 3 days and obtained histological images. PAT and histological images showed the OA progress of similar pattern. These results illustrated the potential for non-invasive diagnosis about the grade of OA using PAT.

8581-163, Session PMon

Study of sickle blood cells by integrated photoacoustic and photothermal confocal microscopy

Dmitry A. Nedosekin, Stephen B. Foster, Univ. of Arkansas for Medical Sciences (United States); Mikhail A. Proskurnin, Lomonosov Moscow State Univ. (Russian Federation); Ekaterina I. Galanzha, Vladimir P. Zharov, Univ. of Arkansas for Medical Sciences (United States)

Sickle-cell disease (or sickle-cell anemia) is a genetic blood disease, which gathered much attention recently. The mutation of a single gene for abnormal hemoglobin (Hb), in this case homozygous HbS, results in precipitation and polymerization of the deoxygenated HbS, which leads to changes to the cell shape. Various methods were developed for clinical blood tests for the presence of abnormal Hb, including: electrophoresis, liquid chromatography and oximetry. However, the study of live sickle cells on a subcellular level with a resolution corresponding to the size of discovered by us Hb clusters (100-250 nm) has not been explored yet. We performed studies of sickle cells using a spectral confocal photothermal (PT) microscope (PTM) platform integrated with photoacoustic (PA) microscopy (PAM) . HbS in sickle red blood cells (RBCs) was analyzed at a subcellular level with a diffraction limited resolution of 240 nm in lateral and 600 nm in axial directions. We demonstrated that PTM is much more sensitive compared to PAM toward HbS clusters in sickle cells. Specifically, we visualized nanosized clusters of HbS in RBCs and found correlation between the observed clustering, oxygenation state and shape of the cell. We also proposed using a novel in vivo fluctuation PA flow cytometry method to analyze blood flow in a mouse model of sickle cell disease, and discovered, particular significant differences in blood heterogeneity as compared to normal nude mice.

8581-164, Session PMon

in vitro universal flow cytometry integrating photoacoustic, fluorescent, and scattering techniques

Dmitry A. Nedosekin, Mustafa Sarimollaoglu, Stephen B. Foster, Ekaterina I. Galanzha, Vladimir P. Zharov, Univ. of Arkansas for Medical Sciences (United States)

Conventional in vitro flow cytometry is a well-established analytical tool that provides quantification of multiple biological parameters of cells, bacteria and viruses at molecular levels, including their functional states, morphology, composition, proliferation, and protein expression. However, only the fluorescence and scattering parameters of the cells or labels are currently available for detection. Cell pigmentation, presence of non-fluorescent dyes or nanoparticles cannot be reliably quantified. We have developed a novel photoacoustic (PA) detection module incorporated into conventional in vitro flow cytometer. We report simultaneous quantification of absorbance, multicolor fluorescence, and light scattering for cells in flow at speeds up to 2 m/s using a nanosecond high pulse repetition rate lasers (up to 500 kHz). We compared various combinations of excitation laser sources for multicolor detection, including simultaneous excitation of PA and fluorescence using a single pulsed laser. The multichannel detection scheme allows simultaneous detection

of up to 8 labels, including 4 fluorescent tags and 4 PA contras agents co-existing in the same spectral region. We demonstrate application of this new tool for studies of gold nanoparticles uptake, for pigmentation analysis of various cells, including natural human melanoma cell line with endogenous melanin or breast cancer cells with genetically encoded melanin. We also show that this tool can be used for direct nanotoxicity studies with simultaneous quantification of nanoparticle content as well as assessment of cell viability using conventional fluorescent apoptosis assays.

8581-165, Session PMon

Improvement in quantifying optical absorption coefficients based on continuous wavelet-transform by correcting distortions in temporal photoacoustic waveforms

Takeshi Hirasawa, Masanori Fujita M.D., Shinpei Okawa, Toshihiro Kushibiki, Miya Ishihara, National Defense Medical College (Japan)

Photoacoustic (PA) signals which have broadband frequency enable to derive the absolute value of optical absorption coefficients of optical absorbers. We fabricated the acoustic detector made of a P(VDF-TrFE) film with a wide frequency bandwidth to acquire broadband frequency components of PA signals. We adopted continuous wavelet-transform to obtain time-resolved frequency spectra of PA signals. However, especially for optical absorption coefficients less than 10cm-1, quantified values were inaccurate. One of reasons for these inaccuracies was a distortion of a measured waveform. This distortion originated mainly from the detector characteristics such as its non-uniform frequency response. In order to calibrate the detector characteristics, we measured its frequency response.

Broadband acoustic sources for the calibration which were generated by PA effect achieved the 12 dB bandwidth of 1-20 MHz. Using this acoustic source, the frequency response of the detector was measured, and its averaged deviation from conventional method less than 15% was demonstrated.

We employed the model described below in order to compare the calibrated PA signals with calculated PA signals. In the model, PA signals were produced from tubes filled with optical absorbers with absorption coefficients ranging to 1-20 cm-1 which emulated blood vessels filled with blood. We will demonstrate improvements of accuracies in optical absorption coefficient quantifications. Improvements of accuracies were expected especially for low optical absorption coefficients by compensating non-uniform frequency response around the cutoff frequencies of the detector.

8581-166, Session PMon

A surprisingly simple analytic reconstruction formula for photoacoustic computed tomography in a spherical geometry

Kun Wang, Mark A. Anastasio, Washington Univ. in St. Louis (United States)

Photoacoustic computed tomography (PACT), also known as optoacoustic tomography, is an emerging imaging modality that has great potential for a wide range of biomedical imaging applications. A variety of exact reconstruction algorithms have been proposed for various measurement geometries that utilize the data function expressed in either real or Fourier domain. In this study, we derive an exact hybrid reconstruction formula where the data function is expressed in a combination of the temporal-frequency and real space domains. This formula explicitly reveals the correspondence between the spatial-frequency components of the object function and the temporal-frequency components of the data function in a spherical geometry in three-dimensions or a circular geometry in two-dimensions. The form of this formula is surprisingly simple comparing with existing Fourier-domain reconstruction formulae and is computationally more efficient than the existing time-domain formulae. Computer-simulation studies have been conducted to investigate the accuracy and stability of the reconstruction formula.

8581-167, Session PMon

Photoacoustic spectromicroscopy beyond the diffraction and spectral limits

Vladimir P. Zharov, Dmitry A. Nedosekin, Ekaterina I. Galanzha, Univ. of Arkansas for Medical Sciences (United States); Alexandru S. Biris, Univ. of Arkansas at Little Rock (United States)

Among the various microscopic methods, fluorescence microscopy remains the most powerful biological tool, able to provide super-resolution imaging of fluorescent molecules. Nevertheless, these techniques are not applicable to critical biological tasks requiring visualization of light-absorbing nanostructures that are weakly fluorescent. As an alternative, photoacoustic (PA) and especially photothermal (PT) microscopy (PAM/PTM) demonstrated the ability to offer label-free detection of single nonfluorescent molecules or single gold nanoparticles of ~1-nm diameter. However, previous applications of these techniques were performed with the limited resolutions of 220-250 nm. Here we e report super-resolution spectral PTM and PAM with spatial resolution down to 50 nm and spectral resolution down to 0.8 nm. These advanced parameters were achieved based on our discoveries of PA and PT spectral resonances and nanobubble-induced signal amplification using time-resolved signal detection. In nonlinear mode, laser-induced nanobubbles around overheated absorbing nanoparticles provide significant (10-100-fold) PT and PA signal amplifications with the simultaneous sharpening of spatial and spectral PT and PA resonances. The principles and new applications of nonlinear PTM and PAM techniques are discussed with focus on spectromicroscopy and spectral hole burning using ultrasharp rainbow plasmonic nanoparticles. In particular, we demonstrated ultrasharp resonances up to a 0.8 nm wide in relatively broad, plasmonic spectra of gold nanorods and golden carbon nanotubes. The sharpening effects can narrow absorption lines of the plasmonic nanoparticles independently from the initial narrowness of the line and physical phenomena limiting its width and line shape in microscopic and spectroscopic applications.

8581-168, Session PMon

Photoacoustic microscopy for ovarian tissue characterization

Tianheng Wang, Yi Yang, Univ. of Connecticut (United States); Molly Brewer, Univ. of Connecticut Health Ctr. (United States); Quing Zhu, Univ. of Connecticut (United States)

Ovarian cancer is the fifth most common cancer among women, and it has the lowest survival rate among all of the gynecologic cancers because it is predominantly diagnosed in late stages due to the lack of early symptoms and the poor sensitivity of screening techniques. As a result, it is necessary to develop more sensitive tools to evaluate ovarian tissue. Photoacoustic microscopy (PAM) is an emerging optical imaging method with high spatial resolution and high contrast. To investigate the feasibility of detection and diagnosis of ovarian cancer during minimally invasive surgery, we have constructed a PAM system and studied ovarian tissue with malignant and benign features ex vivo. The PAM system was validated first by imaging phantoms and mouse ear. PAM images of ovaries showed more detailed blood vessel morphological features and distributions with much higher resolution compared with that obtained from photoacoustic tomography images using ultrasound array transducers. These preliminary results have demonstrated the feasibility of PAM in mapping microvasculature networks in ovarian tissue. The

content and distribution of those high resolution microvasculature networks could be extremely valuable in assisting and guiding surgeons for in vivo evaluation of ovarian tissue during minimally invasive surgery.

8581-169, Session PMon

Iterative reconstruction method for photoacoustic section imaging with integrating cylindrical detectors

Günther Paltauf, Robert Nuster, Gerhild Wurzinger, Sibylle Gratt, Karl-Franzens-Univ. Graz (Austria)

Photoacoustic imaging of selected sections within an object is a useful alternative to full three-dimensional (3D) imaging. Since the sections can be limited to a defined region of interest, data acquisition requires less time and can therefore be achieved with a single, optimized ultrasound detector. Signals for section imaging are usually acquired with a cylindrically focusing transducer that is moved around the object. Recently we could demonstrate the capability of large, integrating cylindrical sensors for reducing artifacts that are related to the size of the detector. Either piezoelectric films on a concave cylindrical surface or elliptical acoustic reflectors in combination with an optical interferometer beam have been used. The image reconstruction employs in both cases the standard inverse Radon transform, owing to the integrating properties of the sensing element.

The focusing properties of the cylindrical detectors are not ideal. For objects lying in the selected plane but outside the focus, distortion of the acoustic signals occurs due to a spread in propagation time from object to sensor within the acoustic aperture. Additionally, there is crosstalk from objects lying outside the selected plane. In this work, both these effects are addressed in reconstruction techniques that use a forward model of signal generation to iteratively improve the reconstruction. The method works in Radon space, meaning that it tends to improve the projections of the initial pressure distribution. It is shown that even the distortions arising from focusing elements with large numerical aperture can be corrected with this method.

8581-170, Session PMon

Photoacoustic monitoring of circulating tumor cells released during medical procedures

Mazen A. Juratli M.D., Ekaterina I. Galanzha, Mustafa Sarimollaoglu, Dmitry A. Nedosekin, James Y. Suen M.D., Vladimir P. Zharov, Univ. of Arkansas for Medical Sciences (United States)

Many cancer deaths are related to metastasis to distant organs due to dissemination of circulating tumor cells (CTCs) shed from the primary tumor. For many years, oncologists believed some medical procedures may provoke metastasis; however, no direct evidence has been reported. We have developed a new, noninvasive technology called in vivo photoacoustic (PA) flow cytometry (PAFC), which provides ultrasensitive detection of CTCs. When CTCs with strongly light-absorbing intrinsic melanin pass through a laser beam aimed at a peripheral blood vessel, laser-induced acoustic waves from CTCs were detected using an ultrasound transducer. We focused on melanoma as it is one of the most metastatically aggressive malignancies. The goal of this research was to determine whether melanoma manipulation, like compression, incisional biopsy, or tumor excision, could enhance penetration of cancer cells from the primary tumor into the circulatory system. The ears of nude mice were inoculated with human melanoma cells. Blood vessels were monitored for the presence of CTCs using in vivo PAFC. We discovered some medical procedures, like compression of the tumor, biopsy, and surgery may either initiate CTC release in the blood which previously contained no CTCs, or dramatically increased (10-30–fold) CTC counts above the initial level. Our results warn oncologists to use caution during physical examination, and surgery. A preventive anti-CTC therapy during or immediately after surgery, by intravenous drug administration could serve as an option to treat the resulting release of CTCs.

8581-171, Session PMon

Fluctuation photoacoustic cytometry with high speed spectral signal analysis

Mustafa Sarimollaoglu, Yulian A. Menyaev, Univ. of Arkansas for Medical Sciences (United States); Coskun Bayrak, Univ. of Arkansas at Little Rock (United States); Ekaterina I. Galanzha, Vladimir P. Zharov, Univ. of Arkansas for Medical Sciences (United States)

One of the main challenges of photoacoustic (PA) scanning and flow cytometry (PAFC) as the integration of microscopy, spectroscopy, and fluidic technologies, is to improve signal analysis to study fast dynamic biological processes. We introduce a novel fluctuation PA cytometry for real-time monitoring of PA signals with fast changes of amplitudes, shapes, rates and short lifetimes. The features, limits, signal-to-noise ratios (SNRs), frequency and time domain analysis of heterogeneous PA signals are discussed. In particular, the SNRs can be improved through extensive averaging of PA waveforms at the expense of the acquisition time, as it is usually done in imaging of static objects. In flow cytometry, however, the objects can be irradiated for only a short period of time resulting in limited gain of SNR by averaging. To overcome this limitation, we explored the possibility of using frequency domain analysis, using an advanced high speed digitizer (analogue to digital converter). Fourier transform was applied to each acquisition of data and coefficients in a particular band of frequencies were recorded as raw data. After averaging of these spectra, the PAFC trace was created by either using the energy in the selected band, or using the time domain signal after inverse Fourier transform of the recorded spectra. The new method was compared to the regular time domain analysis of PA signals in static and flow conditions, in terms of SNR, resulting data size, and performance. Advantages and limitations of both methods were discussed and its new applications using sub-MHz high pulse repetition laser arrays are presented with focus on study of sickle disease, red blood cell aggregation, and immune related cells.

8581-172, Session PMon

Photoacoustic monitoring of clot formation during surgery and blood disorders

Mazen A. Juratli M.D., Ekaterina I. Galanzha, Mustafa Sarimollaoglu, Dmitry A. Nedosekin, James Y. Suen M.D., Vladimir P. Zharov, Univ. of Arkansas for Medical Sciences (United States)

When a blood vessel is injured, the normal physiological response of the body is clot (thrombus) formation to prevent blood loss. Alternatively, even without vessel's injury, the pathological condition called thromboembolism may lead to formation of circulating blood clots (CBCs) that eventually can plug blood vessels; in particular, in the veins of extremities (venous thromboembolism), lungs (pulmonary embolism), brain (embolic stroke), heart (myocardial infarction), kidney, or gastrointestinal tract. Emboli are also common complications of infection, inflammation, cancer, surgery, radiation and coronary artery bypass grafts. Despite clear medical significance of CBCs, however, little progress has been made in the development of methods for real-time detection and identification of CBCs. To overcome these limitations, we developed a new modification of in vivo photoacoustic (PA) flow cytometry (PAFC) for real-time detection of white, red, and mixed clots through a transient decrease, increase or fluctuation of PA signal amplitude, respectively. Using PAFC in the mouse model, we present, for the first time, direct evidence that medical procedures such as conventional or cancer surgery may initiate the formation of CBCs. An

additional therapy such as antithrombotic drug administration during surgery may be an option to treat formed clots. In conclusion, the PA diagnostic platform can be used in real-time, defining risk factors for cardiovascular disease, as well as for prognosis and potential prevention of stroke by using a well-timed therapy or for a clot count as a marker for therapy efficacy.

8581-173, Session PMon

Single wall carbon nanotube/bis carboxylic acid-ICG as a sensitive contrast agent for in vivo tumor imaging in photoacoustic tomography

Saeid Zanganeh, Hai Li, Patrick D. Kumavor, Umar S. Alqasemi, Andres Aguirre, Innus Mohammad, Michael B. Smith, Quing Zhu, Univ. of Connecticut (United States)

Photoacoustic tomography (PAT) is an emerging modality that provides optical absorption contrast at ultrasound resolution. Single Wall Carbon Nanotube (SWCNT) not only has emerged as a new alternative and efficient transporter and translocater of therapeutic molecules but also as an optical imaging agent owing to its strong optical absorption in the near-infrared region. Indocyanine green (ICG) is a FDA approved photosensitive dye for clinical applications. It has considerable absorption and fluorescence in the near-infrared wavelength (NIR) region. Shortly after injection, ICG is eliminated from the circulation. To make an appropriate delivery system, in this study we used a modified ICG (bis carboxylic acid-ICG). This ICG has an improved chemical structure that can be covalently conjugated to the SWCNT. Covalently attaching ICG to the functionalized SWCNT (SWCNT-ICG) provides much stronger bonding and delivers much more ICG to the tumor site. The detection sensitivity of the SWCNT-ICG is demonstrated in vivo using mouse tumor models. In the in vivo study, two groups of experiments with mice injected with ICG and SWCNT-ICG were conducted (n=5 for each group). The statistical analysis of the PAT signals reveals that bis carboxylic acid-ICG is able to provide 38% enhancement in PAT signal strength while SWCNT-ICG yields 220% enhancement. Due to the tubular structure of the SWCNT, the SWCNT-ICG enhancement is shown at the tumor periphery which is extremely valuable for visualization of tumor margins and guiding surgical removal of tumors.

8581-174, Session PMon

Real-time interlaced ultrasound and photoacoustic system for in vivo ovarian imaging

Umar S. Alqasemi, Hai Li, Guangqian Yuan, Patrick D. Kumavor, Quing Zhu, Univ. of Connecticut (United States)

In this presentation, we report an ultrafast co-registered ultrasound and photoacoustic imaging system based on FPGA parallel processing. The system features 128-channel parallel acquisition and digitization, along with FPGA-based reconfigurable processing for real-time co-registered imaging of up to 15 frames per second limited by the laser pulse repetition frequency. We demonstrate the imaging capability of the system with a compact transvaginal probe that includes the PAT illumination using an optic fiber assembly. The system has the ability to assist a clinician to perform transvaginal ultrasound scanning and to localize the ovarian mass, while simultaneously map the absorption of the ultrasound detected mass to reveal its vasculature using the co-registered PAT. The imaging capability of the system is demonstrated with in vivo mice tumor models.

8581-175, Session PMon

Image reconstruction and system optimization for three-dimensional speed of sound tomography using laser-induced ultrasound

Fatima Anis, Washington Univ. in St. Louis (United States); Travis Hernandez, Vyacheslav V. Nadvoretsky, André Conjusteau, Sergey A. Ermilov, Alexander A. Oraevsky, TomoWave Laboratories, Inc. (United States); Mark A. Anastasio, Washington Univ. in St. Louis (United States)

A hybrid imager combining optoacoustic tomography (OAT) and speed of sound tomography (SST) has been constructed and investigated. The system can concurrently yield images depicting both the absorbed optical energy density and acoustic properties (speed of sound) of an object. To accomplish this, we replaced conventional electrical generation of ultrasound waves by laser-induced ultrasound (LU). While earlier studies yielded encouraging results [Manohar, et al., Appl. Phys. Lett, 131911, 2007], they were limited to two-dimensional (2D) geometries. However, 2D image reconstruction algorithms may not yield accurate images, even when the measured data are densely sampled. This is due to the fact that simplified 2D imaging models cannot easily describe transducer focusing and out-of-plane acoustic scattering effects.

Based on computer modeling, the 3D LU imaging system was characterized and optimized. The imager consists of an arc of 128 transducers. The arc has a diameter of 140 mm, placed symmetrically about the central plane and has 150 deg aperture. The number and location of the laser ultrasound emitters, which are constrained to reside on the cylindrical surface opposite to the arc of detectors, were optimized through modeling. In addition to the system parameters, an iterative image reconstruction algorithm was optimized. We demonstrate that high quality volumetric maps of the speed of sound can be reconstructed when only 32 emitters and 128 receiving transducers are employed to record time-of-flight data at 360 tomographic view angles. The implications of the proposed system for small animal and breast-cancer imaging are discussed.

8581-176, Session PMon

Generation of wide-directivity broadband ultrasound by short laser pulses

André Conjusteau, Vyacheslav V. Nadvoretskiy, Sergey A. Ermilov, Alexander A. Oraevsky, TomoWave Laboratories, Inc. (United States)

A three-dimensional imaging system that combines optoacoustic tomography and laser ultrasound has been developed. It features broadband laser ultrasound emitters positioned opposite the array of transducers. This imaging geometry allows reconstruction of images that either depicts the speed of sound distribution from measured time of flight data, or acoustic attenuation from the measured signal amplitude. We have investigated the performance of various laser ultrasound source designs. Laser energy requirements are modest as the efficiency of sound generation is optimized. Novel materials were developed, and laser temporal characteristics were matched to the detection scheme. Image reconstruction through time of flight requires a recognizable sharp wavefront that is consistent through the entire detector array. We show how the resolution of the reconstructed volume is affected by both azimuthal distortion and inhomogeneity in the spatial evolution of the wave front.

8581-177, Session PMon

Towards non-invasive in vivo measurements of nanoparticle concentrations using 3D optoacoustic tomography

Dmitri Tsyboulski, Anton Liopo, Richard Su, Sergey A. Ermilov, Andre Conjusteau, Vyacheslav V. Nadvoretsky, Alexander A. Oraevsky, TomoWave Laboratories, Inc. (United States)

To facilitate development of novel nanotechnology-based theragnostics, preclinical imaging modalities capable of monitoring nanoparticle accumulation and clearance rates in vivo are highly desirable. Also, knowledge of nanoparticle concentrations in specific organs may be important for toxicity studies of nanoparticle based products. In this report, we introduce a methodology, which uses optoacoustic tomography to track biological distribution of optically absorbing agents in major organs of small animals. Aqueous suspensions of single-walled carbon nanotubes (SWCNTs) in Pluronic were used as an example of near-infrared absorbing nanoparticles. Accumulation of nanoparticles in liver, kidney and spleen of mice, visible as the increase in image brightness at those organs, was monitored by imaging live mice before and after intraperitonial administration of nanoparticles using three-dimensional laser optoacoustic imaging system (LOIS-3D). Following optoacoustic imaging, quantitative measurements of nanotube concentrations in harvested organs were performed using intrinsic fluorescence and absorption properties of SWCNTs. The changes of brightness on optoacoustic images of selected organs were correlated to changes in the optical absorption coefficient in these organs caused by SWCNT accumulation. The resulting reference points enable optoacoustic tomography as a modality for non-invasive quantitative analysis of biodistribution of optically absorbing nanoparticles. The results of our efforts towards quantitative optoacoustic tomography will be reported.

8581-178, Session PMon

Magnetic trapping with simultaneous photoacoustic detection of molecularly targeted rare circulating tumor cells

Chen-Wei Wei, Jinjun Xia, Univ. of Washington (United States); Ivan Pelivanov, Univ. of Washington (United States) and Moscow State Univ. (Russian Federation); Xiaoge Hu, Xiaohu Gao, Matthew O'Donnell, Univ. of Washington (United States)

Photoacoustic (PA) imaging has been widely used in molecular imaging to detect diseased cells by targeting them with nanoparticle-based contrast agents. However, the sensitivity and specificity are easily degraded because contrast agent signals can be masked by the background. Magnetomotive photoacoustic (mmPA) imaging uses a new type of multifunctional composite combining an optically absorptive gold nanorod core and magnetic nanospheres, which can potentially accumulate and concentrate targeted cells while simultaneously enhancing their specific contrast compared to background signals. Last year, we reported on magnetic trapping studies with simultaneous detection of micron-scale polystyrene beads coupled with a composite system mimicking targeted rare circulating tumor cells (CTCs) at a flow rate comparable to that in a human radial artery. In this study, HeLa cells molecularly targeted using nanocomposites with folic acid were circulated at a 6 ml/min flow rate for trapping and imaging studies. Preliminary results show that the cells accumulate rapidly in the presence of an externally applied magnetic field produced by a dual magnet system. The sensitivity of the current system can reach up to 1 cell/ml in clear water. By manipulating the trapped cells magnetically, the specificity of detecting cells in highly absorptive ink solution can be enhanced with 16.44 dB background suppression by applying motion filtering on PA signals to remove unwanted background signals insensitive to the magnetic field. The results appear promising for future preclinical studies on a small animal model and ultimate clinical detection of rare CTCs in the vasculature.

8581-179, Session PMon

Iterative image reconstruction in photoacoustic tomography using Kaiser-Bessel windows

Robert W. Schoonover, Kun Wang, Mark A. Anastasio, Washington Univ. in St. Louis (United States)

Photoacoustic computed tomography (PACT), also known as optoacoustic tomography, has great potential for a use in a number of biomedical applications. Iterative image reconstruction algorithms for PACT can improve image quality over that obtained by use of analytic algorithms due to their ability to incorporate accurate models of the imaging physics, instrument response, and measurement noise. Iterative image reconstruction algorithms employ a discrete imaging model that relates the measured data to an estimate of the sought-after object function. This requires an approximation of the object function to be described by use of a finite collection of expansion functions. Conventional choices for expansion functions include uniform cubic or spherical voxels. However, the pressure signals corresponding to these functions have an infinite temporal bandwidth, which presents numerical and computational challenges in practice.

In this work, we investigate a class of spherically symmetric expansion functions for iterative image reconstruction in PACT. Specifically, a closed-form solution for the photoacoustically-induced pressure that would be produced by Kaiser-Bessel functions is employed to develop discrete PACT imaging models. Kaiser-Bessel functions have finite spatial support, are differentiable at the boundaries, and are quasi-bandlimited. Computer simulations are employed to illustrate the use of such expansion functions in iterative reconstruction algorithms. We will quantify the extent to which use of the proposed basis functions in a PACT iterative image reconstruction algorithm can improve the accuracy of reconstructed images and reduce noise levels.

8581-180, Session PMon

Noninvasive optoacoustic system for rapid diagnosis and management of circulatory shock

Irene Y. H. Petrov, Michael Kinsky, Yuriy Y. Petrov, Andrey Petrov, Sheryl N. Henkel, Roger Seeton, Rinat O. Esenaliev, Donald S. Prough, The Univ. of Texas Medical Branch (United States)

Circulatory shock can lead to death or severe complications, if not promptly diagnosed and effectively treated. Typically, diagnosis and management of circulatory shock are guided by blood pressure and heart rate. However, these variables have poor specificity, sensitivity, and predictive value. Early goal-directed therapy in septic shock patients, using central venous catheterization (CVC), reduced mortality from 46.5% to 30%. However, CVC is invasive and complication-prone. We proposed to use an optoacoustic technique for noninvasive, rapid assessment of peripheral and central venous oxygenation. In this work we used a medical grade optoacoustic system for noninvasive, ultrasound image-guided measurement of central and peripheral venous oxygenation. Venous oxygenation during shock declines more rapidly in the periphery than centrally. Ultrasound imaging of the axillary [peripheral] and internal jugular vein [central] was performed using the Vivid e (GE Healthcare). We built an optoacoustic interface incorporating an optoacoustic transducer and a standard ultrasound imaging probe. Central and peripheral venous oxygenation were measured continuously in healthy volunteers. To simulate shock-induced changes in central and peripheral oxygenation, we induced peripheral vasoconstriction in the upper extremity by using a cooling blanket. Central and peripheral venous oxygenation were measured before (baseline) and after cooling and after rewarming. During the entire experiment, central venous oxygenation was relatively stable, while peripheral venous oxygenation decreased by 5-10% due to cooling and recovered after rewarming. The obtained data indicate that noninvasive, optoacoustic measurements of central and peripheral venous oxygenation may be used for diagnosis and management of

circulatory shock with high sensitivity and specificity.

8581-181, Session PMon

Cerebral venous blood oxygenation monitoring during hyperventilation in healthy volunteers with a novel optoacoustic system

Andrey Petrov, Donald S. Prough, Irene Y. H. Petrova, Yuriy Y. Petrov, Sheryl N. Henkel, Roger Seeton, Rinat O. Esenaliev, The Univ. of Texas Medical Branch (United States)

Monitoring of cerebral venous oxygenation is useful to facilitate management of patients with severe or moderate traumatic brain injury (TBI). Prompt recognition of low cerebral venous oxygenation is a key to avoiding secondary brain injury associated with brain hypoxia. In specialized clinical research centers, jugular venous bulb catheters have been used for cerebral venous oxygenation monitoring and have demonstrated that oxygen saturation < 50% (normal range is 55–75%) correlates with poor clinical outcome. We developed an optoacoustic technique for noninvasive monitoring of cerebral venous oxygenation. Recently, we designed and built a novel, medical grade optoacoustic system operating in the near-infrared spectral range for continuous, real-time oxygenation monitoring in the superior sagittal sinus (SSS), a large central cerebral vein. In this work, we designed and built a novel SSS optoacoustic probe and developed a new algorithm for SSS oxygenation measurement. The SSS signals were measured in healthy volunteers during voluntary hyperventilation, which induced changes in SSS oxygenation. Simultaneously, we measured exhaled carbon dioxide tension (ETCO2) using capnography. Good temporal correlation between decreases in optoacoustically measured SSS oxygenation and decreases in ETCO2 was obtained. Decreases of ETCO2 from normal values (35-45 mmHg) to 20-25 mmHg resulted in SSS oxygenation decreases by 3-10%. Intersubject variability of the responses may relate to nonspecific brain activation associated with voluntary hyperventilation. The obtained data demonstrate the capability of the optoacoustic system to detect in real time minor changes in the SSS blood oxygenation.

8581-182, Session PMon

Contour-scanning optical-resolution photoacoustic microscopy

Brian T. Soetikno, Chenghung Yeh, Song Hu, Qiaonan Zhong, Konstantin I. Maslov, Lihong V. Wang, Washington Univ. in St. Louis (United States)

Optical-resolution photoacoustic microscopy (OR-PAM) has drawn increasing attention in vascular and metabolic biology, particularly in the context of ischemic stroke and cancer. However, the depth of focus of OR-PAM (~100 ?m) is often insufficient to cover the uneven surfaces of biological tissues. As a result, the image quality of out-of-focus blood vessels is compromised by the poor resolution and low signal-to-noise ratio. In addition, our recent in vivo experiments have shown noticeable deviations in the measurements of oxygen saturation of hemoglobin (sO2) in out-of-focus vessels.

To address this practical challenge, we have implemented a three-step approach for three-dimensional (3-D) contour scanning, following the uneven surface of the subject to be imaged. Our method begins with a quick scan of the region of interest with a relatively large step size (>40 ?m). A Matlab program for automatic surface detection is then applied to extract the 3-D surface contour map, which is refined using linear interpolation. After that, a high-resolution 3-D scan is performed following the refined contour map.

We have applied our newly developed 3-D contour-scanning OR-PAM for in vivo anatomical and functional (sO2) imaging of mouse brains and tumorous mouse ears with uneven surfaces. The measurements of spatial resolution, signal-to-noise ratio, and sO2 using contour-scanning OR-PAM and conventional OR-PAM are compared. This implementation is expected to have extended impact on sub-wavelength OR-PAM, which has a small depth of focus.

8581-183, Session PMon

Translation of magnetomotive optical coherence tomography to magnetomotive ultrasound for imaging SPIO labeled platelets

Ava G. Pope, Gongting Wu, Elizabeth Merricks, Timothy Nichols, Tomek Czernuszewicz, Caterina Gallippi, Amy L. Oldenburg, The Univ. of North Carolina at Chapel Hill (United States)

The ability to image platelets in vivo can provide insight into blood clotting processes and aid in identifying sites of vascular damage. Furthermore, platelets provide a platform for functional imaging because they readily take up superparamagnetic iron oxide (SPIO) contrast agents, enabling imaging by methods such as magnetomotive optical coherence tomography (MMOCT). MMOCT has been previously used to detect the sub-resolution motion of SPIO labeled platelets induced by a temporally modulated magnetic field gradient. Motivated by the need for greater imaging penetration depth to study blood related diseases, and given the innate similarities between OCT and ultrasonic imaging, we have extended MMOCT techniques toward the development of a clinically feasible magnetomotive ultrasound (MMUS) system. In our setup the exciting magnetic field gradient is produced by two solenoid electromagnets positioned to allow for an arbitrarily large sample while also maintaining portability. As in MMOCT, we employ a phase-sensitive motion detection algorithm for which the displacement at each location in the sample is computed from the phase shift of the acoustic waveform between successive ultrasound frames. With this method we can detect sub-resolution motion on the order of a few microns. We demonstrate the use of this MMUS system for the detection of motion in homogenous tissue phantoms at SPIO concentrations as low as 0.06 mg/ml Fe3O4. Additionally, we show that our system is capable of 3-dimensional imaging of a 1 cm3 tissue phantom inclusion (simulated blood clot) against an otherwise non-magnetic background at biologically feasible SPIO concentrations.

8581-184, Session PMon

Dynamic contrast enhanced 3D photoacoustic imaging

Philip Wong, The Univ. of Western Ontario (Canada); Jeffrey J. L. Carson, Lawson Health Research Institute (Canada); Ivan Kosik, The Univ. of Western Ontario (Canada)

Photoacoustic imaging (PAI) is a hybrid imaging modality that integrates the strengths from both optical imaging and acoustic imaging while simultaneously overcoming many of their respective weaknesses. In previous work, we reported on a real-time 3D PAI system comprised of a 64-element hemispherical array of transducers. Using the system, we demonstrated the ability to capture photoacoustic data, reconstruct a 3D photoacoustic image, and display select slices of the 3D image every 1.4 s, where each 3D image resulted from a single laser pulse. The present study aimed to exploit the rapid imaging speed of the 3D PAI system by evaluating its ability to perform dynamic contrast-enhanced (DCE) imaging. DCE imaging involves the analysis of the time evolution of the voxel-based signal changes produced by a contrast agent. The contrast dynamics can provide rich datasets that contain insight into perfusion, pharmacokinetics and physiology. We captured a series of 3D PA images of a flow phantom before and during injection of Indocyanine Green. We then utilized principal component analysis (PCA) to classify the data according to its spatiotemporal information. Images representative of the first 5 PCA components appeared to separate the flow pattern into distinct early to late arriving components of the flow pattern. The results suggested that PCA analysis can be used to separate a sequence of 3D PA images into a series of images representative of the main features of the spatiotemporal flow dynamics.

8581-61, Session 9

in vivo oxygen sensing using lifetime based photoacoustic measurements

Aniruddha Ray, Univ. of Michigan (United States); Justin R. Rajian, Univ. of Michigan Medical School (United States); Yong-Eun Lee Koo, Univ. of Michigan (United States); Xueding Wang, Univ. of Michigan Health System (United States); Raoul Kopelman, Univ. of Michigan (United States)

Hypoxia is a condition where a region of tissue has less than adequate oxygen. It is of particular importance in tumor biology. The hypoxic core of tumors has been shown to impede the effectiveness of various therapies, such as photodynamic therapy, radiotherapy and chemotherapy. The determination of oxygen saturation levels in blood and other tissues in vivo is critical for ensuring proper body functioning, monitoring status of diseases, e.g. cancer, and predicting the efficacy of therapy.

Previously spectroscopic photoacoustic imaging technology has been used for in vivo blood oxygenation measurements by exploiting the distinct optical absorption spectra of oxygenated- and deoxygenated-hemoglobin. However, the accuracy of such measurements is affected by the heterogeneous light fluence in biological samples. Hemoglobin based spectroscopic measurements are also ineffective in blood devoid tissues such as tumors, especially in the necrosis core. Here we demonstrate, for the first time, a lifetime based photoacoustic technique for the measurement of oxygen saturation in vivo, using a porphyrine based oxygen sensitive dye. This molecular probe aided and lifetime based oxygen sensing technique overcomes the problems mentioned above. The experimental results derived from the main artery in the rat tail indicated that the lifetime of the probe, quantified by the photoacoustic measurement, shows a good linear relationship with the blood oxygenation level in the targeted artery. The upper state lifetime of the probe in the artery changed from 45 microseconds when blood oxygenation was 94% to 158 microseconds when blood oxygenation was 77%.

8581-62, Session 9

Real-time photoacoustic imaging of rat deep brain: hemodynamic responses to hypoxia

Satoko Kawauchi, National Defense Medical College (Japan); Taiichiro Ida, Tomoya Hosaka, Yasushi Kawaguchi, Advantest Corp. (Japan); Hiroshi Nawashiro, Tokorozawa Central Hospital (Japan); Shunichi Sato, National Defense Medical College (Japan)

Hemodynamic response of the brain to hypoxia or ischemia is one of the major interests in neurosurgery and neuroscience. Recent advancement in photoacoustic (PA) imaging method enables in vivo depth-resolved analysis of the brain of small animals, but reports are still limited on the real-time imaging of deep brain through the intact scalp and skull. In this study, we performed real-time transcutaneous PA imaging of the rat brain that was exposed to a hypoxic stress and investigated depth-resolved responses of the brain, including the hippocampus. A linear-array 10-MHz ultrasonic sensor (measurement length, 10 mm) was placed on the shaved scalp. Nanosecond, 532-nm and 605-nm light pulses, both satisfying the MPE requirement, were used to excite PA signals indicating cerebral blood volume (CBV) and blood deoxygenation, respectively. Under spontaneous respiration, inhalation gas was switched from air to nitrogen and then switched again to air, during which real-time PA imaging was performed continuously. The effects of the PA signal reflection with the skull were examined by the phantom study and were taken into account in the analysis. High-contrast PA signals were observed in the depth regions corresponding to the scalp, skull, cortex and hippocampus. After starting nitrogen inhalation, PA signals indicating CBV in the cortex increased transiently, and then decreased. PA signal in the scalp compensatorily decreased after starting hypoxia. The reoxygenation caused gradual recovery of these PA signals. These findings demonstrate the usefulness of the present PA imaging system for real-time, depth-resolved observation of cerebral hemodynamics.

8581-63, Session 9

Mapping tissue oxygen in vivo by photoacoustic lifetime imaging (PALI)

Qi Shao, Ekaterina Morgounova, Jeung-Hwan Choi, Chunlan Jiang, Univ. of Minnesota (United States); John C. Bischof, Univ. of Minnesota, Twin Cities (United States); Shai Ashkenazi, Univ. of Minnesota (United States)

Oxygen plays a key role in the energy metabolism of living organisms. Any imbalance in the oxygen levels will affect the metabolic homeostasis and lead to pathophysiological diseases. Hypoxia is also a key factor in tumor biology as it is highly prominent in tumor tissues. However, clinical tools for assessing tissue oxygenation are limited. Hypoxic tumors are known to be more aggressive and more resistive to chemotherapy and radiotherapy. The gold standard is polarographic needle electrode which is invasive and not capable of mapping (imaging) the oxygen content in tissue.

We have applied the method of photoacoustic lifetime imaging (PALI) of oxygen-sensitive dye to small animal tissue hypoxia research. PALI is new technology for direct, real time, non-invasive imaging of oxygen. The technique is based on mapping the oxygen-dependent transient optical absorption of Methylene Blue by pump-probe photoacoustic imaging. Our studies show the feasibility of imaging of dissolved oxygen distribution in phantoms. Recent in vivo experiments demonstrate that the hypoxia region is consistent with the site of transplanted prostate tumor in mouse with adequate spatial resolution and penetration depth. Our imaging result of tumor hypoxia is verified by needle type oxygen sensor.

In this talk we will introduce the basic principles of the PALI method and its implementation. We will then present our recent results and discuss possible directions for improving imaging quality in small animal tumor hypoxia models. We will conclude by describing routes for translating PALI technology into clinical applications.

8581-64, Session 9

Video-rate functional photoacoustic microscopy of mouse cardiovascular dynamics

Lidai Wang, Konstantin I. Maslov, Wenxin Xing, Alejandro Garcia-Uribe, Washington Univ. School of Medicine in St. Louis (United States); Lihong V. Wang, Washington Univ. in St. Louis (United States)

We report the development of functional photoacoustic microscopy capable of video-rate high-resolution in-vivo imaging in deep tissue. A lightweight photoacoustic probe is made of a single-element broadband ultrasound transducer, a compact photoacoustic beam combiner, and a bright-field light delivery system. Focused broadband ultrasound detection provides 44-μm lateral resolution and 28-μm axial resolution as computed from the signal envelope (15-μm axial resolution based on the raw RF signal). A multimode optical fiber is utilized to deliver laser pulses. The bright-field light delivery system is designed to improve the illumination efficiency, so that the system can image as deep as 4.8 mm in vivo using low excitation pulse energy (28 μJ per pulse, 0.35 mJ/cm2 on the skin surface). The photoacoustic probe weighs 40 grams and is mounted on a voice-coil scanner to acquire 40 two-dimensional B-scan images per second over a 9 mm range. The fast speed effectively improves imaging throughput, reduces motion artifacts, and enables the visualization of highly dynamic biological processes. High-resolution anatomical imaging is demonstrated in the mouse ear and brain. Via fast dual-wavelength switching, the oxygen dynamics of mouse cardio-vasculature are imaged in real time as well.

8581-65, Session 9

Acoustic resolution photoacoustic Doppler blood flow measurements using time-domain cross-correlation

Joanna Brunker, Paul C. Beard, Univ. College London (United Kingdom)

Blood flow measurements have been demonstrated using the acoustic resolution mode of photoacoustic sensing for the first time, enabling penetration depths of several centimetres. This is unlike previous flowmetry methods using the optical resolution mode, which limits the maximum penetration depth to approximately 1mm. Here we describe a pulsed time correlation photoacoustic Doppler technique that is inherently flexible, lending itself to both resolution modes. Doppler time shifts are quantified via cross-correlation of pairs of photoacoustic waveforms generated in moving absorbers using pairs of laser light pulses, and the photoacoustic waves detected using an ultrasound transducer. The acoustic resolution mode is employed by using the transducer focal width, rather than the large illuminated volume, to define the lateral spatial resolution. The use of short laser pulses allows depth-resolved measurements to be obtained with high spatial resolution, offering the prospect of mapping flow within microcirculation. Velocity range and resolution are scalable with excitation pulse separation allowing it be optimised for a wide range of physiologically realistic flow velocities. Whilst our previous work has been limited to a non-fluid phantom, we now demonstrate measurements in more realistic blood-mimicking phantoms incorporating fluid suspensions of microspheres flowing along an optically transparent tube. Flow rates less than 50 mms-1 were measured, and various suspensions and different diameter tubes were evaluated in terms of their effect on the accuracy, resolution and range of measurable velocities. Experiments were also performed with red blood cell suspensions and whole blood and with the tubing in both non-scattering and scattering media. Finally, the technique was applied in vivo in a mouse model.

8581-66, Session 9

Real-time multispectral 3D photoacoustic imaging of blood phantoms

Ivan Kosik, Jeffrey J. L. Carson, The Univ. of Western Ontario (Canada)

Photoacoustic imaging is exquisitely sensitive to blood and can infer blood oxygenation based on multispectral images. However, multispectral measurements can take several seconds to acquire due to delays related to scanning the laser between multiple wavelengths. In this work we present a technique for real time multispectral 3D photoacoustic imaging. We used a custom-built 60-channel hemispherical transducer array to make ultrasonic pressure measurements at a center frequency of 2.6 MHz and a bandwidth of 101%. Two Nd:YAG pumped OPO laser systems (Continuum Inc.) were synchronized to provide double pulse excitation at 680 nm and 900 nm all during a triggered series of ultrasound pressure measurements lasting less than 200 ?s. The information was then mathematically separated into two time series measurements, and with prior knowledge of the imaging operator, the time series were used to reconstruct two 3D images in real time. When interpreted together, the images provided oxygenation-dependent blood contrast. Horizontal in-plane resolution was 0.5 mm while vertical in-plane resolution was approximately 1 mm due to the anisotropic transducer distribution. The system performance was tested using human blood taken from a volunteer, before and after cuffing a finger for 1 minute, which was injected into polyethylene tubing with an I.D. of 0.28 mm. The images exhibited clear oxygenation-dependent contrast at 680 nm, where primarily deoxygenated blood was seen, while at 900 nm both oxygenated and deoxygenated blood was observed. The results demonstrated that 3D PAI is capable of providing relative blood oxygenation maps non-invasively at high speed and resolution.

8581-67, Session 9

Vessel filtering of photoacoustic images

Tanmayi Oruganti, Australian National Univ. (Australia); Jan G. Laufer, Charite Universitätsmedizin Berlin (Germany); Bradley E. Treeby, Australian National Univ. (Australia)

The processing and manipulation of medical images is an integral part of medical image analysis and diagnosis. In particular, vessel filtering algorithms, which can separate tubular structures from 3D images, are often used to process images of the vasculature obtained using CT and MR angiography. Here, the use of vessel filtering for processing photoacoustic images is investigated. First, different filtering approaches are reviewed, including multi-scale vessel enhancement based on eigenvalue decomposition of the local Hessian matrix at each image voxel, and vessel-enhancing diffusion. The effect of these filters on photoacoustic images is then studied using a series of numerical and experimental phantoms. In particular, the impact of the filters on image resolution, feature preservation, and noise is discussed. The classical Hessian filter is shown to be highly effective at removing noise and highlighting vessels, at the expense of reducing the sharpness of vessel edges. These features are better preserved when using vessel-enhancing diffusion, although the noise reduction is less effective. Next, the vessel filters are applied to photoacoustic images of the microvasculature in mice. The filters provide a noticeable qualitative improvement to the images, removing noise and accentuating the vessel features. Filtered images of tumour vasculature are then compared to vascular casts of the same tumour type. Finally, the use of vessel filters as a binary classifier for quantitative photoacoustics is discussed. This classification can be used to reduce the number of unknowns in model-based inversion schemes, and correct for the vessel distortion caused by an uneven light fluence distribution.

8581-68, Session 9

Frequency-based optoacoustic characterization of vascular architecture in an in vivo murine model

Michelle Patterson, Univ. of Prince Edward Island (Canada); Christopher Riley, Atlantic Veterinary College (Canada); Michael C. Kolios, Ryerson Univ. (Canada); William M. Whelan, Univ. of Prince Edward Island (Canada)

A number of organs in the body have unique vascular networks (eg. vessel diameters, densities, etc) including the liver and kidneys. Many solid tumours are also characterized by unique vascular networks compared with normal, healthy tissues.

In our previous in vivo murine study, we found significant differences between the frequencies on tumour versus on healthy surrounding tissues. The relationship, however, between the change in frequency and the characteristics of the target tissue is still unknown. Frequency analysis of optoacoustic signals may hold information on the vascular network of the target tissue. This may allow for in vivo, quantitative diagnosis of the tumour vasculature with good resolution and penetration depth.

Vascular corrosion casting is the standard method for 3D visualization of microvessels. Quantitative analysis of casts can provide the diameters and densities of the blood vessels.

Optoacoustic images of murine liver and kidneys in vivo were acquired at a 775 nm illumination using a reverse-mode imaging system. Vascular corrosion casts of these organs were obtained by inter-cardiac infusion of saline (to flush out the blood), followed by infusion of Mercox resin until the onset of polymerization. Soft tissues were removed by maceration in a 40% KOH solution. Casts were imaged with both our optoacoustic imaging system and a magnetic resonance imaging system for quantitative comparison with the in vivo results. The frequency content of the optoacoustic signals generated in vivo and by casts was determined using ultrasound spectrum analysis methods and will be presented. There

are detectable changes in optoacoustic signal frequency content with vascular architecture, which demonstrates the potential of optoacoustic imaging for characterizing vascular networks.

8581-69, Session 9

Silica-coated gold nanorods for enhanced sensitivity of temperature mapping during photothermal therapy

Yun-Sheng Chen, Wolfgang Frey, Salavat Aglyamov, Stanislav Y. Emelianov, The Univ. of Texas at Austin (United States)

Photothermal therapy uses molecular specific plasmonic nanoparticles to target markers of diseased tissue and plasmonic heating to achieve local thermal ablation of the target, such as a tumor. One of the challenges of photothermal cancer therapy is the precise control of the delivered energy, i.e. the light dosage, to avoid affecting the surrounding healthy tissue. Therefore, a technique to accurately, noninvasively and continuously monitor the spatial temperature distribution during therapy is needed. Nanoparticle-augmented photoacoustic imaging, a noninvasive technique with high penetration depth and near optical resolution, can locally measure the temperature profile, because the photoacoustic amplitude depends on the temperature-dependent thermal properties of the tissue in the immediate vicinity to the nanoparticle. Additionally, the heat transfer process from the particle to the tissue plays an important role and can be used to improve the photoacoustic signal. In this study, we developed the antibody-functionalized silica-coated gold nanorods as both the imaging contrast agents and the temperature sensors. We use the silica shell to increase the heat transfer efficacy and achieve a faster thermoelastic expansion, thus enhancing the sensitivity of the temperature measurement with the same light dosage. Silica-coated gold nanorods were shown to provide a seven times higher signal increment compared to typical nanorods under the same conditions. Targeted silica-coated gold nanorods are not only a superb photoacoustic molecular imaging contrast agent, but their unique thermal properties make them also an excellent nanosized temperature sensor for photoacoustic image-guided photothermal therapy.

8581-70, Session 10

Photoacoustic thermal-strain temperature imaging for plasmonic photothermal therapy

Chia-Chin Li, National Tsing Hua Univ. (Taiwan); Chia-Yu Li, Churng-Ren C. Wang, National Chung Cheng Univ. (Taiwan); Tzu-Chen Yen, Chang-Gung Memorial Hospital (Taiwan); Meng-Lin Li, National Tsing Hua Univ. (Taiwan)

In this study, we developed a photoacoustic (PA) thermal-strain temperature imaging technique based on cross-correlation algorithm for gold-nanorod based plasmonic photothermal therapy (PPTT). Unlike the existing amplitude based PA temperature estimation, the PA thermal-strain temperature estimation is less unaffected by problems such as fluctuation of pulse laser energy and photothermal instability of gold nanorods for PPTT. Computer simulations were used to prove the feasibility of PA thermal-strain temperature imaging and to analyze the effects of different distributions of optical absorbers on the proposed technique. In addition, phantom experiments of PPTT were performed to compare the performance of amplitude based and the proposed thermal-strain based PA temperature imaging on a photoacoustic array imaging system. The experimental results indicated that a temperature resolution of 0.17 degree C within 10 degree C temperature changes can be obtained for the proposed technique. Moreover, the PA thermal-strain temperature estimator is a more stable and accurate temperature monitoring technique for PPTT than the amplitude based one.

8581-71, Session 10

Visualization of focused ultrasound and its cavitation behaviors depending on surface boundary conditions

Taehwa Lee, Hyoung won Baac, Jong G. Ok, L. Jay Guo, Univ. of Michigan (United States)

Pulsed cavitation induced by focused ultrasound generated optically provides with various applications such as biomedical area and mechanical cavitation study, since it is non-invasive due to non-thermal process compared to thermally generated cavitation. Understanding cavitation behaviors depending on different surface conditions is of importance for the applications. Visualization of the focused ultrasound and its cavitation bubble generation allows us to analyze their underlying physics in detail.

The fast-moving objects such as the ultrasound wave (~ 1500 m/s) and bubble behavior are visualized by using the time-resolved laser shadowgraphy technique so that we are able to capture their images with a few ns resolution. The visualization of laser-generated focused ultrasound and its cavitation bubble generation is conducted on different surfaces so that we are able to observe interaction between the focused ultrasound wave and different wall boundaries. Specifically, the focused ultrasound with a small spot size (<100 ?m) hits the solid boundary, and tiny bubbles (several um) within the focal zone are formed at the moment when the focused ultrasound exert high-amplitude pressure on the surface boundaries. The small bubbles are merged into large bubble comparable to the spot size within 1 ?s after the ultrasound arrival, which grows and collapses and eventually form cavitation shock wave. Not only are the cavitation behaviors and bubble generation somewhat different from conventional cavitation generated by thermal process and piezoelectric transducers, but also these are different from one another depending on various surface conditions (hydrophobic, hydrophilic) and ultrasound impedances contrast (high, low contrast) between surfaces and water.

8581-72, Session 10

Thermal treatment monitoring using a novel dual-wavelength photoacoustic technique

Yi-Sing Hsiao, Univ. of Michigan (United States); Xueding Wang, Univ. of Michigan Health System (United States); Cheri X. Deng, Univ. of Michigan (United States)

Safe and effective thermal treatments of biological samples require noninvasive monitoring techniques to provide real-time information on either the temperature distribution or the tissue status. It has been demonstrated that photoacoustic (PA) signals from a biological tissue depend on not only its temperature but also its optical properties which indicates the tissue status. However, since changes in temperature and tissue status usually happen simultaneously during thermal treatments (e.g., high-intensity focused ultrasound (HIFU) ablation), monitoring treatment effects by simply looking at the varying in PA signal intensity cannot differentiate the two changes. We propose a dual-wavelength PA technique to monitor changes in tissue status independent of temperature changes. By dividing PA signal intensities obtained at two wavelengths at the same temperature, the temperature-dependent Grüneisen parameter is eliminated and a ratio which only depends on the optical properties is obtained. PA sensing of ex-vivo porcine myocardium specimens in a temperature-controlled water bath showed a constant ratio (700 nm/800 nm) before coagulation (20 – 45 °C), and a gradual increase at 51 °C, indicating tissue changes. PA sensing on pre-generated HIFU lesions and native tissue showed constant ratios for each tissue status at 20 – 40 °C, while HIFU lesions and native tissue exhibited distinct values. For example, the 700 nm/900 nm ratio yielded a 171% ± 32% contrast between HIFU lesions and native tissue (n = 3, each at 9 temperatures). Our results demonstrated the potential of dual-wavelength PA sensing/imaging in real-time monitoring of thermal treatments by assessing tissue status without being affected by temperature.

8581-73, Session 10

High-precision targeted cell therapy by laser-generated focused ultrasound

Hyoung Won Baac, Yu-Chih Chen, John Frampton, Jong G. Ok, Taehwa Lee, Kyu-Tae Lee, Euisik Yoon, Shuichi Takayama, L. Jay Guo, Univ. of Michigan (United States)

High-amplitude focused ultrasound can provide localized perturbation in liquids and tissues by inducing shock, acoustic cavitation, and heat deposition on focal volumes. Such mechanical and thermal disturbances have been used to deliver targeted impacts on cells and tissues for biomedical therapy: for example, trans-membrane drug delivery, gene transfection, neural activity modulation in brain, and thrombolysis, often relying on acoustic cavitation or externally injected micro-bubbles. Moreover, remarkable progresses have been made in clinical areas of kidney-stone fragmentation as well as ablation-based tumor therapy under high-intensity focused ultrasound. Although the above beneficial effects have been confirmed over a broad range of biomedical applications, their focal accuracy has been typically limited to a few mm in a lateral plane and even >10 mm in an axial plane. This is because the focused ultrasound was typically generated by using low-frequency piezoelectric transducers (a few MHz).

Here, we use laser-generated focused ultrasound (LGFU) to produce high-frequency and high-amplitude acoustic pressure at a tight focal spot (<100 um). We confirmed that a single LGFU pulse is sufficient to induce shock and cavitation effects and therefore useful for a targeted therapy over a few cells. We demonstrate that the localized disruption effects from the LGFU can be used for a single cell surgery to remove cells from substrates and to cut junctions among the neighboring cells. We also confirmed that the targeted disruption enables the cells to open their membranes for molecular delivery. Some experimental examples are shown using cultured cancer cells.

8581-74, Session 10

Enhanced delivery of gold nanoparticles by acoustic cavitation for photoacoustic imaging and photothermal therapy

Yu-Hsin Wang, Ai-Ho Liao, National Taiwan Univ. (Taiwan); Jia-Yu Lin, Cheng-ru Lee, National Chung Cheng Univ. (Taiwan); Tzu-Ming Liu, National Taiwan Univ. (Taiwan); Churng-Ren Wang, National Chung Cheng Univ. (Taiwan); Pai-Chi Li, National Taiwan Univ. (Taiwan)

Gold-nanorods encapsulated within microbubbles (AuMBs) were proposed as a photoacoustic/ultrasound dual-modality contrast agent in our previous study. In the current study, we further explore its potential in molecular imaging and targeted photothermal therapy by exploiting acoustic cavitation for enhanced delivery of gold nanorods. Specifically, with cavitational effects of AuMBs, our hypothesis is that delivery of gold nanorods can be enhanced as cavitation can temporarily change permeability. To test the hypothesis, targeting efficacy is observed macroscopicall by an ultrasound system and a multimodal optical microscope based on a Cr:forsterite laser. The microscope can acquire the third-harmonic generation (THG) signal from gold nanorods and two-photon fluorescence (2PF) from microbubbles. The extended retention of targeted AuMB was observed for 30 minutes in a CT-26 tumor bearing mouse. Also, cavitation induced by time-varying acoustic field can also be applied to disrupt the microbubble and cause increased transient cellular permeability, also known as sonoporation. In vitro examination shows 60% enhancement of 2PF from the cellular uptake of gold nanoparticles with sonoporation. Therefore, acoustic controlled release is feasible and can further improve photothermal therapeutic effects by the nanoparticles.

8581-75, Session 11

Identification of rolling circulating tumor cells using photoacoustic time-of-flight method

Mustafa Sarimollaoglu, Dmitry A. Nedosekin, Ekaterina I. Galanzha, Vladimir P. Zharov, Univ. of Arkansas for Medical Sciences (United States)

Existing optical techniques for in vivo measurement of blood flow velocity are not quite applicable for determination of velocity of individual cells or nanoparticles. A time-of-flight photoacoustic (PA) technique can solve this problem by measuring the transient PA signal width, which is related to the cell velocity passing the laser beam. This technique was demonstrated in vivo using an animal (mouse) model by estimating the velocity of nanoparticles, and red and white blood cells labeled with conjugated gold nanorods (GNRs) in the bloodstream. Here we describe the features and the parameters of novel modifications to the PA time-of-flight method and its new application for real-time monitoring of circulating tumor cells (CTCs), such as melanoma (B16F10) and breast cancer cells (MDA-MB-231) labeled with GNRs. This method provided, for the first time, identification of rolling CTCs in analogy to rolling white blood cells and CTC aggregates. Specifically, monitoring of PA signal widths from CTCs in mouse ear microvessels revealed double maxima in peak-width histograms associated with the fast moving portion of CTCs in central flow and slowly rolling CTCs in analogy to white blood cells. We also developed a two-parameter plot representing PA peak amplitude and peak widths. This method allowed identification of fast-moving individual CTCs, CTC aggregates, and rolling CTCs. The discovery of rolling CTCs in relatively large blood vessels indicates a higher probability of CTC extravasations, further increasing the possibility of metastasis through rolling mechanism in addition to mechanical capturing of CTCs in small vessels.

8581-76, Session 11

Laser-scanning photoacoustic microscopy with ultrasonic phased array transducer

Xiaojing Liu, Fan Zheng, Chi-Tat Chiu, Bill L. Zhou, K. Kirk Shung, The Univ. of Southern California (United States); Hao F. Zhang, Northwestern Univ. (United States); Shuliang Jiao, The Univ. of Southern California (United States)

We report on our latest progress on proving the concept that ultrasonic phased array can improve the detection sensitivity and field of view (FOV) in laser-scanning photoacoustic microscopy (LS-PAM). A LS-PAM system with a one-dimensional (1D) ultrasonic phased array was built for the experiments. The 1D phased array transducer consists of 64 active elements with an overall dimension of 3.2 mm?2 mm. The signals from each element of the array can be acquired independently. By applying the different time delays on the received signals from each channel and summing all the delayed signals (so-called delay-sum beamforming technique), the beam can be steered to and focused at different spatial positions. By performing beamforming the desired signals will be enhanced and the noise will be suppressed simultaneously. The system was tested on imaging a USAF 1951 resolution target and a mouse ear in vivo. Experiments showed a 15 dB increase of the signal-to-noise ratio (SNR) and a significant increase of field of view when 64-channel delay-sum beamforming was employed compared to the images acquired with each single element. For in vivo imaging, with delay-sum beamforming the SNR is greatly improved and more small vessels along the phased array direction can be recognized. The experimental results demonstrated that ultrasonic phased array can be a better candidate for LS-PAM in high sensitivity applications like ophthalmic imaging.

8581-77, Session 11

Reflection-mode multifocal optical-resolution photoacoustic microscopy

Guo LI, Konstantin I. Maslov, Lihong V. Wang, Washington Univ. in St. Louis (United States)

Compared with mechanical scanning single-focus optical-resolution photoacoustic microscopy (OR-PAM), ultrasound-array-based multifocal OR-PAM increases the imaging speed greatly. In multifocal OR-PAM, the time required for mechanical scanning is divided by approximately the number of optical foci. Previously our lab reported a transmission-mode multifocal OR-PAM with a 30 MHz 48-element ultrasound array probe, which used a microlens array to provide 20 linearly distributed focused beams. Experiments showed the transmission mode had increased the imaging speed by 3-4 times, with 1/6 signal multiplexing. However, the transmission mode was limited to imaging only thin biological tissue, such as a mouse ear. This led to the design of a reflection-mode multifocal OR-PAM because it has no similar limitation and thus significantly expands the range of application, such as imaging a mouse brain. The reflection-mode multifocal OR-PAM uses the same microlens array and ultrasound array probe, but employs a new light delivery. This reflection-mode multifocal OR-PAM can image 1000?500?200 voxels within 4 minutes, with a laser repetition rate of 1.35 kHz and 1/6 signal multiplexing. The high imaging speed and reflection-mode flexibility make the reflection-mode multifocal OR-PAM a promising instrument for clinical use.

8581-78, Session 11

Water-Immersible MEMS scanning mirror designed for wide-field fast-scanning photoacoustic microscopy

Junjie Yao, Washington Univ. in St. Louis (United States); Chih-Hsien Huang, Texas A&M Univ. (United States); Catherine Martel, Washington Univ. School of Medicine in St. Louis (United States); Konstantin I. Maslov, Washington Univ. in St. Louis (United States); Lidai Wang, Washington Univ. School of Medicine in St. Louis (United States); Joon-Mo Yang, Liang S. Gao, Washington Univ. in St. Louis (United States); Gwendalyn Randolph, Washington Univ. School of Medicine in St. Louis (United States); Jun Zou, Texas A&M Univ. (United States); Lihong V. Wang, Washington Univ. in St. Louis (United States)

By offering images with high spatial resolution and unique optical absorption contrast, optical-resolution photoacoustic microscopy (OR-PAM) has gained increasing attention in biomedical research. Recent developments in OR-PAM have improved its imaging speed, but have sacrificed either the detection sensitivity or field of view or both. We have developed a wide-field fast-scanning OR-PAM by using a water-immersible MEMS scanning mirror (MEMS-OR-PAM). Made of silicon with a gold coating, the MEMS mirror plate can reflect both optical and acoustic beams. Because it uses an electromagnetic driving force, the whole MEMS scanning system can be submerged in water. In MEMS-OR-PAM, the optical and acoustic beams are confocally configured and simultaneously steered, which ensures uniform detection sensitivity. A B-scan imaging speed as high as 400 Hz can be achieved over a 3 mm scanning range. A diffraction-limited lateral resolution of 2.4 ?m in clear medium and a maximum imaging depth of 1.1 mm in soft tissue have been experimentally determined. Using the system, we imaged the flow dynamics of both red blood cells and carbon particles in a mouse ear in vivo. By using Evans blue dye as the contrast agent, the flow dynamics of lymphatic vessels were also imaged in a mouse tail in vivo. The results show that MEMS-OR-PAM could be a powerful tool for studying highly dynamic and time-sensitive biological phenomena.

8581-79, Session 11

Photoacoustic microscopy of neovascularization in three-dimensional porous scaffolds in vivo

Xin Cai, Washington Univ. in St. Louis (United States); Yu Zhang, Georgia Institute of Technology (United States) and Emory Univ. (United States); Li Li, Massachusetts General Hospital (United States) and Harvard Medical School (United States); Sung-Wook Choi, The Catholic Univ. of Korea (Korea, Republic of); Matthew R. MacEwan, Junjie Yao, Washington Univ. in St. Louis (United States); Chulhong Kim, Univ. at Buffalo (United States); Younan Xia, Georgia Institute of Technology (United States) and Emory Univ. (United States); Lihong V. Wang, Washington Univ. in St. Louis (United States)

It is a challenge to non-invasively visualize in vivo the neovascularization in a three-dimensional (3D) scaffold with high spatial resolution and deep penetration depth. Here we used photoacoustic microscopy (PAM) to chronically monitor neovascularization in an inverse opal scaffold implanted in a mouse model for up to six weeks. The neovasculature was observed to develop gradually in the same mouse. These blood vessels not only grew on top of the implanted scaffold but also penetrated into the scaffold. The PAM system offered a lateral resolution of ~45 μm and a penetration depth of ~3 mm into the scaffold/tissue construct. By quantifying the 3D PAM data, we further examined the effect of scaffold pore size (200 μm versus 80 μm) on neovascularization. At 6 weeks post-implantation, in scaffolds with a pore size of 200 μm, the neovascularization was 2.0–3.5 times better than in scaffolds with a pore size of 80 μm.

8581-80, Session 11

in vivo multi-wavelength optical-resolution photoacoustic microscopy with stimulated Raman scattering fiber-laser source

Parsin Haji Reza, Alexander Forbrich, Wei Shi, Roger J. Zemp, Univ. of Alberta (Canada)

In this paper the potential of a multi-wavelength optical resolution photoacoustic microscopy (MW-OR-PAM) system for in vivo imaging is demonstrated. The multi-wavelength source is generated based on stimulated Raman scattering (SRS) in a length of single-mode fiber. Using a ytterbium doped frequency-doubled fiber laser with 1ns pulse width and 160kHz repetition rate and 4 meters of single mode polarization maintaining (PM) fiber, we demonstrated wavelength peaks at 543nm, 560nm, 570nm, 580nm, 590nm, 600nm with pulse energies about 260nJ, 320nJ, 160nJ, 225nJ, 185nJ, 220nJ respectively. These peaks were selected using band-pass filters. Generating higher wavelengths up to 700nm is possible using slightly different design. The ability of this system is shown by imaging Swiss Webster mouse ear at different wavelengths. The multi-color light at the output of the fiber was collimated and scanned by a 2D scanningmirror system. The scanning light was filtered by a band-pass filter wheel and focused using a microscope objective lens. A 25MHz focused transducer is used to receive the generated photoacoustic signals. A special animal holder was engineered to hold a small amount of water between mouse ear and the transducer. To the best of our knowledge it is the first demonstration of in-vivo OR-PAM imaging using a SRS fiber-laser source. Our system produces orders of magnitude improvement in pulse-energy and imaging speed compared to previous efforts using a microchip laser. We anticipate that this cost effective multi-wavelength source can open up a whole range of possibilities for functional imaging applications.

8581-81, Session 11

Volumetric imaging of single red blood cells using multiphoton photoacoustic microscopy

Ryan L. Shelton, Scott P. Mattison, Brian E. Applegate, Texas A&M Univ. (United States)

While photoacoustic microscopy has demonstrated subcellular resolution in the transverse imaging plane, the resolution along the optical axis is still fundamentally limited to 15-50 microns by the parameters of the ultrasonic transducer used to detect the sound waves. This fundamental limitation restricts the usefulness of ultrahigh resolution PAM implementations and generally results in the integration of the depth information to a single 2D image (maximum amplitude projection). Using a molecular process called transient absorption, we have developed a multiphoton photoacoustic microscope capable of nonlinear optical sectioning in three dimensions, improving the axial resolution over current state-of-the-art photoacoustic microscopes by an order of magnitude. This improvement results in axial resolution of 1.5 microns, equivalent to axial resolutions found in other nonlinear microscopy techniques. The imaging capabilities of this system are validated by capturing a 3D rendered volume of individual red blood cells in a blood smear. The system is then used to capture en face and cross-sectional slices of individual red blood cells in the vasculature of a chick embryo. To our knowledge, this is the first time individual red blood cells have been fully resolved using photoacoustic techniques. This technique is further modified to obtain molecular-specific information from chromophores by measuring ground state recovery time. Characteristic recovery times are measured for a known molecule, Rhodamine 6G, as well as two unknown molecules, oxidized and reduced forms of hemoglobin. Lifetime imaging is demonstrated by differentiating multiple chromophores in an image using the ground state recovery times.

8581-82, Session 11

Non-linear photoacoustic microscopy with optical sectioning

Amos Danielli, Konstantin I. Maslov, Alejandro Garcia-Uribe, Amy M. Winkler, Chiye Li, Lidai Wang, Lihong V. Wang, Washington Univ. in St. Louis (United States)

Photoacoustic microscopy (PAM) is an effective in vivo functional and molecular imaging technique. In conventional optical resolution PAM, the lateral resolution is determined by the numerical aperture (NA) of the optical objective—the tighter the optical focus, the finer the image resolution. For example, Zhang et al. used a water-immersion optical objective with a 1.23 NA to achieve 220 nm lateral resolution at a wavelength of 532 nm. In contrast, the axial resolution in conventional PAM is limited by the bandwidth of the ultrasonic transducer. For example, an ultrasonic transducer with a 75 MHz bandwidth provides 10 μm axial resolution. An axial resolution of 0.5 μm requires a 3 GHz bandwidth ultrasonic transducer, which is difficult to manufacture and handle. Moreover, due to acoustic attenuation in water and tissue, such a broadband ultrasonic transducer is limited to shallow depths.

Here, we show how nonlinear photoacoustic effects provide optical sectioning, as in multi-photon microscopy, which improves the axial resolution dramatically. To demonstrate this improvement, we imaged red blood cells using a 40 MHz ultrasonic transducer and a 1.2 NA objective (beam diameter, 226 nm) at different focal depths, with a step size of 500 nm. In conventional PAM, out of plane objects are blurred but not rejected. Nonlinear PAM, in contrast, is more sensitive to features within the depth of focus (440 nm), yielding an 84-fold improvement in axial resolution over that of conventional PAM. Improvements to the signal-to-noise ratio can further enhance the axial resolution to below 150 nm.

8581-83, Session 11

Photoacoustic microscopy of blood pulse wave

Chenghung Yeh, Song Hu, Konstantin I. Maslov, Lihong V. Wang, Washington Univ. in St. Louis (United States)

Blood pulse wave velocity (PWV) is an important indicator of vascular stiffness. Here we report, for the first time, an electrocardiogram(ECG)-synchronized photoacoustic method for noninvasive quantification of the PWV in peripheral microvessels of living mice. Electrocardiograms were simultaneously recorded with photoacoustic flow measurements and served as references to measure the travel time of the pulse wave between two cross sections of a chosen vessel. Vessel segmentation analysis of photoacoustic images enabled accurate quantification of the travel distance. A robust mathematical procedure was developed for PWV quantification. Photoacoustic flow measurements were divided into single-period segments according to the R-spike of the ECG signal and then averaged. Those segments negatively correlated with the average flow pattern were discarded. The remaining segments were re-averaged, from which the travel time of the pulse wave were computed using a cross-covariance method. Our experimental results showed that the photoacoustic flow measurements in arteries and arterioles exhibited a repeating pattern with the same frequency as the ECG signal, but not those in veins and venules. Moreover, the PWV measured in peripheral arteries and arterioles showed a linear correlation (r-value: 0.999; p-value: 0.012) with the vessel diameter. The slope of the linear regression was 2.77, which is consistent with the values reported in the literature. This technology holds the potential to study a broad range of peripheral cardiovascular diseases, including diabetes and hypertension, by providing a metric of local vascular stiffness and blood pressure.

8581-84, Session 11

Optical-resolution photoacoustic microscopy with dual scanning modes

Song Hu, Chenghung Yeh, Konstantin I. Maslov, Lihong V. Wang, Washington Univ. in St. Louis (United States)

Optical-resolution photoacoustic microscopy (OR-PAM), an emerging complement to mainstay optical microscopy technologies, enables in vivo imaging of optical absorption contrast with cellular resolution and unit sensitivity. However, the under-developed scanning mechanisms of existing OR-PAM systems impose significant limitations on their practical biomedical impacts. Traditional motor-stage based mechanical scanning provides a large field of view, but with a relatively slow scanning speed and a fixed scanning pattern. Newly developed optical scanning techniques dramatically enhance the scanning speed and enrich scanning strategies, but at the expense of the field of view.

To address this outstanding challenge, we have developed a dual-mode scanning OR-PAM system integrating both steering-mirror based real-time optical scanning and motor-stage based wide-field mechanical scanning. Operating in the optical scanning mode, our OR-PAM system can spectroscopically monitor a tissue volume of 50?50?1000 μm3 with a near-video rate of up to 20 frames per second, opening the possibility of monitoring rapid hemodynamics at the single cell level in vivo. While operating in the mechanical scanning mode, our system can cover a field of view of up to 25?25 mm2, well suited for site mapping. Moreover, the additional motorized vertical linear stage in our system enables contour scanning, allowing precise compensation for the out-of-focus effect induced by the curvature of uneven tissue surfaces.

Our dual-modal scanning OR-PAM system has been successfully used for in vivo multi-contrast imaging of tumor microenvironment and ischemic stroke, allowing both real-time visualization of cell trafficking and wide-field monitoring of tumor neovascularization and stroke infarction.

8581-85, Session 11

FRET photoacoustic microscopy

Yu Wang, Lihong V. Wang, Washington Univ. in St. Louis (United States)

Förster (or fluorescence) resonance energy transfer (FRET) provides a ruler to measure intra- and inter-molecular distances between two fluorescence-labeled sites in biological macromolecules in the 1-10 nm range. Widely applied in fluorescence imaging, FRET reveals physicochemical processes in molecular transformations and interactions. In this work, we report photoacoustic imaging of FRET, based on non-radiative decay that produces heat and subsequent acoustic waves. Estimates of the energy transfer efficiency by photoacoustic microscopy were compared to fluorescence confocal microscopy measurements. The experimental results in tissue phantoms show that photoacoustic microscopy provides high resolution FRET imaging at enhanced penetration depth. With its ability to perform multi-scale high-resolution imaging of biological structures, photoacoustic microscopy could be a beneficial biomedical tool to broaden the in vivo application of FRET.

8581-86, Session 11

Focus-free optical-resolution photoacoustic microscopy using an all-fiber Bessel beam generator

Chulhong Kim, Univ. at Buffalo (United States); Sung-Jo Park, Kyungpook National Univ. (Korea, Republic of); Jongki Kim, Sungrae Lee, Yonsei Univ. (Korea, Republic of); Mansik Jeon, Univ. at Buffalo (United States); Jeehyun Kim, Kyungpook National Univ. (Korea, Republic of); Kyunghwan K. Oh, Yonsei Univ. (Korea, Republic of)

Optical-resolution photoacoustic microscopy (OR-PAM) has successfully supplied in vivo morphological, functional, and molecular information of tissues. The key hardware specification of OR-PAM is the fine lateral resolution and fair penetration depth (~1 mm) without using a ultrahigh-frequency ultrasonic transducer. Similar to pure optical microscopic modalities, the lateral resolution of OR-PAM is determined by the tight optical focus using an optical objective. OR-PAM achieves in vivo label-free imaging of intrinsic contrasts (i.e., two types of hemoglobin, melanin, etc). Thus, imaging tumor angiogenesis and diagnosing early-stage melanomas are highly promising in OR-PAM. OR-PAM have been implemented both in transmission and reflection modes. In both modes, at least one optical objective must be used for PA excitation. Thus, accompanying optical components are required to form optical focus. In this proceedings article, for the first time to our knowledge, we have successfully implemented a focus-free OR-PAM (FF-OR-PAM) system in a transmission mode using a compact all-fiber Bessel beam generator. The all-fiber Bessel beam generation was achieved by concatenating hollow optical fiber, coreless silica fiber, and a self-assembled polymer lens in a compact form. Therefore, in the FF-OR-PAM system, no optical objective and associated optics were used for PA excitation. Thus, the system was much compact and less complex compared to exiting OR-PAM systems.

8581-87, Session 11

All-optical photoacoustic microscopy using a MEMS scanning mirror

Sung-Liang Chen, Univ. of Michigan (United States); Zhixing Xie, Univ. of Michigan Medical School (United States); Tao Ling, Univ. of Michigan (United States); Xunbin Wei, Shanghai Jiao Tong Univ. (China); L. Jay Guo, Univ. of Michigan (United States); Xueding Wang, Univ. of Michigan Health System (United States)

It has been studied that a potential marker to obtain prognostic information about bladder cancer is tumor neoangiogenesis, which can be quantified by morphometric characteristics such as microvascular density. Photoacoustic microscopy (PAM) can render sensitive three-dimensional (3D) mapping of microvasculature, providing promise to evaluate the neoangiogenesis that is closely related to the diagnosis of bladder cancer. In most existing PAM imaging systems, bulky apparatuses are used. However, PAM imaging of a bladder using bulky setup to image from the outside of the bladder is not desired due to degraded resolution and sensitivity at deep penetration depth. To improve imaging quality of the bladder by imaging from its inside, the PAM head needs to be engineered to match the transurethral configuration. Previously, we demonstrated laser-scanning PAM systems using piezoelectric transducers to detect photoacoustic signals and galvanometer mirror for laser scanning. Piezoelectric transducers have a trade-off between their size and sensitivity. Besides, the miniaturization is highly restricted due to employing galvanometer scanners. Thus, in this work, we build a PAM system using an optical ultrasound detector and a MEMS scanning mirror, which provides a potential solution for fabricating an endoscopic PAM head capable of high imaging quality of the bladder. The system has high resolutions of 17.5 μm in lateral direction and 20 μm in axial direction at a distance of 3.7 mm. Images of printed grids and the 3D structure of microvasculature in a canine bladder ex vivo by the system are demonstrated.

8581-88, Session 11

Multimodal optoacoustic and multiphoton fluorescence microscopy

Gali Sela, Technion-Israel Institute of Technology (Israel); Daniel Razansky, Technische Univ. München (Germany); Shy Shoham, Technion-Israel Institute of Technology (Israel)

Multiphoton microscopy enables structural and functional imaging with cellular and sub-cellular resolution, deep within biological tissues. It is typically used to measure the fluorescence contrast of specific fluorescent indicators. Optical resolution optoacoustic microscopy also enables cellular and even sub-cellular resolution imaging of absorption contrast utilizing the absorber's non-radiative relaxation properties, thus providing complementary information to that given by the fluorescence.

We have developed a system for simultaneous multimodal optoacoustic and multiphoton fluorescence 3D imaging where both contrasts are obtained within a single scan. The system is based on integrating an ultrasonic transducer into a two-photon laser scanning microscope with a NIR femtosecond laser with a high repetition rate (80MHz). The system is shown to enable the acquisition of multimodal 2D and 3D microscopic images of fluorescently labeled particles and cell cultures infused with carbon particles as well as optoacoustic images of pigmented biological tissue. The observed low frequency optoacoustic signal is characterized and modeled, and the optoacoustic images are shown to be highly correlated with bright-field images.

This multimodal system can provide complementary structural and functional information to the fluorescently labeled tissue, by superimposing optoacoustic images of markers that are highly absorbant in the NIR spectrum. The markers can be both exogenous to the tissue (particles or dyes infused into certain parts of the tissue) or endogenous (melanin deposits, pigmentation).

8582-5, Session 1

Novel insights in photodynamic therapy-generated cancer vaccines *(Invited Paper)*

Mladen Korbelik, The BC Cancer Agency Research Ctr. (Canada)

The development of photodynamic therapy (PDT)-generated cancer vaccines was initiated around ten years ago by the discovery that lysates of PDT-treated tumor cells can act as a prophylactic vaccine for autologous mouse tumor. This was followed by our revelation that in vitro PDT-treated whole-cell tumor cells or tumor tissue can serve as a potent therapeutic cancer vaccine. One of the critical factors contributing to PDT vaccine efficacy is the expression of PDT-induced molecular/biological changes in vaccine cells, particularly those associated with cell death. Pertinent cell death-associated changes are associated with the progression of apoptotic and necrotic death or autophagy processes with the emergence of death signal molecules on the surface of vaccine cells, and the upregulation of genes in vaccine cells responsible for production of important immune response mediators such as heat shock proteins. The process of phagocytic disposal of injected vaccine cells appears pivotal for the optimal presentation of offered antigenic repertoire. The potency of PDT-generated cancer vaccines depends critically on the abundantly expressed cell death-associated molecular patterns (DAMPs) and alternate elements among phagocytic receptors and phagocytic cell types engaged in the process of vaccine cell efferocytosis. Our results show that further improvements in the efficacy of these vaccines can be attained by neutralizing negative immunoregulatory activity of selective engulfment receptors on phagocytes engaged in clearance of vaccine cells, as well as of suppressory effector cells.

8582-6, Session 1

Photodynamic therapy stimulates anti-tumor immune response in mouse models: role of regulatory T-cells, anti-tumor antibodies, and immune attack on brain metastases. *(Invited Paper)*

Michael R. Hamblin, Hoon Chung, Masayoshi Kawakubo M.D., Pawel A. Mroz M.D., Wellman Ctr. for Photomedicine (United States)

We have previously shown that photodynamic therapy mediated by a vascular regimen of benzopophyrin derivative and 690-nm light is capable of inducing a robust immune response in the mouse CT26.CL25 tumor model that contains a tumor-rejection antigen (beta-galactosidase). Here we show that PDT can reduce CD25+, FoxP3+, CD4+ regulatory T-cells (T-regs). For the first time we show that PDT can stimulate the production of serum IgG antibodies against the beta-gal antigen. A common cause of death from cancer (particularly lung cancer) is brain metastases that do not respond to traditional therapies, and are mostly inoperable. If you immune response stimulated by PDT could attack brain metastases, this would be highly significant. We developed a mouse model of brain metastases by injecting CT26.CL25 tumor cells into the brain and under the skin at the same time. When the subcutaneous tumor was treated with PDT, we observed a survival advantage compared to mice that had untreated brain metastases alone.

8582-7, Session 1

Immune responses in topical photodynamic therapy of skin carcinomas in a hairless mouse model

Hongwei Wang, Jingjing Li, Ting Lv, Qingfeng Tu, Xiu-li Wang, Shanghai Skin Diseases and STD Hospital (China); Zheng Huang, Univ. of Colorado Denver (United States)

Objective: To investigate the roles of immune responses in topical photodynamic therapy (PDT) against skin cancer. Materials and Methods: To develop skin squamous cell carcinomas (SCCs), female SKH-1 hairless mice were used as a model animal and back area was exposed to multiple UVB (280-320 nm) at a minimal erythema dose 4 to 5 days/week for up to 22 weeks. ALA cream (8%) was applied to SCC areas for 3 h and followed by light irradiation of 30 J/cm2 at 632.8 nm. Therapeutic effects were examined at various time points after 4 sessions of ALA PDT. Results: Topical PDT could induce a significant reduction in the number and size of SCC lesions without causing noticeable changes in skin pigmentation or structures. PDT also induced a marked increase in TNF? expression and infiltration of CD4+ and CD8+ cells. Conclusion: This preliminary in vivo study demonstrated that ALA PDT could eliminate skin carcinomas. Immune responses may play a role in this process.

8582-9, Session 2

In situ photoimmunotherapy for melanoma

Mark F. Naylor M.D., Dermatology Associates of San Antonio (United States); Robert E. Nordquist, Wound Healing of Oklahoma, Inc. (United States); John A. Lunn M.D., Commonwealth Medical Research Institute (Bahamas); Orn Adalsteinsson, International Strategic Cancer Alliance (United States); Tomas Hode, Immunophotonics, Inc. (United States); Hong Liu, The Univ. of Oklahoma (United States); Wei R. Chen, Univ. of Central Oklahoma (United States)

Immunotherapy is arguably the most effective way of treating advanced melanoma. One of the more promising immunotherapy methods that is being developed for treating advanced (stage III/IV) melanoma and other solid tumors involves in situ treatments of tumor deposits to enhance local immunity and concomitantly, system-wide anti-tumor responses. This treatment paradigm is likely the basis for the abscopal effect which has been observed serendipitously following palliative radiation therapy. A more deliberate approach that achieves this result more reliably combines the use of infrared laser and intralesional glycated chitosan (InCVAX) to induce necrosis of tumor deposits and a subsequent brisk immune response. One technology that is being applied to facilitate this methodology is percutaneous insertion of laser fibers that can be used to reach any location in the body. Recent case reports are presented that demonstrate the step-wise development of this technology for the purpose of demonstrating for the first time, its practical application. Other immunotherapeutic agents such as anti-CTLA4 antibodies can also be used to multiply and enhance these local immune responses to provide more potent system-wide immunological anti-tumor effects that translate into significant anti-tumor responses.

8582-10, Session 2

Survival of late-stage breast cancer patients after the treatment of laser immunotherapy

Tomas Hode, Immunophotonics, Inc. (United States); Orn Adalstensson, International Strategic Cancer Alliance (United

States); Gabriela L. Ferrel M.D., Hospital Nacional Edgardo Rebagliati Martins (Peru); John A. Lunn M.D., Commonwealth Medical Research Institute (Bahamas); Xiaosong Li, Chinese PLA General Hospital (China); Robert E. Nordquist, Wound Healing of Oklahoma, Inc. (United States); Wei R. Chen, Univ. of Central Oklahoma (United States)

Laser immunotherapy (LIT) is a local intervention for late-stage, metastatic cancers. LIT uses laser irradiation, combined with the intratumoral injection of glycated chitosan, a novel immunomodifier. The hypothesized mechanism of LIT is the activation of dendritic cells (DCs) in situ, and subsequent enhancement of uptake and the presentation of antigens by DCs, so that a tumor-specific T-cell response is induced. After we obtained promising pre-clinical results using LIT for the treatment of breast cancer, two overseas (Peru and the Bahamas) clinical studies were carried out. We have followed the treated patients during the past several years. Here we report the survival data of the treated patients. We also report the development of tumors after LIT treatment using different imaging modalities, such as CT, PET-CT, and MRI. A number of no-option patients have had complete responses after LIT. In a number of patients, the distant metastases, such as in the lungs, have been reported shrinking or disappearing. Overall, the preliminary results of LIT in our clinical trials are promising.

8582-11, Session 3

Interstitial laser immunotherapy: a preliminary in vivo study

Cody Bahavar, Jessica D. Goddard, Jessnie Jose, Univ. of Central Oklahoma (United States); Roman F. Wolf D.V.M., Eric Howard, The Univ. of Oklahoma Health Sciences Ctr. (United States); Hong Liu, The Univ. of Oklahoma (United States); Tomas Hode, Immunophotonics, Inc. (United States); Robert E. Nordquist, Wound Healing of Oklahoma, Inc. (United States); Wei R. Chen, Univ. of Central Oklahoma (United States)

Laser immunotherapy (LIT), uses laser irradiation and immunological stimulation to treat metastatic cancers. The current mode of operation of LIT is through dye-enhanced non-invasive irradiation. Though this treatment has given promising results, there are still a number of challenges for using this method, such as limited light penetration for deep tumors and strong light absorption by highly pigmented skins. Interstitial laser immunotherapy (ILIT), using a cylindrical diffuser, is designed to overcome these limitations. In this study, rat tumors were treated by ILIT with different laser powers and different doses of glycated chitosan, an immunological stimulant. The temperature inside tumor was measured by thermocouples. Proton resonance frequency was used to measure the temperature distribution in target tissues during and after interstitial laser irradiation. We have observed long-term survivors of tumor-bearing rats under the treatment of ILIT. The effects of different laser powers and different immunostimulant doses will be reported.

8582-12, Session 3

Biological effects of near-infrared lasers on myofibroblast cellular differentiation and contraction

Melville B. Vaughan, Jessica D. Goddard, Jessnie Jose, Chelsea Spencer, Joseph R. Acquaviva, Wei R. Chen, Univ. of Central Oklahoma (United States)

The ability to modulate the myofibroblast phenotype will have important implications in wound healing, aging and cancer development. Our objective was to determine whether irradiation using a 980-nm laser affects the presence of myofibroblasts and cellular contractility using an attached collagen lattice model. Fibroblasts in type I collagen lattices were allowed to generate tension for 5 days. The laser light stimulation occurred on day 4. Immunostaining was used to determine the total number of cells and percentage of myofibroblasts in the representative image; tension generation was determined by releasing tension and measuring diameter change over time. One treatment demonstrated a slight lattice contraction increase over control, correlated with increased cell number. Myofibroblast percentage was low and was not correlated with lattice contraction. Due to limited sample size and lack of large deviations from the control, we began to try monitoring the cell's biological effects differently to see if this produced varied results. By using an MMT assay kit we were able to more accurately measure cell death. We also used an 805 nm laser to irradiate the cells to see how the wavelength affected results.

8582-13, Session 3

Monitoring tissue temperature distribution for photothermal cancer therapy based on photoacoustic imaging: a simulated analysis

Zhifang Li, Hui Li, Fujian Normal Univ. (China); Wei R. Chen, Univ. of Central Oklahoma (United States)

Laser immunotherapy (LIT) has shown to be a promising treatment modality for metastatic cancers in both pre-clinical and clinical studies. Photothermal effect is a crucial component of LIT, by destroying tumor cells and releasing tumor antigens. LIT employs an in situ light absorbing dye to selectively enhance photothermal effect. However, LIT require effective and reliable temperature determination. In this study, we proposed photoacoustic imaging to monitor the temperature during the phototherapy. Photothermal therapy is carried out by utilizing a continuous wave laser and metal nanocomposites broadly absorbing in the near-infrared optical range. A focusing photoacoustic imaging is interfaced with a nanosecond pulsed laser to images tissue-mimicking phantoms before and during photothermal therapy. The Monte Carlo method is used for simulation of continuous laser light transport in photothermal therapy and nanosecond pulsed laser light for producing photoacoustic signal. The simulated results demonstrated that temperature-induced changes in the photoacoustic signal could reflect optical absorption of tissue during therapeutic procedure. Thus, the photoacoustic imaging is a potential tool to guide photoabsorber-enhanced photothermal therapy.

8582-8, Session 4

in vitro study of combination therapy using specific RNAi and PDT

Yih-Chih Hsu, Chung Yuan Christian Univ. (Taiwan); Leaf Huang, UNC Eshelman School of Pharmacy (United States)

Photodynamic therapy is a non-invasive cancer therapy modality. Photosensitizer or its precursor is given by topical, oral or vein-injection administration. Then photosensitizer accumulates selectively in precancerous or cancerous lesions and is then activated after irradiatiing light. The activated photosensitizer reacts with oxygen to form reactive oxygen species, resulting in tissue destruction of precancerous and cancerous tissue. We established SCC cell line to research on selective RNAi for combination therapy with PDT in vitro. Based on the studies, it demonstrated that combination therapy of specific RNAi and PDT has better antitumor activity effect on SCC in vitro. More studies are needed to further investigate in translational SCC animal model in the near future.

8582-14, Session 4

Folate receptor-mediated tumor-targeted upconversion nanocomplex for photodynamic therapy triggered by near-infrared light

Sisi Cui, Haiyan Chen, China Pharmaceutical Univ. (China); Zhiyu Qian, Nanjing Univ. of Aeronautics and Astronautics (China); Wei R. Chen, Univ. of Central Oklahoma (United States); Yueqing Gu, China Pharmaceutical Univ. (China)

Near-infrared-to-visible upconversion nanoparticles (UCNPs) have been explored as potential photosensitizer carriers and energy donors for photodynamic therapy (PDT). Herein, folate-receptor (FR) mediated tumor-targeted UCNPs (FASOC-UCNPs) were prepared by coating folate-modified amphiphilic chitosan (folate-N-succinyl-N?-octyl chitosan, FASOC) on the oleic acid-capped UCNPs. Photosensitizer Zinc (II) phthalocyanine (ZnPc) was loaded into the UCNPs (FASOC-UCNPs) via hydrophobic interaction to form a novel tumor-targeted nanocomplex (FASOC-UCNP-ZnPc) for in vivo drug delivery and PDT treatment induced by near-infrared (NIR) light. The prepared FASOC-UCNP-ZnPc with an average diameter of 50 nm exhibits excellent optical properties and stability in aqueous phase. Cell viability assays indicate the low cytotoxicity of FA-UCNP-ZnPc on either normal cells or cancer cells. Cellular uptake studies in FR-positive Bel-7402 and FR-negative A549 cancer cells show that folate-conjugation on the UCNP enhances its tumor targeting capacity in FR-positive cells. For in vivo NIR imaging, organic dye ICG-Der-01 was co-encapsulated into the nanocomplex and tumor-targeting ability of FASOC-UCNPs in tumor-bearing mice was monitored. Results indicate that the FR-mediated nanocomplex can be accumulated much more in tumor site in less time, compared to SOC-UCNP without folate-conjugation. Under NIR light irradiation, the detection of singlet oxygen production in cancer cells by fluorescence imaging indicates that ZnPc can effectively generate singlet oxygen excited by the emission from UNCPs, resulted in cell death. All the results demonstrate the promising potential of FA-UCNP-ZnPc for PDT of cancer triggered by NIR light with deeper tissue penetration depth.

Keywords: Upconversion nanoparticles; amphiphilic chitosan; folate-receptor; tumor-targeted; singlet oxygen

8582-15, Session 4

Combined photothermal therapy and chemotherapy in cancer using HER-2 targeted PLGA nanoparticles

Anthony J. McGoron, Supriya Srinivasan, Tingjun Lei, Florida International Univ. (United States); Yuan Tang, Temple Univ. (United States); Romila Manchanda, Florida International Univ. (United States)

Introduction: We previously reported the synergistic effects of hyperthermia by indocyanine green (ICG) and chemotherapy by doxorubicin (DOX) in cancer cells. Here was report the effects of the combined therapy when co-delivered in poly–lactide-co-glycolide (PLGA) nanoparticles (NPs) conjugated to the monoclonal antibody (Ab) for HER-2 targeting. Methods: ICG and DOX loaded PLGA NPs (IDNP) were prepared by o/w emulsion solvent evaporation method and their surface further conjugated with anti- HER-2 monoclonal Ab (referred to as AIDNP). NPs were characterized for their size and zeta potential and evaluated for combined chemotherapy and hyperthermia therapy in three different cell lines, SKOV-3 (HER-2 positive), MESSA/DX5 (negative control for targeting but positive for multidrug resistance) and MESSA (negative control for both targeting and MDR). Hyperthermia treatment was by exposing the nanoparticles to 808 nm NIR laser for 3 min. Results: Ab conjugation efficiency was ~8.9 µg/mg NPs. NPs had an average size of 167 nm (PDI=0.06) which increased to 210 nm (PDI=0.16) after Ab conjugation. Zeta potential increased from -11.8 mV to +1.2 mV after Ab conjugation. Uptake of AIDNP in SKOV-3 was greater than IDNP because of the presence of the HER-2 receptor on SKOV-3 cells and the uptake of DOX via NPs (with or without Ab) was greater than free DOX in MESSA/DX5 because of their ability to bypass the Pgp MDR efflux pump of those cells. AIDNP increased toxicity in SKOV-3 in comparison to IDNP without hyperthermia but when exposed to laser the toxicity was enhanced 3X compared to IDNP.

8582-16, Session 4

Photothermal effects of immunologically modified carbon nanotubes

Wei R Chen, Univ. of Central Oklahoma (United States); Xiaosong Li M.D., Chinese PLA General Hospital (China); Okhil Kumar Nag, Jessica D. Goddard, Joseph Acquaviva, Univ. of Central Oklahoma (United States); Yongqiang Tan, Southwest NanoTechnologies Inc. (United States); Tomas Hode, ImmunoPhotonics, Inc. (United States); Hong Liu, The Univ. of Oklahoma (United States)

Carbon nanotubes have a great potential in the biomedical applications. To use carbon nanotubes in the treatment of cancer, we synthesized an immunologically modified single-walled carbon nanotube (SWNT) using a novel immunomodifier, glycated chitosan (GC), as an effective surfactant for SWNT. This new composition SWNT-GC was stable due to the strong non-covalent binding between SWNT and GC. The structure of SWNT-GC is presented in this report. The photothermal effect of SWNT-GC was investigated under irradiation of a near-infrared laser. SWNT-GC retained the optical properties of SWNT and the immunological properties of GC. Specifically, the SWNT-GC could selectively absorb a 980-nm light and induce desirable thermal effects in tissue culture and in animals. It could also induce tumor cell destruction, controlled by the laser settings and the doses of SWNT and GC. Laser+SWNT-GC treatment could also induce strong expression of heat shock proteins on the surface of tumor cells. This immunologically modified carbon nanotube could be used for selective photothermal interactions in non-invasive tumor treatment.

8582-17, Session 5

in vivo universal flow cytometry for detection of circulating tumor cells in blood, lymph, and cerebrospinal fluid *(Invited Paper)*

Ekaterina I. Galanzha, Univ. of Arkansas for Medical Sciences (United States)

This report introduces in vivo multi-fluid photoacoustic flow cytometry (mPAFC) for the detection and enumeration of circulating tumor cells (CTCs) in the three most important body fluids – blood, lymph and cerebrospinal fluid (CSF). The advantages of the presented approach are (1) improving sensitivity by at least a two-order of magnitude compared to commercial CTC- assays; and (2) significantly extending biomedical applications compared to existing in vivo flow cytometries. Using mouse tumor models of metastatic breast cancer and melanoma, we demonstrated that mPAFC can overcome great challenge in cancer research related to the ability to test lymph, CSF and blood CTCs at the same time points at single-cell levels in the natural microenvironment in vivo over the long-term period of metastatic disease development from early micrometastatic stages to deadly multiple macro-metastasis. The combination of mPAFC with PA lymphography and PA cytometry, as well as with functionalized nanoparticles as high-contrast, low-toxic PA contrast agents, allowed us to define in vivo cross-correlations between lymph, CSF and blood CTCs, size of primary tumor and nodal and distant metastases. We anticipate that this technology with safe for human parameters can be quickly translated to the bedside through the development of a portable multifunctional flow cytometry.

8582-18, Session 5

in vivo flow cytometry visualizes the effects of tumor resection on metastasis by real-time monitoring of rare circulating cancer cells *(Invited Paper)*

Xunbin Wei, Shanghai Jiao Tong Univ. (China)

The quantification of circulating tumor cells (CTCs) is an emerging tool used to diagnose, stratify and monitor patients with metastatic diseases. In vivo flow cytometry (IVFC) has the capability to measure the dynamics of fluorescently labeled CTCs continuously and non-invasively. In this study, we monitored CTC dynamics in a GFP-transfected orthotopic tumor model of metastatic hepatocellular carcinoma (HCC) using IVFC. Our IVFC approach showed a 1.8-fold higher sensitivity than whole blood analysis by conventional flow cytometry and was able to distinguish CTC changes between orthotopic and subcutaneous tumor models. We also used our model to investigate whether liver resection promotes or restricts hematogenous metastasis in advanced HCC. Both the number of CTCs and early metastases decreased significantly after tumor resection. Resection also prominently restricted hematogenous and distant metastases. Importantly, CTC numbers correlated with tumor growth in the orthotopic tumor model, including the number and size of distant metastases. When combined with orthotopic tumor models, the novel IVFC technique presented here offers the capability to elucidate mechanisms that drive hematogenous metastasis and to monitor the efficacy of cancer therapy.

8582-19, Session 5

Real-time monitoring of drug carrier pharmokinetics with ultra-fast photoacoustic flow cytometry

Mustafa Sarimollaoglu, Dmitry A. Nedosekin, Ekaterina I. Galanzha, Vladimir P. Zharov, Univ. of Arkansas for Medical Sciences (United States)

The rapidly growing development and application of nanotechnology-based drug and gene carriers has placed an urgent demand on monitoring their dynamic interactions with blood cells and clearance rates in the vessels of various locations. No clinically relevant method has been developed to address this problem adequately. As most contrast agents and drug carriers have intrinsic or enhanced optical absorption, photoacoustic flow cytometry (PAFC) is an almost ideal tool for real-time, label-free monitoring of their pharmacokinetics. We present here a new multicolor PAFC using a high pulse repetition laser array with different wavelengths (e.g., 532 n, 671 nm, 820 nm, and 1064 nm) to monitor the pharmokinetics of liposomes, nanoparticles coated with drug (e.g., gold-TNF-alpha), nanoparticles with empty core (e.g., golden carbon nanotubes), and conjugated microbubbles. We discovered that after injection of drug carriers or contrast agents, PAFC provides two typical signal trace patterns: an increase in the baseline level above blood background, and strong fluctuations above baseline. The first pattern is associated with homogenous random distribution of nano-objects in circulation, while the second pattern is related with the presence of their aggregates which provide a stronger localized absorption. The clearance rate of most nanoparticles depending on their surface properties was in the range of 0.5-4 hours, while liposomes demonstrated a long term circulation of up to a few days. We revealed dynamic aggregation of nanoparticles in blood flow during and immediately after injection, while prior to injection they demonstrated homogenous, non-clustered patterns. The proposed technique can be useful for the routine evaluation of possible influence of the natural properties of drug careers, the protective materials, and the coating procedures on their clearance. It also allows the minimization of the number of animals used, in contrast to ex vivo methods where periodical blood sampling is required.

8582-1, Session 6

Quantitative analysis of contrast to noise ratio using a phase contrast x-ray imaging prototype

Muhammad U. Ghani, Di Wu, Minhua Kang, Yuhua Li, The Univ. of Oklahoma (United States); Wei R. Chen, Univ. of Central Oklahoma (United States); Xizeng Wu, The Univ. of Alabama at Birmingham (United States); Hong Liu, The Univ. of Oklahoma (United States)

The purpose of this study was to determine the Contrast to Noise Ratio (CNR) of the x-ray images taken with the phase contrast imaging mode and compare them with the CNR of the images taken under the conventional mode. For each mode, three images were taken under three exposure conditions of 100 kVp (2.8mAs), 120 kVp (1.9mAs) and 140kVp (1.42mAs). A 1.61cm thick contrast detail phantom was used as an imaging object. For phase contrast, the source to image detector distance (SID) was 182.88 cm and the source to object (SOD) distance was 73.15 cm. The SOD was the same as SID in the conventional imaging mode. A computed radiography (CR) plate was used as a detector and the output CR images were converted to linear form in relation with the incident x-ray exposure. To calculate CNR, an image processing software was used to determine the mean pixel value and the standard deviation of the pixels in the region of interest (ROI) and in the nearby background around ROI. At any given exposure condition investigated in this study, the CNR values for the phase contrast images were better as compared to the corresponding conventional mode images. The superior image quality in terms of CNR is contributed by the phase-shifts resulted contrast, as well as the reduced scatters due to the air gap between the object and the detector.

8582-2, Session 6

The impact of the motion blur on pathological chromosome image quality: a preliminary study

Yuchen Qiu, Yuhua Li, The Univ. of Oklahoma (United States); Bin Zheng, Univ. of Pittsburgh (United States); Shibo Li M.D., Univ. of Oklahoma Health Sciences Ctr. (United States); Wei R. Chen, Univ. of Central Oklahoma (United States); Hong Liu, The Univ. of Oklahoma (United States)

The purpose of the study is to investigate the impact of motion blur on cytogenetic image quality. During the chromosome scanning, high speed is applied to optimize the efficiency. However, when increasing the scanning speed, the obtained image may be blurred. In this study, the relationship between the scanning speed and image blur is investigated using standard resolution targets. Then clinical cytogenetic sample slides are imaged to examine the impact of the motion blur on the cytogenetic image quality, by subjectively assessing the chromosome band sharpness. The results of this study may be useful for optimizing the efficiency and accuracy of clinical cytogenetic imaging procedures.

8582-3, Session 6

An intrinsic method in characterizing the potential and imaging quality of a phase-contrast tomosynthesis prototype by using phantoms

Di Wu, Hui Miao, Yuhua Li, The Univ. of Oklahoma (United States); Wei R. Chen, Univ. of Central Oklahoma (United States); Xizeng Wu, The Univ. of Alabama at Birmingham (United States);

Hong Liu, The Univ. of Oklahoma (United States)

This research is aimed at studying the advantages of an x-ray phase-contrast tomosynthesis prototype by using ACR and other phantoms. A prototype system is assembled with a micro-focus x-ray source, a rotating stage and a CR detector mounted on an optical rail. In experiments, the phantoms are placed on the rotating stage. Angular projection images are acquired from -20˚ to +20˚ with 2˚ interval. The in-plane slices are reconstructed. The feature groups on the phantom with different dimension are observed. The prototype system provides an intrinsic way to investigate the potential and imaging quality of a phase-contrast tomosynthesis imaging method.

8582-4, Session 6

Application of multi-exposure time laser speckle imaging in mouse ear swelling test for weak allergens

Vyacheslav Kalchenko, Yuri Kuznetsov, Weizmann Institute of Science (Israel); Igor V. Meglinski, Univ. of Otago (New Zealand); Alon Harmelin, Weizmann Institute of Science (Israel)

The multi-exposure time Laser Speckle Imaging approach is used for evaluation of acute skin reaction to allergens and contact irritants. During the test a substance or allergen is applied on the mouse ear for a short period of time and the acute skin reaction is identified as a swelling. We demonstrate that our approach allows significantly improve sensitivity of the preclinical Mouse Ear Swelling Test (MEST) for weak allergens.

8582-20, Session PTues

Immune responses induced by immunologically modified carbon nanotube under NIR laser irradiation

Wei R Chen, Univ. of Central Oklahoma (United States); Feifan Zhou, MOE Key Lab. of Laser Life Science & Institute of Laser Life Science (China); Xiaosong Li M.D., Chinese PLA General Hospital (United States); Jessica D. Goddard, Jessnie Jose, Univ. of Central Oklahoma (United States); Roman F. Wolf D.V.M., Eric Howard, The Univ. of Oklahoma Health Sciences Ctr. (United States); Tomas Hode, ImmunoPhotonics, Inc. (United States); Hong Liu, The Univ. of Oklahoma (United States)

We synthesized an immunologically modified single-walled carbon nanotube (SWNT) using a novel immunomodifier, glycated chitosan (GC), as an effective surfactant for SWNT. SWNT-GC could serve as a light-absorbing agent of a near-infrared light for selective photothermal interaction in cells and in animals, as shown in a previous study. In the current study, this new composition was used as a stimulant to induce immune responses. It could directly activate immune cells, particularly dendritic cells and macrophages. It could also cause T cell proliferation. More importantly, SWNT could carry GC into the tumors cells. In combination with laser irradiation, SWNT-GC could induce further immune activities, such as enhanced interactions between dendritic cells and tumor cells and enhanced antigen presentation to T cells. In animal studies, laser+SWNT-GC treatment tumors caused T cell infiltration to tumor sites. Our results indicated that SWNT-GC, when used in the combination with laser irradiation, could provide a synchronized photothermal and immunological interactions for cancer treatment.

8582-21, Session PTues

Synthesis and aggregation-mediated optical properties of pH-responsive novel conjugated polyampholytes

Okhil K. Nag, The Univ. of Oklahoma Health Sciences Ctr. (United States)

Conjugated polyelectrolytes (CPs) have been highly studied water-soluble molecule for their valuable optoelectronic properties. Due to the easily measureable recognition event using standard optical instruments, CPs are starting to find use in vast area of detecting or sensing of chemicals and biomolecules. In this work we designed and synthesized two novel conjugated polyampholytes (P1QA and P2QA) containing fluorene and 2,1,3-benzothiadiazole (BT, 5% and 10%) moieties in the main chain, and quaternary ammonium ion and carboxylic acid group on the side chains of the polymers. Florescence spectral study of the polymers showed decrease in green (fluorene) and increase in red (BT) emission while pH was changed slowly from 3 to 11. This is perhaps because of the aggregation of the polymer backbone by electrostatic interaction between positively charged quaternary ammonium ions and negatively charged carboxylate ions. This phenomena facilitates the fluorescence resonance energy transfer (FRET) from green to red moieties of the polymers.

8582-22, Session PTues

Assessments of urine cofilin-1 in patients hospitalized in the intensive care units with acute kidney injury

Yi-Jang Lee, National Yang-Ming Univ. (Taiwan); Cheng-Han Chao, National Taiwan Univ. Hospital (Taiwan); Ying-Feng Chang, Chien Chou, Molecular Medicine Research Ctr., Chang Gung Univ. (Taiwan)

Excretion of the actin depolymerizing factor (ADF)/cofilin in urine is found in rats with renal ischemia. Whether urine ADF/cofilin level is correlated to patients with shock during ischemia/reperfusion is unknown. Here, we adopted a high-throughput fiber-optic biosensor based on the gold nanoparticles (GNPs)-enhanced fluorescence technique combined with a sandwich immunoassay to detect the levels of urine cofilin-1 in intensive care units (ICU) hospitalized patients suffered from shock during renal ischemia. Fifty-seven ICU patients and 29 healthy controls were recruited, and the results of measurement showed that the maximum levels of urine cofilin-1 detected in ICU patients and healthy controls were 1.625 and 0.563 after background subtraction, respectively. The mean urine cofilin-1 level of ICU patients with shock was significantly higher than that of healthy controls. An examination of the receiver operating characteristic (ROC) curves showed that cofilin-1 was acceptable for distinguishing ICU patients with shock [area under curve (AUC)=0.700, p=0.004], but not those without shock (AUC=0.619, p=0.154) from the healthy adults. The cell-based study using human proximal tubule cells suggests that ischemia/reperfusion induced oxidative stress may be involved in increase of urine cofilin-1 level. To the best of our knowledge, this is the first reports demonstrated that GNP-conjugated biosensor was able to detect the increased cofilin-1 in urine of ICU patients. This preliminary clinical study suggests that urine cofilin-1 is significantly increased in ICU patients with shock and that it would be important for the clinical diagnosis of related disorders.

8582-23, Session PTues

Gemcitabine induces caspase-dependent apoptosis in A549 cells

Chubiao Zhao, Weijie Gao, Tong-Sheng Chen, South China Normal Univ. (China)

Non Small Cell Lung Cancer (NSCLC) remains the leading cause of cancer-related deaths in the world. Because of its early metastasis and resistance to chemotherapeutic agents, NSCLC is one of the malignant neoplasms with seriously poor prognosis. Gemcitabine (2',2'-difluorodeoxycytidine, dFdC), the standard first-line chemotherapeutic agents in several solid tumors especially NSCLC, is a deoxycytidine analogue. After uptake into cells, Gemcitabine can be activated by deoxycytidine kinase and become into gemcitabine diphosphate and triphosphate (dFdCDP and dFdCTP) that are both active metabolites. dFdCDP can inhibit ribonucleotide reductase effectually, and dFdCTP can arrest DNA synthesis. However, the resistance mechanism of cancers to Gemcitabine, a common problem in the clinical treatment, is not well understood. In this report, we found that Gemcitabine induced A549 cells death via a caspase-dependent apoptotic fashion. CCK-8 assay showed that Gemcitabine exerted a dose- and time-dependent cytotoxicity. Hoechst 33258 staining experiments exhibited that Gemcitabine induced typical apoptotic morphology as chromatin condensation and nucleus shrinkage. AnnexinV-FITC/PI apoptosis detection showed that Gemcitabine mediated A549 cell death mostly via apoptosis. We also found Gemcitabine induced the loss of mitochondrial membrane potential by using Rhodamine 123 staining and pretreatment with caspase inhibitors significantly attenuated the cytotoxicity of Gemcitabine. Collectively, Gemcitabine induces apoptosis of A549 cells through caspase-dependent intrinsic pathway.

8582-24, Session PTues

Paclitaxel crystal in Paclitaxel injection aqueous solution

Tong-Sheng Chen, Jingqin Chen, South China Normal Univ. (China)

Paclitaxel (Taxol) is effective against ovarian cancer and breast cancer. It is clinically administered with polyethoxylated castor oil (Cremophor EL) and ethanol due to its low solubility in water, forming the Paclitaxel Injection (TaxolTM). Recently, we functionalized nano-graphene oxide (NGO) with polyethylene glycol (PEG) to obtain a biocompatible NGO-PEG that is stable conjugate in aqueous solution. The NGO-PEG was used to attach the taxol in TaxolTM non-covalently via π-π stacking. The resulting NGO-PEG-Taxol complex can be applied to the treatment of cancer in vitro and in vivo. We found a phenomenon that some needle crystal precipitation occurred in the aqueous solution of TaxolTM and NGO-PEG after mixing 7 days. The TaxolTM was tried to be dissovled in water solely and saved for 7 days, and the needle crystal precipitation crystallized out of the solution was isolated by ultracentrifugation and confirmed to be taxol by UV-Vis and FT-IR Spectrometer. The taxol concentration dissolved in the solution under various conditions with different temperature, concentration of taxolTM and pH value was measured by UV-Vis Spectrometer after separating the crystal by 0.22 μm filter, and we found that the maximum crystallization rate of taxol appeared in the case of room temperature, 0.2 mg/ml of taxolTM, pH=5 after 7 days, indicating that the aqueous solution of TaxolTM is unsuitable for preserving for long time.

8582-25, Session PTues

Sodium nitroprusside induces apoptosis of rabbit chondrocytes

Qian Liang, Xiao-ping Wang, The First Affiliated Hospital of Jinan Univ. (China); Tong-Sheng Chen, South China Normal Univ. (China)

Osteoarthritis (OA) is characterized by a slowly progressing degradation of the matrix and destruction of articular cartilage. The apoptosis of chondrocyte that is the only cell type present in mature cartilage and solely responsible for the production and maintenance of the extracellular matrix is accounted for the mechanism of OA. Nitric Oxide(NO), as a stimulus, has been shown to activate the matrix metalloproteinases (MMPs), increase the expression of cyclooxygenase 2(COX-2) and the level of prostaglandin E2(PGE2), inhibit the proteoglycan synthesis and type II collagen expression, and induce the apoptosis of chondrocytes. In this study, sodium nitroprusside(SNP) was administered to be the NO donor to explore the mechanism of NO-induced apoptosis of rabbit chondrocytes obtained from six weeks old New Zealand rabbits. CCK-8 assay revealed the inhibitory effect of SNP on cell viability of chondrocytes. We used flow cytometry(FCM) to assess the form of cell death by Annexin-V/PI double staining, and evaluated the change of mitochondrial membrane potential (??m) by confocal microscopy imaging. We found that the NO donor SNP induced apoptosis of chondrocytes in a dose- and time-dependent manner and an observable reduction of ??m. Furthermore, CCK-8 assay was applied to uncover the roles of caspases and whether the SNP-induced apoptosis was caspase-dependent. In conclusion, our findings indicate that SNP induces apoptosis of rabbit chondrocytes via mitochondrial-mediated pathway and dependenting on caspases.

8582-26, Session PTues

Using immunoadjuvant agent glycated chitosan to enhance anti-tumor immunity induced by HIFU

Ying-Ling Chen, National Yang-Ming Univ. (Taiwan); Wei R. Chen, Univ. of Central Oklahoma (United States); Fang-Yi Yang, National Yang-Ming Univ. (Taiwan); Chung-Yi Wang, Cheng Hsin General Hospital (Taiwan); Yi-Jang Lee, National Yang-Ming Univ. (Taiwan)

Thermal therapy is based on the observation that tumor cells are sensitive to increased temperature, and is important for tumor control. In this study, the high intensity focused ultrasound (HIFU) system was used to non-invasively elevate temperature and applied for breast cancer control in the small animal model. Additionally, the immunoadjuvant agent, so-called glycated chitosan(GC), was used to enhance the immunological effects on tumor control.

First, we stably transduced multimodality molecular imaging probes, including mRFP, firefly luciferase and herpes simplex virus 1 thymidine kinase (HSV1-tk) into murine 4T1 breast cancer cell line. The growth and metastatic tumor cells can then be detected using the IVIS system and microSPECT/CT system for fluorescence imaging and radionuclide-based imaging, respectively. Cells were s.c. implanted into the back of female Balb/c mice. When tumor size reached approximately 200 mm3, mice were divided into four different treatment groups. The group treated with 1% GC combining HIFU at a dose of 28W/sec for 2 minutes showed better tumor control than untreated control. The HIFU or GC treated group also exhibited worse tumor control than combined treatment. Two weeks after treatment, we sacrificed mice for immunohistochemical (IHC) staining and H&E staining. Tumor sections were stained with CD4, CD8, CD11 and CTLA4 to validate the accumulation of lymphocytes and macrophages in treated tumors. It showed that highly immune activity in tumors at the group of combined treatments. We also collected plasma from mice with different treatments for investigation of bystander effects in vitro, and the plasma from the group of combined treatments was effective to reduce tumor viability.

The experimental results showed that the HIFU therapy combined GC can enhance the tumor immunogenicity and increase the tumor control.

8582-27, Session PTues

Inhibitory efficacy of the quantified prunellae spica extract on H22 tumor bearing mice

Zhiping Wang, Guangdong Pharmaceutical Univ. (China); Tong-Sheng Chen, South China Normal Univ. (China)

Hepatocarcinoma a malignant cancer, threaten human lives badly. It is a current issue to seek the effective natural remedy from plant to treat cancer due to the resistence of the advanced hepatocarcinoma to chemotherapy. In this report, we assessed the antitumor activity of a prunellae spica extract (PSE) in vitro and in vivo. PSE was quantified by HPLC and UV. The in vitro cytotoxicity of PSE against SMMC-7721 cells was evaluated by MTT assay, and the effects of PSE on cell cycle and cell apoptosis was analyzed by flow cytometry. PSE effectively inhibited the proliferation of SMMC-7721 cells and PSE arrested SMMC-7721 cells in the G2/M cycle. The in vivo anti-tumor activity was assessed by using the mice bearing H22 tumor. In vivo studies showed the higher antitumor efficency of PSE without significant side effect assessed by the reduced tumor volume and tumor weight, and the extended survival time, life span, survival rate, as well as the lower toxicity of PSE to the liver and spleen as well as kidney of the mice bearing H22 solid tumor. Collectively, PSE is a promising Chinese medicinal herb for treating hepatocarcinoma.

8582-28, Session PTues

A bispecific peptide based near-infrared probe for in vivo tumor diagnosis

Yueqing Gu, China Pharmaceutical Univ. (China); Li Ding, China Pharmaceutical Univ. (China); Wei R. Chen, Univ. of Central Oklahoma (United States)

The epidermal growth factor receptor EGFR and HER2 are members of recepeter tyrosine kinase family. Overexpression ofEGFR and HER2 has been observed ina variety of human tumors, making these receptors promising targets for tumor diagnosis. An affibody targeting HER2 and a nanobody targeting EGFR were reported before. In this Manuscript, we describe an bispecific peptide combined with an affibody and a nanonbody through a linker??G4S?3 . And the bispecific peptide was labeled with near-infrared (NIR) fluorochrome MPA for in vivo tumor EGFR and HER2 targeting. Afterwards, the EGFR and HER2 specificity of the fluorescent probe was tested in vitro for receptor binding assay and fluorescence microscopy and in vivo for subcutaneous MDA-MB-231 tumor targeting. The results indicated that the bispecific peptide had a high affinity to EGFR and HER2. Besides, in vitro and in vivo tumor targeting experiment indicated that the MPA-(bispecific peptide) showed excellent tumor activity accumulation. Noninvasive NIR fluorescence imaging is able to detect tumor EGFR and HER2 expression based upon the highly potent bispecific peptide probe.

8582-29, Session PTues

The preparation and characteristic of a drug carrier for hepatocellular carcinoma-selective targeting

Yuxiang Ma, Yuqi Chen, Sisi Cui, China Pharmaceutical Univ. (China); Wei R. Chen, Univ. of Central Oklahoma (United States); Yueqing Gu, China Pharmaceutical Univ. (China)

Asialoglycoprotein receptors distribute on hepatic parenchymal cells can specifically recognize galactose residues, so galactose residues can be applied in hepatocellar carcinoma targeted therapy through binding to the asialoglycoprotein receptors on the membrane of the liver cells.We constructed a drug carrier of PEG-peptide chain-chitosan oligosaccharide-galactose. Due to steric hindrance effect of PEG, drugs will not bind to the normal liver cells and avoid damage to them.

Hepatocellar carcinoma (HCC) cells have a high expression of MMP-2, which can cleavage the peptide chain (Gly-Pro-Leu-Gly-Ile-Ala-Gly-Gln). So antitumor drugs can be distinguished specially targetted to HCC cells. In this paper, we can successfully target the drug to liver cancer cells, and avoid damage to normal liver cells.

8582-30, Session PTues

Novel 2DG-based harmine derivatives for targeted cancer therapy

Aqin Wang, Yuqi Chen, China Pharmaceutical Univ. (China); Wei R. Chen, Univ. of Central Oklahoma (United States); Yueqing Gu, China Pharmaceutical Univ. (China)

Harmine is a beta-carboline alkaloid from the plant Peganum harmala. Previous investigations focused on the effects of carboline alkaloids on the central nervous system (CNS). However, interests in these alkaloids were stimulated by their promising antitumor activities in the recent years. In this study, we designed and synthesized two harmine derivatives #1and #2 modified at position-9 of harmine with ethyl and phenylpropyl, respectively. To improve the tumor targeting capability, #1' and #2' were synthesized by conjugating 2-amino-2-deoxy-D-glucose (2DG) to the derivatives #1and #2, respectively. The synthesis, characterization, comparison, targeting ability of 2DG, and in vitro efficiency and in vivo acute neurotoxicity of these novel complexes were investigated. The MTT assays of all these compounds in vitro against L02, HepG2, Bel-7402, MDA-MB-231, MCF-7 and A549 showed all compounds had low toxicity to normal cells (L02) and significantly enhanced carcinoma cell inhibitory rate compared to harmine. Moreover, the derivative #2' displayed the most significant activity toward hepatocellular carcinoma cell (HepG2, Bel-7402). Cytotoxicity against all five cancer cell lines of compound #1' #2' is higher than #1 #2, and even the compound #2' is better than positive drug 5-FU, which proved the remarkable increasingly anti-tumor and targeting abilities of 2DG. The healthy mice receiving 100mg/kg of #2' gave no any neurotoxic response. The compound #2', a novel 2DG-based harmine derivatives, could become a promising drug for targeted cancer therapy and combination therapy with other antitumor drugs.

8582-31, Session PTues

Role of macrophages in circulating prostate cancer cells studied by in vivo flow cytometry

Xunbin Wei, Shanghai Jiao Tong Univ. (China)

Metastasis is a very complicated multi-step process and accounts for the low survival rate of the cancerous patients. To metastasize, the malignant cells must detach from the primary tumor and migrate to secondary sites in the body through either blood or lymph circulation. Macrophages appear to be directly involved in tumor progression and metastasis. However, the role of macrophages in affecting cancer metastasis has not been fully elucidated. Here, we have utilized a novel technique, namely in vivo flow cytometry (IVFC) to study the depletion kinetics of circulating prostate cancer cells in mice and how depletion of macrophages by the liposome-encapsulated clodronate affects the depletion kinetics. Our results show different depletion kinetics of PC-3 cells between macrophage-deficient group and the control group. The number of circulating tumor cells (CTCs) in macrophage-deficient group decreases in a slower manner compared to the control mice group. The differences in depletion kinetics indicate that the absence of macrophages facilitates the stay of prostate cancer cells in circulation. In addition, our imaging data suggest that macrophages might be able to arrest, phagocytose and digest PC-3 cells. Therefore, the phagocytosis may mainly contribute to the depletion kinetic differences. The developed methods here would be useful to study the relationship between macrophages and tumor metastasis in small animal cancer model.

8582-32, Session PTues

Intravital optical imaging of leucocytes dynamics during the delayed type hypersensitivity reaction

Meijie Luo, Sha Qiao, Qingming Luo, Zhihong Zhang, Britton Chance Ctr. for Biomedical Photonics (China)

The cellular immune response is characterized by large influxes of nonspecific inflammatory cells which attribute to tissue damage and organ dysfunction. Here, we developed a model of delayed-type hypersensitivity (DTH) reaction in the footpad of C57/6L mouse, which elicited by heat aggregated OVA antigen. The monocytes, neutrophils and effector memory T cells (Tem) of the mouse model were labeled with multi-color fluorescence dye, respectively. A significant increase of tissue swelling and leucocytes invasion of neutrophils and monocytes were appeared at 48hr after challenge. The dynamics of monocytes, macrophages/DCs, neutrophils and Tem in the DTH inflammation foci were simultaneously visualized by using two photon microscopy. Neurtrophils crawled with a median velocity of 6.3 ?m/min at 4 hr and reduced to 4.9?m/min at 48hr. Tem cells make constant contact with macrophages/DCs at 4hr and migrate rapidly at 48hr. The recruitment of monocytes and Tem cells are not dependent on the chemokine receptor CX3CR1. Thus CX3CR1 is not essential for DTH inflammation response and the recruitments of both monocytes and neutrophils give targets for modulation of DTH inflammation.

8582-33, Session PTues

Macrophage phagocytosis of cells undergoing HF-LPLI-induced apoptosis

Cuixia Lu, Da Xing, South China Normal Univ. (China)

High fluence low-power laser irradiation (HF-LPLI) provides a new stimulator to trigger cell apoptosis, and it is well known that apoptotic cells provide antigens to effectively trigger recognition by the immune system. In order to investigate the effect of HF-LPLI on the professional antigen-presenting cell (APC) function, in our primary study, we focused our attention on the effect of HF-LPLI-induced apoptotic cells on macrophages recognization and phagocytosis. Flow cytometry analysis experiments showed that HF-LPLI (120-480 J/cm2) induced significantly mouse mammary tumor cells EMT6 apoptosis in a dose-dependent manner. Both confocal microscopy and FACS analysis showed that murine macrophage cells RAW264.7 phagocytized HF-LPLI-induced apoptotic EMT6 cells. Taken together, our results indicate that HF-LPLI-induced apoptotic tumor cells can be effectively recognized by the immune system. The study of HF-LPLI effect on the APC function need to be further studied.

Conference 8583: Design and Performance Validation of Phantoms Used in Conjunction with Optical Measurement of Tissue V

Saturday - Sunday 2 –3 February 2013 • Part of Proceedings of SPIE Vol. 8583
Design and Performance Validation of Phantoms Used in Conjunction with Optical Measurement of Tissue V

8583-1, Session 1

Development of a Qdots 800 based fluorescent solid phantom for validation of NIRF imaging platforms *(Invited Paper)*

Banghe Zhu, Eva M. Sevick-Muraca, The Univ. of Texas Health Science Ctr. at Houston (United States)

Over the past decade, we developed near-infrared fluorescence (NIRF) devices for non-invasive lymphatic imaging using microdosages of ICG in humans and for detection of lymph node (LN) metastasis in animal models mimicking metastatic human prostate cancer. To validate imaging, a NIST traceable phantom is needed so that developed “first-in-humans” drugs may be used with different fluorescent imaging platforms. In this work, we developed a Qdots 800 based fluorescent solid phantom for installation and operational qualification of clinical and preclinical, NIRF imaging devices. Due to its optical clearance, polyurethane was chosen as the base material. Titanium dioxide was used as the scattering agent due to its miscibility in polyurethane. Qdots 800 was chosen owing to its stability and NIR emission spectra. One set of phantoms was constructed for evaluation of the noise floor arising from excitation light leakage, a phenomenon that can be minimized during engineering and design of fluorescent imaging systems. The other set of phantoms was constructed to enable quantification of device sensitivity associated with our preclinical and clinical devices for qualification of new imaging agents. The phantoms have been successfully applied for installation and operational qualification of our clinical and preclinical devices. Assessment of excitation light leakage provides a figure of merit for “noise floor” and imaging sensitivity can be used to benchmark devices for specific imaging agents. We demonstrate the use of the phantoms for qualification of devices specific for an optimized mAb-based agent targeting EpCAM in pre-clinical prostate cancer positive LNs. Supported by NIH U54 CA136404.

8583-2, Session 1

Simulations of light propagation in biological tissues by considering the modelling of light sources and sensors

David Klinger, Jens Kraitl, Hartmut Ewald, Univ. Rostock (Germany)

Simulations of biological tissues are a useful method in detector development for tissue spectroscopy. Usually attention is only paid to the adequate description of tissue structures and the ray trace procedure. The surrounding light source geometry, like output window, reflector and casing is neglected. Instead, the description of light source is usually reduced to incident beam paths. This also applies to detectors and further surrounding tissue connected sensor geometry. We characterized the influence of a complex and realistic description of the light source and detector geometry with the ray tracing software ASAP (Breault Research Organization). Additionally simulations include the light distribution curve in respect to light propagation through the tissue model. We observed that the implementation of the geometric elements of the light source and the detector have direct influence on the propagation paths, average photon penetration depth, average photon path length and detected photon energy. The results show the importance of the inclusion of realistic geometric structures for various light source, tissue and sensor scenarios, especially for reflectance measurements. In reality the tissue surrounding sensor geometry has a substantial impact on surface and subsurface reflectance and transmittance due to the fact that a certain amount of photons is prevented from leaving the tissue model. Further improvement allows a determination of optimal materials and geometry for the light source and sensors to increase the number of light-tissue-interactions by the incident photons.ent allows a determination of optimal materials and geometry for the light source and sensors to increase the number of light-tissue-interactions by the incident photons.

8583-3, Session 1

Reconstructing optical parameters from double integrating sphere measurements using a genetic algorithm

Christoph Böcklin, Dirk Baumann, Jan Klohs, Markus Rudin, Jürg Fröhlich, ETH Zurich (Switzerland)

The exact knowledge of the optical material parameters μa, μs and g are key for the reconstruction of physiological changes in tissue detected by optical techniques. Hence it is of paramount importance, to be able to accurately determine these parameters for any tissue or phantom material. One approach is to use a double integrating sphere measurement system. This approach offers a flexible way to measure various kinds of tissue, liquids and artificial phantom materials yielding three measured values, namely the total reflection Rt, total transmission Tt and unscattered transmission Tc. Accurate measurements can be achieved by technical adjustments and calibration using reflection and transmission standards. No closed form for the determination of the optical parameters μa, μs and g exists up to now. Therefore, an inverse search algorithm combined with an appropriate solver for the solution of the forward problem (calculating Rt, Tt and Tc from μa, μs and g) has to be applied.

When analyzing the resulting fitness landscapes for real tissue and phantom materials, respectively, it becomes apparent, that in general the fitness landscape has several local minima, which calls for a heuristic search strategy. Here, a Genetic Algorithm is used for the reconstruction of the parameters.

Given the challenging preparation of real tissue samples it comes as no surprise that these tissue samples are subject to various uncertainties. In order to perform a robust parameter reconstruction samples of different thickness are used. This adds a further, strong restriction to the possible results from the reconstruction algorithm.

8583-4, Session 1

Dependent scattering effects as measured in high concentration silica beads suspensions

Ton G. van Leeuwen, Duc V. Nguyen, Jeroen Kalkman, Academisch Medisch Ctr. (Netherlands)

By transmission optical coherence tomography measurements we can sperate the non scattered transmission from the multiple scattered light. Using OCT at 1300 nm, we measured the scattering coefficient of high volume concentration silica beads (with diameters of 376, 759, 906 and 1215 nm as determined by TEM, concentrations ranging from 0 to 8-20 volume%) suspended in water. We found that above ~4 vol%, the measured scattering deviated form Mie theory. This non linear relation between the measured scattering coefficient with the concentration fitted perfectly with calculations based on the Percus-Yevick model for all 4 diameters. Thus dependent scattering effects have to be accounted for in highly scattering phantom materials, which can be accuned for by the Percus-Yevick model.

8583-5, Session 2

Optical properties of tissue-like phantoms based on Intralipid and India ink accurately assessed by means of a multi-center study

Lorenzo Spinelli, Consiglio Nazionale delle Ricerche Istituto di Fotonica e Nanotecnologie (Italy); Marcin Botwicz, Norbert Zolek, Michal Kacprzak, Daniel Milej, Piotr Sawosz, Adam Liebert, Institute of Biocybernetics and Biomedical Engineering (Poland); Udo Weigel, Turgut Durduran, ICFO - Institut de Ciències Fotòniques, Parc Mediterrani de la Tecnologia (Spain); Florian Foschum, Alwin Kienle, Institut für Lasertechnologien in der Medizin und Messtechnik, Univ. Ulm (Germany); François Baribeau, Sébastien Leclair, Jean-Pierre Bouchard, Isabelle Noiseux, Pascal Gallant, Ozzy Mermut, INO (Canada); Andrea Farina, Consiglio Nazionale delle Ricerche Istituto di Fotonica e Nanotecnologie (Italy); Antonio Pifferi, Alessandro Torricelli, Rinaldo Cubeddu, Politecnico di Milano (Italy); Hsin-Chia Ho, Industrial Technology Research Institute (Taiwan); Mikhail Mazurenka, Heidrun Wabnitz, Katy Klauenberg, Olha Bodnar, Clemens Elster, Physikalisch-Technische Bundesanstalt (Germany); Magali Bénazech-Lavoué, Yves Bérubé-Lauzière, Univ. de Sherbrooke (Canada); Frédéric Lesage, Ecole Polytechnique de Montréal (Canada); Dmitry Khoptyar, Arman A. Subash, Stefan Andersson-Engels, Lund Univ. (Sweden); Paola Di Ninni, Fabrizio Martelli, Giovanni Zaccanti, Univ. degli Studi di Firenze (Italy)

Optical measurements on tissue at visible and near infrared (NIR) wavelengths are inherently non-invasive, with a potentially high information content. Then, photon propagation through diffusing media like tissues has been investigated in depth for biomedical applications. As optical technologies are being developed towards clinical applications, the assessment of the reliability of the recovered information is an essential issue. Various protocols for the performance standardization assessment of optical instruments have been proposed. For the implementation of standardized procedures, however, the definition of reliable tissue-like phantoms is needed. A multi-center study has been set up to accurately characterize the optical properties of diffusive liquid phantoms based on Intralipid and India ink at NIR wavelengths. Nine worldwide spread research laboratories adopting different measurement techniques, instrumental set-ups, and data analysis methods determined at their best the optical properties and relative uncertainties of diffusive dilutions prepared with common circulating samples of the two compounds. By exploiting a suitable statistical model, comprehensive reference values for the intrinsic reduced scattering coefficient of Intralipid and the intrinsic absorption coefficient of India ink were determined with an uncertainty of about 1% for Intralipid and 2% for ink, at three NIR wavelengths. Availability, low cost, long-term stability of these compounds and the batch-to-batch reproducibility of Intralipid make them the preferable choice to prepare diffusive liquid phantoms with accurately known optical properties. This provides a unique fundamental tool for the calibration and performance assessment of diffuse optical spectroscopy instrumentation intended to be used in laboratory or clinical environment.

8583-6, Session 2

A tissue mimicking phantom model for applications combining light and ultrasound

Avihai Ron, Ilan Breskin, Noam Racheli, Yaakov Metzger, Revital Shechter, Ornim Medical Ltd. (Israel)

We describe a stable and reproducible liquid tissue mimicking phantom optimized for applications involving both ultrasound and light. The phantom has optical and acoustic properties similar to biological tissue as well as a similar decorrelation time. The phantom base material is Glycerol. The Glycerol has low absorption and no scattering in the NIR range. The sound velocity and acoustic impedance of Glycerol (1904 m/s and 234 Kg/(cm2 sec) respectively) are similar to those of tissue. The viscosity of the glycerol provides a decorrelation time similar to that of tissue. Decorrelation time was estimated using ultrasound (US) modulated light by measuring the speckle pattern linewidth at the Ultrasound frequency. For an US frequency of 1MHz, linewidths of 540 ± 10 KHz and 460 ± 10KHs were obtained from the phantom and from a human arm respectively. TiO2 was added to the Glycerol as scattering particles. The phantom's scattering coefficient was measured in transmission mode using a double collimators setup. A concentration of 0.1% TiO2 provided a reduced scattering coefficient ?s' = 11.4 ±1 cm-1. Different dyes were added to obtain desired absorptions in the NIR range. The phantom's optical absorption was measured by Spatially Resolved Spectroscopy in a semi-infinite geometry. Pro-Jet 800TM (Fujifilm) dye at concentrations of 6E-4 % - 9E-4 % provided an absorption coefficient of: ?a = 0.12 - 0.18 ± 0.015 cm-1 @ 830nm. In addition, optical absorption was measured using the acousto-optic effect with Ornim Medical proprietary technology.

8583-7, Session 2

Stable phantoms for characterization of photoacoustic tomography (PAT) systems

Sarah E. Bohndiek, Dominique Van De Sompel, Sandhya Bodapati, Sri-Rajasekhar Kothapalli, Sanjiv S. Gambhir, Stanford Univ. (United States)

Photoacoustic tomography (PAT) is an emerging modality that combines the high contrast of optical imaging, with the spatial resolution and penetration depth of ultrasound, by exploiting the photoacoustic effect. As with any new imaging modality, reliable phantoms are needed to: calibrate instruments; validate performance; optimize signal-to-noise; perform routine quality control; and compare systems. Phantom materials for testing small animal PAT systems should also mimic both the optical and acoustic properties of soft tissue, while for calibration purposes should be resistant to degradation.

Polyvinyl chloride plastisol (PVCP) has previously been demonstrated as a potential phantom material for PAT at 1064nm. We show here that PVCP phantoms enable calibration and performance validation using two PAT systems with distinct designs (Visualsonics Vevo LAZR and Endra Nexus 128) across a wavelength range of 680nm-950nm. Inclusions between 2 and 3.2mm in diameter were fabricated from PVCP using a range of dye concentrations (0% to 0.256% Black Plastic Color, BPC) in a custom mold.

A calibration phantom was imaged repeatedly on both systems, over time scales of minutes, hours and days, to assess system stability. Both systems demonstrated good reproducibility over time, with the coefficient of variation in the measured signal-to-noise ratio (SNR) being less than 2% over the course of 30 days. Imaging performance was optimized by plotting SNR as a function of different system parameters. The visualization of objects embedded in optically absorbing and scattering backgrounds was also assessed. PVCP is easy to work with and provides stable phantoms for assessing PAT system performance.

8583-8, Session 2

Spectrally resolved digital cell phantoms for quantitative blood analysis of malaria infection

Jeeseong Hwang, David W. Allen, National Institute of Standards and Technology (United States); Fuyuki Tokumasu, National Institute of Allergy and Infectious Diseases (United States); Do-Hyun Kim, U.S. Food and Drug Administration (United States); Ji Youn Lee, Maritoni Litorja, Joseph P. Rice, National Institute of Standards and Technology (United States)

As hyperspectral imaging techniques are employed for label-free imaging of endogenous biomarkers, a need for standards is paramount for reliable clinical applications. In blood diagnosis, the standards may be blood samples with properties associated with diseases. However, they are limited by the batch-to-batch variations with a short shelf life. An alternative solution is a digital cell phantom (DCP) which is a medically significant hyperspectral image or scene of single cells with known disease characteristics. The DCPs may serve as measurement references for clinical validation. We will discuss a technique to produce DCPs and its application towards diagnosis of malaria infection.

8583-9, Session 2

OCT phantoms initiative

Anant Agrawal, U.S. Food and Drug Administration (United States); Brendan F. Kennedy, The Univ. of Western Australia (Australia); Guy Lamouche, Conseil National de Recherches Canada (Canada); Peter H. Tomlins, Queen Mary, Univ. of London (United Kingdom); Bobby Mote, Krishan M. Agrawal, Virginia State Univ. (United States)

Given the maturity of OCT and to facilitate clinical translation, there is an imminent need for widely available and standardized tools to benchmark OCT device performance. A variety of phantoms already exist for OCT, but there is no widely used and accepted standard. The OCT Phantoms Initiative has been created to fulfill this need. It is an open initiative to facilitate and accelerate the development of phantoms which are the most relevant to the OCT community. The OCT Phantoms Initiative currently consists of a small group of researchers in academia, industry, and government with interests and experience in developing OCT-specific phantoms.

The first task of the OCT Phantoms Initiative was to carry out a survey to clearly prioritize the need for standardized phantoms in the OCT community. The survey was completed in September 2012. We will present the results of the survey as well as a summary of the related discussions on the OCT Phantoms Initiative forum. The goal is to use this presentation as a means to engage the wider OCT community to foster discussion and plan the next steps towards standardized OCT phantoms.

8583-10, Session 3

Air Force test chart-like phantom for measuring axial and lateral resolution in optical coherence tomography

Ruo Yu Gu, Kristen L. Lurie, Audrey K. Ellerbee, Stanford Univ. (United States)

Optical coherence tomography (OCT) is a widely used technique for imaging biological structures when three-dimensional images are desired. In these images, both lateral and axial resolution are important figures of merit describing the quality of the imaging system. Phantoms such as the United States 1951 Air Force Test Chart (AFTC) can be used to quickly estimate lateral resolution, but these phantoms do not offer a method to measure axial resolution. Conversely, the conventional method for measuring axial resolution with a mirror is both time-intensive and cannot be used to see the degradation of closely-spaced features. To address this, we designed, fabricated and tested an optical phantom based on the AFTC that can be used to directly visualize both axial and lateral resolution.

In this work, we present the design of a polydimethylsiloxane (PDMS) -based phantom fabricated using soft lithography. This design can be used to quickly estimate the axial and lateral resolutions, or alternatively be used to measure the exact resolutions. In addition, we show how the patterned bar structure can be used as a guide to estimate the scattering properties of a medium surrounding the phantom and demonstrate functionality of the phantom on multiple OCT systems possessing a variety of source wavelengths and optical designs (and hence different axial and lateral resolutions). Further, we demonstrate performance of the phantom under a variety of conditions that mimic the absorbing and scattering properties of tissue.

8583-11, Session 3

Realistic phantoms for diffuse optical imaging using totally absorbing objects

Antonio Pifferi, Politecnico di Milano (Italy) and Consiglio Nazionale delle Ricerche (Italy); Fabrizio Martelli, Univ. degli Studi di Firenze (Italy); Davide Contini, Politecnico di Milano (Italy); Lorenzo Spinelli, Consiglio Nazionale delle Ricerche (Italy); Alessandro Torricelli, Politecnico di Milano (Italy); Heidrun Wabnitz, Rainer Macdonald, Physikalisch-Technische Bundesanstalt (Germany); Angelo Sassaroli, Tufts Univ. (United States); Giovanni Zaccanti, Univ. degli Studi di Firenze (Italy)

We propose a general concept for the construction of inhomogeneous diffuse optical imaging phantoms using totally absorbing objects to mimic lesions in tissue. The idea is based on the observation that a totally absorbing sphere of a certain (small) radius yields the same perturbation as a realistic absorption change within a larger volume in time-resolved photon migration measurements. Thus, we can always find a proper volume of a black object that can mimic the effect of any localized optical inhomogeneity. The importance of this Equivalence Principle lies in the fact that black defects are well characterized in terms of the optical properties; therefore experimental errors (due to wrong calibration) are strongly reduced.

Using time-resolved Monte Carlo simulations, we show that this Equivalence Principle is valid for different choices of geometry (source-detector arrangement, position of the inclusion, shape of the homogeneous medium), as well as photon arrival time, and background optical properties.

A possible way to determine the “equivalent” totally absorbing object is proposed using an analytical code for calculation of higher-order perturbation derived from the optical diffusion equation. The code can be easily implemented in a stand-alone freeware program. Using such approach, a conversion plot, mapping a combination of volume and absorption change of the inhomogeneity into the equivalent black object volume is shown. In the time-domain, the conversion plot is independent from the geometry, the photon arrival time, and the background absorption, with a weak dependence on the background scattering.

A practical implementation for the construction of solid/liquid inhomogeneous phantoms is proposed and validated, using black PVC cylinders immersed in a water solution of well-characterized Intralipid and India ink, whereas the same concept is good also for solid/solid structures.

8583-13, Session 3

Spectroscopic measurements and characterization of soft tissue phantoms

Efrain Solarte-Rodriguez, Erick Ipus, Univ. del Valle (Colombia)

Tissue phantoms are important tools to calibrate and validate light propagation effects, measurements and diagnostic test in real biological soft tissue. We produce low cost phantoms using standard commercial jelly, distillated water and Intralipid®, and in a previous work design a procedure to elaborate high purity phantoms which can be used over months. We used the phantom elaboration procedure to produce three different types of phantoms regarding the Intralipid – jelly – water composition: Pure Jelly phantoms, Intralipid in water, and Intralipid in jelly phantoms were produced and different concentrations of Intralipid are used to study optical propagation properties of diffusive mixtures. The phantoms were produced in disposable spectrometer cuvettes for fluorescence studies in order to use all the phantom sides. Measurements were performed using an OceanOptics high resolution spectrophotometer and integrating spheres with photodiode detectors. For the scattering measurements a homemade goniometer with a high resolution angular scale was used and the scattering detector was a linear array of optical fibers, with an angular collimator and connected to the spectrophotometer. White LED and halogen lamps were used as light sources, and the 6328.8 nm HeNe, and 532 Nd:YAG Laser were used for calibration. In this work we present characterization measurements and procedures using spectral reflectance, diffuse and direct spectral transmittance, and small angle scattering measurements. The results of these measurements and their comparison are presented.

8583-14, Session 3

A heterogeneous liquid scattering optical phantom for confocal microscopy

Danni Wang, Ye Chen, Jonathan T. C. Liu, Stony Brook Univ. (United States)

In recent years, there has been increasing interest in translating point-of-care optical microscopes into the clinic to observe the subtle changes in the pathological microenvironment for the early detection and diagnosis of disease. As technologies expand past the stage of prototyping and into testing phases, it is crucial to minimize the variance in performance between imaging devices at various clinics and test sites. Therefore, the development of an appropriate phantom is essential for the verification and validation of these microscope devices. There have been many advances made in optical phantom design in recent years. The existing phantoms, (solid/gel/liquid based), are designed to model different optical properties that are relevant for a specific imaging system and clinical application. In this study, we designed an optical-scattering phantom to verify the performance of a dual-axis confocal (DAC) microscope for imaging unprocessed fresh human skin. The phantom matches the scattering properties of normal human epithelial tissue in terms of effective scattering coefficient and degradation in spatial resolution due to beam-steering caused by tissue micro-architectural heterogeneities.

8583-15, Session 4

Synthetic esophagus phantom with calibrated fluorescent targets for image-based fluorescence quantification

Chenying Yang, Leonard Y. Nelson, Eric J. Seibel, Univ. of Washington (United States)

Background: Fluorescent labeled peptides are being investigated for molecular imaging of adenocarcinoma and high-grade dysplasia in Barrett's esophagus. Cells in Barrett's esophagus express a number of molecular targets on the surface based on amplification and/or overexpression of genes. The peptide biomarker target selectively binds to these species serves to red-flag areas for biopsy. A wide-field endoscopic imaging system is under development for image-guided biopsy of targeted tissue. To quantify the fluorescent intensity of the imaging device, a clinically relevant and reproducible phantom is needed.

Methods: A synthetic phantom was fabricated to mimic both healthy and Barrett's esophagus mucous in adult humans. A photo-stable, dye-doped polymer was fabricated and cut into 750-micrometer thick disks. Fluorescent targets with distinctive shapes were die-cut from disks and embedded onto the inner surface of the phantom to represent fluorescent hot-spots indicating possible biopsy sites. A laser-based ultrathin scanning fiber endoscope (SFE) was used within the phantom for multimodal (reflectance and fluorescence) imaging. A user interface was developed to allow real-time, target/background ratio calculation.

Results: The synthetic esophagus phantom with dye-in-polymer targets represents a reproducible model mimicking human esophagus geometry, mucosal color as well as fluorescence hot-spots. The dye-doped polymer demonstrated a linear relationship between fluorescence emission and dye concentrations which was reproduced with SFE imaging. Real-time RGB white-light reflectance and color-mapped fluorescence imaging and user interface afforded ranking of red-flag sites for biopsy procedures.

Conclusions: Preliminary results show that the developed phantom was able to validate the promise of image-based fluorescence quantification using the SFE.

8583-16, Session 4

Fabrication of a multilayered solid optical skin phantom mimicking human epidermal thin layer and texture

Yunjin Bae, Yonsei Univ. (Korea, Republic of); Youngwoo Bae, Gumi Electronics & Information Technology Research Institute (Korea, Republic of); Heesung Kang, Byungjo Jung, Yonsei Univ. (Korea, Republic of)

Methodologies to fabricate a solid optical skin phantom mimicking epidermal thin layer have been introduced for calibration and performance validation of optical instrument and for in vitro human skin experiments. However, there are cumbersome and time-consuming efforts in fabrication process such as a custom-made casting and calculation of solvent volume before curing process. In previous study, we suggested a new methodology based on spin coating technology in which we fabricated a thin layer analogous to epidermal thickness. In this study, we fabricated a multilayered solid optical skin phantom composed of epidermis and dermis layer for the morphological similarity of human skin and the effect of fine structures in light propagation. The epidermal thin layer with printed skin texture on its surface is spin-coated upon the dermal layer after the defining the optical properties of each layer. The structural characteristics and optical properties of fabricated optical skin phantom were measured by optical coherence tomography and inverse adding doubling algorithms, respectively. In conclusion, we fabricated a multilayered solid optical skin phantom mimicking human epidermal thin layer using spin coating technology and expected to be useful in optical diagnosis and simulation.

8583-17, Session 4

Fabrication of a skin phantom for OCT imaging using two-photon absorption microstereolithography.

Stephen J. Matcher, Piotr Geca, Frederick Claeyssens, The Univ. of Sheffield (United Kingdom)

Optical Coherence Tomography is becoming a popular dermatological imaging tool in research and clinical practice, but establishment of OCT as medical imaging tool will require development of biomimetic skin tissue phantoms (BSTPs) for staff training and calibration.

Recreation of the skin papillary dermis is desirable because its appearance is highly characteristic under OCT, but its geometry has not yet been faithfully reproduced in phantoms.

State-of-the-art structural mimics of papillary dermis have parallel ridges made with photomasking, micromachining or wire layering- all of which result in oversimplified models not replicating 3D structural features which would be visible in volumetric OCT C-scans (i.e. papillary loops).

In our approach we utilised two-photon absorption microstereolithography (TP-STL) system, which is capable of '3D printing' complex microstructures and creating more accurate mimic.

We used Fourier sine series approximation to describe papillae geometry and then fabricated said surface using TP-STL combined with novel control scheme of vertical slicing for greater geometrical accuracy. The geometry was replicated in light-scattering materials using moulding process to create a bi-layer OCT phantom with papillary junction interface.

Our mimic is useful as BSTP component and should be reproducible by other laboratories thanks to increasing availability of short-pulse lasers.

8583-18, Session 4

Development of a corneal tissue phantom for anterior chamber optical coherence tomography (AC-OCT)

T. Scott Rowe, Rowe Technical Design (United States); Robert J. Zawadzki, UC Davis Medical Ctr. (United States)

We document our latest work in developing a corneal tissue phantom designed for demonstrating, validating and comparing anterior chamber ophthalmic Optical Coherence Tomography (OCT) instruments. Corneal tissue phantoms can serve a variety of purposes, including demonstrating OCT imagery, functionality and performance in both the clinic and exhibit hall, validating corneal thickness measurements from different commercial OCT instruments and as an aide for the R&D engineer and field service technician in the development and repair of instruments, respectively. The ideal corneal tissue phantom as viewed with the optical cross-sectional imaging modality would have a volumetric morphology and scattering and absorption properties similar to that of normal human cornea. These include a multi-layered structure of equivalent optical path length to nominal human cornea layers including an epithelium, Bowman's layer, and stroma to demonstrate the layer segmentation and thickness measurements of the OCT system. A completely sealed tissue phantom relieves the user of constant cleaning and maintenance associated with the more common open water bath model eyes. Novel processes have been developed to create an epithelium and Bowman's layer that closely mimic the reflectance and scattering coefficients of the corresponding real layers of the cornea, as imaged by spectral domain OCT.

8583-19, Session 4

Tissue simulating phantoms for optical coherence tomography

Brendan F. Kennedy, The Univ. of Western Australia (Australia); Guy Lamouche, Charles-Etienne Bisaillon, Conseil National de Recherches Canada (Canada); Kelsey M. Kennedy, The Univ. of Western Australia (Australia); Andrea Curatolo, Univ. of Western Australia (Australia); Gord Campbell, Conseil National de Recherches Canada (Canada); David D. Sampson, The Univ. of Western Australia (Australia)

We review progress made on the development of phantoms that simulate the optical and mechanical properties, as well as the complex structures, found in tissue. We concentrate on materials that provide durability of at least one month. We review phantoms based on three materials: silicone, fibrin, and poly(vinyl alcohol) cryogels (PVA-C), which we believe to be the best candidates for the development of versatile, durable tissue-simulating phantoms. Silicone is a convenient base material for flexible and straightforward fabrication of phantoms. It provides ready compatibility with a wide range of suitable scatterers for adjustment of the optical properties. Silicone phantoms have a shelf-life of years. The mechanical properties can be adjusted over a wide range by controlling the amount of cross-linking within the silicone formulation. Silicone is also well suited for fabrication of phantoms with complex structures. Fibrin phantoms provide a transparent organic matrix to which both organic and inorganic scatterers and absorbers may be added. Fibrin is a naturally occurring protein in humans that provides structural support for blood clots. Fibrin is readily synthesized and has a shelf life of up to one month. Poly(vinyl alcohol) have been used extensively to fabricate phantoms for other medical imaging modalities, however they are seldom used in OCT. PVA-C is especially attractive for its mechanical properties, which are readily controllable over the range found in tissue. The strength and weaknesses of the three types of phantoms will be discussed.

8583-20, Session 5

Calibration of fluorescence reflectance reference phantoms *(Invited Paper)*

Jean-Pierre Bouchard, François Baribeau, Ozzy Mermut, INO (Canada)

Exploiting the quantitative intensity information of fluorescence imaging has been shown to improve the diagnostic potential of the technique namely in the field of tumor margin assessment. Calibrating the intensity scale of fluorescence imaging system would be best achieved by imaging a test target of known fluorescence. Before the development of such a reference target, it is important to establish an instrument independent definition of fluorescence response and a mean to measure it. An instrument independent definition of the fluorescence reflectance intensity will be presented. A prototype characterization instrument will be presented along with its calibration procedure and a complete uncertainty analysis.

8583-21, Session 5

Performance assessment of time-domain optical brain imagers: a multi-laboratory study *(Invited Paper)*

Heidrun Wabnitz, Alexander Jelzow, Mikhail Mazurenka, Oliver Steinkellner, Dieter R. Taubert, Rainer Macdonald, Physikalisch-Technische Bundesanstalt (Germany); Antonio Pifferi, Politecnico di Milano (Italy) and Consiglio Nazionale delle Ricerche (Italy); Alessandro Torricelli, Davide Contini, Lucia M. G. Zucchelli, Politecnico di Milano (Italy); Lorenzo Spinelli, Consiglio Nazionale

delle Ricerche Istituto di Fotonica e Nanotecnologie (Italy); Rinaldo Cubeddu, Politecnico di Milano (Italy) and Consiglio Nazionale delle Ricerche (Italy); Daniel Milej, Norbert Zolek, Michal Kacprzak, Piotr Sawosz, Adam Liebert, Institute of Biocybernetics and Biomedical Engineering (Poland); Salavat Magazov, Jeremy C. Hebden, Univ. College London (United Kingdom); Fabrizio Martelli, Paola Di Ninni, Giovanni Zaccanti, Univ. degli Studi di Firenze (Italy)

Common protocols were developed and applied in the European project "nEUROPt" (FP7-HEALTH-2007-201076) to assess and compare performance of instruments for time-domain optical brain imaging as well as related methods of data analysis. As a first step, a number of basic tests were performed. Among these, a specific test was devised to measure the responsivity of the detection system, i.e. the overall efficiency to collect and detect light emerging from tissue. Dedicated solid slab phantoms were developed and quantitatively spectrally characterized to provide sources of known radiance with nearly Lambertian angular characteristics. The responsivity is given by the ratio of photon count rate detected and input radiance.

Another novel protocol was devoted to the assessment of sensitivity, spatial resolution and quantification of absorption changes ("nEUROPt" protocol). It was implemented with liquid phantoms based on Intralipid and ink, with black inclusions and, alternatively, in two-layered geometry. Small black cylinders of various sizes were used to mimic small localized variations of the absorption coefficient. Their position was varied in z (depth) and x-y direction to address contrast and spatial resolution. Two-layered liquid phantoms were used, in particular, to determine depth selectivity, i.e. the ratio of contrasts due to a deep and superficial absorption change of same magnitude.

We give an overview of the results obtained by the four groups of the nEUROPt consortium who developed time-domain optical brain imagers. We discuss potential applications of part of the tests in future standards for fNIRS (functional near-infrared spectroscopy) devices (time-domain, frequency-domain, and continuous wave).

8584-1, Session 1

The complicated mechanisms and fates of nanoparticle-mediated medical applications in the living animal (patient). *(Keynote Presentation)*

Sharon L. Thomsen, Consultant (United States)

Most biological and medical investigations of nanoparticle diagnostic and therapeutic applications have centered on direct infusions of nanoparticle suspensions into cell cultures or tumors with regional placement, attachment and/or ingestion of the particles into the targeted cells/tissues. More recently, intravascular nanoparticle infusions into the systemic circulation of living intact animals and patients have shown a more complicated and sometimes, unwanted distribution pattern of the particles relative to the targeted tissue or lesion. The tissue and organ distributions of nanoparticles appear to be influenced by the chemical and physical composition of the nanoparticle and the complicated physiology of the host and the targeted tissues. In addition, other factors that influence treatment effects, are the limitations imposed by the biological, chemical, pharmacological and external physical stimuli that initiate the treatment mechanisms. Also, the most effective treatment mechanisms in intact, living tissues and organisms may not involve primary direct injury to the targeted cells but may involve more non-specific secondary effects such as disruption of the blood circulation within the targeted treatment volume. Design of effective diagnostic and treatment protocols for nanoparticle applications requires a thorough understanding of these mechanisms and limitations.

8584-2, Session 1

Modification of the tumor vascular barrier to improve magnetic nanoparticle uptake and hyperthermia treatment efficacy *(Keynote Presentation)*

P. Jack Hoopes, Andrew J. Giustini, Alicia A. Petryk, Sarah G. Thappa, Radu V. Stan, Rendall R. Strawbridge, Lionel L. Lewis, Geisel School of Medicine (United States)

The predicted success of nanoparticle based cancer therapy is based, in part, by presence of the inherent leakiness of the tumor vascular barrier, the so-called enhanced permeability and retention (EPR) effect. Although the EPR effect is present in varying degrees, in many tumors, it has not resulted in the level of nanoparticle-tumor uptake enhancement that was initially predicted. Magnetic nanoparticles (iron oxide, mNPs) have many positive qualities, including their inert and nontoxic nature, the ability to be produced in various sizes, the ability to be activated by a deeply penetrating, nontoxic magnetic field that results in cell specific cytotoxic heating. Although a wide variety of functional coatings, including targeting antibodies, can be used, the delivery of adequate numbers of nanoparticles to the tumor site via systemic administration remains challenging. In this study we have used ionizing radiation, cisplatinum chemotherapy, and the anti-tumor endothelial cell molecule (Avastin) to modify the tumor vasculature barrier to improve mNP uptake in rodent tumors.. Preliminary studies suggest the improvement in mNP uptake with each modification modality is less that 5 fold. However, ongoing combination studies indicate a potential for significant enhancement. Study variables include mNP and modification agent dose variance, timing, and mNP coatings. Using histopathology, TEM and ICP-MS, iron levels and spatial location will be assessed in normal and tumor tissue. The pathophysiologic effects of the tumor vasculature /endothelial cell modifying agents on the tumor vasculature /endothelial cell will also be studied and reported in detail. It is anticipated that these techniques will significantly enhance mNP selective delivery to the tumor parenchyma (interstitium and cells).

8584-3, Session 1

Development of a biodegradable iron oxide nanoparticle gel for tumor bed therapy

Benjamin P. Cunkelman, Dartmouth College (United States); P. Jack Hoopes, Dartmouth Medical School (United States); Sarah G. Thappa, Jennifer A. Tate, Alicia A. Petryk, Dartmouth College (United States)

Treatments of the post-operative surgical bed have proven appealing as the majority of cancer recurrence following tumor resection occurs at the tumor margin. A novel, biodegradable pullulan-based gel infused with magnetic iron oxide nanoparticles (IONP) is presented here for surgical bed administration followed by hyperthermia therapy via alternating magnetic field (AMF) activation. Pullulan is a water soluble, film-forming starch polymer that degrades at the post-operative wound site to deliver the IONP payload, targeting the remaining cancer cells. A set of gel formulations containing various %wt of pullulan were tested for IONP elution. Elution levels and amount of gel degradation were measured by immersing the gel in de-ionized water for one hour then measuring particle concentrations in the supernatant and the mass of the remaining gel formulation. The most promising gel formulations will be tested in a murine model of surgical bed resection to assess in vivo gel dissolution and IONP cell uptake kinetics via histology and TEM analysis.

8584-4, Session 1

Preclinical Investigation of Magnetic Fluid Hyperthermia for Thermochemotherapy of Bladder Cancer

Tiago R. Oliveira, Kelly Lee, Etienne Wiguins, Chelsea Landon, Mark W. Dewhirst, Paul R. Stauffer, Duke Univ. (United States)

Despite positive results, thermotherapy is not widely used for clinical oncology. Difficulties associated with field penetration and controlling power deposition patterns in heterogeneous tissue have limited its use for heating deep in the body. Heat generation using iron-oxide superparamagnetic nanoparticles excited with RF magnetic fields has been demonstrated to overcome some of these limitations. The objective of this preclinical study was to investigate the feasibility of treating bladder cancer with magnetic fluid hyperthermia (MFH) by analyzing the thermal dosimetry and biodistribution of nanoparticles in a rat bladder model.

The bladders of twenty female rats were injected with 0.4ml of Actium Biosystems magnetite based namoparticles (Actium Biosystems, Boulder,CO) via catheters inserted in the urethra. Heat treatments were performed with the Actium Biosystems small animal magnetic field applicator with a goal of raising bladder temperature to 42˚C in <10min and maintaining for 60min. Temperatures were measured throughout the rat with eight fiberoptic temperature probes (OpSens Technologies,Quebec) to characterize the ability to localize heat within the bladder. A histological analysis was performed to access the biodistribution of nanoparticles following 60min heat treatment.

Thermal dosimetry data demonstrate our ability to controllably raise temperature of rat bladder >1°C/min to a steady-state of 42˚C while maintaining surrounding tissues less than 41˚C. Histological results demonstrated a tolerable level of iron in the bladder wall and negligible levels in other organs of the heated rats.

Our data suggest that magnetic fluid hyperthermia can be an efficient and well tolerated method to heat bladder cancer.

8584-37, Session 1

New iron-oxide particles for magnetic nanoparticle hyperthermia: An in vivo pilot study of nanoparticle hyperthermia in a mouse xenograft model of a human prostate cancer

Mohammad Hedayati, Anilchandra Attaluri, Michael Armour, Haoming Zhou, Christine Cornejo, Michele Wabler, Yonggang Zhang, Johns Hopkins Univ. School of Medicine (United States); Robert Ivkov, Johns Hopkins Univ. (United States)

Magnetic nanoparticle hyperthermia (mNHP) is regarded as a promising minimally invasive hyperthermic procedure. When an animal or patient is subjected to AMF non-specific Joule heat is deposited into the tissue due to eddy currents. The total non-specific power deposited is proportional to H2f2r2; where H and f are AMF amplitude and frequency, while r is the radius of the eddy current path, and is related to the radius of tissue exposed to AMF. For most iron-oxide nanoparticles (IONPs) the heat generating ability or specific loss power (SLP) is proportional to H2f. Hence, lower AMF frequencies in the range of 100 KHz to 400 KHz are typically used mNPH applications. For mNPH to be effective, the IONPs should generate higher heating at low H-values.

We present results obtained from hyperthermia experiments using a new IONP (JHU-MIONs) formulation having higher SLP at low H-values (< 30 KA/m) compared to commercially available bionized-nanoferrite (BNFs, from micromod Partikeltechnologie, GmbH, Rostock, Germany). Amount of heat deposited during mNHP depends on intratumoral iron-oxide nanoparticle (IONP) concentration and alternating magnetic field (AMF) parameters. Herein, we study the effect of intratumoral JHU-MION concentration (0 to 8 mg Fe/g of tumor) and AMF parameters (17, 29 and 57 KA/m at 160 ± 5 KHz) on temperature elevations in a DU145 human prostate xenograft model for AMF exposure time of 20 min. DU145 tumor xenografts (Male athymic nude mice, n =15) were directly injected with JHU-MIONs when the tumors were in the range of 0.15±0.02 cm3. Fiber-optic temperature probes (FISO Technologies, Inc., Quebec, CA) were used to monitor intratumoral, rectal and skin (contra lateral position to tumor) temperatures. For all AMF parameters intratumor temperature correlated to both nanoparticle concentration and AMF parameters.

Previous mouse studies suggest that rectal temperature change (?TRectal), should be maintained below 5?C, or below 42 °C, for the safety of the animal. Here, we show that at an ideal setting of 29 KA/m and ~ 4 mg Fe/g of tumor, AMF treatment yielded ?TTumor > 10?C while maintaining the ?TRectal< 5?C. While the results obtained are encouraging, we hypothesize that even more effective therapy can be realized with active thermal management of the animal during AMF exposure. Anesthetized mammals generally lose thermo-regulatory control and become hypothermic, while exposure to AMF deposits non-specific heat, potentially creating significant thermal gradients throughout the animal which could be detrimental. If active and homogenizing temperature control can be provided during mNPH, safety may improve allowing increased limits on maximum allowable H-values.

8584-5, Session 2

Microwave tumor ablation: Cooperative academic-industry development of a high-power gas-cooled system with early clinical results *(Invited Paper)*

Christopher L. Brace, Timothy J. Ziemlewicz, James L. Hinshaw, Meghan G. Lubner, Fred T. Lee Jr., Univ. of Wisconsin-Madison (United States); Rick Schefelker, Neuwave Medical (United States)

Microwave tumor ablation continues to evolve into a viable treatment option for many cancers. Current systems are poised to supplant radiofrequency ablation as the dominant percutaneous thermal therapy. Here is provided an overview of technical details and early clinical results with a high-powered, gas-cooled microwave ablation system.

The system was developed with academic-industry collaboration using federal and private funding. The generator comprises three channels that independently produce up to 140W at 2.45GHz synchronously. A mountable power distribution module facilitates CT imaging guidance and monitoring and reduces clutter in the sterile field. Cryogenic carbon-dioxide cools the coaxial applicator, permitting a thin applicator profile (~1.5 mm diameter) and high power delivery.

A total of 106 liver tumors were treated (96 malignant, 10 benign) from December 2010 to June 2012 at a single academic institution. Mean tumor size ± standard deviation was 2.5±1.3cm (range 0.5-13.9cm). Treatment time was 5.4±3.3min (range 1-20min). Median follow-up was 6 months (range 1-16 months). Technical success was reported in 100% of cases. Local tumor progression was noted in 4/96 (4.3%) of malignancies. The only major complication was a pleural effusion that was treated with thoracentesis.

Microwave ablation with this system is an effective treatment for liver cancer. Compared to previous data from the same institution, these results suggest an increased efficacy and equivalent safety to RF ablation. Additional data from the lung and kidney support this conclusion.

8584-6, Session 2

Thermotolerance of human myometrium: Implications for minimally invasive uterine therapies.

Brian T. Grisez, West Virginia Univ. (United States); Kathleen McMillan, gRadiant Research, LLC (United States); Nicholas Chill, Tyler P. Harclerode, Rebecca Radabaugh, James E. Coad, West Virginia Univ. (United States)

Minimally invasive hyperthermic therapies are currently in use or being developed for ablating the intrauterine cavity. This study evaluated the potential for direct thermal injury to ex vivo human myometrium using short term exposures to 45-70C temperatures. The treated tissues were evaluated with both TTC and NBT viability stains. The thermal matrices will be presented to illustrate the boundary of thermal tissue necrosis.

8584-7, Session 2

Determination of the ablation efficiencies of the laser irradiated tissues via rate of temperature change over time

Burcu Tunç, Murat Gülsoy, Bogaziçi Üniv. (Turkey)

The aim of this study was to investigate the relation between ablation efficiency and temperature increase during laser ablation by 1940-nm Tm:fiber laser. The thermal effects of the Tm:fiber laser on the brain tissue was also investigated. The laser beam (200-800 mW) was delivered from a distance of 0-0.1 mm to cortical and subcortical regions of the ex-vivo ovine brain tissue samples via 400 ?m optical fiber. A total of 320 brain samples were irradiated at different settings in continuous-mode or pulsed-mode. In continuous-mode and pulsed-mode doses were changed with exposure time and on-off cycles respectively, in order to achieve the tissue to absorb the same energy 2 joules or 4 joules. During lasing temperature changes of the irradiated tissue were recorded by a thermoprobe (thermoprobe is a system which an optical fiber was embedded into a thermocouple). The radiuses of ablation and coagulation zones were measured under microscope. The ablation efficiencies (100xablation/coagulation radius) and rates of temperature change were calculated. A strong correlation between the ablation efficiency and rate of temperature change was presented (?=0.92293, ?=0.939686, ?= 0.943647, ?= 0.973418 for cortical

continuous-mode, pulsed-mode, subcortical continuous-mode and pulsed-mode respectively). This study revealed that rate of temperature change analysis can be very useful and efficient method to understand and predict the tissue response to the laser investigated. Especially for applications where the collateral thermal damage must be taken into account like brain surgeries to construct a study similar to this will help scientists to achieve more precise and predictable tissue removals.

8584-8, Session 2

Incisional effects of 1940 nm thulium fiber laser on oral soft tissues

Melike Güney, Bogaziçi Üniv. (Turkey) and Istanbul Medeniyet Univ. (Turkey); Burcu Tunç, Murat Gülsoy, Bogaziçi Üniv. (Turkey)

Lasers of different wavelengths are being used in oral surgical procedures with minimal bleeding and pain. Among these wavelengths, those close to 2 μm yield more desirable results on oral soft tissue due to their strong absorption by water. The emission of 1940 nm Thulium fiber laser is well absorbed by water making it a promising tool for oral soft tissue surgery. This study was conducted to investigate the potential of thulium fiber laser as an oral surgical tool for incision and excision purposes.

Ovine tongue has been used as the target tissue due to its similarities to human oral tissues. Laser light obtained from a thulium fiber laser was applied in contact mode onto ovine tongue completely submerged in saline solution in vitro, via a 600μm fiber to form incisions. There were a total of 27 parameters determined by the power (2,5-3- 3,5 W), fiber tip velocity (0,5-0,75-1 mm/s) and number of passes (1-3-5). The samples were stained with H&E for microscopic evaluation.

The depth of incisions increased with increasing power and number of passes, yet widening of the coagulation zone was also observed. Minimum carbonization was observed at 2,5 W however the incision depth could barely reach the muscle layer underneath the mucosa whereas at 3,5 W deep incisions in muscle layer, lined with a thin layer of carbonized tissue, was observed. The ablation depth as well as the coagulation width increased with decreasing fiber tip velocity.

8584-9, Session 3

Numerical models of cell death in RF ablation with monopolar and bipolar probes

Ben M. Bright, John A. Pearce, The Univ. of Texas at Austin (United States)

Radio frequency (RF) is used clinically to treat unresectible tumors. Finite element modeling has proven useful in treatment planning and applicator design. Typically isotherms in the middle 50s °C have been used as the parameter of assessment in these models. We compare and contrast isotherms for multiple known Arrhenius thermal damage predictors including collagen denaturation, vascular disruption, liver coagulation and cell death. Additionally, we compare a recently developed two-state model of cell death in PC3 cells to the more traditional processes. The two-state model more accurately represents cell death processes than Arrhenius models in the early stages of moderate heating. Models for cylindrical and RITA probe geometries are included in the study.

Numerical model results over different heating times in the range of minutes show that the two-state model predicts smaller lesions and narrower 10 - 90% damage bands that the Arrhenius coefficients derived from the same experimental data. Comparison to isotherms is sensible when the activation time is held constant, but varies considerably when heating times vary.

8584-10, Session 3

Predicting tissue division rates for TURP systems using finite element simulations

Arlen K. Ward, Covidien Surgical Solutions (United States); George J. Collins, Colorado State Univ. (United States)

When using simulations to determine electrode geometry and energy deposition patterns for TURP devices, a dominating factor for consideration is the tissue resection rate of the proposed system. While it is well understood that the vaporization of biological tissue is the mechanism of tissue division, previous models have been unable to match experimental results for a given applied power. Whether modeled as direct tissue/electrode contact or through the spatial transform of arcing, the predicted division rate was significantly lower than that observed though experiment.

For the present study, heating rate was again used to determine the vaporization rate during the resection. This model assumes that in order for the wire loop to advance not all of the tissue in front of the electrode must be vaporized but the centerline of the advance must have sufficient energy deposited to divide the tissue. Integrating the volumetric energy deposition rate along this centerline in front of the advancing electrode provides a comparison to the required vaporization energy density resulting in a predicted time necessary for reaching the tissue division threshold.

Using the simulation results for a standard TURP electrode and various power settings, five cases were compared to experimental results using in vitro bovine prostate tissue. Each tested at three cutting rates, evaluating the ability to advance through the tissue. The simulation predicted tissue division rates in good agreement with those seen via experiment, although the predicted values biased slightly higher suggesting that further mathematical model refinements are necessary.

8584-11, Session 3

Numerical model of RF monopolar cutting in heterogeneous tissues *(Invited Paper)*

Dimitry E. Protsenko, Brian Wong, Beckman Laser Institute and Medical Clinic (United States)

Numerical modeling of electrosurgical cutting has generated increasing clinical interest, because electrosurgery is among the most common techniques used in the operational room. However, few studies have investigated effect of tissue heterogeneity such as variations in local thermal, electrical and mechanical properties on cutting rates and thermal damage. The objectives of this study were to: (1) formulate a finite-element model describing electrosurgical cutting in heterogeneous tissue, (2) estimate cutting speeds and thermal damage in tissues with monotonically and abruptly changing material properties, and (3) compare numerical estimations with experimental observations obtained in ex-vivo tissue models.

COMSOL Multiphysics finite element simulation package was used to simulate thermal, electrical and mechanical events during cutting. Tissue mechanical partition was modeled as a result of expansion of vapor bubbles using homogeneous nucleation theory and Rayleigh equation. Dependence of material properties from temperature and tissue compression was considered. Cutting through skin and muscle tissue containing fat and blood vessels was modeled. Verification experiments were performed in porcine and bovine skin and muscle tissue respectively. Size of vapor vacuoles and extent of thermal damage zones were verified using light and polarization microscopy.

A good qualitative correlations between numerical prediction and experimental observation were obtained including: difference in thermal damage size in skin, subcutaneous fat and muscle layers, increase in thermal damage in fatty tissue, increase in thermal damage in the vicinity of small blood vessels. However, to improve model's predictive power more precise material properties values are required.

8584-12, Session 4

Targeting of systemically delivered magnetlc nanoparticle hyperthermia using a noninvasive static external magnetic field *(Invited Paper)*

B. Stuart Trembly, Grayson Zulauf, Andrew J. Giustini, Rendall R. Strawbridge, P. Jack Hoopes, Dartmouth College (United States)

One of the greatest challenges of nanoparticle based cancer therapy is the delivery of adequate numbers of nanoparticles to the tumor site. Magnetic (iron oxide) nanoparticles (mNPs) have many positive qualities, including their inert (nontoxic) nature, the ability to be produced in various sizes, the ability to be activated by a deeply penetrating nontoxic magnetic field, resulting in cell specific cytotoxic heating, and the ability to be successfully coated with a wide variety functional coatings. Although mNPs can be delivered via an intra-tumor injection to some tumors, the resulting tumor nMP distribution is generally inadequate; additionally, local tumor injections do not allow for the treatment of systemic or multifocal disease. Consequently, the ultimate success of nanoparticle based cancer therapy likely rests with successful systemic, tumor-targeted NP delivery. In this study, we used a surface-based, bilateral, noninvasive static magnetic field produced by neodymium-boron-iron magnets (minimum 60 tesla/m between magnets and 480 tesla/m at corners), a rabbit ear model and systemically-delivered starch-coated 110 nm magnetic (iron oxide) NPs to demonstrate a spatially defined 10-fold increase in the local tissue accumulation of MNPs. In this non-tumor model, the mNPs remained within the local vascular space. It is anticipated that this technique can be used to significantly enhance mNP delivery to the tumor parenchyma/cells when this technique is used in a leaky-vasculature setting of a tumor.

8584-13, Session 5

Understanding mNP hyperthermia for cancer treatment at the cellular scale

Robert V. Stigliano, Fridon Shubitidze, Dartmouth College (United States); P. Jack Hoopes, Dartmouth Medical School (United States)

The use of magnetic nanoparticles to induce local hyperthermia has been emerging in recent years as a promising cancer therapy, in both a stand-alone and combination treatment setting. Studies have shown that cancer cells accept and aggregate mNP's more preferentially than normal cells. Once the mNP's are delivered inside the cells, an alternating (~160 kHz) electromagnetic field is used to activate the mNP's. The nanoparticles absorb the applied field and provide localized heat generation at nano-micron scales. The mechanism of nano-scale hyperthermia and temperature distribution at cellular scales is not well understood and requires detailed studies to further optimize mNP hyperthermia. Thus, the main objective of this research is to study mNP hyperthermia at the cellular and subcellular level. A macro-scale heat flow model (Parabolic equation - Fourier model) is not applicable on very small space and time scales. This is simply because the carriers, such as mNP's, undergo too few collisions and heat energy propagates with a finite speed as a wave. To account for this phenomenon, a modified heat transfer model called the Maxwell-Catteneo hyperbolic heat conduction model is needed to be applied at the nano-scale. In this work we use a multi-scale code, based on an unconditional finite-difference scheme, and solve both the classical and modified heat transfer equations at the nano-scale. The comparisons between the classical and modified models are given, and temperature distributions are analyzed at the cellular level for improving cancer treatment via mNP hyperthermia.

8584-14, Session 5

Oxygen microenvironment affects the in vitro uptake and therapeutic response of head and neck tumor cells to magnetic nanoparticle hyperthermia

Sasson Hodge, Katherine Tai, Geisel School of Medicine (United States); Eunice Y. Chen, Dartmouth Hitchcock Medical Ctr. (United States); Kimberley S. Samkoe, Geisel School of Medicine (United States)

Survival of head and neck cancer patients has not improved in several decades despite advances in diagnostic and therapeutic techniques. Tumor hypoxia in head and neck cancers is a critical factor that leads to poor prognosis, resistance to radiation and chemotherapies, and increased metastatic potential. Magnetic nanoparticle hyperthermia (mNPHT) is a promising therapy for hypoxic tumors because nanoparticles (NPs) can be directly injected into, or targeted to, hypoxic tumor cells and exposed to alternating magnetic fields (AMF) to induce hyperthermia. Our preliminary studies indicate that mNPHT can increase therapeutic effect in head and neck cancers by two modes of action: 1) direct killing of hypoxic tumor cells; and 2) increase in tumor oxygenation, which has the potential to make the tumor more susceptible to adjuvant therapies such as radiation and chemotherapy. Although direct killing of hypoxic tumor cells has been observed, we have shown in vitro that the oxygen microenvironment plays a large role in NP uptake by cells. FaDu and SCC25 (squamous cell carcinomas) cells were incubated in hypoxic, normoxic, and hyperoxic conditions with bionized nanoferrite NPs at 0.5 mg Fe/mL for 4 and 24 hours. After incubation, the cells were processed for iron content by ICP-MS. Results indicate that cellular uptake of NPs are diminished in both hypoxic and hyperoxic microenvironments as compared to normoxia, with hyperoxic conditions taking up the least amount of NPs per cell. Furthermore, mNPHT was performed on the cells incubated in differing oxygen microenviroments and response to therapy is compared.

8584-15, Session 5

Biodistribution of antibody-targeted and non-targeted iron oxide nanoparticles in a breast cancer mouse model

Jennifer A. Tate, Warren Kett, Christian NDong, Karl E. Griswold, P. Jack Hoopes, Dartmouth College (United States)

Iron oxide nanoparticle (IONP) hyperthermia is a novel therapeutic strategy currently under consideration for the treatment of various cancer types. Systemic delivery of IONP followed by non-invasive activation via a local alternating magnetic field (AMF) results in site-specific energy deposition in the IONP-containing tumor. Targeting IONP to the tumor using an antibody or antibody fragment conjugated to the surface may enhance the intratumoral deposition of IONP and is currently being pursued by many nanoparticle researchers. This strategy, however, is subject to a variety of restrictions in the in vivo environment, where other aspects of IONP design will strongly influence the biodistribution. In these studies, various targeted IONP are compared to non-targeted controls. IONP were injected into BT-474 tumor-bearing NSG mice and tissues harvested 24hrs post-injection. Results indicate no significant difference between the various targeted IONP and the non-targeted controls, suggesting the IONP were prohibitively-sized to incur tumor penetration. Additional strategies are currently being pursued in conjuncture with targeted particles to increase the intratumoral deposition.

8584-16, Session 5

Cell cycle influence on magnetic nanoparticle uptake

Sarah G. Thappa, Jennifer A. Tate, Dartmouth College (United States); P. Jack Hoopes, Dartmouth Medical School (United States)

Previous studies have shown that cellular uptake of nanoparticles is related to cell cycle phase, with G2/M demonstrating the greatest uptake and G0/G1 the least. However, it is unclear how well this information translates to a wide variety of NPs and cells types. Our own preliminary information using starch coated 100 nm iron oxide NP also suggests a cell cycle influence of NP uptake. Tested in vitro, different cancer cell lines (rodent mammary adenocarcinoma cells: MTG-B and human breast cancer cells: BT-474) were grown and synced using a 72 hour serum-free media starvation incubation. Serum-free media was siphoned off and replaced with serum contained media to re-induce the cell cycle. Data points were collected at different time points after the cell cycle was re-initiated to ensure sampling from a range of cellular phases. Time points were at the 0, 4, 5, 6, 8, 10, 12, 14, 16, 18, 20, 22, 24, and 26 hour. Samples from each time point were taken from one 6-well plate of cells with serum-media and one 6-well plate of cells with serum-media and magnetic nanoparticles. While final results remain understudy, ICP-MS iron analysis and flow cytometry staining based cell cycle analysis suggest cell cycle defined IONP uptake in rodent mammary adenocarcinoma cells (MTGB) has well defined cell cycle uptake parameters. The understanding of cell cycle based nanoparticle uptake has very significant consequences for primary or adjuvant IONP cancer therapy. For example, delivery of nanoparticles could be coordinated with tumor cell cycle synchronization thereby increasing the temporal knowledge of cancer cell delivery and uptake and the ability to enhance the tumor-normal tissue therapeutic ratio. Final results will contain a quantification of cell iron levels through an understanding of cell cycle uptake kinetics, as well as the synchronized cell cycle.

8584-17, Session 5

Influence of cancer cell intracellularization on iron oxide nanoparticle hyperthermia cytotoxicity

Jennifer A. Tate, Dartmouth College (United States); P. Jack Hoopes, Dartmouth Medical School (United States)

Based on their nano-scale size and their ability to be activated non-invasively by a high-frequency local alternating magnetic field (AMF), magnetic iron oxide nanoparticles can induce cell-specific hyperthermia-based cytotoxicity. Our studies compare the cytotoxic effectiveness of intracellular IONP versus extracellular IONP hyperthermia at the same IONP/Fe dose/volume. MTGB murine adenocarcinoma cells were incubated with 110nm, starch-coated IONP for up to 72 hours before AMF activation. Clonogenic assays, trypan blue counting and flow cytometry were used to assess cytotoxicity of the intracellular IONP compared to extracellular IONP administered without any incubation. Preliminary results demonstrate enhanced cytotoxicty with intracellular particles when a threshold level of intracelluar Fe is achieved. Additional variables including incubation time, cell type and cell density are also influential and being studied.

8584-18, Session 5

Iron oxide nanoparticles as a radiation enhancer

Courtney Mazur, Jennifer A. Tate, Dartmouth College (United States); Rendall R. Strawbridge, P. Jack Hoopes, Dartmouth Medical School (United States) and Dartmouth Hitchcock Medical Ctr. (United States)

Iron oxide nanoparticles (IONPs) have been investigated as a promising means for inducing tumor cell-specific hyperthermia. However, generation of nanoparticles that are biocompatible, tumor specific, and have the ability to produce adequate cytotoxic heat at biologically feasible, intravenously-administered concentrations has proven challenging. This has led to the consideration of IONP hyperthermia as an adjunct therapy, which will allow sub-lethal heat doses to act synergistically with conventional therapy to improve the therapeutic index. Due to their high-Z characteristics, intracellular IONPs are here considered as a potential radiation enhancer.

In order to quantify intracellular IONPs, their uptake kinetics in murine breast adenocarcinoma (MTG-B) cells were studied in vitro. Intracellular iron levels were measured with ICP-MS, and the amount of intracellular iron was shown to increase with time through 72 hours. To test the efficacy of IONPs as radiation enhancers, cells with and without intracellular IONPs were irradiated at 4 Gy, and cytotoxicity was determined by clonogenic assay. Preliminary results demonstrate that cells irradiated with intracellular IONPs experienced a 1.2 fold increase in radiation-induced cytotoxiciy over irradiated cells without IONPs. These results suggest that intracellular IONPs may act to decrease the necessary dose of radiation, thereby increasing the therapeutic ratio of a combination of radiation and IONP-induced hyperthermia. Ongoing studies will determine the relationship between intracellular iron levels and cytotoxicity as well as whether the addition of IONP hyperthermia to radiation creates a synergistic effect.

8584-19, Session 6

Hypothesis for thermal activation of the caspase cascade in apoptotic cell death at elevated temperatures *(Keynote Presentation)*

John A. Pearce, The Univ. of Texas at Austin (United States)

Apoptosis, one form of Programmed Cell Death (PCD), is an especially important process affecting disease states from HIV-AIDS to auto-immune disease to cancer. Cancer cells, for example, are able to avoid apoptosis in the presence of pro-apoptotic signals. A cascade of initiator and executioner capsase functional proteins is the hallmark of apoptosis. When activated the various caspases, or cysteine aspartic proteases, activate other caspases or cleave structural proteins of the cytoskeleton, resulting in “blebbing” of the plasma membrane forming apoptotic bodies that completely enclose the disassembled cellular components. Containment of the cytosolic components differentiates apoptosis from necroptosis and necrosis, both of which release fragmented cytosol into the intracellular space.

Biochemical models of caspase activation reveal the extensive feedback loops characteritic of apoptosis. They explain the failure of Arrhenius models to give accurate predictions of cell survival curves in hyperthermic heating protocols: Arrhenius models describe single first-order reactions and these systems involve at least eight state-space equations.

Nevertheless, each of the individual reaction velocities can reasonably be assumed to follow Arrhenius kinetics. The thermal sensitivity of the reaction velocity to temperature elevation is given by: ∂k/∂T = Ea [k/RT^2]. Consequently, particular reaction steps described by higher activation energies, Ea, are more thermally-sensitive than lower energy reactions. These reactions among either the caspase or Inhibitor of Apoptosis Protein (IAP) family may initiate apoptosis in the absence of other stress signals.

8584-20, Session 6

Evolution of pathology techniques for evaluating energy-based tissue effects *(Keynote Presentation)*

James E. Coad, Brian T. Grisez, West Virginia Univ. (United States)

Over the last decade, histopathology techniques for evaluating tissue effects associated with minimally invasive energy-based medical devices have substantially progressed. These techniques have evolved from hematoxylin and eosin and collagen staining on fixed tissues to membrane and enzymatic viability staining in fresh tissue. Further, immunohistochemistry has advanced the detection of apoptosis over the TUNEL and FLICA assays in intact tissue samples. As a result, these techniques have enhanced our ability to evaluate tissues following both hyperthermic and cryothermic tissue treatments.

8584-21, Session 6

Tissue fusion bursting pressure and the role of tissue water content

James D. Cezo, Univ. of Colorado at Boulder (United States); Kenneth D. Taylor, ConMed Electrosurgery (United States); Virginia L. Ferguson, Mark E. Rentschler, Univ. of Colorado at Boulder (United States)

Tissue fusion is a complex, poorly understood process which bonds collagenous tissues together using heat and pressure. The goal of this study is to elucidate the role of hydration in bond efficacy. Hydration of porcine splenic arteries (n=12) was varied by pre-fusion treatments: 12-hour immersion in isotonic, hypotonic, or hypertonic baths. Treated arteries were fused in several locations using Conmed's Altrus thermal fusion device and the bursting pressure was measured. Artery sections were then weighed before and after lyophilization, to quantify water content. Histology (H&E, EVG staining) and confocal Second Harmonic Generation Imaging enabled visualization of the bonding interface. Bursting pressure was significantly greater ($p=9.5$ E-5) for the hypotonic group (840 ± 270 mmHg), while there was no significant difference existed between the isotonic (532 ± 220 mmHg) and hypertonic (383 ± 142 mmHg) treatment groups. Total water content varied ($p=1.4$ E-8) from low water content in the hypertonic samples (75.5% weight ± 1.3), to high water content in the hypotonic samples (84.8% weight ± 1.7), while the isotonic samples contained 80.0% weight ± 0.9. Strength differences imply that bound water driven from the tissue during fusion may reveal available collagen crosslinking sites to facilitate fusion bond formation. Therefore when the tissue contains greater bound water volumes, more crosslinking sites may become available during fusion, creating a stronger bond. This study provides an important step towards understanding the chemistry underlying tissue fusion and the mechanics of tissue fusion as a function of bound water within the tissue.

8584-22, Session 6

Thermal spread associated with tissue sealing devices: a comparison of histologic methods for detecting adventitial collagen denaturation

Ryan H. Livengood, Brian T. Grisez, James E. Coad, West Virginia Univ. (United States)

Twenty-eight ex-vivo fresh porcine carotid arteries were harvested and sealed using a commercially available FDA approved tissue sealing device, in accordance with the manufacturer's Instructions for Use. Following sealing, the arteries were marked to maintain orientation of the top vs bottom of the device and fixed in 10% neutral buffered formalin. Each artery was midline bisected longitudinally through the seal. After routine processing and paraffin-embedding, two 5 micron sections were prepared for H&E and trichrome staining. The H&E section was evaluated by bright field (H&E detected collagen denaturation) microscopy and polarized light (loss of birefringence detected collagen denaturation). The trichrome stained section was evaluated by bright field microscopy. For the top and bottom side of each seal, two collagen denaturation measurements were made using a calibrated ocular micrometer: 1) along the path of the adventitia as it arcs away from the seal (adventitial collagen denaturation) and 2) midline measurement made along the axis of the vessel lumen (midline collagen denaturation). The measurements were made by two pathologists on separate occasions. For each assessment method (H&E, birefringence, trichrome), the mean, standard deviation, median, minimum and maximum collagen denaturation lengths for the four measurements were determined. The adventitial and midline collagen denaturation lengths for both top and bottom device sides will be presented and decreased in magnitude from H&E to birefringence to trichrome methods. When comparing the H&E and trichrome results and birefringence and trichrome results, the differences were statistically significant ($p < 0.01$). The lengths of detectable thermal spread, as represented by collagen denaturation, are technique dependent. The lengths of collagen denaturation were significantly less with the trichrome method than with the H&E and birefringence methods. Based on these results, the H&E method appears to be more representative of true thermal spread that that determined with the trichrome method.

8584-23, Session 7

Overview of plasma technology used in medicine *(Invited Paper)*

Thomas P. Ryan, Kenneth R. Stalder, Jean Woloszko, ArthroCare Corp. (United States)

Plasma Medicine is a growing field that is having an impact in several important areas in therapeutic patient care, combining plasma physics, biology, and clinical medicine. Historically, plasmas in medicine were used in electrosurgery for cautery and non-contact hemostasis. Presently, non-thermal plasmas have attained widespread use in medicine due to their compatibility with biological systems.

The paper will give a general overview of how low temperature, nonequilibrium, gas plasmas operate, both from physics and biology perspectives. Plasma is described as the fourth state of matter and is typically comprised of charged species, active molecules and atoms, as well as a source of UV and photons. The most active areas of plasma technology applications are in wound treatment; tissue regeneration; inactivation of pathogens, including biofilms; treating skin diseases; and sterilization.

There are several means of generating plasmas for use in medical applications, including plasma jets, dielectric barrier discharges, capacitively or inductively coupled discharges, or microplasmas. These systems overcome the former constraints of high vacuum, high power requirements and bulky systems, into systems that use room air and other gases and liquids at low temperature, low power, and hand-held operation at atmospheric pressure. Systems will be discussed using a variety of energy sources: pulsed DC, AC, microwave and radiofrequency, as well as the range of frequency, pulse duration, and gas in an air environment. The ionic clouds and reactive species will be covered in terms of effects on biological systems. Lastly, several commercial products will be overviewed in light of the technology utilized, health care problems being solved, and clinical trial results.

8584-24, Session 7

Some physics and chemistry of Coblation electrosurgical plasma devices *(Invited Paper)*

Kenneth R. Stalder, ArthroCare Corp. (United States)

Electrosurgical devices employing plasmas to ablate, cut and otherwise treat tissues have been in widespread use for decades. Following d'Arsonval's 19th century work on the neuromuscular response from high-frequency excitation of tissue, Doyen treated skin blemishes with a spark-gap generator in 1909. In the late 1920's, physician Harvey Cushing and physicist William Bovie developed an electrosurgical device and power source that eventually became a standard of care for cutting, coagulating, desiccating, or fulgurating tissue. Beginning in the 1990's a new class of low-voltage electrosurgical devices employing electrically-conducting saline fluids were developed by ArthroCare Corp. These modern Coblation® devices are now widely used in many different surgical procedures, including those in arthroscopic surgery, otorhinolayrngology, spine surgery, urology, gynecological surgery, and others.

This talk will include an introductory review of some of the research we have been doing over the last decade to elucidate the physics and chemistry underlying Coblation® electrosurgical devices. Electrical-, thermal-, fluid-, chemical- and plasma-physics all play important roles in these devices and give rise to a rich variety of observations. Experimental techniques employed include optical and mass spectroscopy, fast optical imaging, and electrical voltage and current measurements. Many of the features occur on fast time scales and small spatial scales, making laboratory measurements difficult, so coupled-physics finite-element-modeling can also be employed to glean more information than has been acquired so far through physical observation.

8584-25, Session 7

Clinical applications of plasma based electrosurgical systems *(Invited Paper)*

Jean Woloszko, Thomas Ryan, Kenneth R. Stalder, ArthroCare Corp. (United States)

Over the past 18years, several electrosurgical systems generating a low temperature plasma in an aqueous conductive solution have been commercialized for various clinical applications and have been used in over 7 million patients to date. The most popular utilizations are in arthroscopic surgery, otorhinolaryngology surgery, spine and neurosurgery, urology, wound care and others.

These devices can be configured to bring irrigating saline to the tip and to have concomitant aspiration to remove by-products and excess fluid. By tuning the electrode geometry, waveform and fluid dynamic at the tip of the devices, tissue resection and thermal effects can be adjusted individually. This allows one to design products that can operate as very precise tissue dissector for treatment of articular cartilage or debridement of chronic wound, as well as global tissue debulking devices providing sufficient concomitant hemostasis for applications like tonsillectomies. Effects of these plasma based electrosurgical devices on cellular biology, healing response and nociceptive receptors has also been studied in various models.

This talk will include a review of the clinical applications, with product descriptions, results and introductory review of some of the research on the biological effects of these devices.

8584-26, Session 8

Stable microwave radiometry system for long term monitoring of deep tissue temperature *(Invited Paper)*

Paul R. Stauffer, Sara Salahi, Dario B. Rodrigues, Duke Univ. (United States); Erdem Topsakal, Mississippi State Univ. (United States); Tiago Ribeiro, Aniruddh Prakash, Duke Univ. (United States); Douglas Reudink, Thermimage Corp. (United States); Brent W. Snow, The Univ. of Utah (United States); Paolo F. Maccarini, Duke Univ. (United States)

There are numerous clinical applications for non-invasive monitoring of deep tissue temperature. We present the design and experimental performance of a miniature radiometric thermometry system for measuring volume average temperature of tissue regions located up to 4cm deep in the body.

We constructed a miniature sensor consisting of EMI-shielded log spiral microstrip antenna with high gain on-axis and integrated high-sensitivity 1.35GHz total power radiometer. We tested performance of the radiometry system in multilayer phantom models of three intended clinical measurement sites: i) brown adipose tissue (BAT) depots within 4cm of surface, ii) 3-5cm deep kidney, and iii) human brain underlying intact scalp and skull. These models included layers of circulating tissue-mimicking liquids controlled at different temperatures to characterize our ability to quantify small changes in target temperature at depth under normothermic surface tissues.

We report SAR patterns that characterize sense region of a 2.5cm diameter receive antenna, and radiometric power measurements as a function of deep tissue temperature that quantify radiometer sensitivity. The data demonstrate our ability to accurately track temperature rise in three realistic tissue targets such as: i) 0.5°C rise of 1-2cm3 volumes of BAT up to 4cm deep, ii) 2-5°C rise of 30ml urine inside kidney located 3-5cm deep, and 2-10°C rise of brain underlying normothermic scalp and skull .

A non-invasive sensor consisting of 2.5cm diameter receive antenna and integral 1.35GHz total power radiometer has demonstrated sufficient sensitivity to track clinically significant changes in temperature of deep tissue targets underlying normothermic surface tissues.

8584-27, Session 8

Numerical 3D modeling of heat transfer in human tissues for microwave radiometry monitoring of brown fat metabolism

Dario B. Rodrigues, Duke Univ. (United States) and Univ. Nova de Lisboa (Portugal); Paolo F. Maccarini, Duke Univ. (United States); Sara Louie, ANSYS, Inc. (United States); Tiago R. Oliveira, Duke Univ. (United States); Pedro J. S. Pereira, Instituto Superior de Engenharia de Lisboa (Portugal); Paulo Limao-Vieira, Univ. Nova de Lisboa (Portugal); Paul R. Stauffer, Duke Univ. (United States)

Brown adipose tissue (BAT) plays an important role in whole body metabolism in a way that could potentially mediate weight gain and insulin sensitivity. Although some imaging techniques allow BAT detection within the body, there are currently no viable methods for continuous acquisition of BAT energy expenditure. We present a non-invasive technique for long term monitoring of BAT metabolism using microwave radiometry.

A 3D computational model was created using Avizo® by segmenting CT images of an adult human, delimiting BAT from surrounding tissues. The segmented regions were imported into ANSYS® to create an accurate model for heat transfer analysis. SAR patterns of a miniature 2.5cm receive antenna were calculated in HFSS™, validated in an SAR scan tank, and combined with the simulated thermal distribution to predict radiometric signal expected from an ultralownoise 1.35GHz radiometer. A phantom model of the human torso was constructed and the radiometer tested for detection of different levels of BAT metabolism.

Simulations of SAR patterns and heat transfer correlated well with experiments and showed direct correspondence between BAT temperature variation and radiometric signal. The radiometer demonstrated the ability to sense 0.5°C changes (corresponding to five-fold increase in metabolism) in 1-2cm3 regions of BAT to 4cm depth.

Results demonstrated the ability to detect thermal radiation from small volumes (1-2 cm3) of BAT to 4cm depth and monitor changes in temperature typical of the range of BAT metabolism. The developed miniature 1.35GHz radiometer appears suitable for non-invasive long term monitoring of BAT metabolism.

8584-28, Session 8

in situ treatment of liver using catheter based therapeutic ultrasound with combined imaging and GPS tracking system *(Invited Paper)*

E. Clif Burdette, Goutam Ghoshal, Tamas Heffter, Acoustic Medsystems, Inc. (United States); Laurie Rund, John M. Ehrhardt, Univ. of Illinois (United States); Chris J. Diederich, Univ. of California, San Francisco (United States)

Extensive surgical procedure or liver transplant still remains the gold standard for treating slow-growing tumors in liver. But only few candidates are suitable for such procedure due to poor liver function, tumors in unresectable locations or presence of other liver diseases. In such situations minimally invasive surgery may be the best therapeutic procedure. The use of RF, laser and ultrasound ablation techniques has gained considerable interest over the past several years to treat liver diseases. The success of such minimally invasive procedure depends on accurately targeting the desired region and guiding the entire procedure. The purpose of this study is to use ultrasound imaging and GPS tracking system to accurately place a steerable acoustic ablator and multiple temperature sensors in porcine liver in situ. Temperature sensors were place at eight different locations to estimate thermal distribution in the three-dimensional treated volume. Acoustic ablator of center frequency of 7 MHz was used for the experiments. During therapy a maximum temperature of 60-65 °C was observed at a distance 8-10 mm from the center of the ablation transducer. The dose distribution was analyzed and compared the gross pathology of the treated region. Accurate placement of the acoustic applicator and temperature sensors were achieved using the combined image-guidance and the tracking system. By combining ultrasound imaging and GPS tracking system accurate placement of catheter based acoustic ablation applicator can be placed accurately in livers in situ.

8584-29, Session 8

Targeted hyperthermia in prostate with an MR-guided endorectal ultrasound phased array: patient specific modeling and preliminary experiments

Vasant A. Salgaonkar, Punit Prakash, Viola Rieke, John Kurhanewicz, I. C. J. Hsu, Chris J. Diederich, Univ. of California, San Francisco (United States)

Introduction: Feasibility of hyperthermia delivery to the prostate with a commercially available MR-guided endorectal ultrasound (ERUS) phased array ablation system (ExAblate by Insightec) was assessed through computer simulations and ex vivo experiments. Methods: The simulations included a 3D FEM-based model of Pennes equation, and acoustic field calculations for the ExAblate phased array (2.3 MHz, 2.3?4.0 cm2) using the rectangular radiator method. Array beamforming strategies were investigated to deliver 30-min hyperthermia (>41 oC) to focal regions of prostate cancer, identified from MR or CT images in representative patient cases (n=6). ExAblate's hardware and software constraints on power densities, sonication durations and switching speeds were incorporated in the models. The preliminary experiments included beamformed sonications in tissue mimicking phantom material under MRI-based temperature monitoring at 3T (GRE TE=7.2 ms, TR=15 ms, BW=10.5 kHz, FOV=20 cm, matrix 256x128, FA=40º). Results: T>41 oC was calculated in 10–20 cm3 for sonications with planar or diverging beam patterns at 1.2–1.7 W/cm2, and in 3-9 cm3 for curvilinear (cylindrical) or multifocus beam patterns at 1.3–3.3 W/cm2, potentially useful for treating focal disease in a single posterior quadrant. Bilateral targets required scanned sonications. Conformable hyperthermia may be delivered by tailoring power deposition along the array length and angular expanse. MR-temperature rises of 4-8 oC were induced in a phantom with the ExAblate array, consistent with calculated values and lower power settings (~1.3 W/cm2).

Conclusions: MRgERUS HIFU systems can be controlled for continuous hyperthermia in prostate to augment radiotherapy and drug delivery [NIH R01 122276, 111981].

8584-30, Session 9

Preliminary experimental and theoretical assessment of MR-guided thermal therapy of pancreatic tumors with endogastric and transgastric catheter-based ultrasound devices

Punit Prakash, Vasant A. Salgaonkar, Serena J. Scott, Univ. of California, San Francisco (United States); Graham Sommer, Stanford Univ. School of Medicine (United States); Chris J. Diederich, Univ. of California, San Francisco (United States)

The objectives of this study were to use theoretical and experimental techniques to evaluate endogastric and transgastric approaches for MR-guided thermal therapy of pancreatic tumors with catheter-based ultrasound devices. The transgastric approach involves direct endoscopic or percutaneous placement of a 14 g interstitial ultrasound applicator into the pancreas. The endogastric approach, based on an ultrasound transducer assembly enclosed in a cooling balloon, endoscopically positioned within the stomach/duodenum, can sonicate pancreatic targets from within the GI tract. A 3D bioacoustic-thermal model was implemented to calculate acoustic energy distributions and transient temperature and thermal dose profiles in tissue. These models were used to determine transducer dimensions, operating frequency, and power levels needed for ablating 1-3 cm diameter pancreatic targets. Theoretical models indicated that unsectored and sectored interstitial ultrasound applicators could be used to ablate (t43>240min) tumors measuring up to 2.3-3.4 cm in diameter, with applied power levels of 20-30 W/cm2 at 7 MHz for 5-10 min. Endogastric applicators with planar and curvilinear transducers operating at 3-4 MHz could be used to ablate tumors up to 20-25 mm deep from the stomach wall within 5 min. Endogastric devices with sectored tubular transducers (10 mm OD, 3-4 MHz) could ablate tumors up to a depth of 13-18 mm. Proof-of-concept devices were fabricated and successfully integrated into the MRI environment for heating experiments in tissue phantoms under real-time thermometry and closed-loop feedback control. Ongoing efforts include evaluation of endoscopic device placement and targeting in an in vivo animal model. [NIH R21CA137472 and P01CA159992].

8584-31, Session 9

Non-invasive estimation of thermal tissue properties by high-intensity focused ultrasound *(Invited Paper)*

Sunil Appanaboyina, Medical Univ. of South Carolina (United States); Ari Partanen, Philips Medical Systems (Finland); Dieter Haemmerich, Medical Univ. of South Carolina (United States)

Background: Magnetic Resonance guided Focused Ultrasound System (MRgFUS) locally heat tissue via ultrasound, and record tissue temperature profiles via MR-Thermometry. The goal was to investigate the use of a computational technique based on inverse heat-transfer modeling for the non-invasive measurement of thermal tissue properties via data collected from a MRgFUS system.

Methods: Heating and cooling data of a Agar-Silica gel using a MR-guided High-Intensity Focused Ultrasound (HIFU) system with a 1.2 MHz-transducer was obtained, where a single focal spot was heated for 30 s at 120 W. Temperature profile in a sagittal slice was recorded at 3 s intervals, with in-slice resolution of 2.5mm x 2.5mm and 7mm slice

thickness. The specific absorption rate (SAR) was calculated from the experimental data, and subsequently synthetic data sets were generated with 15s and 30s heating times by solving the bioheat transfer equation (BHTE). Thermal conductivity was varied between 0.3 - 0.7 W/m/K, and perfusion was varied between 0.002 - 0.018 ml/ml/s. Gaussian random noise (standard deviation 1°C) was added to these temperature data. The cool-down data was then used as input data with unknown thermal properties. A simplex optimization scheme and solution of the BHTE was used to estimate thermal conductivity and perfusion of the synthetic data sets.

Results: Estimated thermal conductivity was between 80-100% higher than actual values. Estimated perfusion was ~10 % lower than actual value at 0.018 ml/ml/s (=normal liver perfusion), and ~40 % lower at 0.002 ml/ml/s.

Conclusion: MR-thermometry data acquired during HIFU may allow estimation of local tissue perfusion non-invasively via inverse modeling. This method may provide patient-specific data to optimize thermal treatments, as well as drug delivery to tumors.

8584-32, Session 9

Incorporating tissue absorption and scattering in rapid ultrasound beam modeling *(Invited Paper)*

Douglas A. Christensen, Univ. of Utah (United States); Scott Almquist, The Univ. of Utah (United States)

We have developed a new approach for modeling the propagation of an ultrasound beam in inhomogeneous tissues such as encountered with focused ultrasound surgery (FUS) for treatment of various diseases. This method, called the hybrid angular spectrum (HAS) approach, combines propagation steps in both the space and the spatial frequency domains throughout the inhomogeneous regions of the body; the use of spatial Fourier transforms makes this technique considerably faster than other modeling approaches (a few seconds for a 201 x 201 x 201 model). Of prime importance in FUS thermal treatments is the acoustic absorption property of the tissues, which leads to temperature rise and the achievement of the desired thermal dose at the treatment site. We have recently added to the HAS method the capability of independently modeling tissue absorption and scattering, the two components of acoustic attenuation. This improves the predictive value of the beam modeling and more accurately describes the thermal conditions expected during a therapeutic ultrasound exposure. The speed of the technique also allows its use in optimization routines that determine changes in tissue properties that accompany thermal exposures. Some anatomically realistic examples that demonstrate the importance of independently modeling absorption and scattering will be given, including propagation through the human skull for noninvasive brain therapy and in the human breast for treatment of breast lesions.

8584-33, Session 9

Catheter-based therapeutic ultrasound treatment of urinary tract disorders *(Invited Paper)*

E. Clif Burdette, Acoustic Medsystems, Inc. (United States); Chris J. Diederich, Jeffrey Wooton, Univ. of California, San Francisco (United States); Emery M. Williams, Paul Neubauer, Lance Frith, Bruce Komadina, Acoustic Medsystems, Inc. (United States)

The overall objective of this research is to examine the suitability and develop specific devices and methodology for treatment of urinary tract disorders and specifically urinary incontinence via thermally-induced modification of targeted tissues. A high degree of selectivity is required to induce tissue remodeling to increase tissue density at the base of the bladder neck and endopelvic region supporting the urethra. Incontinence is a significantly greater problem in females than males. In females, primary factors contributing to incontinence are bearing children and age. In males, the primary factor is loss of sphincter control at the bladder neck. These are pervasive problem, with some references putting the prevalence at over 16 million annually in the U.S. alone. Our objectives have been to assess the anatomy and critical structures involved, determine the specific targets for treatment, perform modeling and analysis of achievable thermal treatment profiles, perform design analysis, fabricate devices specific to the desired treatment targets, and determine feasibility of achieving the desired treatment conditions in ex-vivo tissues. Each of these objectives were achieved and results were consistent with producing the desired treatment dose delivery and resulting therapeutic conditions. New devices were designed, implemented, and tested via both modeling and through tissue treatments with measured thermal dose results. These devices were highly directional, multisectored acoustic transducers capable of high power output and selective treatment of the targeted treatment volumes, with temperatures 55-60oC in target and <45o in nearby structures. Experimental results and modeling confirming feasibility will be presented.

8584-34, Session 9

Interstitial ultrasound ablation of tumors within or adjacent to bone: contribution of preferential heating at the bone surface

Serena J. Scott, Punit Prakash, Peter D. Jones, Richard N. Cam, Univ. of California, San Francisco (United States); E. Clif Burdette, Acoustic Medsystems, Inc. (United States); Chris J. Diederich, Univ. of California, San Francisco (United States)

Preferential heating of bone due to high ultrasound attenuation may enhance thermal ablation with catheter-cooled interstitial ultrasound applicators in or near bone, while thermally and acoustically insulating cortical bone may protect sensitive structures nearby. 3D acoustic and biothermal transient finite element models were developed to simulate temperature and thermal dose distributions during 7 MHz catheter-cooled interstitial ultrasound ablation near bone. Experiments in ex vivo tissues and phantoms were performed to validate the models and to quantify the temperature rises and ablated volumes for various distances between the interstitial applicator and the bone surface. 3D patient-specific models selected to bracket the range of clinical usage were developed to investigate what types of tumors could be treated, applicator configurations, insertion paths, safety margins, and other parameters. Experiments show that preferential heating at the bone surface decreases treatment times and that when placed up to 2 cm away from bone, all tissue between an applicator and the bone can be ablated. Simulations indicate that a 3-4 mm safety margin of normal bone is needed to protect (t43<6 min and T<45°C) sensitive structures behind ablated bone. In 3D patient-specific simulations, tumors 1.0-3.8 cm (L) and 1.3-3.0 cm (D) near or within bone were ablated (t43>240 min) within 10 min without damaging the nearby spinal cord, lungs, esophagus, trachea, or major vasculature. Preferential absorption of ultrasound by bone may provide improved localization, faster treatment times, and larger treatment zones in tumors in and near bone compared to other heating modalities. (NIHR44CA112852)

8584-35, Session 10

Magnetic nanoparticle hyperthermia: predictive model for temperature distribution

Robert V. Stigliano, Fridon Shubitidze, Dartmouth College (United States); P. Jack Hoopes, Dartmouth Medical School (United States)

Magnetic nanoparticle (mNP) hyperthermia has developed into a promising adjuvant cancer therapy. mNP's are injected, either intravenously or directly into a tumor, and are heated by applying

an alternating magnetic field (AMF). The mNP's are, in many cases, sequestered by cells and packed into endosomes. The proximity of the mNP's has a strong influence on their ability to heat due to inter-particle magnetic interaction effects. This is an important point to take into account when modeling the mNP's. Generally, more mNP heating can be achieved using higher magnetic field strengths. The factor which limits the maximum field strength applied to clinically relevant volumes of tissue is the heating caused by eddy currents, which are induced in the noncancerous tissue. A coupled electromagnetic and thermal model has been developed to predict dynamic thermal distributions during AMF treatment. The EM model is based on the method of auxiliary sources and the thermal modeling is based on the Pennes bioheat equation. The results of our phantom study are used to validate the model which takes into account nanoparticle heating, interaction effects, particle spatial distribution, particle size distribution, EM field distribution, and eddy current generation in a controlled environment. Once fully developed and validated, the model will have applications in experimental design, AMF coil design, and treatment planning.

8584-36, Session 10

Infrared thermography analysis of thermal diffusion induced by RF magnetic field on agar phantoms loaded with magnetic nanoparticles

Jose Bante-Guerra, Ctr. de Investigación y de Estudios Avanzados (Mexico)

Recently, several treatments for fighting malignant tumors have been designed. However these procedures have well known inconveniences, depending on their applicability, tumor size and side effects, among others. Magnetic hyperthermia is a safe and non-invasive method for cancer therapy. This treatment is applied via elevation of target tissue temperature by dissipation of heat from Magnetic Nanoparticles (MNPs), previously located within the tumor. The induction of heat causes cell death and therefore the removal of the tumor.

In this work the thermal diffusion in phantoms of agar loaded with magnetic nanoparticles (MNPs) is studied using the infrared thermography technique, which is widely used in biology/medicine (e.g. skin temperature mapping). Agar is one of the materials used to simulate different types of body tissues, these samples are known as "phantoms". Agar is of natural origin, low cost and high degree of biocompatibility. In this work the agar gel was embedded with MNPs by co-precipitacion and placed in an alternating magnetic field radiation. As a consequence, the energy from the radiation source is dissipated as heat and then transferred from the MNP to the gel, increasing its temperature.

For the temperature analysis, the samples of agar gel were stimulated by RF magnetic field generated by coils. Heating was measured with infrared thermography using a Thermovision A20M infrared camera. Thermographic images allowed obtaining the dependence of thermal diffusion in the phantom as a function of the magnitude of the applied RF magnetic field and the load of magnetic particles.

8585-1, Session 1

THz photoconductive devices: tried and true *(Keynote Presentation)*

Elliott R. Brown, Wright State Univ. (United States)

Ultrafast photoconductors (PCs) continue to captivate materials scientists, device engineers, and THz researchers worldwide because of their fascinating solid-state physics at the sub-ps time scale and their unique ability to make ultra-wideband THz sources, be it pulsed (PC switches) or tunable cw (photomixers). Arguably, ultrafast PC devices have been the most successful THz device technology during the past decade, becoming the heartbeat of several THz systems such as time- and frequency-domain spectrometers. They are relatively simple to fabricate, operate at room temperature, require modest electric but no magnetic bias, and benefit directly from continual advances in the photonic components used to drive them – especially fiber mode-locked lasers, and single-frequency diode (e.g., DFB) lasers. Fundamentally, they are subject to a gain-bandwidth product, similar to transistors, but this product is much more lenient in PC devices partly because the role of the metallic gate or base in transistors is replaced by the photon flux in PC devices, which entails no metal contact and thus adds no capacitance. This talk will address the evolution of the various types of THz PC devices over the past two decades, starting with heavily ion-implanted Si, LTG-GaAs, ErAs:GaAs, and ditto for InGaAs lattice-matched to InP. Special attention will be given to the most promising recent 1550-nm-driven PC devices, such as InGaAs/InAlAs superlattice, Fe cold-implanted InGaAsP, and extrinsic-photoconductive ErAs:GaAs. This is because 1550-nm devices can be readily scaled to 2D arrays, and enable other fiber-optoelectronic integrated circuits that would make THz power and control much more affordable.

8585-2, Session 1

Nonlinear optical THz generations and applications *(Invited Paper)*

Kodo Kawase, Nagoya Univ. (Japan); Shin'ichiro Hayashi, Hiroaki Minamide, RIKEN (Japan)

We report on the development of a high-peak-power (> 1kW), single-longitudinal-mode and tunable injection-seeded terahertz-wave parametric generator (is-TPG) using MgO:LiNbO3, which operates at room temperature. The experimental setup consists of a pumping source, amplifiers, seeding source (ECDL) and the nonlinear crystal (MgO:LiNbO3). The pumping source is a diode end-pumped single-mode microchip Nd:YAG laser passively Q-switched by Cr:YAG saturable absorber. In this experiment, the pumping beam from the microchip laser was amplified by two tandem Nd:YAG amplifiers in double-pass configuration. The pumping beam diameter on the crystal is about 1 mm (FWMH). We used a 50-mm-long nonlinear MgO:LiNbO3 crystal with a Si-prism coupler. The terahertz-wave output was measured using a calibrated pyroelectric detector (SpectrumDetector Inc.: SPI-A-65 THZ). The pumping energy was 14 mJ/pulse (28 MW at peak) and the seeding power was 500 mW (CW). The observed maximum peak power of terahertz-wave was about 1 kW (@ 1.7 THz). This peak power was the highest in our research. The tuning curve (1.0 - 2.8 THz) has a flat region around 1.4 - 2.2 THz. The small footprint size are suitable for a variety of applications. We also report other novel nonlinear optical THz sources and real-life applications.

8585-3, Session 1

Potential for biomedical sensing using broadband terahertz devices *(Invited Paper)*

René Beigang, Fraunhofer-Institut für Physikalische Messtechnik (Germany); Michael Theuer, Technische Univ. Kaiserslautern (Germany); Garik Torosyan, Fraunhofer-Institut für Physikalische Messtechnik (Germany); Daniel Molter, Marco Rahm, Benjamin Reinhard, Technische Univ. Kaiserslautern (Germany)

Terahertz (THz) radiation in a frequency range between 100 GHz and 10 THz is, in principle, well suited for biomedical sensing applications as almost all biomolecules show characteristic absorptions in this frequency range. However, the particular properties of THz radiation together with the requirement to allow detection in a natural environment containing water and other solvents ask for specific sensors. In particular, there is need for sensitive sensors to detect even very small amounts of biomolecules without additional labelling.

In this contribution we discuss the use of broadband THz radiation for biomedical sensing applications. Different THz sensors are presented, including ATR devices, waveguide sensors and sensors based on propagating surface waves on metamaterial surfaces. In ATR sensors the evanescent field of a THz pulse at the surface during total internal reflection is used to determine properties of the "external" medium. The interaction length is determined by the extension of the evanescent wave. A compact fiber coupled sensor will be presented which is well suited for the investigation of liquids. In sensors based on waveguides or other resonant structures the frequency response on the coverage of the surface with different adsorbates is exploited. The measurement of frequency shifts instead of amplitude changes makes these devices insensitive to amplitude fluctuations of the THz source. Metamaterial structures on a surface can be used to launch propagating surface waves. The resonance conditions of these propagating surface waves can be tailored to resonances of the biomolecules under investigation. Typical examples for these sensors will be presented.

8585-4, Session 1

Biological applications of terahertz near-field microscope *(Invited Paper)*

Koichiro Tanaka, Kyoto Univ. (Japan)

Bio-application of terahertz (THz) wave is an important issue and many efforts have been paid in these days. Especially, THz imaging has been expected as an alternative technique for conventional imaging techniques, since THz waves can be transmitted through many materials that block visible light and give much higher imaging resolution than microwaves. Especially, much attention has been paid for the biological applications, because THz wave can interact sensitively with liquid waters and large bio-related molecules such as proteins and DNAs. In this sense, a THz microscope for the biological tissues has been eagerly anticipated. However, there is a severe problem existing in the space resolution, that is, diffraction limit.

We achieve high spatial resolution on a large area by combining two novel techniques: terahertz generation by tilted-pulse-front excitation and electro-optic (EO) balanced imaging detection using a thin crystal. We took visible and THz images of a metallic mask directly deposited on top of the EO crystal. We found a spatial resolution of 10 ?m with a 3-?m-thick LiNbO3 x-cut crystal, corresponding to ?/150 for a center frequency at 0.2 THz. The extracted visible profile confirms that the optical elements do not restrict the THz spatial resolution. We measured near-field images of THz metamaterials with metallic dipole antennas or split-ring resonators that are expected to be a biosensor. The structures show clear field enhancement at specified positions in the structure. By THz near-field imaging in time-domain, we confirmed time-development and enhancement of the electric field in near-field regime.

8585-5, Session 1

Development of terahertz (THz) microfluidic devices for lab-on-a-chip applications *(Invited Paper)*

Hao Xin, The Univ. of Arizona (United States)

No Abstract Available

8585-6, Session 1

Terahertz sensing with meta-surfaces and integrated circuits *(Invited Paper)*

Marco Rahm, Benjamin Reinhard, Klemens Schmitt, Tassilo Fip, Martin Volk, Jens Neu, Anna-Katharina Mahro, René Beigang, Technische Univ. Kaiserslautern (Germany)

Many applications in the realms of terahertz research are concerned with electromagnetic sensing of substances such as drugs, chemical compounds, explosives and much more. While standard techniques mostly rely on terahertz time domain spectroscopy, the technological demands for high data acquisition speed and the economic affordability of the measurement systems often require alternate and less sophisticated methods. While the cost can be significantly reduced by the use of continuous wave terahertz sources instead of ultrashort pulse lasers, the data acquisition time can be considerably optimized when only the amplitude of the THz fields is measured and phase information is obsolete for the measurement principle.

In this respect, meta-surfaces can be used as highly sensitive near-field sensors. Meta-surfaces are artificially structured metallic surfaces whose electromagnetic response can be designed at purpose. By exploiting the dependence of the resonance frequency of specifically devised meta-surfaces to substances in the vicinity of the near-field of the surface, it is possible to implement highly sensitive chip-based terahertz sensors. As an example, we show that such sensors can be used to determine the thickness of ultra-thin layers of silicon on top of the sensors. The maximum thickness resolution was of the order of wavelength ?/16000. Moreover, the sensors were used to measure the refractive index of liquids and liquid mixtures in refractometry experiments. We also show that meta-surfaces support tailored, tightly bound surface waves which can be guided along the surface at will. By this methodology, terahertz chip-based circuits can be implemented for interferometric sensing applications.

8585-7, Session 1

Terahertz quantum cascade laser based optical coherence tomography *(Invited Paper)*

Alan W. M. Lee, LongWave Photonics LLC (United States); Tsung-Yu Kao, Qing Hu, Massachusetts Institute of Technology (United States)

Terahertz frequency (300 GHz to 10 THz) tomography of thin-films has found recent practical applications for the characterization of polymers. The opacity of these polymers at near-infrared and visible frequencies precludes the use of more mature infrared or visible wavelength technologies, justifying the expense and complexity of the non-linear generation mechanisms of current commercial terahertz systems. As an alternative, quantum-cascade lasers (QCLs) are a promising fundamental source of terahertz frequency radiation for their multi-milliwatt power levels, electrical operation and absence of optical alignment. However, the use of QCLs for tomography of dielectric films is challenging due to the lack of picosecond pulsed sources necessary for time-of-flight tomography, or practical frequency tuning mechanisms necessary for interferometry-based tomography. In this talk we report a frequency agile QCL source and the demonstration of tomography using the swept source optical coherence tomography (SS-OCT) technique.

In this talk we will present recently obtained results on the measurement of interfaces of a dielectric sample using SS-OCT using recently developed QCL arrays at 2.1 to 2.4 THz as well as arrays covering 4.7 to 5 THz. These arrays have shown excellent single mode operation, with good beam patterns and power levels of ~100 uW. A compact closed cycle cryocooler system has been developed as well as specialized electronics for rapidly switching the active device, allowing fast frequency scanning. Applications for these arrays will be discussed.

8585-8, Session 1

Terahertz and mid-infrared photoexpansion nanospectroscopy

(Invited Paper)

Mikhail A. Belkin, Feng Lu, The Univ. of Texas at Austin (United States); Mohammed Salih, Paul Dean, Suraj P. Khanna, Lianhe H. Li, Giles Davies, Edmund H. Linfield, Univ. of Leeds (United Kingdom)

We report a method of taking mid-infrared and terahertz spectra on nanoscale using compact mW-level sources, such as quantum cascade lasers, and a standard atomic force microscope (AFM). Light absorption is detected via deflection of an AFM cantilever due to local sample thermal expansion. The spatial resolution is principally determined by the diameter of the high-intensity spot in the vicinity of a sharp metalized AFM tip, and is below 50nm. To enable detection of minute sample expansion, the repetition rate of the laser pulses is moved in resonance with the cantilever mechanical frequency. The technique requires no optical detectors.

8585-9, Session 1

Hydration dynamics in biomolecules probed by time-domain spectroscopy *(Invited Paper)*

Gun-Sik Park, Da-Hye Choi, Heyjin Son, Seoul National Univ. (Korea, Republic of)

Recently, terahertz (THz) spectroscopy has been proposed for observing ultrafast hydration water dynamics. Water molecules form labile hydrogen-bond collective networks which are constantly changed on a picosecond time scale (1 ps-1 = 1 THz). The constant breaking and forming of hydrogen-bonds results in the fluctuations of the water dipole moments, and the THz spectrum is sensitive to the motion. As a consequence, THz spectroscopy measures the subtle change of water molecules by the presence of solutes. By using terahertz time domain spectroscopy (THz-TDS), Hishida et al. recently revealed the long-range hydration effect of lipid on the sub- ps time scale. The measured time scale of previous studies was relatively slow (10-9 ~ 10-11 s) so that it only observed more tightly bound short-range water molecules. In spite of many efforts to understand the lipid hydration, clear picture about a relation between hydration water dynamics and lipid dynamics is still lacking. To investigate such possible relations we follow the lipid dynamics and hydration water dynamics at different temperatures. We observed the temperature dependent dynamics change of lipids and water molecules with FTIR and THz-TDS respectively, and found the global water dynamics and lipid dynamics is closely related. The hydration dynamics of DNA will be also discussed in this presentation.

8585-10, Session 2

Watching the dance of ions and molecules in the THz *(Keynote Presentation)*

Martina Havenith, Ruhr-Univ. Bochum (Germany)

In recent years a new frequency window has been opened: The THz range. In pioneering studies it could be shown that THz absorption spectroscopy is a new tool to study the solvation dyncamics of biomolecules [1]. THz spectroscopy probes sensitively the fast (sub-psec) collective network dynamics of bulk water. Accompanying ab initio MD simulation unravel the underlying molecular motions: In contrast to the mid infrared regime -where the absorption peaks can be assigned to intramolecular motions- in the frequency regime below 1000 cm-1 intermolecular motions with concerted particle motions dictate the spectrum [2]. Precise measurements of absorption coefficients of solvated solutes in the THz regime allow now a precise view on changes in hydration dynamics of solutes:

The discussion about the solvation mechanism of different salts has been initiated over a century ago by introduction of the Hofmeister series; however the molecular picture of ion hydration is still part of a controversial scientific debate. Ion hydration is a fundamental question in chemistry with many implications for biology –ranging from ion transport in membrane channels to ion transports in electrolytes. The concept of water “structure breaking” and “structure making” still provides the basis for the interpretation of experimental observations, in particular the stabilization/destabilization of bio-molecules. Recent studies either challenge or support some key points of the structure maker/breaker concept, specifically regarding long-ranged ordering/disordering effects. We will report the results of a systematic terahertz absorption spectroscopy and molecular dynamics simulation study, which adds a new piece to the puzzle [3].

Furthermore, the development of Kinetic THz Absorption (KITA) spectroscopy allows to follow changes in hydration dynamics in real time during biological function [4,5]. Thereby we could show that changes in the hydration dynamics go along with the initial step in protein folding. Using a combination of time resolved X-ray studies and THz absorption studies we find that, as enzyme–substrate binding develops, but before a full complex is formed, the movement of water near the pro¬tein is retarded. Crudely put, it is as if the water ‘thickens’ towards a more glassy form, which in turn calms the fluctuations of the sub¬strate so that it can become locked securely in place.

All these results offer an astonishing picture of how finely biomolecules manipulate their associated water molecules to perform their function.

[1] S. Ebbinghaus, S.J. Kim, M. Heyden, X. Yu, U. Heugen, M. Gruebele, D.M. Leitner, M. Havenith, “An extended dynamical solvation shell around proteins,” Proc. Natl. Acad. Sci. USA, 104, 20749 (2007).

[2] M. Heyden, J. Sun, S. Funkner, G. Mathias, H. Forbert, M. Havenith, D. Marx Dissecting the THz spectrum of liquid water from first principles via correlations in time and space. Proc. Natl. Acad. Sci. USA, 107, 12068 (2010).

[3] D.A. Schmidt, Ö. Birer, S. Funkner, B. Born, R. Gnanasekaran, G. Schwaab, D.M. Leitner, M. Havenith, Rattling in the cage: Ions as probes of sub-ps water network dynamics, J. Am. Chem. Soc., 131(51), 18512-18517 (2009)

[4] S.J. Kim, B. Born, M. Havenith, M. Gruebele, Real-time detection of protein-water dynamics upon protein folding by terahertz absorption, Angewandte Chemie Intl. Edition 47 (34), 6486-6489 (2008).

[5] M. Grossmann, B. Niehues, M. Heyden, D. Tworowski, G.B. Fields, I. Sagi, M. Havenith (2010), Correlated structural kinetics and retarded solvent dynamics at the metalloprotease active site, Nature Structural & Molecular Biology, published online 18.9.2011; doi:1038/nsbm.2120

8585-11, Session 2

Terahertz-frequency transition from disorder to order in amorphous condensed matter *(Keynote Presentation)*

Peter U. Jepsen, Technical Univ. of Denmark (Denmark)

Terahertz spectroscopy of condensed matter systems in the amorphous phase, including glasses and biological materials, typically reveals a dielectric loss spectrum with absorption strength monotonously increasing with frequency. This universal behavior is caused by extremely strong disorder-induced scattering of acoustic waves in the material. In the THz frequency range, the consequence is that most amorphous materials display very similar dielectric spectra, making quantitative spectroscopic investigations very challenging. At higher frequencies, however, the universal behavior breaks down, and the dielectric response is dominated by well-defined vibrational modes of the material. In this regime, acoustic modes are well described as plane waves, and material disorder has much less influence on the dielectric properties. In this keynote talk I will review recent advances in ultrahigh-bandwidth terahertz time-domain spectroscopy (THz-TDS) that have allowed the direct observation of the transition from disorder to order in amorphous materials.

8585-12, Session 2

Molecular modeling of membrane modifications after exposure to nanosecond, pulsed electric fields *(Keynote Presentation)*

Paul T. Vernier, The Univ. of Southern California (United States)

Structural modifications of cell membranes are among the primary consequences of exposure to intense nanosecond pulsed electric fields. These alterations can be characterized indirectly by monitoring changes in electrical conductance or small molecule permeability of artificial membranes or suspensions of living cells, but direct observations of the membrane-permeabilizing structures remain out of the reach of experiments. Molecular dynamics simulations provide an atomically detailed view on the nanosecond time scale of the sequence of events that follows the application of an external electric field to a system containing an aqueous electrolyte and a phospholipid bilayer, a simple approximation of a cell membrane. This biomolecular perspective, which correlates with experimental observations of electroporation (electropermeabilization) in many respects, points to the key role of water dipoles, driven by the electric field gradients at the membrane interface, in the initiation and construction of the membrane defects which evolve into conductive pores. We describe a method for stabilizing these lipid electropores in phospholipid bilayers, and for characterizing their stability and ion conductance, and we show how the properties of these nanoscale structures connect with continuum models of electroporation and with experimental results.

8585-13, Session 2

Protein-water network dynamics during metalloenzyme hydrolysis observed by kinetic THz absorption (KITA) *(Invited Paper)*

Benjamin P. Born, Weizmann Institute of Science (Israel)

For long, the contribution of water network motions to enzymatic reactions was enigmatic due to the complexity of biological systems and to experimental limitations. Thanks to the development of new powerful THz emitters and detectors in the last decades, it is now possible to detect the fast making and breaking of water hydrogen bond during biochemical reactions. For this purpose, we developed a kinetic terahertz absorption (KITA) spectrometer which combines the strength of THz radiation (~1 THz = 1 ps) to directly probe collective picosecond protein-water dynamics with the fast mixing properties of a stopped-flow apparatus which initializes a biochemical reaction within milliseconds. With KITA, we analyzed the collective water dynamics during substrate hydrolyses by a human matrix-metalloproteinase. In addition, we studied the reorganization and electrostatic changes at the catalytic zinc-ion from the enzyme active site and performed molecular dynamics simulations of the enzyme-substrate-water system. Our results revealed a systematic gradient of water network motions: From the active site to the bulk water surrounding hydrogen bond dynamics increased from 7 ps (active site) to 1ps (bulk water) prior to substrate binding and hydrolysis. The approaching substrate perturbs the dynamic water gradient resulting in an overshoot of KITA signal which than relaxes back during onset

of substrate hydrolyses. Our findings suggest that collective water dynamics may contribute to effective substrate alignment and binding to enzyme active sites and could be induced by the charge of the catalytic zinc-ion residing at the active site.

8585-14, Session 2

Determination of the optical properties of melanin-pigmented human skin equivalents using terahertz time-domain spectroscopy

Dawn Lipsomb, Ibtissam Echchgadda, Air Force Research Lab. (United States); Xomalin G. Peralta, The Univ. of Texas at San Antonio (United States); Gerald J. Wilmink, Air Force Research Lab. (United States)

Several studies have used terahertz time-domain spectroscopy (THz-TDS) methods to characterize the optical properties of skin components (i.e., water, collagen, and keratin). However, experiments have not yet been performed to examine the influence of melanin pigment on skin's optical properties. In this study, we used human skin equivalents with different pigmentation levels to investigate melanin's contribution. In vitro skin equivalents, with or without normal human melanocytes, were cultured for three weeks to promote gradual melanogenesis. Skin spectra were collected at various time intervals using a THz-TDS system operating in transmission geometry. Frequency-domain analysis techniques were performed to determine the index of refraction (n) and absorption coefficient (?a) for each skin sample over the frequency range of 0.1-2.0 THz. We found that for all samples as frequency increased, n decreased exponentially and the ?a increased linearly. Additionally, we observed that skin samples with higher levels of melanin exhibited greater n and ?a values than the non-pigmented samples. Our results indicate that skin's level of melanin-pigmentation contributes to the measured optical properties. Future studies will be performed to examine the optical properties of in vivo human skin.

8585-15, Session 3

Nanoelectroablation for human carcinoma therapy *(Keynote Presentation)*

Richard Nuccitelli, Mark Kreis, Brian Athos, Ryan Wood, Kaying Lui, Joanne Huynh, Pamela Nuccitelli, BioElectroMed Corp. (United States)

The use of nanosecond pulsed electric fields to ablate tumors (nanoelectroablation) is now well established in the murine xenograft model system. We have identified the appropriate pulse parameters to ablate melanomas, basal cell carcinomas and human carcinomas in mice with a single treatment. Our next goal is to bring this therapy into the clinic for the treatment of human tumors. This requires that we develop both a reliable and easily used pulse generator as well as delivery electrodes to target the tumors to be treated. We will provide an update on our progress towards these goals.

PulseCure® Pulse Generator Model MBR-1: We are developing a pulse generator to be used in the medical environment that stores and analyzes each pulse and determines if it meets the required rise time and amplitude. PulseCure simultaneously displays and stores both the voltage applied and the current delivered to the patient.

NanoBlate® Delivery Electrode: We have developed an electrode for treating human skin lesions using a parallel array of needles to penetrate the stratum corneum and deliver current to the dermis. We have used the NanoBlate® to ablate several types of human skin lesions.

Clinical Trial Data treating basal cell carcinoma: We have been conducting the first human clinical trial using nanoelectroablation to treat basal cell carcinomas with the NanoBlate® yielding excellent results. Only 100 pulses of 30 kV/cm 100 ns in duration are needed to ablate BCCs scarlessly.

8585-16, Session 3

Understanding terahertz data for medical applications

Emma Pickwell-MacPherson, Hong Kong Univ. of Science and Technology (Hong Kong, China); Vincent P. Wallace, Anthony Fitzgerald, The Univ. of Western Australia (Australia)

Failure to remove the entire cancer during breast conserving surgery with an adequate margin of normal tissue can occur in over 40% of cases, resulting in an increased risk of local recurrence unless a second operation is undertaken to remove additional tissue. This potentially causes further morbidity, a poorer cosmetic result, a delay in giving adjuvant therapy, increased risk of wound infection, a potential reduction in survival rates and increased cost to healthcare systems. Thus, there is a clinical need to accurately define regions of tumor during surgery so as to conserve normal tissue and minimize the number of second surgical procedures. We are now at the point that a hand-held intraoperative THz probe is being tested in clinical trials. Statistically significant heuristic parameters are chosen from both time and frequency domain reflected data to classify tissues into diseased and normal using the Support Vector Machine (SVM) method. The best classification accuracy was achieved using ten parameters extracted from the reflected THz data resulting in an accuracy of 92%. However, further understanding of the connection between physiology, tissue structure and the terahertz data parameters is required. We use a finite difference time domain (FDTD) model to simulate the interaction of THz radiation breast tumours and predict the expected values of the tissue classification parameter; allowing us to further develop our understanding of the interaction of THz radiation with human tissues.

8585-17, Session 3

Hemorrhage control by short electrical pulses

Yossi Mandel M.D., Stanford Univ. (United States); Guy Malki, Eid Adawi, Tel Aviv Univ. (Israel); Richard Manivanh, Stanford Univ. School of Medicine (United States); Ofer Barnea, Tel Aviv Univ. (Israel); Daniel V. Palanker, Stanford Univ. (Israel)

Trauma is a leading cause of death among young individuals, and uncontrolled hemorrhage is the leading cause of preventable death. Controlling a hemorrhage from a solid organ may be challenging in military as well as in civilian settings. We describe the in-vivo effects of short electric pulses on blood vessels and solid organs with a goal of minimizing the bleeding following injury in an animal model.

Short (1?s) electric pulses were applied to the femoral and mesenteric arteries and veins in rats. Threshold amplitude for vasoconstriction increased with shorter pulses, with decreased treatment time and with larger vessel diameters. Pulses were applied at 1 Hz repetition rate. Vessel diameter started decreasing within 20 seconds after the beginning of the procedure, and reached full constriction after about 2 minutes. It then remained steady for the duration of the treatment, and dilated back to its original dimensions within 20-30 minutes after the end of treatment. Longer pulses and higher electric field caused permanent occlusion of blood vessels, which was associated with endothelial damage.

Electric pulses of 25 and 50µs in duration were used to treat liver after penetrating injury in rats and rabbits. Intra-abdominal bleeding volume was reduced by 60% and 36% with pulses of 50 and 25 ?s, respectively, as compared to an untreated control group ($P<0.001$). Histological evaluation found intravascular thrombosis with localized cellular injury.

Vasoconstriction induced by short electrical pulses offers a promising approach to hemorrhage control after trauma and for reduction in bleeding during standard surgical procedures.

8585-18, Session 3

Using a portable terahertz spectrometer to measure the optical properties of in vivo human skin

Gerald J. Wilmink, Jessica E. Grundt, Air Force Research Lab. (United States)

Terahertz time-domain spectroscopy (THz-TDS) systems are excellent tools for the noninvasive assessment of skin health and hydration; however, most conventional systems prove too cumbersome for limited-space environments. We previously demonstrated that a portable, compact THz-TDS (Zomega mini-Z) device permitted measurement of porcine skin optical properties that were comparable to those collected with conventional spectrometers. The goal for this study was to collect in vivo skin measurements on human subjects. Spectra were collected from 0.1-2 THz, and measurements were made on the inner wrist, forearm, and palm. Prior to each THz measurement, we used a multiprobe adapter system to measure each subjects' skin hydration levels, transepidermal waterloss (TEWL), skin color, sebum content, and degree of melanin pigmentation. Our results suggest that the measured optical properties were wide-ranging, and varied considerably for skin tissues with different hydration and melanin levels. These data provide a novel framework for accurate human tissue measurements using THz-TDS in limited-space environments.

8585-19, Session 3

Identification of tissue interaction of terahertz radiation toward functional tissue imaging

William Baughman, Ho-Yun Won, Hamdullah Yokus, David S. Wilbert, Patrick Kung, Seongsin M. Kim, Univ. of Alabama (United States)

In recent years, many applications have been recognized for biomedical imaging techniques utilizing terahertz frequency radiation. This is largely due to the capability of unique tissue identification resulting from the nature of the interaction between THz radiation and the molecular structure of the cells. By THz identification methods, tissue changes in tooth enamel, cartilage, and malignant cancer cells have already been demonstrated. Terahertz Time-Domain Spectroscopy (THz-TDS) remains one of the most versatile methods for spectroscopic image acquisition for its ability to simultaneously determine amplitude and phase over a broad spectral range.

In this study we investigate the use of THz imaging techniques to uniquely identify damage types in tissue samples for both forensic and treatment applications. Using THz-TDS imaging in both transmission and reflection schemes, we examine tissue samples which have been damaged using a variety of acids, thermal burns, and other chemical compounds. Each method of damage causes structural deterioration to the tissue by a different mechanism, thus leaving the remaining tissue uniquely changed based on the damage type. We correlate the change in frequency spectra , phase shift for each damage type to the mechanisms and severity of injury. Once these correlations are established, we further investigate the forensic viability of these techniques by allowing natural rotting to damage the cellular structures so that the time window of effectiveness for this identification method can be determined.

8585-20, Session 3

In vivo assessment of skin burns using terahertz radiation *(Invited Paper)*

M. Hassan Arbab, Dale P. Winebrenner, Trevor C. Dickey, Antao Chen, Matthew B. Klein, Pierre D. Mourad, Univ. of Washington (United States)

We present experimental results from terahertz time-domain spectroscopy of in vivo 2nd and 3rd degree burns in a survival study over the 72 hour period post injury. We will show the dynamic nature of burns by the evolution of the terahertz spectroscopic response of the tissue over the in vivo study period. We will discuss the animal model and experimental burn protocol in detail. Furthermore, we will show an example of the wide range of the burn grades that must be characterized during triage using noninvasive methods by presenting the histological section images. Moreover, we will introduce an image processing approach to objectively quantify the density of skin structures (DOS), such as microvasculature, sweat glands, hair follicles, etc. The severity of the burn is related to the number of the normal skin structures that survive after the burn injury. We will show that the terahertz response of different burn grades is not only an indication of the overall water content in the tissue, but also it depends upon the density of these discrete scattering structures within the skin layers. Therefore, the scattering level of terahertz radiation by the skin structures post-burn can be used to non-invasively probe the DOS metric. These observations suggest that a new diagnosis criterion for clinical discrimination burn injuries can be proposed based on the THz response of the tissue.

8585-21, Session 4

Electric stimulation using subnanosecond pulses *(Invited Paper)*

Shu Xiao, Old Dominion Univ. (United States)

The exposure of biological cells to electric pulses can induce the change of membrane potential, permeabilization of membrane or even cell death. These processes generally originate from cell membrane charging provided that the pulse duration is longer than the membrane charging time constant, approximately 100 ns. Shorter pulses of a few hundred picoseconds induce negligible membrane charging and therefore new mechanism of cell-electric field interaction can be expected. We investigate the possibility of using subnanosecond pulses to stimulate neurons. Single 200 ps pulses with electric field intensity of approximate 100 kV/cm will be used. We also study the possibility of lowering the stimulation threshold by applying more pulses at high repetition rate. The delivery of subnanosecond pulses can be done through impulse radiating antennas. We will report an antenna for delivering subnanosecond pulses to the brain for deep-zone stimulation. The antenna is a prolate-spheroidal reflector antenna from which high voltage subnanosecond pulses are emitted. A dielectric lens consists of multiple layers of dielectrics is used in conjunction with the antenna. Through the use of such novel antenna and lens, the electromagnetic simulation shows the penetration depth of subnanosecond pulses is on the order of 6 cm.

8585-22, Session 4

Reversible modulation of neuronal activity in the leech ganglion by focal 60 GHz irradiation *(Invited Paper)*

Sergii Romanenko, Peter H. Siegel, California Institute of Technology (United States); Victor Pikov, Huntington Medical Research Institutes (United States)

This study provides in-depth evaluation of a novel method for modulation of neuronal activity using non-invasive focal irradiation with millimeter waves. Millimeter waves (MMW) at 60 GHz and incident power density of 100-600 μW/cm2 were applied to freshly-dissected segmental ganglia of the adult leach, and neuronal activity was recorded from individual neurons using the intracellular glass electrode. Dose-dependent changes in several parameters of neuronal activity were observed, including the resting membrane potential, amplitude and width of the action potential, ratio of the rising and falling slopes of the action potential, and the firing rate. Detailed comparison of MMW-induced effects with the equivalent thermal heating revealed that 1) similar slight resting membrane hyperpolarization was induced by MMWs and thermal heating; 2)

some of the action potential characteristics, such as the ratio of the rising and falling slopes, were differentially affected by the MMWs and thermal heating. The results provide strong evidence for the feasibility of modulating neuronal excitability using non-invasive delivery of millimeter waves, and suggest an existence of non-thermal component in the MMW interaction with the neurons.

8585-25, Session 4

The effects of terahertz radiation on cellular bioenergetics and mitochondrial respiration

Cesario Z. Cerna, Kimberly Greer, Ibtissam Echchgadda, Bennett L. Ibey, Jessica E. Grundt, Gerald J. Wilmink, Air Force Research Lab. (United States)

Cytochrome c is a small heme protein found in the mitochondria. Cytochrome c is an essential player in the electron transport chain, which is the primary site for oxidative phosphorylation and Adenosine-5'triphosphate (ATP) production. Recent spectroscopic studies show that cytochrome c exhibits a high absorption coefficient at terahertz (THz) frequencies. Given this finding, we hypothesize THz radiation may directly interact with cytochrome c, resulting in changes in cellular metabolism and ATP production. To test this hypothesis, we exposed human dermal fibroblast cells to high power THz radiation and used Seahorse technology to evaluate cellular bioactivity and mitochondria responses. Specifically, we used these physiologic cell-based assays to determine basal oxygen consumption, glycolysis, ATP turnover, and expiration capacity rates in a single experiment.

8585-37, Session 4

Effects of nanosecond electrical pulses (nsEPs) on cell cycle progression and susceptibility at various phases

Megan Mahlke, U.S. Air Force (United States); Bennett L. Ibey, Air Force Research Lab. (United States); Christopher Navara, U.S. Air Force (United States)

No Abstract Available

8585-26, Session 5

Intense picosecond THz pulses affect DNA and alter gene expression in human skin tissue in vivo

Lyubov Titova, Ayesheshim Ayesheshim, Frank A. Hegmann, Univ. of Alberta (Canada); Dawson Fogen, Andrey Golubov, Rocio Rodriguez-Juarez, Jody Filkowski, Anna Kovalchuk, Emmanuel Ojefua, Olga Kovalchuk, Univ. of Lethbridge (Canada)

Pulsed THz imaging has been suggested as a novel high?resolution, non?invasive medical diagnostic tool. In fact, the use of THz imaging for the detection of several types of tumors, such as breast and skin cancer, has been demonstrated. However, little is known about the influence of THz radiation on human tissue, i.e., its genotoxicity and effects on cell activity and cell integrity. An understanding of THz-induced cellular and molecular responses is crucial for not only for assessing potential health risks associated with exposure to this type of radiation but also for development of THz-based cancer diagnostic tools. We have carried out a comprehensive investigation of the biological effects of THz radiation on human skin tissue using a high power THz pulse source and in-vivo full-thickness human skin tissue model. Intense THz pulses with picosecond duration, 1 kHz repetition rate, and pulse energy variable up to 1 ?J are generated by optical rectification of tilted-pulse-front optical pulses in LiNbO3. We analysed the effects of THz exposure on gene expression and DNA damage. We have observed that THz irradiation led to a significant induction of H2AX phosphorylation, indicating that THz irradiation may indeed cause DNA damage in the exposed skin tissue. Moreover, THz exposure has also led to alterations in the levels of cell cycle regulatory proteins and caused changes in the global gene expression profiles of human skin tissue. The new model of biological effects of THz radiation will be presented and discussed.

8585-27, Session 5

Changes in protein expression of U937 and Jurkat cells exposed to nanosecond pulsed electric fields

Erick K. Moen, The Univ. of Southern California (United States); Caleb C. Roth, General Dynamics Information Technology (United States); Bennett L. Ibey, Larry Estalck, Caesar Z. Cerna, Gerald J. Wilmink, Air Force Research Lab. (United States)

The use of nanosecond pulsed electric fields (nsPEF) as a novel stressor for cellular studies has yielded several unique effects that may prove technologically useful. These pulses cause repairable damage to plasma membranes through the creation of nanopores and appear to activate intracellular signaling pathways in addition to agitating various organelles inside the cell. The underlying mechanism(s) controlling these effects and how they progress in time, however, is still unknown. In an effort to understand the physiological processes induced by applying nsPEFs, we explored the full genetic, proteomic, and metabolic responses of Jurkat and U937 cells at various time intervals up to 8 hours post-exposure to high intensity nsPEFs. Exposures were designed to match viability to both cell lines as well as overall dose using a custom Blumlien line pulser system. Previous studies have reported transient activation of select signaling pathways involving mitogen-activated protein kinases (MAPKs), protein phosphorylation and downstream gene expression as a result of nsPEF application. These results are verified and expanded upon via a complete protein analysis using Luminex and metabolomics analysis through a Seahorse XF Extracellular Flux Analyzer. In so doing, we intend to provide a more complete documentation of the cell's response to this type of stimuli.

8585-28, Session 5

Measurement of changes in plasma membrane phospholipid polarization following nanosecond pulsed electric field exposure

Samantha K. Franklin, Univ. of Texas at San Antonio (United States); Kelly L. Nash, The Univ. of Texas at San Antonio (United States); Hope T. Beier, Bennett L. Ibey, Air Force Research Lab. (United States)

The plasma membrane of mammalian cells is, in part, comprised of phospholipids which are arranged in a bilayer. This highly organized arrangement has been shown to be very sensitive to ambient temperature. Disruption of this arrangment by nanosecond pulsed electric fields (nsPEF) has been shown to create nanopores in the plasma membrane at room temperature that reseal over minutes. It remains unknown how such long-lived small pores in the plasma membrane are formed and resealed at biologically relevant temperatures. In this paper, we use the temperature dependent, membrane fluorescent dyes, 6 - Dodecanoyl - 2 – Dimethylaminonaphthalene (LAURDAN) and 6-Propionyl-2-Dimethylaminnoaphthalene (PRODAN), to monitor the disruption of the plasma membrane in Jurkat cells following nsPEF exposure at temperatures ranging from 20-40°C. Membrane fluorescence was measured every two minutes after exposure to capture the impact of nanopore formation and rate of resealing. Corresponding nsPEF

exposures were performed on cells in the presence of Propidium iodide (PI) and YO-PRO-1dyes to confirm pore formation and size. We identified that nsPEF exposure indeed caused a change in PRODAN expression equal to that of a 5°C temperature rise. Subsequent cellular swelling increased this observed change suggesting a multifaceted impact on the plasma membrane from nsPEF exposure. Future work will utilize a high speed optical system to capture the observed change during and after the nsPEF exposure.

8585-29, Session 5

Role of cytoskeleton and elastic moduli in cellular response to nanosecond pulsed electric fields

Gary L. Thompson, National Research Council (United States); Caleb C. Roth, General Dynamics Information Technology (United States); Gleb Tolstykh, National Research Council (United States); Marjorie Kuipers, Bennett L Ibey, Air Force Research Lab. (United States)

Nanosecond pulsed electric fields (nsPEFs) perturb the membranes of cultured cells and increase plasma membrane permeability. These effects occur in a dose-dependent manner with different types of cells exhibiting characteristic survival rates. Survivability does not depend on cell size; instead, smaller, non-adherent Jurkat cells are less robust than larger, naturally adherent HeLa cells, suggesting additional parameters are required for prediction of the effects of nsPEFs on cells. As previous work has focused on whole-cell nsPEF exposures, electrodeformation may contribute to cellular responses. Here, we consider elasticity of cells as a nsPEF-relevant parameter. Elastic moduli of freshly-deposited Jurkat, U937 and CHO cells on a poly-D-lysine (PDL) surface have been calculated using a Hertzian model fit along indentation sections of atomic force microscopy (AFM) force curve data acquired with a 5 mm-diameter borosilicate spherical probe tip positioned over the center of each cell. For an indentation of 0.5 mm, average elastic moduli are lowest for Jurkat and highest for CHO cells. This trend is consistent with experiments showing much lower survivability of Jurkat cells than U937 and CHO cells for a given nsPEF dosage regime. To distinguish any cytoskeletal foundation for these observations, agonistic and antagonistic cytoskeletal reagents were applied. Preliminary results show that 1.2 mM Latrunculin A, which inhibits actin polymerization, significantly depresses average CHO cell membrane stability upon exposure at 150 kV/cm with 300 pulses of 10 ns pulse width as determined by relative propidium iodide uptake and phosphatidylserine externalization.

8585-30, Session 5

T-ray nerve stimulation: a novel approach to trigger neural activity using terahertz radiation

Theodore E. Schomay, Robert J. Thomas, Gerald J. Wilmink, Air Force Research Lab. (United States)

Pulsed laser stimulation approaches using infrared (IR) wavelengths have been shown to be useful tools for direct stimulation of nerves. Recent reports indicate that optical stimulation is mediated via a highly general, thermally-mediated, capacitance-based, electrostatic mechanism. Since this mechanism is triggered by the rapid, local heating of bulk water molecules, we believe that other forms of electromagnetic radiation, which are strongly absorbed by both bulk and free water molecules, may be useful nerve stimulation tools. In this study, we hypothesized that since interfacial water molecules that coat the surface of plasma membranes exhibit absorption maxima at a frequency of 2.5 terahertz (THz), it may feasible that pulsed THz laser sources may be particularly well-suited for precise nerve stimulation. To test this hypothesis, we developed computational stimulation tools to model the interaction of both IR and THz radiation with neurons in vitro. In addition, we developed advanced models to simulate the temperature-dependent ion distribution near the cell membrane, and the effects that changing ion distribution have on membrane potential. We also used these models to predict the optimal IR and THz exposure parameters for stimulating action potentials in neurons. Our results show that THz radiation technologies can be used to excite neural activity. These findings suggest that THz stimulation methods may become useful neuroscience tools.

8585-31, Session 6

The penetration depth enhancement method of the THz wave in fresh tissue using a THz tissue-clearing agent

Seung Jae Oh, Sang-Hooh Kim, Yong-Min Huh, Kiyoung Jeong, Yeonji Park, Yonsei Univ. College of Medicine (Korea, Republic of); Joo-Hiuk Son, The Univ. of Seoul (Korea, Republic of); Jin-Suck Suh, Yonsei Univ. College of Medicine (Korea, Republic of)

The high sensitivity of the terahertz (THz) wave in water molecules enables diagnostic imaging of cancer and burn, but the penetration depth of this wave is limited in skin tissues. Several methods in which the interstitial water is replaced with paraffin or frozen water have been reported to depress the water effect of tissues and enhance the penetration depth. However, these methods cannot be applied in the fresh tissue of a body. We propose a THz tissue-clearing agent (THz TCA) to improve the penetration depth into fresh tissue in vivo. THz TCA is a biocompatible material with a lower absorption constant than that of water in the THz frequency range and can be easily absorbed into tissue. When THz TCA is applied to a tissue such as the skin or mucosa, some interstitial water from the tissue is replaced with THz TCA, and the THz wave permeates more deeply. Herein, we obtained THz images of a metal target below the skin using THz TCA and compared them with THz images obtained without using THz TCA. We also evaluated the permeation of THz TCA into skin tissue using THz tomography imaging. Skin tissues were extracted from the abdomen of 5–8-week-old male BALB/c-nude mice. THz images obtained using THz TCA displayed the metal target below the skin clearly; however, THz images obtained without using THz TCA rarely displayed the target below the skin. The time-dependent permeation of THz TCA was observed by THz tomography.

8585-32, Session 6

Reflective terahertz (THz) imaging: system calibration using hydration phantoms

Yoon Kyung Lee, Univ. of California, Los Angeles (United States); Neha Bajwa, Ctr. for Advanced Surgical and Interventional Technology (United States)

The aim of this research is to fabricate hydration phantoms to calibrate and characterize the hydration sensitivity of a novel, reflective Terahertz (THz) imaging system. THz radiation, sub millimeter wave energy (1 mm - 0.1 mm) with frequencies between 0.1 to 10 THz in the electromagnetic spectrum, has demonstrated potential for medical imaging applications. Given the modality's high sensitivity to water composition in tissues, it's applications in burn imaging, corneal diseases, and corneal transplantation rejections are of interest. To facilitate the translation of our technology for clinical studies, system calibration and characterization with hydration targets that mimic in vivo tissue structure and hydration are necessary. Current THz calibration phantoms consist of materials such as carbon monoxide (CO) gas, copper, silver, silicone, and other rigid polymers. To improve and quantify THz hydration sensitivity to water content, this paper presents a calibration technique using hydration phantoms made of agarose, polyhydroxyethylmethacrylate (PHEMA), and other polymer gels. These materials, in the form of hydrogels, are characterized by homogenous distributions of water, and therefore are suitable for THz calibration studies. The data acquired from the hydration

phantoms generates calibration curves over the range of 80-99.5% water concentrations at 0.5% increments and allow calibration of THz images. These preliminary hydration experiments may provide a new and improved calibration method of water sensitivity measurement for cornea and burn wound.

8585-33, Session 6

Reflectivity measurements of water and dioxane mixtures using a GHz Gunn diode source

Ashkan Maccabi, Univ. of California, Los Angeles (United States)

Terahertz (THz) sensing has shown potential as a novel imaging modality in medical applications due to its high water sensitivity. The design of medical THz sensing systems and their successful application to applications in vivo has attracted recent interest to the field, and highlighted the need for improved understanding of the interaction of THz waves with biological tissues. This paper explores the modeling of composite materials which combine strongly-interacting water with weakly-interacting species such as those that are common to biological tissues. The Bruggeman, Maxwell-Garnett, and power law effective media models are introduced and discussed. A reflection-mode 100 GHz Gunn diode sensing system was used to measure the reflectivity of solutions of water and dioxane as a function of relative concentration, and the results were compared with the predictions the Maxwell-Garnett, power law, and Bruggeman mixing theories. The Maxwell-Garnett model provided a bad goodness of fit on near-equal mixtures of water and dioxane, but well when the concentration of water exceeded~55% or was below ~15%. The first-order power law model implemented poorly except at near-pure solutions. Power law models employing 1/2 and 1/3 terms behaved well at all concentration values, but did not match the accuracy of the Bruggeman model. The Bruggeman model provided a better goodness of fit in compare to the Maxwell-Garnett and the power models and accurately predicted the solution reflectivity through the whole range of concentrations. This analysis supports the choice of the Bruggeman model in developing simulation tools for THz reflectometry of hydrated biological tissues.

8585-34, Session 6

Terahertz metamaterials perfect absorbers for sensing and imaging

David S. Wilbert, Mohammad Parvinnezhad Hokmabadi, Joshua Martinez, Patrick Kung, Seongsin M. Kim, Univ. of Alabama (United States)

Devices operating at THz frequencies have been continuously expanded in many areas of application and major research field, which requires materials with suitable electromagnetic responses at THz frequency ranges. Unlike most naturally occurring materials, novel THz metamaterials have proven to be well suited for use in various devices due to narrow and tunable operating ranges. In particular, near perfect electromagnetic absorbers which can be realized by some clever tuning of the electric and magnetic responses, where both electric and magnetic energy can be absorbed by the same metamaterial structure, enables the possibility of efficient sensing devices and THz photonic components. Metamaterial absorbers are typically designed to reduce or eliminate impedance mismatch with the surrounding atmosphere.

In this work, we present results of two THz metamaterial absorber structures aiming two important device aspects; polarization sensitivity and broad band absorption. The absorbers were simulated by finite element method and fabricated through the combination of standard lift-off photolithography and electron beam metal deposition. Both designs consist of a conducting Cu ground plane, a polyimide dielectric spacer layer with arrays of the periodic, and patterned Cu resonator structures on top. The fabricated devices were characterized by reflection mode THz time domain spectroscopy. The narrow band absorber structures exhibit up to 95% absorption with a bandwidth of 0.1 THz to 0.15 THz. The broadband absorbers show 60% absorption over a bandwidth of 0.7 THz. Possible future uses of these structures include implementation in applications such as bolometric detection devices and THz photonic filters.

8585-35, Session 6

Terahertz spectroscopy of methemoglobin: implications for novel medical imaging and therapeutics

Ogan Gurel M.D., Samsung Advanced Institute of Technology (Korea, Republic of) and Sungkyunkwan Univ. (Korea, Republic of); Jaehun Park, Pohang Accelerator Lab. (Korea, Republic of); Seong Eon Ryu, Hanyang Univ. (Korea, Republic of)

Met-hemoglobin from bovine blood was used in a lyophilized powder form (Sigma-Aldrich). Tightly packed power samples were placed within a 2mm thick crystalline quartz-lined carrier. Measurements (all at 3% humidity) were taken of both the protein and control (ambient air, no protein). Full details of the electron-linac based femtosecond terahertz beamline at PAL (60MeV electron linac beameline producing coherent femtosecond THz pulses) has been previously described. The radiation extends up to 3 THz with a pulse width of <200 fs and pulse energy up to 10?J. Time-domain THz transients were generated and detected through two sets of experiments (repeated three times): one with the hemoglobin sample, the other with ambient air as reference.

The amplitude spectrum demonstrated a clear difference between the control and sample protein (confirmed with three experimental repetitions). This confirms the hypothesis, at least for met-hemoglobin, that proteins absorb electromagnetic radiation in the terahertz band.

The results can be summarized as encompassing three specific spectroscopic patterns: (1) broad absorption at relatively high terahertz frequencies, greater than 1.5THz, (2) two relatively specific mid-range absorptions at 1.3THz and 0.8THz, and (3) Low-frequency emissions that may represent a Stokes shift phenomenon. The latter may constitute internal energy transfer within the protein by which energies absorbed at the higher frequencies become channeled into the lower-frequency modes. This interpretation fits with the known characteristics of protein motions, which include a broad spectrum of higher frequency motions, extending to the infrared domain, in addition to the functionally significant lower frequency modes.

8585-36, Session 6

High resolution field distributions in metamaterial structures using apertureless terahertz near-field imaging

William Baughman, Zachary Smithson, David S Wilbert, Patrick Kung, Seongsin M. Kim, Univ. of Alabama (United States)

Terahertz based spectroscopy and imaging has become an active field of research in the past decade for a wide number of applications including security screening, contraband identification, biomedical imaging, chemical analysis, and investigation of carrier dynamics. Several advantages exist for the use of THz techniques since investigation of a sample can be performed without contact or ionization; however, fine detail is difficult to determine due to the diffraction limit of the radiation. The resolution limit of THz imaging and sensing can be overcome by the incorporation of near-field optical techniques; which can allow image resolution as fine as tens of nanometers at THz frequencies. With this expanded resolution capability, THz imaging can decipher micro- and nano-structural information which, when coupled with the non-contact features of these techniques, makes THz spectroscopy ideal for the analysis micro and nano-optical devices.

In this study, we perform Terahertz Time-Domain Spectroscopic (THz-

TDS) imaging using an aperture-less near-field technique consisting of a tungsten scattering tip held close to the sample surface. The tungsten tip scatters the near-field, non-propagating radiation directly beneath it, and the tip offset is held constant from the sample plane by use of a piezoelectric motor. Thus by observing changes in the detected signal resultant from the scattered field, the THz response unique to the region below the tip is distinguished. Using this technique, we determine the field localization behaviors observed in THz frequency metamaterial structures and compare the observed field distributions to those determined through FEA simulations.

8585-36, Session 6

Water revisited: unifying a myriad of beliefs

Paul Ben Ishai, The Hebrew Univ. of Jerusalem (Israel); Eugene Mamontov, Oak Ridge National Lab. (United States); Alexei Sokolov, Oak Ridge National Lab. (United States) and Univ. of Tennessee (United States); Jon Nickels, Univ. of Tennessee (United States); Kodo Kawase, Nagoya Univ. (Japan); Yuri Feldman, The Hebrew Univ. of Jerusalem (Israel)

Diverse communities have diverse views on what constitute the true behavior of water. When considering the THz behavior of water it is common to consider the behavior as a superposition of fundamental Debye relaxations. Yet the view held by many in the Soft Condensed Matter community is that water is a glass former and that a simple Debye laws will not adequately describe its dynamic behavior. This is partly because the role of the cluster structure, reorientation and its relationship to the H-bond network has not been fully explored up to the higher frequencies. We attempt to marry THz spectroscopy and traditional dielectric spectroscopy to provide a complete picture of the dynamics of water and also of aqueous salt solutions, in the frequency range covering all reorientation and transport phenomena. Additional microscopic information is gained from neutron scattering. Consequently we hope to span two sometimes opposing world views and lead to a unified discussion on what water really does in the higher frequency spectrum of THz. The talk will present dielectric measurements carried out in the Hebrew University of Jerusalem and THz results measured in the University of Nagoya. The microscopic picture will be further probed by considering Neutron Scattering on aqueous salt solutions, carried out in Oak Ridge National Laboratory.

8586-1, Session 1

Optogenetics: development and application *(Keynote Presentation)*

Karl Deisseroth, Stanford Univ. (United States)

No Abstract Available

8586-2, Session 1

High-speed optogenetic circuit mapping *(Invited Paper)*

George Augustine, Duke Univ. School of Medicine (Singapore)

Scanning small spots of laser light allows mapping of synaptic circuits in brain slices from transgenic mice expressing channelrhodopsin-2 (ChR2). These light spots photostimulate presynaptic neurons expressing ChR2, while postsynaptic responses can be monitored in neurons that do not express ChR2. Correlating the location of the light spot with the amplitude of the postsynaptic response elicited at that location yields maps of the spatial organization of the synaptic circuits. This approach yields maps within minutes, which is 10,000 times faster than can be achieved with conventional paired electrophysiological methods. We have applied this high-speed technique to map local circuits in many brain regions. In cerebral cortex, we observed that maps of excitatory inputs to pyramidal cells were qualitatively different from those measured for interneurons within the same layers of the cortex (PNAS 104: 8143). In cerebellum, we could use this approach to quantify the convergence of molecular layer interneurons on to Purkinje cells and found that at least 7 interneurons form functional synapses with a single Purkinje cell. The number of converging interneurons is reduced by treatment with gap junction blockers, indicating that electrical synapses between interneurons contribute substantially to the spatial convergence. Remarkably, gap junction blockers affect convergence in sagittal cerebellar slices but not in coronal slices, indicating sagittal polarization of electrical coupling between interneurons. By measuring limb movement, this approach also can be used in vivo to define motor maps non-invasively (J. Neurosci. Meth. 179: 258). In summary, ChR2-mediated high-speed mapping promises to revolutionize our understanding of brain circuitry.

8586-3, Session 1

Near-infrared in vivo optogenetic stimulation

Kamal Dhakal, The Univ. of Texas at Arlington (United States); Ling Gu, The Univ. of Texas at Arlington (United States) and Univ. of Texas (United States); Torry Dennis, The Univ. of Texas at Arlington (United States); Ting Li, Univ. of Electronic Science and Technology of China (China); Linda Perrotti, Samarendra K. Mohanty, The Univ. of Texas at Arlington (United States)

Optical stimulation (or inhibition) of genetically-targeted cells (optogenetics) is proving to be a powerful tool in controlling cellular functions. While visible (blue-yellow) low-power light sources are sufficient for causing optogenetic modulation, strong absorption and scattering of visible light by tissue may limit non-invasive in-depth application of this technology especially for in-vivo situations. Further, single-photon visible light based stimulation does not provide localized stimulation. To overcome these limitations, near-infrared ultrafast laser beam has been demonstrated in-vitro to provide highly localized optogenetic stimulation. Here, we report near-infrared in-vivo optogenetic stimulation of neurons in mouse models with a focus on in-depth stimulation capability. These results are supported by Monte Carlo simulation of light propagation in visible and near-infrared spectrum. In contrast to single photon approach, the near-infrared in-vivo optogenetic stimulation, as demonstrated by us, will lead better probing of the in-vivo neural circuitry.

8586-4, Session 1

GaN-based micro-LED arrays on flexible substrates for optical cochlear implants

Christian Goßler, Colin Bierbrauer, Rüdiger Moser, Katarzyna Holc, Wilfried Pletschen, Klaus Köhler, Joachim H. Wagner, Fraunhofer-Institut für Angewandte Festkörperphysik (Germany); Michael Schwärzle, Patrick Ruther, Oliver Paul, Albert-Ludwigs-Univ. Freiburg (Germany); Victor Hernandez, Gerhard Hoch, Georg-August-Univ. Göttingen (Germany); Tobias Moser, Univ. Göttingen (Germany); Ulrich T. Schwarz, Fraunhofer-Institut für Angewandte Festkörperphysik (Germany) and Univ. of Freiburg (Germany)

Currently available cochlear implants are based on electrical stimulation of the spiral ganglion neurons. Optical stimulation with arrays of micro-sized light-emitting diodes (LEDs) promises to increase the number of distinguishable frequencies. The development of a flexible GaN-based micro-LED array as an optical cochlear implant is reported. The device is designed for optogenetic stimulation in the mouse model.

The (AlGaIn)N LED structure is grown on a sapphire substrate. In our thin film approach, the semiconductor layer stack with a typical thickness of 5 µm is transferred to a flexible polyimide-on-silicon substrate by wafer bonding and subsequent laser lift-off. The fabrication of 20 µm thin and highly flexible devices is enabled by the combination of sapphire laser lift-off and the flexible substrate technology. The realized probes exhibit a width of 200 µm to fit into the mouse cochlea. The single 50?50 µm? LEDs are individually addressable via patterned structured conducting paths on both p- and n-side of the LEDs. During processing, the LEDs are mechanically and electrically separated while still on sapphire using laser processing as well as standard lithography techniques. This is necessary to avoid subsequent fracture of the GaN layer while bending the probe. We employ a low temperature gold-indium based solid-liquid interdiffusion bonding process to ensure process compatibility with the flexible polyimide substrate.

Individual LEDs driven at 2 mA and 40 mA emit 0.1 mW and 2.0 mW, respectively, at a wavelength of 440 nm. Functional GaN micro-LED probes were successfully furled with a radius of curvature of 500 µm and are therefore suited for implantation in the mouse cochlea.

8586-5, Session 1

Label free optical detection of optogenetic activation of cells

Niloy Choudhury, Michigan Technological Univ. (United States) and GE India Technology Ctr. (India); Zhaoqiang Zhang, Feng Zhao, Michigan Technological Univ. (United States); Ling Gu, Samarendra K. Mohanty, The Univ. of Texas at Arlington (United States)

In optogenetic stimulation, chemically-identical neurons can be activated by (blue) light with high temporal and spatial resolution by the introduction of light activated molecular channels (e.g., channelrhodopsin-2, ChR2), by genetic targeting. However, for detection of neural activity the usual methods used are either mechanically intrusive (e.g., use of micro-electrodes) or chemically invasive (e.g., calcium imaging). In order to achieve complete non-invasiveness in optogenetic stimulation, there is a need to record cellular activation in addition to cell

specific gene-delivery and light activation. A toolbox that has can achieve cell-specific stimulation and simultaneous detection of neural activity will be of great importance for simultaneous input-output interrogation of excitable cells. This will allow us to non-invasively investigate how cell controls and converts information in diseased state and normal state, and so on.

We have developed a phase-sensitive Fourier domain optical coherence tomography (PSFD-OCT) system to detect cellular activity. PSFD-OCT is used to measure nano-motion by analyzing the phase changes in the measured spectral interferograms. A monolayer of transfected HEK293 cells were put in a cell culture dish and activated by a blue laser diode operating at 473 nm. Using a PSFD-OCT signal we were able to detect the nanoscale optical path length change due to optogenetic activation of ChR2-transfected HEK 293 cells. Use of PSFD-OCT system enables intrinsic detection of neural activity without addition of calcium dyes or insertion of microelectrodes. In conclusion, this label-free non-invasive optical method for detection of neuronal activity in combination with light-assisted activation brings us a valuable approach to study and better understand the nervous system.

8586-6, Session 1

Distributed light delivery and detection for fluorescence recording and optical stimulation

Ramin Pashaie, Ehsan Majidi, Univ. of Wisconsin-Milwaukee (United States)

Design and analysis of a passive fiber optic component is discussed which is capable of delivering light at different depths within the brain tissue. For this purpose, finite length tilted fiber gratings are designs to be embedded within the core of a single mode fiber and function as electromagnetic cavities that resonate at specific wavelengths and radiate the selected optical power in the medium surrounding the fiber. By changing the design of the tilted gratings, different wavelengths can be delivered or detected at different depths inside the tissue using only one optical fiber and without physical movement of any component. This device can be used for delivery of the excitation and stimulation light for fluorescence detection and/or optical modulation of neural activities including optogenetic applications or detection of fluorescence emission signals. Simplicity of this design makes the device highly appropriate for implementation of optoelectronic neuroprosthetic systems. In such systems, a large array of this fibers should be integrated to implement a mechanism for three dimensional distribution of light within the brain tissue. Design and performance of this device is presented in the article.

8586-7, Session 1

Multifractal detrended fluctuation analysis of optogenetic modulation of neural activity

Satish Kumar, Indian Institute of Science Education and Research Kolkata (India); Ling Gu, The Univ. of Texas at Arlington (United States); Nirmalya Ghosh, Indian Institute of Science Education and Research Kolkata (India); Samarendra K. Mohanty, The Univ. of Texas at Arlington (United States)

Here, we introduce a computational procedure to examine whether optogenetically activated neuronal firing recordings could be characterized as multifractal series. Optogenetics is emerging as a valuable experimental tool and a promising approach for studying a variety of neurological disorders in animal models. The spiking patterns from cortical region of the brain of optogenetically-stimulated transgenic mice were analyzed using a sophisticated fluctuation analysis method known as multifractal detrended fluctuation analysis (MFDFA). We observed that the optogenetically-stimulated neural firings are consistent with a multifractal process. Further, we used MFDFA to monitor the effect of chemically induced pain (formalin injection) and optogenetic treatment used to relieve the pain. In this case, dramatic changes in parameters characterizing a multifractal series were observed. Both the generalized Hurst exponent and width of singularity spectrum effectively differentiates the neural activities during control and pain induction phases. The quantitative nature of the analysis equips us with better measures to quantify pain. Further, it provided a measure for effectiveness of the optogenetic stimulation in inhibiting pain. MFDFA-analysis of spiking data from other deep regions of the brain also turned out to be multifractal in nature, with subtle differences in the parameters during pain-induction by formalin injection and inhibition by optogenetic stimulation. Characterization of neuronal firing patterns using MFDFA will lead to better understanding of neuronal response to optogenetic activation and overall circuitry involved in the process.

8586-8, Session 2

in vivo optical stimulation of and electrical read-out from neural circuits in non-human primates and rodents by chronically implanted devices *(Invited Paper)*

Arto V. Nurmikko, Jing Wang, Travis May, Ilker Ozden, Carlos Vargas, Brown Univ. (United States)

For applications of optogenetics for studying brain function in non-human primates, we have conceived a suite of integrated dual-function optoelectronic devices for combined optical stimulation and electrophysiology. These devices have been deployed to induce both behavioral and neural circuit modulation (action potential and field potentials) in Rhesus Macaques performing assigned tasks, and freely moving rats.

Key device requirements for optical “write-in” and electrical “read-out” devices are (i) their precise targeting to reach optogenetically transduced cortical or deeper brain areas, (ii) biophysical modeling and design for understanding the size of both optical and electrical volumes relative to transduction, (iv) estimating safety limits for light delivery, and (v) robustness and biocompatibility for eventual long term chronic implants.

In this presentation we describe the design, fabrication and implementation of two such integrated devices developed in our laboratories for primate and rodent optogenetics studies: a single-element device, the “coaxial optode”, and a multi-element device, the polymer optical fiber-microelectrode array (“POF-MEA”). The former has been deployed usefully in primate work at both Brown and collaborators at Stanford to show optically induced modulation of primate behavior, while the latter has been useful in freely moving rats in population dynamical studies of optically perturbed cortical circuits – while making a transition to primates.

Close collaboration with the groups of Karl Deisseroth (Stanford), Krishna Shenoy (Stanford), John Donoghue (Brown) and David Sheinberg (Brown) is gratefully acknowledged. Research supported by DARPA under Repair program, and the National Science Foundation.

8586-9, Session 2

A precise and minimally invasive approach to optogenetics in the awake primate

Jonathan J. Nassi, Ali H. Cetin, The Salk Institute for Biological Studies (United States); Anna W. Roe, Vanderbilt Univ. (United States); Edward M. Callaway, The Salk Institute for Biological Studies (United States); Karl Deisseroth, Stanford Univ. (United States); John H. Reynolds, The Salk Institute for Biological Studies (United States)

Optogenetics has proven to be a powerful tool for understanding the function of specific cell types and circuits within the central nervous system and establishing a causal link between their activity and behavior. Its application in non-human primates has been slow to develop. One

challenge has been the damage caused by transdural delivery of viruses and light to the brain. Here, we report optogenetic activation of neuronal responses in the alert and behaving monkey after replacement of the native dura with a transparent artificial dura. This approach enables the use of fine glass micropipettes to inject virus with minimal damage and transdural illumination, obviating the damage that would otherwise occur as a result of lowering optical fibers into the brain. It also permits visualization of the underlying cortical micro-vasculature, which has proven to be helpful in targeting electrodes and laser illumination to the virus location. We have injected several viruses into distinct locations within macaque primary visual cortex (V1), including AAV5 and VSVg-pseudotyped lentivirus, which were engineered to preferentially express the opsin C1V1 in local excitatory neurons. Several weeks after virus injections, light delivered to V1 of an alert, fixating monkey through an optical fiber positioned above the artificial dura modulated the firing rate of recorded neurons. We describe the magnitude and efficacy of this firing rate modulation as a function of the irradiance, frequency and duty cycle of light stimulation. This approach promises to greatly assist in the dissection of cortical circuits underlying visual perception and behavior.

8586-10, Session 2

A combinatorial optogenetic approach to medial habenula function

Yun-Wei Hsu, Seattle Children's Research Institute (United States); Si Wang, Seattle Children's Research Institute (United States); Glenn Morton, Seattle Childrens Research Institute (United States); Aguan Wei, Seattle Children's Research Institute (United States); Hatim Zariwala, Univ. of Washington (United States); Hongkui Zeng, Allen Institute for Brain Science (United States); Eric E. Turner, Seattle Childrens Research Institute (United States)

The habenula is a dorsal thalamic nucleus consisting of medial and lateral subnuclei, both of which connect to the ventral midbrain via a prominent projection, the fasciculus retroflexus. The lateral habenula (LHb) makes direct projections to inhibitory neurons in the ventral tegmental area (VTA). Recent studies have begun to define a circuit through the LHb that signals negative reward by inhibiting dopamine (DA) release, mediating a "disappointment" signal. In contrast, the medial habenula (MHb) projects almost exclusively to the interpeduncular nucleus (IP), which in turn projects to brainstem raphe and dorsal tegmental nuclei. The MHb can be further divided into two principal subnuclei, the peptidergic dorsal MHb (dMHb) and the cholinergic ventral MHb (vMHb), which have specific projections to the lateral and medial IP, respectively. Although this anatomy has been described for 30 years, little is known about the function of these MHb-IP-brainstem pathways.

Here we describe a combinatorial optogenetic approach to the function of the MHb. By interbreeding Cre-driver lines targeting specific populations of MHb neurons and Cre-inducible optogenetic effector lines, we have specifically targeted Chr2 expression to the dMHb, the vMHb and the projections of these nuclei. Targeted expression of Chr2 supports robust activation of MHb neurons in brain slice preparations. The small size, subnuclear structure, and medial location of the habenula present special challenges for in vivo optogenetics, and custom fiber optic cannulas have been designed for this purpose. Using these methods we show that the dMHb mediates a reward signal in a self-stimulation paradigm.

8586-11, Session 2

Evaluating cerebellar functions using optogenetic transgenic mice

John P. Welsh, Seattle Children's Research Institute (United States) and Univ. of Washington (United States); Josef Turecek, Seattle Children's Research Institute (United States) and Univ. of Washington (United States)

Synaptic mechanisms of cerebellar function have remained elusive despite the fact that the cerebellum is among the best described systems in the vertebrate brain. A major afferent of the cerebellum is the inferior olive (IO), which exerts a high degree of control over cerebellar output by its monosynaptic relation with Purkinje cells. All models of the cerebellum recognize a fundamental role for the IO in cerebellar function, either as a guide for synaptic scaling involved in learning, or as a time-keeping device for on-line motor/cognitive control. IO neurons are pacemakers determined by ionic conductances that drive sinusoidal subthreshold membrane potential oscillations (STOs). To better understand the role of STOs in cerebellar functions, we generated transgenic mice that expressed channelrhodopsin-2 in inferior olive neurons (ptf1a-ChR2 mice; progeny of ptf1a-cre and Ai27/32 mice obtained from the Allen Brain Institute). Whole-cell patch clamp recordings in acute brainstem slices demonstrated 159 ± 10 pA inward current and 9.3 ± 0.7 mV membrane potential depolarizations driven by a 40-µm diameter 473 nm light column (<0.06 mW/µm2) or by single neuron activation produced by 2-photon excitation (<0.5 mW/µm2). Selective activation of the IO using a light-guide/extracellular recording electrode in vivo demonstrated that rhythmic pulses can drive coherent spike and LFP oscillations, synchronized postsynaptic responses in Purkinje cells, and coherent muscle activations similar to the clinical condition of essential tremor. We will discuss advantages of optogenetic experiments of cerebellar function using transgenic mice and new insights so obtained for resolving mechanisms of cerebellar function.

8586-12, Session 2

Two-photon optogenetics of dendritic spines and neuronal circuits in three dimensions *(Invited Paper)*

Rafael Yuste M.D., Columbia Univ. (United States)

Optogenetic techniques can be used to effectively manipulate the activity of genetically defined populations of neurons but they mostly rely on one-photon activation, which has poor spatial resolution in living brain tissue. Consequently, optogenetics has not yet capitalized on the advantages of non-linear excitation, such as two-photon microscopy, for precise optical access in scattering tissue. In particular, selective optogenetic activation of individual neurons within a circuit, or subcellular compartments within a cell, remains a challenge. While two-photon excitation of channelrhodopsin can be achieved, it requires complex illumination strategies to ensure neuronal firing and has therefore limited practical utility.

To develop a viable two-photon optogenetic method, we explore the use of C1V1, a novel red-shifted opsin that generates significant currents after two-photon excitation, enough to generate action potentials in neurons with single cell precision. We report the application of C1V1 for optical mapping of synaptic circuits and to specifically activate small dendritic regions, including single dendritic spines. Finally, using a spatial light modulator (SLM), we multiplex the laser beam onto multiple neurons to perform, for the first time, simultaneous optogenetic activation of selected neurons in three dimensions. Two-photon activation of C1V1, combined with SLM microscopy, opens the way for optical manipulations of neuronal circuits in three dimensions, from the level of networks down to individual spines.

8586-13, Session 2

Optogenetic stimulation of the auditory nerve for cochlear implants with increased number of frequency channels and dynamic range

Ulrich T. Schwarz, Fraunhofer-Institut für Angewandte Festkörperphysik (Germany) and Univ. of Freiburg (Germany); Christian Goßler, Fraunhofer-Institut für Angewandte

Festkörperphysik (Germany); Michael Schwärzle, Patrick Ruther, Oliver Paul, Albert-Ludwigs-Univ. Freiburg (Germany); Victor Hernandez, Gerhard Hoch, Kirsten Reuter, Georg-August-Univ. Göttingen (Germany) and Bernstein Focus for Neurotechnology, Univ. Göttingen (Germany); Nicola Strenzke, Georg-August-Univ. Göttingen (Germany); Tobias Moser, Univ. Göttingen (Germany) and Bernstein Focus for Neurotechnology, Univ. Göttingen (Germany)

Cochlear implants (CIs) based on direct electrical stimulation of spiral ganglion neurons (SGNs) are highly successful neuro-prostheses, even though they allow only to address a limited number of frequency channels (up to 22 in commercial products) and narrow dynamic range (max. 20 dB). The limitation in the number of frequency channels can be lifted by optical stimulation, as light can be better focused to stimulate a narrow range of nerve cells when compared to the widespread current flow from a stimulating electrode. With the help of optogenetics it is possible to transfect nerve cells expressing channelrhodopsin-2 (ChR2) which can be stimulated with low levels of blue light.

In a proof-of-principle experiment we demonstrate the optogenetic restoration of hearing, working with mouse models of acute and chronic human deafness. SGNs expressing the light-gated ion channel ChR2 were activated by optical stimulation, and optogenetic auditory brainstem responses (oABR) were recorded with a minimum latency of 80 Hz and a dynamic range of more than 20 dB.

The geometry of the cochlea, limits to local heating (thermal losses) and energy consumption (electrical losses) have to be considered in the use of LEDs in cochlear implants. Arrays of micro-LEDs (light emitting diodes) emitting in the blue spectral range have the potential to overcome these limitations. Activation of the auditory pathway was confirmed by inferior colliculus recordings. Telemetric activation of oABR was achieved using a micro-LED-based implanted optical stimulator.

8586-14, Session 2

Laser speckle contrast reveals cerebral blood flow dynamics evoked by optogenetically controlled neuronal activity

Nan Li, F.M. Kirby Research Ctr. for Functional Brain Imaging, Kennedy Krieger Institute (United States) and Johns Hopkins Univ. (United States); Nitish V. Thakor, Johns Hopkins Univ. (United States); Galit Pelled, F.M. Kirby Research Ctr. for Functional Brain Imaging, Kennedy Krieger Institute (United States) and Johns Hopkins Univ. (United States)

As a critical basis of functional brain imaging, neurovascular coupling describes the link between neuronal and hemodynamic changes. The majority of in vivo neurovascular coupling studies are performed by inducing sensory stimulation via afferent inputs. Unfortunately such an approach results in recruiting of multiple types of cells, which confounds the explanation of neuronal roles in stimulus evoked hemodynamic changes.

Recently optogenetics has emerged to provide immediate control of neurons by exciting or inhibiting genetically engineered neurons expressing light sensitive proteins. However, there is a need for optical methods capable of imaging the concurrent hemodynamic changes.

We utilize laser speckle contrast imaging (LSCI) to obtain high resolution display of cerebral blood flow (CBF) in the vicinity of the targeted neural population. LSCI is a minimally invasive method for imaging CBF in microvessels through thinned skull, and produces images with high spatiotemporal resolution, wide field of view. In the integrated system light sources with different wavelengths and band-passing/blocking filters are used to allow simultaneous optical manipulation of neuronal activities and optical imaging of corresponding CBF. Experimental studies are carried out in a rodent model expressing ChR2 or eNpHR in excitatory neurons in the somatosensory cortex (S1).

The results demonstrated significant increases of CBF in response to ChR2 stimulation (exciting neuronal firing), and decreases of CBF with eNpHR stimulation (inhibiting neuronal firing) in response to contralateral forepaw stimulation.

The approach promises to be an exciting minimally invasive method to study neurovascular coupling. This complete system provides a novel approach for broad neuroscience applications.

8586-15, Session 2

Comparison between Bessel and Gaussian beam propagation for in-depth optogenetic stimulation

Ting Li, Univ. of Electronic Science and Technology of China (China); Samarendra K. Mohanty, The Univ. of Texas at Arlington (United States)

Optogenetics technology has opened new landscapes for neuroscience research by allowing targeted (cell type-specific), fast (millisecond-scale) control of precise defined events in biological systems as complex as freely moving mammals. Due to its non-diffracting and self-healing nature, Bessel beam has potential to improve in-depth optogenetic stimulation and therefore recently been attempted. A detailed understanding of Bessel beam propagation, as well as its superiority over commonly-used Gaussian beam, is essential for delivery and control of light irradiation for optogenetics. We developed an algorithm for modeling Bessel beam propagation in layered tissue and coded it into the widely-used Monte Carlo code for multilayered tissue (MCML). By carrying out a full amount of simulations, we compared Bessel and Gaussian beam propagation in two-layered mice brain under variance of multiple variables (i.e., wavelength, numerical aperture, and beam size). Bessel beam was found out to be significantly advantageous over Gaussian beam for in-depth optogenetics stimulation. Our research quantified the potential of Bessel beam in improving optogenetic stimulation and thus will lead to development of less-invasive probes for therapeutic applications.

8586-16, Session 3

Light-gated ion channels and pumps as optogenetic tools in neuro- and cell biology *(Keynote Presentation)*

Ernst Bamberg, Max-Planck-Institut für Biophysik (Germany)

Microbial Rhodopsins are widely used in these days as optogenetic tools in neuro and cell biology. We were able to show that rhodopsins from the unicellar alga Chlamydomonas reinhardtii with the 7 transmembrane helix motif act as light-gated ion channels, which we named channelrhodopsins(ChR1,2). Together with the light driven Cl-pump Halorhodopsin ChR2 is used for the non-invasive manipulation of excitable cells and living animals by light with high temporal resolution and more important with extremely high spatial resolution The functional and structural description of this new class of ion channels is given (electrophysiology, noise analysis ,flash photolysis and 2D crystallography). New tools with increased spatial resolution and extremely enhanced light sensitivity in neurons are presented. Based on our recent results a perspective for new optogenetic constructs with increased light sensitivity and modified ionic selectivity is given.

Literature:

Nagel et al. (2002) Science 296 2395-2398

Nagel et al. (2003) PNAS 100 13940-13945

Nagel et al. (2005) Current Biology 15 2279-2284

Zhang et al (2007) Nature 446 633-639

Bamann et. al. (2007) J. Mol. Biol. 375 686-694

Feldbauer, K. et.al. (2009). Proc Natl Acad Sci USA 106 12317-12322

Bamann, C. et. al. (2010). Biochemistry 49, 267-278 14

Kleinlogel, S. et.al.(2011). Nature Neuroscience 14 513-51
Kleinlogel S. et al. (2011) Nature Methods 8 1083-1087

8586-17, Session 3

Expression and function of channelrhodopsin 2 in mouse outer hair cells

Fangyi Chen, Tao Wu, Teresa Wilson, Oregon Health & Science Univ. (United States); Hrebesh M. Subhash, National Univ. of Ireland, Galway (Ireland); Irina Omelchenko, Michael Bateschell, Lingyan Wang, John Brigande, Zhigen Jiang, Alfred L. Nuttall, Oregon Health & Science Univ. (United States)

Outer hair cell (OHC) is widely accepted as the origin of cochlear amplification, a mechanism that accounts for the extreme sensitivity of the mammalian hearing. The key process of the cochlear amplification is the reverse transduction, where OHC changes its length under electrical stimulation. In this study, this electro-mechanical transduction is modulated with an optogenetic approach based on channelrhodopsin 2 (ChR2), a direct light-activated non-selective cation channel (NSCC). We specifically transferred ChR2 gene to the mouse cochlea OHCs through in uterus injection of adenovirus vector with ChR2 in fusion with fluorescent marker tdTomato. We also transfected ChR2(H134R), a point mutant of ChR2, with plasmid to an auditory cell line (HEI-OC1). With whole cell recording, we found that blue light (470 nm) elicited the typical NSCC current of ChR2 with reversal potential around zero in both mouse OHCs and HEI-OC1 cells and generated significant depolarization in both cell types. We also performed in vivo experiments on the cochlea of tranfected ChR2 mouse. In this experiment, tones were applied to the mouse ear to elicit the cochlear receptor and neuronal evoked potentials , which were recorded with a silver electrode placed at the edge of the round window. Blue light was focused on the hook region of the cochlea through round window. The effect of the blue light was analyzed by observing the amplitude of the cochlear potential changes under the light stimulation.

8586-18, Session 3

Temporally precise control of intracellular calcium activity in non-excitable cells by optogenetic techniques

Chao Wang, Yue Zhuo, Jihye Seong, Yingxiao Wang, Stephen A. Boppart, Univ. of Illinois at Urbana-Champaign (United States)

The high complexity of multiple calcium (Ca2+) entry mechanisms in non-excitable cells requires optical control of Ca2+ activity with greatest flexibility. This in vitro study demonstrates temporally-precise control of intracellular calcium elevation [Ca2+]i in HEK293T cells expressing channelrhodopins-2 (ChR2) in comparison to the same cell line lacking this photoreceptor. By Ca2+ imaging of individual cells sufficiently expressing ChR2, observed plateau-like [Ca2+]I indicates a quasi-instantaneous response to single pulse stimulation of 300 milliseconds in duration (at 475 nm from Xenon-lamp; average power at 159 ?W and 1.24 mW). With insufficient ChR2 expression or shortened stimulation, some plateau-like [Ca2+]I profiles (maybe preceded by a time-lag) converge to baseline while others exhibit significantly prolonged responses. These observations highlight the importance of an optimal dosage in optogenetics (optimal stimulation power/duration and sufficient ChR2 expression). These plateau-like [Ca2+]I levels featured by their oscillatory profiles may reflect differential cross-talk between membrane and capacitative Ca2+ entry mechanisms. These responses, mostly induced by rapid and massive Ca2+ influx via voltage-gated Ca2+ channels, are subject to co/cascaded activation of light-gated ChR2 and voltage-gated Na+ channels. Graded-potential variations localized to the soma facilitate light-induced Ca2+ activity which could also be saturated. At low stimulation doses, quasi [Ca2+]I oscillations are observable, likely modulated by intracellular Ca2+ store discharge/charge triggered by impulsive Ca2+ leakage through low-voltage-sensitive Ca2+ channels in the endoplasmic reticulum. Our custom-designed broadband stimulation scheme with state-of-the-art optical techniques shows its promise for optical control of Ca2+ activity in non-excitable cells with high precision and effectiveness.

8586-19, Session 3

Optical control in microbial rhodopsins, especially channelrhodpsin *(Invited Paper)*

Klaus B. Gerwert, Ruhr-Univ. Bochum (Germany)

Channelrhodopsin is becoming the crucial tool in optogenetics. It belongs to microbial rhodopsins as bacteriorhodopsin. In order to elucidate the molecular reaction mechanism time-resolved FTIR spectroscopy in combination with biomolecular simulations (MD and QM/MM) is applied as before in bacteriorhodopsin. (1,2). A protonated water complex, working as “proton diode” at the release site determines the direction of the proton flow (1,2). This approach is recently extended to channelrhodopsin (4). Deprotonation of E-90 is identified as crucial gate for water invasion, and proposed to be the key residue in the channel gating and selectivity mechanism. Unpublished FTIR experiments and MD simulations on channelrhodopsin will be discussed.

References

(1) Garczarek, F., Gerwert, K. Functional Waters in Protein Proton Transfer Nature, 439, 109-112 (2006)

(2) Wolf, S., Freier, E., Potschies, M., Hofmann, E. and Gerwert, K. Directional Proton Transfer in Membrane Proteins Achieved through protonated Protein-Bound Water Molecules: A Proton-Diode Angew. Chem. Int. Ed., 49, 6889-6893 (2010)

(3) Freier, E., Wolf, S., Gerwert, K. Proton transfer via a transient linear water-molecule chain in a membrane protein PNAS 108 (28), 11435-11439 (2011)

(4) Eisenhauer K., Kuhne J., Ritter E., Berndt, A., Wolf S., Freier E., Bartl F., Hegemann P., Gerwert K. In channelrhodopsin-2 E90 is crucial for ion selectivity and is deprotonated during the photo-cycle Journal of Biological Chemistry, 287 (9), 6904-6911 (2012)

8586-20, Session 3

Optogenetic control of ATP release

Matthew Lewis, The Univ. of Texas Southwestern Medical Ctr. at Dallas (United States); Bipin Joshi, Ling Gu, The Univ. of Texas at Arlington (United States); Andrew Feranchak, The Univ. of Texas Southwestern Medical Ctr. at Dallas (United States); Samarendra K. Mohanty, The Univ. of Texas at Arlington (United States)

Controlled release of ATP can be used for understanding of the extracellular purinergic signaling. While coarse mechanical forces and hypotonic-stimulation have been utilized in the past to initiate ATP release from cells, these methods are neither spatially-accurate nor temporarily precise. Further, these methods cannot be utilized in a highly effective cell-specific manner. To mitigate the uncertainties regarding cellular-specificity and spatio-temporal release of ATP, we herein demonstrate use of optogenetics for ATP release. ATP release in response to optogenetic stimulation was monitored by Luciferin-Luciferase assay using luminometer as well as mesoscopic imaging. Our result demonstrates repetitive release of ATP subsequent to optogenetic stimulation. It is thus feasible that purinergic signaling can be directly detected via imaging if the stimulus can be confined to single cell or in a spatially-defined group of cells. This study opens up new avenue to understand the mechanism of purinergic signaling.

8586-21, Session 3

The spatial pattern of light determines the kinetics and guide backpropagation of optogenetic action potentials

Nir Grossman, Imperial College London (United Kingdom)

Optogenetics offers an unprecedented ability for spatially targeted stimulation of neural cells. This study investigated for the first time, via simulation, how the spatial pattern of excitation affects the response of channelrhodopsin-2 (ChR2) expressing neurons. We compared four most commonly considered illumination strategies (somatic, dendritic, axonal and whole cell) in a paradigmatic model of a cortical layer V pyramidal cell. We show that the spatial pattern of illumination has an important impact on the efficiency of stimulation and the kinetics of the spiking output. Whole cell illumination synchronizes the depolarization of the dendritic tree and the soma and evokes spiking characteristics with a distinct pattern including an increased bursting rate and enhanced back propagation of APs. This type of illumination is the most efficient as a given threshold irradiance was achievable with only 6% of ChR2 density needed in the case of somatic illumination. Targeting only the AIS requires a high ChR2 density to achieve a given threshold irradiance and a prolonged illumination does not yield sustained spiking. We also show that patterned illumination can be used to modulate the back propagating APs and hence spatially modulate the direction and amplitude of spike time dependent plasticity protocols. We further found the irradiance threshold to increase in proportion to the de-myelination level of an axon, suggesting that measurements of the irradiance threshold (for example relative to the soma) could be used to remotely probe a loss of neural myelin sheath, which is a hallmark of several neurodegenerative diseases.

8586-22, Session 3

Adrenergic modulation of gamma cortical oscillations

Jevin J. Jackson, The Univ. of Texas at Dallas (United States); Hector D. Tejeda, Kamal Dhakal, Samarendra K. Mohanty, The Univ. of Texas at Arlington (United States); Marco Atzori, The Univ. of Texas at Dallas (United States)

Gamma oscillations are sub-threshold changes in neuronal resting potential in the 30-70 Hz frequency bandwidth, associated with synaptic summation leading to perception, and transfer of highly processed information between distant brain areas. Both excitatory and inhibitory synaptic transmissions are necessary for physiological gamma oscillations. The global neuromodulator norepinephrine (NE) has been proposed to enhance attention and other cognitive functions by acting on both excitatory and inhibitory synapse. NE might enhance the amplitude of gamma oscillations by a combined action on glutamatergic, excitatory synapses, and GABAergic, inhibitory synapses. Gamma oscillations were previously induced either by brief trains of electrical stimulation or by exogenous applications of the neurotoxin kainic acid, both of which are highly un-physiological. Here, we will present induction of gamma oscillations in brain slices of prefrontal cortex by light-stimulation of ensembles of either pyramidal neurons or GABAergic interneurons. Comparison of the adrenergic modulation of optogenetically-induced gamma oscillations to that obtained by electric stimulation or by stimulation with kainic acid, will be presented.

8586-28, Session 4

Optogenetics without the genetics: photochemical tools for biomedical manipulation of endogenous ion channels and neuronal firing *(Invited Paper)*

Richard Kramer, Univ. of California, Berkeley (United States)

We have been developing synthetic photosimerizable molecules that enable optical manipulation of neuronal activity without requiring exogeneous gene delivery. These “photoseitch” molecules have theraapeutic potential for non-invasive manipulation or restoration of neural signaling in neuropathic or neurodegenerative disorders. Retinitis pigmentosa (RP) and age-related macular degeneration (AMD) are degenerative blinding diseases caused by the death of rods and cones in the retina, leaving the remainder of the visual system intact but unable to sense light. AAQ, a synthetic small molecule photoswitch, can restore light sensitivity to the retina and mediate behavioral responses in vivo in mouse models of RP. Hence AAQ and related photoswitch molecules present a new drug strategy for restoring retinal function in degenerative blinding diseases. A second photoswitch molecule, named QAQ, is targeted specifically to nociceptive neurons, nerve cells specialized to respond to noxious stimuli. These neurons are responsible for pain sensation, thus QAQ can be used to alleviate pain signaling in a light dependent manner. By enabling rapid and precise photoregulation of nociceptors, QAQ will help identify where chronic pain originates and may have clinical use as an analgesic that is much more rapidly reversible than currently available drugs.

8586-29, Session 4

Photothermal control of cellular systems

Samarendra K. Mohanty, The Univ. of Texas at Arlington (United States)

The influence of photons on cellular systems can be enhanced via use of photothermal agents. While this interaction has been primarily utilized for destruction of cells, there exists significant potential in applying photothermal agents for microinjection and stimulation of cells. Here, we report near-infrared laser based optoporation approach for delivering plasmids encoding channelrhodopsin-2 into spatially-selected cells. Use of carbon nanoparticles as photothermal agent minimized the required laser dose for microinjection of plasmids into cells. Propagation of near-infrared light for in-depth transfection was evaluated using Monte Carlo simulation. The photothermal method allowed in-vivo transfection of selected regions of living tissue. The advantages of the photothermal delivery method over viral transfection include spatial selectivity and potential to inject large size plasmids. Use of photothermal effect as a cue for axonal navigation and stimulation of cells will also be discussed.

8586-30, Session PSun

Design and implementation of a high performance fluorescence tomography system for brain studies

Ramin Pashaie, Mehdi Azimipour, Univ. of Wisconsin-Milwaukee (United States)

No Abstract Available

8586-31, Session PSun

Miniaturized LED sources for in vivo optogenetic experimentation

Isaac P. Clements, Plexon Inc. (United States)

Recently developed optogenetics techniques have enabled researchers to modulate the activity of specific cell types. Complex neural pathways previously regarded as black boxes can now be directly probed, yielding a steadily increasing understanding of the basic neural circuits that underlie health and disease.

For in vivo experimentation, fiber-coupled lasers are typically used to illuminate internal brain regions, via an optical fiber that penetrates through overlying tissue. Though able to deliver intense fiber-coupled light, lasers are costly and face limitations in output beam stability and temporal precision during modulated outputs. A laser-driven system also necessitates the use of an optical commutator for experiments with unrestricted behaving animals. Optical commutators are also costly due to their complex and high precision optics, and result in light attenuation, varying light output during rotation, and limitations in the number of signals that can be transmitted. Furthermore, for experiments with combined optical stimulation and electrophysiology, a hybrid electrical / optical commutator is required.

Here we report and characterize an alternative light delivery solution, based on a high intensity fiber-coupled LED that is miniaturized for placement on the rotating end of an electrical commutator or for mounting directly onto the animal. Chronic stimulation experiments were performed to validate the function of this LED based system in in vivo recording scenarios. In behavioral experimentation, LED modules were used to deliver 465nm light through optical fibers (200µm core) ending in a connector able to attach to the animal for chronic experiments. Light was delivered to the behaving animals and optogenetically induced behavior was assessed.

8586-32, Session PSun

TBA

Bishorup Banjara, Nelson Cardenas, Samarendra K. Mohanty, The Univ. of Texas at Arlington (United States)

Stimulation and inhibition of chemically-identical group of cells in a cell population using optogenetic means has made great stride in modulating and controlling cellular function. However, We hypothesize that optogenetic modulation can lead to changes in subtle morphological (shape/refractive index) changes in the cell that can be detected with high resolution imaging. While conventional AFM and other scanning probe techniques are highly sensitive to morphological changes, these invasive-methods also suffer from low temporal resolution and restrictive field of view leading to reduced throughput. Here we present integration of a wide-field, label-free, non-invasive optical imaging technique with optogenetic stimulation for all optical stimulation and detection with high spatial and temporal resolution. This is achieved by dynamic monitoring of cell's phase (height x integrated refractive index) using quantitative phase microscopy of cells with and without expression of ChR2 and light stimulation. The fluctuation of phase in optogenetically stimulated cells are found to be higher than the control. With spatially-modulated optogenetic stimulation and wide-field quantitative phase imaging, we believe the method has potential to screen effectiveness of different opsins and stimulation parameters as well as cellular function under different physiological environments.

8586-23, Session 5

Development of optics with micro-LED arrays for improved opto-electronic neural stimulation

Lionel Chaudet, Mark Neil, Patrick Degenaar, Imperial College London (United Kingdom); Kamyar Mehran, Rolando Berlinguer-Palmini, Newcastle Univ. (United Kingdom); Brian Corbet, Pleun Maaskant, Tyndall National Institute (Ireland); David Rogerson, Peter Lanigan, Scientifica Ltd. (United Kingdom); Ernst Bamberg, Max-Planck-Institut für Biophysik (Germany); Boton Roska, Friedrich Miescher Institute (Switzerland)

The breakthrough discovery of a nanoscale optically gated ion channel protein, Channelrhodopsin 2 (ChR2), and its combination with a genetically expressed ion pump, Halorhodopsin, allowed the direct stimulation and inhibition of individual action potentials with light alone. This work reports developments of ultra-bright electronically controlled optical array sources with enhanced light gated ion channels and pumps for use in systems to further our understanding of both brain and visual function. This work is undertaken as part of the European project, OptoNeuro.

Micro-LED arrays permit spatio-temporal control of neuron stimulation on sub-millisecond timescales. However they are disadvantaged by their broad light emission distribution and low fill factor. We present the design and implementation of a projection and micro-optics system for use with a micro-LED array consisting of a 16x16 matrix of 25 ?m diameter micro-LEDs with 150 ?m centre-to-centre spacing and an emission spectrum centred at 470 nm overlapping the peak sensitivity of ChR2. The projection system images the micro-LED array onto micro-optics to improve the fill-factor from 2 % to more than 78 % by capturing a larger fraction of the LED emission and directing it correctly to the sample plane. This approach allows low fill factor arrays to be used effectively, which in turn has benefits in terms of thermal management and electrical drive from CMOS backplane electronics. The entire projection system is integrated into a microscope prototype to provide stimulation spots at the same size as the neuron cell body (~10 ?m).

8586-24, Session 5

Optogenetics to target actin-mediated synaptic loss in Alzheimer's

Atena Zahedi, Iryna Ethell, Univ. of California, Riverside (United States)

Numerous studies in Alzheimer's animal models have shown that overproduction of A? peptides and their oligomerization can distort dendrites, damage synapses and decrease the number of dendritic spines. Actin-regulating proteins, such as Rac1 and Cofilin, govern the growth and disassembly of F-actin and ultimately, the density and shape of dendritic spines. Excessive activation of actin-severing protein cofilin can trigger the formation of a non-dynamic actin bundles, called rods, which block transport and cause loss of synapses. Furthermore, A?1-42 oligomers inhibit an opposing pathway that suppresses cofilin phosphorylation through Rac1- mediated activations of LIMK1. Therefore, spatial regulation of actin-regulating proteins in dendritic spines can aid in preventing the synapse/spine loss associated with AD neuropathology.

Lack of spatial and temporal control of the activity of these proteins is a key limitation to their use. Recently, advances in Optogenetics have provided researchers with convenient light-activating versions such as photoactivatable Rac (PA-Rac). Our studies confirm feasibility of using PA-Rac to trigger actin-reorganization in dendritic spines. Cultured primary hippocampal neurons were transfected with an mCherry construct containing PA-Rac and the mCherry-expressing cells were identified and imaged under an inverted fluorescence microscope. Activation of Rac was achieved by irradiation with blue light (480nm) and live changes in dendritic spine morphology were observed using a different wavelength (587nm). PA-Rac activation resulted in rapid growth of spines and filopodia, which was observed in irradiated cells but not in control cells. We are currently assaying the signaling events activated by PA-Rac and F-actin dynamics through biochemical and immunostaining techniques.

8586-25, Session 5

Optofluidic control of axonal guidance

Ling Gu, Bryan Black, Simon Ordonez, Samarendra K. Mohanty, The Univ. of Texas at Arlington (United States)

Significant efforts are being made for control on axonal guidance due to its importance in nerve regeneration and in the formation of functional neuronal circuitry in-vitro. These include several physical (topographic modification, optical force, and electric field), chemical (surface functionalization cues) and hybrid (electro-chemical, photochemical etc) methods. Here, we report comparison of the effect of linear flow versus microfluidic flow produced by an optically-driven micromotor in guiding retinal ganglion axons. A circularly polarized laser tweezers was used to hold, position and spin birefringent calcite particle near growth cone, which in turn resulted in microfluidic flow. The flow rate and resulting shear-force on axons could be controlled by a varying the power of the laser tweezers beam. The calcite particles were placed separately in one chamber and single particle was transported through microfluidic channel to another chamber containing the retina explant. In presence of flow, the turning of axons was found to strongly correlate with the direction of flow. Turning angle as high as 900 was achieved and such long-range controlled optofluidic guidance of neurons allowed formation of in vitro neuronal circuits. Optofluidic-manipulation can be applied to other types of mammalian neurons and also can be extended to stimulate mechano-sensing neurons.

8586-26, Session 5

Micro mirror arrays as high-resolution spatial light modulators for photoactivation and optogenetics

Florian Rückerl, Jean-Yves Tinevez, Institut Pasteur (France); Jörg Heber, Fraunhofer-Institut für Photonische Mikrosysteme (Germany); Spencer L. Shorte, Institut Pasteur (France)

The ability to control the illumination and imaging paths of optical microscopes is an essential part of advanced fluorescence microscopy, and a powerful tool for optogenetics. In order to maximize the visualization and the image quality of the objects under observation we use programmable, ultra-fast Micro Mirror Arrays (MMA) as high-resolution Spatial Light Modulators (SLMs). Using two 256x256 MMAs in a mirror based illumination setup allows for fast angular-spatial control at a wide range of wavelengths (300-1000nm). Additionally, the illumination intensity can be controlled in at 10-bit resolution.

The setup allows selective illumination of subcellular regions of interest enabling the precise, localized activation of fluorescent probes and the activation and deactivation of subcellular and cellular signaling cascades using photo-activated ion-channels. Furthermore, inasmuch as phototoxicity is dependend on the rate of photo illumination [1] we show that our system providing fast, compartmentalized illumination is minimally phototoxic.

[1] Tinevez et al., A Quantitative Method for Measuring Phototoxicity of a Live Cell Imaging Microscope. Methods in Enzymology, Vol. 506,? 2012, pp. 291-309.

8586-27, Session 5

Glass optrode array for optical neural stimulation

Tanya Vanessa F. Abaya, Melany Moras, Mohit Diwekar, Steve Blair, Loren Rieth, Prashant Tathireddy, Gregory A. Clark, Florian Solzbacher, Univ. of Utah (United States)

Early-generation penetrating waveguide arrays made of glass were micromachined for infrared (IR) neural stimulation and optogenetics in able to provide comprehensive and selective access to distributed targets in three dimensions. We characterized the light delivery and loss mechanisms of the device in order to facilitate design optimization. The glass optrodes were formed by dicing, etching, and annealing. A fused silica/quartz substrate was used to produce 10x10 arrays of optrodes with constant geometry having a pyramidal tip at the end of a straight-edge shank; length, width, spacing, tip angle, and even array size can be varied indepedently. This substrate has a refractive index matching that of an optical fiber and is able to transmit the visible and near-IR spectrum.

Light transmission efficiency of optrodes was investigated with input from different optical fibers as well as a collimated beam. With a 150-um wide and 1.5-mm long optrode having a tip taper angle of 45 degrees with respect to the optical axis, 70% of visible and IR light from a butt-coupled 105-um multimode fiber is transmitted out of the optrode tips. These results match ray-tracing simulation data. The normalized output power decreases according to the cross-sectional area mismatch between optrode shank and input fiber. Shank length and tip taper does not affect the output power. Output beam profiles in the red and IR were also measured; wider optrodes emit wider beams, while going from a tip taper angle of 45 degrees to 30 degrees increases the full-angle divergence from 15 degrees to 55 55 degrees and offers a wider field of illumination.

Analysis reveals that the dominant source of loss is from total internal reflection within the tips. Insertion tests in tissue were also performed and had been successful.

8587-1, Session 1

Multimodality imaging in an orthotopic mammary window chamber mouse model

Rachel Schafer, The Univ. of Arizona (United States); Hui Min Leung, College of Optical Sciences, The Univ. of Arizona (United States); Arthur F. Gmitro, The Univ. of Arizona (United States)

Window chamber models have been utilized for many years to investigate cancer development and the microenvironment. More recently, an orthotopic mammary window chamber model was developed as an alternative to the original ectopic dorsal skin fold window chamber model. Orthotopic window chamber models, due to the native environment, support more realistic growth and tumor behavior than the ectopic models. The work by other groups thus far utilizing mammary window chamber models has focused solely on optical imaging techniques, limited to probing the first few millimeters of tissue. These techniques do not take full advantage of the unrestricted, three-dimensional tumor growth the model supports. We have developed a custom plastic structure compatible with multimodality imaging. We present in this work the implementation of our custom window chamber into a mouse model and the successful imaging of the window chamber cancer environment with MRI and nuclear imaging in addition to traditional optical techniques. MRI provides a full three-dimensional view of the tumor growth and allows for additional potentially clinically translatable approaches to be utilized in investigating the cancer microenvironment. Nuclear imaging is detected using the novel approach of the beta imager, demonstrated previously in a window chamber model. The beta imager detects photons after the interaction of a single gamma ray with a scintillator, instead of the coincidence detection of annihilation gamma ray pairs. We utilized the radioisotope glucose analog, 2-deoxy-2-(18F)fluoro-D-glucose or FDG, with the beta imager to obtain information on the glycolytic metabolism of the tumor and surrounding region.

8587-2, Session 1

Synthesis, calibration, and application of a novel tissue-permeable phosphorescence lifetime-based near-infrared ratiometric optical oxygen sensor with single-cell resolution

Alexander J. Nichols, Harvard Univ. (United States) and Massachusetts Institute of Technology (United States)

Recent work has suggested that hypoxic regions in cancerous tumors harbor a pernicious population of therapy-resistant cells. These cells evade death during therapy and often go on to reform untreatable, therapy-resistant tumors. In spite of hypoxia's known role in therapeutic resistance, few tools currently exist that allow high-resolution spatial mapping of oxygen tension in living systems. In one approach, known as phosphorescence lifetime imaging (PLI), certain photoexcited triplet emitters, such as porphyrins, can be used to generate optical contrast through the oxygen sensitivity of their excited triplet state lifetime. At present, such porphyrin-based "dendrimer" sensors are only compatible with intravascular imaging, rendering them inherently incapable of penetrating into solid tumors that host hypoxic environments. Furthermore, the majority of PLI systems are slow, expensive, and incapable of providing the 3D, cellular-level resolution required to comprehensively understand oxygen distribution in tumors. In contrast, porphyrin sensors based on a ratiometric platform, in which the oxygen sensitive signal is referenced to an oxygen-independent emission generated by a different chromophore within the same dendrimer, can be imaged using straightforward confocal microscopy. Here we report the synthesis, characterization, and application of a near-infrared (NIR) oxygen sensor based on a palladium(II)-tetrabenzoporphyrin core that is capable of penetrating into large in vitro 3D models of metastatic ovarian cancer. Using a custom-assembled laser scanning confocal microscope specially optimized to collect low-levels of NIR phosphorescence, we demonstrate fully calibrated ratiometric oxygen measurements in living cells.

8587-3, Session 1

Quantitative analysis of three-dimensional in vitro ovarian cancer model by optical coherence tomography

Yookyung Jung, Wellman Ctr. for Photomedicine (United States) and Harvard Medical School (United States) and Massachusetts General Hospital (United States); Oliver J. Klein, Wellman Ctr for Photomedicine (United States) and Massachusetts General Hospital (United States); Conor L. Evans, Wellman Ctr. for Photomedicine (United States) and Harvard Medical School (United States) and Massachusetts General Hospital (United States)

Visualizing and quantifying cellular and tumoral responses to therapy in metastatic ovarian cancer (OvCa) is highly challenging, as the disease often manifests as disseminated lesions that coat peritoneal surfaces. The difficulty in following cellular treatment response in OvCa precludes critical studies needed to improve patient survival and quality of life. To circumvent many of the difficulties encountered in vivo, 3D in vitro models of OvCa have been used that recapitulate many of the features found in human disease. While optical microscopies have been used to visualize the treatment response of 3D models, longitudinal studies of in vitro models by current technologies can be difficult due to the perturbative nature of sample preparation. Furthermore, the attenuation of light in tumor nodules prevents most optical microscopy techniques from visualizing details throughout large and complex tumor models. Optical coherence tomography (OCT) is a powerful approach for visualizing 3D in vitro model systems, where treatment-induced cellular and tumoral changes result in alterations in both light attenuation and scattering. Here, we present automated OCT and time-lapse OCT (TL-OCT) studies investigating therapeutic response in an in vitro model of ovarian cancer. To quantify therapeutic response data collected over multiple days, we have developed morphometric and segmentation analysis routines that longitudinally compute parameters such as nodule volume and surface area. By using such values on a nodule-by-nodule basis, we can create metrics that track very well with cellular death, and report cellular responses to frontline and photodynamic therapies throughout tumor nodules without staining.

8587-4, Session 1

The effect of copper on eumelanin photophysics and morphology

David J. Birch, Jens Sutter, Univ. of Strathclyde (United Kingdom)

Despite being an important pigment in skin, hair, the eye and the brain, melanin remains one of the most enigmatic of pigments. Melanin exists predominantly in two forms, the red pigment pheomelanin and the more common brown-black pigment eumelanin. Although the main constituents of eumelanin are well-known to be dihydroxyindoles, its detailed structure has so far eluded decades of research. This lack of knowledge is a barrier to progress in several areas, perhaps most notably in understanding the role melanin plays in melanoma, the most aggressive form of skin cancer.

Melanin's optical spectroscopy is complex. Its broad absorption spectrum underpins its sun-screening properties, but is open to different explanations, and its intrinsic fluorescence is weak and offers little insight. Recently we have used the fluorescent probe Thioflavin T to provide further evidence of a sheet-like structure for eumelanin and to monitor its synthesis from the auto-oxidation of 3, 4-dihydroxy-L-phenylalanine (L-DOPA)[1]. In an attempt to glean further knowledge of melanin's structure we have also fabricated unusual fibrils formed upon dying eumelanin and studied their photophysics [2].

In plant and animals tyrosinase is a copper-containing enzyme that catalyzes the production of melanin by oxidation of tyrosine to form L-DOPA. In this work we have arrested the usual synthesis of eumelanin from L-DOPA, prior to completion, by the addition of copper ions. We will report how adding copper ions simplifies the fluorescence kinetics and modifies the end products, giving some degree of control and understanding of the complex photophysics and morphology of eumelanin.

1. Eumelanin kinetics and sheet structure. J Sutter, T Bidláková, J Karolin and D J S Birch. App. Phys. Letts., 100, 113701, 2012.

2. Eumelanin fibrils. R McQueenie, J Sutter, J Karolin and D J S Birch. J. Biomed. Optics. In press.

8587-5, Session 1

Single shot white light interference microscopy with color fringe analysis for quantitative phase imaging of biological cells

Vishal Srivastava, Dalip S. Mehta, Indian Institute of Technology Delhi (India)

Recently there has been enormous research and development in the field of quantitative phase microscopy which provides the quantitative information about the transparent biological cells, such as structure, morphology and composition and that can be obtain from phase-based analysis. There are various methods to obtain the quantitative information about the objects, such as, Fourier phase microscopy [1], Hilbert phase microscopy [2], digital holographic microscopy [3] and Diffraction phase microscopy [4] and most of these microscopic techniques use laser as a light source which causes spurious fringes and speckles. As we know refractive index (RI) of biological sample is a vital parameter for determining the average cell mass, thickness and haemoglobin concentration in RBC etc. For quantitative phase imaging we use low coherence white light source which is a mixture of red, green and blue colour of light and RI of a material is wavelength dependent [5]. We record a single white light interferogram by a colour CCD camera and then decompose it into the red, green and blue colour wavelength components and processed it by Hilbert transform colour fringe analysis to find out the RI for different colour wavelengths.The present methods is very useful for dynamic processes where path-length changes in nano-meter and are at millisecond level due to its single shot nature and its acquisition time is only limited by CCD camera or recording device. Experimentally obtained quantitative phase maps and RI profiles of both the onion film and human RBC will be presented later.

8587-6, Session 1

Ophthalmic adaptive optics by digital holography

Myung K. Kim, Changgeng Liu, Univ. of South Florida (United States)

We are developing adaptive optics (AO) systems for aberration corrections in retinal imaging based on digital holography (DH). Compared to existing technologies of adaptive optics, our systems do not have hardware components such as lenslet arrays or deformable mirrors. Instead, wavefront sensing and correction are done by acquisition and numerical manipulation of optical phase by digital holography, thereby substantially reducing hardware complexity and introducing novel imaging capabilities.

We are studying two distinct DH-based AO systems (DHAO) that we have recently proposed, incorporating DH of coherent or incoherent sources. We describe and compare our recent progress on the development of these two types of holographic adaptive optics systems. In either system, the DHAO is a two-step process, consisting of acquisition of holograms with guide-star and full-field illuminations. The two complex holograms, containing the amplitude and phase profiles of the corresponding optical fields, are numerically combined to determine and compensate for the effect of aberration in the optical path. A main difference between the two systems is the manner in which the complex holograms are extracted. With a coherent source, the holographic interference between the object and reference automatically contain the necessary complex field information. On the other hand, with the incoherent source, the self-interference between two copies of spherical wavefronts from each source point results in Fresnel zone pattern, which in turn is combined with phase shifting technique for extraction of the complex field. We have demonstrated that both systems exhibit efficient and robust aberration compensation of artificial targets. We are carrying out systematic studies of imaging sensitivity and noise characteristics of the two systems, both theoretically and experimentally, with the goal of achieving high-quality imaging with retinal cone mosaic resolution.

8587-7, Session 1

Lensless imaging system to quantify cell proliferation

Srikanth Vinjimore Kesavan, Cédric P. Allier, Fabrice P. Navarro Y Garcia, Frédérique Mittler, CEA-LETI (France); Bernard Chalmond, ETIS/ENSEA Univ. de Cergy-Pontoise-CNRS (France); Jean-Marc Dinten, CEA-LETI (France)

Owing to its simplicity, 'Lensless Imaging System' is adept at continuous monitoring of adherent cells inside the incubator. The setup consists of a CMOS sensor with pixel pitch of 2.2 µm and field of view of 24 mm?. LED with a dominating wavelength of 525 nm, along with a pinhole of 150 µm is used as the source of illumination. The in-line hologram obtained from cells depends on the degree of cell-substrate adhesion. Drastic difference is observed between the holographic patterns of floating and adherent cells. In addition, the well-established fact of cells losing contact with the substrate during cell division is observed with our system based on corresponding spontaneous transition in the holographic pattern. Here, we demonstrate that by recognizing this specific holographic pattern, number of cells undergoing mitosis in a cell culture with a population of approximately 5000 cells, can be estimated in real-time. This method also proves efficient with confluent cell cultures. The method is assessed on comparison with Edu-based proliferation assay. We monitored cell culture for more than 24 hours inside the incubator. The approach is straightforward and it eliminates the use of markers to estimate the proliferation rate of a given cell culture. Unlike classic proliferation assay, the cells are not removed from the substrate, leaving the cell culture unmodified. Changes in proliferation rate over a period can also be obtained which could prove effective in the quantification process of dyes, drugs, etc.

8587-8, Session 1

Internal and external fingerprint reconstruction using optical coherence tomography (OCT)

Richelle Hoveling, Maurice C. Aalders, Academisch Medisch Ctr. (Netherlands)

Fingerprint identification of suspects is currently the most common procedure in biometry. Various methods for acquiring fingerprints are

available. However, the quality of the fingerprints heavily depends on influences like pressure of the finger and perspiration. Worse, when fingertips are altered, by e.g. abrasion, burning or scarring the fingertip, it is impossible to obtain fingerprints. These types of self-inflicted damage to the fingertips are frequently encountered in the judicial field. [1] Hence, to overcome these disadvantages we developed a method to obtain fingerprints from the external and internal structure of the skin of the fingertips. Using swept-source Optical Coherence Tomography (OCT) scans we were able to detect both the transition from air to the stratum corneum as well as from the stratum corneum to the stratum granulosum. The results show a high similarity between the prints obtained from the two skin layers. These "internal prints" therefore show high potential to be used for identification of individuals with damaged fingerprints. By immersing a cadaver finger we were able to detach the epidermis to uncover the structure of the dermis, enabling OCT scanning for dermal print reconstruction. The preliminary results confirm our ideas on the double ridge structure of the dermis and its suitability for identification, e.g. in case of extreme damage or absence of the epidermal layer.

Moreover, the non-invasive OCT technique can be used to detect pore activity, an indication whether the fingerprint donor is alive, and identify 'fake skin'. OCT therefore shows great potential in the field of biometrics.

Reference:

[1] Vij, K., (2011). Textbook of Forensic Medicine and Toxicology: Principles and practice (Fifth edition). India: Elsevier.

8587-9, Session 1

Multimodal in vitro toxicity testing by quantitative phase digital holographic imaging

Christina E. Rommel, Christian Dierker, Angelika Vollmer, Steffi Ketelhut, Björn Kemper, Jürgen Schnekenburger, Westfälische Wilhelms-Univ. Münster (Germany)

In vitro toxicity testing of drugs, chemicals or nanomaterials involves the measurement of cellular endpoints like stress response, cell viability, proliferation or cell death. The common assay systems determine enzyme activity or protein expression by optical read out of enzyme substrates or marker protein labeling. These standard procedures have several disadvantages. Cellular processes have to be stopped at a distinct time point for the read out, where usually only parts of the cells were affected by the treatment. Only one parameter is analyzed and detection of cellular processes requires several time consuming incubations and washing steps.

Here we have applied Digital Holographic Microscopy (DHM) for a multimodal analysis of drug toxicity. NIH 3T3 cells were incubated with 1 µM Taxol for 24 h. The recorded quantitative phase images were analyzed for cellular refraction index, cell volume, cell height and cell migration. Taxol treated cells showed a rapid freezing of cell motility as measure of cell viability. A short increase in cell height and cell volume indicated cell division in control cells, whereas Taxol treatment resulted in a long increase in cell height followed by a rapid decrease and a decrease of cellular refraction index as indicators of cell death.

DHM analysis of drug treatment allows direct and marker free detection of several toxicity parameters in parallel. DHM can record cellular reactions over a time period and analyze kinetics of delayed cellular responses. Our results demonstrate Digital Holographic Microscopy as a valuable tool for multimodal toxicity testing.

8587-10, Session 1

Label free quantitative imaging of the effects of estrogen on breast cancer cell growth

Mustafa A. Mir, Anna Bergamaschi, Benita S. Katzenellenbogen, Gabriel Popescu, Univ. of Illinois at Urbana-Champaign (United States)

Cancer is an uncontrolled proliferation of cells due to abnormal cell-cycle regulation or deregulation of cell signaling machinery and accounts for over 13% of all human deaths. Traditional methods for assessing this proliferation do not provide single cell level information, are generally tedious, require specialized materials and instrumentation and usually provide indirect measures. It is becoming increasingly clear that to truly understand the nature of cancer cell proliferation and the efficacy of drugs in controlling it, quantitative information on cell growth and morphology is required at the single cell level. Here we show that Spatial Light Interference Microscopy (SLIM), a recently developed broadband, common path, quantitative phase imaging method is ideal for such measurements. SLIM has femtogram level sensitivity to changes in dry mass and can simultaneously provide this information at both the single cell and population level. Furthermore, since SLIM is an imaging modality, changes in cell morphology, motility, and interactions between cells can also be quantified with little additional effort. In this work we used SLIM to measure the effects of Estrodiol, Tomaxafin and the estrogen receptor antagonist, ICI on MCF-7 breast cancer cells. These results provide information on the effects of these widely used agents on cell growth rates, morphology, dynamics and heterogeneity in the temporal response to the treatment amongst cells. These studies will undoubtedly improve our understanding of the effects of commonly used drugs at the single cell level, paving the way for designing more targeted and efficient cancer therapies.

8587-11, Session 2

Label free imaging of human neural progenitor differentiation

Mustafa A. Mir, Univ. of Illinois at Urbana-Champaign (United States); Anirban Majumder, The Univ. of Georgia (United States); Steven Stice, Univ. of Georgia (United States); Gabriel Popescu, Univ. of Illinois at Urbana-Champaign (United States)

Characterizing and quantifying the phenomenon of stem cell differentiation is of fundamental importance to our understanding of developmental biology. In this work we followed the differentiation of human neural progenitor cells to neurons over the course of two weeks using a Spatial Light Interference Microscope (SLIM). SLIM provides quantitative measurements of the dry mass (non-aqueous content) density at each spatial location in an image with femtogram level accuracy. This information is used to quantify changes in the overall cell mass over the two weeks to provide insight on how the cell growth dynamics change over the course of the differentiation process. In addition, fluctuations in the dry mass density map are also used to measure the inter- and intra-cellular mass transport characteristics of the population. Since SLIM is an imaging modality, we have simultaneous access to morphological and motility information providing a detailed picture of the differentiation process. The results from this study indicate that it may be possible to establish signatures for the level of differentiation a single cell has undergone based on mass growth and transport measurements, effectively removing the need for the complicated labeling procedures that are currently used. Such a technique to assess the differentiation state of single cells will be invaluable to biologists in rapidly assessing the effects of various treatments in a practical and non-invasive manner.

8587-12, Session 2

Microscopic analysis of cell death by metabolic stress-induced autophagy in prostate cancer

Austin Changou, UC Davis Medical Ctr. (United States); Balpreet S. Ahluwalia, Univ. of Tromsø (Norway); R. Holland Cheng, Univ. of California, Davis (United States); Richard Bold, Hsing-Jien Kung, Frank Y. Chuang, UC Davis Medical Ctr. (United States)

Autophagy promotes cellular survival against environmental stress and nutritional starvation. We have recently shown that some prostate cancers undergo metabolic stress and caspase-independent cell death following exposure to arginine deiminase (ADI, an enzyme that degrades arginine in tissue). The aims of our current investigation into the application of ADI as a novel therapy are to identify the components mediating tumor cell death, and to determine the role of autophagy (stimulated by ADI and/or rapamycin) on cell death. Using advanced fluorescence microscopy techniques including 3D deconvolution and structured-illumination superresolution imaging, we show that prostate tumor cells treated with ADI for extended periods, die exhibiting a morphology that is distinct from caspase-dependent apoptosis; and that autophagosomes forming as a result of ADI stimulation contain DAPI-stained nuclear material. Fluorescence imaging (as well as cryo-electron microscopy) show a breakdown of both the inner and outer nuclear membranes at the interface between the cell nucleus and aggregated autophagolysosomes. Finally, the addition of N-acetyl cysteine (or NAC, a scavenger for reactive oxygen species) effectively abolishes the appearance of autophagolysosomes containing nuclear material. We hope to continue this research to understand the processes that govern the survival or death of these tumor cells, in order to develop methods to improve the efficacy of cancer pharmacotherapy.

8587-13, Session 2

Fast spatial light interference microscopy (fSLIM) for dynamic biomedical imaging

Basanta Bhaduri, David Wickland, Gabriel Popescu, Univ. of Illinois at Urbana-Champaign (United States)

Quantitative phase imaging (QPI), i.e. mapping the phase distribution of an image field, has become a rapidly emerging area of study. Spatial light interference microscopy (SLIM) is a highly sensitive QPI method which is capable of unprecedented structure studies in biology and beyond. SLIM combines Zernike's phase contrast method by revealing the intrinsic contrast of transparent samples, with Gabor's holography by rendering quantitative phase maps across the sample. In addition to the π/2 shift introduced in phase contrast between the scattered and unscattered light from the sample, further 4 phase shifts are generated, by increments of π/2 using a reflective liquid crystal phase modulator (LCPM). As 4 phase shifted images are required to produce a quantitative phase image, the switching speed of the LCPM and the acquisition rate of the camera limit the acquisition rate and, thus, SLIM's applicability to highly dynamic samples.

In this paper we present a new SLIM setup which can image at a rate of 50 frames per second and provide in real-time, 5 megapixel size quantitative phase images at 50/4=12.5 frames per second. We use a spatial light modulator (Boulder Nonlinear Systems) which can refresh its frames up to 150 per second for phase shifting and a CMOS camera (Andor, Neo sCMOS) which is capable of imaging up to 98 frames at full size (5MP). To demonstrate the capability of the new system, we'll present dynamic QPI of beating cardiomyocyte cell.

8587-14, Session 2

Measuring uptake dynamics of multiple identifiable carbon nanotube species via high-speed confocal Raman imaging of live cells

Jeon Woong Kang, Massachusetts Institute of Technology (United States); Freddy T. Nguyen, Univ. of Illinois at Urbana-Champaign (United States); Niyom Lue, Ramachandra R. Dasari, Peter T. C. So, Massachusetts Institute of Technology (United States); Daniel A. Heller, Memorial Sloan-Kettering Cancer Ctr. (United States)

Carbon nanotube uptake was measured via high-speed confocal Raman imaging. Two cell-intrinsic, as well as 9 nanotube-derived Raman modes were measured simultaneously, resulting in multiplexed imaging which allowed spatial and temporal tracking of specific endogenous and exogenous features. Transient uptake experiments resolved single nanotube species, as denoted by the presence of spectra bearing single nanotube radial breathing modes (RBMs), as well as their locations relative to the cell position, which was denoted by cell-intrinsic Raman peaks. This work portends the real-time molecular imaging of live cells and tissues using Raman spectroscopy, affording complete photostability and much greater multiplexing ability.

Dynamics of the macrophage uptake of nanotubes were measured by quantifying cell-localized nanotube Raman signals across images over the course of the experiment. The mapping process involved the rapid scanning of a 17 ? 17 μm area containing the cell by acquiring 900 (30 ? 30) spectra with an integration time of 50 milliseconds. With minimal interval between time frames, 40 frames were imaged repeatedly and the experiments produced 36,000 (30 ? 30 ? 40) Raman spectra. All Raman spectra were fit with a linear combination of normalized basis spectra with non-negative restriction. Basis spectra were generated with known center wave numbers from previous studies. Fitting coefficient of each basis spectra represents the relative strength of each component and used to reconstruct images. We have demonstrated the first transient cellular uptake imaging of nanomaterials and the first transient imaging of carbon nanotubes with the ability to distinguish multiple pristine SWNT species.

8587-15, Session 2

Cantilever-assisted two-beam interference microscopy for the observation of stratum corneum swelling

Shin-ichiro Yanagiya, Hiroshi Katayama, Hiroshi Katayama, Nobuo Goto M.D., Nobuo Goto M.D., Univ. of Tokushima (Japan)

We have studied two-beam interference phenomena, which are observed on an atomic force microscope cantilever bar using a laser confocal microscope. Although this technique, which we named cantilever-assisted interference microscopy (CAIM), is a kind of simple Fizeau type interferometry, it has a feature of quite a small 3D space for the measurement. In vertical direction, the height corresponds to the height of the atomic force microscope (AFM) cantilever cantilever tip (~10 ?m). In addition, the measurement field along the horizontal axis is also small (several hundreds square microns) because the interval between interference fringes is around 1 ?m. This technique covers transparent materials. In this study, we studied the swelling process of stratum corneum (SC) by CAIM.

The SC was obtained from a cultured human epidermis, which was purchased from J-TEC Co. The SC was cut into 2–3 mm pieces and stuck on a glass plate. The sample was observed using the combination of an AFM (NanoWizard II, JPK Instruments) and an LCM (IX-71 and FV-300, Olympus Co.). We used a triangular AFM cantilever, which was used as the interference mirror. The LCM was operated using a green He–Ne laser (543 nm). Interference imaging was taken every 30 s for 30 min.

The fringe interval was almost the same during the experiments. Conversely, the fringe moved right and the speed decreased with time. According to theoretical calculations, the tilt angle was about 11° and the SC swelled with the speed of hundreds nm/min.

8587-16, Session 2

Characterization and validation of an optical platform for in vivo circulating cell quantification in adult zebrafish

Li Zhang, Massachusetts General Hospital (United States) and Fudan Univ. (China); Vera Binder, Harvard Medical School (United

States) and Children's Hospital Boston (United States); Clemens Alt, Wellman Ctr. for Photomedicine (United States); Pulin Li, Richard M. White, Leonard I. Zon, Harvard Medical School (United States) and Children's Hospital Boston (United States); Xunbin Wei, Shanghai Jiao Tong Univ. (China); Charles P. Lin, Wellman Ctr. for Photomedicine (United States)

Zebrafish is a powerful animal model for drug discovery, cancer and stem cell research. A recently developed optically clear strain of zebrafish, named casper, is transparent as adults therefore greatly facilitates the detailed imaging of cell migration, metastasis, and kinetics of stem cell engraftment and tumor growth.

An optical platform has been developed to track and count circulating blood cells in live adult casper fish. This instrument is an integrated multi-color, multi-channel laser scanning confocal microscope (LSCM) and an in vivo flow cytometer (IVFC), which allows simultaneous detection of multiple cell populations or imaging of different tissues.

Here we have characterized the sensitivity of the instrument using microbeads of different fluorescent intensities. The system was then validated to read out ratio of two-color cell populations, for the purpose of evaluating drug effect in competitive transplantation assay using Zebrafish,

This novel platform permits longitudinal imaging of competitive transplantation engraftment with zebrafish mutants hematopoietic stem cells (HSCs) and chemical effects on homing, engraftment, and self-renewal. Furthermore it provides unprecedented opportunities of tracing stem cells and cancer cells at a single cell level within the living adult zebrafish.

8587-17, Session 2

Label-free volume determination using differential interference contrast microscopy: quantification of in vitro platelet aggregate and thrombus volumes under physiological shear rates

Sandra M. Baker, Kevin G. Phillips, Owen J. T. McCarty, Oregon Health & Science Univ. (United States)

Differential interference contrast (DIC) microscopy has become an indispensable resource in the label free investigation of microorganisms and cellular structures on the micron scale. High numerical aperture (NA) Kohler illumination coupled with DIC enables the visualization of distinct planes through the specimen along the optical axis. We combine a Hilbert transform technique, introduced by Arnison et al. to make DIC contrast amenable to thresholding in 3D image cubes, with Fourier spatial filtering to perform 3D optical sectioning of weak index contrast specimens for volume determination. The method is validated on polystyrene spheres (n = 1.596) suspended in fluoromount G (n = 1.4) imaged at 540 nm ranging in diameter from 0.1 up to 10 microns. We then applied the technique to the quantification of platelet aggregate and thrombus volumes under low (200 s^-1) and high (1000 s^-1) physiological shear rate conditions.

8587-18, Session 2

Cell cycle imaging with quantitative differential interference contrast microscopy

Piotr Kostyk, Shelley Phelan, Min Xu, Fairfield Univ. (United States)

The cell cycle is a series of events which lead to the growth, replication, and division of cells. The cell cycle has a vital role in many life processes, such as the development of a unicellular zygote to a multicellular organism, as well as the renewal of epithelial tissue, haematocytes, and organs. Furthermore, the cell cycle has a significant role in the development of cancer. A notable characteristic of cancer cells is their rapid progression through the cell cycle. Recent studies suggested that the population of cancer cells in post-DNA replication phases of the cell cycle in a tissue correlates with its aggressiveness.

Here, we report a microscopic approach for determining whether cells are actively proliferating or quiescent from the optical path length (OPL) within the cells' nuclear regions measured by quantitative differential interference contrast (DIC) microscopy at wavelengths of 450nm to 700nm. It enables differentiation between cells in pre-DNA replication phases and cells in post-DNA replication phases without the use of chemical treatments. The approach is validated by the excellent agreement between the proportion of proliferating-to-quiescent breast cancer epithelial MCF7 cells obtained from DIC microscopy, and that from a standard immunofluorescence assay for the nuclear protein Ki-67. The potential of this approach for determination of cell cycles inside tissue in situ and in vivo is discussed at the end.

8587-19, Session 2

Dynamic spectroscopic phase microscopy for red blood cells

Jaeduck Jang, Yunhun Jang, YongKeun Park, KAIST (Korea, Republic of)

Molecular concentration in living cells is crucial role to understand the cellular pathophysiology. Optical techniques such as fluorescence imaging, Raman spectroscopy, and interferometry microscopy are exploited to measure molecular concentrations. Fluorescence imaging technique that utilizes exogenous agents including fluorescent molecules have been used for labeling to target molecules inside cells and quantifies molecular concentrations of interest. Although fluorescence image provides high molecular sensitivity, the use of staining agents requires careful consideration of non-specific binding and photo-bleaching/blinking. Raman spectroscopy is non-invasive technique based on confocal microscopy that provides a means of determining the molecular concentration in cells. However, Raman signal needs long integration time and expensive laser sources. Refractive index (RI) as an intrinsic optical property can be used for measuring molecular concentration of target molecule. Currently, quantitative phase microscopy (QPM) has been employed to measure the molecular concentrations of target molecules in cells.

We present dynamic spectroscopic phase microscopy (dSPM) that can simultaneously measure the molecular concentration and volumes at high speed. dSPM integrates three different coherent lasers and a Bayer patterned color CCD. Our approach to measure the molecular concentrations is to introduce two different immersion media with different refractive indexes in order to decouple the refractive index and the thickness of the red blood cells (RBC). The wavelength-dependent RI, obtained by dSPM, has been employed to determine the molecular concentration in RBC, to decouple the molecular concentration of hemoglobin proteins and cellular thickness from the phase delay induced by a sample. Moreover, the proposed technique offers the dynamically changing of molecular concentration and volume in intact RBC.

8587-20, Session 3

Manipulating freely diffusing single 20-nm particles in an anti-Brownian electrokinetic trap (ABELtrap)

Michael Börsch, Friedrich-Schiller-Univ. Jena (Germany); Nawid Zarrabi, Monika G. Düser, Univ. Stuttgart (Germany)

Conformational changes of individual fluorescently labeled proteins can be followed in solution using a confocal microscope. Two fluorophores attached to selected domains of the protein report fluctuating conformations. Based on Förster resonance energy transfer (FRET) between these fluorophores on a single protein, sequential distance

changes between the dyes provide the real time trajectories of protein conformations. Freely diffusing proteins are not affected by potential surface influences. However, observation times are then limited by the Brownian motion through the confocal detection volume. A. E. Cohen and W. E. Moerner have invented and built microfluidic devices with 4 electrodes for an anti-Brownian electrokinetic trap (ABELtrap). Here we present an ABELtrap based on a laser focus pattern generated by a pair of acousto-optical beam deflectors and controlled by a programmable FPGA chip. Fluorescent 20-nm beads in solution were used to mimic freely diffusing large proteines like FOF1-ATP synthase. The ABELtrap could hold these nanobeads for about 10 seconds at the given position. Thereby, the observation times of a single particle were increased from 10 ms without trapping by a factor of 1000.

8587-21, Session 3

Activation of cell signaling via optical manipulation of gold-coated liposomes encapsulating signaling molecules

Gabriel V. Orsinger, Sarah J. Leung, Marek Romanowski, The Univ. of Arizona (United States)

Many diseases involve changes in cell signaling cascades, as seen ubiquitously in drug resistant cancers. To better understand these intricate signaling events in diseased cells and tissues, experimental methods of probing cellular communication at a single to multi-cell level are required. We recently introduced a general platform for activation of selected signaling pathways by optically controlled delivery and release of water soluble factors using gold-coated liposomes. In the example presented here, we encapsulated inositol trisphosphate (IP3), a ubiquitous intracellular secondary messenger involved in GPCR and Akt signaling cascades, within 100 nm gold-coated liposomes. The high polarizability of the liposome's unique gold pseudo-shell allows stable optical trapping for subcellular manipulation in the presence of cells. We take this optical manipulation further by optically injecting IP3-containing liposomes into the cytosol of a single cell to initiate localized cell signaling. Upon optical injection of liposomal IP3 into intestinal epithelial cells (IEC), we observed spatiotemporal activation of a single cell as reported by changes in Indo-1 fluorescence intensity. With established gap junctions between the injected IEC and neighboring IECs, we monitored propagation of this signaling to and through nearby cells. We also demonstrated the ability to modulate cell signaling by, for example, varying the number of IP3-containing gold-coated liposomes injected into a single cell. By combining optical trapping with gold-coated liposomes encapsulating signaling molecules, we present a unique in vitro tool for studying cell signaling.

8587-22, Session 4

Classification of atherosclerotic patients with different Gensini score by cytome data from polychromatic (10-color) flow cytometry immunophenotyping *(Invited Paper)*

Jozsef Bocsi, Frank Beutner, Kay Olischer, Aniko Szabo, Gerhard Schuler, Joachim Thiery, Ingo Dähnert, Attila Tarnok, Univ. Leipzig (Germany)

Cardiac infarction is one of the leading causes of death in the western hemisphere. Activation of leukocyte adhesion molecules occurs after coronary intervention and the level of activation have predictive value. Previously, we demonstrated that surface expression level of leukocyte adhesion molecules assessed by flow cytometry (FCM) can predict restenosis after stenting and advanced coronary artery disease (CytometryB 2003;53:63). Here, we hypothized that complex cytome data from immunophenotyping can identify atherosclerotic individuals. As proof of concept, we analyzed patients from the cluster of excellence project "Leipzig research center for civilization disease – LIFE"(http://www.uni-leipzig-life.de/). Blood samples were drawn before diagnosis from 25 adults who suffered from chest pain (angina pectoris) without myocardial infarction undergoing diagnostic cardiac catheterization and immunophenotyped by polychromatic (10-color) FCM. These cytome data were tested for their predictive value for athrosclerosis. Patients were grouped according to their Gensini score (range:0-85) into a low (score=0, n=10) and a high (score>8.5, mean=34.9, n=10) atherosclerotic group and statistically analyzed by discriminant analysis and systems biology tools. The low and high score group was 100% correctly classified in a learning data set by cell count and marker expression on lymphocyte subclasses and clustered by discriminant analysis based on 12 parameters. Furthermore, a set of test individuals (n=5) with known score but not used in the learning set was 100% correctly identified. Our results show that cell systems biological instruments may help to predict atherosclerosis. This approach is substantially more cost effective than cardiac catheterization and could in future help to identify risk patients.

8587-23, Session 4

Label-free imaging of fatty acid content within fungal samples using stimulated Raman scattering microscopy

Natalie Garrett, Julian J. Moger, Univ. of Exeter (United Kingdom)

There are an estimated 1.5 million species of fungus, although only 5% of these have been formally classified. Of these, it is the species which are pathogenic to plant crops and to humans that have received the most scientific scrutiny. The devastating losses to crop yields as a direct result of fungal infection have a direct impact on the global economy and have a knock-on detrimental effect on human health. Lipid metabolism is a key target for the development of fungicides, therefore effective mapping of lipid distribution within fungi is vital.

To improve our understanding of lipid distribution and metabolism within fungi, scientists have thus far relied on biochemical analysis of whole cell contents and fluorescence microscopy using lipid-specific staining or green fluorescent protein (GFP) tagged proteins associated with lipid droplets. These approaches have clear drawbacks: whole-cell biochemical analysis provides average data of all lipids present in the cell without any spatial or single-cell information. On the positive side, detailed specifications on carbon chain length, degree of saturation, etc. are readily obtained. The lipid staining and protein tag approaches provide single-cell and morphological information on the lipid droplets. However, staining is an indirect and invasive method with potential side effects such as altered chemical and physical properties of the lipids, photo-induced damages and uncertainties in the labelling/expression efficacy.

With recent advances in nonlinear microscopy, it is now possible to non-invasively obtain contrast from intrinsic chemical bonds within live samples using chemically-specific spectroscopy techniques probing Raman-active resonances. We present SRS microscopy as a means to identify lipid species and to quantify the degree of lipid saturation within individual living fungi by probing Raman resonances of the CH stretch between 2850cm?1 and 3015cm?1.

8587-24, Session 4

Ball lens hollow Raman probe and Fourier transform infrared applied for studying non-clinic samples colorectal tumor models

Bibin B. Andriana, Kwansei Gakuin Univ. (Japan); Norio Miyoshi, Univ. of Fukui (Japan); C. Linda R. Soeratman, The Univ. of Tokyo (Japan); Mika Ishigaki, Yashuhiro Maeda, Akinori Taketani, Kwansei Gakuin Univ. (Japan); Leenawaty Limantara, Univ. Ma Chung (Indonesia); Hidetoshi Sato, Kwansei Gakuin Univ. (Japan)

Ball-lens hollow Raman Probe (BHRP) and FTIR spectroscopy were main tools in this study. BHRP was purposed exploring the biochemical

alteration in the living animal, mean while FTIR spectroscopy clarifies BHRP result. In this study, both equipments detected the alteration of antisymmetric and symmetric P=O stretching vibration within our mice colorectal tumor models. Some differences of spectra due to randomly the edge of each BHRP and FTIR attached the surface of tumor during measurements. Meanwhile, the application of FTIR potentially differentiates the grade levels of non-clinic samples colorectal tumor models at four different grades (normal, grade 1, grade 2 and grade 3). Detailed investigation of the spectra in the fingerprint region is 1800-700 cm-1 for BHRP and 4000–500 cm-1 for FTIR exposed some discrete peaks and shoulders, most of which were assignable to wave numbers that publicized to represent biochemical alteration within the tissue. Differences in peak ratios and peak heights indicated differences in biochemical composition of cancer from different grade level. It was possible to distinguish between their grades. However, all collected colorectal tumor model at different peak was distinguishable, where antisymmetric stretching of CH2, antisymmetric and symmetric P=O stretching of DNA (represents more DNA in cell) were imaged and mapped clearly. Therefore, both of equipments spectral analysis in combination with calibration curve might be used to distinct cancer grade. Extension of this method to other cancer type may be of great interest for cancer grade determination.

8587-25, Session 4

Raman-based in vitro and in vivo visualization of heat and radiation-induced damage in collagen

Iwan W. Schie, UC Davis Medical Ctr. (United States); Cindy Thomas, Lawrence Livermore National Lab. (United States); Paul F. Wilson Jr., Brookhaven National Lab. (United States); Thomas R. Huser, Univ. Bielefeld (Germany) and Univ. of California at Davis (United States); Matthew A. Coleman, Lawrence Livermore National Lab. (United States) and Univ. of California at Davis (United States)

Novel techniques are needed for detecting and measuring the appearance of ionizing radiation specific changes in humans that are predictors of tissue injury. Spontaneous Raman spectroscopy is ideal for non-invasive identification of robust signatures of radiation exposure and tissue injury. We used spontaneous Raman spectroscopy to measure signatures of induced damage in collagen. First, we compared spectra from purified collagen type I to spectra from pig skin surface, and proved that the majority of the spectral signature is identical to collagen type I. Second, we determined the effects of temperature and irradiation on collagen type I. The difference spectra of exposed and non-exposed collagen was used to illustrate changes in the spontanious Raman signature. Several spectral features were shared between the heated and irradiated samples. One can see the exposure dependent decrease of the peak intensity of the 1668cm-1 peak that is correlated to the C-C bond of the protein backbone (amide I bonds), which indicates the degradation of the protein backbone. This data is in agreement with earlier Raman spectroscopy-based studies that illustrated the ability to see other exposure differences. The importance of our approach is our ability to visualize heat and irradiated based exposures. Additional data will be needed to quantify the precision of the spectra and its association with tissue specific damage in vivo. These studies will form the foundation for establishing rapid, precise, high-throughput assay systems that are practical in a variety of radiation exposure scenarios in order to triage and treat exposed individuals.

8587-26, Session 4

Diagnosis and subclassification of breast pathologies using mosaicked large-field two-photon microscopy

Yuankai K. Tao, Osman O. Ahsen, Massachusetts Institute of Technology (United States); Dejun Shen, The Univ. of Alabama at Birmingham (United States); Yury Sheykin, Beth Israel Deaconess Medical Ctr. (United States); Alex E. Cable, Thorlabs Inc. (United States); James L. Connolly, Beth Israel Deaconess Medical Ctr. (United States); James G. Fujimoto, Massachusetts Institute of Technology (United States)

Local recurrence following breast cancer surgery is strongly correlated to tumor involvement at the surgical margin. Unfortunately, conventional histology requires long tissue processing times and intraoperative evaluation requires frozen-section analysis, which introduces processing artifacts, is limited in sampling area, has reduced accuracy and compromises specimen integrity. The molecular-specificity of two-photon microscopy (TPM) is particularly well-suited for visualizing subcellular-resolution biomarkers of disease, such as nuclear size and shape, and morphological changes, such as reorganization of collagen. TPM can allow for rapid non-destructive optical assessment of specimen surfaces in real-time. Furthermore, TPM fields can be mosaicked in post-processing to extend the imaging field-of-view (FOV) to improve coverage.

In a prospective study, 178 surgical breast specimens from 48 patients were imaged to evaluate the diagnostic accuracy of TPM relative to H&E histology in bulk, freshly excised human breast tissue. Specimens were rapid stained with Acridine Orange and imaged using 100fs excitation pulses. Specimens were imaged with dual-channel detection for two-photon fluorescence and second-harmonic-generation to detect both nuclear and stromal contrast, respectively. Overlapping TPM images were mosaicked in post-processing using a scale-invariant feature transform and nonlinear intensity blending to extend the FOV, and the dual acquisition channels were remapped to a pseudo-H&E colormap to generate composite images comparable to that of conventional histology. A double-blinded reading of the TPM images by three trained breast pathologists yielded 96.7% and 91.1% sensitivity and specificity, respectively, for distinguishing between normal and malignant tissue. These results suggest that TPM can be used for real-time assessment of surgical margins.

8587-27, Session 4

Hyperspectral angular domain imaging for ex vivo breast tumor detection

Fartash Vasefi, SMI (United States); Bozena Kaminska, Simon Fraser Univ. (Canada); Muriel Brackstone, Jeffrey J. L. Carson, Univ. of Western Ontario (Canada)

Purpose: To determine the performance of angular domain hyperspectral imaging for delineation of ex-vivo breast tumor margins after lumpectomy.

Materials and methods: Angular domain hyperspectral imaging system was built and used to test fresh breast tissue samples with a thickness of 2 mm. The hyperspectral system consisted of a halogen lamp, collimation optics, scanning stage with controller, a silicon micro-machined micro channel array, and a pushbroom spectrometer. The system operated within the spectral range of 650 - 900 nm. An angular filter array (AFA) consisting of a series of parallel micro-channels was placed between the sample and the imaging spectrometer. The AFA preferentially selected for ballistic and quasi-ballistic (snake) photons, which retain their original trajectories and rejected scattered photons to a large extent.

Results: The hyperspectral imager was able to acquire hyperspectral 2 cm line scans of the trans-illuminated tissue specimens, which were built up into 3D data cubes by mechanically scanning over the tissue sample. As a proof of concept, spectral data cubes acquired from the tissue samples were input into principal component analysis and linear discriminant analysis (PCA- LDA). The resulting maps provided visible discrimination between normal fat and cancerous tissue.

Conclusion: We have developed a hyperspectral transillumination imager which mostly accepts non and weakly scattered photons to form hyperspectral shadowgrams. The PCA-LDA analysis results suggested that the system could be used to distinguish between normal and

cancerous tissues obtained from lumpectomy procedures. We propose that the transformation vectors acquired from the training set can be used to construct a set of classifiers to enable tumor detection in samples representative of the surgical margin.

8587-28, Session 4

Interplay between inflammatory cells and demyelination in a model of multiple sclerosis

Benoit Aubé, Ctr. de Recherche de l'Univ. Laval Robert-Giffard (Canada) and Ctr. d'optique, photonique et laser (Canada) and Univ. Laval (Canada); Yves De Koninck, Steve Lacroix, Ctr. de Recherche de l'Univ. Laval Robert-Giffard (Canada) and Univ. Laval (Canada); Daniel Côté, Ctr. de Recherche de l'Univ. Laval Robert-Giffard (Canada) and Ctr. d'optique, photonique et laser (Canada) and Univ. Laval (Canada)

The infiltration of blood-derived inflammatory cells as well as the recruitment and activation of resident microglia into the central nervous system (CNS) are critical components of the immune response taking place over the course of Multiple Sclerosis (MS). Differentiating monocytes (macrophages) and microglia both possess the potential to be destructive agents to axons and their insulating myelin sheaths, hallmarks of the disease and its animal model, EAE. However, the absence of a specific marker for discriminating both cell populations in vivo has hindered their simultaneous investigation.

We use the EAE model in the lysM-eGFP mouse strain, in which blood-borne myeloid cells express eGFP. This allows us to look specifically at their role in the demyelinating process with minimal disturbance to their environment. The results obtained thus far demonstrate that the latter accumulate in the meninges at the early stages of the physical disabilities, with earlier appearance on the ventral region of the spinal cord. In order to visualize myelin, or the lack thereof, we use CARS microscopy. This label-free technique takes advantage of the endogenous contrast provided by the lipid content of myelin, thereby allowing to monitor with maximum context its health status. Combining these modalities with chronic in vivo imaging, we characterize the interplay between the potential destructive agents and their targets during the onset of the pathology. Immunohistochemistry for microglial markers, such as iba-1, is also performed to describe their activation status relatively to the presence of lesions or cellular infiltrates.

8587-29, Session 4

In vivo skin chromophore mapping using a multimode imaging dermoscope (SkinSpect™)

Nicholas B. MacKinnon, Fartash Vasefi, Eugene Gussakovsky, Gregory H. Bearman, Daniel L. Farkas, SMI (United States)

Purpose: To evaluate the performance of a new multimode dermoscope (SkinSpect™) for extracting skin chromophore concentrations in vivo.

Materials and methods: Our SkinSpect™ imaging system combines fluorescence, polarization control and hyperspectral imaging technologies with >35 wavelength bands (450 - 1000 nm). The reflected photons are divided in collinear and cross polarized image paths and the hyperspectral data sets are stored for further analysis. Multiple volunteer normal skin samples with pigmented mole regions are imaged.

Results: Pseudo-optical density data-cubes were input to a wavelength dependent linear model to extract the relative contribution of light scattering and chromophores according to Beer-Lambert. The total hemoglobin concentration, oxygen saturation, concentrations of eumelanin, pheomelanin and optical pathlength by the proposed algorithm using collinear and cross polarization data cubes were compared for normal and pigmented mole regions. The extracted optical properties are compared to diffuse reflectance point spectroscopy with source-detector separated fiber optic probe and high resolution spectrometer.

Conclusion: We built, characterized and used SkinSpect™ polarization-sensitive hyperspectral imager for in vivo skin analysis. The acquired reflection spectral image sets from skin samples suggest that the system is useful for extracting and quantifying scattering and chromophore concentrations in tissues, in a topologically resolved manner.

8587-30, Session 4

In vivo hyperspectral imaging in the extended near infrared (800 -1600 nm)

Mikhail Y. Berezin, Qian Cao, Steven Wang, Natalia Zhegalova, Walter J. Akers, Washington Univ. School of Medicine in St. Louis (United States)

To minimize scattering and absorption of photons in deep tissues while increasing the penetration depth, we explored the feasibility of imaging in the previously unexplored extended NIR spectral region at 800 - 1600 nm. This region, also known as Optical Window II, is weakly dominated by absorption of water and free from other endogenous chromophores, leaving this spectral range absorption transparent with virtually no autofluorescence. To investigate the applicability of the Optical Window II in bioimaging we build a scanning imager featuring a fiber-optic based, linear-diode array with a detector aligned with a broad light source in transmission geometry. Based on the differences in depth penetration of photons with various energies in the tissue, we developed an algorithm for processing the acquired 3D "datacube". The obtained images of a mouse head revealed sufficient resolution and anatomical structures consistent with the anatomy of the mouse brain. The potential of contrast enhanced imaging using optical contrast probes absorbing and emitting in extended NIR range is also discussed.

8587-31, Session 4

An aberration free spectrograph for improved imaging and spectra of biological samples

Brian C. Smith, Jason McClure, Princeton Instruments (United States)

Traditional Czerny-Turner (CT) imaging spectrographs suffer from optical aberrations including field astigmatism, spherical aberration, and coma that reduce spectral and spatial resolution and diminish the usable portion of the instrument's focal plane array detector. We have developed a novel variant of the traditional CT spectrograph, called the Schmidt-Czerny-Turner (SCT) spectrograph, which is astigmatism free and with greatly reduced levels of spherical aberration and coma. The improved spectral and spatial resolution of this spectrograph gives crisper, cleaner images of samples, and improved signal-to-noise ratios for spectral measurments such as Raman spectroscopy. It will be shown how the high quality data generated by this spectrograph is used to learn more about biological samples such as tissues and cells.

8587-32, Session 5

Single-shot multispectral quantitative phase microscopy

Niyom Lue, Jeon Woong Kang, Timothy R. Hillman, Ramachandra R. Dasari, Zahid Yaqoob, Massachusetts Institute of Technology (United States)

Quantitative phase imaging (QPI) [1,2] is a technique for accurately measuring the structure and function of transparent biological samples without the addition of extrinsic contrast agents. In the last few years, QPI has gained acceptance as a new label-free tool for studying cellular

processes such as nerve displacement during an action potential [3], single cell volume measurements [4], cell growth [5], and dynamics of pathogen infection [6,7].

Typically, conventional QPI acquires sample's two-dimensional optical-path-length profile at a single wavelength; it therefore lacks the ability to provide molecular-specific information, limiting the range of biological problems to which it can be applied. In this context, multi-spectral QPI can be used for optical dispersion measurements of biological samples, which can in turn provide the information about the underlying biochemical state of the sample. Moreover, multi-spectral QPI can also be used to advance mathematical modeling of light scattering and absorption, and to improve the image quality in high-resolution optical imaging systems. Recent efforts in this regard include the development of wide-field QPI based on serial selection of wavelengths [8]. Simultaneous two- and three-wavelength QPI based on Mach-Zehnder configurations has also been demonstrated [9,10].

In this paper, we will report the development of a single-shot common-path multi-spectral phase microscope with the capability to acquire wide-field quantitative phase information of a sample under observation at multiple wavelengths simultaneously. Using this proposed spectroscopic phase microscopy system, comprehensive and direct measurement of the average refractive index of live cells as a function of wavelength will be demonstrated.

References:

[1] P. Ferraro, A. Wax, and Z. Zalevsky, Coherent Light Microscopy: Imaging and Quantitative Phase Analysis, 1st edition (Springer, New York, 2011).

[2] G. Popescu, Quantitative Phase Imaging of Cells and Tissues, 1st edition (McGraw, Hill New York, 2011).

[3] C. Fang-Yen, M. C. Chu, H. S. Seung, R. R. Dasari, and M. S. Feld, Opt. Lett. 29, 2028 (2004).

[4] C. L. Curl, C. J. Bellair, P. J. Harris, B. E. Allman, A. Roberts, K. A. Nugent, and L. M. Delbridge, Cell Physiol. Biochem. 17, 193 (2006).

[5] M. Mir, Z. Wang, Z. Shen, M. Bednarz, R. Bashir, I. Golding, S. G. Prasanth, and G. Popescu, Proc. Natl. Acad. Sci. U. S. A. 108, 13124 (2011).

[6] Y. K. Park, M. Diez-Silva, G. Popescu, G. Lykotrafitis, W. S. Choi, M. S. Feld, and S. Suresh, Proc. Natl. Acad. Sci. U. S. A. 105, 13730 (2008).

[7] S. Lee, Y. R. Kim, J. Y. Lee, J. H. Rhee, C. S. Park, and D. Y. Kim, J. Biomed. Opt. 16, 036004, (2011).

[8] Y. Park, T. Yamauchi, W. Choi, R. Dasari, and M. S. Feld, Opt. Lett. 34, 3668 (2009).

[9] C. J. Mann, P. R. Bingham, V. C. Paquit, and K. W. Tobin, Opt. Exp. 16, 9753 (2008).

[10] M. T. Rinehart, N. T. Shaked, N. J. Jenness, R. L. Clark, and A. Wax, Opt. Lett. 35, 2612 (2010).

8587-33, Session 5

Stoichiometric FRET imaging by fluorescence lifetime excitation-emission matrix confocal microscopy

Ming Zhao, College of Optical Sciences, The Univ. of Arizona (United States); Sung-Eun Kim, Boston Children's Hospital (United States) and Harvard Medical School (United States); Xi He, Children's Hospital Boston (United States) and Harvard Medical School (United States); Leilei L. Peng, College of Optical Sciences, The Univ. of Arizona (United States)

Macromolecular interactions play a central role in the complex cellular machineries of all living organisms. Among various techniques for studying molecular interactions, Förster resonant energy transfer (FRET) is unique in its ability to measure intra- and inter-molecular distances in vivo within 10 nm. However, quantification FRET results often suffer from large spatial and cell-to-cell heterogeneity due to concentration heterogeneity of donors and acceptors. We report a novel imaging method, named fluorescence lifetime excitation-emission matrix (FLEEM) confocal microscopy to perform stoichiometric fluorescence lifetime imaging of FRET. Operated under the principle of Fourier multiplexed lifetime spectroscopy [1], FLEEM acquires confocal lifetime images of all three excitation-emission combinations of a dual-labeled FRET sample (donor, acceptor and FRET synthetized emission) in parallel. We demonstrate the FLEEM analysis of co-existing homo- and hetero-FRET through stoichiometric analysis of the oligomerization/polymerization of Axin, a negative regulator of the Wnt signaling pathway [2]. The oligomerization or polymerization of the Axin scaffolding protein is observed through two-color FRET of GFP-Axin and Axin-mCherry. GFP quenching due to homo- and hetero- FRET in Axin oligomer or polymer are simultaneously quantified in highly heterogeneous cell population.

[1] M. Zhao and L. Peng, "Multiplexed fluorescence lifetime measurements by frequency-sweeping Fourier spectroscopy," Optics Letters 35, 2910 (2010).

[2] B. T. Macdonald, K. Tamai, and X. He, "Wnt ?-Catenin Signaling: Components, Mechanisms, and Diseases," Developmental Cell 17, 9-26 (2009).

8587-34, Session 5

Quantifying the optical properties and chromophore concentrations of turbid media using polarization sensitive hyperspectral imaging: optical phantom studies

Fartash Vasefi, SMI (United States); Rolf B. Saager, Anthony J. Durkin, Beckman Laser Institute and Medical Clinic (United States); Nicholas B. MacKinnon, Eugene Gussakovsky, Daniel L. Farkas, SMI (United States)

Purpose: To determine the performance of a polarization-sensitive hyperspectral imaging system for extracting scattering properties and chromophore concentrations from tissue-mimicking phantoms.

Materials and methods: A hyperspectral imaging system employs spectrally-programmable linearly-polarized light source in the wavelength range 500nm - 950 nm. The diffusely reflected photons are separated in collinear and cross polarized image paths and the hyperspectral data sets are stored for further analysis. A fabrication process is presented for polydimethylsiloxane-based phantoms with titanium dioxide as a scattering agent and mixture of coffee, nigrosin, and naphtol green pre-characterized using an integrating sphere with spectrometer setup. Phantoms were produced with both smooth and rough textured surfaces.

Results: Multiple tissue-mimicking phantoms with various scattering and absorption levels were fabricated for optical system calibration and performance testing. The absorption and scattering levels were designed to mimic the optical properties of normal skin as well as pigmented light and dark moles. Phantom properties were characterized and validated using a two-distance, broadband frequency-domain photon migration system. Pseudo-optical density data-cubes were input to a wavelength dependent linear model to extract the relative contribution of light scattering and chromophores according to Beer-Lambert. The extracted chromophore and scattering values by the proposed algorithm using collinear and cross polarization data cubes were compared for different surface textures.

Conclusion: We have built and used a polarization sensitive hyperspectral imager for tissue imaging. The acquired reflection spectra results from tissue-mimicking phantoms suggest that the system is useful for extracting and quantifying scattering and chromophore concentrations in tissues.

8587-35, Session 5

High throughput 3D widefield spectral imaging based on HiLo microscopy and imaging fourier transform spectrometer

Heejin Choi, Peter T. C. So, Massachusetts Institute of Technology (United States)

We have developed a depth resolved wide field spectral imaging system for high throughput imaging cytometry. This system is designed to acquire 3D image stack of 1000 adherent cells per second. At this rate, one million cells can be acquired in 20 minutes providing statistical power similar to flow cytometry but with significantly greater structural information. This device was realized by combining several key components. First, the depth resolved widefield imaging is implemented with HiLo microscopy first proposed by the Mertz group. This method requires only two images to generate depth-resolved image increasing speed with minimal sensitivity to motion artifacts. Second, the high speed depth scanning is implemented using the remote depth scanning scheme first proposed by the Wilson group. Conventional depth resolved imaging by scanning the objective lens is limited in its bandwidth due to the heavy weight of the objective lens. However, in this technique, the depth scanning is performed by moving small mirror, which substantially increase the speed of the depth scanning. In addition, the large field of view, high NA objective lens and the recently introduced large pixelation, high frame rate sCMOS camera enables high resolution images of a large population of cells at the same time. For the wide field spectroscopic resolved imaging, we further implemented a Fourier transform imaging spectrometer using a Sagnac design. This system combines the advantages of high speed flow cytometer with structural information 3D microscopy.

8587-36, Session 5

Quantitative functional assessment of tumor microenvironment using photoacoustic imaging in pre-clinical breast tumor model

Melissa Yin, Sunnybrook Health Sciences Ctr. (Canada); Minalini Lakshman, VisualSonics Inc. (Canada); F. Stuart Foster, Sunnybrook Health Sciences Ctr. (Canada) and Univ. of Toronto (Canada)

Altered tumor microenvironment confers with aggressive cancer phenotype, and photoacoustic (PA) imaging combined with contrast enhanced ultrasound (CE-US) can track this phenotype in vivo in a non-invasive manner. This study investigates changes in oxygen saturation and tumor perfusion as a measure of altered tumor microenvironment, and validates the sensitivity of PA and CE-US with histology.

Primary orthotopic tumors were surgically implanted in nude SCID mice using the 231/LM2-4 breast cancer cell line. Mice with tumors of an approximate volume of 200mm3 were given either a single dose of 50mg/kg of Oxi-4503 or 0.9% saline. US imaging was performed using the VevoLAZR system with integrated PA probe at 21MHz; pre-, and 4 and 48 hours post-vascular shut down. Relative tissue oxygen saturation was measured with PA imaging, and indices of relative blood volume and flow was assessed with CE-US. Post-sacrifice, tumour tissue was excised and fixed for histology.

Functional changes in the tumor vasculature were evident at 4 hours post-treatment as shown by a decrease in blood volume (-77%), flow (-72%), and oxygen saturation (-9%). Histological confirmation of subsequent molecular changes included positive CD31 staining for vessels and CA9 staining for hypoxia at the tumor core. While functional changes persisted with further decrease in oxygen saturation (-16%), histology confirmed hypoxia closer to the tumor periphery at 48 hours post-treatment. This may have resulted from the development of a necrotic tumor core. Taken together, PA imaging and CE-US are potentially a sensitive tool for quantitative functional assessments of breast tumor models.

8587-37, Session 6

Mesenchymal stem cell interactions with 3D ECM modules fabricated via multiphoton excited photochemistry

Paul J. Campagnola, Ping-Jung Su, Quyen A. Tran, Jimmy Fong, Kevin W. Eliceiri, Univ. of Wisconsin-Madison (United States); Brenda M. Ogle, Univ. of Wisconson-Madison (United States)

To understand complex micro/nanoscale ECM stem cell interactions, reproducible in vitro models are needed that can strictly recapitulate the relative content and spatial arrangement of native tissue. Additionally, whole ECM proteins are required to most accurately reflect native binding dynamics. To address this need, we use multiphoton excited (MPE) photochemistry to create 3D whole protein constructs or “modules” to study how the ECM governs stem cell migration. Similar to MPE fluorescence microscopy, MPE photochemistry has intrinsic 3-dimensionality with submicron fabrication capabilities. Here “modules” in the form of a series of arch-like structures were created to provide a 3D environment, into which mesenchymal stem cells (MSCs) could migrate and proliferate. The modules, designed using a rapid prototype approach, were created from mixtures of BSA/laminin (LN) and BSA alone, whose comparison afforded studying how the migration dynamics are governed from the combination of morphological and ECM cues. We characterized the pore size properties by electron microscopy and also swell-shrinking analysis and found they were similar for both compositions. We found that MSCs interacted for significantly longer durations with the BSA/LN constructs than pure BSA, pointing to the importance of binding cues of the LN. Time-lapse videos showed that MSCs successfully proliferated inside the modules. Critical to this work was the development of an automated system with feedback based on fluorescence imaging to provide quality control when synthesizing multiple identical constructs. We suggest this approach could be used to induce stem cell differentiation into desired lineages.

8587-38, Session 6

Real-time image processor for detection of rare cells and particles in flow at 37 million line scans per second

Ali Ayazi, Keisuke Goda, Cejo K. Lonappan, Jost Adam, Jagannath Sadasivama, Daniel R. Gossett, Elodie Sollier, Ali M. Fard, Soojung Claire Hur, Coleman Murray, Chao Wang, Nora Brackbill, Dino Di Carlo, Bahram Jalali, Univ. of California, Los Angeles (United States)

Optical microscopy is the gold standard for cell and tissue-based diagnostics and identification of rare cancer cells in blood. Combination of microscopy with a method for delivering focused fast moving cells holds great promise for screening of large cell populations. However, due to its low throughput, conventional microscopy is incapable of providing large enough data sets needed to identify rare cell subpopulations without pre-concentration. This is due to the limited frame rate and shutter speed of continuous-running cameras needed for this purpose, as well as lack of hardware and software that can capture and process millions of images per second in real-time. Low throughput limits the number of cells that can be analyzed and, due to Poisson noise, compromises the statistical accuracy.

In this paper, we describe a real-time image processor that has enabled a new automated flow through microscope to screen cells in flow at 100,000 cells/s with a record false positive rate of one in a million. This unit is integrated with an ultrafast optical imaging modality known as serial time-encoded amplified microscopy (STEAM) for blur-free imaging of particles in high-speed flow. We show real-time image-based identification and screening of budding yeast cells and rare breast cancer cells in blood. The system generates E-slides (an electronic version of glass slides) on which particles of interest are digitally analyzed.

8587-39, Session 6

Dual wavelength diffuse fluorescence flow cctometer for detecting and localizing rare circulating cells in mice in vivo

Noah Pestana, Vivian E. Pera, Dwayne Vickers, Shashi K. Murthy, Northeastern Univ. (United States); Charles P. Lin, Massachusetts General Hospital (United States) and Harvard Medical School (United States); Mark J. Niedre, Northeastern Univ. (United States)

There are many areas in biomedical research where it is important to quantify rare cells in circulation in small animals, for example in the study of early-stage metastasis of cancer. Although a number of cell enumeration strategies are presently used for this (including extraction of peripheral blood samples or in vivo flow cytometry) more sensitive tools are required to non-invasively detect and count very rare circulating cell populations. We recently developed a new approach to this problem, termed “diffuse fluorescence flow cytometry” (DFFC) that potentially offers orders of magnitude improvement in sensitivity since it allows detection and localization of individual fluorescently-labeled cells from relatively large tissue volumes – with relatively large blood vessels - in a mouse tail or hind-limb.

In this presentation, we discuss recent advances in our instrument and data processing approaches that have improved the detection sensitivity and tomographic imaging accuracy compared to our previous prototype. In particular, mouse limbs were illuminated with dual sequentially modulated 640 nm lasers and an array of six optodes coupled to photomultiplier tube detectors operating in photon counting mode. Each optode utilized concurrent dual-wavelength detection for estimation and removal of autofluorescence and movement artifacts. Use of rapidly acquired tomographic data sets allowed localization of cells in the limb cross section with 100-200 ?m accuracy using sparse image reconstruction strategies. Most recently we demonstrated the high detection sensitivity of our DFFC instrument by detection of less than 1e4 cells per mL fluorescently-labeled Mesenchymal Stem Cells in nude mice in vivo.

8587-40, Session 7

High-speed multispectral confocal imaging *(Invited Paper)*

Gary E. Carver, Sarah A. Locknar, William A. Morrison, Omega Optical, Inc. (United States); Daniel L. Farkas, SMI (United States)

A new approach for generating high-speed multispectral images has been developed. The central concept is that spectra can be acquired for each pixel in a confocal spatial scan by using a fast spectrometer based on optical fiber delay lines. Since the spectrometer is fiber-based, the face of the entrance fiber can act as the pinhole in a confocal microscope. This concept merges fast spectroscopy with standard spatial scanning to create datacubes in real time. The spectrometer is based on a serial array of reflecting spectral elements, delay lines between these elements, and a single element detector. After excitation by a laser pulse, broadband fluorescence from a biological tissue sample propagates into the array, light of the first wavelength band reflects from the first element, and light of the Nth wavelength band reflects from the Nth element. Each wavelength is mapped into a specific time slot. The spectral elements can be fabricated in two ways - fiber tips can be coated with interference filters to create 10 to 20 nm wide spectral slices, while fiber Bragg gratings can be written into the fiber core to create 1 to 2 nm wide spectral slices. Most spectrometers employ one grating that disperses light spatially across N detectors or pixels. Our approach employs N tips or gratings that distribute the light temporally against one detector. The spatial, spectral, and temporal resolution of the instrument is described including multispectral images of laser-induced fluorescence. (Funded by NIH Grant 5R44CA124036-03)

8587-41, Session 7

Mesoporous silica nanoparticles for treating spinal cord injury at the single cell level *(Invited Paper)*

Desiree White, Riyi Shi, James F. Leary, Purdue Univ. (United States)

An estimated 12,000 new cases of spinal cord injury (SCI) occur every year in the United States. A small oxidative molecule responsible for secondary injury, acrolein, is an important target in SCI. Acrolein attacks essential proteins and lipids, creating a feedforward loop of oxidative stress in both the primary injury area and the surrounding areas. A small molecule used for hypertension, hydralazine, has been found to “scavenge” acrolein after injury, but its delivery and short half-life hinder its application for SCI. Nanomedical systems broaden the range of therapeutic availability and efficacy over conventional medicine. They allow for targeted delivery of therapeutic molecules to cells and tissues of interest, reducing side effects of wayward therapies in unwanted areas. Nanoparticles made from silica form porous networks that can carry therapeutic molecules throughout the body. To attenuate the acrolein cascade and improve therapeutic availability, we have used a one-step, modified Stober method to synthesize two types of silica nanoparticles. Both particles are stealth-coated with poly(ethylene) glycol (PEG), which is also a therapeutic agent for SCI by facilitating membrane repair. One nanoparticle type contains an amine-terminal PEG (SiNP-mPEG-Am) and the other possesses a terminal hydrazide group (SiNP-mPEG-Hz). The former allows for exploration of hydralazine delivery, loading, and controlled release. The latter group has the ability to react with acrolein, allowing the nanoparticle to scavenge directly. The nanoparticles have been characterized and will be explored using neuronal PC-12 cells in vitro, demonstrating the potential of novel silica nanoparticles for use in attenuating secondary injury to single cells after SCI.

8587-42, Session 7

AFM combined with near field techniques for probing trans-membrane protein dynamics

Sina Amini, Texas A&M Univ. (United States); Zhe Sun, Gerald A. Meininger, Univ. of Missouri-Columbia (United States); Kenith E. Meissner, Texas A&M Univ. (United States)

Trans-membrane protein dynamics in cell signaling is studied using evanescent wave (EW) and Förster Resonance Energy Transfer (FRET) techniques. These methods provide different axial resolutions (~100 nm for EW and ~10 nm for FRET) and are used to axially limit the collection region to near-membrane and trans-membrane proteins. In these experiments, Quantum Dot (QD) modified microspheres are coated with fibronectin and brought into contact with HeLa cells possessing red fluorescent protein (RFP) labeled integrin. Upon binding of fibronectin to integrin and activation of integrin leading to formation of focal adhesions, fluorescent signals are collected using the EW and FRET techniques. For FRET measurements, the photobleaching technique is used. QDs are coated on the surface of 5 µm silica microspheres and HeLa cells are labeled with RFP-integrin constructs. In this case, QDs serve as the donors and RFP serve as the acceptors in the FRET pair. For the EW technique, QDs are embedded inside 10 µm polystyrene microspheres where whispering gallery modes are generated by the micro-spherical cavity. The EW generated at the surface of the cavity is used to excite the RFP-labeled integrins and the signal is collected by an EMCCD. Atomic Force Microscopy (AFM) is used in conjunction with the optical techniques to control the sample contact area and pressure. In both methods, the modified microsphere is mounted on an AFM cantilever which provides mobility to the micro-spherical probe. The results obtained from both methods show the clustering and activity of the integrins and are in good agreement with each other.

8587-43, Session 7

Large-field-of-view chip-scale Talbot fluorescence microscopy

Shuo Pang, Chao Han, Changhuei Yang, California Institute of Technology (United States)

The fluorescence microscope is one of the significant tools in modern clinical diagnosis and biological science. However, its expense, size, and field-of-view (FOV) are becoming the bottlenecks in some key applications, such as large-scale phenotyping and low-resource-setting diagnostics. In this work, we demonstrate a fluorescence chip-scale microscopy method, termed Fluorescence Talbot Microscopy (FTM), which is based on the Talbot effect. The FTM method utilizes the Talbot effect to project a grid of focused excitation light spots onto the sample. The sample rests on a filter-coated CMOS sensor chip. The fluorescence emissions associated with each focal spot are collected by the sensor chip and are composed into a sparsely sampled fluorescence image. By raster scanning the Talbot focal spot grid across the sample and collecting a sequence of sparse images, we can then reconstruct a filled-in high-resolution fluorescence image. In contrast to a conventional microscope, the collection efficiency, resolution, and FOV are not tied to each other for this technology. The FOV of FTM is directly scalable. Our FTM prototype has a demonstrated resolution of 1.2 ?m, and a collection efficiency equivalent to a conventional microscope with a 0.70 N.A. objective. Its FOV is 3.9?3.5 mm2, which is 100 times larger than that of a 20X/0.4 N.A. conventional microscope objective. Due to its large FOV, high collection efficiency, compactness, and its potential for integration with other on-chip devices, FTM is suitable for diverse applications, such as point-of-care diagnostics, large-scale functional screens, and long-term automated imaging.

8587-44, Session 7

Optical quantification of cellular mass, volume, and density of circulating tumor cells identified in an ovarian cancer patient

Kevin G. Phillips, Oregon Health & Science Univ. (United States); Carmen Ruiz Valesco, Julia Li, Anand Kolatkar, Madelyn Luttgen, The Scripps Research Institute (United States); Kelly Bethel, Bridgette Duggan, Scripps Health (United States); Peter Kuhn, The Scripps Research Institute (United States); Owen J. T. McCarty, Oregon Health & Science Univ. (United States)

Cancer metastasis, the leading cause of cancer-related deaths, is facilitated in part by the hematogenous transport of circulating tumor cells (CTCs) through the vasculature. Clinical studies have demonstrated that CTCs circulate in the blood of patients with metastatic disease across the major types of carcinomas, and that the number of CTCs in peripheral blood is correlated with overall survival in metastatic breast, colorectal, and prostate cancer. While the potential to monitor metastasis through CTC enumeration exists, the basic physical features of CTCs remain ill defined and moreover, the corresponding clinical utility of these physical parameters is unknown. To elucidate the basic physical features of CTCs we present a label-free imaging technique utilizing differential interference contrast (DIC) microscopy to measure cell volume and to quantify sub-cellular mass-density variations as well as the size of subcellular constituents from mass-density spatial correlations. DIC measurements were carried out on CTCs identified in a breast cancer patient using the high-definition (HD) CTC detection assay. We compared the biophysical features of HD-CTC to normal blood cell subpopulations including leukocytes, platelets, and red blood cells. HD-CTCs were found to possess larger volumes, decreased mass-density fluctuations, and shorter-range spatial density correlations in comparison to leukocytes. Our results suggest that HD-CTCs exhibit biophysical signatures that might be used to potentially aid in their detection and to monitor responses to treatment in a label-free fashion. The biophysical parameters reported here can be incorporated into computational models of CTC-vascular interactions and in vitro flow models to better understand metastasis.

8587-45, Session 7

Nano-confined protein anchors structured by STED lithography probed by dSTORM

Jaroslaw Jacak, Richard Wollhofen, Johannes Kepler Univ. Linz (Austria); Kurt Schilcher, Upper Austria Univ. of Applied Sciences (Austria); Thomas A. Klar, Johannes Kepler Univ. Linz (Austria)

The ability to place individual proteins into nano-confined spaces plays a constantly growing role in bioscience, from basic studies in biology to the development of nanosensoric devices. One of the possibilities to generate submicrometer sized structures is direct laser writing lithography (DWL), a process which can be enhanced by stimulated emission depletion (STED) lithography for assembly of polymeric structures down to several tens of nanometers in any desired geometry [1, 2]. The fluorescent properties of the photoinitiators can be used for an quantification of the structure size via STED microscopy. The structures show good biocompatibility and allow an easy biofuctionalzation with proteins down to a single protein level. For characterization of the binding properties of proteins to the polymer nano-structures, we use direct stochastic optical reconstruction microscopy (dSTORM), which enables determination of protein cluster properties at a nanoscale level [3]. Combining the STED lithography/imaging with dSTORM fluorescent microscopy approach allows us to produce well characterized, biocompatible structures, applicable to many biological assays.

1. Klar, T.A., et al., Fluorescence microscopy with diffraction resolution barrier broken by stimulated emission. Proc Natl Acad Sci U S A, 2000. 97(15): p. 8206-10.

2. Fischer, J., G. von Freymann, and M. Wegener, The materials challenge in diffraction-unlimited direct-laser-writing optical lithography. Adv Mater. 22(32): p. 3578-82.

3. van de Linde, S., et al., Multicolor photoswitching microscopy for subdiffraction-resolution fluorescence imaging. Photochem Photobiol Sci, 2009. 8(4): p. 465-9.

8587-46, Session 7

in situ 3D monitoring of collagen fibrillogenesis using SHG microscopy

Stéphane Bancelin, Ecole Polytechnique (France) and Ctr. National de la Recherche Scientifique (France) and INSERM (France); Vaia Machairas, Etienne Decencière, Mines ParisTech (France); Claire Albert, Univ. Pierre et Marie Curie (France) and Collège de France (France) and CNRS (France); Thibaud Coradin, Carole Aimé, Univ. Pierre et Marie Curie (France) and Collège de France (France) and Ctr. National de la Recherche Scientifique (France); Marie-Claire Schanne-Klein, Ecole Polytechnique (France) and Ctr. National de la Recherche Scientifique (France) and INSERM (France)

Type I collagen is synthesized by cells as triple helices that self-assemble into fibrils in vivo and in vitro to form three-dimensional networks. Thorough characterization of collagen fibrillogenesis is crucial to understand the biological mechanisms of tissue formation and tissue remodeling and to design new biomaterials. In this study, we developed time-lapse in situ Second Harmonic Generation (SHG) microscopy to continuously monitor the formation of collagen fibrils [Bancelin et al, Biomed. Opt. Express 2012]. Fibrillogenesis was triggered in a controlled way by increasing the pH in a dilute solution of collagen I from rat tail. We then performed time-lapse SHG imaging for a few hours and quantified the increase of the fibril density in the imaged volume. Our results showed reproducible dynamics of fibrillogenesis that could be changed by tuning the pH. We also monitored the growth of single fibrils and

quantified the length increase over time, which has never been reported before using an optical technique. Finally, we investigated surface-mediated fibrillogenesis by adding silica nanoparticles to the solution. We used Two-Photon excited fluorescence (2PEF) microscopy to visualize the stained nanoparticles and quantified the self-assembly of collagen around these nanoparticles.

Compared to confocal microscopy, SHG microscopy advantageously exhibits greater structural specificity for fibrillar collagen and can be easily combined to 2PEF. Compared to electron microscopy, it advantageously exhibits a larger field of view and enables in situ visualization of samples in solution. SHG microscopy is therefore a powerful technique for in situ monitoring of collagen fibrillogenesis, in a non invasive way.

8587-47, Session 7

Real time blood testing using quantitative phase imaging

Hoa V. Pham, Univ. of Illinois at Urbana-Champaign (United States); Krishnarao V. Tangella, Christie Clinic (United States) and Univ. of Illinois at Urbana-Champaign (United States); Gabriel Popescu, Univ. of Illinois at Urbana-Champaign (United States)

We demonstrate a quantitative phase imaging system used for blood screening which reconstructs phase images, analyzes and calculates many morphology parameters of red blood cells at single cell level, all in real time. The system is capable of very high throughput imaging which allows imaging easily several thousand cells per sample. We measured blood samples of a healthy patient and patients with macrocytic and microcytic anemia. The resulted MCV distributions show an excellent agreement with results from Beckman-Coulter counter. Furthermore, we show statistics of several other morphology parameters, which are unavailable with current automatic analyzers used in clinical settings.

8587-48, Session 7

Quantitative birefringence imaging using quadra-wave interferometry

Sherazade Aknoun, Institut Fresnel (France) and PHASICS S.A. (France); Pierre Bon, Serge Monneret, Institut Fresnel (France); Benoit F. Wattellier, PHASICS S.A. (France)

Phase contrast imaging can be considered as a powerful method for the label-free imaging of semi-transparent biological samples. Recent techniques not only improve image contrast but give access to a quantitative measurement of optical thickness.

Changes in the refractive index inside the samples are the main contrast sources in living cells. However some biological structures inside cells are optically anisotropic and thus scatter light differently depending on the illumination light polarization. In polarized light microscopy, the contrast created by anisotropic elements has been widely used to reveal ordered fibrous structures of biological samples without any staining or labelling. So, measurement of phase shifts introduced with different incident polarization angles, on an anisotropic sample, would give access to quantitative values of both its linear birefringence and preferential orientation of its optical axes.

We propose here to use a quadri-wave lateral shearing interferometer wave front sensor to measure a set of polarization-dependent phase shifts, in order to reveal collagen fibers and amyloid fibrils structure. This high-resolution wave front sensor is mounted on a commercial non-modified transmission microscope to measure characteristic optical path difference (OPD) of the sample [1]. A single rotating polarizer placed in the illumination light path before the sample allows to record one quantitative phase image for each excitation polarization angle. The set of those images is then numerically computed to obtain what we call “Quantitative Birefringence Images” which represents specific local birefringence and orientation of the sample. Results with collagen fibers and amyloid fibrils will be presented.

References :

[1] Pierre Bon, Guillaume Maucort, Benoit Wattellier and Serge Monneret, ``Quadriwave lateral shearing interferometry for quantitative phase microscopy of living cells,” Optics Express 17(15): 13080-13094 (2009).

8587-49, Session 7

Immunolabeling of latent fingermarks

Annemieke van Dam, Academisch Medisch Ctr. (Netherlands); Maurice C. Aalders, Univ. van Amsterdam (Netherlands); Ton G. Leeuwen, S.A.G. Lambrechts, Academisch Medisch Ctr. (Netherlands)

Fingermarks are an important type of evidence that can be found during criminal investigations. Nowadays, only the skin ridge pattern of the fingermark and DNA content are used for identification purposes. But a fingermark contains a lot more information that only thin skin ridge impression. The chemical composition of the mark is individual and contains specific profiling information of the donor. A method to identify the secretions from the donor is immunolabeling. Antibodies are able to detect specific components and can therefore by used to obtain additional information from fingermarks.

We investigated the use of different antibodies to detect multiple components in a single fingermark. Fluorophores were coupled to specific antibodies. Fluorescence microscopy was used to visualize the presence of fluorophores and thus the presence of the antigens. To proof the principle two general antigens were selected that can be found in almost all fingermarks, dermcidin and albumin. Dermcidin is an antimicrobial peptide and one of the most abundant proteins in sweat. Albumin is the most abundant protein in human serum.

Multiplex immunolabeling was performed successfully. Dermcidin and albumin could be detected simultaneously in single fingermarks. Additionally, high quality images could be obtained from the multiple labeled fingermarks, whereby the pore position and the ridge flow could be visualized and also can be used for identification purposes.

This method can be used to obtain additional information about the donor of the fingermark and can therefore be of great forensic value.

8587-50, Session 8

An XML based systems approach to a shared standard for cytometry and pathology

Robert C. Leif, Stephanie H. Leif, Newport Instruments (United States)

Purpose: To create a continuum of interoperable XML standards for flow and image cytometry that can be used by cytometry researchers and clinicians, primarily pathologists. Wherever possible, these standards should be based on existing standards, specifically those of the International Society for Advancement of Cytometry, ISAC, and Digital Imaging and Communication in Medicine, DICOM. In principle, the simplest and most efficient means to communicate the contents of XML metadata to humans is to encapsulate them in HTML5.

Methods: The schemas are written in the XML Schema Definition (XSD1.1) language and validated to demonstrate adherence to XSD1.1. Their content was tested by translating specific XSD elements into XML and filling in the values of the objects contained therein. The use of an element based implementation of relationships permits bidirectional and multiple relationships between two objects to be expressed. The use of XSD1.1 permitted XML elements to be interspersed in an XHTML5 page.

Results: An XML based system that includes the DICOM specified separation of series and instances and includes relationships has been created. Very preliminary data indicates that these XML data-types can be used with XHTML5, which would permit the creation of a medical

informatics system that has access to the full power of the Internet.

Conclusions: This design together with the use of an EPUB container could serve as a reliable efficient means for the transmission of research and medical data.

8587-51, Session 8

Quantitative segmentation of fluorescence microscopy images of heterogeneous tissue: application to the detection of residual disease in tumor margins

Jenna L. Mueller, Zachary T. Harmany, Jeffrey K. Mito, Joseph Geradts, David G. Kirsch, Rebecca M. Willett, Duke Univ. (United States); J. Quincy Brown, Tulane Univ. (United States); Nirmala Ramanujam, Duke Univ. (United States)

Fluorescent contrast agents combined with microscopy is a powerful technique to obtain images of tissue histology at the point-of-care, without the need for fixing and sectioning. The potential of these technologies lies in the identification of robust methods for image segmentation and quantitation, particularly in heterogeneous tissues. Most approaches within the microscopy community depend on subjective observer interpretation, gray level intensity information or setting a threshold at a particular intensity level to isolate features of interest. However, these simple schemes have limited utility in thick tissues that exhibit a high degree of non-uniform background heterogeneity. To address this important need, sparse component analysis (SCA) is applied to monochrome images of fluorescently-stained microanatomy to segment and quantify distinct tissue types. Unlike other image processing techniques, the strategy described here does not rely heavily on intensity information, which can be compromised by excess background signal or calibration errors. Additionally, SCA does not discard image content but rather retains all of the information inherent in the image to preserve spatial relationships between tissue types, which is essential for proper interpretation. SCA is demonstrated to be vastly superior to traditional thresholding, one of the most widely used methods of image segmentation to perform quantitative pathology. The clinical utility of our approach is demonstrated by imaging excised margins and the tumor bed in vivo in a cohort of mice after surgical resection of a sarcoma. Any clinical application in which the pathological state of disease needs to be assessed during a procedure could benefit from this combination of approaches.

8587-52, Session 8

Feature-based algorithms for predicting tissue necrosis using near-infrared fluorescence angiography

Gabriel Brat, Johns Hopkins Univ. (United States); Ravi Starzl, Carnegie Mellon Univ. (United States) and Johns Hopkins Univ. (United States); Alexandros Afthinos, Joani M. Christensen, Kate J. Buretta, Damon S. Cooney, W.P. Andrew Lee M.D., Gerald Brandacher, Justin M. Sacks M.D., Johns Hopkins Univ. (United States)

Near-infrared fluorescence imaging is an area of intense study in reconstructive surgery. This interest has been fueled by the fact that Indocyanine Green (ICG) is a versatile FDA-approved dye that can be used to detect poor tissue perfusion. This project aims to improve upon standard imaging analytics and design automated intra-operative algorithms to predict long-term tissue necrosis.

A cephalad-caudal 8x2cm random flap was created on the back of eight-week Lewis rats fitted with jugular venous ports. Dissection was performed to the muscle and a layer of silicone sheeting was placed at all sides of the flap and sutured into position. Near-infrared imaging using a commercially available device was performed after injection of approximately 0.05mg/kg of ICG. Imaging was performed at post-operative hour 2 and 3 and 7 days after surgery. At day 7, masks of tissue necrosis were generated to superimpose on intra-operative image stacks. Computational algorithms were iteratively optimized to analyze each voxel in relation to the ultimate tissue fate.

Retrospective optimization of intensity-based algorithms (baseline) led to a sensitivity and specificity of 82% and 83%, respectively, when evaluating poor perfusion border regions. Feature-based algorithms integrated novel curve-fitting and machine learning classifiers to differentiate voxels based on long-term tissue survival. These algorithms improved predictive capability by 10-20% to a maximum of 92% and 86% sensitivity and specificity, respectively.

Feature-based algorithms surpass intensity-based algorithms in their predictive capabilities in the rat model are now being validated using human imaging data.

8587-53, Session 8

Image processing for drift compensation in fluorescence microscopy

Steffen B. Petersen, International Iberian Nanotechnology Lab. (Portugal) and Aalborg Univ. (Denmark); Thiagarajan Viruthachalam, Isabel Coutinho, Gnana P. Gajula, International Iberian Nanotechnology Lab. (Portugal); Maria Teresa Neves-Petersen, International Iberian Nanotechnology Lab. (Portugal) and Aalborg Univ. (Portugal)

Fluorescence microscopy is characterized by low background noise, thus a fluorescent object appear as an area of high signal/noise. Here, we developed an image processing methodology in order to obtain an image with better resolution using the Zeiss LSM 780 confocal microscope. A total of 1000 images of a human embryonic kidney (HEK 293) cell nucleus labeled with Hoechst 33342 were acquired with a pixel size of 30 nm. The acquisition time for each image was approximately 1 second. The sub-pixel accuracy computed centroid track over 1000 frames indicates the single path direction with the drift of 510 nm along X-axis and 240 nm along Y-axis. Using these 1000 images, we can in principle measure drifts down to approximately 1 nm in size and a drift-compensated image can be reconstructed. Reconstructed image leads to better resolution in order to observe the fine details of the image. In principle we can only compensate for inter-image drift – thus the drift that takes place during the acquisition time for the individual image is not corrected. We believe our results are of general applicability in microscopy and other types of imaging. A prerequisite is the presence of a track-able object in the image. The present methodology was successfully applied to a simple spherical object and we believe that more complex objects such as microtubules may be tracked using other types of feature detection algorithms.

8587-54, Session 8

Automated segmentation of laser irradiated engineered skin in 3D OCT

Taeho Kim, Ulsan National Institute of Science and Technology (Korea, Republic of) and Univ. of Ulsan (Korea, Republic of); Jungbin Ahn, Areun Kim, Ulsan National Institute of Science and Technology (Korea, Republic of); Jeehyun Kim, Kyungpook National Univ. (Korea, Republic of); Woonggyu Jung, Ulsan National Institute of Science and Technology (Korea, Republic of)

The laser therapy of skin has become widely used for the treatment of acne and wrinkle. Major interest of current laser therapy is to achieve precise tissue removal, minimal side effect such as thermal damage, and fast healing process. However, mechanisms for laser-tissue interaction and healing improvement have not yet been completely. In order to

address fine laser therapy, it is required to observe and quantify the structure change of skin before and after laser irradiation. In this study, we developed the automated segmentation algorithm in 3D OCT images to monitor wound healing process of laser irradiated tissue. There already exist various automated segmentation methods in OCT images. However, most of works were focused on cornea and retina, and it has restriction to be applied to 3D random morphological change happening in wound healing process. Our method utilized typical segmentation process such as noise reduction, labeling algorithm, and edge detection. The most featured work is that whole process applies to the every horizontally and vertically acquired 2D OCT images, and the combination of the measured result generates the 3D voxel of holes. Since it compared two axis images simultaneously, it improves the accuracy to segmentation line along laser hole and pit. In order to evaluate the performance of our method, engineered skins were irradiated by Fraxel laser and analyzed by developed system and software. The accuracy of automated algorithm for volume segmentation was within a mean and median volume fraction of 5% compared to the volume measured by manual calculation.

8587-55, Session 8

Automatic cell nuclei counting: a protocol to acquire images and to compare results between color and multispectral images

Mohamed Bouzid, Univ. de Bourgogne (France) and Institut Supérieur de Biotechnologie de Sfax (Tunisia); Ali Khalfallah, Institut Supérieur de Biotechnologie de Sfax (Tunisia); André Bouchot, Univ. de Bourgogne (France); Mohamed-Salim Bouhlel, Institut Supérieur de Biotechnologie de Sfax (Tunisia); Franck S. Marzani, Univ. de Bourgogne (France)

The application described here is the cell nuclei or cell counting. High-throughput screening in histology and analysis need a necessary automatic cell counting. Current methods and systems based on grayscale or color images give results with counting errors. We suggest using multispectral imaging (with more than three bands) rather than color one for cells counting.

We considered two types of samples: a histological section of rat brain and one of rat colon carcinoma cells. For our experiment, we acquired color and multispectral images of 10 areas for each sample. We used a Programmable Light Source (PLS) capable of generating different wavelengths in the visible spectrum. So, one color image and four multispectral images have been acquired for each sample. The four multispectral images contained respectively 3 bands, 5 bands, 7 bands and 10 bands. To make a proper comparison of data, several considerations must have be taken, like camera linearity, intensity difference between the wavebands from the SLP and non uniformity of the light intensity range in the images. So, a set of measures were done for calibrating the system.

We chose to use an automatic counting method based on ellipse fitting and watershed on color images. An extension of this method is proposed in order to be applied to multispectral images. The original and the extended method are then applied to the data previously acquired to have first results regarding the effect of using multispectral images rather than color ones.

8587-57, Session 8

Retrieving spatio-temporal resolved Jones matrix using polarization holographic microscopy

Jaeduck Jang, YoungChan Kim, Joonwoo Jung, Mahn Won Kim, YongKeun Park, KAIST (Korea, Republic of)

Polarization is one of fundamental properties of light that illustrates the orientation of an oscillating electric-field. Polarization microscopy has been used for probing molecular structures and orientations in anisotropic materials. Generally polarization of light can be described in field-based formalism with Jones matrices with complex vectors, and thus, coherent light must be treated with Jones formalism rather than Stokes-Muller formalism which is based on the intensity-based framework. Recently, quantitative phase imaging techniques have been presented to quantitatively measure polarization sensitive phase information from birefringence samples. However, the Jones matrix information could not be extracted; the previous polarization sensitive holographic measurements have been thus used to retrieve birefringence phase and Strokes parameters. More recently, Z. Wang et al. reported the Jones phase microscopy (JPM) based on a Mach-Zehnder heterodyne interferometer, which can extract the spatially resolved Jones matrix for transparent and anisotropic samples However, JPM is not suitable for studying dynamics in birefringence samples since four measurements with different polarization states are required to extract one spatially resolved Jones matrix map.

Here, we present a novel field-based polarization microscopy technique, referred to as polarization holographic microscopy (PHM), capable of extracting the spatially resolved Jones matrix associated with anisotropic samples. PHM employs the principle of common-path interferometry to quantitatively retrieve both the amplitude and phase information of a polarized light field. More importantly, the spatially resolved Jones matrix information can be measured at a speed of 31 Hz. We demonstrate the features of PHM with quantitatively imaging the dynamics of liquid crystal droplets at a video rate.

8587-58, Session 9

Phase relief imaging with confocal laser scanning system

Tong Peng, Hao Xie, Yichen Ding, Peking Univ. (China); Weichao Wang, Shanghai Jiao Tong Univ. (China); Zhiming Li, Wenzhou Medical College (China); Dayong Jin, Macquarie Univ. (Australia); Yuanhe Tang, Xi'an Univ. of Technology (China); Qiushi Ren, Peng Xi, Peking Univ. (China)

Confocal laser scanning microscopy (CLSM) has become one of the most important biomedicalresearch tools today due to its noninvasive and 3-D abilities. It enablesimaging in living tissue with better resolution and contrast,andplays a growing role among microscopic techniquesutilized for investigatingnumerous biological problems.In some cases, the sample was phase-sensitive, thus we introduce a novel method named laser oblique scanning optical microscopy (LOSOM) which could obtain a relief image in transparent sample directly.

Through the LOSOM system, mouse kidney and Hela cells sample were imaged and 10x,20x and 40x magnify objective imaging resultswere realized respectively.Also, we comparedthe variation of pinhole sizeversus imaging result.One major paraments of LOSOM is the distance between fluorscence medium and the sample. Previously, this distance was set to 1.2 mm, which is the thickness of the slide.The experiment result showed that decreasing d can increase the signal level for LOSOM phase-relief imaging.To study this effect quantitatively, we set each depth of 0.17mm by designing a stack ofhollow coverglasses, andthe result demonstrated the signal strength versus the fluorescence medium distance.

8587-56, Session PMon

The development of high-speed confocal laser scanning microscopy

Sanghoon Choi, Yong J. Lee, Donghyeon Kwak, Ho Lee, Kyungpook National Univ. (Korea, Republic of)

The confocal laser scanning microscopy and two-photon microscopy was implemented based on a single laser source and an objective lens. And these laser scanning microscopes were made of two axis scanning

mirrors (polygonal rotating mirror or galvanometer mirror) for two dimensional laser beam scanning. The imaging speed of laser scanning microscopy was dependence on two dimension scanning speed. So, we develop the high speed confocal laser scanning microscopy and two-photon microscopy using the enhanced two dimension laser beam scanning system. The enhanced two dimension laser beam scanning system was consisted of polygon scanning mirror(x-axis) and galvanometer mirror(y-axis). The polygon scanning mirror has more number of mirror facets and better rotation speed. Moreover, the galvanometer mirror was able to scan the laser beam adjust to polygon mirror scanning speed. For the acquisition of image signal, we applied the photomultiplier tube which has high frequency bandwidth up to 50MHz. Along with we employ the practicable high sampling rate A/D converting card. Using the high speed two dimension scanning system, we could obtain the high speed confocal and two photon microscopy images for in vivo applications. And we could observe the high speed blood flow and the unit of msec biological phenomenon using the high speed Confocal microscopy and two photon microscopy.

8587-59, Session PMon

Differences in activity profile of bacterial cultures studied by dynamic speckle patterns

Evelio E. Ramírez Miquet, Isabel Otero, Dania Rodriguez, Juan G. Darias, Andres Combarro, Orestes R. Contreras, Ctr. de Aplicaciones Tecnologicas y Desarrollo Nuclear (Cuba)

We outline the main differences in the activity profile of bacterial cultures studied by dynamic laser speckle (or biospeckle) patterns. The activity is detected in two sorts of culture mediums. The optical setup and the experimental procedure are presented. Experimentally obtained images are processed by the temporal difference method and a qualitative assessment is made with the time history of speckle patterns of the sample. The main differences are studied after changing the culture medium composition. We conclude that the EC medium is suitable to detect the E. coli bacterial presence in early hours and that Mueller Hinton agar delays some additional hours to make possible the assessment of bacteria in time.

8587-60, Session PMon

Observation of silicon-mediated alleviation of cadmium stress in maize (Zea mays L.) seedlings via LED-induced chlorophyll fluorescence

Artur S. Gouveia-Neto, Elias A. Silva Jr., Airon J. da Silva, Clístenes W. A. Nascimento, Univ. Federal Rural de Pernambuco (Brazil)

Soil contamination with heavy-metals due to human activity is one of the most important global environmental subjects of research lately. Overabundance of metal in soil causes harm to human, animal and plant health and is an environment problem that requires effective and affordable remediation techniques. The study of metal contamination in soil evaluates tolerance of certain plant spieces to high metal concentrations for application in soil phytoremediation. For optimal concentrations some metals are essential for plant nutrition, and when the concentrations reach supraoptimal values, toxic effects and metabolic desorder occurs. Nevertheless, plants capable of retaining high metal concentrations in their shoots are potential candidates for soil decontamination through phytoextraction. Cadmium in the soils, derived mainly from industrial processes, mining, and agricultural application of fertilizers, is extremely toxic to living cells even at low concentrations. Cadmium severely damages plants health, and may cause death by disturbing the nutrient uptake and inhibiting photosynthesis through degradation of chlorophyll and inactivation of enzymes involved in the CO2 fixation. Chlorophyll fluorescence spectroscopy permits detection, monitoring, and evaluation of abiotic stresses upon healthy plants. The technique relies upon the fluorescence light generated by chlorophyll molecules in the photosynthesis process which convey information on the physiological state of higher plants. LED-induced chlorophyll fluorescence analysis is exploited to observe, and monitor the time evolution of silicon-induced alleviation of toxicity in mayze (Zea mays L.) seedlings in cadmium contaminated soil. Red, and far-red emissions were examined as a function of cadmium-silicon concentrations, during the 30 days period of the seedlings growing process. The chlorophyll fluorescence spectral analysis provided detection, and evaluation of the damage imposed by the metal stress in the early stages of the plant growing process. The technique also provided the time evolution evaluation of the silicon-induced tolerance enhancement of mayze plants to Cadmium, which is not viable using conventional in vitro spectral analysis

8587-62, Session PMon

Determining the influence of age and diabetes on the second-harmonic generation strength of dermal collagen fibers in vivo

Wei-Chun Hung, Chi-Kuang Sun, Argon Chen, National Taiwan Univ. (Taiwan)

It is commonly believed that the skin aging is associated with the change of the collagen structures. The influence of the diabetes on the skin collagen is also considered to be similar to aging. Moreover, second-harmonic-generation (SHG) in collagen fibers is considered to reflect the detailed collagen structures. It is thus highly valuable to adopt the SHG intensity as a collagen structure indicator. With the help of SHG, recently one can achieve in vivo imaging which provides the information of what really happens beneath the human skin. However, when analyzing the images, the SHG brightness of each pixel highly depends on the illumination condition, the depth of the SHG source, and the voltage of PMT. Therefore, it is important to calibrate these factors before statistical analysis. In this talk, we present our recent development that calibrates the in vivo SHG images by using noises. We first determine the regions of signals and noises by setting a threshold relating to the standard deviation of the image. By using the assumption that the noise was amplified by PMT with an amplification ratio the same as the SHG signal, we can define the brightness of the noise region as a parameter representing the voltage of PMT, and use this parameter to calibrate all SHG images. After calibrating, we can then compare different images from volunteers and analyze the influence of aging and diabetes on the SHG intensity from collagen fibers, even if the voltage of PMT was not fixed.

8587-63, Session PMon

Tumor-stem cells interactions by fluorescence imaging

Aleksandra V. Meleshina, Elena Cherkasova, Nizhny Novgorod State Univ. (Russian Federation); Marina V. Shirmanova, Nizhny Novgorod State Medical Academy (Russian Federation); Ekaterina A. Sergeeva, Institute of Applied Physics (Russian Federation); Ekaterina Kiseleva, Erdem Dashinimaev, Koltzov Institute of Developmental Biology (Russian Federation); Ilya V. Turchin, Institute of Applied Physics (Russian Federation); Elena V. Zagaynova M.D., Nizhny Novgorod State Medical Academy (Russian Federation)

Recently, great deal of interest is investigation the function of the stem cells (SC) in tumors. In this study, we investigated «recipient–tumor–fluorescent stem cells » system using the methods of in vivo imaging and LSM.

We used in our work adipose-derived adult stem (ADAS) cells of human

liposome transfected with the gene of fluorescence protein Turbo FP635. The objects of research were nude mice with transplanted tumor HeLa Kyoto (human cervical carcinoma). ADAS were administrated into the experimental animals at different stages of tumor growth (0-8 days) intravenously or into tumor.

In vivo imaging was performed on the experimental setup for epi – luminescence bioimaging (IAP RAS, Nizhny Novgorod). Results of image processing show unambiguous localization of fluorophore tagged stem cells in animals spleen of different groups on day 5-9 after injection. The sensitivity of the technique may be improved by spectral separation self-fluorescence and fluorescence of stem cells.

We compared results obtained on the setup for epi – luminescence bioimaging and on the confocal laser scanning microscopy LSM 510 META (Carl Zeiss, Germany). Internal organs of animals and tumor tissues were investigated. It was shown that with i.v. injection of ADAS, bright fluorescent structures with spectral characteristics corresponding to TurboFP635 protein are locally accumulated in the marrow, lungs and tumor tissues of animals.

These findings indicate, that ADAS cells integrate in the animal organism with transplanted tumor and can be identified by the surface bioimaging techniques and LSM.

8587-64, Session PMon

Water content distribution imaging of skin tissue using near-infrared camera and measurement depth analysis

Hidenobu Arimoto, National Institute of Advanced Industrial Science and Technology (Japan); Mariko Egawa, Shiseido Co., Ltd. (Japan)

Wavelength-dependent light penetration depth in the measurement of water distribution of the skin tissue is analyzed. Near-infrared imaging enables 2-D water content map on the skin tissue because water absorbs light strongly in the near-infrared region particularly around the wavelengths of 1,460 and 1,920 nm. However, the depth of the light penetration depends largely on wavelength as the absorption coefficient of water changes considerably in the near-infrared range. We investigate the measurement depth of the water content mapping with a near-infrared camera and bandpass filters at the wavelengths of 1,300, 1,450 and 1,920 nm. Analysis is performed with Monte Carlo light scattering simulation adopting the depth profile of the water contents measured by the confocal Raman microscopy. It is found that the near-infrared image at 1,920 nm shows the shallowest water distribution and is the most sensitive to the water content changes that occurred in the stratum corneum layer. The calculated results are verified with the near-infrared camera images which measure volunteers.

8587-65, Session PMon

Investigation of the mechanical property of individual cell using axial optical tweezers

Mary-Clare C. Dy, Tadao Sugiura, Kotaro Minato, Nara Institute of Science and Technology (Japan)

Optical tweezers is a technique that can trap and manipulate small objects using a highly focused laser beam. Because optical tweezers can also be used to measure small forces, it has been extensively used for the measurement of the mechanical forces of cells, wherein particles are used as probes to study and investigate cell elasticity. However, previous research works typically study particle manipulation and cell force measurement in the lateral direction, hence excluding valuable insights about the axial mechanical properties of cells. Other works that investigate axial cell force measurements utilize spatial light modulators and other devices that are expensive and complicate the setup. Thus, in our study, we designed a simple scheme that can axially manipulate particles by adjusting the position of one lens, called L1-lens, in our setup. Image processing techniques were utilized to determine the changes in the axial particle translation, providing nanometer sensitivity. We investigated the capability of our system using two different-sized particles and results show that for a given L1-lens default position and movement, a 2.10?m particle and a 4.26?m particle were moved axially for 2.56?m and 4.83?m, respectively. Axial trapping stiffness was also measured for the stated bead sizes in different magnification. Using the computed trapping stiffness, we will investigate the axial reactive forces of cells, wherein we will axially probe the cells. Finally, this scheme will be incorporated to our existing Cell Palpation system to create a three-dimensional particle manipulation and cell force measurement system.

8587-66, Session PMon

Kinetic identification of protein ligands in a 50,000 small-molecule library using microarrays and label-free ellipsometric scanning microscopes

James P. Landry, Andrew P. Proudian, Galina Malovichko, Xiangdong Zhu, Univ. of California, Davis (United States)

Drug discovery begins by identifying protein-small molecule binding pairs. Afterwards, binding kinetics and biofunctional assays are performed, to reduce candidates for further development. High-throughput screening, typically employing fluorescence, is widely used to find protein ligands in small-molecule libraries, but is rarely used for binding kinetics measurement because: (1) attaching fluorophores to proteins can alter kinetics and (2) most label-free technologies for kinetics measurement are inherently low-throughput and consume expensive sensing surfaces. We addressed this need with polarization-modulated ellipsometric scanning microscopes, called oblique-incidence reflectivity difference (OI-RD). Label-free ligand screening and kinetics measurement are performed simultaneously on small-molecule microarrays printed on relatively inexpensive isocyanate-functionalized glass slides. As a microarray is reacted, an OI-RD microscope tracks the change in surface-bound macromolecule density in real-time at every spot. We report progress applying OI-RD to screen purified proteins and virus particles against a 51,200-compound library from the National Cancer Institute. Four microarrays, each containing 12,800 library compounds, are installed in four flow cells in an automated OI-RD microscope. The slides are reacted serially, each giving 12,800 binding curves with ~30 sec time resolution. The entire library is kinetically screened against a single probe in ~14 hours and multiple probes can be reacted sequentially under automation. Real-time binding detection identifies both high-affinity and low-affinity (transient binding) interactions; fluorescence endpoint images miss the latter. OI-RD and microarrays together is a powerful high-throughput tool for early stage drug discovery and development. The platform also has great potential for downstream steps such as in vitro inhibition assays.

8587-68, Session PMon

TPEF-SHG study of myofibril disassembly in live adult cardiomyocytes during dedifferentiation

Honghai Liu, Clemson Univ. (United States); Yonghong Shao, Shenzhen Univ. (China); Wan Qin, Zhonghai Wang, Huaxiao Yang, Clemson Univ. (United States); Thomas K. Borg, Medical Univ. of South Carolina (United States); Bruce Z. Gao, Clemson Univ. (United States)

The primarily cultured adult cardiomyocytes have been widely used as an in vitro model of adult myocardium and shown increasing importance in the research of cardiology and cardiopathology. The freshly dissociated adult cardiomyocytes undergo dedifferentiation while they are cultured in-vitro: they lose their rod-shape morphology, striated myofibril structure, and their normal physiological functions, which has been

proposed to serve as an in-vitro pathologic model of the cardiomyocytes in myocardium. However, the detailed structural changes during the dedifferentiation at molecular level are unclear, which hinder the application of such a model in biological research.

Based on hybrid on-stage-incubating TPEF-SHG imaging and immunocytological techniques, we studied dedifferentiation of the live adult cardiomyocytes isolated from 4-week-old Sprague-Dawley rats. The length change of sarcomere in the cardiomyocytes was analyzed during their dedifferentiation: The myofibrils first shrunk to shorten the sarcomere length, the striated structure of myofibrils was wrecked from the cell ends, then to the entire cell. Our results demonstrate that the striated patterns of different sarcomeric components do not disassemble simultaneously and synchronously during dedifferentiation. The striated pattern of myosin filaments was wrecked first at the cell ends, while the striated pattern of alpha-actinin faded away first at the center of the cell and was recruited close to the cell membrane during the dedifferentiation of adult cardiomyocytes. Our present results suggest that the end-by-end connection of the fresh isolated adult cardiomyocytes is necessary to maintain the original striated myofibrillar structure and rod-shape morphology in building the in vitro culture model of adult cardiomyocytes.

8587-69, Session PMon

Study of virus by micro-Raman spectroscopy

Kamila Moor, Yusuke Nishimoto, Masanori Sawa, Hodaka Kitamura, Kiyoshi Ohtani, Hidetoshi Sato, Kwansei Gakuin Univ. (Japan)

It is reported that the viruses is one of the major causes of tumor. Some viruses are found in high rate in some human tumors. It is very important to develop an easier and more efficient method to its detection. Conventional testing method for virus is expensive and time-consuming. It requires experienced technicians too. Hence, Raman spectroscopy will offer a new direction to study viruses. In the present study, we employed a confocal Raman microscopy. It has enough high spatial resolution to measure the spectra of single cell. Raman spectroscopy is one of the vibrational spectroscopies, which allow one to identify molecules in the sample in nondestructive manner. It is suitable to monitor the molecular alteration without labeling of live cells. We employed cancer cell and virus. Some viruses contain oncogenes which lead to tumoral transformation of cell in a genome. Therefore, this virus can proliferate only in this cell, cannot do in normal cells. The Raman microscope was applied to observe cancer cell and virus infection into the cell. The Raman observation was carried out 24 hours and 7 days after the virus infection. It seems that the cytopathic effects are observer during the total destruction of the cell. Principal component analysis (PCA) was used to classify and detect the effect due to the virus infection. The infectivity was confirmed with fluoroimmunoassay and confocal fluorescent microscopy. TEM (transmission electron microscopy) is employed to observe the cytopathic effect and the virus proliferation.

8587-70, Session PMon

Automated in vivo sensing and tracking of rare circulating cells in wide-field macroscopic fluorescence image sequences with high background Autofluorescence

Stacey Markovic, Binlong Li, Mario Sznaier, Octavia I. Camps, Mark J. Niedre, Northeastern Univ. (United States)

Background: Observing, quantifying and tracking rare circulating cells in vivo is an important problem in many biomedical research areas. Microscopy-based in vivo flow cytometry approaches allow non-invasive sensing of cells, but are limited in sensitivity because they rely on sampling of small blood vessels; in principle, a larger blood volume can be sampled by using a wide-field (“macroscopic”) fluorescence imaging approach but this yields image sequences with substantial image noise and autofluorescence content. Methods: We used widefield illumination of a mouse ear with a 660 nm laser, and imaged a 4mm2 area with an electron multiplied CCD fitted with a low magnification objective. We injected very low concentrations (about 5e3/mL) of fluorescently labeled multiple myeloma (MM) cells. At this concentration, less than 1 cell per minute was observed, necessitating automated cell detection. Substantial removal of background noise – due to the high gain EMCCD camera, widefield collection area and high laser power – was required to isolate moving cells. To achieve this, we implemented a multi-step computer vision image processing algorithm that first removed non-specific background to identify cell candidates, and then identified moving cells by dynamically searching image sequences for candidates that could be merged into cell trajectories. Results and Discussion: This approach allowed tracking of cells with an order of magnitude improvement in sensitivity versus current approaches and despite high background yielded a false alarm rate of less than 0.73 per minute. Further, cell motility patterns were characterized by analyzing cell tracks to extract, e.g. cell velocities and trajectories.

8587-73, Session PMon

Synthesize dye-bioconjugates to visualize cancer cells using fluorescence microscopy

Yang Pu, Wubao Wang, The City College of New York (United States); Rui Tang, Baogang Xu, Duanwen Shen, Sharon Bloch, Mingzhou Zhou, Washington Univ. in St. Louis (United States); Samuel Achilefu, Washington Univ. School of Medicine in St. Louis (United States); Robert R. Alfano, The City College of New York (United States)

Until now, the confirmation of most cancers still depends on biopsy samples, which are randomly taken from the suspected organ. The histology slide is used to diagnose the precursors and stages of cancers based on phenotypic markers, such as nuclear to cytoplasmic ratio, appearance of cell nuclei. Optical fluorescence microscopy techniques can be functioned as “optical biopsy” to view these features in vivo.

In this study, near infrared dyes-bovine serum albumin (BSA) conjugates were synthesized by adding 0.4 mg EDC and 1 mg Sulfo-NHS in 1 ml activation buffer: 0.1 M MES, 0.5 M NaCl. The conjugate was purified on a Sephadex G-25 column with 1X PBS buffer. Fractions were evaluated using SDS - PAGE. The absorption and fluorescence spectral of the dye-bioconjugates were measured shown to exist in the NIR “tissue optical window” between 650 nm and 900 nm. The peak positions of both absorption and fluorescence for new compounds were observed to be similar to that of free corresponding dyes. Fluorescence microscopy outfitted with far red to NIR light sources and filters of dye-bioconjugates-stained different cell lines were performed for visual confirmation of internalization and pinocytosis of the synthesized compound in MCF-7, DU-145 and PC-3 cells. DAPI was used to stain cell nuclei. The time and concentration dependence of compound in cell staining were systemically studied to obtain the optimal concentration and staining time scale. This research serve as a step forward to the in vivo histological microscopy of “optical biopsy”.

8587-74, Session PMon

Polarised Raman imaging of living cells for chemical contrast manipulation

Liang-da Chiu, Almar F. Palonpon, Keisaku Hamada, Satoshi Kawata, Osaka Univ. (Japan); Mikiko Sodeoka, RIKEN (Japan); Katsumasa Fujita, Osaka Univ. (Japan)

Raman spectroscopy is now gaining more and more attention in biological studies because it can extract chemical information from living cells in a label-free manner. One of the main challenges in the Raman spectroscopic studies of living cells is that the spectrum is usually dominated by a few strong Raman bands such as the amide I band around 1650 cm-1, CH2 bend around 1445 cm-1 or the amide III

band around 1300 cm-1 and it is not easy to get chemical contrast from other Raman bands that overlap with them. In this study, we succeeded in manipulating the chemical contrast in a living cell by exploiting the polarisation effects in Raman spectroscopy. Raman bands with less symmetry of vibrations are known to have higher depolarisation coefficient. In case of organised molecular structures, such as the lipid membrane bilayer in cells, the molecular orientation also affects the polarisation of the observed Raman bands. Certain molecules, such as the haem group in cytochromes, even possess inverse polarisation Raman bands that rotates the polarisation of the incident light by 90? under resonance enhanced conditions. By imaging the cells at different polarisations, we are able to manipulate the chemical contrast of the Raman image even at the same Raman shift and extract more chemical information than what we could before.

8587-75, Session PMon

The microstructure of collagen hydrogels has a very strong effect on differentiation of embryonic stem cells

Yu Jer Hwang, Julia G. Lyubovitsky, Univ. of California, Riverside (United States)

This talk will describe the effect of microstructure of collagen hydrogels on the process of early differentiation of G-Olig2 embryonic stem cells into a neural lineage. We monitored the G-Olig2 embryonic stem cell behaviors separately in a 3D encapsulated and topographic collagen hydrogel models. For the encapsulated model, the cells were polymerized within hydrogels assembled from either 2 g/l or 4 g/l initial collagen concentration and differentiated in situ. For a topographic model, cells were differentiated on top of the 2 g/l hydrogels cross-linked with EDC, EDC/NHS or genipin and on the 2 g/l and 4 g/l 37 °C or 27 °C assembled materials. In the encapsulated model, embryonic stem cells differentiated faster in 2 g/l collagen materials than in 4 g/l materials. In the topographic 3D model, both the initial concentration as well as the cross-linking affected the G-Olig2 embryonic stem cells differentiation rate and remodeling of collagen hydrogels. On top of unmodified 2 g/l 37 °C collagen hydrogels, the cellular differentiation was concomitant with migration and subsequent aggregation into clusters. The collagen of the supporting extracellular matrix aligned at the periphery of the formed cluster. On top of the cross-linked 2 g/l materials, the G-Olig2 differentiated stem cells remained scattered. For the materials modified with EDC the cells aligned collagen fibers while making a clearance and no fiber alignment for the EDC/NHS and genipin modified gels. The data and methods developed provide an outline to monitor the extent of differentiating cells and degradation of collagen-based substrates in tissue engineering applications.

8587-76, Session PMon

Actin motility confinement on micro/nanostructured surfaces

Jenny L. Aveyard, Joanna Hajne, Univ. of Liverpool (United Kingdom); Alf Mansson, Malin Persson, Linnaeus Univ. (Sweden); Falco C. M. van Delft, J. van Zijl, Jaap Snijder, Eric Van Den Heuvel, MiPlaza, Philips Research (Netherlands); Dan V. Nicolau, Univ. of Liverpool (United Kingdom)

In this work, microfabricated silicon oxide pillars and lines with z-nanoscale heights of 20, 40 and 80 nm on planar silicon coated wafers were functionalized with trimethylchlorosilane (TMCS) vapour to allow attachment of heavy meromyosin (HMM). The motility of fluorescently labeled actin filaments was then monitored to determine if the structured surfaces could 1) support motility 2) contain the filament and 3) control the directionality of the filaments during a motility assay as these three factors are amongst the most important considerations when designing molecular motor-based devices.

8587-77, Session PMon

Multiple parallel actin/myosin motility assays on a microfluidic platform

Jenny L. Aveyard, Harm van Zalinge, Univ. of Liverpool (United Kingdom); Alf Mansson, Malin Persson, Linnaeus Univ. (Sweden); Falco C. M. van Delft, M. M. den Dekker, MiPlaza, Philips research (Netherlands); Dan V. Nicolau, Univ. of Liverpool (United Kingdom)

Outside of the cell, motility assays are traditionally used to study molecular motors. In these assays, motors such as myosin are immobilized on a functionalized surface and labeled cytoskeletal filaments such as actin glide over the assembly. The movement is observed under the light microscope using fluorescence markers or high-contrast techniques. For device applications one particular challenge is the development of high-throughput assays that allow the multiplexed analysis of the effects of different analytes or different concentrations of analytes on physiological motor function (production of motion/force) rather than simpler binding studies or assays for catalytic activity. As a result we are developing a system for performing a number of simultaneous motility assays in the presence of a range of different analytes. This test system is miniaturized in order to limit the substance cost and highly parallel for high throughput

In this work a simple microfluidic platform is described that enables the study of the effects of different concentrations of chemical species, including Ethylenediaminetetraacetic acid (EDTA) and ATP, simultaneously on the velocity of heavy meromyosin (HMM) propelled actin filaments. The device consists of Polydimethylsiloxane (PDMS) microchannels each feeding an array of micron sized holes running through a quartz plate. The design allows the diffusion of a plume of analyte solution from each channel through the holes in the plate into an area of a flow cell which contains motility assay components.

8587-78, Session PMon

The application of motile microorganisms and microfluidics to solve complex simulations

Ben Libberton, Marie Binz, Univ. of Liverpool (United Kingdom); Falco C. M. van Delft, A. F. Jos J. van de Ven, Jaap Snijder, Harold H. A. J. Roosen, Philips Innovation Services (Netherlands); Harm van Zalinge, Dan V. Nicolau, Univ. of Liverpool (United Kingdom)

Bacteria are abundant in the environment. The propulsion mechanisms of motile bacteria vary and cause different species to have different locomotive properties. Traditionally these properties have not been studied in spatial confinement, despite the fact that many bacteria naturally reside in spatially confined habitats. Recent work shows that spatial confinement of microorganisms can change properties of their movement.

Here we investigated the behaviour of motile microorganisms in complex microfluidic networks of different diameters and architectures. Microfluidic networks were constructed using standard microlithography techniques from the biocompatible polymer, polydimethylsiloxane. The networks were then filled with different growth media to create microenvironments with the capacity to initiate different measurable responses from the motile bacterial cells. The cells were visualised using light microscopy and their responses observed in replicate trials.

Bacterial cells were able successfully navigate the complex microfluidic networks and the direction of their motility could be controlled by the introduction of specific architectural features of the networks such as junctions between channels. The direction and velocity of locomotion was also shown to be affected by stimuli that could either attract or repel the microorganisms, as well as the viscosity of the media within the microfluidic channels.

We then used the information about the motility of different species in

confined spaces and applied it to real world problems. We showed that bacteria could be used in microfluidic channels to simulate complex processes.

8587-79, Session PMon

Microscopic imaging of glyceraldehydes-induced tissue glycation with intrinsic second harmonic generation and two-photon fluorescence contrasts

Yu Jer Hwang, Joseph Granelli, Univ. of California, Riverside (United States); Manasa Tirumalasetty, Univ of California Riverside (United States); Julia G. Lyubovitsky, Univ. of California, Riverside (United States)

The biomimetic and bioinspired approaches to tissue strengthening and preservation rely on non-toxic cross-linking agents one of which is glyceraldehyde. In this study we used multiphoton microscopy that employs second harmonic generation (SHG) contrast to evaluate collagen microstructures and two-photon fluorescence (TPF) contrast to monitor the progress of cross-linking upon treatment of tissues with glyceraldehyde. We examined collagen hydrogels assembled at 37 C and 27 C, bovine scleral and corneal tissues as well as rat tail tendons and evaluated glyceraldehyde treatments. The results show a difference in the effect of glyceraldehyde on the collagen microstructures within the above tissues. We observed that this effect depends on the original microstructural assembly of collagen within a specific tissue. This presentation will highlight the benefits of monitoring the progression of collagen cross-linking and the effects of cross-linking on fiber microstructures as imaged with SHG and TPF signals.

8587-72, Session 11

Sparse-sampling parallel Raman/SERS microspectroscopy for high-throughput molecular analysis of micro and nanoparticles

Wei-Chuan Shih, Univ. of Houston (United States)

Raman/SERS spectroscopy can provide molecular information via inelastic light scattering without physical contact. Coupled with microscopic imaging, Raman/SERS microspectroscopy is a powerful technique for material analysis, for example, stress and temperature measurement in silicon, compositional analysis of polymer microparticles, plasmonic nanoparticles and biological cells. However, due to the small scattering cross-section and spectroscopic nature of data, the single-point spectrum acquisition time is significantly longer than other optical modalities. The traditional design of conventional charge coupled detector (CCD) readout electronics introduces additional latency, resulting in low imaging throughput.

In this paper, we present a novel parallel Raman/SERS microspectroscopy scheme based on programmable patterned illumination. This technique enables semi-random, sparse sampling of micro and nanoparticles within a ~ 100 x 100 ?m2 field of view without mechanical scanning. We demonstrate the performance of this scheme using uniform samples, trapped polymer microparticles and fixed polymer microparticle with mixed molecular composition, colloidal nanoshells functionalized with various thiolated hydrocarbons, and trapped and fixed bacteria cells. We show that the throughput of this scheme can be orders of magnitude faster than a single-point scan-and-readout scheme, is significantly more flexible than the line-scan approach, and maintains smaller power fluctuation compared to time-sharing of a single-point illumination.

8588-1,

Enhanced resolution and sensitivity in fluorescence fluctuation measurements using multi-modal data acquisition and global analysis *(Keynote Presentation)*

Keith M. Berland, Neil R. Anthony, Emory Univ. (United States)

Fluorescence correlation spectroscopy (FCS) and related fluctuation spectroscopy and microscopy methods have become important research tools that enable detailed investigations of the chemical and physical properties of molecules and molecular systems in a variety of complex environments. When analyzed successfully fluctuation measurements often provide unique information that is otherwise difficult to measure, such as molecular concentrations and interaction stoichiometry. However, information recovery via curve fitting of fluctuation data can present challenges due to limited resolution and/or problems with fitting model verification. We discuss a new approach to fluctuation data analysis coupling multi-modal fluorescence measurements and global analysis, and demonstrate how this approach can provide enhanced sensitivity and resolution in fluctuation measurements. We illustrate the approach using a combination of FCS and fluorescence lifetime measurements, here called ?FCS, and demonstrate the capability to recover the concentration of two independent molecular species in a two component mixture even when the species have identical diffusion coefficients and molecular brightness values. This work was partially supported by NSF grants MCB0817966 and DMR0907435.

8588-2,

Promising new wavelengths for multi-photon microscopy: thinking outside the Ti:Sapphire box *(Keynote Presentation)*

Gail McConnell, Greg Norris, Rumelo C. Amor, John Dempster, Univ. of Strathclyde (United Kingdom); William B. Amos, MRC Lab. of Molecular Biology (United Kingdom)

Multi-photon excitation (MPE) imaging is dominated by the Ti:Sapphire laser as the source for excitation. However, it is limited when considering 3PE of common fluorophores and efficient 2PE of UV dyes which require wavelengths beyond the range of the Ti:Sapphire. Two ultra-short pulsed sources are presented as alternatives: a novel optical parametric oscillator (OPO) geometry (1400–1600nm) and the sum-frequency mixing of an OPO and Yb-doped fibre laser, providing a tunable output (626-635nm).

For long wavelengths, we report three-photon laser scanning microscopy (3PLSM) using a bi-directional pumped optical parametric oscillator (OPO) with signal wavelength output at ? =1500 nm. This novel laser was used to overcome the high optical loss in the infrared spectral region observed in laser scanning microscopes and objective lenses that renders them otherwise difficult to use for imaging. To test our system, we performed 3PLSM auto-fluorescence imaging of live plant cells at ?=1500 nm, specifically Spirogyra, and compared performance with two-photon excitation (2PLSM) imaging using a femtosecond pulsed Ti:Sapphire laser at ?=780 nm. Analysis of cell viability based on cytoplasmic organelle streaming and structural changes of cells revealed that at similar peak powers, 2PLSM caused gross cell damage after 5 minutes but 3PLSM showed little or no interference with cell function after 15 minutes. The ?=1500 nm OPO was thus shown to be a practical laser source for live cell imaging.

For short wavelengths, we report the use of an all-solid-state ultra-short pulsed source specifically for two-photon microscopy at wavelengths shorter than those of the conventional Ti:Sapphire laser. Our approach involved sum-frequency mixing of the output from the long-wavelength OPO described above with residual pump radiation to generate fs-pulsed output in the red spectral region. We demonstrated the performance of our ultra-short pulsed system using fluorescently labelled and autofluorescent tissue, and compared with conventional Ti:Sapphire excitation. We observed a more than 3-fold increase in fluorescence signal intensity using our visible laser source in comparison with the Ti:Sapphire laser for two-photon excitation at equal illumination powers of 22 mW or less.

8588-3,

Stimulated Raman scattering microscopy: coming of age *(Keynote Presentation)*

X. Sunney Xie, Harvard Univ. (United States)

Recent advances in stimulated Raman scattering microscopy, a label free and noninvasive have opened up exciting new possibilities for biological research and medical diagnostics. Latest results including DNA imaging will be discussed.

8588-4, Session 1

Functional broadband coherent Raman imaging *(Invited Paper)*

Marcus T. Cicerone, Charles H. Camp, Evangelos Gatzogiannis, Christopher Hartshorn, Young Jong Lee, National Institute of Standards and Technology (United States)

I will report on recent advances from our lab in broadband coherent Raman imaging. We have been developing broadband coherent anti-Stokes Raman (CARS) and stimulate Raman Scattering (SRS) as noninvasive contrast mechanisms for microscopy of chemically complex materials as well as biological cells and tissues. These coherent processes provide high spatial resolution, high sensitivity, and spectral sensitivity over the “fingerprint” frequency range of (500 to 1800) cm-1. Using new laser technologies we have improved our spectral image acquisition speed by more than 10X, and now obtain full spectra in < 1 ms, facilitating high-resolution chemical tracking of biological processes.

8588-5, Session 1

Quantitative vibrational imaging by pulse shaping based hyperspectral stimulated Raman scattering microscopy and multivariate curve resolution analysis

Delong Zhang, Ping Wang, Mikhail N. Slipchenko, Dor Ben-Amotz, Andrew M. Weiner, Ji-Xin Cheng, Purdue Univ. (United States)

Spectroscopic imaging has been an increasingly critical approach for unveiling specific molecules in biological environments. Towards this goal, we demonstrate hyperspectral stimulated Raman scattering (SRS) imaging by intra-pulse spectral scanning through a femtosecond pulse shaper. The hyperspectral stack of SRS images is further analyzed by a multivariate curve resolution (MCR) method to reconstruct a quantitative concentration image for each individual component and retrieve the corresponding vibrational Raman spectra. Using these methods, we demonstrate quantitative mapping of dimethyl sulfoxide concentration in aqueous solutions and in fat tissue. Moreover, MCR is performed on SRS images of breast cancer cells to generate maps of principal chemical components along with their respective vibrational spectra. These results

show the great capability and potential of hyperspectral SRS microscopy for quantitative imaging of complicated biomolecule mixtures with overlapped Raman bands.

8588-6, Session 1

Label-free observation of tissues by high-speed stimulated Raman spectral microscopy and independent component analysis *(Invited Paper)*

Yasuyuki Ozeki, Osaka Univ. (Japan) and Japan Science and Technology Agency (Japan); Yoichi Otsuka, Shuya Sato, Hiroyuki Hashimoto, Canon Inc. (Japan); Wataru Umemura, Kazuhiko Sumimura, Osaka Univ. (Japan); Norihiko Nishizawa, Nagoya Univ. (Japan); Kiichi Fukui, Kazuyoshi Itoh, Osaka Univ. (Japan)

We have developed a video-rate stimulated Raman scattering (SRS) microscope with frame-by-frame wavenumber tunability. The system uses a 76-MHz picosecond Ti:sapphire laser and a subharmonically synchronized, 38-MHz Yb fiber laser. The Yb fiber laser pulses are spectrally sliced by a fast wavelength-tunable filter, which consists of a galvanometer scanner, a 4-f optical system and a reflective grating. The spectral resolution of the filter is ~ 3 cm^-1. The wavenumber was scanned from 2800 to 3100 cm^-1 with an arbitrary waveform synchronized to the frame trigger. For imaging, we introduced a 8-kHz resonant scanner and a galvanometer scanner. We were able to acquire SRS images of 500 x 480 pixels at a frame rate of 30.8 frames/s. Then these images were processed by principal component analysis followed by a modified algorithm of independent component analysis. This algorithm allows blind separation of constituents with overlapping Raman bands from SRS spectral images. The independent component (IC) spectra give spectroscopic information, and IC images can be used to produce pseudo-color images. We demonstrate various label-free imaging modalities such as 2D spectral imaging of the rat liver, two-color 3D imaging of a vessel in the rat liver, and spectral imaging of several sections of intestinal villi in the mouse. Various structures in the tissues such as lipid droplets, cytoplasm, fibrous texture, nucleus, and water-rich region were successfully visualized.

8588-7, Session 1

When is stimulated Raman scattering microscopy more sensitive than spontaneous Raman scattering microscopy?

Wei Min, Columbia Univ. (United States)

Stimulated Raman scattering (SRS) microcopy has recently emerged as a powerful label-free chemical imaging technique for live cells, tissues, organisms and humans. However, when compared to the conventional spontaneous Raman microscopy, the sensitivity performance of SRS microscopy has not been quantitatively examined in the literature. In particular, it is not clear as to whether SRS is always superior to the spontaneous Raman, and if not, at what conditions SRS can be more sensitive than the spontaneous counterpart. Here we perform a theoretical treatment to compute the ultimate (shot-noise-limited) sensitivities in imaging configurations. A two-dimensional phase-diagram-like plot is constructed (using the number of vibrational oscillators and the number of incident Stokes photons) to describe the sensitivity behavior of both SRS and spontaneous Raman microscopies. Our study provides a theoretical basis for evaluating the relative performance of these two closely related Raman imaging techniques under comparable experimental conditions.

8588-8, Session 1

Nonlinear nearfield microscopy *(Invited Paper)*

Annika M. Enejder, Henning Hagman, Juris Kiskis, Chalmers Univ. of Technology (Sweden)

Higher order nonlinearity of light–matter interactions, such as second and third harmonic generation (SHG & THG) and Coherent anti-Stokes Raman Scattering (CARS) can be used for improving spatial resolution in far-field imaging as a consequence of the spatial confinement of the nonlinear polarization. However, the resolution is limited to ~300 nm, not sufficient to resolve macromolecules or nanostructures of interest in the bio-, life- and nano-sciences. In the strive to push the resolution beyond the diffraction limit, allowing for nanoscale imaging, we have equipped a nonlinear optical microscope with a scanning-probe setup operated in tapping-mode feedback. A tapered single-mode fiber with an aperture diameter of ~50 nm is scanned over the sample, probing the nonlinear nearfield generated by free-beam excitation. First nonlinear coherent Raman nearfield images of biological macromolecules and metallic nanostructures will be shown. Limitations and future challenges with nonlinear nearfield microscopy will be discussed.

8588-9, Session 1

Circularly polarized coherent anti-Stokes Raman scattering microscopy for background-free tissue imaging

Jian Lin, Paul Kumar Upputuri, Gong Li, Haifeng Wang, Zhiwei Huang, National Univ. of Singapore (Singapore)

The existence of non-resonant background severely decreases the image contrast and may overwhelm the resonant signal from small scatterers in coherent anti-Stokes Raman scattering (CARS) microscopy imaging. In this study, we found that by using circularly polarized pump and Stokes excitations with inverse rotation directions, the non-resonant as well as the resonant CARS generation from molecules with symmetry can be totally suppressed, whereas the resonant CARS signal from asymmetric molecules preserves. This unique property of circularly polarized CARS is useful for high-contrast imaging of asymmetric samples without the interference of non-resonant background, which is demonstrated by the imaging of natural silk fibers.

8588-10, Session 1

Surface selective coherent Raman scattering microscopy *(Invited Paper)*

Eric O. Potma, Yong Wang, Xuejun Liu, Univ. of California, Irvine (United States)

Many chemical and biological processes occur at surfaces. To probe these processes optically, a technique with intrinsic surface selectivity is desirable to suppress the contributions from the bulk. Coherent Raman scattering (CRS) techniques, however, probe the third-order susceptibility of the material, which renders these techniques sensitive to bulk optical properties. We show that surface-selective CRS can be achieved when evanescent excitation fields are used instead of free-space excitation light. We demonstrate that plasmon-enhanced CRS signals can be generated on glass coverslips coated with a thin layer of gold, enabling direct visualization of surface bound objects without contributions from the bulk. By utilizing newly designed plasmonic lenses, we achieve evanescent excitation fields that are confined to tight focal spots and suitable for precise excitation of Raman active molecules. We present chemical and biological applications of this surface-selective imaging capability.

8588-11, Session 2

Spectroscopic SRS imaging with a time-lens source synchronized to a femtosecond pulse shaper

Ke Wang, Cornell Univ. (United States); Delong Zhang, Purdue Univ. (United States); Kriti Charan, Cornell Univ. (United States); Mikhail N. Slipchenko, Ping Wang, Ji-Xin Cheng, Purdue Univ. (United States); Chris Xu, Cornell Univ. (United States)

Though single-color coherent Raman microscopy has been widely used for vibrational imaging of isolated Raman bands, it is still challenging to visualize molecules having overlapping Raman bands. We address this issue by developing a spectroscopic SRS microscope with a time-lens laser source synchronized to a femtosecond laser. The time-lens source provides 2-ps pulse at the wavelength of 1064 nm. A pulse shaper is installed for intra-pulse spectral scanning of the femtosecond laser output. By electronically modulating the time-lens source at MHz frequency, spectroscopic stimulated Raman loss (SRL) images were obtained on a laser-scanning microscope. Using this microscope, we have been able to detect 0.2% DMSO in aqueous solution. Spectroscopic SRL images of prostate cancer cells were obtained. Multivariate curve resolution analysis was further applied to decompose the SRL images into concentration maps of proteins and lipids. With high sensitivity and high spectral resolution, this method offers exciting potential in label-free imaging of live cells using fingerprint Raman bands.

8588-12, Session 2

Development of CARS spectrometer using dual-wavelength electronically tuned laser

Yasuhiro Maeda, Yusuke Nishimoto, Hidetoshi Sato, Kwansei Gakuin Univ. (Japan)

In recent year, non-chromosomal spectroscopy or imaging, such as raman spectroscopy, are used for investigating the chemical or biological dynamics in living cells or tissues. In particular, Coherent Anti-Stokes Raman Scattering (CARS) attracts much attention for more sensitive non-chromosomal spectroscopy or imaging in biological fields, because CARS signal has higher intensity, we can obtain clear spectrum with high signal to noise ratio. However, two wavelengths are required to obtain the CARS signal, so that they need complex laser system and difficult operations. Furthermore, the stability of laser intensity is most important and required factor to obtain more clear spectrum of living samples..

In this study, we are developing more easy-operated CARS system with high stability for biological spectroscopy using a dual-wavelength oscillation electronically tuned laser based on Ti:Sapphire laser.The laser has an acousto-optic tunable filter (AOTF) in the cavity as a tuning element. Fast (1 ms) and random-access tuning was realized by applying radio frequency (rf) to the AOTF. We can select any wavelength in the tuning range from 700 nm to 1000 nm by changing a frequency of the rf, and output power of the laser is controlled by adjusting the rf power without any mechanical movements. Moreover the laser can oscillate two different wavelengths simultaneously by applying the two different rf to the AOTF. Using these features of this laser, we achieved easily-operated CARS spectrometer. We measured the CARS spectrum of polystyrene beads to estimate the performance, including the stability of this CARS system.

8588-13, Session 2

All-fiber laser system for CRS microscopy by optical synchronization of two power-amplifiers

Christian W. Freudiger, Harvard Univ. (United States) and Invenio Imaging, Inc. (United States); Wenlong Yang, Gary R. Holtom, Harvard Univ. (United States); Nasser N. Peyghambarian, The Univ. of Arizona (United States); X. Sunney Xie, Harvard Univ. (United States); Khanh Q. Kieu, The Univ. of Arizona (United States)

Coherent Raman scattering (CRS) microscopy allows biomedical imaging based on vibrational spectroscopy without the need for dye staining or fluorescent labeling. By virtue of stimulated excitation of vibrational transitions with two laser beams, the CRS signal is amplified by up to five orders of magnitude compared to spontaneous Raman scattering. This requirement for two synchronized and precisely tunable lasers poses a challenge; existing solutions are expensive and require specialized optical tables. Fiber technology has the potential to overcome this problem as telecom components are inexpensive and light-guiding by the fiber core avoids misalignment. Our laser design is based on the realization that the difference frequency of the two major fiber gain media, Erbium and Ytterbium, corresponds to the high-wavenumber region of Raman spectra, where most CRS imaging is performed. We achieve robust temporal synchronization by optical synchronization of two power-amplifiers using super-continuum generation, demonstrate all-fiber implementation, and have stringently optimized the laser parameters for high-speed narrowband CRS. To demonstrate that this “affordable” CRS laser source does not compromise performance, we present sensitive tissue imaging with contrast from lipids, protein, and DNA with acquisition speeds of up to one frame per second.

8588-14, Session 2

Broadly tunable high-energy spectrally focused CARS microscopy with chemical specificity and high resolution for biological samples

Craig Brideau, Kelvin W. Poon, Peter K. Stys, Univ. of Calgary (Canada)

The current trend in laser sources for Coherent Anti-Stokes Raman Scattering (CARS) microscopy consists of picosecond optical parametric oscillators (OPO)s and femtosecond-pumped fiber supercontinuum sources. While both methods are proven CARS performers, restricted wavelength tuning range and low power limit the Raman lines and types of samples that may be practically interrogated. To address these limitations, we present a novel; highly tunable spectrally focused femtosecond Optical Parametric Amplifier (OPA) and microscope system optimized for CARS microscopy. The laser source consists of an amplified ytterbium fiber laser driving a pair of semi-independent OPAs producing two femtosecond outputs that are tunable from 650 to 1300 nm. Each OPA may be tuned independent of the other over its entire range, allowing the addressing of any arbitrary wavenumber from 0 to 7700 cm-1. Additionally, the complete freedom of tuning allows one beam to be set at the optimal wavelength for a complimentary technique, such as two-photon fluorescence or second harmonic generation, while the second beam is then tuned to the desired wavenumber difference for CARS. The femtosecond pulses are chirped out to the picosecond regime, reducing non-resonant background and providing improved spectral resolution.

Typically, OPA systems are limited to kHz repetition rates, making them impractical for imaging applications. Conversely, the presented OPA system is driven at 1 MHz, providing a sufficient pulse rate for high-resolution imaging at rates of 1-2 frames per second. The 1 MHz rate preserves good pulse energy while reducing average power, thus limiting sample photo damage.

8588-15, Session 2

Fiber bundle based probe with polarization for coherent anti-Stokes Raman scattering microendoscopy imaging

Zhengfan Liu, Beijing Institute of Technology (China) and The Methodist Hospital Research Institute (United States); Zhiyong Wang, Xi Wang, Xiaoyun Xu, Xu Chen, Jie Cheng, Xiaoyan Li, The Methodist Hospital Research Institute (United States); Shufen Chen, Beijing Institute of Technology (China); Jianguo Xin, Stephen T. C. Wong, The Methodist Hospital Research Institute (United States)

The ability to visualize cellular structures and tissue molecular signatures in a live body could revolutionize the practice of surgery. Specifically, such technology is promising for replacing tissue extraction biopsy and offering new strategies for a broad range of intraoperative or surgical applications, including early cancer detection, tumor margin identification, nerve damage avoidance, and surgical outcomes enhancement. Coherent anti-Stokes Raman scattering (CARS) microendoscopy offers a way to achieve this with label-free imaging capability and sub-cellular resolution. However, efficient collection of epi-CARS signals and reduction of nonlinear effects in fibers are two major challenges encountered in the development of fiber-based CARS microendoscopy. To circumvent this problem, we designed and developed a fiber bundle for a CARS microendoscopy prototype. The excitation lasers were delivered by a single multimode fiber at the center of the bundle while the epi-CARS signals were collected by multiple MMFs surrounding the central fiber. A polarization scheme was employed to suppress the four-wave mixing (FWM) effect in the excitation fiber. Our experimental results suggest that, with this fiber bundle and the polarization FWM-suppressing scheme, the signal-to-noise ratio of the CARS images was greatly enhanced through a combination of high collection efficiency of epi-CARS signals, isolation of excitation lasers, and suppression of FWM. The three dimensional scanning capability of the microendoscopy prototype was also demonstrated by ex vivo imaging on mouse tissues. This fiber bundle-based CARS microendoscopy prototype, with the polarization FWM-suppressing scheme, offers a promising platform for constructing efficient fiber-based CARS microendoscopes for label free intraoperative imaging applications.

8588-17, Session 3

Seeing the unseen in cell machinery based on multiplex SRS microscopy *(Invited Paper)*

Ji-Xin Cheng, Mikhail N. Slipchenko, Purdue Univ. (United States)

We will present our latest advances in the development of stimulated Raman scattering microscopy and its application to single cell analysis. In particular we will demonstrate a novel approach for a multiplex SRS microscope based on lock-in free detection. Such a microscope is critical for mapping of overlapped Raman bands. Combination of ps/fs laser source and multiplex heterodyne detection of spectrally dispersed SRS signal allows fast acquisition of a SRS spectrum at the speed of a few μs, which enables fast spectroscopic mapping of live cells. For simultaneous lock-in free detection of multiple spectral channels from a photodiode array we have designed and built a 32-channel tuned amplifier. Fast spectroscopic mapping of living cells by multiplex SRS microscopy opens a new window to monitor biochemistry in important cellular processes such as proliferation and apoptosis.

8588-18, Session 3

Integrated stimulated Raman scattering, two-photon fluorescence, and third harmonic generation microscopy revealed acetowhitening mechanistic phenomenon in living cells

Jianan Y. Qu, Seng Khoon Teh, Hong Kong Univ. of Science and Technology (Hong Kong, China)

Tissue acetowhitening phenomenon, as a result of instillation of acetic acid onto the epithelia, is currently being actively explored for early neoplasia detection in various epithelial organ sites. Despite the widespread application of acetic acid instillation for precancer and cancer tissue detection, the underlying mechanism remains elusive. In this study, we investigate the acetowhitening phenomenon at the subcellular level using multimodal nonlinear optical (NLO) microscopy techniques. Specifically, an unique multimodal NLO microscopy that can simultaneously probe stimulated Raman scattering-induced CH3 stretching of proteins/lipids information (2950 cm-1), third harmonic generation (THG) signals from regions of optical heterogeneity, and two-photon excited fluorescence (TPEF) of tryptophan from the proteins was developed and employed for biological cells characterization. Cervical cancer cells lines (i.e., SiHa) were monolayered cultured and utilized as a living cell model. We examined the SRS, THG and TPEF signals alterations within the monolayer cultured living SiHa cell lines during the treatment of medium with acetic acid at various concentrations. THG reveals acetic acid treatments results in significant optical heterogeneity within the entire cell. Colocalization analysis of the images from THG with SRS and TPEF shows proteins and lipids to contribute significantly towards cellular regions of optical heterogeneity within the cytoplasm and nucleus. The multimodal NLO microscopy, for the first time, provided evidences that proteins and/or lipids aggregation induced by acetic acid contributed towards increased optical heterogeneity within cellular cytoplasm and nucleus. The results explain the observations of previous study based on light scattering spectroscopy and reveal the mechanism of acetowhitening phenomenon.

8588-19, Session 3

Agrochemical application of stimulated Raman scattering (SRS) microscopy

Julian J. Moger, Jessica C. Mansfield, Univ. of Exeter (United Kingdom)

The growing world population is putting ever-increasing pressure on plant and agrochemical scientists to increase agricultural yields. Despite recent progress, research in this area would greatly benefit from a new generation of analytical tools capable of providing in-situ quantitative biochemical analysis in living plants. The label-free chemical specificity, high spatial resolution and non-invasive nature makes techniques based on Raman scattering highly attractive. However, their application in plant science is severely limited by the overwhelming autofluorescence of plant tissues.

We propose that, by overcoming the issues associated with Raman analysis in plant tissues, Stimulated Raman Scattering (SRS) microscopy is an exciting new analytical tool for agrochemical research. This presentation will discuss how the high optical absorption and autofluorescence of plant tissues affect coherent Raman scattering microscopy and explore how they may be minimised with SRS. Finally, examples of how SRS can be used to perform biochemical analysis of intact plant tissues and their interaction with agrochemical formulations will be shown.

8588-20, Session 3

Visualizing cold treatment response of sebaceous glands in vivo with CARS microscopy

Yookyung Jung, H. Ray Jalian, Joshua Tam, R. Rox Anderson M.D., Conor L. Evans, Wellman Ctr. for Photomedicine (United States)

It has long been observed that lipid-rich cells appear to be especially sensitive to cold-induced injury. For example, inflammatory damage and necrosis in subcutaneous fat tissue has been described in young children after they suck on ice or popsicles – a phenomenon known as "popsicle panniculitis". Recently we have exploited this cold-sensitivity of fat tissue to develop a novel method for subcutaneous fat removal, called "cryolipolysis". By non-invasive cooling at the skin surface, an acute lobular panniculitis is induced in subcutaneous fat tissue, resulting in fat mass reduction with no measurable disturbances to surrounding tissues or to serum lipid profile. While the effects of cold exposure on sebocytes and sebaceous glands have not been specifically studied, it has been reported that sebaceous glands in a canine model became necrotic within 1 week after freezing of the skin to sub-zero temperatures. We hypothesize that freezing of sebum (human sebum is reported to freeze at 15-20 ºC) could be a means to selectively damage sebocytes and sebaceous glands, which could lead to new treatment options for acne.

To study the effect of cold treatment on sebaceous glands, we carried out longitudinal studies visualizing the sebaceous glands in the ears of treated mice using coherent anti-Stokes Raman scattering (CARS) microscopy. CARS microscopy enabled 3D imaging of the lipid-rich sebaceous glands with cellular resolution, allowing for detailed studies of sebaceous gland morphological changes in vivo. We will present both long-term visualization of damaged sebaceous glands after cold treatment as well as the dose-dependent changes observed.

8588-21, Session 3

Label-free detection of microscopic brain tumor boundaries using stimulated Raman scattering microscopy *(Invited Paper)*

Daniel A. Orringer M.D., Univ. of Michigan Health System (United States); Minbiao Ji, Christian W. Freudiger, Harvard Univ. (United States); Shakti Ramkissoon M.D., Dana Farber/Harvard Cancer Ctr. (United States); Alexandra Golby M.D., Nathalie Agar, Brigham and Women's Hospital (United States); Marika Hayashi, Dana Farber/Harvard Cancer Ctr. (United States); Darryl Lau, Univ. of Michigan Medical School (United States); X. Sunney Xie, Harvard Univ. (United States); Oren Sagher M.D., Univ. of Michigan Health System (United States)

Surgery remains essential in the treatment of brain tumors. However, surgeons lack a reliable method for delineating tumor from normal brain during surgery. Here we describe the use of stimulated Raman scattering (SRS) microscopy as a label-free means of differentiating healthy brain from tumor-infiltrated brain on a cellular level. SRS microscopy delineates tumor from normal brain based on histologic and biochemical differences. Moreover, SRS microscopy is capable of differentiating tumor from normal brain both ex vivo and in vivo in infiltrative human glioblastoma xenograft models. In vivo studies demonstrate the ability of SRS microscopy to reveal tumor margins that are invisible under the standard operative conditions used today by neurosurgeons. These results demonstrate the potential of SRS microscopy as an intraoperative method for differentiating tumor from normal brain. By providing the surgeons with a real-time histologic assessment of the operative field, SRS microscopy may ultimately improve the safety and accuracy of cancer surgeries where tumor boundaries are visually indistinct.

8588-22, Session 3

Local myelin in vivo health analysis in a multiple sclerosis mouse model with a two-dimensional Fourier approach

Steve Begin, Erik Belanger, Sophie Laffray, Ctr. de Recherche de l'Univ. Laval Robert-Giffard (Canada); Steve Lacroix, Ctr. de Recherche de l'Univ. Laval (Canada); Yves De Koninck, Daniel Côté, Ctr. de Recherche de l'Univ. Laval Robert-Giffard (Canada)

The very high amount of heterogeneities in spinal cord lesions during multiple sclerosis (throughout the cord and across different animals) makes studying the early stages of the disease very difficult. This calls for a local, objective, and fast assessment of myelin in order to identify and follow potential early lesions. Myelin is visualized through the use of Coherent Anti-Stokes Raman Scattering microscopy (CARS), a label-free technique that takes advantage of the endogenous contrast provided by their lipid content.

We present an automated two-dimensional discrete Fourier transform approach to analyse the organization and health state of myelinated axons in the spinal cord. CARS microscopy was used ex vivo and in vivo to observe multiple sclerosis-like lesions in an animal model (Experimental Autoimmune Encephalomyelitis (EAE)). The acquired images are separated in subdomains which are then fourier-transformed in order to find the average orientation of the fibers within the domains. The correlation between orientations of adjacent domains is then used to evaluate tissue health, find lesions and quantitatively characterize them. This procedure, compatible with live animal imaging, is developed for performing local in situ evaluation of myelinated axons afflicted by EAE.

8588-23, Session 3

A microfluidic platform for high-throughput label-free cellular imaging and screening

Aaron M. Streets, Tao Chen, YanYi Huang, Peking Univ. (China)

Progress in quantitative image analysis has evolved microscopy into a powerful tool for systems biology studies. As automated image collection and processing techniques are able to quantitatively manage larger and larger volumes of two-dimensional and three-dimensional image data, biological image analysis has been able to approach the experimental throughput of chemical screening. Here we present a microfluidic platform for parallel, label free cellular imaging with stimulated Raman scattering (SRS) microscopy. SRS microscopy is a quantitative technique which achieves label free cellular imaging with chemical specificity and low background by exploiting vibrational resonances in chemical bonds. Microfluidic technology enables precise and dynamic titration of chemicals into nanoliter reaction chambers and provides an ideal platform for screening of chemical conditions. A SRS microscope is integrated with a microfluidic device that consists of an array of parallel, independently addressable cell chambers. This system is used to monitor lipid metabolism by quantifying intercellular lipid droplet morphology while varying the extracellular chemical environment. With this platform lipid droplet dynamics can be observed in response to titrations of exogenous fatty acids or other chemical stimuli. With automated image collection and processing, this platform demonstrates the potential for a systems approach to studying lipid droplet biology.

8588-24, Session 3

Combining multiphoton and CARS microscopy for skin imaging

Hans G. Breunig, Univ. des Saarlandes (Germany) and JenLab GmbH (Germany); Martin Weinigel, Marcel Kellner-Höfer, Rainer Bückle, JenLab GmbH (Germany); Maxim E. Darvin M.D., Jürgen M. Lademann, Charité Universitätsmedizin Berlin (Germany);

Karsten König, Univ. des Saarlandes (Germany) and JenLab GmbH (Germany)

Non-invasive in vivo imaging of tissue with subcellular resolution, high sensitivity and chemical discrimination is highly desirable for modern biomedical research. We present in vivo imaging of human skin with a combined CARS (coherent anti-Stokes Raman scattering) and multiphoton tomograph. The combination of both imaging modalities enables label-free imaging with both chemical discrimination and subcellular resolution. CARS is utilized to image lipid-rich structures inside the skin, while the multiphoton imaging modality can detect intrinsic skin fluorophores like keratin, melanin and NAP(P)H and in addition second harmonic generation (SHG) light from the skin collagen network. Multiphoton imaging is realized with single beam excitation. CARS imaging employs a second excitation pulse train obtained by spectrally broadening of the fs pulses with a photonic crystal fiber setup. Out of the broadband continuum an appropriate spectral part for the CARS excitation is selected. Imaging examples of different skin layers as well as skin conditions are presented.

8588-25, Session 3

Applications of hyperspectral coherent Raman scattering microscopy

Erik T. Garbacik, Andrew L. Fussell, Roza P. Korai, Jeroen P. Korterik, Cornelis Otto, Jennifer L. Herek, Herman L. Offerhaus, Univ. Twente (Netherlands)

Using system that we recently developed for hyperspectral coherent Raman scattering (CRS) microscopy we have analyzed samples from a number of fields that have not yet been extensively explored with coherent Raman techniques. Expansion of CRS imaging into these fields has been stymied partly by the paradigm of multi-spectral imaging, in which only a few images are acquired at pre-determined frequencies. Artifacts in these images, arising from effects such as the polarization dependencies of crystalline materials, can result in misleading interpretations of the results. Our method, which utilizes a picosecond optical parametric oscillator and a laser-scanning microscope, is to quickly record a large number of individual frames across a range of equally-spaced vibrational frequencies and then apply a different color to each frame. Additive mixing of all spectral points per spatial pixel produces a single image in which the majority compounds are qualitatively represented by separate colors. Chromatic ambiguities are resolved by using multiple color look-up tables for each hyperspectral data cube, so that each spectrum is represented by a unique set of three colors. We will present results from samples across multiple disciplines, including biomedical, pharmaceutical, and botanical sciences. In particular, we note that the presence of multiple polymorphs of one compound in a sample can be readily detected and characterized with hyperspectral CRS microscopy, and that distinctions between vibrational and electronic resonances can be made without complicated detection or data-processing techniques.

8588-26, Session 3

Raman microspectroscopy for visualization of peripheral nerves

Takeo Minamikawa, Yoshinori Harada, Noriaki Koizumi, Tetsuro Takamatsu, Kyoto Prefectural Univ. of Medicine (Japan)

The peripheral nervous system plays an important role in motility, sensory, and autonomic functions of the human body. Preservation of peripheral nerves in surgery is essential for improving quality of life of patients. To preserve peripheral nerves, detection of fine peripheral nerves that cannot be identified by human eye or under white light imaging is necessary. In this study, we sought to provide a proof-of-principle demonstration of a label-free detection technique of peripheral nerve tissues against adjacent tissues that employs spontaneous Raman microspectroscopy. A line-illumination confocal Raman microscope was used for the experiment. A laser operating at the wavelength of 532 nm was used as an excitation laser light. We obtained Raman spectra of peripheral nerve, fibrous connective tissue, skeletal muscle, blood vessel, and adipose tissue of Wistar rats, and extracted specific spectral features of peripheral nerves and adjacent tissues. By applying multivariate image analysis, peripheral nerves were clearly detected against adjacent tissues without any preprocessing neither fixation nor staining. These results suggest the potential of the Raman spectroscopic observation for noninvasive and label-free nerve detection, and we expect this method could be a key technique for nerve-sparing surgery.

8588-59, Session PSun

Chemical-contrast imaging with pulse-shaping based pump-probe spectroscopy

Daniel C. Flynn, Amar R. Bhagwat, Jennifer P. Ogilvie, Univ. of Michigan (United States)

The introduction of pump-probe spectroscopy to the field of microscopy has enabled high contrast imaging of non-fluorescent species in vivo. Endogenous species such as heme proteins show rich nonlinear spectroscopic signatures of excited state absorption, stimulated emission and ground-state bleaching. Commercially available octave-spanning Ti:sapphire oscillators offer new opportunities for imaging based on pump-probe contrast. While large spectral bandwidth enables nonlinear excitation of a wide range of chemical species, it also limits the ability to selectively excite and obtain chemical contrast of molecular structures with similar spectral properties. Pulse shaping techniques using spatial light modulators can help overcome these challenges. Here we present two-color pump-probe microscopy of heme proteins. Via two-photon excitation we excite the Soret band with the pulse-shaped output from a Venteon Pulse: One Ti:sapphire oscillator. Using pulse-shaped second harmonic light from the oscillator we probe via one-photon transitions. Images are acquired using a raster scanning piezo stage and lock-in amplification of pump modulation transfer to the transmitted probe light. The approach enables selective imaging of a wide range of chemical species via multiphoton excitation followed by probing of nonlinear spectroscopic signals of stimulated emission, ground-state-bleach, and excited state absorption. We present two-color pump-probe imaging of proteins and discuss conditions for achieving optimum contrast based on pulse-shaping. Finally, we discuss future applications of this technique to in vivo studies.

8588-73, Session PSun

Optical metabolic imaging of macro-suspension tumor cultures predicts tumor therapeutic response

Alex J. Walsh, Rebecca S. Cook, Carlos L. Arteaga, Melissa C. Skala, Vanderbilt Univ. (United States)

The standard of care for breast cancer patients includes treatment with antiestrogens, HER2 inhibitors, and chemotherapy; however, no accurate method exists to assess early responders vs. non-responders. Therapeutic efficacy, both clinically and in drug-development studies, is measured by tumor size assessed weeks after treatment. However, molecular changes may occur within the tumor cells early, perhaps within hours after treatment. The oncogenic drivers targeted by therapeutic agents often regulate cellular metabolism. We hypothesize that both the intensity and fluorescence lifetime of NADH and FAD, two coenzymes of metabolism, are potent biomarkers of therapeutic response. In this study, we used two-photon auto-fluorescence imaging of NADH and FAD in breast tumor macro-suspensions (3D cell cultures) retaining all cellular components of a tumor to assess therapeutic response. The novel macro-suspension model allows in vitro culture of tumors in a physiologically relevant 3D matrix. Upon treatment with the antiestrogen, fulvestrant, and epidermal growth factor receptor (EGFR) inhibitors, A4

and AMG-888, the redox ratio of responsive cells decreases ($p<0.001$) and is further reduced when these therapies are combined ($p<0.001$). Furthermore, the NADH fluorescence lifetime decreases in macro-suspensions treated with EGFR inhibitors ($p<0.05$). Therefore, the application of optical metabolic imaging techniques described herein to assess tumor macro-suspensions in high-throughput drug screens may be a feasible approach to guide clinical therapy selection and to expedite pre-clinical studies.

8588-74, Session PSun

Stimulated Raman microscopy without ultrafast lasers

Zhaokai Meng, Georgi I. Petrov, Vladislav V. Yakovlev, Texas A&M Univ. (United States)

Stimulated Raman scattering (SRS) microscopy is a powerful tool for chemically-sensitive non-invasive optical imaging. However, the short-pulse laser sources, which are currently being employed for this imaging technique, are still expensive and require substantial maintenance to provide temporal and spectral overlap. SRS imaging, which utilizes cw laser sources, has a major advantage over pulsed lasers, as it eliminates the possibility of cell damage due to exposure to high-intensity light radiation, while substantially reducing the cost and complexity of the set-up and keeping a sub-cellular spatial resolution. As a proof-of-principle, we demonstrate microscopic imaging of dimethyl sulfoxide using two independent, commonly used and inexpensive lasers: a diode-pumped, intracavity doubled 532 nm laser and a He-Ne laser operating at 633 nm. In our demonstration, dimethyl sulfoxide acts as a contrast agent providing Raman scattering signal. The 532 nm and 633 nm lasers act as excitation and probe sources, respectively. Multi-dimensional images are obtained over scanning processes [1].

References:

[1] Z. Meng, G. I. Petrov, and V. V. Yakovlev, Opt. Lett. (2012) Submitted.

8588-75, Session PSun

Second harmonic imaging to distinguish grana and starch inside an intact leaf

Mei-Yu Chen, Guan-Yu Zhuo, Po-Fu Chen, Pei-Chun Wu, Yuan Tsung Hsieh, Tzu-Ming Liu, Shi-Wei Chu, National Taiwan Univ. (Taiwan)

Photosynthesis is one of the most important chemical reactions on earth. The main functional structure for photosynthesis is the grana, which is located inside the chloroplasts of plant. To study the position and the arrangement of grana, we used multiphoton microscopy, with simultaneously acquisition of two photon fluorescence (TPF) and second harmonic generation (SHG) signals. The TPF imaging indicates the distribution of chlorophyll, while SHG shows the location of ordered orientation structures inside a chloroplast. It has been shown that grana exhibit SHG due to its layered packing, so ideally we should be able to identify grana by SHG imaging. However there is another structure inside chloroplast that can also give strong SHG emission: the starch granule. Starch granule is the main product of photosynthesis and the energy storage for plants. The size of starch in chloroplast is on the order of micrometer, similar to grana. Therefore our purpose is to distinguish starch and grana inside an intact leaf. Since there is no autofluorescence from starch, whereas strong autofluorescence is expected from grana, our method is to compare the SHG images with TPF images, which filtered out specifically the fluorescence band of chlorophyll. As a result, there are two types of SHG structures in the image. One is collocated with strong TPF, and the other is complementary to TPF. The former corresponds to grana while the latter should correspond to starch. Consequently, we have demonstrated a straightforward noninvasive method to identify the distribution of grana and starch inside a mesophyll.

8588-76, Session PSun

Imaging molecular structure with Stokes-polarimeter based second harmonic generation microscopy

Nirmal Mazumder, Jianjun Qiu, Chih-Wei Hu, Fu-Jen Kao, National Yang-Ming Univ. (Taiwan)

We have developed a polarization resolved four channel photon counting based Stokes vector polarimeter to work with second harmonic generation microscopy. In this work, the four channels Stokes-polarimeter can measure all four Stokes parameters of SHG signal and reconstruct the corresponding images of degree of polarization (DOP), degree of linear polarization (DOLP), degree of circular polarization (DOCP) and polarization anisotropy. By applying the Stokes parameters based image analysis techniques SHG images of biomolecules, such as potato starch, collagen, and skeletal muscle. From these reconstructed images, we are able to quantify the polarization state of SH light and the corresponding molecular orientation of the biomolecules. The SHG polarization images clearly indicate the presence of birefringence and reflect the samples' structural information from their polarization properties. The DOLP indicates the crystalline alignment of molecules and are parallel to the linear polarization states. The DOCP is a measure of how effectively the medium flips the helicity of the scattered light. The observation from the polarization parameters reveals that these biomolecules are highly anisotropic, coincides with the known pitches of distinct helices within the coil structures of fibers.

We analyze the influence of the polarization states and different polarization properties of molecular and biological samples through four channel polarization resolved microscopy imaging. We have demonstrated that birefringence and chirality from biological samples is accounted for in polarization resolved SHG imaging through DOLP and DOCP. Birefringence is present in increasing depths, which can tell us about the symmetry, orientational disorder of molecular and biomolecular assemblies.

8588-77, Session PSun

Ultra-deep penetration and remote scanning of temporally-focused two-photon excitation

Gali Sela, Hod Dana, Shy Shoham, Technion-Israel Institute of Technology (Israel)

Temporal focusing (TF) nonlinear microscopy enables simultaneous illumination of relatively large areas while maintaining optical sectioning, by relying on the sensitivity of multiphoton processes to pulse duration. Line illumination temporal focusing (LITF) combines temporal focusing in the axial direction (xz plane) and spatial focusing in the lateral direction (xy). The additional spatial focusing improves optical sectioning compared to wide field temporal focusing and exhibits improved performance in scattering medium.

Two photon microscopy's ultimate depth of penetration is limited by out-of-focus excitation, and it is interesting to explore whether TF and particularly LITF can be used to address this limitation. Here, we present theoretical and experimental results displaying the feasibility of ultra-deep penetration two-photon excitation in scattering media (>>1mm) using LITF without significant distortions or out-of-focus-excitation. Our experimental setup is based on an amplified 800nm ultrafast laser where a dual-prism grating (DPG) is used as a diffractive element, allowing light to propagate on-axis throughout the optical setup as well as a higher diffraction efficiency. We also show (theoretically and experimentally) that this "on axis" design enables to remotely scan the LITF plane by linearly moving the DPG.

These results present new opportunities for ultra deep, optically sectioned 3D two photon imaging and stimulation within scattering biological tissue.

8588-78, Session PSun

Maximum imaging depth comparison in porcine vocal folds using 780-nm vs. 1550-nm excitation wavelengths

Murat Yildirim, Onur Ferhanoglu, The Univ. of Texas at Austin (United States); James B. Kobler, Steven M. Zeitels M.D., Massachusetts General Hospital (United States); Adela Ben-Yakar, The Univ. of Texas at Austin (United States)

Vocal fold scarring is one of the major cause of voice disorders and may arise from overuse or post surgical wound healing. One promising treatment utilizes the injection of soft biomaterials aimed at restoring viscoelasticity of the outermost vibratory layer of the vocal fold, superficial lamina propria (SLP). However, the density of the tissue and the required injection pressure impair proper localization of the injected biomaterial in SLP. To enhace treatment effectiveness, we are investigating a technique to image and ablate sub-epithelial planar voids in vocal fold using ultrafast laser pulses to better localize the injected biomaterial. However, it is crucial to find an optimized wavelength to perform imaging and ablationat depths suitable for clinical use.

We present a comparison of maximum imaging depth using two-photon autofluorescence, second harmonic generation and third harmonic generation imaging modalities with superior porcine vocal fold. We use a home-built one channel inverted nonlinear laser scanning microscope together with a high repetition rate (300 kHz- 2 MHz) ultrafast fiber laser (Raydiance Inc.). We acquire both second harmonic generation and two photon autofluorescence images using 780 nm wavelength and third harmonic generation images with using 1550 nm wavelength. Our imaging depth observed with combined two-photon autofluorescence and second-harmonic generation at 780 nm wavelength was significantly improved from 140 µm to 250 µm when third-harmonic generation was employed using 1550 nm, without any observable damage in the tissue.

8588-79, Session PSun

Two-photon-based structured illumination microscopy applied for superresolution optical biopsy

Chia-Hua Yeh, Szu-Yu Chen, National Central Univ. (Taiwan)

Wide-field structured illumination microscopy (WF-SIM) is known to provide at least 2-fold improvement in lateral resolution by extending the effective optical transfer function of the imaging system. However, its applications are limited in thin tissues since it possesses no optical sectioning power. To overcome this limitation, we introduce a system, two-photon grid scanning pattern microscopy (TP-GPSM), which combines the concept of SIM with two-photon microscopy (TPM). By utilizing the nonlinearity of two-photon excitation, optical sectioning can be achieved due to the confined excitation volume. To meet the two-photon excitation requirements, wide-field illumination was replaced by a laser scanning scheme, while a femtosecond laser was used for excitation. The grid two-photon illumination patterns were effectively produced by using an acousto-optic modulator and a pair of scanning mirrors to temporally and spatially modulate the excitation light, respectively; a 2D couple-charge device was used to record the two-photon fluorescence images. Since the 2D grid illumination pattern can induce frequency shift of the object information in four directions in Fourier domain, five phase-stepped images should be obtained to solve the unknown frequency components. To achieve resolution improvement in all directions, two orientations of the grid pattern were needed so that at least nine images were required to accomplish the image reconstruction. Based on this system scheme, TP-GPSM was demonstrated to provide a 2-fold improvement in lateral resolution compared with the traditional TPM. With the optical sectioning capability, TP-GPSM was shown to have the potential for super-resolution imaging in thick tissues.

8588-80, Session PSun

Auto-balancing detector for fiber laser based stimulated Raman scattering (SRS) imaging

Wenlong Yang, Christian W. Freudiger, Gary R. Holtom, X. Sunney Xie, Harvard Univ. (United States)

SRS allows label-free chemical imaging of cells and tissue. Previously we have been working with free-space solid state laser excitation and implemented a modulation transfer scheme to detect the relatively small signal from the transmitted laser beams. Using high-frequency modulation (10 MHz) we achieved close to shot-noise limited sensitivity by avoiding the low-frequency 1/f noise. In applying this approach to inexpensive and more robust fiber laser sources, we realized significant high frequency noise prevent us from obtaining a good SRS image. Here we report a high dynamic range balanced detector with 35dB RF noise suppression capability to overcome this problem and demonstrated shot-noise limited sensitivity of 163.5 dBc/Hz for our current fiber laser system. To compensate for quickly varying sample transmission in beam-scanning microscopy, we further implemented high speed auto-balancing with a feedback time constant of 500ns, which is faster than the pixel dwell-time but slower than the 10MHz SRS signal. We demonstrate label-free imaging of mouse skin with high sensitivity and high speed (1fps).

8588-81, Session PSun

Label-free detection of microscopic brain tumor boundaries using stimulated Raman scattering microscopy

Minbiao Ji, Harvard Univ. (United States); Daniel A. Orringer, Univ. of Michigan Medical School (United States)

Surgery remains essential in the treatment of brain cancer. However, surgeons lack a reliable method for delineating tumor from normal brain during surgery. Here we describe the use of stimulated Raman scattering (SRS) microscopy as a label-free means of differentiating healthy brain and from tumor-infiltrated brain on a cellular level. SRS microscopy effectively delineates tumor from normal brain based on histologic and biochemical differences. Traditional hematoxylin and eosin light microscopy confirms that SRS microscopy can accurately identify microscopic infiltration of tumor cells into adjacent brain. Moreover, SRS microscopy is capable of differentiating tumor from normal brain both ex vivo and in vivo in infiltrative human glioblastoma xenograft models. These results demonstrate the potential of SRS microscopy as a method for delineating tumor from normal brain during surgery.

8588-82, Session PSun

Rapid multi-color stimulated Raman scattering microscopy using OPO with electro-optical Lyot filter

Lingjie Kong, Minbiao Ji, Gary R. Holtom, Christian W. Freudiger, X. Sunney Xie, Harvard Univ. (United States)

Stimulated Raman scattering (SRS) microscopy, a label-free chemically specific technology with high sensitivity, has seen great developments recently. However, spectral specificity of the narrowband implementation in current SRS microscopy is a limitation for chemically complex samples. Methods for quantitative imaging multiple species have been developed, employing spectrally tailored excitation, modulation multiplexing, or spectrally resolved detection. However, by using synchronized broadband and narrowband lasers, all these schemes are complex and of limited spectral resolution. The most straightforward method for resolving samples with overlapping spectra is sequential tuning, which is followed by a transformation using linear algebra to convert the mixed sample information into concentration maps of

individual chemical constituents. For N chemical species, at least N different vibrational frequencies should be probed. To minimize motion blurring and allow quantitative analysis, the wavelength should be tuned as fast as the galvo line scanning (typically in the milisecond scale), thus a series of whole images at different Raman shifts can be acquired simultaneously.

Here we demonstrate SRS microscopy with a fast wavelength tuning OPO. With an intracavity electric-optical tunable Lyot filter, SRS images are taken with line-by-line wavelength tunability (about 2 ms/line, synchronized with trigger signals from the microscope). With 3-color sequential wavelength tuning line-by-line, we show imaging of mixed beads (melamine, PMMA, and polystyrene), and ex vivo imaging of fresh mouse skin tissue, mapping distributions of lipid, protein, and blood.

8588-83, Session PSun

Two-photon fluorescence imaging of intracellular reactive oxygen species H2O2

Hengchang Guo, Univ. of Maryland, College Park (United States) and Weill Cornell Medical College (United States); Hossein Aleyasin, Burke Medical Research Institute (United States); Scott S. Howard, Cornell Univ. (United States); Vivian Lin, Univ. of California, Berkeley (United States); Chao-Wei Chen, Jianting Wang, Univ. of Maryland, College Park (United States); Renee E. Haskew-Layton, Burke Medical Research Institute (United States); Christopher J. Chang, Univ. of California, Berkeley (United States) and Howard Hughes Medical Institute (United States); Chris Xu, Cornell Univ. (United States); Rajiv R. Ratan, Burke Medical Research Institute (United States); Yu Chen, Univ. of Maryland, College Park (United States)

The reactive oxygen species (ROS) H2O2, recognized intracellular second messenger, acts as a signaling molecule in a variety of signaling transduction processes. It is also an oxidative stress indicator related to cancer, diabetes, and neurodegenerative diseases [1-2]. A substantial challenge in elucidating its diverse roles in complex biological environments is determine the spatial and temporal dynamics of this ROS metabolite in living systems.

To monitor the production of intracellular H2O2 in situ, we developed a biophotonic technique including a home-made two-photon fluorescence (TPF) microscope and chemoselective fluorescent probes Peroxyfluor-6 acetoxymethyl ester (PF6-AM) [2-3] and Mitochondria Peroxy Yellow 1 (MitoPY1) [4]. We developed these fluorescent probes based on boronate-switch mechanism for selective detection of intracellular H2O2 with improved sensitivity. PF6-AM was designed with the intracellular acetoxymethyl ester functionalities allowing for cell membrane-permeability [2-3]. MitoPY1 was designed with a mitochondrial-targeting phosphonium moiety for detection of H2O2 localized to cellular mitochondria [4]. Two-photon absorption (TPA) spectra of PF6AM and MitoPY1 were measured with a mode-locked Ti:sapphire laser in the wavelength range of 720-1040 nm. The peak TPA cross section values of PF6-AM and MitoPY1 are comparable to that of fluorescein, which is sufficiently large for the TPF imaging to detect localized endogenous H2O2 production in living cells.

To characterize this technique, we genetically modified brain cells with D-amino acid oxidase (DAAO) to enable controllable production of H2O2 [1]. The study demonstrates that TPF imaging is capable of visualizing intracellular H2O2 production in brain cells.

ACKNOWLEDGEMENT

H.G., C.W.C, J.T.W and Y.C. are supported by National Institutes of Health (NIH) grant R21DK088066 and R21EB012215. H.A., R.H.L. and R.R.R. are supported by NIH Grants NS04059 and NS39170. S.H. and C.X. are supported by NIH R01 CA133148. C.J.C. is an Investigator with the Howard Hughes Medical Institute.

REFERENCES

[1] R.E. Haskew-Layton, J.B. Payappilly, N.A. Smirnova, T.C. Ma, K.K. Chan, T.H. Murphy, H.C. Guo, B. Langley, R. Sultana, D.A. Butterfield, S. Santagata, M.J. Alldred, I.G. Gazaryan, G.W. Bell, S.D. Ginsberg and R.R. Ratan, “Controlled enzymatic production of astrocytichydrogen peroxide protects neurons from oxidative stress via an Nrf2-independent pathway”, Proc Natl Acad Sci USA, Vol. 107 (40), pp. 17385–17390, October 2010.

[2] B.C. Dickinson, J. Peltier, D. Stone, D.V. Schaffer and C.J. Chang, “Nox2 redox signaling maintains essential cell populations in the brain”, Nat. Chem. Biol., vol. 7 (2), pp. 106-112, February 2011.

[3] H.C. Guo, H. Aleyasin, S. Howard, B.C. Dickinson, R. Haskew-Layton, D. Kobat, V. Lin, D.R. Rivera, C.J. Chang, R.R. Ratan, and C. Xu, “Two-photon Imaging of Intracellular Hydrogen Peroxide with a Chemoselective Fluorescence Probe”, Optical Molecular Probes, Imaging and Drug Delivery (OMP) 2011 paper: OTuD3.

[4] B.C. Dickinson and C.J. Chang, “A Targetable Fluorescent Probe for Imaging Hydrogen Peroxide in the Mitochondria of Living Cells”, J Am. Chem. Soc., Vol. 130 (30), pp. 9638–9639, July 2008.

8588-84, Session PSun

Coherent Raman scattering microscopy with a compact Er:fiber laser

Adil T. Gorgulu, Rabia Gorgulu, Andreas Zumbusch, Claudius Riek, Alfred Leitenstorfer, Univ. Konstanz (Germany)

Coherent Raman Scattering (CRS) microscopy is a nonlinear microscopy technique which draws a great deal of attention for many biological applications. Wide distribution of CRS microscopy has been hampered by the necessity to use complex laser systems.

Here we present a compact, stable and cost-effective Er:fiber system. A two-color ps Er:fiber based laser has been developed in order to improve the overall performance of the existing CRS microscopy schemes. It is a self-starting passively mode locked oscillator which seeds two parallel fiber amplifiers. Since the pulses of the both amplifiers originate from the same seed, synchronization with attosecond precision can be realized. The system can be applied for both Coherent anti-Stokes Raman Scattering (CARS) and for Stimulated Raman Scattering (SRS) microscopy. In the latter case, only minor changes to the laser are necessary in order to implement efficient modulation. Biological as well as material scientific applications will be demonstrated.

8588-85, Session PSun

Random addressing FLIM with acousto-optic deflectors

Jing Qi, Yonghong Shao, Wang Yan, Kaige Wang, Junle Qu, Niu Hanben, Shenzhen Univ. (China)

Fluorescence Lifetime Imaging Microscopy (FLIM) is becoming a widely used tool in biomedicine. By measuring the fluorescence lifetime of each point in the sample, FLIM can provide 2D or 3D information on the microenvironment of the fluorophores. However, FLIM system generally uses galvanometer-driven mirror to scan the laser beam. The imaging speed is usually too slow to record the fast process in biological samples. The mechanical scanning device also limits the flexibility of FLIM to image the sites or regions of interest. In this paper, we developed a fluorescence lifetime imaging microscope which uses a pair of acousto-optic deflectors (AODs) to scan the laser beam and a Time-Correlated Single Photon Counting (TCSPC) module to measure the lifetime. By using AOD device to provide inertia-free beamsteering and address the sites or regions of interests in the sample for lifetime measurement, a random addressing fluorescence lifetime imaging microscope has been achieved. We perform system characterization and validation experiment using standard fluorescent dyes and biological samples.

8588-86, Session PSun

Evaluation of the oxidative stress of psoriatic fibroblasts based on spectral two-photon fluorescence lifetime imaging

Dimitrios Kapsokalyvas, Victoria Barygina, Univ. degli Studi di Firenze (Italy); Riccardo Cicchi, Univ. degli Studi di Firenze (Italy) and Consiglio Nazionale delle Ricerche (Italy); Claudia Fiorillo, Consiglio Nazionale delle Ricerche (Italy); Francesco S. Pavone, European Lab. for Non-linear Spectroscopy (Italy)

Psoriasis is an autoimmune disease of the skin characterized by hyperkeratosis, hyperproliferation of the epidermis, inflammatory cell accumulation and increased dilatation of dermal papillary blood vessels. Metabolic activity is increased in the epidermis and the dermis. Oxidative stress is high mainly due to reactive oxygen species (ROS) originating from the skin environment and cellular metabolism. We employed a custom multiphoton microscope coupled with a FLIM setup to image primary culture fibroblast cells from perilesional and lesional psoriatic skin in-vitro. Two-photon excited fluorescence images revealed the morphological differences between healthy and psoriatic fibroblasts. Based on the spectral analysis of the NADH and FAD components the oxidative stress was assessed and found to be higher in psoriatic cells. Furthermore the fluorescence lifetime properties were investigated with a TCSPC FLIM module. Mean fluorescence lifetime was found to be longer in psoriatic lesional cells. Analysis of the fast (?1) and slow (?2) decay components revealed a decrease of the ratio of the contribution of the fast (?1) component to the contribution of the slow (?2) component. The fluorescence in the examined part of the spectrum is attributed mainly to NADH. The decrease of the ratio (?1)/ (?2) is believed to correlate strongly with the anti-oxidant properties of NADH which can lead to the variation of its population in high ROS environment. This methodology could serve as an index of the oxidative status in cells and furthermore could be used to probe the oxidative stress of tissues in-vivo.

8588-87, Session PSun

Clinical multiphoton endoscopy with FLIM capability

Martin Weinigel, Hans G. Breunig, Peter Fischer, Marcel Kellner-Höfer, Rainer Bückle, JenLab GmbH (Germany); Karsten König, Univ. des Saarlandes (Germany) and JenLab GmbH (Germany)

Multiphoton tomography is an excellent method for non-invasive imaging of living tissue without any need of additional contrast agents. For increased accessibility and endoscopic application of this imaging method the distal focusing optics of multiphoton tomographs can be miniaturized to a diameter of less than 1.4 mm and a numerical aperture (NA) of 0.8. Based on the excitation of endogenous fluorophores (like reduced nicotinamide adenine dinucleotide (NADH)) and second-harmonic generation (SHG) by the dermal collagen network these endoscopes allow to perform multimodal imaging (autofluorescence and SHG simultaneously) without the need of staining with exogenous contrast substances. With an effective length from seven to 20 mm multiphoton endoscopy can be applied for intra-corporal imaging as well as for the examination of hard-to-access tissue areas.

A further imaging modality which had not been realized before with these endoscopes is fluorescence lifetime imaging (FLIM). As a temporal based contrast mechanism FLIM allows to perform functional imaging which can be used for example to investigate the metabolic activity of the tissue. Especially interesting with these endoscopes can be the research of the healing mechanism of chronic wounds and the corresponding cell metabolism.

We performed first in vivo measurements using FLIM endoscopy with a combination of a gradient-index-endoscope and the motorized computer controlled scanhead of the clinical multiphoton tomograph MPTflex.

8588-88, Session PSun

Next generation TCSPC detection

Uwe Ortmann, Hans-Jürgen Rahn, Felix Koberling, Benedikt Krämer, Marcelle König, PicoQuant GmbH (Germany); Samantha Fore, PicoQuant Photonics North America, Inc. (United States); Peter Kapusta, Michael Wahl, Rainer Erdmann, PicoQuant GmbH (Germany)

More than 20 years ago single photon counting based single molecule detection started with cooled photomultiplier tubes (PMT). Already 5 years later the single photon avalanche photodiode (SPAD) started to replace the PMT especially due to its higher detection efficiency and became the workhorse in ultrasensitive confocal microscopy. In the last decade step by step SPAD technology improvements enabled to meet most of the requirements of modern Time-Correlated Single Photon Counting (TCSPC) based microscopy, especially when sub millimeter detection areas are not a limitation.

Recently a new detector module was made available which allows to merge the millimeter sized detection area of the PMT with the photon processing efficiency of the SPAD. We incorporated this novel hybrid photomultiplier detector module in a cooled, self-contained housing hosting the complete electronics for TCSPC yielding a plug and play device with a detection sensitivity down to single molecules. Beneath standard confocal detection we developed an universal approach to integrate this detector also for multichannel non-descanned detection (NDD) in existing commercial microscopes. This will for example noticeably increase the detection efficiency for time-resolved deep-tissue FLIM imaging.

We present several examples highlighting the outstanding performance of the new device like the narrow and ultrastable IRF, low darkcounts and almost negligible afterpulsing and afterglow. These features make it ideally suited for FLIM, FCS as well as polarization resolved (anisotropy) imaging.

8588-89, Session PSun

Two-photon raster image cross-correlation spectroscopy (RICCS) with a supercontinuum light source and pulse phase control

David J. Graham, The Univ. of Texas Southwestern Medical Ctr. at Dallas (United States); George Alexandrakis, The Univ. of Texas at Arlington (United States)

Raster image correlation spectroscopy (RICS) is a technique for obtaining fluorescence correlation data from images acquired with a standard confocal or two-photon microscope. RICS uses the correlations between pixels and the time differences in their acquisition due to the raster scan. This can be extended to Raster image cross-correlation spectroscopy (RICCS) by measuring the correlations between two images acquired simultaneously for two different fluorophores, which can allow the detection of interactions between molecules in live cells.

We will present a RICCS system where a single femtosecond laser is used to excite two fluorophores with coherent control allowing their relative brightness to be selected. For our apparatus a highly nonlinear photonic crystal fiber is pumped with a Ti:Sapphire laser to produce a supercontinuum spectrum. A pulse shaper then controls the spectral phase of the light to compress the pulses to below 20 femtoseconds and allow coherent control by selecting the wavelengths at which two photon effects occur. These short broadband pulses allow efficient excitation of both the GFP and DsRed fluorescent proteins. The brightness of the two fluorophores can be adjusted separately to optimize the SNR of the RICCS measurement. Selectively excitation of one of the fluorescent proteins allows the cross talk between channels to be measured and corrected for. This system will be used to study the interaction of DNA repair proteins in vitro and in live cells.

8588-90, Session PSun

The development of fluorescence lifetime imaging microscopy system based on a streak camera

Lixin Liu, Xidian Univ. (China); Heng Li, Shenzhen Univ. (China); Yahui Li, Xidian Univ. (China); Yonghong Shao, Junle Qu, Shenzhen Univ. (China)

Fluorescence microscopy has become an important tool in biomedicine. Like fluorescence spectrum, fluorescence lifetime is a characteristic of a given fluorescent molecule and can be used for contrasting different fluorophores and distinguishing different molecular species in a sample. Moreover, fluorescence lifetime is very sensitive to the microenvironment of the fluorophores, i.e. a change in the fluorescence lifetime of a fluorophore reflects a change in its local environment. Thus a lot of physiological parameters including pH, Ca2+, Na+ and pO2 can be quantified from fluorescence lifetime measurement. Fluorescence lifetime imaging microscopy (FLIM) combines time-resolved fluorescence spectroscopy to imaging microscopy and aims to analyze quantitative parameters of fluorescence at a cell or tissue level. Generally, there are three main implementation methods for FLIM, including time-gated image intensifier, time-correlated single-photon counting (TCSPC) and streak camera. In this paper, we present the development of fluorescence lifetime imaging microscopy system based on a streak camera (streak-FLIM), which couples ultrafast infrared laser for multiphoton excitation and a streak camera for lifetime measurements. The streak-FLIM system was calibrated with an F-P etalon and several standard fluorescent dyes. Preliminary experimental results on fluorescence lifetimes of plant leaves are obtained. The streak-FLIM system may have potential applications in the diagnosis of cancer tissue and fluorescence resonance energy transfer (FRET) imaging of living cells.

8588-91, Session PSun

Multi-color femtosecond source for simultaneous excitation of multiple fluorescent proteins in two-photon fluorescence microscopy

Ke Wang, Cornell Univ. (United States); Tzu-Ming Liu, Juwell Wu, Wellman Ctr. for Photomedicine (United States) and Massachusetts General Hospital (United States); Nicholas G. Horton, Cornell Univ. (United States); Charles P. Lin, Wellman Ctr. for Photomedicine (United States) and Massachusetts General Hospital (United States); Chris Xu, Cornell Univ. (United States)

Simultaneous imaging of cells expressing multiple FPs is of particular interest in applications such as mapping neural circuits, tracking multiple immune cell populations, etc. To visualize both in vivo and ex vivo tissue morphology and physiology at a cellular level deep within scattering tissues, two-photon fluorescence microscopy (2PM) is a powerful tool that has found wide applications. However, simultaneous imaging of multiple FPs with 2PM is greatly hampered by the lack of proper ultrafast lasers offering multi-color femtosecond pulses, each targeting the two-photon absorption peak of a different FP. Here we demonstrate simultaneous two-photon fluorescence excitation of RFP, YFP, and CFP in human melanoma cells engineered to express a “rainbow” pallet of colors, using a novel fiber-based source with energetic, three-color femtosecond pulses. The three-color pulses, centered at 775 nm, 864 nm and 950 nm, are obtained through second harmonic generation of the 1550 nm pump laser and SHG of the solitons at 1728 nm and 1900 nm generated through soliton self-frequency shift (SSFS) of the pump laser in a large-mode-area (LMA) fiber. The resulting wavelengths are well matched to the two-photon absorption peaks of the three FPs for efficient excitation. Our results demonstrate that multi-color femtosecond pulse generation using SSFS and a turn-key, fiber-based femtosecond laser can fulfill the requirements for simultaneous imaging of multiple FPs in 2PM, opening new opportunities for a wide range of biological applications where non-invasive, high-resolution imaging of multiple fluorescent indicators is required.

8588-92, Session PSun

Analysis of spectrally resolved autofluorescence images by support vector machines

Anton Mateasik, Dusan Chorvat Jr., Alzbeta Chorvatova, International Laser Ctr. (Slovakia)

Redox fluorimetry and spectrally resolved imaging based on the mitochondrial autofluorescence (AF) provides an efficient tool for noninvasive assessment of functional and structural characteristics of the living cells and can be used for evaluation of overall health state of the cells. The key factor for successful application of AF signal as an intermediary of changes in mitochondrial metabolism is the knowledge of dependencies between detected AF intensities, spectral AF profiles and/or molecular events occurring in mitochondria [1]. Mitochondrial AF is primarily based on the fluorescence of FAD and NAD(P)H molecules. In this study, we focused on the spectral analysis of AF images of isolated cardiac cells to identify spectral components corresponding to fluorescence of FAD or NADPH, applying a blind source separation approach. Non-negative matrix factorization method was used for identification of sources [2]. This approach iteratively estimates the coefficient and fluorophore contribution from the global AF signal in each pixel of images. The non-negativity constraint was enforced on each component allowing only assumption of additive combinations. The output of this method was the extraction of quasi-orthogonal basic components that fully renders the AF signal. The extraction was independently done for different groups of cardiac cells exposed to various modulators of cell metabolism and respiration to mimic changes in mitochondrial metabolic state. The estimated spectral components were used for semi- automatic classification of metabolic state of cells applying support vector machine method: a supervised method decomposed in two steps [3]. The first – learning step consists of computing an optimal linear separator between learning classes. As an input, we have used the spectral fingerprints calculated in the blind source separation stage. The second step consists of the classification of the whole image data set by evaluating the distance of each pixel to the separator. In this step, manual parametric specification was established by choosing training pixels on each image corresponding to mitochondria localization and threshold them manually to obtain suitable classification parameter. Classification was done in respect to the responses of AF to metabolic modulators. The effectiveness and correctness of classification of AF images was the tested on approximately 1000 different sample images (original from experiment or modified by addition of noise, blur, spatial distortion, etc.). The success of correct classification was close to 90%, suggesting that this approach can be used for evaluating the FAD or NAD(P)H AF images. The main advantage of this approach is that with the sufficient training data, the AF images can be evaluated without need of spectral decomposition [4].

References

[1]. Chorvat D. Jr., Kirchnerova J., Cagalinec M., Smolka J., Mateasik A., Chorvatova A. Biophys. J 89 (2005) L55-57.

[2]. Lee D. D., Seung H. S. Proc. Neur. Inf. Proc. Syst. 13 (2000) 556-562.

[3]. Pal M., Mather P. M. Int. J. Remote Sens. 26 (2005) 1007-1011.

[4]. Authors acknowledge support from EC’s 7FP project LaserLab Europe III (grant agreement n° 284464), ERDF project Intelinsys (ITMS code 26240220072) and project VEGA-1/0296/11

8588-93, Session PSun

Two photon fluorescence stereomicroscopy with Bessel beams

Yan Long Yang, Juanjuan Zheng, Runze Li, Tong Ye, Xi'an Institute of Optics and Precision Mechanics (China)

Optical sectioning method is commonly used in multiphoton fluorescence laser scanning microscopy. Though the lateral scan rates can reach up to several kHz, the relatively slow z scan compromise the speed of real-time imaging of a volume. Here, we use axicon generated Bessel beams to replace Gaussian beams in multiphoton microscopy. The extended depth of field allow recording a volume of cells without scanning the depth. The depth information can be retrieved by recording a pair of parallax views of the same volume. We have also demonstrated that it is possible to add the stereoscope capability to multiphoton microscopy.

An axicon was used to convert a collimated beam to a Bessel beam, which projected a ring on a pair of galvonometer scanning mirrors. The rings were then relayed by two lenses to the back aperture of a microscope objective. The specimen was imaged by scanning the Bessel beam at a focal region that could be up to several hundred micrometers in depth. By slightly shifting the axicon in the lateral direction (<0.5mm), we were able to introduce a small displacement to the projected ring at the back aperture of the objective, which caused a tilted point spread function at the focus. The generated fluorescence in the specimen was collected by the objective and detected by a photomultiplier tube as in a general two-photon microscopy. For maximizing fluorescence collection efficiency, a configuration of filber bundle is used to detect the photons outside the light cone of the objective lens.

This technique can be incorporated to a two-photon fluorescence laser scan microscope. Without sacrificing the lateral resolution, the stereoscopic views of the specimen can be achieved with just two scanned frames.

8588-94, Session PSun

Two-photon microscopy for real-time monitoring of focused ultrasound-mediated drug delivery to the brain in a mouse model of Alzheimer's disease

Alison Burgess, Naomi B. Eterman, Sunnybrook Research Institute (Canada); Isabelle Aubert, Kullervo H. Hynynen, Sunnybrook Research Institute (Canada) and Univ. of Toronto (Canada)

There is substantial evidence that focused ultrasound (FUS) in combination with microbubble contrast agent can cause disruption of the blood-brain barrier (BBB) to aid in drug delivery to the brain. We have previously demonstrated that FUS efficiently delivers antibodies against amyloid-? peptides (A?) through the BBB, leading to a reduction in Alzheimer's pathology at 4 days. In the current study, we use two-photon microscopy to characterize the delivery of A? antibodies to the plaques in real time. Mice are anesthetized and a cranial window is made in the skull. A custom-built ultrasound transducer is fixed to a coverslip and attached to the skull, covering the cranial window. MethoxyX-04 [2mg/kg] delivered intravenously 1 hr prior to the experiment clearly labels the A? surrounding the vessels and the amyloid plaques in the cortex. Dextran conjugated Texas Red (70kDa) administered intravenously, confirms BBB disruption. At the ultrasound pressures tested in vivo, we observe that the disruption of the BBB occurs at vessels of similar in size in wild-type and transgenic mice, which have cerebral amyloid angiopathy. However, the time required for the BBB to repair itself following FUS is longer when the blood vessels are covered with amyloid. We have conjugated A? antibody BAM10 to the fluorescent molecule FITC for real time monitoring of the antibody distribution in the brain. We are currently optimizing the parameters to achieve maximal fluorescent intensity of the BAM10 antibody at the plaque surface. Two-photon microscopy is a valuable tool for evaluating the efficacy of FUS mediated drug delivery, including antibodies, to the Alzheimer brain.

8588-95, Session PSun

Detection of calcium waves in mice heart tissue with multispot two-photon imaging

Claudio de Mauro, Carlo A. Cecchetti, Domenico Alfieri, Light4Tech Firenze S.r.l. (Italy); Giulia Borile, Andrea Urbani, Marco Mongillo M.D., Venetian Institute of Molecular Medicine (Italy); Francesco S. Pavone, Univ. degli Studi di Firenze (Italy)

The highest limitation of multiphoton imaging is its acquisition speed because the laser beam scans the specimen with a raster pattern. A field of investigation requiring an improvement in acquisition speed is the study of Ca2+ signal propagation inside the cell and between cells. The technology of Multispot Multiphoton Microscopy (MCube) exploiting a diffractive optic element (DOE) allows increasing frame rate without losses in both spatial and axial resolution of acquired images. By exploiting the three operating mode, single beam, 16 beamlets or 64 beamlets, the best experimental conditions can be found by adapting the power per beamlet. This MCube system has been characterized in thick tissue samples, and subsequently used for the first time for Ca2+ imaging of acute heart slices. A test sample with fixed mice heart slices with embedded sub-resolution fluorescent beads has been used to test the capability of optical axial resolution up to ~200 microns in depth. Radial and axial resolutions of 1.2 microns and 3 microns have been respectively obtained with a 20X water immersion objective, getting close to the theoretical limit. Then images of heart slices cardiomyocites, loaded with Fluo4-AM have been acquired. The formation of Ca2+ waves during electrostimulated beating has been observed, and the possibility of easily acquire full frame images at 16Hz (16 beamlets) has been demonstrated, towards the in vivo study of time resolved cellular dynamics and arrhythmia trigger mechanisms in particular. The research leading to the results has received funding from the European Community's Seventh Framework Programme FP7/2007-2013 under grant agreement N° HEALTH-F2-2009-241526, EUTrigTreat.

8588-96, Session PSun

Visualization of pathological development for Alzheimer's model using multiphoton-excited multi-mode microscope

Gaixia Xu, Ming Ying, Hanben Niu, Jiazuan Ni, Shenzhen Univ. (China)

Alzheimer's disease (AD) is the most common cause of dementia in the elderly. It has been known that AD is associated with structural and morphological changes in the brain which induce the abnormal behavors of patients. Thus, to visualization of pathological changes of Alzheimer's disease is important for us to understand the disease development. The intrinsic optical emissions, such as autofluorescnece and harmonic generation are potentially useful for functional imaging and biomedical diseae diagnosis for biological samples.

In this work, a multimode microscope, detecting the signals of autofluorescence intensity, autofluorescence lifetime and second harmonic generation (SHG)?was used to visualize the sophisticated changes in brain slices harvested from 2-month, 4-month, 6-month, 8-month and 12-month triple-transgenic Alzheimer's models. The autofluorescence and SHG were characterized by their emission spectra. The results indicated that the autofluorescnece intensity pointed out the location of senile plaques, and the SHG provided the information of the neurofibrillary tangles (NFT). What's more, autofluorescence lifetime imaging indicated the different binding status of NADH, an intrinsic fluorescent molecule and ubiquitous metabolic co-enzyme. It is notable that all the signals varied according to the different ages of mice. The results suggested that such multimode microscope could provide valuable information about the disease development and metabolic states in pathological materials, which was useful to understand the AD diagnosis and therapy.

8588-97, Session PSun

Two-photon microscopy and Spectral phasor to monitor intrinsic fluorophores in normal and cancer 3D culture

Hoa H. Truong, Helene Knaus, Farzad Fereidouni, Gerhard A. Blab, Hans C. Gerritsen, Utrecht Univ. (Netherlands)

Nicotinamide Adenine Dinucleotide (NADH) and Flavin Adenine Dinucleotide (FAD) are important metabolic coenzymes to study cancer progression and cell death (1,2) via two-Photon Fluorescence Lifetime imaging (FLIM) system. In the general direction, we developed a novel approach of imaging and measuring NADH/FAD in 3D culture by combining two-photon microscopy with fluorescence anisotropy (FA) and spectral phasor (representing the spectra by polar representation, 3). Our goal is to exploit this technique to characterize cancer and non-cancer cellular spheroids (cell aggregates) by un-mixing and quantifying the intrinsic fluorphores based on their emission spectrum and FA. It has been reported spheroid of ~300-500 um contains several layers of cells at different stages of growth and activities. As expected, our preliminary data showed spheroids of >500 um was excited with 740 nm wavelength (in which NADH and FAD can be detected) displayed shift in spectrum, changed in NADH/FAD concentration, and FA with each increasing layer. This approach is more feasible than the standard histological assessment (a “snap-shot” of disease development) because it provides dynamic information of apoptotic stages and metabolic activities during cancer progression. Moreover, it reduces the use of exogenous fluorescence-labeled proteins (a common biological tool) that can modify cellular behaviors (e.g. unwanted cell death & disrupted protein function) or introduces artifacts, which does not normally occur with intrinsic fluorophores.

(1) Skala MC et al. J Biomed Opt. 2007 Mar-Apr;12(2):024014.

(2) Wang HW et al. J Biomed Opt. 2008 Sep-Oct;13(5):054011.

(3) Fereidouni F, Bader AN, Gerritsen HC. Opt Express. 2012 Jun 4;20(12):12729-41.

8588-98, Session PSun

Demonstration of near-bandwidth-limited 7-fs pulses at the foci of high-NA microscope objectives

Gabriel Tempea, FEMTOLASERS Produktions GmbH (Austria); Stefan Gomes da Costa, Wan Hui, Hilton B. de Aguiar, Andreas Volkmer, Univ. Stuttgart (Germany)

We demonstrate that near-bandwidth-limited pulses with 7 fs durations can be systematically achieved at the focus of commonly used, high-numerical-aperture microscope objectives, for which the control of both the group delay dispersion (GDD) and the third-order dispersion (TOD) of the setup was of paramount importance. We coupled 6.4-fs laser pulses (central wavelength at 820 nm) from an all-dispersive-mirror Ti:Sapphire oscillator into a Olympus IX71 inverted microscope via an ultra-broadband dispersive mirror compressor with a TOD/GDD ratio of 0.5 fs. This setup proved to be optimal for the compensation of several different high-NA objectives and paves the way for ultrafast (femtosecond) micro-spectroscopy.

8588-99, Session PSun

Wide dynamic range intensity sensitive SPR imaging biosensor based on the wavelength-scanning technique

Yan Li, Kai Zhang, Junle Qu, Shenzhen Univ. (China); Ho-Pui A. Ho, The Chinese Univ. of Hong Kong (China); Hanben Niu, Yonghong Shao, Shenzhen Univ. (China); Dayong Gu, Health Care Ctr. of Shenzhen International Travel (China)

Surface plasmon resonance (SPR)-based biosensing is one of the most advanced label free, real time detection technologies. Traditional intensity sensitive SPR biosensor technology has been commercialized and SPR biosensors have become an important tool for characterizing and quantifying biomolecular interactions. However, mechanically scanning an incident angle in these SPR sensors brings the hardware difficulty and reduces the stability. Moreover, its small dynamic range also limits its applications in microarray analysis. In this paper, we present a novel intensity sensitive SPR imaging based on a liquid crystal tunable filter (LCTF). A typical Kretschmann configuration is used in the system. The SPR cell is composed of an equilateral prism made of BK7 glass, a microscope glass slide coated with 46nm thick gold film and a flow chamber allowing different sample solutions to contact with the gold film. A white-light source is used for SPR excitation and the corresponding SPR intensity changes at different coupling wavelengths is recorded by an area CCD camera while the incidence angle is fixed. SPR intensity images at different optimized wavelengths can be acquired without any change to the hardware. Especially, compared to the traditional spectral SPR sensors, our SPR technique has both a wide dynamic range, high sensitivity and high throughput. The final dynamic range can be enlarged by the number of times which is determined by the spectral width of light source and incident angle. Our SPR imaging biosensor could have potential applications in microarray analysis.

8588-100, Session PSun

A study on the application of chirped photonic crystal fiber in multiphoton microscopy

Jiali Yu, The Univ. of British Columbia (Canada); Haishan Zeng, Harvey Lui M.D., The Univ. of British Columbia (Canada) and The BC Cancer Agency Research Ctr. (Canada) and Vancouver Coastal Health Research Institute (Canada); Julia S. Skibina, N.G. Chernyshevsky Saratov State Univ. (Russian Federation); Günther Steinmeyer, Max-Born-Institut für Nichtlineare Optik und Kurzzeitspektroskopie (Germany); Shuo Tang, The Univ. of British Columbia (Canada)

Multiphoton microscopy (MPM) has developed into a powerful technique for high resolution imaging from biological samples. However, most current MPM instruments are based on bench-top microscopes which greatly limit their clinical applications for in vivo imaging. Therefore, considerable efforts are made to develop fiber-based multiphoton endoscopes due to their flexibility and miniaturization. One major challenge of fiber-based MPM endoscopes is the efficient delivery of ultrashort pulses through the fiber in the near infrared region. Recently, a specially-designed chirped photonic crystal fiber (CPCF) can almost eliminate the pulse broadening effects in a broad transmission window because cell-size radial chirp in the cladding structure of CPCF, similar with principle of chirped mirror, localizes the reflection of different wavelengths in different resonant layers of the cladding. In contrast, traditional hollow core fiber (HCF) consists of several layers of identical holes that produce the substantial third-order dispersion. The feasibility of applying a novel CPCF to MPM imaging is studied in this paper. The propagation properties of CPCF for delivery of femtosecond pulses are compared with commercial HCF. Our experimental results indicate significantly lower dispersion and a larger transmission band of the CPCF compared to a HCF. And the extended bandwidth towards short wavelength of CPCF appears useful for enhancing the MPM signals for specific fluorophores (e.g. NADH, DAPI, etc.). Since nonlinear effects also affect the pulsewidth, the corresponding pulsewidths at different power levels are investigated for CPCF and HCF. The good performance of CPCF applied in MPM imaging is validated by images of fluorescent beads, potassium dihydrogen phosphate (KDP) and biological samples. We see a clear effect of increased image intensity for all images by CPCF illumination due to lower dispersion and extended bandwidth.

In conclusion, the extremely low dispersion of the CPCF over a wide transmission window is promising in fiber delivering of femtosecond pulses for high-resolution multiphoton endoscopy.

8588-101, Session PSun

Corneal refractive index measurement using a combined multiphoton microscopy and optical coherence tomography system

Tom Lai, Shau Poh Chong, Yifeng Zhou, Gregory Moloney, Shuo Tang, The Univ. of British Columbia (Canada)

Refractive index (RI) is a useful optical property that describes the physiological condition of the cornea. It is especially important for most ocular surgeries such as LASIK. In this study, we will calculate the corneal RI using a combined multiphoton microscopy (MPM) and optical coherence tomography (OCT) system. MPM excites and detects non-linear signals including two photon excitation fluorescence (TPEF) and second harmonic generation (SHG). TPEF signals are observed from NADH in the cytoplasm, allowing MPM to image the cellular structures in the corneal epithelium and endothelium. SHG signals are observed from collagen, an abundant connective tissue found in the stroma. Optical coherence tomography (OCT) produces cross-sectional, structural images based on the interferences fringes created by the reflected light from the sample and reference arms. Our system uses a single sub-10 fs Ti:sapphire laser source which is good for both MPM's excitation and OCT's resolution. The MPM and OCT images are co-registered when they are taken successively because their axial resolutions are similar and because the system shares the laser source and the scanning unit. We can calculate the RI by measuring the physical thickness and the optical path length of the cornea from the MPM and OCT images respectively. We have imaged and calculated the RI of human, piscine, and murine corneas. We were able to see the epithelial, stromal, and endothelial layers and compare their relative thicknesses and the organization of the stromal collagen lamellae. Our preliminary results showed that our system can provide both functional and structural information about the cornea and measure the RI of multi-layered tissues.

8588-102, Session PSun

Two-photon imaging in Z axis without moving the objective lens

Long Yan, Zaki Moustafa, Jason M. Christie, James Schummers, Max Planck Florida Institute (United States)

Multiphoton microscopy is widely used for depth-resolved imaging in biological applications due to its inherent optical sectioning capability. Traditionally, the optical axis of focus is altered by repositioning the objective lens relative to the specimen, which is not only slow but can also cause vibration if images are acquired during repositioning. Recently, a new method to change the axial (z) location of focus without moving the objective lens has been demonstrated using an electrically tunable lens (ETL) immediately above the objective (Grewe et al. 2011). We present a modification of this design in which the ETL is repositioned away from the objective and into the excitation beam path. The advantages of this design are: 1) it doesn't affect the collection path, 2) it places no constraints on the objective lens used and 3) it can be implemented easily.

8588-103, Session PSun

Monitoring glucose oxidase immobilization processes by means of two-photon microscopy

Ines Delfino, Univ. degli Studi della Tuscia (Italy); Marianna Portaccio, Gianluigi Manzo, Mario De Rosa, Maria Lepore, Seconda Univ. degli Studi di Napoli (Italy)

The enzyme immobilization processes is of fundamental importance both for technological applications and for understanding protein interactions in solid state phase. The enzyme distribution on different supports can be experimentally evaluated by coupling microscopic techniques with staining radioactive or fluorescence labelling. Unfortunately, the nonuniformity in protein-labelling methods is a potential source of errors in these studies. Moreover fluorescence labelling alters the enzyme structure, with consequential changes in protein adsorption and in other physicochemical properties. Also Fourier Transform Infrared (FT-IR) microscopy has been recently proposed for the quantitative determination of an immobilized protein's spatial distribution throughout supporting media without the need for protein modification or staining. However, FT-IR can give information only on very thin superficial layers and with a spatial resolution not less than tens of micron. In the present report we used a standard de-scanned two-photon microscope for monitoring glucose oxidase (GOD) immobilization processes on different supports using endogeneous FAD fluorescence. In particular we investigated sol-gel supports and various kinds of functionalized beads by means of a two-photon microscope based on a modified confocal scanhead (Olympus Fluoview 300) with internal detectors and a Ti:sapphire laser (Chameleon Ultra). The obtained results show that GOD immobilization processes can be successfully monitored and also interaction with glucose can be studied in order to develop new biosensing schemes

8588-104, Session PSun

3D microrheology using wide-field two photon microscopy

Naveen K. Balla, National Univ. of Singapore (Singapore) and Singapore MIT Alliance for Research and Technology (Singapore); Elijah Y. Yew, Singapore-MIT Alliance (Singapore); Hayden K. Taylor, Nanyang Technological Univ. (Singapore); Peter T. C. So, SMART-Singapore MIT Alliance for Research & Technology (Singapore) and Massachusetts Institute of Technology (United States)

Two particle microrheology, which is based on tracking multiple particles, allows measurement of mechanical properties of soft materials using wide-field microscopy. This technique has given us new insights into the roles played by mechanical forces in biological systems. Different types of cells respond differently to mechanical forces acting on them. Mechanical forces are actively involved in important physiological process like cancer metastasis, angiogenesis, and stem cell differentiation. Conventional single photon wide-field microscopy lacks axial sectioning ability and therefore two particle microrheology studies have been carried out primarily on 2D samples. Biological processes occur in 3D environments and to probe mechanical properties of these environments we need a wide-field imaging tool with axial sectioning ability. Wide-field two photon microscopy meets this criterion. We built a wide-field two photon microscope which is capable of imaging 100 µm x 100 µm regions with an axial resolution of 1.6 µm. Using this microscope, we have demonstrated that we can track fluorescent beads embedded in collagen matrix over a period of time. The tracking data was used to calculate viscosity modulus (G') and elasticity modulus (G") of the gels. To demonstrate microrheology in 3D, we measured the viscoelastic properties of two different types of collagen gels stacked on top of one another. Thus, our system can be used to monitor mechanical changes in 3D tissue cultures over extended periods of time.

8588-106, Session PSun

in vivo imaging of dermal collagen in skin burn by collagen-sensitive second-harmonic-generation microscopy

Takeshi Yasui, Univ. of Tokushima (Japan) and Osaka Univ. (Japan); Ryosuke Tanaka, Osaka Univ. (Japan); Eiji Hase, Univ. of Tokushima (Japan); Shuichiro Fukushima, Tsutomu Araki, Osaka Univ. (Japan)

Burn, which is caused by excessive thermal invasions, such as flame, hot liquids or hot solids, is a common and significant injury in skin. Since a therapeutic method to the burn largely differs depending on the invasion depth, an assessment of the burn depth is a key step to determine the clinical treatment plan of burn. Optical probe methods are attractive for such assessment because of a simple, non-contact, and low invasion to the patient. If one can obtain biological information closely related with the skin burn by optical probe methods, optical burn assessment will be achieved. One biological change caused by the burn is structural transition of collagen molecule from triple helix to random coil. Therefore, second-harmonic-generation (SHG) microscopy is one potential method for non-invasive assessment of skin burn because it is sensitive to structural asymmetry of materials in the order of optical wavelength. In this paper, we evaluated a potential of SHG microscopy for assessment of skin burn through in vivo imaging of dermal collagen in animal skin. Animal model of burn was prepared following well-established protocols of Walker and Mason and the experimental protocol was approved by Bioethics Committee for Animal Experiment at Osaka University, Japan. We confirmed in SHG image that the cracked structure was appeared and its size become finer with respect to increase of the invasion depth as well as decreased intensity of SHG light. These results imply a high potential of SHG microcopy for optical burn assessment.

8588-107, Session PSun

in vivo imaging of collagen fiber orientation with rapid polarization-resolved SHG microscopy

Yuji Tanaka, Osaka Univ. (Japan); Eiji Hase, Univ. of Tokushima (Japan); Shuichiro Fukushima, Osaka Univ. (Japan); Takeshi Yasui, Univ. of Tokushima (Japan); Tsutomu Araki, Osaka Univ. (Japan)

Second-harmonic-generation (SHG) microscopy has attracted attentions as a powerful tool for in vivo imaging of dermal collagen fiber because SHG light is specifically generated by asymmetric triple-helix structure of collagen molecule. Interestingly, when the laser light is linearly polarized, the emission efficiency of SHG light depends on a relation between polarization angle of incident laser light and orientation angle of collagen fiber. Therefore, polarization-resolved SHG microscopy can be used to visualize the distribution of collagen fiber orientation in tissue. For example, polarization-resolved SHG microscopy using two perpendicularly, linearly polarized laser lights indicated that wrinkle direction in UVB-exposed skin was predominantly parallel to the orientation of dermal collagen fibers. However, long data acquisition time in previous polarization-resolved SHG microscopy, resulting from mechanical rotation of a half-wave plate, makes the microscopy sensitive to artifacts such as pulsation or breath of subjects; this hinders in vivo application of polarization-resolved SHG microscopy. In this paper, to achieve in vivo measurement without influence of artifacts, we introduced an electro-optic modulator (EOM) into polarization-resolved SHG microscopy. Polarization angle of linearly polarized laser light was switched between vertical and horizontal directions at a rate of several tens kHz by EOM. The rapidly polarization-switched laser light was used to acquire a pair of data set of SHG intensity under vertical and horizontal polarization pixel-by-pixel. The effectiveness of this microscopy was demonstrated by in vivo imaging of collagen fiber orientation in animal skin and human one.

8588-108, Session PSun

Noninvasive polarization second harmonic generation of oral epithelial dysplasia

Gracie Vargas, Kert Edward, Jinping Yang, Siumin Qiu, The Univ. of Texas Medical Branch (United States)

Epithelial neoplastic transformation is associated with alterations of the basement membrane and lamina propria, including changes in the organization and orientation of fibrillar collagen. Polarization sensitive second harmonic generation (PSHG) has been exploited as a technique for orientation characterization of type I collagen in pathological conditions such as atherosclerosis. However, this technique has not been utilized for the non-invasive characterization of oral neoplasia. In this study, we used PSHG to investigate the fibrillar collagen organization and anisotropy differences in normal and dysplastic oral epithelium.

In vivo PSHG imaging was performed on the buccal pouch of the 9,10-dimethyl-1,2-benzanthracene (DMBA) hamster model for oral carcinogenesis (8-12 weeks;n=6) and mineral oil controls (n=2). During imaging, the polarization of the incident light was varied in increments of 10 degrees for full rotation with an SHG image acquired at each increment. Subsequent processing and fitting analysis was performed for determination of the angular distribution of collagen fiber orientation and anisotropy calculation using MATLAB code developed in-house.

Results indicated a distinct difference between normal and dysplasia in angular distribution with additional intensity peaks observed in the latter and indicating increased disorganization. The tri-helix orientation angle was the same for both groups and consistent with previously published results. Significantly greater anisotropy was observed in dysplastic oral mucosa compared to normal.

8588-109, Session PSun

Applying tattoo dye as third-harmonic generation contrast agent for in vivo optical biopsy of human skin

Ming-Rung Tsai, National Taiwan Univ. (Taiwan); Yi-Hua Liao M.D., National Taiwan Univ. Hospital (Taiwan); Chi-Kuang Sun, National Taiwan Univ. (Taiwan)

In vivo harmonic-generation microscopy (HGM) has been reported to provide an extraordinary performance on human skin. In human skin, third-harmonic generation (THG) microscopy can provide intrinsic contrasts in elastic fibers, cytoplasmic membrane, nucleus, lipid bodies, hemoglobin, and melanin. For advanced molecular imaging, it is sometime required to develop exogenous contrast agents to trace the function of a specific molecule. Tattooing has been practiced for centuries in many cultures spreading throughout the world. In this paper, we demonstrate that tattoo dye can serve as a THG contrast agent for in vivo molecular imaging in skin due to the principles of multiphoton resonant enhancement. Spectroscopy and microscopy experiments of tattoo dyes were performed on cells, in vivo mouse skin, and eventually in human skin in vivo. To test whether the tattoo dye could be used for contrast enhancement, tattoo dyes were transfected into cultured cells and the THG enhancement of membrane can be found. In addition, we confirmed the THG enhancement of tattoo dye from in vivo HGM of mouse and human skin. Taking advantage of the weak multiphoton fluorescence of a specific tattoo dye, in vivo molecular THG microscopy of human skin by using a tattoo dyes is achieved. In comparison with hematoxylin or nanoparticles as exogenous THG contrast agents, tattoo dyes are with a bio-compatible characteristic for future clinical applications. Our result indicates that tattoo dyes provide a high potential to serve as a THG exogenous contrast agent for in vivo optical biopsy of human skin.

8588-111, Session PSun

Stimulated emission reduced fluorescence microscopy for high-resolution deep-tissue imaging

Wei Min, Lu Wei, Zhixing Chen, Columbia Univ. (United States)

Two-photon fluorescence microscopy has become an indispensable tool for imaging scattering biological samples by detecting scattered fluorescence photons generated from a spatially confined excitation volume. However, this optical sectioning capability breaks down eventually when imaging much deeper, as the out-of-focus fluorescence gradually overwhelms the in-focal signal in the scattering samples. The resulting loss of image contrast defines a fundamental imaging-depth limit, which cannot be overcome by increasing excitation efficiency. Herein we propose to extend this depth limit by performing stimulated emission reduced fluorescence (SERF) microscopy in which the two-photon excited fluorescence at the focus is preferentially switched on and off by a modulated and focused laser beam that is capable of inducing stimulated emission of the fluorophores from the excited states. The resulting image, constructed from the reduced fluorescence signal, is found to exhibit a significantly improved signal-to-background contrast and sharper spatial resolution owing to its overall higher-order nonlinear dependence on the incident laser intensity. We demonstrate this new concept by both analytical theory and numerical simulations. For brain tissues, SERF is expected to extend the imaging depth limit of two-photon fluorescence microscopy by a factor of about 2. The simplicity of required instruments and the biocompatibility of the relatively weak stimulated emission beam promise the utility of this new technique in two-photon high-resolution deep tissue imaging.

8588-112, Session PSun

Study of aging-related photosynthesis pathway change in the plant

Yongjoon Joo, Taejun Wang, Eunjoo Lee, Yumi Kim, HongGil Nam, Ki Hean Kim, Pohang Univ. of Science and Technology (Korea, Republic of)

Photosynthesis is an important process in the plant. To absorb lights of various wavelengths, there exists light harvesting complex 2 which contains many pigments like chlorophyll a/b and carotenoid. These pigments have different absorption spectra and different excitation pathways which we can distinguish by fluorescence time. We'd like to study the changes of these photo-excitation pathways related with aging by imaging plant leaves at different ages. To see the chloroplast itself, we will use confocal microscopy and two-photon microscopy will be used to see two different excitation paths. Regardless of which pigments are excited, what we see are chlorophylls as pigments will transfer the absorbed energy. At 850nm, chlorophyll b excitation path will be imaged and carotenoid excitation will be imaged at 1200nm. Carotenoid mostly absorbs lights in blue-green region, but when it is two-photon excited, it can absorb 1200nm (same as 600nm in single photon excitation) and rise to an energy state unavailable in single photon excitation. Arabidopsis, whose genetic information is well known, will be used for imaging. Various mutant Arabidopsis plants related with aging will be imaged as well. Two-photon microscopy and confocal fluorescence microscopy will measure the excitation spectra of chloroplasts to provide functional information of individual pathways. Confocal reflectance microscopy will be used to provide size information of chloroplasts.

8588-114, Session PSun

Fluorescence lifetime imaging with pulsed diode laser enabled stimulated emission

Jianhong Ge, Cuifang Kuang, Zhejiang Univ. (China); Shin-Shian Lee, National Yang-Ming Univ. (United States); Fu-Jen Kao, National Yang-Ming Univ. (Taiwan)

We present a stimulated emission based fluorescence lifetime imaging (FLI) scheme using a pair of synchronized diode lasers operating at gain switched pulse mode. Two semiconductor lasers, with wavelengths at 635 nm and 700 nm, serve as the excitation and the stimulation light sources for the Atto647N labeled sample, respectively. FLI is readily achieved with their relative delay controlled electronically. The coherent nature of the stimulated emission signal also allows FLI at long working distance. In this way, a high performance all-semiconductor fluorescence lifetime module is realized in a compact, robust, and cost effective configuration.

8588-115, Session PSun

Multiphoton phosphorecence lifetime imaging microscopy (MP-PLIM): tissue-friendly lifetime imaging on the microsecond domain with platinum (II) complexes

Elizabeth Baggaley, Univ. of Sheffield (United Kingdom); Stanley Walter Botchway, Rutherford Appleton Lab. (United Kingdom); John W. Haycock, The Univ. of Sheffield (United Kingdom); Igor V. Sazanovich, Univ. of Sheffield (United Kingdom); J. A. Gareth Williams, Durham Univ. (United Kingdom); Julia A. Weinstein, The Univ. of Sheffield (United Kingdom)

Non-invasive detection and tracking of bio-molecules is key to understanding biological processes which underpin complex biological systems. Developments in imaging technologies over recent years has seen the emergence of femtosecond red and near infra red lasers that enable effective tissue penetration via multiphoton excitation, and thus high-resolution, in vivo imaging. The powerful technique of multiphoton excitation, combined with lifetime imaging on the previously unprecedented microsecond time domain, has recently been made a reality with a series of novel [PtLCl] complexes, where L represents a tridentate, N^C^N-coordinated ligand, based on 1,3-di(2-pyridyl) benzene.

The long emission lifetimes of [PtLCl] complexes in vitro have already enabled autofluorescence-free imaging using Time Resolved Emission imaging Microscopy (TREM)1,2 and phosphorescence lifetime mapping of living cells and histological tissue via time correlated single photon counting (TCSPC).3

The recent emergence of a combined FLIM / PLIM system (Becker & Hickl GmbH) in conjunction with these biologically compatible microsecond [PtLCl] emitters has widened the scope of lifetime imaging. Simultaneous collection of kinetic data from both short and long lived probes / dyes has the potential to provide a wealth of information from the local biological environment, whilst also making autofluorescence-free imaging a reality.

Simultaneous two-photon, FLIM / PLIM imaging, with [PtLCl] dyes on live cells and histological tissue will be presented along with the potential applications in life sciences and diagnostics.

8588-116, Session PSun

Fluorescence Lifetime Imaging (FLIM) for mapping intracellular polarity

James A. Levitt, Pei-Hua Chung, Gilbert O. Fruhwirth, Klaus Suhling, King's College London (United Kingdom)

We demonstrate that TCSPC-based two-photon-excitation spectrally-resolved Fluorescence Lifetime Imaging (FLIM) allows mapping of polarity in living HeLa cells. We have used the hydrophobic, solvatochromic dye Nile Red, which is taken up into hydrophobic cellular compartments, most notably into lipid droplets. Fluorescence lifetime measurements of the dye as a function of the dielectric constant (?) in isotropic media

served as calibration plots, which were then used to create dielectric constant maps for the cells. Our data reveal an average of ?≈12 in lipid droplets and ?≈20 in other stained internal membranes, consistent with intensity-based spectrally-resolved confocal microscopy measurements. We also show that spectrally-resolved fluorescence lifetime measurements reveal emission wavelength dependent fluorescence decay kinetics of Nile Red. The average fluorescence lifetime is found to increase with increasing emission wavelength. Finally, we discuss the origins of multi-exponential fluorescence decays from Nile Red and the potential of this dye for use as a probe for multiple cellular properties (polarity and viscosity) simultaneously.

8588-27, Session 4

Monitoring subunit rotation in single FRET-labeled FOF1-ATP synthase in an anti-Brownian electrokinetic trap *(Invited Paper)*

Michael Börsch, Hendrik Sielaff, Anja Korn, Marc Renz, Friedrich-Schiller-Univ. Jena (Germany); Nawid Zarrabi, Univ. Stuttgart (Germany)

FOF1-ATP synthase is the membrane proteine catalyzing the synthesis of the 'biological energy currency' adenosinetriphosphate ATP. The enyzme uses internal subunit rotation for the mechanochemical conversion of a proton motive force into the chemical bond. We have used single-molecule Förster resonance energy transfer (FRET) to monitor subunit rotation in the two coupled motors F1 and FO. Therefore, enzymes were reconstituted into 120-nm sized lipid vesicles. The observation times in a confocal microscope for subunit rotation are now extended by capturing single vesicles in an modified anti-Brownian electrokinetic trap (ABELtrap, invented by A. E. Cohen and W. E. Moerner). Hidden Markov Models are applied to identify the dwells and substeps of the rotary motors running at low ATP concentrations.

8588-28, Session 4

FLIM with near-infrared dyes *(Invited Paper)*

Wolfgang Becker, Vladislav I. Shcheslavskiy, Becker & Hickl GmbH (Germany)

Near-infrared (NIR) dyes are used as fluorescence markers in small-animal imaging and in diffuse optical tomography of the human brain. It is therefore important to know whether these dyes bind to proteins or other tissue constituents, and whether they report anything about the metabolic state of the tissue via their fluorescence lifetimes. Unfortunately, neither the lasers nor the detectors of commonly used confocal and multiphoton laser scanning microscopes allow for excitation and detection of NIR fluorescence. We therefore upgraded existing confocal FLIM systems with NIR lasers and NIR sensitive detectors. In multiphoton systems we used the Ti:Sa laser as a one-photon excitation source in combination with an NIR-sensitive detector in the confocal beam path. We tested a number of NIR dyes in cells and tissue. Most of them showed clear lifetime changes depending on the location in the cells. We therefore believe that NIR FLIM can deliver molecular information that is not available by steady-state imaging techniques.

8588-29, Session 4

Two photon fluorescence imaging of lipid membrane domains and potentials using advanced fluorescent probes

Yves Mely, Zeinab Darwich, Olexandr Kucherak, Pascal Didier, Andrey Klymchenko, Univ. de Strasbourg (France)

Biomembranes are ordered and dynamic nanoscale structures critical for cell functions. The biological functions of the membranes strongly depend on their physicochemical properties, such as electrostatics, phase state, viscosity, polarity and hydration. These properties are essential for the membrane structure and the proper folding and function of membrane proteins. To monitor these properties, fluorescence techniques and notably, two-photon microscopy appear highly suited due to their exquisite sensitivity and their capability to operate in complex biological systems, such as living cells and tissues. In this context, we have developed a series of multiparametric environment-sensitive fluorescent probes tailored for precise location in the membrane bilayer. We notably developed probes of the 3-hydroxychromone family, characterized by an excited state intramolecular proton transfer reaction, which generate two tautomeric emissive species with well-separated emission bands. As a consequence, the response of these probes to changes in their environment could be monitored through changes in the ratios of the two bands, as well as through changes in the fluorescence lifetimes. Using two-photon ratiometric imaging and FLIM, these probes were used to monitor the dipolar and surface membrane potentials, and were applied to image apoptotic cells and membrane rafts 1, 2. Moreover, by coupling the solvatochromic fluorescent dye Nile Red with an amphiphilic anchor group, we developed a membrane probe showing a reversible redox switching of its fluorescence at one leaflet using sodium dithionite, which allows monitoring its flip-flop3. This probe binds exclusively to cell plasma membranes and can be used to monitor cholesterol depletion.

1. Shynkar VV, Klymchenko AS, Kunzelmann C, Duportail G, Muller CD, Demchenko AP, Freyssinet JM, Mely Y, J Am Chem Soc, 2007, 129, 2187.

2. Demchenko AP, Mély Y, Duportail G, Klymchenko AS. Biophys. J., 2009, 96, 3461.

3. Kucherak OA, Oncul S, Darwich Z, Yushchenko DA, Arntz Y, Didier P, Mély Y, Klymchenko AS. J Am Chem Soc, 2010, 132, 4907.

8588-30, Session 4

Polarization resolved confocal imaging to study rotation dynamics, clustering and absolute orientations in biological sample *(Invited Paper)*

Volker Buschmann, Benedikt Krämer, PicoQuant GmbH (Germany); Samantha Fore, PicoQuant Photonics North America, Inc. (United States); Felix Koberling, PicoQuant GmbH (Germany); Joerg Nikolaus, Humboldt Univ. (Germany); Uwe Ortmann, PicoQuant GmbH (Germany); Roland Schwarzer, Joanna Ziomkowska, Humboldt Univ. (Germany); Andreas Herrmann, Humboldt-Univ. zu Berlin (Germany); Rainer Erdmann, PicoQuant GmbH (Germany)

While the fluorescence intensity and color is routinely measured in commercial laser scanning microscopes, measurements of the fluorescence polarization are addressed much less frequently, in spite of numerous applications where this technique can be usefully applied. A few examples are: Measurements of molecular rotations through polarization resolved fluorescence correlation analysis or investigating the molecular orientation in membrane studies. Different subpopulations can be resolved using a multiparameter analysis approach in single molecule studies.

A very important application for anisotropy measurements is HOMO-FRET, Förster Resonance Energy Transfer between two equal molecules. HOMO-FRET results in a decreased anisotropy and thereby makes the anisotropy an ideal indicator for molecular clustering.

We have developed an easy and robust way to upgrade a commercial CLSM for polarization resolved measurements, using a retractable polarizing beam splitter that allows to split the fluorescence light into its two perpendicular polarized components. In combination with Time-Resolved Single Photon Counting (TCSPC), it allows also time-resolved

anisotropy measurements on a confocal microscope.

We present several applications for anisotropy analysis. Measurements of fluorescently labeled Giant Unilamellar Vesicles (GUVs) reveal the order of membrane domains by fluorescence lifetime and anisotropy imaging, as well as the orientation of the fluorophores within the membrane. Studying the location of cluster formation of a viral membrane protein through Homo-FRET can help to clarify the molecular mechanisms of virus proliferation. As well, the orientation of immobilised single molecules imaged on a substrate can be investigated.

8588-31, Session 5

Improving fluorescence guided diagnosis using spectral and time resolved methods *(Invited Paper)*

Angelika C. Rueck, Univ. Ulm (Germany)

Fluorescence guided diagnosis of tumour tissue is in many cases insufficient, because false positive results are interfering with the outcome. Discrimination between tumour and inflammation could be therefore difficult. Improvement of fluorescence diagnosis by introducing time resolved methods could be the solution. However, in the case of autofluorescence a complex combination of fluorophores give rise to the emission signal. Also in PDD (photodynamic diagnosis) different photosensitizer metabolites contribute to the fluorescence signal. Therefore, the fluorescence decay in many cases does not show a simple monoexponential profile. In those cases a considerable improvement could be achieved when time-resolved and spectral-resolved techniques are simultaneously incorporated. Global analysis and new algorithms were successfully implemented (Strat et al., 2011).

This paper discusses various possibilities which FLIM ("fluorescence lifetime imaging") and SLIM ("spectral resolved fluorescence lifetime imaging") offers for improving fluorescence guided diagnosis, as well as successfully realized applications. Special attention is focused on the detection of NADH, FAD and 5-ALA (5-aminolevulinic acid) induced porphyrins. With respect to NADH and FAD the discrimination between protein bound and free coenzyme was investigated in squamous carcinoma cells from different origin. These measurements allowed a deeper understanding of the metabolic state of the cells. The redox ratio, which can be correlated with the fluorescence lifetimes of NADH and FAD also changed depending on the state of the cells.

Most of our investigations were done in monolayer cell cultures. However, in order to get information from a more realistic in vivo situation we additionally used the chorioallantoismembrane (CAM) of fertilized eggs where tumour cells or biopsies were allowed to grow. The results of theses measurements will be discussed as well.

Literature:

D. Strat, F. Dolp, B. von Einem, C. Steinmetz, C.A.F. von Arnim and A. Rueck „Spectrally resolved fluorescence lifetime imaging microscopy (SLIM): FRET Global Analysis with a one- and two-exponential donor model", JBO 16(2), 026002 (February 2011).

8588-32, Session 5

Time-resolved spectroscopy of endogenous NAD(P)H in Gluconobacter oxydans *(Invited Paper)*

Julia Horilova, Katarina Kromkova, International Laser Ctr. (Slovakia) and Comenius Univ. in Bratislava (Slovakia); Marek Bucko, Aniko Illesova, Slovak Academy of Sciences (Slovakia); Anton Mateasik, Dusan Chorvat Jr., International Laser Ctr. (Slovakia); Alica Vikartovska, Institute of Chemistry, Slovak Academy of Sciences (Slovakia); Vladimir Stefuca, Axxence Slovakia s.r.o (Slovakia); Alzbeta Chorvatova, International Laser Ctr. (Slovakia)

The genus Gluconobacter comprises some of the most frequently used microorganisms when it comes to biotechnological and/or nanotechnological applications [1, 2]. It belongs to the group of acetic acid bacteria, which are characterized by their ability to incompletely oxidize a wide range of carbohydrates and alcohols resulting in production of NAD(P)H in electron transport chain [3]. In most cases, the reactions are catalyzed by dehydrogenases connected to the respiratory chain. Our goal was to evaluate whether the endogenous NAD(P)H fluorescence, used for evaluation of the oxidative capacity and sensitivity of the oxidative metabolic state in mammalian cells [4], can be also recorded in Gluconobacter oxydans (GOX). Endogenous NAD(P)H fluorescence of GOX was investigated in bacteria, resuspended in phosphate buffer (50 mM, pH 7). We measured excitation/emission spectra by steady-state fluorimetry (Fluorolog 3-11, SPEX, USA). For time-resolved measurements we used TCSPC setup and excitation by 375nm pulsed diode laser (Becker&Hickl, Germany). We evaluated the concentration dependence of the bacterial endogenous fluorescence, temperature-dependent changes and finally spectral changes induced by metabolic modulation of GOX. In temperature studies, the cuvette was heated by temperature bath (RE106, Lauda) from 22°C to 35°C. Fresh bacteria (up to 5 hours after isolation), as well as de-freezed ones (after freezing at -20°C) were studied. NAD(P)H fluorescence increased linearly with the concentration of bacteria. Freezing have little effect on the endogenous fluorescence or viability of bacteria. Sodium cyanide (10 mM) provoked significant rise in the NAD(P)H fluorescence, while dinitrophenol (200 μM) induced its decrease, confirming the bacterial fluorescence sensitivity to modulators of electron transport chain. Gathered preliminary results demonstrate that endogenous NAD(P)H fluorescence can be successfully recorded in the bacterial strain GOX using time-resolved measurements. The obtained data were subjected to numerical analysis. GOX represents an interesting model system for nano/bio-technological applications, such as synthesis of aromatic substances, being encapsulated in polyelectrolyte microcapsules in the process of production of natural flavors. We show that combined approach of lifetime- and spectrally-resolved detection of their autofluorescence can provide viable information about their activity and metabolic conditions, which can be further used in conditioning, adaptation and control of their properties in bioreactors [5].

References

[1]. Muynck C., Pereira C.S.S, Naessens M., Parmentier S., Soetaert W., Vandamme E.J. Critical Reviews in Biotechnology 27 (2007) 147-171.

[2]. Svitel J., Tkac J., Vostiar I., Navratil M., Stefuca V., Bucko M., Gemeiner P. Biotechnology Letters 28 (2006) 2003-2010.

[3]. Deppenmeier U., Hoffmeister M., Prust C., Appl Microbiol Biotechnol, 60 (2002) 233-242.

[4]. Chorvat D. Jr. and Chorvatova A. Laser Phys. Letters 6 (3) (2009) 175–193.

[5]. Authors acknowledge support from EC's 7FP project LaserLab Europe III (grant agreement n° 284464), project VEGA-1/0296/11 and project APVV-0302-10.

8588-33, Session 5

A freely triggerable picosecond supercontinuum laser source for fluorescence lifetime spectroscopy

Kristian Lauritsen, Thomas Schönau, Torsten Siebert, Sebastian Tannert, Romano Haertel, Thomas Eckhardt, Rainer Erdmann, PicoQuant GmbH (Germany)

An all-fiber picosecond supercontinuum laser is presented that is specifically designed to meet the requirements of a light source for fluorescence lifetime spectroscopy by time-correlated single-photon counting (TCSPC). The key features include the capability of flexible acquisition rates with a uniform spectral profile and equivalent pulse characteristics of the supercontinuum over variable repetition rates from 1 to 40 MHz in the spectral range from 480 to 700 nm. This is achieved with a balanced three-stage Yb3+fiber-amplification scheme of a freely

triggerable gain-switched laser diode at 1062 nm that maintains constant peak power of the amplified signal for equivalent supercontinuum generation in a photonic crystal fiber (PCF) over the full range of repetition rates. The nonlinear propagation in the PCF is scaled to avoid significant dispersion for maintaining nearly analytical pulse profiles at sub 150 ps, while simultaneously guaranteeing the highest power density in all the spectral channels of the supercontinuum. In order to provide free wavelength selection, two spectral filtering techniques are presented that allow for a contrast better than five orders of magnitude in a desire spectral channel of variable bandwidth. This offers flexible acquisition rates, high time-resolution and high contrast wavelength selection to single photon counting applications for which selected applications are presented in order to illustrate the capabilities of this supercontinuum laser source. The unique feature of the external pulse trigger allows for the incorporation of this tunable source into multi-color excitation schemes like PIE or ALEX for single molecule FRET measurements with very high precision.

8588-34, Session 5

Development of a fast TCSPC FLIM-FRET imaging system

Simon P. Poland, Simao Coelho, King's College London (United Kingdom); Nikola Krstajic, David Tyndall, Richard Walker, The Univ. of Edinburgh (United Kingdom); David U. Li, Univ. of Sussex (United Kingdom); Robert K. Henderson, The Univ. of Edinburgh (United Kingdom); Simon M. Ameer-Beg, King's College London (United Kingdom)

Forster/Fluorescence resonant energy transfer (FRET) has become an extremely important technique to explore biological interactions in cells and tissues. As the non-radiative transfer of energy from the donor to acceptor occurs typically only within 1-10nm, FRET measurement allows the user to detect localisation events between protein-conjugated fluorophores.

The use of time correlated single photon counting (TCSPC) to measure fluorescence lifetime (FLIM) has become the gold standard for measuring FRET interactions in cells. The technique is fundamentally superior to all existing techniques due to its near ideal counting efficiency, inherent low excitation light flux (reduced photobleaching and toxicity) and time resolution. Unfortunately due to its slow acquisition time when compared with other techniques, such as Frequency-domain lifetime determination or anisotropy, this makes it impractical for measuring dynamic protein interactions in cells. The relatively slow acquisition time of TCSPC FLIM-FRET is simply due to the system usually employing a single-beam scanning approach where each lifetime (and thus FRET interaction) is determined individually on a voxel by voxel basis.

In this paper we will discuss the development a microscope system which will parallelise TCSPC for FLIM-FRET in a multi-beam multi-detector format. This will greatly improve the speed at which the system can operate, whilst maintaining both the high temporal resolution and the high signal-to-noise for which typical TCPSC systems are known for. Using a beamlet array generated using a spatial light modulator (SLM) and a single photon avalanche detector (SPAD) array, some examples highlighting the capability of the system will be shown.

8588-35, Session 5

A fiber-laser-based stimulated Raman scattering spectral microscope

Keisuke Nose, Yasuyuki Ozeki, Tatsuya Kishi, Kazuhiko Sumimura, Yasuo Kanematsu, Kazuyoshi Itoh, Osaka Univ. (Japan)

Stimulated Raman scattering (SRS) spectral microscopy is a powerful technique for label-free biological imaging because it allows us to distinguish chemical species with overlapping Raman bands. Here we present a SRS spectral microscope based only on fiber lasers (FL's), which offer the possibilities of downsizing and simplification of the system. Femtosecond figure-8 Er-FL pulses at a repetition rate of 54.4 MHz are used to generate pump pulses. After amplifying by an Er doped fiber amplifier, 4-ps second harmonic pulses are generated by a 25-mm long periodically poled Mg:LiNbO3 crystal. As Stokes pulses, femtosecond Yb-FL pulses at a repetition rate of 27.2 MHz are used. These lasers are synchronized by a phase locked loop, which consists of a two-photon absorption photodetector, a loop filter, a phase modulator in the Er-FL cavity, and a piezo transducer in the Yb-FL cavity. The intensity noise of pump pulses is reduced by the collinear balanced detection (CBD) technique, based on delay-and-add fiber lines. Experimentally, we confirmed the intensity noise level of probe pulses was close to the shot noise limit. The pump pulses are introduced to a wavelength tunable band pass filter (BPF), which consists of a galvanometer mirror, a 4-f optical system, a reflective grating, and a collimator. This system is able to scan the wavenumber from 2850 cm-1 to 2950 cm-1 by tuning the BPF. We succeeded in the spectral imaging of a mixture of polystyrene beads and poly(methyl methacrylate) beads.

8588-36, Session 5

Sensitive NDD-FLIM and multidimensional fluorescence analysis for laser scanning microscopes

Benedikt Krämer, Uwe Ortmann, PicoQuant GmbH (Germany); Samantha Fore, PicoQuant Photonics North America, Inc. (United States); Ingo Gregor, Georg-August-Univ. Göttingen (Germany); Marcelle König, Volker Buschmann, Steffen Ruettinger, Michael Wahl, PicoQuant GmbH (Germany); Jörg Enderlein, Georg-August-Univ. Göttingen (Germany); Felix Koberling, Rainer Erdmann, PicoQuant GmbH (Germany)

The fluorescence lifetime of fluorophores is strongly dependent on their photophysical properties and local environment. Together with the emission profile detected in different spectral channels the fluorescence decay can act as a fingerprint for a dye in a certain condition. We present a 32 channel spectral TCSPC detector together with a new pattern-matching analysis technique that allows to identify selected patterns consisting of fluorescence decays in different spectral excitation and detection channels. The technique is easy to apply and allows for an excellent separation of different fluorophores and their discrimination from autofluorescence in biological samples.

Additionally, a new hybrid photomultiplier detector (PMA Hybrid) combines high detection efficiency together with excellent timing performance and a nearly afterpulsing free photon detection. These features make it ideally suited for FLIM and FCS. We will present a universal approach to integrate this detector in laser scanning microscopes also for non-descanned detection (NDD). This will noticeably increase the detection efficiency for time-resolved deep-tissue FLIM imaging. Confocal, NDD and polarisation resolved measurements can be performed with one modular detection unit having up to four detection channels.

Unparalleled speed of data analysis is accomplished by a new 64 bit software architecture, which processes even large data files directly in the computer memory. Resource demanding processes like FLIM fitting, or FCS calculations are now parallelized and make use of all processor cores available in the PC.

8588-37, Session 6

Ultra-deep imaging of turbid samples by enhanced photon harvesting *(Invited Paper)*

Enrico Gratton, Viera Crosignani, Alexander S. Dvornikov, Univ. of California, Irvine (United States)

We constructed an advanced detection system for two-photon fluorescence microscopy that allows us to image in biological tissue and tissue phantoms up to the depth of a few millimeters with 1 micron resolution. The innovation lies in the detection system which is much more sensitive to low level fluorescence signals than the fluorescence detection configuration used in conventional two-photon fluorescence microscopes. A wide area photocathode PMT was used to detect fluorescence photons directly from a 1 inch area of the turbid sample, as opposed to the photon collection by the microscope objective which can only collect light from a very small area of the sample. The optical path between the sample and the photocathode is refractive index matched to curtail losses at the boundaries due to reflections. The system has been successfully employed in the imaging of tissue phantoms simulating brain optical properties, murine small intestine and colon (ex vivo and in vivo), xenograft subcutaneous tumors in mice, and in vivo vasculature in a rodent dorsal chamber. The system has fluorescence lifetime imaging (FLIM) capabilities and is also well suited for SHG signal detection (such as collagen fibers and muscles), due to the intrinsically forward-directed propagation of the signal.

8588-38, Session 6

Investigation of the tumor microenvironment in live tumor-bearing mice by in vivo multiphoton tomography *(Invited Paper)*

Aisada Uchugonova, Univ. des Saarlandes (Germany); Robert M. Hoffman, Anticancer, Inc. (United States); Karsten König, Univ. des Sarlaandes (Germany) and JenLab GmbH (Germany)

The novel high-resolution multiphoton tomograph MPTflex with an optical arm for NIR femtosecond laser pulses was employed to study intratissue tumor and stromal cells as well as the extracellular matrix in living tumor-bearing mice. The two-photon fluorescence of ds-red and green fluorescent proteins as well as of the endogenous coenzyme NAD(P)H was detected with a compact dual detector device with single photon counting sensitivity. In addition, extracellular matrix protein-collagen has been imaged by second harmonic generation (SHG).

Interestingly, high resolution imaging revealed that collagen structures were organized scaffolding structures to support cancer growth. Ds-red/GFP and autofluorescence imaging provided the possibility to monitor single cancer cells, cancer killing bacteria and tumor-associated stromal cells within the tumor tissue with submicron resolution.

8588-39, Session 6

Clinical studies of pigmented lesions in human skin by using a multiphoton tomograph *(Invited Paper)*

Mihaela Balu, Beckman Laser Institute and Medical Clinic (United States); Kristen M. Kelly M.D., Univ. of California, Irvine School of Medicine (United States); Christopher B. Zachary M.D., Ronald M. Harris M.D., Univ. of California, Irvine (United States); Tatiana B. Krasieva, Beckman Laser Institute and Medical Clinic (United States); Karsten König, JenLab GmbH (Germany) and Univ. des Saarlandes (Germany); Bruce J. Tromberg, Beckman Laser Institute and Medical Clinic (United States)

In-vivo imaging of pigmented lesions in human skin was performed with a clinical multiphoton microscopy-based tomograph (MPTflex, JenLab, Germany). Two-photon excited fluorescence (TPEF) was used for visualizing endogenous fluorophores such as NADH/FAD, keratin, melanin in the epidermal cells and elastin fibers in the dermis. Collagen fibers were imaged by second harmonic generation (SHG). Our study involved in-vivo imaging of benign melanocytic nevi, dysplastic nevi and pigmented lesions with irregular shape and pigment distribution suspected of melanoma. Comparison with histopathology was performed for the biopsied lesions. Benign melanocytic nevi were characterized by the presence of nevus cell nests at the epidermal-dermal junction. In dysplastic nevi, features such as cytological atypia, lentiginous hyperplasia and nests of nuclear pleomorphic cells were imaged and compared with histopathology results. In melanoma, migration of melanocytes and pagetoid spread of large pleomorphic cells in the upper layers of the epidermis were typically observed by multiphoton microscopy and compared to histopathology results A summary of sensitivity and specificity diagnostic criteria for melanocytic nevi, dysplastic nevi and melanoma will be presented. All in vivo measurements were conducted according to an approved institutional protocol, and with informed consent by all participants.

8588-40, Session 6

Optical clearing and multiphoton imaging of paraffin-embedded specimens

Jesse W. Wilson, Simone Degan, Martin C. Fischer, Warren S. Warren, Duke Univ. (United States)

New labeling, imaging, or analysis tools could provide new retrospective insights when applied to archived samples. For example, a growing concern among dermatopathologists is the need for better diagnostic criteria that can predict whether a 'pre-cancerous' lesion will eventually develop into a melanoma, or whether an early-stage melanoma is capable of producing metastases. Imaging of pigmentation chemistry with novel pump-probe microscopy tools could help develop these criteria by studying archived specimens, for which the ultimate patient outcomes are known.

However, serial sectioning these specimens is generally impractical and the optical scattering properties of paraffin wax (used as an embedding medium in standard histology procedures) prevents whole-block high-resolution imaging. While various clearing protocols have been developed for imaging freshly excised tissue, these either involve chemicals that dissolve melanin or require special tissue preparation techniques that are incompatible with prior paraffin embedding. Here we present an optical clearing protocol to enable deep-tissue imaging of archived specimens with multiphoton microscopy.

In order to clear paraffin specimens, we remove the paraffin, and then infiltrate the tissue with a mixture of glycerol and mineral oil. We tested a variety of murine tissue specimens including skin, lung, spleen, kidney, and heart, acquiring multiphoton autofluorescence and second-harmonic generation images. In these samples we have imaged depths in excess of 200 microns, approximately restoring what can be achieved in fresh tissue.

We will report on progress on optimization of imaging depth and discuss prospects for re-paraffinization after imaging, thus restoring the sample to its original state.

8588-41, Session 7

High contrast in vivo bioimaging using multiphoton upconversion in novel rare-earth-doped fluoride upconversion nanoparticles *(Invited Paper)*

Chunhui Yang, Harbin Institute of Technology (China); Guanying Chen, Paras N. Prasad, Univ. at Buffalo (United States)

Upconversion in rare-earth ions is a sequential multiphoton process that efficiently converts two or more low-energy photons, which are generally near infrared (NIR) light, to produce anti-Stokes emission of a higher energy photon (e.g., NIR, visible, ultraviolet) using continuous-wave (cw) diode laser excitation.1 Here, we show the engineering of small-sized upconversion nanoparticles with controlled size, shape, emissions, and surface chemistry. In particular, novel, efficient, and biocompatible NIRin-to-NIRout upconversion nanoparticles are developed for biomedical imaging with both excitation and emission being within the "optical

transparency window" of tissues. The small animal whole-body imaging with exceptional contrast (signal-to-noise ratio of 310) was shown using BALB/c mice intravenously injected with aqueously dispersed nanoparticles. An imaging depth as deep as 3.2-cm was successfully demonstrated using thick animal tissue (pork) under cw laser excitation at 980 nm.

1P. N. Prasad, "Introduction to Nanomedcine and Nanobioengineering", Wiley, New Jersey (2012)

8588-42, Session 7

Latest advances in ultra-fast laser sources for multi photon microscopy

Philip G. Smith, Spectra-Physics®, a Newport Corp. Brand (United States)

The advent of compact, fully automated, and widely wavelength-tunable ultrafast oscillators has triggered an explosive growth in their use in a broad array of multiphoton imaging techniques. Over the past decade laser manufacturers have constantly improved the performance characteristics of these sources to meet the requirements of the user community. We will review the latest advances at Newport / Spectra-Physics in this field and discuss new ways of optimizing key parameters for efficient deep-tissue fluorescence generation, including turn-key, automated second order dispersion compensation that allows for optimization of the pulse width at the sample over a wide wavelength range, without compromising beam pointing and other critical beam parameters.

8588-43, Session 7

Advanced ultrafast lasers for nonlinear microscopy

Marco F. Arrigoni, Coherent, Inc. (United States); Darryl McCoy, Coherent, Inc. (United Kingdom)

Recent developments in Multiphoton Excitation microscopy are in the direction of multimodal images with minimum damage and maximum imaging depth, obtained with the combination of multiple wavelengths, increasingly extending above 1 micron. Longer wavelengths (i.e. above ~ 900-1,000 nm) have been widely demonstrated to reduce photo-damage and increase depth of penetration for imaging purposes. In turn the availability of these longer wavelengths enables the use of an extended set of fluorescent probes and the extension of non-linear imaging to harmonic generation microscopy and CARS/SRS. Additional benefits are gained when multiple and independent wavelengths at suitable powers are available at the same time, thus enabling low damage, multimodal and in-depth imaging. As the required performance of these laser sources is becoming more advanced and demanding, these sources are also expected to provide unprecedented reliability. In this presentation we will discuss performance improvement and reliability testing of Coherent's lasers for non-linear imaging applications. Performance improvements include availability of high power outputs extending to over 1.5 microns and laser systems able to generate multiple wavelengths that are independently tunable covering in excess of 3.5 micron of tuning range . These laser outputs are designed for simplicity of transport, management and delivery on the sample and enable new applications both in imaging and spectroscopy. Multiple-variable reliability testing and stress screening result in extended lifetimes and minimal failure rates enabling operations also in non-conventional environments.

8588-44, Session 7

Multibeam multiphoton microscopy with adaptive optical correction

Simao Coelho, Simon P. Poland, King's College London (United Kingdom); David U. Li, Univ. of Sussex (United Kingdom); Nikola Krstajic, Robert K. Henderson, The Univ. of Edinburgh (United Kingdom); Simon M. Ameer-Beg, King's College London (United Kingdom)

Multiphoton microscopy has significantly contributed to in vivo imaging of fundamental biological processes in living systems. The improvement in optical penetration of infrared light compared with linear excitation due to Rayleigh scattering and low absorption have provided imaging depths of up to 1mm in brain tissue but significant image degradation occurs as samples distort (aberrate) the infrared excitation beam.

Multiphoton fluorescence lifetime imaging microscopy (FLIM) using the time-correlated single photon counting technique is well established as a method for obtaining functional, high resolution images of biological structures. In particular, the use of FLIM to determine protein-protein interactions is well advanced in our lab, and others, using fluorescence resonance energy transfer (FRET).

We report the development of a Multibeam Multiphoton Microscope (MMM) titled MegaFLI capable of incorporating adaptive optical correction. MMM is a promising solution to the limiting imaging speed and sensitivity practiced in multiphoton microscopy. Multiphoton beam parallelization performed via a 2D Gerchberg–Saxton algorithm using a Spatial Light Modulator (SLM) increases data rate by the amount of beamlets produced with the added benefit of flexible adaptive optical correction. The Tscherning wavefront sensing technique has been developed as an iterative optimization to correct for system and sample aberrations via zonal reconstruction. Sample fluorescence is imaged onto a single-photon avalanche diode (SPAD) array designed for FLIM applications.

8588-45, Session 7

In vivo multiphoton microscopy with low power continuous wave sources using dendritic upconverting nanoparticles

Sergei A. Vinogradov, Tatiana V. Esipova, Univ. of Pennsylvania (United States); Sava Sakadzic, Massachusetts General Hospital (United States); Xingchen Ye, Univ. of Pennsylvania (United States); Josh E. Collins, Intelligent Material Solutions Inc. (United States); Emiri T. Mandeville, Massachusetts General Hospital (United States); Christopher B. Murray, Univ. of Pennsylvania (United States)

Lanthanide-based upconverting nanoparticles (UCNPs) form a new class of imaging agents with unique non-linear optical properties. Here we show that non-covalent modification of UCNPs with polyanionic dendrimers converts them into stable, water-soluble, non-toxic imaging probes. Exceptionally high apparent multiphoton absorption cross-sections of dendritic UCNPs combined with their excellent bio-compatibility make them directly suitable for physiological imaging. Using a low power continuous wave (CW) laser for excitation we performed mapping of mouse cortical vasculature with micron-scale resolution down to 400 um under the brain surface, setting the first precedent of true in vivo two-photon microscopy with CW sources.

8588-46, Session 7

Multiphoton cryo microscope with sample temperature control

Hans G. Breunig, Univ. des Saarlandes (Germany) and JenLab GmbH (Germany); Aisada Uchugonova, Univ. des Saarlandes (Germany); Karsten König, Univ. des Saarlandes (Germany) and JenLab GmbH (Germany)

Understanding temperature induced effects in plants and cells is desired

to improve the knowledge of low temperature behavior for cryobiology and cryopreservation. We present a multiphoton microscope system which combines the advantages of multiphoton imaging with precise sample temperature control. The microscope provides online insight into the temperature-induced changes and effects during cooling and thawing processes of plant tissue and animal cells with subcellular resolution. Imaging is possible non-invasively based on multiphoton fluorescence intensity and fluorescence lifetime (FLIM) of externally applied or intrinsic fluorophores in the range from liquid nitrogen temperature up to +600°C. In addition, micro spectra from the imaged regions can be recorded. The cryomicroscope can be used to investigate in detail freezing and thawing effects of animal and plant cells for basic research as well as to improve cryopreservation protocols. We present measurement results from plant leave samples as well as Chinese hamster ovary (CHO) cells.

8588-47, Session 7

in vivo reactive neural plasticity investigation by means of correlative two photon: electron microscopy *(Invited Paper)*

Francesco S. Pavone, Anna Letiza Allegra Mascaro, European Lab. for Non-linear Spectroscopy (Italy); Paolo Cesare, Istituto Nazionale di Neuroscienze (Italy); Leonardo Sacconi, European Lab. for Non-linear Spectroscopy (Italy); Giorgio Grasselli, Georgia Mandolesi, Fondazione Santa Lucia (Italy); Bohumil Maco, Graham Knott, Ecole Polytechnique Fédérale de Lausanne (Switzerland); Vincenzo De Paola, Imperial College London (United Kingdom); Piergiorgio Strata, Istituto Nazionale di Neuroscienze (Italy)

In the adult nervous system, different population of neurons corresponds to different regenerative behavior. Although previous works showed that olivocerebellar fibers are capable of axonal regeneration in a suitable environment as a response to injury (Rossi et al., 2001), we have hitherto no details about the real dynamics of fiber regeneration. We set up a model of singularly axotomized Climbing Fiber (CF) to investigate the reparative properties of these axons in the adult Central Nervous System (CNS) in vivo. Time lapse two photon imaging has been combined to laser nanosurgery (Allegra Mascaro et al., 2010) to define a temporal pattern of the degenerative event and to follow the structural rearrangement after injury. In order to characterize the damage and the CF plasticity (possible formation of new synaptic contacts on the sprouted branches) we combined two-photon in vivo imaging with electron microscopy (FIB-SEM). We will describe the approach followed for correlative light-electron microscopy, which allowed the characterization of the molecular mechanism of reactive plasticity after injury.

8588-48, Session 8

Probing the spatiotemporal relationship between intracellular Ca2+ release and action potential propagation in cardiomyocytes by ultrafast multi-photon random access microscopy *(Invited Paper)*

Leonardo Sacconi, Claudia Crocini, European Lab. for Non-linear Spectroscopy (Italy); Raffaele Coppini, Cecilia Ferrantini, Chiara Tesi, Elisabetta Cerbai, Corrado Poggesi, Univ. degli Studi di Firenze (Italy); Francesco S. Pavone, European Lab. for Non-linear Spectroscopy (Italy)

Action potential (AP) driven Ca2+ current via the transverse axial tubular system (TATS) synchronously trigger Ca2+ release from the sarcoplasmic reticulum (SR) rapidly activating contraction throughout the cardiomyocyte. Here we combine the advantage of an ultrafast random access multi-photon (RAMP) microscope with a double staining approach to optically record AP in several TATS elements and, simultaneously, the corresponding local Ca2+ transient. Isolated cardiomyocytes were labeled with a novel red-shifted voltage sensitive dye and a green calcium indicator. A single wavelength was used to excite both optical probes while the two-photon fluorescence signals were detected simultaneously. RAMP microscope rapidly scans between lines drawn across the TATS of the cardiomyocyte to perform a multiplexed measurement of the two fluorescence signals. A spectral unmixing procedure was then applied to eliminate the crosstalk between the emission spectra of the two probes. In healthy cardiomyocytes, we found uniform AP propagation within the TATS and homogeneous Ca2+ release throughout the whole cell. The capability of our technique in probing spatiotemporal relationship between Ca2+ and electrical activity was then explored in a model of acute detubulation in which failure to conduct AP in disconnected TATS introduces local delay of Ca2+ transient rise, leading to non-homogenous Ca2+ release.

8588-49, Session 8

Extending the fundamental imaging-depth limit of two-photon fluorescence microscopy by imaging with photo-activatable fluorophores and fluorescent proteins

Wei Min, Zhixing Chen, Lu Wei, Xinxin Zhu, Columbia Univ. (United States)

It is highly desirable to be able to optically probe biological activities deep inside live organisms. By employing a spatially confined excitation via a nonlinear transition, two-photon fluorescence microscopy has become indispensable for imaging scattering samples. However, as the incident laser power drops exponentially with imaging depth due to scattering loss, the out-of-focus fluorescence eventually overwhelms the in-focal signal. The resulting loss of imaging contrast defines a fundamental imaging-depth limit, which cannot be overcome by increasing excitation intensity. Herein we propose to significantly extend this depth limit by multiphoton activation and imaging (MPAI) of photo-activatable fluorophores. The imaging contrast is drastically improved due to the created disparity of bright-dark quantum states in space. We demonstrate this new principle by both analytical theory and experiments on tissue phantoms labeled with synthetic caged fluorescein dye or genetically encodable photoactivatable GFP.

8588-51, Session 8

Combined two-photon microscopy and angiography optical coherence tomography for in vivo tissue study

Bumju Kim, Ki Hean Kim, Qingyun Li, Yeoreum Yoon, Taejun Wang, Yongjoon Joo, Jun Ho Lee, Peng Xiao, Pohang Univ. of Science and Technology (Korea, Republic of)

A combination of two-photon microscopy (TPM) and optical coherence tomography (OCT) is useful for in vivo tissue study by providing comprehensive information of tissues at both the cellular, molecular, and structural levels. A combined system was previously developed by using separate optimal light sources: a Ti-Sapphire laser, which are wavelength-tunable, for TPM and wavelength swept-source centered at 1300 nm for OCT. Vasculature is an important parameter to understand the physiology of tissues including lesions. Especially cancer metastasis requires the growth of a new network of blood vessels to get supply of oxygen and nutrient, and it is called as angiogenesis. Vasculature in the cancer is known to have irregular and tortured shapes, and the cancer can be distinguished from the normal based on the shape of vasculature. There are many anti-cancer drugs which inhibits angiogenesis. Therefore, it is natural to add the functionality of vasculature visualization into the combined system for the study of tissues including cancer. Intensity

variance method was adapted for vasculature visualization: 5 cross-sectional images were acquired in the same location and the standard deviation was calculated. The vasculature of mouse ear was imaged in vivo as demonstration. OCT had the field of view (FOV) of 2.25 mm x 2.25 mm and the imaging speed of 90 frames per second with the cross-sectional image of 512 x 512 pixels. Meanwhile, TPM has the FOV of 300 ?m x 300 ?m with the image of 512 x 512 pixels and the imaging speed of 40 frames per second maximum.

8588-52, Session 8

New developments in clinical CARS

Martin Weinigel, Hans G. Breunig, Peter Fischer, Marcel Kellner-Höfer, Rainer Bückle, JenLab GmbH (Germany); Jürgen M. Lademann, Charité Universitätsmedizin Berlin (Germany); Karsten König, JenLab GmbH (Germany) and Univ. des Saarlandes (Germany)

Nonlinear optical imaging methods like multiphoton (MP) microscopy and coherent anti-Stokes Raman scattering (CARS) microscopy are excellent for non-invasive imaging of living tissue without any need of additional contrast agents.

We combined both methods MP- and CARS-imaging within a single hybrid multiphoton tomograph (CARS-DermaInspect) for in vivo imaging of human skin. The clinically certified MP/CARS system enables simultaneous imaging of endogenous fluorophores like reduced nicotinamide adenine dinucleotide (NADH), melanin or keratin with MP together with non-fluorescent substances like lipids or water with CARS.

The stokes laser for a two-beam configuration of CARS was realized in two different setups. One is based on an optical parametric oscillator (OPO) and the other is based on frequency conversion of femtosecond laser pulses within a photonic crystal fiber (PCF).

We performed first clinical measurements including patients suffering from psoriasis and cancer.

8588-53, Session 8

Temporally focused wide-field two-photon microscopy: From the paraxial to the vectorial *(Invited Paper)*

Elijah Y. Yew, Singapore-MIT Alliance (Singapore); Peter T. C. So, Massachussetts Institute of Technology (United States)

We present a vectorial approach to temporally focused wide-field two-photon microscopy. In the first instance, an paraxial approach is used to derive an analytical solution which has the advantage of being able to describe temporal focusing in a general and intuitive manner. In this approach, it is found that better resolution in the z direction is given through the use of objectives of high numerical aperture (NA). As a result, the description of temporally focused wide-field two-photon microscopy is better described using a vectorial approach. We start with the vectorial pupil function and from there evaluate the electric-field at the focus and compare the effects of high NA focusing with that of the paraxial approach.

8588-54, Session 8

Photon reassignment of scattered emission photons in multifocal multiphoton microscopy (MMM) *(Invited Paper)*

Vijay Raj Singh, Singapore-MIT Alliance (Singapore); Jae Won Cha, Elly Nedivi, Peter T. C. So, Massachusetts Institute of Technology (United States)

Multifocal multiphoton microscopy (MMM) uses a lenslet array or a diffractive optical element (DOE) to generate multiple foci at the same time and scanned together. Within the limit of the laser power, the number of foci can be maximized and the imaging speed is improved in proportion to the number of foci. The sub-images generated by the foci are combined as montage to form the final image. Use of imaging detectors, such as CCD cameras, results in a degradation of image signal-to-noise-ratio (SNR) due to the scattering of emitted photons into neighbor pixels limiting image depth. To overcome these limitations, MMM with descanning detection configuration using the Multi-anode Photo Multiplier Tube (MAPMT) has been developed. However, with the presence of scattering of turbid specimen this image generation results as degradation of final image due to the scattering of emission photons to neighbor anodes which results as ghost images. The cross-talk between different anodes can be quantified by a scattering matrix that can be measured a priori. But, a priori measurement of the scattering matrix is cumbersome as scattering cross-talk depends on specimen type, location and depth. In this paper, we present the methodology of the photon reassignment process established based on the maximum likelihood (ML) estimation for the quantification of the cross talk between the anodes of MAPMT. The method provides the reassignment of the photons generated by the ghost images to the original spatial location thus increases the SNR of the final reconstructed image.

8588-55, Session 8

Multiphoton microscopy of cleared human tissue for 3D histology

Michael J. Levene, Sam Vesuna, Richard Torres M.D., Yale Univ. (United States)

Histological evaluation of tissue samples is the backbone of disease diagnosis and evaluation of surgical resections, and although there have been advances in staining protocols, the basic approach of imaging thin slices of tissue has remained constant. Meanwhile, diagnostic radiology has benefited from great advances in imaging technology, with computed tomography (CT) bringing the 3rd dimension to X-ray imaging while MRI and PET scanners have provided powerful additions to the 3D imaging arsenal. These imaging tools have greatly enhanced the ability of radiologists to assess a wide range of medical conditions and opened the door to advanced image processing algorithms for quantitative assessment of disease. Yet, pathologists have remained mired in 2 dimensions, dependent on their imaginations for extrapolating from 2D images to the 3D nature of disease. The necessarily sparse sampling of conventional tissue processing complicates the evaluation of tumor margins and needle-in-haystack markers of disease. We propose to bring pathology into the 3rd dimension through complete imaging of entire resected tissue samples using multiphoton microscopy and optical clearing. We present multiphoton images of human biopsies that are 1.5 mm thick. Combining intrinsic fluorescence, second harmonic generation, and the use of extrinsic dyes provides contrast similar to standard histological stains. Further, we show that optical clearing and multiphoton microscopy are completely compatible with traditional approaches to histology, enabling the use of specialty stains and immunohistochemistry where necessary.

8588-56, Session 8

Photon number absorption in step-wise multi-photon activation of melanin and graphite

Zhenhua Lai, Josef Kerimo, Charles A. DiMarzio, Northeastern Univ. (United States)

Previous research has shown that melanin performs step-wise three-photon fluorescence when activated with high laser power. We have conducted further research using even higher laser power for the activation and shown the possibility of higher than third order multi-photon activation. Graphite which has a well-known molecular structure and organization is a strong absorber and is shown to have a similar

kind of step-wise multi-photon activation process. This article discusses the relationship between the number of photon absorbed and the input laser power for both melanin and graphite. The step-wise multi-photon fluorescence spectra of melanin and graphite are also compared in the article.

8588-57, Session 8

Multimodal nonlinear optical microscopy used to discriminate human colon cancer

Javier F. Adur M.D., Univ. Estadual de Campinas (Brazil) and Univ. Nacional de Entre Rios (Argentina); Vitor B. Pelegati, Univ. Estadual de Campinas (Brazil); Mariana Bianchi, Univ. Nacional de Entre Rios (Argentina); André A. de Thomaz, Mariana O. Baratti, Hernandes F. Carvalho, Univ. Estadual de Campinas (Brazil); Victor H. Casco, Univ. Nacional de Entre Rios (Argentina); Carlos Lenz-Cesar, Univ. Estadual de Campinas (Brazil)

Colon cancer is one of the most diffused cancers in the Western World, ranking third worldwide in frequency of incidence after lung and breast cancers. Even if it is curable when detected and treated early, a more accurate premature diagnosis would be a suitable aim for both cancer prognostic and treatment. Combined multimodal nonlinear optical (NLO) microscopies, such as two-photon excitation fluorescence (TPEF), second-harmonic generation (SHG), third harmonic generation (THG), and fluorescence lifetime imaging microscopy (FLIM) can be used to detect morphological and metabolic changes associated with stroma and epithelial transformation in colon cancer disease.

NLO microscopes provide complementary information about tissue microstructure, showing distinctive patterns between normal and malignant human colonic mucosa. Using a set of scoring methods significant differences both in the content, distribution and organization of stroma collagen fibrils, and lifetime components of NADH and FAD cofactors of human colon mucosa biopsies were found. Our results provide a framework for using NLO techniques as a clinical diagnostic tool for human colon cancer, and also suggest that the SHG and FLIM metrics could be applied to other intestinal disorders, which are characterized by abnormal cell proliferation and collagen assembly.

8588-58, Session 8

Nonlinear spectral imaging of fungal metabolism

Helene Knaus, Farzad Fereidouni, Gerhard A. Blab, Hans C. Gerritsen, Han A. B. Wösten, Utrecht Univ. (Netherlands)

Nonlinear microscopy combined with fluorescence spectroscopy is known as nonlinear spectral imaging (NLSI), providing simultaneously the specimen morphology and (auto)fluorescence spectra. Hence, it allows deducing the biochemical composition, while distinguishing different parts of the tissue. Combined with a new data analysis method, the spectral phasor (F. Fereidouni et al. 2012), data processing is enhanced as it allows quick semi-blind spectral analysis. The spectral phasor is a polar representation of the spectral data (first harmonic of the Fourier transformation), where each emission spectrum is represented as a vector and its position is determined by the emission maximum and the spectral width.

We introduce NLSI in combination with the spectral phasor as a novel minimum-invasive method to monitor the state of “fungal cells” (hyphae). Fungi are consumables and are utilized to produce industrial and pharmaceutical compounds, requiring quality control. As an example we will present NLSI to monitor the freshness of mushrooms. This will show the potential of this user-friendly method capable of addressing a broad range of microbiological questions. Moreover it can be implemented in diagnostics for fungi commonly encountered in clinics.

8588-110, Session 8

Two-photon excited endogenous fluorescence for label-free in vivo imaging ingestion of disease-causing bacteria by human leukocytes

Yan Zeng, Hong Kong Univ. of Science and Technology (Hong Kong, China); Bo Yan, Hong Kong Univ. of Science and Technology (China); Qiqi Sun, Seng Khoon Teh, Wei Zhang, Zilong Wen, Jianan Y. Qu, Hong Kong Univ. of Science and Technology (Hong Kong, China)

Infection plays an important role in the development of diverse diseases. Real time and in vivo monitoring leukocyte behavior provides unique information to understand the physiological and pathological processes of infection. Our recent study demonstrated that two-photon excited reduced nicotinamide adenine dinucleotide (NADH) fluorescence provides intrinsic contrast for neutrophil trafficking in vivo. In addition, the NADH fluorescence signal could be potentially used for imaging the morphology and functionality of leukocytes. In this work, we first study the two-photon excited endogenous fluorescence of various blood cells. Hemoglobin fluorescence enables imaging erythrocytes while leukocytes and platelets can be clearly visualized by NADH and tryptophan fluorescence. The polymorphonuclear structure of granulocyte and mononuclear feature of agranulocyte can be identified in the sectioning NADH fluorescence images (Fig.(a)), and tryptophan fluorescence only shows homogenous patterns. For the first time (to our knowledge), by using spectral and time-resolved NADH fluorescence, we studied the immune response of bacterial infection (Escherichia coli) with human neutrophils. The morphological changes of resting neutrophils (round shape) to activated neutrophils (ruffle shape) during phagocytosis have been clearly revealed. The NADH fluorescence lifetime of neutrophils decreases significantly after ingesting Escherichia coli. This is due to the alteration of relative contribution of free and bound NADH in energy metabolism through glycolysis, which was further verified by the red-shift of NADH fluorescence spectra. The results show that two-photon excited NADH fluorescence provides morphological and biochemical information for monitoring leukocyte behaviors. More importantly, the findings of this work demonstrate a potentially new label-free optical technique to investigate various inflammatory processes in vivo.

8588-60, Session 9

Directional and polarization resolved SHG as a robust means to quantify changes in collagen architecture and isoform distribution in ovarian cancer: a translation approach of human tissues, animal models, and in vitro models *(Invited Paper)*

Paul J. Campagnola, Karissa B. Tilbury, Chi-Hsiang Lien, Manish Patankar, Univ. of Wisconsin-Madison (United States)

We show that characteristic changes in the architecture of collagen (concentration, fibril/fiber structure) and isoform distribution in ovarian cancer can be probed quantitatively by Second Harmonic Generation (SHG) imaging microscopy. Using forward-backward (F/B) directional measurements and polarization anisotropy measurements, we found that the stromal collagen is extensively remodeled by the synthesis of new collagen. To better understand this process, we have created both in vitro and animal models. 3D F/B measurements were utilized to measure changes in the fibril/fiber assembly in self-assembled gel models of the stroma, which consisted of mixtures of type I (Col I) and type III (Col III) collagen, where up-regulation of the latter has been implicated in ovarian cancer. Increasing concentration of Col III resulted in smaller fibers and weaker SHG intensity, corresponding to decreased organization. The F/B concurrently becomes smaller, consistent with the morphological

changes. These results are further consistent with observations of Col III having faster turnover and defective crosslinking in ovarian cancer. We also use polarization resolved SHG to successfully differentiate gels of differing Col III concentration, where the premise is that Col III has a different respective ?-helical pitch angle than Col I. Lastly, we performed F/B measurements on mouse xenografts created by injection of SKOV-3 and ECC-1 human ovarian cancer cells (cell lines), and found that the F/B ratios were consistent with the morphological structure. Taken together, changes in collagen may be an important biomarker in ovarian cancer that can be measured by SHG directional measurements and polarization analysis.

8588-61, Session 9

The arrangement of fibrous collagen in cornea using second harmonic generation (SHG) microscopy *(Invited Paper)*

Yair J. Mega, Charles A. DiMarzio, James P. McLean, Northeastern Univ. (United States)

This study maps the micro-structural organization of corneal collagen using second harmonic generation (SHG) microscopy. A mosaic of SHG images were gathered at a regular sampling rate from human as well as bovine corneas. The images were then analyzed using a novel technique to quantify the orientation of the fibers in the cornea samples. The two-dimensional data was processed to obtain the overall orientation from the entire stack of the sample. The overall results are in agreement with previously reported measurements of the corneal fibrous arrangement. The use of SHG as a method to quantify the organizational information improves on non imaging techniques by enabling researchers to obtain new information on the arrangement of the fibers in the transition regions between the sheets of collagen as well as the process of fibrillogenesis of corneal collagen. Transitional region between the sheets of corneal collagen is of particular importance because of its role in the progression of keratoconus, a disease resulting in degradation of the cornea due to weakness in the collagen matrix.

8588-62, Session 9

Hierarchical model of fibrillar collagen distribution for polarization-resolved SHG microscopy

Adam E. Tuer, Univ. of Toronto Mississauga (Canada) and Institute for Optical Sciences (Canada); Margarete K. Akens, Sunnybrook Health Sciences Ctr. (Canada); Serguei Krouglov, Univ. of Toronto Mississauga (Canada); Daaf Sandkuijl, Univ. of Toronto Mississauga (Canada) and Institute for Optical Sciences (Canada); Brian C. Wilson, Ontario Cancer Institute (Canada); Cari M. Whyne, Sunnybrook Health Sciences Ctr. (Canada); Virginijus Barzda, Univ. of Toronto Mississauga (Canada) and Institute for Optical Sciences (Canada)

A hierarchical model of the organization of fibrillar collagen is developed and its implications on polarization-resolved second harmonic generation (SHG) microscopy are investigated. A “ground-up” approach is employed to develop the theory for understanding of the origin of SHG from fibrillar collagen. The effects of fiber ultra-structure and fiber macroscopic organization on the second-order polarization properties of fibrillar collagen are presented in conjunction with recent ab initio results performed on a collagen triple-helix model (-GLY-PRO-HYP-)n. Various tissues containing fibrillar collagen are quantified using a polarization-resolved SHG technique, termed polarization-in, polarization-out (PIPO) and interpreted in light of the aforementioned theory. The method involves varying the incident laser polarization, while monitoring the SHG intensity through an analyzer. From the SHG polarization data the orientation of the fibers, in biological tissue, can be deduced. Unique PIPO signatures are observed for different tissues (rat-tail tendon, rat skeletal tissue, rat skin, rat cornea, and rabbit tibia) and interpreted in terms of the collagen composition, fiber ultra-structure, and macroscopic organization. Similarities and discrepancies in the second-order polarization properties of different collagen types and ultra-structures will be presented. PIPO SHG microscopy shows promise in its ability to quantify the organization of collagen in various tissues. The ability to characterize the structure of collagen in various tissue microenvironments will aid in the study of numerous collagen related biological process, including tissue diseases, wound repair, and tumour development and progression.

8588-63, Session 9

SHG quantitative imaging of collagen fibrillogenesis

Stéphane Bancelin, Ecole Polytechnique (France) and CNRS (France) and INSERM (France); Carole Aimé, Thibaud Coradin, Univ. Pierre et Marie Curie (France) and Collège de France (France) and CNRS (France); Marie-Claire Schanne-Klein, Ecole Polytechnique (France) and CNRS (France) and INSERM (France)

Collagen is a major structural protein in mammals that self-assembles into fibrils in vivo and in vitro to form three-dimensional (3D) networks. Investigation of collagen fibrillogenesis in a 3D environment is crucial to gain insight into the biological mechanisms of tissue formation and tissue remodeling, and for the rational design of collagen-based biomaterials. In this work, we overcame the limitations of conventional techniques, which are either invasive or lack specificity, by using time-lapse in situ Second Harmonic Generation (SHG) microscopy [Bancelin et al, Biomed. Opt. Express 2012]. We triggered the formation of fibrils by increasing the pH in a dilute acidic solution of collagen I from rat tail. This strategy allowed monitoring the dynamics of fibrillogenesis by quantifying the volume density of voxels with non vanishing signal in SHG 3D images acquired sequentially overnight. We obtained reproducible characteristic times of fibrillogenesis for different pHs, illustrating the robustness of this approach. In addition, we monitored the growth of isolated collagen fibrils and quantified their length increase over time. Finally, we compared our SHG images with images obtained by Transmission Electron Microscopy by blocking fibrillogenesis at various stages and drying the samples. It showed that SHG microscopy allows imaging of fibrils with a diameter of 60-100 nm, below the optical resolution. In conclusion, SHG microscopy enables sensitive and well contrasted 3D imaging of collagen fibrillogenesis, in a non invasive way.

8588-64, Session 9

Multiphoton microscopy based cryo-imaging of inflated frozen human lung sections at -60C in healthy and COPD lungs

Thomas Abraham, Damian Kayra, Masaru Suzuki M.D., John McDonough, W. Mark Elliott, The Univ. of British Columbia (Canada); Joel Cooper, Univ. of Pennsylvania (United States); James C. Hogg M.D., The Univ. of British Columbia (Canada)

Lung is a complex gas exchanger with interfacial area (where the gas exchange takes place) is about the size of a tennis court. Respiratory function is linked to the biomechanical stability of the gas exchange or alveolar regions which directly depends on the spatial distributions of the extracellular matrix fibers such fibrillar collagens and elastin fibers. It is very important to visualize and quantify these fibers at their native and inflated conditions to have correct morphometric information on differences between healthy and diseased states. This can be only achieved in the ex vivo states by imaging directly inflated frozen lung specimens Multiphoton microscopy, uses ultra-short infrared laser pulses as the excitation source, produces multiphoton excitation fluorescence (MPEF) signals from endogenously fluorescent proteins (e.g. elastin)

and induces specific second harmonic generation (SHG) signals from non-centrosymmetric proteins such as fibrillar collagens in fresh human lung tissues [J. Struct. Biol. (2010)171,189-196]. Here we report 3D image data obtained directly from thick frozen inflated lung specimens (~0.7 millimeter thick) visualized at -60C without prior fixation or staining in healthy and diseased states. Lung specimens (n=4) donated for transplantation and released for research when no appropriate recipient was identified served as controls, and diseased lung specimens donated for research by patients receiving lung transplantation for very severe COPD (n=4) were prepared as previously described [N. Engl. J. Med. (2011) 201, 1567]. Lung slices (approximately n=8/lung) evenly spaced between apex and base were examined using multiphoton microscopy while maintained at -60°C using a temperature controlled cold stage with a temperature resolution of 0.1C. Infrared femto-second laser pulses tuned to 880nm, dry microscopic objectives, and non-de-scanned detectors/spectrophotometer located in the reflection geometry were used for generating the 3D images/spectral information. At least five 3D stack images (representing 1.2 millimeter X 1.2 millimeter X ~0.7 millimeter thick lung volume) with optical slice thickness of approximately 2.5 microns were captured from each specimen. The volume fractions of fibrillar collagens and the elastin, the alveolar wall thickness, and fiber size distributions were estimated from the 3D images. In conclusion, the SHG and MPEF methods were successfully performed on the inflated rapidly frozen lung specimens at -60C without prior fixation or staining. We found that this novel imaging approach can provide spatially resolved 3D images with spectral specificities from frozen inflated lungs that are sensitive enough to identity and quantify the micro-structural details of fibrillar collagens and elastin in alveolar walls in both control and diseased tissues.

8588-65, Session 10

Imaging leukocytes in vivo with third harmonic generation microscopy

Cheng-Kun Tsai, Chien-Kuo Chen, Yu-Shing Chen, Pei-Chun Wu, Yuan Tsung Hsieh, Han-Wen Liu, Chiou-Yueh Yeh, Win-Li Lin, Jean-San Chia, Tzu-Ming Liu, National Taiwan Univ. (Taiwan)

In vivo study of leukocytes is challenging due to its nature of fast trafficking, multiple lineages, frequent cell-cell interactions, and dynamic activation or maturation in a process of immune response. People commonly used confocal or multiphoton fluorescence microscopy to label cells and study in vivo dynamics and microenvironments of immune system at a high spatial and temporal resolution. But for future clinical application, a labeling free method is required.

In this report, without a labeling, we demonstrated that granules in leukocytes have distinctive third harmonic generation (THG) contrast. Excited by a 1230nm femtosecond laser, THG signals were generated at a significantly higher level in neutrophils than other mononuclear cells, whereas signals in agranular lymphocytes were one order smaller. These characteristic THG features can also be observed in vivo to trace the recruited leukocytes following lipopolysaccharide (LPS) challenge. Furthermore, using video-rate THG microscopy, we also captured images of blood cells in human capillaries. Quite different from red-blood-cells, every now and then, round and granule rich blood cells with strong THG contrast appeared in circulation. The corresponding volume densities in blood, evaluated from their frequencies of appearance and the velocity of circulation, fall within the physiological range of human white blood cell counts. These results suggested that labeling-free THG imaging may provide timely tracing of leukocyte movement and hematology inspection without disturbing the normal cellular or physiological status.

8588-66, Session 10

Determination of the origin of SHG from starch granules by PIPO SHG microscopy and ab initio calculations

Richard Cisek, Danielle B. Tokarz, Adam E. Tuer, Virginijus Barzda, Univ. of Toronto (Canada) and Univ. of Toronto Mississauga (Canada)

Nonlinear optical laser scanning microscopy was combined with ab initio calculations to determine the origin of the intense second harmonic generation (SHG) from starch granules. Starch is very important for biological function, providing storage of the chemical energy derived from photosynthesis in the form of starch granules in plants. Imaging SHG of starch granules has been performed with a home built laser scanning microscope modified with automated half-wave plate and analyzer for modulation of the polarization of the excitation laser, and polarization analysis of the outgoing polarized harmonic signal. The microscope was coupled to a femtosecond Yb:KGW laser radiating at 1030 nm with a pulse repetition rate of 15 MHz. Direct measurement of tensor element ratios of the first hyperpolarizability was achieved in bio-crystalline regions of starch granules using polarization-in-polarization-out (PIPO) SHG microscopy. PIPO measurements could differentiate between amylose A and B type crystallinity. The difference in the measured hyperpolarizability was investigated via ab initio time-dependent Hartree Fock (TDHF) calculations using the GAMESSUS software on the SciNet supercomputer at the University of Toronto. TDHF calculations performed on the crystal structures of amylose A and B revealed that SHG originates from the hydroxide and hydrogen bonds in the starch granules. The conclusion was supported by PIPO experiments of starch granules at different hydration conditions. The research suggests that anisotropic ordering of water inside starch granules plays a role in intense SHG generated by starch granules, and could be potentially applied to measure other biological structures that contain ordered water.

8588-67, Session 10

Multicolor two-photon and multimodal tissue imaging using synchronized pulses

Emmanuel Beaurepaire, Pierre Mahou, Maxwell Zimmerley, Ecole Polytechnique (France); Karine Loulier, Katherine Matho, Institut de la Vision (France); Guillaume Labroille, Ecole Polytechnique (France); Xavier Morin, Ecole Normale Supérieure (France); Willy Supatto, Ecole Polytechnique (France); Jean Livet, Institut de la Vision (France); Delphine Débarre, Ecole Polytechnique (France)

Systems biology issues in neuroscience and development require tissue-scale measurements of cell anatomy, dynamics and functional parameters. Several multicolor genetic labeling strategies are currently emerging to reconstruct connectivity and tracking cell migrations or lineage during development [1]. However, although multiphoton microscopy has proven efficient for tissue studies, simultaneous multiparametric imaging of live samples has remained challenging so far. We present here advances in multicolor and multimodal multiphoton imaging [2,3]. We demonstrate a strategy that provides optimal and simultaneous two-photon excitation of three chromophores with distinct absorption spectra using a single femtosecond laser and an OPO [2]. The two beams generate separate multiphoton processes, and their spatiotemporal overlap provides an additional two-photon excitation route with submicrometer overlay of the color channels. We report volume and live multicolor imaging of ‘Brainbow’-labeled chick and mouse tissues using this approach. We show that this strategy also enables the efficient combination of third-harmonic generation (THG) imaging with 2PEF imaging, and we present simultaneous three-color fluorescence and third-harmonic imaging of developing Drosophila embryos. Finally, we report efficient multimodal imaging combining two-photon-excited-fluorescence (2PEF), second- and third-harmonic generation (SHG, THG), and four-wave mixing (FWM) in small organisms.

[1] Livet et al, Nature (2007)

[2] Mahou et al, Nature Methods (2012)

[3] Mahou et al, Biomed Opt Express (2011).

8588-68, Session 10

Nonlinear optical microscopy and microspectroscopy of oral precancers and early cancer

Gracie Vargas, Kert Edward, Liang Ma, Suimin Qiu, Vicente Resto M.D., Susan McCammon M.D., The Univ. of Texas Medical Branch (United States)

Multiphoton autofluorescence microscopy (MPAM) and second harmonic generation microscopy (SHGM) offer the ability to assess morphometry similar to that of pathologic evaluation as well as biochemical information from endogenous fluorophores which are altered with neoplastic transformation. In this study the nonlinear optical spectroscopic properties of normal and neoplastic oral mucosa were evaluated in a layer-resolved manner toward the goal of identifying image/spectroscopic based indicators of neoplastic transformation using nonlinear optical microscopy.

A hamster model for oral carcinogenesis involving the tri-weekly topical application of 9,10-dimethyl-1,2-benzanthracene (DMBA) to the buccal pouch was used for these studies. Areas of the buccal pouch were imaged in vivo by MPAM/SHGM with excitation wavelengths in the 780-890 nm range and detection of broadband emission and appropriate SHG wavelength. Multiphoton microspectroscopy was performed in each layer of the oral mucosa (stratum corneum, epithelium, lamina propria) at three sites per imaged area. Spectra were obtained at four excitation wavelengths between 780nm to 890nm. Imaged sites were biopsied immediately after imaging/microspectroscopy and processed for histology then graded by a pathologist. Image based and spectroscopic parameters were correlated to pathological grade.

Results showed statistically significant differences in spectral features between normal, dysplastic/neoplastic mucosa for all layers. Spectra of dysplastic mucosa were blue-shifted relative to normal, with magnitude of the shift decreasing with increasing wavelength and depth; tumors had an additional 630 nm peak. Redox based differences were quantified. The combination of spectroscopy with morphometric features obtained from these endogenous nonlinear optical signals are promising for delineating normal from neoplastic epithelium.

8588-69, Session 10

Towards the label-free purification of stem cell-derived cardiomyocytes using second harmonic generation

Samir Awasthi, NSF Ctr. for Biophotonics Science and Technology (United States); Dennis L. Matthews, NSF Ctr. for Biophotonics Science and Technology (United States) and Lawrence Livermore National Lab. (United States); Ronald A. Li, Mount Sinai School of Medicine (United States) and The Univ. of Hong Kong (Hong Kong, China); Nipavan Chiamvimonvat M.D., Deborah K. Lieu, Univ. of California, Davis (United States); James W. Chan, NSF Ctr. for Biophotonics Science and Technology (United States) and Univ. of California, Davis (United States)

Cardiomyocytes derived from pluripotent stem cells (PSC-CMs) are being widely investigated as a source of cells, with regenerative capacity, that have the ability to restore contractile function to damaged heart tissue. Furthermore, by serving as realistic, patient- and disease-specific models, PSC-CMs may significantly enhance the process of cardiac drug discovery and side-effect screening. In order to use PSC-CMs for transplantation-based regenerative therapies or for cardiac drug discovery, one must be able to control the phenotype, number and purity of CMs used so that reproducible and clinically acceptable results are achieved. However, a label-free, sensitive method for analyzing, counting and sorting human PSC-CMs of varied maturity has not yet been developed. We have taken the first steps toward realizing a label-free PSC-CM sorting methodology by utilizing the second harmonic generation (SHG) signal emanating from the rod domains of sarcomeric myosin. SHG intensity, when integrated over entire cell volumes, is strongly dependent on the maturity of PSC-CMs. Additionally, a PSC-CM's capacity for SHG is retained even after single cells have been retained in suspension for two hours. Furthermore, it is shown that other cells that arise in a typical cardiac-directed stem cell differentiation protocol, including smooth muscle cells, do not generate SH signals. In the interest of constructing an SHG-activated flow cytometer, we have developed a Bessel-beam excitation scheme that is capable of exciting SHG in PSC-CMs, yet retains a longitudinal extent suitable for integration with microfluidic cell-sorting devices.

8588-70, Session 10

Chirality study inside biological tissue by second harmonic generation circular dichroism

Kuo-Jen Hsu, Hsuan Lee, Guan-Yu Zhuo, Shi-Wei Chu, National Taiwan Univ. (Taiwan)

Many biological systems consist of chiral molecules and their functions depend strongly on molecular chirality. For example, most amino acids are of left-handed chirality while most polysaccharides are of right-handed chirality. Both of them are vital for human life so chiral detection inside biological tissues is very important. Conventionally, optical method for chiral detection of molecules is by circular dichroism (CD), which measures the absorption difference between right- and left-circularly polarized light after it goes through experimental samples. However, CD has poor signal contrast and does not provide spatial discrimination in axial direction. Also, it needs longer collection time up to minute level for doing CD experiment. Fortunately, nonlinear optical method such as second-harmonic-generation circular-dichroism (SHG-CD) provides higher chiral contrast and better spatial discrimination in axial direction. On the other hand, it is known that SHG imaging provides deep penetration depth inside thick biological tissue with good optical sectioning capability. To our best of knowledge, there is no research group has used SHG-CD as a method in doing image. In this report, we combined SHG-CD and SHG-imaging as a novel imaging contrast in thick biological tissues for the first time, unraveling local molecular chirality within a sub-femtoliter volume. Experimentally, the radial and axial chiral distribution of collagen in ligament and amylopectin in starch is revealed with sub-micrometer spatial resolution by SHG-CD microscopy. Our method will expand the horizon of chirality study from simplified surface/solution environment into complicated biological tissues.

8588-71, Session 10

Adaptive multiphoton and harmonic generation microscopy for whole tissue imaging

Marie Caroline Muellenbroich, Univ. of Strathclyde (United Kingdom); Ewan J. McGhee, The Beatson Institute for Cancer Research (United Kingdom); Niall McAlinden, Univ. of Strathclyde (United Kingdom); Kurt I. Anderson, The Beatson Institute for Cancer Research (United Kingdom); Keith Mathieson, Univ. of Strathclyde (United Kingdom)

Multiphoton microscopy (MPM) is capable of imaging biological tissue non-invasively with sub-micrometre resolution in three dimensions. For efficient MP signal generation, it is necessary to focus high power, ultra-fast laser pulses into a volume of femtolitres. Aberrations introduced either by the system's optical setup or the sample under investigation cause a broadening of the diffraction limited focal spot and hence the signal intensity and resolution of the image to deteriorate. Adaptive optics (AO) provides a means to compensate for these aberrations and

is capable of restoring resolution and signal strength to surface quality when imaging at depth. Additionally, the incident laser power can be reduced which decreases the risk of photobleaching and improves sample viability. We describe the use of a MEMS deformable membrane mirror in a multiphoton adaptive microscope. The aberration correction is determined in a wavefront sensorless approach by rapidly altering the mirror shape with a random search algorithm until the fluorescence or second harmonic signal intensity is satisfactorily improved. We demonstrate the benefits of wavefront compensation for system- and sample induced aberrations in a variety of samples. For example, the imaging of fluorescent beads, organotypic samples and whole mouse tissue are compared with and without aberration correction. We investigate the possibility of optimising on an intrinsic second harmonic signal providing an optimisation procedure which is not limited by photobleaching therefore allowing many algorithm iterations. This optimised mirror shape can then be stored in a look-up-table and called upon for multiphoton imaging at a specific depth.

8588-72, Session 10

3D quantitative Fourier analysis of second harmonic generation microscopy images of collagen structure in cartilage

Elisabeth I. Romijn, Magnus B. Lilledahl, Norwegian Univ. of Science and Technology (Norway)

One of the main advantages of nonlinear microscopy is that it provides 3D imaging capability. Second harmonic generation is widely used to image the 3D structure of collagen fibers, and several works have highlighted the modification of the collagen fiber fabric in several important diseases. Examples are osteoarthritis, cancer, and atherosclerosis. Several authors have also presented results on automated and semi-quantitative analysis of SHG images. One example is the analysis of the Fourier transformed images which has been widely used for 2D analysis However, no robust 3D analysis methods have been developed, and thus one of the main advantages of NLOM, the three dimensional imaging capability, is not utilized. We have extended the 2D Fourier transform to 3D Fourier transforms of 3D images (image stacks). One of the main challenges in achieving 3D quantitative imaging is the difference in the axial and lateral resolution in the images. However, by preprocessing using deconvolution and using an ellipsoidal specific fitting technique of the Fourier transformed image, we show that the 3D direction of the collagen fibers can be robustly determined. The effect of the point spread function is filtered out in the Fourier space. The technique is validated using synthetic fiber images as well as images of the same sample volume measured from different directions.

Conference 8589: Three-Dimensional and Multidimensional Microscopy: Image Acquisition and Processing XX

BiOS SPIE Photonics West

Tuesday - Thursday 5 –7 February 2013 • Part of Proceedings of SPIE Vol. 8589 Three-Dimensional and Multidimensional Microscopy: Image Acquisition and Processing XX

8589-1, Session 1

Imaging properties of an extended depth of field microscopy system based on the single-shot focus scanning technique

Sheng- Huei D. Lu, Hong Hua, College of Optical Sciences, The Univ. of Arizona (United States)

Although the single-shot focus scanning technique has been experimentally demonstrated for extended depth of field (EDOF) imaging, few work has been performed to characterize its imaging properties and limitations. We investigated and experimentally verified several of the key imaging properties of an EDOF microscopy system based on this technique. We integrated a Lister-type microscope objective with a liquid lens placed at the rear focal plane of the objective to enable the focus scanning without moving parts. The clear aperture of the liquid lens served as the system stop for accomplishing an object-space telecentric configuration, which ensured that the image magnification was maintained constantly during focus scanning to keep the invariance of impulse function at the plane. The focus plane of the system was optically scanned through an extended depth range during a single exposure, and a sharp EDOF image was recovered via a single-step deconvolution process. Through a series of controlled experiments, we experimentally examined the image quality of recovered EDOF images in related to the extended depth position, scan range, and optical telecentricity. The results confirmed the predictions of our analytical modeling that the achievable EDOF was equivalent to the scan range with great versatility, though noticeable image degradation was observed near the edge of focus. We further demonstrated, in exchange for degrading image quality of the best focus, the noticeable image degradation near the edge could be improved by increasing the scanning range. These can be used as the guidance for optimizing image quality with the depth of interest.

8589-2, Session 1

A new expanded point information content design approach for 3D live-cell microscopy at video rates

Ramzi N. Zahreddine, Robert H. Cormack, Carol J. Cogswell, Univ. of Colorado at Boulder (United States)

A new expanded information content (EPIC) biological microscope has been designed that demonstrates how the primary capabilities of confocal and widefield deconvolution system can be achieved with a much simpler optical design approach and easily installed in a conventional microscope. The new microscope is able to record sharply focused images over an extended depth of field and at the same time axially super locate features in complex biological objects to an accuracy of at least 75nm. To achieve this, the new microscope utilizes a combination of novel point spread function (PSF) engineering and computational algorithms. The engineered PSF is axially asymmetric, being focus invariant (i.e. having extended depth of field properties) on one side of best focus, and creating depth-varying rings (i.e. encoded axial localization information) on the other side of focus. By observing both sides of focus simultaneously and utilizing updated iterative processing algorithms the new EPIC microscope is capable of extracting the full x-y-z position information over an extended depth of field. The engineered PSF also creates a patterned signal that can be computationally separated from shot and detector noise, thus improving image quality in low light applications. This data can then be combined to create high-resolution, low-noise, quantitatively accurate 3D animations of complex, live-cell biological specimens. This technique can be applied to a number of different microscope modalities such as fluorescence, brightfield, and DIC. In addition it has the potential for improving the low light imaging performance of multi-photon, confocal, and other microscopes.

8589-3, Session 1

Fuzzy logic components for iterative deconvolution systems

Brian M. Northan, True North Image Processing (United States)

Iterative deconvolution is a technique used to remove blur from three-dimensional wide-field images. Iterative approaches include Richardson Lucy and Landweber among others. In isolation these approaches have been rigorously tested. In practice these algorithms are integrated within a larger system that can include pre-processing (psf and first guess generation, noise reduction, volume partitioning, edge extension), inter-iteration-processing (adaptive PSF updates, noise reduction, evaluation of a stopping criteria, iteration acceleration) and post processing (volume reconstruction).

Practical deconvolution systems tend to be ad-hoc. Even if each individual component is rigorously tested and understood, it is impossible to rigorously test and understand all possible permutations of components. For every choice in the system there are a multitude of sub-choices. For example, the PSF can be theoretical or measured. The theoretical PSF can then be calculated using several different models and the measured PSF can also be preprocessed countless ways. So in practice, deconvolution systems rely heavily on expert knowledge and would benefit from approaches that capture this expert knowledge.

Fuzzy logic is an approach that is used to capture expert knowledge rules and then produce outputs that range in degree. This paper presents a fuzzy-deconvolution-system that integrates traditional Richardson Lucy with fuzzy components. The system is intended for restoration of 3D widefield images taken under conditions of refractive index mismatch. The system uses a fuzzy rule set for calculating sample refractive index, a fuzzy median filter for inter-iteration noise reduction, and a fuzzy rule set for stopping criteria.

8589-4, Session 1

Heavy atom optics solving the inverse problem of optical imaging

Aaron Lewis, The Hebrew Univ. of Jerusalem (Israel)

This presentation describes an approach to a solution of inverse problems in imaging with application to optical, electron/ion beam, x-ray and other imaging modalities. The approach is based on a nanoscopically controllable nanoscopic delta function reference source integrated into one of these imaging approaches. We show that it is possible to obtain, with such a method, an exact solution to the inverse problem of phase both experimentally and theoretically. Our method is based on the breakthrough that crystallography experienced in phase retrieval for large molecular entities by Max Perutz's introduction of "heavy atoms" using the method of isomorphous replacement. The availability of scanning probe microscopy and its full integration with various microscopies allows us to apply these X-ray concepts and to implement "heavy atom" restoration of phase to phase retrieval. In analogy to the heavy atom method, we acquire Fourier intensities in place of an X-ray diffraction pattern, and in place of the heavy atom, we utilize a nanometrically translatable point reference source, coherently related to the far-field illumination. We show that in optics such a reference delta function can readily be implemented with our development of near-field scanning optical microscopy (NSOM) and the associated control imposed on an NSOM probe using atomic force microscopy. This unifying integration

of NSOM/AFM technology with far-field imaging and interferometry achieves robust phase retrieval independent of external parameters without iteration, leading to 3D optical imaging. The methodology has super-resolution potential.

8589-5, Session 1

A low light imaging method that enables parameter estimation with near-best accuracies

Jerry Chao, Sripad Ram, The Univ. of Texas at Dallas (United States); Elizabeth S. Ward, The Univ. of Texas Southwestern Medical Ctr. at Dallas (United States); Raimund J. Ober, The Univ. of Texas at Dallas (United States)

Imaging under low light conditions represents an important means for acquiring information in diverse areas of research. Examples include the imaging of faint stars in astronomy and fluorescent proteins in single molecule microscopy where, respectively, interstellar distances and intracellular particle positions can be determined from the resulting images. A key objective in these parameter estimation studies is to extract the desired quantities with the highest accuracy possible. In single molecule microscopy, for example, the performance of the techniques for superresolution image reconstruction and three-dimensional particle tracking depends directly on how accurately the position of a particle can be estimated. Here, we describe a method of low light imaging that enables ultrahigh accuracy parameter estimation by minimizing corruption of the acquired image by the widely used electron-multiplying charge-coupled device (EMCCD) detector. Our method is based on the allocation of the acquired photons over the pixels of the EMCCD detector, in a way that minimizes the deteriorative effect of detector noise and maximizes the information content of the resulting image. By doing so, it allows the estimation of a parameter with an accuracy that approaches what would only be possible if the image were acquired with a hypothetical detector that introduces no noise. We present the information-theoretic principle behind the method, and describe two implementation approaches. Additionally, by applying it to the point source localization problem which is of central importance to single molecule microscopy, we demonstrate the significant advantage gained by using this method instead of conventional low light EMCCD imaging.

8589-6, Session 2

Intensity-based segmentation and visualization of cells in 3D microscopic images using GPU

Misun Kang, Ewha Womans Univ. (Korea, Republic of); Jeong-Eom Lee, Korea Institute of Science and Technology (Korea, Republic of); Woong-Ki Jeon, Heung-Kook Choi, Inje Univ. (Korea, Republic of); Myoung-Hee Kim, Ewha Womans Univ. (Korea, Republic of)

3D microscopy images contain abundant astronomical data, rendering 3D microscopy image processing time-consuming and laborious on a central processing unit (CPU). To solve these problems, many people crop a region of interest (ROI) of the input image to a small size. Although this reduces cost and time, there are drawbacks at the image processing level, e.g., the selected ROI strongly depends on the user and there is a loss in original image information.

To mitigate these problems, we developed a 3D microscopy image processing tool on a graphics processing unit (GPU). Our tool provides efficient and various automatic thresholding methods to achieve intensity-based segmentation of 3D microscopy images. Users can select the algorithm to be applied. Further, the image processing tool provides visualization of segmented volume data and can set the scale, transportation, etc. using a keyboard and mouse.

However, the 3D objects visualized fast still need to be analyzed to obtain information for biologists. To analyze 3D microscopic images, we need quantitative data of the images. Therefore, we label the segmented 3D objects within all 3D microscopic images and obtain qualitative information on each labeled object. This information can use the classification feature. A user can select the object to be analyzed. Our tool allows the selected object to be displayed on a new window, and hence, more details of the object can be observed.

Finally, we validate the effectiveness of our tool by comparing the CPU and GPU processing times by matching the specification and configuration.

8589-7, Session 2

GPU Based image registration in aperture correlation microscopy and reflection mode correlation microscopy

Lionel Fafchamps, Mark A. Neil, Imperial College London (United Kingdom); Rimas Juskaitis, Univ. of Oxford (United Kingdom)

Aperture Correlation microscopy is a structured illumination microscopy technique capable of producing wide-field optically sectioned fluorescence images in real-time. A disk etched with a pattern is placed in critical illumination and return light is imaged to 2 separate cameras: one containing wide-field plus confocal information, and the other containing wide-field minus confocal. A confocal image can then be recovered by subtracting the camera frames from each-other. However, sub-pixel registration is needed for this operation and a simple global affine transformation is insufficient, with distortions in the optical systems often requiring true elastic registration.

Here we describe a method for high-speed registration of images using the graphics processing unit (GPU) in OpenGL. This technique relies on the ability of the GPU to innately perform affine transforms and interpolations quickly, and uses a custom pixel shader to enable image subtraction during the drawing process. Overall raw frame processing rates of over 100 fps are easily achievable for 1.3MPixel images on even modest hardware.

Additionally, a new reflection mode correlation microscope is introduced which extends spinning disk microscopy to reflective samples. The disk is placed flat in the critical plane of the microscope and imaged onto a single camera. This camera then captures alternate widefield+confocal and widefield frames. Using a modified version of the previous software, this system should also be capable of real time confocal operation using large images with the aid of the GPU, and the addition of separate sectors on the disk for confocal and widefield acquisition.

8589-8, Session 2

Phasor analysis for pump-probe microscopy

Francisco E. Robles, Jesse W. Wilson, Martin C. Fischer, Warren S. Warren, Duke Univ. (United States)

Pump-probe microscopy provides molecular information by probing transient, excited state dynamic properties of samples. In this technique signals are acquired as a function of time-delay between the pump and probe pulses, which may display positive (absorptive) and/or negative (gain) multi-exponential dynamics, resulting form a broad range of physical mechanisms. The primary challenges in analyzing such signals are to distinguish between multiple pigments with as few time-delay data points as possible to increase imaging speeds, and to do so without a priori information.

Typically, signals are analyzed using principal component analysis (PCA) or multi-exponential fitting; unfortunately these methods are not always practical or feasible. For example, PCA gives inadequate results when two or more pigments with non-orthogonal signals are present. Similarly, multi-exponential fitting requires high signal-to-noise ratios and a priori

information regarding the physical model (e.g., number of exponentials), neither of which is always available.

In this work we will present an adaptation of phasor analysis to pump-probe imaging, characterizing the approach with respect to the unique concerns of pump-probe microscopy. In phasor analysis the data are decomposed into two components, g and s, that are related to the real and imaginary parts of the signals' Fourier transform. The presentation will include a theoretical treatment, which yields an alternate definition of the phasor components, as well as analyses of experimental results from cutaneous and ocular pigmented samples, and pigments in historical art work. The results demonstrate that this approach provides an intuitive, robust, and fit-free method for analyzing pump-probe signals.

8589-9, Session 2

High numerical aperture (NA=0.9) and wide-field on-chip microscopy

Wei Luo, Alon Greenbaum, Ahmet F. Coskun, Uzair Y. Sikora, Aydogan Ozcan, Univ. of California, Los Angeles (United States)

Lensfree holographic on-chip microscopy is a computational imaging modality that does not use any lenses to image a specimen. The lack of lenses in its design is compensated using holographic image reconstruction and phase-recovery algorithms. In general, lensfree imaging has several advantages over bright-field-microscopy such as portability, cost-effectiveness and wide field-of-view (e.g., ~20-30mm2), thus making it alluring to applications that require rapid imaging of large areas/volumes. However, its resolution is limited by the pixel-size of the image sensor-array, which samples the holographic diffraction patterns of the objects under unit fringe-magnification.

Meanwhile, there is a growing demand for smaller pixel-size image sensors in consumer electronics market mostly for cell-phone cameras. In this work, we utilized a state-of-the-art color (RGB) CMOS sensor-array along with pixel-super-resolution algorithms to demonstrate a half-pitch resolution of ~300nm and a numerical-aperture (NA) of ~0.9 while also achieving a wide field-of-view of >20mm2. This high NA is achieved by shifting a partially-coherent source in discrete steps, which effectively shift the lensfree holograms of the objects by sub-pixel distances on the sensor-array. By digitally merging these sub-pixel shifted lensfree holograms, a wide-field image of the specimen can be reconstructed with >0.9 gigapixels and an NA of 0.9. These results constitute the highest NA and resolution reported for lensfree on-chip imaging so far. The use of color image-sensors that are constantly being deployed in cellphone cameras would further improve both the cost-effectiveness and the performance of lensfree microscopy and could open new avenues for various bio-medical applications that require high-resolution and wide field-of-view imaging.

8589-10, Session 2

Comparison of computational methods developed to address depth-variant imaging in fluorescence microscopy

Muhammad Mizanur Rahman, Univ. of Memphis (United States); Lutz Schaefer, Advanced Imaging Methodology Consultation (Canada); Dietwald Schuster, Univ. of Applied Sciences (Germany); Chrysanthe Preza, Univ. of Memphis (United States)

In this study, we present a quantitative comparison among different image restoration techniques developed based on a depth-variant (DV) imaging model for fluorescence microscopy [1, 2, 3]. The models employed by these methods approximate DV imaging by either stratifying the object space or image space so that only a small number of DV PSFs are needed for the computations. The DV model proposed in [1] is using non-overlapping strata in object space and a sum in image space, which is comparable to the Discrete Fourier Transformed (DFT) overlap-add method on a stratified DFT [5]. On the other hand, other methodologies such as the Enhanced Merging Masks Algorithm (EMMA) [3] employ stratification in the image space which is comparable to the DFT overlap-save method on a stratified DFT. We compare algorithm implementations based on expectation maximization for maximum likelihood estimation [1], Richardson-Lucy algorithm with total variation regularization (RLTV) [4], and inverse filtering using both the "overlap-add" and "overlap save" approaches in order to assess their impact on the restoration methods. In addition these methods are also directly compared with the two recently proposed methods [2]. Overall, simulations show that for widefield microscopy imaging better restoration results are achieved with methods implemented using the overlap-add method than with their implementation using the overlap-save method.

References

[1] C. Preza and J.A. Conchello, "Depth-variant maximum-likelihood restoration for three-dimensional fluorescence microscopy," JOSA A, vol. 21, no. 9, pp. 1593–1601, 2004.

[2] S. Ben Hadj, L. Blanc-Féraud, "Depth-variant image restoration in 3d fluorescence microscopy: Two approaches under Gaussian and Poissonian noise conditions," ISBI, IEEE, ISSN. 1945-7928, pp. 1671 – 1674, 2012

[3] Elie Maalouf, Bruno Colicchio, Alain Dieterlen, "Fast deconvolution with non-invariant PSF for 3-D fluorescence microscopy", Proc. of SPIE, Vol. 7000, 70001K-1, 2008

[4] Nicolas Dey, Laure Blanc-Freraud, Christophe Zimmer, Pascal Roux, Zvi Kam, "Richardson-Lucy algorithm with total variation regularization for 3D Confocal Microscope Deconvolution," Wiley Liss Inc., Microscopy research and technique, 69, pp. 260-266, 2006

[5] Press, W., Teukolsky, S., Vetterling, W. and Flannery, B., "Numerical recipes in C. The art of scientific computing," Cambridge University Press, 1992

8589-11, Session 3

Gigavoxel imaging with a single beam laser scanning microscope

Urs Utzinger, The Univ. of Arizona (United States)

Imaging of biologic processes, such as cell migration, require time series imaging over a large field of view to capture relevant processes. We study the angiogenic vessel sprouting of adipose derived microvessels in collagen hydro gels. Long-term incubation on the microscope stage was achieved for 4-5 days on a regular upright microscope. A single time point in our measurements consists of 2 gigavoxels. For each voxel we record three measurement channels. We image our model system for 4-5 days with up to 60 time points. Such an imaging event produces in the order of 1 million files and 500 gigabytes of data which poses challenges in data storage, transmission and processing. Our approach to this challenge consists of an in-house built data storage server using a zetabyte file system allowing for stepwise storage expansion. Data Grid software tools were deployed for intra and inter university data transmission using the iRODS framework. High throughput computing was utilized in our university's research data center for processing data using Matlab and filters to enhance tubular structures. Image processing was optimized to run on multiple twelve core processing nodes with the parallel processing toolbox. Total usable storage of 48 terrabytes was produced at nominal hardware costs. Inter university transfer rate reached 50 megabytes/second, while the local gigabit network was saturated at 100 megabytes/second. Matlab CPU usage was increased from 20% to 80% using parallel computing toolbox and bricking our data. Datasets in excess of the computer's available memory were visualized.

8589-12, Session 3

Assessment of robust reconstruction algorithms for compressive sensing spectral-domain optical coherence tomography

Daguang Xu, Jin U. Kang, Johns Hopkins Univ. (United States)

Application of compressed sensing (CS) on optical coherence tomography (OCT) imaging has been studied for several years. In this paper, we performed an in-depth assessment of current state-of-the-art CS reconstruction algorithms for applications in CS-OCT. They can be roughly classified as algorithms solving constraint problem: YALL1, CSALSA, NESTA, SPGL1, and algorithms solving unconstraint problem: TwIST, SpaRSA. A brief description of mentioned algorithms and criteria in assessing performance between constraint and unconstraint algorithms are presented. The study used well-defined artificial noiseless OCT A-scan data sets. Reconstruction error, computation time, noise tolerance and reliability of each algorithm are used as key metrics. The performance of all algorithms is assessed on a set of artificial A-scan signals with different spatial-domain dynamic range. Every algorithm has its own stopping criterion and reconstruction error. In order to make a fair assessment on speed of these algorithms, instead of modifying stopping criterion which changes their intrinsic structure, value of object function, residual, relative error of reconstruction, and computation time are recorded for each iteration of each algorithm. Plots of first three values versus time give a better overview about which algorithm converges faster, especially when requirement on reconstruction error is loose. Finally, all algorithm are assessed using real OCT B-scan data in terms of computation time, SNR and local contrast. Our results show that YALL1 has moderately better performance among these algorithms.

8589-13, Session 3

Modeling and optimization of pupils for line-scanning confocal microscopy

Christopher Glazowski, Milind Rajadhyaksha, Memorial Sloan-Kettering Cancer Ctr. (United States)

Line-scanning confocal microscopy (LSCM) has the potential to provide a simple and low-cost approach for imaging of human tissues. Cellular-level resolution is possible for imaging in either reflectance or fluorescence. However, relative to the standard point-scanning confocal microscope, full-pupil LSCM suffers from reduced contrast and sectioning performance, due to lack of confocality in one dimension and the resulting stronger multiply-scattered background collected across the linear detection array. However, it is known that separated illumination and detection pupils allow significant recovery of optical sectioning and contrast.

To realize the potential of LSCM, we developed a numerical model to study the paraxial diffraction-limited performance with various pupil configurations. The model is able to report the coherent and incoherent sectioning ability for pupil configurations, and can be parameterized in terms of numerical aperture and wavelength. With this model, we have theoretically optimized the axial sectioning performance of divided-pupil and annular-pupil configurations to enable imaging with high quality in tissue.

Also, for the divided-pupil configuration, we show that the divider width, between the illumination and detection sub-apertures, along with the detection slit-width can be jointly optimized for both axial sectioning and speckle-noise reduction for coherent reflectance imaging. With a bench-top LSCM, we present experimental results that validate the model along with in-vivo human skin images and video. Design maps for potential divided-pupil LSCM systems adhering to these optimizations are also presented.

8589-14, Session 3

Modeling coherent effects in optical phase conjugation of ultrasonically encoded signal

Joseph L. Hollmann, Charles A. DiMarzio, Northeastern Univ. (United States)

Focusing light in tissue is limited to one transport mean free path due to strong scattering. However, the use of adaptive optics has been shown to suppress these scattering effects. A focused ultrasound beam serves as a guidestar by frequency shifting light that has traversed its waist. Optical phase conjugation of the sidebands then forces light to retrace its trajectory and focus back at the US beam waist.

We analyze this technique utilizing a Finite-Difference Time-Domain (FDTD) simulation to propagate an optical signal in a synthetic skin model. The US beam is simulated as perturbing the indicies of refraction by an amount proportional to the acoustic pressure for four equally spaced phases. By the Nyquist criterion, this is sufficient to capture the carrier and first US sidebands.

Though optical propagation in a highly scattering medium like tissue is commonly modeled as a diffusive wave, optical energy can travel along coherent paths for long distances. We analyze these coherent paths and their effect on optical phase conjugation of a US encoded optical beam.

8589-15, Session 4

Single-shot optical sectioning using polarised illumination coded Structured Illumination Microscopy (picoSIM)

Daniel Appelt, King's College London (United Kingdom); Kai Wicker, Friedrich-Schiller-Univ. Jena (Germany) and Institut für Photonische Technologien e.V. (Germany); Rainer Heintzmann, Friedrich-Schiller-Univ. Jena (Germany) and Institut für Photonische Technologien e.V. (Germany) and Randall Div of Cell & Molecular Biophysics, King's College London (United Kingdom)

The conventional epi-fluorescent wide-field microscope features a uniform illumination of an extended sample region. A problem arises with this setup since light from out-of-focus fluorophores is also detected. The result is poor quality in the final image, as out-of-focus structures appear blurred; furthermore, their emission light contributes to the background and leads to a reduction in image contrast.

Removing out-of-focus light yields an optically sectioned image: a thin slice of a thick sample that only contains in-focus information. Taking a stack of such sectioned images allows for a three-dimensional view of the specimen.

Conventional Structured Illumination Microscopy (cSIM) is a method to obtain optically sectioned data, similar to that obtained from the widely used confocal microscope. However, cSIM suffers from a limited acquisition rate, as at least three individual images need to be acquired.

We propose the technique of polarised illumination coded Structured Illumination Microscopy (picoSIM), which combines high temporal and high spatial resolution. Our technique encodes the three individual light patterns needed for cSIM in the polarisation of the illumination light. This allows the simultaneous acquisition of the three images required for a computational reconstruction of a sectioned image in one single exposure, allowing optical sectioning with in principle arbitrary temporal resolution. Although optical sectioning on this timescale is possible with other technique like e.g. SPIM (Selective plane illumination microscopy), our method has the advantage of an ameliorated z-resolution in the sub-micrometer range.

Experimental results will be shown.

[Wicker K, Heintzmann R (2010) Single-shot optical sectioning using polarization-coded structured illumination. J Opt 12:084010]

8589-17, Session 4

Structured oblique illumination microscopy for enhanced resolution imaging of non-fluorescent, scattering samples

Shwetadwip Chowdhury, Hafeez Dhalla, Joseph A. Izatt, Duke Univ. (United States)

Many biological samples contain features of interest beyond the diffraction limited resolution of conventional microscopy, rendering them physically unobservable using conventional means. Visualizing such features requires image resolutions exceeding this physical limit and can only be achieved with application of super-resolution techniques. To this end, super-resolution techniques have found tremendous success in fluorescent imaging and have allowed imaging of nano-sized structures well beyond the diffraction limit. However, such techniques are limited to fluorescence, and achieving comparable resolutions in samples that are highly scattering, but not fluorescent, remains difficult. Here, we introduce a non-fluorescent extension to structured illumination microscopy (SIM), termed structured oblique illumination microscopy (SOIM), where we use simultaneous oblique illuminations of the sample to multiplex high spatial-frequency content into the frequency support of the system. We present theory describing how to demodulate this multiplexed information to reconstruct an image with a greater frequency support than allowed by the diffraction limit, and we show how this enhanced resolution is analogous to the super-resolution offered by conventional linear SIM. We experimentally confirm this approach by performing enhanced-resolution imaging of a reflection test chart and show quantitative measures for the resolution gain beyond the diffraction limit achieved by this technique. We next apply this technique to image more biologically relevant samples at high (1.4) NA and achieve resolutions comparable to those reached by conventional linear SIM. Our approach thus allows imaging of non-fluorescent samples at resolutions previously attainable predominantly in fluorescence microscopy.

8589-18, Session 4

Time-resolved wide-field optically sectioned fluorescence microscopy

Guillaume Dupuis, Univ. Paris-Sud 11 (France) and CNRS (France); Nadia Benabdallah, Aurélien Chopinaud, Univ. Paris-Sud 11 (France); Sandrine Lévêque-Fort, Univ. Paris-Sud 11 (France) and CNRS (France)

Fluorescence Lifetime Imaging Microscopy (FLIM) is widely applied in biology and medicine to study both the structure and dynamic processes in live cells. However, when implemented in a point scanning approach (confocal or two-photon excitation), the slow acquisition rate can be a major drawback. Therefore, we present the implementation of a fast wide-field optical sectioning technique called HiLo microscopy on a time-gated fluorescence lifetime imaging microscope. HiLo microscopy is based on the fusion of only two images, one with structured illumination and another with standard uniform illumination. Optically sectioned images of desired thicknesses are then digitally generated thanks to a fusion algorithm that requires only a single adjusting parameter. HiLo images have been shown to be comparable in quality with confocal 3-D images of the same samples but they can be acquired faster, up to a near video-rate and over larger fields of view. We used a digital micro-mirror device to rapidly switch from structured to standard uniform illumination, and a high-rate imager optically coupled to a CCD camera to sample the fluorescence decay. The microscope objective is equipped with piezo-electric scanning to enable in-depth imaging. Four-dimensional (4D) imaging is obtained by combining HiLo optical sectioning, time-gated detection, and z displacement. We illustrate time-resolved capabilities of this set-up on the live-cell imaging of dynamic neurobiological processes.

8589-19, Session 4

A comparison of methods for optical sectioning using structured illumination microscopy

Peter A. Kner, Benjamin Thomas, The Univ. of Georgia (United States)

Structured Illumination Microscopy is a simple and effective way to remove out-of-focus light in widefield fluorescence microscopy. Neil et al originally proposed a simple square-law method for calculating the optically sectioned image from the three raw images with the structured illumination pattern super-imposed. However, the Neil method does not make the most efficient use of the three raw images. The three structured illumination images can also be used to separate three copies of the image covering shifted regions of frequency space in a similar manner to that developed by Gustafsson et al. These can then be combined using a generalized wiener filter to create an image with a well-behaved optical transfer function in which the missing cone has been filled in, providing optical sectioning. Here, we compare the Neil and Gustafsson methods and show that the Gustafsson method provides an image with higher fidelity and a better Signal to Noise Ratio (SNR) at low photon counts. Imaging antibody labeled septins in Aspergillus nidulans, the SNR is a factor of 5 better using the Gustafsson method. The Gustafsson method requires knowledge of the grid spacing, but we show that it is easy to determine the grid spacing from the raw data and a simple search algorithm.

8589-20, Session 4

Total-variation constrained image reconstruction for structure illumination microscopy

Kaiqin Chu, Stephen M. Lane, NSF Ctr. for Biophotonics Science and Technology (United States); Jay Yin, Paul C. Goodwin, Applied Precision, Inc. (United States)

In the structure illumination microscopy, Wiener-type filter is used for reconstructing the super resolved images. Due to high SNR requirement of the filter, photo-bleaching often happens, particularly in the case of thick sample. We propose to use the total variation as a constraint during the reconstruction. This enables high quality reconstruction even with much lower SNRs in the raw data. With lower requirement on SNR, the photo-bleaching can be avoided.

8589-58, Session 4

Phase imaging with partially coherent light

Laura Waller, Univ. of California, Berkeley (United States)

No Abstract Available

8589-21, Session 5

Stochastic near field 3D microscopy using Brownian metallic nanoparticles

Ariadna Martinez Marrades, Institut Langevin (France); Nathalie Bardou, Stéphane Collin, Lab. de Photonique et de Nanostructures (France); Michel Gross, L2C, CNRS (France); Gilles Tessier, Institut Langevin, ESPCI, CNRS (France)

We present a fast, full-field, three-dimensional microscopy technique based on heterodyne digital holography for the localization of metallic nanoparticles in liquid environments with sub-diffraction accuracy. Tens

of particles down to diameters of 60nm can be localized simultaneously and selectively by the numerical reconstruction of a single hologram acquired in 5ms, consequently allowing real time reconstruction by taking advantage of the huge computing power of PC graphic cards for parallel calculations.

This imaging tool, which has recently been applied to the characterization of Brownian motion, is now being used to develop a novel type of near field microscope, using gold particles in a microfluidic chamber as local scatterers of the optical field, therefore acting as multiple stochastic near field probes. The random motion of the particles allow for a complete exploration of the sample and a measurement of its optical near field. Moreover, frequency domain studies are also available thanks to heterodyne holography, giving access to the rotation frequency of anisotropic nanoparticles like rods, and therefore the temperature and viscosity of their local environment.

The major applications of our imaging technique are thus the local electromagnetic characterization of water-based systems -which are mostly inaccessible to electronic microscopy or local probes microscopies such as AFM- present in many emerging microfluidics studies involving plasmonic nanostructures, as well as the detection and sub-diffraction tracking of biological specimens labeled with gold nanoparticles, freely moving in an aqueous volume. Images of local hot spots on gold nanostructures on glass substrates will be presented.

8589-22, Session 5

Improved quantitative phase contrast in self-interference digital holographic microscopy and sensing dynamic refractive index changes of the cytoplasm using internalized microspheres as probes

Björn Kemper, Robin Schubert, Sebastian Dartmann, Angelika Vollmer, Steffi Ketelhut, Gert von Bally, Westfälische Wilhelms-Univ. Münster (Germany)

Self-interference digital holographic microscopy (DHM) [1] has been found particular suitable for simplified quantitative phase imaging of living cells and usage in multifunctional microscopy platforms. However, a main draw back of the self-interference DHM principle are scattering patterns that are induced by the coherent nature of the laser light and which affect the resolution for the detection of optical path length changes. We present a simple and efficient technique for the reduction of coherent disturbances in quantitative phase images. The principle is based on amplitude and phase modulation of the sample illumination and has been found in particular convenient with the self-interference DHM concept. Results from the characterisation of the method are presented and its performance for enhanced quantitative phase imaging of living cells is illustrated. Moreover, the application of self-interference DHM for sensing of dynamic refractive index changes of adherent cells and its usage with microfluidics is demonstrated. Therefore, silica microspheres which are internalized by living cells due to phagocytosis are used as probes to determine the refractive index of the cytoplasm from single quantitative phase images. The reliability of this approach for dynamic refractive index retrieval is shown by data from a comparative study on adherent and suspended human tumor cells and the refractive index response of adherent cancer cells to repeated osmotical stimulation in a microfluidic channel.

[1] B. Kemper, A. Vollmer, C. Rommel, J. Schnekenburger, G. von Bally, “Simplified approach for quantitative digital holographic quantitative phase contrast imaging of living cells”, J. Biomed. Opt. 16, 026014 (2011).

8589-23, Session 5

Digital holographic confocal microscope

Alexandre S. Goy, Demetri Psaltis, Ecole Polytechnique Fédérale de Lausanne (Switzerland)

We demonstrate experimentally a laser scanning confocal microscopy technique based on the capture of an off-axis digital hologram for each scanned spot. The data collected in this way contains all the necessary information to digitally produce three-dimensional images. The fact that the data is available in the digital domain provides a great flexibility. We show, in particular, how to improve the quality of images acquired in transmission by dynamically placing the confocal detection pinhole. Other metrics than the filtering by a pinhole can be devised to build the image. For example, we perform the correlation between the image of the focus in the sample and the image of an undistorted focus. In transmission, the correlation corrects for part of the sample-induced aberrations that would affect a conventional confocal microscope. We show examples of reflection and transmission images of epithelial cells and mouse brain tissue. The scanning speed is limited only by the frame rate of the camera recording the holograms. The computations, consisting mainly in fast Fourier transforms, can be be performed in real time considering the speed of current graphic processing units. This method enables a convenient implementation of confocal microscopy, especially in the transmission geometry as no beam tracking device is required to pass the light through the detection pinhole. We believe that the data collected with the scanning digital holographic set-up is a complete record of the information that can be gathered within a given numerical aperture, from the scattering by the object of the coherent field.

8589-24, Session 5

Quantitative phase reconstruction and holographic volume imaging with diffuse illumination

Walter H. Harm, Alexander Jesacher, Stefan Bernet, Monika Ritsch-Marte, Innsbruck Medical Univ. (Austria)

We demonstrate quantitative reconstruction of complex objects and multisectional imaging in the visible regime from a single diffraction pattern. Digital in-line holography is a well established alternative to lens-based imaging. Sufficiently coherent light is scattered by the specimen and the interfering scattered and unscattered waves are captured by a digital sensor. Image reconstruction is performed by numerically propagating the measured intensity distribution to the sample volume, providing large depth of field. However, the loss of phase information introduces an ambiguity that results in the occurrence of a mostly undesired phase conjugated image, the twin image, that is superimposed on the real image. Also axially overlapping objects cannot be resolved seperately by conventional digital in-line holography.

One possibility to suppress undesired diffraction orders is to employ phase retrieval algorithms. We propose a method to significantly improve the performance of a Gerchberg-Saxton type algorithm in optical imaging. The method relies on introducing a specially designed phase object into the specimen plane during the image recording, which serves as a constraint in the subsequent phase retrieval algorithm. This leads to faster algorithm convergence and improved final accuracy. Quantitative imaging can be performed by a single recording of the resulting diffraction pattern in the camera plane, without using lenses or other optical elements. Results from numerical simulations and experiments confirm a high accuracy which can be comparable to that of phase-stepping interferometry. Holographic volume imaging with high sectioning capability can be performed by inserting a phase object in the specimen plane, which increases the effective numerical aperture in the illumination path.

8589-25, Session 5

Molecular specificity and digital coherence gating in quantitative phase spectroscopy

Matthew T. Rinehart, Adam Wax, Duke Univ. (United States)

Quantitative phase spectroscopy (QPS) has been developed as a method of investigating the wavelength-dependent refractive index of semitransparent microscopic samples with high spectral and spatial resolution. Here, we present novel wavelength illumination patterns for acquiring holographic data as well as algorithms for digital coherence gating and ratiometric imaging of multiple absorptive species in a single sample. Light from a supercontinuum source spanning from 450nm to 750nm is filtered with a rapidly-tunable custom spectral filter to a bandwidth of <1nm, allowing wide-field off-axis interferometry without suffering from coherence effects at the edges of the field of view. The spectral filter is tuned to arbitrary center wavelengths in <1ms and synchronized with a high-speed camera. We have developed two operating modes for this QPS instrument: (i) high-resolution spectral sweeps for detailed imaging spectroscopy of novel samples, (ii) high-speed ratiometric molecular imaging. In spectroscopy mode, the instrument is also capable of digitally gating the coherence window to interrogate the spectral content of the sample at different time delays. In the ratiometric imaging mode, the instrument is capable of detecting multiple absorptive and dispersive species at high speeds (>100Hz) using a sparse set of scanned illumination wavelengths. We will present validation results of these techniques by imaging thick samples with embedded absorptive objects and also samples with multiple absorbers present.

8589-26, Session 5

Spatial filter encoded volume holographic gratings in PQ-PMMA for spatial-spectral imaging

Yuan Luo, National Taiwan Univ. (Taiwan); Jui-Chang Tsai M.D., National Taiwan Univ. Hospital (Taiwan); George Barbastathis, Massachusetts Institute of Technology (United States) and Singapore-MIT Alliance for Research and Technology Ctr. (Singapore); SeBaek Oh, KLA-Tencor Corp. (United States)

Spatial-spectral volume holographic (VH) imaging incorporating multiplexing techniques has been developed for a variety of imaging applications. The gratings formed in a thick holographic recording material are utilized in the Fourier plane of a 4-f imager to have strong wavefront filtering properties. Therefore, VHI can obtain spatial images and spectral information of an object. However, as is well known from microscopy and biology, many objects of interest are composed of weak phase features, which are largely transparent; thus they are in very poor contrast and barely observable for conventional VH systems in imaging. We present a design of embedded spatial filters in a volume holographic three-dimensional pupil, providing advantages in terms of image contrast and strong filtering properties to acquire unstained, weak phase information of biological structures. The design utilizes a spatial filter recorded through the entire volume of the volume holographic pupil in phenanthrenquinone-doped polymethyl methacrylate (PQ-PMMA) bulk recording material. This results in stronger filtering to significantly improve weak phase features of an object. Further, we show experimental results demonstrating this technique to enhance unstained features of spatial-spectral images of human endothelial cells.

8589-27, Session 6

Tunable thin-film optical filters for hyperspectral microscopy

Peter F. Favreau, Thomas C. Rich, Univ. of South Alabama (United States); Prashant Prabhat, Semrock, Inc. (United States); Silas J. Leavesley, Univ. of South Alabama (United States)

Hyperspectral imaging was originally developed for use in remote sensing applications. More recently, it has been applied to biological imaging systems, such as fluorescence microscopes. The ability to distinguish molecules based on spectral differences has been especially advantageous for identifying fluorophores in highly autofluorescent tissues. A key component of hyperspectral imaging systems is wavelength filtering. Each filtering technology used for hyperspectral imaging has corresponding advantages and disadvantages. Recently, a new optical filtering technology has been developed that uses multi-layered thin-film optical filters that can be rotated, with respect to incident light, to control the center wavelength of the pass-band. Compared to the majority of tunable filter technologies, these filters have superior optical performance including greater than 90% transmission, steep spectral edges and high out-of-band blocking. Hence, tunable thin-film optical filters present optical characteristics that may make them well-suited for many biological spectral imaging applications.

An array of tunable thin-film filters was implemented on an inverted fluorescence microscope (TE 2000, Nikon Instruments) to cover the full visible wavelength range. Images of a previously published model: GFP-expressing endothelial cells in the lung were acquired using a charge-coupled device camera (Rolera EM-C2, Q-Imaging). This model sample presents fluorescently-labeled cells in a highly autofluorescent environment.

Linear unmixing of hyperspectral images indicates that thin-film tunable filters provide equivalent spectral discrimination to our previous acousto-optic tunable filter–based approach, with increased signal-to-noise characteristics. Hence, tunable multi-layered thin film optical filters may provide greatly improved spectral filtering characteristics and therefore enable wider acceptance of hyperspectral widefield microscopy.

8589-28, Session 6

Lensfree multispectral holographic microscopy using sunlight

Ikbal Sencan, Uzair Y. Sikora, Aydogan Ozcan, Univ. of California, Los Angeles (United States)

Newton's experiments with a pair of prisms decomposed sunlight into its colors and combined it back to explain the refraction and dispersion of sunlight through a glass prism interface. Since this milestone experiment, the use of sunlight as a source in optical experiments continued to be quite common until other light sources such as incandescent light bulbs were invented. Providing us an easy-to-access and rather broad spectral content, the sunlight still presents a rich source that could potentially be used in multispectral imaging to extract the wavelength-dependent features of microscopic objects of interest. Toward this end, here we demonstrate a field-portable lensfree multispectral holographic microscopy platform, which utilizes the Sun as its light source.

In this compact and light-weight partially-coherent holographic imaging geometry, the objects are placed at ~0.5 mm away from the active region of a color (RGB) CMOS sensor-array and are homogenously illuminated by the sunlight, which is first collected by a simple light condenser adapted from conventional solar cell technologies. After the sunlight passes through a plastic diffuser, it is spatially filtered by a 0.1 mm diameter pinhole/aperture. This pinhole is positioned at ~7.5cm away from the objects, and is controlled using a simple screw-based x-y translation stage, which permits capturing of slightly shifted in-line holograms of the objects. These lensfree images captured under sunlight are digitally combined using pixel super-resolution algorithms to form a finely sampled in-line hologram per color channel (i.e., at red, green and blue channels). These pixel-super-resolved holograms are then processed with the knowledge of the spectral response curves of the sensor-array as well as the spectral content of the sunlight to digitally remove the cross-talk between color channels and retrieve the multispectral spatial features of the objects. We demonstrate the performance of this field-portable sunlight-based multispectral microscopy platform with a spatial resolution of <2μm over a wide field-of-view of e.g., 15-30 mm2.

8589-29, Session 6

Spatial-spectral coupling in hyperspectral CARS microscopy image formation

Aaron M. Barlow, Steacie Institute for Molecular Sciences (Canada) and Univ. of Ottawa (Canada); Marco Andreana, Steacie Institute for Molecular Sciences (Canada) and Univ. of Ottawa (Canada); Konstantin Popov, Univ. of Ottawa (Canada); Douglas J. Moffatt, Andrew Ridsdale, Steacie Institute for Molecular Sciences (Canada); Aaron D. Slepkov, Trent Univ. (Canada); Adrian F. Pegoraro, Harward Univ. (United States); Rune Lausten, Benjamin J. Sussman, Steacie Institute for Molecular Sciences (Canada); Albert Stolow, Steacie Institute for Molecular Sciences (Canada) and Univ. of Ottawa (Canada) and Queen's Univ. (Canada)

Hyperspectral Coherent Anti-Stokes Raman Scattering (CARS) microscopy has provided an imaging tool for extraction of 3-dimensional volumetric information, as well as chemically-sensitive spectral information. These techniques have been used in a variety of different domains including biophysics and material science [1]. The measured CARS spectrum results from interference between the Raman response of the sample and a non-resonant background from which the Raman response can be extracted using such methods as Kramers-Kronig transformations [2] and maximum entropy [3]. However, the resulting three dimensional images are distorted by interference, some of which arises because of the Gouy phase shift. This type of interference can be observed as a function of the axial position of the Raman resonant object in the laser focus [4]. We studied how the Gouy phase manifests itself in the spectral domain by collecting four dimensional data sets (three spatial dimension, plus spectra) of spherical and planar objects in a CARS microscope and extracting the Raman response. Through experimental results and numerical calculation using finite-difference time-domain (FDTD) methods we were able to understand the relationship between the spatial configuration of the sample and the CARS response in a three dimensional space as well as Raman frequency.

1. A. Zumbusch, G. R. Holtom, and X. S. Xie, "Three-Dimensional Vibrational Imaging by Coherent Anti-Stokes Raman Scattering," Phys. Rev. Lett 82, 4142–4145 (1999).

2. Y. Liu, Y. J. Lee, and M. T. Cicerone. "Broadband CARS spectral phase retrieval using a time-domain Kramers–Kronig transform," Optics Letters, 34, 1363-1365 (2009)

3. E. M. Vartiainen, H. A. Rinia, Mi. Müller, and M. Bonn, "Direct extraction of Raman line-shapes from congested CARS spectra," Optics Express, 14, 3622-3630 (2006)

4. K. I. Popov, A. F. Pegoraro, A. Stolow, and L. Ramunno, "Image formation in CARS microscopy: Effect of the Gouy phase shift," Optics Express, 19, 5902-5911 (2011)

8589-30, Session 6

Application of non-negative matrix factorization to multispectral FLIM data analysis

Paritosh Pande, Javier A. Jo, Texas A&M Univ. (United States)

Current method of interpreting fluorescence lifetime microscopy (FLIM) images is based on comparing the intensity and lifetime values obtained from the sample time-resolved fluorescence measurements with those of known fluorophores. This method becomes unwieldy and subjective in many practical applications where there are several fluorescing species contributing to the bulk fluorescence signal, and even more so in the case of multispectral FLIM. Non-negative matrix factorization (NMF) is a multivariate data analysis technique that is aimed at extracting non-negative signatures of pure components and their non-negative abundances from an additive mixture of those components. In this paper, we present the application of NMF to multispectral time-domain FLIM data to obtain a new set of FLIM features (fractional abundance of each constituent fluorophore). These features are more intuitive and easier to interpret than the standard fluorescence intensity and lifetime values. Unlike several FLIM data analysis methods, the proposed approach is not limited by the number of constituent fluorescing species and their possibly complex decay dynamics. Moreover, the new set of FLIM features can be obtained by processing the raw multispectral FLIM intensity data rendering time deconvolution unnecessary, resulting in lesser computational time and relaxed SNR requirements. The performance of the NMF method was validated on simulated and experimental multispectral time-domain FLIM data. The NMF features were also compared against the standard intensity and lifetime features, in terms of their ability to discriminate between different types of atherosclerotic plaques.

8589-31, Session 7

Rapid wavefront corrections for deep tissue imaging

Reto P. Fiolka, Ke Si, Meng Cui, HHMI Janelia Farm Research Campus (United States)

Random scattering in tissue causes the ballistic focus to decay exponentially with increasing depth, limiting the penetration of optical imaging techniques to a few scattering path lengths. Adaptive optics has the potential to drastically increase the penetration depth, light efficiency and resolution in deep tissue imaging.

Here we present two approaches for microscopy based AO, coherent optical adaptive technique (COAT) [1] and the k-space method [2] that both allow rapid wavefront corrections for highly scattering media.

In COAT, originally invented to focus light through atmospheric turbulence, individual elements of a spatial light modulator (SLM) are phase modulated each at a unique frequency, enabling parallelized wavefront correction.

COAT can be advantageously applied to 2 photon microscopy [3] and we demonstrate its potential by imaging through brain tissue with a high speed segmented MEMS deformable mirror. Combining COAT with optical coherence microscopy (OCM) enables wavefront corrections using only backscattered light. We apply this technique to focus through tissue phantoms and 500 micron fixed brain tissue.

In the k-space method, two mirrors rapidly visit different optical modes in reciprocal space. At each scan position, the beating with a frequency shifted reference beam is measured and the phase for the corresponding optical mode is determined. Once a sufficient number of optical modes are characterized, the corresponding wavefront is displayed on an SLM. This approach enables high speed (1ms per optical mode) and flexibility (number of modes can be adjusted to the scattering media).

[1] W.B. Bridges et al, Applied Optics, Vol. 13, Issue 2, pp. 291-300 (1974)

[2] M. Cui, Optics Express, Vol. 19, Issue 4, pp. 2989-2995 (2011)

[3] J. Tang, PNAS, Vol.109, Issue 22, pp. 8434-8439 (2012)

8589-32, Session 7

Light sheet adaptive optics microscope for 3D live imaging

Cyril J. T. Bourgenot, Jonathan M. Taylor, Christopher D. Saunter, John M. Girkin, Gordon D. Love, Durham Univ. (United Kingdom)

We report on the incorporation of adaptive optics (AO) into the imaging arm of a selective plane illumination microscope (SPIM). SPIM has recently emerged as an important tool for life science research due to its ability to deliver high-speed, optically sectioned, time-lapse microscope images from deep within in vivo selected samples. SPIM provides a very interesting system for the incorporation of AO as the illumination and imaging paths are decoupled and AO may be useful in both paths.

In this paper, we will report the use of AO applied to SPIM, demonstrating significant improvement in image quality of a 3D z-stack of a GFP-labelled transgenic zebrafish embryo using a wavefront modal sensorless AO system on the imaging path. These experimental results will be linked to a computational model showing that significant aberrations are produced by the tube holding the sample in addition to the aberration from the biological sample itself. We will also discuss the use of AO when imaging a live zebrafish heart, whose beating cycle has been synchronized with the SPIM illumination, enabling image acquisition without motion effects.

Finally, we will examine the possibility of using the separated illumination arm to generate a localised artificial guide star within the field of view.

8589-33, Session 7

Adaptive optics device for improvement of the spinning disk imaging

Audrius Jasaitis, Grégory Clouvel, Xavier Levecq, Imagine Optic SA (France); Vincent Fraisier, Jean Salamero, Institut Curie (France)

The spinning disk confocal fluorescence microscopy is becoming more and more popular in the in vivo imaging thanks to its high speed of acquisition, lower toxicity for live samples and the improved imaging depth. Unfortunately, as all other optical imaging techniques, the confocal microscopy is also affected by optical aberrations. These aberrations can be induced by the tiny misalignment of the static elements inside the confocal microscope, like lenses and mirrors. Moreover, the mismatch of the refractive indexes when oil (n=1.5) immersion objective is used to image biological samples (mostly water, n=1.33) introduces additional aberrations. Moreover, when the actual biological sample (cell culture or a sample of tissue) is placed in the microscope it induces additional aberrations. This second source of aberrations becomes more significant when deeper layers of the sample are imaged. To correct for the most of these aberrations we propose to use adaptive optics elements. Our device (MicAO) is capable to correct for all the static system aberrations using the Shack-Hartmann type wave-front sensor and the deformable mirror. Moreover, we use genetic and 3N algorithms to correct for the sample induced aberrations. Those algorithms are especially useful, when it is imaged deeper in the sample. We will also discuss the influence of the adaptive optics correction on the excitation pathway and the emission pathway.

8589-34, Session 7

Superresolution microscopy through thick tissue using adaptive optics

Brian Patton, Daniel Burke, Univ. of Oxford (United Kingdom); Travis J. Gould, Joerg Bewersdorf, Yale Univ. (United States); Martin Booth, Univ. of Oxford (United Kingdom)

Superresolution microscopes have been able to resolve features on the scale of tens of nanometers and lower. These microscopes - including scanning methods (STED, RESOLFT, etc.) and stochastic wide field methods (PALM, STORM, GSDIM, etc.) - all suffer from the effects of aberrations that compromise resolution, signal and consequently image quality. Adaptive optics has been demonstrated in a range of diffraction-limited resolution microscope modalities to compensate for system and specimen-induced aberrations. However, the use of adaptive optics in superresolution microscopes presents new challenges. We investigate how aberrations affect the properties of superresolution microscopes and develop new adaptive optics schemes to measure and correct the aberrations. In particular we show how the commonly-used 2D STED configuration is robust to aberrations, whereas the 3D STED configuration is particularly sensitive. A new scheme is presented that permits the adaptive compensation of aberrations in the 3D STED microscope through optimization of a new image quality metric incorporating both image brightness and sharpness information. This system is used to perform three-dimensionally resolved superresolution imaging through thick (~10 to 50 micrometre) specimens. Significant improvements in resolution and image intensity are achieved. The adaptive correction of specimen-induced aberrations in this manner will be an essential step to the wider use of superresolution methods in a wider range of biologically relevant specimens.

8589-35, Session 8

Wide-field microscopy using microcamera arrays

Daniel L. Marks, David S. Kittle, Seo Ho Youn, Jungsang Kim, David J. Brady, Duke Univ. (United States)

We adapt a unique microcamera array architecture from a multiscale gigapixel camera to wide-field microscopy. The imaged surface may be curved or irregular as each microcamera may be individually focused.A resolution of 3 microns or better over 1000 square millimeters can be recorded in a snapshot. Applications include screening for skin lesions, microsurgical imaging, and microscopic cytometry.

8589-36, Session 8

Photothermal imaging of melanin

Josef Kerimo, Charles A. DiMarzio, Zhenhua Lai, Northeastern Univ. (United States)

We present the first photothermal images of melanin using modulation with two near-infrared CW lasers. The melanin from several samples including Sepia officinalis, black human hair, and human tissue were imaged with a high signal-to-noise ratio. Two laser beams with different wavelengths (one with amplitude modulation) were focused collinearly on the sample and the scattering of one of the beams, at the modulation frequency, was detected. Strong absorption of the modulated beam leads to an increase in temperature and changes in the refractive index in melanin and the modulated scattering of the second laser beam. Although the dual-beam photothermal method has been used in the past to image single metal nanoparticles and semiconductor nanocrystals, it appears to be practical for imaging and detecting melanin. The melanin can be detected without interference from the background scattering since it is suppressed efficiently by the modulation scheme. The imaging can also be done for an extended period of time without photoactivation or photodamage to the melanin since the laser power is lower. Furthermore, the signal is stable and does not suffer from the photobleaching effects normally seen in fluorescence-based detection. The nature of the photothermal image is discussed including the image resolution, dependence on the laser power, wavelength, and modulation frequency. The new photothermal imaging method is promising and can be easily implemented in a low-cost CW laser-scanning system.

8589-37, Session 8

Supercritical self-interference fluorescence microscopy for full-field membrane imaging

Thomas Barroca, Institut Langevin (France); Pierre Bon, Institut Langevin, Ctr. d'Imageries Plasmoniques Appliquées (France) and Institut des Sciences Moléculaires d'Orsay (France); Sandrine Lévêque-Fort, Institut des Sciences Moléculaires d'Orsay and Centre de photonique Biomédicale (CLUPS) (France); Emmanuel Fort, Institut Langevin, Ctr. d'Imageries Plasmoniques Appliquées (France)

We have developed a full-field imaging technique based on Supercritical Angle Fluorescence (SAF) emission for cell membrane imaging. It takes advantage that only fluorophores in the vicinity of the glass slide emit

light above the critical angle [1]. This supercritical emission sharply decays with the fluorophore/surface distance z over a characteristic length of about 100 nm while the Undercritical Angles Fluorescence (UAF) is no z-dependent. Hence, selecting the supercritical emission provides an efficient way to perform axial filtering.

We have shown that the use of a simple mask to block the UAF components induces a loss of lateral resolution [2]. To avoid this drawback, we have developed an original method, where the surface image is obtained by the subtraction of two images: one with both the UAF and SAF, the other with the UAF only [3]. This image principally originates in the interference term between UAF and SAF components. However, this operation also adds a term (second order) that reduces the sensibility.

Here, we propose a new approach to hugely enhance the interference term using a phase plate. We have implemented a dual-channel optical system to instantly perform the subtraction of the two images: one with the (SAF+UAF), the other with the (SAF-UAF). The PSF engineering, resulting from this operation, performs an axial filtering of about 100 nm. This setup can be connected on any standard fluorescence microscope equipped of a simple white lamp to simultaneously follow dynamic events both at the surface and more in-depth.

[1] J. D. Jackson, “Classical Electromagnetism”, 3rd ed., Chap. 9, Wiley, New York (1998).

[2] T. Barroca, K. Balaa, J. Delahaye, S. Lévêque-Fort and E. Fort, “Full-field supercritical angle fluorescence microscopy for live cell imaging”, Optics letters 36, 3051 (2011).

[3] T. Barroca, K. Balaa, S. Lévêque-Fort and E. Fort, “Full-field Near-field optical microscope for Cell Imaging”, Phys. Rev. Lett., 108, 218101 (2012).

8589-38, Session 8

Wide field high resolution light sheet microscopy using Airy beams

Tom Vettenburg, Heather I. C. Dalgarno, Tomá? ?i?már, Frank J. Gunn-Moore, Kishan Dholakia, Univ. of St. Andrews (United Kingdom)

Single plane illumination microscopy (SPIM) boasts a myriad of unique advantages. Orthogonal detection allows rapid imaging of large, three-dimensional, samples of living tissue. Illumination with a thin sheet of light ensures high contrast by minimizing the fluorescent background. Moreover, by restricting the sample exposure to a single plane, photo-bleaching and damage are minimized, crucial when imaging photo-sensitive samples over a larger period of time. Recent enhancements to the original technique attempt to overcome the inherent trade off between axial resolution and field-of-view of conventional light sheet microscopy, either by employing four objectives to illuminate and image the sample from various directions, by relying on two-photon excitation, or by introducing elements of structured illumination or confocal scanning. To date, this was only achieved by compromising on one or more of its key advantages: high contrast, time-resolution, or minimal sample exposure. We present Airy beam light sheet microscopy, which employs a peculiar curved light sheet to overcome all of these limitations simultaneously. Such a light sheet is readily created by introducing a phase mask in the illumination path, a surprisingly straightforward modification to existing apparatus. Counter-intuitively, the curved light sheet, nor its side-lobes, do not preclude high lateral and axial resolution. We show that a single scan of such a light sheet yields high resolution images of a volume extended by an order of magnitude making it the optimal choice for single photon light sheet studies. We demonstrate the potential of the method by resolving fluorescent mitochondria in an array of HEK cells.

8589-53, Session PWED

Dual detection confocal fluorescence microscopy: depth imaging without depth scanning

Dong-Ryoung Lee, Young-Duk Kim, Hyeong-Jun Jeong, KAIST (Korea, Republic of); Jong-Min Lee, Hanyang Univ. (Korea, Republic of); DaeGab Gweon, KAIST (Korea, Republic of); Hongki Yoo, Hanyang Univ. (Korea, Republic of)

We propose a new method for three-dimensional fluorescence imaging without depth scanning that we refer to as the dual detection confocal fluorescence microscopy (DDCFM). Compared to conventional beam-scanning confocal fluorescence microscopy, where the focal spot must be scanned either optically or mechanically to collect a three-dimensional images, DDCFM is able to obtain depth information without depth scanning. DDCFM utilizes two photo multiplier tubes (PMTs) in the confocal detection system. The emitted fluorescence is divided by the beam splitter and received by the two PMTs through pinholes with different size. Each PMT signal generates different axial response curve according to the pinhole diameter, which decides stiffness of the curve. Since the PMT signal is determined by the intensity of the fluorescent emitter and the distance from the focal point, we can acquire depth position of a fluorescent emitter by comparing two intensity signals from the PMTs. Since the depth information can be obtained by a single excitation without depth scanning, DDCFM has many advantages. The measurement time is dramatically reduced for volume imaging. Also, photo-bleaching and photo-toxicity can be minimized. The system can be easily miniaturized because no mechanical depth scan is needed. Here, we demonstrate the feasibility of the proposed method by phantom study using fluorescent beads.

8589-54, Session PWED

An optimized two-photon method for in vivo lung imaging reveals intimate cell collaborations during infection

Daniel Fiole, Pierre Deman, Institut de Recherche Biomédicale des Armées (France); Julien Douady, Lab. Interdisciplinaire de Physique (France); Jean-Nicolas Tournier, Institut de Recherche Biomédicale des Armées (France)

Lung tissue motion arising from breathing and heart beating has been described as the largest annoyance of in vivo imaging. Consequently, infected lung tissue has never been imaged in vivo thus far, and little is known concerning the kinetics of the mucosal immune system at the cellular level. We have developed an optimized post-processing strategy to overcome tissue motion, based upon two-photon and second harmonic generation (SHG) microscopy.

In contrast to previously published data, we have freed the lung parenchyma from any strain and depression in order to maintain the lungs under optimal physiological parameters. Excitation beams swept the sample throughout normal breathing and heart movements, allowing the collection of many images. Given that tissue motion is unpredictably, it was essential to sort images of interest. This step was enhanced by using SHG signal from collagen as a reference for sampling and realignment phases. A normalized cross-correlation criterion was used between a manually chosen reference image and rigid transformations of all others. Using CX3CR1+/gfp mice this process allowed the collection of high resolution images of pulmonary dendritic cells (DCs) interacting with Bacillus anthracis spores, a Gram-positive bacteria responsible for anthrax disease. We imaged lung tissue for up to one hour, without interrupting normal lung physiology. Interestingly, our data revealed unexpected interactions between DCs and macrophages, two specialized phagocytes. These contacts may participate in a better coordinate immune response. Our results not only demonstrate the phagocytizing task of lung DCs but also infer a cooperative role of alveolar macrophages and DCs.

8589-55, Session PWED

Using liquid crystal variable retarders for fast modulation of bias and shear direction in quantitative differential interference contrast (DIC) microscope

Michael I. Shribak, Marine Biological Lab. (United States)

Conventional DIC microscope shows the two-dimensional distribution of optical path length gradient encountered along the shear direction between two interfering beams. It is therefore necessary to rotate unknown objects in order to examine them at several orientations. We built new DIC beam shearing assembly, which allows the bias to be modulated and shear directions to be switched rapidly without any mechanically rotating the specimen or the prisms. The assembly consists of two standard DIC prisms with liquid crystal cell in between. Another liquid crystal cell is employed for modulating a bias. All components do not require a special design and are available on the market. We describe techniques for measuring parameters of DIC prisms and calibrating liquid crystal cells. One beam-shearing assembly is added to the illumination path and another one to the imaging path of standard microscope. Two sets of raw DIC images at the orthogonal shear directions and two or three different biases are captured and processed within a second. Then the quantitative image of optical path gradient distribution within a thin optical section is displayed on a computer screen. The obtained data are also used to compute the quantitative distribution of optical phase, which represents refractive index gradient or height distribution. It is possible to generate back the enhanced regular DIC images with any desired shear direction. New DIC microscope can be combined with other techniques, such as fluorescence and polarization microscopy.

8589-56, Session PWED

Quantitative phase analysis through scattering media by depth-filtered digital holography

Sebastian R. Goebel, Technische Fachhochschule Georg Agricola Bochum (Germany); Volker Jaedicke, Nektarios Koukourakis, Helge Wiethoff, Adamou Adinda-Ougba, Nils C. Gerhardt, Ruhr-Univ. Bochum (Germany); Hubert Welp, Technische Fachhochschule Georg Agricola Bochum (Germany); Martin R. Hofmann, Ruhr-Univ. Bochum (Germany)

Phase analysis in digital holography (DH) provides axial resolutions in the nanometer range. However, this technique is not applicable to structures located in scattering media since the interference patterns are disturbed by light from different depth regions. We propose a method using optical coherence tomography (OCT) to synthesize interference patterns for isolated depth regions allowing the phase analysis of structures inside scattering media. In our experiments we used this approach to reconstruct holograms of a reflective surface through a scattering layer. Our results demonstrate a proof-of-principle, as the quantitative phase-profile could be recovered and separated from scattering influences.

8589-57, Session PWED

In vivo deep tissue FRET imaging with multi-color fluorescence lifetime excitation-emission matrix optical projection tomography

Ming Zhao, College of Optical Sciences, The Univ. of Arizona (United States); Weibin Zhou, Univ. of Michigan (United States); Leilei L. Peng, College of Optical Sciences, The Univ. of Arizona (United States)

We present a deep tissue multi-color fluorescence lifetime imaging method based on Fourier fluorescence lifetime excitation-emission matrix (FLEEM) spectroscopy [1] and scanning laser optical projection tomography [2]. The method is capable of simultaneous multi-color lifetime imaging of multiple fluorophores and enables imaging of FRET sensors in live transgenic zebrafish embryos. The FLEEM spectroscopy uses a Michelson interferometer with a high-speed optical delay line to modulate a multi-wavelength continuous-wave laser source in a high-speed frequency sweep. Fluorescence emissions associated with different excitation wavelengths are separated in the frequency domain. With a multi-color PMT array, the system measures fluorescence lifetimes simultaneously in all channels of an excitation-emission matrix at a speed of 46 microsecond/pixel. The lifetime spectrometer is combined with scanning laser optical tomography to perform 3D fluorescence lifetime imaging. The modulated laser output of the interferometer is focused to a 15 micron beam waist and incident onto the sample to excite fluorophores along the projection line. The beam is scanned by a galvo mirror to obtain an X-Y projection. The sample is then rotated to obtain projections at 360 degrees. 3D image reconstruction is realized with a back-projection algorithm based on the inverse Radon transform, followed by lifetime analysis of all EEM channels. The 3D fluorescence lifetime and intensity information allows quantitative analysis of Forster resonant energy transfer inside live samples. We demonstrate the method with live transgenetic zebrafish embryos with cAMP FRET sensors. The method allows functional 3D imaging in vivo for the investigation of cellular functions in whole organisms.

[1] M. Zhao and L. Peng, Optics Letters. 35,2910. (2010)

[2] R. A. Lorbeer, et al., Optics Express. 19,5419. (2011)

8589-39, Session 9

Portable low-coherence interferometer for quantitative phase microscopy of live cells

Natan T. Shaked, Pinhas Girshovitz, Tel Aviv Univ. (Israel)

We present a highly portable and inexpensive interferometer for obtaining spatial interferograms of microscopic biological samples, without the strict stability and the highly-coherent illumination that are usually required for interferometric microscopy setups. The device is built using off-the-shelf optical elements and can easily operate with low-coherence illumination, while being positioned in the output of a conventional inverted microscope. The interferograms are processed into the quantitative amplitude and phase profiles of the sample. Based on the phase profile, the optical thickness or optical path delay profile of the sample is obtained with temporal stability of 0.18 nm and spatial stability of 0.42 nm. We show several configurations of this interferometer that are suitable for both on-axis and off-axis holographic geometries, and present various experimental results of imaging live cells in a non-contact label-free manner. Since the interferometer can be ported in the output of any inverted microscope and operate in a simple way, without involvement of an expert user with a knowledge in optics and without complicated alignment prior to every experiment, and still obtain a remarkably high accuracy, we believe that this new setup will make interfeometeric phase microscopy more accessible and affordable for biologists and clinicians, while significantly broadening its range of applications.

8589-40, Session 9

Three-dimensional intracellular phase imaging

Frank Helderman, Vrije Univ. Amsterdam (Netherlands); Bryan Haslam, Massachusetts Institute of Technology (United States); Mattijs de Groot, Johannes F. de Boer, Vrije Univ. Amsterdam (Netherlands)

Optical coherence tomography has been applied to the microscope domain to develop a three dimensional microscopy technique with a

resolution on a sub micrometer scale. A common-path setup that uses for example the reflection of a cover glass as a local phase reference can sense optical path displacements smaller than a nanometer. Herewith, the motion of objects within the focal volume can be studied.

The need for detecting the cover glass limits the possibilities to use high numerical aperture objectives and thus the resolution, because the depth of field would become too short. Therefore, we designed a setup with a dual beam sample arm.

A polarizing beam splitter divides the sample beam into s- and p-polarized states that travel the same path, but in opposite directions through a Sagnac interferometer. There, a 4:1 telescope (f = -25 mm and f = 100 mm, Thorlabs) magnifies the width of the p-polarized beam and narrows the width of the s-polarized beam. The two beams share a common path towards the microscope. The broad beam will be focused into the sample for spatially specific phase information. The narrow beam with a long depth of field can detect the phase at the cover glass as a local reference.

The lateral resolution was 0.42 µm and the axial point spread function was 0.84 µm. The phase stability of 0.02 radians enabled detection of optical path displacements of 0.9 nm. This setup allows for three-dimensional intracellular phase imaging.

8589-42, Session 9

Interferometric phase imaging with multiple broadband sources for increasing measurement range

Jae Seok Park, In Hee Shin, Hyeong Ju Park, Joo Beom Eom, Byeong Il Lee, Korea Photonics Technology Institute (Korea, Republic of)

Phase imaging techniques from the interferometric signal have been widely developed to measure sub-wavelength variation in a sample. Those techniques show nanometer scale resolution with fast data acquisition rate and therefore can be applied for the imaging of cellular dynamics in biological samples or the surface inspection of integrated devices. However those suffer from the limited measurement range. It is related to 2 pi ambiguities or phase wrapping artifacts when phase variations are larger than any of the wavelength of light source. Software or hardware based methods have been attempted to avoid phase ambiguities but require complex optical setups or intensive calculations. In this research, we report a simple phase imaging technique to overcome 2 pi ambiguities using multiple broadband sources. A home-made spectral filter was prepared to generate multiple broadband sources by dividing original broadband light source into several spectral regions with same bandwidth. Data sets of phase values can be extracted from the acquired interferometric signal by using our multiple sources. After conducting simple calculations, we could increase measurement range of phase imaging to hundreds of micrometers in principle without adding other noise values. The results corresponded with those of standard measurement instruments. Our approach may be applied for other phase imaging modalities where require broadband light source.

8589-43, Session 9

Supercritical scattering microscoy for quantitative phase imaging in the vicinity of a lamella

Pierre Bon, Institut Langevin, ESPCI, CNRS (France) and Institut des Sciences Moléculaires d'Orsay (France); Thomas Barocca, Institut Langevin, ESPCI, CNRS (France); Sandrine Lévêque-Fort, Univ. Paris-Sud 11 (France); Emmanuel Fort, Institut Langevin, ESPCI, CNRS (France)

We describe here the use of quadri-wave lateral shearing interferometry (QWLSI) [1] to make quantitative phase imaging of object near a lamella. Using Super Angle Fluorescence (SAF) idea [2], we are able to image objects in contact with the lamella without any use of fluorescence. This approach gives cell membrane images avoiding problems of photo-bleaching, sample modification or dedicated microscope.

[1] Bon, Maucort, Wattellier, and Monneret, "Quadriwave lateral shearing interferometry for quantitative phase microscopy of living cells," Opt. Express 17, 13080-13094 (2009)

[2] Barroca, Balaa, Leveque-Fort, Fort, "Full-Field Near-Field Optical Microscope for Cell Imaging", Phys. Rev. Letters, 18, 2012

8589-44, Session 10

Swept-source phase microscopy based on wavelength-swept laser beam

Hyojin Kim, Hyung Seok Lee, Myung-Yong Jeong, Chang-Seok Kim, Pusan National Univ. (Korea, Republic of)

Spectral domain phase microscopy (SDPM) has been used to obtain depth-resolved phase information for 3D nanometer-scale imaging based on the coherence gating of broadband light source. In general, area CCD detector is used to obtain the 3 D surface profiling of SDPM; one axis of CCD detector is to provide a spectral interferometer signal (for Z- direction) and the other axis is for the spatial information on the sample (for X-direction). Thus, a scanning of light beam (for Y-direction) is necessary to construct the X-Y-Z 3 D surface profile of SDPM.

In this work, the swept-source phase microscopy (SSPM) is newly proposed using the area beam of wavelength-swept laser. Since the depth-resolved phase information can be obtained from the wavelength-swept laser (for Z- direction), both axes of CCD detector are involved to provide the 2-dimensional spatial information on the sample (for X and Y-directions). It means that the 3 D surface profile can be easily measured without any mechanical movement of light beam on the sample. In order to use a Si-type CCD detector, which shows a larger number of pixel, faster response time and lower price, compared to the InGaAs-type CCD detector, it is critically helpful to build a novel wavelength-swept laser with a center wavelength of 840 nm, a sweeping bandwidth of 70 nm and an output intensity of 20 mW.

To demonstrate a stable and high speed 3D imaging, a large area beam over 80 mm2 is applied on the sample of standard resolution target (R3L3S1P, Thorlabs) to lead with the CCD detector with the pixels of 2040 x 1088 and the speed of 128 frames/sec. It corresponds to 1 volume/sec for a 2040 x 1088 x 128 voxel element (X-Y-Z) of 3D SDPM imaging. It is important to stabilize the wavelength-swept laser to improve the depth resolution of SDPM less than nm order.

In conclusion, we demonstrate a novel SSPM system, which is ideal for a stable and high speed nano-scale imaging with no mechanical movement.

8589-45, Session 10

Tomographic incoherent phase imaging, a diffraction tomography alternative for any white-light microscope

Pierre Bon, Institut Fresnel - CNRS (France) and Institut Langevin - CNRS (France); Sherazade Aknoun, Institut Fresnel - CNRS (France) and Phasics S.A. (France); Julien Savatier, Institut Fresnel - CNRS (France); Benoit F. Wattellier, PHASICS S.A. (France); Serge Monneret, Institut Fresnel - CNRS (France)

Quantitative phase imaging (QPI) is a powerful method to visualize a semi-transparent sample in a quantitative manner, in particular for thin samples. In standard setups, coherent illumination only gives access to limited object frequencies, in particular along the optical axis, avoiding accurate 3D visualization of thicker samples. In diffraction tomography, the object frequency space is filled thanks to a full set of images that are

recorded by rotating the plane-wave illumination angle. This technique requires either a very stable setup during the whole acquisition of about 1000 angles [1] or less angles but a much more time consuming inversion algorithm with some a priori knowledge about the sample [2].

We propose here to use a well-known property of standard intensity imaging to generate optical sectionning : a spatially incoherent beam makes the sample illuminated by a large number of incidence angles. This also leads to a lateral resolution increase compared to classical coherent illumination.

We have shown that it was possible to apply spatially incoherent illumination to QPI using quadri-wave lateral shearing interferometry (QWLSI) [3]. A z-stack is recorded in order to reconstruct the 3D object structure and then the use of simulation tools [4] allows us to get access to the local complex refractive index of the sample.

The main advantages of our approach are its implementation simplicity compared to the other state-of-the-art diffraction tomographic setups and its speed allowing living sample imaging.

In this presentation, we will present the theoretical background of Tomographic Incoherent Phase Imaging (TIPI). We will propose accurate tomographic reconstruction of model samples (beads) and living COS-7 cells.

[1] Debailleul, Georges, Morin, Simon, Haeberlé, “High resolution three-dimensional tomographic diffraction microscopy of transparent inorganic and biological samples”, optics letters, 34 (1), 2009

[2] Ruan, Bon, Murdry, Maire, Chaumet, Giovannini, Belkebir, Talneau, Wattellier, Monneret, Sentenac, “Tomographic diffraction microscopy with a wavefront sensor”, optics letters, 37 (10), 2012

[3] Bon, Maucort, Wattellier, and Monneret, “Quadriwave lateral shearing interferometry for quantitative phase microscopy of living cells,” Opt. Express 17, 13080-13094 (2009)

[4] Bon, Wattellier, Monneret, “Modeling quantitative phase image formation under tilted illuminations”, optics letters, 37(10), 2012

8589-46, Session 10

Stain-free 3D imaging flow cytometry

Yongjin Sung, Niyom Lue, Ramachandra R. Dasari, Zahid Yaqoob, Massachusetts Institute of Technology (United States)

In this study, we present a stain-free, imaging flow cytometry to provide the 3-D refractive index map of flowing samples. Our method is a phase imaging technique based on digital holography; therefore, it does not require any extra contrast agent. On the contrary to the existing methods that require the sample to be stationary during the measurement, our method can provide the 3-D refractive index map of the samples flowing in a small channel. For this, we focus the beam onto a line in a microfluidic chamber, and record the angular spectra while the sample is flowing across the line. A line-focused beam can be decomposed into plane waves, which are incident onto the sample with different illumination angle. Therefore, by summing up the line-focused beams illuminating different parts of the sample, we can synthesize the plane wave using the Huygens principle. Using this method and with the projection approximation, our group published a work to provide the 3-D refractive index map of the sample translated on a stage across a line-focused beam. However, the previous technique had limited depth of focus due to the projection approximation, and thus it was hard to be applied to flowing samples. In this study, we overcome this limitation by adopting a diffraction tomography-based algorithm. We demonstrate this technique by adopting a specially designed micro-fluidic chamber, and providing the 3-D refractive index map of the flowing samples. Our technique can be easily incorporated into the existing flow cytometry configuration, and the speed of our technique is only limited by the camera speed. Using polystyrene beads, we present the measurement accuracy of our technique, and we try to monitor the drug response of multiple myeloma cells based on the measured refractive index map.

8589-47, Session 10

Processing improvements in dynamic quantitative phase microscope

Katherine Creath, Goldie L. Goldstein, 4D Technology Corp. (United States) and The Univ. of Arizona (United States)

This paper describes recent advances in developing an spatio-temporal unwrapping and hardware advances for a new, novel interference microscope system and presents images and data of live biological samples. The specially designed optical system enables instantaneous 4-dimensional video measurements of dynamic motions within and among live cells without the need for contrast agents. “Label-free” measurements of biological objects in reflection using harmless light levels are possible without the need for scanning and vibration isolation. This instrument utilizes a pixelated phase mask enabling simultaneous measurement of multiple interference patterns taking advantage of the polarization properties of light enabling phase image movies in real time at video rates to track dynamic motions and volumetric changes. Optical thickness data are derived from phase images. This data is processed with automated processing routines that locate, track and isolate objects, and then correct phase unwrapping from frame to frame across time lapse measurements. In addition we will review various hardware improvements we have made in the last year.

8589-48, Session 11

Parallel localization of multiple emitters for fast localization microscopy

Yina Wang, Tingwei Quan, Shaoqun Zeng, Zhen-li Huang, Huazhong Univ. of Science and Technology (China)

Localization-based super-resolution fluorescence microscopy (also called localization microscopy) employs clever strategy to separate close-packed fluorescence emitters into hundreds or even thousands of image frames, so that the locations of individual emitters can be obtained precisely through further molecule localization. These locations are then used to reconstruct a final image whose resolution is not limited by far-field diffraction but by photon-counting statistics. Unfortunately, localization microscopy naturally scarifies its temporal resolution to obtain ultra-high spatial resolution, thus limits the versatility of this technique in studying dynamic processes inside living samples. High-density localization microscopy is a promising approach to minimize this limit by increasing the density of active emitters in each image frame, and thus is capable of enhancing the temporal resolution of localization microscopy while maintaining a desired spatial resolution. However, the widespread use of high-density localization microscopy is thus far mainly obstructed by the slow image analysis speed.

In this talk we will present our recent progress on high-density localization methods. Especially, we will introduce a newly developed method, termed PALMER for “PArallel Localization of Multiple Emitters via Bayesian information criterion Recommendation”. This method comes from the combination of GPU parallel computation, multiple-emitter fitting, and optimal model recommendation via Bayesian Information Criterion (BIC). Compared to conventional localization microscopy, high-density localization microscopy based the PALMER method allows a speed gain of up to ~14-fold in data acquisition with the same desired Nyquist resolution. We believe that this PALMER method has great potentials in pushing forward the field of fast localization microscopy.

8589-49, Session 11

Nonphoto-bleachable, 3D-organized, sub-micron fluorescent patterns for the calibration and the alignment of fluorescence microscopes

Arnaud Royon, Argolight (France); Philippe Legros, Bordeaux Imaging Ctr. (France); Gautier Papon, Argolight (France); Thierry Cardinal, Institut de Chimie de la Matière Condensée de Bordeaux (France); Lionel S. Canioni, Univ. Bordeaux 1 (France)

Fluorescence microscopes equip many laboratories and platforms, not only in biology and medicine, but also in materials science. More and more, these laboratories and platforms want to pursue a quality approach. To achieve this goal, the performances of the microscopes must be guaranteed. However, these instruments are sold as “imaging tools” and not “measurement tools”, because the different devices composing the microscope cannot be calibrated altogether.

We have developed a new process that enables the inscription of non-photo-bleachable fluorescent patterns with sub-micrometer sizes in three dimensions inside glass. In this paper, we present, based on this new process, a fluorescent multi-dimensional (space, intensity, spectrum, lifetime) ruler adapted for the calibration and the alignment of fluorescence microscope (usual, confocal, epi, multiphoton) components.

Non-exhaustively, this new tool enables the measurement of:

- The repositioning of the translation stages with a resolution higher than the optical one.

- The dynamics of the detectors, thanks to up to sixteen well-discriminated fluorescence intensity levels.

- The field and illumination homogeneities of the microscope objective.

- The lateral and axial resolutions of the microscope objective with an uncertainty of 200 nm and 1 µm, respectively.

- The spectral response (spectrum, intensity and lifetime) of the system.

This device is guaranteed not to photo-bleach, it can be used for a long period of time (> 5000 hours), and can be stored without any particular precaution. Thus, measurements can be carried out at different times and can be compared, to follow, for example, the performances of a microscope in time and/or detect any malfunction.

8589-50, Session 11

Polarization sensitive full-field optical coherence tomography based on bi-stable polarizaton switch

Kwan Seob Park, Byeong Ha Lee, Gwangju Institute of Science and Technology (Korea, Republic of); Woo June Choi, Korea Basic Science Institute (Korea, Republic of); Tae Joong Eom, Gwangju Institute of Science and Technology (Korea, Republic of)

We present the polarization-sensitive full-field optical coherence tomography (PS-FF-OCT) that is based on a bi-stable polarization switch (BSPS) device. The proposed PS-FF-OCT is a Linnik type interference microscope and allows getting both the birefringence-induced phase retardation and the intensity images of biological samples with high resolutions using a pair of micro objectives and a BSPS device. Two orthogonal polarization states were formed at a regular interval by the BSPS device which can produce changes of polarization direction of light in a short time by switching their optic axes. Therefore, both the horizontally polarized light signal and the vertically polarized light signal from the sample could be detected by a single camera. For getting a phase retardation image in real-time, the BSPS device is synchronized with the CCD camera and a piezoelectric transducer. The proposed method makes easy the implementation of the polarization-sensitive FF-OCT system without the needs of complex alignment process and using two identical CCD cameras. The experimental results confirm the feasibility of the system.

8589-51, Session 11

Towards diabetes imaging based on optical coherence microscopy and confocal fluorescence imaging

Corinne Berclaz, Christophe Pache, Arno Bouwens, Antonio Lopez, Ecole Polytechnique Fédérale de Lausanne (Switzerland); Anne Grapin-Botton, The Danish Stem Cell Ctr. (Denmark); Theo Lasser, Ecole Polytechnique Fédérale de Lausanne (Switzerland)

In vivo and in situ imaging of islets of Langerhans represents an important subject in diabetes research and diagnostic. Many imaging concepts aiming in vivo imaging of ?-cells are limited in imaging speed, penetration depth and resolution. In addition, missing contrast agents with high specificity for ?-cells prevented PET, SPECT and MRI imaging for future diabetic imaging.

Extended-focus OCM allows visualizing the pancreas in vivo and ex vivo with high spatial resolution. In this study, we investigate the specificity of Cy5.5-exendin-3, an agonist of glucagon-like peptide 1 receptor which is expressed on ?-cells, both at the cellular level and in vivo inside the pancreas. In vitro imaging of cells has been achieved based on dark field OCM. These in vitro images clearly differentiate between complete internalization of the protein at 37°C whereas only membrane binding of these labels occurs at 4°C.

Complemented by small animal imaging, right after intravenous injection of Cy5.5-exendin-3, this protein can be detected inside the vascular architecture of the pancreas along with its accumulation over time inside islets of Langerhans. These results show the feasibility to use OCM coupled with simultaneous fluorescence imaging as a technological platform for tracer characterization for ?-cell imaging in vitro and in vivo. This dual system integrating OCM and confocal fluorescence imaging has been used as a technological platform for tracer characterization in view of ?-cell imaging. This opens the door to overcome the resolution limits of PET/SPECT and MRI imaging based on OCM selected labels for future clinical applications.

8589-52, Session 11

Z-microscopy for parallel axial imaging with micro mirror array

Chuan Yang, Kebin Shi, Mingda Zhou, Siyang Zheng, Shizhuo Yin, Zhiwen Liu, The Pennsylvania State Univ. (United States)

In conventional laser scanning optical microscopy, many techniques have been developed to achieve high-speed scanning in lateral (x-y) dimensions. However, to achieve three-dimensional imaging, slow mechanical scanning of the objective lens or the specimen itself in the axial (z) direction is typically required, which impedes the development of the capability for imaging fast processes in the axial direction. Here we propose and demonstrate a method for high-speed z-microscopy. By utilizing an array of 45°-tilted micro mirrors arranged along the axial direction, fluorescence signals emitted from different axial positions of a specimen can be orthogonally reflected and spatially separated on an image sensor for parallel detection. Further, each micro-mirror behaves effectively as a confocal pinhole due to its finite dimension, providing optical sectioning capability. We have performed numerical analysis, which shows that nearly diffraction limited axial resolution can be achieved. In addition, micro mirror arrays are fabricated by using photolithography, and coated with silver to enhance the reflectivity. Z-imaging of multiple microspheres located at different axial positions is experimentally demonstrated.

8590-4, Session 1

Optimization of multiplexed fluorescence correlation spectroscopy confinement and application using an array of optical fibers

Fiona Quinlan-Pluck, Mouhamadou Sy, Emmanuel Fort, Institut Langevin (France); Neso Sojic, Univ. Bordeaux 1 (France); Sandrine Lévêque-Fort, Univ. Paris-Sud 11 (France); Catherine K. Marquér, Ctr. de Recherche de l'Institut du Cerveau et de la Moelle (France); Marie-Claude Potier, Ctr. deRrecherche de l'Institut du Cerveau et de la Moelle (France); Samuel Gresillon, Institut Langevin (France)

Fluorescence correlation spectroscopy (FCS) is currently playing an ever more important role in the area of life science, with recent advances in both the technique - combining FCS to lifetime fluorescence or cross-correlation - and for the measurement of transport properties within the living cell or membrane. However, improving both resolution and speed together remains a challenge. We present multiplexed FCS (mFCS) at high concentrations using an electron multiplying charge coupled device camera, a microscope and an ordered array of etched optical fibers. When illuminated, an independent observation volume with sub wavelength confinement is created at the end of each optical fiber. Using a camera, fluorescence is detected through the array of fibers and correlation is performed on each fiber. Physical separation of the observation volume on the sample side avoids unwanted cross talk between the correlation signals. With fast acquisition modes on the camera, we perform multiplexed fluorescence correlation with a time resolution better than 0.1 milliseconds and observation volume smaller than standard confocal volume. We show optimized measurements of increasingly smaller bodies as well as comparisons between the sample concentration limits for our multiplexed system versus standard FCS. Excitation volume simulations are compared to volumes measured by mFCS to show that our mFCS results in an excitation volume more axially confined than the classical Gaussian volume. Initial mFCS detection of cholera toxin linked HEK cell membranes is also shown.

8590-5, Session 1

Dynamics of protein folding revealed by fluorescence lifetime correlation spectroscopy

Ingo Gregor, Phillip Kroehn, Qui Van, Jörg Enderlein, Georg-August-Univ. Göttingen (Germany)

Proper folding of proteins from the native amino-acid chain to the functional bio-machine is still one of the most fascinating processes in nature. In recent years, sp-FRET studies provided ground-breaking evidence in order to elucidate the nature of the fundamental principles driving this process [1]. One of the key characteristics for any process is the rate at which the turnover or transition takes place. Unfortunately, it turned out that the transition-rate in protein folding is just too high to be resolved using the classical analysis methods.. This is related to the fundamental limit of photon statistics in single molecule spectroscopy. Usually, photons in a single molecule burst are detected at a rate of several 10 to 100 kHz. The time between photon is therefore in the order of some 10 µs which gives the upper limit for observable rate constants for these methods. The photon-by-photon estimators developed by Gopich et al. [2] provides a valuable approach to elucidate hidden dynamics by simulating the expected variables and a reveals the most likely kinetic parameters for the given experimental data.

However, it is well known that much faster processes can be resolved quite easily using FCS. Being based on single-molecule events, FCS overcomes the limit in temporal resolution by averaging over many events. Applying FCS to FRET experiments requires a criterion that decides which of the events can be averaged. The donor fluorescence lifetime well suited to report the state of a FRET-pair and therefore provides this criterion. Fluorescence lifetime correlation spectroscopy (FLCS) [3] takes advantage of exactly this parameter. It not only sorts the events accordingly, but additionally allows monitoring transitions in the fluorescence lifetime by computing the cross-correlation functions.

[1] Schuler B., Eaton W.A. (2008) Protein folding studied by single-molecule FRET. Curr Opin Struct Biol 18:16–26.

[2] Gopich I.V., Szabo A. (2012) Theory of the energy transfer efficiency and fluorescence lifetime distribution in single-molecule FRET. PNAS 109: 7747–7752.

[3] Gregor I.; Enderlein J. (2007) Time-resolved methods in biophysics. 3. Fluorescence lifetime correlation spectroscopy. Photochem Photobiol Sci 6:13-18.

8590-6, Session 1

Detection of Hyaluronidase activity using fluorescence lifetime correlation spectroscopy to separate diffusing species and eliminate autofluorescence

Ryan M. Rich, Mark Mummert, Univ. of North Texas Health Science Ctr. at Fort Worth (United States); Zygmunt K. Gryczynski, Univ. of North Texas Health Science Ctr. at Fort Worth (United States) and Texas Christian Univ. (United States); Julian Borejdo, Ignacy Gryczynski, Univ. of North Texas Health Science Ctr. at Fort Worth (United States); Thomas J. Sorensen, Bo W. Laursen, Univ. of Copenhagen (Denmark); Rafal Fudala, Univ. of North Texas Health Science Ctr. at Fort Worth (United States)

The over-expression of hyaluronidase has been linked to many types of cancer, and thus we present here a technique for hyaluronidase detection and quantification using Fluorescence Correlation Spectrsocopy (FCS). Our probe consists of Hyaluronan macromolecules (HAs) heavily loaded with fluorescein dye to the extent that the dye experiences self-quenching, and these HAs are detected as very bright and slowly moving particles by FCS. Hyaluronidase cleaves HAs into HA fragments, increasing the concentration of independent fluorescent molecules diffusing through the detection volume. The cleavage of HAs releases the self-quenching so that intensity of emission is drastically increased. Both the concentration and intensity are measured simultaneously. Furthermore, a time correlated system, such as that used in this report allows one to assess the heterogeneity of the HA solution. The overall fluorescence decay will consist of a short component (large, quenched HA molecules) and a long component (smaller, unquenched HA molecules). Filters are constructed that weight the collected photons in favor of one component or the other, and the FCS fittings may be conducted to quantify concentration and intensities of quenched and unquenched molecules individually. In other words, subpopulations may be isolated based upon their lifetime for individual study by FCS. Scattered excitation light and afterpulsing artifacts are removed by this technique as well, and since there is no spectral separation, all this may be done using one detector.

8590-7, Session 1

Exploring the physics of single molecules of charged macromolecules by fluorescence correlation spectroscopy

Jiang Zhao, ShuangJiang Luo, Qingbo Yang, Institute of Chemistry (China)

In this talk, we will summarize recent advances in the study of charged polymers by fluorescence correlation spectroscopy. The high sensitivity at single molecule level of fluorescence correlation spectroscopy (FCS) enables measurements of charged polymer molecules at extreme dilution condition, which has been a difficulty for conventional techniques as dynamic light scattering. By FCS, the conformation transition of single chain of polyelectrolytes is clearly exposed: the first-order conformation transition by pH of poly 2-vinylpyridine, the scaling analysis of polystyrene sulfonate shows a change from rod-like conformation to random coil conformation with the increase of the molecular weight. Photon count histogram (PCH) helps to determine the electric potential of single charged polymer molecules, explaining the important contribution of the counterion distribution: the breakdown of “conterion condensation”. FCS is a very important method for the study of charged polymers and bio-macromolecules.

8590-8, Session 2

Optical coherence correlation spectroscopy (OCCS)

Stephane Broillet, Lab. d’Optique Biomédicale, École Polytechnique Fédérale de Lausanne (Switzerland); Stefan Geissbühler, Akihiro Sato, Christophe Pache, Arno Bouwens, Daniel Szlag, Theo Lasser, Marcel Leutenegger, Ecole Polytechnique Fédérale de Lausanne (Switzerland)

A classical technique to monitor dynamical processes at the single-molecule level is fluorescence correlation spectroscopy (FCS). However, FCS requires fluorescent labels that are typically limited by photobleaching and saturation. We present a new method, optical coherence correlation spectroscopy (OCCS), based on noble-metal nanoparticles that overcome those photobleaching and saturation limitations.

OCCS is a correlation spectroscopy technique based on dark-field optical coherence microscopy (dfOCM), a Fourier domain optical coherence microscopy technique. OCCS is based on the amplified backscattered light caused by diffusing nanoparticles. Due to the interferometric principle of OCCS, several sampling volumes along the optical axis are measured simultaneously with high detection sensitivity. This adds the possibility to assess axial flow, which is similar to a lateral flow measurement in dual-focus fluorescence correlation.

Using a mode-locked Ti:Sapphire laser (780nm central wavelength) we performed experiments with nanoparticles down to 30nm in diameter. We present these first experimental results and an associated theoretical fit model allowing the extraction of the particles’ concentrations and diffusion parameters. The experimental determination of the diffusion time and concentration of gold nanoparticles based on this method is presented as a proof of principle and shows the potential of this technique.

In the near future, we aim at investigating smaller gold nanoparticles assessing biological phenomena. As a first application we apply this method to membrane receptor interaction using functionalized nanoparticles.

8590-9, Session 2

Correction of bleaching artifacts in high content fluorescence correlation spectroscopy (HCS-FCS) data

Jeffrey J. Lange, Christopher J. Wood, William A. Marshall, Lucinda E. Maddera, Qingfeng E. Yu, William D. Bradford, Brian R. Slaughter, Jay R. Unruh, Winfried Wiegraebe, Stowers Institute for Medical Research (United States)

For large-scale protein-protein interaction screens, we developed an automated Fluorescence Correlation and Cross-Correlation Spectroscopy (HCS-FCS/FCCS) platform. In addition, we measured molecular diffusion and protein concentration and localization in vivo. We were able to obtain FCS and FCCS data from tens of thousands of individual yeast cells expressing one or two tagged proteins of interest at the endogenous level. It is well known, that measured results of FCS/FCCS experiments are strongly influenced by fluorophore photobleaching. Here, we used large experimental and simulated datasets to explore the effect of photobleaching and to propose ways to correct for these effects.

We employed wavelet based raw trajectory detrending before we calculated the autocorrelation and cross-correlation curves. We developed bleaching dependent correction factors for concentration, diffusion times, and binding kinetics. We tested our approach systematically using both in vivo control samples and simulated data with different bleaching rates.

We developed an ImageJ plugin to simulate three dimensional diffusion of a set number of fluorophores with defined bleaching rate. The detrended and corrected measurements should give the same results independent of simulated bleach rate. Based on the same idea, we measured large numbers of live yeast cells, using different excitation laser powers. This resulted in fluctuation curves with different bleach rates. Again, our results should be independent of laser power and thus bleaching rate.

Finally, we discuss the merits and limits of this approach. Our solution makes automated high-content FCS robust. In addition, these results will guide the interpretation of manual FCS experiments.

8590-10, Session 2

Detecting molecular interactions at distances larger than 100 Å. Application of FRET to study dynamics of Annexin A2 complexing with plasminogens

Zygmunt K. Gryczynski, Univ. of North Texas Health Science Ctr. at Fort Worth (United States) and Texas Christian Univ. (United States); Ryan M. Rich, Univ. of North Texas Health Science Ctr. at Fort Worth (United States); Dmytro Shumilov, Texas Christian Univ. (United States); Anindita Mukerjee, Amalendu P. Ranjan, Julian Borejdo, Ignacy Gryczynski, Rafal Fudala, Univ. of North Texas Health Science Ctr. at Fort Worth (United States); Badri P. Maliwal, Univ. of North Texas Health Science Ctr. at Forth Worth (United States); Sangram Raut, Jamboor K. Vishwanatha, Univ. of North Texas Health Science Ctr. at Fort Worth (United States)

At the core of biological function lies the ability of proteins to interact and associate with each other. In cell the essential activities are spatially and/or temporally dependent on the assembly/disassembly of transient complexes of macromolecules.

Stable complexes like proteasomes for molecular degradation and ribosomes for protein synthesis, as well as the formation of transient complexes during signaling initiated by hormones and growth factors (transductosomes) or simply membrane trafficking are a few examples of the many biological processes precisely regulated by macromolecular interactions. Many such transient complexes are much larger than 10 nm (100 Å) and the separations between involved macromolecules are much

over 100 Å. Today, available technologies capable of high resolution in-vivo studies of molecular complexes exclusively rely on optical methods. These methods are inherently limited by optical resolution and even the most sophisticated super-resolution imaging microscopy cannot reach bellow 30 nm (300 Å). From the other end Förster resonance energy transfer (FRET) has been limited to distances bellow 100 Å. The gap between limits of optical resolution and the range of FRET covers a large range of proteins and macromolecular complexes never explored before.

We recently realized that significant increase of FRET range is possible when a single donor molecule interact with a horde of acceptor molecules randomly localized on a single small body like protein/ antibody. In this paper we present and test a new method suitable for detecting proteins proximity at distances over 100 Å within macromolecular complexes.

We use example of Annexin A2 which is a cell surface receptor that plays essential role as tissue plasminogen activator and generation of cell surface proteases (like plasmin) fundamental to a wide variety of in-vivo biological processes. We use FRET approach to monitor plasminogen activator and plasminogen assembly on membrane embedded Annexin II tetramer a system much larger than 100 Å.

8590-11, Session 2

Subunit rotation in single FRET-labeled F1-ATPase hold in solution by an anti-Brownian electrokinetic trap

Michael Börsch, Thomas Heitkamp, Marc Renz, Friedrich-Schiller-Univ. Jena (Germany); Nawid Zarrabi, Univ. Stuttgart (Germany)

The F1 part can be separated from the enzyme FOF1-ATP synthase by biochemical methods. F1 acts as an ATP hydrolyzing enzyme. ATP hydrolysis is associated with stepwise subunit rotation, that is, with rotation of the gamma and epsilon subunits. Since 15 years, this rotary motion was studied in great detail using single F1 complexes attached to surfaces. Subunit rotation of gamma was monitored by videomicroscopy of bound fluorescent actin filaments, nanobeads or nanorods, or single fluorophores. Alternatively, we have applied single-molecule Förster resonance energy transfer (FRET) to monitor subunit rotation in the holoenzyme FOF1-ATP synthase reconstituted in liposomes. Here, we aim to extend the observation times of single FRET-labeled F1 parts in solution using a modified version of the anti-Brownian electrokinetic trap (ABELtrap) invented by A. E. Cohen and W. E. Moerner. Monte Carlo simulations indicated the FRET signal-to-noise ratio changes due to an increased background caused by the microfluidics of the ABELtrap. This allowed for testing our automated FRET data analysis by Hidden Markov Models for the three 120 degree rotary steps in F1-ATPase as well as substeps expected at low [ATP] concentrations. In addition, we evaluated the use of FRET-FCS to analyze the fast fluctuations of the FRET signals in F1 at high [ATP] concentrations.

8590-12, Session 2

Effect of the HIV-1 nucleocapsid protein on reverse transcriptase pause sites revealed by single molecule microscopy

Yves Mely, Armelle Jouonang, Frédéric Przybilla, Julien Godet, Univ. de Strasbourg (France); Tobias Restlé, Univ. zu Lübeck (Germany); Hugues de Rocquigny, Cyril Kenfack, Pascal Didier, Univ. de Strasbourg (France)

During reverse transcription, the HIV-1 viral RNA is converted into proviral DNA in the cytoplasm of infected cells. This process is directed by the HIV-1 reverse transcriptase (RT) which possesses two functions, namely a DNA- and RNA-dependent DNA polymerase activity and a ribonuclease H activity. RT is assisted by the HIV-1 nucleocapsid (NC) protein that chaperones key nucleic acid conformational changes required for efficient synthesis of proviral DNA [1]. Indeed, during reverse transcription, RT encounters a number of pause sites that can lead to premature termination of polymerization. NC increases the ability of RT to synthesize DNA through pause sites [2]. In the present work, we studied by single molecule FRET the effect of NC on the binding of RT to nucleic acid substrates that correspond to two pause sites. Oligonucleotides labeled with Cy5 were immobilized on glass slides and RT-Cy3 was added in solution [3]. Our data show that in the absence of NC, RT binds oligonucleotides in three different conformations. Moreover, analysis of the dissociation kinetic rate constants indicates that the residence time of RT depends on the sequence of the pause sites. When NC is added to the complexes, we observe a subsequent modification in the distribution of RT/ oligonucleotide conformations, as well as a decrease of the residence time of RT on one of the pause sites. These results give direct insight into the molecular mechanism by which NC increases the efficiency of reverse transcription at the pause sites.

REFERENCES

[1] D. Grohmann et al., Biochemistry, 2008, 47, p. 12230-40

[2] X. Ji, G. J. Klarmann, and B. D. Preston, Biochemistry, 1995, 35, p. 132-43

[3] I. Rasnik, S. A. McKinney, T. Ha, Nat Methods, 2006, 3, p. 891-3

8590-13, Session 2

Single molecule FRET using the FRET pair DRONPA/PhotoActivable mCherry

Viviane Devauges, Elena Ortiz-Zapater, Christina Efthymiou, Melanie D. Keppler, Jody Barbeau, King's College London (United Kingdom); Daniel R. Matthews, The Univ. of Queensland (Australia); James Monypenny of Pittmilly, King's College London (United Kingdom); Daniel Rolfe, Science and Technology Facilities Council (United Kingdom); Tony C. Ng, Simon M. Ameer-Beg, King's College London (United Kingdom)

Photoswitchable or photoactivable proteins such as Dronpa and PhotoActivable mCherry (PA-mCherry) are powerful tools to perform high resolution microscopy (PALM/STORM) or to study fast molecule dynamics. Dronpa, a GFP-like fluorescent protein mutant, can achieve reversible photoswitching between emissive and non-emissive states. In principle, irradiation at 488nm switches Dronpa to a dark state, and short irradiation at 405nm switches it to its green emitting state. In comparison, PA-mCherry switches irreversibly from a dark state to a red emitting state with high contrast and good photostability after irradiation at 405nm. These two photoswitchable proteins have been used to perform FRET (Förster Resonance Energy Transfer) imaging. At the single molecule level, FRET also permits access to information about the structure and dynamics of molecules. A FRET standard construct consisting of Dronpa and PA-mCherry separated by seven amino acids was expressed in MCF7 breast cancer cells. Membrane localization was assured by adding a CAAX sequence to the C-terminal fragment of the construct. Ensemble FRET experiments (measured by FLIM) were performed. We observed low FRET efficiency of the photoswitchable FRET standard compared to a similar construct with a non-switchable acceptor (mCherry). That could suggest the existence of two populations of FRET competent/ incompetent fluorophore pairs. In single molecule experiments, we have optimised irradiation conditions at 488 and 405 nm, given Dronpa's complex photophysical properties and its preswitched emissive state. We discuss strategies for observing FRET at the single molecule level with photoactivatable proteins by monitoring modifications in the donor and acceptors emissive states.

8590-1, Session 3

Förster resonance energy transfer between fluorescent proteins at single-molecule resolution *(Invited Paper)*

Alexander P. Savitsky, A.N. Bach Institute of Biochemistry (Russian Federation); Maria G. Khrenova, Lomonosov Moscow State Univ. (Russian Federation); Alexander S. Goryashenko, A.N. Bach Institute of Biochemistry (Russian Federation); Alexander V. Nemukhin, Lomonosov Moscow State Univ. (Russian Federation)

Förster resonance energy transfer (FRET) is applied as a powerful tool to analyze changes in protein conformations, protein interactions and enzymatic activity in vitro and in vivo. Fluorescent proteins are excellent partners to construct practically important FRET systems because of their low toxicity, relatively small size and suitable optical properties.

Herein we present the cooperative experimental and theoretical study which relies on fluorescence lifetime correlation spectroscopy (FLCS) and precise computational quantum chemical methods for accurate characterization of the specific FRET system. The system under consideration is the fuse protein composed of fluorescent protein TagRFP that acts as an energy donor and photoswitchable protein KFP that is an energy acceptor linked by the 23 amino-acid oligopeptide with a specific DEVD motif. The latter can be specifically cleaved by caspase-3. We obtained the fluorescence lifetime distribution of the fuse protein based on the data of FLCS. The data is collected from the single molecule experiments and thus characterizes the system's properties at the molecular level unlike approaches using averaged values obtained from the statistic ensemble. The data obtained are described in terms of conformational dynamics of the fuse protein that employed the results of molecular dynamics simulation, combined with the results of quantum chemical calculations of transition dipole moments of the TagRFP and KFP . We demonstrate that the observed distribution is well characterized in theoretical approaches.

8590-2, Session 3

Single-molecule FRET experiments with the new red-enhanced custom technology SPADs

Francesco Panzeri, Politecnico di Milano (Italy); Niusha Sarkhosh, Antonino Ingargiola, Ron R. Lin, Univ. of California, Los Angeles (United States); Angelo Gulinatti, Ivan Rech, Massimo Ghioni, Sergio Cova, Politecnico di Milano (Italy); Shimon Weiss, Xavier Michalet, Univ. of California, Los Angeles (United States)

Single-molecule fluorescence spectroscopy of freely diffusing molecules in solution is a powerful tool used to investigate the properties of individual molecules, providing the ability of obtaining information otherwise not available due to ensemble averaging.

This technique is made possible by the use of sensitive single-photon detectors, which can detect the weak and brief fluorescence of single-molecules diffusing rapidly through a focused excitation spot. Single-Photon Avalanche Diodes (SPAD) are the detectors of choice for these applications. Two different types of SPADs are currently available: (i) thick SPADs have excellent quantum efficiency but show limited timing resolution and suffer from variable instrument response functions (IRFs); (ii) thin SPADs have excellent timing performances and can be manufactured in array geometry, but suffered until recently from lower quantum efficiency in the red and infrared part of the spectrum.

Recently an evolution of the thin SPAD, named red-enhanced SPAD, was introduced, with better sensitivity throughout the visible spectrum and preserving excellent timing performance. Here we present a complete characterization of these new detectors for single-molecule fluorescence spectroscopy, using two-color single-molecule FRET (smFRET) experiments on a series of doubly-labeled DNA molecules. Both intensity-based (?s-ALEX) and lifetime-based (ns-aLEX) measurements are presented and compared to identical measurements performed with standard thick SPADs.

These new detectors appear as serious contenders for single-molecule fluorescence spectroscopy, due to their robustness, excellent timing characteristics and good sensitivity throughout the visible spectrum.

8590-3, Session 3

8-spot single diffusing molecule FRET analysis using two 8-pixel SPAD arrays

Antonino Ingargiola, Niusha Sarkhosh, Univ. of California, Los Angeles (United States); Francesco Panzeri, Angelo Gulinatti, Ivan Rech, Massimo Ghioni, Politecnico di Milano (Italy); Shimon Weiss, Xavier Michalet, Univ. of California, Los Angeles (United States)

Single-molecule Förster resonance energy transfer (smFRET) techniques are widely used to address outstanding problems in biology and biophysics. In order to study freely diffusing molecules, current approaches consist in exciting a low concentration (<100 pM) sample within a single confocal spot using one or more lasers and detecting the induced single-molecule fluorescence in one or more spectral/polarization channels (e.g. donor and acceptor) using single-pixel Single Photon Avalanche Diodes (SPADs). A sufficient number of single-molecule bursts must be accumulated in order to compute FRET efficiencies with sufficient statistics. As a result, the timescale of observable phenomena is constrained by the minimum acquisition time needed for accurate measurements, typically a few minutes or more, limiting this approach mostly to equilibrium studies. Increasing smFRET analysis throughput would allow studying dynamics with shorter timescales.

We recently demonstrated a new multispot excitation approach, employing a novel multipixel SPAD array, using a simplified dual-view setup in which a single detector was used to collect FRET data from 4 independent spots.

In this work we extend our results to 8 spots by using two 8-SPAD arrays to collect donor and acceptor photons and demonstrate the capabilities of this system by studying a series of doubly labeled dsDNA samples with different donor-acceptor distances ranging from low to high FRET efficiencies. Results show that it is possible to enhance the throughput of smFRET measurements in solution by almost one order of magnitude, opening the way for studies of single-molecule dynamics with fast timescale once larger SPAD arrays become available.

8590-23, Session 3

Biodegradable molecular photoswitches for super-resolution fluorescent imaging

Ming-Qiang Zhu, Guofeng Zhang, Chong Li, Wen-Liang Gong, Huazhong Univ. of Science and Technology (China)

Biodegradable spiropyran-conjugated polymers and their nanoparticles with spiropyran integrated into the hydrophobic PCL matrix exhibit green-red dual-color intrinsic fluorescence switching upon UV/Vis alternate illumination. Green emission from SP in SP-PCL nanoparticles is observed before UV irradiation while red emission from MCs in MC-PCL nanoparticles after UV irradiation. For both SP-PCL and MC-PCL nanoparticles, the critical excitation wavelength is determined at 420 nm, at which the photo-induced interconversion of MC- and SP-forms are found to achieve the equilibrium. Positive and inverse photoisomerizations monitored using time-dependent fluorescence spectra show that blue light excitation above 420 nm yields green emission of SPs in SP-PCL nanoparticles while UV irradiation below 420 nm imparts photoisomerization (SP to MC) and thus red emission of MCs in MC-PCL nanoparticles. Green and red fluorescence can be optically switched and imaged under fluorescent microscopy. The SP-PCL biodegradable nanoparticles are demonstrated to be promising photoswitchable fluorophores for localization-based super-resolution

microscopy, evidencing by resolving nanostructures with sub-50 nm resolution in polyvinyl alcohol (PVA) film and live cells.

8590-14, Session 4

Role of the amyloid region in the formation and propagation of Als adhesive nanodomains on Candida albicans *(Invited Paper)*

David A. Alsteens, Univ. Catholique de Louvain (Belgium)

Unravelling the structure-function relationships of the yeast cell wall is a major challenge in current microbiology. A key question is to understand how cell wall proteins respond to mechanical force and how they assemble to form nanodomains.

By combining single-molecule atomic force microscopy (AFM) with the tools of genetics and cell biology, we showed that the precise delivery of piconewton forces on Candida albicans yeast adhesins triggers the formation of adhesion nanodomains on live cells (Alsteens et al., 2009; Alsteens et al., 2010; Garcia et al., 2011). We showed that Als5p nanodomains resulted from protein redistribution triggered by force-induced conformational changes in the initially probed proteins, rather than from non-specific cell wall perturbations. Using AFM and fluorescence microscopy, we also found that nanodomains are formed within ~30 min, and migrate at a speed of ~20 nm.min-1, thus indicating that domain formation and propagation are slow, time-dependent processes.

In a next step, we measure the mechanical properties of amyloids formed by the cell adhesion protein Als5p from the pathogen C. albicans. We show that stretching Als proteins through their amyloid sequence yields characteristic force signatures corresponding to the mechanical unzipping of ?-sheet interactions formed between surface-arrayed Als proteins. The unzipping probability increases with contact time, reflecting the time necessary for optimal inter ?-strand associations. These results demonstrate that amyloid interactions provide cohesive strength to a major adhesion protein from a microbial pathogen, thereby strengthening cell adhesion. We suggest that such functional amyloids may represent a generic mechanism for providing mechanical strength to cell adhesion proteins.

What is the mechanism underlying domain formation? We suggest that, in the initial stage, stretching and unfolding of Als5p with the AFM tip extend conformations in which homologous hydrophobic interactions are favored. Fast hydrophobic interactions between extended tandem repeats would first promote Als5p self-associations and the recruitment of further neighboring proteins. Next, slower interactions would take place between the stimulated proteins, such as amyloid interactions between threonine-rich regions, and then propagate across the entire surface (Lipke et al., 2012)

Collectively, our experiments demonstrate that AFM is a powerful platform for analyzing the localization and mechanics of individual yeast cell wall proteins. Our data shed new light into the mechanical response of yeast adhesins, and contribute to refine our understanding of the molecular bases of cell adhesion. The results are also of medical relevance since they offer exciting prospects in therapeutics for developing new antimicrobial strategies to fight pathogens.

Alsteens, D., V. Dupres, et al. (2009). “Unfolding individual Als5p adhesion proteins on live cells.” ACS Nano 3: 1677-1682.

Alsteens, D., M. C. Garcia, et al. (2010). “Force-induced formation and propagation of adhesion nanodomains in living fungal cells.” Proc Natl Acad Sci U S A 107(48): 20744-20749.

Garcia, M. C., J. T. Lee, et al. (2011). “A Role for Amyloid in Cell Aggregation and Biofilm Formation.” PLoS ONE 6(3): e17632

Lipke, P. N., M. C. Garcia, et al. (2012). “Strengthening relationships: amyloids create adhesion nanodomains in yeasts.” Trends Microbiol 20(2): 59-65.

8590-15, Session 4

Expanding the excitation range of confocal microscopy from UV to IR

Felix Koberling, Marcelle König, Steffen Ruettinger, Benedikt Krämer, Sebastian Tannert, Thomas Schönau, PicoQuant GmbH (Germany); Ingo Gregor, Georg-August-Univ. Göttingen (Germany); Michael Wahl, Marcus Sackrow, Kristian Lauritsen, PicoQuant GmbH (Germany); Jörg Enderlein, Georg-August-Univ. Göttingen (Germany); Rainer Erdmann, PicoQuant GmbH (Germany)

Today, detecting the fluorescence of a single molecule is straight forward, not least because of the availability of turn-key microscope systems with single molecule sensitivity. However, even these boundaries of confocal fluorescence microscopy can be pushed further, especially as we will show for:

Extension of excitation wavelengths into the deep UV: 266 nm grants access to the intrinsic fluorescence of tryptophan-containing proteins enabling label-free FLIM with biological cells where the aromatic amino acids within the proteins become visible. As a first benchmark, UV-FCS with organic fluorophores is shown.

Just opposite in the IR wavelengths region two photon absorption offers to eliminate the bleaching in out of focus regions. The excitation region in axial direction already being restricted by the two photon process allows to detect the fluorescence right after the objective without the need of a confocal pinhole. For non-descanned detection the new hybrid PMT (PMA-Hybrid) detector shifts the detection efficiency for the first time towards real single molecule sensitivity combined with its superior fluorescence lifetime resolution.

The fluorescence lifetime of a dedicated fluorophore is strongly dependent on its photophysical properties and its environment. Together with its emission profile detected in different spectral channels the fluorescence decay can act as a fingerprint for a dye in a certain condition. We present a pattern-matching technique that allows to identify selected patterns consisting of fluorescence decays in different spectral channels. The technique allows an excellent separation of fluorophores in FLIM images and their discrimination from autofluorescence.

8590-17, Session 4

Enhancement of single molecule fluorescence using conical micromirrors

Annette C. Grot, Aaron J. Rulison, Janice Yujuan Cheng, Austin Tomaney, Pei-Lin Hsiung, Ravi Saxena, Mathieu E. Foquet, Paul Lundquist, Joyce Y. Huang, Mark McDonald, Pacific BioSciences (United States)

Single molecule fluorescence signaling systems using subwavelength metal apertures require efficient illumination and collection optics. On-chip micromirror structures are of interest for increasing coupling efficiency between the subwavelength metal apertures, and external fluorescence illumination, and collection optics, thus simplifying several aspects of instrument design including optics, optomechanics, and thermal control. Techniques are required for modeling and experimentally verifying the illumination and collection gains of practically-fabricated micromirrors used with subwavelength metal apertures. A combination of ray based and finite difference time domain models is used to optimize conical micromirrors for use with subwavelength metal apertures for the case where the illumination light interacts strongly with the micromirror and for NA 0.5 collection optics. Experimental methods employing free diffusing and immobilized dye molecules are used to measure the illumination and collection efficiencies of micromirror prototypes. Overall fluorescence gains of ~100 comprising flood illumination efficiencies ~20 and collection efficiencies ~5 were predicted and experimentally verified. Conical micromirrors optimized for use with single molecule

fluorescence in subwavelength metal apertures greatly simplify external instrumentation.

8590-18, Session 4

Comparison of Gaussian and Poisson noise models in a hybrid least squares and principal components analysis algorithm for Raman spectroscopy

Dominique Van de Sompel, Ellis Garai, Cristina L. Zavaleta, Sanjiv S. Gambhir, Stanford Univ. (United States)

Raman spectra are most commonly analyzed using the ordinary least squares (LS) method. However, LS is sensitive to variability in the spectra of the analyte and background materials. We previously addressed this problem by successfully proposing a novel hybrid least squares and principal components (HLP) algorithm. HLP extends LS by allowing the reference spectra to vary in accordance with the principal components observed in calibration sets. Previously, HLP assumed zero-mean Gaussian measurement noise. In this work, we show that the noise in fact follows a Poisson distribution, and update the mathematical framework of HLP accordingly. The performance of the Gaussian and Poisson noise models is compared using both simulated and measured spectra. The simulated spectra were computed by adding various concentrations of Raman-enhanced gold-silica nanoparticles to three different backgrounds (paraffin, glass and quartz). The measured spectra were acquired from a serial dilution of gold-silica nanoparticles placed on an excised pig colon. For the simulated spectra, the Poisson model consistently outperformed the Gaussian model, on average reducing the mean absolute concentration error as well as its standard deviation by ~15-20%. For the measured data, the Gaussian and Poisson noise models yielded similar concentration estimates. Further, more rigorous performance comparisons were precluded by the lack of exact knowledge of the nanoparticle concentrations, which differed from the serial dilution values due to diffusion into the mucus layer. As already demonstrated by the simulation results, however, the optimization of noise models is an important topic warranting further investigation, capable as it is of improving the detection accuracy of Raman spectroscopy.

8590-16, Session 5

Development of an integrated Raman scanned probe microscope for TERS imaging.

Aaron Lewis, The Hebrew Univ. of Jerusalem (Israel); Yossi Bar-David, Rimma Dekhter, Hesham Taha, Nanonics Imaging Ltd. (Israel)

Research will be described that has focused on optimizing the essential components of instrumentation and probes for tip enhanced Raman scattering (TERS) and associated techniques based on full integration of scanned probe microscopy with microRaman spectroscopy. The results of this research effort have allowed for a general TERS solution that can be applied for both opaque and transparent samples and employing exciting developments of multiprobe scanned probe microscopy. It also permits for integration with all upright, inverted and dual 4 Pi microscope solutions. The probes that have worked best have been those that are based on single gold nanoparticles at the exposed tip of a low dielectric glass probe. These probes were originally designed for use in tip enhanced non-linear optical microscopy (TEN)1. Such probes will be compared to other solutions in the literature especially those based on etched wires of gold or silver or coated silicon probes. The data indicate that gold or silver nanostructures isolated in low dielectric probes provide artifact free TERS results generally applicable to a wide variety of studies from semiconductor thin films to carbon nanotubes and graphene. As part of this research it has been necessary to define samples which have specific properties to demonstrate the nature of the TERS effect. This aspect of the research has identified the factors that maximize enhancement and minimize the optical interference that can be parasitic to the TERS signal. In addition it will be shown that these TERS developments are compatible with exciting new directions in multiprobe scanned probe microscopy

1. Barsegova et al, “Controlled Fabrication Of Silver Or Gold Nanoparticle Atomic Force Probes: Enhancement Of Second Harmonic Generation,” Applied Physics Letters 81, 3461-63 (2002)

8590-19, Session 6

Localization, structure and dynamics: exploring live bacteria cells at the single molecule level *(Invited Paper)*

Julie S. Biteen, Univ. of Michigan (United States)

High-resolution, non-destructive methods for examining subcellular events have opened up an exciting new frontier: the study of macromolecular localization and dynamics in cells by direct, physical approaches. By determining the position and tracking the motion of individual, isolated emitters, single-molecule fluorescence imaging brings the resolution of optical microscopy down to the nanometer scale of the proteins themselves. Such investigations allow us to unlock the mysteries of how biomolecules work together to achieve the complexity that is a cell.

We have developed novel methods for single-molecule investigations of live bacterial cells under physiologically relevant conditions, and used these techniques to investigate thee important prokaryotic systems. By examining the dynamics of TcpP, the membrane-bound transcription activator in the infectious Vibrio cholerae, we uncover several modes of protein motion and quantify the amount of time spent in each corresponding confirmation. By resolving the response to starch of pairs of Bacteroides thetaiotaomicron Starch Utilization System proteins, we determine that these outer-membrane proteins form a complex and investigate the mechanism of carbohydrate catabolism in this human gut symbiont. By tracking the motion of the Bacillus subtilis DNA mismatch repair protein MutS relative to the replication fork, we determine how MutS locates mismatched base pairs to assure survival of the species. Each system presents unique challenges, and here we discuss the important methods developed for each system, in particular, a comparison of membrane-bound and soluble proteins, extensions to two-color and 3D imaging, and adaptations for studying live anaerobic cells.

8590-20, Session 6

The double-helix point spread function enables precise and accurate measurement of 3D single-molecule localization and orientation

Mikael P. Backlund, Matthew D. Lew, Adam S. Backer, Stanford Univ. (United States); Ginni Grover, Rafael Piestun, Univ. of Colorado at Boulder (United States); W. E. Moerner, Stanford Univ. (United States)

Single-molecule-based super-resolution fluorescence microscopy has recently been developed to surpass the diffraction limit by roughly an order of magnitude. These methods depend on the ability to precisely and accurately measure the position of a single-molecule emitter, typically by fitting its emission pattern to a symmetric estimator (e.g. centroid or 2D Gaussian). However, single-molecule emission patterns are not isotropic, and depend highly on the orientation of the molecule’s transition dipole moment, as well as its z-position. Failure to account for this fact can result in localization errors on the order of tens of nm for in-focus images, and ~50-200 nm for molecules at modest defocus. The latter range becomes especially important for three-dimensional (3D) single-molecule super-resolution techniques, which typically employ

depths-of-field of up to ~2 ?m. To address this issue we report the simultaneous measurement of precise and accurate 3D single-molecule position and 3D dipole orientation using the Double-Helix Point Spread Function (DH-PSF) microscope. We are thus able to significantly improve dipole-induced position errors, reducing standard deviations in lateral localization from ~2x worse than photon-limited precision (48 nm vs. 25 nm) to within 5 nm of photon-limited precision. Furthermore, by averaging many estimations of orientation we are able to improve from a lateral standard deviation of 116 nm (~3x worse than the precision, 28 nm) to 34 nm (within 6 nm).

8590-21, Session 6

New approach to double-helix point spread function design for 3D super-resolution microscopy

Ginni Grover, Rafael Piestun, Univ. of Colorado at Boulder (United States)

Advances in super-resolution microscopy over the last decade have enabled imaging of intracellular structures with resolution beyond the optical diffraction limit. Super-resolution methods like STORM/PALM are based on localization of individual fluorescent molecules in 2D or 3D to provide less than 50 nm resolution in all three dimensions. To achieve 3D localization, a double-helix point spread function (DH-PSF) has been used. A DH-PSF refers to a PSF that instead of producing a single lobe, displays two lobes in a transverse plane which rotate with defocus. Therefore, the axial shifts of a point source are now encoded in the rotation of the two-lobed pattern. A DH-PSF is generated by inserting a specific spatial phase modulation element in the pupil plane of the imaging system.

We report on a new analytic method to generate different DH-PSFs for specific applications- localization, tracking, and ranging. The new method allows control of the characteristics such as efficiency, rotation rate, depth-of-field and transverse size. A PSF suitable to high background 3D super-resolution microscopy is designed and experimentally demonstrated. An information-theoretical comparison of this PSF with other DH-PSFs and 3D methods shows that this design is most suitable for 3D imaging with backgrounds upto 50 photons/pixel. With this PSF, 3D super-resolution imaging over a depth of 1.2 µm is shown without scanning. Single-molecule localization precision of (?x, ?y, ?z)= (6, 9, 39) nm (FWHM) with 6000 collected photons is demonstrated with the new PSF design. The new design method thus provides more freedom and flexibility for extended depth-of-field super-resolution microscopy.

8590-22, Session 6

SOFI of GABA-B neurotransmitter receptors in hippocampal neurons elucidates intracellular receptor trafficking and assembly

Anja Huss, Georg-August-Univ. Göttingen (Germany); Omar Ramírez, Felipe Santibáñez, Andrés Couve, Steffen Härtel, Univ. de Chile (Chile); Jörg Enderlein, Georg-August-Univ. Göttingen (Germany)

The synaptic efficacy of neurons depends on the number of neurotransmitter receptors in the plasma membrane. The availability of these receptors is controlled by their specific intracellular trafficking routes. GABA-B receptors (GABA-B Rs) are heteromeric proteins consisting of GABA-B R1 and GABA-B R2 subunits. These receptors are found at the plasma membrane of dendritic postsynaptic sites.

It is unknown whether the assembly of the subunits occurs directly in the somatic endoplasmic reticulum (ER) followed by vesicular transport, or whether the assembly occurs after the separate transport of the subunits to the dendritic ER compartment.

To address this question we have studied the assembly of the GABA-B Rs in hippocampal neurons with dual-color, 3D Stochastic Optical Fluctuation Imaging (SOFI). SOFI is a fluorescence imaging modality which yields super-resolved spatial resolution, 3D-sectioning and high image contrast. First, we compare the performance of SOFI on neurons with QDot-labeled GABA-B R subunits with that of conventional confocal microscopy. Next, we use the SOFI images to quantify the distribution of the GABA-B R subunits in the plasma membrane and in the dendritic intracellular compartments.

Finally, we want to apply quantitative co-localization analysis to determine the compartments in which the assembly of the GABA-B R subunits occurs.

8590-44,

Nanoscopy with focussed light *(Keynote Presentation)*

Stefan W. Hell, Max-Planck-Institut für Biophysikalische Chemie (Germany)

No Abstract Available

8590-24, Session 7

Two-color 3D super-resolution imaging of bacterial protein ultrastructures with the double-helix point-spread function microscope

Andreas Gahlmann, Stanford Univ. (United States); Ginni Grover, Univ. of Colorado at Boulder (United States); Jerod L. Ptacin, Lucy Shapiro, Stanford Univ. (United States); Rafael Piestun, Univ. of Colorado at Boulder (United States); W. E. Moerner, Stanford Univ. (United States)

Recently, a new 3D super-resolution imaging methodology has been introduced which produces a double-helical point-spread-function (DH-PSF) using transmissive optical phase masks. With the DH-PSF, the microscope's optical system generates two focused spots on the detector for a single molecule emitter and these two spots revolve around each other as a function of axial z defocus. The full 3D position of any molecule within a ~2 µm depth of field can then be extracted from the angular orientation of the line connecting the two spots (z position), and the midpoint of that line (x,y position). In this work, we implement a two-color version of this approach for imaging of protein ultrastructures in bacteria. Locally adaptive 3D image registration during post-processing enables quantitative multicolor 3D super-resolution reconstructions. We apply this multicolor DH-PSF methodology using genetically encoded fluorescent protein fusions in live Caulobacter crescentus cells and visualize the subcellular organization of critical cell-cycle dependent proteins, e.g. PopZ, at the cell pole. We show that the precision in distance measurements between any imaged fluorescent proteins within the same cell is chiefly limited by the localization precision of the individual single-molecule fluorophores themselves. Finally, we sample the cell surface using the PAINT technique to position the fluorescent protein localizations within the 3D spatial context of the cell's boundaries.

8590-25, Session 7

Fiber amplified and frequency doubled gain-switched diode laser at 766 nm as a depletion source for high resolution STED microscopy

Kristian Lauritsen, Thomas Schönau, Torsten Siebert, Romano Haertel, Thomas Eckhardt, Dietmar Klemme, Rainer Erdmann,

PicoQuant GmbH (Germany)

For the depletion of fluorescence in classical STED microscopy, pulsed lasers with pulse energies of several nanojoules and pulse widths of picoseconds are essential. To synchronize with the excitation source and optionally to a scanning device, electrically triggerable depletion sources are desirable.

We present a picosecond pulsed laser, based on a fiber amplified and frequency doubled gain-switched laser diode. Gain switched laser diodes give the opportunity to trigger singles pulses from an arbitrary electrical signal source. Pulses out of a 1532nm DFB gain-switched laser diode with an energy of a few picojoules are amplified in a multi-stage Er-doped fiber amplifier to energy levels as high as 25 nanojoules. A periodically poled Lithium Niobate crystal converts the amplified IR-pulses to 766nm pulses with energies of more than 3 nanojoules.

This freely triggerable laser source can operate in a wide range of repetition frequencies from 1 MHz up to 80 MHz which makes it easy to adapt the pulse period to different fluorescence lifetimes.

The wavelength of 766nm is appropriate for the depletion of fluorescent dyes like ATTO 633 or Abberior STAR 635 and can be easily combined with a gain-switched diode laser at 635 nm as an excitation source. Both lasers can be driven by a multi-channel picosecond electrical pulse generator with variable delays which makes the setup of synchronized excitation and depletion sources for STED easy.

8590-26, Session 7

Confocal spinning disk image scanning microscopy

Olaf Schulz, Christoph M. Pieper, Jörg Enderlein, Georg-August-Univ. Göttingen (Germany)

Fluorescence microscopy is one of the main techniques for functional imaging in biology and life sciences. In the past years, multiple approaches to enhance the resolution of optical microscopy have been developed. While, in principle, resolutions of under 10nm can be reached using these super-resolution methods, they are often restricted to the use of particular fluorophores, or require elaborate optical setups. Here, we present an approach for enhancing the resolution that is based on standard spinning disk confocal microscopy. Our method is a modification of Image Scanning Microscopy (ISM) which employs a confocal microscope equipped with a CCD instead of a pinhole and point detector. By using a simple algorithm, the intensity distribution on the CCD can be used to extract spatial information that would correspond to an infinitely small pinhole, thus resulting in an enhancement of the resolution of about 1.4 fold. Using deconvolution of the image with an assumed point spread function increases this factor to about 2 fold. In the spinning disk confocal microscope, multiple foci, corresponding to the pinhole pattern on the spinning disk, are imaged onto a CCD simultaneously. By synchronizing a short (microseconds) laser pulse with the rotation of the disk, we generate a point pattern that is scanned through the sample by shifting the offset between laser pulse and disk rotation. The images from these scans are analyzed using the ISM algorithm. We present 3D-images of fluorescently labeled cells to show the viability of the method.

8590-27, Session 8

Low power super resolution fluorescence microscopy *(Invited Paper)*

Angus J. Bain, Richard J. Marsh, Siân Culley, Univ. College London (United Kingdom)

We demonstrate a new and experimentally simple method for obtaining sub-diffraction resolution in fluorescence microscopy with low on-sample laser powers. The technique involves the analysis of the time evolution of fluorescence images in the presence of weak and unstructured continuous wave (CW) stimulated emission. A sub-diffraction limited point spread function (PSF) is obtained by the recombination of time segments of the evolving image. Theoretical modelling and experimental results are presented for 20nm fluorescent nanospheres in agar and live HEK cells. A sub-diffraction limited PSF is obtained with ca. 7.5mW CW stimulated emission with no discernable changes to cell morphology and viability.

8590-28, Session 8

Plasmon-enhanced fluorescence intensities and rates permit super-resolution imaging of enhanced local fields

Esther Wertz, Jessica E. Donehue, Christopher Hayes, Julie S. Biteen, Univ. of Michigan (United States)

Single-molecule fluorescence imaging is a powerful tool for imaging structures below the standard diffraction limit of light. The resolution gain comes from fitting isolated fluorophore emission, and localization accuracy improves with number of photons detected. Here, we control single-molecule emission by coupling to gold nanoparticle local plasmon resonances. These resonances are generated by the interaction of light with particles smaller than the incident wavelength and are strongly localized electromagnetic modes. We have characterized the photophysics of isolated fluorophores in the near field of gold nano-island arrays through wide-field single-molecule epifluorescence microscopy, and we observe up to five-fold enhancements in emission intensity, a doubling of the width of the distribution of intensities and up to a seven time increase in photostability of single molecules. Furthermore, since fluorescence intensity is proportional to local electromagnetic field intensity, these changes in emission properties serve as a read-out of the field intensity. By using random motion of single dyes in solution to stochastically scan the surface, and by assessing plasmon-enhanced emission as a function of position, we have imaged the electromagnetic field profile about gold nano-islands and determined its dependence on distance from the nano-island surface with better than 10 nm precision. By yielding brighter, longer-lived probes, plasmon-enhanced fluorescence has important implications for bio-imaging, and the ability to image the local field provides an in situ probe for measuring the electromagnetic field of intricate plasmonic substrates on the nanometer scale, and offers important insight into the enhancement profile of rough metallic surfaces.

Young Investigator best paper competition BO403

8590-29, Session 8

Breaking the diffraction limit in pump-probe microscopy of non-fluorescent species

Pu Wang, Mikhail N. Slipchenko, James I. Mitchell, Xianfan Xu, Ji-Xin Cheng, Purdue Univ. (United States)

Breaking the diffraction limit in far-field fluorescence microscopy has been achieved by multiple technologies, such as stimulated emission depletion (STED) microscopy, structure illumination microscopy (SIM), photoactivated localization microscopy (PALM) and stochastic optical reconstruction microscopy (STORM). These current super-resolution technologies require fluorescent samples. To break the diffraction limit in imaging of non-fluorescent species, herein we demonstrate saturated transient absorption microscopy (STAM) for far-field sub-diffraction-limit imaging of non-fluorescent nanostructures. Our method is based on a pump-probe microscope where a modulated pump beam perturbs the charge-carrier density in a sample, thus modulating the transmission of a probe beam. To achieve sub-diffraction-limit, we add a doughnut-shaped suppression beam, with the same wavelength as the pump beam and much higher intensity. The suppression pulses transiently saturate the charge-carrier density in the doughnut-shape region, leaving the modulated portion only at the focal center for the sequential probe pulses. Sub-diffraction-limit images were obtained by raster scanning of the three collinearly aligned beams. Nano-defects on epitaxial graphene and graphite nano-platelets were imaged. A resolution of

?/4 was achieved. This method opens new opportunities in studies of nanoparticle-cell interaction, characterization of nanoelectronics devices, and imaging of non-fluorescent chromophores in live cells.

8590-30, Session 8

Nanoscale imaging of heterochromatic proteins in human embryonic stem cells using light sheet microscopy

Ying S. Hu, Quan Zhu, Inder M. Verma, Hu Cang, The Salk Institute (United States)

Using a light sheet microscope configured with a slant sample stage (3S light sheet microscope), we demonstrate for the first time nanometer-resolution images of the heterochromatic protein distribution in human embryonic stem (hES) cells. The direct visualization provides essential information in the epigenetic processes of gene regulation.

Up to date, light sheet microscopy largely relies on thick sheets that do no allow sectioning of a single cell. This limitation is intrinsic to the current design concept where excitation and illumination objective lenses cannot be placed in close proximity due to their bulky physical footprint. Inspired by the highly inclined laminated optical sheet (HILO) microscopy, we introduce the 3S light sheet microscope that relaxes this limitation. 3S light sheet microscopy improves the field of view by overlapping the excitation plane with the focal plane of the objective lens while simultaneously achieving high signal-to-noise performance using a thin light sheet. Combined with the Bayesian blink and bleach algorithm and the super computing power at the National Energy Research Scientific Computing Center (NERSC), we reconstruct and reveal the unprecedented superresolution images of the heterochromatic protein 1 distribution in H1 hES cells.

8590-31, Session 9

In depth 3D PALM/STORM/SPT adaptive device

Xavier Levecq, Imagine Optic SA (France); Xavier Darzacq, Ignacio Izeddin, Maxime Dahan, Ecole Normale Supérieure (France); Audrius Jasaitis, Gregory Clouvel, Imagine Optic SA (France)

Fluorescence microscopy is widely used in biology as a basic tool to investigate cellular and molecular processes. The 2D nanometric localization precision provided by single molecule detection techniques like single particle tracking and single-molecule based super-resolution microscopy (PALM, STORM and its derivates) has revolutionized cell imaging and set new standards in fluorescence microscopy. While it is relatively easy to locate a molecule in the image plane (with a typical resolution of 10 to 50 nm), it is difficult to do so along the optical axis with comparable resolution. Moreover, as all other optical techniques, it is affected by optical aberrations. These aberrations can be induced by two different ways: various optical elements along the optical path and the difference of the refractive index between the objective immersion medium and the region studied in the sample. This second source of aberrations becomes more significant when imaged deep in the biological sample and degrades the signal significantly. In this communication we present the application of an adaptive device, which performs 1) Correction of the residual aberrations, 2) Correction of the aberrations induced by the sample deep in the biological sample, and 3) Controled and tunable induced astigmatism (or other known PSF deformations) which enables the nanometric axial resolution in the PALM/STORM microscopy, also deeper in the sample. We show how the adaptive optics device recovers the image, discuss the accuracy of this adaptive optics technique in comparison with previous strategies (cylindrical lens, double helix psf etc), especially deep in the sample. We also show how the configurability of this technique allows us to improve the imaging resolution in all three dimentions.

8590-32, Session 9

Super-resolution localization microscopy with an sCMOS camera: opportunities and challenges

Fan Long, Hongyu Zhu, Hongqiang Ma, Shaoqun Zeng, Huazhong Univ. of Science and Technology (China); Zhen-li Huang, Britton Chance Ctr. for Biomedical Photonics (China)

Low-light detectors are essential for fluorescence imaging of single molecules, and thus in realizing several innovative localization-based super-solution microscopy (or called super-resolution localization microscopy) imaging techniques, which rely on repeated detection and localization of single fluorescent molecules to reconstruct a final super-resolution image. Currently, Electron Multiplying Charge Coupled Device (EMCCD) cameras are widely accepted as the image sensors of choice in super-resolution localization microscopy, because EMCCD cameras utilize electron multiplication processes to effectively eliminate camera read noise and thus are capable of detecting the weak fluorescence signal from single molecules.

However, even since their launch in 2010, there is a hot debate among industry and academic researchers that whether the newly developed scientific-grade complementary metal oxide semiconductor (sCMOS) cameras, which offer simultaneously low read noise (1~2 e-) at extremely rapid readout rate (up to 560 MHz), could become a technology replacement for EMCCD cameras in super-resolution localization microscopy, since the imaging performance of this kind of sCMOS cameras already approaches the key requirements crucial for single molecule detection.

In this talk, we will present our recent investigations on the opportunities and challenges of replacing EMCCD using sCMOS cameras in super-resolution localization microscopy. Especially, we will discuss our experimental findings on the imaging performance of several commercial available sCMOS and EMCCD cameras in single molecule detection and localization. Finally, we will show our results on using a commercial sCMOS camera in high-throughput super-resolution localization microscopy.

8590-33, Session 9

Multiemitter colocalization with likelihood maximization for 3D superresolution fluorescence microscopy

Yi Sun, Yang Pu, The City College of New York (United States); Mitchell Schaffler, The City Univ. of New York (United States)

The recent nanoscope technique including STED, RESOLFT, STORM, PALM, and SOFI can break the diffraction barrier to provide a spatial superresolution about ten nanometers. STORM requires that the diffraction regions of two simultaneously activated fluorophores do not overlap. Consequently, the activation probability must be as low as one thousandth and the total imaging time is significantly long. In applications such as viewing bio-activities in a live cell, not only high spatial resolution but also short imaging time is desired. In this study, we develop an approach, named multiemitter colocalization (MEC), to reduce the required imaging time. Multiple fluorophores with distances less than the size of the diffraction pattern are allowed to be activated simultaneously and their 3-D locations are jointly determined. First, the number of activated fluorophores and their 3-D locations in a region are initially estimated. From an acquired 2-D image the location of an activated fluorophore is estimated, and its fluorescent image is reconstructed and is subtracted from the acquired image in a sequential mode. Second, initialized with the sequentially estimated fluorophore locations, the multiple fluorophores are colocalized with likelihood maximization using gradient search. Third, the resolved multiple fluorophore locations are accepted if the mean squared error between the acquired image and the image reconstructed by the resolved fluorophores is close to the noise variance. Simulation results demonstrated that MEC can reduce the

imaging time by a factor of five or more while retaining the same spatial resolution.

8590-34, Session 9

Nonlinear structured illumination microscopy with Surface Plasmon Resonance (SPR) enhanced Stimulated Emission Depletion (STED)

Han Zhang, The Univ. of Arizona (United States)

Nonlinear structured illumination microscopy (SIM) allows full-field imaging at resolutions <100 nm. Saturated (SSIM) and photoswitchable SIM had been demonstrated. We report a new nonlinear SIM technique that utilizes the full-field STED effect. Resolution and sensitivity simulation shows that STED-SIM may serve as a better alternative to SSIM and photoswitchable SIM.

To generate strong STED field at a large area, we use SPR enhancement of evanescence field near a dielectric-metal-dielectric interface. 10 times STED beam field enhancement is achieved on an optimized glass-silver-glass-water planar structure. We further use two SPR-enhanced STED fields propagating at opposite direction at the glass- water interface. Interference between two STED field generate a 1D structured STED field. Combined with a uniform excitation field, the structure STED field allows full field total internal reflection imaging with an enhanced resolution along the structured dimension. Resolution enhancement along the structured dimension is verified with on fluorescence beads of sub-diffraction-limit sizes.

A STED-SIM microscope with 2D structured STED field is under development. Future research will ally the microscope to image membrane resident or near membrane structure at super-resolution over time in live cells.

8590-35, Session 9

Fundamental limits to superresolution fluorescence microscopy

Alex Small, California State Polytechnic Univ., Pomona (United States)

Superresolution fluorescence microscopy techniques such as PALM, STORM, STED, and Structured Illumination Microscopy (SIM) enable imaging of live cells at nanometer resolution. The common theme in all of these techniques is that the diffraction limit is circumvented by controlling the states of fluorescent molecules. Although the samples are labeled very densely (i.e. with spacing much smaller than the Airy distance), not all of the molecules are emitting at the same time. Consequently, one does not encounter overlapping blurs. In the deterministic techniques (STED, SIM) the achievable resolution scales as the wavelength of light divided by the square root of the intensity of a beam used to control the fluorescent state. In the stochastic techniques (PALM, STORM), the achievable resolution scales as the wavelength of light divided by the square root of the number of photons collected. Although these limits arise from very different mechanisms (parabolic beam profiles for STED and SIM, statistics for PALM and STORM), in all cases the resolution scales inversely with the square root of a measure of the number of photons used in the experiment.

We have developed a proof that this relationship between resolution and photon count is universal to techniques that control the states of fluorophores using classical light. Our proof encompasses linear and nonlinear optics, as well as computational post-processing techniques for extracting information beyond the diffraction limit. If there are techniques that can achieve a more efficient relationship between resolution and photon count, those techniques will require light exhibiting non-classical correlations.

8590-36, Session PSUN

Pushing the boundaries of single molecule detection

Marcelle König, Steffen Ruettinger, Sebastian Tannert, Thomas Schönau, PicoQuant GmbH (Germany); Olaf Schulz, Arizona State Univ. (United States); Michael Wahl, Marcus Sackrow, Kristian Lauritsen, Felix Koberling, PicoQuant GmbH (Germany); Robert Ros, Arizona State Univ. (United States); Rainer Erdmann, PicoQuant GmbH (Germany)

Single molecule based techniques made their way from the early idea to overcome ensemble averaging via studies of biological dynamics and conformations, towards DNA sequencing and ultra high-resolution imaging. Most of these experiments were typically carried out with confocal or widefield microscopes in the visible wavelength region. Here we present new modalities to shift the single molecule detection into the UV and to improve the single molecule localisation by an AFM based nanomanipulation.

Confocal microscopy with 266nm excitation: Driven by the idea to access the intrinsic fluorescence of tryptophan-containing proteins we will show as a first benchmark FCS with organic fluorophores in the deep UV. Also label-free Fluorescence Lifetime Imaging (FLIM) with biological cells becomes feasible where the aromatic amino acids within the proteins become visible.

Combination of time-resolved fluorescence detection with Atomic Force Microscopy (AFM): The open architecture of the MicroTime 200 microscope allows for the integration of sample-scanning AFMs from selected manufacturers. The precise coalignment of the confocal observation volume with the AFM tip and the straightforward synchronization of the Time-Correlated Single Photon Counting (TCSPC) detection with the AFM scanning allows to obtain simultaneously fluorescence and AFM images.

Integration of a new hybrid PMT (PMA Hybrid): For VIS measurements, we report on the integration of the PMA Hybrid and highlight in a comparison with actual SPAD type detectors some of its unique properties for single molecule applications concerning e.g. sensitivity, timing performance and afterpulsing behaviour.

8590-37, Session PSUN

Issues in the benchmarking of image analysis algorithms for superresolution microscopy

Shane P. Stahlheber, Alex Small, California State Polytechnic Univ., Pomona (United States)

Superresolution localization microscopy requires accurate and precise localization algorithms. We have developed a plugin for ImageJ, called M2LE, which can localize molecules quickly and distinguish between single-molecule and multiple-molecule images using a shape test that requires only a single iteration. Localization is accomplished via a fast maximum-likelihood algorithm that uses the separable property of the Gaussian to independently fit two 1-D Gaussians along the x- and y-directions. To assess the performance of M2LE, we tested the plugin with realistic simulated images of single and multiple molecule images. We first found the optimal shape test parameters that accept most single-molecule images, and then the optimal signal-to-noise cutoff parameter for identifying potential molecules from noise. These two parameters have the greatest impact on what parts of the image go on to be analyzed. Using these optimal parameters, we then assessed (1) the tendency of the algorithm to find molecules from the tail of a point-spread function in high signal-to-noise cases, (2) the effects of regions-of-interest size and overlap tolerances, (3) the ability of shape tests to identify multi-molecule images as a function of molecular separation and ratio of photon counts from two molecules, and (4) the performance of the entire process--the number of molecules identified and their corresponding localization precision and accuracy. These methods and results can be used to identify the optimal M2LE parameters to

use for experiments, as well as to compare the performance with other localization microscopy software.

8590-38, Session PSUN

Surface plasmon enhanced spatially activated fluorescence imaging based on optical nanoapertures for super-resolution microscopy

Wonju Lee, Youngjin Oh, Kyujung Kim, Donghyun Kim, Yonsei Univ. (Korea, Republic of)

Surface plasmons (SPs) are longitudinal coherent oscillations of electrons at dielectric-metal interface. Evanescent electromagnetic field associated with SP exponentially decays in amplitude within typically 100 nm from the surface under total internal reflection (TIR) condition. By using subwavelength optical nanoapertures, electromagnetic near-field can be spatially modified, creating locally amplified hot spots in the evanescent region. These hot spots have been used for SP resonance (SPR) biosensors to detect bio-molecular interactions and can also be useful for breaking Abbe's diffraction limit of conventional microscopy based on the enhancement of fluorescence signals for plasmon-enhanced TIR fluorescence (TIRF) imaging techniques.

In this paper, we investigate spatially activated SP-enhanced fluorescence imaging based on periodic optical nanoapertures for sub-diffraction limited super-resolution microscopy. We have explored switching light incidence conditions to obtain varied local hot spots at nanoaperture surface and also studied the effect of the shape and other geometrical parameters of nanoapertures on the spatial activation of fluorescence. We have analyzed spatial activation of fluorescence based on two- and four-channel switching of light incidence at gold nanogratings and nanoposts with dimensions of 100-200 nm. The resolution of spatially activated fluorescence microscopy was demonstrated to be under 100 nm and can be further reduced by increasing the number of channels.

8590-39, Session PSUN

Molecular modeling of the Förster resonance energy transfer between FusionRed and Dedushka fluorescent proteins

Maria G. Khrenova, Lomonosov Moscow State Univ. (Russian Federation) and A.N. Bach Institute of Biochemistry (Russian Federation); Alexander S. Goryashenko, A.N. Bach Institute of Biochemistry (Russian Federation) and Lomonosov Moscow State Univ. (Russian Federation); Alexander V. Nemukhin, Lomonosov Moscow State Univ. (Russian Federation); Alexander P. Savitsky, A.N. Bach Institute of Biochemistry (Russian Federation)

Förster resonance energy transfer (FRET) is a powerful tool to investigate biochemical and biophysical processes in vitro and in vivo. We present the computational study of a novel FRET system, namely, a fuse protein that is composed of two far-red fluorescent proteins FusionRed and Dedushka joined with a linker. The latter contains a tetrapeptide DEVD motif which can be specifically cleaved by caspase-3. FusionRed acts as an energy donor and Dedushka as an energy acceptor in this pair. We carried out the comprehensive study of the factors that influence FRET efficiency, including, in particular, distances between donor and acceptor, as well as relative orientations of transition dipole moments from donor to acceptor. We started from the primary structure of the proteins and also used available data on the similar ?-barrels to construct the full-atom 3D structure. At the first stage, we used a protein-protein docking procedure to construct the tetramer structure of the fuse protein. Next, we performed molecular dynamics simulation for the best candidates proposed by molecular docking. Finally, we used combined quantum mechanics / molecular mechanics approaches to find equilibrium geometry configurations for FusionRed at the first excited potential energy surface and Dedushka at the ground state potential energy surface and to calculate transition dipole moments. Combining these results with the experimentally available information on the overlap of the absorption spectrum of Dedushka and emission spectrum of FusionRed we report the distribution of conformations and characteristic lifetimes in this FRET system.

8590-41, Session PSUN

Total internal reflection fluorescence correlation spectroscopy with structured light illumination using a digital micromirror device

Jong-Ryul Choi, Taewoong Lee, Donghyun Kim, Yonsei Univ. (Korea, Republic of)

Fluorescence correlation spectroscopy (FCS) provides valuable dynamic information of molecular interactions based on the correlation analysis of fluorescent intensity fluctuations in biological and chemical processes. While typical FCS detection uses confocal measurement, it has a disadvantage of low spatial resolution limited by the size of a laser beam waist which is bounded by diffraction limit. One of the methods to reduce the imaging volume in FCS is to perform FCS under total internal reflection fluorescence (TIF) condition. Such TIR-FCS uses an evanescent field, which is only 50 to 100 nm in axial depths, in which fluorescent fluctuation is excited, so the imaging volume is axially sub-diffraction limited with a decrease that is three times or larger than that of confocal FCS. In this presentation, we describe further reduction of imaging volume with structured light illumination using a digital micromirror device (DMD). A DMD consists of pixelated micromirrors that can be controllable between on and off-state. To employ a DMD in the illumination part of TIR-FCS, spatially modulated light with de-magnifications was illuminated to samples. Samples are designed with nanostructures, which if individually illuminated, can excite subwavelength plasmonic hot spots. Since imaging volume is mainly determined by the dimensions of the hot spots, significant volume reduction can be feasible. In this proof-of-concept study, we have confirmed that spatially modulated illumination by a DMD can create light modulation patterns to produce excite individual near-field distribution associated with designed nanostructures. Assessment of the concept in TIR-FCS is also discussed.

8590-42, Session PSUN

Two-color CW STED nanoscopy

Yujia Liu, Shanghai Jiao Tong Univ. (China); Eric Alonas, Philip J. Santangelo, Georgia Institute of Technology (United States); Dayong Jin, James A. Piper, Macquarie Univ. (Australia); Qiushi Ren, Peng Xi, Peking Univ. (China)

Fluorescent microscopy has become an essential tool to studybiological molecules, pathways and events in living cells, tissuesand animals. Meanwhile even the most advanced confocal microscopy can only yield optical resolution approaching Abbe diffraction limit of ~200 nm. This is still larger than many subcellular structures, which are too small to be resolved in detail.Theselimitations have driven the development of super-resolution opticalimaging methodologies over the past decade.

In stimulated emission depletion (STED) microscopy, the excitation focus is overlapped by an intense doughnut-shaped spotto instantly de-excitemarkers from their fluorescent state to the ground stateby stimulated emission. This effectively eliminates the periphery of the Point Spread Function (PSF), resulting in a narrower focal region, or super-resolution. Scanning a sharpened spot through the specimen renders images with sub-diffraction resolution. Multi-color STED imaging can present important structural and functional information for protein-protein interaction.

In this work, we presenteda dual color, synchronization-free STED

microscopy with a Ti:Sapphire oscillator. The excitation wavelengths were 532nm and 635nm, respectively. With pump power of 4.6 W and sample irradiance of 310 mW, we achieved super-resolution as high as 71 nm. A series of biological specimens were imaged with our dual-color STED.

8590-43, Session PSUN

STED microscopy with nano-axial resolution

Siddharth Sivankutty, Institut des Sciences Moléculaires d'Orsay (France); Thomas Barroca, Institut Langevin (France); Guillaume Dupuis, Le Ctr. de Photonique BioMedicale (France); Christophe Lefumeux, Institut des Sciences Moléculaires d'Orsay (France); Céline Mayet, Le Ctr. de Photonique BioMedicale (France); Arnaud Dubois, Lab. Charles Fabry (France); Catherine K. Marquér, Ctr. de Recherche de l'Institut du Cerveau et de la Moelle (France); Sandrine Lécart, Le Ctr. de Photonique BioMedicale (France); Marie-Claude Potier, Ctr. de Recherche de l'Institut du Cerveau et de la Moelle (France); Emmanuel Fort, Institut Langevin (France); Sandrine Lévêque-Fort, Institut des Sciences Moléculaires d'Orsay (France)

Monitoring cells structures and dynamical events occurring at the membrane is crucial to understand numerous cell mechanisms. To achieve this selectivity both lateral and axial resolution needs substantial improvements. Recent developments in super-resolution microscopies, like Stimulated Emission Depletion (STED) microscopy, provide lateral resolution well below the diffraction limit. However, the performances on axial resolution are less impressive and require additional complex developments. Combining STED with Total Internal Reflection Fluorescence (TIRF) microscopy has recently been proposed to achieve both high axial confinement and a non diffraction-limited lateral resolution. Here, we propose an alternative technique to improve significantly the axial resolution close to the glass interface, by combining STED microscopy with fluorescence emission filtering. These two complementary techniques associate the performances of both excitation and collection engineering.

Moreover, by taking advantage of the amount of fluorescence emitted at supercritical angles it is possible to evaluate the distance between the fluorophores and the glass interface. This approach allows one to retrieve additional axial information at the nanometric scale. We will present the current state of development and first biological results of this new supercritical STED microscope.

8591-1, Session 1

Polarimetric glucose sensing in vitro: a high frequency approach to improving signal-to-noise ratio

Casey W. Pirnstill, Daniel T. Grunden, Gerard L. Coté, Texas A&M Univ. (United States)

Diabetes affects millions of people worldwide annually. Current blood finger-stick methods for glucose sensing are invasive and can be painful which often leads to poor patient compliance. Recently, using optical polarimetry as a method to monitor glucose levels in the aqueous humor has shown promise as a way to noninvasively ascertain blood glucose concentration. One of the major limiting factors to optical polarimetric approaches for glucose monitoring is time varying birefringence due to motion artifact. The presence of this birefringence confounds the optical activity due to glucose and must be accounted for in order to accurately predict glucose levels in the anterior chamber of the eye. Several optical polarimeters used for glucose monitoring consist of separate air-core Faraday rotator (FR) elements for both modulation and compensation. This air-core FR approach has been limited to low modulation frequencies of roughly 1kHz and the use of two devices for modulation and DC-compensation. In this report, we present a modulation approach for real-time closed-loop polarimetry that is capable of glucose monitoring in vitro at optical modulation frequencies of tens of kHz that includes the DC-compensation in a single device. To achieve this, a single high permeability ferrite based magneto-optic modulation device was designed, built, and tested. The new polarimetric design, setup, and in vitro glucose measurements will be presented demonstrating the sensitivity and accuracy of the system at these higher frequencies. Such higher frequency modulation has the potential benefit of improving the signal-to-noise ratio of the system in the presence of motion artifacts.

8591-2, Session 1

The development of an integrated Faraday modulator and compensator design for continuous polarimetric glucose monitoring

Brandon W. Clarke, Brent D. Cameron, The Univ. of Toledo (United States)

In recent years, significant advances have been made in the development of noninvasive polarimetric glucose detection systems, salutary for the treatment of our rapidly increasing diabetic population. This area of research utilizes the aqueous humor as the detection medium for its strong correlation to blood glucose concentration and highlights three major features: the optical activity of glucose, minimal scattering of the medium, and the ability to detect sub-millidegree rotation in polarized light. However, many of the current polarimetric systems are faced with size constraints based on the paramount optical components. As a step toward developing a low cost hand-held design, our group has designed a miniaturized integrated single-crystal Faraday modulator/compensator. This device is capable of replacing the traditional two component arrangement that has been widely reported on in many Faraday-based polarimetric configurations. In this study, the newly designed prototype is compared with a theoretical model and its performance is evaluated experimentally under both noninvasive static and dynamic glucose monitoring conditions. The combined rotator can achieve modulation depths above 1°, and when operating in a compensated closed-loop configuration, it has demonstrated glucose prediction errors of 3 mg/dL and 8 mg/dL under hypoglycemic and hyperglycemic conditions, respectively. These results demonstrate that such an integrated design can perform similar if not better than its larger two-part predecessors. This technology could also be extended to facilitate the use of multispectral polarimetry by considerably reducing the required number of physical components. Such multispectral techniques have demonstrated usefulness for in vivo and multi-analyte noninvasive sensing.

8591-3, Session 1

Limitations of current fluorescent glucose sensing assays based on competitive binding

Brian M. Cummins, Javier T. Garza, Gerard L. Coté, Texas A&M Univ. (United States)

Diabetes Mellitus is a disease that is characterized by the body's inability to regulate blood glucose concentrations. Its management requires the frequent monitoring of blood-glucose levels, and innovative optical approaches are being investigated to maximize patient compliance. Fluorescent sensing assays serve as one of these techniques, using light to obtain glucose concentrations once embedded within the dermal layers of tissue. Competitive binding chemistries using Concanavalin A and various competing ligands are being engineered to have different fluorescent properties when they are bound together. The degree this complex forms can be designed to vary with physiological glucose concentration, making the chemistry's collective fluorescence dependent on glucose concentration. However, to date these assays have been plagued by either low sensitivity or low reversibility for what many have believed to be an inherent attribute of the protein.

In this report, we explore the apparent trade-off between the sensitivity and reversibility in fluorescent competitive binding assays that use multivalent competing ligands. As chelation between multivalent molecules has been shown to increase the perceived affinity via the 'glycoside cluster effect,' we determine the affinity between multivalent assay components for varying degrees of chelation and show fluorescent glucose responses for aggregative systems. These responses display a hysteresis-like effect that introduces significant error and subsequently explain the aforementioned tradeoff no matter the optical approach. Considering these findings, we will discuss an alternative competing ligand approach coupled with Forster Resonance Energy Transfer that could offer improvement to the sensitivity and reversibility of such sensors.

8591-4, Session 1

Enzymatic glucose sensor compensation for variations in ambient oxygen concentration

Bradley B. Collier, Texas A&M Univ. (United States); Michael J. McShane, Texas A&M Univ. (United States) and Texas A&M Univ. (United States)

Due to the increasing prevalence of diabetes, research toward painless glucose sensing continues. Oxygen sensitive phosphors with glucose oxidase (GOx) can be used to determine glucose levels indirectly by monitoring oxygen consumption. This is an attractive combination because of its speed and specificity. Packaging these molecules together in "smart materials" for implantation will enable non-invasive glucose monitoring. As glucose levels increase, oxygen levels decrease; consequently, the luminescence intensity and lifetime of the phosphor increase. Although the response of the sensor is dependent on glucose concentration, the ambient oxygen concentration also plays a key role. This could lead to inaccurate glucose readings and increase the risk of hyper- or hypoglycemia. To mitigate this risk, the dependence of microparticle glucose sensor response on oxygen levels was investigated and compensation methods explored. Sensors were calibrated at different oxygen concentrations using a single generic logistic equation, such that trends in oxygen dependence were determined as varying parameters in the equation. Each parameter was found to be a function of oxygen concentration, such that the correct glucose calibration

equation can be calculated if the oxygen level is known. Accuracy of compensation will be determined by developing an overall calibration, using both glucose and oxygen sensors in parallel, correcting for oxygen fluctuations in real time by intentionally varying oxygen, and calculating the error in actual and predicted glucose levels. While this method was developed for compensation of enzymatic glucose sensors, in principle it can also be implemented with other kinds of sensors utilizing oxidases.

8591-6, Session 2

Non-invasive measurement of blood and tissue parameters based on VIS-NIR spectroscopy

Jens Kraitl, Ulrich Timm, Univ. Rostock (Germany); Axel Kulcke, Senspec GmbH (Germany); Hartmut Ewald, Univ. Rostock (Germany)

Currently, invasive methods are used to measure the hemoglobin concentration and the most hemoglobin-derivatives, whereby blood is taken from the patient and subsequently analyzed. The noninvasive method presented here allows pain free continuous on-line patient monitoring with minimum risk of infection and facilitates real time data monitoring allowing immediate clinical reaction to the measured data. Visible and near infrared (VIS-NIR) spectroscopy in combination with the photo-plethysmography (PPG) is used for a detection of human tissue properties and the measurement of hemoglobin concentration in whole blood and the hemoglobin derivatives. The absorption, scattering and the anisotropy of blood and tissue is a function of the irradiated wavelengths. This fact is used to calculate the optical absorbability characteristics of blood and tissue which is yielding information about blood components like hemoglobin-concentration (cHb), carboxy-hemoglobin (CoHb), met-hemoglobin (MetHb) and arterial oxygen saturation (SaO2). The measurement is based on a new developed Micro-Spectrometer with a broadband Micro-LED as transmitter. The new Spectrometer-Sensor is implemented in special finger clip housing and is measuring the tissue and blood spectra with a high time- and frequency-resolution. The ratio between the PPG peak to peak pulse amplitudes for each wavelength is used in combination with a dynamic spectrum extraction. The prediction of the blood- and tissue-parameters is based on a Principal Component Regression (PCR) method. The non-invasive sensor system is calibrated with a lab based artificial blood circulatory system and with data from clinical studies during dialyses sessions.

8591-7, Session 2

Optical modeling toward optimizing monitoring of intestinal perfusion in trauma patients

Tony J. Akl, Texas A&M Univ. (United States); Mark A. Wilson M.D., Univ. of Pittsburgh (United States) and VA Pittsburgh Healthcare System (United States); Milton N. Ericson, Oak Ridge National Lab. (United States); Gerard L. Coté, Texas A&M Univ. (United States)

Trauma is the number one cause of death for people under the age of 44 in the United States. In addition, according to the Centers of Disease Control and Prevention, injury results in over 31 million emergency department visits annually. Minimizing the resuscitation period in major abdominal injuries increases survival rates by correcting impaired tissue oxygen delivery. Optimization of resuscitation requires a monitoring method to determine sufficient tissue oxygenation. Oxygenation can be assessed by determining the adequacy of tissue perfusion. In this work, we present the design of a wireless perfusion and oxygenation sensor based on photoplethysmography. Through optical modeling, the benefit of using the visible wavelengths 470, 525 and 630nm (around the 525nm hemoglobin isobestic point) for intestinal perfusion monitoring is compared to the typical near infrared (NIR) wavelengths (805nm isobestic point) used in such sensors. Specifically, it is demonstrated that NIR wavelengths penetrate through the thin intestinal wall (~4mm) leading to high background signals. However, these visible wavelengths have three times shorter penetration depth. Monte-Carlo simulations show that the transmittance of the three selected wavelengths is lower by 1 to 5 orders of magnitude depending on the perfusion state. Due to the high absorbance of hemoglobin in the visible range, the perfusion signal carried by diffusely reflected light is also enhanced by an order of magnitude while oxygenation signal levels are maintained the same. In addition, short source-detector separations (2 to 3mm) proved to be beneficial for limiting the probing depth to the thickness of the intestinal wall.

8591-8, Session 2

Effects of local cold spray on subcutaneous and intramuscular blood flow and oxygenation

Babak Shadgan M.D., W. Darlene Reid, The Univ. of British Columbia (Canada)

Topical cold spray (CS) is one of the most common Cryotherapy modalities in sports medicine and rehabilitation that is individually used to control pain and soft tissue inflammation in acute musculoskeletal injuries. It is believed that CS relieves pain, inflammation, swelling and muscle spasm following acute soft tissue trauma by freezing soft tissue and reducing local blood flow. It is while the evidence to support this theory has been highly controversial and unconvincing. Furthermore, it remains unclear whether the physiological effects of CS on reducing local blood flow are only limited to the subcutaneous layers or can be extended to the intramuscular level too. The purpose of this study was to investigate the effects of CB on subcutaneous and intramuscular blood flow using near infrared spectroscopy (NIRS), a noninvasive optical method that monitors changes in local tissue hemodynamics and oxygenation. Using a two-channel continuous-wave NIRS device changes in oxygenated (O2Hb), deoxygenated (HHb) and total hemoglobin (tHb) at two depths of 10 and 25 mm over the vastus medialis muscle in 12 adult healthy subjects were monitored before and after applying cold spray. Significant decrease in subcutaneous tHb and HHb started after 30 seconds of CS application and lasted for two minutes ($P<0.05$). Changes in intramuscular tHb, HHb and O2Hb were not significant at any time after CS. This study suggests that physiological effects of CS on reducing local blood flow and tissue oxygenation are superficial and transient.

8591-9, Session 2

Portable multiwavelength frequency-domain diffuse optical instrument

Keunsik No, Bruce J. Tromberg, Albert E. Cerussi, Beckman Laser Institute and Medical Clinic (United States)

Frequency domain photon migration (FDPM) methods can perform non-invasive, measurements of tissue hemoglobin concentrations and oxygenation states. Tissue optical properties (absorption coefficient ?a and reduced scattering coefficient, ?s') can be measured independently by measuring the phase and amplitude of diffusive photon density waves. There are a variety of FDPM instruments that feature a wide array of spectral, temporal and spatial information content. We have constructed a second-generation board-based FDPM instrument that has four laser diodes (660, 690, 785, and 830nms) that are intensity-modulated at frequencies ranging from 50 to 500MHz. The device is stand alone unit, with a built-in Avalanche Photo Diode (APD) module that can be fiber coupled or the unit can be used with an external APD placed on the tissue for the recovery of deeper tissue signals. An optical probe and computer are all that are needed to acquire data. The unit can also be coupled with continuous-wave broadband source/detectors to amplify the spectral content, and multiple units can be linked together to amplify

the spatial information content.

We have tested this new design in a series of tissue-simulating phantoms and compared them with our established FDPM devices that are being tested in a national clinical trial. The device is further tested in measuring pulsatile signals from the finger, with full recovery of tissue absorption and scattering several times within the pulse period. This self-contained portable system can measure tissue oxygenated and deoxygenated hemoglobin concentrations and the fast measurement capability can be used for exploring new applications.

8591-10, Session 3

The study of esophageal cancer in an early stage by using Raman spectroscopy

Mika Ishigaki, Akinori Taketani, Yasuhiro Maeda, Bibin B. Andriana, Kwansei Gakuin Univ. (Japan); Ryu Ishihara, Osaka Medical Ctr. for Cancer and Cardiovascular Diseases (Japan); Hidetoshi Sato, Kwansei Gakuin Univ. (Japan)

The esophageal cancer is a disease with a high mortality. In order to lead a higher survival rate after the treatment, it is expected to develop a new method to diagnose the early stage cancer and to support the therapy during the treatment. Raman spectroscopy is one of the powerful techniques for the purpose. It is possible to record information less-invasively of the molecular composition in the tissue without labeling. In the present study, we collect the Raman spectra from ex vivo esophageal tissue using a portable Raman system with a miniaturized Raman probe. The system consists of a 785nm diode laser, Raman spectrometer, CCD detector and miniaturized Raman probe. The Raman measurements are carried out before the histopathological examinations. The spectrum has strong background due to auto-fluorescence but characteristic bands are observed. The spectra are analyzed by chemometrics techniques to extract interesting information. In this report, the early esophageal cancer is analyzed to find out a characteristic changes to that of normal tissues, especially difference between the cancer and the benign tumor.

8591-11, Session 3

Label-free identification of single cell-derived vesicles by Raman microspectroscopy

Edwin van der Pol, Univ. van Amsterdam (Netherlands) and Academisch Medisch Ctr. (Netherlands); Chi M. Hau, Academisch Medisch Ctr. (Netherlands) and Univ. van Amsterdam (Netherlands); Aufried T. M. Lenferink, Univ. Twente (Netherlands); Auguste Sturk, Rienk Nieuwland, Academisch Medisch Ctr. (Netherlands) and Univ. van Amsterdam (Netherlands); Cornelis Otto, Univ. Twente (Netherlands); Ton G. van Leeuwen, Academisch Medisch Ctr. (Netherlands) and Univ. van Amsterdam (Netherlands)

Background: Human blood contains cell-derived vesicles, which are spherical particles enclosed by a phospholipid bilayer. These vesicles originate from blood cells, bone marrow cells, stem cells, and endothelial cells, and their function, origin, and composition is disease (state) dependent. Therefore, vesicles can be potentially used for prognosis, therapy, and biomarkers for disease. However, due to their small size (30 nm – 1 ?m), detection of vesicles is cumbersome. The cellular origin of vesicles is usually established by fluorescent antibody labeling, which is laborious, expensive, and involves practical problems. We have applied Raman microspectroscopy to distinguish normal vesicles from tumor-derived vesicles in solution without labeling.

Methods: Platelet and erythrocyte vesicles were isolated from blood bank concentrates and tumor-derived vesicles were isolated from a human pancreatic adenocarcinoma cell line. Vesicles were isolated using differential centrifugation and analyzed by transmission electron microscopy, resistive pulse sensing, and Raman microspectroscopy. For Raman microspectroscopy, a 100-mW krypton ion laser operating at a wavelength of 647 nm was focused to a probe volume of 1 fL, which overlaps with the dimension of vesicles. The Stokes shift from light scattered by optically trapped vesicles was measured using a spectrograph dispersing in the range 646–849 nm.

Results: The Raman spectra of single optically trapped vesicles showed spectral transitions characteristic of phospholipids. Erythrocyte vesicles exhibited more fluorescence compared to platelet vesicles, whereas tumor-derived vesicles showed additional Raman peaks compared to normal vesicles.

Conclusions: For the first time, single tumor-derived vesicles were distinguished from normal vesicles without labeling using Raman microspectroscopy.

8591-12, Session 3

Urinary tract infection (UTI) multi-bacteria multi-antibiotic testing using surface enhanced Raman spectroscopy (SERS)

Evdokia Kastanos, Univ. of Nicosia (Cyprus); Katerina Hadjigeorgiou, Costas Pitris, Univ. of Cyprus (Cyprus)

Bacterial resistance to antibiotics is a major health care problem mostly caused by the inappropriate use of antibiotics. At the root of the problem lies the current method for determination of bacterial susceptibility to antibiotics which requires overnight cultures. Physicians suspecting a bacterial infection usually prescribe an antibiotic without waiting for the antibiogram results. This practice aggravates the problem of bacterial resistance. In this work, a rapid method of diagnosis and antibiogram for a bacterial infection was developed using Surface Enhanced Raman Spectroscopy and silver nanoparticles. For antibiotic sensitivity testing, SERS spectra of five species of gram negative bacteria, namely Escherichia coli, Proteus spp., Klebsiella spp., Enterobacter spp., and Citrobacter spp. were obtained after a 4 hour exposure to the following antibiotics: amoxicillin, amoxicillin/clavulanic acid, ciprofloxacin, cefaclor, cefuroxime, ceftriaxone, cefazoline, amikacin and gentamycin. Spectral analysis revealed clear separation between bacterial samples exposed to antibiotics to which they were sensitive and samples exposed to antibiotics to which they were resistant. SERS was also used to determine the concentration of a bacterial culture. SERS spectra of serial dilutions of various gram negative bacteria (103-108 cells/ml), isolated from urine cultures, showed a linear correlation between spectral intensity and concentration. With the enhancement provided by SERS, the technique can be applied directly to urine or blood samples, bypassing the need for overnight cultures. This technology can become the basis for the development of rapid methods of diagnosis and antibiogram for a variety of bacterial infections.

8591-13, Session 3

Cholesterol accumulation in the cornea and in the aorta: imaging using europium chlortetracycline complex fluorescent probe

Lilia C. Courrol, Univ. Federal de São Paulo (Brazil); Leticia B. Sicchieri, Instituto de Pesquisas Energéticas e Nucleares (Brazil); Daliane C. Silva, Univ. Federal de São Paulo (Brazil)

The Europium-Chlortetracycline complex (EuCTc) presents interesting optical properties, such as absorption around 400 nm and a large Stokes shift that originates an emission around 615 nm with a fluorescent lifetime of a few microseconds, which differs from the lifetimes of biological tissues.With the addition of small amounts of low density lipoproteins (LDL) there is an increase in the Europium emission intensity at 615 nm in solutions with neutral pH. The europium complex EuCTc-LDL emission lifetime increases to 50 microseconds due to a reduction in the luminescence quenching by energy transfer. The EuCTc complex is easily synthesized, operates at neutral pH, has high stability and low cost. Such

characteristics provide high sensitivity and specificity in the detection of LDL. Low-density lipoproteins (LDL) are atherogenic and represent a high cardiovascular risk factor. LDL in its modified form contributes to inflammation as well as to macrophages evolution to foam cells. Our main challenge is to test if the method of LDL quantification, using the probe europium Chlortetracycline, is valid in tissue. For this purpose, the cornea and aorta fluorescence analysis of rabbits subjected to high-cholesterol diets was performed by fluorescence microscopy and by using the EuCTc complex as fluorescent probe, following the development of the hypercholesterolemia framework. Cholesterol deposition in the peripheral cornea and vessel wall are also similar in that deposition is accelerated in both tissues by elevated levels of atherogenic lipoproteins such as low density lipoproteins (LDL). Arcus and atherosclerotic coronary artery disease increase with high-cholesterol diets. Determining the origin of this lipid is helpful to learning why this lipid accumulates and also how this lipid may accelerate atherosclerosis.

8591-14, Session 3

Application of optical methods for characterizing the vascular structure in psoriasis patients

Jürgen M. Lademann, Charité Universitätsmedizin Berlin (Germany); Rami Archid, Charité Universitätsmedizin Berlin (Germany) and Univ. Tübingen (Germany); Bernhard Kleffner, Fraunhofer Institut für Biomedizinische Technik (Germany); Robert M. Lemor, Ctr. de Recherche Public Henri Tudor (Luxembourg) and Kibero GmbH (Germany); Katharina Ossadnik, Wolfram Sterry, Alexa Patzelt M.D., Charité Universitätsmedizin Berlin (Germany)

Psoriasis is a common disease worldwide. As all systemically and topically applied drugs may entail severe side effects, efforts are made to reduce the application period of these drugs to minimize them. Consequently, psoriasis is treated only until the skin surface appears healthy again. Using in vivo laser scanning microscopy and opto-acoustic imaging it could be shown that even if the skin surface appears cured, the pathological status of the underlying vascular structure can still exist. While healthy capillaries exhibit a single-loop structure, the structure of pathological capillary vessels shows double or triple loops. If therapy is discontinued as soon as the skin surface appears healthy, although the condition of the underlying vascular structure is still pathological, recurrences will occur soon. Using an in vivo laser scanning microscope in reflection mode at 830nm wavelength, the changes of the pathological capillary vessels until complete healing were visualized up to a tissue depth of 150µm.

Opto-acoustic methods provide non-invasive anatomical and functional images in a clinical setting. In opto-acoustic mode, signals are generated by absorption of laser pulses of 532nm. Due to the high absorption coefficient of hemoglobin in this spectral range, cutaneous blood vessels can be investigated up to a depth of 2mm below the skin surface. These non-invasive opto-acoustic measurements are far better suited to characterize human vascular structures in vivo.

8591-15, Session 4

A novel optical thromboelastography (OTEG) for coagulopathy assessment

Markandey M. Tripathi, Seemantini K. Nadkarni, Harvard Medical School (United States) and Massachusetts General Hospital (United States)

Coagulopathies are closely associated with increased mortality and hospital length of stay following acute trauma, illness, and surgery. Point-of-care (POC) devices for coagulation assessment are critical in guiding and monitoring hemostasis therapy, and determining therapeutic end-points. Devices such as, thromboelastography (TEG) and rotational thromboelastometry (ROTEM) have been developed that involve mechanically stirring blood and measuring changes in clot stiffness during coagulation. The large size and requirement for specialized operators have limited the utility of these devices for POC diagnosis. Here we present a novel approach, termed Optical Thromboelastography (OTEG) to measure the coagulation status of blood in real-time at the POC.

In OTEG, an imaging chamber containing small amount of blood sample is illuminated by a laser light (690 nm, 4 mW). Time-varying speckle pattern is captured at a frame rate of 400 fps using a high-speed CMOS camera. During coagulation, changes in the viscoelastic properties of the clot restrict the Brownian motion of the scattering particles altering the rate of speckle modulations in the captured speckle pattern. Hence, the time varying changes in clot stiffness can be measured by relating the rate of speckle fluctuations with the viscoelastic properties of the sample using dynamic light scattering techniques. Samples (N=10) of normal and hypocoagulable human blood were measured using OTEG and compared with clinical findings (INR, aPTT, and TEG measurements). The OTEG measurements showstrong correlation with the clinical measurements ($R = 0.86$, $P < 0.001$). These results demonstrate the potential of OTEG for accurate assessment of the coagulopathies.

8591-16, Session 4

Sensing cocaine in saliva with infrared laser spectroscopy

Kerstin M. C. Hans, Michele Gianella, Matthias Müller, ETH Zurich (Switzerland); Philip Wägli, Joab Di Francesco, Ecole Polytechnique Fédérale de Lausanne (Switzerland); Markus W. Sigrist, ETH Zurich (Switzerland)

If the police stops a car due to the suspicion of driving under the influence of drugs (DUID) like cocaine, the initial screening method is usually based on the analysis of urine or saliva with the help of immunoassays. However, despite their sufficient sensitivity, most of these tests do not yield quantitative data and a second blood test is thus necessary to confirm positive results. As an alternative approach for an on-the-road-side test we propose a sensing device based on infrared laser spectroscopy. Initial broadband studies with an FTIR spectrometer combined with total attenuated reflection (ATR) demonstrated that the preferred spectral region for detecting cocaine occurs around 1750 cm-1 where cocaine exhibits strong absorption peaks with least spectral interferences from potential diluents, masking substances (such as mouthwash), medicine, common soft drinks, caffeine, alcohol and saliva itself [1]. However, since water exhibits a strong background absorption, we developed a simple one-step method to efficiently extract cocaine from saliva into a weakly absorbing diluent. Using a CW quantum cascade laser (QCL) at 1750 cm-1 as light source and either ATR or transmission spectroscopy with a specially developed cell with a pathlength of 5 mm and volume of only ~1.5 ml we achieved a detection limit of ≤ 1 ?g/ml. Since our extraction scheme is also feasible with microfluidics we currently implement a microfluidic chip and waveguides to further lower the sample volume and the detection threshold to the required limit of ~20 ng/ml. First results of this novel sensor will be presented.

[1] K. M.-C. Hans, S. Müller and M.W. Sigrist: Drug Testing and Analysis, 4: 420-429, (2012)

8591-17, Session 4

NANODEM and CAREMAN European projects: continuous therapeutic drug monitoring and sepsis monitoring using the POCT format

Francesco Baldini, Ambra Giannetti, Cosimo Trono, Istituto di Fisica Applicata Nello Carrara (Italy)

CARE-MAN (HealthCARE by Biosensor Measurements And Networking) is an European project ended in April 2011 finalised to the development of a diagnostic POCT device for the multi parameter detection of analytes of clinical interests defined by doctors. In particular a fluorescence-based stand-alone platform was developed for the detection of bioanalytes for sepsis diagnosis. The heart of the platform is a plastic 13-microchannel chip carrying the necessary chemistry for the implementation of the assay on its surface. Both sandwich and competitive assays were implemented for the determination of procalcitonin (PCT), C-reactive protein (CRP) and neopterin. Limit of detections of 0.8 ?g L-1, 2 ?g L-1 and 0.3 ?g L-1 were achieved for CRP, PCT and neopterin, respectively.

NANODEM (Nanophotonic device for multiple therapeutic drug monitoring) is a starting STREP project, with the aim of developing a novel therapeutic drug monitoring point-of-care-testing device for the measurement of immunosuppressants and related metabolites in transplanted patients. The new device will allow the measurements of therapeutic drugs and metabolites characterized by a narrow therapeutic range and serious potential side effects. Clinical benefit will be an optimized dosage of the respective therapeutical drug. The patient will be connected to the device by an intravenous microdialysis catheter to allow 48-h online measurements. Based on this minimally-invasive approach, the therapeutic drugs and related metabolites will be monitored at short time intervals.

8591-18, Session 4

Developing point of care microarray fluidics using stressed polystyrene

Matthew A. Coleman, Lawrence Livermore National Lab. (United States) and Univ. of California, Davis (United States); Ehson M. Ghandehri, Dennis L. Matthews, Univ. of California, Davis (United States); Jane P. Bearinger, Corporos Inc. (United States); Eric Douss, Lawrence Livermore National Lab. (United States)

The potential of portable, disposable, and inexpensive devices capable of quantitative and sensitive molecular diagnostics in Point-of-Care (PoC) settings has drawn the attention of many researchers. Conventional clean-room fabrication strategies have been widely used for PoC chip fabrication, but reducing device cost necessitates incorporating novel materials and fabrication techniques. Pre-stressed Polystyrene (PS) material has been successfully used for fabricating low-cost, functional PoC microfluidic devices. In this research, we demonstrate that PS chips were adaptable templates for multiple biodetection formats. First, we constructed a PS immunoassay for detecting the standard curve of C-reactive protein (CRP), with a dynamic range of 2 ?g/mL- 2 mg/mL concentration (3 logs) and detection limit of 2.5 ?g/mL. These results were compared to the CRP detection on conventional aminosilanated glass, and the results showed a correlation of 76±3%. Second, we designed and constructed a four-inch lateral flow device by embedding standard conjugated and detection pads for CRP into a PS microchip. The device was capable of detecting CRP along with an IgG control molecule. Third, the PS chip surface was used in a combination with a cell-phone camera for fluorescent-based detection. This was demonstrated by surface spotting IgG-flour, BSA-biotin, and IgG-Cy3 biomolecules. The fluorescence signals were detectable and comparable to a commercial scanner. Finally, we printed electrical circuits on top of PS surfaces using electrically conductive inks. Combined, our approach to prefab, detection, and prototyping is an effective process for building inexpensive PoC microdevices capable of quantitative and sensitive molecular diagnostics.

8591-19, Session 4

A cellphone-based polarizing microscope for in-vitro detection of the malaria-pigment

Itay Remer, Alberto Bilenca, Ben-Gurion Univ. of the Negev (Israel)

Malaria is an infectious disease caused by parasites (transmitted by mosquitoes) that invade host liver cells and red blood cells. More than one billion people are at risk for malaria worldwide, and an estimated one million deaths occur annually. Conventional Giemsa microscopy of blood samples is the current gold standard for the diagnosis of malaria, but it requires phlebotomy, clinical laboratory infrastructures and trained technicians, which are rare in most regions where malaria occurs. The need for point-of-care diagnostic tests for malaria has led to the development of rapid diagnostic tests of finger-prick blood. These tests are simple, but are invasive and use antibody-labeled strips which tend to degrade in the tropics where malaria is endemic. It is therefore imperative to develop inexpensive, portable and easy-to-use devices that can diagnose malaria noninvasively and accurately in field settings.

In this talk, we present the development of a polarizing microscope based on a standard camera cellphone to detect beta-hematin crystals (a synthesized analog of hemozoin - the malaria pigment) in transparent and scattering media. The microscope was used in transmission-mode to image various concentrations of beta-hematin in PBS and Intralipid solutions at 30 frames/sec. The results show that beta-hematin concentrations as low as 1 ?g/ml were detectable in samples with mu_s'l=1, thus implying that cellphone polarizing microscopes may offer diagnosis of malaria at parasitemia as low as ~0.03%. Potential application of the cellphone-based microscope to point-of-care diagnostics and severity monitoring of malaria will be also discussed.

8591-20, Session 4

Crowd-sourced biogames toward distributed microscopic image analysis and tele-diagnosis

Sam Mavandadi, Stoyan Dimitrov, Steve Feng, Frank Yu, Richard Yu, Uzair Y. Sikora, Aydogan Ozcan, Univ. of California, Los Angeles (United States)

We present a crowd-sourcing framework for tele-diagnosis of microscopic medical images. We specifically focus on conditions that require a binary decision (i.e., infected vs. uninfected) and discuss our results for a malaria diagnosis case-study.

Since optical microscopy is the traditional gold-standard methodology for identifying the existence of malaria parasites in human red blood cells (RBCs), the task of analyzing a patient's blood smear sample can be rather time-consuming, especially for cases where there is no infection since the medical expert must inspect thousands of individual cells under high magnification. Therefore, one can look at the task of diagnosing malaria as a large-scale pattern-recognition problem.

We propose to tackle the malaria diagnosis problem by crowd-sourcing the microscope-captured RBC images of patients' blood samples through entertaining games to individuals (experts and non-experts) around the world. The malaria game that we created for this purpose was designed to be played over the web and through Apps on Android phone and tablets. To this end we developed a digital gaming platform (http://biogames.ee.ucla.edu/) through which we allow an unlimited number of gamers from any location to diagnose RBC images with potential P. falciparum infection. In less than two months we received more than 1.5 million individual diagnosis decisions on approximately 8,500 microscopic images of RBCs. Combining these decisions through a Maximum a priori Probability framework, we were able to achieve an overall accuracy of 98.13% and a false positive rate less than 5% when compared to the diagnosis labels assigned by medical experts.

We believe that this telemedicine platform presents a viable framework for tackling an emerging Big-Data problem in diagnostics medicine.

8591-5, Session PWed

Tunable mid-infrared laser spectroscopy based on fiber-optic sensor for glucose measurement

Songlin Yu, Dachao Li, Kexin Xu, Tianjin Univ. (China)

The application of tunalbe Mid-infrared laser spectroscopy to regent-free quantification of glucose concentration in PBS solution was first presented. Tunable carbon dioxide (CO2) laser was employed as the light source, and all the laser emission wavelengths, including 1081?1076?1051?1041 and 1037 cm-1, locate in 950 ~ 1200 cm-1 band named as the “finger print spectrum”. The concentration of glucose was quantified by method of fiber-based attenuated total reflection spectrosopy, and the sensor cell was builded with silver halide fiber inserted into a micro tube. Dual path was applied to overcome the laser power fluctuation and obtain high SNR in this study. In our experiments, absorbance at the five wavenumbers correlates strongly well with the glucose concentration (R2>0.999, SD<0.0004, P<0.0001) in PBS solution, and noise-equivalent concentration as low as 3.2 mg/dL was achived. Compared with the conventional FT-IR spectrometer, higher sensitivity was aquired because of the laser higher power and spectral resolution, and it is about 4 times higher than that of FT-IR. All the results of this investigation suggested that the tunable CO2 laser spectroscopy is a powerful method for glucose measurement. Especialy, the multiple measurement wavelengths, which makes it possible for glucose determination in blood or interstitial fluide with complicated components. And the room-temprature measurement system, including CO2 laser, fiber-based sensor, and pyreoelectric detectors, make it sutable for glucose measurement. In the future, the fiber-optic sensor will be further mimiaturized and implanted into subcutanious tissue for continuous monitoring of glucose.

8591-21, Session PWed

Blood circulatory system for noninvasive diagnostics

Dirk Fricke, Jens Kraitl, Hartmut Ewald, Univ. Rostock (Germany)

Based on the human circulatory system an artificial blood circulatory system was developed to allow a controlled variation of the blood parameter as total hemoglobin concentration (ctHb), oxyhemoglobin (O2Hb) methemoglobin (MetHb) and carboxyhemoglobin (COHb). The optical properties of the blood were observed by online spectrometer measurements. The purpose was to observe the absorption, transmission and scattering properties of human whole blood in a wavelength range from 400 to 1700 nm. All the noninvasive measurements of the whole blood transmission-spectra were compared with sample results obtained by a Blood Gas Analyzer (BGA) to validate the results. For all measurements donor erythrocyte concentrates were used. The concentration of hemoglobin was changed by adding fixed amounts of blood plasma to the erythrocyte concentrate. Oxygen saturation and COHb were adjusted by a continuous flow of N2, N2-CO and compressed air through a hollow fiber membrane oxygenator. Different methemoglobin concentrations were adjusted by using natrium nitrite. The blood temperature was kept constant at 37 °C via a tube heating mechanism and a separate water circulation through the Oxygenator. Temperature and pressure of the system were automatically controlled and monitored. The model was also used to test new noninvasive measurement systems and for this reason special cuvettes were designed to imitate human tissue and generate plethysmographical signals.

In future the blood circulatory system should be used for testing, validating and also for calibrate newly developed optical prototype devices and for further investigations of interested blood components.

8591-22, Session PWed

Software-assisted live visualization system for subjacent blood vessels in endonasal endoscopic approaches

Peter Hartmann, Christopher Taudt, Benjamin Lempe, Markus Ernstberger, Jeannette Grüning, Ronny Maschke, Fabiola Basan, Tobias Baselt, Westsächsische Hochschule Zwickau (Germany); Ronny Grunnert, Fraunhofer Institut für Werkzeugmaschinen und Umformtechnik (Germany)

Minimal invasive surgery methods have received growing attention in recent years. In vital important areas, it is crucial for the surgeon to have a precise knowledge of the tissue structure.

Especially the visualization of arteries is desirable, as the destruction of the same can be lethal to the patient. In order to meet this requirement, the study presents a novel assistance system for endoscopic surgery. While state-of-the art systems rely on pre-operational data like computer-tomographic maps and require the use of radiation, the goal of the presented approach is to provide the clarification of subjacent blood vessels on live images of the endoscope camera system.

Based on the transmission and reflection spectra of various human tissues, a prototype system with a NIR illumination unit working at 800 nm was established. Several image filtering, processing and enhancement techniques have been investigated and evaluated on the raw pictures in order to obtain high quality results. The most important were increasing contrast and thresholding by difference of Gaussian method. Based on that, it is possible to rectify a fragmented artery pattern and extract geometrical information about the structure in terms of position and orientation. By superposing the original image and the extracted segment, the surgeon is assisted with valuable live pictures of the region of interest. The whole system has been tested on a laboratory scale. An outlook on the integration of such a system in a clinical environment and obvious benefits are discussed.

8591-23, Session PWed

Direct model for thin wetting film focusing

Daniel Migliozzi, Ecole Polytechnique (France); Cédric P. Allier, Yves Hennequin, Jean-Guillaume Coutard, Jean-Marc Dinten, CEA-LETI-Minatec (France)

We demonstrated that thin wetting film focusing allows detection of single micro-meter sized object with 24mm2 lensfree imaging. In order to refine the technique and push the limit of detection down to nanometer dimensions, a deep insight in the imaging mechanisms is necessary. We constructed an optical model taking into account thin wetting film physics. We considered a phase object of which the thickness follows a logarithmic law and light propagation according to the Fresnel function. This model fits well the intensity measurements acquired on micrometer-sized objects with our lensfree imaging setup. When the particle diameter is 1?m, a microlens is formed by a liquid surface deformation of about 100nm in height over few microns radial distance. The measured point spread function of the light deflected by such conical microlens presents constant propagated beam intensity over a long range, between z=-50?m and z=-250?m from the object plane. This is very similar to what is obtained from illuminating an axicon with a Gaussian beam, i.e. the central beam propagates for several Rayleigh ranges without appreciable divergences. In the lensfree imaging setup, the detector plane is far apart from the object (z=500?m). It is thus a true advantage to form axicon lens that can propagate strong intensity beam till the detector plane. Most important, the model predicts that the detection of smaller particle needs thinner film. Our results are important to envisage the detection of virus with lensfree imaging technique.

8591-24, Session PWed

Novel algorithm for background correction of the quantitative spectroscopic tomography of the biogenic substances

Pradeep K. W. Abeygunawardhana, Wei Qi, Ichirou Ishimaru, Kagawa Univ. (Japan)

The non-invasive blood sugar sensor is to be realized by using imaging-type 2-dimensional Fourier spectroscopy. For the quantitative analysis with high accuracy, the light-source fluctuation and the phase-shift error should be corrected. This paper proposes an algorithm to correct those errors. Light source fluctuation will be corrected using process of Fourier transform then filtering and finally inverse Fourier transform. Then, Phase shift error is corrected using phase angle calculated by self-convoluted interferogram. Inverse Fourier transforms of imaginary parts will gives phase spectrum. Convolution of phase spectrum with recorded data will result the phase corrected interferogram.

8591-25, Session PWed

A glucose concentration measurement method by surface plasmon resonance with borate polymer binding

Dachao Li, Peng Wu, Jia Yang, Tianjin Univ. (China)

Minimally-invasive human blood glucose detection can be realized by measuring the glucose concentration of interstitial fluid to predict the blood glucose level. As the volume of transdermally extracted interstitial fluid is minimal and its composition is complex, a surface plasmon resonance (SPR) glucose measuring method based on PAA-ran-PAAPBA polymer binding is proposed. The SPR measurement has high accuracy by optical refractive measurement and the polymer PAA-ran-PAAPBA can adsorb glucose molecule specifically. The polymer is chemically stable and easy to be synthesized which can extend the life of the sensor and simplify the binding process compared to other chemicals. The polymer was immobilized on the gold surface of SPR sensor using nano layer-by-layer self-assembly technique to realize the specific detection of glucose molecules and improve the measurement sensitivity. In order to verify the feasibilities of the glucose measurement method, including measurement limitation, dynamic dissociation and stability, a series of experiments were conducted. 2~1000mg/dL glucose solutions were injected into the equipment, and the measurement results were fitted with their corresponding glucose concentrations using quadratic curve. The fitting degrees of refractive index difference ?RU and glucose concentration are 0.90177 and 0.99509 in the glucose concentration range of 2~10mg/dL and 25~1000mg/dL, respectively. And the dynamic dissociation process of glucose molecules from PAA-ran-PAAPBA is verified. The performance of the polymer bonded to SPR sensor has no much difference after one month, which proves the stability of polymer. All results indicate this method can satisfy the requirement of the human blood glucose continuous monitoring in clinics.

8591-26, Session PWed

Deep UV Raman spectroscopy of solutions

Vladislav V. Yakovlev, Maria Troyanova-Wood, Georgi I. Petrov, Texas A&M Univ. (United States)

Deep UV Raman spectroscopy is one of the most effective ways to collect chemically-specific information about complex samples. The availability of inexpensive and reliable light sources in the spectral region below 250 nm has been always considered a major bottleneck problem on the way of a widespread of this powerful spectroscopic technique to biomedical applications. We report on a simple set-up, which allows generation of several mW's of average power at 237 nm and permits collection of high-quality, fluorescence-free spectra of micromolar concentrations of biologically significant substances in solution. The system is based on a microchip, diode-pumped 946 nm laser, which is subsequently converted in two stages to the fourth harmonic. The measured spectral bandwidth of the excitation laser is less than 10 cm^-1, allowing high-resolution spectral recording. Using as little as 1 mW incident power, the signal to noise ratio as high as 30 was recorded for 1-s acquisition time of the water Raman band.

8591-27, Session PWed

Raman spectroscopy is paving the way towards molecular understanding of drug interaction in malaria research

Torsten Frosch, Friedrich-Schiller-Univ. Jena (Germany) and Institut für Photonische Technologien e.V. (Germany); Juergen Werner, Stefan Hanf, Jürgen Popp, Institut für Photonische Technologien e.V. (Germany)

Raman spectroscopy has unique potential for identification of biological targets and elucidation of drug-target-interactions within living cells [1-4]. This is true because Raman spectroscopy can be applied for a non-invasive, marker-free investigation of molecules in the biological environment, while water does not cause a strong Raman signal [3]. The vibrational spectra are very sensitive for subtle chances of the molecular structure and are therefore a very sensitive probe for the environment of the molecules [2, 4]. In our case we are mostly interested in changes in the Raman spectra which are caused by interactions between target molecules and antimalaria active agents. The interpretation of these Raman bands will help in an understanding of the molecular interaction and for the tailored design of new effective active agents.

In this contribution we exploit techniques for highly frequency resolved Raman spectroscopy in order to investigate the chemical influence of drugs to the biological target structures in detail. By utilizing a unique Raman difference spectrometer [1], it is demonstrated, that the weak interaction of haematin and antimalarial agents cause variations of the Raman spectrum, more precisely shifts of the haematin macro ring vibrations. These shifts are characteristic for an interaction with a defined stoichiometric ratio of haematin to agent.

References

[1] Frosch, T.; Meyer, T.; Schmitt, M.; Popp, J., Anal. Chem. (2007), 79(16) 6159-6166;

[2] Frosch, T.; Popp, J., J. Mol. Struct. (2009), 924-926, 301;

[3] Frosch, T.; Koncarevic, S.; Becker, K.; Popp, J., Analyst (2009) 134, 1126-1132;

[4] Frosch, T.; Popp, J., J. Biomedical Optics (2010) 15, 041516

8591-28, Session PWed

Optical imaging of oxidative stress in rodent model of retinitis pigmentosa

Zahra Ghanian, Sepideh Maleki, Reyhaneh Sepehr, Sandeep Gopalakrishnan, Janis T. Eells, Mahsa Ranji, Univ. of Wisconsin-Milwaukee (United States)

Objective: In this study, the metabolic state of the retina in a rodent model of Retinitis Pigmentosa (RP) is investigated using a cryofluorescence imaging technique. Oxidative stress (OS) in the RP model, which is the most common cause of inherited blindness, is evaluated using the autofluorescence of mitochondrial metabolic coenzymes NADH (Nicotinamide Adenine Dinucleotide) and FAD (Flavin Adenine Dinucleotide). Here, NADH redox ratio (RR), the ratio of these two coenzymes (NADH/FAD) is used a marker of OS and expected to decrease in the presence of RP.

Materials and methods: The mitochondrial redox in retina from the RP rat model is measured using cryoimager and compared to that of normal

model. The eyes are harvested from heterozygous P23H-1 transgenic rats, the model of retinal degeneration in Sprague-Dawley (SD) rats. After harvesting, eyes are frozen quickly, embedded in a black mounting medium and kept at -80oC prior to cryoimaging. The cryoimager sequentially sections tissue and acquires fluorescent images. For this study, an axial resolution of 10?m is used, which results in ~ 300 z-slices per eye. Fluorescent images from each group of eyes are processed to extract NADH RR values using MATLAB.

Results: The NADH RR mean values are 1.11 ± 0.03 in the SD normal and 0.841 ± 0.01 in the P23H retina with a decrease of 24% due to OS. Comparing these mean intensities, reveals decrease in NADH RR translated to increase in OS of the P23H retina. This result demonstrates a dysfunctional electron transport chain due to increased OS that likely contributes to the observed loss of photoreceptor functions in the P23H retina.

8591-29, Session PWed

Determining the amounts of urea and glucose by near-infrared Raman spectroscopy in urine of patients with renal complications from diabetes mellitus and hypertension

Jeyse A. M. Bispo, Landulfo Silveira Jr., Camilo Castelo Branco Univ. (Brazil); Elzo E. S. Vieira, Adriana B. F. Moretti, Univ. Camilo Castelo Branco (Brazil)

Diabetes Mellitus and Hypertension diseases are frequently found in the same patient, which if untreated predispose to atherosclerotic and kidney diseases. The objective of this study was to identify potential biomarkers in the urine of diabetic and hypertensive patients through dispersive near-infrared Raman spectroscopy. Urine samples were collected from patients with low and high degree of complications, and control ones: one fraction was submitted to biochemical tests and another one was stored frozen (-80ºC) until spectral analysis. Samples were warmed up and placed in an aluminum sample holder for Raman spectra collection using a dispersive spectrometer (830 nm wavelength, 300 mW laser power and 20 s exposure time). Spectra were then submitted to Principal Components Analysis. The PCA loading vectors 1 and 3 revealed spectral features of urea and glucose, respectively; the PCA scores showed that patients with complications (low and high grade) had higher amount of glucose in the urine compared to the normal group ($p < 0.05$), which can bring serious consequences to patients. Also, the PCA scores showed that the amount of urea decreased in the groups with complications ($p < 0.05$), which generates the same concern as it is a marker that has a strong importance in the metabolic changes induced by such diseases. These results, applied to the analysis of urine of patients with diabetes and hypertension, can lead to early diagnostic information of complications and a possible disease prognosis in the patients where no complications from diabetes and hypertension were found.

8591-30, Session PWed

Profilometry and subsurface imaging in point of care diagnosis in ocular and meoplastic disease

Samir I. Sayegh, The Eye Center (United States); Alphonse Taghian, Massachusetts General Hospital (United States) and Harvard Medical School (United States)

Breast cancer-related lymphedema (BCRL) can be irreversible with profound negative impact on patients' quality of life. Programs that provide screening and active surveillance for BCRL are essential to determine whether early detection and intervention influences the course of lymphedema development.

Established methods of quantitatively assessing lymphedema at early stages include "volume" methods such as perometry and bioimpedance spectroscopy. In this work we demonstrate

1) The use of topographical techniques analogous to those used in corneal topography as an extension and refinement to volume based methods

2) The development of point-of-care lymphedema detection and characterization based on off-the-shelf hardware

3) The role of subsurface imaging

4) Demonstration of multimodal diagnostics techniques and integration yielding higher sensitivity/ specificity

8592-1, Session 1

Myoglobin saturation in free-diving whales: optical sensor development

Walfre Franco, Enoch Gutierrez-Herrera, Paulino Vacas-Jacques, R. Rox Anderson M.D., Warren M. Zapol, Massachusetts General Hospital (United States)

Mass strandings of live whales have been explained by proposing many natural or human-related causes. Recent necropsy reports suggest a link between mass stranding of beaked whales and the use of naval mid-frequency sonar. Surprisingly, whales experienced symptoms similar to those caused by inert gas bubbles in human divers. Our goal is to develop an optical sensor to monitor the consumption of myoglobin-bound oxygen stores in the muscle of freely diving whales. To this end we implemented a near-infrared (NIR), dual-wavelength, frequency-resolved technique in reflectance mode to probe tissue oxygenation. The probe contained two laser diodes (735 nm, 810 nm) as light sources and one avalanche photodetector. Changes in oxygenation are monitored by tracking and quantifying changes in phase-shift in the probing signal modulated at 70 MHz. Analytical expressions derived from diffusion theory were used to determine the absorption of chromophores in tissue phantoms. Comparisons with reported values for similar tissue phantoms were used to validate and characterize the sensor response. Since the absorption spectra of hemoglobin and myoglobin are very similar at NIR wavelengths, we used blood as a substitute for in vitro testing. Results show that the optical sensor tracked induced changes in saturation of the heme-containing proteins accurately, as compared with a blood gas analyzer. The significance of our physiological tag is to improve the understanding of the cardiovascular responses during natural dives and, subsequently, enhance our ability to determine if sonar disrupts management of gases in whales.

8592-2, Session 1

Precise sizing of particle suspensions on an unmodified cell phone using elastic light scattering

Zachary J. Smith, Kaiqin Chu, Sebastian Wachsmann-Hogiu, UC Davis Medical Ctr. (United States)

We report on the construction of a Fourier plane imaging system attached to a cell phone. In the Fourier plane, scattering angle at the sample is mapped to position. By illuminating aqueous particle suspensions with a collimated beam from an inexpensive 1 mW, 655 nm diode laser, angularly resolved scattering patterns (measuring scattering from approximately 5 to 20 degrees) are imaged by the phone's camera. To prevent unscattered laser light from overwhelming the camera, a beam stop consisting of a square of black aluminum foil was placed in the center of the Fourier plane. Analyzing the scattering patterns with Mie theory results in predictions of size distributions of the particles in suspension. Despite using consumer grade electronics, we extracted size distributions of sphere suspensions with 12 nm accuracy. The total cost of the system (excluding the cost of the camera phone) is approximately $50, and could be further reduced by volume production. We also show results from lipid droplets in milk, yeast cells, and red blood cells. Performing these measurements on a portable device presents opportunities for field-testing of food quality, process monitoring, and medical diagnosis. These and continuing results will be presented.

8592-3, Session 1

Oblique polarized reflectance spectroscopy for depth sensitive measurements in the epithelial tissue

Maria Jimenez, Leonid Fradkin, The Univ. of Texas at Austin (United States); Sylvia Lam, The BC Cancer Agency Research Ctr. (Canada); Bobby Knight, The Univ. of Texas at Austin (United States); Calum E. MacAulay, Catherine F. Poh D.D.S., The BC Cancer Agency Research Ctr. (Canada); Konstantin Sokolov, The Univ. of Texas M.D. Anderson Cancer Ctr. (United States) and The Univ. of Texas at Austin (United States)

Optical spectroscopy has been shown potential as tool for precancer detection by discriminating alterations in the optical properties within epithelial tissues. Identifying depth-dependent alterations associated with the progression of epithelial cancerous lesions can be especially challenging in the oral cavity due to the variable thickness of the epithelium and the presence of keratinization. Optical spectroscopy of epithelial tissue with improved depth resolution would greatly assist in the isolation of optical properties associated with cancer progression. Here, we report a fiber optic probe for oblique polarized reflectance spectroscopy (OPRS) that is capable of depth sensitive detection by combining multiple beveled fibers, oblique collection geometry, and polarization gating. We analyze how probe design parameters are related to improvements in collection efficiency of scattered photons from superficial tissue layers and to increased depth discrimination within epithelium. We have demonstrated that obliquely-oriented collection fibers increase both depth selectivity and collection efficiency of scattering signal. Currently, we evaluate this technology in a clinical trial of patients presenting lesions suspicious for dysplasia or carcinoma. We use depth sensitive spectroscopic data to develop automated algorithms for analysis of morphological and architectural changes in the context of the multilayer oral epithelial tissue. Our initial results show that OPRS has the potential to improve the detection and monitoring of epithelial precancers in the oral cavity.

8592-4, Session 2

In-line holographic Fourier-transform light scattering and its applications on cytometry and biophysical studies

Kyoohyun Kim, YongKeun Park, KAIST (Korea, Republic of)

Static and dynamic light scattering techniques have been widely used for studying morphology and dynamics of scatters. Normally, ensemble-averaged light scattering signals from bulk samples are measured by rotating detectors with specific angles. For that reason, until recently, it has been known that it is hard to measure static and dynamic light scattering signals from individual micrometer-sized samples. Recently developed Fourier-transform light scattering (FTLS), however, has provided a means to measure static and dynamic light scattering signals over the large range of scattering angles with high sensitivity. In FTLS, measured electric field at the sample plane, typically measured by quantitative phase imaging, is numerically propagated to the far field by applying Fourier transformation. This technique has been applied in various fields, especially in biological samples and clustering particles. However, measuring electric field, mainly performed by off-axis holography like diffraction phase microscopy, requires complicated optics setup and careful alignment; thus it has limitations for practical applications.

We develop a simple and effective method of measuring static and light scattering signals using a typical optical imaging setup. FTLS is integrated with digital in-line holography, which does not need for a separate beam path for a reference. We show that in-line holography

can measure both static and dynamic light scattering signals effectively. The FTLS measurement of static light scattering signals from polystyrene beads quantified the size and refractive index distribution. In addition, we present the measurement of static and dynamic light scattering patterns of human red blood cells, and biomechanical parameters of RBCs are quantified.

8592-5, Session 2

Optical diffraction tomography for the study of malaria-infected human red blood cells and hemozoin crystals

Kyoohyun Kim, HyeOk Yoon, YongKeun Park, KAIST (Korea, Republic of)

Refractive index (RI) distribution of biological cells gives useful information about various physiological or pathological states of the cells. Rather than other biomarkers such as fluorescent dyes, the RI distribution is an intrinsic property that is sensitive to the chemical composition and structure of samples. For example, the RI measurement of malaria-infected RBCs has been utilized for studying malaria diagnosis and treatment. Malaria-infected human red blood cells (RBCs) undergo severe structural and biochemical modifications by metabolic activities of malaria parasites inside the RBCs. Recently, 3D RI distributions of malaria-infected RBCs are reconstructed using the filtered backpropagation method. However, details of highly diffractive internal structures of the infected RBCs are difficult to be imaged because the back-propagation method considers samples weakly scattering phase materials.

We implement optical diffraction tomography for the measurement of 3D RI distribution of malaria-infected RBCs in high resolution. Diffraction tomography based on the First Rytov approximation of the scattered field reveals details of internal morphological changes of RBCs in intraerythrocytic stages of P. falciparum malaria parasites. Advantage of using the diffraction tomography over filtered back-propagation method is clearly seen when revealing highly scattering internal components of infected RBCs like hemozoin in late malaria stages. Shape distortion of samples in the defocus plane from the projection method is also corrected by the diffraction method, and physiological parameters such as cytoplasmic volume and hemoglobin concentration of samples and hemozoin are calculated.

8592-6, Session 2

Solving inverse scattering problems using quantitative phase imaging *(Invited Paper)*

Gabriel Popescu, Univ. of Illinois at Urbana-Champaign (United States)

The principle of diffraction tomography applied to semitransparent objects has been formulated theoretically more than 50 years ago by Wolf [1]. The approach relies on far-zone measurements of the field scattered by the object, assumed to fulfill the conditions of the Born approximation.

Recently, we demonstrated that quantitative phase imaging [2] can generate light scattering data with unprecedented sensitivity. This approach, termed Fourier transform light scattering (FTLS), can retrieve scattering over broad angular scales from extremely weakly scattering, such a single micron-sized particle or subcellular structure [3]. We used FTLS to retrieve the scattering parameters associated with tissue slices and blood smears.

In this presentation, we review FTLS and demonstrate a version of diffraction tomography, where the 3D structure of the semitransparent object is reconstructed via an imaging measurement, rather than scattering. Thus, instead of illuminating the object at various angles and collecting the scattered field on the Ewald sphere, we translate the object through the focus of an imaging system. The theoretical description and proof of principle data will be presented.

8592-7, Session 3

Chronic imaging of cortical microcirculation using multi-exposure speckle imaging

Syed M. S. Kazmi, Andrew K. Dunn, The Univ. of Texas at Austin (United States)

We recently developed a new Multi Exposure Speckle Imaging (MESI) technique based on Laser Speckle Contrast Imaging (LSCI) that enables quantitative determination of acute blood flow changes. We now demonstrate that the MESI technique more accurately estimates blood flow from speckle contrast images compared to single exposure LSCI and thus provides a quantitative assessment of flow that can be used for chronic imaging. We evaluate the accuracy of the MESI flow estimates by using dynamic Red Blood Cell (RBC) reflectance tracking as an absolute flow calibration in mice over several days. The flow measures computed using the MESI and LSCI techniques were found to be on average 10% and 27% deviant (n = 8 mice) from velocity changes estimated using RBC tracking, respectively. We also used MESI to map CBF dynamics after photo-thrombosis of selected cortical microvasculature, akin to studies that induce neurovascular pathology. Chronic flow changes estimated using MESI were more correlated with RBC tracking (R = 0.87) than LSCI (R = 0.63), enabling accurate characterization of CBF dynamics up to two weeks from baseline. With the increased accuracy, we envision MESI can provide a quantitative platform for studying the efficacy of stroke therapies aimed at flow restoration.

8592-8, Session 3

Tissue dynamic imaging of ex vivo ovarian cancer tumors

Ran An, John J. Turek, Purdue Univ. (United States); Daniela E. Matei, Indiania Univ. (United States); David D. Nolte, Purdue Univ. (United States)

Tissue Dynamic Imaging (TDI) is a pixel-based version of tissue dynamic spectroscopy (TDS) [1, 2]. It uses subcellular dynamics as an endogenous imaging contrast agent of living tissue. With the help of a short coherence gate, it collects digital holograms of dynamic speckle from selected depths in the living tissue. TDI generates voxel-based frequency versus time differential spectrograms, and creates functional spectral response fingerprints to identify cellular behaviors. Previously, TDS and TDI were applied to in vitro targets showing the cellular responses to environmental perturbations and anti-cancer drugs. In this paper TDI is applied for the first time to living ex vivo targets: human ovarian cancer exgrafts from nude mice. Ovarian cancer is the most lethal gynecologic cancer due to its propensity to metastasize early and to its inherent ability to acquire resistance to chemotherapy [3]. TDI successfully demonstrated a differential motility in proliferating tumor vs. normal tissues. Cisplatin is the standard of care for ovarian cancer. We observed strong sensitivity to cisplatin in cell line A2780, but complete drug resistance to cisplatin in the modified cell line CP70. TDI's ability to identify, distinguish and monitor drug sensitivity and resistance inside 3-D tissue exgrafts demonstrates its potential for clinical cancer diagnosis and cancer therapy selection.

[1] Nolte, D. D., An, R., Turek, J. J., and Jeong, K. (2011) J. Biomed. Opt. 16, 087004

[2] Nolte, D. D., An, R., Turek, J. J., and Jeong, K. (2011) J. Assoc. Lab. Auto. 5, 002

[3] Guarneri, V., Piacentini, F., et al. (2010) Gynecol Oncol 117, 152-158

8592-9, Session 3

Correcting for absorption in laser speckle rheology of blood

Zeinab Hajjarian Kashany, Seemantini Nadkarni, Harvard Medical School (United States)

Viscoelastic properties of blood are altered during the progression of various pathological conditions. Tools that enable characterizing blood viscoelasticity are invaluable to multiple diagnostic and therapy monitoring applications. Laser Speckle Rheology (LSR) is a novel optical approach, capable of evaluating tissue biomechanics, in situ. In LSR, the sample is illuminated with a coherent laser beam and the resulting speckle pattern is recorded by a high speed CMOS camera. Speckle fluctuations are modulated by displacements of endogenous scattering particles and, hence, are related to mechanical susceptibility of the environment. Nonetheless, interpreting speckle dynamics in terms of sample mechanics is complicated since variations in absorption and scattering properties also modify speckle fluctuations. Moreover, for light absorbing bio fluids, the simplifying diffusion approximation cannot be used to model light propagation and assess the impact of optical properties on speckle dynamics. We have developed an innovative ray tracing algorithm to explain the transport and correlation transfer of light in a medium with arbitrary absorption and scattering coefficients. Along with accurate estimation of optical properties, this algorithm enables correct interpretation of LSR measurements and evaluation of particular displacement. In the current study, LSR estimations of complex viscoelastic modulus, G*(?) for fresh and clotted swine blood samples are compared with mechanical rheology. A close correspondence is observed between the evaluated G*(?) values for fresh (R=0.98, P<10-4) and clotted (R=0.96, P=10-4) blood. These results demonstrate the immense potential of LSR for microrheology of light absorbing bio-fluids, such as blood.

8592-10, Session 4

Real-time turbidity compensation of biological tissue in motion by a process of three waves mixing optical phase conjugation

Fabrice Devaux, Eric Lantz, Univ. de Franche-Comté (France)

In the context of medical imaging, many non-invasive imaging methods through biological tissues using non-ionizing radiation were studied for twenty years. The consistent methods are based on the principle of interaction between a wave passing through the scattering medium and one or more waves of references. Recent significant advances in this field were carried out with devices using phase conjugation [1] and numerical holography [2]. However in these works, static scattering media are studied because of the relatively long time scales needed for reconstruction of the wave through the scattering medium. Indeed, these devices require that the position of the scatterers do not vary between the outgoing and returning light in the scattering medium. Now living biological tissues are dynamic scattering media with characteristic correlation time of about 1 ms making these methods inoperable at the moment for application to medical imaging. In addition these devices use visible light outside of the therapeutic window. This restricts to a few hundred microns thickness of scattering media traversed. In this context we present our work of imaging through scattering media by a method of real time optical phase conjugation based on three wave mixing nonlinear interaction [3] in order to restore an image transmitted through a biological tissue in motion (slice of chicken breast). Furthermore, we show how the motion of the scattering medium is used to improve the signal to noise and the resolution in restored images.

8592-11, Session 4

Real-time quantitative structural imaging of label-free objects

Yang Liu, Sergey A. Alexandrov, Shikhar Uttam, Rajan K. Bista, Univ. of Pittsburgh (United States); Chengquan Zhao, Univ. of Pittsburgh Medical Ctr. (United States)

Microscopic imaging and accurate quantification of the internal structures of a label-free three-dimensional (3D) object are of great importance in biology and medicine. We developed a novel imaging approach based on the spectral encoding of spatial frequency (SESF) principle for quantitative real-time structural imaging and nanoscale structural characterization. As the structure of a complex object can be rigorously described by a distribution of spatial frequencies in the Fourier space, the SESF encodes each local spatial frequency of an object with a corresponding spectral wavelength (color) at each image point. Thus such image not only presents a superior contrast, the local structure of a label-free object can also be visualized as a true-color map in real time (i.e., Rt-SESF image) and simultaneously quantified by correlating each color with its corresponding dominant axial spatial frequency of the object at the nanoscale sensitivity. We experimentally showed the ability of the SESF approach to perform real-time quantitative structural imaging of complex 3D objects using multilayer nanosphere aggregates with different sizes and the nanoscale size differences are clearly presented as distinct colors in the Rt-SESF images. Further, using human cervical cytology specimens, we found that axial spatial period of intra-nuclear structures of high-grade pre-cancerous cells exhibit a significantly larger dominant axial spatial period (size) compared with those of normal cells. This technique shows the potential to detect the structural changes in pre-cancerous cells that are not visible using conventional microscopy.

8592-12, Session 4

Assessing axial birefringence heterogeneity in bi-layered turbid media using polarized light imaging

Sanaz Alali, Rain Wang, I. Alex Vitkin, Univ. of Toronto (Canada)

Biological tissues are often composed of layers of cells or connective tissues aligned in specific ways, giving rise to tissue anisotropy [1]. These alignments manifest as optical birefringence in the different tissue layers, and can be obtained via polarized light imaging by measuring the tissue Mueller matrix (MM) from different depths [2]. Here, we propose using the MM itself to obtain information about the axial (depth) uniformity of the birefringence in turbid media such as tissues. Using polarization-sensitive Monte Carlo simulations and selected experimental validations, we show that the elements of the MM of a homogenous anisotropic media exhibit symmetry properties that differ from heterogeneous anisotropic media.

Polarization sensitive Monte Carlo code was modified to model turbid bi-layered media with arbitrary birefringence (magnitude and direction) of the two layers. Bi-layered samples (of same optical properties) with the same birefringence magnitude but different relative orientations were modeled and their MM images were constructed. The effective retardance (birefringence) and orientation of each sample were then calculated using polar decomposition [3,4]. The heterogeneous samples were compared to their equivalent homogenous (i.e., uniformly birefringent samples), which have the same effective values of retardances and ordinations. An asymmetry degree (ASD) between the off-diagonal MM elements was calculated for all samples. ASD in heterogeneous samples was higher than the ASD in the equivalent homogenous ones. We also offer experimental validation of this methodology, showing ASD increase in heterogeneous bi-layered polyacrylamide phantoms. This ability to distinguish between isotropic and anisotropic tissues, and whether the latter are uniformly anisotropic or heterogeneously so, should prove useful for quantitative assessment of striated/aligned biological tissues.

References:

[1] Alali et al, " Assessment of anisotropy in ex vivo rat bladders during distension", to be published in J. Biomed. Opt.

[2] Jiao et al, Opt. Lett. 27, 101-103, 2002.

[3] Lu and Chipman, J. Opt. Soc. Am. A. 13 , 1106-1113 ,1996.

[4] Wood et al, J. Biomed. Opt. 15(4), 047009-9,2010.

8592-13, Session 4

Controlling the spectral properties of light through turbid media

Jung-Hoon Park, Chunghyun Park, Hyunseung Yu, Yong-Hoon Cho, YongKeun Park, KAIST (Korea, Republic of)

Since the emergence of the field of molecular cell biology, the importance of different functionalities of individual organelles comprising a single cell has finally been grasped. Imaging has played an important role in this field by directly observing the different organelles in action. This was possible due to the advances in the techniques of staining specific molecules using fluorescent dyes or proteins. However, one of the main restrictions that these methods face is that they can only be applied to cellular specimens that have been cultured or extracted in vitro. This is mainly due to scattering rather than absorption which is minimal in biological tissues. Multiple scattering from the highly inhomogeneous biological structures result in random scattering which deteriorates image quality for in vivo bio imaging.

In contrast to common sense, we demonstrate that scattering can be used in our favor to actively spectral filter polychromatic sources to excite specific target samples beyond turbid media. We adapt and improve the wavefront shaping technique first developed by Vellekoop et al. and take advantage of the wavelength dependent scattering paths to selectively focus multiply foci with different wavelengths at different positions. This is based on the dispersion of the refractive index of multiple scatterers comprising the turbid media. It is shown that a single polychromatic wavefront impinged on turbid media can result in multiple foci with different colors based on the linearity of the transmission matrix. We also demonstrate applications of active spectral filtering in realistic biological systems.

8592-14, Session 4

Linear classifier and textural analysis of optical scattering images for tumor classification during breast cancer extraction

Alma Eguizabal, Univ. de Cantabria (Spain); Ashley M. Laughney, Thayer School of Engineering at Dartmouth (United States); Pilar Beatriz García-Allende, Helmholtz Zentrum München GmbH (Germany); Venkataramanan Krishnaswamy, Thayer School of Engineering at Dartmouth (United States); Wendy A. Wells, Dartmouth Hitchcock Medical Ctr. (United States); Keith D. Paulsen, Dartmouth Hitchcock Medical Ctr (United States) and Thayer School of Engineering at Dartmouth (United States); Brian W. Pogue, Thayer School of Engineering at Dartmouth (United States); José M. López-Higuera, Olga M. Conde, Univ. de Cantabria (Spain)

Texture analysis of light scattering in tissue is proposed to obtain diagnostic information from breast cancer specimens. Light scattering measurements are minimally invasive, and allow the estimation of tissue morphology to guide the surgeon in resection surgeries. The usability of scatter signatures acquired with a microsampling reflectance spectral imaging system was improved utilizing an empirical approximation to the Mie theory to estimate the scattering power on a per-pixel basis. Co-occurrence analysis is then applied to the scattering power images to extract the textural features. A stochastic analysis of the features demonstrated the suitability of the autocorrelation for the classification of not-malignant (normal epithelia and stroma, benign epithelia and stroma, inflammation), malignant (DCIS, IDC, ILC) and adipose tissue, since it reveals morphological information of tissue. Non-malignant tissue shows higher autocorrelation values while adipose tissue presents a very low autocorrelation on its scatter texture, being malignant the middle ground. Consequently, a fast linear classifier based on the consideration of just one straightforward feature is sufficient for providing relevant diagnostic information. A leave-one-out validation of the linear classifier on 48 regions of interest showed classification accuracies of 98.74% on adipose tissue, 82.67% on non-malignant tissue and 72.37% on malignant tissue, in comparison with the biopsy gold standard. This demonstrates that autocorrelation analysis of scatter signatures is a very computationally efficient and automated approach to provide pathological information in real-time to guide surgeon during tissue resection.

8592-15, Session 4

Signature of Stokes vector on the Poincare sphere for cancerous and non- cancerous tissues: computer modeling and experiment

Callum M. Macdonald, Alexander Doronin, Igor V. Meglinski, Univ. of Otago (New Zealand)

A Monte Carlo based computational approach for imitation of interaction of coherent circularly polarized laser light with biological tissues is developed. The technique is used for simulation the signature of Stokes vector depicted on Poincare sphere for cancerous and non- cancerous tissues. The model is also applied to establish optimal parameters of the experimental system developed for cancer detection. The results of modeling and its cross-validation with the phantom studies by using water solutions of polystyrene microspheres of a known size and concentration, as well as the results of measurements for cancer and non-cancer samples in vitro are presented. We also show that changes of size and concentration of scattering particles can be easily observed by tracking the Stoke's vector of scattered polarized light on the Poincare sphere.

8592-16, Session 5

Modeling microsphere axial displacement in optical projection tomographic microscopy to analyze effects on filtered backprojection reconstruction

Ryan L. Coe, Eric J. Seibel, Univ. of Washington (United States)

A computationally efficient method of simulating illumination in Optical Projection Tomographic Microscopy (OPTM) is presented to analyze the effect of microsphere axial displacement on image reconstruction using the filtered backprojection. OPTM reconstructs three-dimensional images of single cells from two-dimensional projection images in a fashion similar to Computed Tomography. Projection images are acquired from circumferential positions around the cell by scanning the objective focal plane through the cell, while the condenser focal plane remains stationary. Unlike CT, the cell rotates between the source and detector in a microcapillary where it is not necessarily positioned at the optical axis. As the cell rotates, its axial position changes relative to the condenser focal plane for every projection. These differences in illumination have an impact on the overall reconstruction that cannot be understood experimentally. The computational model presented in this work relies on an alternative method of calculating illumination using a matrix formalism with near-field Mie theory. This method provides the ability to calculate the response of a microsphere illuminated with plane waves propagating from different directions. The response from each plane wave is subsequently summed to determine the total response. The

power of this method is provided by the ability to arbitrarily choose the microsphere position after calculating the plane wave response, meaning illumination for all axial displacements can be computed in approximately the same time as a single position. Projection images are computed for microspheres at intervals away from the optical axis to understand how the axial displacement degrades the reconstructed image.

8592-17, Session 5

FullMonte: a framework for high-performance Monte Carlo simulation of light through turbid media with complex geometry

Jeffrey Cassidy, Vaughn Betz, Lothar D. Lilge, Univ. of Toronto (Canada)

Emerging clinical applications require fast and accurate modelling of light propagation through tur- bid media with complex geometries. One important example is bioluminescence imaging, which requires many forward solutions of light propagating through tissue in order to solve the inverse problem determining the source. Accuracy and speed are both critical to the success of this tech- nique.

Monte Carlo simulations are widely recognized as the standard for high-quality modelling of light propagation in turbid media, at the cost of high computational requirements. We present Full- Monte: a flexible, extensible software framework for Monte Carlo modelling of light transport from arbitrary extended light sources through general 3D turbid media including anisotropic scattering and refractive index changes. The problem geometry is expressed using a tetrahedral mesh, which gives accurate surface normals and hence avoids the reflection and refraction interface artifacts in- troduced by voxel approaches. Compared to previous tetrahedral models, FullMonte offers higher performance, more general source geometry, and more flexible options for capturing, visualizing, and analyzing results.

FullMonte exploits multi-core CPUs via multithreading, and also incorporates novel performance enhancements: Intel SSE vector instructions and optimized data structures. The software was designed for portability to higher-performance computational devices such as GPUs and custom FPGA hardware for maximum performance and efficiency. We discuss the design features that enable such implementations.

Existing implementations (TIM-OS, MCML, CUDAMCML) are used for functional validation and performance benchmarking. Accuracy and speed results are shown for forward solutions of bioluminescence imaging using the Digimouse dataset for a variety of source configurations.

8592-18, Session 5

Analytic phase-function corrected diffusion model for diffuse reflectance of an oblique pencil beam Incident on a semi-infinite turbid medium

Roger J. Zemp, Univ. of Alberta (Canada)

Oblique incidence reflectometry is an established technique for estimation of tissue optical properties, however, it typically requires a footprint of a few transport mean-free paths to reliably estimate the centroid of diffuse-reflectance. Smaller-footprint probes would require improved light-propagation models and inversion schemes for diffuse reflectance close to the point-of-entry but might enable micro-endoscopic form factors for clinical assessments of cancers and pre-cancers. Recently Vitkin et al. (Nat. Comm. 2011) found that the radiative transport equation with normally-incident collimated pencil-beam entering a semi-infinite turbid medium could be approximated as two equations: one that follows the diffusion approximation and one that serves as a phase-function-correction term. Analytical solutions to the diffuse reflectance from a pencil beam normally-incident on a semi-infinite turbid medium was presented and validated with excellent accuracy against Monte Carlo simulations and experimental data in situations where the diffusion approximation fails including near the point of entry. In this paper we extend the phase-function corrected diffusion-theory to the case of pencil beams obliquely incident on a semi-infinite turbid medium. The analytical expressions for diffuse reflectance require only minimal computational complexity and agree within 2% error of Monte Carlo simulations for tissue-realistic parameters including absorption and reduced scattering coefficients of 0.1 and 10 cm-1. The analytical model is used in a nonlinear fitting algorithm to demonstrate recovery of optical properties using a footprint that is smaller than needed for the previous diffusion-regime models.

8592-19, Session 5

Illumination area dependent coherent backscattering cone shape

Renzhe Bi, Jing Dong, Kijoon Lee, Nanyang Technological Univ. (Singapore)

Coherent backscattering (CBS) is a beautiful physical phenomenon that takes place in a highly scattering medium, which has potential application in noninvasive optical property measurement. The current model that explains the CBS cone shape, however, assumes the incoming beam diameter is infinitely large compared to the transport length. Though our study, when beam size becomes submillimeter the CBS cone shape begins to show distortion, which is quite similar to low-coherence enhanced backscattering (LEBS), and this effect should not be ignored in general.

By time-reversal photon pair model, when infinite illumination area assumption is taken, all the constructively interfering photon pairs will contribute to the coherent peak. However under small beam condition, the long path length photon pairs will not exist, leaving only the short path length photon pairs, which is similar to LEBS by illumination of short spatial coherence light source. A finite integration model is used to describe this phenomenon and Monte Carlo study is conducted. The simulation result and experimental result show good correlation.

In small beam CBS, the beam size serves similarly as spatial coherence length in LEBS. Comparing with control of spatial coherence length, laser beam size is much easier to adjust. And by using narrow beam, high spatial resolution can be achieved, which will enable us to make scanning map of the sample.

Besides, small beam size effect shows significantly broader CBS cone, thus has high potential to be applied in biological tissue study, where the narrow CBS angular profile remains a great challenge.

8592-20, Session 5

Maximal energy transport through disordered media with the implementation of transmission eigenchannels

Moonseok Kim, Youngwoon Choi, Changhyeng Yoon, Wonjun Choi, Korea Univ. (Korea, Republic of); Jaisoon Kim, Myongji Univ. (Korea, Republic of); Q-Han Park, Wonshik Choi, Korea Univ. (Korea, Republic of)

A disordered medium, however high its degree of disorder becomes, is a linear system. When two incident waves propagate simultaneously through the medium, the total transmitted wave is a linear summation of the two transmitted waves. Therefore the input-output response of a disordered medium can be described by a transmission matrix which relates free modes at the input to those at the output. One of the fascinating aspects of the transmission matrix that has yet to be fully explored is transmission eigenchannels. According to random matrix theory, the transmittance of the eigenchannels can reach unity in an ideal condition. The underlying physical description is that a proper choice

of eigenchannel as an incident wave can induce strong constructive interference of scattered waves at the opposite side of the medium.

In this study, we report the first experimental implementation of individual transmission eigenchannels for a highly disordered medium. To this end, we experimentally record a transmission matrix of the disordered medium for a limited numerical aperture (0.32 NA) and acquire its transmission eigenchannels. Using a wavefront shaping method, we generate an optical wave corresponding to each eigenchannel and record its transmission. In doing so, we have demonstrated that the eigenchannel with the maximum transmittance transports 3.99 times more energy than the uncontrolled waves, which is the best experimental record reported so far. Our study will open up new avenues for enhancing light energy delivery to biological tissues for medical purposes and controlling the lasing threshold in random lasers.

8592-21, Session 6

The contribution of specific organelles to side scatter *(Invited Paper)*

Judith R. Mourant, Oana C. Marina, Claire K. Sanders, Los Alamos National Lab. (United States)

Side scattering and backscattering from cells is often attributed to mitochondria. To determine if this is a valid assumption for a variety of cells types, wide angle side-scattering was simultaneously imaged with fluorescence from cells stained with nuclear, mitochondrial, and lysosomal fluorophores. Thousands of epithelial and fibroblast cells were imaged using an imaging flow cytometer. The intensity of side-scatter was spatially correlated with fluorescence from the stained organelles to understand the origin of side-scattering. Lysosomes scatter similarly to mitochondria, while the side-scatter from nuclei is in some cases stronger than from any other organelle.

8592-22, Session 6

Single versus coincidence detection of cell-derived vesicles by flow cytometry

Edwin van der Pol, Univ. van Amsterdam (Netherlands); Martin J. C. van Gemert, Auguste Sturk, Rienk Nieuwland, Ton G. van Leeuwen, Academisch Medisch Ctr. (Netherlands)

Background: Body fluids contain cell-derived vesicles ranging from 30 nm to 1 µm in diameter. The function, origin, and composition of these vesicles is disease dependent and therefore vesicles contain clinical information. The most common method to detect vesicles is flow cytometry, which guides vesicles through a laser beam in a hydrodynamically focused fluid stream. The unknown relationship between the measured light scattering intensity and the vesicle diameter resulted in unexplained contradictions between expected and observed results.

Methods: We combined light scattering measurements of polystyrene and silica beads with Mie calculations using an estimated refractive index of vesicles.

Results: We established the relationship between measured light scattering and the diameter of vesicles. We show that common gating strategies based on beads select vesicles (and cells) ranging from 800 to 2400 nm in diameter. For our flow cytometer, the smallest detectable silica beads were 204 nm, corresponding to vesicles ranging from 300 to 700 nm in diameter. However, we demonstrated that multiple vesicles <220 nm or multiple 89-nm silica beads were counted as a single event at sufficiently high concentrations.

Conclusions: Vesicle detection by flow cytometry relies on two mechanisms: (1) detection of single, relatively large, vesicles that scatter more light than the detection limit; and (2) coincidence detection – i.e. multiple relatively small vesicles are simultaneously illuminated by the laser beam and counted as a single event. Coincidence detection allows the detection of smaller vesicles than previously thought possible and explains why flow cytometry underestimates the concentration of vesicles typically 1,000-fold.

8592-23, Session 6

Analyzing the effect of absorption and refractive index on image formation in high numerical aperture transmission microscopy of single cells

Ryan L. Coe, Eric J. Seibel, Univ. of Washington (United States)

Transmission bright-field microscopy is the clinical mainstay for disease diagnosis where image contrast is provided by absorptive and refractive index differences between tissue and the surrounding media. Different microscopy techniques often assume one of the two contrast mechanisms is negligible as a means to better understand the tissue scattering processes. This particular work provides better understanding of the role of refractive index and absorption within Optical Projection Tomographic Microscopy (OPTM) through the development of a generalized computational model based upon the Finite-Difference Time-Domain method. The model mimics OPTM by simulating axial scanning of the objective focal plane through the cell to produce projection images. These projection images, acquired from circumferential positions around the cell, are reconstructed into isometric three-dimensional images using the filtered backprojection normally employed in Computed Tomography. The model provides a platform to analyze all aspects of bright-field microscopes, such as the degree of refractive index matching and the numerical aperture, which can be varied from air-immersion to high NA oil-immersion. In this preliminary work, the model is used to understand the effects of absorption and refraction on image formation using micro-shells and idealized nuclei. Analysis of absorption and refractive index separately provides the opportunity to better assess their role together as a complex refractive index for improved interpretation of bright-field scattering, essential for OPTM image reconstruction. This simulation, as well as ones in the future looking at other effects, will be used to optimize OPTM imaging parameters and triage efforts to further improve the overall system design.

8592-24, Session 6

Optical scatter imaging as an apoptosis assay for cells undergoing ALA-mediated photodynamic therapy in vitro

Vincent M. Rossi, Oregon State Univ. (United States) and Oregon Health & Science Univ. (United States); Steven L. Jacques, Oregon Health & Science Univ. (United States)

Aminolevulinic acid (ALA) is converted to protoporphyrin-IX (PpIX) within mitochondria, causing the assumption that ALA-mediated photodynamic therapy (PDT) results in mitochondrial damage and therefore an apoptotic response. Mitochondria within apoptosing cells swell, forming pores in their outer mitochondrial membranes which release cytochrome-c, triggering apoptosis. Optical scatter imaging (OSI) makes use of scattered fields in order to indicate the morphology of subcellular components, and is used here in order to measure changes in mitochondrial size as a response to ALA-mediated PDT. Two images of the same field of view are spatially filtered in the Fourier plane of a 4-F system. Both spatial filters block directly transmitted light, while accepting different angles of scattered light through an adjustable iris. The optical scatter image ratio (OSIR) of the local intensities of these two spatially filtered images is indicative of scattering particle size. Mie theory is used to calculate the predicted OSIR as a function of scattering particle size. In this fashion, the OSI system is calibrated using polystyrene microspheres of know sizes. Comparison of the measured OSIR from cellular images to theoretical values predicted for mitochondria then serves as an indication as to whether cells are apoptosing. Cells are treated at varying concentrations of ALA and

varying exposures of 635 nm light and imaged at varying time points in order to develop a broader understanding of an apoptotic response of cells undergoing ALA mediated PDT. Cells are also analyzed using standard apoptosis assays for comparison.

8592-25, Session 6

Size- and position-dependent angular scattering interferometry

Dustin W. Shipp, Ruobing Qian, Andrew J. Berger, Univ. of Rochester (United States)

Integrated Raman and Angular-scattering Microscopy (IRAM) has demonstrated the ability to interrogate single cells and measure changes over time. Raman spectroscopy reveals chemical information about the sample, while organelle sizes can be extracted from angular scattering. However, measuring the angular scattering from single cells presents unique challenges. The scattered light from individual organelles interferes coherently. This interference creates speckle patterns that undermine the ability to perform theoretical fits. Because the cells and their organelles are stationary, the speckle cannot be removed through simple time-averaging. Instead, several methods are being explored to reduce the effect of this interference. The cell can be “virtually rotated” in three dimensions by varying the illumination polarization and central incidence angle. This virtual rotation rearranges the scatterer locations and thereby changes the speckle pattern. Also, the coherent effects can be reduced by illuminating with a broader collection of wavelengths, thus reducing the coherence of the source. Finally, the speckle pattern can be suppressed digitally by using Fourier filtering to selectively remove small, high-frequency features caused by coherent interference while leaving the smoother features of the scattering pattern intact. The results from each of these methods, along with their advantages and limitations, will be discussed.

8592-26, Session 6

Analyzing subcellular structure with optical Fourier processing based on Gabor filters *(Invited Paper)*

Nada N. Boustany, Heidy Sierra, Rutgers, The State Univ. of New Jersey (United States)

Label-free measurement of subcellular morphology can be used to track dynamically cellular function under various conditions and has important applications in cellular monitoring and in vitro cell assays. We show that optical filtering of scattered light by two-dimensional Gabor filters allows for direct and highly sensitive measurement of sample structure. The Gabor filters, which are defined by their spatial frequency, orientation and Gaussian envelope, can be used to track locally and in situ the characteristic size and orientation of structures within the sample. Our method consists of sequentially implementing a set of Gabor filters via a spatial light modulator placed in a conjugate Fourier plane during optical imaging and identifying the filters that yield maximum signal. Using this setup, we show that Gabor filtering of light forward-scattered by spheres yields an optical response which varies linearly with diameter between 100nm and 2000nm. The optical filtering sensitivity to changes in diameter is on the order of 20nm and can be achieved at low image resolution. We use numerical simulations to demonstrate that this linear response can be predicted from scatter theory and does not vary significantly with changes in refractive index ratio. By applying this Fourier filtering method in samples consisting of diatoms and cells, we generate false-color images of the object that encode at each pixel the size of the local structures within the object. The resolution of these encoded size maps in on the order of 0.36um. The pixel histograms of these encoded images directly provide 20nm resolved “size spectra”, depicting the size distribution of structures within the analyzed object. We use these size spectra to differentiate the morphology of apoptosis-competent and bax/bak null apoptosis-resistant cells during cell death. We also utilize the sensitivity of the Gabor filters to object orientation to track changes in organelle morphology, and detect mitochondrial fission in cells undergoing apoptosis.

8592-27, Session 7

Application of angle-resolved low coherence interferometry to cervical dysplasia *(Invited Paper)*

Tyler K. Drake, Steven K. Yarmoska, Duke Univ. (United States); Yizheng Zhu, Virginia Polytechnic Institute and State Univ. (United States); Rex C. Bentley, Fidel A. Valea, Adam Wax, Duke Univ. (United States)

Angle-resolved low coherence interferometry (a/LCI) is an optical biopsy technique used to measure the average size and optical density of cell nuclei in epithelial tissue in order to determine tissue health. The angular distribution of elastically scattered light from cell nuclei and other small scatterers in the target tissue is collected and compared to Mie Theory. a/LCI obtains depth-resolved measurements without the use of exogenous contrast agents, with submicron accuracy. Fourier domain a/LCI allows parallel collection of multiple scattering angles allowing for subsecond data acquisition. a/LCI has successfully been used to detect the presence of dysplasia in Barrett’s Esophagus patients as well as in ex vivo human intestinal tissue with high sensitivity and specificity. Here we use a/LCI in a pilot study of ex vivo cervical tissue from subjects undergoing cervical cone biopsies and hysterectomy procedures to test the ability of a/LCI in correctly identifying cervical dysplasia. A fiber bundle probe was used to scan the tissue, and nuclear size and optical density measurements obtained from the basal layer of the epithelium (200-300 ?m deep). These measurements were then compared to pathological diagnosis from co-located physical biopsies in order to determine a correlation between nuclear morphology and the presence of dysplasia. This pilot study assesses the application of a/LCI to the detection of cervical dysplasia and future in vivo studies will be conducted to further investigate a/LCI as a novel cervical screening platform.

8592-28, Session 7

Diffuse reflectance spectroscopy: a clinical study of tuberculin skin tests reading

Anne Koenig, Commissariat à l’Énergie Atomique (France); Sophie Grande, Karima Dahel, Unité de recherche Clinique en Immunologie Lyon Sud (France); Anne Planat-Chrétien, Vincent Poher, Commissariat à l’Énergie Atomique (France); Catherine Goujon, Unité de recherche Clinique en Immunologie Lyon Sud (France); Jean-Marc Dinten, Commissariat à l’Énergie Atomique (France)

In this paper, we present the development of a low-cost optical instrument, usable in a clinical environment for skin test readings in order to detect changes of physiological parameters within skin tissue thickness. We choose the spatially resolved diffuse spectroscopy method to interrogate tissue, and particularly to determine skin optical properties at various wavelengths (450-900 nm). A method based on the comparison of the measurements to a Monte Carlo forward model provides absorption and diffusion optical coefficients. A change of optical properties of the examined tissue, or more precisely variations of diffusion and quantity variations of the main chromophores present in the skin (melanin, oxyhemoglobin, deoxyhemoglobin, lipid and water), reflects the reaction to study. We present the system and the method we developed for the application of skin test readings firstly pre-clinically validated on Yorkshire pigs. We detail the dedicated probe geometry we choose. Then, we present results on an ongoing clinical study for skin tests readings (patients were injected with tuberculin causing a delayed hypersensitivity reaction). Tuberculin or purified protein derivative (PPD)

has been used worldwide as a skin test reagent to support the diagnosis of tuberculosis. We demonstrate that an early detection of the reaction only 16 to 18 hours after the injection of the reagent is possible using this system, as the clinical reading is usually done 72 hours after injection. The extension of the method will enable to address other reactions and will open the fields to other applications in skin disease diagnostics.

8592-29, Session 7

In vivo determination of scattering properties of healthy and malignant breast tissue by use of multi-diameter-single fiber reflectance spectroscopy (MDSFR)

Ute A. Gamm, Erasmus MC (Netherlands)

Elastic scattering of light in tissue offers a natural biologic contrast that can be used to classify tissue and its ultrastructure for diagnostic purposes.

There are 2 important parameters that characterize light scattering in tissue; the reduced scattering coefficient μs' and the scattering phase function p(?).

For a single fiber reflectance spectroscopy setup, which uses a single multimode optical fiber with diameter dfib for both illumination and detection, our group has previously reported a relationship between the single fiber reflectance (SFR) signal and the dimensionless scattering (μs'dfib). Based on this relationship we developed the multi-diameter single fiber reflectance method (MDSFR), that allows the extraction of μs' and a phase function dependent parameter ?=(1-g2) / (1-g1) from tissue by taking multiple SFR measurements with different fiber diameters. Parameters g1 and g2 are the first two Legendre moments of the phase function and g1 is the anisotropy.

We have recently discussed the limitations and the sensitivity of the MDSFR analysis and showed that as few as 2 fiber diameters are required for a successful extraction of μs' and ?. In a subsequent phantom study we have validated the feasibility of the MDSFR method experimentally.

We present data from an in-vivo clinical study utilizing MDSFR to determine tissue scattering properties of healthy and malignant breast tissue, on patients undergoing biopsy of a suspicious lesion found during mammographic breast screening. Here MDSFR measurements are performed with a custom made disposable probe, incorporating two fiber diameters (0.4 and 0.8 mm), which is inserted through the biopsy needle before the biosy is taken, allowing in vivo spectroscopic measurements of tumor centre, tumor margin and healthy tissue.

8592-30, Session 7

Determination of scattering coefficient and anisotropy of scattering of Murine tissues using reflectance-mode confocal microscopy

Ravikant V. Samatham, Steven L. Jacques, Oregon Health & Science Univ. (United States)

Optical properties of turbid media, like tissue, are measured by different techniques. These techniques can be used to measure absorption coefficient (μa) and reduced scattering coefficient (μs(1-g)). Separation of the lumped parameter μs' into scattering coefficient (μs) and anisotropy of scattering(g) can be accomplished by goniometry and collimated transmission methods, but this requires preparation of micro-sections of tissue sample that can be cumbersome and alter tissue properties. A technique to determine scattering properties of bulk tissue from depth dependent decay of the reflectance-mode confocal scanning laser microscopy (rCSLM) data is developed. This report presents anisotropy of scattering (g) and scattering coefficient (μs) of 5 different mouse tissue from rCSLM data. Types of tissue tested are: White matter of Brain, Gray matter of Brain, Skin, Liver and Muscle. Tissues are extracted from mouse and three dimensional images were captures. The depth of imaging was changed according to the signal from the tissue. The rCSLM signal decays exponentially as the focus moved deeper into the tissue. The exponential decay as a function of depth of the rCSLM signal is modeled as R (z) = ? exp (-μz) where μ [cm-1] is the exponential decay constant and ?(dimensionless, ?=1 for mirror) is the local reflectivity. The theoretical model theory was developed to deduce optical scattering properties μs and g (at 488nm and 632.8nm wavelength), from the experimentally determined μ and ? values. This technique needs minimal tissue processing and can be used to determine optical properties of tissue in vivo.

8592-31, Session 7

Multispectral imaging of scatter features to assess feasibility of margin imaging during breast conserving surgery *(Invited Paper)*

Brian W. Pogue, Ashley M. Laughney, Venkataramanan Krishnaswamy, Keith D. Paulsen, Thayer School of Engineering at Dartmouth (United States); Richard J. Barth M.D., Wendy A. Wells M.D., Geisel School of Medicine at Dartmouth (United States); David J. Cuccia, Bruce J. Tromberg, Univ. of California, Irvine (United States)

Two localized spectroscopic imaging methods were evaluated to image the surface of excised breast tissues, with the goal of determining which would provide optimal descrimination of tissue status in a surgical setting. The application is to eventually design a system which would image resected tissue during surgery, and guide the surgeon to regions of cancer or DCIS involved tissue, allowing them to remove more tissue a the time of surgery. This would improve resection completeness during standard breast conservative surgery.

The first system was a scanning in situ spectroscopy platform, designed to explore the diagnostic potential of nearly coherent light scatter imaging to quantify the localized spectral-spatial signatures of breast pathologies. The light transport in the tissue was limited in this system, by a restricted spot size, and the scanning-beam approach to spectral image acquisition rapidly sampled localized reflectance over a 1cm x 1cm field of view. Spectroscopic-imaging features were diagnostically discriminant, quantifying known tissue heterogeneities and texture and shape signatures of breast pathologies.

A second, specialized near-infrared planar imaging technique, spatial frequency domain imaging (SFDI), was also examined to quantify sub-surface tissue scattering and absorption across resected specimens by analyzing its spatial modulation transfer function. Structured illumination patterns enhance signal localization in this relatively diffuse acquisition geometry and the spatial frequency dependence of the modulation amplitude was used to uniquely separate absorption and scattering effects. Disease-specific contrast was distinguished when spectral absorption and scattering signatures were interpreted together.

For both acquisition geometries, the optical parameters were quantified according to analytical models of light transport. Shape and texture parameters extracted from spectroscopic images revealed new contrast mechanisms and enhanced discrimination between breast pathologies. Diagnostic classification demonstrated high specificity and was mainly limited by sensitivity to under-represented pathologies. A feature-ranking algorithm was developed to determine which parameters contributed most significantly to a diagnosis to inform guidelines for the next generation of interventional spectroscopic imaging systems. Both systems present as good options for rapid tissue scanning, although the SFDI system has the distinct advantage of being non-contact and potentially images a wider field of view in a shorter time. Whereas the scanning system has the advantage of higher spatial resolution and direct tissue contact. Taken together the two systems could be built as a single unit, with the SFDI as a wide field survey unit, and the scanning system as a localized spot sampling follow up.

8592-32, Session 8

Spectroscopic microscopy for quanitification of nanoscale refractive index fluctuations *(Invited Paper)*

Lusik Cherkezyan, Ilker R. Capoglu, Hariharan Subramanian, Dhwanil Damania, Vadim Backman, Northwestern Univ. (United States)

Optical microscopy techniques are used in a variety of biophotonics and medical applications for the study of biological cells and tissues. Nevertheless, the spatial resolution of optical microscopy is diffraction limited and this imposes a constraint on the degree of detail it can provide. Emerging "spectroscopic microscopy" (SM) techniques such as partial wave spectroscopic (PWS) microscopy, confocal light scattering and absorption spectroscopy (CLASS), spectroscopic optical coherence microscopy (SOCM), etc. take advantage of the spectroscopic content in the detected light in addition to the imaging benefits of an optical microscope to overcome the diffraction limit. Here we demonstrate that spectroscopic analysis of an image obtained by a conventional inverted bright field microscope can reveal the statistics of refractive index distribution beyond the diffraction limit. Using the Born approximation, we establish that the spectral variance of intensity reflectance from a sample with weak refractive index fluctuations (such as biological cells) is a quantitative characteristic of the sample's internal nanostructure. Although the theory and derivations are valid for an arbitrary functional form of refractive index distribution, here we present a closed-form solution for the special case of exponential refractive index distribution. The analytical formula is validated using 3-D finite difference time domain (FDTD) simulations for a range of a) exponential correlation lengths, b) sample thicknesses, and c) numerical apertures of the instrument. The herein proposed spectroscopic analysis can be done on histological samples to provide an insight into microscopically invisible intracellular structures.

8592-33, Session 8

On alterations in the refractive index and scattering properties of biological tissue caused by histological processing

Htet Aung, Bianca DeAngelo, John Soldano, Piotr Kostyk, Braulio Rodriguez, Min Xu, Fairfield Univ. (United States)

Clinical tissue processing such as formalin fixing, paraffin-embedding and histological staining alters significantly the optical properties of the tissue. To improve the accuracy of optical diagnosis of tissue specimens and translate optical biopsy into clinical settings, it is critical to understand the alterations in the optical properties (refractive index, the scattering coefficient, the reduced scattering coefficient, and the anisotropy factor) of a specimen resulting from tissue processing and compensate for these changes in the diagnosis algorithm.

Here, we first report the comparison of the optical properties in the 450nm to 700nm spectral range of fresh frozen sections, paraffin-embedded unstained sections, and paraffin-embedded Hematoxylin and Eosin (H&E) stained sections from a serial cut of prostate cancer tissue obtained by quantitative differential interference contrast (DIC) microscopy. Our approach was validated by the excellent agreement between the measured optical properties of plain and dyed polystyrene spheres and those predicted by Mie theory. The alterations in the optical properties of nuclei, cytoplasm, lumen, and stroma due to tissue processing will be documented. A simple model will then be presented to explain these alterations.

8592-34, Session 8

Fractal analysis of scatter imaging signatures to distinguish breast pathologies

Alma Eguizabal, Univ. de Cantabria (Spain); Ashley M. Laughney, Venkataramanan Krishnaswamy, Thayer School of Engineering at Dartmouth (United States); Wendy A. Wells M.D., Dartmouth Hitchcock Medical Ctr. (United States); Keith D. Paulsen, Dartmouth Hitchcock Medical Ctr. (United States) and Thayer School of Engineering at Dartmouth (United States); Brian W. Pogue, Thayer School of Engineering at Dartmouth (United States); José M. López-Higuera, Olga M. Conde, Univ. de Cantabria (Spain)

Fractal analysis combined with a label-free scattering technique is proposed for describing the pathological architecture of tumors. Clinicians and pathologists are conventionally trained to classify abnormal features such as structural irregularities or high indices of mitosis. The potential of fractal analysis lies in the fact of being a morphometric measure of the irregular structures providing a measure of the object's complexity and self-similarity. As cancer is characterized by disorder and irregularity in tissues, this measure could be related to tumor growth. Fractal analysis has been probed in the understanding of the tumor vasculature network, in the analysis of OCT breast images, etc. This work addresses the feasibility of applying fractal analysis to the scattering power map provided by a localized reflectance spectroscopic system. Disorder, irregularity and cell size variation in tissue samples is translated into the scattering power magnitude and its fractal dimension is correlated with the pathologist assessment of the samples. Box-counting and correlation techniques are compared for fractal dimension computation and key parameters such as window size of analysis are discussed. Results show that scattering analysis of ex-vivo fresh tissue samples exhibits separated ranges of fractal dimension in non-malignant breast tissue and in malignant tissue (DCIS, ILC, IDC). This contrast trend would help in the discrimination of tissues in the intraoperative context and may serve as a useful adjunct to surgeons.

8592-35, Session 8

Three models of light transport at subdiffusion lengthscales measured with coherent backscattering spectroscopy

Andrew J. Radosevich, Nikhil N. Mutyal, Jeremy D. Rogers, Vadim Backman, Northwestern Univ. (United States)

Coherent backscattering (CBS) manifests itself as an angular intensity peak centered in the backscattering direction. Through a Fourier transform relation, the angular CBS peak can be used to acquire measurements of diffuse reflectance at subdiffusion lengthscales (i.e. source-detector separations less than a transport mean free path) with spatial resolution of approximately 10 microns and spatial extent of several millimeters. Because of this sensitivity to subdiffusion lengthscales, the shape of the CBS peak is largely dependent on the scattering phase function which is in turn dependent on the physical composition of the sample. As such, when modeling the CBS peak it is necessary to choose a scattering phase function which accurately approximates the composition of the sample under observation. In this work, we begin by presenting the experimental methodologies used to measure the diffuse reflectance profile using CBS. We then detail three models of light scattering which can be applied to different types of biological tissue. First, Mie theory can be applied when the medium is composed primarily of homogeneous spherical particles such as occurs in adipose tissue. Second, the Whittle-Matèrn model can be applied when the medium is composed of a continuous distribution of refractive index fluctuations such as occurs in a large number of tissues including colon, liver, brain, etc. Finally, a model based on Fresnel's equations can be applied to biological structures formed in the process of biomineralization. Choosing between these three models should be made based on a priori knowledge of the sample composition.

8592-43, Session PSun

Depolarization of light by rough surface of scattering phantoms

Lioudmila Tchvialeva, The Univ. of British Columbia (Canada); Tim K. Lee, The BC Cancer Agency Research Ctr. (Canada); Alexander Doronin, Igor V. Meglinski, Univ. of Otago (New Zealand)

The growing interest in biomedical optics to the polarimetric methods suffers from a lack of understanding the processes of scattered light depolarization in and on the surface of biological tissues. In current study depolarization of linearly polarized light propagated in semi-transparent silicone phantoms is considered. The solid phantoms with variety of surface roughness and bulk optical properties were specially designed to imitate scattering of laser light on collagen fibres in human skin along with the diffuse reflectance on the skin surface. Utilizing parallel (Ip) and perpendicular (Ix) measurements from two free-space speckle patterns the spatial distribution of depolarization ratio for scattered light D = (Ip - Ix)/(Ip + Ix) is analyzed. The Monte Carlo model developed in house has been applied to assess the fraction of light maintaining its initial linear polarization and a part of light scattered form superficial layers of the medium. The spatial distribution of D vs. phantom roughness, scatterer concentration and scatterer size in far zone is analysed. A weak depolarization and negligible response to scattering of the medium are observed for phantoms with smooth surfaces, whereas for the surface roughness in order to the mean free path the depolarization ratio decreases and reveals dependence on the bulk scattering coefficient. In conclusion, the surface roughness could be a key factor triggering the ability of tissues' characterization by depolarization ratio.

8592-44, Session PSun

Reflection matrix measurement of a highly scattering media

HyeonSeung Yu, Jung-Hoon Park, YongKeun Park, KAIST (Korea, Republic of)

We measured the optical reflection matrix (RM) of a highly scattering media. Recently it has been shown that the transmission matrix of a complex media is a great tool for generating a focus or delivering an object image through a scattering media. However, the reflection matrix is not fully measured experimentally so far. The measurement of RM is important in the aspect of real biological imaging, since beam illumination and detection must be done in the same side of a highly scattering biological tissue for diagnostic purposes. This report shows the first measurement of large optical reflection matrix and optical properties are investigated.

Optical field images are acquired by full-field interferometric microscopy. The basis of input and output channels is spatial frequency, which was accessed using a rotating galvano mirror. The numbers of the input and output channels are set comparable to the number of theoretically resolvable channels in the region of interest. The large statistical information from the measured RM gives the way to study the property of the light transport. We analyze the eigenvalue distribution of the matrix and compare it with random-matrix theory. The effect of the limitation of the optical system is theoretically examined, especially determined by the numerical aperture. Furthermore, we investigate field optimization and imaging application in reflection geometry, which has been fruitfully shown in transmission configuration. The possibility of finding the signature of coherent enhanced backscattering is also discussed.

8592-45, Session PSun

Numerical re-evaluation of the Mcdonald-Vaughan model for Raman depth profiling

Jacob Caro, Dennis Leenman, Jeroen Heldens, Technische Univ. Delft (Netherlands)

Raman spectroscopy, i.e. inelastic scattering of light by vibrational modes of molecules, is increasingly used in biomedical applications, for example in diagnostics of human tissue. It is fast, non-destructive and label free, and for a number of situations already has a proven capability to discriminate between healthy and unhealthy tissue and cells. As for the spatial resolution of confocal Raman spectroscopy, it is usually assumed to be on the order of the focal volume of the focused laser beam used for excitation. Depth profiling studies of layered structures, however, indicate that the resolution question cannot be properly answered in this simple way.

In this contribution we re-evaluate the Macdonald-Vaughan model for Raman depth profiling [J. Raman Spectrosc. 38, 584 (2007)]. The model is an intuitive geometrical description of the spatial regions which generate Raman signal in a confocal geometry, indicating that Raman signal also originates from far outside the focal volume. Based on simple but just assumptions, correct shapes of profiles were obtained for various measured structures. Quantitatively, however, the results were not satisfactory, since the fitted extinction coefficients of the incoming and scattered light were off by a factor 1E5. The re-evaluation, based on our own numerical implementation, indicates that the model not only predicts the proper shape of the profiles but also yields the right extinction coefficients. Based on this result, we believe that the model now is highly useful for description of depth profiles and thus is also very suitable for interpretation of depth profiles of biomedical samples.

8592-46, Session PSun

Determination of optical properties of biological tissue through the diffuse reflectance curves using adjustment by Fourier series expansion

Aaron A. Munoz, Univ. de Carabobo (Venezuela) and Instituto Nacional de Astrofísica, Óptica y Electronica (Mexico); Sergio Vázquez-Montiel, Instituto Nacional de Astrofísica, Óptica y Electrónica (Mexico)

The determination of optical parameters of biological tissues is essential for the application of optical techniques in the diagnosis and treatment of diseases. Diffuse Reflection Spectroscopy is a widely used technique to analyze and optical characterize of biological tissues. In this work we show that by using the diffuse reflectance spectra and a new mathematical model we can retrieve the optical parameters by applying an adjustment of the data with nonlinear least squares. In our model we represent the spectra using a Fourier series expansion finding mathematical relations between the coefficients of the polynomial and the optical parameters. In this first paper we use spectra generated by the Monte Carlo Multilayered Technique to simulate the propagation of photons in turbid media. Using these spectra we determine the behavior of Fourier series coefficients when varying the optical parameters of the medium under study. With this procedure we find mathematical relations between Fourier series coefficients and optical parameters. Finally, the results show that our method can retrieve the optical parameters of biological tissues with accuracy adequate for medical applications.

8592-47, Session PSun

Active polarization control through turbid media

Jung-Hoon Park, Chunghyun Park, Hyeonseung Yu, Yong-Hoon Cho, YongKeun Park, KAIST (Korea, Republic of)

Polarization is an important aspect of light that has found use in both imaging and manipulation techniques. The conventional scheme of obtaining a highly polarized light field depends on placing polarizing optical components in the beam path prior to the sample. However, this is only applicable for ex vitro studies where there is no scattering layer between the probe and sample. When multiple scattering is present, even the accumulation of isotropic scattering results in a speckle of random polarized states. In this work we choose a turbid random medium as a model system for scattering in biological tissues and control the relative phases of the scattering paths to manipulate the polarization properties of a focused beam after multiple scattering events. This is based on the fact that the transmission matrix which describes the entire scattering process is a function dependent on polarization states.

In contrast to the common knowledge that scattering scrambles the polarization properties of the incident wavefront, the present approach demonstrates repolarization of light through highly scattering media; the polarization of an optimized focus beyond a scattering layer can be actively controlled with no limitations given by the polarization of the incident beam. Dynamic polarization control of the optimized focus can also be achieved with no moving mechanical parts by simply imposing appropriate relative phase delays to two orthogonal polarization states. After the proof of principle demonstration using white paint as a dynamic waveplate, applications in real biological systems are demonstrated.

8592-48, Session PSun

Fourier-transform light scattering of individual colloidal aggregates

Hyeonseung Yu, HyunJoo Park, YoungChan Kim, Mahn Won Kim, YongKeun Park, KAIST (Korea, Republic of)

We presents the experimental measurement of the light scattering of individual aggregated polymethyl methacrylate spheres in dimer, trimer, and tetrahedron shapes. The measurement of light scattering from a single colloidal particle is extremely difficult in traditional goniometer-based measurement, because (i) it is difficult to isolate individual clusters without imaging clusters in microscopic scale; (ii) a highly sensitive detector is required to measure the low scattered power from a single cluster; and (iii) choosing the major axes of the cluster and polarization sensitive measurement are difficult since its orientation is unknown. Here we present the light scattering from individual colloidal clusters using Fourier-transform light scattering. The electric field at the sample plane is measured via quantitative phase imaging with diffraction phase microscopy. Then by numerically propagating the sample field to the far-field scattering plane, which is corresponding to the Fourier-transform of the sample field, the two-dimensional light scattering patterns from individual clusters are effectively and precisely retrieved. The obtained scattering patterns clearly reflect the configuration of dimer, trimer, and tetrahedron shapes.

We also quantitatively compared the angular light scattering along the primary axis and auxiliary axis between the measured light scattering patterns and simulated patterns calculated by multi-particle Mie solution.

8592-49, Session PSun

Optical monitoring of photopolymerization for medical hydrogel-implant design

Andreas Schmocker, Azadeh Khoushabi, Salma Farahi, Pierre-Etienne Bourban, Jan-Anders E. Månson, Christophe Moser, Ecole Polytechnique Fédérale de Lausanne (Switzerland)

The placement of implants requires extensive surgery. The currently available minimally invasive surgical options are geometrically strongly limited and surgeons are looking towards more effective, but still physiological solutions. A particularly attractive option is to replace tissues with a synthetic in situ polymerized and tailored material.

Yet, for applications with restricted physical access and illumination time, such as an intervertebral disc replacement, photopolymerization of volumes with a large volume/illumination-area ratio becomes highly challenging. During the reaction, the material's absorption and scattering coefficients change and directly influence local polymerization rates. By controlling and understanding such polymerization patterns local material properties can be built up, custom materials be designed within the human body and reactions be monitored. Thus, it is essential to better understand and model photopolymerization reactions.

Using a double integrating sphere setup, the optical properties of suitable hydrogel samples are measured dynamically during polymerization. Scattering, absorption and monomer conversion rates are connected using a Monte Carlo approach for inverse parameter identification. Validation is done by polymerizing a hydrogel in a sphere like volume using an optical fiber for light delivery. The results are used to study and predict 3D polymerization patterns for different illumination configurations. Moreover, real tests are done on bovine intervertebral discs.

The results provide insights for the development of novel endoscopic light-scattering polymerization probes paving the way for a new generation of implantable scaffolds.

8592-36, Session 9

Low-coherence spectroscopy measurements of scattering and backscattering coefficients

Nienke Bosschaart, Maurice C. G. Aalders, Ton G. van Leeuwen, Dirk J. Faber, Univ. van Amsterdam (Netherlands)

Optical property measurements reflect the composition and organization of healthy and diseased tissue on a sub-micrometer scale. Quantitative measurements of light scattering properties can be used to detect the changes in cellular and sub-cellular organization that occur during disease progression, e.g. cancer development. Despite the existence of many spectroscopic methods, it is still a challenge to do non-invasive, quantitative measurements of the scattering properties in vivo over a large wavelength range.

Low-coherence spectroscopy (LCS) simultaneously quantifies scattering (?s) and backscattering (?b) coefficients between 480 and 700 nm. In addition, LCS offers the possibility to do depth resolved measurements of these coefficients within very confined tissue volumes (axial x lateral resolution: 22 x 9 µm). Recently, we have shown that our measurements of ?s and ?b are in good agreement with Mie calculations for small particles and low volume concentrations. However, multiple scattering and dependent scattering effects may influence LCS measurements on higher particle concentrations and larger particle sizes. Therefore, in this presentation we will show measurements on polystyrene spheres with diameters ranging from 200-1000 nm with expected scattering coefficients up to 40 mm-1. We will analyze our data in the first Born approximation using a Percus-Yevick model to calculate the structure factor.

In conclusion, we can state that LCS is a promising technique for non-invasive, quantitative, localized in vivo measurements of tissue scattering properties.

8592-37, Session 9

Low coherence light scattering from gold micro- and nano- rods to study diffusion using optical coherence tomography

Raghav K. Chhetri, The Univ. of North Carolina at Chapel Hill (United States); Wei-Chen Wu, Joseph B. Tracy, North Carolina State Univ. (United States); Amy L. Oldenburg, The Univ. of North Carolina at Chapel Hill (United States)

The dynamics of micro- and nano- sized particles are reflective of fundamental physical and biochemical processes and are of significance in fields including microrheology, microfluidics, soft condensed matter, and drug delivery. In light scattering techniques, the Brownian dynamics of an ensemble of particles lead to temporal fluctuations of the scattered optical field which can be related to the particles' diffusion coefficients. For biomedical applications, there is considerable interest in resolving thermal diffusion of probes within a heterogeneous sample. Here we investigate the use of Optical Coherence Tomography (OCT) to provide path-length-resolved diffusion imaging of gold microrods and nanorods. The high scattering cross section and high albedo of gold rods make them ideal probes for use with OCT. Using OCT, we demonstrate that polarized backscattering from these anisotropic probes simultaneously registers their rotational and translational dynamics. We employed gold microrods (69 nm by 565 nm) and gold nanorods (18 nm by 62 nm) coated with a non-adherent polyethylene glycol layer to study diffusion in Newtonian fluids (glycerol-water), complex fluids (polyethylene oxides) and viscoelastic gels (collagen I). We found that several factors dictate the choice of probe for a given application, including the desired dynamic range of rheological properties, and the relative probe size compared to the inherent mesh size of the complex fluid or solid. Finally, we demonstrate diffusion imaging in 3D tissue cultures of breast cancer, and find that probes freely diffusing in the collagen extracellular matrix can be monitored with OCT, highlighting their application-driven utilities in biomedical studies.

8592-38, Session 9

Quantifying the tissue structural changes under the field effect of colorectal cancer by inverse spectroscopic optical coherence tomography

Ji Yi, Northwestern Univ. (United States); Hemant K. Roy, NorthShore Univ. Health Systems (United States); Vadim Backman, Northwestern Univ. (United States)

Field effect states that the formation of a tumor is a consequence of a chronic condition on the entire organ, rather than a sudden and isolated event. Thus there may be subtle structural change detectable at locations apart from the eventual site of tumorgenesis. The field effect provides means to detect cancer at an early stage via an easily accessible portion of the organ, for example, detect colorectal cancer (CRC) through anus measurement. Although multiple optical modalities have been developed for CRC field effect detection, the physical mechanism is still eluded. Here a novel method called inverse spectroscopic optical coherence tomography (ISOCT) is developed to locally quantify the structural properties under CRC field effect. Optical and structural properties from the epithelium and the extracellular matrix (ECM) ex vivo are quantified and correlated with CRC development.

In ISOCT, tissue is modeled as a medium with continuously varying refractive indices (RI), and the spatial autocorrelation function of the varying RI (RI correlation function) is described by the Whittle-Matern functional family. By measuring the optical quantities by ISOCT, the RI correlation function can be inversely deduced. We find that the backscattering spectrum extracted by ISOCT exhibits a power law form and the exponent (often called the scattering power) is sensitive to the change of correlation function at length scale down to ~30nm. At the mean time, the 3D imaging capability of OCT provides a guide so that different components of the tissue such as epithelium and ECM can be separated and analyzed individually.

8592-39, Session 9

Fast high-resolution imaging through turbid media by optical parametric amplification of ballistic photons *(Invited Paper)*

Youbo Zhao, Benedikt W. Graf, Steven G. Adie, Stephen A. Boppart, Univ. of Illinois at Urbana-Champaign (United States)

Ballistic photons offer opportunities to reconstruct high-resolution images of targets behind or within turbid media. Optical parametric amplification (OPA) was proposed as a promising technology to detect ballistic photons in the early 1990s. Technically, however, a long-standing challenge has been to apply OPA to biomedical imaging, where sub-cellular resolution and fast real-time visualization are always preferred. In this work, we employed a special OPA scheme to detect ballistic photons, which enabled fast scanning and high-resolution imaging of objects through highly scattering (turbid) media. Particular strategies include employment of high repetition-rate (250 kHz) laser pulses (800 nm, 100 fs), tight focusing of both the pump and signal beams inside the crystal (1 mm BBO), and a double-pass amplification scheme. The high repetition-rate laser supports fast imaging speed of a few minutes per image in sample scanning mode (or possibly up to video rate if a high-speed beam scanner is used). The focused OPA scheme not only provides sufficient optical intensity to support an efficient OPA process, but also automatically forms a non-linear confocal filter (virtual pinhole). The double-pass amplification scheme enables signal gains of more than 35 dB. Near diffraction-limited resolutions were obtained when imaging samples through turbid media (either several sheets of lens tissue or a certain thickness of biological tissue) of up to 10 mean-free-paths, enabled by the efficient detection of ballistic photons using the high-gain, femtosecond time-gated OPA setup. We compared the OPA-based ballistic photon imaging method with optical coherence microscopy, showing its advantages when imaging through thick turbid media where ballistic light is extremely weak and multiple scattering is dominant.

8592-40, Session 9

Detection of hemoglobin In thick scattering samples with multispectral multiple scattering low coherence interferometry

Thomas E. Matthews, Michael G. Giacomelli, Adam Wax, Duke Univ. (United States)

Low coherence interferometry is a powerful technique for sensitively detecting light scattered from tissue and making a precise determination of its time of flight, which corresponds to the optical path it followed. This depth sectioning typically has a resolution on the order of a few micrometers, which is higher than that offered by other time gating methods, and has the additional benefit of interferometric gain. Both of these characteristics make it an ideal way to selectively detect scattered light from tissue based on path length to separate ballistic photons, multiple low angle scattered light ("snake" photons) and diffuse scattered photons.

We have implemented multiple scattering low coherence interferometry (ms/LCI) in the Fourier domain, using a supercontinuum light source. This increases both the speed of the system and gives access to rich spectroscopic information. Interferometric detection was achieved with a custom imaging spectrometer, designed to have high spectral resolution (17 pm) resulting in large imaging depth range (greater than 6 mm). By using an imaging spectrometer, parallel detection of a spectral reference and the sample is enabled, reducing the noise associated with supercontinuum sources. Angle resolved detection is used to reduce the diffuse background signal, and features 1 cm deep in a scattering

phantom were detected. The signal from these features was processed with the dual¬ window technique to generate depth resolved spectra from deep within a scattering phantom. The dual-window technique is a mathematical method which utilizes two short¬ time Fourier transforms with narrow and broad spectral windows to extract a time frequency distribution from one A scan with high spectral and axial resolution, avoiding tradeoffs previously inherent in spectroscopic LCI techniques. Visible wavelengths in the 600-660 nm region were chosen, which allowed detection of biologically relevant chromophores, including oxyhemoglobin and deoxyhemoglobin.

8592-41, Session 9

Spectroscopic optical coherence tomography with graphics processing unit based analysis of three dimensional data sets

Volker Jaedicke, Semih Agcaer, Sebastian R. Goebel, Ruhr-Univ. Bochum (Germany); Helge Wiethoff, Technische Fachhochschule Georg Agricola zu Bochum (Germany); Nils C. Gerhardt, Ruhr-Univ. Bochum (Germany); Hubert Welp, Technische Fachhochschule Georg Agricola zu Bochum (Germany); Martin R. Hofmann, Ruhr-Univ. Bochum (Germany)

Spectroscopic optical coherence tomography (OCT) is an extension of the standard strength of backscattering analysis of OCT. It enables depth resolved monitoring of molecular and structural differences of tissue. A drawback of most methods to calculate and process the spectroscopic data is the long processing time. Also systematic and stochastic errors make the interpretation of the results challenging. Our approach combines modern signal processing tools with powerful graphics processing unit programming. The processing speed for the spectroscopic analysis is nearly 3 mega voxel per second. This allows us to analyze multiple B-Scans in a few seconds and to display the results as a three dimensional data set. Our algorithm contains the following steps additional to the conventional processing for frequency domain OCT: a threshold based quality map to exclude noisy parts of the data, spectral analysis by Short Time Fourier Transform, feature reduction by Principal Component Analysis, unsupervised pattern recognition with K-means and rendering of the gray scale backscattering OCT data which is superimposed with a colormap that is based on the results of the pattern recognition algorithm. Our set up provides a spectral range from 650-950nm and is optimized to suppress chromatic errors. In a proof-of-principle attempt, we already achieved additional spectroscopic contrast in phantom samples including scattering microspheres of different sizes and ex vivo biological tissue. This is an important step towards a system for real time spectral analysis from OCT data, which would be a powerful diagnosis tool for many diseases e.g. cancer detection.

8592-42, Session 9

Simulating the optical coherence tomography via numerical solutions of Maxwell's equations

Snow H. Tseng, Yu-Ting Hung, National Taiwan Univ. (Taiwan)

Here we attempt to simulate the macroscopic light scattering phenomenon of Optical Coherence Tomography. Numerical solutions of Maxwell's equations are calculated to accurately account for phase and amplitude of light. The reported simulation enables qualitative and quantitative characterization that may provide important information for future development of this technique.

8593-1, Session 1

Novel role of cardiac function in the development of congenital heart defects associated with Fetal Alcohol Syndrome

Ganga H. Karunamuni, Shi Gu, Lindsy M. Peterson, Zhao Liu, Yves T. Wang, Quinn McHale, Katherine Mai, Michael W. Jenkins, Michiko Watanabe, Andrew M. Rollins, Case Western Reserve Univ. (United States)

Over 500,000 American women per year report drinking alcohol during pregnancy, and even low levels of prenatal alcohol/ethanol exposure can produce birth defects. 54% of live-born children with Fetal Alcohol Syndrome (FAS) present with cardiac anomalies, including valvuloseptal defects. While the mechanisms of ethanol exposure have been studied extensively, most studies fail to consider the role of altered cardiac function in producing congenital heart defects. It is already known that changes in hemodynamics can profoundly affect cardiac development. We hypothesize that ethanol exposure affects cardiovascular hemodynamics early, and thus contributes to the development of cardiac structural defects at late stages. We employed optical coherence tomography, allowing us to accurately map hemodynamic changes and the resultant structural abnormalities in the live embryo at very early stages, when the trajectory to heart defects can begin. In our studies, avian embryos were exposed to ethanol during gastrulation stages, when the embryos were most vulnerable for the induction of cardiac birth defects. Our preliminary data indicate that ethanol exposure results in increased retrograde flow and increased oscillatory shear stress, leading to smaller cardiac cushions and eventually abnormal valve phenotypes. These studies will demonstrate that function analyses can be used as early, sensitive gauges of cardiac normalcy and abnormalities, and clarify the role of abnormal cardiac function in producing FAS-related congenital heart defects.

8593-2, Session 1

High-resolution time-resolved 3D optical microscopy inside the beating zebrafish heart using prospective optical gating

Jonathan M. Taylor, Christopher D. Saunter, John M. Girkin, Gordon D. Love, Durham Univ. (United Kingdom)

The ability to image inside the naturally-beating zebrafish heart is becoming increasingly attractive for developmental and functional biological investigations. From an optical perspective this presents two challenges: not only is high resolution 3D imaging in bulk living tissue difficult due to optical aberrations and phototoxic considerations, but in the heart there is the additional difficulty that the tissue is constantly moving due to the heartbeat. This requires some form of synchronization in order to acquire consistent 3D datasets.

We will show results from our real-time synchronized selective plane illumination microscope (SPIM), demonstrating time-resolved 3D fluorescence images ("4D" imaging) of the naturally-beating embryonic zebrafish heart. This promises new potential for studying cardiac development due to the non-invasive character of our technique. We will describe our solution to the synchronization problem for 3D imaging, which requires particular refinements to maintain precise synchronization while scanning through the sample, and compare it to alternative techniques based around post-acquisition processing. We will also describe the extension of this technique to synchronized optical intervention, where a focused laser beam is used to optically switch or selectively damage localized regions of tissue for optogenetic and injury recovery studies.

Our robust technique for real-time optical gating in the beating heart opens up the ability to perform a wide range of optical imaging and intervention procedures on the beating zebrafish heart exactly as if the heart had been artificially stopped, but sidestepping this undesirable interference with the heart and instead allowing the heart to beat as normal.

8593-3, Session 1

Measurement of contractile wave propagation in the developing heart tube using OCT

Lindsy M. Peterson, Shi Gu, Ganga H. Karunamuni, Yves T. Wang, Pei Ma, Michael W. Jenkins, Andrew M. Rollins, Case Western Reserve Univ. (United States)

Alterations to the contraction wave of the developing heart can greatly influence the hemodynamics in the heart, which can lead to congenital heart defects later in development. To better understand changes in contraction in vivo, a non-invasive 3-D imaging method is needed capable of measuring the entire heart tube. We previously measured contraction by acquiring 2-D longitudinal sections through the center of the heart. However a 2-D plane cannot section the exact center, throughout the heart. Through the acquisition of multiple 3-D OCT volumes we are able to accurately obtain sections along the centerline of the heart tube. These sections are then used to calculate the contractile wave velocity at each position along of the heart tube. To validate these metrics, the calculated contraction wave velocities are compared with conduction velocities obtained from optical mapping of excised embryonic hearts of similar stages, showing no significant differences. This metric can be used to analyze changes in the developing heart that result from various perturbations without the need to sacrifice the embryo. As an example, stage 14 embryonic hearts were imaged prior to and during optical pacing (at 50% above intrinsic rate). The measurements showed no significant changes in the velocity of the contraction wave at the ventricle of the heart tube, consistent with a normal, intrinsic beat. This metric will be utilized in longitudinal investigations of various disease models, such as fetal alcohol syndrome.

8593-4, Session 1

in vivo functional imaging of blood flow and wall strain rate in developing outflow tract using ultrafast spectral domain optical coherence tomography

Peng Li, Xin Yin, Univ. of Washington (United States); Liang Shi, Sandra Rugonyi, Oregon Health & Science Univ. (United States); Ruikang Wang, Univ. of Washington (United States)

During cardiac cycle, cardiac wall and flowing blood constantly interact with each other, which determines the biomechanical environment that in turn regulates cardiac development. However, a dilemma exits when studying the dynamic interaction between cardiac wall and blood flow because the motion of cardiac wall is relatively slow compared to the fast flow of blood. The slow motion of the cardiac wall requires the OCT system operating at a slower imaging speed, whereas the fast motion of blood demands a faster imaging speed. In this study, we report the use of an ultrafast 1310 nm dual-camera spectral domain optical coherence tomography (SDOCT) system to characterize/image, in parallel, the dynamic radial strain rate (SR) of the myocardial wall and the Doppler velocity of the flowing blood within an in vivo beating chick embryo. The OCT system operates at 184 kHz line scan rate, providing the flexibility of imaging the fast blood flow (up to ~43.95 mm/s Doppler velocity) and the slow tissue deformation (-2.2 to 2.4 s-1 strain rate) within one scan.

We use the phase-shift between adjacent B-scans to quantify the slow wall motion, while the imaging speed of the system is not sacrificed to measure the velocity of the fast blood flow that is assessed by the phase shift between adjacent A-lines within a B-scan. The ability to simultaneously characterize cardiac wall and blood flow provides a useful approach to quantitatively understand the interactions between wall dynamics and hemodynamics during cardiac development. Particularly, the biomechanical characterization of cardiac wall is of fundamental importance to predict the hemodynamic behavior.

8593-5, Session 1

Changes in strain and blood flow in the outflow tract of chicken embryo hearts observed with spectral domain optical coherence tomography after outflow tract banding

Zhenhe Ma, Linlin Du, Xiaoxiao Jiang, Qiaoyun Wang, Zhongdi Chu, Xuan Zang, Fengwen Wang, Northeastern Univ. at Qinhuangdao (China); Ruikang Wang, Univ. of Washington (United States)

Optical coherence tomography (OCT) is a non-invasive imaging modality with high resolution (5 to 20μm), suited to study early cardiovascular development. Alterations in hemodynamic conditions during early development are known to lead to cardiac defect, presumably as a result of changes in cardiac biomechanics produced by the alternations. In this paper, we demonstrate the use of a spectral domain OCT in visualizing and quantifying changes in cardiac wall strain and blood-flow velocities under normal and altered hemodynamic conditions in chicken embryos at an early stage of development, focusing on the heart outflow tract (OFT). The OCT system employed acquired simultaneously structural and blood-flow images at a rate of 140 frames/s with a axial resolution of ~14μm. OCT imaging allowed in vivo evaluation strain and strain rate of the myocardium of the OFT through analyzing the periodic variation of the myocardial wall thickness calculated from real-time serial OCT images. We found that alterations in hemodynamic conditions, through OFT banding, Changed strain and blood-flow velocities through the OFT, as expected. Our results therefore establish the utility of spectral domain OCT to study the influence of hemodynamic conditions on heart development in vivo chicken embryo models.

8593-6, Session 2

High resolution optical mapping of optically paced embryonic quail hearts

Yves T. Wang, Shi Gu, Case Western Reserve Univ. (United States); Andreas A. Werdich, MetroHealth Medical Ctr. (United States); Andrew M. Rollins, Michael W. Jenkins, Case Western Reserve Univ. (United States)

Recently, we demonstrated pacing of intact embryonic hearts using a near-infrared laser as an alternative to electrical point stimulation, which creates artifacts that impede recording in small tissues due to millimeter-long electrical space constants in cardiac tissue. Here, for the first time, we demonstrate that optical mapping of surface electrical activity can be accomplished in embryonic hearts that are paced with optical point stimulation.

Excised embryonic quail hearts were stained with voltage-sensitive di-4-anepps and contractions were stopped with cytochalasin D. Pacing was achieved using a 1440-nm diode laser coupled through a single mode fiber and focused to a 10-?m spot near the inflow tract. High resolution optical mapping under both sinus and paced conditions was obtained using a microscope with a 10x objective and a 128x128-element CCD camera.

Surface action potentials under paced conditions were obtained away from the pacing site. Action potential shape was similar between paced and unpaced hearts. Electrical activity near the pacing site was obscured due to a thermal lensing artifact with a length constant of 56?m. However, some of the action potentials affected can be recovered with additional processing.

Surface electrical activity from embryonic hearts can be obtained with optical mapping during optical pacing. The artifact from optical pacing was an order of magnitude smaller than the electrical artifact from traditional pacing. Additionally, optical pacing allows for easily positioned point stimulation. The protocol developed here can be used to further study the electrophysiology of developing hearts.

8593-7, Session 2

Optical mapping of freely beating embryonic hearts

Pei Ma, Yves T. Wang, Shi Gu, Michael W. Jenkins, Andrew M. Rollins, Case Western Reserve Univ. (United States)

Optical mapping is a common technique for measuring electrical activity using voltage-sensitive fluorescent dyes (e.g. di-4-ANEPPS). Because heart motion changes the location of signal sources during imaging, making Action Potential traces ambiguous, optical mapping conventionally uses an excitation-contraction (EC) uncoupler (e.g. cytochalasin D, blebbistatin) to stop motion by abolishing the contraction. However, in data interpretation we must take into account the possibility that EC uncouplers can also affect calcium handling, ion channel kinetics and action potential characteristics. Although previous motion correction schemes for optical mapping have been attempted in adult hearts, they have had limited success and not been attempted in early-stage embryo hearts. We will, for the first time, demonstrate optical mapping at high resolution (128x128 pixels, 880 ?m field of view, 500 fps) of a freely beating embryonic quail heart (Hamburger-Hamilton stage 13). The 2-D motion correction algorithm employs a B-spline non-rigid image registration that is based on a normalized cross-correlation similarity metric. This correction allows us to recover the upstroke of the action potential, thus enabling the calculation of activation maps and conduction velocities. The activation maps taken before and after the administration of cytochalasin D are very similar. In addition, the conduction velocities in the ventricle (13.82 mm/sec) and outflow tract region (2.91 mm/sec) are comparable to the stopped heart (15.36 and 2.67 mm/sec respectively). Overall, this method has shown great promise in obtaining meaningful measurements in freely beating embryonic hearts and may have potential future use allowing in vivo studies with a variety of fluorophores.

8593-8, Session 2

Hemoglobin contrast subtraction angiography reveals quantitative defects in embryo heart function generated by targeted sarcomere gene knockdown

Engin Deniz M.D., Yale Univ. (United States); Stephan Jonas, Yale School of Medicine (United States) and RWTH Aachen (Germany); Mustafa K. Khokha M.D., Michael A. Choma M.D., Yale School of Medicine (United States)

Although in vivo cross-sectional imaging of embryo hearts is of increasing importance, microangiography is infrequently used. Barriers to the widespread use of microangiographic methods are (a) the technically challenging microinjection of exogenous contrast agents and (b) the lack of quantitative methods for extracting physiological measures from microangiographic movies. We recently demonstrated a novel, noninvasive technique called hemoglobin contrast subtraction angiography (HCSA) that overcomes these barriers in optically-accessible embryo hearts. HCSA uses the wavelength-varying absorption of hemoglobin in a subtraction angiography framework as source of flow

contrast. Here, we validate HCSA in quantitative flow imaging and demonstrate the use of quantitative HCSA in phenotyping intermediate physiological defects in genetically-modified Xenopus embryo hearts. We used the Otsu method on HCSA images to classify pixels as blood or background based on (a) the intensity histogram of the pixels and (b) an assumption of two underlying populations of pixels. This approach yields a receiver-operator characteristic curve with an area under the curve of ~95%. After incorporating our processing methods into an HCSA software package, we characterized physiological defects in Xenopus embryo hearts after knocking down expression of myosin heavy chain 6, a sarcomeric protein associated with congenital heart defects. At moderate doses, morpholino knockdown moderately reduces ejection fraction, while at higher doses ejection fraction is severely impaired. Thus, HCSA can be used to quantify defects in embryo heart physiology in the setting of targeted genetic manipulation. Ongoing work includes modifying candidate genes for congenital cardiomyopathies and quantifying embryonic heart response to pharmacological treatment.

8593-9, Session 2

Ultra-high frequency ultrasound biomicroscopy and high throughput cardiovascular phenotyping in a large scale mouse mutagenesis screen

Xiaoqin Liu, Richard J. B. Francis, Kimimasa Tobita, Univ. of Pittsburgh (United States); Andrew J. Kim, Univ. of Pittsburgh School of Medicine (United States); Linda Leatherbury, Children's National Medical Ctr. (United States); Cecilia W. Lo, Univ. of Pittsburgh (United States)

Ultrasound biomicroscopy (UBM) is ideally suited for phenotyping fetal mice for congenital heart disease (CHD), as imaging can be carried out noninvasively to provide both hemodynamic and structural information essential for CHD diagnosis. Using the UBM (Vevo 2100; 40Hz) in conjunction with the clinical ultrasound system (Acuson Sequioa C512; 15Hz), we developed a two-step screening protocol to scan 46,270 fetuses derived from 1318 G1 ENU mutagenized pedigrees. We detected cardiac defects in 1,722 (3.7%) fetuses. A high incidence (40.8%) of prenatal lethality was observed in fetuses with cardiac defects. A wide spectrum of CHD was detected by the UBM, which were subsequently confirmed with follow-up necropsy and histopathology examination with episcopic fluorescence image capture. CHD observed included outflow anomalies, left/right heart obstructive lesions, septal/valvular defects and cardiac situs anomalies (all $P<0.01$). Most commonly found was ventricular septal defect, while double outlet right ventricle/overriding aorta was the most prevalent complex CHD found. Surprisingly, 54.4% of mutant lines exhibited laterality defects, with 92.3% of fetuses with heterotaxy exhibiting complex CHD. Most striking was recovery of the first mutant mouse models of hypoplastic left heart syndrome. Overall, 90 mutant lines with CHD were recovered, 81 of which were identified by fetal ultrasound. Our analyses showed the UBM was better at assessing cardiac structure and blood flow profiles, while conventional ultrasound allowed higher throughput low-resolution screening. Our study showed the integration of conventional clinical ultrasound imaging with the UBM for fetal mouse cardiovascular phenotyping can maximize the detection and recovery of CHD mutants.

8593-10, Session 3

In vivo imaging of zebrafish from embryo to adult stage with optical projection tomography

Andrea Bassi, Luca Fieramonti, Cosimo D'Andrea, Gianluca Valentini, Rinaldo Cubeddu, Sandro De Silvestri, Giulio Cerullo, Politecnico di Milano (Italy); Efrem Foglia, Franco Cotelli, Univ. degli Studi di Milano (Italy)

Optical Projection Tomography (OPT) is a three-dimensional imaging technique, which is particularly suitable for studying millimeter sized biological samples and organisms. Similarly to x-ray computed tomography, OPT is based on the acquisition of several optical transmission images of the sample at different orientations. The acquired projections are processed to reconstruct three-dimensionally the volume of the sample, typically using a back-projection algorithm.

This technique has been recently applied to in-vivo imaging of zebrafish (Danio rerio). The instrument and the protocol for in vivo imaging of a whole zebrafish embryo are presented here. Moreover, a method for label-free reconstruction of its vasculature is described.

Nevertheless, in vivo OPT is usually limited by tissue light scattering, especially when zebrafish at the juvenile and adult stage are under study. To reduce this problem, we present Time-Gated Optical Projection Tomography (TGOPT), a technique able to reconstruct adult zebrafish internal structures without staining or chemical clearing procedures. The use of a time gating mechanism, based on non-linear optical upconversion of an infrared ultrashort laser pulse, allows the rejection of multiply scattered photons and the exclusive detection of ballistic ones within a 100 fs temporal gate. This results in a strong increase of contrast and resolution with respect to conventional OPT. Artifacts in the reconstructed images are reduced as well. We show that TGOPT is suited for imaging the skeletal system and nervous structures of adult zebrafish.

8593-11, Session 3

3D whole animal imaging of zebrafish at cellular resolution using synchrotron microCT

Keith C. Cheng, Xuying Xin, Penn State Hershey (United States); Darin P. Clark, Penn State Hershey (United States) and Duke Univ. (United States); Xianghui Xiao, Francesco De Carlo, Argonne National Lab. (United States); Gordon Kindlmann, The Univ. of Chicago (United States); Patrick J. La Riviere, The Univ. of Chicago Medical Ctr. (United States)

We are optimizing 3D imaging of a whole vertebrate animal at peri-micron voxel resolution to facilitate phenotypic analysis. Light-based imaging at such cell resolutions is impeded by greater than about 200 micron imaging depth, and by pigmented cells. These limitations do not affect tomographic tomographic X-ray imaging. Since monochromaticity and parallel beam physics can enhance resolution, and high flux enhances speed, microCT imaging is being pursued at the 7.4 GeV synchrotron at Argonne National Labs. We are imaging zebrafish because of its power as an experimental model, and a size that makes whole-animal imaging possible. Heavy metal staining of fixed samples and tomographic projections at 1500 angles over 180 degrees has allowed us to achieve isotropic voxel resolutions of 0.743 and 1.43 um, at fields of view of ~1.5 and 2.9 mm, respectively; these resolutions are sufficient to reveal the identity of most cell types. From merged, multiple image segments into whole animal files, we have generated complete sets of two-dimensional digital slices at multiple orthogonal orientations, and created movie visualizations. To our knowledge, this represents the first example of a whole vertebrate animal 3D imaging at cell resolutions beyond embryogenesis. It is possible to view every slice of a fish at multiple orientations. Improvements in optics, high throughput sample preparation, and sample handling, and the development of high-throughput computational image processing, segmentation, and phenotyping tools would greatly increase the value and throughput of morphological phenotyping for phenome projects for probing the functions of genes and the toxicity of chemicals.

8593-12, Session 3

Confocal episcopic fluorescence image capture (CEFIC) provides unparalleled 3D imaging of both anatomical development and molecular signaling within the developing embryo

Richard J. B. Francis, Univ. of Pittsburgh (United States); Rod Bunn, Vashaw Scientific, Inc. (United States); Andy Reidler, Leica Microsystems Inc. (United States); Cecilia W. Lo, Univ. of Pittsburgh (United States)

Confocal laser microscopy provides excellent visualization of cells and tissues, but the shallow laser penetration depth restricts its use in visualizing complex tissue architecture. In this study, we developed the combined use of confocal imaging with automated histological serial sectioning to generate high resolution registered 2D histological image stacks suitable for anatomical and/or molecular phenotyping of whole animals, embryos, or tissue/organ systems.

A custom CEFIC system was fabricated by adapting a Lecia LSI confocal scan head onto a Lecia SM2500 microtome. Paraffin embedded tissue samples were sectioned and imaged using the CEFIC system using endogenous tissue autofluorescence. Serial 2D image stacks obtained from imaging the block face were digitally resliced and reconstructed using the Osirix software package. Using CEFIC 2D image stacks and 3D volumes, we can detect a wide spectrum of structural birth defects in fetal/neonatal mice, including malformations difficult to ascertain by standard histology, such as tracheoesophageal fistulas, and small atrial/ventricular septal defects. We also showed the use of CEFIC to examine the complex anatomy of zebrafish adult animals and embryos, and demonstrate the feasibility to combine CEFIC with whole mount immunostaining or the imaging of fluorescently tagged proteins to delineate gene/protein expression profile in 3D dimensions for characterizing cell lineage and molecular signaling profile.

In summary, CEFIC can provide high-resolution 3D anatomical information that can be combined with cell and molecular profiling to delineate cell and molecular signaling profile. Such studies will prove invaluable for elucidating the developmental etiology of disease.

8593-13, Session 3

Living pupa imaging with high-resolution FFOCT during the 96 hours of metamorphosis

Adriano Burcheri, Ecole Supérieure de Physique et de Chimie Industrielles (France); Thomas Riemensperger, Univ. Göttingen (Germany); Serge Birman, A. Claude Boccara, Ecole Supérieure de Physique et de Chimie Industrielles (France)

Visualizing the dynamic formation of organs in Drosophila melanogaster has so far been limited by the highly scattering pupal case surrounding the insect during its metamorphosis (i.e the transition from larva to adult fly).

Current optical methods such as confocal microscopy remain inadequate for in-vivo imaging over an extended period of time; limitations include vast amounts of laser light, photo-bleaching, or heat. Alternative approaches either require tedious reconstruction of postmortem specimens or are still trading resolution for penetration depth (e.g. mesoscopic fluorescence tomography or MRI techniques).

We present a study showing the feasibility of Full-Field OCT to perform in-vivo measurements at 80 µm in depth with a 1.5 µm resolution during the four days of metamorphosis. To our knowledge, these are the first images able to visualize the dynamic series of events at the micron-scale in a living pupa.

The method requires to maintain the insect's environment stable during the four days of measurements. The combination of a thin layer of olive oil and an appropriate pressure were key factors. In addition, a precise control of the illumination was crucial to avoid overexposure to light and heat, although the beam projects only 2 mW/mm2 of light power intensity. It was done by short illumination periods every 6 hours.

Results allow to identify the development of undifferentiated nest of cells (i.e. imaginal discs) to fully formed adult organs (e.g. leg discs or maxillary palps) with an unprecedented micron-scale resolution.

8593-14, Session 3

OCT guided microinjections for mouse embryonic research

Kirill V. Larin, Univ. of Houston (United States); Saba H. Syed, Baylor College of Medicine (United States); Andrew J. Coughlin, Duke Univ. (United States); Shang Wang, Univ. of Houston (United States); Jennifer L. West, Duke Univ. (United States); Mary E. Dickinson, Irina V. Larina, Baylor College of Medicine (United States)

Optical coherence tomography (OCT) is gaining popularity as live imaging tool for embryonic research in animal models. Recently we have demonstrated that OCT can be used for live imaging of cultured early mouse embryos (E7.5-E10) as well as later stage mouse embryos in utero (E12.5 to the end of gestation). Targeted delivery of signaling molecules, drugs, and cells is a powerful approach to study normal and abnormal development, and image guidance is highly important for such manipulations. Here we demonstrate that OCT can be used to guide microinjections of gold nanoshells (OCT contrast agent) and fluorescent markers in live mouse embryos. This approach can potentially be used for variety of applications such as guided injections of contrast agents, signaling molecules, pharmacological agents, cell transplantation and extraction, as well as other image-guided micromanipulations.

8593-15, Session 4

Computational recognition and quantification of ciliary beat patterns from high-speed digital videomicroscopy

Shannon Quinn, John Durkin, Maliha Zahid, Univ. of Pittsburgh (United States); Richard J. B. Francis, Cecilia W. Lo, Univ. of Pittsburgh Medical Ctr. (United States); Chakra Chennubhotla, Univ. of Pittsburgh (United States)

Primary ciliary dyskinesia (PCD) is a rare disorder in which motile cilia in the airway show abnormal dyskinetic motion that can cause mucus clearance defects and sinopulmonary disease. The current diagnostic standard relies on manual inspection of nasal biopsies using high-speed videomicroscopy to identify abnormal ciliary motion. However, this process is laborious, subjective, and error-prone due to variability in normal/abnormal motion phenotypes. Here we present a novel computational approach for visual recognition and quantitative identification of ciliary motion phenotypes using automated imaging and machine learning algorithms. Ciliary motion closely resembles familiar motion in nature, such as flickering flames or rippling water. Using well-established computer vision and machine learning algorithms, we analyzed such dynamic textures. In particular, we use image velocity invariants at each pixel, computed from ciliary motion videos. Some of these videos are manually annotated to provide a basis for evaluating our algorithm, but significant variability of motion patterns present in each region of interest (ROI) precluded associating a single motion type with the video. This motivates the proposed computational pipeline where we perform a series of unsupervised clustering steps on the image velocity invariants, both within one ROI and then across multiple ROIs, to establish a small number of canonical motion signatures associated with each phenotype. Our clustering pipeline allows us to i) define the different types of ciliary motion, ii) identify the locations in each video where such motion types exist, and iii) classify the motion patterns in new, unannotated videos, enabling the objective diagnosis of PCD.

8593-16, Session 4

Quantitative imaging of the development of directional cilia-driven fluid flow using optical coherence tomography (OCT)-based particle tracking velocimetry

Brendan Huang, Stephan Jonas, Mustafa K. Khokha M.D., Michael A. Choma M.D., Yale School of Medicine (United States)

Development of a ciliated respiratory epithelium is important for respiratory health but is incompletely understood. One important feature is the emergence of directional fluid flow, which occurs in specific developmental timeframes. Establishment of directionality depends upon a well-defined planar cell polarity (PCP) and coupling of hydrodynamic forces, both demonstrated using the ciliated skin of Xenopus embryos. We have previously shown quantification of ciliary performance using optical coherence tomography (OCT)-based particle tracking velocimetry. This technique is advantageous over traditional fluorescent microscopy-based methods because OCT is cross-sectional, allowing quantification of vectorial flow fields and related parameters (e.g. shear forces), as well as more detailed quantification of laminar flow that is highly dependent upon distance from a ciliated surface. Building on this work, we investigated flow-field dynamics in Xenopus embryos. We first showed that increasing viscosity by a factor of 2 and 3 leads to a 2.3- and 3.1-fold decrease, respectively, in flow tangential to the surface, a derived parameter that reflects transport along a surface. We next quantified cilia-generated flow in embryos from Nieuwkoop-Faber stages 20 to 28, the period over which PCP is established. We calculated velocities through orthogonal cross sections, allowing us to assess flow polarity along all three anatomic axes. We found that a ventral-dorsal and anterior-posterior flow begins at stage 23-24 and rapidly increases to an average tangential speed of 150-200 micrometers/s at stage 28. Our results are consistent with the rapid establishment of PCP. Ongoing work includes manipulation of motor proteins and PCP genes.

8593-17, Session 4

Label free quantitative analysis of developing neural networks

Mustafa A. Mir, Univ. of Illinois at Urbana-Champaign (United States); Anirban Majumder, Steven Stice, The Univ. of Georgia (United States); Gabriel Popescu, Univ. of Illinois at Urbana-Champaign (United States)

The growth and formation of neural networks is a highly complex and dynamic process and although it is of fundamental importance to neuroscience it is poorly understood. To date, the mostly widely used method for studying this process is through the use of fluorescence labeling which usually requires fixation and the effects of which on the culture itself are unknown. However, it is known that neural networks are far from static, with connections constantly being made and lost, especially during the early stages of development. Thus, to truly understand this process it is necessary to use a method that allows for constant long term monitoring at the single cell, cluster and population levels. Here we show that Spatial Light Interference Microscopy (SLIM), a recently developed, broadband, quantitative phase imaging method is ideal for understanding this phenomenon. Using SLIM, we followed a population of human stem cell derived neurons for 24 hours after they were plated. During this time the culture shows a marked evolution from small unconnected clusters to a well-established and relatively stable network. We quantified this evolution in terms of dry mass growth, light scattering, mass transport signatures and cell motility. The results show that SLIM can be used to characterize the maturity of a neural network in terms of spatial organization, growth rate and level of connectivity. Such a label-free technique will allow for a deeper understanding of neural development while being more practical and accessible than current approaches.

8593-18, Session 4

Effect of alcohol exposure on fetal brain development

Narendran Sudheendran, Univ. of Houston (United States); Shameena Bake, Texas A&M Health Science Ctr. (United States); Karishma Prasad, Univ. of Houston (United States); Rajesh C. Miranda, Texas A&M Health Science Ctr. (United States); Kirill V. Larin, Univ. of Houston (United States)

Alcohol consumption during pregnancy can be detrimental to the brain development in fetuses. This study investigates effects on embryonic brain development, whose mother were intragastrically gavaged with ethanol. These embryos were fixed and imaged using a swept-source optical coherence tomography (SSOCT) system. 3D images of alcohol-treated and control embryo brains were obtained and the volume of the right and left ventricles were measured to be 0.35 and 0.15 mm3, respectively. The results suggest that the ventricle volumes of brain are much larger in the alcohol treated embryos as compared to control embryos indicating alcohol-induced developmental delay.

8593-19, Session 5

Time-lapse imaging of live embryos reveals tissue movements drive cardiac progenitor displacements during avian heart morphogenesis

Anastasiia Aleksandrova, Andras Czirok, The Univ. of Kansas Medical Ctr. (United States); Rusty Lansford, Children's Hospital Los Angeles (United States); Charles D. Little, Brenda Rongish, The Univ. of Kansas Medical Ctr. (United States)

Transformation of planar cardiac progenitor fields into a midline tubular heart, involves cellular and tissue movements in three dimensions. Despite much investigation, the driving forces behind the cardiac progenitor movements are not understood. We investigated the motion of fluorescently-tagged myocardial progenitors in live quail embryos using wide-field time-lapse imaging and custom imaging code. The fibronectin ECM environment for myocardial movement was visualized with microinjected fluorescent antibodies, while endocardial progenitors were labeled with transgenic expression of Tie1::H2B-YFP. The imaging period encompassed the motion of myocardial progenitors from primary heart field(s) to the midline and continued through early heart looping. We used computational methods to calculate the relative contribution of cell autonomous motility versus convective tissue movements in the assembly of the myocardial tube using object tracing and particle image velocimetry. These quantitative data indicate the degree of cell autonomous motility displayed by myocardial progenitors is limited, with convective tissue movements driving their displacements to the midline. Further, concomitant with the onset of cardiac tube bending, myocardial primordia undergo a coordinated displacement in the posterior-ventral direction ("rotation"), suggesting a possible connection between these two processes. Interestingly, this rotation was abrogated following the introduction of exogenous VEGF165, but proceeded in separated primordia following incision-induced cardia bifida. Ongoing studies using myocardial-specific expression of dominant negative and constitutively active isoforms of RhoA will assess the relationship between myocardial progenitor displacements and concomitant regression of the anterior intestinal portal. This work seeks to elucidate the cellular and tissue mechanisms driving the bulk movement of cardiac progenitors.

8593-20, Session 5

Combined lineage mapping and fate profiling with NLOM-OCM using sub-10-fs pulses

Holly Gibbs, Colin R. Dodson, Yuqiang Bai, Arne C. Lekven, Alvin T. Yeh, Texas A&M Univ. (United States)

We have developed a combined NLOM-OCM method using ultrashort sub-10-fs pulses to study the behavior of cell lineages and their gene expression profiles in zebrafish. First, time-lapse NLOM is used to capture both embryo morphology (broadly excited autofluorescence) and cell lineage dynamics (eGFP reporter). The embryo is then fixed and an in situ hybridization performed, the final step being the deposition of the NBT-BCIP stain where a gene of interest is being expressed. Combined NLOM-OCM is then used to capture the expression pattern with three dimensional resolution (OCM) and morphology (NLOM). These two data sets independently acquired from the same embryo can then be merged using morphological landmarks. We are currently using this approach to study the dynamics of the wnt1 lineage at the midbrain-hindbrain boundary (MHB) and to understand fate alterations of this lineage in the ace(fgf8a) mutant background. It is already known that wnt1 expression is lost at the anterior ring of cells at the MHB, and our preliminary results from lineage tracing with NLOM-OCM suggest these wnt1 cells migrate from the MHB into the midbrain. Presumably as they do so, these cells acquire a new fate reflected by changes in gene expression. After lineage tracing, we will perform combined NLOM-OCM with a set of midbrain gene markers to more precisely determine the altered fate of the wnt1 MHB lineage in the absence of fgf8a. The accuracy of co-registration will be tested with combined in-situ hybridization and immunohistochemistry for eGFP.

8593-21, Session 5

Tissue dynamic imaging of live porcine cumulus-oocyte complexes

Ran An, John J. Turek, Zoltan Machaty, David D. Nolte, Purdue Univ. (United States)

Freshly-harvested porcine oocytes are invested with cumulus granulosa cells in cumulus-oocyte complexes (COCs). The cumulus cell layer is usually too thick to image the living oocyte under a conventional microscope. Therefore, it is difficult to assess the oocyte viability. The low success rate of implantation is the main problem for in vitro fertilization [1]. In this paper, a new dynamic imaging technique called Tissue Dynamic Imaging (TDI) provides a non-invasive way to monitor the COCs before and after maturation. TDI shows a change of intracellular activity during oocyte maturation, and a measures dynamic contrast between the cumulus granulosa shell and the oocytes. TDI also shows a difference in the response spectrograms between oocytes that were graded into quality classes. TDI is based on short-coherence digital holography. It uses intracellular motility as the endogenous imaging contrast of living tissue. Localized dynamic speckle is used to generate localized frequency versus time voxel spectrograms to produce functional spectral responses as the fingerprint of cellular motility [2]. TDI presents a new approach for cumulus-oocyte complex assessment.

[1] A. Van Soom, B. Mateusen, J. Leroy, and A. De Kruif, “Assessment of mammalian embryo quality: what can we learn from embryo morphology?,” Reprod Biomed Online, vol. 7, pp. 664-670, 2003.

[2] D. D. Nolte, R. An, J. Turek, and K. Jeong, “Holographic tissue dynamics spectroscopy,” Journal of Biomedical Optics, vol. 16, Aug 2011.

8593-22, Session 5

Bioconjugated gold nanomarkers for imaging in cytology and reproduction biology

Stephan Barcikowski, Christoph Rehbock, Daniel Werner, Lisa Gamrad, Univ. Duisburg-Essen (Germany); Ulrike Taylor, Wilfried Kues, Detlef Rath, Friedrich-Loeffler-Institut (Germany)

Due to their high quantum yield, Au nanoparticles (NPs) are excellent nanomarkers which exhibit an enhanced bleaching stability and biocompatibility compared to organic dyes and quantum dots. In this work mono- and bivalently conjugated AuNPs were examined for their applicability as nanomarkers in cell imaging and sperm sexing experiments. The NPs were functionalized with cell penetrating peptide (CPP) to cross the cell membrane and with nucleotides for hybridization with specific DNA sequences. This hybridization leads to a selective particle aggregation, which may result in a detectable shift of the plasmon resonance band [1] and the aggregates may even be detected by confocal microscopy provided their size exceeds 60 nm [2]. Particularly sperm cell penetration is challenging due to complex membrane structures and therefore high ligand loads on the NPs may be required. For this reason NP synthesis was done using an advanced laser based method providing particles with highly charged ligand-free surfaces, which provided 5 times higher ligand loads during bioconjugation compared to chemically synthesized particles functionalized using ligand exchange [3]. Additionally, bioconjugation with different CPPs was thoroughly and systematically studied. Particularly the influence of the peptide´s sequence, length, charge, and concentration on bioconjugate stability and cell-penetrating properties were examined.

[1] Klein et al., J. Biomed. Opt. 15, 3 (2010)

[2] McKenzie et al., 2367-2369 (2008)

[3] S. Petersen, S. Barcikowski. J. Phys. Chem. C. 113, 19830-19835 (2009)

8593-23, Session PSun

Computational analysis of the spatial distribution of mitotic spindle angles in mouse developing airway

Nan Tang, Wallace F. Marshall, Univ. of California, San Francisco (United States)

Investigating the spatial information of cellular processes in tissues during mouse embryo development is one of the major technical challenges in development biology. Many imaging methods are still limited to small volumes of tissue due to tissue opacity, light scattering and the availability of advanced imaging tools. For analyzing the mitotic spindle angle distribution in developing mouse airway epithelium, we determined spindle angles in mitotic epithelial cells on serial sections of whole airway of mouse embryos. We then developed a computational image analysis method to optimally align sections so as to obtain spindle angle distribution in three dimensional airways reconstructed from the data obtained from all serial sections. From this study, we were able to understand how mitotic spindle angles are distributed in a whole airway tube. This analysis provides a potentially fast, simple and inexpensive alternative method to quantitatively analyze cellular process at subcellular resolution. Furthermore, this analysis is not limited to the size of tissues, which allows us to obtain three dimensional and high resolution information of cellular processes in cell populations deeper inside intact organs.

8593-24, Session PSun

Birefringence analysis of cultured and imitation pearls using polarization-sensitive swept-source OCT

Jae Hwi Lee, Eun Jung Min, Kwan Seob Park, Byeong Ha Lee, Gwangju Institute of Science and Technology (Korea, Republic of)

We present a birefringence analysis method based on polarization-sensitive swept-source optical coherence tomography (PS-SS-OCT) for distinguishing pearls. To evade intricacy of the polarization control of a

fiber-based PS-SS-OCT system, the system was constructed in a bulk type. And for the sample scanning, since pearls are in a round shape, a rotation stage was used. With the system, the birefringence of some cultured pearls, such as south sea and Akoya pearls, and imitation pearls are analyzed and compared. PS-SS-OCT surely shows well developed birefringence pattern with the cultured pearls; whereas interestingly, in the imitation pearls birefringence pattern is not appeared. Therefore, PS-SS-OCT could be used to identify the cultured pearls from imitation pearls. In addition, it is thought that the phase retardation information including the optical intensity profile of PS-SS-OCT can distinguish among various cultured pearls also. The growth condition of a pearl gives rather unique birefringence pattern.

8593-25, Session PSun

Multicolor two-photon excitation and wavefront control for imaging developing tissues

Emmanuel Beaurepaire, Pierre Mahou, Maxwell Zimmerley, Jun Zeng, Ecole Polytechnique (France); Karine Loulier, Katherine Matho, Institut de la Vision (France); Marie-Claire Schanne-Klein, Ecole Polytechnique (France); Xavier Morin, Ecole Normale Supérieure (France); Jean Livet, Institut de la Vision (France); Willy Supatto, Delphine Débarre, Ecole Polytechnique (France)

Understanding the dynamics at play in embryogenesis requires tissue-scale measurements of cell dynamics and function. Multiphoton microscopy is attractive for deep imaging, but multiparametric imaging of evolving tissue remains challenging. We discuss advances in multicolor multiphoton excitation [1] and aberration correction [2].

A number of multicolor genetic labeling methods are currently emerging for reconstructing connectivity and tracking cell migrations or lineage during development [3]. Efficient live/volume imaging methods compatible with these methods are required. We introduce a strategy that provides optimal and simultaneous two-photon excitation of three chromophores with distinct absorption spectra using a single femtosecond laser and an OPO [1]. The two beams generate separate multiphoton processes, and their spatiotemporal overlap provides an additional two-photon excitation route with submicrometer overlay of the color channels. We present volume/live multicolor imaging of 'Brainbow'-labeled chick and mouse tissues, and simultaneous three-color fluorescence and third-harmonic imaging of Drosophila embryos.

Another common limitation in deep tissue imaging is the loss of image quality due to tissue-induced aberrations. Adaptive optics can partially address this issue, but its efficiency needs to be characterized in practical situations. We implemented image-based correction methods compatible with dynamic embryo imaging [4], and extended this approach for mapping optical aberrations in 3D samples. We report 3D aberration maps in skin biopsies and mouse brain tissue and show that aberrations are linked to tissue structure [2]. These data reveal region sizes over which aberrations can be uniformly corrected, and pave the way towards efficient correction strategies.

[1] Mahou, Nature Methods (2012) ; [2] Zeng, Biomed Opt Express (2012); [3] Livet, Nature (2007) ; [4] Olivier, Opt Lett (2009).

8593-26, Session PSun

High-throughput phenotyping of structural birth defects using micro-computed tomography and magnetic resonance imaging

Andrew J. Kim, Richard J. B. Francis, Xiaoqin Liu, George Gabriel, Univ. of Pittsburgh School of Medicine (United States); William A. Devine, Univ. of Pittsburgh School of Medicine (United States) and Childrens Hospital of Pittsburgh (United States); Wendy Shung, Chien-Fu Chang, Deborah R. Farkas, Shane Anderton, Heather Lynn, Youngsil Kim, Li Yin Wong, Univ. of Pittsburgh School of Medicine (United States); Jovenal San Agustin, Gregory J. Pazour, Univ. of Massachusetts Medical School (United States); Linda Leatherbury, Children's National Medical Ctr. (United States); Kimimasa Tobita, Univ. of Pittsburgh School of Medicine (United States) and Children's Hospital of Pittsburgh (United States); Cecilia W. Lo, Univ. of Pittsburgh School of Medicine (United States)

Phenotype-driven forward genetic screening in mice provides the opportunity to recover mouse models with a wide range of structural anomalies for modeling structural birth defects (SBDs) in humans. This requires high-throughput imaging tools for the detection and analysis of SBDs. Necropsy and histopathology are the gold standards for SBD phenotyping, but these are time-consuming and are incompatible for large-scale high-throughput screening. Here, we evaluated the efficacy of post-mortem micro-computed tomography (micro-CT) and magnetic resonance imaging (micro-MRI) in identifying fetal/neonatal mice with SBDs as part of a large-scale mouse mutagenesis screen. Fetal and newborn mice were formalin-fixed, stained with iodine or gadolinium, and then scanned using high-resolution micro-CT or micro-MRI. A wide range of SBDs was detected from the scanning of 3112 ENU mutagenized fetal/newborn mice. The most prevalent SBDs are eye defects (n=205; 6.59%) (anophthalmia, micropthalmia, enophthalmia), kidney defects, including agenesis (n=18; 0.58%), duplication (n=57; 1.83%), hydronephrosis/hydroureter (n=64; 2.06%), and cleft palate (n=90; 2.89%). Also observed were brain malformations (holoprosencephaly, microcephaly, hydrocephalus), airway/lung defects (pulmonary isomerism, cysts, tracheoesophageal fistula), herniation (diaphragmatic, hiatal), congenital heart defects, agenesis of the thymus, gut abnormalities (obstruction/shortening, enlarged colon), and visceral organ situs anomalies. These SBD findings were verified by necropsy and/or histopathology examinations. Overall, these findings show micro-CT/MRI have high detection sensitivity for a wide spectrum of SBDs. When combined with ENU mutagenesis, phenotyping by microCT/MRI imaging can provide a powerful strategy to recover mutant mouse models for investigating the genetic and developmental etiology of SBD.

8593-27, Session PSun

A new method of deep UV LED microscopy using galvano-mirror scanning system for label-free live cell imaging

Joo Hyun Park, Korea Research Institute of Standards and Science (Korea, Republic of); Sang-Won Lee, Jae Yong Lee, Eun Seong Lee, Korea Research Institute of Standards and Science (Korea, Republic of)

Recently, a light emitting diode (LED) has been actively used in fluorescence microscopy because the LED are inexpensive, compact, and easy to use, compared with the other light sources such as xenon arc, tungsten halogen lamp, and laser. The LED can also provide the enough intensity for fluorescence microscopy in the specific wavelength. In a label-free imaging with a deep ultraviolet LED (DUV-LED) for proteomics, it is needed to use an expensive UV-sensitive CCD camera because a standard CCD camera is insensitive below 400 nm. However, the photomultiplier tube (PMT), a typical detector used in confocal laser scanning microscopy (CLSM), has the higher quantum efficiency (QE) compared with the CCD camera in the UV region. We present a fluorescence imaging system with the DUV-LED and the PMT as a new method by using a 2D galvano-mirror scanning system. We simply modified the scan head of a commercial CLSM. A light from the DUV-LED was incident into the specimen and made a transmitted fluorescence image plane. The transmitted fluorescence image plane was delivered and swept around a detection pinhole by the 2D galvano-mirror scanner and several lenses. The fluorescence signal of a specific point in the swept fluorescence image plane was passed via the pinhole and detected by the PMT. We could obtain a label-free live cell image from tryptophan (an excitation absorption at 280 nm), which is one of intrinsic fluorescence proteins.

Conference 8594: Nanoscale Imaging, Sensing, and Actuation for Biomedical Applications IX

Wednesday - Thursday 6 –7 February 2013
Part of Proceedings of SPIE Vol. 8594 Nanoscale Imaging, Sensing, and Actuation for Biomedical Applications X

8594-1, Session 1

Application of phase shift ring down spectroscopy to microcavities for biosensing *(Keynote Presentation)*

M. Imran Cheema, McGill Univ. (Canada); Usman A. Khan, Tufts Univ. (United States); Andrea M. Armani, The Univ. of Southern California (United States); Andrew G. Kirk, McGill Univ. (Canada)

Microcavities are widely used for sensing applications. In these applications, binding events induce changes to the effective refractive indices of the cavity modes, which are then detected primarily by tracking the change in the resonant wavelength of microcavities. Such a measurement suffers from a variety of noise mechanisms e.g. laser intensity noise and laser frequency jitter. A binding event will also impact the quality factor (Q) of microcavities. By using a phase shift ring down measurement approach (PS-CRDS), we have developed a real time biosensor which can simultaneously track the quality factor Q and the resonant wavelength ? of microcavities as a function of the biodetection event. In such a sensor many noise mechanisms are also minimized in Q measurement. Both of these parameters (Q and ?) carry information about the biological event and can be combined to provide an accurate estimate about the event. We have developed a mathematical model to predict the binding event with high accuracy by utilizing the information from these two physical parameters (Q and ?). Experiments have been conducted to validate the model. Hence, the PS-CRDS biosensor in conjunction with the estimation model, will pave the way for highly sensitive measurements of biological entities (e.g. proteins, DNA, virus etc) and processes (e.g. association and disassociation constants) ranging from micron to nano scale.

8594-2, Session 1

Hybrid sensing device using direct plasmon detection

Hossein Shokri Kojori, Univ. of Miami (United States); Juhyung Yun, Univ. at Buffalo (United States); Joondong Kim, Korea Institute of Machinery & Materials (Korea, Republic of); Wayne A. Anderson, Univ. at Buffalo (United States); Sung Jin Kim, Univ. of Miami (United States)

Surface plasmon based sensors are successfully used in various applications, since this optical phenomenon provides extreme sensitivity and robustness. Conventional SPR sensors consist of a thin metal surface or nanoparticle structure, excitation light source and detectors with controlled optical geometry. Since it uses multiple components and long optical path for better resolution, it is difficult to have multiplexing capability in an integrated device. To achieve highly sensitive and integration capable plasmon sensor, we introduce a novel hybrid sensing device using direct plasmon detection from gold nanoparticles. The device is fabricated using a wide bandgap semiconductor material and gold nanoparticles. The integrated hybrid structure enables the plasmon energy from the gold nanoparticles transferred to semiconductor film. This energy transfer appears as a change of current in the semiconductor layer. The wide bandgap material is used to avoid the overlap of absorbance spectra between metallic nanoparticle and semiconductor film. We successfully demonstrated direct current measurement of plasmon induced current which is well matched with the absorbance of gold nanoparticles. This novel hybrid plasmon sensor has several advantages such as extremely small size for integration and multiplexing, no need of complex optical geometry and robust operation.

8594-3, Session 2

Ultra-sensitive nanodetection using a whispering gallery microcavity laser

Tao Lu, Univ. of Victoria (Canada); Hansuek Lee, Tong Chen, California Institute of Technology (United States); Steven Herchak, Univ. of Victoria (Canada)

An ultra-high Q whispering gallery microcavity displays a Rayleigh scattering induced mode splitting. The resulting frequency difference between the split modes is proportional to the size of particle bound to the cavity surface and immune to common mode noises, making it suitable for nanodetection. The splitting frequency of a passive cavity has a linewidth in the order of MegaHertz. This limits the detection sensitivity to a 12.5nm-radius polystyrene bead in an aqueous environment. To enhance the sensitivity, we fabricated an Ytterbium doped microtoroid laser displaying the mode splitting structure in both air and an aqueous environment. Due to its self-referencing nature, the common mode frequency noises are eliminated, leaving the resulting linewidth close to the Schawlow-Townes limit. The resulting split frequency tones reside in the microwave region and have a linewidth as narrow as 21 Hz in air and 905 Hz in an aqueous environment. In addition, a split frequency fluctuation in the order of several kilohertz is obtained under both conditions. This microlaser provides sufficient sensitivity for in-vivo detection of single protein molecule binding events without the need for a fluorescence label. We first present single polystyrene particle sensing down to an 11.5nm radius where a record signal-to-noise ratio is achieved. We further report the detection of a single protein molecule binding event. Both results display split frequency steps larger than predicted by the reactive shift theory, suggesting the existence of a thermal-optical enhancement to the resulting split frequency change.

8594-4, Session 2

Label-free imaging of live cell using large-scale photonic crystal nanolaser array

Hiroshi Abe, Michimasa Narimatsu, Shota Kita, Kosuke Nakamura, Satoshi Ota, Yasushi Takemura, Toshihiko Baba, Yokohama National Univ. (Japan)

In this study, we fabricated large-scale photonic crystal nanolaser array, and applied it to label-free live cell imaging. In the live-cell imaging, label-free methods have been desired because they greatly simplify the sample preparation and avoid the invasiveness. Semiconductor photonic crystal nanolasers we have developed so far are easily fabricated by e-beam lithography and ICP dry etching and operated by photo-pumping. They can be used as a sensor chip of the environmental index, which is detected through the laser wavelength shift. The index resolution for liquids is the order of 10^-5 RIU, and the detection limit concentration of BSA protein is as low as of 100 fM order. Since the single device is approximately 10 ?m^2 in size, we can integrate many devices in an array configuration. It is applicable to acquiring real-time images of the index profile of live cells directly attached on the nanolaser array without labels. In this experiment, we fabricated 441 nanolasers array in a (100 ?m)^2 area, and cultured HeLa cells on it. By continuously mapping the wavelengths of all nanolasers, we successfully observed the time-dependent images displaying the cell behaviors. Reagents were injected to stimulate the cells, and the observation was continued until the cell reaction was saturated. The results show the reasonable behaviors against the reagents.

8594-5, Session 2

Optical sensing characteristics of nanostructures supporting multiple localized surface plasmon resonances

Neha Nehru, J. Todd Hastings, Univ. of Kentucky (United States)

Noble metal nanoparticles supporting localized surface plasmon resonances (LSPR) have been extensively investigated for label free detection of various biological and chemical interactions. When compared to traditional propagating surface plasmon based sensors, LSPR sensors offer extensive wavelength tunability, greater electric field enhancement and sensing in reduced volumes. However, these sensors also suffer from a major disadvantage – LSPR sensors remain highly susceptible to interference because they respond to both solution refractive index changes and non-specific binding as well as specific binding of the target analyte. These interactions can compromise the measurement of the target analyte in a complex unknown media and hence limit the applicability and impact of the sensor. Despite the extensive amount of work done in this field, there has been an absence of optical techniques that make these sensors immune to interfering effects. Recently, our group experimentally demonstrated a multi-mode LSPR sensor that exploits three resonances of a U-shaped gold nanostructure to differentiate the target interaction from bulk and surface interfering effects. In this paper,we provide a comprehensive description of the electric field profiles of the three resonances of the U-shaped nanostructure. We will also evaluate the sensitivities of the nanostructure to the various bulk and surface interactions using numerical simulations. Finally, we report an optimized U-shaped nanostructure based multi-mode sensor that provides improved sensitivities and limits of detection.

8594-6, Session 2

(Ho3+,Yb3+,Tm3+):KLu(WO4)2 nanoparticles, an efficient thermometry sensor in the biological range.

Oleksandr A. Savchuk, Joan Josep Carvajal Marti, E. William Barrera, Maria Cinta Pujol, Xavier Mateos Ferre, Rosa M. Solé, Jaume Massons, Magdalena Aguilò Diaz, Francesc Díaz, Univ. Rovira i Virgili (Spain)

In recent years up-conversion processes have been intensively studied for photonics applications. Since the efficiency of this effect is highly temperature dependent so thus it can be used for temperature determination at the nanometer scale. The most common technique is based on the measurement of the ratio between fluorescence intensities from two energy levels which are considered to be thermally coupled, named the fluorescence intensity ratio technique. Lanthanide doped materials are widely used as temperature sensors as they have the capability to generate efficient up-conversion emission through absorbing near-infrared light and converting it in visible emission. The most studied lanthanide ion for this specific application is Er3+. We studied a novel rare earth doped material, (Ho3+,Yb3+,Tm3+):KLu(WO4)2 nanoparticles for applications in thermometry. The KLu(WO4)2 host has several advantages for lanthanide ions, being the most important the high absorption and emission cross section that these ions present in this host.

One of the main innovations of this system is that it can be excited at different wavelengths, for instance by pumping Yb3+ at 980 nm or by pumping Tm3+ at 802 nm. The response observed in both cases is different, and it allows to use this material for different thermometry applications. Thus, while pumpint at 980 nm allows to use this material in the range of temperatures between 293 and 673 K, pumping at 802 nm leads to a high sensitivity in the biological range of temperatures.

8594-7, Session 3

Porous silicon biosensors using quantum dot signal amplifiers *(Invited Paper)*

Girija Gaur, Dmitry S. Koktysh, Sharon M. Weiss, Vanderbilt Univ. (United States)

In this work, we demonstrate highly sensitive labeled detection of biotin molecules in streptavidin-functionalized porous silicon (PSi) films using colloidal quantum dots (QDs) as signal amplifiers. QDs are conjugated to target biotin molecules, giving rise to both a distinct fluorescent signal and a significantly enhanced refractive index change upon capture by streptavidin probes pre-immobilized in the sensor. Compared to label-free detection of the target biotin molecules in a functionalized PSi film, QD-labeled biotin detection leads to a 10-fold increase in the effective optical thickness of the film, and a three order of magnitude improvement in detection limit from 2 pg/mm2 to 0.5 fg/mm2. In this work, we will present not only characterization of the sensor performance, including reflective interferometric spectroscopy, fluorescence, and FTIR spectroscopy, but also a detailed analysis about the properties of the PSi films that lead to the high sensitivity detection of QD-bioconjugates. In particular, we will report on the relationship between different PSi formation conditions and the resulting pore size distributions and internal surface area available to capture small target molecules. Additionally, we will discuss the quantification of surface area coverage of different sized QDs in the pores and the efficiency with which different sized QDs are infiltrated and detected in PSi films with different pores sizes and depths. Our demonstration of a novel, rapid, dual-mode optical sensing scheme is likely to provide an important stepping-stone for the realization of multiplexed optofluidic sensor arrays for highly sensitive, rapid, low cost, point-of-care diagnostics.

8594-8, Session 3

Enhanced magnetic resonance contrast of iron oxide nanoparticles embedded in a porous silicon nanoparticle host

Joseph Kinsella, McGill Univ. (Canada); Shalini Ananda, Univ. of California, San Diego (United States); Jennifer Andrew, Univ. of Florida (United States); Joel Grondek, Miao-Ping Chien, Miriam Scandeng, Nathan Gianneschi, Erkki Ruoslahti, Michael Sailor, Univ. of California, San Diego (United States)

In this report, we prepared a porous Si nanoparticle with a pore morphology that facilitates the proximal loading and alignment of magnetite nanoparticles. We characterized the composite materials using superconducting quantum interference device magnetometry, dynamic light scattering, transmission electron microscopy, and MRI. The in vitro cytotoxicity of the composite materials was tested using cell viability assays on human liver cancer cells and rat hepatocytes. An in vivo analysis using a hepatocellular carcinoma (HCC) Sprague Dawley rat model was used to determine the biodistribution properties of the material, while naïve Sprague Dawley rats were used to determine the pharmocokinetic properties of the nanomaterials. The composite material reported here demonstrates an injectable nanomaterial that exploits the dipolar coupling of superparamagnetic nanoparticles trapped within a secondary inorganic matrix to yield significantly enhanced MRI contrast. This preparation successfully avoids agglomeration issues that plague larger ferromagnetic systems. A Fe3O4:pSi composite formulation consisting of 25% by mass Fe3O4 yields an maximal T2* value of 556 mM Fe?1 s?1. No cellular (HepG2 or rat hepatocyte cells) or in vivo (rat) toxicity was observed with the formulation, which degrades and is eliminated after 4–8 h in vivo. The ability to tailor the magnetic properties of such materials may be useful for in vivo imaging, magnetic hyperthermia, or drug-delivery applications.

8594-9, Session 3

Self-referenced resonance-based biosensors for multiplexed toxin detection using glycans surface coatings at visible wavelengths

Farshid Ghasemi, Ali A. Eftekhar, David S. Gottfried, Georgia Institute of Technology (United States); Xuezheng Song, Richard D. Cummings, Emory Univ. (United States); Ali Adibi, Georgia Institute of Technology (United States)

Compact, sensitive, and low-cost sensing devices are of great interest for portable sensing applications. On-chip photonic microring arrays offer a viable solution for monolithic lab-on-chip biosensing due to their small footprint and scalability. However, despite their high sensitivity, temperature variations and laser instability hinder attaining low limit-of-detection (LOD).

We report on application of on-chip referencing to improve the LOD for compact multiplexed biosensors based on silicon nitride (SiN) microring arrays. Silicon nitride is transparent at visible wavelength, which enables incorporation of parallel sensing modalities such as fluorescence detection. Furthermore, lower thermo-optic coefficient of SiN compared to silicon, leads to a smaller sensitivity to temperature variations.

Microring resonators with a 20 x 20 ?m footprint are fabricated using e-beam lithography and fluorine-based etching. Reference resonators are covered with SU-8, and the sensing resonators are coated by glycans, GM1 and NA2 as specific ligands for certain proteins. Using pin-based printing, less than 10 pL of glycan solution is consumed per microring. Microrings are designed to have 600 pm spectral spacing between adjacent resonances. A visible tunable laser (? ~ 652-660 nm) is used to measure the real-time shifts in the resonance wavelengths caused by the binding of analyte to the resonator. Using the proposed self-referencing approach, multiplexed recognition of Cholera Toxin Subunit B (CTB) and Ricinus Communis Agglutinin I (RCA I) is demonstrated.

The details of the sensor design, fabrication, and characterization as well as its optimal application to the multiplexed toxin detection with high sensitivity will be presented in this talk.

8594-10, Session 3

Light-activated endosomal escape using upconversion nanoparticles for enhanced delivery of drugs

Muthu Kumara Gnanasammandhan Jayakumar, Akshaya Bansal, Yong Zhang, National Univ. of Singapore (Singapore)

Nanoparticle-based delivery of drugs has gained a lot of prominence recently but the main problem hampering efficient delivery of payload is the clearing or degradation of nanoparticles by endosomes. Various strategies have been used to overcome this issue and one such effective solution is Photochemical Internalization (PCI). This technique involves the activation of certain photosensitizing compounds by light, which accumulate specifically in the membranes of endocytic vesicles. The activated photosensitizers induce the formation of reactive oxygen species which in turn induces localized disruption of endosomal membranes. But the drawback of this technique is that it needs blue light for activation and hence confined to be used only in in-vitro systems due to the poor tissue penetration of blue light. Here, we report the use of Upconversion nanoparticles (UCNs) as a transducer for activation of the photosensitizer, disulfonated meso-tetraphenylporphine (TPPS(2a)). NIR light has good tissue penetrating ability and thus enables PCI in greater depths. Highly monodisperse, uniformly-sized, sub-100 nm, biocompatible upconversion nanoparticles were synthesized with a mesoporous silica coating. These UCNs activated TPPS(2a) efficiently in solution and in cells. Paclitaxel, an anti-cancer drug was used as a model drug and was loaded into the mesoporous silica coating. B16F0 cells transfected with drug-loaded UCNs and irradiated with NIR showed significantly higher nanoparticle uptake and in turn higher cell death caused by the delivered drug. This technique can be used to enhance the delivery of any therapeutic molecule and thus increase the therapeutic efficiency considerably.

8594-11, Session 4

Optical microscopy with super-resolution capability by liquid-immersed high-index microspheres

Arash Darafsheh, The Univ. of North Carolina at Charlotte (United States); Gary F. Walsh, Luca Dal Negro, Boston Univ. (United States); Vasily N. Astratov, The Univ. of North Carolina at Charlotte (United States)

We demonstrate that the super-resolution imaging of samples containing sub-diffraction limited features can be achieved by using high-index microspheres in a liquid environment. By using barium titanate glass microspheres (2-125 μm diameters) with refractive index ~1.9-2.1 totally immersed in liquids such as isopropanol alcohol (with index 1.37) we demonstrate ~?/7 far field resolution, where ?=550 nm is the peak wavelength of the white-light illumination system. Microspheres with diameters >50 μm were found to have smaller resolution (~?/4), but provide an extraordinary wide (>30 μm) super-resolution field-of-view. The results of this work can be used in biomedical microscopy, microfludics and nanophotonics applications for imaging individual cells and/or nanoparticles in a liquid environment.

8594-12, Session 4

Rare Earth doped nanoparticles in imaging and PDT

Brian G. Yust, Dhiraj K. Sardar, Lawrence C. Mimun, Ajith K. Gangadharan, Andrew Tsin, The Univ. of Texas at San Antonio (United States)

Nanocrystalline hosts doped with rare earth ions for biomedical imaging and infrared photodynamic therapy (IRPDT) have been synthesized, characterized, and compared. Specifically, these nanoparticles utilize two primary modalities: near infrared excitation and emission for imaging, and near infrared upconversion for photodynamic therapy. Near infrared light is ideal for biomedical imaging because of the low absorption and scattering power of most tissues within this region which leads to better image quality and lower necessary excitation intensities. Photodynamic therapy is achieved in the same particle through conjugating a photosensitive agent, such as zinc phthalocyanine, to the nanoparticle so that energy from upconversion fluorescence is resonantly transferred and activates the drug. The upconversion is achieved through exciting the erbium-ytterbium or thulium-ytterbium codoped systems with a 980nm laser while the imaging is achieved through near infrared downconversion. The upconversion emission intensity profiles are engineered through controlling the composition and phase of the nanocrystals such that the energy transfer to the photodynamic agent is optimized, resulting in more efficient IRPDT. Finally, these nanoparticles are tested for toxicity, imaged in cells using the near infrared emission pathway, and used for selective killing of cells through the upconversion driven IRPDT.

8594-14, Session 4

Atomic force imaging microscopy investigation of the interaction of ultraviolet radiation with collagen thin films

Andreas Stylianou, Dido M. Yova, Eleni Alexandratou, Aspasia G. Petri, National Technical Univ. of Athens (Greece)

Collagen is the major fibrous protein in the extracellular matrix and consist a significant component of skin, bone, cartilage and tendon. Due to its unique properties it has been widely used as scaffold or culture substrate for tissue regeneration or/and cell-substrate interaction studies. The ultraviolet light-collagen interaction investigations are very crucial for many reasons such as the application of UV rays in the field of biomaterials as sterilizing and cross-linking method. The aim of this paper was to investigate the mechanism of UV-collagen interactions by developing a collagen-based well characterized surface with controlled topography of collagen thin films in the nanoscale range. The methodology was to quantify the surface modification induced in collagen by ultraviolent radiation and correlate it with changes induced in cells. Surface nanoscale characterization was performed by Atomic Force Microscopy (AFM) which is a powerful tool and offers quantitative and qualitative information with a non-destructive manner. In order to investigate cells behavior, the irradiated films were used for in vitro cultivation of human skin fibroblasts and the cells morphology, migration and alignment were assessed with optical microscopy imaging and image processing methods. The clarification of the role of the UV light on collagen thin films and the cells behavior to the different modifications that UV induced to the collagen-based surfaces will contribute to the better understanding of cell-matrix interactions in the nanoscale and will assist to the appropriate use of UV light for developing biomaterials.

8594-15, Session 4

Detection of apoptosis caused by anticancer drug paclitaxel in MCF-7 cells by confocal Raman microscopy

Hamideh Salehi, Elodie Middendorp, Nano Science-Bio Health Lab., Univ. Montpellier 1 (France); Attila-Gergely Végh, Institute of Biophysics (Hungary); Sathish Kumar Ramakrishnan, Csilla Gergely, Lab. Charles Coulomb, Univ. Montpellier 2 (France); Frederic J. G. Cuisinier, Nano Science-Bio Health Lab., Univ. Montpellier 1 (France)

Confocal Raman microscopy, a non-invasive, label free and high spatial resolution imaging technique is used to study apoptosis in living MCF-7 cells . The images are obtained based on the Raman spectra of cells components and drug and are treated by K-mean cluster analysis method to localize drug in cell. Distribution of paclitaxel in cells is verified by calculating the correlation coefficient between the reference spectrum of the paclitaxel and the Raman spectra of the whole image. Our results show that the drug is distributed all over in the cytoplasm , that is in good agreement with other recent researches suggesting a new picture of the pharmaceutical action of this drug based on rapid binding of crystallized paclitaxel to free tubulin.(Ref:1,2) Finally cell apoptosis is monitored by tracing cytochrome c apparition and distribution in cytoplasm.

1 J. S. Castro, P. A. Deymier, B. Trzaskowski, and J. Bucay., Colloid. Surface B 76, 199 (2010).

2 M. Foss, B. W. L. Wilcox, G. B. Alsop, and D. Zhang, PLoS ONE 3, e1476 (2008).

8594-16, Session 5

Selective detection of sub-atto-molar streptavidin in 10^13 fold impure sample using nanoslot photonic crystal nanolaser

Shoji Hachuda, Shota Otsuka, Shota Kita, Yokohama National Univ. (Japan); Toshinari Isono, Yokohama City Univ. (Japan); Keisuke Watanabe, Toshihiko Baba, Yokohama National Univ. (Japan)

Biosensors which can selectively detect a very small amount of biomarker protein in human blood are desired towards early diagnoses of severe diseases. However no methods simultaneously satisfy the requirements such as high sensitivity, high selectivity, simple detection, and immediacy. We succeeded in detecting ultra-low concentration streptavidin (SA) even in a highly impure sample using nanoslot photonic crystal (PC) nanolasers. This nanolaser consists of GaInAsP semiconductor slab with a periodic airhole array. Since the total device area is only (10 ?m)^2, high-throughput fabrication is possible even using e-beam lithography. Moreover, it is easy to operate by photopumping through free-space optics. Since the evanescent wave of the laser mode penetrates from the PC slab, the laser wavelength changes sensitively to the environmental index. In the sensing experiment, we first functionalized the devices with biotin, and then measured the wavelength in ultrapure water before and after immersion in solutions with various concentration SA. As a result, we evaluated that the detection limit of SA is 16 zM. In another experiment, we put 1 ?M BSA into the solution as a contaminant, and repeated the same measurement. We detected 100 zM SA even in the impure solution, meaning a selectivity ratio (BSA / SA) of 10^13. Thus this device achieves unprecedented high sensitivity and selectivity in addition to the simple fabrication and fast sensing. It is very promising as a point of care device for medical diagnoses.

8594-17, Session 5

DNA nanosensor surface grafting and salt dependence

Bruna G. Garvalho, Jaciara Fagundes de Souza Martins, Airton A. Martin, Leandro J. Raniero, Priscila P. Favero, Univ. do Vale do Paraíba (Brazil)

Metallic nanoparticles applied as DNA sensors have been used to identify and describe the symptoms that are caused by different organisms contaminations. This is the case of the fungus Paracoccidoides brasiliensis that can be breath in and installed in the lungs. As its symptoms are similar to tuberculosis the fungus diagnosis is usually incorrect. In order to avoid these errors, DNA sensors are applied in such a way that just PB's DNA are detected. The DNA functionalized nanoparticles sensors are based on colorimetric technique that is quick, accurate and easy to be manipulated. Although this diagnosis technique has already succeeded in our laboratory, this application shows that it is dependent on nanoparticle's environment like pH and salt concentration. In order to optimize the technique, we study the DNA strand interaction with nanoparticles surface and the environment role via density function theory applied in the Vienna Ab-initio Simulation Package (VASP). We propose different models for representing the gold nanoparticle surface: the plane and the curved surface. Our results indicate that the plane surface is a more representative model than the curved surface as it presented unpredictable properties. The simple strand of the fungus DNA is represented by the first nucleotide functionalized (Tymine and SH + C6H12). By the adsorption energy calculation of first and second DNA we estimate the DNA grafting and concentration of colloidal solution when it is applied to nanoparticle. In addition, we conclude that the strands of DNA desorption due to the presence of salt concentration is unlikely.

8594-18, Session 5

Analysis of DNA nanosensors interaction via density function theory

Aline A. Bidoul, Airton A. Martin, Leandro J. Raniero, Priscila P. Favero, Univ. do Vale do Paraíba (Brazil)

Paracoccidoides brasiliensis (PB) is a fungus that is usually found on the soil. It can be breath in and installed in the lungs. The symptoms manifested by these contamination are initially similar to tuberculosis, therefore, are usually wrongly diagnosed. This error can result in an inefficient cure procedure and also in a subestimation of disease cases quantity. In order to improve the fungus diagnosis, a DNA sensor was developed based on a gold nanoparticle functionalized with the PB's DNA. The test result is based on colorimetric technique and is very simple to be interpreted: red means positive and blue means negative to

the disease investigation. Although this diagnosis technique has already succeeded in our laboratory, we verify that environment characteristics as pH and salt concentration can change the nanoparticles interaction and can result in a false diagnostic. Motivated by this cases, we have studied nanoparticles interaction and the environment role via density functional theory (DFT) using the software Vienna Ab-initio Simulation Package (VASP). The used models consist of gold nano-spheres with 520 atoms and two hemispheres of 260 atoms each, adsorbed with tiol group. We calculate the spatial electrical potential projected at a Z direction produced by the nanosphere and by the two hemispheres. The electronic charge density and electrical potential are evaluated as a dependence of the distance between the nanoparticles and salt concentration that there is in between them. By this evaluation, we calculated the change of charge interaction between nanoparticles due to the salt presence and the dipole formation.

8594-19, Session 5

ZnO light-emitting nanoprobes for tumor detection

Yung-Tsan Chen, Yi-Chun Shen, Sheng-Chieh Yang, National Taiwan Univ. (Taiwan); Tsung-Lin Yang, National Taiwan Univ. (Taiwan) and Research Ctr. for Developmental Biology and Regenerative Medicine, National Taiwan Univ. (Taiwan); Jian-Jang Huang, National Taiwan Univ. (Taiwan)

Tumor detection is a significant health issue, but it is still a limit to identify cancer cells during tumor resection by using traditional methods such as fluorescence. In this study, zinc oxide (ZnO) nanorods bonded to antibodies was investigated as nanoprobes for sensing cancer cells. The result shows that antibodies toward epidermal growth factor receptor (EGFR) can be connected to ZnO nanorods and EGFR receptors of squamous cell carcinoma (SCC). The cancer cells can be recognized via the observation of purple light emission from these probes by using naked eye or an optical microscope. By contrast, the HS68 cells with less EGFR expression had no purple light emission as the probes were washed off. Besides, from the photoluminescent spectra, the intensity ratio between the purple light (from ZnO nanorods) and green band (from the autofluorescence of cells) is much higher in SCC than in HS68 cells, which suggest that the cancer cells can be detected by comparing the peak intensity ratio. The probes have the potential clinical application for real-time tumor detection, and the cancer cells can be excised more precisely with the help of purple light emission.

8594-20, Session 5

Partially embedded gold nanoislands in a glass substrate for SERS applications

Mohammad T. Yaseen, Yia-Chung Chang, Min-Hsiung Shih, Academia Sinica (Taiwan)

In this work, we present a SERS substrate based on gold nanoislands partially embedded in a transparent substrate to generate SERS hot spots in a large area. Partially embedded gold nanoislands were fabricated by the thermal annealing of an initial gold thin layer, which was deposited on the glass substrate using E-gun evaporator, near the melting temperature of the glass substrate. The annealed samples were optically characterized by using spectroscopic ellipsometry. After that, the experimental results were compared with theoretical model to understand their optical response. The SERS performance has been successfully shown with the Rhodamine 6g at nanomolar concentration level. For the proposed SERS substrate, high hot spot density due to the localized field, simple and low cost preparation procedure could make this SERS substrate a good candidate for SERS detection at single molecule level.

8594-21, Session 6

Colloidal nanostructures characterization via monochromatic x-ray microtomography

Michael K. Rafailov, Univ. of Alberta (Canada); Victor Asadchikov, Russian Academy of Sciences (Russian Federation); Svetlana Rubtsova, Nano-technology Ctr. (Russian Federation)

Here we report work done toward detection and characterization of micro-and nano-structures containing V, Co, Mo, Re Ni in colloidal mixture. X-ray micro-tomograph with monochromatic radiation has been used to detect nano-and-microstructures containing metal-organics formed with these metals. In order to detect and characterize nano- and micro-structures with metal-organics the tomograph's operational wavelength was tuned to a wavelength of absorption in X-ray spectrum of the metals. Contrast between resonant X-ray absorption of specific metal and average colloidal mixture absorption provides a tool for measurement of metal mass concentration in the structures as well as distribution of micro-and nano structures not only on surface but in thelume. Work specifically has been focused at measurement of oil disperse system containing porphyrines where concentration of metals changing as a function of asphalten concentration changing along oil processing.

8594-22, Session 6

Near-field optical fluorescence correlation spectroscopy

Aaron Lewis, Yosef Y. Kuttner, The Hebrew Univ. of Jerusalem (Israel); Rimma Dekhter, Nanonics Imaging Ltd. (Israel); Mila Polhan, The Hebrew Univ. of Jerusalem (Israel)

The technique of fluorescence correlation spectroscopy has become a very important tool in cell biology. The technique was first developed in the 1970s when it was shown that it had the ability to monitor the rate of molecular diffusion and the rate of chemical reactions. Nonetheless, the technique remained effectively dormant over many years until the 1990s when Eigen and Rigler realized that if the detection volume was reduce using confocal techniques and the number density of the fluorophore was made to be low (10 nM) then, high quantum efficiency detectors could address important problems in cell biology [1]. Thus, FCS is a single-molecule analytical technique sensitive to the fluctuations of fluorescence in the focal beam. Statistical analysis of these fluctuations is used in order to interpret various dynamic molecular events, such as chemical and biochemical reactions, diffusion or conformational fluctuations of biomolecules etc. A problem with such methodology however has been the extremely low concentrations that were required for effective signal to noise with confocal detection. The first paper to apply conventional fiber apertured near-field scanning optical microscopy (NSOM) techniques to fluorescence correlation spectroscopy was by Lewis et al (2). These authors realized that by applying conventional NSOM technology the excitation volume could be drastically reduced and thus one could increase the concentration of the molecular species being investigated.

In essence with NSOM probes zeptoliter excitation volumes can be achieved with the crucial benefit of force feedback ultra-stability that resolves many issues in conventional FCS and adds topographic correlation. The results suggest that NSOM FCS has considerable potential for applications of FCS in membrane, near-membrane, solution and even within cell environments. The latter is achieved through atomic force feedback controlled penetration of tapered cantilevered metal coated glass fibers into cells that will also be reported.

1. Eigen M., and Rigler R. Proc Natl Acad Sci USA (1994) 91:5740

2. Lewis A., Kuttner Y. Y,, Dekhter R., and Polhan M. (2007) Isr J Chem 47:171

8594-23, Session 6

Visualization of lipid rafts in normal or AD hippocampus neurons with nano-resolution

Danni Chen, Lei Liu, Yingdong Huo, Bin Yu, Hanben Niu, Shenzhen Univ. (China)

Visualization, tracking and analyzing molecules and their events in cells are critical in understanding a complex biological system. So, as a tool being capable of visualizing the dynamic processes inside cells, optical microscopy has to meet the following requirements, namely molecule identification, nano-resolution, single molecule detection sensitivity, and temporal resolution as high as microseconds even picoseconds. The last two requirements are mainly determined by the detector used during experiment. At present, the first requirement is easy to be met for the fluorescence microscopy, because fluorescent labels can be specifically attached with the aimed molecules. As an optical imaging method, the spatial resolution of a fluorescence microscopy is limited by the diffraction. However, with the development of laser techniques, label material, label techniques, and weak signal detection techniques, more and more imaging methods are put forward and realized, and traditional resolution which is limited by the diffraction has been broken through by means of different approaches, such as single-molecule-localization based microscopy. Lipid rafts are sphingolipid- and cholesterol-enriched membrane domain (10-200nm) floating in the plasma membrane. Rafts have been implicated to participate in the pathogenesis of a variety of conditions, such as HIV, Alzheimer's disease (AD), Parkinson's disease (PD) and prion disease. To date, however, lipid-raft field is still at a technical impasse due to the lack of suitable techniques with nano-resolution and higher imaging speed for directly observing lipid rafts in living cells. Therefore, we investigated the characterization of the labeled lipid rafts in normal or AD hippocampus neurons using our home-built super-resolved single-molecule-localization fluorescence nanoscopy.

8594-24, Session 6

Bilipid membrane phase characterization by reflectance anisotropy

spectroscopy (RAS)

Priscila P. Favero, Univ. do Vale do Paraíba (Brazil); Armando C. Ferraz, Maurício S. Baptista, Univ. de São Paulo (Brazil); Ronei Miotto, Univ. Federal do ABC (Brazil)

Cell membrane models have received a great deal of attention in the last century. Despite it, more molecular level membrane studies are required, especially those involving molecules bound to the membrane surface or embedded within the membrane. These informations are fundamental to a molecular understanding of disease and hence in the design of new biomolecules for use in treatment, molecular medicine. In this work we propose the use of experimental and theoretical reflectance anisotropy spectra (RAS) (using Kohn-Sham density functional theory (KS-DFT)) as a new tool to identify structural and dynamical aspects of the bilipid membrane and its various constituent molecules. The role of geometric details at the atomic level and macroscopic quantities, such as the membrane curvature and tilt for the different gel phases, in the theoretical RAS spectra are presented, and the results are compared to the experimentally measured spectra taken from other techniques. In addition, the role and contribution of the cholesterol molecules to the optical properties of the membrane have also been calculated. Our results indicate that RAS KS-DFT level spectroscopic simulations are capable of determining the orientation of the cholesterol hydroxyl functional group with respect to the membrane surface. Therefore we suggest this methodology can be used to study the binding of drug molecules, ligands, and ions to the membrane surface and their transport through the membrane itself. In addition the technique presents a selectivity capable of detecting the properties of atoms that comprise the membrane surface, neglecting effects due to the bilayer inner atoms.

8594-25, Session 7

Control of molecular motors-driven nano-level motion on thermo-chips *(Invited Paper)*

Michael Berndt, Till Korten, Max Planck Institute for Molecular Cell Biology and Genetics (Germany); S. Syed, Harm van Zalinge, Univ. of Liverpool (United Kingdom); S. Diez, Max Planck Institute for Molecular Cell Biology and Genetics (Germany); Dan V. Nicolau, Univ. of Liverpool (United Kingdom)

Motility-systems based on linear molecular motors, such as microtubule-kinesin systems, are ubiquitous natural nano-machines. They can be used to mimic the function of the natural biological nanodevices that operate in a cellular environment, where molecular motors move cargo (target biomolecules) towards (probe) molecules in solution.

In order to control the activity of motor proteins on the surface of a biodevice, the motor proteins were embedded in a layer of thermo-responsive poly(N-isopropylacrylamide) (PNIPAM polymers). These molecules can display two states, a tightly coiled molecule at temperatures above 35 °C and elongated at lower temperatures. When the PNIPAM is present in the combination of kinesin motor proteins the state of the PNIPAM will determine whether or not a microtubule will be able to attach to the kinesin and whether motility can occur.

A combinatorial set of electrodes with varying lengths and widths, which according to different currents will produce different temperatures, was fabricated. From the simulation of the current density it can be concluded the heat development will preferentially occur in the constricting areas. During a first test without PNIPAM present a current was successfully applied. This current heated up the structure as indicated by the increase in microtubule gliding speed. This speed increase corresponds to a temperature increase of 9˚C which is sufficient for switching of PNIPAM. However the temperature increase was not very localized. According to numeric simulations done for structured silicon chips, this global increase is caused by a lack of heat dissipation into the surrounding air leading to heat accumulation.

8594-26, Session 7

Optical tweezers based measurement of PLGA-NP interaction with cancer cells

Argha Mondal, Thea Blesener, Jyothi Menon, Kytai Nguyen, Samarendra K. Mohanty, The Univ. of Texas at Arlington (United States)

Biodegradable and biocompatible, poly(lactic-co-glycolic acid) (PLGA) nanoparticles (NPs) are emerging as agents of choice for controlled and targeted drug delivery for control of cancer. Here, we report use of optical tweezers for measurement of binding and rupture force of different (size, surface properties) PLGA-NPs with prostate cancer cells. The force of interaction between the NP and cell membrane was found to increase with time. For similar interaction time the force was higher for larger size NPs. Further, the rupture force measurements showed that the binding between PLGA-NPs and prostate cancer cells is significantly enhanced by coating the NPs with cancer-specific targeting peptide. These results will lead to optimization of designed NPs for drug delivery into cancer cells.

8594-27, Session 7

The molecular nanotweezer: nanomanipulation taken to new lows

Bernardo Cordovez, Robert Hart, David Erickson, Optofluidics (United States)

By exploiting near field optical forces, the Molecular NanoTweezer can optically trap the smallest nanoparticles to date including

individual proteins and quantum dots. This breakthrough is being commercialized and will produce the first system to allow for direct optical manipulation of biologically relevant nanoparticles. This new system enables completely new experiments including surface-tether-free immunoassays, simplified single molecule analysis and enhancing localized concentration of solution-phase biomolecules. In the quest of optically trapping smaller objects, traditional optical free space tweezers run into the diffraction limit, which places a lower limit on the size of the beam waist, and an upper limit on the gradient forces that can be generated to trap small objects, making it an almost impossible task to trap objects smaller than 100 nm in size. Shortening the operating wavelength can improve their performance, but at the cost of undue heating and chemical damage. The Molecular NanoTweezer overcomes the lower size limit imposed by diffraction (thus the current barrier faced by traditional optical tweezers) by exploiting near field optical effects using waveguides and optical resonators patterned on semiconductor chips. Furthermore, the operating Molecular NanoTweezer operates in the infrared, avoiding heating and chemical damage of the probed particles. To date, this technology has been used to trap some of the smallest matter including quantum dots, clinically relevant globular proteins, lambda DNA and polystyrene microspheres, with particle sizes ranging from 5 nm to 3 μm in size. We will finalize our talk by describing our commercialization efforts.

8594-28, Session 7

Electric field modulation of the motility of actin filaments on myosin-functionalised surfaces

Laurence C. Ramsey, Jenny Aveyard, Harm van Zalinge, Univ. of Liverpool (United Kingdom); Malin Persson, Alf Mansson, Linnaeus Univ. (Sweden); Dan V. Nicolau, Univ. of Liverpool (United Kingdom)

We investigated the difference in electrically guided acto-myosin motility on five surfaces. Rabbit skeletal muscle heavy meromyosin (HMM) was absorbed onto surface coatings Nitrocellulose (NC), Polystyrene (PS), Poly(methyl methacrylate) (PMMA), Poly(tertbutyl methacrylate) (PTBMA), Poly(butyl methacrylate) (PBMA), and Trimethylchlorosilane (TMCS). A modified in vitro motility assay with sealed chambers for the insertion of electrodes allowed an electrical field to be applied across the flow cell. On all surfaces a small increase in velocity and general guidance of the actin filaments towards the positive electrode is seen at field strengths in the range of ~3000 – 4000V/m. A large increase in velocity was observed at ~5000V/m and a significant change in the velocity of the actin filaments present in field strengths higher than this. TMCS supported the highest percentage of motile filaments and at a field of 8000V/m reached ~80%. PBMA and PTBMA however supported the least percentage of motile filaments and irregular motility was observed even at higher fields where guidance was expected to be strong. The change in velocity in the range of fields tested varied significantly on the surfaces with TMCS displaying a 136% increase from 0 to 8000V/m whereas on PMMA this value was just 39%.

8594-29, Session 7

Simulation of actin filament motility on myosin-functionalised surface in electric field

Aleksandr Chichenkov, Laurence Ramsey, Jenny Aveyard, Harm van Zalinge, Univ. of Liverpool (United Kingdom); Dan V. Nicolau, McGill Univ. (Canada)

Actin-myosin motility has been generally attributed to cyclic interactions between actin filaments and myosin molecules, which produce force as a result of structural changes during the ATPase cycle. The values of the force during the motility as well as without ATP have previously been determined using complicated optical trapping techniques. We have developed a model wherein the protein interaction is directly mimicked according to cross-bridge activity. Motion is only produced when the lever arm of a myosin is in a, what is referred to, strong-bind state and is able to overcome resistive forces or when the filament is subjected to an external force produced by an electric field. An in vitro motility assay has been used to experimentally investigate the effect of the external electric field on directionality and velocity of a negatively charged filament on different surfaces – Nitrocellulose (NC) and Poly (methyl methacrylate) (PMMA). These results were then used in a simulation to determine the number of active and inactive myosin molecules that interact with the filament to accommodate obtained velocities. Moreover the concentration of motors, immobilized on each surface is determined. Finally, by inputting the amount of myosin determined from quartz crystal microbalance and ATPase experiments, the force exerted by active and inactive motors have been determined to be 10.2-11.8 pN and 3.6-4.4 pN respectively.

8595-1, Session 1

Colloidal inorganic nanoparticles: functionality and bio-applications *(Invited Paper)*

Otto L. Muskens, Antonios G. Kanaras, Dorota Bartczak, Rute Fernandes, Agathi Christofidou, Tracey Newman, Neil Smyth, Timothy M. Millar, Michael R. Ardern-Jones, Univ. of Southampton (United Kingdom); Simone Nitti, Istituto Italiano di Tecnologia (Italy)

In this presentation we discuss the interactions of advanced types of inorganic nanoparticles with several biological structures including different types of popular cells and larger organs (i.e. skin). We will particularly highlight how the appropriate selection of ligands and the intrinsic properties of nanoparticles can influence biological functions.

8595-2, Session 1

O6-alkylguanine-DNA transferase (SNAP) as capture module for site-specific covalent bioconjugation of targeting protein on nanoparticles

Serena Mazzucchelli, Sacco Hospital (Italy); Miriam Colombo, Univ. degli Studi di Milano-Bicocca (Italy); Elisabetta Galbiati, Univ. degli Studi di Milano-Bicocca (Italy) and Univ. degli Studi di Milano-Bicocca (Italy); Fabio Corsi, Sacco Hospital (Italy); Josè M Montenegro, Philipps-Univ. Marburg (Italy) and Philipps-Univ. Marburg (Germany); Wolfgang J. Parak, Philipps-Univ. Marburg (Germany); Davide Prosperi, Univ. degli Studi di Milano-Bicocca (Italy)

The design of multifunctional nanoparticles (MFN) combining optical and magnetic properties with a focused targeting action is a primary challenge in cancer diagnostics. The selectivity in targeting cancer cell is usually achieved immobilizing biomolecules with high affinity for cancer biomarkers on MFN. Here we report an novel strategy that involves the use of fusion proteins containing a small enzyme (i.e. human O6-alylguanine-DNA alkyltransferase, SNAP) capable of cross-reacting with a suicide inhibitor anchored to the solid surface. This approach let us to finely control ligand arrangement on nanoparticle surface. A further advantage is that the immobilized ligand is a small molecule that binds the enzyme in a quick, specific and irreversible manner under physiological condition. Moreover, this binding system involves monovalent recognition partners, which overcomes crosslinking side-effects.

SNAP irreversibly transfers the alkyl group from its substrate, O6-alkylguanine-DNA, to one of its cysteine residues, and is highly reactive also toward alternative non-natural nucleobases, including O6-benzylguanine derivatives. Therefore, we reasoned that a pegylated O6-alkylguanine derivative could be a good candidate to mediate the covalent, site-specific immobilization of SNAP fusion proteins on MFN. As a proof of concept , we designed a bimodular genetic fusion (SNAP-scFv) comprising a bioactive scFv mutant selective for HER2 receptor in breast cancer cells as a targeting module, and SNAP as MFN capture module. We demonstrate the utility of this method for protein nanoconjugation and cellular imaging by evaluating the effects of the treatment of HER2-positive breast cancer cells with MFN covalently bound to SNAP-scFv.

8595-3, Session 1

Tailoring surface biofunctionalization of nanoparticles to improve targeting efficiency *(Invited Paper)*

Davide Prosperi, Univ. degli Studi di Milano-Bicocca (Italy); Serena Mazzucchelli, Luisa Fiandra, Fabio Corsi, Sacco Hospital (Italy); Miriam Colombo, Univ. degli Studi di Milano-Bicocca (Italy)

The design of ideal targeted multifunctional nanoparticles (MFN) needs careful optimization of fundamental features including uniform size and shape, surface charge, optical and magnetic properties, and efficient functionalization with suitable homing ligands to improve the signal amplification and target selectivity toward malignant cells. The selectivity in targeting cancer cells is usually accomplished exploiting the modification of MFN with biomolecules endowed with high affinity for specific cell membrane receptors.

A greatest challenge in designing MFN functionalized with homing peptides resides in the possibility to control the ligand orientation on the nanoparticle surface. To illustrate the potential of controlling the surface organization of biomolecules on MFN, we present a multidisciplinary approach to the design and synthesis of a universal hybrid nanosystem consisting of Fe3O4 nanocrystals, displaying narrow size distribution, a high magnetic T2 relaxivity and a bioactive protein shell. Magnetite nanoparticles are conjugated to a newly designed recombinant monodomain protein A fragment, which has been bioengineered to present a cysteine tripod at the C-terminal end. As protein A recognizes the Fc portion of IgGs, it mediates an orderly Fc site-specific antibody immobilization on MFN resulting in a target-directed Fab presentation. The same approach is very effective also in the preparation of immunogold nanoparticles. As a case study for the development of tumor-targeting nanoprobes, we focus on trastuzumab, a monoclonal antibody that can bind the HER2 receptor in breast cancer cells with high affinity. This novel targeted nanoparticle model is assessed by fluorescence analysis, MRI and ultrastuctural investigation.

The work was supported by Regione Lombardia (NanoMeDia Project) and Fondazione “Romeo ed Enrica Invernizzi”.

8595-5, Session 1

Functionalized nanoparticles and negatively charged ligands as inhibitor for viral vectors *(Invited Paper)*

Maria Pelliccia, European School of Molecular Medicine (Italy) and Univ. degli Studi di Milano (Italy); Gianluca Deflorian, IFOM-IEO (Italy); Randy P. Carney, Paulo J. Silva, Ecole Polytechnique Fédérale de Lausanne (Switzerland); Patrizia Andreozzi, Istituto Neurologico Carlo Besta (Italy); Federica Pezzimenti, IFOM-IEO (Italy); Francesco Stellacci, Ecole Polytechnique Fédérale de Lausanne (Switzerland); Silke Krol, Istituto Neurologico Carlo Besta (Italy)

Viral diseases are becoming an increasing burden on the global health system as they are frequently causing chronic disease and requiring permanent treatment or leave the patients handicapped.

In the present study we investigated the interaction of surface-functionalized (striped and non-structured) nanoparticles of different sizes or single molecules, so-called ligands with enveloped viruses such as lentivirus or naked viruses such as adenoviruses. Moreover we included a nanotoxicology assay in order to face safety issues of the nanoparticles in the light of a potentially use as antiviral drug.

The experiments with the enveloped lentivirus mainly confirmed previous findings by other groups [1-5] that the transfection efficacy of enveloped

viruses can be efficiently blocked by sulfonated nanoparticle surfaces or direct interaction with the sulfonated ligand molecules. Nanotoxicology assays indicate that the nanoparticles express a very low toxicity profile towards their target cells.

References

1. Baram-Pinto et al. (2009) Bioconjugate Chem., 20, 1497–1502

2. Baram-Pinto et al. (2010) Small, 6, 1044–1050

3. Di Gianvincenzo et al. (2010) Bioorg. Med. Chem. Lett., 20, 2718–2721

4. Witvrouw et al. (1997) Gen. Pharmacol. 29, 497-511

5. Moulard et al. (2000) J. Virol. 74, 1948-1960

8595-6, Session 1

Applying a hydrophobic shield to diminish non-specific interactions of gold nanoparticles

Timothy A. Larson, Angel Zubieta, The Univ. of Texas at Austin (United States); Konstantin V. Sokolov, The Univ. of Texas M.D. Anderson Cancer Ctr. (United States)

Polyethylene glycol (PEG) is often used to prevent unwanted protein adsorption to gold nanoparticles (GNP). While GNP-PEG are indeed more stable in biological media compared to GNP coated by citrate or other charged molecules, they are still eventually internalized into macrophage cells. This work suggests a new mechanism by which gold nanoparticle surfaces are disrupted by cysteine and cystine. Evidence is presented to support the hypothesis that cysteine can penetrate PEG layers and replace methoxy-PEG-thiol via ligand exchange. Cysteine and cystine are present in both blood plasma and in cell culture media, and thus will lead to the slow degradation of surface of GNP-PEG over time. Additionally, protein adsorption to PEGylated gold nanoparticles in cell culture medium is found to occur over a period of 48 hours; this adsorbed protein layer mediates cellular interactions with macrophage cells. We address this problem by incorporating a hydrophobic shield layer between the thiol and the outer hydrophilic PEG layer. A simple synthesis for thiol-dodecane-PEG is presented, the mPEG-alkyl-thiol coating greatly reduces protein adsorption on GNPs that leads to a diminished cellular uptake in RAW macrophage cells, even after five days of incubation in cell culture medium. This work suggests a new way to understand gold nanoparticle interactions with biological media and a way to improve their stability.

8595-7, Session 2

Plasmonic gold nanocrosses with multidirectional excitation and strong photothermal effect *(Invited Paper)*

Ming-Yong Han, A*STAR Institute of Materials Research and Engineering (Singapore)

Surface plasmons propagate on the surface of metals (silver, gold, palladium, etc.) whose optical properties are determined by their surface geometry at nanoscale. Recent advancement in controlling the surface shape/morphology of metal nanostructures has demonstrated the great capability to engineer their localized surface plasmon resonance (LSPR). In order to tune the LSPR from visible to near-infrared, metal nanostructures need to have a size comparable to the optical wavelength in one or more dimensions. For example, metal nanorods, nanoprisms and nanoplates have red-shifted LSPR by increasing length or edge size, and metal nanoshells, nanorings and nanocages have red-shifted LSPR by changing core/cavity diameter and shell thickness. Recently, the successful fabrication of structurally more complex metal nanostructures including semishells, multishells, split rings, helixes and gammadions can greatly enrich surface plasmonic properties, and the closely spaced arrays of various metal nanostructures on substrates can further enhance these properties through interparticle coupling. In this talk, we present a facile chemical synthesis of free-standing multiple-branched gold nanocrosses, which exhibit a pronounced near- and middle-infrared LSPR. The colloidal production of such well-defined gold nanocrosses in a controlled fashion was a challenging task due to the symmetric face-centered-cubic lattice of gold, and the copper-induced formation of single or double twins in the center of gold nanocrosses in this research is important in determining the unique habit of the final morphology (e.g. D2h and C2v symmetries). Theoretical investigations indicate that an entire nanocross gets excited along any branches and these plasmonically coupled branches lead to synergistic enhancement in local electric fields, which enable applications in sensing, surface-enhanced spectroscopy, nonlinear optics, imaging, therapeutics, and medicine. For example, the highly branched gold nanocrosses have exhibited strong photothermal effect for effective photothermal destruction of cells, and this can be integrated with two-photon luminescence imaging to understand cell damage process for tumor therapies.

8595-8, Session 2

Star-like gold nanoparticles as higly active subtrate for surface enhaced Raman spectroscopy

Carlo Morasso, Dora Mehn, Renzo Vanna, Marzia Bedoni, Elena Forvi, Fondazione Don Carlo Gnocchi (Italy); Davide Prosperi, Univ. degli Studi di Milano-Bicocca (Italy); Furio Gramatica, Fondazione Don Carlo Gnocchi (Italy)

Star like Gold Nanoparticles (SGN) have been recently proposed as new reliable nanostructures as substrate for Surface Enhanced Raman Spectroscopy experiments. They combine the remarkable plasmonic properties usually typical of silver nanostructure with the stability and biocompatibility of gold.

Despite the great interest, the synthesis of this kind of structure is still laborious. Here we present a procedure to prepare SGN with a diameter of 70 nm by a simple one-step, room temperature procedure not involving the use of any seeds, surfactants, polymers or organic solvents. The procedure is entirely based on chemical reduction of Gold ions and do not require any special physical technique.

Particles produced according this method have excellent properties for SERS and are able to enhance signal in a remarkable broad range of wavelength, from green to near infra-red. When compared with spherical nanoparticles with similar dimension and concentration, SGN shows enhancing factors from 10 to 50 times higher depending from the dye and the wavelength employed.

Based on these data and on their good physicochemical characteristics we expect that SGN could be used for the further development of highly specific and sensible SERS based assays for the detection of biomarkers.

8595-9, Session 2

Image theory for plasmon-modified luminescence near nanospheres

Zhe Zhang, Derrick Lim, Rodolfo E. Diaz, Arizona State Univ. (United States)

We present a semi-electrostatic method to model the interaction between dipolar emitting molecule and a plasmon-metal nano-sphere. Based on the Image theory, we model the nano-spheres by dipole images of the molecule. The retardation effect is taken into account by XXX. The expressions of the radiative rate, the non-radiative rate and the quantum efficiency for the molecules are derived. Our image method indicates the strong distance-dependant and frequency-dependant enhancement on both radiative and non-radiative rate. The coupling effect between the molecule and its image is investigated by analyzing multipole expressions of the image dipole. We demonstrates that the high order modes and the

radiation pattern of the molecule/image system, is strong consistency with the exact electromagnetic theory while they were not described by the old electrostatic Gerstern-Niztan Model.

8595-10, Session 2

DNA-templated nanoantennas ready for biological applications *(Invited Paper)*

Guillermo P. Acuna, Phil Holzmeister, Friederike Möller, Susanne Beater, Birka Lalkens, Philip Tinnefeld, Technische Univ. Braunschweig (Germany)

We report on the development of a bottom-up nanoantenna to enhance the fluorescence intensity in a reduced hot-spot, ready for biological applications. We use self-assembled DNA origami structures as a breadboard where different gold nanoparticle systems consisting of dimers and monomers are positioned with nanometer precision. The dependence of the fluorescence enhancement on nanoparticle size is studied and compared to numerical simulations. A maximum of 100fold intensity enhancement is obtained using 100 nm gold nanoparticles at a gap of 23 nm between the dimer. Additionally, the binding and unbinding of short DNA strands on the hotspot of the nanoantenna is realized, showing the compatibility of this technique with biomolecular assays. The combination of metallic nanoparticles with DNA origami structures with docking points for biological assays paves the way for the development of bottom up inexpensive enhancement chambers for single molecule measurements at high concentrations where processes like DNA sequencing occurs.

8595-11, Session 2

One phase growth of in-situ functionalized gold and silver nanoparticles and luminescent nanoclusters

Fadi H. Aldeek, Habeeb M. Muhammed, Xin Ji, Goutam Palui, Naiqian Zhan, Hedi Mattoussi, Florida State Univ. (United States)

Metallic non-luminescent nanoparticles (NPs) and non-metallic luminescent nanoclusters (NCs) of gold and silver are two exciting groups of nanomaterials that exhibit entirely different optical, physical and chemical properties. Owing to their unique properties, a great interest has been generated in these systems over the past few years. We report the growth of an array of stable gold and silver NPs and fluorescent NCs using one-step reduction of Au and Ag precursors in aqueous media and in the presence of bifunctional ligands; these ligands are made of bidentate anchoring groups (lipoic acid) appended with either poly(ethylene glycol), LA-PEG, or Zwitterion (LA-ZW). The particle size can be discretely controlled by varying the metal-to-ligand molar ratios.

We found that while high ratios promote the formation of NPs, low ratios exclusively favour the formation of small size and highly fluorescent nanoclusters. The NCs primarily emit in the red and near infrared (NIR) region of the optical spectrum. Furthermore, the ligands enhance the optical properties of the NPs and NCs and improve their long term colloidal stability to pH changes and excess electrolytes, while reducing the nonspecific interactions in biological media.

The growth strategy further permitted the in-situ functionalization of the NCs with reactive groups (e.g., carboxylic acid or amine) that are compatible with common coupling chemistries, such as carbodiimide and cysteine-maleimide reactions. We will describe the growth method and provide structural and optical characterization of these materials. We will also discuss the integration of the materials in biological hybrids and their effectiveness in energy transfer processes when combined with luminescent quantum dots.

8595-12, Session 3

Colloidal gold nanorings for improved photodynamic therapy through field-enhanced generation of reactive oxygen species

Yue Hu, Yamin Yang, Hongjun Wang, Henry Du, Stevens Institute of Technology (United States)

Au nanostructures that exhibit strong localized surface plasmon resonance (SPR) have excellent potential for photo-medicine, among a host of other applications. Here, we report the synthesis and use of colloidal gold nanorings (GNRs) in photodynamic therapy of breast cancer. The GNRs were fabricated via galvanic replacement reaction of sacrificial Co nanoparticles in gold salt solution with low molecular weight (Mw = 2,500) poly(vinylpyrrolidone) (PVP) as a stabilizing agent. The GNRs were characterized by scanning electron microscopy and high-resolution transmission electron microscopy. The size and the opening of the GNRs were controlled by the diameter of the starting Co particles and the concentration of the gold salt. UV-Vis absorption measurements indicated the tunability of the SPR from 560 nm to 780 nm via varying the physical dimension of the GNRs. MTT assay showed that the GNRs were non-toxic and biocompatible when they were incubated with breast cancer cells as well as healthy cells for control. The GNRs conjugated with 5-ALA photosensitizer precursor led to elevated formation of reactive oxygen species in and improved efficacy (by 40%) of photodynamic therapy of breast cancer cells under light irradiation compared to photosensitizer. These results can be attributed to significantly enhanced localized electromagnetic field of the GNRs, consistent with the observed high SERS activity of GNRs in our Raman measurements.

8595-13, Session 3

Bioanalytics using single plasmonic nanostructures *(Invited Paper)*

Ondrej Stranik, Dublin City Univ. (Ireland); Thomas Schneider, Norbert Jahr, Janina Wirth, Frank Garwe, Andrea Csaki, Wolfgang Fritzsche, Institut für Photonische Technologien e.V. (Germany)

Plasmonic nanostructures promise to provide sensing capabilities with the potential for sensitive and robust assays in a high parallelization. We present here the use of individual nanostructures for the detection and manipulation of biomolecules such as DNA based on optical approaches.

The change in localized surface plasmon resonance of individual metal nanoparticles is utilized to monitor the binding of DNA directly or via DNA-DNA interaction. The influence of different size (length) as well as position (distance to the particle surface) is thereby studied.

Holes in a Cr layer present another interesting approach for bioanalytics. They are used to detect individual plasmonic nanoparticles as labels or to sense the binding of DNA on these particles. This hybrid system of hole and particle allows for simple (just using RGB-signals of a CCD) but a highly sensitive (one nanoparticle sensitivity) detection. On the other hand, the binding of molecular layers around the particles can be detected using spectroscopic features of just an individual one of these systems.

Besides sensing, individual plasmonic nanostructures can be also used to manipulate single biomolecular structures such as DNA. Attached particles can be used for local destruction or cutting as well as coupling of energy into (and guiding along) the molecular structure.

8595-14, Session 4

The biocompatibility of nanosized materials: intracellular nanoparticle stability and effects on toxicity and particle functionality *(Invited Paper)*

Stefaan J. Soenen, Stefaan C. De Smedt, Kevin Braeckmans, Univ. Gent (Belgium)

The interest in using nanoparticles for biomedical applications is vastly increasing. However, for most particles, their use in live cells and animals remains limited, which is largely due to the potential toxicity of these particles which remains an issue of debate.

Here, a recently established multiparametric protocol is presented to investigate the cytotoxic effects of various types of nanomaterials, including gold nanoparticles, quantum dots or fluorescent silica particles on multiple cell types. Parameters studied include cell viability, generation of reactive oxygen species and secondary effects, cell division, intracellular nanoparticle quantification and localization, cell morphology and cell functionality. Special emphasis is on the intracellular stability of nanoparticles against the degradative endosomal environment. Using this extensive panel of tests allows to reveal the mechanisms involved in nanoparticle toxicity and to define the concentrations at which no negative effects are observed. Furthermore, as all work is done under well-defined conditions, results obtained for various types of nanomaterials can be easily compared to other particles tested under identical conditions. For the different particles, highly variable results were obtained, where Au particles were highly persistent within cells whereas quantum dots degraded rapidly, impeding cell viability and reducing the particle's quantum yield.

These data highlight the importance of a multiparametric methodology to assess nanoparticle cytotoxicity as particles were found to affect cell homeostasis by various mechanisms. Also, the behaviour of the particles in their final biological micro-environment must be studied carefully as well as the effect of the particles as a function of time.

8595-16, Session 4

Additive-free gold nanoparticles as toxicity reference materials in reproduction biology *(Invited Paper)*

Stephan Barcikowski, Christoph Rehbock, Vivian Merk, Lisa Gamrad, Univ. Duisburg-Essen (Germany); Ulrike Taylor, Wilfried Kues, Detlef Rath, Friedrich-Loeffler-Institut (Germany)

The toxicological effect of nanoparticles (NPs) emitted from coated medical implants on germ cell function and embryo development is a growing matter of concern as in reproduction medicine already one compromised cell may have severe effects. Requirements for NP reference materials suited for cytotoxicity assays are a reduced material toxicity (e.g. Au), ligand-free surfaces, controlled particle sizes and stability in biological media. Unfortunately chemically synthesized Au-NPs are always contaminated with artificial ligands from synthesis which cannot be quantitatively removed [1] and might interfere with toxicity assays [2].

In this work AuNP reference materials are synthesized using a laser-based method, which does not require artificial surfactants and provides colloids of high purity [3]. To rule out side-effects in toxicity assays all additives used are cell culture components. In this respect low ionic strengths of inorganic salts (phosphate buffer, NaCl) were used to successfully tune the particle size in a range from 6-20 nm. To achieve stability in biological media the particles were coated with the model protein BSA. These experiments clearly indicate an increased NP stability with BSA concentrations far below the physiological level. Additionally an improved long-term stability in biological systems was found. The thus optimized NPs are applied in toxicity assays with gametes, where their impact on sperm motility, fertilization and embryo development is examined.

[1] J. A. Lopez-Sanchez et al., Nat. Chem., 3, 551–556 (2011)

[2] Uboldi et al., Part. Fibre Toxicol. 6:18 (2009)

[3] Petersen, Barcikowski., J. Phys.Chem.C 113, 19830-19834 (2009)

8595-17, Session 4

Excretion and toxicity of gold-iron nanoparticles

David L. Halaney, James T. Jenkins, The Univ. of Texas Health Science Ctr. at San Antonio (United States); Konstantin V. Sokolov, The Univ. of Texas M.D. Anderson Cancer Ctr. (United States); Li Leo Ma, The Univ. of Texas at Austin (United States); Heather J. Shipley, The Univ. of Texas at San Antonio (United States); Smridhi Mahajan, Christopher L. Louden, Reto Asmis, The Univ. of Texas Health Science Ctr. at San Antonio (United States); Thomas E. Milner, Keith P. Johnston, The Univ. of Texas at Austin (United States); Marc D. Feldman, The Univ. of Texas Health Science Ctr. at San Antonio (United States)

Introduction: Macrophages are of great interest for imaging due to their critical roles in the progression of atherosclerosis and modulation of cancer. Gold nanoparticles are an ideal contrast agent for imaging in vivo macrophages. Although gold nanoparticles have been considered bio-inert, some recent studies have demonstrated their toxicity. One strategy to reduce toxicity is to enhance excretion from the body. Thus, we developed a nanoclustering of gold and iron oxide as a nanoparticle (nanorose) with peak light absorption in the near-infrared (NIR), which biodegrades into subunits to facilitate rapid excretion.

Methods: In vitro studies consisted of HCl acid degradation and macrophage lysosomal biodegradation of nanorose and were assessed through UV-vis absorption spectrometry and light scattering hyperspectral microscopy, respectively. Excretion was evaluated in vivo by i.v. injection of nanorose into C57BL/6 mice (n=14). Inductively coupled plasma optical emission spectrometry (ICP-OES) was used to quantify 31 day reduction in gold concentration in 11 tissues. Nanorose toxicity was investigated through hematology and blood chemistry.

Results: Both in vitro studies demonstrated acid degradation of nanoroses at pHs similar to lysosomes via blueshift of peak light absorption and scattering. In vivo studies demonstrated a reduction from 46.2±14.4 to 10.5±2.7 percent injected gold ($p<0.01$), more rapid than the excretion of competing gold nanoparticles in ten publications. Hematology and chemistry showed no toxicity in nanorose-injected mice up to 14 days.

Conclusion: We conclude that the clustering design of nanorose enhances its excretion, and is a viable strategy to limit toxicity of gold nanoparticles for clinical applications.

8595-18, Session 4

Antimicrobial photodynamic effect of protoporphyrin IX in the prescence of gold nanoparticles and hydrogen peroxide against staphylococcus aureus

Fathi A. Taha, Anna Univ. Chennai (India); Chandrasekaran Ramprasath, Narayanasamy Mathivanan, Univ. of Madras (India); Prakasarao Aruna, Singaravelu Ganesan, Anna Univ. Chennai (India)

Staphylococcus aureus is one of the human pathogens, which causes a wide range of diseases such as syptic arthritis, osteomyelitis, wound infections, and endocarditis . Methicillin-resistant S. aureus (MRSA) strains are considered to be the most dangerous, as they cause and

develop infections very efficiently and they are also exhibit resistant to all types of ?-lactam antibiotics and other antimicrobials.

Although Photodynamic Therapy (PDT) is most commonly used for various oncological applications, it has been considered for many non-oncological applications. Antimicrobial PDT (APDT) is one of the non-oncology applications. APDT is used against a wide range of bacteria, viruses and fungi, which are extremely harmful.

The effectiveness of APDT with Protoporphyrin IX (PPIX) in the presence of Gold nanoparticles (GNPs) and hydrogen peroxide (H2O2) against Staphylococcus aureus was studied. Fluorescence spectroscopy was used to characterize the damage at protein level. Results showed that PPIX with H2O2 has showed higher bactericidal effect than that of PPIX alone and PPIX with GNPs. Fluorescence spectroscopic characterization showed considerable change in the intensity of protein emission and excited state kinetics of tryptophan emission from the microorganism due to pre and post APDT protein damage is one of the reasons of bactericidal effect.

8595-19, Session 5

Nanoprecipitation versus two step desolvation technique for the preparation of gelatin nanoparticles *(Invited Paper)*

Saeed A. Khan, Univ. des Saarlandes (Germany) and Kohat Univ. of Science and Technology (Pakistan); Marc Schneider, Univ. des Saarlandes (Germany)

The delivery of hydrophilic macromolecules to the desired site of the body has always been a challenging task; since they are sensitive compounds requiring protection from the biological environment and cannot easily cross the biological barriers. As a consequence, their efficacy to reach the target site is reduced. Several approaches have been utilized so far, for the delivery of macromolecule, among which nanoparticulate delivery systems has offered great promise [1]. The usage of hydrophobic polymers may induce unfolding and loss of biological activity [2]. Therefore, hydrophilic biopolymers are gaining interest, as carrier nanomaterial for the delivery of labile biopharmaceutics.

Gelatin is a protein obtained by hydrolysis of collagen commonly used for pharmaceutical and medical applications. It has been widely used as biomaterial for drug delivery system. The biocompatibility, biodegradability offers large potential also as a nanomaterial. Various techniques have been used for preparation of gelatin nanoparticles highlighting the two step desolvation, which is the most widely used method. We established nanoprecipitation [3] as a new approach and compared the results, as both methods rely on different mechanisms for nanoparticle formation. In this scenario, we focus on a comparative study of nanoprecipitaiton and two step desolvation. Size and colloidal stability was monitored. It was observed that two step desolvation resulted in smaller particles using the same gelatin concentration. Nevertheless no substantial increase in size was observed during the course of crosslinking, in both the cases. Last but not the least, FITC-dextran was employed as a model macromolecule, to see the comparative efficiency of both techniques for encapsulation of macromolecules.

References

1. Janes, K.A., P. Calvo, and M.J. Alonso, Polysaccharide colloidal particles as delivery systems for macromolecules. Advanced Drug Delivery Reviews, 2001. 47: p. 83-97.

2. Bilati, U., E. Allémann, and E. Doelker, Development of a nanoprecipitation method intended for the entrapment of hydrophilic drugs into nanoparticles. European Journal of Pharmaceutical Sciences, 2005. 24(1): p. 67-75.

3. Lee, E., S. Khan, and K. Lim, Gelatin Nanoparticle Preparation by Nanoprecipitation. Journal of biomaterials science. Polymer edition, 2010. 22(4-6): p. 753-771.

8595-20, Session 5

Synthesis and optical trapping of a biocompatible gold nanoparticle/DNA origami hybrid

Jaekwon Do, Robert Schreiber, Andrey A. Lutich, Tim Liedl, Jessica Rodríguez Fernández, Jochen Feldmann, Ludwig-Maximilians-Univ. München (Germany)

Designing complex nanoscale objects having the potential to undergo light-controlled motion in biological environments is an important challenge of nanotechnology. Light-controlled motion of a given object requires some degree of three-dimensional control. The focused light of laser tweezers can provide the trapping force needed to hold an object in a convenient position [1] and also the flux needed to rotate it by generating an optical torque on it [2,3]. Gold nanoparticles are attractive nanoscale building-blocks for light-controlled motion in biological environments. They can be synthesized with tailored morphologies and sizes; they are chemically robust; their surface can be derivatized with biocompatible molecules; and they can be 3D-trapped with a tightly focused laser beam under optimal conditions [4]. Some examples on light-driven motion of various types of gold nanoparticles (mainly consisting of as-synthesized nanoparticles, and their randomly-formed aggregates) have been reported [5]. However reports dealing with gold-based nanostructures having a complex, hybrid-like morphology, a biocompatible character, and the potential for light-driven motion have remained elusive to-date.

In an effort to fill this gap, in this communication we present the design and synthesis of a biocompatible nanoscale hybrid (referred hereafter as 'Au@DNA origami') having a complex morphology, and the potential for light-driven motion under biological conditions [6]. Our nanoscale hybrid consists of a DNA-functionalized spherical gold nanoparticle (ca. 60 nm diameter) containing self-assembled two-dimensional square-like DNA sheets (80?80 nm) on its surface, prepared by the highly versatile DNA origami technique [7]. The spatial arrangement of the DNA sheets on the Au surface provides the hybrid with a propeller-resembling shape. The DNA sheets, and hence the Au@DNA origami hybrids, are biocompatible and stable in biological buffers. As a first step towards the possible utilization of these Au@DNA origami hybrids as light-driven nanoscale motors in biological media, we show that they can be efficiently trapped with a non-resonant near-IR laser beam, and that under realistic trapping conditions (< 200 mW, < 51°C) optothermal effects can be minimized, and thus, their propeller-like morphology, preserved.

[1] Ashkin, A., Dziedzic, J. M., Bjorkholm, J. E. & Chu, S. Observation of a single-beam gradient force optical trap for dielectric particles. Opt. Lett. 11, 288-290 (1986).

[2] Friese, M. E. J., Nieminen, T. A., Heckenberg, N. R. & Rubinsztein-Dunlop, H. Optical alignment and spinning of laser-trapped microscopic particles. Nature 394, 348-350 (1998).

[3] Paterson, L. et al. Controlled Rotation of Optically Trapped Microscopic Particles. Science 292, 912-914 (2001).

[4] Ohlinger, A., Nedev, S., Lutich, A. A. & Feldmann, J. Optothermal Escape of Plasmonically Coupled Silver Nanoparticles from a Three-Dimensional Optical Trap. Nano Lett. 11, 1770-1774 (2011).

[5] Tong, L., Miljkovic, V. D. & Käll, M. Alignment, Rotation, and Spinning of Single Plasmonic Nanoparticles and Nanowires Using Polarization Dependent Optical Forces. Nano Lett. 10, 268-273 (2009).

[6] Do, J., Schreiber, R., Lutich, A. A., Liedl, T., Rodríguez-Fernández, J., Feldmann, J., 2012, Submitted.

[7] Gu, H. Z., Chao, J., Xiao, S. J. & Seeman, N. C. A proximity-based programmable DNA nanoscale assembly line. Nature 465, 202-U286 (2010).

8595-21, Session 6

Inorganic/organic core-shell colloids: synthesis, characterization and potential applications *(Invited Paper)*

Matthias Karg, Univ. Bayreuth (Germany)

The synthesis and characterization of metal and metal oxide nanoparticles has attracted enormous scientific interest within the last decades. Not at last from an application point of view the stability of such particles plays an important role. Hence, ligand exchange strategies or polymer coatings are often applied to enhance the colloidal stability and to introduce new functionalities. Multifunctional materials can be prepared if inorganic nanoparticles are combined with responsive polymer materials[1,2,3].

In this contribution we present a versatile protocol to coat metal nanoparticles such as gold, silver and platinum with cross-linked, thermoresponsive polymer shells. Our synthetic approach allows control over the shell dimensions, the responsivity of the shell as well as the introduction of functional groups. These multifunctional inorganic/organic hybrid colloids are colloidally stable in different dispersion media also at extremely high volume fractions. In case of plasmonic nanoparticle cores UV-vis spectroscopy has been used to investigate the optical properties of these colloids. The size, polydispersity and thermoresponsive behavior was studied by means of Dynamic Light Scattering, whereas the internal structure of the polymer shell was analyzed by Small Angle Neutron Scattering. As an example for potential applications we demonstrate SERS sensing using self-assembled core-shell particles with different sized and shaped gold cores[4].

[1] M. Karg, Colloid Polym. Sci. 2012, 290 (8), 673-688

[2] M. Karg, T. Hellweg, J. Mater. Chem. 2009, 19, 8714-8727

[3] M. Karg, T. Hellweg, Current Opinion in Colloid & Interface Science 2009, 14, 438-450

[4] M. Mueller, M. Tebbe, D.V. Andreeva, M. Karg, R.A. Alvarez Puebla, N. Pazos Perez, A. Fery, Langmuir 2012, 28, 9168-9173

8595-22, Session 6

Synthesis and application of fluorescent gold nanocluster's probes *(Invited Paper)*

Walter H. Chang, Jhih-Liang Li, Po-Wen Lee, To-Yuan Chen, Ching-Ta Chen, Fang-Yu Shao, Chia-Hui Lin, Yu-Yu Wu, Cheng-An J. Lin, Chung Yuan Christian Univ. (Taiwan)

Fluorescent nanoprobes are rapidly gaining popularity, and will soon replace more traditional bio-markers – such as organic fluorescent dyes, fluorescent proteins and quantum dots – as the most commonly used contrast for imaging in the field of biomedical technology. Fluorescent gold nanoclusters (FGNCs) hold particular interest, as they are known for their superior optical properties, high biocompatibility, as well as great resistance to photobleaching. However, FGNCs have low quantum yield and bind nonspecifically when tested in vivo. In response to these flaws, we first show that using dodecanethiol (DDT) as the surface modifier can increase the quantum yield of these clusters. Secondly, to combat the lack of specificity of FGNCs, we ultimately modify the surface of the cluster to have a distearyl acyl phosphatidyl ethanolamine – polyethylene glycol – folic acid (DSPE-PEG-Folate) shell. Using a facile, efficient method, we synthesized biocompatible hydrophilic structured FGNCs from toxic, hydrophobic clusters with a diameter of two nanometers through the use of microemulsion. This simple phase conversion process can not only be used to modify any organic hydrophobic nanoparticle or cluster into a hydrophilic structure, it also increases the efficiency of binding DSPE-PEG-Folate to the gold nanocluster. This counters the lack of specificity of FGNCs by allowing the particles to target certain folate receptors on cancers cells and illuminate their locations. Using a generic microemulsifier, we can decrease the biological toxicity and increase binding specificity of any nanomaterial through phase conversion technology and thus enhance the regenerative medical applications of nanotechnology.

8595-23, Session 6

Colloidal ZnO nanoparticles for nonlinear optical probes and selective cell destruction

Ben E. Urban Jr., Univ. of North Texas (United States)

Nanoparticles have numerous properties that can be used for imaging. Nonlinear optical properties of certain nanoparticles make their use as biological probes especially interesting.

High crystalline quality ZnO nanoparticles exhibit efficient multiphoton excitation luminescence (MPE) and second harmonic generation (SHG) properties. SHG is particularly efficient in ZnO nanoparticles, has a wide range in the NIR and does not generate heating effects in cells. TPE, however, leads to large amounts of localized heating. Cells that have ingested ZnO can be imaged using the large antistokes shift of the SHG process and selectively destroyed using the localized heating effects of TPE.

The selective toxicity of ZnO nanoparticles, depending on density and size, has also let to its study for potential use in nanomedicines. Oxide rich nanoparticles tend to create oxidative stress in cells that ingest them. Cancer cells are especially susceptible to oxidative stress due to their inability to process the peroxidation effect that it leads to inside the cell, where as healthy cells are less susceptible to peroxidation. By controlling the density and size of the ZnO being delivered to the cancer, it is possible to deliver lethal doses to the mutant cells, while leaving healthy counterparts functional.

However, delivering semiconductor nanoparticles to cells is difficult. Attaching antibodies or cell specific microRNA to the surface is not possible without chemical surface treatments, which degrade crystal properties and lead to higher toxicity. In this presentation, we present a cheaper alternative to delivering ZnO nanoparticles directly to cancer cells without affecting the properties of the ZnO nanoparticles. By integrating ZnO with a 'smart' biological component, we can specifically attack types of cancer cells, while not interacting with healthy cells. A presentation of our experiments and most recent progress follows.

8595-24, Session 7

Raman confocal microscopy studies of biotoxicity and biodistribution of modified magnetic nanoparticles for biomedical applications *(Invited Paper)*

Irantzu Llarena, CIC BiomaGUNE (Spain); Camila Messias, Sebastiao W. Da Silva, Univ. de Brasilia (Brazil); Maria Echeverría, CIC BiomaGUNE (Spain); Sergio E. Moya, CIC BiomaGUNE (Spain) and Lab. of Macromolecular Synthesis and Functionalization, Zhejiang Univ. (China); Paulo C. Do Morais, Univ. de Brasilia (Brazil)

Understand the effects of nanoparticles (NPs) and nanostructured materials is of major interested for human health, because of the increasing interest of this kind of materials as medical tools for sensing, drug delivery or imaging.

The effect of the different functionalization in the biodistribution and toxical effect on in vitro systems is studied by means of the Raman confocal microscopy technique, taking advantage of the free label character of technique. Systems in which prevail their magnetic properties and combine reduce toxicity with specific targeting are promising candidates for in vitro studies and magnetic resonance imaging probes in animal models.

Magnetic iron oxide nanoparticles functionalized with different charged polymers, as poly allylaminochloride (PAH) and poly acrylic acid (PAA), using Layer by layer technique (LbL) had been characterized mediated different techniques such as Ultraviolet-Visible and FT-Infrared spectroscopy, Dynamic Light Scattering (DLS) and Surface Enhance Raman Spectroscopy (SERS). Further modification using the LbL system as scaffold provide the possibility of incorporating different coatings as

Polyetheylene glycol (PEG) and Folic acid which can reduce toxicity and improve specificity. The biodistribution of the NPs and the toxical effects in vitro is studied using confocal raman microscopy.

8595-25, Session 7

Multiplexed color encoded nanospheres (MENs) on stepwise encapsulation of nanocrystals into SiO2

Quian Ma, Ivan Castelló-Serrano, Emilio J. Palomares, ICIQ - Institut Català d'Investigació Química (Spain)

Quantum dot (QDs) multicode silica nanospheres were prepared by employing a micro-emulsion method. This method allows the successful preparation of SiO2 layer-by-layer with the encapsulation of hydrophobic QDs. This novel procedure has several main features. Firstly, it is facile and straightforward, avoiding complex chemical reactions that may quench the CdSe/ZnS Qds luminescence, Secondly, QDs loading and composition can be controlled simply through the number of silica layers and QDs selection respectively, thereby providing a means to tune the nanospheres optical properties. Finally, the use of inert silica for coating QDs avoids the leakage of heavy metal ions into the environment and enhances the chemical stability of CdSe QDs. We have employed the nanospheres as pH chemiodosimeters and found a superb stability between pH 5 to pH 7 for more than 160 hours. Moreover, the multicode spheres can be used to determine the pH value in the range of pH between 4 to pH 9. The implications of these results to measure intracellular pH are also discussed.

8595-26, Session 7

Multiphoton imaging of three-dimensional cancer models using upconverting lanthanide nanoparticles

Christian F. Gainer, Marek Romanowski, The Univ. of Arizona (United States)

While upconverting lanthanide nanoparticles have numerous advantages over other exogenous contrast agents used in scanned multiphoton imaging, their long luminescence lifetimes cause images collected with non-descanned detection to be greatly blurred. We demonstrate herein the use of Richardson-Lucy deconvolution to deblur luminescence images obtained via multiphoton scanning microscopy. Images were taken of three dimensional models of colon and ovarian cancer following incubation with NaYF4:Yb,Er(Tm) nanoparticles functionalized with an antibody for EGFR and folic acid respectively. Following deconvolution, images had a lateral resolution on par with the optimal performance of the imaging system used, ~1.2 um, and an axial resolution of ~5 um. Due to the relatively high multiphoton excitation efficiency of these nanoparticles, it is possible to follow binding of individual particles in tissue. In addition, their extreme photostability allows for prolonged imaging without significant loss in luminescence signal. With these advantageous properties in mind, we also discuss the potential application of upconverting lanthanide nanoparticles for tracking of specific, cancer relevant receptors in tissue.

8595-28, Session 7

Multifunctional rare-earth vanadate nanoparticles: luminescent probes, hydrogen peroxide sensors, and MRI contrast agents

Mouna Abdesselem, Markus Schöffel, Isabelle Maurin, Ecole Polytechnique (France); Olivier Clément, Paris Ctr. de Recherche Cardiovasculaire (France); Pierre-Louis Tharaux, Institut National de la Santé et de la Recherche Médicale (France); Jean-Pierre Boilot, Cédric Bouzigues, Antigoni Alexandrou, Ecole Polytechnique (France)

Europium-doped nanoparticles (Y0.6Eu0.4VO4) show red photo-stable and non-blinking luminescence1, ideal for single-biomolecule labeling and tracking2. Moreover, recent work showed that they can be photo-reduced reversibly. The luminescence recovery is correlated to oxidant concentration which opens the possibility for powerful oxidant sensing. Intracellular signaling pathways involving hydrogen peroxide were successfully investigated quantitatively with both temporal and spatial resolution3.

Furthermore, gadolinium introduction yields 10 or 40-nm Gd0.6Eu0.4VO4 particles and opens the way for multimodal medical imaging. Indeed. relaxivity measurements showed that these particles are efficient T1-contrast enhancers for magnetic resonance imaging (MRI) (r1= 8.2 mM-1s-1at 20 MHz, higher than that of Dotarem®: r1=3.6 mM-1s-1). In addition, these particles retain their luminescent and oxygen sensing properties.

Carboxymethyl-dextran-coated nanoparticles were injected in living mice. MRI experiments confirmed a positive contrast enhancement and showed an accumulation of the particles in the bladder 30 minutes after injection. These particles combine the advantages of a long blood circulation, a low leaching rate of Gd3+ ions, which are highly toxic in free form, by embedding them in a solid matrix, and facile functionalization. For specific targeting of inflammation sites, we successfully performed ex vivo macrophage loading with Gd0.6Eu0.4VO4 nanoparticles, demonstrated by fluorescence microscopy. The promising combination of three modalities can provide wealthy information about hydrogen peroxide involvement and macrophage recruitment dynamics in inflammatory reactions.

1. Beaurepaire E., et al. Nano Lett. 4, 2079-2083 (2004)

2. Türkan S., et al. Biophys. J., 102, 2288–2298 (2012)

3. Casanova, D., et al. Nature Nanotechnol.,4(9):581–585 (2009)

8595-29, Session 7

Gold nanosensitisers for dual-modal fluorescent and SERS bioimaging

Vijaya Raghavan Ayanam Parthasarathy, Hai Ming Fan, Malini C. Olivo, National Univ. of Ireland, Galway (Ireland)

Multi-modal nanosensitisers have attracted much attention because of their superior chemical and physical properties that have great potential for early diagnostics and treatment of cancer. In this work, complex multi-branched gold nanocrystals, known as nanostars, have been used to construct dual-modal fluorescent (FL) and surface enhanced Raman spectroscopy (SERS) probes for detecting and photodynamic treatment (PDT) of cancer. The nanosensitiser is constructed by a multilayer technique in which Raman reporter, DTTCi (3, 3'-Diethylthiatricarbocyanine iodide), and photosensitiser (Hypericin) are controllably coated onto the gold nanostars. By elaborate adjusting of the layer space, these coating can endow both SERS and enhanced FL capabilities for the multi-branched gold nanocrystals. Cellular uptake and cytotoxicity of nanosensitisers are performed using SK-BR-3 and MDA-MB-231 cell lines. Cell localization of these nanosensitisers will be investigated using dual-modal confocal Raman/FL imaging. In-vitro studies of photodynamic treatment using SK-BR-3 cell lines are also demonstrated and therapeutic function of nanosensitisers can be achieved by the means of switching wavelength of excitation light. The development of such dual-modal SERS/FL nanosensitiser in current work will offer a useful tool for non-invasive, high-accuracy, single-node diagnosis and therapy of cancers.

8595-30, Session 7

Uptake and processing of semiconductor quantum dots in living cells studied by fluorescence lifetime imaging microscopy (FLIM)

Jay L. Nadeau, Lina Carlini, McGill Univ. (Canada)

Carboxylate-terminated and dopamine-conjugated CdSe/ZnS quantum dots (QDs) are imaged in living fibroblasts using fluorescence lifetime imaging microscopy (FLIM). Changes in lifetime are observed as the QDs are processed in the cells, and are consistent with lifetime measurements in bulk solution using buffer compositions that are expected to correspond to different cellular regions. However, some new features are seen that are not observed in bulk solution, such as qualitatively different lifetime values as the concentration of QDs is increased. This is the first report of the use of FLIM to study QD processing in cells, and demonstrates the utility of the technique and its caveats.

8595-31, Session 8

Capsules-based fluorescent ratiometric sensors to investigate the cellular environment *(Invited Paper)*

Loretta L. del Mercato, Marzia M. Ferraro, Consiglio Nazionale delle Ricerche (Italy); Azhar Z. Abbasi, Markus Ochs, Wolfgang J. Parak, Philipps-Univ. Marburg (Germany); Rosaria Rinaldi, Consiglio Nazionale delle Ricerche (Italy) and Univ. del Salento (Italy)

Fluorescent ratiometric sensors based on particles platforms are of great interest in the bioanalytical field. In this context, polyelectrolyte capsules may prove to be viable tools as their architecture and composition can be properly tuned for measuring the concentration of different species in the cellular environment through ratiometric measurements. This talk will discuss a few opportunities in the synthesis and applications of prototype biosensors based on multilayer polymer capsules for in-vitro sensing of intracellular ions. In particular, a methodology recently developed for assembling quantum-dots barcoded polyelectrolyte capsules for multiplexed sensing of protons, sodium and potassium ions will be described1. Finally, the use of pH-sensitive capsules for measuring pH changes that occurs in the endocytic pathways of cells in which the functionality of the V-ATPase proton pump have been altered will be shown. The reported examples demonstrate that polymer capsules are promising carrier matrixes for optical sensing of target biological analytes.

8595-32, Session 8

Voltage clamped single gold nanoparticles: sensors for anions and pH *(Invited Paper)*

Thomas A. Klar, Cynthia Vidal, Martin Djiango, Calin Hrelescu, Johannes Kepler Univ. Linz (Austria)

Recently, we have shown that optical dark field spectroscopy of voltage-clamped single gold nanoparticles is an excellent tool to observe the interaction of anions with the nanoparticles. [1] Hereby, the nanoparticle plasmon resonance (NPPR) of gold nanoparticles in aqueous solution can be damped reversibly by applying a potential more positive than the point of zero charge but below the onset of oxidation. This damping leads to a spectral broadening of the NPPR. In addition, a pronounced spectral shift of the NPPR is observed. Interestingly, both cannot be simply explained by a refractive index effect nor by a pure charging effect. Instead, both can conclusively be explained by the opening of additional damping channels for the plasmon resonance and a voltage dependent nanoparticle capacitance due to the adsorption of anions.

In the current contribution, we will discuss how this effect can be applied to gain further insight in the nano-local electro-chemistry on the surface of a single gold nanoparticle. For instance, different anions from the Hofmeister series give different spectroscopic signals and it is also possible to use single gold nanoparticles as nanoscale pH-meters. Our findings can be useful in designing nano-local chemical and biological sensors. More general, the voltage-induced chemical surface damping needs to be accounted for in all situations where molecules in aqueous solutions come in close contact with metal nanoparticles. These include bio-diagnostics and surface enhanced Raman scattering.

[1] SK Dondapati et al.; Nano Letters 12, 1247 (2012)

8595-33, Session 8

Nanoparticle-functionalized microcapsules for delivery and sensing in the context of health and medicine applications

Wolfgang J. Parak, Philipps-Univ. Marburg (Germany)

Inorganic nanoparticles such as magnetic nanoparticles, fluorescent quantum dots, and plasmonic nanoparticles can be used as building blocks for designing multifunctional systems based on polymeric capsules. The properties of the inorganic nanoparticles hereby are harnessed to provide additional functionality to the polymer capsules. Biological applications towards sensing and delivery are discussed. Examples will be given in which magnetic nanoparticles are used to direct capsules with magnetic field gradients, colloidal quantum dots are used to identify capsules via the formation of optical barcodes, and gold nanoparticles are used as light-controlled heat-sources for opening capsules and releasing macromolecules from their cavity upon optical excitation. This demonstrates that combination of inorganic nanoparticles and organic / polymeric molecules as carrier matrices allow for tailoring multifunctional hybrid particles for practical applications.

8595-34, Session 8

Optical microscopy and spectroscopy of analyte-sensitive functionalized gold and silver nanoparticles in microfluidic systems *(Invited Paper)*

Martinus Werts, Julien Navarro, Ecole Normale Supérieure de Cachan (France); Vincent Raimbault, Institut de Chimie de la Matière Condensée de Bordeaux (France); Matthieu Loumaigne, Ecole Normale Supérieure de Cachan (France) and Lab. Aimé Cotton (France); Anne Débarre, Lab. Aimé Cotton (France); Laurent Griscom, Olivier Français, Bruno Le Pioufle, Ecole Normale Supérieure de Cachan (France)

Microfluidic technology offers interesting perspectives when combined with functionalized optically responsive colloidal nanoparticles. On one hand, it offers a highly controllable hydrodynamic environment which may be used for nanoparticle synthesis, functionalization, purification and in situ characterization through optical spectroscopies. On the other hand, the strong optical response of certain types of colloidal particles may be harnessed for the implementation of optical (bio)sensing schemes adapted to microfluidic volumes.

Our work concerns the combination of functionalized plasmonic gold nanoparticles with microfluidics for the development of novel (bio) analytical detection schemes, as well as the study of the physical chemistry of colloidal gold and silver particles in fluidic microsystems.

Building on microfluidic methodology that we have developed recently, we analyze molecularly functonalized metal nanoparticles addressing the detection (and removal) of desorbed ligands. This is combined with fluorescence spectroscopies and the measurement of plasmonic light

scattering. We will furthermore demonstrate the great utility of resonant light scattering spectroscopy for studying interparticle interactions by applying it to a model system of analyte-sensitive functionalized gold nanoparticles in a microfluidic device.

8595-35, Session 8

Sensitive detection of NaYF4: Yb/Tm nanoparticles using suspended core microsctructured optical fibers

Erik P. Schartner, The Univ. of Adelaide (Australia); Dayong Jin, Jiangbo Zhao, Macquarie Univ. (Australia); Tanya M. Monro, The Univ. of Adelaide (Australia)

Rare-earth doped upconversion nanocrystals are emerging as the next-generation luminescent biomaterials. Here we load NaYF4: Yb/Tm upconversion nanocrystals into a soft-glass suspended-core optical fiber dip sensor, allowing sensitive measurements to be performed. Power-dependent optimization of the Tm doping concentration (thousands of Tm ions per nanocrystal) provides high signal brightness from the nanocrystals. This, in combination with negligible background autofluorescence from the glass fibre when using infrared excitation has provided a significant improvement in terms of sensitivity over what has previously been demonstrated using an optical fiber dip sensor.

Suspended-core fibers especially have found extensive use in sensing applications. These combine the high evanescent overlap comparable to that of a nanowire, with the robust handling characteristics and long interaction length of a conventional fiber. The fiber sensor platform allows measurements to be performed using minimal sample volumes (<20 nL) while still maintaining sensitivity of the platform. Trials have demonstrated detection using concentrations as low as 3.9 fM, with a total sample volume filled within the fiber of ~20 nL. This corresponds to ~47 upconversion nanocrystals filled within the fiber, of which a portion are available for detection within the evanescent field in the fiber. Multiple trials showed discrete fluorescent signal intensities, with a peak signal level of either ~30 (background) or ~250 (signal) counts, strongly suggesting that this platform has reached a level where single nanoparticles can be detected in a solution measurement. This offers good opportunities for bio-sensing if the particles are functionalized with appropriate antibodies for detection.

8595-36, Session 8

Examination of pterins using surface-enhanced Raman spectroscopy using low-volume samples

Sam Mehigan, Ciarán Smyth, Eithne M. McCabe, Trinity College Dublin (Ireland)

Surface-enhanced Raman spectroscopy (SERS) is a useful technique for the investigation and quantification of biological compounds. It is based on the adsorption of the molecules to metal surfaces, such as to metal colloids, with a subsequent enhancement of the Raman spectrum. The analysis of biological compounds often demands the use of small sample volumes, and as such the use of 6?L sample droplets will be considered here, while still maintaining sufficient reproducibility in the resultant SERS response. Silver colloids in solution were typically employed in this work, and these have also been optimised as to their response to the pterins. Any variation in the SERS response, both laterally and vertically, over the sample droplet is also considered, as is the impact of the substrate type on the shape of the droplet.

8595-37, Session 9

Biomedical tools based on magnetic nanoparticles *(Invited Paper)*

Maria F. Casula, Anna R. Saba, Paula M. Castillo, Univ. degli Studi di Cagliari (Italy); Elvira Fantechi, Claudio Sangregorio, Univ. degli Studi di Firenze (Italy); Alessandro Lascialfari, Univ. degli Studi di Milano (Italy); Andrea Sbarbati, Univ. degli Studi di Verona (Italy); Alberto Casu, Istituto Italiano di Tecnologia (Italy); Andrea Falqui, Univ. degli Studi di Cagliari (Italy)

Magnetic and superparamagnetic colloids represent a versatile platform for the design of composite nanostructures which may act as multifunctional tools for biomedicine, being active in cancer therapy, tissue imaging and magnetic separation.

In this work, multifunctional spinel ferrites of general formula MFe2O4 coated by either biopolymers, non-toxic commercial dispersants, silica or gold were tested as contrast enhancers in magnetic resonance imaging (MRI) and as magnetic hyperthermia mediators.

XRD, TEM, FT-IR, TGA, N2-Physisorption and DLS techniques were used to gain insights on the structural and morphological features of the materials as well as on the features of the coating. SQUID magnetometry has been used to investigate the magnetic behaviour of the nanoparticles by zero field cooled-field cooled measurements as well as the field dependence of the magnetization at low temperature. NMR-Dispersion (NMRD) profiles, i.e., the measurements of proton nuclear r1 (longitudinal) and r2 (transverse) relaxivities as a function of frequency were collected in order to gain insights on the ability of the materials to act as contrast agents for MRI.

Specific Absorption Rate (SAR) measurements were performed to test the potential of the nanostructures in cancer treatment by magnetic hyperthermia.

8595-38, Session 9

Self-assembled colloidal nanocrystal clusters for bioseparation

Yadong Yin, Univ. of California, Riverside (United States)

It has been a challenge in developing bioseparation methods that are reproducible and with high throughput and quantitative accuracy. We have recently developed a class of novel porous nanostructured materials for the efficient separation of proteins, peptides, and DNA strands. Nanoparticles of various materials with controllable size, shape, and surface properties are self-assembled into three-dimensional clusters containing well-defined mesoscale pores. This new system shows a few advantages in the selective enrichment of biomolecules. First, the pore sizes of shell can be tuned to limit the size of biomolecules that can enter the inside of the clusters. The hydrophilic nature of the nanoparticle clusters also prevents the nonspecific binding of many hydrophobic protein/peptides. Further size exclusion can also be achieved by controlling the dimension of the pores produced by the stacking of the clusters. The surface property of the nanocrystal clusters can be varied to attract the target biomolecules. Additional functional ligands can also be introduced to the particle surfaces to enhance the selectivity. We also demonstrate the incorporation of magnetic nanocrystals into the clusters to enable convenient and efficient magnetic separation.

8595-39, Session 9

Localized magnetic nanoparticle heating for cell stimulation and control *(Invited Paper)*

Arnd Pralle, Heng Huang, Katherine Spoth, Univ. at Buffalo (United States)

Remote, contact-less control of cellular processes would open the large

array of applications from basic research, such as the study of neuronal network response to the activation of specific neurons, to medicine, e.g. the release or production of a drug deep inside the body.

We have developed magnetogenetics, a remote stimulation method based on radio-frequency magnetic field heating of supra-paramagnetic nanoparticles targeted to temperature-sensitive cation channels in cells. Upon application of the RF magnetic fields, the channels are thermally activated, permitting calcium influx into the cells, which in neurons leads to action potentials or in other cells may be used to trigger gene transcription. Precise localized heating is required to achieve fast activation of the channels without inducing cellular damage. We have developed fluorophores as molecular thermometers and use fluorescence lifetime measurements to show that the induced temperature increase is highly localized. We will present theoretical modeling and experimental measurements of temperature distributions around single nanoparticles, two-dimensional arrays and nanoparticle solutions, and discuss the optimal arrangement.

8595-40, Session 9

Water soluble iron oxide nanocubes with high values of specific absorption rate for cancer cell hyperthermia treatment *(Invited Paper)*

Pablo Guardia, Istituto Italiano di Tecnologia (Italy); Riccardo Di Corato, Instituto Italiano di Tecnologia (Italy) and National Nanotechnology Lab. of CNR-NANO (Italy); Leniac Lartigue, Claire Wilhelm, Florence Gazeau, Univ. Paris 7-Denis Diderot (France); Liberato Manna, Istituto Italiano di Tecnologia (Italy); Teresa Pellegrino, Istituto Italiano di Tecnologia (Italy) and National Nanotechnology Lab. of CNR-NANO (Italy)

Magnetic nanoparticles (MNPs) provide a valuable platform with unique properties that are potential exploitation in biomedicine. MNPs have been proposed as magnetic guidance in drug delivery and magnetic separation, as contrast agents in magnetic resonance imaging (MRI) or as heat mediators in hyperthermia treatments. The latter represents a novel therapeutic concept to cancer treatment and is based on the evidence that cancer cells are more sensitive than healthy cells to temperatures higher than 41 °C. Among the various approaches to raise the body temperature, magnetically mediated hyperthermia is based on the generation of heat via an oscillating magnetic field exploiting MNPs as heating foci. Iron oxide nanocrystals (IONCs) are appealing heat mediator nanoprobes in magnetic mediated hyperthermia for cancer treatment. In this work, specific absorption rate (SAR) values are reported for cube-shaped water-soluble IONCs prepared by a one-pot synthesis approach in a size range between 13 and 40 nm. The SAR values were determined as a function of frequency and magnetic field applied, spanning also technical conditions which are considered biomedically safe for patients. Among the different sizes tested, IONCs with an average diameter of 19±3 nm had significant SAR values in clinical conditions and reached SAR values up to 2452 W/gFe at 520 kHz and 29 kAm-1, which is one of the highest values so far reported for IONCs. In vitro trials carried out on KB cancer cells treated with IONCs of 19 nm have shown efficient hyperthermia performance, with cell mortality of about 50% recorded when an equilibrium temperature of 43 °C was reached after 1 hour of treatment.

8595-41, Session 9

Cleaning blood: applications of ultra-strong metal nanomagnets in nanomedicine *(Invited Paper)*

Inge K. Herrmann, Andrea A. Schlegel, Martin Urner, Christoph M. Schumacher, Wendelin J. Stark, Beatrice Beck-Schimmer, ETH Zurich (Switzerland)

Nanomagnets with metal core have recently been shown to be promising candidates for magnetic drug delivery and hyperthermia due to superior magnetic properties compared to commonly used iron oxide beads. We present the direct removal of harmful substances from human whole blood by the use of functionalized magnetic nanoparticles. As a successful application strongly relies on a safe implementation, a particular focus is put on possible interactions of nanomagnets with the vascular compartment. The presentation will also discuss the implementation of the technology into an extracorporeal blood purification device and further steps in the direction of a clinical application of the concept.

The applicability of the concept is demonstrated utilizing three examples: The removal of a heavy metal (lead), a steroid drug (digoxin) and whole proteins (Interleukin-6 and Interleukin-1b) is achieved by spiking human whole blood with the contaminant and applying appropriately functionalized magnetic beads for the detoxification. The contaminant concentration in intoxicated whole blood could be significantly decreased in a dose-dependent manner using a magnetic separation-based blood purification technology. The integrity of the blood was not affected by the process as depicted by monitoring a series of clinically important parameters.

Noxious compounds differing in chemical nature (ions, small molecule drugs, and proteins) can be efficiently and selectively removed from whole blood without being limited by filter cut-offs or slow pore diffusion. Combined with existing therapies, these results may have major implications for the treatment of severe intoxications (digoxin, barbiturates), sepsis (specific filtering of cytokines or toxins), metabolic disorders or auto-immune diseases.

8595-42, Session 9

Hybrid magnetic/plasmonic nanocarriers for capture and photoacoustic detection of circulating tumor cells

Chun-Hsien Wu, Jason R. Cook, Stanislav Y. Emelianov, The Univ. of Texas at Austin (United States); Konstantin V. Sokolov, The Univ. of Texas at Austin (United States) and The Univ. of Texas M.D. Anderson Cancer Ctr. (United States)

Detection of disseminated tumor cells in human fluids such as blood, urine, and saliva can provide an opportunity to develop an accessible tool for cancer detection, prognosis and monitoring the effectiveness of therapy. However, the technical challenge of identifying CTCs in whole blood is their extremely low abundance - one CTC per billions blood cells. Currently assays techniques can provide desirable sensitivity; however, they are cumbersome and require multiple processing steps to minimize background contribution of non-cancerous cells. Here we present a one-step assay for the detection of cancer cells in an unpurified human specimen, such as blood. The assay is based on technological advances in immunotargeted hybrid magnetic/plasmonic nanocarriers and photoacoustic (PA) imaging. We synthetized antibody targeted core-shell plasmonic nanoparticles with a magnetic core and a gold shell to simultaneously capture and detect cancer cells; the nanoparticles are targeted to receptor molecules that are overexpressed in cancer cells. Cancer cells interact with the molecular specific magnetic nanoparticles and are separated from normal blood cells by magnetic force. Then, PA imaging is used to image and quantify the number of cancer cells. The specificity of PA detection of cancer cells is based on the effect of receptor mediated aggregation of the hybrid plasmonic nanoparticles that leads to a strong increase in the absorbance of labeled cancer cells in the red-NIR region. This method has been evaluated in spiked experiments in cell culture and in the whole blood.

8595-43, Session 10

Quantum dots as versatile biosensors for FRET-based multiplexed diagnostics

Niko Hildebrandt, David Wegner, Stina Linden, Zongwen Jin, Univ. Paris-Sud 11 (France); W. Russ Algar, The Univ. of British Columbia (Canada); Igor L. Medintz, U.S. Naval Research Lab. (United States)

The combination of semiconductor quantum dots (QDs) and Förster Resonance Energy Transfer (FRET) offers many advantages for multiplexed diagnostics [1-3]. QDs can be used as FRET donors and acceptors in combination with many different luminophores such as organic dyes, fluorescent proteins or lanthanide complexes. Different QD colors allow spectral multiplexing whereas different luminescence lifetimes provide temporal multiplexing. In this contribution we will present various QD-based FRET-biosensors using antibodies, peptides and oligonucleotides as biological recognition molecules for the multiplexed sensitive detection of tumor markers, proteases and DNA hybridization [4, 5]. Time- and spectrally-resolved optical analysis of FRET from Tb complexes (TCs) with long luminescence lifetimes (up to several milliseconds) to QDs and multistep FRET from TCs to QDs to organic dyes allows spectro-temporal multiplexing with very high sensitivity (sub-nanomolar detetion limits) in simple homogeneous non-amplified bioassays. Our results demonstrate the possibility of very sensitive multiplexed detection of several individual biological events, an important issue for many biosensing applications using optical spectroscopy and imaging of in vitro and in vivo biological systems.

References:

[1] B. Hötzer, I.L. Medintz, N. Hildebrandt. Fluorescence in Nanobiotechnology – Sophisticated Fluorophores for Novel Applications. Small 2012, DOI: 10.1002/smll.201200109, published online.

[2] Z. Jin, N. Hildebrandt. Quantum dots for in vitro and in vivo sensing. Trends Biotechnol. 2012, 30 (7), 394-403.

[3] N. Hildebrandt. Biofunctional Quantum Dots: Controlled Conjugation for Multiplexed Biosensors. ACS Nano 2011, 5(7), 5286–5290.

[4] W. R. Algar, D. Wegner, A. L. Huston, J. B. Blanco-Canosa, M. H. Stewart, A. Armstrong, P. E. Dawson, N. Hildebrandt and I. L. Medintz. Quantum Dots as Simultaneous Acceptors and Donors in Time-Gated Förster Resonance Energy Transfer Relays: Characterization and Biosensing. J. Am. Chem. Soc. 2012, 134, 1876?1891.

[5] D. Geißler, L.J. Charbonnière, R.F. Ziessel, N.G. Butlin, H.-G. Löhmannsröben, N. Hildebrandt, Quantum Dot Biosensors for Ultra-Sensitive Multiplexed Diagnostics, Angew. Chem. Int. Ed. 2010, 49(8), 1396-1401.

8595-44, Session 10

Highly photostable hydrophilic quantum dots prepared with a new family of designer pyridine-appended multidentate polymers *(Invited Paper)*

Kimihiro Susumu, Eunkeu Oh, U.S. Naval Research Lab. (United States) and Sotera Defense Solutions, Inc. (United States); James B. Delehanty, Kelly L. Boeneman-Gemmill, Alan L. Huston, Igor L. Medintz, U.S. Naval Research Lab. (United States)

Biocompatible nanoparticles have recently attracted significant attention due to increasing interest in their use for cellular labeling and in vivo imaging. Semiconductor quantum dots (QDs) with good colloidal stability as well as small hydrodynamic volumes are particularly useful within these applications. While surface ligands with multidentate thiol anchoring groups have significantly enhanced the colloidal stability of QDs, it still remains beneficial to develop surface ligands with new anchoring groups which function to keep the QDs less susceptible to air and light. Pyridine is one of the more promising anchoring groups for QDs since it has been known to bind on QD surfaces. However, its utility to prepare hydrophilic QDs has not been fully realized. We have designed a new class of poly(acrylic acid)-based compact multifunctional ligands with both pyridine and short poly(ethylene glycol) (PEG) pendant groups incorporated for aqueous solubility and biocompatibility. Carboxyl groups were also incorporated in the polymer to allow for covalent bioconjugation to the QD surface. The QD dispersions coated with the new polymer ligands were found to be colloidally stable and remained highly fluorescent over a wide range of pHs. Hydrodynamic sizes of the polymer-coated QDs are comparable to those of DHLA-PEG-coated QDs, suggesting that multiple pyridine groups are efficiently bound on the QD surface. The QD dispersions were also colloidally stable in an extremely dilute condition at room temperature under room light over months. We will discuss the details of ligand design, synthesis, characterization and colloidal stability of the QDs, along with biological applications for these hydrophilic QDs.

8595-45, Session 10

Tailoring lanthanide nanocrystals for nanomedicine

Timothy T. Tan, Nanyang Technological Univ. (Singapore)

Lanthanide nanocrystals have demonstrated strong potentials in nanomedicine due to its upconversion and strong magnetic properties, and low toxicity. The current talk will focus on the synthesis and demonstration of lanthanide nanostructures for bioimaging, drug delivery and cancer cells killing. In particular, it will discuss various strategies to achieve strong and simultaneous T1 and T2 MRI contrast without compromising upconversion emission. The tuning of ultrasensitive sub-10 micron lanthanide nanocrystals for pure red or near-infrared chromatic upconversion fluorescence in the presence of Mn2+ dopant will also be presented. Finally, a new lanthanide-based nanostructure capable of generating radicals through an upconversion mechanism, and its demonstration in triggered drug delivery and cancer cells killing will be featured.

8595-46, Session 10

Highly efficient MnSe/ZnSeS quantum dots for biomedical applications

Leisha M. Armijo, Brian A. Akins, John B. Plumley, Antonio C. Rivera, Nathaniel C. Cook, Gennady A. Smolyakov, Marek Osinski, The Univ. of New Mexico (United States)

Quantum dots emitting in the visible spectral range are of interest for many biomedical applications, including bioimaging, drug targeting, and photodynamic therapy. However, a significant limitation is that QDs typically contain cadmium, which makes prospects for their FDA approval very unlikely. Recent research has focused on cadmium-free QDs, which are anticipated to exhibit lower cytotoxicity. For example, InP was considered as an alternative semiconductor material for QDs. However, quantum efficiency on InP QDs is rather low (~5%), and they were reported to be cytotoxic due to generation of reactive oxygen species by photoexcited electrons and holes that escape to the QD surface. As an alternative, we have synthesized high quantum efficiency (~50%) MnSe/ZnSeS QDs. Incorporation of manganese imparts magnetic properties on the QDs, which makes them attractive as a potential contrast agent for magnetic resonance imaging (MRI). We will present results of comprehensive structural, optical and magnetic characterization of these novel QDs.

8595-47, Session 10

Single molecule quantum confined stark effect measurements of semiconductor nanoparticles at room temperature

KyoungWon Park, Univ. of California, Los Angeles (United States); Zvicka Deutsch, Weizmann Institute of Science (Israel); J. Jack Li, Univ. of California, Los Angeles (United States); Dan Oron, Weizmann Institute of Science (Israel); Shimon Weiss, Univ. of California, Los Angeles (United States)

We investigated the quantum confined Stark effect (QCSE) of semiconductor nanoparticles (NPs) on the single molecule level at room temperature. Eight different NPs with different geometries, material compositions and electronic structures were examined. It was found that suppression of the coulomb interaction between electron and hole by asymmetric type-II heterostructure is critical for an enhanced QCSE. For example, ZnSe-CdS and CdSe(Te)-CdS-CdZnSe asymmetric nanorods (type-II) display ?2 ~ ?3 larger QCSE as compared to a type-I QD (CdSe) or quasi type-II nanorods (CdSe-CdS). In addition, a wavelength blue shift was observed for asymmetric type-II heterostructures. In contrast to the conventional red shift in QCSE (due to charge separation that opposes the applied electric field), blue shift occurs when the applied field 'pushes' both electron and hole towards the type-II interface. As a result, asymmetric type-II nanorods exhibit a roughly linear ?E-F (energy shift vs. applied electric field) relation which affords the determination of the field polarity. We reproduced the ?E and ?E-F experimental results in self-consistent quantum mechanical simulations. Both simulations and experiments suggest that the magnitude of the QCSE is predominantly determined by the degree of initial charge separation (and the associated exciton binding energy) in these structures.

8595-48, Session 11

Thermolabile molecules on iron oxide nanoparticles: sub-nanometer local temperature probes and drug release modulators *(Invited Paper)*

Andreas Riedinger, Teresa Pellegrino, Pablo Guardia, Liberato Manna, Istituto Italiano di Tecnologia (Italy)

Local heating can be produced by iron oxide nanoparticles (IONPs) when exposed to an alternating magnetic field (AMF). To measure the temperature profile at the nanoparticle surface with a sub-nanometer resolution, small thermolabile molecules can be bound through spacers to IONPs. Significant local heating was found at very close vicinity to the nanoparticles surface, which decays rapidly with increasing distance. These findings can be implemented in AMF-triggered drug release system in which doxorubicin was covalently linked at different distances from the IONP surface bearing the same thermo-labile molecule. The AMF triggered distance dependent release of the drug was assessed by a cytotoxicity assay on KB cancer cells..

8595-49, Session 11

Layered double hydroxides as carriers for quantum dots@silica nanospheres *(Invited Paper)*

Georgiana Stoica, Iván Castelló Serrano, Emilio Palomares, ICIQ - Institut Català d'Investigació Química (Spain)

Quantum dot-layered double hydroxides (LDH) nanoplatforms were successfully prepared at ambient conditions via a one-pot approach from the individual components without any additional treatment. Total quantum dots uptake proceeds very fast, i.e. 4 h. The novel materials were extensively characterized by X-ray diffraction, thermogravimetry, infrared spectroscopy, transmission electron microscopy, true color fluorescence microscopy, photoluminescence, and nitrogen adsorption. The quantum dot-hydrotalcite nanomaterials display extremely high stability in mimicking physiological media such as saline serum (pH 5.5) and PBS (pH 7.2). Yet, quantum dot release from the solid structure is noted. Remarkably, the optical properties of quantum dots changed from orange to green-yellowish. This blue shift was attributed to several factors like the quantum dot-hydrotalcite interaction, magnesium dissolution and ultimate doping at the quantum dot surface. However, their effect is reversible upon the dissolution of the solid host. It can be concluded that the blue shift originates from the surface changes only, while the bulk core is not affected. In order to prevent the leaking of quantum dots we have developed a novel strategy which consists on using tailor made LDH as protecting shells for quantum dots embedded into silica nanospheres (QDs@silica core / LDH shell). This combination is reported herein for the first time and leads to efficient barrier for leaching processes of the QDs in biological alike media. Additionally, the optical properties transitions were stopped. In overall, we created advanced nanostructured inorganic scaffolds that will prevent cytotoxicity and will permit multimodal imaging and simultaneous diagnosis in advanced therapeutically systems.

References

G. Stoica et al., Nanoscale 2012, DOI:10.1039/C2NR31550E.

8595-50, Session 11

A self-assembled DNA nanostructure for the transport of immunostimulatory CpG oligonucleotides *(Invited Paper)*

Verena J. Schueller, Simon Heidegger, Ludwig-Maximilians-Univ. München (Germany); Carole Bourquin, Univ. Fribourg (Switzerland); Tim Liedl, Ludwig-Maximilians-Univ. München (Germany)

DNA nanotechnology enables the construction of highly programmable and biocompatible nanostructures as new platforms for the precise organization of biochemical molecules [1]. Currently, DNA nanostructures are explored as potential vehicles for effective cellular transport and drug delivery. In particular the recently established DNA origami method is suited for this endeavor asfunctional DNA nanostructures of arbitrary shapes can be reliably produced with high yields [2]. Using this technique, we created a hollow 30-helix DNA origami tube capable of transporting up to 62 immunostimulative cytosine-phosphate-guanine (CpG) oligonucleotides to freshly isolated murine spleen cells. The DNA tubes entered these cells and initiated an immune response which was characterized by specific cytokine production [3]. Our devices triggered a higher immunostimulatory activity than equal amounts of CpG Oligonucleotides associated with a standard carrier system while showing no detectable cytotoxicity. This approach could inspire the development of new designs for vaccines and tailored adjuvants.

[1] Seeman, N.C. DNA in a material world, Nature 421, 427-431 (2003).

[2] Rothemund, P.W.K. Folding DNA to create nanoscale shapes and patterns, Nature 440, 297-302 (2006).

[3] Schüller, V.J., Heidegger, S., Sandholzer, N., Nickels, P.C., Suhartha, N.A., Endres, S., Bourquin, C., Liedl, T. Cellular Immunostimulation by CpG-Sequence-Coated DNA Origami Structures, ACS nano 5, 9696–9702 (2011).

8595-51, Session 11

Effectiveness of Tobramycin conjugated to iron oxide nanoparticles in treating cystic fibrosis

Yekaterina I. Brandt, Leisha M. Armijo, Nathaniel C. Cook,

Gennady A. Smolyakov, The Univ. of New Mexico (United States); Hugh D. Smyth, The Univ. of Texas at Austin (United States); Marek Osinski, The Univ. of New Mexico (United States)

Tobramycin is the antibiotic of choice in treating cystic fibrosis (CF) patients whose lungs contain opportunistic bacteria Pseudonomas aeruginosa. CF is a genetic disorder that affects about 30,000 people in the US (70,000 worldwide). CF causes the body to produce unusually thick, sticky mucus that clogs the lungs and leads to life-threatening lung infections. The viscous mucus caused by CF makes it easy for a common bacterium P. aeruginosa to infect the lungs. For people with CF, P. aeruginosa is responsible for most lung infections. The effectiveness of treatment is limited by the mucus barrier, which protects the bacteria from the exposure to drug. We are pursuing a novel drug delivery scheme, whereby the drug is attached to a superparamagnetic iron oxide nanoparticle (SPION), which then is heated up in an alternating magnetic field to reduce the mucus viscosity and diffuse across the barrier. An important question is whether the drug retains its effectiveness while attached to a SPION, or whether it should be detached from the nanoparticle in order to perform its therapeutic role. In this paper, we will report on our in vitro experiments aimed at determining therapeutic effects of Tobramycin on P. aeruginosa when attached to SPIONs, and compare these results to the free drug effects without the nanoparticles.

8595-52, Session 12

Targeted delivery of peptide-conjugated biocompatible gold nanoparticles into cancer cell nucleus

Wei Qian, IMRA America, Inc. (United States); Taeyjuana Curry, Univ. of Michigan (United States); Yong Che, IMRA America, Inc. (United States); Raoul Kopelman, Univ. of Michigan (United States)

Novel therapeutic strategies (for example, gene therapy), enabled by safe and efficient delivery of drug molecules and nanoparticles into the nucleus, are heralded by many as the ultimate treatment for severe and intractable diseases. However, most nanomaterials and macromolecules are incapable of reaching the cell nucleus on their own, because of biological barriers carefully honed by evolution including cellular membrane and nuclear envelope. In this presentation, we have demonstrated an approach of fabrication of biocompatible gold nanoparticle (Au NP)-based vehicles which can entering into cancer cell nucleus by modifying Au NPs with both PEG 5000 and two different peptides (RGD and nuclear localization signal (NLS) peptide). The Au NPs used were fabricated via femtosecond laser ablation of Au bulk target in deionized water. The Au NPs produced by this method provide chemical free, virgin surface, which allows us to carry out “Sequential Conjugation” to modify their surface with PEG 5000, RGD, and NLS. “Sequential Conjugation” described in this presentation is very critical for the fabrication of Au NP-based vehicles capable of entering into cancer cell nucleus as it enables the engineering and tuning surface chemistries of Au NPs by independently adjusting amounts of PEG and peptides bound onto surface of Au NPs so as to maximize their nuclear targeting performance and biocompatibility regarding the cell line of interest. Both optical microscopy and transmission electron microscopy (TEM) are used to confirm the targeted nuclear delivery of peptide-conjugated biocompatible Au NPs in vitro by showing their presence in the cancer cell nucleus.

8595-53, Session 12

Fluorescent nanocolloids for differential labeling of the endocytic pathway and drug delivery applications *(Invited Paper)*

James B. Delehanty, Christopher M. Spillmann, Jawad Naciri, W. Russ Algar, Banahalli R. Ratna, Igor L. Medintz, U.S. Naval Research Lab. (United States)

The demonstration of fine control over nanomaterials within biological systems, particularly in live cells, is integral for the successful implementation of nanoparticles (NPs) in biomedical applications. Here, we show the ability to differentially label the endocytic pathway of mammalian cells in a spatiotemporal manner utilizing fluorescent nanocolloids (NCs) doped with a perylene-based dye. EDC-based conjugation of green- and red-emitting NCs to the iron transport protein transferrin resulted in stable bioconjugates that were efficiently endocytosed by HEK 293T/17 cells. The staggered delivery of the bioconjugates allowed for the time-resolved, differential labeling of distinct vesicular compartments along the endocytic pathway in a nontoxic manner. We further demonstrated the ability of the NCs to be impregnated with the anticancer therapeutic, doxorubicin. Delivery of the drug-doped nanoconjugates resulted in the intracellular release and nuclear accumulation of doxorubicin in a time- and dose-dependent manner. We discuss our results in the context of the utility of such materials for NP-mediated drug delivery applications.

8595-55, Session 13

Methods for the determination of the optical properties and the surface chemistry of fluorescent particles *(Invited Paper)*

Ute Resch-Genger, Christian Würth, Bundesanstalt für Materialforschung und -prüfung (Germany); Andreas Hennig, Thomas Behnke, Soheil Hatami, BAM Federal Institute for Materials Research and Testing (Germany); Katrin Hoffmann, BAM Federal Institute for Material Research and Testing (Germany); Angelika Hoffman, Alexandra Huber, Christian Jaeger, BAM Federal Institute for Materials Research and Testing (Germany); Heike Borcherding, Thomas Thiele, Uwe Schedler, PolyAn GmbH (Germany)

Fluorescent nanometer- and micrometer-sized particles ranging from polymeric beads to nanocrystalline materials like quantum dots and upconversion phosphors are important tools and platforms for bioanalysis and clinical diagnostics [1]. Accordingly, there is an increasing need for versatile procedures for particle preparation and for analytical tools that enable the determination of the number of fluorophores per bead and the quantification of surface functionalities [2-5]. Additionally, procedures for the characterization of the signal-relevant optical properties of such materials like the fluorescence quantum yields and brightness values per bead in application-relevant matrices are needed [4, 6, 7].

This encouraged us to develop versatile one-step procedures for the preparation of nanometer- and micrometer-sized fluorescent polymer particles from a broad variety of vis and NIR fluorophores and simple, fast, and cost-efficient analytical tools for the determination of the total and the accessible number of surface groups. For the characterization of the optical properties of these fluorescent particles and the quantification of surface functionalities with fluorophore labeling strategies, we designed two custom-built integration sphere setups for the ultraviolet (UV),visible (vis), and near-infrared (NIR) spectral region that enable measurements of absolute fluorescence quantum yields as well as transmission and reflection spectra of transparent solutions and scattering bead suspensions [7]. Here, we present different examples for the optical and analytical characterization of nm- and ?m-sized particles employed as optical probes and nanosensors or as platform for fluorescence assays.

References. [1] Resch-Genger, U. (ed), Standardization and Quality Assurance in Fluorescence Measurements II Bioanalytical and Biomedical Applications, Springer-Verlag: Berlin Heidelberg, 2008. [2] Sapsford, K. E.; Tyner, K. M.; Dair, B. J.; Deschamps, J. R.; Medintz, I. L., Anal. Chem. 2011, 83, 4453-4488. [3] Hennig, A.; Hoffmann, A.; Borcherding, H.; Thiele, T.; Schedler, U.; Resch-Genger, U., Anal. Chem. 2011, 83, 4970-4974. [4] Huber, A.; Behnke, T.; Würth, C.; Jaeger, C.; Resch-Genger, U., Anal. Chem. 2012, 84, 3654-3661. [5] Hennig, A.; Borcherding,

H.; Jaeger, C.; Hatami, S.; Würth, C.; Hoffmann, A.; Hoffmann, K.; Thiele, T.; Schedler, U.; Resch-Genger, U., J. Am. Chem. Soc. 2012, 134, 8268-8276. [6] Russin, T. J.; Altinoglu, E. I.; Adair, J. H.; Eklund, P. C., J. Phys. Cond. Mat. 2010, 22, 334217. [7] Würth, C.; Pauli, J.; Lochmann, C.; Spieles, M.; Resch-Genger, U., Anal. Chem. 2012, 84, 1345-1352.

8595-56, Session 13

Stiffness measurement of a biomaterial by optical manipulation of microparticle

Waleed Muhammad, Jung-Dae Kim, Yong-Gu Lee, Gwangju Institute of Science and Technology (Korea, Republic of)

Since the discovery of the trapping nature of laser beam, optical tweezers have been extensively employed to measure various parameters at micro/nano level. Optical tweezers show exceptional sensitivity to weak forces making it one of the most sensitive force measurement devices. In this work, we present a technique to measure the stiffness of a biomaterial at different points. For this purpose, a microparticle stuck at the bottom of the dish is illuminated by the trapping laser and respective QPD signal as a function of the distance between the focus of the laser and the center of the microparticle is monitored. After this, microparticle is trapped and manipulated towards the target biomaterial and when it touches the cell membrane, QPD signal shows variation. By comparing two different QPD signals and measuring the trap stiffness, a technique is described to measure the stiffness of the biomaterial at a particular point. We believe that this parameter can be used as a tool to identify and classify different biomaterials.

8595-57, Session 13

Opto-acoustic characterization of chitosan based gold nanoparticles (GNPs) synthesized in the presence of monovalent salt

Samantha K. Franklin, Kelly L. Nash, Zannatul Yasmin, The Univ. of Texas at San Antonio (United States); Saher Maswadi, The Univ. of Texas Health Science Ctr. at San Antonio (United States)

Several studies, over recent years, focus on the use of chitosan, a biocompatible macromolecule, to form gold nanoparticles (GNPs). In this study, gold nanoparticles were synthesized using chitosan and chloroauric acid (HAuCl4), under stirring which cause micro/nano-gels to form. Ultraviolet (UV) light is used to reduce the Au ions in the solution into gold nanoparticles, in which the resulting biocompatible nanoparticles upon reduction. In an effort to study the influence of the chitosan on the nanoparticles shape and size, different concentrations of monovalent salt, were added to the chitosan solution during synthesis. Morphology of the resulting particles are studied using electron microscopy and optical spectroscopy techniques. To study the variations in the nanoparticles morphology the optical absorption of the nanoparticles are probed with an optoacoustic setup based on a probe beam deflection technique. Using this sensitive technique we are able to study very dilute concentrations of the Au NPs to give a morphological dependent optical response which may normally be outside of a spectrophotometer response. The optoacoustic measurements are compared to the absorption spectra of the Au NPs at higher concentrations. The overall goal of this study is to investigate the influence of chitosan, with the addition of the monovalent salt, on the formation of the biocompatible gold nanoparticles. This characterization will aid in the preparation of measurements to be made on these particles in other portions of the electromagnetic spectrum such as radio frequencies.

8595-58, Session 13

Thermo-optical properties of magic-sized nanocrystals in aqueous solutions

Sthanley R. Lima, Viviane Pilla, Acácio A. Andrade, Anielle C. A. Silva, Noelio O. Dantas, Univ. Federal de Uberlândia (Brazil)

CdSe/ZnS and CdSe/CdS core-shell semiconductor nanocrystallites are II-VI semiconductor systems and Type I Quantum Dots (QDs) [1]. In such core-shell nanocrystals, the shell provides an efficient passivation of the surface trap states, giving rise to a strongly enhanced fluorescence quantum yield. The ideal QDs for use in nanobiotechnology trials should be thermodynamically stable and have homogeneous dispersion, high radiative quantum efficiency, a very broad absorption spectrum, low levels of nonspecific links to biological compounds and, most importantly, stability in aqueous media. Recently, a new class of CdSe QDs called magic-sized nanocrystals (MSNs), with sizes from 1 to 2 nm and well-defined structures, has attracted considerable attention because of its novel physical properties [1]. The solvent used to suspend the solute samples can exert important influence on such properties as the radiative quantum efficiency and thermal parameters [2] of the investigated materials. In this way, for a nanostructure to be a candidate for practical applications, it is important to characterize their thermo-optical properties. The present work reports the thermo-optical properties of CdSe/CdS MSNs and CdSe/ZnS in aqueous solutions measured with two techniques: the well-known Thermal Lens (TL) technique and an alternative method called thermal spatial self-phase modulation (TSPM) technique [1].

[1] V. Pilla et al., Photothermal spectroscopic characterization in CdSe/ZnS and CdSe/CdS Quantum Dots: A Review and New Applications, Quantum Dots - A Variety of New Applications, InTech (2012) ISBN: 978-953-51-0483-4.

[2] V. Pilla et al., Optics Communications 280 (2007) 225.

8595-59, Session 13

Effect of surface modification on protein corona formation and uptake of 5-nm Au NPs *(Invited Paper)*

Blair D. Johnston, Martin J. D. Clift, The Adolphe Merkle Institute (Switzerland); Martin Schäffler, Helmholtz Zentrum München GmbH (Germany); Christian Pfeiffer, Philipps-Univ. Marburg (Germany); Simon Ristig, Univ. Duisburg-Essen (Germany); Jose Maria Montenegro Martos, Philipps-Univ. Marburg (Germany); Stefanie Hauck, Helmholtz Zentrum München GmbH (Germany); Hakan Sarioglu, Helmholtz Zentrum München GmbH (Germany); Alke Petri-Fink, The Adolphe Merkle Institute (Switzerland); Matthias Epple, Univ. Duisburg-Essen (Germany); Pilar Rivera Gil, Philipps-Univ. Marburg (Germany); Wolfgang J. Parak, Philipps-Univ. Marburg (Germany); Peter Wick, Materials-Biology Interactions, EMPA (Switzerland); Wolfgang Kreyling, Helmholtz Zentrum München GmbH (Germany); Barbara Rothen-Rutishauser, The Adolphe Merkle Institute (Switzerland)

After contact with biological fluids at epithelial interfaces (i.e. alveolar sac in the mammalian lung), a protein corona will adsorb to the core nanoparticles (NPs) and help to determine their bioavailability and toxicokinetic profile. The design of nanomaterial drug-delivery systems that effectively cross biological barriers (i.e. air-blood) and target specific cells or cellular compartments would help guide the development of new nanomaterials for biomedical applications and aid our understanding of the possible impacts of nanomaterials to human and environmental health. Little is known about the factors that determine the composition and configuration of the protein corona in vivo. Modification of the surface of the NP (by differential ligand binding) can alter the composition and equilibrium kinetics of protein binding to the NP. These modifications

may alter core NP circulation parameters and internal transport. In this study, 5 nm Au NPs with one of several different surface coatings (citrate-stabilised, triphenylphosphine, PEG-NH2, CH3O-PEG-SH, and Poly (isobutylene-maleic acid anhydride), were incubated with serum or BAL from C 57 BL/6 mice. Proteins were separated by SDS-gel electrophoresis and identified by Orbitrap Mass-Spectrometry. NP size and geometry were measured with spin-disc centrifugation (SDC), atomic force microscopy (AFM), UV-Vis spectrophotometry, dynamic light scattering (DLS) and small angle X-ray scattering (SAXS). NPs with adsorbed proteins were also exposed in an air-liquid interface co-culture system (ALICE) and in vitro uptake imaged with confocal microscopy. Differences in protein corona composition, configuration and corresponding toxicokinetic profiles between the differentially ligated NPs will be discussed.

8595-60, Session 14

Nanoparticles for diagnostics and laser medical treatment of cartilage in orthopaedics

Olga I. Baum, Yulia Soshnikova, Alexander I. Omelchenko, Emil N. Sobol, Institute on Laser and Information Technologies (Russian Federation)

Laser regeneration of cartilage has opened new opportunities in orthopedics for minimally invasive treatment of arthritis and degenerated spine discs. The aims of the paper is to provide spatial specificity for laser regeneration of cartilage by introducing nanoparticles (NP) into the cartilage which can decrease incident laser dose compared to that used in existing treatment protocols. 20 minipigs were used for in-vivo animal experiments.

Two types of porcine joint cartilage have been impregnated with Ferric oxide NP of about 20 nm in size into: (1) healthy cartilage and (2) damaged cartilage. Size and mass distribution of NP was studied using dynamic light scattering and ultracentrifugation techniques. Laser radiation and magnetic field have been applied to accelerate NP impregnation.

AFM, electron microscope and Mossbauer spectroscopy were used for examination of cartilage impregnated with NP. We have shown that: (1) NP penetrate by diffusion into the damaged cartilage, but do not infiltrate healthy cartilage. That can be used for early diagnostics of cartilage diseases. (2) Ferric oxide NP might be used to provide spatial specificity of laser regeneration. When damaged, the regions of cartilage impregnated with NP have higher absorption of laser radiation than that for healthy areas. (3) Regions containing NP form target sites to generate laser-induced thermomechanical stress leading to regeneration of cartilage of hyaline type.

8595-61, Session 14

Optimizing nanoparticles for brain tumor immunotherapy *(Invited Paper)*

Jacob M. Berlin, Yiming Weng, Huaqing Wang, Anna Carvalho da Fonseca, Anil K. Suresh, Leying Zhang, Ian Zhang, Behnam Badie, City of Hope National Medical Ctr. (United States)

Even when treated with aggressive current therapies, most patients with primary or metastatic malignant brain tumors survive less than two years. Although immunotherapy is being studied as a potential treatment, the blood-brain barrier and local tumor immunosuppressive milieu may prevent penetration of cytotoxic antibodies or immune cells into the brain. Local delivery of immunostimulatory molecules such as CpG can overcome this suppressive environment, but at high doses may also cause toxic brain inflammation. Thus, there is a pressing need for a safer, more effective targeted strategy to enhance CNS immune responses to malignant brain tumors. We recently demonstrated that carbon-nanotubes (CNTs) are efficient nontoxic carriers of macromolecules into tumor inflammatory cells, and when conjugated with CpG (CNT-CpG), result in robust activation of inflammatory cells. Remarkably, even a single low-dose injection of CNT-CpG (but not free CpG) eradicated brain tumors in animal models and protected surviving animals from tumor rechallenge. These findings suggest that enhanced delivery of immunostimulatory molecules into the brain can induce a strong local and systemic anti-tumor response. Here we describe optimizing this novel immunotherapy strategy for treatment of human brain tumors. We have evaluated other nanoparticles as carriers for the CpG as well as progressed towards Good Manufacturing Practices preparation of the CNT-CpG in preparation for translation to humans. If successful, the nanoparticle-CpG developed here can be used in human clinical trials for treatment of not only glioma, but also cancers that metastasize to the brain, thereby greatly benefiting patients with these devastating diseases.

8595-62, Session 14

Magnetized endothelial progenitor cells as angiogenic activators *(Invited Paper)*

Anna Roig, Consejo Superior de Investigaciones Científicas (Spain)

Magnetic nanoparticles are continuously receiving growing interest in nanomedicine. Judicious design in terms of their size, shape and magnetic properties makes them unique for several diagnosis and therapeutic treatments of human diseases.

Endothelial Progenitor Cells (EPC) are good candidates for cell-based therapies to treat ischemia by inducing angiogenesis. We propose that EPCs can be magnetized with iron oxide superparamagnetic nanoparticles enabling their guidance and engrafting into specific brain areas by an external magnet. Magnetized cells could be further tracked by Magnetic Resonance Imaging (MRI).

This study focuses on the preparation of anionic magnetic colloids for the above mentioned application. Transmission electron microscopy was used to investigate the internalization of the particles by the cells while magnetometry was used as quantitative approach to evaluate their iron uptake. No toxicity and no remarkable changes in cell morphology were noticed at used concentrations (under 100 ?g/ml). It will be shown that magnetized EPC are fully functional since they shaped vessel-like structures into matrigel matrices and the secretion of important growth factors (such as VEGF or FGF) is enhanced compared to non-magnetized EPCs. Moreover, in-vivo MRI studies showed that brain tissue accumulated hypointense signals consistent with magnetized EPCs engraftment when an external magnetic field was applied.

8595-63, Session 14

Multifunctional nanocarriers for biomedical applications *(Invited Paper)*

Michael Maskos, Institut für Mikrotechnik Mainz GmbH (Germany); Regina Bleul, Raphael Thiermann, Bundesanstalt für Materialforschung und -prüfung (Germany); Olga Koshkina, Institut für Mikrotechnik Mainz GmbH (Germany)

Polymeric, amphiphilic nanoparticles are of growing interest due to their increasing potential for application. Examples are the employment as drug delivery system, as markers, as nano-containers or nano-reactors. Different routes and types of reactions are being used to synthesize particles with dimensions between several nanometers up to approximately 100 nm. Especially challenging is the combination of different properties in the very same particles, such as marking (e.g. fluorescently or magnetically labelled), targeting (typically achieved by e.g. attachment of targeting functionalities to the particle surface) and specific carrier properties (e.g. triggered release or catalytic activity). In addition, the characterization and analysis of the structure-property-relations, especially in solution, are extremely challenging due to the small size of the particles. State-of-the-art techniques include

light scattering techniques, field-flow fractionation techniques (FFF), cryogenic transmission electron microscopy (cryo-TEM) and atomic force microscopy (AFM).

We present an example of a multi-functional core-shell type nanoparticles system based on polyorganosiloxanes and discuss their properties, especially related to biological environments.

8595-64, Session 14

Radiation dose enhancement using lanthanide fluoride nanoparticles on human pancreatic cancer cells in vitro

Nathan J. Withers, Yekaterina I. Brandt, Jacqueline M. Sugar, Antonio C. Rivera, Nathaniel C. Cook, Leisha M. Armijo, John B. Plumley, Brian A. Akins, Gennady A. Smolyakov, Marek Osinski, The Univ. of New Mexico (United States)

Lanthanide fluoride colloidal nanocrystals offer a way to improve radiation therapy and diagnostics of cancer through the enhanced absorption of X- and gamma rays. Cerium fluoride nanocrystals co-doped with lanthanum and terbium and capped with polyethylene glycol (PEG) were synthesized in water as platelets 20-40 nm in diameter and 1-3 nm thick. These nanocrystals were characterized by transmission electron microscopy, muffle furnace ashing, absorbance spectroscopy, dynamic light scattering, zeta potential measurements, and photoluminescence spectroscopy. Following characterization, the nanocrystals were suspended in deionized water and Eagles minimum essential media (MEM). The nanocrystals were then used in radiation experiments using a human pancreatic cancer cell line, purchased from ATCC. Various cell mortality and clonogenic assays were used to assess the dose enhancement effects.

Conference 8596: Reporters, Markers, Dyes, Nanoparticles, and Molecular Probes for Biomedical Applications

Monday - Wednesday 4 –6 February 2013 • Part of Proceedings of SPIE Vol. 8596
Reporters, Markers, Dyes, Nanoparticles, and Molecular Probes for Biomedical Applications V

8596-1, Session 1

Super-enhanced permeability and retention (SUPR) effect induced by photo-immunotherapy (PIT) can accommodate nano-sized reagents deep into cancer tissue. *(Invited Paper)*

Hisataka Kobayashi, National Institutes of Health (United States)

Photo-immunotherapy (PIT) is a newly developed molecularly-targeted cancer photo-therapy based on conjugating a near infrared phthalocyanine dye, IR700, to a humanized monoclonal antibody (MAb) targeting cancer-specific cell-surface molecules. When exposed to NIR light, the conjugate induces a highly-selective necrotic cell death only in MAb-IR700 bound cancer cells. This target-specific necrotic cell death occurs within 5 minutes of exposure to NIR light and results in rapid morphologic changes including cellular swelling, bleb formation, and rupture of vesicles indicating necrotic cell death. Meanwhile, immediately adjacent receptor-negative cells are unharmed. Because it damages cells behind the tumor vasculature, PIT results in dramatically enhanced nano-particle delivery to cancer tissue an effect termed “super-enhanced permeability and retention (SUPR)”. Any nano-sized reagents including macromolecules (dendrimers), particles (quantum dots, iron oxide nano-particles), and liposomes up to 300 nm in diameter rapidly enter and are retained within the tumor space following PIT. Therefore, although PIT is unlikely to eliminate all cancer cells, its SUPR effects allow the delivery of relatively high concentrations of nano-sized anti-cancer reagents such as, daunorubicin containing liposome (Daunoxome) which can provide synergistic therapeutic effects. In conclusion, target-selective PIT can induce a SUPR effect leading to the accumulation of relatively high concentrations of nano-sized reagents at the site of treatment resulting in synergistic effects while minimizing off-target side-effects.

8596-2, Session 1

ICG-loaded polymeric nanocapsules functionalized with anti-HER2 for targeted fluorescence imaging and photdestruction of ovarian cancer cells

Baharak Bahmani, Yadir A. Guerrero, Valentine I. Vullev, Univ. of California, Riverside (United States); Sheela P. Singh, Vikas Kundra, The Univ. of Texas M.D. Anderson Cancer Ctr. (United States); Bahman Anvari, Univ. of California, Riverside (United States)

Optical nano-materials present a promising platform for targeted molecular imaging of cancer biomarkers and its phototdestruction. Our group is investigating the use of polymeric nanoparticles, loaded with indocyanine green, an FDA-approved chromophore, as a theranostic agent for targeted intraoperative optical imaging and laser-mediated destruction of ovarian cancer. These ICG-loaded nanocapsules (ICG-NCs) can be functionalized by covalent attachment of targeting moieties onto their surface. Here, we investigate ICG-NCs functionalized with anti-HER2 for targeted fluorescence imaging and laser-mediated destruction of ovarian cancer cells in vitro. ICG-NCs are formed through ionic cross-linking between polyallylamine hydrochloride chains and sodium phosphate ions followed by diffusion-mediated loading with ICG. Before functionalization with antibodies, the surface of ICG-NCs is coated with single and double aldehyde terminated polyethylene glycol (PEG). The monoclonal anti-HER2 is covalently coupled to the PEGylated ICG-NCs using reductive amination to target the HER2 receptor, a biomarker whose over-expression is associated with increased risk of cancer progression. We quantify uptake of anti-HER2 conjugated ICG-NCs by ovarian cancer cells using fluorescent confocal microscopy and flow cytometery. The in-vitro laser-mediated destruction of SKOV3 cells incubated with anti-HER2 functionalized ICG-NCs is performed using an 808 nm diode laser. Cell viability is assessed using Trypan blue staining following laser irradiation. Our results are promising since they suggest that anti-HER2 functionalized ICG-NCs can be used as theranostic agents for optical molecular imaging and photodestruction of ovarian cancer.

8596-3, Session 1

Imaging of tumor vascular endothelial cells in living mice

Dawen Zhao, Jason H. Stafford, Heling Zhou, Philip E. Thorpe, The Univ. of Texas Southwestern Medical Ctr. at Dallas (United States)

Phosphatidylserine (PS), normally restricted to the inner leaflet of the plasma membrane, becomes exposed on the outer surface of viable (non-apoptotic) endothelial cells in tumor blood vessels, probably in response to oxidative stresses present in the tumor microenvironment. In the present study, we optically imaged exposed PS on tumor vasculature in vivo using PGN635, a novel human monoclonal antibody that targets PS. PGN635 F(ab')2 was labeled with the near infrared (NIR) dye, IRDye 800CW. Human glioma U87 cells or breast cancer MDA-MB-231 cells were implanted subcutaneously or orthotopically into nude mice. When the tumors reached ~5 mm in diameter, 800CW-PGN635 was injected via a tail vein and in vivo dynamic NIR imaging was performed. For U87 gliomas, NIR imaging allowed clear detection of tumors as early as 4 h later, which improved over time to give a maximal tumor/normal ratio (TNR = 2.9 ± 0.5) 24 h later. Similar results were observed for orthotopic MDA-MB-231 breast tumors. Localization of 800CW-PGN635 to tumors was antigen specific since 800CW-Aurexis, a control probe of irrelevant specificity, did not localize to the tumors, and pre-administration of unlabeled PGN635 blocked the uptake of 800CW-PGN635. Fluorescence microscopy confirmed that 800CW-PGN635 was binding to PS-positive tumor vascular endothelium. Our studies suggest that tumor vasculature can be successfully imaged in vivo to provide sensitive tumor detection.

Acknowledgments: We thank Peregrine Pharmaceuticals Inc., Tustin, CA, for the provision of PGN635 antibody. This work was supported in part by NCI 1R21 CA141348-01A1 and by the Meredith D. Chesler Foundation, Dallas, TX.

8596-4, Session 2

NIR fluorescent dyes: versatile vehicles for marker and probe applications *(Invited Paper)*

Gabor Patonay, Gala Chapman, Garfield Beckford, Maged Henary, Georgia State Univ. (United States)

The binding characteristics of NIR dyes to biomolecules are possibly controlled by several factors, including hydrophobicity, size and charge among others. Upon binding to biomolecules significant fluorescence enhancement can be observed. This fluorescence amplification facilitates the detection of the NIR dye and enhances its utility as NIR reporter. Our research group synthesized asymmetric NIR dyes using a new approach that eliminates symmetrical byproducts. These asymmetric dyes exhibited binding and fluorescence behavior very different from their symmetric counterparts. One application discussed in this presentation is the use of NIR dyes to report on enzymatic activities. Carbocyanines containing alkenesulfonate moieties do not exhibit significant fluorescence change upon binding to biomolecules however otherwise

identical dyes that contain alkene moiety at the same position do. This can be used for the detection of alkenesulfonate monooxygenase activity in vitro and in vivo. Upon cleavage of the sulfonate moiety NIR dye fluorescence diminishes in aqueous buffer solution. For labeling applications the fluorescence intensity of the NIR fluorescent label can significantly be increased by enclosing several dye molecules in nanoparticles. To decrease self quenching dyes that have relatively large Stokes' shift needs to be used. This is achieved by substituting meso position halogens with amino moiety. This presentation reports on the preparation of NIR fluorescent silica nanoparticles. Silica nanoparticles that are modified with aminoreactive moietiues can be used as bright fluorescent labels in bioanalytical applications. Examples of silica nanoparticles containing visible and NIR fluorophores are presented along with applications requiring bright fluorescent labels.

8596-5, Session 2

Covalent IR820-PEG diamine conjugates: characterization and in vivo biodistribution

Alicia Fernandez-Fernandez, Nova Southeastern Univ. (United States) and Florida International Univ. (United States); Romila Manchanda, Florida International Univ. (United States); Denny A. Carvajal, Mount Sinai Medical Ctr. (United States) and Florida International Univ. (United States); Tingjun Lei, Anthony J. McGoron, Florida International Univ. (United States)

Introduction: IR820 is a near-infrared probe with potential applications in optical imaging and hyperthermia. Its chloro-substituted cyclohexene makes it amenable forming conjugates as multifunctional probes. Our group prepared a novel covalent IR820/PEG-diamine (IRPDcov) nanoconjugate. Methods: IRPDcov was prepared using IR820 and 6kDa PEG-diamine, characterized by DLS, H-NMR, spectrophotometry, and spectrofluorometry; and studied in vitro and in vivo. Mice (n=36) were used to explore the biodistribution of IRPDcov compared to IR820 and indocyanine green (ICG) after i.v. injection of a 0.24 mg/kg dose of dye, with plasma samples collected at 15-30-60 minutes and 24 hours. The plasma curves were fit to a biexponential curve following a two compartment model. Organ samples were collected at 24-hours. Results and Discussion: IRPDcov retained the ability to fluoresce for in vivo optical imaging and also to generate heat, and was significantly more stable than IR820 in aqueous solution over a period of 72 hours. IRPDcov and IR820 demonstrated significantly longer ($p<0.05$) plasma half-lives, elimination half-lives, and area-under-the-curve values compared to ICG. This could pose an advantage in therapeutic probe applications such as hyperthermia or drug delivery. Both IR820 and IRPDcov showed a very strong signal in the liver and lower-intensity signal in the kidneys 24 hours after injection, whereas the predominant signal for ICG was weak and located in the intestines, demonstrating a much more rapid GI elimination. IR820 showed signal in the lungs, which was not present in IRPDcov subjects indicating that IRPDcov may have been able to escape detection by alveolar macrophages.

8596-6, Session 2

Near-infrared light-triggered dissociation of block copolymer micelles for controlled drug release

Jie Cao, Shanshan Huang, Yuqi Chen, Siwen Li, Sisi Cui, China Pharmaceutical Univ. (China); Samuel Achilefu, Washington Univ. School of Medicine in St. Louis (United States); Yueqing Gu, China Pharmaceutical Univ. (China); Zhiyu Qian, Nanjing Univ. of Aeronautics and Astronautics (China)

In this manuscript, a new near-infrared (NIR) light-breakable amphiphilic block copolymer containing light-sensitive triggering group on the hydrophobic block was developed. By encapsulating NIR dye cypate inside micelles of poly (N-succinyl-N'-4-(2-nitrobenzyloxy)-succinyl chitosan) and exposing the micellar solution to 765.9 nm light, the photo-cleavage reaction was activated and leading to the dissociation of micelles and release of co-loaded hydrophobic species. The UV-vis absorption spectra, fourier transform infrared (FTIR) spectra and 1H nuclear magnetic resonance (1H NMR) spectra of micelles were characterized. Triggered burst release of the payload upon NIR irradiation and subsequent degradation of the micelles were observed by transmission electron microscopy (TEM). This system represents a general and efficient method to circumvent the need for UV or visible light excitation that is a common drawback for light-responsive polymeric systems developed for potential biomedical applications.

8596-7, Session 2

Near-infrared Imaging (NIR) loaded polymeric nanoparticles: In vitro and In vivo studies

Tingjun Lei, Romila Manchanda, Yen-Chih Huang, Florida International Univ. (United States); Alicia Fernandez-Fernandez, Karina Bunetska, Karina Bunetska, Andrew Milera, Andrew Milera, Azael Sarmiento, Azael Sarmiento, Anthony J. McGoron, Florida International Univ. (United States); Alicia Fernandez-Fernandez, Florida International Univ. (United States) and Nova Southeastern Univ. (United States)

Introduction: Research has been focused on developing new biomaterials used for delivery of imaging agent and drugs. In our study, we report a new biocompatible and biodegradable polymer, termed poly(glycerol-co-malic-dodecanoate) (PGMD), which was then used for synthesis of nanoparticles (NPs) and loading of NIR dyes.

Methods: IR820 was chosen for NIR dye and PGMD polymer was synthesized via thermal condensation method and was characterized by FTIR. The NPs were synthesized via o/w single emulsion technique. The loading efficiency of IR820 in PGMD NPs was measured by spectrophotometer. The release of IR820 was estimated with spectrofluorometer in different pH buffer saline. The cytotoxicity of NPs was estimated through Sulforhodamine B colorimetric assay.

Results and Discussion: Void PGMD NPs and IR820-PGMD NPs have mean size around 120nm and 130nm, respectively. FTIR showed that polyester bonds were forming in PGMD polymer. The release of IR820 was increased in acidic buffer (pH=5.0) as compared to neutral buffer (pH=7.4), indicating the release of IR820 is controllable. Cellular uptake studies showed comparable fluorescence of IR820-PGMD NPs to free IR820 (5μM) after 24-h exposure. The cytotoxicity profile of void PGMD NPs showed no toxicity up to 0.1mg/ml in all the cell lines tested. IR820-PGMD NPs after laser exposure induce significant cancer cell killing due to the photodynamic effect of the dye.

Conclusions and future work: We expect that ease of synthesis and good biocompatibility make PGMD a good candidate for numerous imaging agent and drug delivery applications. The IR820-PGMD NPs have the ability to be used for both imaging and hyperthermia purpose. In the future, its in vivo biodistribution will be studied in animal model.

8596-8, Session 3

Evaluation of inflammatory response to acute ischemia using near infrared fluorescent reactive oxygen sensors *(Invited Paper)*

Walter J. Akers, Selena Magalotti, Tiffany P. Gustafson, Mikhail Y. Berezin, Dana Abendschein, Richard Pierce, Washington Univ. School of Medicine in St. Louis (United States)

Post-ischemia processes associated with generation of inflammatory molecules such as reactive oxygen species (ROS) are difficult to detect at the acute stage before physiologic and anatomic evidence of tissue damage is present. Evaluation of the inflammatory and healing response early after an ischemic event in vivo will aid in treatment selection and

patient outcomes. We introduce a novel near-infrared hydrocyanine molecular probe for detection of ROS as a marker of tissue response to ischemia and a precursor to angiogenesis and remodeling. The synthesized molecular probe, initially non-fluorescent hydrocyanine conjugated to a high molecular weight polyethyleneglycol, converts to a highly fluorescent cyanine reporter upon oxidation. The probe was applied in a preclinical mouse model for myocardial infarction, where ligation and removal of a portion of the femoral artery in the hindlimb resulted in temporary ischemia followed by angiogenesis and healing. The observed increase in fluorescence intensity was approximately 6-fold over 24 hr in the ischemic tissue relative to the uninjured control limb and was attributed to the higher concentration of ROS in the ischemic tissue. These results demonstrate the potential for non-invasive sensing for interrogating the inflammatory and healing response in ischemic tissue.

8596-9, Session 3

Fluorescent proteins as singlet oxygen photosensitizers: mechanistic studies in photodynamic inactivation of bacteria

Rubén Ruiz-González, Univ. Ramon Llull (Spain); John H. White, The Univ. of Edinburgh (United Kingdom); Aitziber L. Cortajarena, Instituto Madrileño de Estudios Avanzados (Spain); Montserrat Agut, Santi Nonell, Univ. Ramon Llull (Spain); Cristina Flors, Instituto Madrileño de Estudios Avanzados (Spain)

Antimicrobial photodynamic therapy (aPDT) combines a photosensitizer, light and oxygen to produce reactive oxygen species (ROS), mainly singlet oxygen (1O2), to photo-oxidize important biomolecules and induce cell death. aPDT is a promising alternative to standard antimicrobial strategies, but its mechanisms of action are not well understood. One of the reasons for that is the lack of control of the photosensitizing drugs location. Here we report the use of genetically-encoded 1O2 photosensitizers to address the latter issue. First, we have chosen the red fluorescent protein TagRFP as a photosensitizer, which unlike other fluorescent proteins such as KillerRed, is able to produce 1O2 but not other ROS (Ragàs et al, ChemPhysChem 12, 161, 2011). TagRFP photosensitizes 1O2 with a small, but not negligible, quantum yield of 0.004. In addition, we have used miniSOG, a more efficient 1O2 photosensitizing fluorescent flavoprotein that has been engineered from phototropin 2 (Shu et al, Plos Biol. 9, e1001041, 2011). We have genetically incorporated these two photosensitizers into the cytosol of E. coli and demonstrated for the first time that intracellular 1O2 is sufficient to kill bacteria (Ruiz-González et al, Photochem. Photobiol. Sci. DOI: 10.1039/c2pp25126d). Additional assays have provided further insight into the mechanism of cell death. Photodamage seems to occur primarily in the inner membrane, and extends to the outer membrane if the photosensitizer's efficiency is high enough. These observations are different to those reported for external photosensitizers, suggesting that the site where 1O2 is primarily generated proves crucial for inflicting different types of cell damage.

8596-10, Session 3

Investigating real-time activation of adenosine receptors by bioluminescence resonance energy transfer technique

Yimei Huang, Hongqin Yang, Liqin Zheng, Jiangxu Chen, Yuhua Wang, Hui Li, Shusen Xie, Fujian Normal Univ. (China)

Adenosine receptors play important roles in many physiological and pathological processes, for example regulating myocardial oxygen consumption and the release of neurotransmitters. The activations of adenosine receptors have been studied by some kinds of techniques, such as western blot, immunohistochemistry, etc. However, these techniques cannot reveal the dynamical response of adenosine receptors under stimulation. In this paper, bioluminescence resonance energy transfer technique was introduced to study the real-time activation of adenosine receptors by monitoring the dynamics of cyclic adenosine monophosphate (cAMP) concentration which is the action target of adenosine receptors. The results showed that there were significant differences between adenosine receptors on real-time responses under stimulation. Moreover, the dynamics of cAMP demonstrated that competition between adenosine receptors existed. Taken together, our study indicates that monitoring the dynamics of cAMP using bioluminescence resonance energy transfer technique could be one potential approach to investigate the mechanism of competitions between adenosine receptors.

8596-11, Session 3

Assessment of surgical margins in an orthotopic colorectal cancer model by optical imaging

Tauseef Charanya, Gail P. Sudlow, Washington Univ. in St. Louis (United States); Kyle Gullicksrud, Washington Univ. School of Medicine in St. Louis (United States); Kexian Liang, Washington Univ. in St. Louis (United States); Nalinikanth Kotagiri, Walter J. Akers, Deborah C. Rubin, Samuel Achilefu, Washington Univ. School of Medicine in St. Louis (United States)

Dissemination of tumor cells from the colon during tumor resection is known to significantly increase the risk of local recurrence and tumor metastasis. It is important to accurately distinguish between healthy mucosa and surrounding precancerous-cancerous lesions. Although there has been significant developments in numerous imaging technologies for visualizing pathological conditions, the high specificity and sensitivity coupled with low energy of radiation makes optical imaging an attractive method for molecular imaging. We have developed a peptide based targeted near infrared (NIR) fluorescent molecular probe that can aid in accurate identification of tumor margins for surgical resection. An orthotopic colorectal cancer model was employed where HT-29 human colon carcinoma cells were implanted in the cecal wall. Time-course in-vivo fluorescence imaging conducted using small animal imaging system demonstrated the enhanced specificity of this probe in identifying the proliferating tumor edges after 24 hours of administration. The results demonstrate the potential of using this integrin-targeted probe for detecting tumor margins in colorectal cancer model for improved surgical resection.

8596-12, Session 4

Probing intra-cellular drug release event using activatable (OFF/ON) CdS:Mn/ZnS quantum dots *(Invited Paper)*

Swadeshmukul Santra, UCF NanoScience Technology Ctr. (United States)

Quantum dot (Qdot) nanotechnology has strong potential to strengthen modern drug discovery research in at least two ways – confirming delivery of therapeutic drug cargoes intra-cellularly and quantifying the amount of cargoes delivered. Extensive research has been done in the past decade using Qdots as bioimaging probes for both in vitro and in vivo studies. Significant research has been done towards developing water-soluble bright and photostable Qdots. Studies have shown that Qdots with appropriate surface coating minimizes surface defects, improving quantum efficiency and photostability. In this talk, I will focus on design, synthesis and study of activatable CdS:Mn/ZnS Qdots. Qdot surface was modified with suitable ligands which are capable of quenching Qdot luminescence ("OFF" state) via electron transfer process. Qdot luminescence was restored ("ON" sate) when electron transfer process was stopped. This was done by removing the quencher ligands or by exchanging with suitable non-quencher ligands. Using the "OFF"/"ON" strategy we have developed Qdot sensing probes for

the detection of glutathione. Following similar strategy, Qdot-iron oxide based multimodal/multifunctional biosensing probe that is optically and magnetically imageable, targetable and capable of reporting on intracellular drug release events have been developed. Specifically, the probe has a core-shell structure consisting of a superparamagnetic iron oxide nanoparticle core and a CdS:Mn/ZnS Qdot shell. Qdots were further conjugated to an anti-cancer drug, vitamin folate (as targeting agent) and m-polyethylene glycol (a dispersing agent). The Qdot luminescence was quenched due to electron/energy transfer processes. Upon intracellular interaction with glutathione Qdot luminescence was restored, reporting drug release event.

8596-13, Session 4

Lanthanide-doped nanoparticles for hybrid x-ray/optical imaging

Sudheendra Lakshmana, Gautom K. Das, Changqing Li, Simon R. Cherry, Ian M. Kennedy, Univ. of California, Davis (United States)

Nanoparticles comprised of a hexagonal NaLnF4 matrix and containing ytterbium sensitizer and Er3+/Tm3+ activators have been studied in the past for their well known near-infrared (NIR) up-conversion. Because of their high atomic number the lanthanide elements also absorb X-rays efficiently and hence are well-suited to X-ray luminescence optical tomography, which takes advantage of the fact that some lanthanides can re-emit the absorbed X-ray radiation in the visible-NIR spectrum range via a down-conversion mechanism. We have studied a series of Gd3+ and Eu3+ compositions in lanthanide fluorides to optimize the emission of Eu3+ ions upon X-ray excitation. Our results suggest that 15% molar concentration of Eu3+ in NaGdF4:Eu3+ showed good down-conversion emission following X-ray excitation. Similar to NIR to visible up-conversion, the hexagonal crystal structure was more efficient than the cubic structure with X-ray excitation. Furthermore, the X-ray down-conversion efficacy of broad-band sensitizers such as Ce3+ and Pr3+ on Er3+/Tm3+ and Yb3+ emitters is reported. In addition to lanthanide concentration, we also explored external coating effect such as gold coating [1,2] on the X-ray conversion to NIR radiation. The use of Er3+/Tm3+ and Yb3+ emitters as X-ray down-converters opens up the possibility of achieving high resolution and high sensitivity in-vivo molecular imaging through contrast agents that combine X-ray absorption and optical emission.

1. L. Sudheendra, Volkan Ortalan, Sanchita Dey, Nigel D. Browning and I.M. Kennedy Chem. Mater., 23 (2011) 2987

2. Wei Deng, L Sudheendra, Jiangbo Zhao, Junxiang Fu, Dayong Jin, Ian M Kennedy and Ewa M Goldys, Nanotechnology 22(2011) 325604

8596-15, Session 4

Multimodal microspheres for targeted PET and Cerenkov luminescence-excited fluorescence imaging of angiogenesis

Joanne Li, Lawrence W. Dobrucki, Marina Marjanovic, Eric J. Chaney, Stephen A. Boppart, Univ. of Illinois at Urbana-Champaign (United States)

Recently, it has been demonstrated that positron-emitting radionuclides used for PET can generate Cerenkov luminescence (CL). This discovery has led to the development of a new molecular imaging modality, known as CL imaging (CLi). The limitations of CLi used for imaging of biological tissues, however, include weak intensity and low tissue penetration. We present the method of fabricating radiolabeled multimodal microspheres that can convert CL to higher-intensity, higher penetrating near-infrared fluorescence through excitation of quantum dots (Qdots, Invitrogen). We also report the feasibility of using these microspheres as dual-modality targeted agents for both nuclear and optical imaging.

The microspheres have an ultrasonically-stabilized BSA shell and a vegetable oil core filled with near-infrared Qdots (300-600 nm excitation/800 nm emission). In these experiments, the microspheres were labeled with copper-64 isotope. This design allows the high refractive index oil core to act as a medium to enhance CL and to excite the encapsulated Qdots within the core. In addition, the BSA shell prevents direct contact of the Qdots with the biological tissue, reducing the risk of biotoxicity. These microspheres were further functionalized with PEG and cyclic RGD peptides and used for in vivo tumor targeting in a carcinogen-induced rat mammary tumor model. Tumor-bearing animals were imaged post-injection using both a microPET-CT scanner (Siemens Inveon) and an actively-cooled and sensitive CCD camera for detection of CL and CL-excited fluorescence. RGD-targeted radiolabeled Qdot microspheres have the potential as a more sensitive multimodal imaging agent for angiogenesis in a variety of diseases, including cancer and atherosclerosis.

8596-33, Session PMon

Perfluorinated near-IR dye labeled flourescent micelle for imaging of tumor hypoxia

Seong Ho Pahng, Washington Univ. in St. Louis (United States)

Hypoxia presents a challenge in cancer therapy because the poor oxygenation state renders solid tumors high resistance to radiation therapy and chemotherapy. Because of this therapeutic implication, many imaging methods have been investigated for early detection of tumor hypoxia. Most imaging probes are often based on hypoxia biomarkers and thus rely on a single molecular recognition event. Despite accuracy of such methods, these probes are limited by slow diffusion rate and reaction mechanism. More importantly, it fails to convey information at tissue-level, which is of interest to clinicians. We present a noble noninvasive hypoxia-sensing reporter near-IR fluorescent (NIRF) dye labeled oxygen-transport system to overcome such limitation. Due to overconsumption of oxygen, tumor tissues exhibit low oxygen tension in surrounding region. Herein, this oxygen partial pressure differential is used as a tissue-at-large indicator of tumor hypoxia by combining perfluorocarbon (PFC) compound's hitherto use as a blood substituent and quenching effect of oxygen. Micelle was prepared from perfluoro amphiphile and mixed with oxygen-trapping perfluorooctylbromide (PFOB) and PFC-conjugated cypate near-IR dye. Size of the micelle was characterized by DLS and TEM image. Upon saturation of oxygen, the fluorescence of the micelle was effectively quenched in fluorescence spectrophotometer study. For in vivo study, oxygen-saturated micelles were injected to tumor-induced mice. In the post injection scan, recovery of the fluorescence signal was only observed in hypoxic tissue region. Due to the excessive vascularization of tumor, the observed fluorescence also determined the size of the affected tissue.

8596-34, Session PMon

Mechanism of the first reversible photobleaching step in red fluorescent proteins

Mikhail Drobizhev, Thomas E. Hughes, Montana State Univ. (United States); Yuriy Stepanenko, Pawel Wnuk, Institute of Physical Chemistry (Poland); Kieran O'Donnell, J. Nathan Scott, Patrik Callis, Alexander Mikhaylov, Leslie Dokken, Aleksander K. Rebane, Montana State Univ. (United States)

Many red fluorescent proteins (RFPs) are not photostable, which limits their use in imaging. The first step of their complex photobleaching kinetics is related to isomerization of chromophore involving rotation around either one of two exocyclic bonds bridging phenol and imidazolinone groups. The detailed mechanism of this process and the role of the protein matrix are not understood. Here we show that the rate (k) associated with the first photobleaching step in a series of 13 RFPs varies by almost 2 orders of magnitude and strongly correlates with the change of the permanent electric dipole moment upon excitation (d).

Experimental dependence of k on d is a symmetric function, reaching a minimum at d0 = 2.9D and showing two exponentially increasing branches from both sides of the minimum. To describe this behavior, we present a model which assumes that the barrier for rotation around one of the exocyclic bonds increases linearly with the bond order. We treat the chromophore in a protein as a linear combination of two limiting resonating structures whose relative weights depend on the local electric field in a protein. The model predicts a linear dependence of d and bond length alternation (BLA) in the bridge region, which we indeed confirm experimentally. Using this model we evaluate the rotational barriers for each bridge bond and every protein. Our results present experimental evidence for the dominance of electronic effects in conformational dynamics of the RFP chromophore and provide useful guidelines for designing more photostable proteins.

8596-35, Session PMon

Single molecule interactions studied by using a modified DNA sequencer: a comparison with surface plasmon resonance and microarray data

Jens Sobek, ETH Zurich (Switzerland)

We studied the hybridization of an oligonucleotide immobilized at the bottom of a nanowell in a commercial DNA sequencer (“RS”, Pacific Biosciences). We investigated the influence of duplex length, salt concentration, and labeling dye on the binding constant. Kinetic data are compared with results obtained from SPR (Biacore) and from microarray experiments.

8596-36, Session PMon

Real-time point-of-care measurement of impaired renal function in a rat acute injury model employing exogenous fluorescent tracer agents

Richard B. Dorshow, MediBeacon LLC (United States); Sevag Demirjian M.D., Cleveland Clinic Lerner Research Institute (United States); Richard M. Fitch, John N. Freskos, Amruta R. Poreddy, Raghavan Rajagopalan, Jeng J. Shieh, Karen P. Galen, Jolette K. Wojdyla, Covidien (United States)

Renal function assessment is needed for the detection of acute kidney injury and chronic kidney disease. Glomerular filtration rate (GFR) is now widely accepted as the best indicator of renal function, and current clinical guidelines advocate its use in the staging of kidney disease. The optimum measure of GFR is by the use of exogenous tracer agents. However current clinically employed agents lack sensitivity or are cumbersome to use. An exogenous GFR fluorescent tracer agent, whose elimination rate could be monitored noninvasively through skin would provide a substantial improvement over currently available methods. We developed a series of novel aminopyrazine analogs for use as exogenous fluorescent GFR tracer agents that emit light in the visible region for monitoring GFR noninvasively over skin. In rats, these compounds are eliminated by the kidney with urine recovery greater than 90% of injected dose, are not broken down or metabolized in vivo, are not secreted by the renal tubules, and have clearance values similar to a GFR reference compound, iothalamate. In addition, biological half-life of these compounds measured in rats by noninvasive optical methods correlated with plasma derived methods. In this study, we show that this noninvasive methodology with our novel fluorescent tracer agents can detect impaired renal function. A 5/6th nephrectomy rat model is employed.

8596-37, Session PMon

A molecular dynamics study of phospholipid biomacromolecules using a coarse-grained model

Olga E. Glukhova, Irina V. Kirillova, Elena L. Kossovich, N.G. Chernyshevsky Saratov State Univ. (Russian Federation)

Characteristic features of the phospholipid molecule structure, rigidity and rotary mobility are studied using a coarse-grained (CG) model [1] slightly modified by authors. An original molecular dynamics method of the specific Ring software was utilized for the macro-molecule modeling. It was established for the first time that the phospholipid spiral-like structure can be presented as a spring with a rigidity of 27.68 kN/m. A rotary mobility of the phospholipid molecule was also studied. It was found that the molecule is rotating around an axis located at one of its ‘head’ atoms. The rotational frequency depends on the temperature. It equals to 0.9 GHz at the temperature of 293 K and increases up to 1.2 GHz at 309K. In the water, which is also modeled as four water molecules gathered into one CG virtual atom, the rotation frequency of phospholipid decreases down to 0.11 GHz, which is a well-known value of phospholipid molecule natural rotational frequency.

The micelle and bilayer aggregation processes were studied for the CG models of phospholipids. It was established that, at the constant temperature, the micelle aggregation time does not depend on the molecules amount, and at the temperature of 309 K it is 0.1 ns. Along with the temperature increase, the aggregation time decreases by the logarithmic law. Under the condition of the lower temperatures (less than 309 K) the assembly process depends also on the molecules positioning and the distance between the neighboring ones, at which these molecules will be involved in the aggregation process. The critical value of distance between the neighboring molecules decreases with the temperature.

Bibliography

1. Marrink, S.J. Coarse Grained Model for Semiquantitative Lipid Simulations / S.J. Marrink, A.H. de Vries, A.E. Mark // Journal of Physical Chemistry .B. – 2004. Vol. 108. – P. 750-760

8596-38, Session PMon

Development of the terahertz emitter model based on nanopeapod in terms of biomedical applications

Olga E. Glukhova, Anna S. Kolesnikova, N.G. Chernyshevsky Saratov State Univ. (Russian Federation); Igor S. Nefedov, Aalto Univ. School of Science and Technology (Finland)

It is known that the receipt of terahertz radiation sources is necessary for medical diagnostic purposes. It is important to get a miniature radiation sources that range. There are currently developed sources of terahertz time has two significant drawbacks: they have very little power, they are very bulky size. Therefore, actual problem is the creation of small system with an acceptable level of energy characteristics.

In this paper we were carried out simulation of terahertz emitter based on peapod filled with fullerenes C60. Investigation of the parameters under which the terahertz range is observed, was performed using a molecular-mechanical method.

An open nanotube (10,10) was used to model nanoscale emitter. Three fullerenes C60 related by the chemical bond between themselves and with the wall of nanotubes (fullerenes chains) were placed on both edges of the nanotube. Distance between these fullerenes chains was equal to 4.3 nm. Fullerene C60 was related in the space of the nanotube between fullerenes chains.

It is shown that terahertz radiation sources has nanometer dimensions (length of 3.10 nm and radius of 1.35 nm) and the average power expended on the motion of the fullerene is 0.6?kW. It is necessary that charge fullerene C60 was equal to +6e and the charge of tube was equal

to -6e for creating the small external field. The terahertz radiation sources operates at a frequency 0.267 THz with condition charge of nanotube and fullerene and with the field strength 106 V / cm. Power consumed fullerene to exit the potential well is equal to 2.210-8 W.

8596-39, Session PMon

Carbon nanotube+graphene quantum dots complex for biomedical applications

Olga E. Glukhova, Igor N. Saliy, Anna S. Kolesnikova, Michael M. Slepchenkov, N.G. Chernyshevsky Saratov State Univ. (Russian Federation)

The results of the theoretical investigation of influence of the graphene quantum dots on the properties of the carbon nanotubes (CNT) are presented in the current work. The mathematical model of the CNT+graphene quantum dot complex was built in the course of investigation. This model based on the quantum-mechanical presentation of the nanotube, realized within the semi-empirical tight-binding model. The atomic structure of the CNT with quantum dot was constructed on basis of the single-layer nanotube and graphene flake. Graphene flake was attached to CNT by means of the armchair edge.

On example of the interaction between carbon nanotube and graphene flakes was shown:

1) The stability of the atomic structure for CNT+graphene quantum dot complex increases at the increase of number of the graphene flakes.

2) The configuration of the CNT+graphene quantum dot complex, where graphene flakes form chemical bonds around both side of nanotube, is energetically favorable.

3) The conductivity of the CNT increases at the attachment of the graphene flakes.

The unique physical properties of the quantum dots make their the ideal tool for the supersensitive multicolored registration of the biological objects, and also for medical diagnostics. Experimental investigations revealed that the graphene quantum particles begin to luminesce at the excitation of the ultraviolet radiation. Taking into account the obtained in this work results, one can propose that nano-dimensional sensors based on the CNT+graphene quantum dot complex can be made for medicine and biology.

8596-40, Session PMon

Docosahexaenoic acid conjugated near infrared flourescence probe for in vivo early tumor diagnosis

Siwen Li, Jie Cao, China Pharmaceutical Univ. (China); Samuel Achilefu, Washington Univ. School of Medicine in St. Louis (United States); Yueqing Gu, China Pharmaceutical Univ. (China)

Docosahexaenoic acid(DHA) is an omega-3 C22 natural fatty acid with six cis double bonds and as a constituent of membranes used as a precursor for metabolic and biochemical path ways. In this manuscript,we describe the synthesis of near-infrared(NIR) flourescence ICG-Der-01 labeled DHA for in vitro and vivo tumor targeting.The structure of the probe was intensively characterized by UV and MS. The in vitro and vivo tumor targeting abilities of the DHA-based NIR probes were investigeted in MCF-7 cells and MCF-7 xenograft mice model differently by confocal microscopy and CCD camera. The cell cytotoxicity were tested in tumor cells MCF-7 and normal liver cells L02 in vitro. The results shows that the DHA-based NIR probes have high affinity with the tumor both in vitro and vivo.In addition ,we also found that the DHA-based NIR probes have the apparent cytotoxicity on MCF-7 cells but less in L02.which demonstrated that DHA was conjugated with other antitumor drug could increase the abilities of antirumor efficacy but less damage in normal human cells. So DHA-ICG-Der-01 is a promising optical agent for diagnosis of tumors especially in their early stage.

8596-41, Session PMon

MUC1 aptamer based near infrared fluorescence probes for tumor diagnosis

Juan Zhao, China Pharmaceutical Univ. (China); Samuel Achilefu, Washington Univ. School of Medicine in St. Louis (United States); Yueqing Gu, China Pharmaceutical Univ. (China)

Mucin?1?(MUC1) is a cell surface mucin?broadly expressed in mucosal?tissues. The aberrant expression of MUC1 under-glycosylated forms has been reported in various carcinomas of the epithelium, such as breast, pancreatic and ovarian cancers. Using the Systematic Evolution of Ligands by Exponential Enrichment (SELEX) methodology, aptamers previously selected against MUC1 glycoprotein with high affinities and specificities. In this study, we developed two targeted near-infrared fluorescent probes for tumor in-vivo diagnostics using a MUC1 aptamer(APT) as targeted ligand and near-infrared fluorescent dye (ICG-Der-02) as labelling. MUC1 aptamer conjugated ICG-Der-02 (APT-ICG-Der-02) displayed a great selectivity to MUC1 positive cell line MCF7 and MCF7 xenograft-bearing nude mice. To improve the high targeting of the probe to the tumor cells, PEG, with high biocompatibility, non immunogenicity and long circulation, was conjugated to the probe .The new probe (APT-PEG-ICG-Der-02) showed better tumour uptake and clearance, and also displayed a great selectivity to MCF7 tumor-bearing nude mice. Data obtained demonstrate a high potential of the targeted near-infrared fluorescent probes in cancer early diagnosis.

8596-42, Session PMon

Thermal-lens study of semiconductor nanoparticles embedded in restorative dental resin

Viviane Pilla, Univ. Federal de Uberlândia (Brazil); Leandro P. Alves, Adalberto N. Iwazaki, UNICASTELO (Brazil); Paulo R. Barja, Univ. do Vale do Paraíba (Brazil); Egberto Munin, UNICASTELO (Brazil)

Quantum Dots (QDs) or nanostructured semiconductors are materials in continuous development that hold potential for a variety of new applications, including uses in fluorescent labels for biomedical science, photonic devices and sensor materials [1,2]. In biomedical applications, several nanodiagnostic assays have been developed that use QDs. They have been applied to diagnostics, the treatment of diseases, bioimaging, drug delivery, engineered tissues and biomarkers [2,3]. The matrix used to suspend the solute samples can exert important influence on optical and thermal properties as thermal diffusivity and the thermal coefficient of the refractive index of the investigated materials.For a nanoparticle to be a candidate for practical applications, it is important to know their thermo-optical properties. The present work reports the thermo-optical properties of cadmium selenide/zinc sulfide (CdSe/ZnS) core-shell QDs embedded in restorative dental resins measured with thermal lens (TL) technique [4]. Transient TL measurements were performed using the mode-mismatched dual-beam (excitation and probe) configuration. Thermo-optical study was performed in QDs with different core sizes and concentrations embedded in commercial composite resins. The results obtained from TL technique were compared with the fluorescence and photoacoustic measurements.

[1] M. Bruchez Jr et al., Science 281, 2013-2016 (1998).

[2] N. Sounderya and Y. Zhang, Recent Patents Biomed Eng 1, 34-42 (2008).

[3] L. P. Alves et al., J Dentistry 38, 149-152 (2010).

[4] V. Pilla et al., Opt Commun 280, 225-229 (2007).

8596-43, Session PMon

NIR quantum dots as contrast agents for the detection of colorectal cancer

Jordan L. Carbary, Jennifer K. Barton, Urs Utzinger, The Univ. of Arizona (United States)

Optical Coherence Tomography/Laser Induced Fluorescence (OCT/LIF) dual-modality imaging has been shown to provide more information on colorectal cancer imaging in mice than either one alone. Ideally, the contrast agent used for this system should not compete with autofluorescence of the tissue or with the OCT wavelength range. NIR quantum dots (QD) have great potential as contrast agents for this dual-modality approach. As a preliminary ex vivo investigation into their efficacy, NIR quantum dots (705nm emission) targeted to endothelial growth factor receptor, which has been shown to be upregulated in colon neoplasms, were applied in vivo to the colon of carcinogen or saline treated mice and allowed to incubate for 20 or 40 minutes. At the end of the incubation, the colon was explanted and imaged using wide-field fluorescence microscopy for an en face image, and multiphoton microscopy to obtain images through the thickness of the neoplasms and colon. This presentation will include contrast analysis on the images obtained from the wide-field fluorescence microscopy, as well as determination of the location of QDs through the thickness of the tissue. The contrast analysis provides the ability to elucidate the efficacy of the QDs as contrast agents for an in vivo pre-clinical study, whereas the movement of the quantum dots through the thickness of the tissue provides information on the ideal incubation time to yield the maximal number of quantum dots at the surface of the colon, as it is imaged using OCT/LIF.

8596-44, Session PMon

Fluorescence resonance energy transfer in systems of zinc-pthalocyanines in the presence of CdSe quantum dots

Adamo F. Monte, Univ. Federal de Uberlândia (Brazil); Tamiris S. Souza, Univ. Federal de Uberlândia (Brazil) and Univ. Federal de Uberlândia (Brazil); Arnaldo F. Reis, Djalmir N. Messias, Guilherme A. Alves, Univ. Federal de Uberlândia (Brazil)

Several processes leading to energy transfer between inorganic and organic systems have gained much attention nowadays, because of their potentials appearing in biological applications, including photodynamic therapy, design of biosensors, and the analysis of biomolecular conformation and interaction. In this work, fluorescence resonance energy transfer (FRET) in CdSe–ZnS semiconductor nanocrystals (FRET donors) and organic chromophores (FRET acceptors) was explored. Zinc-pthalocyanines (Zn-Pc) as organic chromophores were prepared in the presence of core-shell CdSe-ZnS quantum dots (QDs) in dimethyl sulfoxide (DMSO) colloidal solutions. The photophysical properties of the Pcs in the presence of QDs were enhanced, and the FRET mechanism represents an efficient way for the study of their physical and chemical properties, and also for the detection of interactions between the photosensitizer molecules. The main results were obtained by using the microluminescence surface scan technique (MSST), which is based on the spatial analysis of the fluorescence distribution compared to the excited area by a tightly focused optical beam normal to the surface. These measurements provide spatial accuracy for the analysis of the energy transfer process. By measuring the spatial energy migration (fluorescence distribution) and its wavelength dependence it is possible to understand the whole dynamics of the QD-organic system. The concomitant decrease of the fluorescence spatial distribution width indicates that the excitation of the Pc molecules occurs not only through reabsorption but also through FRET. This also demonstrates that the FRET in such a hybrid system occurs even without chemical conjugation of the donor and the acceptor.

8596-46, Session PMon

Combination of near infrared (808-nm) laser and selective gold nanorods in antimicrobial action on staphylococcus aureus

Elena S. Tuchina, Pavel O. Petrov, N.G. Chernyshevsky Saratov State Univ. (Russian Federation); Fulvio Ratto, Istituto di Fisica Applicata Nello Carrara (Italy); Sonia Centi, Univ. degli Studi di Firenze (Italy); Roberto Pini, Istituto di Fisica Applicata Nello Carrara (Italy); Valery V. Tuchin, N.G. Chernyshevsky Saratov State Univ. (Russian Federation)

We investigated the action of near infrared laser irradiation on S. aureus 209 P threated with cojugates of gold nanoparticles and suitable immunoglobulins. Microbial cells overexpressing protein A were targeted with 40 nm length ? 10 nm diameter Au nanorods in concentration 0.4 mM Au, which were conjugated with human IgG. The rationale behind this choice originates from the high affinity between protein A and the Fc domain of human IgG, which belongs to the defense of S. aureus against opsonization and phagocytosis. Proper controls included the use of other immunoglobulins with different affinity for protein A. For irradiation, NIR laser (808 nm, 100 mW/cm2) in the CW mode with exposures 5, 10, 15 and 30 min was used.

It was shown that combination of NIR laser light and Au nanorods-human IgG effectively supresses growth of bacterial population. After 30 min irradiaton reduction in number of S. aureus 209 P colony forming units above 90% was noted.

8596-16, Session 5

Concept of nanoparticle clustering in biomedical applications *(Invited Paper)*

Konstantin V. Sokolov, The Univ. of Texas M.D. Anderson Cancer Ctr. (United States); Justina O. Tam, Avinash Murthy, Soon Joon Yoon, Timothy A. Larson, Bobby Stover, Stanislav Y. Emelianov, Keith P. Johnston, The Univ. of Texas at Austin (United States)

Previously, our group has shown that targeted plasmonic nanoparticles can change optical signatures in the presence of cells overexpressing a biomolecule of interest. This effect is associated with specific interactions between targeted gold nanoparticles and a biomolecule of interest such as EGF receptors that results in receptor mediated aggregation of nanoparticles. The closely spaced nanoparticles exhibit the effect of plasmon resonance coupling that leads to a profound increase in absorbance of nanoparticles in the red-NIR region.

Here we extend the concept of plasmon resonance coupling to synthesis of hybrid nanomaterials for in vivo biomedical imaging and therapy. We use weakly adsorbing biodegradable polymers and primary sub-5nm ligand coated gold nanoparticles to produce metal/polymer biodegradable nanoclusters with controllable sizes ranging from ca. 25 to 100 nm with strong NIR absorbance. We showed that these nanoclusters can degrade into primary sub-5nm nanoparticles in slightly acidic environment of cellular endosomes; this degradation process can lead to efficient clearance of the nanoclusters from the body through a combination of clearance pathways such as biliary and renal clearance. Furthermore, clusters of small primary particles can exhibit significantly different physicochemical properties as compared to solid nanoparticles of the same size; this is due in part to a different distribution of the near electromagnetic field in a cluster vs. a solid nanoparticle. In this presentation we will discuss how unique properties of metal nanoparticle clusters can be optimized for biomedical applications including efficient delivery, multimodal molecular imaging and therapy, biodegradation, and clearance.

8596-17, Session 5

Fast and reliable luminescence quantum yield determination for efficient fluorescent probes developement

Steffen Ruettinger, Felix Koberling, Sebastian Tannert, PicoQuant GmbH (Germany); Christian Würth, Federal Institute for Research and Testing (BAM) (Germany); Katrin Hoffmann, Ute Resch-Genger, Bundesanstalt für Materialforschung und -prüfung (Germany); Rainer Erdmann, PicoQuant GmbH (Germany); Markus Grabolle, Jutta Pauli, Bundesanstalt für Materialforschung und -prüfung (Germany); Ute Resch-Genger, Bundesanstalt für Materialforschung und -prüfung (Germany)

Besides molar absorption coefficient and excited state lifetime, the photoluminescence quantum yield is the key parameter to be optimized for highly efficient and bright fluorescent probes. An easy and reliable way to determine the quantum yield is therefore the prerequisite for modern fluorescent probe development.

Photoluminescence quantum yield measurements are typically done by comparing the emission intensity of the target compound with a standard of known quantum yield, under identical measurement conditions. This method is well established and precise, but also time consuming. In addition target compound and reference have to have similar absorption and emission spectra. For those cases where a suitable standard is not available; when the measurement of the absorption is cumbersome, when the determination speed is an issue, or generally for scattering samples, the use of an integrating sphere to measure the absolute photoluminescence quantum yield is mandatory.

Here we show that absolute photoluminescence quantum yield measurements of solutions as well as solid samples can be easily realized using a simple integrating sphere accessory for a conventional fluorescence lifetime spectrometer. This allows to acquire all relevant fluorescence characteristics with one instrument, therefore streamlining the characterization workflow and keeping all calibration schemes simple.

For the validation of our new assembly, selected quantum yield standards have been measured and the data were compared to literature data previously determined with a calibrated spectrofluorometer and two calibrated integrating sphere setups. Procedures for the determination of the instrument's spectral sensitivity and attainable precision of the results will be discussed.

8596-18, Session 5

Design and synthesis of novel photoswitchable nanoparticles for imaging

Ming-Qiang Zhu, Guo-Feng Zhang, Huazhong Univ. of Science and Technology (China)

Both photoswitchable fluorescent nanoparticles and photoactivatable fluorescent proteins have been used for super-resolution far-field imaging at the nanometer scale, but the photo-activating wavelength for such photo-chemical events generally falls in the near-UV region (NUV < 420 nm) that is not preferred in cellular imaging. Using two near IR (NIR) photons, lower in energy, however, we can circumvent such problems and replace NUV single-photon excitations (e.g., 390 nm) with NIR two-photon excitations (e.g., 780 nm). Thus, we demonstrated that alternating 780-nm NIR two-photon and 488-nm single-photon excitations had induced reversible on-off fluorescence switching of immunotargeted nanoparticles in the human breast cancer cell line SK-BR-3. Herein, two-photon absorption not only caused spiropyran-merocynine photoisomerization within the particles but also imparted red fluorescence. When compared to single-photon NUV excitations, two-photon NIR laser excitations can potentially reduce absorption-related photodamage to living systems because cellular systems absorbs much weakly in the NIR. Interstingly, the novel photoswitchable nanoparticles show great potential in super-resolution imaging.

8596-19, Session 6

Molecular and nano-thermometers for potential applications in thermal ablation procedures *(Invited Paper)*

Mikhail Y. Berezin, Tiffany P. Gustafson, Natalia Zhegalova, Qian Cao, Alex Aydt, Steven Wang, Washington Univ. School of Medicine in St. Louis (United States)

Precise monitoring of temperature to minimize the damaging effects of medical thermal ablation methods is essential for the efficacy and safety of these procedures. We present several principles of measuring the temperature on a micro scale with temperature sensitive fluorescent constructs and nanoparticles. In one of the presented methods two fluorophores emitting at different wavelengths are covalently bound to form a reversible optical thermometer. One fluorophore serves as a sensor, while the second fluorophore serves as a reference point. Temperature sensitivity of such construct is measured ratiometrically. In another approach non- or minimally fluorescent nanoparticles are prepared to become irreversibly fluorescent when the temperature inside the target reaches a critical temperature. These approaches introduce new possibilities for measuring and controlling temperature during thermal ablation procedures.

8596-20, Session 6

Dendritic up-converting nanoparticles: pH nanosensors

Sergei A. Vinogradov, Tatiana V. Esipova, Xingchen Ye, Univ. of Pennsylvania (United States); Josh E. Collins, Intelligent Material Solutions Inc. (United States); Christopher B. Murray, Univ. of Pennsylvania (United States)

Lanthanide-based upconverting nanoparticles (UCNPs) form a new class of imaging agents with unique non-linear optical properties. However, utilization of UCNPs in biomedical arena has been hampered by the lack of robust methods of their solubilization and surface functionalization. Here we show that non-covalent modification of UCNPs with polyanionic dendrimers converts them into stable, water-soluble, non-toxic imaging probes. When dendrimers contain chromophoric cores, UCNP-to-dendrimer excitation energy transfer enables analyte-sensitive detection by upconverted luminescence. As an example we demonstrate that UCNP/porphyrin-dendrimers make up ratiometric pH nanosensors for physiological pH range.

8596-47, Session 6

Integrated in vivo modeling of cancer biology using avian embryos: a role for intravital imaging *(Invited Paper)*

John Lewis, Univ. of Alberta (Canada)

Recent innovations in microscopy and imaging technologies have increased the utility of optical imaging approaches for the study of tumor progression and metastasis, and this has been coupled with the development of highly sensitive and specific contrast agents that has enabled the visualization of structural and functional information using intravital imaging. Metastasis is an complex multi-step process, and one that has a significant impact on cancer mortality. The success of metastatic dissemination is determined by a tumour cell's ability to travel to a distant site, arrest, extravasate into the stroma surrounding the vasculature and grow in a new microenvironment. Tumor cell extravasation is an integral step of cancer metastasis but the mechanisms that regulate this dynamic process are unclear. Using a 3D intravital imaging approach in ex ovo avian embryos, we show that cancer cells that have arrested in secondary organs will

migrate intravascularly, during which protrusive structures probe the microvasculature prior to the initiation of extravasation at endothelial junctions. We demonstrate that these invasive structures are in fact invadopodia, and they play a critical role in facilitating transendothelial migration in vivo. Inhibition of structural and functional components of invadopodia, including cortactin, Tks4, and Tks5 significantly abrogate the extravasation of tumor cells in vivo and the subsequent establishment of metastatic colonies. This establishes cancer cell extravasation as a critical rate-limiting step of metastasis, and a potentially important therapeutic target for anti-metastasis strategies.

8596-21, Session 7

Suppressing inflammation from inside out with novel NIR visible perfluorocarbon nanotheranostics

Jelena M. Janjic, Sravan K. Patel, Erin DiVito, Michael Cascio, Duquesne Univ. (United States); Michael Patrick, Carnegie Mellon Univ. (United States); John A. Pollock, Duquesne Univ. (United States)

Highly innovative multimodal perfluorocarbon (PFC) nanoreagents are presented. They serve simultaneously as dual mode imaging reagents (near infrared and 19F magnetic resonance) and drug delivery vehicles for water insoluble cyclooxgenase-2 (COX-2) inhibitors. This feature qualifies them as true theranostic nanoreagents. Cancer progression and metastasis are highly influenced by tumor microenvironment and inflammation. Infiltration of primary tumors with inflammation-promoting cells (e.g. macrophages) is a negative prognostic factor for cancer patient survival. We postulate that suppression of COX-2 enzyme in macrophages by theranostic PFC nanoemulsions will result in change of macrophage levels of accumulation in tumors and/or their phenotype, which can suppress their tumor promoting activity. Presented PFC nanoemulsions are drug delivery vehicles, 19F magnetic resonance (MR) tracers and near infrared (NIR) imaging agent carriers. 19F MRI is used to quantitatively assess the distribution of the injected anti-inflammatory PFC theranostic in the peritumoral area and measure tumor associated inflammation, while 1H MRI is used to provide anatomical context. NIR is used as a complementary imaging technique in vitro and in vivo. We will present in detail design rationale for PFC theranostics carrying varied COX-2 inhibitors, the in vitro evaluation and in vivo NIR and 19F MR images in a mouse tumor model. We are developing PFC nanoemulsions to simultaneously treat and image inflammation associated with tumors. Targeting macrophages with specific agents to change their behavior in vivo is crucial novelty in the presented theranostic designs.

8596-22, Session 7

Core-shell polymeric nanoparticles: spectroscopic assessment of micelle CST, assembly and dye binding

Tiffany Gustafson, Young Lim, Shiyi Zhang, Gyu-Seong Heo, Alexander T. Lonnecker, Jeffery E. Raymond, Karen L. Wooley, Texas A&M Univ. (United States)

Core-shell crosslinked nanoparticles (SCKs) have been shown to be viable candidates for targeted drug delivery and targeted contrast agents. The majority of reports focus on polymer synthesis, purification and application, with little said about assembly and cross-linking kinetics. In this work, we will detail how block co-polymer systems and block-brush co-polymer systems of polylactic acid and polystyrene can be monitored by raman and fluorescence to determine assembly and cross-linking kinetics during the SCK formation process. Similarly, the effects on assembly associated with concentration and temperature control will be detailed. It will be shown that careful assessment of these intermediate states leads to better size regularity, lower amounts of side product, higher assembly efficiency and better control of morphology through a more detailed understanding of micelle formation and cross-linking.

8596-24, Session 7

Time-resolved fluorescence spectroscopy of cationic polymer/DNA complex stained with SYBR Green I

Cosimo D'Andrea, Daniele Pezzoli, Chiara Malloggi, Andrea Bassi, Giulio Capelli, Alessandro Volonterio, Paola Taroni, Gabriele Candiani, Politecnico di Milano (Italy)

Gene therapy depends on the capability of carriers to efficiently internalize genetic material into target cells. Non-viral gene delivery system such as cationic polymer/DNA complex (polyplex) are drawing significant attention due to the possibility to overcome some drawbacks shown by the most commonly adopted viral vectors, even if transfection efficiency still remain a limiting factor. In order to optimize non-viral vectors, there is a strong request of analytical tools to study and predict their performance (e.g. DNA binding ability, complexation, DNA release dynamics, serum resistance, etc). Time-resolved fluorescence spectroscopy technique has been recently demonstrated to provide useful information for the transfection process characterization. The key idea is to monitor the fluorescence lifetime of a DNA dye (e.g. Et:Br , SYBR Green I) to get insights into the state of the DNA in the polyplex. In this work, a more extensive study has been carried out to monitor the fluorescence lifetime of SYBR Green I with different polyplexes at various Nitrogen to Phosphate (N/P) ratios. In particular, a novel copolymer (chitosan-graft-branched polyethylenimine, Chi-g-bPEI), which showed high transfection efficiency and low cytotoxicity, was studied and compared with the basic polymer block (2 kDa bPEI) and the gold standard polymeric transfectant 25 kDa bPEI. The fluorescence lifetime values were correlated with measurements of Dynamic Light Scattering, Zeta Potential and transfection efficiency. Finally, measurements were performed to dynamically follow the process of polyplex formation and decomplexation once Heparin was added.

8596-25, Session 8

Engineering a methylene-blue dual activatable probe for photoacoustic imaging

Ekaterina Morgounova, Qi Shao, Benjamin Hackel, Shai Ashkenazi, Univ. of Minnesota (United States)

High-resolution, high-penetration depth activatable probes are needed for in-vivo imaging of enzyme activity. In this talk we will describe the design and development of a new dual-labeled photoacoustic contrast agent that changes its lifetime upon activation. The excitation decay of methylene blue (MB), an FDA approved chromophore, is probed by a photoacoustic lifetime imaging (PALI) system. The monomer of the dye presents a high-quantum yield of intersystem-crossing and long lifetime (70 ?s) whereas the dimer is statically quenched with a short lifetime (a few nanoseconds). This forms the basis of a highly sensitive contrast mechanism between monomers and dimers. A dimerization model using sodium dodecyl sulfate as a cross-linker between MB molecules was applied to mimick the conditions of activation of the probe. Preliminary results show that the photoacoustic signal of a dimer solution is efficiently suppressed (20 dB) due to their short lifetime compared to the monomer sample. Flash-photolysis of the same solutions reveals a 99% phosphorescence decrease confirming those results. We are developing a dual-methylene blue probe bound by a cleavable peptide linker specific for MMP2, a molecular marker for cancer progression of the Matrix Metalloproteinase (MMP) family. When the probe is cleaved by its target, the dyes will separate by diffusion and recover their long excitation lifetime enabling their detection by PALI. Our long-term goal is to investigate MMP-specific imaging in small animals and establish pre-clinical data for translational research and implementation of the technology in clinical applications.

8596-26, Session 8

Polyacrylamide based ICG nanocarriers for enhanced fluorescence and photoacoustic imaging

Aniruddha Ray, Hyung Ki Yoon, HeeJu Ryu, Yong-Eun Koo Lee, Gwangseong Kim, Univ. of Michigan (United States); Xueding Wang, Univ. of Michigan Health System (United States); Raoul Kopelman, Univ. of Michigan (United States)

Indocyanine green (ICG) is an FDA approved tricarbocyanine dye. This dye, with a strong absorbance in the near infrared (NIR) region, has been extensively used for fluorescence and photoacoustic imaging in vivo. ICG in its free form, however, has a few drawbacks that limit its in vivo applications: (i) In its free form, ICG cannot be specifically targeted to any cell or tissue. (ii) Depending on the local concentration, ICG aggregates to form dimers, changing its optical properties. (iii) Free ICG gets easily degraded in biological environments due to the loss of its double bond. (iv) Free ICG has a very short plasma lifetime. (v) The fluorescence and absorbance intensities of ICG significantly decrease at body temperature compared to those at room temperature.

In order to bypass the above mentioned drawbacks and make ICG a contrast agent suitable for in vivo applications, we demonstrate a special type of polyacrylamide based nanocarrier that was particularly designed to carry the negatively charged ICG molecules. These nanocarriers are biodegradable, biocompatible and can be specifically targeted to any cell or tissue. Using these nanocarriers we not only avoid all the problems associated with free ICG, such as degradation, aggregation and short plasma lifetime, but also enhance the photoacoustic signal intensity due to the interaction of ICG molecules with the positively charged free amine groups inside the matrix. The photoacoustic spectrum of the nanocarriers containing ICG shows a maximum signal enhancement of 90% in the NIR region from 700 to 810 nm.

8596-27, Session 8

Carotenoids as biological labels for third harmonic generation microscopy

Danielle B. Tokarz, Richard Cisek, Ulrich Fekl, Virginijus Barzda, Univ. of Toronto Mississauga (Canada)

Third harmonic generation (THG) microscopy is a valuable technique currently used for imaging biological organisms without dyes, however, structural specificity can be achieved by labeling intracellular structures with molecules that demonstrate large third-order nonlinear optical properties. Molecular labels which enhance the THG signal intensity of stained structures are referred to as harmonophores. We studied the third-order nonlinear susceptibility (?(3)) of ?-carotene, but also other carotenoids found in nature including: violaxanthin, neoxanthin, lutein, zeaxanthin, canthaxanthin and astaxanthin as well as chlorophylls: chlorophyll a and chlorophyll b. Measurements were taken in solution by the THG ratio method which is based on measuring the THG intensity from two interfaces using a harmonic generation microscope. Second hyperpolarizability (?) values of carotenoids and chlorophylls were extracted from ?(3) measurements including the refractive index at fundamental and third harmonic wavelengths. Early investigations revealed that the difference in refractive index at both wavelengths largely influenced the calculation of ? values when harmonophores have absorption near the third harmonic or fundamental wavelength. In particular, the magnitude of the ? value of chlorophylls were found to be two orders of magnitude larger than the ? value of carotenoids as well, the sign of ? for chlorophylls was found to opposite in sign of ? for carotenoids. Lastly, carotenoids were demonstrated as harmonophores by labeling the cell membrane of Drosophila Schneider 2 cells by liposome cell fusion experiments. This study demonstrates that THG enhancement by carotenoids and chlorophylls can be used for nontoxic in vivo labeling of subcellular structures.

8596-28, Session 8

Photothermal based detection of the contrast properties of polypyrrole nanoparticle using optical coherence tomography

Deepa K. Kasaragod, Kin Man Au, Zenghai Lu, David Childs, Steven Armes, Stephen J. Matcher, The Univ. of Sheffield (United Kingdom)

We report on a photothermal modulation detection scheme developed using a swept source based optical coherence tomography (OCT) system centred at 1315nm. Photothermal detection gives an improved technique to study the contrast properties of exogenous contrast agents like microsphere and nanoparticles used with OCT imaging, taking into account their absorption properties [1-2]. The swept source based OCT system has a wavelength sweep rate of 10 kHz which is used for the phase modulation detection of different concentrations of polypyrrole (PPy) nanoparticles. PPy nanoparticles have been recently reported to be a promising candidate for OCT imaging owing to the strong absorption spectrum shown by them in the wavelength range from 700–1300nm and beyond. PPy nanoparticles are synthesized via aqueous dispersion polymerisation of pyrrole using a poly vinyl alcohol stabilizer and studies have also confirmed their biocompatibility and low long term cytotoxicity [3]. Phase sensitive detection of the photothermal modulation signal is carried out using pump laser beam of wavelength 975nm at two different modulation frequencies of 80Hz and 120Hz for different concentrations of PPy nanoparticles in 2% intralipid phantom, imaged over a depth of 225microns with a coverslip on top of the sample in order to account for the phase fluctuations in the swept source based system. This study strengthens the use of PPy nanoparticle as a potential biocompatible contrast agent in OCT imaging, quantitatively.

References:

[1] Zhou, C., Tsai, T. H., Adler, D. C., Lee, H. C., Cohen, D. W., Mondelblatt, A., Wang, Y. H., Connolly, J. L., and Fujimoto, J. G., “Photothermal optical coherence tomography in ex vivo human breast tissues using gold nanoshells,” Optics Letters, 35(5), 700-702 (2010).

[2] Guan, G. Y., Reif, R., Huang, Z. H., and Wang, R. K. K., “Depth profiling of photothermal compound concentrations using phase sensitive optical coherence tomography,” Journal of Biomedical Optics, 16(12), (2011).

[3] Au, K. M., Lu, Z. H., Matcher, S. J., and Armes, S. P., “Polypyrrole Nanoparticles: A Potential Optical Coherence Tomography Contrast Agent for Cancer Imaging,” Advanced Materials, 23(48), 5792-5795 (2011).

8596-29, Session 9

Mechanisms of multiphoton photobleaching of red fluorescent proteins

Caleb Stoltzfus, Aleksander K. Rebane, Mikhail Drobizhev, Thomas E. Hughes, Kelsey March, Montana State Univ. (United States)

Red fluorescent proteins (FPs) should be incredibly useful for multiphoton microscopy involving thick samples of living tissue: they are brighter than green FPs and they absorb at optimal wavelengths for live imaging, however they photobleach remarkably quickly. In order to engineer better two-photon red FPs the mechanisms causing this photobleaching must be understood. Here we have studied photobleaching for five red FPs of the mFruits series using a 75 MHz femtosecond Ti:Sapphire laser in a two-photon excited fluorescence microscope setup. E. coli bacteria colonies expressing the FP are imaged in the focal plane the microscope and the fluorescent signal is then recorded as a function of time for various laser powers. Earlier it was reported that the decay kinetics is strongly non-monoexponential and that the rate of the decay increases with the incident power. We obtain the power dependence of the initial photobleaching rate measured shortly after the fs laser beam is switched on. For most of the FPs the power dependence can be described using

the sum of a quadratic term and a fourth order term. We have found that the quantum efficiency corresponding to the first term is similar to that previously found by us using single photon excitation. The mechanism of this reaction, starting from the first excited state was related to reversible chromophore isomerization. The second (fourth order power dependence) term is most probably due to four-photon ionization of the chromophore. This information allows us to better understand the photobleaching mechanisms of different FPs.

8596-30, Session 9

Predicting errors from spectral overlap in multi-probe and multi-laser flow cytometry

Mary J. Potasek, Simphotek Inc. (United States) and New York Univ. (United States); Gene Parilov, Karl Beeson, Simphotek Inc. (United States)

In flow cytometry a group of cells labeled with a fluorescent probe molecule or dye is focused into a single cell stream passing through a laser light source. The fluorescent light is filtered and sampled by an array of detectors. In many cases a single light source and one probe/dye molecule have been used. But additional information can be obtained if several different laser wavelengths and multiple probes fluorescing at other wavelengths are used. We consider four lasers at 488nm, 532nm, 640nm and 785nm which occur near the peak absorptions of common fluorescent probes, Alexa488, Alexa532, Alexa647 and Alexa750, respectively. In some cases overlapping of the various fluorescent spectra occur. This effect can be mitigated by checking the emitted signals in individual wavelength channels. But residual amounts of fluorescence and phosphorescence may not be completely taken into account because of the photodetector sensitivity. Using a unique numerical method we developed to calculate both the fluorescence and phosphorescence intensities in a multi-laser and multi-probe case we determine quantitatively the extent of possible false positive signals that may occur. The total intensities of the fluorescent state and phosphorescent state are calculated for a range of laser powers from 5mW to 100mW. Our numerical calculation enables users not only to select the best possible combination of probes, but also correct for any spectral overlap not detected by standard techniques.

8596-31, Session 9

Intracellular delivery of molecular beacons by PMMA nanoparticles and carbon nanotubes for mRNA sensing

Sara Tombelli, Francesco Baldini, Istituto di Fisica Applicata Nello Carrara (Italy); Marco Ballestri, Istituto per la Sintesi Organica e la Fotoreattività (Italy); Sara Carpi, Univ. di Pisa (Italy); Silvestro G. Conticello, Fondazione IRCCS Istituto Nazinoale dei Tumori (Italy); Giambastiani Giuliano, Istituto di Chimica dei Composti OrganoMetallici (Italy); Ambra Giannetti, Istituto di Fisica Applicata Nello Carrara (Italy); Andrea Guerrini, Istituto per la Sintesi Organica e la Fotoreattività (Italy); Raffaella Mercatelli, Istituto dei Sistemi Complessi (Italy); Paola Nieri, Univ. di Pisa (Italy); Franco Quercioli, Istituto Nazionale di Ottica (Italy); Francesco Severi, Fondazione IRCCS Istituto Nazinoale dei Tumori (Italy); Giovanna Sotgiu, Istituto per la Sintesi Organica e la Fotoreattività (Italy); Cosimo Trono, Istituto di Fisica Applicata Nello Carrara (Italy); Giulia Tuci, Istituto di Chmica dei Composit OrangoMetallici (Italy); Greta Varchi, Istituto per la Sintesi Organica e la Fotoreattività (Italy)

Nanomaterials have been explored in many biomedical applications, such as biosensing or molecular imaging, because their properties and functions provide a plethora of advantages for these specific applications. Due to these advantages coupled to the optimum dimensions, the delivery of fluorescent agents or probes to cells and tissues by using NPs or other nanomaterials is currently receiving a growing interest to examine cellular mechanisms without interferences.

We describe here the synthesis, characterization and application of fluorescently labeled carbon nanotubes (CNTs) and cationic core–shell nanoparticles (NPs), made up of a core of polymethylmethacrylate (PMMA), surrounded by a shell bearing cationic groups. These intracellular delivery nanomaterials have been modified with particular fluorescent DNA probes, molecular beacons (MB), for the detection and localization of the mRNA of survivin, a protein member of the inhibitor of apoptosis family, highly expressed in most types of cancer.

NPs and CNTs were modified with –NH2 groups and they were also functionalized, during the synthesis, with fluoresceine or HiLyte Fluor™ 488, for reference purposes. The MB was anchored to their surface via a commercial sulfhydryl-reactive heterobifunctional crosslinker. Survivin MB was characterized by hybridization studies to prove its functionality both free in solution and once immobilized onto NPs and nanotubes.

The functionality and specificity of the MB was also tested in living cells by transfection with a classical lipid agent, Lipofectamine.

8596-32, Session 9

Quantified tomographic macro-micro multi-modal molecular imaging of Ber-Ep4 on cutaneous basal cell carcinoma

Bahar Dasgeb, Memorial Sloan-Kettering Cancer Ctr. (United States); Aleksandr V. Smirnov, Yasaman Ardershirpour, Amir Gandjbakhche, National Institutes of Health (United States); Allan C. Halpern, Memorial Sloan-Kettering Cancer Ctr. (United States); Jay R. Knutson, Darius Mehregan, National Institutes of Health (United States); Milind Rajadhyaksha, Memorial Sloan-Kettering Cancer Ctr. (United States); Dan L. Sackett, National Institutes of Health (United States)

Basal cell carcinoma (BCC) is the most common cancer in humans. Morphologically, BCCs may appear macroscopically and/or microscopically similar to many other skin lesions, which makes differential diagnosis difficult. We are developing an approach for quantified molecular imaging ofBer-EP4, a trans-membrane biomarker for cutaneous BCC, to increase precision and accuracy of diagnosis

We used collagen microspheres (60 micron) as a phantom, on which carcinoma cell lines (BCC, colon, breast), proved to express Ber-EP4Ag by flow-cytometry, were cultured. Melanoma and keratinocyte were selected as -ve control. Ber-EP4+ve and –ve control microspheres were labeled with Alexa-750-Ber-EP4 Antibody and Alexa-750-non-specific Ab separately. Near-infrared macro spectroscopy showed a quantifiable increased in fluorescent signals from Ber-EP4+ve microspheres compared with -ve control. Ber-EP4+ve and -ve phantoms were also imaged with multimodal 2photonTED/1photon confocal microscopy. We detected signals from Alexa-750-Ber-EP4 Ab on cell membranes of Ber-EP4+ve phantoms and lack of signal from –ve control. The negative predictive value was confirmed with backscattered confocal microscopy to show the presence of Ber-EP4–ve cells. In addition, increased signal was detected when 2photon microscopy and 1photon confocal images were co-registered. Ber-EP4+ve and –ve phantoms, incubated with non-specific Ab, lacked fluorescent signals. In conclusion, near-infrared labeled Ber-EP4 Ab can be used as a diagnostic probe to image micro-tumor phantoms of Ber-EP4+ve carcinoma cell lines quantifiably by macro and tomographically my micro optical modalities. As the next step, we will apply this approach to mice models in-vivo.

8597-1, Session 1

Surface enhanced Raman scattering on grating-type patterned nanoporous gold films

Yang Jiao, Judson D. Ryckman, Sharon M. Weiss, Vanderbilt Univ. (United States)

We report an effective and highly reproducible surface enhanced Raman scattering (SERS) substrate based on grating-type patterned nanoporous gold (P-NPG) films, which supports both localized surface plasmon (LSP) and surface plasmon polariton (SPP) modes for SERS enhancement. P-NPG substrates consisting of two dimensional (2D) periodic gratings surrounded by a densified NPG network are fabricated via a straightforward imprinting technique – Direct Imprinting of Porous Substrates (DIPS). Previous SERS studies on bare or modified NPG films have only focused on nanoscale surface roughness and the LSP effect. In our P-NPG substrates, in addition to the LSP effect associated with NPG and densified NPG, the imprinted 2D grating structures with properly chosen grating periods can directly couple the incident light into a SPP mode, which significantly enhances the SERS signal over a large area. By tuning the duty cycle and height of the grating, the SPP resonance as well as the resulting SERS response can be systematically engineered. Our experimental results show that deeper gratings with appropriate grating period and duty cycle lead to the effective activation of a SPP mode which covers both excitation and scattered Raman light. With contributions from both LSP and SPP effects, our P-NPG substrate is demonstrated to provide a uniform enhancement factor of 1.2?10^8(±10%) over a 1mm2 area for detection of benzenethiol.

8597-2, Session 1

Disposable plasmonic plastic SERS sensor

Swe Z. Oo, Martin D. B. Charlton, Univ. of Southampton (United Kingdom); Samuli Siitonen, Ville Knotturi, Nanocomp Oy Ltd. (Finland); David Eustace, Renishaw Diagnostics Ltd. (United Kingdom); Jarkko Tuominen, Rousu Sanna, VTT Technical Research Ctr. of Finland (Finland)

Surface-enhanced Raman scattering (SERS) based sensors are popular for biosensing, chemical identification and homeland security applications because of high sensitivity and rapid label-free identification.

The ‘KlariteTM’ SERS sensor platform consisting of an array of inverted square pyramid with gold nanofilm patterned onto a silicon substrate has over the last decade become the industry standard providing highly reproducible SERS signals.

Last year we reported development of an optimized SERS substrate based on the Klarite design which was demonstrated to provide 786% improvement in sensitivity to a standard Benzenethiol test molecule over standard production Klarite.

In this paper, we report successful transfer of the optimized SERS substrate design from silicon to plastic base platform. Transfer is achieved using roll to roll UV nanoimprint fabrication techniques. The new generation plastic SERS sensors provide the added benefit of cheap low cost mass-manufacture, and easy disposal.

The plastic replicated SERS sensors are shown to provide a similar level of performance as the original silicon based sensors (>10E6 enhancement factor).

8597-3, Session 1

A reliability analysis for molecular diagnostics with multiplexed SERS-coded nanoparticles

Steven Y. Leigh, Madhura Som, Anushree Srivastava, Jonathan T. C. Liu, Stony Brook Univ. (United States)

Surface-enhanced Raman scattering (SERS) nanoparticles have been engineered to generate unique fingerprint spectra and are potentially useful as bright contrast agents in molecular diagnostics. One promising application for biomedical diagnostics and imaging is to functionalize various particle flavors, each emitting a unique spectral signature, to target a large multiplexed panel of protein biomarkers. While SERS particles emit narrow spectral features that allow them to be easily separable under ideal conditions, the presence of competing noise sources and background signals such as detector noise and autofluorescence confounds the reliability of demultiplexing algorithms. Results obtained during time-constrained in vivo imaging experiments may not be reproducible nor accurate. Therefore, our goal is to provide experimentalists with a fitting metric that may be monitored to ensure a desired level of measurement accuracy within a user-defined confidence bound. We have defined a spectral reliability index (SRI), obtained directly from the results of a direct classical least-squares (DCLS) demultiplexing routine, which provides a measure of the reliability of the computed nanoparticle concentration ratios. We present simulations and experiments to demonstrate the validity of this strategy, which can be generalized to a range of instruments and applications involving multiplexed SERS nanoparticles.

8597-4, Session 1

Combined SERS probes and super-resolution imaging for studying molecular interactions

Albert Lee, The Univ. of Texas at Austin (United States)

Molecular interactions govern a myriad of normal and pathologic human processes. Development of methods that will allow us to visualize interactions between biomolecules in live cells will lead to better understanding of the cellular and molecular underpinnings of many devastating diseases such as cancer.

Recently, significant advances have been made in super-resolution optical imaging that allow localization of individual fluorophores with better than 5 nm spatial resolution. However, these methods suffer from irreversible photobleaching and blinking of fluorescent probes that complicates data analyses and limits the possibility of long-term imaging. Also, multiplexing capabilities for imaging multiple interacting biomolecules is severely limited in fluorescent imaging due to broad emission spectra. Emergence of molecular specific probes for surface-enhanced Raman scattering (SERS) can provide multiplexed labeling capabilities that are unmatched by any other labeling techniques. In SERS probes, the Raman scattering from a molecule located close to a plasmonic nanoparticle surface is enhanced by 10^4 – 10^9. This enhancement can be increased by more than an order of magnitude in so-called “hot-spots” at the junction between adjacent nanoparticles. In addition, SERS is excitation-wavelength independent, does not suffer from photo-bleaching or blinking, and has comparable or better signal-to-noise than any fluorescent tags, including quantum dots. Therefore, SERS probes provide an extremely attractive alternative for detection and imaging of molecular interactions.

Here, we will present development of molecular specific SERS probes in combination with super-resolution imaging methodologies to study molecular interactions between growth factor receptors in cell culture models of lung cancer.

8597-5, Session 2

Intracellular SERS probes for distinction of cell phenotypes

Anna Huefner, William Kuan, Roger A. Barker, Sumeet Mahajan, Univ. of Cambridge (United Kingdom)

So far, discriminating closely related cell phenotypes by non-invasive imaging techniques like optical microscopy is impossible both in vitro and in vivo. We employ surface-enhanced Raman spectroscopy (SERS) for cellular imaging to address this problem. Raman scattering is a vibrational spectroscopic technique which gives a molecular fingerprint of detected molecules. Though, Raman scattering is a very weak process, significant enhancement can be achieved by bringing metal nanoparticles into close vicinity of the molecule of interest which is known as SERS. In contrast to conventional spectroscopic methods, SERS is label-free, non-invasive and does not need fluorescent markers for imaging molecules inside cells.

We have used spherical gold nanoparticles as intracellular SERS transducers in neuronal cells (SH-SY5Y). Aggregated nanoparticles inside cells allow for SERS imaging revealing a chemical map of the cell. Data achieved in only a single scan contains information about the intracellular distribution of various biochemical compounds such as lipids and proteins.

Furthermore, we are able to distinguish between progenitor and differentiated neuronal cells using intranuclear SERS spectra. Functionalisation of gold nanoparticles with the nuclear localisation signal peptide sequence [1] was used to target the cell nucleus. As the relative amount of nuclear DNA/ RNA varies with the state of cellular differentiation, SERS spectra from the nucleus allow for distinction between progenitor and differentiated cells. Furthermore, we found that the level of protein increases during differentiation [2]. Thus, targeted SERS nanoparticles provide an appropriate probe for intracellular imaging by preserving the integrity of the biological system and showing many advantageous over conventional spectroscopic techniques.

[1] A. G. Tkachenko, H. Xie, D. Coleman, W. Glomm, J. Ryan, M. F. Anderson, S. Franzen, D. L. Feldheim, Journal of the American Chemical Society 125, 4700-4701, 2003.

[2] A. Huefner and S. Mahajan, NanoScale Feature Article, in preparation.

8597-6, Session 2

Gold nanoparticle dimers For SERS-based tumor detection and therapy

A. Swarnapali De Silva Indrasekara, Laura Fabris, Prabhas V. Moghe, Dominik J. Naczynski, Bryan Paladini, Rutgers, The State Univ. of New Jersey (United States)

The research presented herein is focused on the development of a new biocompatible nanoparticle-based platform that combines the advantages of fluorescence- and surface enhanced Raman scattering (SERS)-based microscopy for tumor detection. In this system, dimeric assemblies of spherical gold nanoparticles (Au NS) were achieved using a small Raman-active dithiolated linker molecule that also acts as a SERS reporter, and are envisioned as the main tool to enable highly localized optical cell imaging. Au NS dimers are also functionalized with specific cancer cell targeting moieties and fluorescent tags that allow the simultaneous cancer cell targeting and imaging.

Combined analysis of U87 glioblastoma cells dosed with as-functionalized Au NS dimers via confocal fluorescence microscopy and SERS spectroscopy demonstrated specific cell targeting and cellular internalization of the SERS-active Au NS dimers. Most importantly, they enabled highly selective SERS-based detection more efficiently than what obtained with fluorescent tags, they remained stable under physiological conditions for a long period of time, and did not undergo enzymatic cleavage upon endocytosis. In addition, the investigation of the potential of Au NS dimers as an agent for efficient photothermal tumor treatments is underway. These results provide a strong evidence for the potential widespread application of this nanoparticle platform for highly sensitive SERS-based biological imaging, setting the basis for their use in photothermal therapy.

8597-7, Session 2

Dynamic SERS imaging with gold nanoparticles transported in a living cell

Katsumasa Fujita, Jun Ando, Nicholas I. Smith, Satoshi Kawata, Osaka Univ. (Japan)

Surface enhanced Raman scattering (SERS) has been used to detect molecules at a low concentration. Although the SERS provided a strong Raman signal from biological samples, the motion of SERS agents, such as gold nano particle, in a living cell causes a strong fluctuation in SERS spectra and makes it difficult to analyze the spectra for extracting useful information from the measurements. In our research, we developed a rapid Raman imaging system which can image dynamic activity of SERS agents and the SERS spectra. Synchronization of EM-CCD imaging frames and laser scanning enables us to obtain SERS image in a few seconds with about 100, 500 and 1000 pixels for x, y and wavenumbers, respectively. By combining dark-field microscopy, the system can also be used to track a single particle moving in a cell and detect SERS spectra from the particle with a temporal resolution of 50 msec. By using the developed microscope systems, we observed the motion of 50 nm gold nanoparticles, taken up into the interior of a macrophage or HeLa cell through an endocytosis, and monitored the molecular finger prints associated cell transportation functions. In particular with tracking system, we achieved molecular map of cellular transport pathways with spatial resolution of ~65 nm, segmented into three types of motion behavior, indicating the correspondence with the cellular functions, such as organelle transportation, lysosomal accumulation and digestion.

8597-8, Session 2

Plasmonic Coupling Interference

No Abstract Available

8597-9, Session 3

Controlling the nanopore fabrciation using high energy electron beam exposure

Seong Soo Choi, Sun Moon Univ. (Korea, Republic of); Myoung Jin Park, Sun Moon Univ (Korea, Republic of); Tokutaro Yamaguchi, Sun Moon Univ. (Korea, Republic of); Namkyoo Park, Seoul National Univ. (Korea, Republic of)

Recently there have been tremendous interests about the dynamical sequence of the fabrication of the solid state nanopore due to the capability of the solid state nanopore as a single molecule sensor. Depending upon the instruments such as transmission electron microscopy (TEM) and field emission scanning electron microscopy(FESEM). Initially, the nanopores with ~ 50 nm diameter on the top of the pyramidal apex were fabricated using conventional Si microfabrication techniques followed by wet isotropic etching of the oxide, metal deposition followed by the Focued ion beam drilling. Under the TEM electron beam exposure, for the aperture diameter greater than 50 nm, no shrinking effect of the nanopore was observed. For the aperture diameter less than 50 nm, the widening and shrinking phenomena were observed. However, for the high scanning electron beam exposure with scan rate of 100 microsecond, the only shrinking phenomena were observed. We do believe these phenomena as liquid phase transition for TEM electron beam and adiabatic solid state phase transition for high scanning FESEM. Due to very high energy input from the high scan rate, the energy spike into the electron penetration area will be delivered without enough escape time to surrounding area. Then, the

solid phase surface modification would occur. In addition, the thickness of the nanomembrane was measured with calibrating the electron counts on the detector on the TEM instruments. This will be inportant for understaning the liquid phase nanopore formation.

8597-10, Session 3

Plasmonic properties of weakly interacting silver nanocubes on high refrective index substrates

Anatoli I. Ianoul, Adam Bottomley, Daniel Prezgot, Alyssa Staff, Carleton Univ. (Canada)

In the present work we investigated the refractive index sensitivity (RIS), surface enhancement of the Raman signal (SERS), fluorescence quenching, and photocatalytic activity for monolayers of weakly interacting monodisperse silver nanocubes deposited on thin silicon film. We demonstrated that such properties can be qualitatively modified in a very well controlled manner if the supporting silicon film thickness is varied. The fine tunability results from the strong dependence of the nanocube plasmonic modes on the refractive index of the supporting film. For example, the dipolar (D) plasmon mode can be red shifted by more than 200 nm when the silicon film thickness is increased from zero to 40 nm, whereas the quadrupolar plasmon mode remains unchanged. The silicon supported nanocubes demonstrated a significant improvement of RIS via the Q mode with a figure of merit greater than 6.5. The RIS was found to be sensitive to the silicon film thickness. We also observed an order of magnitude enhancement of the SERS signal due to the stronger electric field created by the D mode red shifted to coincide with the Raman label electronic transition. Such substrates also showed ~10 times decrease in rhodamine 6G fluorescence as well as the rates of amorphous carbon formation suggesting the presence of additional non-radiative de- excitation pathways for the silicon supported nanocubes. The study proposes a new way to design and engineer plasmonic nanostructures.

8597-11, Session 3

Optical properties of strongly interacting supported silver nanocube monolayers

Daniel Prezgot, Anatoli I. Ianoul, Carleton Univ. (Canada)

Plasmonic properties of monolayers of strongly interacting silver nanocubes with controlled interparticle spacing are investigated. Uniform monolayers with controlled particle densities are made using the Langmuir-Blodgett technique with passive phosopholipid spacers, such as dioleoyl phosphatidylcholine (DOPC). Both extinction intensity and wavelength of dipole-dipole coupling modes are tuned via particle spacing. The refractive indices of the substrates are used to tune dipolar and interparticle coupling modes via deposition onto thin films of silicon (0 - 25nm). By varying silicon film thickness it is possible to shift and control peak widths for both the dipole and interparticle dipole-dipole coupling modes. Control of plasmon shifts and interparticle gap size is applied towards the optimization of SERS substrates. SERS substrates using a Rhodamine B or Rhodamine 6G label are tuned at different excitation wavelengths which are in resonance with either the plasmon dipole, fluorescent dye, or interparticle coupling. Substrates display reproducible enhancement across multiple sites. Reduced photodecomposition of the Raman active dye is also noted on silicon thin film substrates. This work presents methodology to design and optimize uniform silver nanocube SERS substrates through tuning of plasmon shifts and particle spacing.

8597-12, Session 3

A plasmonics nanoparticle super-resolution lens

Hu Cang, The Salk Institute (United States); Yuan Wang, Xiang Zhang, Univ. of California, Berkeley (United States)

The resolution of a lens is limited to about half the wavelength of light. This resolution reflects the drawback of current optic designs, which were pioneered by the French mathematician Fermat. Essentially unchanged for hundreds of years, Fermat's optic design method has failed to capture super-resolution, sub-wavelength scale information. As biology has entered a molecular era, this resolution is becoming increasingly inadequate to researchers' needs. The demand now is for a lens with nanometer-scale resolution. We propose a novel method that can extend Fermat's theory down to the nanoscale. By inducing a slowly varying surface plasmon, we can 'reduce' the wavelength of light in a slow and gradual manner. We show that if the variation is slow enough, Fermat's theory can be pushed beyond the limit of the wavelength. To demonstrate this new method, we demonstrate a few designs using single nanoparticles to make a super-resolution lens with a resolution of 10s of nanometers. Unlike near-field optical scanning microscopy (NSOM), which requires a raster scanning of an object to form an image, this new type of super-lens doesn't require scanning; rather, it can form image with a simple camera in the same way as a normal lens, but with much improved optical resolution.

8597-13, Session 3

Single LSPR particle sensor array för single molecule biosensing

Si Chen, Mikael Käll, Chalmers Univ. of Technology (Sweden)

Sensitive biosensors are essential in early and accurate diagnostics. The ultrasensitive biosensor should have a detection limit of a single molecule. Localized surface plasmon resonance (LSPR) particles which are only sensitive towards the refractive index change around the nanoparticles provide an excellent platform for single molecule sensing due to its small sensing volume that are comparable to the sizes of biomolecules. We have utilized single localized surface plasmon particle arrays as the nanosensors to combine with an enzymatic precipitation reaction in a similar fashion as in ELISA methods to reach single molecule detection limit. The enzyme that binds to the particle is capable of producing a precipitate that is larger than the protein itself which greatly increases the peak shift from a single particle. In combination of the enzymatic enhancement, we also used spectra imaging technique to extract the spectra and peak shifts of up to a thousand of single LSPR particle simultaneously which increases accuracy and dynamic range of the sensor platform. This could really pave the road to a massive parallelization of single particle sensors which was already predicted at the birth of LSPR sensors.

8597-14, Session 4

Monolithic porous gold nanostructures as surface-enhanced Raman spectroscopy substrates for molecular and biosensing

Wei-Chuan Shih, Univ. of Houston (United States)

Surface-enhanced Raman spectroscopy (SERS) has been widely used for high-sensitivity molecular detection and identification. When a molecule of interest is near the nanostructured surface of a noble metal such as gold or silver, the localized surface plasmon resonance (LSPR) effect can boost the Raman scattering by many orders of magnitude. Because the LSPR is a near-field phenomenon and decays rapidly with increased separation distance between the molecule and the nanostructure, the SERS signal primarily arises from the molecules residing within a few

nanometers of the nanostructured surface. Therefore, it is advantageous for a SERS substrate to have a large surface-to-volume ratio from the standpoint of optical sampling efficiency. In this paper, we show that monolithic porous gold nanostructures such as nanofilms and nanodisks can be effective SERS substrates with large surface area. The average enhancement factor of the nanodisk and nanofilm substrates have been determined using benzenethiol self-assembled monolayers to be ~70 million and 0.5 million, respectively. Variability on the order of 40% has been observed by large area SERS mapping. A single nanodisk coated with benzenethiol self-assembled monolayer (~10 attmoles) can provide SERS spectrum with a signal-to-noise ratio ~400, resulting in an estimated detection limit in the range of zeptomoles. We have applied these substrates to the label-free detection of DNA molecules and their hybridization.

8597-15, Session 4

Biosensor based on degree of coherence of paired surface plasma waves

Chien Chou, Chang Gung Univ. (Taiwan); Chien-Wa Ho, National United Univ. (Taiwan); Sheng-Yi Chang, Ming Chi Univ. of Technology (Taiwan); Nai-Chuan Chen, Ying-Feng Chang, Chang Gung Univ. (Taiwan); Li-Chen Su, National Central Univ. (Taiwan)

A novel 'degree of coherence paired surface plasma wave biosensor' (DOC-PSPWB) is proposed wherein the principle of detection involves the degree of coherence of highly correlated surface plasma waves when these are excited on a metal/dielectric interface within the DOC-PSPWB. Using the sensor, the concentration of total PSA (t-PSA) in a phosphate-buffered saline solution was measured, and a detection limit of 0.015pg/mL was determined experimentally. Finally, the dynamic range of the DOC-PSPWB when used on samples with ultralow molecular concentrations is discussed.

8597-16, Session 4

Real time monitoring in-vivo micro-environment through the wound heal mechanism

Jack Yan, AnnA I2P (Canada)

One of the In-vivo system's challenge is real time display the sensing information. Usually Ultrasound, CT, MRI, PET are used to get the internal information, this thesis proposed another approach to address the display challenge. Special nano-particles are in-taken or injected to living subject (usually into blood circulation) to sense and collect psychological information when the active particles pass through the tissues of interest. Using the wound healing mechanism, these activated particles (Information collected) can be drifted out to the wound area and adhibited close to the skin, then skin can show different colour if the activated particles are concentrated enough in the specific area to create a skin screen. The skin screen can display the blood status, internal organ's temperature, pressure depending the nano-particles' function and their pathway. This approach can also be used to display in-body video if the particles are sensitive and selective enough. In the future, the skin screen can be bio-computer's monitor.

The wound healing in an animal model normally divides in four phase: Hemostasis, Inflammation, Proliferation and Maturation. Hemostasis phase is to form a stable clot sealing the damaged vessel. Inflammation phase causes the blood vessels to become leaky releasing plasma and PMN's (polymorphonucleocytes) into the surrounding tissue and provide the first line of defense against infection. Proliferation phase involves replacement of dermal tissues and sometimes subdermal tissues in deeper wounds as well as contraction of the wound.Maturation phase remodels the dermal tissues mainly by fibroblast to produce greater tensile strength. The skin screen wound will be carefully controlled to be triggered at dermis layer.

8597-17, Session 4

An integrated platform for biomolecule interaction analysis

Pei-I Tsai, National Taiwan Univ. (Taiwan)

We integrated surface plasmon resonance (SPR) and an ellipsometry technique to a biosensor chip platform to measure a biomolecular interaction mechanism. A conductive ITO (indium-tin-oxide) film was introduced to the bio-sensor platform chip to expand the dynamic range and improve the measurement accuracy. The thickness of the conductive film and the suitable voltage constants were identified to enhance performance. A circularly polarized ellipsometry configuration was introduced onto the newly developed platform to measure the label-free interactions of recombinant human C-reactive protein (CRP) with immobilized biomolecule target monoclonal human CRP antibody at various concentrations. CRP was chosen as it is a cardiovascular risk biomarker, as well as an acute phase reactant and a specific prognostic indicator after inflammation. We found that the sensitivity of a phase-interrogation SPR is predominantly dependent on optimizing the incidence angle of the samples. The effect of the ITO layer effective index change under DC and AC effects as well as the optimal modulation associated with a testing was verified experimentally. The experimental data shows that the modulated dynamic range for phase detection was 10E-2 RIU based on current effect, and was 10E-4 RIU based on potential effect; a 0.55 (°/RIU) measurement was found by angular-interrogation. Our results show that performance of our newly developed metrology platform possesses higher sensitivity and less dynamic range when compared to a traditional full-field measurement system. In addition, our new metrology platform can detect real-time changes in both the phase-interrogation and the intensity modes of SPR.

8597-18, Session 4

Aptamer-based surface plasmon resonance sensing of glycated human blood proteins

Nathan Reaver, Rui Zheng, Dong-Shik Kim, Brent D. Cameron, The Univ. of Toledo (United States)

The concentration ratio of glycated to non-glycated forms of various blood proteins can be used as a diagnostic measure in diabetes to determine a history of glycemic compliance. Depending on a protein's half-life in blood, compliance can be assessed from a few days to several months in the past which can then be used to provide additional therapeutic guidance. Current glycated protein detection methods are limited in their ability to measure multiple proteins and are susceptible to interference from other blood pathologies. In this study, we developed a series of DNA aptamer-based Surface Plasmon Resonance (SPR) sensors to assess specific blood proteins which include both hemoglobin and albumin. The aptamers were developed by way of a modified Systematic Evolution of Ligands by Exponential Enrichment (SELEX) process which selects DNA sequences that have a high binding affinity to a specific protein. Polymerase Chain Reaction (PCR) is then used to amplify the sequences and the process is repeated until an acceptable degree of specificity is achieved. The resulting DNA products are then sequenced and the aptamers are synthesized. This process was performed for both glycated and non-glycated forms of the blood proteins. The aptamers are then immobilized as biomolecular recognition units on the plasmonic surfaces. The developed sensors were evaluated using both single and confounding blood protein samples and current results demonstrate both a high degree sensitivity and selectivity. This technology has the potential to deliver low-cost and immediate glycemic compliance assessment in either a clinical or home setting.

8597-19, Session 4

Nano-imprint-based on substrate fabrication of bio-conjugated Au nanoring solution for biomedical applications

Hung-Yu Tseng, Wei-Fan Chen, Yean-Woei Kiang, Chih-Chung Yang, National Taiwan Univ. (Taiwan)

We show the preparation of Au nanoring (NRI) solutions based a novel on-substrate technique and demonstrate their localized surface plasmon (LSP) characteristics. Au NRIs are fabricated first on a nano-imprint polymer stamp and then transferred into water solution. This approach shows its advantages in the process of bio-conjugation. The conventional bio-conjugation procedures of Au nanoparticles (NPs) in solution include several steps of centrifuge and sonication during the reaction process to prevent aggregation. Such steps will lead to NP loss and reduce the yield. If the bio-conjugation procedures can be undertaken when Au NPs are still attached to a substrate, those steps are not needed. In this situation, we can simply immerse the sample substrate in the reaction solution and then rinse it in water to remove the residues. The procedures of Au NRI fabrication based on the nano-imprint technique include the following. First, a Si mold is used to form a pillar array on a polymer stamp. Then, oxygen plasma is applied to reduce the size and shape of the pillars. After Au deposition and secondary sputtering with reactive ion etching to form NRIs, oxygen plasma is applied again to remove polymer inside the NRIs and form a pillar structure under an NRI. Then, the bio-conjugation processes are applied to the sample stamp. After sonication, the Au NRIs are transferred into water solution. We will also show the control of the LSP resonance wavelength of the NRI solution by adjusting the NRI geometry through the aforementioned etching processes.

8597-20, Session 5

Plasmon-enhanced emission from single fluorescent proteins

Jessica E. Donehue, Esther Wertz, Courtney Taliscka, Julie S. Biteen, Univ. of Michigan (United States)

Single-molecule fluorescence (SMF) imaging is a powerful tool for noninvasive imaging of biological systems and structures with nanometer-scale resolution. This super-resolution technique localizes isolated fluorophores with accuracy far better than the standard diffraction limit of light. Indeed, this accuracy is limited only by the number of detected photons, and in vitro implementations of SMF have achieved 1.5-nm localization accuracies. Unfortunately, the resolution of SMF imaging in cells is generally limited to 20-40 nm, in part due to the limited brightness of fluorescent proteins (FPs), the genetically encodable labels widely used for bio-imaging. We therefore seek to improve FP photophysics with plasmonic substrates, as fluorophores coupled to resonantly excited plasmonic nanoparticles can demonstrate enhanced optical properties, such as increased brightness and photostability.

In this work, we use evaporated gold nanoparticle films and colloidal gold nanorod monolayers as substrates for plasmon-enhanced imaging of two FPs, mCherry and YFP. Through single-molecule epifluorescence microscopy, we show enhancement of single FP emission in the presence of both plasmonic substrates. The gold-coupled FPs demonstrate emission up to four times brighter and seven times longer lived, yielding order of magnitude enhancements in total photons detected. Ultimately, this results in increased localization accuracy for single-molecule imaging. Furthermore, we introduce preliminary results for enhancement of mCherry-labeled TcpP membrane proteins inside live Vibrio cholerae cells coupled to gold substrates. Our work indicates that plasmonic substrates are uniquely advantageous for super-resolution imaging, and that plasmon-enhanced imaging is a promising technique for improving live cell single-molecule microscopy.

8597-21, Session 5

Enhancing fluorescence properties with microhole array substrates

Hugo-Pierre Poirier Richard, Jean-François Masson, Univ. de Montréal (Canada)

A possible metal enhanced fluorescence (MEF) phenomenon on gold microhole arrays was investigated in propagating SPR and in fluorescence microscopy to achieve coupling of both techniques in a single portable instrument. This work relies on gold microhole arrays that are ultra-sensitive SPR substrates for bioanalysis. These new plasmonic materials exhibit a greater sensitivity towards refractive index changes compared to classic SPR substrates due to coupling of a localized and propagating SP modes supported by microhole arrays. The fluorescence signal on the microhole arrays of a rhodamine B excited at 532 nm was collected with a 100x (0.9 NA) Nikon LU plan fluor microscope objective and a scanning stage. Thereby, the localization of the enhanced fluorescence was assessed on the substrates. Combination of SPR and fluorescence spectroscopy aims to improve the sensitivity and minimize the impact of non-specific binding of a biological assay for prostate specific antibody (PSA) quantification. Together, the fluorescence and SPR spectroscopies will improve the confidence for the results obtained by greatly reducing the false positives rate. It is a crucial aspect in the development of biomedical tools of greater sensitivity for the detection of biomarkers with sandwich assays.

8597-22, Session 5

Nanometric axial imaging with time-resolved surface plasmon-mediated fluorescence microscopy

Olivier Loison, Ecole Supérieure de Physique et de Chimie Industrielles de la Ville de Paris (France) and Univ. Paris 7-Denis Diderot (France); Viviane Devauges, Institut des Sciences Moléculaires d'Orsay (France); Emmanuel Fort, Ecole Supérieure de Physique et de Chimie Industrielles (France) and Univ. Paris 7-Denis Diderot (France); Sandrine Lévêque-Fort, Institut des Sciences Moléculaires d'Orsay (France) and CNRS (France)

Surface Plasmon-Mediated Fluorescence Microscopy (SPMFM) is a new imaging technique which takes the advantage of surface plasmon (SP) properties of a metallic thin-film to selectively excite and detect fluorophores in a restricted specimen region immediately adjacent to the metallic/sample interface. This technique is particularly suitable for cell membrane imaging. SP mediated-excitation and emission provide many advantages over other competing techniques. When compared to standard TIRF microscopy, the molecular detection efficiency is enhanced and the confinement is increased. Besides, the additional distance dependant emission filter resulting from the near-field coupling of the fluorophore emission to the SP provides an enhanced signal to noise ratio. In cell imaging, it limits the background noise increased resulting from the scattering effect of the excitation light by the sample.

The presence of the metallic surface in the vicinity of the fluorophores induces significant modifications of the fluorescence lifetime. The coupling to the metallic surface provides additional relaxation processes which decreases the fluorescence lifetime by several order of magnitude. These variations depend strongly on the fluorophore/metal distance d and on the molecular orientation of the emission dipole in the range $d<200$ nm.

We will show that it is possible to retrieve nanometric axial positioning of the fluorophores from lifetime measurements on biological samples.

8597-23, Session 5

DNA detection using a plasmon-enhanced nanoparticle architecture: synthesis and characterization

Olivier Ratelle, Univ. Laval (Canada); Danny Brouard, Univ. Laval (Canada) and Héma-Québec (Canada); Félix-Antoine Lavoie, Denis Boudreau, Univ. Laval (Canada)

The development of fluorescence-based DNA detection methods is considered a hot topic in numerous active fields such as the diagnosis of infectious diseases, identification of genomic mutations (SNPs) and forensic analyses, where different strategies are being developed and implemented. Unfortunately, in many cases, the number of targets available is very low and one needs to rely on enzymatic amplification (PCR) to raise the analyte concentration above the detection threshold. To circumvent PCR, alternative methods based on the amplification of the analytical signal generated upon the transduction of a recognition event are being investigated.

In this context, we are developing a plasmon-enhanced DNA biosensor based on an optical polymeric transducer complexed with probe-grafted core-shell silver-silica nanoparticles. Hybridization of a target sequence at the surface of the nanoparticles allows the excitation light to be coupled to acceptor fluorophores located in the outer silica layer through Resonant Energy Transfer (RET). This plasmonic architecture enhances the luminosity and photostability of fluorophores, leading to increased detectability.

The synthesis and characterization of the fluorescent nanoparticles by transmission electron microscopy, time-resolved fluorescence and optical microscopy will be shown. Moreover, the results obtained for low level DNA detection using flow cytometry will be presented.

8597-24, Session 5

A comprehensive study on metallic nano-hole arrays with a surface plasmon energy matching property

Mohamadreza Najiminaini, Fartash Vasefi, The Univ. of Western Ontario (Canada); Bozena Kaminska, Simon Fraser Univ. (Canada); Jeffrey J. L. Carson, The Univ. of Western Ontario (Canada)

An array of periodic holes perforated in an opaque metal film has shown a unique optical transmission property [the so-called extraordinary optical transmission (EOT)], which is not predicted by standard aperture theory. The EOT phenomenon results from an interaction of light with the surface plasmon (SP), where oscillations of free electrons occur at an interface between metal and dielectric materials. The EOT properties of a nano-hole array (NHA) structure depend greatly on the dielectric materials on the top and the bottom of the metal film. For instance, a change in a dielectric material on the top or bottom of a NHA structure results in a shift of the spectral position of the EOT to shorter or longer wavelengths. The resonance shift has been employed in Surface Plasmon Resonance (SPR) sensing of various bio-molecules and chemicals.

Recently, a NHA structure with a dynamic SP energy matching property demonstrated a higher SPR sensitivity compared to a conventional NHA. In this work, we present more comprehensive numerical and experimental studies on the performance of a NHA structure with a dynamic SP energy matching property as a bulk-SPR sensor. We fabricated NHAs with different cavity depths and periodicities using electron beam lithography (EBL). We then characterized the optical transmission of each structure during a bulk-SPR sensing experiment where various refractive index liquids were deposited on to the structure. The experimental results were analyzed and compared to the numerical results. Both sets of results demonstrated higher SPR sensitivity for structures with the dynamic SP energy matching property.

8597-25, Session 5

Wide-field interferometric phase imaging of plasmonic nanoparticles at the subcellular level

Nir A. Turko, Ania Peled, Natan T. Shaked, Tel Aviv Univ. (Israel)

We present a new wide-field quantitative photothermal (PT) imaging method of gold nanoparticles

(AuNPs) in live cells. To obtain this goal, we built a reflection-mode wide field interferometric phase microscope and modified it for the excitation of plasmonic resonance in AuNPs, while recording the resulting phase signatures. On the first stage, the AuNPs were conjugated to a glass coverslip and excited with a laser at a wavelength corresponding to their absorption spectral peak. We then acquired an image sequence of the sample phase profile in time and analyzed the entire field of view using a Fourier analysis, creating a map of the locations of the AuNPs without the need for lateral scanning.

We obtained a strong PT signal around the AuNPs central locations, where the signal is exponentially dependent on the distance from the center of the AuNPs, enabling identification of their locations.

Moreover, the PT signals showed a linear relation to the illumination intensity, distinguishing the AuNPs from the background noise and the out-of-focus particles. On the next stage, AuNPs were conjugated to breast cancer cells using EGFR antibodies. We recorded a PT signal from the cell membrane, which was not present on non-cancerous cells of the control group. To the best of our knowledge, we are the first to record wide-field PT signals at the subcellular level without the need of either lateral scanning or integrating total-internal-reflection prisms to the system.

8597-26, Session 6

Plasmon saturation induced super-resolution imaging

Hsuan Lee, Tung-Yu Su, National Taiwan Univ. (Taiwan); Yasuo Yonemaru, Masahito Yamanaka, Osaka Univ. (Japan); Ko-Fan Huang, National Taiwan Univ. (Taiwan); Satoshi Kawata, Katsumasa Fujita, Osaka Univ. (Japan); Shi-Wei Chu, National Taiwan Univ. (Taiwan) and Molecular Imaging Ctr. (Taiwan)

Traditionally, far-field optical imaging is limited by diffraction of light; hence the best optical resolution can only reach about half of light wavelength. During the last decade, such diffraction barrier was successfully overcome by manipulating the on/off switching of fluorophores, or by saturation of fluorescence emission, resulting in resolution below 100 nm. However, fluorescence exhibits intrinsic photobleaching issue. The on/off switching techniques require repeated excitation of a single fluorophore while the saturation techniques need strong incident power, both leading to faster and easier bleaching of labeling. Therefore, it will be more than desirable to develop super-resolution imaging modality based on an alternative contrast agent without bleaching, such as scattering. Here, we demonstrate novel super-resolution imaging based on scattering saturation of particles.

One of the most appealing candidates is the extraordinarily strong scattering from structures of surface plasmon resonance (SPR), which has attracted extensive interests due to its wide applications.

To our knowledge, neither saturation nor switching of scattering from SPR structures has been reported, but there are plenty of reports on saturable absorption of plasmonic nanoparticles embedded in dielectric matrix. Since scattering and absorption are related to the real and imaginary parts of electric susceptibility, respectively, and the two parts are closely linked via Kramers-Kronig relation, we set out to examine saturable scattering in a single gold nanoparticle. As a result, the saturation of scattering in a single gold nanoparticle (GNP) was observed for the first time. With spectral studies, we have confirmed the saturation is directly linked to SPR effect. With the aid of saturation excitation

microscopy (SAX), plus field concentration due to nonlinear plasmon resonance, we have achieved optical resolution below 80-nm based on scattering. Our study will open up a completely new paradigm for super-resolution microscopy.

8597-27, Session 6

Molecularly defined plasmonic engineering to visualize individual binding events by eye

Alasdair W. Clark, Jonathan M. Cooper, Univ. of Glasgow (United Kingdom)

We report a new plasmonic biosensing technique allowing visualization of single biomolecular binding events via engineered colorimetry. Combining direct-write fabrication with molecular nanopatterning, we use molecular interaction to position individual Ag nanoparticles around single, pre-fabricated metallic nanostructures, changing the plasmonic resonance of the structure and effecting a visible color-shift in plasmonic scattering.

Plasmonic colorimetry relies on electron coupling of discrete nanostructures, brought into proximity by molecular binding, in order to produce a visible color-shift. These techniques traditionally rely on aggregation of nanoparticle suspensions, or blanket-binding of nanoparticles onto pre-fabricated surface structures. Although molecular lithography has seen great progress recently, significant challenges remain in controlling the size and placement of molecular nanopatterns in order to create complex surface structures. Here, we bridge the gap between the versatility of direct-write nanolithography, and the resolution of molecular self-assembly, combining both techniques to create a novel biosensor.

Our engineered approach allows us to dictate, with protein-scale resolution (~5 nm), the patterning of biomolecules around individual nanostructures (using two electron-beam-lithography processes). In doing so, we create distinctive color-shifts, corresponding to individual nanoparticle binding events, which can be observed by simple, low-magnification dark-field-microscopy of single nanostructures, or, in the case of denser arrays, by the naked eye.

By fabricating complex nano-geometries with a variety of independent plasmonic modes, different color-shifts can be triggered dependent on nanoparticle binding position. This enables multiplexed sensing, to report molecular binding at sensitivities far exceeding that of other colorimetric methods, and without the need for spectrometry or electron-microscopy.

8597-28, Session 6

Nanoplasmonic co-localization for highly sensitive surface plasmon resonance detection of molecular interactions

Youngjin Oh, Yonghwi Kim, Wonju Lee, Donghyun Kim, Yonsei Univ. (Korea, Republic of)

Surface plasmon resonance (SPR) biosensors have been used extensively for detecting bio-molecular interactions because it allows quantitative real-time monitoring. However, traditional thin film-based SPR detection suffers from moderate limit of detection. For this reason, many studies have been attempted for the sensitivity enhancement. Recently, SP localization based on nanostructures has been successfully employed for modulation of surface near-fields whereby detection sensitivity of SPR biosensors can be improved. In this research, we study further sensitivity enhancement by co-localizing specific target distribution with localized near-fields using various two-dimensional sub-wavelength nanostructures. Experimentally, we performed oblique evaporation of ITO to create shadow areas in which target molecules can be localized. Localized near-fields (hot spots) can be created near the shadow area to enable co-localization of hot spots and target molecules. For numerical evaluation, surface near-field distribution was calculated using rigorous coupled-wave analysis. The concept was tested by measuring DNA hybridization and biotin/streptavidin binding as model bio-molecular interactions using a custom-built angle scanning SPR set-up. Nanopatterns of various shapes such as nanogratings, nanoholes, nanopillars, and nanotriangles have been used for the measurement with various pattern concentration. Result shows that nanotriangles produced the largest optical signatures and that co-localized detection improves the detection sensitivity by at least two orders of magnitude. From the experimental data, it is suggested that detection of less than 104 ssDNA molecules may be feasible with this approach. These results are expected to open up a new way of bio-molecular detection in SPR sensing.

8597-29, Session 6

ROS-mediated plasmonic killing of malignant cells using femtosecond laser pulses

Limor Minai, Daniella Yeheskely-Hayon, Lior Golan, Dvir Yelin, Technion-Israel Institute of Technology (Israel)

Ultrashort laser pulses irradiating malignant cells targeted by gold nanoparticles have been shown effective in causing high cell damage that leads to cell death. While the exact mechanism causing cell death is often unknown, membrane or internal organelle rupture due to the acoustic shock wave emanating from the particles is currently the most common hypothesis. In this study, we show that Burkitt lymphoma (BJAB) and epithelial breast cancer (MDA 468) cells targeted by gold nanospheres and irradiated by resonant femtosecond pulses exhibit elevated concentrations of reactive oxygen species (ROS). While free radicals are essential for various cellular processes and are normally found at low concentrations in living cells, at sufficiently high concentrations ROS are known to effectively trigger cellular death. ROS level was found to increase in correlation with the increasing number of irradiating pulses; the percentage of cells with high levels of ROS increased from 1.8% for two pulses up to 26.7% following six pulses. Higher number of pulses caused immediate apparent damage to the cells (i.e. necrosis or cells fusion), resulting with a drop in the total ROS level within the cells. We will discuss the possible mechanisms that could lead to ROS production and compare our technique to other methods in which cellular damage is mediated by ROS, including chemotherapy, radiation therapy, and photodynamic therapy.

8597-30, Session 7

Plasmonic nanosensors in the detection and remedy of cancerous cells

Saikat Das, Univ. of Eastern Finland (Finland)

The aim of this study is to develop some nanosensors based on the phenomenon of surface plasmon resonance, which can act not only as sensors but also can be used for the detection and remedy of cancer. So, the target of our study can be divided into two parts.

In the first part, we will discuss about the development of these plasmonic nanosensors. Now as discussed in the introduction part, we know that the phenomenon of surface plasmon resonance can take place at metallic interfaces. So, we selected an interface, one side of which is a metal and the other a dielectric. In our study, we took optical fibers as the base medium or platform of the nanosensors. The reason behind the selection of optical fibers as the base medium of nanosensors is that we want to use the same nanosensors for treatment of cancer and that the technology of fiber optics will serve the purpose of transfer and guidance of conglomerate nanobubble based cancer treatment as well as diminish the adverse effects of optical scattering on tissues in our body (our main strategy to be discussed in the second part). Then we coated these optical fibers with a thin film of silver layer (metal) of the order of nanometers. The metal layer was then surrounded by a dielectric layer. This dielectric actually acts as the sensing medium (a change in refractive index of dielectric layer immediately brings about a change in surface plasmon resonance angle) in these nanosensors. These nanosensors can have large number of sensing applications like detection of food quality,

environmental monitoring etc.

Now, we wanted to add a new feather to the performance of these nanosensors by making these same nanosensors usable for detection and healing of cancer, which can be categorized as the second part of the target of our study. For this, we now harnessed the metallic layer in these nanosensors to form nanorods, nanospheres and nanoshells. Then these nanoparticles were assorted in batches to form nanoparticle clusters, which were optically activated by laser pulses to form vapour nanobubbles.

Then we introduced a completely new strategy, the conglomerate technique, which exploits simultaneous merged result of many surface plasmon resonances in one particular nanoparticle cluster, to increase the lifespan and to decrease the energy of each laser pulse beyond the threshold energy level for germination of the nanobubbles. These conglomerate nanobubbles will actually play a crucial role in our way of treatment of cancer.

8597-31, Session 7

Controlled release of rituximab from gold nanoparticles for phototherapy of malignant cells

Daniella Yeheskely-Hayon, Gili Bisker, Limor Minai, Dvir Yelin, Technion-Israel Institute of Technology (Israel)

Releasing drug molecules at their targets with high spatial and temporal accuracy could aid numerous clinical applications which require low systemic damage and low side effects. Nano-carriers of drugs are an attractive solution for such task, allowing specific accumulation in tumors and gradual release of their payload. The unique optical and chemical properties of gold nanoparticles make them excellent potential candidates for carrying and releasing drugs under external optical signals.

In this study, we utilize gold nanospheres conjugated to Rituximab, an anti-CD20 monoclonal antibody-based drug, for carrying and releasing the drug upon irradiation of specifically tailored femtosecond laser pulses at the plasmonic wavelength. We demonstrate that the released anti-CD20 molecules retain their functionality and ability of triggering complement-dependent cytotoxicity (CDC) on malignant human B cells followed by incubation with active serum containing CDC-related proteins. This effect comes in addition to cell necrosis caused by the plasmonic nanometric shock waves emanating from the nanospheres and rupturing the plasma membranes. The dual roles of both the nanospheres, as drug carriers and phototherapy mediators, and of the antibodies, as targeting agents and activators of the CDC mechanism, is quantified by measuring the amount and functionality of the released antibody, and demonstrated by studying light-induced necrosis in cells targeted by the nano-conjugates. The main advantages of the presented technique include high spatial and temporal resolutions in the drug release, low toxicity, and high repeatability and consistency due to the morphological stability of the nanospheres.

8597-32, Session 7

Enhancing antimicrobial action of PDT in Candida albicans cultures by silver-pectin nanoparticles

Luciana De Melo, Flávio Bonfim, Adriana de Souza, José Filho, Armando Marsden, Renato de Araujo, Univ. Federal de Pernambuco (Brazil)

Photodynamic therapy (PDT) is a medical technique which explores photosensitizing drugs and light to induce selective damage on the target tissue. Photosensitizer molecules, as riboflavin, can activate singlet oxygen generation through a triplet interaction with ground-state molecular oxygen. In particular the riboflavin photosensitizer molecule is a water solved vitamin and is also known as B2 vitamin. In PDT, an inefficient production of singlet oxygen and free radicals, to react with biological targets, can limit the use of the technique. Recently a new phenomenon named metal enhanced singlet oxygen generation was demonstrated on a silver island film. Here we explore localized plasmon resonance on the interaction of silver nanoparticles, in a solution base platform, and riblofavin to enhance antimicrobial action on Candida albicans culture. Silver nanospheres, with 13 nm diameter, enclosed by a pectin layer were synthesized and it interaction with riboflavin molecule was analyzed. Pectin, a complex carbohydrate found in plants primary cell walls, was used to improve metal enhanced singlet oxygen generation of the colloid. The photochemical process in the microorganism culture were induced by blue LEDs (415 nm) in irradiation chamber. We observed a 300% enhancement of the Candida albicans elimination on photodynamic therapy by exploring localized plasmon effect.

8597-33, Session 7

Selective cell copuling and fusion using gold nanoparticles and femtosecond pulses

Daniella Yeheskely-Hayon, Limor Minai, Lior Golan, Eldad J. Dann, Dvir Yelin, Technion-Israel Institute of Technology (Israel)

Stimulating the immune system effector cells to mediate cell lysis is a promising alternative to traditional therapies that directly target invading cells using chemical agents; currently, the main approach for coupling between immune system and specific cells uses various genetic engineering methods for generating bispecific molecules. In this study, we present an alternative approach for enhancing the association between tumor cells and dendritic cells, a key component of the immune system, by using dual antibody-coated gold nanospheres designed to simultaneously bind to both target cells. We show that heterogeneous cell cultures incubated with the dual-coated nanoparticles exhibited high efficiency coupling between tumor and dendritic cells. But, attachment of a tumor and a dendritic cell would not, by itself, be sufficient for the stimulation of the immune system; cell fusion must take place so that the tumor-related antigen will be presented by the dendritic cells. To initiate fusion, the entire cell culture was irradiated by a short sequence of high intensity femtosecond pulses whose wavelength was tuned to the plasmonic resonance of the particles, causing nano-scale ruptures of the cells' plasma membranes and promoting fusion between neighboring cells. The dual role of the bispecific gold nanoparticles, both as conjugating agents and as fusion mediators would offer a potential bypass of immune system inhibition employed by cancer cells, and would improve the treatment of various cancers and other related diseases. The presentation will describe the fabrication and characterization of the dual-coated nanoparticles, and discuss the advantages and potential applications of this approach.

8597-34, Session 7

Combined SERS sensing and photodymanic treatment using gold nanostars

Hsiangkuo Yuan, Tuan Vo-Dinh, Duke Univ. (United States)

No Abstract Available

8597-35, Session 8

Planar chiral metamaterials for biosensing applications

Sangeeta Murugkar, Israel De Leon, Matthew Horton, Hammam Qassim, Jonathan Leach, Robert W. Boyd, Univ. of Ottawa (Canada)

There has been a considerable effort recently in the development of planar chiral metamaterials. Owing to the lack of inversion symmetry, these materials have been shown to display interesting physical properties such as negative index of refraction and giant optical activity. However, the biosensing capabilities of these chiral metamaterials have not been fully explored. Ultrasensitive detection and structural characterization of proteins adsorbed on chiral plasmonic substrates was demonstrated recently using UV-visible circular dichroism (CD) spectroscopy. Second harmonic generation microscopy is an extremely sensitive nonlinear optical probe to investigate the chirality of biomaterials. In this study, we investigate the effects on the second harmonic generation – circular dichroism (SHG-CD) response from biomolecules adsorbed on chiral nanostructured substrates. These planar chiral metamaterials, fabricated by electron-beam lithography, consist of right-handed and left-handed gold gammadions of length 400 nm and thickness 100nm, deposited on a glass substrate and arranged in a square lattice with a periodicity of 800nm. The results of the SHG-CD measurements are compared to the results of the CD measurements on the same samples.

8597-36, Session 8

Tissue radiation dose measurement using viscoelastic shear wave at thermal steady state

Sheng-Yi Chang, Ming Chi Univ. of Technology (Taiwan); Chien Chou, Chang Gung Univ. (Taiwan); Chien-Wa Ho, National United Univ. (Taiwan); Tong-Sheng Hsieh, Taipei Veterans General Hospital (Taiwan); Li-Ping Yu, Chang Gung Univ. (Taiwan)

A novel bio-dosimeter based on measuring attenuated harmonic oscillation frequency of the viscoelastic shear wave (VSW) in porcine dermis via transverse displacement at fixed location under ionization radiation is proposed. The porcine dermis is converted into an isotropic and homogeneous viscoelastic medium after ionization radiation. This results in the change of oscillation frequency of VSW in porcine dermis due to variation of the complex shear modulus or mass density of porcine dermis which is sensitive to ionization radiation. It is in contrast to normal porcine dermis which shows optical properties of anisotropic and inhomogeneous. A polarized heterodyne interferometer was setup which is able to precisely measure the vertical displacement at 0.3 nm. The proposed VSW bio-dosimeter was demonstrated experimentally where the oscillation frequency of VSW was measured based on real time monitoring its transverse displacement at fixed position on porcine dermis under thermal steady state condition. Linear dependent of the absorbed dose and oscillation frequency of VSW was clearly observed. In this experiment, the detection limit on absorbed dose of proposed VSW dosimeter using porcine dermis is 1 cGy by use of a linear accelerator (6 MV). The linear range of (a) 0-60cGy and (b) 80-500cGy versus oscillation frequency of VSW in porcine dermis are demonstrated. Additionally, the recovered ability of the optical properties of porcine dermis after ionization radiation at low absorbed dosage was shown. Meanwhile, the temperature effect which induces the change of mass density of porcine dermis, on oscillation frequency of VSW of porcine dermis was presented and discussed.

8597-37, Session 8

Real-time detection of toxins using localized surface plasmon resonance (LSPR) sensing

Reza Abbaspour, Maysamreza Chamanzar, Mahmoud Mahmoud, Farshid Ghasemi, Georgia Institute of Technology (United States); Yi Lasanajak, Xuezheng Song, Emory Univ. (United States); Mostafa El-Sayed, Georgia Institute of Technology (United States); Richard Cummings, Emory Univ. (United States); Ali Adibi, Georgia Institute of Technology (United States)

We demonstrate real-time detection of different toxins using localized surface plasmon resonance (LSPR) sensing through immobilizing novel plasmonic gold nanocages on a glass surface. The surface of these nanoparticles are functionalized using different purified glycans such as pentasaccharide GM1 and nonasaccharide NA2 as specific ligands in order to detect different toxins such as the B-subunit of Cholera Toxin (CTB) and Ricinus Communis Agglutinin I (RCA I). Toxins are captured by the glycans on the surface of the plasmonic nanoparticles and result in a red-shift in the LSPR peak wavelength. The shift in the extinction peak of the LSPR mode of the plasmonic nanoparticle (that is proportional to the level of the binding events) is used to track the toxin-glycan binding dynamics using our sensor in a custom-made microabsorption spectrophotometer, we can measure the extinction spectrum with high signal-to-noise ratio (SNR) with steps of only 300 msec. Using this system, we have been able to resolve the binding kinetics of 200 nM CTB to GM1 over a period of 400 sec. The transducer sensitivity is separately measured using different bulk analytes with different refractive indices and a large sensitivity of 300 nm/RIU is obtained. In this paper, we will outline the details of the design, implementation, and experimental characterization of the sensor including the integration of microfluidic circuitry with the plasmonic device. We will also demonstrate the sensing scenarios to detect different toxins with high sensitivity and specificity. Furthermore, we will discuss the possibilities for making an array of such sensors for multiplex toxins screening in complex analyte media.

8597-38, Session 8

Spectro-angular optical biosensor based on surface plasmon resonance operating in the visible spectrum

Sandrine Filion Côté, Philip J. R. Roche, Andrew G. Kirk, McGill Univ. (Canada)

Surface plasmon resonance (SPR) sensing is one of the most widely used methods to implement biosensors due to its sensitivity and capacity for label-free detection. Most conventional SPR sensors measure the change in reflectance at a metal-dielectric interface as a function of either angle or wavelength. However, it has recently been shown that an increase in sensitivity and a greater robustness against noise can be achieved by measuring reflectivity in both domains simultaneously, in a so-called spectro-angular SPR biosensor. This provides a surface plasmon dispersion curve on an image sensor that is tracked in real time. A single value decomposition method is used to project the dispersion curve onto a basis set and allows the image obtained from an unknown refractive index sample to be compared very accurately with a pre-calculated reference set. The objective of the current work is to further improve the detection limit of the spectro-angular biosensor. Simulations have shown that the spatial resolution and numerical precision of the image sensor have a significant impact on the accuracy of the refractive index change measurement. Therefore, upgrading the cameras used for the data acquisition could significantly improve the detection limit of the SPR biosensor. In this work, simulation results are presented to justify the modifications of the experimental system and to estimate the expected improvement in the detection limit of the spectro-angular biosensor by using higher spatial resolution and higher data precision cameras. Experimental results will be presented showing the improvement with respect to the previous design.

8597-39, Session 8

Surface-enhanced infrared absorption from nano-ellipse arrays fabricated using nanospherical-lens lithography

Sih-Chen Lu, Yun-Chorng Chang, National Cheng Kung Univ. (Taiwan)

Nanospherical-Lens Lithography (NLL) is an economic fabrication technique that is capable of fabricating nanodisk arrays that cover large

area. It utilizes polystyrene nanospheres as focusing lenses to focus the incoming ultraviolet light and exposure the underlying photoresist layer. Photoresist hole arrays form after developing. Metal nanodisk arrays can be fabricated following metal evaporation and lifting-off process. Nanodisk arrays with diameter less than 100 nm and cover an area as large as 1 cm2 are being fabricated using NLL in our research group.

In this study, NLL is used to fabricate nano-ellipse arrays by replacing the light source with a commercial ultraviolet lamp. The UV light from the lamp is propagating differently between the directions perpendicular and parallel to the lamp and therefore demonstrates different focusing behavior. We discovered that the ratio between the lengths of long axis to the short axis of the fabricated nano-ellipse is related to the diameters of the nanospheres. The large the nanosphere, the ratio becomes higher. By using nanospheres with diameter of 2 micron, the ratio is close to 3 and we were able to fabricate nano-cross arrays by performing an additional exposure after rotating the lamp for 90 degree. This fabricating process is very economic and fast. The Localized Surface Plasmon Resonance (LSPR) of the nano-ellipse arrays dependes on the long-axis of the nano-ellipse. The response is in infrared region when the long-axis length exceeds 1 micron. Therefore, the nano-ellipse arrays fabricated using NLL is a strong candidate for surface-enhanced infrared absorption (SERIA).

8597-40, Session 8

Label free plasmonic slot waveguide biosensor for biochemical sensing

Tuffail Dar, Muttukrishnan Rajarajan, The City Univ. (United Kingdom)

The finite element method based on the full-vectorial H-field formulation has been employed to achieve the maximum field penetration in the sensing medium of the plasmonic slot waveguide based ring resonator biosensor. The use of nanometer scale guiding structure where optical mode is confined in a low-index region permits a very compact sensor with high optical intensity in the region, which makes it possible to detect minimum refractive index change, and offers higher sensitivities. We analyse the change in effective refractive index of mode, sensitivity and power confinement of proposed plasmonic slot waveguide based ring resonator biosensor for biochemical sensing applications.

8597-41, Session 8

Gold nanocrescents for temperature sensing and local heating

Michael Levy, Institut Langevin (France); Xuan Hoa Vu, Institut Langevin (France) and Thai Nguyen Univ. (Viet Nam); Thomas Barroca, Emmanuel Fort, Institut Langevin (France)

Controlling and measuring the local temperature of complex media at the nanometer scale presents an increasing interest in several nanotechnology applications including nanoscale catalysis and photothermal therapeutic medicine. On a more fundamental level, it also represents a key factor to study local thermal processes as physicochemical and biochemical reactions. Consequently, different strategies have been developed during the last decade to perform high resolution thermal mapping. Nevertheless, these techniques only probe the local temperature. They do not perform to actively control it by heating or cooling the media.

In the present study we design specific nano-objects commonly called nanocrescents and consisting in gold semi-coated nanoparticles in order to simultaneously act as thermal nano-probes and as local nano-heaters remotely activated. Such a double function is made possible by combining the unique plasmon resonance properties of metallic nanostructures with the anisotropic optical signature of a gold semi-shell.

The local temperature is actually evaluated studying the rotational Brownian motion of an individual particle by rotational scattering correlation spectroscopy. Because of the particle anisotropic optical signature, the rotational diffusion makes it blink erratically and the autocorrelation of such a blinking intensity give access to the temperature surrounding the particle. By focusing on rotational diffusion instead of translational one our method free itself from potential troubling currents in the environment and may be applied even in complex biological media where the translational diffusion is confined.

The heating efficiency of our particles proceeds from their well-established plasmonic properties and more precisely from their strong absorption cross-section. Using an incident laser at the wavelength of a plasmon resonance we induce heat dissipation around an individual particle, generating a local hyperthermia.

Here we give evidence that nanocrescents can induce a local and remote control heating of their surroundings and that using rotational scattering correlation spectroscopy is an efficient way to probe the reached temperature.

8597-42, Session 8

Transmission resonance of a three-dimensional nanostructure with a localized surface plasmon property

Mohamadreza Najiminaini, Fartash Vasefi, Lawson Health Research Institute (Canada); Bozena Kaminska, Simon Fraser Univ. (Canada); Jeffrey J. L. Carson, Lawson Health Research Institute (Canada)

The interaction of light with a nano-hole array (NHA) structure in an opaque metal film results in extraordinary optical transmission (EOT). The EOT phenomenon occurs due to the coupling of incident light to the surface plasmon (SP), where the NHA structure allows momentum matching between light and the SP at certain wavelengths with respect to the grating geometry and incident angle of the light. However, the electric field intensity nearby each nano-hole at the EOT position was not as great as the electric field nearby a nano-disk of similar size due to the propagating SP property of NHAs versus the localized SP (LSP) property of nano-disks. A structure that could provide for a resonance transmission mediated by the LSP effect could potentially outperform a structure that provides for SP effects alone (such as a standard NHA).

We designed and fabricated a gold NHA membrane, where each hole was co-registered with a nano-disk on the substrate with a nano-scale separation between them. This structure provided a new resonance transmission due to the LSP interaction between each hole and co-registered disk. The LSP resonance properties of the structure were experimentally and numerically investigated for different hole and disk diameters and various separation distances. A high electric field intensity between each hole and disk was observed, when the separation distance between each hole and co-registered disk was less than 100 nm. Also, the LSP resonance position was greatly dependent on the hole and co-registered disk diameter as well as their separation distance.

8598-1, Session 1

Digital cameras in bio-inspired designs: from humans to flies *(Keynote Presentation)*

John A. Rogers, Univ. of Illinois at Urbana-Champaign (United States)

Imaging systems found in biology exploit design principles that enable fields of view, uniformity in illumination, acuity to motion and levels of aberration that are difficult or impossible to realize using conventional technologies. This talk describes our work on cameras that adopt curvilinear layouts inspired by eyes found in mammals and insects. We explain the underlying materials science and mechanics of these approaches, and illustrate the imaging characteristics through modeling and experimental studies. Working cameras in geometries that mimic eyes in humans and flies demonstrate the ideas.

8598-2, Session 2

Protein-based photonic devices: 1. lasers

Malte C. Gather, Technische Univ. Dresden (Germany) and Wellman Ctr. for Photomedicine (United States) and Harvard Medical School (United States); Seok Hyun Yun, Wellman Ctr. for Photomedicine (United States) and Harvard Medical School (United States)

The invention of the laser has enabled a vast variety of novel technologies and today lasers play an integral role in data storage, communications, materials processing, various measurements and sensing techniques, as well as in biomedicine. However, while lasers are clearly omnipresent, lasing has remained a man-made phenomenon and lasing is non-existent in natural, biological systems.

Here, we present a new type of laser that is based on the biologically produced green fluorescent protein, GFP, and show that this novel laser material can support lasing in various device configurations. Different lasers based on recombinant solutions of GFP are investigated and compared in terms of their performance and characteristics. Besides the fundamental significance of being able to generate laser light in biologically produced materials, we expect that these bio-lasers will also become enabling tools for new biomedical applications.

8598-3, Session 2

Multi-layered liposomes as optical resonators

Derrick Yong, A*STAR Singapore Institute of Manufacturing Technology (Singapore) and Nanyang Technological Univ. (Singapore); Xia Yu, A*STAR Singapore Institute of Manufacturing Technology (Singapore); Chi Chiu Chan, Nanyang Technological Univ. (Singapore)

Light propagation and amplification within biological systems have always been challenges to imaging and therapy due to the high absorptivity and scattering effects of biological tissues. These have led to the devise of circumventing techniques such as the use of deeply penetrating near-infrared light sources and additional introduction of amplifying or transducing nanoparticles. Notably, the recent demonstration of biological lasers (by M. C. Gather and S. H. Yun) has opened an entirely new avenue for potential light delivery in vivo. Their successful demonstration of lasing action from single-cells in vitro, however, required the presence of external resonators (cavity mirrors), which sandwich GFP-expressing cells. Miniaturizing these external resonators, as highlighted by the authors, would therefore allow for in vivo lasing. With considerations of maintaining cellular integrity and limiting the introduction of non-biological components, we propose the use of multilayered phospholipid membrane structures as optical resonators. As explored and demonstrated by numerous groups, multilayered microspheres possess cavities capable of confining light and energy of particular wavelengths with high Q-factors. These properties, in particular, can then be tuned by altering the refractive index profile and periodicity of the multilayered structure. Their inorganic nature has however restricted applications in vivo, requiring surface modifications and size restrictions. On the other hand, the biological disposition and inherent ability for self-assembly of liposomes render them ideal organic platforms for mimicking the described multilayered microspheres. We therefore aim to achieve Bragg reflection or a bandgap effect by fabricating and studying liposomes with alternating refractive index layers and specific layer-layer separation distances.

8598-4, Session 2

Biological photonic structures and their bio-inspired stimuli-responsive adaptive optical counterparts *(Invited Paper)*

Mathias Kolle, Joanna Aizenberg, Harvard Univ. (United States)

Nature's brightest colors result from the interaction of light with intricate compositions of periodic hierarchical micro- and nanostructures, found in the scales, and wing cases of many insects, the feathers of birds or in the skin of some mammals. Knowledge of the interplay between the morphology, composition and optical appearance of such biological photonic systems can provide broad inspiration for novel artificial photonic elements. The detailed analysis of biophotonic systems can yield inspiration and even detailed design templates for man-made photonic structures. In this talk we identify a number of organic and inorganic biophotonic architectures bound to surfaces or confined within fibrous geometries. We then discuss possible approaches to transfer the key elements of these role model biological structures into artificial stimuli-responsive bio-inspired photonic systems. In particular, we will present the investigation of bio-inspired elastic band-gap tunable photonic fibers and discuss the unique optical properties of bio-inspired thermo-responsive micro-diffraction grating arrays.

8598-5, Session 2

Study of nano-architecture of the wings of Paris Peacock Butterfly

Ekata H. Ghate, Gauri R. Kulkarni, Sudha V. Bhoraskar, Univ. of Pune (India)

Butterflies are one of the most colorful creatures in animal Kingdom. Wings of the male butterfly are brilliantly colored to attract females. Color of the wings often plays an important role in camouflage.

Study of the structural colors in case of insects and butterflies are important for their biomimic and biophotonic applications. Structural color is the color which is produced by physical structures and their interaction with light.

Paris Peacock butterfly or Papilio paris belongs to the family Papilionidae. The basis of structural color of this butterfly was investigated in the present study. The upper surface of the wings in this butterfly is covered with blue, green and brown colored scales. Nano-architecture of these scales was investigated with scanning electron microscope(SEM) and environmental scanning electron microscope (ESEM). Photomicrographs were analyzed using image analyzing software.

Goniometric color or iridescence in blue and green colored scales of this butterfly was observed and studied with the help of gonio-spectrophotometer in the visible range. No iridescence was observed in brown colored scales of the butterfly. Hues of the blue and green color

were measured with spectrophotometer and were correlated with nano-architecture of the wing.

Results of electron microscopy and reflection spectroscopy are used to explain the iridescent nature of blue and green scales.

Sinusoidal grating like structures of these scales were prominently seen in the blue scales. It is possible that the structure of these wings can act as a template for the fabrication of sinusoidal gratings using nano-imprint technology.

8598-6, Session 3

Biopolymer-based optical waveguides for photochemical tissue bonding

Sedat Nizamoglu, Myunghwan Choi, Malte C. Gather, Robert W. Redmond, Massachusetts General Hospital (United States); Seok Hyun Yun, Wellman Ctr. for Photomedicine (United States)

Photochemical tissue bonding (PTB) is an emerging technique for wound closure, which is fast and safe and leaves less scarring than conventional sutures [1]. In PTB, an FDA-approved dye, such as Rose Bengal, is applied, and green activation light is illuminated to induce dye-assisted cross-linking between collagen fibers of the tissues [2]. Although PTB of superficial skin incisions has been successfully demonstrated, bonding thicker tissues has been challenging due to the limited light penetration depth (<2 mm) in the tissue. To solve this problem, we propose and demonstrate waveguide-assisted PTB. We have fabricated thin mesh-type optical waveguides using various types of transparent biopolymers, such as PEG, PLLA, and PVP, and measured a wide range of light extraction efficiencies (dB/mm). Using a biopolymer waveguide we demonstrate PTB on full-thickness skin incisions (>1 cm) in animal models.

References

[1] S. Tsao et. al., “Light-activated tissue bonding for excisional wound closure: a split-lesion clinical trial,” British Journal of Dermatology, 166, 555-563 (2012).

[2] Y. Kamegaya et. al., “Evaluation of photochemical tissue bonding for closure of skin incisions and excisions,” Lasers in Surgery and Medicine, 37, 264-270 (2005).

8598-7, Session 3

Implantable optical waveguide for light-controlled cell therapy

Myunghwan Choi, Harvard Medical School (United States) and KAIST (Korea, Republic of); Jin Woo Choi, Wellman Ctr. for Photomedicine (United States); Sedat Nizamoglu, Massachusetts General Hospital (United States); Seok Hyun Yun, Wellman Ctr. for Photomedicine (United States) and KAIST (Korea, Republic of) and Harvard-MIT Health Sciences and Technology (United States)

Optogenetic technology enables control of cellular activities through exposure to light by genetically introducing light-sensitive proteins into the cell. Such cells can be further engineered to transmit the optogenetic signal to a targeted cellular physiology, such as secretion of a therapeutic protein for cell therapy. In this approach, poor penetration of light into tissues is considered as a barrier to the development toward its clinical applications. The current gold standard to mitigate the light delivery problem is to use an optical fiber. While the point illumination from the tip of the fiber is adequate for certain scenarios, most applications require uniform illumination over large volume. Here we report novel use of a hydrogel as both an optical waveguide and a cell scaffold, where light delivered via an optical fiber is distributed uniformly over the cells encapsulated within the hydrogel. We tested poly-ethylene glycol hydrogels with different monomer sizes and concentrations to optimize both optical transmittance for light-guiding and mechanical stability for implantation. The higher monomer size resulted in better optical transmittance but reduced mechanical stability. After establishing the optimal composition, we confirmed long-term maintenance of light transmittance and cellular viability of implanted hydrogel. Cells engineered to express glucagon-like protein-1 in response to light were encapsulated into the hydrogel waveguide and implanted into diabetic mice. The mice showed markedly enhanced glucose homeostasis in glucose tolerance test when light is delivered. Our results demonstrate the proof of concept of the implantable hydrogel waveguide for light-controlled cell therapy.

8598-8, Session 3

Micro-encapsulated implantable bio-markers for assessment of oxidative stress in aquatic organisms in vivo

Anton V. Sadovoy, Cathleen Teh, A*STAR Institute of Materials Research and Engineering (Singapore); Marc Escobar, A*STAR Institute of Medical Biology (Singapore); Vladimir Korzh, Institute of Molecular and Cell Biology (Singapore); Igor V. Meglinski, Univ. of Otago (New Zealand)

We develop micro-encapsulated implantable bio-marker for assessment of oxidative stress in aquatic organisms in vivo. The bio-compatible poly-electrolyte micro-capsules are used to deliver fluorescent dyes sensitive to amount of reactive oxygen spices in tissues. Micro-encapsulation prevents dye diffusion in tissue that makes use toxic dyes possible. The encapsulated fluorescent dyes injected in zebrafish larvae have been monitored by using hybrid laser scanning imaging system combined with the fluorescent microscope. The obtained results show that micro-capsules are stable and naturally circulating through brain, liver, and other organs with no blood flow disruptions or any other disturbances that can affect cardiac or organ functions. Current approach has a great potential to use such micro-encapsulated bio-markers as a diagnostic tool in vascular biology as well as for monitoring of aquatic pollution and ecological risk assessment in eco-toxicological studies.

8598-9, Session 3

Biomolecule microdroplets on superhydrophobic biopolymer substrates: a biomaterial laser

Sedat Nizamoglu, Malte C. Gather, Massachusetts General Hospital (United States); Seok Hyun Yun, Wellman Ctr. for Photomedicine (United States)

Light sources based on biologically safe materials have the potential to serve as an important building block for new implantable devices for optical diagnosis and therapies. In particular, an interesting device is a laser made of biocompatible and biodegradable biomaterials, as such a laser can be used as a sensor on its own [1] or integrated as a light source into a more complex, implantable photonic device. Under the strategy of optical pumping, a number of organic dyes approved for human use, such as indocyanine green can serve as the gain medium. A notable example is the “edible” laser, where a drop of fluorescein gelatin-dye solution dangling from a glass pipet was used [2]. A number of droplet lasers via microdrop liquid jet [3], electrodynamical trap [4] and superhydrophobic surface [5] have been reported. In this study, we demonstrate a biomaterial-based laser using flavin mononuclotide (FMN) biomolecule microdroplets encapsulated in superhydrophobic polylactic acid (PLLA) biopolymer microwells. Vitamin microdroplets with diameters of 10-30 micrometer were formed in situ on a superhydrophobic substrate (with a contact angle of 154 degree). These droplets supported the oscillation of whispering gallery modes with quality factors of ~3000. The laser exhibits a threshold energy of 32 nJ/pulse and quasi-isotropic emission.

References

1. Y. Sun, J. Liu, G. Frye-Mason, S. Ja, A. K. Thompson, and X. Fan, Optofluidic ring resonator sensors for rapid DNT vapor detection, Analyst 134, 1386–1391 (2009).

2. T. Hansch, M. Pernier, A. Schawlow, Laser action of dyes in gelatin, IEEE Journal of Quantum Electronics, 7, 45-46 (1971).

3. S. X. Qian, J. B. Snow, H. M. Tzeng, R. K. Chang, Lasing Droplets: Highlighting the Liquid-Air Interface by Laser Emission, Science 231, 486 (1986).

4. M. Tona, M. Kimura Novel Lasing Modes Observed in a Levitated Single Dye-Doped Microdroplet. J. Phys. Soc. Jpn. 69, 3533 (2000).

5. A. Kiraz, A. Kurt, M. A. Dündar, A. L. Demirel, Simple largely tunable optical microcavity, Appl. Phys. Lett. 89, 081118 (2006).

8598-10, Session 3

Nanoconstructs for biomedical multifunctional imaging *(Invited Paper)*

Paolo Decuzzi, The Methodist Hospital Research Institute (United States)

Nanoconstructs are multifunctional, particle-based devices for the 'smart' delivery of therapeutic and imaging agents. In this lecture, first, an integrated approach will be presented for the rational design of nanoconstructs with high level of accumulation within the diseased tissue and minimal sequestration by the organs of the reticulo-endothelial system (liver, spleen, kidneys, lungs). Second, a new class of multifunctional nanoconstructs will be described offering superior contrast enhancement for MR imaging and thermal ablation potential under non invasive electromagnetic fields.

The integrated approach for the rational design of nanoconstructs combines together the in-silico mathematical modeling for the vascular transport and adhesion of blood-borne nanoparticles, in-vitro microfluidic-based assays and in-vivo intravital microscopy analysis in small animals. The multifunctional nanoconstructs are based on mesoporous silicon and hydrogel-based particles exhibiting a variety of size and shape combinations, loaded with Gd-based contrast agents (Magnevist®; Gd-nanotubes and Gd-fullerenes) for T1-based MRI and SuperParamagnetic iron oxide (SPIOs) for T2-based MRI. In the presence of non-invasive electromagnetic fields, these nanoconstructs could also generate thermal toxicity for tissue ablation and/or triggered drug release.

8598-11, Session 4

Bio-inspired microlenses and their biomedical applications *(Invited Paper)*

Hongrui Jiang, Univ. of Wisconsin-Madison (United States)

Optical detection and imaging have wide applications in biomedicine and biological and chemical analyses. With continuing miniaturization effort to realize integrated microsystems, micro-scale optical components become more and more important. For any optical system, lenses are critical elements. In this talk, I will present our work on liquid microlenses. I will first introduce a few types of microlenses and microlens arrays, including tunable liquid microlenses actuated by temperature-, pH- and infrared light-responsive hydrogels. Then, I will discuss about potential applications of these lenses in medical instruments. I will describe miniaturized cameras capable of multiple viewpoints, and prototype flexible endoscopes implementing infrared-light responsive liquid microlenses at their distal ends.

8598-12, Session 4

Novel photodynamic therapy based on bioluminescence energy

Yi Rang Kim, Seonghoon Kim, KAIST (Korea, Republic of); Jin Woo Choi, Wellman Ctr. for Photomedicine (United States); Gou Young Koh, KAIST (Korea, Republic of); Seok Hyun Yun, Wellman Ctr. for Photomedicine (United States) and KAIST (Korea, Republic of)

Photodynamic therapy(PDT) uses visible light to activate the drug called a photosensitizer. While PDT is clinically used to treat such diseases as age-related macular degeneration and esophageal cancer, applications of PDT in other areas have been limited by the poor penetration of light into tissues. For example, current PDT is ineffective to treat large tumors with sizes greater than the typical optical penetration depth (a few mm's) or even small tumors located within the tissue at depths greater than the penetration depth. Here, we present new PDT technique using bioluminescence energy. We found that the resonant nonradiative energy transfer from bioluminescence molecules, but not bioluminescence emission, is sufficient to activate the photosensitizers. Tumor growth was markedly suppressed in mice treated with the administration of bioluminescence molecules and photosensitizers. Our new approach was more effective to treat deep and large size tumors than conventional PDT using external illumination.

8598-13, Session 4

Biomimetic polydopamine coating on gold nanorods for biofunctionalization, imaging, and photothermal therapy

Kvar C. Black, Washington Univ. School of Medicine in St. Louis (United States); Ji Yi, Jose Rivera, Daria Zelasko-Leon, Phillip B. Messersmith, Northwestern Univ. (United States)

A versatile biomimetic polydopamine (PD)-based strategy was employed for presenting antibodies and metals on gold nanorods (NRs) to target either cancer cells or bacterial cells for use in photothermal therapy. With regard to cancer, PD was polymerized onto gold NRs, and epidermal growth factor receptor antibodies (anti-EGFR) were immobilized onto the layer. Cell-binding affinity and light activated cell death of cancer cells incubated with anti-EGFR-PD-NRs were quantified by optical imaging. PD was successfully deposited onto gold NRs, and antibodies were bound to PD-coated NRs. Anti-EGFR-PD-NRs were stable in media, and specifically bound to EGFR-overexpressing cells. Illumination of cells targeted with anti-EGFR-PD-NRs enhanced cell death compared to non-irradiated controls and cells treated with antibody-free NRs. To create a multifunctional antibacterial NR, silver and antibacterial antibodies were immobilized onto the biomimetic PD layer surrounding gold NRs. NRs were identified on bacteria through optical and electron microscopies. Irradiation with light of cells targeted with NRs produced substantial heating and release of silver from the layer, which caused a significant synergistic bacterial killing effect. Overall, PD facilitates the surface functionalization of gold NRs with biomolecules and metals, allowing cell targeting and photothermal killing of cancer or bacterial cells. PD can potentially coat a large variety of nanoparticles with targeting ligands as a strategy for biofunctionalization of diagnostic and therapeutic nanoparticles.

8598-14, Session 4

Imaging through turbid media *(Invited Paper)*

Wonshik Choi, Dept. of Physics, Korea Univ. (Korea, Republic of)

"Turbidity" caused by multiple scattering interrupts the propagation of waves and thus undermine optical imaging. For example, translucent biological tissues limit imaging depth and significantly attenuate energy

transmission. In this talk, I will describe the counterintuitive finding that optical turbidity, rather than being a hindrance to imaging, can in fact dramatically improve both the spatial resolution and the field of view of the target images. These improvements are based on our new method of extracting the original image information from the image distorted by the multiple scattering, which we call turbid lens imaging (TLI)[1-2]. With the use of TLI, we achieve the resolution enhancement by more than five times over the diffraction limit and the extension of view field over the physical area of the camera.

In addition, I will introduce our recent work that realizes maximal energy transport through disordered media[3]. However high the degree of disorder becomes, it is possible in principle to enhance the delivery of energy to the far side of the medium. Similar to the resonator modes in the linear optical cavities, specific modes called eigenchannels exist for a disordered medium which have extraordinarily high transmission. We reported the first experimental realization of the transmission eigenchannels in a disordered medium and showed that an eigenchannel transport 3.99 times more energy than uncontrolled waves, which is the best experimental record reported so far. Our study will open up new avenues for enhancing light energy delivery to biological tissues and for improving imaging depth in biomedical imaging.

Reference

1. Y. Choi, T. D. Yang, C. Fang-Yen, P. Kang, K. J. Lee, R. R. Dasari, M. S. Feld, and W. Choi, “Overcoming the Diffraction Limit Using Multiple Light Scattering in a Highly Disordered Medium,” Phys Rev Lett 107, 023902 (2011).

2. Y. Choi, M. Kim, C. Yoon, T. D. Yang, K. J. Lee, and W. Choi, “Synthetic aperture microscopy for high resolution imaging through a turbid medium,” Opt Lett 36, 4263-4265 (2011).

3. M. Kim, Y. Choi, C. Yoon, W. Choi, J. Kim, Q-H. Park, W. Choi, “ Maximal energy transport through disordered media with the implementation of transmission eigenchannels,” Nature Photonics, DOI: 10.1038/NPHOTON.2012.159 (2012).159

8598-15, Session 5

Photonic biosensors for mild traumatic brain injury-biomimetic indicators and field portable biomarker diagnostics

Mark A. Mentzer, U.S. Army Aberdeen Test Ctr. (United States)

While there is much focus upon the high prevalence of brain traumas experienced in both military scenarios as well as contact sports we lack adequate means for instrumenting live fire tests to assess mild traumatic brain injury (mTBI). This prevents effective mitigation or prevention of mTBI, through improved personal protective equipment, or by early diagnosis in the field, coupled with appropriate therapeutic intervention. This situation represents an opportunity to solve a serious problem using microfluidics and biosensors. We therefore describe a biomimetic indicator of mTBI, as well as a microfluidic platform for detection of blood based biomarker panels for identification of neuropathological cascades and therapeutic opportunity. The sensor construct is a self-assembled liposome encapsulating self-quenching dye. Disruption of the liposomes encapsulating self quenching calcein dyes produces a colorimetric change proportional to the traumatic event. The proposed complementary microfluidic platfrom will provide multi-antibody protein detection.

8598-17, Session 5

Bioinspired photonic materials and technologies at the U.S. Defense Threat Reduction Agency and the U.S. DoD *(Invited Paper)*

Viktoria Greanya, Defense Threat Reduction Agency (United States)

The Defense Threat Reduction Agency’s (DTRA) Chemical and Biological Defense Department funds critical research and technology development to counter the country’s current and future chemical and biological (CB) threats. Efforts span from innovative basic research to impactful advanced technology demonstrations to enable new DoD capabilities. The Department of Defense (DoD) has a long history of interest in bioinspired and biomimetic approaches. Recent investment in bioinspired photonics has centered in general on fabrication, sensors, camouflage, displays, and diagnostics technologies. This presentation will provide a broad picture of existing and potential future interests in the area of bioinspired photonics at DTRA as well as other DoD agencies.

8598-18, Session 6

Protein-based photonic devices: 2. sensors

Malte C. Gather, Technische Univ. Dresden (Germany) and Wellman Ctr. for Photomedicine (United States) and Harvard Medical School (United States); Seok Hyun Yun, Wellman Ctr. for Photomedicine (United States) and Harvard Medical School (United States)

The discovery and development of fluorescent proteins represents a major breakthrough for biomedical research and has enabled non-destructive monitoring and imaging of various biological processes in-vivo. Based on our recent finding that the green fluorescent protein, GFP, can not only serve as a fluorescent probe but is also capable of generating stimulated emission in an efficient manner, we discuss possibilities to use fluorescent protein-based cell lasers and other protein based devices as sensors.

8598-19, Session 6

Imaging and analysis of single chromatin molecules *(Invited Paper)*

Harold Craighead, Cornell Univ. (United States)

8598-20, Session 6

Silicon nanophotonic ring resonator sensors integrated in reaction tubes

Cristina Lerma Arce, Tom Claes, Katarzyna Komorowska, Peter Bienstman, Univ. Gent (Belgium)

Enzyme-linked immunosorbent assay (ELISA) is the most popular immunoassay technique performed every day in hospitals and laboratories and it is used as a diagnostic tool in medicine and plant pathology, as well as a quality-control check in various industries. [1] However, complex labeling techniques are required to be able to perform the assay and non-specific binding and endpoint timing are difficult to optimize. These issues could be solved by label free techniques such as silicon nanophotonic microring resonator sensors we studied earlier [2], but this platform requires complex microfluidics, which is still very much removed from the daily practice in e.g. hospital labs, which still relies to a large degree on platforms like 96-well microtiter plates, or reaction tubes. To address these issues, here, we propose the combination of a simple and compatible reaction tube platform with label free silicon-on-insulator (SOI) photonic biosensors. The device consists of a reaction tube in which bottom a silicon photonic chip has been integrated. This chip contains an array of well-known microring resonators sensors [2] which will be in contact with the fluid under analysis. The main difference with our previous work is that now light from a tunable laser is coupled into the microring resonator through the chip substrate. A shift in the resonance wavelength of the ring is measured when a binding event is produced on the surface of the sensors. This device allows real time

detection and analysis. Its great flexibility and small footprint make it ideal for an easy handling in any laboratory.

8598-21, Session 6

Directed self-assembly of synthetic proteins nanowires: structural control and excited-state dynamics of Pi-conjugate amyloids

William L. Wilson, Univ. of Illinois at Urbana-Champaign (United States)

Supramolecular materials with electronic function driven by π-conjugated organic subunits are a technologically exciting option for nanomaterials in the size regime (1-100nm). While much work has focused on the self-assembly of molecular π-conjugated components from organic solvents, to generate π-stacked aggregates that mimic transport properties of their conjugated polymer counterparts, the formation supramolecular species in aqueous, i.e., more physiological environments is far less developed. This class of self-assembling molecules contain π-conjugated elements directly embedded within peptide backbones. Aqueous assembly in solution leads to the formation of π-stacked synthetic proteins with well-defined nanoscale and potentially aligned macroscale structures. These peptide-based electronic materials undergo self-assembly into hydrogels as well-defined one-dimensional nanomaterials. We have harnessed amyloid assembly to construct nanomaterials, and used microfluidic device structures to control structural morphology. This important size regime in aqueous media is comparable to the scale of the extracellular matrix, and potentially bridges to the biotic interface. The peptide sequences attached to the π-electron cores allow for a rich diversity of structural and functional tunability impacting solubility, hydrogen-bonding structure, intermolecular π-electron delocalization, and exciton dynamics. Understanding the details of this physics is critical for realizing advanced technologies with these energy transporting nanomaterials. We discuss the photophysical and exciton dynamics of these assembled proteins characterized using Fluorescence Lifetime Imaging (FLIM), and Confocal Fluorescence Microscopy. The data indicates that the details of the assembly control the excited-state dynamics, moreover subtle changes is residue structure impacts the secondary structures formed and excited-state behavior observed.

8598-26, Session 6

Transient Fourier holography with bacteriorhodopsin films for breast cancer diagnostics

Gopal L. N. Rao, Univ. of Massachusetts Boston (United States)

X-ray mammography is the current gold standard for breast cancer screening. Microcalcifications and other features which are helpful to the radiologist for early diagnostics are often buried in the noise generated by the surrounding dense tissue. So image processing techniques are required to enhance these important features to improve the sensitivity of detection. We demonstrated a novel technique of recording a hologram of the mammogram. It is recorded on a thin polymer film of Bacteriorhodopsin (bR) as photo induced isomerization grating containing the interference pattern between the object beam containing the Fourier spatial frequency components of the mammogram and a reference beam. The hologram contains all the enhanced features of the mammogram. A significant innovation of the technique is that the enhanced components in the processed image can be viewed by the radiologist in time scale. The diffraction efficiency of the recorded hologram is optimum when the intensity of the spatial frequency component in the object beam is matched to the reference beam. The Fourier hologram is recorded matching the intensity of the reference beam to the high spatial frequency band corresponding to microcacifications. When the radiologist looks at the recorded movie, he would see the microcalcifications as the brightest and last long in time. He would also observe lesions with intensity decreasing as their size increases and decay faster. The movie is recorded using a CCD camera and the radiologist can conveniently look at the various features as they reveal in time scale, freezing the frame as and when desired. Within a few minutes, the recorded hologram in the bR film is completely erased and the film is ready for recording another hologram. The experimental arrangement is verasile and can be used for mammograms either in analog or digital format.

8598-22, Session PSUN

Lensed fiber bundle probe for fluorescence imaging

Joo Beom Eom, In Hee Shin, Jae Seok Park, Byeong Il Lee, Korea Photonics Technology Institute (Korea, Republic of)

A lensed fiber bundle probe has been made with a ball lens, which was packaged in a metal. By forming a focusing ball lens directly connected fiber bundle probe which was made with 61 multi mode fibers. Fiber bundle probe consists three parts of sample, source and detector region. We employed a proper ball lens diameter and distance between ball lens and fiber bundle probe. A working distance of up to 6 mm was achieved with the implemented lensed fiber bundle probe which is directly manufactured on to the fiber bundle probe connected by anti-reflection coated ball lens. We use 760 nm laser diode and ICG(Indocyanine Green) to demonstrate the feasibility of this lensed fiber bundle probe for fluorescence imaging. A lensed fiber bundle probe could be use in handheld fluorescence imaging system

8598-23, Session PSUN

A glucose fluorescent biosensor for glucose delay detection in interstitial fluid and blood

Ting Shi, Dachao Li, Kexin Xu, Tianjin Univ. (China); Lou Lu, Univ. of California, Los Angeles (United States)

Based on the high related relationship between the glucose concentration in blood and in interstitial fluid, more and more people try to realize the real-time continuous monitoring of blood glucose by the real-time continuous monitoring of glucose concentration in interstitial fluid. The major issue is the physiological lag existing between these two kinds of glucose concentration. Therefore, we have designed a fluorescent biosensor based on borate polymer to monitor the glucose dynamic changes both in blood and in interstitial fluid both in vitro and in vivo. In vitro, glucose concentration curve is established according to the known glucose concentration and its responding fluorescent intensity. In vivo, biosensor is injected into mice's subcutaneous tissue to monitor interstitial fluid glucose concentration. At the same time, blood glucose concentration is measured by biosensor in wells using tail blood. From the results we know that the response tracked blood glucose changes by this biosensor have same tendency with the measurement taken by glucose meter. Both the glucose concentration in blood and interstitial fluid can be monitored continually by fluorescent biosensor with same diffusion and association rate between biosensor and glucose. The physiological delay time is the difference constant time between blood and interstitial fluid glucose concentration, which comply with the computer model results.

8598-24, Session PSUN

Surface-enhanced Raman scattering on diatom biosilica photonic crystals

Fanghui Ren, Jeremy Campbell, Xiangyu Wang, Dihan Hasan, Gregory L. Rorrer, Alan X. Wang, Oregon State Univ. (United States)

Diatoms are a group of single-celled photosynthetic algae that make skeletal shells of hydrated amorphous silica, called frustules, which

possess hierarchical nanoscale photonic crystal features made by a bottom-up approach at ambient temperature and pressure. Such low cost, bio-inspired nanophotonic structures could potentially revolutionize the fabrication of photonic devices for optical communication, biomedical detection, chemical analysis, and energy harvesting. In this paper, we theoretically and experimentally investigate diatom biosilica photonic crystal as a platform for ultra-sensitive Surface-Enhanced Raman Scattering (SERS). We compare electric field enhancements of plasmonic nanoparticles on a flat glass substrate and on top of a diatom skeletal shell. Because of the localized electric field induced by the photonic crystal structure, plasmonic resonances at the surface of metallic nanoparticles are enhanced by a factor of ~2? at 532 nm wavelength. To experimentally determine whether the diatom substrates will increase the SERS sensitivity, we prepare a uniform layer of diatom shells on two glass substrates. Then we coat one of the substrates with thermally evaporated 10 nm thick silver film, and the other by self-assembling for high-density nanoparticle arrays on the diatom surfaces. We use confocal Raman microscope to measure the SERS signals of Rhodamine 6G. For the sample prepared by self-assembled nanoparticles, diatoms show ~2? stronger Raman signals than flat glass substrates for R6G concentration from 0.1?M to 1mM; for samples prepared by evaporated silver film, diatoms show single-molecule-detection capability with strong signature peaks of R6G, while we cannot observe any clear signal on flat glass substrates.

8598-25, Session PSUN

pH induced switching in hydrogel coated fiber Bragg grating sensor

B.N. Shivananju, Manish K. Priydarshi, Gopalkrishna M. Hegde, D. Roy Mahapatra, Sundarrajan Asokan, Indian Institute of Science (India)

Hydrogels are soft polymers which undergo either swelling or shrinkage in response to small changes in stimuli or applied field. The stimulus may include pH, temperature, electric field, magnetic field, UV / visible light, ion concentration, urea, antibody etc. Optical Fiber Bragg Grating (FBG) sensors have been used to sense temperature, strain, load, refractive index, humidity, gases like hydrogen and ammonia etc. In this paper we report a novel hydrogel functionalized FBG sensor based on chemo-mechanical-optical sensing and demonstrate its specific application in pH activated process monitoring. The sensing mechanism is based on the osmotic pressure difference between the gel and the contact environment (fluid). This pressure gradient causes the hydrogel to deform which in turn induces secondary strain on the FBG sensor resulting in shift in the Bragg wavelength. A simple dip coating method to coat a thin layer of hydrogel on the FBG has been established. Gel formation is observed in real-time by continuously monitoring the Bragg wavelength shift. We have demonstrated pH swelling and deswelling behavior of FBG functionalized with hydrogel by alternate dipping between acidic and base solutions. It is observed that the behavior is reversible and the Bragg wavelength undergoes reversible pH dependent switching. This phenomenon is likely to find enormous important applications in shape memory materials, microfluidics, Lab-on-chip, new pacemakers, bioseperation, self-walking actuators, drug delivery systems. Also this phenomenon will help to understand some of the natural biological motions like heart beat, lungs movement, brainwaves, pulsatile potential of nerve cells etc.